INSIGHTS IN HEMATOLOGIC MALIGNANCIES: 2021

EDITED BY: Alessandro Isidori
PUBLISHED IN: Frontiers in Oncology

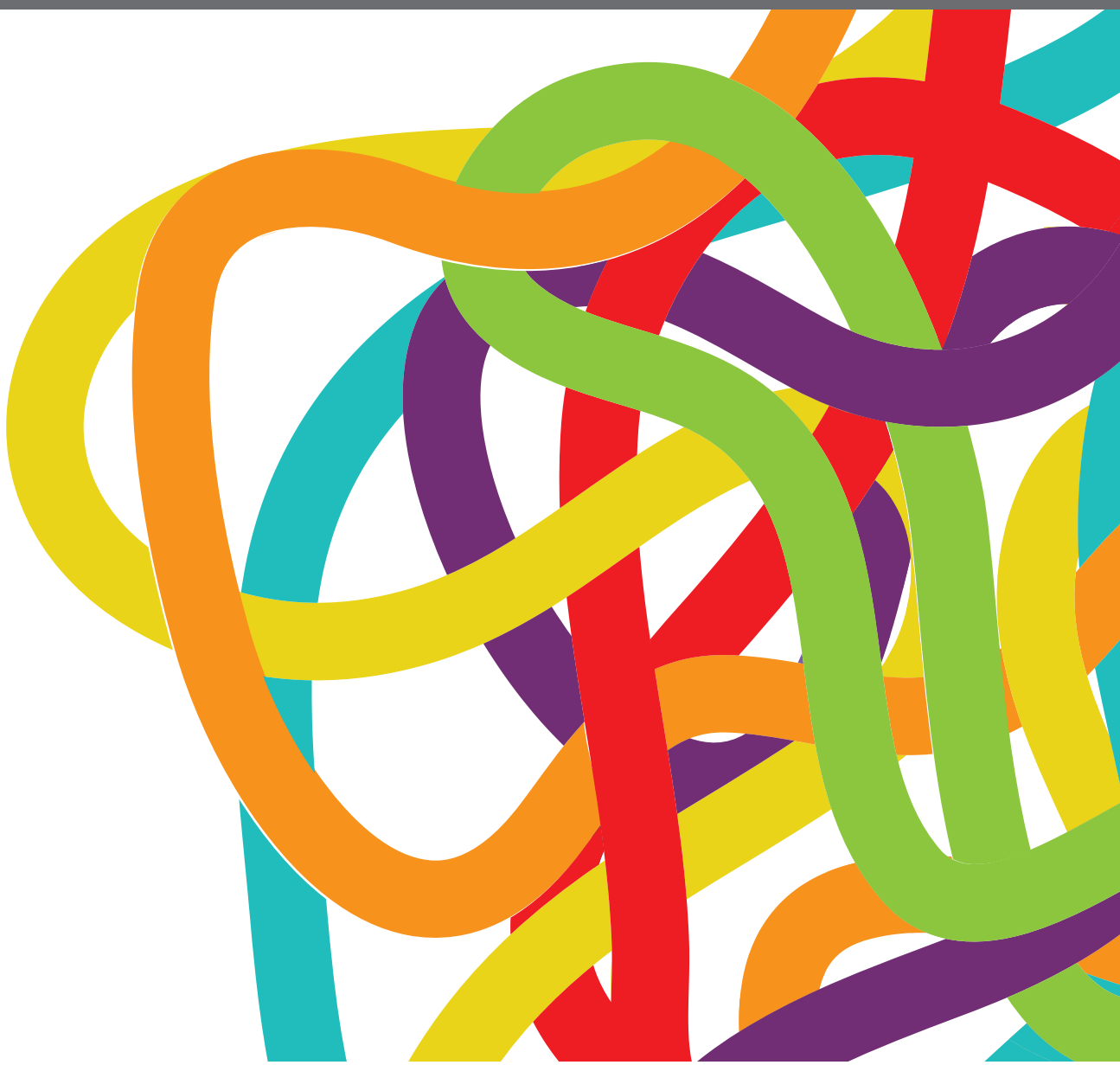

frontiers Research Topics

frontiers

ISSN 1664-8714
ISBN 978-2-88976-751-9
DOI 10.3389/978-2-88976-751-9

About Frontiers

Frontiers is more than just an open-access publisher of scholarly articles: it is a pioneering approach to the world of academia, radically improving the way scholarly research is managed. The grand vision of Frontiers is a world where all people have an equal opportunity to seek, share and generate knowledge. Frontiers provides immediate and permanent online open access to all its publications, but this alone is not enough to realize our grand goals.

Frontiers Journal Series

The Frontiers Journal Series is a multi-tier and interdisciplinary set of open-access, online journals, promising a paradigm shift from the current review, selection and dissemination processes in academic publishing. All Frontiers journals are driven by researchers for researchers; therefore, they constitute a service to the scholarly community. At the same time, the Frontiers Journal Series operates on a revolutionary invention, the tiered publishing system, initially addressing specific communities of scholars, and gradually climbing up to broader public understanding, thus serving the interests of the lay society, too.

Dedication to Quality

Each Frontiers article is a landmark of the highest quality, thanks to genuinely collaborative interactions between authors and review editors, who include some of the world's best academicians. Research must be certified by peers before entering a stream of knowledge that may eventually reach the public - and shape society; therefore, Frontiers only applies the most rigorous and unbiased reviews.
Frontiers revolutionizes research publishing by freely delivering the most outstanding research, evaluated with no bias from both the academic and social point of view. By applying the most advanced information technologies, Frontiers is catapulting scholarly publishing into a new generation.

What are Frontiers Research Topics?

Frontiers Research Topics are very popular trademarks of the Frontiers Journals Series: they are collections of at least ten articles, all centered on a particular subject. With their unique mix of varied contributions from Original Research to Review Articles, Frontiers Research Topics unify the most influential researchers, the latest key findings and historical advances in a hot research area! Find out more on how to host your own Frontiers Research Topic or contribute to one as an author by contacting the Frontiers Editorial Office: frontiersin.org/about/contact

INSIGHTS IN HEMATOLOGIC MALIGNANCIES: 2021

Topic Editor:
Alessandro Isidori, Hematology and Stem Cell Transplant Center, AORMN Hospital, Italy

Citation: Isidori, A., ed. (2022). Insights in Hematologic Malignancies: 2021. Lausanne: Frontiers Media SA. doi: 10.3389/978-2-88976-751-9

Table of Contents

frontiers in Oncology

ORIGINAL RESEARCH
published: 28 April 2021
doi: 10.3389/fonc.2021.674492

Altered T Follicular Helper Cell Subsets and Function in Chronic Lymphocytic Leukemia

Xun Wu[1†], *J. Ernesto Fajardo-Despaigne*[1†], *Christine Zhang*[1], *Vishala Neppalli*[2], *Versha Banerji*[3,4], *James B. Johnston*[3,4], *Spencer B. Gibson*[1,3,4] *and Aaron J. Marshall*[1,3,4,5*]

[1] Department of Immunology, Max Rady College of Medicine, Rady Faculty of Health Sciences, University of Manitoba, Winnipeg, MB, Canada, [2] Hematopathology Laboratory, Shared Health Manitoba, Winnipeg, MB, Canada, [3] Research Institute in Oncology and Hematology, CancerCare Manitoba, Winnipeg, MB, Canada, [4] Department of Internal Medicine, Max Rady College of Medicine, Rady Faculty of Health Sciences, University of Manitoba, Winnipeg, MB, Canada, [5] Department of Biochemistry and Medical Genetics, Max Rady College of Medicine, Rady Faculty of Health Sciences, University of Manitoba, Winnipeg, MB, Canada

OPEN ACCESS

Edited by:
Dimitar G. Efremov, International Centre for Genetic Engineering and Biotechnology, Italy

Reviewed by:
Martina Seiffert, German Cancer Research Center, Germany
Angelika Muchowicz, Medical University of Warsaw, Poland

***Correspondence:**
Aaron J. Marshall
aaron.marshall@umanitoba.ca

[†]These authors have contributed equally to this work

Specialty section:
This article was submitted to Hematologic Malignancies, a section of the journal Frontiers in Oncology

Received: 01 March 2021
Accepted: 06 April 2021
Published: 28 April 2021

Citation:
Wu X, Fajardo-Despaigne JE, Zhang C, Neppalli V, Banerji V, Johnston JB, Gibson SB and Marshall AJ (2021) Altered T Follicular Helper Cell Subsets and Function in Chronic Lymphocytic Leukemia. Front. Oncol. 11:674492. doi: 10.3389/fonc.2021.674492

Follicular helper T cells (T_{FH}) have specialized properties in promoting normal B cell activation but their role in chronic lymphocytic leukemia (CLL) is unknown. We find that T_{FH} cells are elevated in CLL patients and are phenotypically abnormal, expressing higher levels of PD-1, TIGIT, CD40L, IFNγ and IL-21, and exhibiting abnormal composition of $T_{FH}1$, $T_{FH}2$ and $T_{FH}17$ subsets. Frequencies of CD4-positive T cells expressing $T_{FH}1$ markers and IL-21 were positively correlated with patient lymphocyte counts and RAI stage, suggesting that accumulation of abnormal T_{FH} cells is concomitant with expansion of the leukemic B cell clone. Treatment with ibrutinib led to normalization of T_{FH} frequencies and phenotype. T_{FH} cells identified in CLL bone marrow display elevated expression of several functional markers compared to blood T_{FH} cells. CLL T cell-B cell co-culture experiments revealed a correlation of patient T_{FH} frequencies with functional ability of their CD4-positive T cells to promote CLL proliferation. Conversely, CLL cells can preferentially activate the T_{FH} cell subset in co-culture. Together our results indicate that CLL development is associated with expansion of abnormal T_{FH} populations that produce elevated levels of cytokines and costimulatory molecules which may help support CLL proliferation.

Keywords: chronic lymphocytic leukemia (CLL), T follicular helper (Tfh) cell, interleukin 21 (IL-21), ibrutinib, TIGIT, coculture assay, bone marrow

HIGHLIGHTS

1. Follicular helper T cells with altered cytokine and receptor profiles are progressively expanded in CLL and normalized upon treatment.
2. CLL B cells can preferentially activate follicular helper T cells, promoting $CD4^+$ T cell-driven CLL B cell proliferation *in vitro*.

INTRODUCTION

Monoclonal B cell lymphocytosis (MBL) and chronic lymphocytic leukemia (CLL) are lymphoproliferative disorders characterized by the presence of abnormal numbers of CD5+ monoclonal B lymphocytes in the blood or tissues (1). MBL is the precursor to CLL, with approximately 1% of high-count cases requiring therapy each year following progressing to CLL (2). The clinical course of CLL patients is heterogeneous and prognostic markers have been developed to predict which patients may have aggressive disease (3). Independent prognostic markers for CLL include Rai stage, age, *IGVH* mutational status, β2-microglobulin level and TP53 loss-of-function (1, 3), which are used to calculate the International Prognostic Index (4). Within tissue microenvironments, CLL B cells come into close contact with other cells such as stromal cells, which provide signals that promote survival and drug resistance (5). The lymphoid tissue environment also promotes activation of B cell antigen receptor (BCR) signaling pathways and CLL proliferation (6).

Although CLL has historically been characterized as a disease of enhanced cell survival, active signaling and proliferation within lymphoid tissue is now appreciated to be an important factor determining disease prognosis (7, 8). Within bone marrow, spleen and lymph nodes, CLL proliferation occurs in "proliferation centers" where CLL cells interact directly with T cells, myeloid cells and stromal cells and display markers of active signaling (9). CLL patients showing highly active proliferation centers exhibit aggressive disease and poor prognosis (10). Inhibitors of Bruton's Tyrosine Kinase (BTK) have proven to be efficacious in treating CLL *via* interrupting BCR signaling as well as the supportive cell:cell interactions within the lymphoid tissue microenvironment (11). BTK inhibitor treatment of CLL patients frequently results in a transient increase in circulating malignant cells after treatment, concomitant with dramatic loss of leukemic cells from lymph nodes (12), suggesting that these treatments trigger a rapid dissolution of proliferation centers.

Autologous human T cells were found to be required for CLL proliferation in a mouse xenograft model (13), suggesting they play an essential role distinct from stromal cells. Normal B cell follicles, as well as germinal centers containing activated B cells, are known to depend on a specialized subset of CD4+ T cells called follicular helper T cells (T_{FH}). These CD4+ T cells express the chemokine receptor CXCR5 (14, 15), that allows them to migrate toward its ligand CXCL13, the B cell follicle chemokine made by follicular dendritic cells (16, 17). Normal T_{FH} cells produce a unique spectrum of cytokines and costimulatory molecules and provide essential co-stimulatory signals to sustain B cell survival and proliferation within germinal centers (18). Functionally distinct T_{FH} subpopulations have been identified based on their differential expression of CXCR3 and CCR6 (19, 20). Abnormalities in T_{FH} populations have been observed in a number autoimmune diseases, where considerable evidence implicates them as drivers of pathological B cell responses (19). While substantial evidence indicates that T cell populations are altered in CLL (21–23), a full assessment of T_{FH} populations across the spectrum of MBL and CLL has not previously been reported.

Here we report a comprehensive assessment of T_{FH} populations and associations of their frequency and phenotypes with CLL biomarkers, clinical stage and immune dysfunction. We find evidence that CLL T_{FH} exhibit an increased functional capacity to produce co-stimulatory receptors and cytokines linked to CLL survival and proliferation and skewing to a $T_{FH}1$-like phenotype in advanced stage patients. Finally, we find that CLL cells can preferentially activate T_{FH} cells *in vitro* and observe an association of T_{FH} frequencies with the ability of activated CD4+ T cells to trigger CLL proliferation. These results define alterations in T_{FH} phenotype and function in CLL and indicate a potential role for these cells as part of the dysfunctional immune microenvironment in this disease.

METHODS

Patient Samples and Clinical Biomarkers

Peripheral blood and bone marrow aspirates were obtained from CLL patients attending the CLL clinic at CancerCare Manitoba. Informed consent of patients and control subjects was obtained under a protocol approved the Research Ethics Board at the University of Manitoba. Rai staging was determined using standard clinical criteria. Clinical biomarkers including CD38, IgM, IgG, IgA and lymphocyte count were determined using standard protocols and obtained from the Manitoba Tumor Bank and CAISIS database. Mononuclear cells were isolated using Ficoll-Paque density gradient and cryopreserved in 10% DMSO medium prior to analysis. Lymph node biopsies were formalin-fixed and paraffin-embedded prior to sectioning.

T Cell Phenotyping

For assessment of T_{FH} subpopulations, peripheral blood or bone marrow mononuclear cells were stained for the markers CD3, CD4, CD14, CD19, CXCR5, PD-1, ICOS, CD45RA, CCR7, CXCR3, CCR6, TIGIT (antibody details in **Supplementary Table 1**) and LIVE/DEAD™ Fixable Aqua viability dye (Invitrogen™) at room temperature for 30 minutes. Stained cells were run on a Beckman Coulter Cytoflex instrument. T_{FH} populations were quantified as percent of the singlet, CD4+, Dump (CD19/CD14/LiveDead) negative population as illustrated in **Supplementary Figure 1**.

Production of Costimulatory Molecules and Cytokines

For assessment of cytokine production, cryopreserved peripheral blood mononuclear cells (PBMC) were cultured overnight and then stimulated for 6 hours with 50ng/ml PMA and 1μg/ml ionomycin (Selleck Chemicals), with 10μg/ml Brefeldin A (Selleck) added for the last 4 hours. Cells were then cell surface stained for CD3, CD14, CD19, CXCR5, CCR6, CXCR3 as described above, fixed and permeabilized using eBioscience™ Fixation/Permeabilization buffer and stained intracellularly for CD4, IFNγ, IL-21 and CD40L at room temperature for 45 minutes. Intracellular CD4 staining was utilized to improve

discrimination of CD4+ cells, as cell surface CD4 is downmodulated upon treatment with PMA+ionomycin. Antibody details are provided in **Supplementary Table 1**.

Immunofluorescence Microscopy

Lymph node tissue sections were deparaffinized, rehydrated and boiled for 20 minutes in Target Retrieval Solution, Citrate pH 6.1 (Agilent). After washing, serial tissue sections were blocked with 1% BSA and 2% FBS in PBS followed by staining with unconjugated primary antibodies at 4°C overnight. After washing, sections were incubated with secondary antibodies for 4 hours at room temperature with shaking, washed and then stained with directly conjugated primary antibodies at 4°C overnight. Following a final wash, sections were air dried and mounted with ProLong™ Gold antifade reagent (Invitrogen) and kept at -20°C until analysis. Antibody details are provided in **Supplementary Table 2**. Images were captured with a CSU-X1M5000 spinning disc confocal microscope (Carl Zeiss) equipped with 405/488/561/635nm lasers.

CD4 T Cell: CLL B Cell Co-Culture Assay

Autologous CD4 T cells and CLL B cells were purified from PBMC using EasySep™ Human CD4+ T Cell Isolation Kit and EasySep™ Human B Cell Enrichment Kit II without CD43 Depletion (both STEMCELL Technologies), respectively. Purified CD4 T cells were suspended at 1x10^6 cells/mL in RPMI 1640 media (GE Healthcare) with 10% FBS (Life Technologies). T cells were cultured overnight in 24-well plates with/without addition of ImmunoCult™ Human CD3/CD28/CD2 T Cell Activator (STEMCELL Technologies) at 25 µL cocktail/mL of cells. B cells were cultured overnight in U-bottom 96-well plates at 1x10^6 cells/well, in the presence of sCD40L+IL-4 (both 50ng/mL; R&D Systems). After 14-16 hours incubation, cells were washed to remove stimuli. B cells were stained with carboxyfluorescein succinimidyl ester (CFSE) (Sigma-Aldrich) at 0.3 µM in PBS for 5min at room temperature, then washed with culture media. T cells (with or without pre-activation) were co-cultured together with CFSE-labelled autologous CLL-B cells in U-bottom 96-well plates, using 2x10^5 T and 1x10^6 B cells per well. T and B cells alone were included as controls. Starting at day 2 of co-culture, 100 µL of culture medium was gently taken out and fresh medium added to each well daily. At indicated times, wells were harvested and flow cytometry analyses were carried out using the panel detailed in **Supplementary Table 1**. Briefly, cells were stained for CD4, CD19, CXCR5, CXCR3, CCR6, CCR7, CD69, CD25, CD134/OX40, PD-1, CD38 and LIVE/DEAD™ Fixable Aqua viability dye (Invitrogen™). Following wash, cells were fixed and permeabilized as above and stained for Ki-67 at room temperature for 45 min.

Data Analysis and Statistics

Flow data were analyzed by FlowJo® V10 (FlowJo, LLC). Statistical analysis was performed with GraphPad Prism (GraphPad Software Inc). Confocal images were processed by ImageJ (V1.47). Box and whisker plots illustrate the median, interquartile range and 10-90% percentile values. Statistical tests used are indicated in figure legends and differences were considered to be statistically significant at values of *($p<0.05$), **($p<0.01$), ***($p<0.001$) and ****($p<0.0001$).

RESULTS

Follicular Helper T Cells Are Expanded and Phenotypically Distinct in CLL Patients

Peripheral blood mononuclear cells collected from CLL patients, MBL patients or age-matched controls were analyzed by multicolor flow cytometry to assess T follicular helper (T_{FH}) cell populations. Gating on CD4+CXCR5+CD19-CD14- live lymphocytes (**Figure S1**) revealed a significant elevation in both T_{FH} frequencies and overall T_{FH} numbers in CLL but not MBL patients (**Figure 1A**). CLL T_{FH} express higher levels of T_{FH}-associated activation markers PD-1 and ICOS than corresponding non-T_{FH} CD4 T cells and more PD-1 than control T_{FH} (**Figure 1B**). Compared to control T_{FH}, CLL T_{FH} populations contain a higher proportion of CD45RA-/CCR7- effector memory cells and fewer CD45RA-CCR7+ central memory cells (**Figure S2**). Within the T_{FH} population we further examined $T_{FH}1$, $T_{FH}2$ and $T_{FH}17$ subset composition based on expression of chemokine receptors CXCR3 and CCR6 (24) and found that CLL patients demonstrate significant skewing towards the CXCR3+CCR6- $T_{FH}1$ population (**Figure 1C**). The increased $T_{FH}1$ skewing in CLL patients was accompanied by significantly reduced frequencies of the $T_{FH}2$ population, whereas no significant change in $T_{FH}17$ cells was observed (**Figure 1C**). Together these results indicate that T_{FH} cells are expanded and phenotypically altered in CLL.

Association of Follicular Helper T Cells With Disease Burden

Within the spectrum of CLL patients in the cohort analyzed, we examined whether T_{FH} frequencies were associated with clinical parameters or established biomarkers of disease. Strikingly, we found that both frequency of T_{FH} among CD4+ T cells and $T_{FH}1$ skewing were positively correlated with blood lymphocyte counts (**Figure 2A**). T_{FH} expression of PD-1 or ICOS were also positively correlated with lymphocyte count (**Figure S3**). Frequencies of T_{FH} and skewing to $T_{FH}1$ were significantly elevated in high risk CLL (Rai 3-4) relative to low risk CLL (Rai 0) and CD38+ CLL patients showed more $T_{FH}1$ skewing than CD38- patients (**Figure 2B**). The latter is consistent with a report that CD38 expression is driven by the T_H1 cytokine IFNγ[25]. Interestingly, T_{FH} frequency was inversely correlated with plasma IgM and IgG levels (**Figure 2C**). Together these results suggest that T_{FH} accumulation and selective skewing to a $T_{FH}1$ phenotype occurs in parallel with expansion of the leukemic B cell clone and decline in normal B cell function.

Impact of Ibrutinib Treatment on T_{FH} Populations

To determine how CLL treatment impacts T_{FH} populations, we examined patients during the first year of ibrutinib treatment.

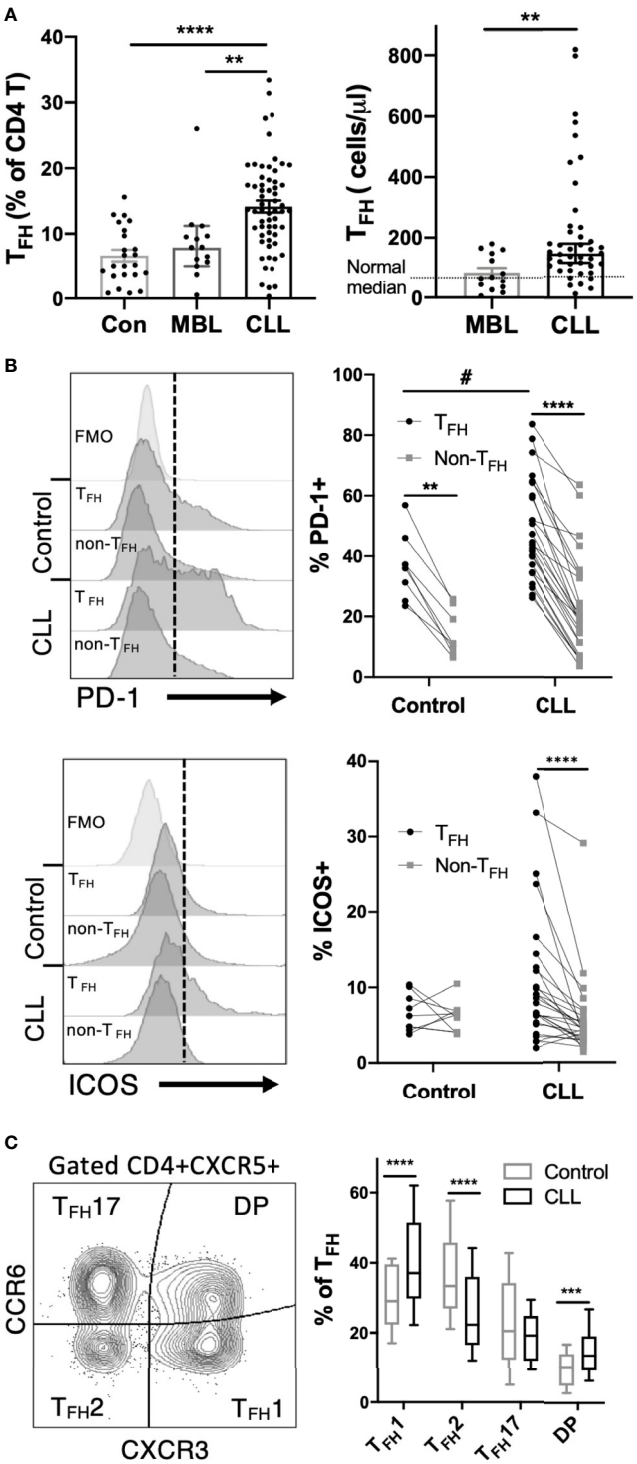

FIGURE 1 | T_{FH} cells are expanded and phenotypically altered in CLL patients. Peripheral blood mononuclear cells (PBMC) were isolated from CLL and MBL patients or control donors and analyzed by flow cytometry. For complete gating strategy see **Supplementary Data**. **(A)** T_{FH} frequency and absolute numbers are significantly increased in CLL patients. N=23 for controls, 14 for MBL and 61 for CLL. All graphs illustrate the individual patient values, median, and 95% confidence interval. Mann-Whitney U test, **(p<0.01), ****(p<0.0001). **(B)** Expression of PD-1 or ICOS on T_{FH} and non-T_{FH} CD4+ T cell populations. T_{FH} were gated as CD4+ CXCR5+CD45RA- cells. Individual patients or control values are connected by lines. Histograms labeled FMO show fluorescence minus one staining controls. *denotes significance by Wilcoxon paired t test, ****(p<0.0001). #denotes significance by Mann-Whitney U test, #(p<0.05). **(C)** Proportions of $T_{FH}1$, $T_{FH}2$ and $T_{FH}17$ sub-populations as determined by CCR6 and CXCR3 expression. Mann-Whitney U test, ***(p<0.001), ****(p<0.0001).

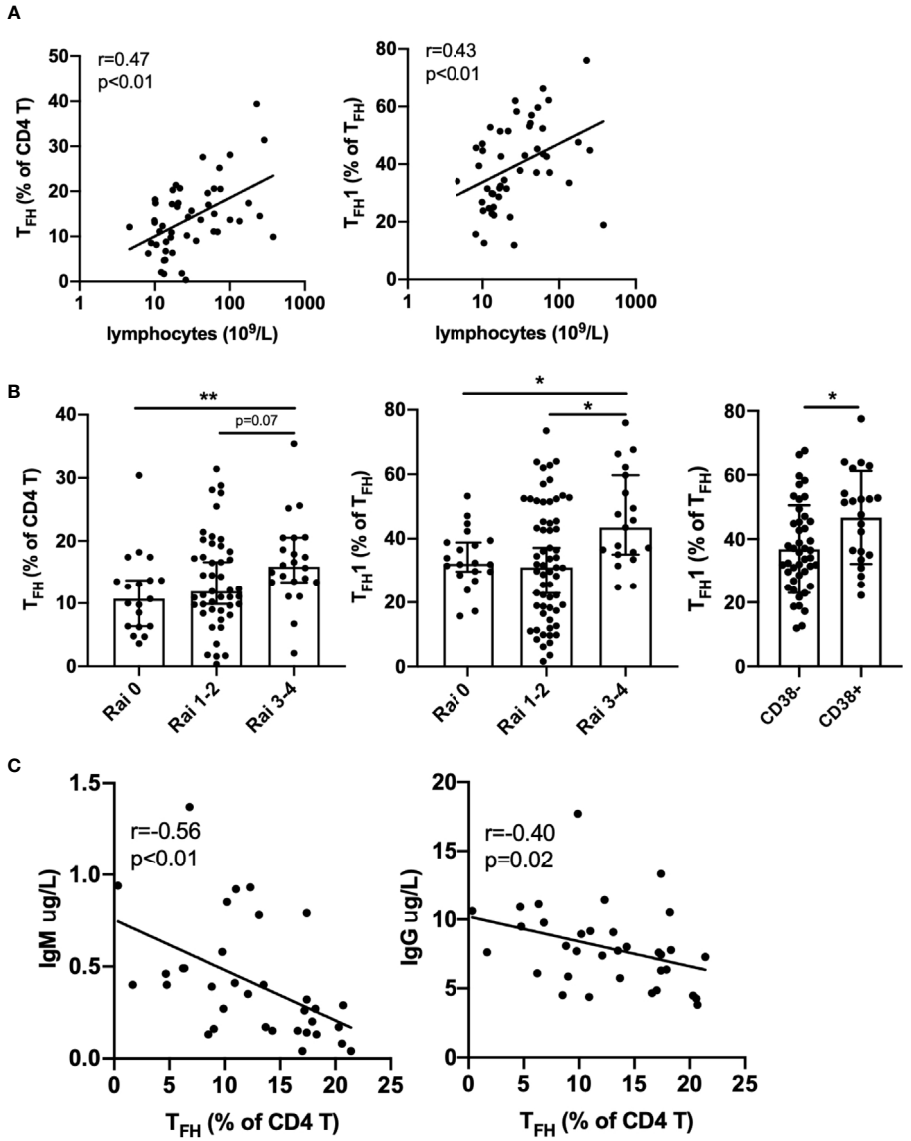

FIGURE 2 | Association of T_{FH} with disease burden and immune deficiency in CLL patients. **(A)** T_{FH} frequency and $T_{FH}1$ skewing are positively correlated with lymphocyte count. **(B)** T_{FH} frequency or $T_{FH}1$ skewing are elevated in advanced Rai stage patients and $T_{FH}1$ frequency is increased in CD38 positive versus CD38 negative patients. All graphs illustrate the individual patient values, median, and 95% confidence interval. **(C)** T_{FH} frequency is negatively correlated with plasma IgM and IgG levels. Significance was determined by Spearman correlation **(A, C)** or Mann-Whitney test, *(p<0.05), **(p<0.01) **(B)**.

Ibrutinib treatment led to a gradual decline in the frequency of T_{FH} cells over time, in parallel with a decline in total lymphocyte count (**Figure 3A**). In one patient who exhibited prolonged lymphocytosis after treatment, there was a concurrent transient increase in the T_{FH} population prior to normalization. Notably, T_{FH} composition changed post-ibrutinib treatment, with patients exhibiting a gradual re-balancing of $T_{FH}1$, $T_{FH}2$, and $T_{FH}17$ subsets (**Figure 3A**). Significant reductions in both T_{FH} frequencies and $T_{FH}1$ skewing were observed after 40 weeks of treatment (**Figure 3B**). This was accompanied by increased frequencies of CXCR3-CCR6- $T_{FH}2$-like cells, while $T_{FH}17$ frequencies were not altered (**Figure 3C**). These results suggest that ibrutinib treatment can normalize T_{FH} subsets concomitant with reduction in disease burden.

CLL T_{FH} Cells Produce High Levels of CD40L, TIGIT, IFNγ and IL-21

We further examined expression of costimulatory molecules and cytokines by CLL T_{FH} cells. We found that T_{FH} express higher levels of CD40L than non-T_{FH} in both CLL patients and controls, however CLL T_{FH} exhibit a strikingly elevated expression of CD40L (approximately 5-fold on average) relative to control T_{FH} (**Figure 4A**). In addition, we found that CLL T_{FH} express high levels of TIGIT (**Figure 4A**), an inhibitory immunoreceptor

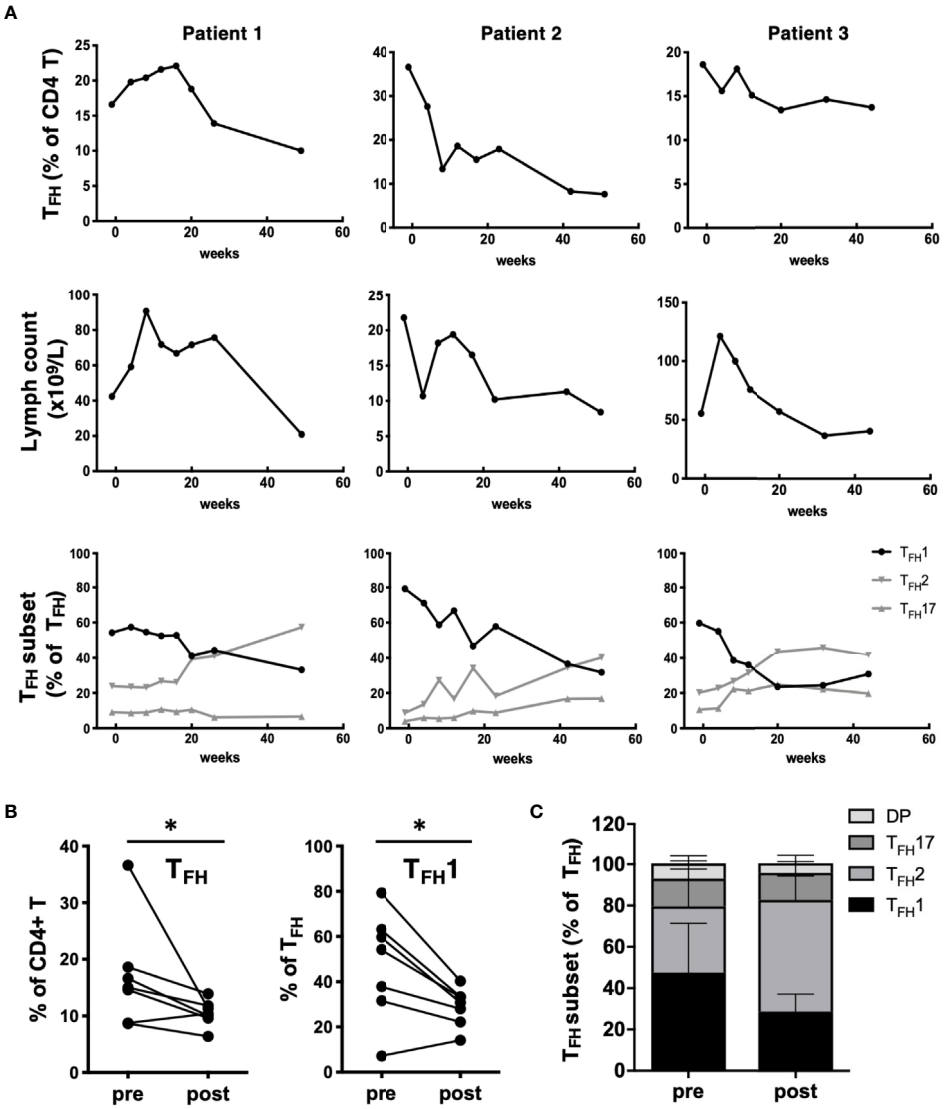

FIGURE 3 | Impact of ibrutinib treatment on T_{FH} populations. **(A)** PBMC samples were collected from CLL patients prior to starting treatment with ibrutinib and at multiple time points over a one-year follow-up. Changes in T_{FH} frequencies, lymphocyte counts or T_{FH} subset frequencies for 3 representative patients over time after ibrutinib treatment for three representative patients are shown. **(B)** Graphs showing pre/post treatment (>40 wk) frequencies of T_{FH} or $T_{FH}1$ subsets, with individual patient data connected by a line (*p<0.05, Wilcoxon test). **(C)** Stacked bar graph summarizing the average composition of four T_{FH} subpopulations pre and post ibrutinib treatment (N=7).

previously thought to function in T:B cell interactions (25, 26). We examined the ability of CLL T_{FH} to produce the canonical Type 1 cytokine IFNγ and the T_{FH}-associated cytokine IL-21 (**Figure 4B**). Remarkably, we observed a substantial increase in both the frequency IL-21 producing and IL-21/IFNγ double-producing cells in CLL patients, with the CLL T_{FH} population containing significantly more IL-21 and double-producing cells than control T_{FH} cells (**Figure 4B**). $T_{FH}1$ cells produced significantly more IL-21 and IFNγ than other T_{FH} subsets, but interestingly produced slightly less CD40L (**Figure S4**). We further assessed whether levels of CD40L, TIGIT or IL-21 expression by T_{FH} are associated with disease burden or stage. Interestingly, while CD40L and TIGIT expression did not show strong associations, IL-21 expression by T_{FH} was significantly associated with lymphocyte count and Rai stage (**Figure 4C**). These results indicate that CLL T_{FH} cells produce abnormally high levels of costimulatory molecules and cytokines known to stimulate CLL survival and proliferation and the expression of IL-21 by these cells is associated with adverse biomarkers and disease burden.

Activated $T_{FH}1$-Like Cells Are Present in CLL Lymphoid Tissues

CLL cells are present at varying levels in the bone marrow and lymph nodes, and signals present in these microenvironments are thought to drive CLL proliferation. To investigate whether circulating T_{FH} cells may represent the counterpart of T_{FH}

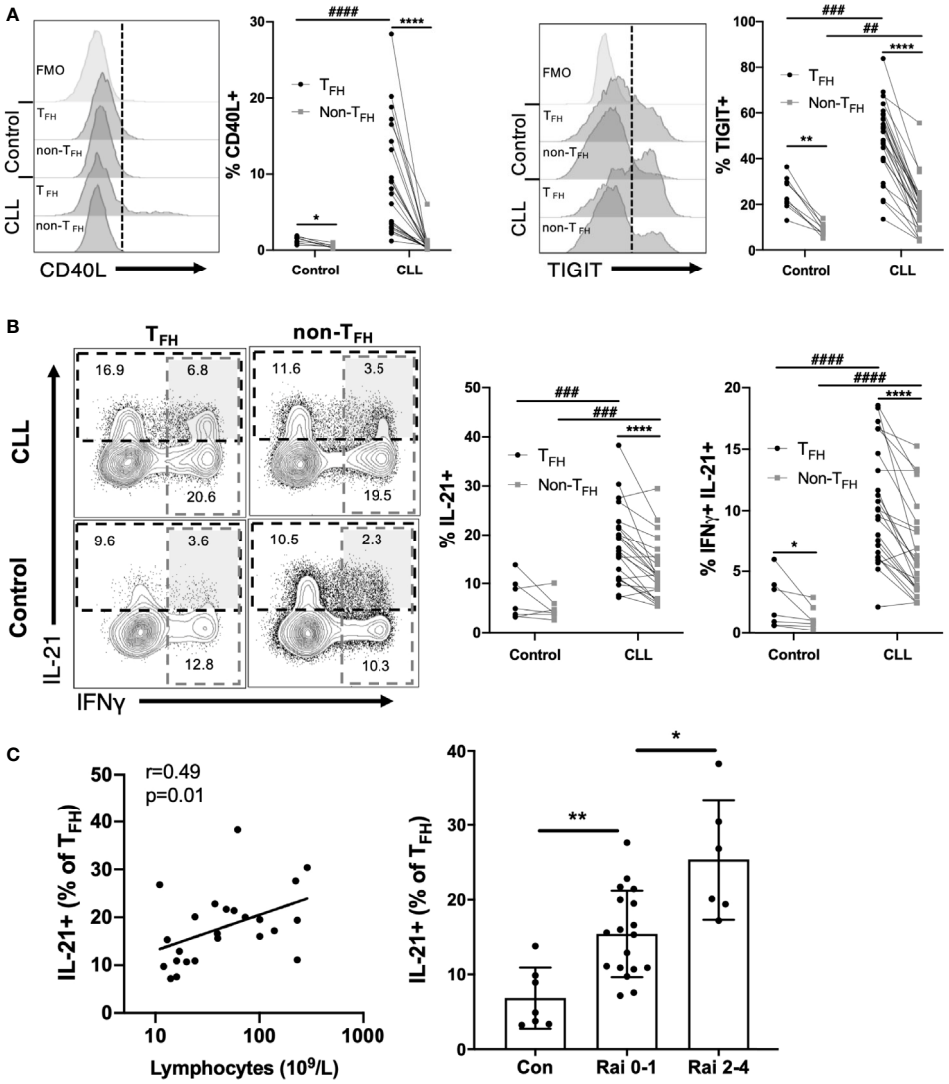

FIGURE 4 | CLL T_{FH} cells express abnormally high levels of CD40L, TIGIT, IFNγ and IL-21. **(A)** Expression of CD40L or TIGIT within T_{FH} and non-T_{FH} CD4+ T cell populations from controls and CLL patients. Left panels show representative staining histograms within the indicated cell populations. Histograms labeled FMO show fluorescence minus one staining controls. Right graphs show percent CD40L or TIGIT positivity among T_{FH} or non-T_{FH} populations, with individual subjects connected by lines. **(B)** Intracellular staining of IFNγ and IL-21 in T_{FH} or non-T_{FH} cell populations. Representative flow plots illustrate gating (left panels). Gated IL-21+ or IFNγ+/IL-21+ cell frequencies within the indicated groups (right panels). In **(A, B)** *denotes significance by Wilcoxon paired t test, ****(p<0.0001); #denotes significance by Mann-Whitney U test, ##(p<0.01), ###(p<0.001), ####(p<0.0001). **(C)** T_{FH} cell expression of IL-21 is associated with lymphocyte count and Rai stage. Left panel, Spearman correlation; Right panel, Mann-Whitney U test, *(p<0.05), **(p<0.01).

populations present within lymphoid tissues, paired blood and bone marrow samples from CLL patients were analyzed. We found a significant correlation between blood and marrow T_{FH} and $T_{FH}1$ cell frequencies from the same patients (**Figure 5A**). Interestingly, T_{FH} populations in bone marrow showed increased activation status relative to those in peripheral blood of the same patients, expressing significantly more IL-21, IFNγ and IL-21/IFNγ double-producing cells (**Figure 5B**). While levels of PD-1 was also elevated, CD40L and TIGIT were similar in bone marrow and peripheral blood T_{FH} (**Figure 5C**). We further examined lymph node tissue sections from CLL patients using immunofluorescent staining and could identify T cells present within proliferation centers expressing the $T_{FH}1$ markers CD3, CD4, CXCR5, CXCR3 and PD-1 (**Figure 6**). These results suggest that T_{FH} cells are present in both circulation and within lymphoid tissues, with the latter showing similar skewing to $T_{FH}1$ and a highly activated phenotype.

Autologous Activated CD4 T Cells Can Promote CLL B Cell Survival, Activation and Proliferation

We developed an *in vitro* system to study CLL B cell interaction with autologous CD4+ T cells. CD4 T cells were isolated from

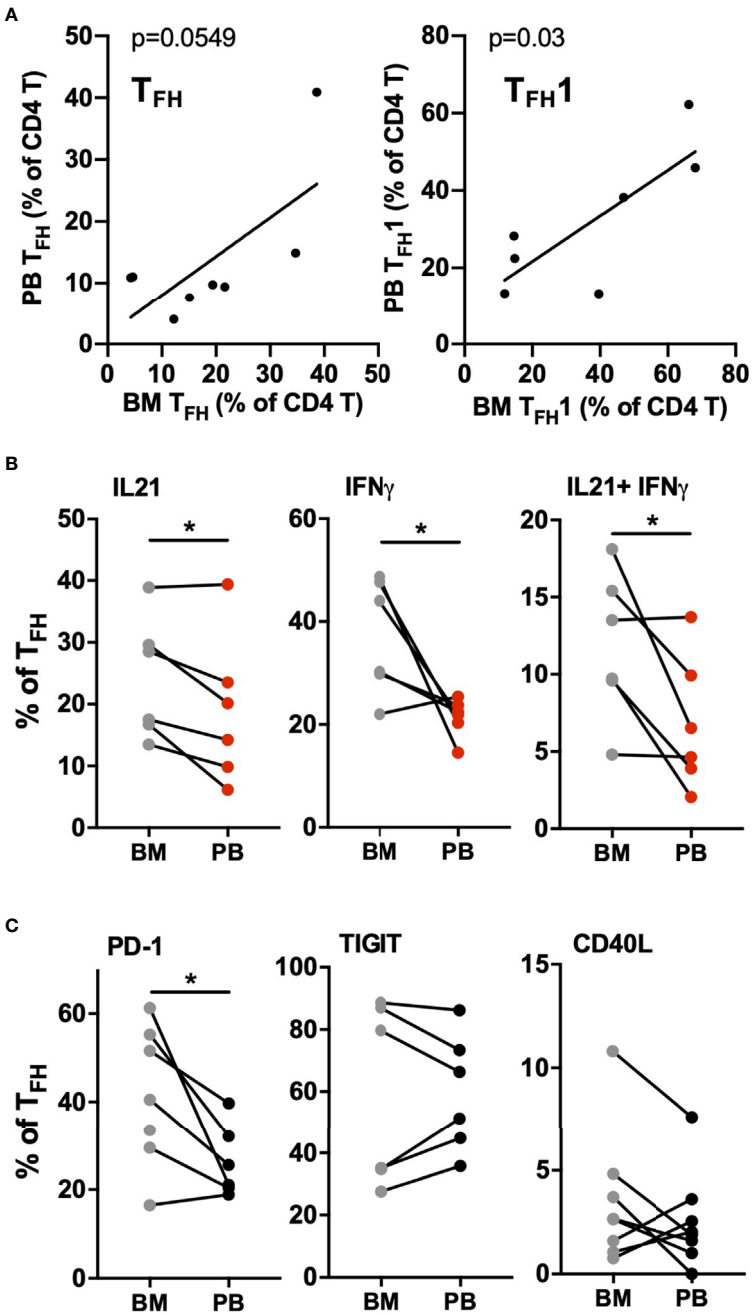

FIGURE 5 | CLL bone marrow contains high levels of activated $T_{FH}1$ cells. Mononuclear cells isolated from bone marrow aspirates (BM) and peripheral blood samples (PB) of the same patients were analyzed by flow cytometry. **(A)** Correlation between T_{FH} (left) or $T_{FH}1$ (right) frequencies in marrow versus matched blood samples **(B)** Comparison of cytokine production in marrow versus blood T_{FH} populations. **(C)** Comparison of activation/costimulatory markers in marrow versus blood T_{FH} populations. * denotes significance by Wilcoxon paired t test, *($p<0.05$).

patient PBMC, pre-cultured overnight with a T cell-activation cocktail or medium alone, then washed and co-cultured with B cells isolated from the same patient that were labeled with cell division tracking dye CFSE. Resulting CLL-B cell division, and expression of activation markers by B and T cells, were assessed after 2 and 6 days of co-culture. At day 2, a significant increase in CLL B cell expression of CD69 and nuclear proliferation antigen Ki-67 was observed in the presence of activated CD4 T cells, compared to co-cultures with non-activated T cells or B cells alone (**Figure 7A**). Activated CD4 T:B cell co-culture also promoted an increase in CD25 activation marker expression among B cells and increased CLL B cell survival at this time

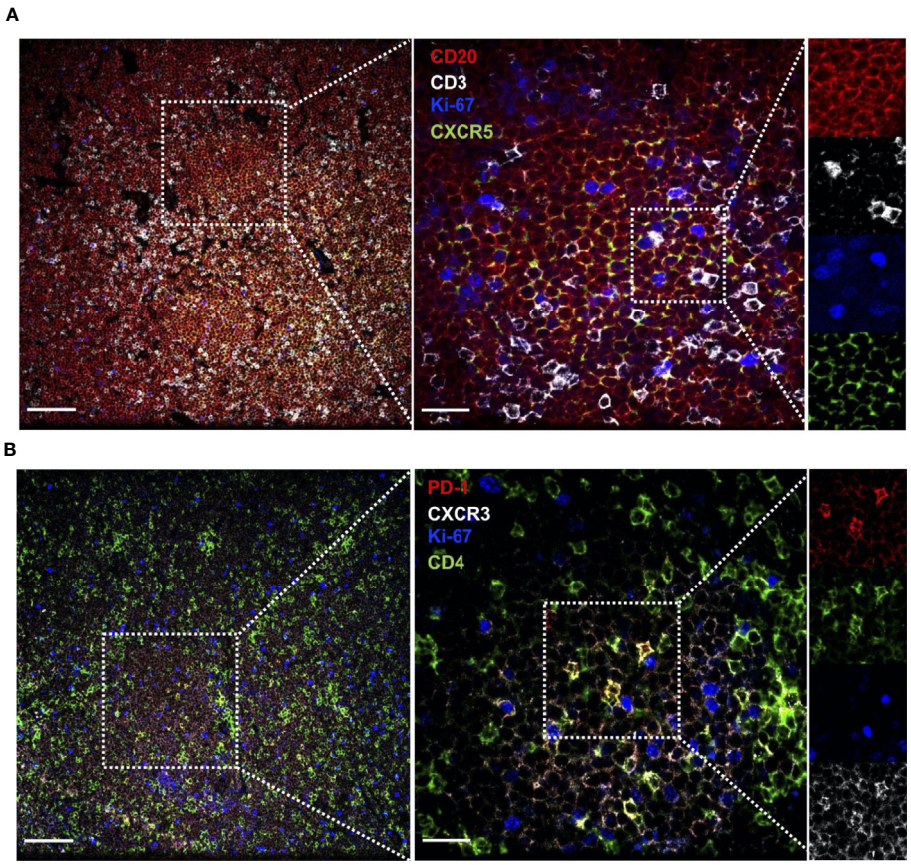

FIGURE 6 | CLL lymph nodes contains cells expressing activated $T_{FH}1$ markers. Lymph node sections from CLL patients were stained with the indicated labelled antibodies and imaged by confocal microscopy. **(A)** Section stained for CLL B cell marker CD20, T cell marker CD3, proliferation marker Ki67 and CXCR5 (expressed on CLL B cells and T_{FH}). **(B)** Section stained for activation marker PD-1, T cell marker CD4, proliferation marker Ki67 and CXCR3 (expressed at low levels on CLL B cells and high levels on $T_{FH}1$ cells). Several magnifications are shown (Left panel scale bar = 100μm, right panel scale bar = 25μm) to illustrate T cell presence within CLL B cell clusters containing proliferating cells, and close contact between CLL cells and T cells expressing CD3, CD4, CXCR5, PD-1 and CXCR3.

point, whereas increased CD38 expression or cell division (as assessed by CFSE dilution) were not observed at day 2 (**Figure S5A**). After 6 days of co-culture, CLL-B cell division was observed (**Figure 7B**) and most divided cells also expressed Ki-67 (**Figure S5B**). At day 6, CLL B cells also exhibited significant upregulation of the activation marker CD25 (**Figure 7B**) as well as CD38 and CD69 (**Figure S5C**) when co-cultured with activated CD4 T cells. Notably, there was a positive correlation between patient T_{FH} frequency and the frequency of divided, Ki-67+ and CD25+ CLL B cells observed in co-cultures (**Figure 7C**), consistent with a potential role for T_{FH} cells in driving CLL-B cell activation and proliferation.

CLL Cells Activate T_{FH} Cells in Co-Culture

During CLL:T cell interactions, CLL-B cells can also impact CD4+ T cell activation (27), but it is unclear whether particular cell subsets are preferentially targeted. In order to assess CLL B cell-dependent activation of CD4+ T cell subsets in co-culture, CD4 T cells untreated with activation cocktail were assessed for their expression of various activation markers in the presence or absence of autologous CLL cells. It was found that the presence of CLL B cells led to an increase in expression of activation markers in a small fraction (less than 15%) of autologous CD4 T cells (**Figure 8A**). This upregulation was significant for CD25, CD69 and PD-1 within 2 days of co-culture (**Figure 8A**). The frequency of CD4 T cells co-expressing both CD25 and OX40, associated with antigen-specific T cell recall responses (28), was also increased in the presence of the B cells at both timepoints (**Figure 8A**). To determine whether T_{FH} cells were preferentially activated by CLL-B cells, we assessed activation marker expression on T_{FH} and non-T_{FH} fractions. The presence of B cells provoked an increase in CD69+ cells in both populations, however the fold increase in expression was significantly higher for T_{FH} (**Figure 8B**). In addition to CD69, T_{FH} cells showed greater fold increases in expression of CD25, CD25/OX40 and PD-1 than non-T_{FH} cells when co-cultured with CLL (**Figure 8B**). T_{FH} cell expression of activation markers CD25 and OX40 increased between day 2 and day 6 of culture, while no further increase in CD69 or PD-1 were observed after day 2 (**Figure 8C**). We noted that while the patient-specific

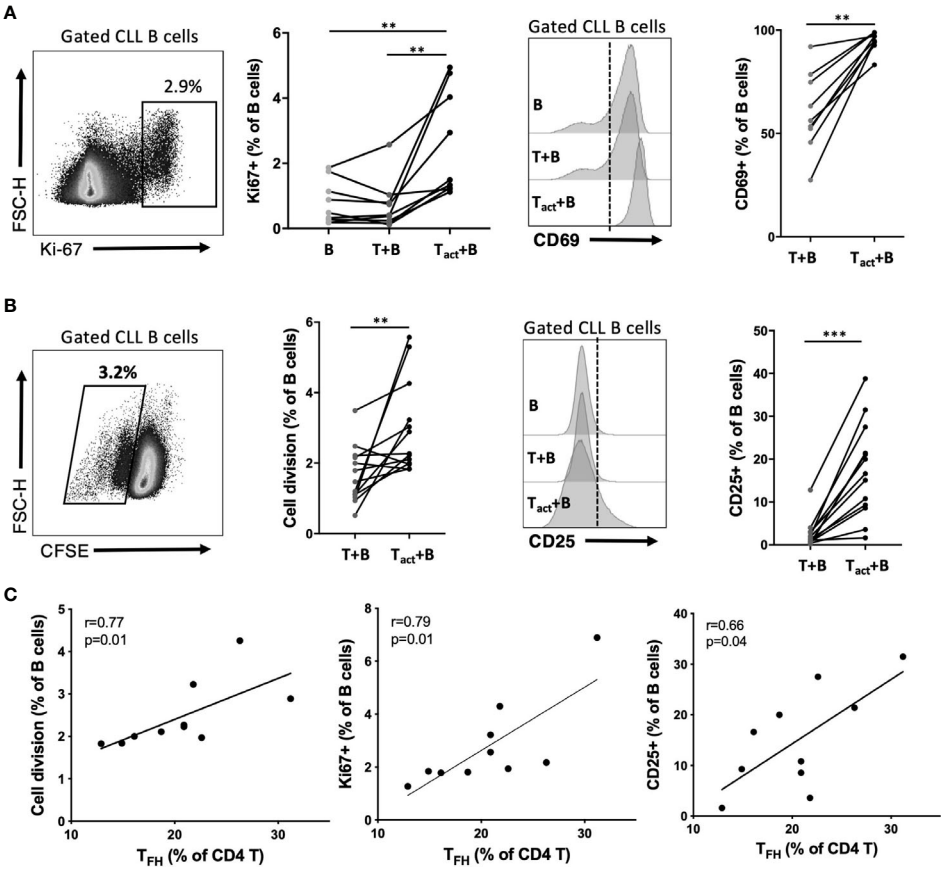

FIGURE 7 | Impact of activated autologous CD4+ T cells on CLL activation and proliferation. Purified CLL cells were co-cultured with purified autologous CD4+ T cells from the same PBMC sample. Prior to co-culture, CLL cells were labeled with CFSE and T cells were briefly exposed to an activation cocktail (T_{act}) or kept in medium alone (T). After 2 or 6 days of co-culture, cells were analyzed by flow cytometry to determine cell division and expression of activation markers. B cells were gated as live CD19+CD4- cells. **(A)** Expression of nuclear proliferation antigen Ki67 or activation marker CD69 at day 2 of culture. **(B)** CLL cell division assessment based on CFSE dilution and expression of activation marker CD25 at day 6 of culture. In **(A, B)** *denotes significance by Wilcoxon paired t test, **(p<0.01), ***(p<0.001). **(C)** Correlation of observed B cell division, Ki67 expression or CD25 expression with the frequency of T_{FH} within CD4 T cells for each patient sample cultured (Spearman correlation).

frequencies of T_{FH} cells were very stable over the first two days of culture, they began to decline by day 6 in cultures without B cells but were well maintained in the presence of CLL B cells (**Figure 8D**). Taken together, these results indicate that in this co-culture system, CLL-B cells can promote T_{FH} cell activation and maintenance.

DISCUSSION

Abnormalities in T cell subsets and function in CLL have been reported in a number of studies, including changes in CD4/CD8 ratios, expansion of the Treg population, loss of naïve and increased memory populations, and increased expression of exhaustion markers (23, 29, 30). Here we report an in-depth analysis of follicular helper T cell subsets and functional status as well as their association with disease progression, immune status and ibrutinib treatment. Our results are partially consistent with studies from Asian and UK patients which also observed elevated T_{FH} frequencies in CLL (31, 32). Our study reveals that elevation in T_{FH} cells is first observable in Rai 0 CLL patients, whereas no increase was apparent in the MBL group. These previous studies reported lack of association with IgVH mutation status (31, 32) and we also found no association with either IgVH mutation status or ZAP-70 status (data not shown). Our study demonstrates a significant positive correlation between T_{FH} frequencies and total lymphocyte counts, indicating that increasing acquisition of the T_{FH} phenotype among CD4+ T cells occurs in tandem with expansion of the malignant B cell clone. A previous study found increased T_{FH} frequencies in Binet C versus A/B patients (32), consistent with our observed trends of higher T_{FH} frequencies, in the Rai 3-4 group. Surprisingly, we further find that expanded T_{FH} populations in advanced stage CLL exhibit significant $T_{FH}1$ skewing. Strikingly, increased expression of PD-1, ICOS and IL-21 by T_{FH} cells were associated with disease burden, and CLL T_{FH} cells were also

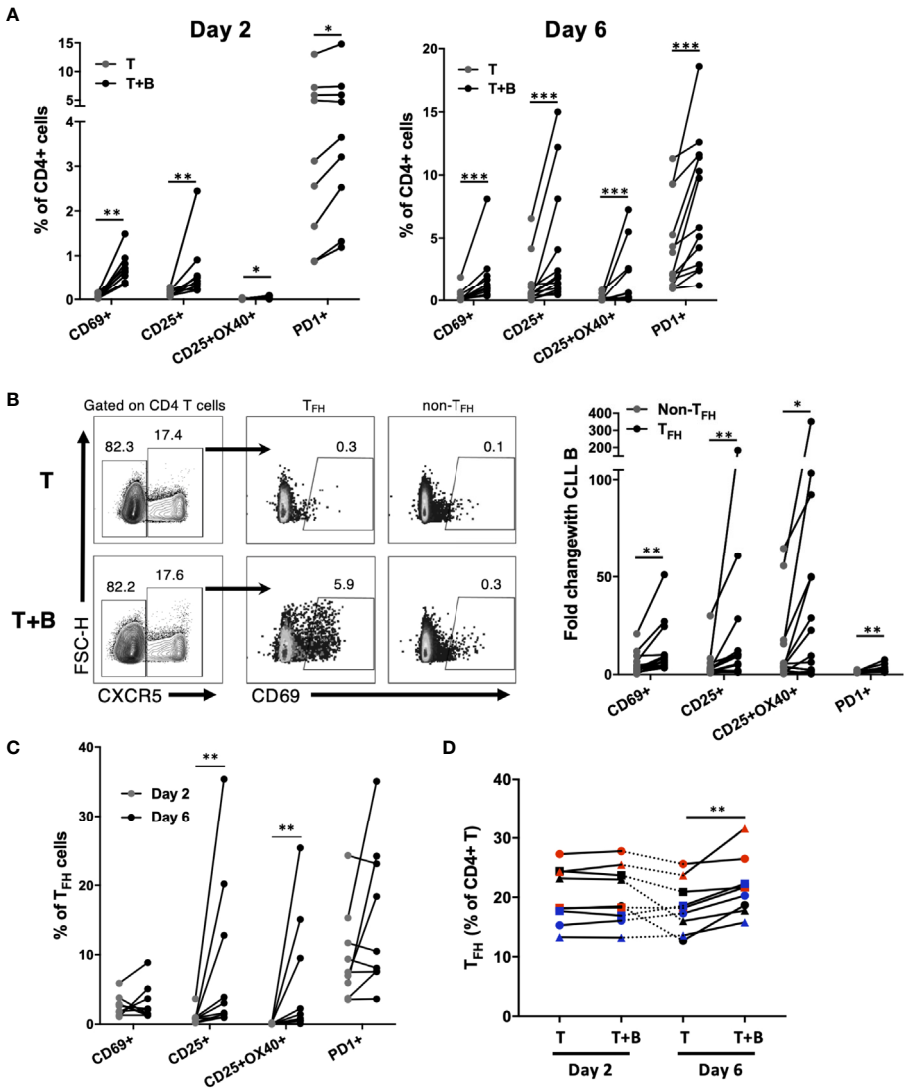

FIGURE 8 | Impact of CLL B cells on activation of autologous CD4+ T cell subsets. Purified CLL cells were co-cultured with purified autologous CD4+ T cells that were not pre-activated. **(A)** Expression of activation markers on CD4+ T cells after 2 days or 6 days of co-culture. **(B)** Example flow cytometry analysis showing expression of CD69 on T_{FH} or non-T_{FH} CD4+ T cells. Data in right panel is expressed as fold change in activation marker expression among T_{FH} or non-T_{FH} (calculated as percent expression in T+B cell co-culture/percent expression in T cell only culture). **(C)** CD25 and OX40 expression increase on T_{FH} cells co-cultured with CLL B cells between day 2 and day 6. **(D)** Patient-specific frequencies of T_{FH} are maintained in CLL B cell co-culture. Individual patients are connected by lines. *denotes significance by Wilcoxon paired t test, *(p<0.05), **(p<0.01), ***(p<0.001).

found to over-express other stimulatory molecules such as IFNγ, TIGIT and CD40L.

Together our findings indicate that CLL T_{FH} express more PD-1 than either non-T_{FH} CD4+ T cells from CLL patients or T_{FH} from controls. PD-1 is a marker for chronically-activated or exhausted T cells, and was previously reported to be elevated in CLL CD4+ T cells (33). Our results are consistent with this finding, and further define the CD4 sub-populations abnormally expressing this marker. In the context of the T_{FH} literature, the PD-1+ T_{FH} phenotype which we describe here (PD-1+CXCR5+ CCR7low) is not associated with functional exhaustion but rather has been previously associated with recent T_{FH} activation in tissues and enhanced functional capacity for providing B cell help (34, 35). However, we found evidence that T_{FH} frequencies are *negatively* correlated with IgM and IgG levels. This finding is consistent with these T_{FH} cells being dysfunctional in relation to their normal supportive roles for antibody responses; or alternatively it may reflect the association of T_{FH} expansion with expansion of the CLL clone, and concomitant disruption of normal B cell niches within tissues.

Our results indicate that ibrutinib can normalize T_{FH} frequencies and activation gradually over several months of treatment. These results are partially consistent with previous studies which found that ibrutinib can reduce T cell expression of

PD-1 as well as memory markers (36, 37). The effects of ibrutinib on T cells may be due to inhibition of the kinase ITK expressed in T cells, since treatment with acalabrutib, which does not inhibit ITK, showed lesser impact on T cells (37). Patients with BTK mutations were found to have severe deficiency in T_{FH} cells (38), suggesting the possibility that BTK itself may be required for T_{FH} development and/or maintenance. Alternatively, ibrutinib may indirectly affect T_{FH} cell populations *via* depletion of the CLL B cell clone and/or its other effects on the immune microenvironment.

Previous studies have provided considerable evidence that blood T_{FH} are clonally related to T_{FH} in lymphoid tissues. We found cells expressing markers of activated T_{FH} cells within proliferation centers in lymph nodes and in bone marrow, suggesting they are in direct contact with CLL B cells within these microenvironments. T_{FH} cells present in the bone marrow expressed a more activated phenotype than peripheral blood T_{FH}, including highly elevated PD-1 and IL-21/IFNγ expression in some patients, indicating that lymphoid tissues are likely their primary site of activation. Given that IFNγ can impair hematopoietic stem cell function and contribute to bone marrow failure (39), it is possible that the presence of these activated T cells in marrow may directly participate in disruption of marrow function in advanced stage disease.

CLL T_{FH} cells exhibit elevated expression of B cell stimulatory molecules CD40L and IL-21. Numerous studies have shown that the culture with CD40L-expressing T or stromal cell lines promotes CLL-B cell proliferation (40–42). The addition of IL-21 to CD40L-stimulated CLL-B cells increases the frequency of divided cells and the average number of divisions (31, 42). Our study provides evidence that T_{FH} cells are the predominant T cell subset producing these CLL stimulatory factors *in vivo*. Additionally, we observed that CLL T_{FH} cells expressed high levels of TIGIT, molecule that has been linked to CLL-B cell survival (43). $T_{FH}1$ cells are reported to be relatively poor helpers for normal B cell responses (24), however it is possible that the abnormal $T_{FH}1$-like cells in CLL are adapted to support malignant CLL B cells. A study using a mouse xenograft model found that T cells driving CLL cell proliferation had a T_H1 phenotype (44), indicating the potential of these cells to serve as supportive cells in the microenvironment. Some studies have implicated IFNγ as a supportive cytokine for human CLL cells (27, 45). Together, our data demonstrate that abnormal T_{FH} present in CLL patients over-produce multiple factors that could potentially support CLL survival and proliferation in tissues.

Our *in vitro* co-culture studies revealed evidence that CLL cells can preferentially activate T_{FH} and that T_{FH} expansion is associated with ability of activated CD4+ T cells to trigger CLL proliferation *in vitro*. Activated autologous CD4 T cells promoted CLL cell activation marker expression and division in line with other studies showing that the expression of activation markers by CLL cells is increased after 2-3 days of co-culture with T cells (27, 45), while CLL division is only observed after 4 days (27, 40, 46). To our knowledge, this is the first study to report this functional activity of purified autologous CD4 T cells in CLL, without addition of other factors such as stromal cells or cytokines. We observe that reactivation of CD4+ T cells using anti-CD3/28 is required to observe affects on CLL B cells, which may reflect that blood T_{FH}, like blood CLL cells, are relatively quiescent compared to their counterparts in lymphoid tissues. Notably, the frequency of T_{FH} cells within the CD4 T cell pool positively correlated with CLL-B cell division; however we were unable to purify sufficient numbers of T_{FH} from CLL patient blood to carry out co-culture studies. Thus, while our data are consistent with a role of T_{FH} cells in driving CLL proliferation, it remains possible that increased frequency of T_{FH} could be associated with other alterations in CD4 T cell or autologous CLL cell populations that are critical for proliferation under these conditions.

Notably, the reciprocal activation of T_{FH} cells by CLL cells in co-culture included induction of CD25/OX40 double positive T_{FH} cells. Co-expression of these activation markers has been shown to be dependent on antigen-specific stimulation (28). Previous studies have raised the possibility of antigen-specific cognate interactions between CLL and CD4+ T cells leading to oligoclonal expansions (47), however the phenotype of these oligoclonal T cells has not been determined. One study found that CLL : CD4 T cell interactions *in vitro* can be abrogated by an anti-pan-MHC II antibody (27), consistent with cognate interaction. In addition to induction of activation marker expression on T_{FH}, we found that CLL cells could maintain T_{FH} frequencies during *in vitro* culture, resulting in significantly higher T_{FH} frequencies in the presence of CLL after 6 days. These results suggest that direct bi-directional interactions between CLL cells and abnormal T_{FH} cells is a significant feature of the dysfunctional CLL immune microenvironment.

Together, our findings suggest that alterations in T_{FH} frequencies, activation status, subset distribution and costimulatory molecule expression can serve as alternative biomarkers in CLL reflective of lymphoid tissue involvement and disease progression. T_{FH} cells may represent significant sources of CLL stimulatory molecules and play roles in disrupting normal immune function and promoting CLL proliferation.

DATA AVAILABILITY STATEMENT

The raw data supporting the conclusions of this article will be made available by the authors, without undue reservation.

ETHICS STATEMENT

The studies involving human participants were reviewed and approved by Research Ethics Board at the University of Manitoba. The patients/participants provided their written informed consent to participate in this study.

AUTHOR CONTRIBUTIONS

XW and JF performed research, analyzed data, performed statistical analyses and wrote the manuscript. CZ performed research and analyzed data. SG, VN, VB and JJ designed research

and collected CLL patient samples. AM designed research, analyzed and interpreted data, supervised trainees and wrote the manuscript. All authors contributed to the article and approved the submitted version.

FUNDING

XW and JF received graduate studentship funding from Research Manitoba. This study was supported by the Manitoba Tumour Bank, a member of the Canadian Tissue Repository Network, funded in part by the CancerCare Manitoba Foundation and the Canadian Institutes of Health Research. This study was supported by grants from the Leukemia and Lymphoma Society of Canada and Research Manitoba.

ACKNOWLEDGMENTS

The authors thank Mandy Squires for help with the patient database, Laurie Lange and Yun Li for blood sample biobanking and retrieval, Dr. Jie Li for preparing lymph node sections, Donna Hewitt and Linda Davidson with help obtaining healthy blood donor sample and Ahmed Ali and Sen Hou for advice and technical support.

SUPPLEMENTARY MATERIAL

The Supplementary Material for this article can be found online at: https://www.frontiersin.org/articles/10.3389/fonc.2021.674492/full#supplementary-material

REFERENCES

1. Hallek M, Cheson BD, Catovsky D, Caligaris-Cappio F, Dighiero G, Dohner H, et al. Iwcll Guidelines for Diagnosis, Indications for Treatment, Response Assessment, and Supportive Management of CLL. *Blood* (2018) 131 (25):2745–60. doi: 10.1182/blood-2017-09-806398
2. Strati P, Shanafelt TD. Monoclonal B-Cell Lymphocytosis and Early-Stage Chronic Lymphocytic Leukemia: Diagnosis, Natural History, and Risk Stratification. *Blood* (2015) 126(4):454–62. doi: 10.1182/blood-2015-02-585059
3. Shanafelt TD, Geyer SM, Kay NE. Prognosis At Diagnosis: Integrating Molecular Biologic Insights Into Clinical Practice for Patients With CLL. *Blood* (2004) 103(4):1202–10. doi: 10.1182/blood-2003-07-2281
4. International CLLIPIwg. An International Prognostic Index for Patients With Chronic Lymphocytic Leukaemia (CLL-IPI): A Meta-Analysis of Individual Patient Data. *Lancet Oncol* (2016) 17(6):779–90. doi: 10.1016/S1470-2045(16)30029-8
5. Burger JA, Ghia P, Rosenwald A, Caligaris-Cappio F. The Microenvironment in Mature B-Cell Malignancies: A Target for New Treatment Strategies. *Blood* (2009) 114(16):3367–75. doi: 10.1182/blood-2009-06-225326
6. Herishanu Y, Perez-Galan P, Liu D, Biancotto A, Pittaluga S, Vire B, et al. The Lymph Node Microenvironment Promotes B-Cell Receptor Signaling, NF-Kappab Activation, and Tumor Proliferation in Chronic Lymphocytic Leukemia. *Blood* (2011) 117(2):563–74. doi: 10.1182/blood-2010-05-284984
7. Murphy EJ, Neuberg DS, Rassenti LZ, Hayes G, Redd R, Emson C, et al. Leukemia-Cell Proliferation and Disease Progression in Patients With Early Stage Chronic Lymphocytic Leukemia. *Leukemia* (2017) 31(6):1348–54. doi: 10.1038/leu.2017.34
8. Burger JA, Li KW, Keating MJ, Sivina M, Amer AM, Garg N, et al. Leukemia Cell Proliferation and Death in Chronic Lymphocytic Leukemia Patients on Therapy With the BTK Inhibitor Ibrutinib. *JCI Insight* (2017) 2(2):e89904. doi: 10.1172/jci.insight.89904
9. Herreros B, Rodriguez-Pinilla SM, Pajares R, Martinez-Gonzalez MA, Ramos R, Munoz I, et al. Proliferation Centers in Chronic Lymphocytic Leukemia: The Niche Where NF-Kappab Activation Takes Place. *Leukemia* (2010) 24 (4):872–6. doi: 10.1038/leu.2009.285
10. Gine E, Martinez A, Villamor N, Lopez-Guillermo A, Camos M, Martinez D, et al. Expanded and Highly Active Proliferation Centers Identify a Histological Subtype of Chronic Lymphocytic Leukemia ("Accelerated" Chronic Lymphocytic Leukemia) With Aggressive Clinical Behavior. *Haematologica* (2010) 95(9):1526–33. doi: 10.3324/haematol.2010.022277
11. Burger JA, Tedeschi A, Barr PM, Robak T, Owen C, Ghia P, et al. Ibrutinib as Initial Therapy for Patients With Chronic Lymphocytic Leukemia. *N Engl J Med* (2015) 373(25):2425–37. doi: 10.1056/NEJMoa1509388
12. Herman SE, Niemann CU, Farooqui M, Jones J, Mustafa RZ, Lipsky A, et al. Ibrutinib-Induced Lymphocytosis in Patients With Chronic Lymphocytic Leukemia: Correlative Analyses From a Phase II Study. *Leukemia* (2014) 28 (11):2188–96. doi: 10.1038/leu.2014.122
13. Bagnara D, Kaufman MS, Calissano C, Marsilio S, Patten PE, Simone R, et al. A Novel Adoptive Transfer Model of Chronic Lymphocytic Leukemia Suggests a Key Role for T Lymphocytes in the Disease. *Blood* (2011) 117 (20):5463–72. doi: 10.1182/blood-2010-12-324210
14. Breitfeld D, Ohl L, Kremmer E, Ellwart J, Sallusto F, Lipp M, et al. Follicular B Helper T Cells Express CXC Chemokine Receptor 5, Localize to B Cell Follicles, and Support Immunoglobulin Production. *J Exp Med* (2000) 192 (11):1545–52. doi: 10.1084/jem.192.11.1545
15. Schaerli P, Willimann K, Lang AB, Lipp M, Loetscher P, Moser B. CXC Chemokine Receptor 5 Expression Defines Follicular Homing T Cells With B Cell Helper Function. *J Exp Med* (2000) 192(11):1553–62. doi: 10.1084/jem.192.11.1553
16. Vinuesa CG, Linterman MA, Goodnow CC, Randall KL. T Cells and Follicular Dendritic Cells in Germinal Center B-Cell Formation and Selection. *Immunol Rev* (2010) 237(1):72–89. doi: 10.1111/j.1600-065X.2010.00937.x
17. Cyster JG, Ansel KM, Reif K, Ekland EH, Hyman PL, Tang HL, et al. Follicular Stromal Cells and Lymphocyte Homing to Follicles. *Immunol Rev* (2000) 176:181–93. doi: 10.1034/j.1600-065X.2000.00618.x
18. Crotty S. Follicular Helper CD4 T Cells (TFH). *Annu Rev Immunol* (2011) 29:621–63. doi: 10.1146/annurev-immunol-031210-101400
19. Ueno H, Banchereau J, Vinuesa CG. Pathophysiology of T Follicular Helper Cells in Humans and Mice. *Nat Immunol* (2015) 16:142–52. doi: 10.1038/ni.3054
20. Schmitt N, Bentebibel S-E, Ueno H. Phenotype and Functions of Memory Tfh Cells in Human Blood. *Trends Immunol* (2014) 35:436–42. doi: 10.1016/j.it.2014.06.002
21. Gorgun G, Holderried TA, Zahrieh D, Neuberg D, Gribben JG. Chronic Lymphocytic Leukemia Cells Induce Changes in Gene Expression of CD4 and CD8 T Cells. *J Clin Invest* (2005) 115(7):1797–805. doi: 10.1172/JCI24176
22. Ramsay AG, Clear AJ, Fatah R, Gribben JG. Multiple Inhibitory Ligands Induce Impaired T-Cell Immunologic Synapse Function in Chronic Lymphocytic Leukemia That Can Be Blocked With Lenalidomide: Establishing a Reversible Immune Evasion Mechanism in Human Cancer. *Blood* (2012) 120(7):1412–21. doi: 10.1182/blood-2012-02-411678
23. Forconi F, Moss P. Perturbation of the Normal Immune System in Patients With CLL. *Blood* (2015) 126(5):573–81. doi: 10.1182/blood-2015-03-567388
24. Morita R, Schmitt N, Bentebibel S-E, Ranganathan R, Bourdery L, Zurawski G, et al. Human Blood CXCR5+CD4+ T Cells are Counterparts of T Follicular Cells and Contain Specific Subsets That Differentially Support Antibody Secretion. *Immunity* (2011) 34:108–21. doi: 10.1016/j.immuni.2010.12.012
25. Godefroy E, Zhong H, Pham P, Friedman D, Yazdanbakhsh K. TIGIT-Positive Circulating Follicular Helper T Cells Display Robust B-Cell Help Functions: Potential Role in Sickle Cell Alloimmunization. *Haematologica* (2015) 100(11):1415–25. doi: 10.3324/haematol.2015.132738
26. Yu X, Harden K, Gonzalez LC, Francesco M, Chiang E, Irving B, et al. The Surface Protein TIGIT Suppresses T Cell Activation by Promoting the Generation of Mature Immunoregulatory Dendritic Cells. *Nat Immunol* (2009) 10(1):48–57. doi: 10.1038/ni.1674

27. Os A, Burgler S, Ribes AP, Funderud A, Wang D, Thompson KM, et al. Chronic Lymphocytic Leukemia Cells are Activated and Proliferate in Response to Specific T Helper Cells. *Cell Rep* (2013) 4(3):566–77. doi: 10.1016/j.celrep.2013.07.011
28. Havenar-Daughton C, Reiss SM, Carnathan DG, Wu JE, Kendric K, Torrents de la Pena A, et al. Cytokine-Independent Detection of Antigen-Specific Germinal Center T Follicular Helper Cells in Immunized Nonhuman Primates Using a Live Cell Activation-Induced Marker Technique. *J Immunol* (2016) 197(3):994–1002. doi: 10.4049/jimmunol.1600320
29. Riches JC, Davies JK, McClanahan F, Fatah R, Iqbal S, Agrawal S, et al. T Cells From CLL Patients Exhibit Features of T-Cell Exhaustion But Retain Capacity for Cytokine Production. *Blood* (2013) 121(9):1612–21. doi: 10.1182/blood-2012-09-457531
30. Rissiek A, Schulze C, Bacher U, Schieferdecker A, Thiele B, Jacholkowski A, et al. Multidimensional Scaling Analysis Identifies Pathological and Prognostically Relevant Profiles of Circulating T-Cells in Chronic Lymphocytic Leukemia. *Int J Cancer* (2014) 135(10):2370–9. doi: 10.1002/ijc.28884
31. Ahearne MJ, Willimott S, Pinon L, Kennedy DB, Miall F, Dyer MJ, et al. Enhancement of CD154/IL4 Proliferation by the T Follicular Helper (Tfh) Cytokine, IL21 and Increased Numbers of Circulating Cells Resembling Tfh Cells in Chronic Lymphocytic Leukaemia. *Br J Haematol* (2013) 162(3):360–70. doi: 10.1111/bjh.12401
32. Cha Z, Zang Y, Guo H, Rechlic JR, Olasnova LM, Gu H, et al. Association of Peripheral CD4+ CXCR5+ T Cells With Chronic Lymphocytic Leukemia. *Tumour Biol* (2013) 34(6):3579–85. doi: 10.1007/s13277-013-0937-2
33. Palma M, Gentilcore G, Heimersson K, Mozaffari F, Nasman-Glaser B, Young E, et al. T Cells in Chronic Lymphocytic Leukemia Display Dysregulated Expression of Immune Checkpoints and Activation Markers. *Haematologica* (2017) 102(3):562–72. doi: 10.3324/haematol.2016.151100
34. Locci M, Havenar-Daughton C, Landais E, Wu J, Kroenke MA, Arlehamn CL, et al. Human Circulating PD-1+CXCR3-CXCR5+ Memory Tfh Cells are Highly Functional and Correlate With Broadly Neutralizing HIV Antibody Responses. *Immunity* (2013) 39(4):758–69. doi: 10.1016/j.immuni.2013.08.031
35. He J, Tsai LM, Leong YA, Hu X, Ma CS, Chevalier N, et al. Circulating Precursor CCR7(Lo)PD-1(Hi) CXCR5(+) CD4(+) T Cells Indicate Tfh Cell Activity and Promote Antibody Responses Upon Antigen Reexposure. *Immunity* (2013) 39(4):770–81. doi: 10.1016/j.immuni.2013.09.007
36. Kondo K, Shaim H, Thompson PA, et al. Ibrutinib Modulates the Immunosuppressive CLL Microenvironment Through STAT3-Mediated Suppression of Regulatory B-Cell Function and Inhibition of the PD-1/PD-L1 Pathway. *Leukemia* (2018) 32(4):960–70. doi: 10.1038/leu.2017.304
37. Long M, Beckwith K, Do P, Mundy BL, Gordon A, Lehman AM, et al. Ibrutinib Treatment Improves T Cell Number and Function in CLL Patients. *J Clin Invest* (2017) 127:3052–64. doi: 10.1172/JCI89756
38. Ma CS, Wong N, Rao G, Avery DT, Torpy J, Hambridge T, et al. Monogenic Mutations Differentially Affect the Quantity and Quality of T Follicular Helper Cells in Patients With Human Primary Immunodeficiencies. *J Allergy Clin Immunol* (2015) 136(4):993–1006.e1001 doi: 10.1016/j.jaci.2015.05.036.
39. Morales-Mantilla DE, King KY. The Role of Interferon-Gamma in Hematopoietic Stem Cell Development, Homeostasis, and Disease. *Curr Stem Cell Rep* (2018) 4(3):264–71. doi: 10.1007/s40778-018-0139-3
40. Asslaber D, Grossinger EM, Girbl T, Hofbauer SW, Egle A, Weiss L, et al. Mimicking the Microenvironment in Chronic Lymphocytic Leukaemia - Where Does the Journey Go? *Br J Haematol* (2013) 160(5):711–4. doi: 10.1111/bjh.12151
41. Hamilton E, Pearce L, Morgan L, Robinson S, Ware V, Brennan P, et al. Mimicking the Tumour Microenvironment: Three Different Co-Culture Systems Induce a Similar Phenotype But Distinct Proliferative Signals in Primary Chronic Lymphocytic Leukaemia Cells. *Br J Haematol* (2012) 158 (5):589–99. doi: 10.1111/j.1365-2141.2012.09191.x
42. Pascutti MF, Jak M, Tromp JM, Derks IA, Remmerswaal EB, Thijssen R, et al. IL-21 and CD40L Signals From Autologous T Cells Can Induce Antigen-Independent Proliferation of CLL Cells. *Blood* (2013) 122(17):3010–9. doi: 10.1182/blood-2012-11-467670
43. Catakovic K, Gassner FJ, Ratswohl C, Zaborsky N, Rebhandl S, Schubert M, et al. TIGIT Expressing CD4+T Cells Represent a Tumor-Supportive T Cell Subset in Chronic Lymphocytic Leukemia. *Oncoimmunology* (2017) 7(1): e1371399. doi: 10.1080/2162402X.2017.1371399
44. Patten PE, Ferrer G, Chen SS, Simone R, Marsilio S, Yan XJ, et al. Chronic Lymphocytic Leukemia Cells Diversify and Differentiate In Vivo Via a Nonclassical Th1-Dependent, Bcl-6-Deficient Process. *JCI Insight* (2016) 1(4). doi: 10.1172/jci.insight.86288
45. Burgler S, Gimeno A, Parente-Ribes A, Wang D, Os A, Devereux S, et al. Chronic Lymphocytic Leukemia Cells Express CD38 in Response to Th1 Cell-Derived IFN-Gamma by a T-Bet-Dependent Mechanism. *J Immunol* (2015) 194(2):827–35. doi: 10.4049/jimmunol.1401350
46. Patten PE, Buggins AG, Richards J, Wotherspoon A, Salisbury J, Mufti GJ, et al. CD38 Expression in Chronic Lymphocytic Leukemia is Regulated by the Tumor Microenvironment. *Blood* (2008) 111(10):5173–81. doi: 10.1182/blood-2007-08-108605
47. Zaborsky N, Holler C, Geisberger R, Asslaber D, Gassner FJ, Egger V, et al. B-Cell Receptor Usage Correlates With the Sensitivity to CD40 Stimulation and the Occurrence of CD4+ T-Cell Clonality in Chronic Lymphocytic Leukemia. *Haematologica* (2015) 100(8):e307–310. doi: 10.3324/haematol.2015.124719

Conflict of Interest: VB and JJ: Consultant and research funding from Astra Zeneca, Abbvie, Janssen and Gilead unrelated to this work. VB: Received fees from BIOGEN for compounds unrelated to this work. SG: Research funding from Gilead, Abbvie and Janssen unrelated to this work.

The remaining authors declare that the research was conducted in the absence of any commercial or financial relationships that could be construed as a potential conflict of interest.

frontiers in Oncology

ORIGINAL RESEARCH
published: 02 June 2021
doi: 10.3389/fonc.2021.684396

Adrenomedullin Expression Characterizes Leukemia Stem Cells and Associates With an Inflammatory Signature in Acute Myeloid Leukemia

Giorgia Simonetti[1], Davide Angeli[2], Elisabetta Petracci[2], Eugenio Fonzi[2], Susanna Vedovato[3], Alessandra Sperotto[4], Antonella Padella[1], Martina Ghetti[1], Anna Ferrari[1], Valentina Robustelli[5,6], Rosa Di Liddo[7], Maria Teresa Conconi[7], Cristina Papayannidis[5], Claudio Cerchione[8], Michela Rondoni[9], Annalisa Astolfi[10,11], Emanuela Ottaviani[5], Giovanni Martinelli[12] and Michele Gottardi[13]*

[1] Biosciences Laboratory, IRCCS Istituto Romagnolo per lo Studio dei Tumori (IRST) "Dino Amadori", Meldola, Italy, [2] Unit of Biostatistics and Clinical Trials, IRCCS Istituto Romagnolo per lo Studio dei Tumori (IRST) "Dino Amadori", Meldola, Italy, [3] Department of Clinical and Experimental Medicine, University of Padova, Padua, Italy, [4] Hematology and Transplant Center Unit, Dipartimento di Area Medica (DAME), Udine University Hospital, Udine, Italy, [5] IRCCS Azienda Ospedaliero-Universitaria di Bologna, Istituto di Ematologia "Seràgnoli", Bologna, Italy, [6] Dipartimento di Medicina Specialistica, Diagnostica e Sperimentale, Università di Bologna, Bologna, Italy, [7] Department of Pharmaceutical and Pharmacological Sciences, University of Padova, Padua, Italy, [8] Hematology Unit, IRCCS Istituto Romagnolo per lo Studio dei Tumori (IRST) "Dino Amadori", Meldola, Italy, [9] Hematology Unit & Romagna Transplant Network, Ravenna Hospital, Ravenna, Italy, [10] "Giorgio Prodi" Cancer Research Center, University of Bologna, Bologna, Italy, [11] Department of Morphology, Surgery and Experimental Medicine, University of Ferrara, Ferrara, Italy, [12] Scientific Directorate, IRCCS Istituto Romagnolo per lo Studio dei Tumori (IRST) "Dino Amadori", Meldola, Italy, [13] Onco Hematology, Department of Oncology, Veneto Institute of Oncology IOV, IRCCS, Padua, Italy*

OPEN ACCESS

Edited by:
Alessandro Isidori, AORMN Hospital, Italy

Reviewed by:
Adrián Mosquera Orgueira, University Hospital of Santiago de Compostela, Spain
Sara Galimberti, University of Pisa, Italy
Paolo Sportoletti, University of Perugia, Italy

***Correspondence:**
Giorgia Simonetti
giorgia.simonetti@irst.emr.it

Specialty section:
This article was submitted to Hematologic Malignancies, a section of the journal Frontiers in Oncology

Received: *23 March 2021*
Accepted: *23 April 2021*
Published: *02 June 2021*

Citation:
Simonetti G, Angeli D, Petracci E, Fonzi E, Vedovato S, Sperotto A, Padella A, Ghetti M, Ferrari A, Robustelli V, Di Liddo R, Conconi MT, Papayannidis C, Cerchione C, Rondoni M, Astolfi A, Ottaviani E, Martinelli G and Gottardi M (2021) Adrenomedullin Expression Characterizes Leukemia Stem Cells and Associates With an Inflammatory Signature in Acute Myeloid Leukemia. Front. Oncol. 11:684396. doi: 10.3389/fonc.2021.684396

Adrenomedullin (ADM) is a hypotensive and vasodilator peptide belonging to the calcitonin gene-related peptide family. It is secreted *in vitro* by endothelial cells and vascular smooth muscle cells, and is significantly upregulated by a number of stimuli. Moreover, ADM participates in the regulation of hematopoietic compartment, solid tumors and leukemias, such as acute myeloid leukemia (AML). To better characterize ADM involvement in AML pathogenesis, we investigated its expression during human hematopoiesis and in leukemic subsets, based on a morphological, cytogenetic and molecular characterization and in T cells from AML patients. In hematopoietic stem/progenitor cells and T lymphocytes from healthy subjects, *ADM* transcript was barely detectable. It was expressed at low levels by megakaryocytes and erythroblasts, while higher levels were measured in neutrophils, monocytes and plasma cells. Moreover, cells populating the hematopoietic niche, including mesenchymal stem cells, showed to express *ADM*. *ADM* was overexpressed in AML cells *versus* normal $CD34^+$ cells and in the subset of leukemia compared with hematopoietic stem cells. In parallel, we detected a significant variation of *ADM* expression among cytogenetic subgroups, measuring the highest levels in inv(16)/t(16;16) or complex karyotype AML. According to the mutational status of AML-related genes, the analysis showed a lower expression of *ADM* in *FLT3*-ITD, *NPM1*-mutated AML and *FLT3*-ITD/*NPM1*-mutated cases compared with wild-type ones.

Moreover, *ADM* expression had a negative impact on overall survival within the favorable risk class, while showing a potential positive impact within the subgroup receiving a not-intensive treatment. The expression of 135 genes involved in leukemogenesis, regulation of cell proliferation, ferroptosis, protection from apoptosis, HIF-1α signaling, JAK-STAT pathway, immune and inflammatory responses was correlated with *ADM* levels in the bone marrow cells of at least two AML cohorts. Moreover, *ADM* was upregulated in $CD4^+$ T and $CD8^+$ T cells from AML patients compared with healthy controls and some *ADM* co-expressed genes participate in a signature of immune tolerance that characterizes $CD4^+$ T cells from leukemic patients. Overall, our study shows that *ADM* expression in AML associates with a stem cell phenotype, inflammatory signatures and genes related to immunosuppression, all factors that contribute to therapy resistance and disease relapse.

Keywords: acute myeloid leukemia, adrenomedullin, hematopoiesis, inflammation, leukemia stem cells

INTRODUCTION

Adrenomedullin (ADM) is a 52-amino acid hormone belonging to the amylin/calcitonin gene-related peptide (CGRP) super-family, that has been originally identified in the extracts of human pheochromocytoma (1). It is produced by cleavage of an immature precursor that is synthesized by the *ADM* gene. ADM binds to calcitonin receptor-like (CALCRL), associated with modulating proteins with a single transmembrane domain, named receptor activity-modifying protein 2 (RAMP-2) or RAMP-3 (2).

ADM has been detected in many human tissues, including the endothelium, the nervous, cardiovascular, digestive, excretory, respiratory systems, the endocrine and reproductive organs (3). Despite its original definition as a hypotensive and vasodilator agent (1, 4), ADM is involved in a number of physiological processes, including angiogenesis (5), cell proliferation, migration (6), apoptosis (7, 8) and differentiation (9), with potential promoting and inhibitory functions depending on the cell type. Moreover, ADM production increases during infection, since it acts as an anti-microbial peptide against Gram-positive and Gram-negative bacteria (10), and during inflammation. Indeed, inflammatory molecules, as lipopolysaccharide (LPS) and 12-O-Tetradecanoylphorbol-13-acetate (TPA), and cytokines, including TNF-α and IL-1α force ADM secretion (11), and NF-κB binding sites have been identified on the *ADM* promoter (12). Once released, ADM can exert local and systemic anti-inflammatory actions by regulating cytokine secretion (13) and immune system properties, with beneficial effects on inflammatory conditions as gastric ulcers (14) and bowel diseases (15). Additional stimuli, as cell-to-cell interaction (16), growth factors, steroids, hormones, and physical factors, including oxidative stress and hypoxia, can induce *ADM* expression (3).

In the hematopoietic system, ADM is produced and secreted by peripheral blood monocytes, monocyte-derived macrophages and granulocytes (17). Moreover, mononuclear hematopoietic cells of the cord blood express *ADM* transcript (18) and ADM, in combination with growth-promoting cytokines, was able to enhance clonal growth and expansion of cord blood hematopoietic stem cells (18–20) and progenitor cells, respectively (20).

In contrast with the protective and therapeutic activity demonstrated in different diseases, ADM has pro-tumorigenic functions. It is over-expressed in a number of malignancies, including breast cancer, melanoma, tumors of the eye, of the respiratory, nervous, urogenital and gastroenteric system (21). Despite its relevance in hematopoietic stem cells and in the myeloid lineage, little is known about ADM in acute myeloid leukemia (AML). Previous studies on AML cellular models showed that HL60 (22) and THP1 cells produce ADM, though at low levels, and respond to a number of stimuli, including TPA, LPS, TNF-α by increasing its expression (17, 23). The elevated ADM production was associated with increased expression of markers of monocyte/macrophage differentiation (17). Conversely, exposure to exogenous ADM had no evident effects on cell differentiation that was instead induced by treatment with an ADM receptor antagonist. Exogenous ADM promoted AML cell proliferation through the ERK/MAPK pathway and induced CD31 upregulation, which could enhance their transendothelial migration capacity.

Here we analyzed the expression of the *ADM* gene across human hematopoietic cell differentiation and in AML, including its morphological, cytogenetic and molecular subtypes, cell subpopulations and T cell subsets from leukemic patients, and we investigated *ADM* impact on prognosis and its related transcriptional network.

MATERIALS AND METHODS

Sample Collection and Cell Preparation

Samples were obtained from AML and acute lymphoblastic leukemia (ALL) patients after written informed consent, as approved by the institutional ethics committees (Comitato Etico Indipendente di Area Vasta Emilia Centro, protocol 112/2014/U/Tess and Comitato Etico della Romagna, protocol 5805/2019), in accordance with the Declaration of Helsinki.

Mononuclear cells from bone marrow (n = 7) or peripheral blood (n = 5) of adult (non-M3) AML patients at diagnosis were collected by density gradient centrifugation using Lymphosep (Biowest). $CD34^+$ leukemic blasts were enriched by immunomagnetic separation (CD34 MicroBead Kit, Miltenyi Biotec). Healthy hematopoietic stem-progenitor cells ($CD34^+$) from bone marrow specimens (n = 3) were obtained by STEMCELL Technologies Inc.

Gene Expression Datasets

Gene expression data were obtained from the BLUEPRINT consortium (http://dcc.blueprint-epigenome.eu/#/home) (24) and the Gene Expression Omnibus (GEO) repository [https://www.ncbi.nlm.nih.gov/gds, GSE98791 (25), GSE24759 (26), GSE24006 (27), GSE63270 (28), GSE158596 (29), GSE117090 (30), GSE14924 (31), GSE14468 (32), GSE6891 (33), GSE13159 (34)]. Array data from 61 AML bone marrow samples (blasts ≥80%) and 29 Philadelphia-negative (Ph−) B-ALL have been generated by the Next Generation Sequencing platform for targeted Personalized Therapy of Leukemia (NGS-PTL) project, as previously described (35, 36). The Beat AML (37) and The Cancer Genome Atlas (TCGA) project on AML (38) transcriptomic cohorts were obtained from https://portal.gdc.cancer.gov (projects BEATAML1.0-COHORT and TCGA-LAML), respectively. The datasets used in the manuscript are described in **Supplementary Table 1**.

Transcriptomic Data Analysis

Data quality control and normalization (signal space transformation robust multi-array average) of NGS-PTL data (Affymetrix Human Transcriptome Array 2.0) were carried out by Expression Console software (version 1.4.1, Affymetrix, Thermo Fisher Scientific). Raw data from GSE24006, GSE14468, GSE6891, GSE13159 (all Affymetrix U133 Plus 2.0 array), were normalized by Transcriptome Analysis Console Software (version 4.0.1) using robust multi-array average normalization. Normalized data from GSE98791 (Agilent-021441 NCode Human Long Non-coding RNA), GSE117090 (Affymetrix Human Transcriptome Array 2.0), GSE14924, GSE63270 (Affymetrix U133 Plus 2.0 array) and GSE24759 (Affymetrix HT-HG-U133A Early Access) were retrieved from GEO. BLUEPRINT RNA-seq data were normalized in Transcript Per Million (TPM) by RSEM (39). RNA-Seq data from TCGA-LAML and Beat AML are available in the form of HTSeq read counts. Those were transformed into Counts Per Million (CPM) with Trimmed Mean of M values (TMM), using calcNormFactors (method = "TMM") function in edgeR (40) (v3.24.1), then log2-transformed. RNA-seq data from GSE158596 were normalized using the median of ratios method of DESeq2 (41). Supervised gene expression analysis was performed by Student's t-test or Welch's t-test [R package stats, v3.4.1 (42)—python v3.6.5 (43) package scipy v1.5.2 (44)] in order to compare expression of *ADM*, its co-expressed and interacting genes. *ADM* interacting proteins were identified by STRING (version 11.0). Pathway enrichment analysis was carried out by Enrich R (45) on Gene Ontology Biological Processes, KEGG and Reactome annotations. The ClueGO package (version 2.5.7) from the Cytoscape software platform (version 3.8.1) was used for functional network analysis. Gene set enrichment analysis (GSEA) was performed with GSEA software (Broad Institute) (46).

qRT-PCR

After TRIzol extraction, RNA was reverse transcribed into cDNA (PrimeScript Reag Kit with gDNA Eraser, Takara). TaqMan gene expression for *ADM* mRNA (Hs00181605_m1, ThermoFisher Scientific) was performed on $CD34^+$ cells from AML and control samples, using *HPRT1* (Hs02800695_m1) as reference gene, on the Applied Biosystems 7500 Real-Time PCR System (ThermoFisher Scientific). Gene expression was quantified by the $2^{-\Delta\Delta Ct}$ method, using the average expression of healthy $CD34^+$ cells as calibrator.

Statistical Analyses

Data were reported as median and minimum-to-maximum values for continuous variables and as natural frequencies and percentages for categorical ones. The Shapiro–Wilk test was used to assess if continuous variables were normally distributed. The association between one continuous and one categorical variable was performed using the Student t-test or the Analysis of Variance (ANOVA) or the analogous Wilcoxon–Mann–Whitney test or Kruskal–Wallis test, as appropriate. In case of a significant result (p-value ≤0.05) from an omnibus test for the comparison of more than two categories, post-hoc test p-values were adjusted using the Bonferroni method. The association between two categorical variables was assessed by means of the Chi-square test or the Fisher's exact test, as appropriate. Correlation among genes was studied through the Pearson correlation coefficient. To investigate the association between *ADM* expression and overall survival (OS), a Cox proportional hazards model was used. Hazard ratios (HRs) and 95% confidence intervals (CIs) were reported. To assess the presence of outliers or influential observations as well as the functional form of *ADM* in relation to the hazard function, the Deviance and the Martingale residuals were used, respectively. Overall survival analysis was performed firstly on each cohort separately and then on an integrated dataset to explore the prognostic role of *ADM* in specific subgroups otherwise characterized by very low frequency. Such integrated dataset was obtained applying the Blom transformation to the normalized expression data of *ADM* (47). Such rank-based transformation backtransforms the uniformly distributed ranks to a standard normal distribution. Statistical analyses were performed using R statistical language version 3.6.1 and STATA 12.0 (College Station).

RESULTS

ADM Expression Is a Characteristic of the Myeloid Differentiation Program

To deeply investigate *ADM* expression in the hematopoietic system, we analyzed its mRNA levels at different stages of

hematopoiesis and in the microenvironment in the BLUEPRINT dataset. *ADM* transcript was barely detectable in hematopoietic stem cells (HSC) and almost undetectable in hematopoietic multipotent progenitor cells (MPP) (**Figure 1A**). In the myeloid differentiation program, *ADM* was not expressed by common myeloid progenitor cells (CMP) and granulocyte-monocyte progenitor cells (GMP). It was barely detectable in megakaryocytes and erythroblasts, while increasing in dendritic cells (DC) and, especially, during neutrophilic differentiation and in monocytes (**Figure 1A**). Monocyte-derived macrophages showed low *ADM* levels. However, *ADM* expression was significantly enhanced by LPS stimulation (**Supplementary Figure 1**), in line with previous reports (49). In the lymphoid lineage, *ADM* was not expressed by common lymphoid progenitors (CLP) and by T cells at any stage of differentiation (thymocytes, memory T cells and regulatory T cells, **Figure 1A**). *ADM* expression remained close to undetectable during B lymphocyte differentiation (naïve, germinal center and memory B cells), while increasing in terminally-differentiated plasma cells (**Figure 1A**). Of note, *ADM* was highly expressed by cells populating the hematopoietic niche and/or interacting with the hematopoietic system, including endothelial progenitor and mature cells, bone marrow mesenchymal stem cells (MSC) and osteoclasts (**Figure 1A**).

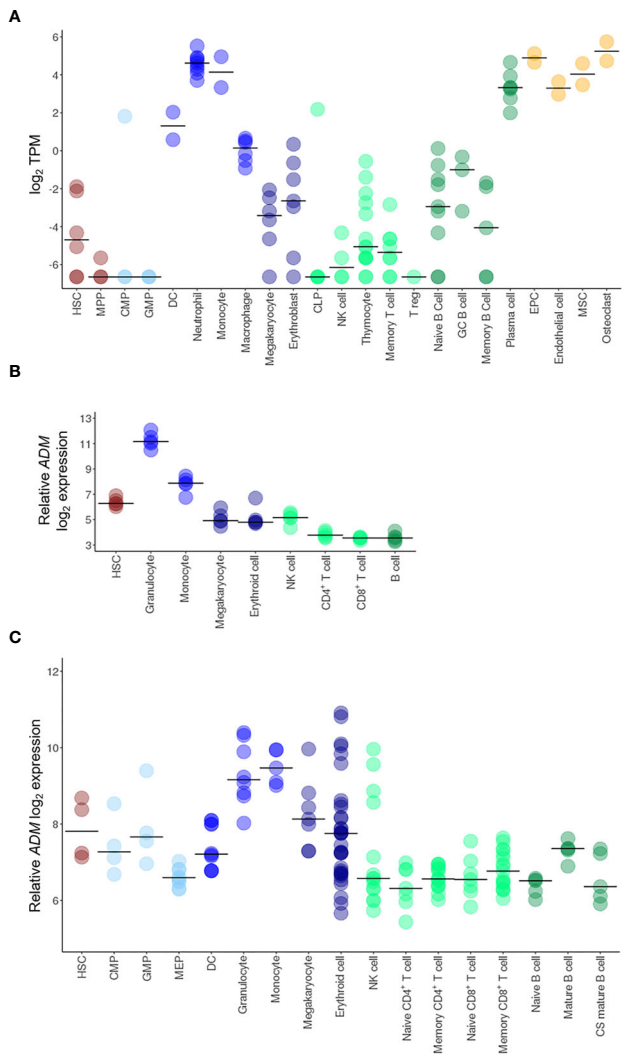

FIGURE 1 | *ADM* expression in HSC and in the hematopoietic system. Transcriptional analysis of *ADM* expression in hematopoietic cells from the BLUEPRINT **(A)**, the GSE98791 **(B)** and the GSE24759 **(C)** datasets. Scatter plots were generated with the R package ggplot2 (48) (version 3.3.1). Each dot indicates one sample and the bar represents the median value (HSC, hematopoietic stem cells; MPP, hematopoietic multipotent progenitor cells; CMP, common myeloid progenitors; GMP, granulocyte–monocyte progenitors; DC, conventional dendritic cells, CLP, common lymphoid progenitors; NK, natural killer; T reg, regulatory T cells; GC, germinal center; EPC, endothelial progenitor cells; MSC, mesenchymal stem cells; MEP, megakaryocyte-erythroid progenitors; CS, class-switched; TPM, Transcripts Per Million).

To validate these data in independent cohorts, we analyzed the GSE98791 and GSE24759 datasets, containing hematopoietic and immune cell populations. The results were largely overlapping, showing very low *ADM* levels in CMP, GMP, B cells, $CD4^+$ and $CD8^+$ T lymphocytes (naïve, mature and memory), low expression in HSC, erythroid cells and megakaryocytes and higher *ADM* transcript in monocytes and granulocytes (**Figures 1B, C**).

Taken together, these data indicate that in the normal hematopoietic system, *ADM* expression is a hallmark of mature myeloid cells.

Leukemia Stem Cells Express *ADM*

It was previously reported that the expression of the ADM binding receptor CALCRL is a prognostic marker in AML (50). However, both CGRP and ADM bind to the same receptor. To understand whether ADM may be involved in CALCRL signaling in AML, we analyzed its expression in three different datasets of leukemic and hematopoietic cells at different stages of differentiation, including stem and progenitor cells, defined on a surface phenotype base (GSE24006, GSE117190 and GSE63270).

ADM was overexpressed in leukemic stem cells (LSC) compared with HSC (GSE24006, $p = 0.017$; GSE117190, $p = 0.023$, GSE63270, $p = 0.052$) or MPP (GSE24006, $p = 0.018$; GSE63270, $p = 0.002$, **Figures 2A–C**). Elevated levels were also detected in leukemic compared with hematopoietic progenitor cells (GSE24006, $p = 0.051$; GSE117190, $p < 0.001$, GSE63270, $p = 0.003$; **Figures 2A–C**). Moreover, *ADM* expression was maintained in AML blast cells that showed similar levels compared with more undifferentiated AML cells (GSE24006, **Figure 2A**). The elevated *ADM* expression in AML was confirmed in our qRT-PCR analysis of $CD34^+$ AML cells *versus* bone marrow hematopoietic stem-progenitor cells (HSPC, $p = 0.017$, **Figure 2D**) and in the GSE158596 dataset, by comparing leukemic blasts with G-CSF mobilized HSPC ($p < 0.001$, **Figure 2E**).

We then asked whether *ADM* expression differs between AML and ALL. We observed higher *ADM* expression in AML *versus* ALL (GSE13159, $p < 0.001$, **Figure 2F**). This result was confirmed by comparing AML with T-ALL ($p < 0.001$, **Figure 2G**) or B-ALL

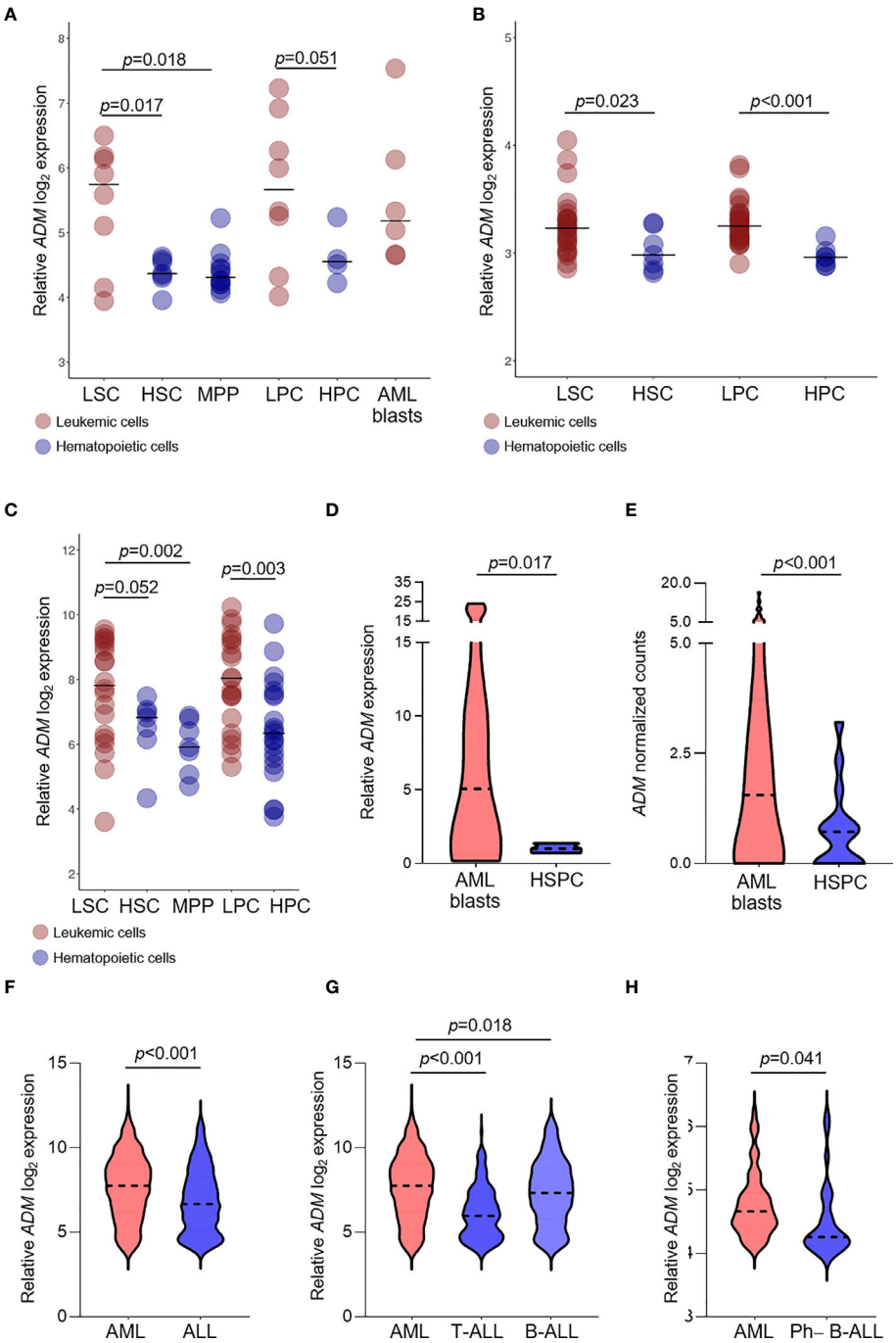

FIGURE 2 | *ADM* expression is elevated in leukemic compared with hematopoietic stem and progenitor cells and in AML compared with ALL. **(A–C)** Comparison of *ADM* levels between leukemic cells subpopulations and normal stem and progenitor cells in the GSE24006 **(A)**, the GSE117090 **(B)** and the GSE63270 **(C)** datasets. Subpopulations according to their surface phenotype: leukemia stem cells (LSC): (Lin^-)$CD34^+CD38^-(CD90^-)$, hematopoietic stem cells (HSC): $Lin^-CD34^+CD38^-CD90^+(CD45RA^{+/-})$, hematopoietic multipotent progenitor cells (MPP): $Lin^-CD34^+CD38^-CD90^-CD45RA^-$, leukemia progenitor cells (LPC): (Lin^-) $CD34^+CD38^+(CD90^-)$, hematopoietic progenitor cells (HPC): $Lin^-CD34^+CD38^+(CD90^+)$, AML blasts: Lin^-CD34^-. Scatter plots were generated with the R package ggplot2 (48) (version 3.3.1). Each dot indicates one sample and the bar represents the median value. **(D)** Comparison of *ADM* levels between AML blasts (n = 12) and healthy $CD34^+$ bone marrow cells (n = 3, hematopoietic stem-progenitor cells, HSPC, qRT-PCR) and **(E)** between AML blasts (n = 60) and healthy G-CSF mobilized HSPC (n = 16) from the GSE158596 dataset. **(F)** *ADM* transcript levels in AML (n = 505) and ALL (n = 784, GSE13159), **(G)** separated in T-ALL (n = 173) and B-ALL (n = 441) and **(H)** in AML (n = 61) *versus* Ph–B-ALL (n = 29, NGS-PTL). Violin plots were generated with GraphPad Prims (version 8.4.3). The plots represent the frequency distribution of *ADM* levels (from minimum to maximum) and the dotted line indicates the median value.

(p = 0.018, **Figure 2G**), separately. When analyzing the NGS-PTL B-ALL cohort, we observed that *ADM* expression was increased in AML compared with Ph-negative (Ph–) B-ALL (NGS-PTL, p = 0.041, **Figure 2H**). Overall, these data suggest that *ADM* is generally higher in AML compared with ALL.

High *ADM* Expression Associates With Specific Cytogenetic Features in AML

We then asked whether *ADM* expression levels changed among AML molecular and biological subgroups and investigated the association between *ADM* levels and disease features, including age, morphology, cytogenetics, and genomic lesions. To this aim, we analyzed six independent datasets of newly-diagnosed AML (excluding M3 cases, age ≥18 years) and focused on bone marrow samples (GSE6891, n = 68; Beat AML, n = 142; TCGA-LAML, n = 135, GSE13159, n = 458, NGS-PTL, n = 61), except for GSE14468 cohort that included mixed bone marrow and peripheral blood samples (n = 459, tissue not specified, **Table 1** and **Supplementary Table 2**).

Elderly patients (aged ≥60 years) expressed significantly higher *ADM* transcript in the GSE14468 cohort (p = 0.034) and this comparison was close to significance in the TCGA-LAML dataset (p = 0.056). *ADM* expression showed a significant variation according to French–American–British classification (GSE6891, p = 0.001, GSE14468, p <0.001), with high levels in the immature M0 cytomorphology, in the monocytic types (FAB M4/M5) and in erythroid leukemia (M6). Moreover, we observed a significant variation among cytogenetic subgroups (Beat AML, p = 0.001; TCGA-LAML, p = 0.001, GSE14468, p <0.001; GSE13159, p <0.001), with elevated levels in complex karyotype and inv(16)/t(16;16) AML and low expression in t(8;21) cases.

The analysis of *ADM* expression according to genetic alteration of AML-related genes revealed no association with the mutational status of *IDH1*, *IDH2*, *KRAS*/*NRAS*, *RUNX1*, *ASXL1*, *DNMT3A* and *TP53*. Moreover, no significant differences were observed among ELN 2010 risk categories (**Table 1**). Conversely, we detected lower expression in *FLT3*-ITD AML (GSE6891, p = 0.023; TCGA-LAML, p = 0.001; GSE144468, p = 0.009) compared with *FLT3*-ITD-negative AML and in *NPM1*-mutated *versus* wild-type cases in the TCGA-LAML dataset (p = 0.034). Accordingly, when considering *FLT3*-ITD and *NPM1* mutation simultaneously, we observed a significant difference among the subgroups, with the wild-type cases expressing the highest *ADM* levels and the *FLT3*-ITD/*NPM1*-mutated ones expressing the lowest ones (GSE6891, p = 0.004; TCGA-LAML, p = 0.009).

We then asked whether *ADM* may have a prognostic role in terms of OS, but no statistically significant association was observed. This analysis was performed on the Beat AML, TCGA-LAML, GSE6891 and NGS-PTL cohorts that had the information related to the OS. Bone marrow and peripheral blood samples were included in order to increase the cohort size and allow subgroup analyses. Considering the integrated dataset, the associations between *ADM* and AML molecular and biological features observed on the single cohorts were confirmed (**Table 2**). Moreover, the integrated dataset suggested the association with ELN 2010 risk classification (p = 0.006, **Table 2**). In details, *ADM* expression was elevated in the favorable and adverse risk categories, compared with the intermediate ones, in line with the cytogenetic features. Additional analyses showed that high *ADM* expression had a negative impact on OS within the patients' subgroup characterized by favorable ELN 2010 risk (HR for a one-unit increase in *ADM* = 1.28; 95% CI: 1.02–1.61, p = 0.031, **Figure 3A**). Adjusting for age (<60, ≥60 years) that resulted either significantly associated to *ADM* and to affect the OS, the HR for a one-unit increase in *ADM* was equal to 1.22 (95% CI: 0.97–1.53, p = 0.083). Conversely, high *ADM* expression seemed to have a positive impact on OS within the subgroup receiving a not-intensive treatment (azacytidine, decitabine, targeted therapies; HR = 0.65, 95% CI: 0.43–0.97 p = 0.037, **Figure 3A**). In this cohort, the prognostic role of *ADM* was independent from other biological and clinical factors.

The *ADM* Gene Network Is Enriched of Inflammatory Signatures in Leukemic Cells and of Immunomodulatory Genes in T Cells From AML Patients

To understand the biological features associated with *ADM* expression in AML, we analyzed genes co-expressed and interacting with it. We defined 135 genes whose expression positively correlated with *ADM* (absolute value of Pearson correlation coefficient ≥0.5 and p value ≤0.05) in at least two out of the five cohorts of bone marrow samples (**Figure 3B** and **Supplementary Table 3**). Moreover, we identified the top-scoring *ADM* interactors (protein–protein interaction enrichment p <1.0e−16, **Supplementary Figure 2**), that are mainly involved in G protein-coupled receptor signaling.

Genes co-expressed with *ADM* were involved in regulation of cell growth and proliferation (e.g. *CDKN2D*, *SDCBP*, *BTG1*, *PTPRJ*, *SGK1*), ferroptosis (*FTH1*, *CYBB*, *SAT1*, *FTL*), protection from apoptosis (e.g. *HCK*, *RNF144B*, *BCL2A1*, *BIRC3*), HIF-1α signaling (e.g. *CDKN1A*, *EDN1*, *PFKFB3*, *CYBB*), JAK-STAT pathway (*SOCS3*, *IL6*, *CDKN1A*, *IL10RA*, *IL21R*) and response to stimuli, including lipids, LPS, cytokines and chemokines (**Supplementary Table 4**). Three of these genes were confirmed in four out of five cohorts, thus representing high-fidelity *ADM* co-expressed genes. They were the p53 transcriptional target *SAT1*, that is involved in polyamine metabolism and functions as a metabolic mediator of ferroptotic cell death (51), the BCL2 family member *BCL2A1*, that has been recently shown to confer resistance to Venetoclax treatment (52, 53), and *IER5*, that regulates LPC proliferation (54) (**Figure 3B** and **Supplementary Table 3**).

Four *ADM* co-expressed genes were also upregulated in LSC compared with HSC in two analyzed datasets (GSE24006, **Figure 3C** and GSE117090, **Figure 3D**). The Src family kinase HCK is strongly expressed in a significant proportion of AML patients (55), is known to be upregulated in leukemic compared to normal stem cells and is a potential therapeutic target (56, 57).

TABLE 1 | Association between *ADM* expression levels and clinical/molecular data across public datasets.

Variable	GSE6891 (n=68)			GSE14468 (n=459)			Beat AML (n=142)			TCGA-LAML (n=135)		
	n (%)	median [min-max]	*p*	n (%)	median [min-max]	*p*	n (%)	median [min-max]	*p*	n (%)	median [min-max]	*p*
Age			**-**			**0.034**			0.653			0.056
<60-years	–	–		383 (83.8)	159.8 [57.7-3848.3]		60 (42.3)	9.5 [0.2-313.9]		72 (53.3)	1.3 [0.0-23.1]	
≥60-years	63 (100.0)	196.7 [93.4-4451.3]		74 (16.2)	238.2 [98.4-442.9]		82 (57.7)	11.4 [0.3-151.7]		63 (46.7)	2.0 [0.0-57.1]	
missing	5			2			–			–		
FAB			**0.001**			**<0.001**			0.057			0.591
M0	2 (3.6)	229.7 [188.7-270.6]		18 (4.1)	135.3 [80.5-477.7]		4 (7.8)	4.0 [1.2-6.1]		14 (10.5)	2.1 [0.0-5.5]	
M1	11 (19.6)	122.7 [97.0-206.5]		97 (22.2)	134.8 [57.7-3396.9]		6 (11.8)	1.3 [1.0-118.2]		35 (26.1)	1.2 [0.0-12.4]	
M2	23 (41.1)	148.1 [92.4-1024.0]		123 (28.2)	147.0 [71.0-2936.7]		5 (9.8)	6.4 [0.9-63.6]		38 (28.4)	1.3 [0.1-17.2]	
M4	9 (16.1)	221.3 [172.4-4451.3]		83 (19.0)	205.1 [84.5-3848.3]		16 (31.4)	19.0 [3.5-159.1]		29 (21.6)	2.0 [0.1-12.8]	
M5	10 (17.9)	448.6 [166.6-4451.3]		109 (24.9)	183.6 [83.9-4482.2]		19 (37.3)	4.3 [0.3-151.7]		15 (11.2)	1.1 [0.0-57.1]	
M6	1 (1.8)	843.4		7 (1.6)	171.3 [123.6-849.2]		–	–		2 (1.5)	2.3 [1.9-2.7]	
M7	–	–		–	–		1 (2.0)	5.9		1 (0.8)	1.4 [1.4-1.4]	
missing	12			22			91			1		
Cytogenetic group			0.063			**<0.001**			**0.001**			**0.001**
t(8;21)	3 (5.0)	104.0 [96.3-126.2]		32 (9.8)	137.2 [92.4-451.9]		3 (2.1)	7.3 [0.9-15.1]		7 (5.3)	0.2 [0.1-1.0]	
inv(16)/t(16;16)	4 (6.7)	516.6 [182.3-2256.7]		33 (10.1)	210.1 [125.4-2164.8]		9 (6.4)	18.9 [5.1-98.7]		10 (7.6)	1.9 [1.2-7.0]	
NK	23 (38.3)	188.7 [96.3-4451.3]		139 (42.4)	149.1 [57.7-3848.3]		75 (53.6)	7.5 [0.2-313.9]		60 (45.5)	1.2 [0.0-57.1]	
CK	4 (6.7)	178.1 [92.4-4451.3]		27 (8.2)	133.4 [95.7-2740.1]		19 (13.6)	35.6 [1.2-130.8]		18 (13.6)	3.4 [0.3-17.2]	
KMT2A-r	1 (1.7)	179.8		15 (4.6)	116.2 [84.5-1782.9]		8 (5.7)	2.0 [0.3-39.3]		8 (6.1)	0.5 [0.0-1.8]	
Other	25 (41.7)	229.1 [114.6-2019.8]		82 (25.0)	169.5 [74.5-3304.0]		26 (18.6)	13.8 [0.4-159.1]		29 (22.0)	1.9 [0.0-12.8]	
missing	8			131			2			3		
***FLT3*-ITD**			**0.023**			**0.009**			0.062			**0.001**
FLT3-ITD$^+$	18 (26.5)	145.5[96.3-1024.0]		112 (28.3)	144.5 [57.7-2091.0]		27 (20.3)	4.2 [0.4-118.2]		27 (20.5)	0.4 [0.0-23.1]	
FLT3-ITD$^-$	50 (73.5)	247.3 [92.4-4451.3]		283 (71.7)	167.7 [68.1-3848.3]		106 (79.7)	14.5 [0.2-313.9]		105 (79.6)	1.9 [0.0-57.1]	
missing	–			64			9			3		
***NPM1* status**			0.127			0.249			0.064			**0.034**
NPM1-mut	20 (29.4)	151.2 [96.3-2019.8]		135 (34.2)	313.9 [57.7-3743.1]		37 (27.8)	4.2 [0.6-313.9]		38 (28.8)	0.6 [0.0-57.1]	
NPM1-wt	48 (70.6)	244.0 [92.4-4451.3]		260 (65.8)	164.9 [68.1-3848.3]		96 (72.2)	13.8 [0.2-159.1]		94 (71.2)	1.8 [0.0-16.8]	
missing	–			64			9			3		
FLT3*-ITD/*NPM1			**0.004**			0.070			0.086			**0.009**
–/wt	40 (58.8)	244.7 [92.4-4451.3]		218 (55.2)	168.9 [68.1-3848.3]		81 (60.9)	15.1 [0.2-159.1]		84 (63.6)	2.0 [0.0-16.8]	
+/wt	8 (11.8)	281.9 [97.0-1024.0]		42 (10.6)	147.5 [83.3-2091.0]		15 (11.3)	8.9 [0.4-118.2]		10 (7.6)	0.8 [0.2-12.4]	
–/mut	10 (14.7)	305.0 [120.3-2019.8]		65 (16.5)	163.2 [71.0-3743.1]		25 (18.8)	9.4 [0.6-313.9]		21 (15.9)	1.5 [0.0-57.1]	
+/mut	10 (14.7)	123.8 [96.3-166.6]		70 (17.7)	140.6 [57.7-1758.3]		12 (9.0)	2.7 [0.8-46.5]		17 (12.9)	0.3 [0.0-23.1]	
missing	–			64			9			3		
ELN 2010			0.448			0.255			0.104			0.114
Favorable	11 (18.3)	221.3 [96.3-2256.7]		115 (35.3)	172.4 [67.2-2179.8]		38 (27.1)	10.8 [0.5-313.9]		40 (30.8)	1.3 [0.0-57.1]	
Int-I	19 (31.7)	148.1 [96.3-4451.3]		89 (27.3)	140.1 [57.3-3875.1]		49 (35.0)	7.7 [0.2-151.7]		37 (28.5)	1.2 [0.1-23.1]	
Int-II	18 (30.0)	201.6 [117.8-2019.8]		74 (22.7)	160.9 [70.0-3327.0]		26 (18.6)	10.2 [0.3-159.1]		22 (16.9)	1.5 [0.0-12.8]	
Adverse	12 (20.0)	237.3 [92.4-4451.3]		48 (14.7)	150.1 [83.7-2019.8]		27 (19.3)	21.8 [0.4-130.8]		31 (23.9)	2.8 [0.3-17.2]	
missing	8			133			2			5		

CK, complex karyotype; Int, Intermediate; ITD, internal tandem duplication; KMT2A-r, KMT2A-rearranged; min-max, minimum-to-maximum value; mut, mutated; n, number; NK, normal karyotype; p, p value; wt, wild-type.
$p \leq 0.05$ are highlighted as bold text.

TABLE 2 | Association between *ADM* expression levels and clinical/molecular data in the overall AML cohort after normalization.

Variable	Beat AML+TCGA-LAML+GSE6891+NGS-PTL (n=903)		
	n (%)	median [min-max]	*p*
Age			**<0.001**
<60-years	578 (64.9)	-0.1 [-3.0-2.6]	
≥60-years	313 (35.1)	0.2 [-2.8-2.9]	
missing	12		
FAB			**<0.001**
M0	40 (6.0)	-0.4 [-2.2-1.1]	
M1	147 (21.9)	-0.4 [-3.0-2.4]	
M2	175 (26.1)	-0.2 [-2.6-2.2]	
M4	143 (21.3)	0.2 [-1.9-2.9]	
M5	154 (23.0)	0.02 [-2.3-2.9]	
M6	9 (1.3)	0.1 [-0.6-1.4]	
M7	3 (0.5)	-0.1 [-0.4-0.4]	
missing	232		
Cytogenetic group			**<0.001**
t(8;21)	50 (6.2)	-0.5 [-1.6-1.1]	
inv(16)/t(16;16)	68 (8.4)	0.3 [-0.6-2.3]	
NK	360 (44.4)	-0.2 [-3.0-2.9]	
CK	89 (11.0)	0.4 [-1.7-2.9]	
KMT2A-r	38 (4.7)	-0.9 [-2.8-1.9]	
Other	205 (25.3)	0.1 [-2.6-2.8]	
missing	93		
FLT3-ITD			**<0.001**
FLT3-ITD$^+$	200 (24.3)	-0.4 [-3.0-2.3]	
FLT3-ITD$^-$	622 (75.7)	0.1 [-2.8-2.9]	
missing	81		
***NPM1* status**			**<0.001**
NPM1-mut	241 (30.4)	-0.3 [-3.0-2.6]	
NPM1-wt	572 (69.6)	0.1 [-2.8-2.9]	
missing	81		
FLT3*-ITD/*NPM1			**<0.001**
–/wt	486 (59.1)	0.2 [-2.8-2.9]	
+/wt	86 (10.5)	-0.2 [-2.1-1.7]	
–/mut	136 (16.6)	-0.01 [-2.6-2.6]	
+/mut	114 (13.9)	-0.6 [-3.0-2.3]	
missing	81		
ELN 2010			**0.006**
Favorable	224 (30.1)	0.1 [-2.7-2.6]	
Int-I	218 (29.3)	-0.2 [-3.0-2.9]	
Int-II	162 (21.7)	0.02 [-2.6-2.3]	
Adverse	141 (18.9)	0.4 [-2.8-2.9]	
missing	158		

CK, complex karyotype; ITD, internal tandem duplication; KMT2A-r, KMT2A-rearranged; min–max, minimum-to-maximum value; mut, mutated; n, number; NK, normal karyotype; p, p value; wt, wild-type.
p ≤ 0.05 are highlighted as bold text.

Along with the metabolic mediator *SAT1*, an additional gene functions as regulator of cell homeostasis, namely the lysosomal thiol reductase *IFI30*, that facilitates degradation of unfolded proteins, thus controlling endoplasmic-reticulum stress. *IFI30* is also a predictor of response to combined Mitoxantrone, Etoposide, Cytarabine and the proteasome inhibitor Ixazomib in relapsed/refractory AML (58). Moreover, *FCER1G* is an immune regulator. Indeed, it is an adapter protein that transduces activation signals from various immunoreceptors and has been shown to prime T cells toward T-helper 2 and T-helper 17 cell subtypes (59).

Remarkably, network analysis of the *ADM* co-expressed genes across AML datasets highlighted the enrichment of transcripts involved in immune and inflammatory response, including myeloid leukocyte activation, regulation of their differentiation, neutrophil migration, toll-like receptor signaling, mononuclear cell migration, regulation of leukocyte proliferation (**Figure 4** and **Supplementary Table 4**), suggesting an association between high *ADM* levels and an inflammatory status in leukemic cells.

Since *ADM* has been previously linked with immune response under physiological and pathological conditions (60–63), we compared its expression in T cell subsets from AML patients and healthy controls. We observed increased *ADM* expression in CD4$^+$ T cells (GSE14924, p <0.001, **Figure 5A**) and in CD8$^+$ T lymphocytes (GSE117090, p <0.001, **Figure 5B**) from AML patients. Moreover, 40 and six *ADM* co-expressed genes were upregulated in CD4$^+$ T (**Figure 5C**) and CD8$^+$ T cells (**Figure 5D**) from AML patients compared with cells from healthy controls, respectively. When studied by GSEA, CD4$^+$ T cells from AML patients were enriched of signatures related to regulatory T (Treg) cells (**Figure 5E**). Of note, some *ADM* co-expressed genes, including *JUNB*, *CDKN1A*, *ANXA5*, *CYBB*, *NFKBIZ*, that were upregulated in CD4$^+$ T cells from AML patients compared with cells from healthy controls (**Figure 5B**), are known to participate to the Treg phenotype (65–69).

DISCUSSION

ADM is a circulating hormone that also functions as a local paracrine and autocrine mediator, with involvement in a number of different cellular responses. We here studied *ADM* expression in the hematopoietic system and in AML and analyzed the transcriptional program associated with it both in leukemic cells and the immune microenvironment.

ADM is upregulated in a variety of human cancers compared with normal tissues and its mRNA expression correlated with high protein expression in the majority of them (21). In AML, we observed elevated levels in cell subpopulation defined, on the basis of their surface phenotype, as LSC and LPC compared with their normal counterparts that showed undetectable-to-barely-detectable levels.

ADM expression is also elevated in AML compared with ALL, in line with the observation that *ADM* expression is a main feature of the myeloid differentiation program. Accordingly, among AML FAB subtypes, monocytic (M4/M5) and erythroid (M6) leukemia had the highest expression, together with the immature M0 phenotype. These data reflect the distribution of *ADM* expression across the cytogenetic subgroups, with complex karyotypes, that frequently have an undifferentiated phenotype and inv(16)/t(16;16) AML, that characterizes the myelomonocytic cytomorphology, showing the strongest *ADM* positivity. This feature may also explain the lack of prognostic relevance of *ADM* in AML in general, that has been reported in other solid tumors (70–76). Conversely, high *ADM* levels showed a potential negative impact on overall survival in the favorable ELN 2010 risk class, that also includes inv(16)/t(16;16) cases. In AML, *ADM* expression is related to the disease molecular features, both in terms of genomic rearrangements and

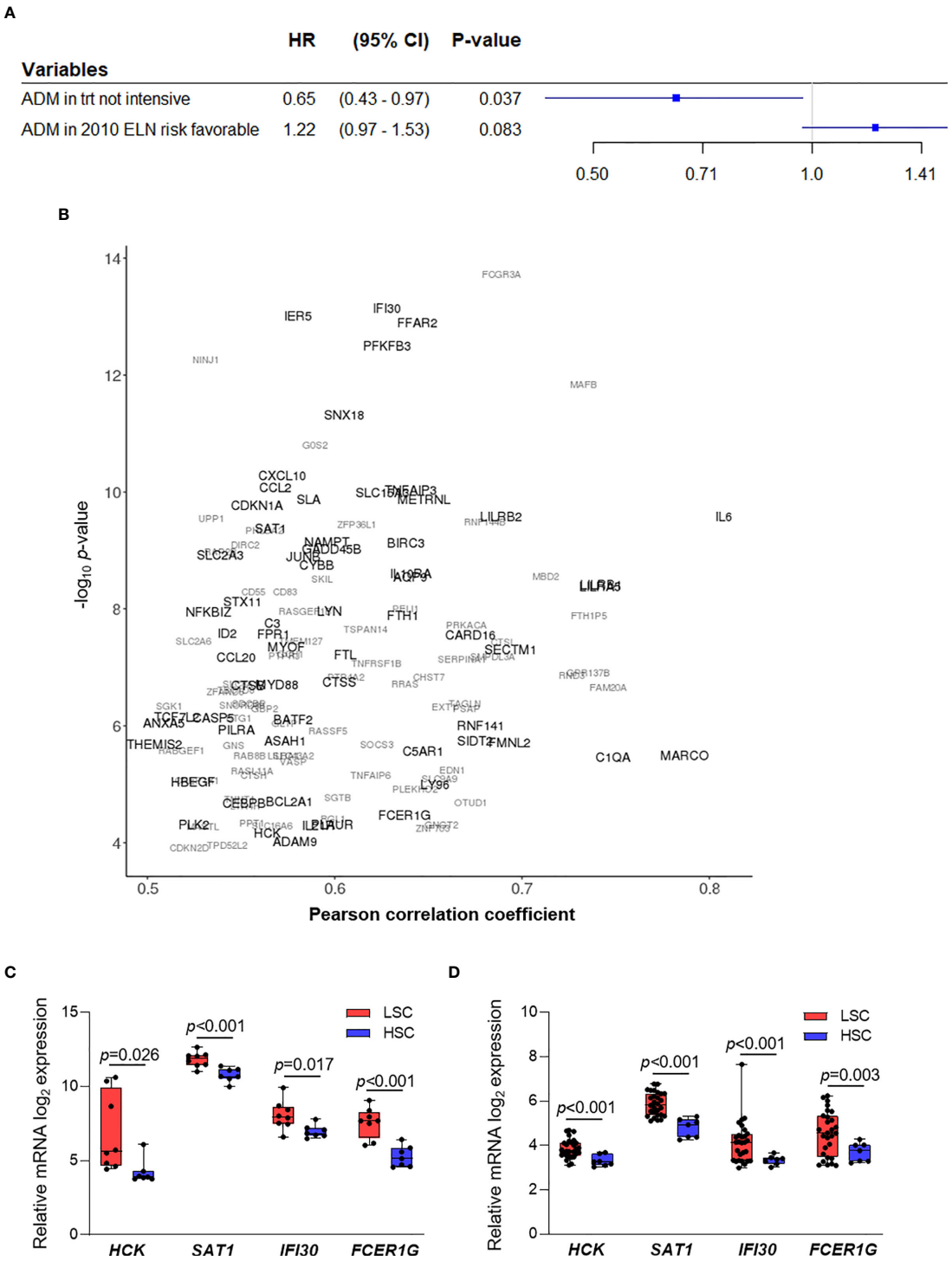

FIGURE 3 | *ADM* prognostic role and co-expressed genes in AML. **(A)** Results from two separate Cox regression models within the subgroup with 2010 ELN favorable risk (adjusting for age, n = 214) and within the subgroup receiving a not-intensive treatment (n = 64, HR, Hazard ratio, CI, confidence interval, trt, treatment). **(B)** Correlation analysis between *ADM* expression and the AML transcriptome across bone marrow samples from five AML datasets (GSE6891, GSE13159, Beat AML, TCGA-LAML, NGS-PTL). Genes showing an absolute value of Pearson correlation coefficient ≥0.50 and a *p* value ≤0.05 in at least two cohorts were reported. Genes are represented according to the weighted arithmetic mean of the correlation coefficient and *p* value across the datasets. The scatter plot was generated with the R package ggplot2 (48) (version 3.3.1). **(C)** Transcriptional analysis of *ADM* co-expressed genes in LSC compared with HSC in the GSE24006 and **(D)** in the GSE117090 datasets (fold change ≥1.5 and *p* ≤0.05 were set as cut off). The boxes extend from minimum to maximum values, each individual value is plotted and the line represents the median value.

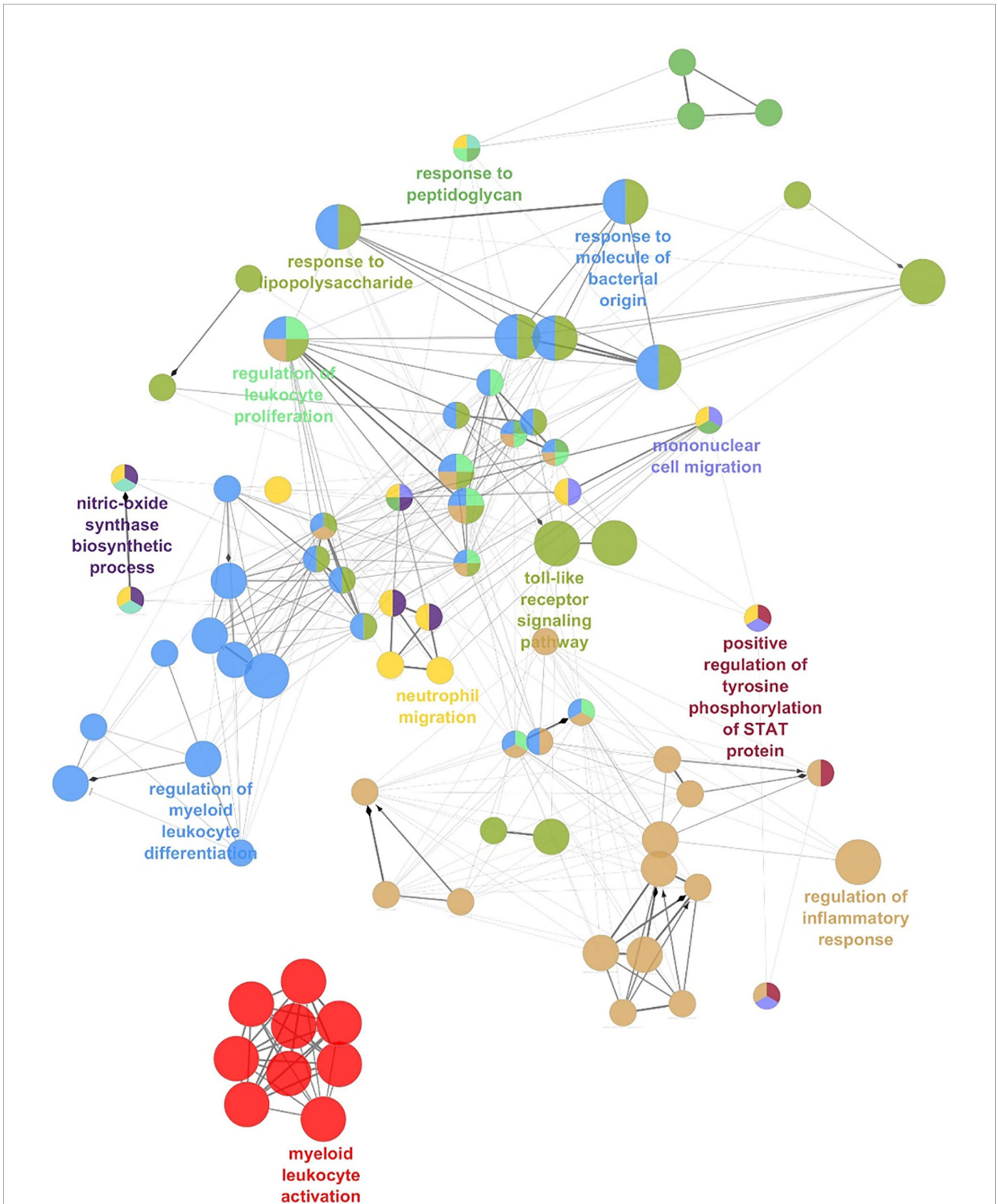

FIGURE 4 | The network of *ADM* co-expressed genes in AML. Network analysis of the Gene Ontology Biological Processes pathways enriched by *ADM* co-expressed genes in AML (ClueGO). Colors indicate functionally-related pathways; one representative pathway for each subnetwork is specified.

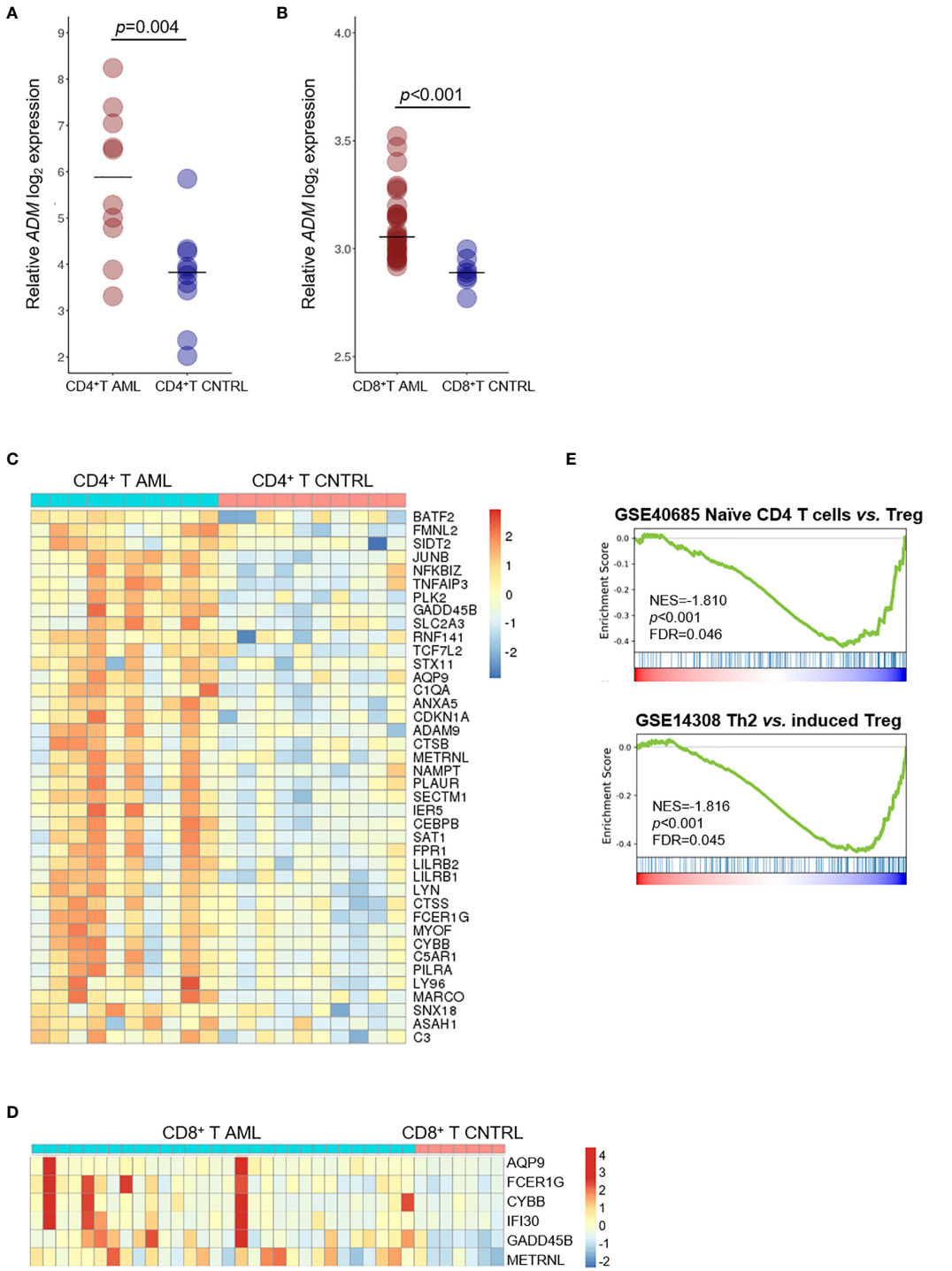

FIGURE 5 | *ADM* is overexpressed in the T cell compartment of AML patients and associates with a tolerogenic gene signature. **(A)** Comparison of *ADM* levels between $CD4^+$ T cells from AML patients and healthy subjects (GSE14924) and **(B)** between $CD8^+$ T cells from AML patients and healthy subjects (GSE117090). Scatter plots were generated with the R package ggplot2 (48) (version 3.3.1). Each dot indicates one sample and the bar represents the median value (CNTRL: healthy subjects). **(C)** Heatmap of *ADM* co-expressed genes that are differentially expressed between $CD4^+$ or **(D)** $CD8^+$ T lymphocytes isolated from AML patients and from healthy subjects. Columns represent patients/subjects. Data were standardized through a z-score transformation. Color changes within a row indicate expression levels relative to the mean and rescaled on the transcript standard deviation. Genes are grouped according to average linkage hierarchical clustering. Heatmaps were built with R package pheatmap (64) (version 1.0.12). **(E)** GSEA of $CD4^+$ T cells from AML patients compared with healthy subjects showing the enrichment of tolerance signatures (NES, normalized enrichment score, FDR, false discovery rate; Th2, T-helper 2, Treg, regulatory T cells).

mutational status. Indeed, *FLT3*-ITD or *NPM1*-mutated cases displayed lower *ADM* levels compared with the wild-type ones and the expression was particularly low when the two alterations co-occurred. Several lines of evidence may explain this observation. First, two tyrosine kinases, namely *LYN* and *HCK*, show a positive correlation with *ADM*, suggesting alternative ways of signaling activation. Moreover, *ADM* is co-expressed with *SLAP*, that binds to FLT3 and modulates receptor stability and downstream signaling (77), likely favoring its activation even in the absence of the internal tandem duplication. Regarding *NPM1*-mutated AML, an inflammatory transcriptional program, characterized by enrichment of genes belonging to IFN-γ response, IL6 signaling and complement cascade (78) has been already associated with this genomic subgroup, and PRDM16 upregulation contributes to it (79). Functional studies on AML genomic subtypes will clarify in the future the role of ADM in specific leukemic cell contexts, thus overcoming the limitation of the currently available studies that analyzed generic AML models. Moreover, some of the identified associations and ADM function in AML cells under the pressure of not-intensive treatment regimens (e.g. hypomethylating agents), deserve further validation and investigation.

Our data suggest that the *ADM*-related transcriptional network has a role in cell proliferation, it negatively regulates apoptosis and, remarkably, it is involved in the inflammatory response. Moreover, some of the *ADM* co-expressed genes are already known for their leukemia-related role, including the anti-apoptotic gene *BIRC3*, the signaling molecules *HCK*, *LYN* (tyrosine kinases), *SLA* (Src kinase-like-adapter protein) and *PLAUR* (urokinase plasminogen activator surface receptor), the transcriptional regulators *TCF7L2* (WNT pathway) and *ID2*, the metabolism-related genes *FTH1*, *FTL* (ferritin heavy and light chain, respectively), *PFKFB3* (glycolytic regulator), *NAMPT* (NAD biosynthesis pathway), *SLC15A3* (solute carriers transporting histidine) and *FFAR2* (free fatty acid receptor). Among *ADM* interacting genes, *EDN1*, that mediates VEGF-C-induced proliferation and chemoresistance in AML (80), showed a positive correlation with *ADM* expression. Several co-expressed genes and enriched pathways point towards an AML inflammatory phenotype, characterized by expression of *IL6*, *IL10RA*, *CXCL10*, *THEMIS2*, *TNFAIP3*, *LILRA5*, *LILRB2*. *ADM* was also upregulated in the $CD4^+$ and $CD8^+$ T cell subsets from AML patients compared with healthy controls and *ADM* correlating genes that were identified in AML, participate in a signature of immune tolerance in $CD4^+$ T cells. We could not perform the correlation analysis on the $CD4^+$ and $CD8^+$ T cells due to the low number of samples, which would have hampered data significance and robustness.

In our analysis, none of the genes belonging to the ADM receptor complex (CALCRL, RAMP2, RAMP3) showed a correlation with endogenous *ADM* expression. However, it has been recently reported that CALCRL, the receptor of ADM and CGRP, is also overexpressed in LSC and its genomic ablation impaired the clonogenic capacity of AML cell lines (50) and the frequency of chemotherapy-resistant cells able to initiate leukemia relapse in preclinical models (81). In contrast to *ADM*, CALCRL was highly expressed in *NPM1*-mutated cases also carrying the *FLT3*-ITD (50). This difference reinforces the notion that the receptor expression is not controlled by the basal ADM levels, rather by changes in the extracellular ADM availability (22). We can therefore hypothesize an intrinsic capacity of leukemic cells to respond to ADM-mediated microenvironmental and self-stimulation, as also supported by the high level of *ADM* expression observed in MSC and osteoclasts.

Overall, our results suggest multiple biological roles of ADM in AML. Indeed, it may support LSC and may be involved in the maintenance of a leukemic cell inflammatory phenotype *via* autocrine and paracrine signaling, thus contributing to drug resistance and relapse. Moreover, ADM may exert an anti-inflammatory action when released in the blood and may promote immune tolerance by direct expression in the $CD4^+$ T cell subset and by uptake from the tumor microenvironment, as indicated by data from murine models of autoimmune disorders (63). This evidence, along with the observation that an antagonistic ADM peptide induced differentiation of leukemic cell lines (22), suggest that targeting ADM may carry therapeutic potentials in AML. However, given the pleiotropic effects of ADM, a therapeutic strategy to deplete it may have serious side effects and toxicities. Therefore, encapsulated formulations aimed to deliver ADM neutralizing antibodies in targeted cells may be required. Alternatively, combination strategies blocking the *ADM*-related network (e.g. HCK, LYN, NAMPT inhibitors) may be investigated for their effect on AML cases expressing high *ADM* levels.

DATA AVAILABILITY STATEMENT

TThe NGS-PTL gene expression array AML dataset is available in the Gene Expression Omnibus repository under the accession number GSE161532.

ETHICS STATEMENT

The studies involving human participants were reviewed and approved by Comitato Etico Indipendente di Area Vasta Emilia Centro (CE-AVEC), Bologna, Italy, and Comitato Etico della Romagna (CEROM), Meldola (FC), Italy. The patients provided their written informed consent to participate in this study.

AUTHOR CONTRIBUTIONS

GS designed the research, analyzed the data and wrote the manuscript. DA and EF analyzed transcriptomic data and prepared the figures. EP performed statistical analysis and revised the manuscript. SV and AS analyzed the data and revised the manuscript. AP, MGh, AF, VR, AA, and EO performed experiments. RL and MC helped in data

interpretation. CP, CC, and MC provided patients' specimens and data. GM supported the study design and data interpretation. MGo designed the research, analyzed the data and revised the manuscript. All authors contributed to the article and approved the submitted version.

FUNDING

This study was supported by TrevisoAIL.

ACKNOWLEDGMENTS

We thank the HOVON study group for sharing clinical data.

SUPPLEMENTARY MATERIAL

The Supplementary Material for this article can be found online at: https://www.frontiersin.org/articles/10.3389/fonc.2021.684396/full#supplementary-material

REFERENCES

1. Kitamura K, Kangawa K, Kawamoto M, Ichiki Y, Nakamura S, Matsuo H, et al. Adrenomedullin: A Novel Hypotensive Peptide Isolated From Human Pheochromocytoma. *Biochem Biophys Res Commun* (1993) 192:553–60. doi: 10.1006/bbrc.1993.1451
2. McLatchie LM, Fraser NJ, Main MJ, Wise A, Brown J, Thompson N, et al. RAMPS Regulate the Transport and Ligand Specificity of the Calcitonin-Receptor-Like Receptor. *Nature* (1998) 393:333–9. doi: 10.1038/30666
3. Schönauer R, Els-Heindl S, Beck-Sickinger AG. Adrenomedullin – New Perspectives of a Potent Peptide Hormone. *J Pept Sci* (2017) 23:472–85. doi: 10.1002/psc.2953
4. Nuki C, Kawasaki H, Kitamura K, Takenaga M, Kangawa K, Eto T, et al. Vasodilator Effect of Adrenomedullin and Calcitonin Gene-Related Peptide Receptors in Rat Mesenteric Vascular Beds. *Biochem Biophys Res Commun* (1993) 196:245–51. doi: 10.1006/bbrc.1993.2241
5. Nikitenko LL, MacKenzie IZ, Rees MCP, Bicknell R. Adrenomedullin Is an Autocrine Regulator of Endothelial Growth in Human Endometrium. *Mol Hum Reprod* (2000) 6:811–9. doi: 10.1093/molehr/6.9.811
6. Miyashita K, Itoh H, Sawada N, Fukunaga Y, Sone M, Yamahara K, et al. Adrenomedullin Promotes Proliferation and Migration of Cultured Endothelial Cells. *Hypertens Res* (2003) 26:S93–8. doi: 10.1291/hypres.26.S93
7. Uzan B, Ea H-K, Launay J-M, Garel J-M, Champy R, Cressent M, et al. A Critical Role for Adrenomedullin-Calcitonin Receptor-Like Receptor in Regulating Rheumatoid Fibroblast-Like Synoviocyte Apoptosis. *J Immunol* (2006) 176:5548–58. doi: 10.4049/jimmunol.176.9.5548
8. Uzan B, Villemin A, Garel JM, Cressent M. Adrenomedullin Is Anti-Apoptotic in Osteoblasts Through CGRP1 Receptors and MEK-ERK Pathway. *J Cell Physiol* (2008) 215:122–8. doi: 10.1002/jcp.21294
9. Hinson JP, Kapas S, Smith DM. Adrenomedullin, a Multifunctional Regulatory Peptide. *Endocr Rev* (2000) 21:138–67. doi: 10.1210/er.21.2.138
10. Allaker RP, Grosvenor PW, McAnerney DC, Sheehan BE, Srikanta BH, Pell K, et al. Mechanisms of Adrenomedullin Antimicrobial Action. *Peptides* (2006) 27:661–6. doi: 10.1016/j.peptides.2005.09.003
11. Sugo S, Minamino N, Shoji H, Kangawa K, Kitamura K, Eto T, et al. Interleukin-1, Tumor Necrosis Factor and Lipopolysaccharide Additively Stimulate Production of Adrenomedullin in Vascular Smooth Muscle Cells. *Biochem Biophys Res Commun* (1995) 207:25–32. doi: 10.1006/bbrc.1995.1148
12. Ishimitsu T, Kojima M, Kangawa K, Hino J, Matsuoka H, Kitamura K, et al. Genomic Structure of Human Adrenomedullin Gene. *Biochem Biophys Res Commun* (1994) 203:631–9. doi: 10.1006/bbrc.1994.2229
13. Wu R, Zhou M, Wang P. Adrenomedullin and Adrenomedullin Binding Protein-1 Downregulate TNF-Alpha in Macrophage Cell Line and Rat Kupffer Cells. *Regul Pept* (2003) 112:19–26. doi: 10.1016/S0167-0115(03)00018-1
14. Fukuda K, Tsukada H, Oya M, Onomura M, Kodama M, Nakamura H, et al. Adrenomedullin Promotes Epithelial Restitution of Rat and Human Gastric Mucosa in Vitro. *Peptides* (1999) 20:127–32. doi: 10.1016/S0196-9781(98)00146-6
15. Ashizuka S, Kita T, Inatsu H, Kitamura K. Adrenomedullin: A Novel Therapy for Intractable Ulcerative Colitis. *Inflammation Bowel Dis* (2013) 19:E26–7. doi: 10.1002/ibd.22891
16. Hojo Y, Ikeda U, Ohya K, Ichida M, Kario K, Takahashi M, et al. Interaction Between Monocytes and Vascular Endothelial Cells Induces Adrenomedullin Production. *Atherosclerosis* (2001) 155:381–7. doi: 10.1016/S0021-9150(00)00607-9
17. Kubo A, Minamino N, Isumi Y, Kangawa K, Dohi K, Matsuo H. Adrenomedullin Production Is Correlated With Differentiation in Human Leukemia Cell Lines and Peripheral Blood Monocytes. *FEBS Lett* (1998) 426:233–7. doi: 10.1016/S0014-5793(98)00349-4
18. Del Pup L, Belloni AS, Carraro G, De Angeli S, Parnigotto PP, Nussdorfer GG. Adrenomedullin Is Expressed in Cord Blood Hematopoietic Cells and Stimulates Their Clonal Growth. *Int J Mol Med* (2003) 11:157–60. doi: 10.3892/ijmm.11.2.157
19. De Angeli S, Del Pup L, Febas E, Conconi MT, Tommasini M, Di Liddo R, et al. Adrenomedullin and Endothelin-1 Stimulate in Vitro Expansion of Cord Blood Hematopoietic Stem Cells. *Int J Mol Med* (2004) 14:1083–6. doi: 10.3892/ijmm.14.6.1083
20. Chute JP, Muramoto GG, Dressman HK, Wolfe G, Chao NJ, Lin S. Molecular Profile and Partial Functional Analysis of Novel Endothelial Cell-Derived Growth Factors That Regulate Hematopoiesis. *Stem Cells* (2006) 24:1315–27. doi: 10.1634/stemcells.2005-0029
21. Larráyoz IM, Martínez-Herrero S, García-Sanmartín J, Ochoa-Callejero L, Martínez A. Adrenomedullin and Tumour Microenvironment. *J Transl Med* (2014) 12:339–53. doi: 10.1186/s12967-014-0339-2
22. Di Liddo R, Bridi D, Gottardi M, De Angeli S, Grandi C, Tasso A, et al. Adrenomedullin in the Growth Modulation and Differentiation of Acute Myeloid Leukemia Cells. *Int J Oncol* (2016) 48:1659–69. doi: 10.3892/ijo.2016.3370
23. Nakayama M, Takahashi K, Kitamuro T, Murakami O, Shirato K, Shibahara S. Transcriptional Control of Adrenomedullin Induction by Phorbol Ester in Human Monocytic Leukemia Cells. *Eur J Biochem* (2000) 267:3559–66. doi: 10.1046/j.1432-1327.2000.01384.x
24. Stunnenberg HG, Abrignani S, Adams D, de Almeida M, Altucci L, Amin V, et al. The International Human Epigenome Consortium: A Blueprint for Scientific Collaboration and Discovery. *Cell* (2016) 167:1145–9. doi: 10.1016/j.cell.2016.11.007
25. Schwarzer A, Emmrich S, Schmidt F, Beck D, Ng M, Reimer C, et al. The Non-Coding RNA Landscape of Human Hematopoiesis and Leukemia. *Nat Commun* (2017) 8:218–34. doi: 10.1038/s41467-017-00212-4
26. Novershtern N, Subramanian A, Lawton LN, Mak RH, Haining WN, McConkey ME, et al. Densely Interconnected Transcriptional Circuits Control Cell States in Human Hematopoiesis. *Cell* (2011) 144:296–309. doi: 10.1016/j.cell.2011.01.004
27. Gentles AJ, Plevritis SK, Majeti R, Alizadeh AA. Association of a Leukemic Stem Cell Gene Expression Signature With Clinical Outcomes in Acute Myeloid Leukemia. *JAMA - J Am Med Assoc* (2010) 304:2706–15. doi: 10.1001/jama.2010.1862
28. Jung N, Dai B, Gentles AJ, Majeti R, Feinberg AP. An LSC Epigenetic Signature Is Largely Mutation Independent and Implicates the HOXA Cluster In AML Pathogenesis. *Nat Commun* (2015) 6:8489–500. doi: 10.1038/ncomms9489
29. Lux S, Blätte TJ, Gillissen B, Richter A, Cocciardi S, Skambraks S, et al. Deregulated Expression of Circular Rnas in Acute Myeloid Leukemia. *Blood Adv* (2021) 5:1490–503. doi: 10.1182/bloodadvances.2020003230
30. Radpour R, Riether C, Simillion C, Höpner S, Bruggmann R, Ochsenbein AF. CD8+ T Cells Expand Stem and Progenitor Cells in Favorable But Not

Adverse Risk Acute Myeloid Leukemia. *Leukemia* (2019) 33:2379–92. doi: 10.1038/s41375-019-0441-9
31. Le Dieu R, Taussig DC, Ramsay AG, Mitter R, Miraki-Moud F, Fatah R, et al. Peripheral Blood T Cells in Acute Myeloid Leukemia (AML) Patients At Diagnosis Have Abnormal Phenotype and Genotype and Form Defective Immune Synapses With AML Blasts. *Blood* (2009) 114:3909–16. doi: 10.1182/blood-2009-02-206946
32. Wouters BJ, Löwenberg B, Erpelinck-Verschueren CAJ, Van Putten WLJ, Valk PJM, Delwel R. Double CEBPA Mutations, But Not Single CEBPA Mutations, Define a Subgroup of Acute Myeloid Leukemia With a Distinctive Gene Expression Profile That Is Uniquely Associated With a Favorable Outcome. *Blood* (2009) 113:3088–91. doi: 10.1182/blood-2008-09-179895
33. Verhaak RGW, Wouters BJ, Erpelinck CAJ, Abbas S, Beverloo HB, Lugthart S, et al. Prediction of Molecular Subtypes in Acute Myeloid Leukemia Based on Gene Expression Profiling. *Haematologica* (2009) 94:131–4. doi: 10.3324/haematol.13299
34. Kohlmann A, Kipps TJ, Rassenti LZ, Downing JR, Shurtleff SA, Mills KI, et al. An International Standardization Programme Towards the Application of Gene Expression Profiling in Routine Leukaemia Diagnostics: The Microarray Innovations in Leukemia Study Prephase. *Br J Haematol* (2008) 142:802–7. doi: 10.1111/j.1365-2141.2008.07261.x
35. Simonetti G, Padella A, do Valle IF, Fontana MC, Fonzi E, Bruno S, et al. Aneuploid Acute Myeloid Leukemia Exhibits a Signature of Genomic Alterations in the Cell Cycle and Protein Degradation Machinery. *Cancer* (2018) 125:712–25. doi: 10.1002/cncr.31837
36. Salvestrini V, Ciciarello M, Pensato V, Simonetti G, Laginestra MA, Bruno S, et al. Denatonium as a Bitter Taste Receptor Agonist Modifies Transcriptomic Profile and Functions of Acute Myeloid Leukemia Cells. *Front Oncol* (2020) 10:1225. doi: 10.3389/fonc.2020.01225
37. Tyner JW, Tognon CE, Bottomly D, Wilmot B, Kurtz SE, Savage SL, et al. Functional Genomic Landscape of Acute Myeloid Leukaemia. *Nature* (2018) 562:526–31. doi: 10.1038/s41586-018-0623-z
38. The Cancer Genome Atlas. Genomic and Epigenomic Landscapes of Adult De Novo Acute Myeloid Leukemia the Cancer Genome Atlas Research Network. *N Engl J Med* (2013) 368:2059–74. doi: 10.1056/NEJMoa1301689
39. Li B, Dewey CN. RSEM: Accurate Transcript Quantification From RNA-Seq Data With or Without a Reference Genome. *BMC Bioinf* (2011) 12:323–38. doi: 10.1186/1471-2105-12-323
40. Robinson MD, McCarthy DJ, Smyth GK. Edger: A Bioconductor Package for Differential Expression Analysis of Digital Gene Expression Data. *Bioinformatics* (2009) 26:139–40. doi: 10.1093/bioinformatics/btp616
41. Love MI, Huber W, Anders S. Moderated Estimation of Fold Change and Dispersion for RNA-Seq Data With Deseq2. *Genome Biol* (2014) 15:550–70. doi: 10.1186/s13059-014-0550-8
42. R Core Team 2019. R: A Language and Environment for Statistical Computing. *R Found Stat Comput Vienna Austria* (2019). http://www.R-project.org/.
43. van Rossum G, Drake FL. *Python 3 Reference Manual* (2009).
44. Virtanen P, Gommers R, Oliphant TE, Haberland M, Reddy T, Cournapeau D, et al. Scipy 1.0: Fundamental Algorithms for Scientific Computing in Python. *Nat Methods* (2020) 17:261–72. doi: 10.1038/s41592-019-0686-2
45. Kuleshov MV, Jones MR, Rouillard AD, Fernandez NF, Duan Q, Wang Z, et al. Enrichr: A Comprehensive Gene Set Enrichment Analysis Web Server 2016 Update. *Nucleic Acids Res* (2016) 44:W90–7. doi: 10.1093/nar/gkw377
46. Subramanian A, Tamayo P, Mootha VK, Mukherjee S, Ebert BL, Gillette MA, et al. Gene Set Enrichment Analysis: A Knowledge-Based Approach for Interpreting Genome-Wide Expression Profiles. *Proc Natl Acad Sci USA* (2005) 102:15545–50. doi: 10.1073/pnas.0506580102
47. Zwiener I, Frisch B, Binder H. Transforming RNA-Seq Data to Improve the Performance of Prognostic Gene Signatures. *PloS One* (2014) 9:e85150–62. doi: 10.1371/journal.pone.0085150
48. Ginestet C. Ggplot2: Elegant Graphics for Data Analysis. *J R Stat Soc Ser A* (2011) 174:245–6. doi: 10.1111/j.1467-985X.2010.00676_9.x
49. Nakayama M, Takahashi K, Murakami O, Murakami H, Sasano H, Shirato K, et al. Adrenomedullin in Monocytes and Macrophages: Possible Involvement of Macrophage-Derived Adrenomedullin in Atherogenesis. *Clin Sci* (1999) 97:247–51. doi: 10.1042/CS19990108
50. Angenendt L, Bormann E, Pabst C, Alla V, Görlich D, Braun L, et al. The Neuropeptide Receptor Calcitonin Receptor-Like (CALCRL) Is a Potential Therapeutic Target in Acute Myeloid Leukemia. *Leukemia* (2019) 33:2830–41. doi: 10.1038/s41375-019-0505-x
51. Ou Y, Wang SJ, Li D, Chu B, Gu W. Activation of SAT1 Engages Polyamine Metabolism With P53-Mediated Ferroptotic Responses. *Proc Natl Acad Sci USA* (2016) 113:E6806–12. doi: 10.1073/pnas.1607152113
52. Zhang H, Nakauchi Y, Köhnke T, Stafford M, Bottomly D, Thomas R, et al. Integrated Analysis of Patient Samples Identifies Biomarkers for Venetoclax Efficacy and Combination Strategies in Acute Myeloid Leukemia. *Nat Cancer* (2020) 1:826–39. doi: 10.1038/s43018-020-0103-x
53. Bisaillon R, Moison C, Thiollier C, Krosl J, Bordeleau ME, Lehnertz B, et al. Genetic Characterization of ABT-199 Sensitivity in Human AML. *Leukemia* (2020) 34:63–74. doi: 10.1038/s41375-019-0485-x
54. Nakamura S, Nagata Y, Tan L, Takemura T, Shibata K, Fujie M, et al. Transcriptional Repression of Cdc25B by IER5 Inhibits the Proliferation of Leukemic Progenitor Cells Through NF-YB and P300 in Acute Myeloid Leukemia. *PloS One* (2011) 6:e28011–25. doi: 10.1371/journal.pone.0028011
55. Dos Santos C, Demur C, Bardet V, Prade-Houdellier N, Payrastre B, Récher C. A Critical Role for Lyn in Acute Myeloid Leukemia. *Blood* (2008) 111:2269–79. doi: 10.1182/blood-2007-04-082099
56. Dos Santos C, Mcdonald T, Ho YW, Liu H, Lin A, Forman SJ, et al. The Src and C-Kit Kinase Inhibitor Dasatinib Enhances P53-Mediated Targeting of Human Acute Myeloid Leukemia Stem Cells by Chemotherapeutic Agents. *Blood* (2013) 122:1900–13. doi: 10.1182/blood-2012-11-466425
57. Roversi FM, Pericole FV, Machado-Neto JA, da Silva Santos Duarte A, Longhini AL, Corrocher FA, et al. Hematopoietic Cell Kinase (HCK) Is a Potential Therapeutic Target for Dysplastic and Leukemic Cells Due to Integration of Erythropoietin/PI3K Pathway and Regulation of Erythropoiesis: HCK in Erythropoietin/PI3K Pathway. *Biochim Biophys Acta - Mol Basis Dis* (2017) 1863:450–61. doi: 10.1016/j.bbadis.2016.11.013
58. Advani AS, Cooper B, Visconte V, Elson P, Chan R, Carew J, et al. A Phase I/II Trial of MEC (Mitoxantrone, Etoposide, Cytarabine) in Combination With Ixazomib for Relapsed Refractory Acute Myeloid Leukemia. *Clin Cancer Res* (2019) 25:4231–37. doi: 10.1158/1078-0432.CCR-18-3886
59. Liang Y, Yu B, Chen J, Wu H, Xu Y, Yang B, et al. Thymic Stromal Lymphopoietin Epigenetically Upregulates Fc Receptor Γ Subunit–Related Receptors on Antigen-Presenting Cells and Induces TH2/TH17 Polarization Through Dectin-2. *J Allergy Clin Immunol* (2019) 144:1025–35. doi: 10.1016/j.jaci.2019.06.011
60. Makino Y, Nakamura H, Ikeda E, Ohnuma K, Yamauchi K, Yabe Y, et al. Hypoxia-Inducible Factor Regulates Survival of Antigen Receptor-Driven T Cells. *J Immunol* (2003) 171:6534–40. doi: 10.4049/jimmunol.171.12.6534
61. Rullé S, Ah Kioon MD, Asensio C, Mussard J, Ea HK, Boissier MC, et al. Adrenomedullin, a Neuropeptide With Immunoregulatory Properties Induces Semi-Mature Tolerogenic Dendritic Cells. *Immunology* (2012) 136:252–64. doi: 10.1111/j.1365-2567.2012.03577.x
62. Pedreño M, Morell M, Robledo G, Souza-Moreira L, Forte-Lago I, Caro M, et al. Adrenomedullin Protects From Experimental Autoimmune Encephalomyelitis At Multiple Levels. *Brain Behav Immun* (2014) 37:152–63. doi: 10.1016/j.bbi.2013.11.021
63. Gonzalez-Rey E, Chorny A, O'Valle F, Delgado M. Adrenomedullin Protects From Experimental Arthritis by Down-Regulating Inflammation and Th1 Response and Inducing Regulatory T Cells. *Am J Pathol* (2007) 170:263–71. doi: 10.2353/ajpath.2007.060596
64. Kolde R. Package 'Pheatmap'. *Bioconductor* (2012), 1–6. https://mran.microsoft.com/snapshot/2017-09-01/web/packages/pheatmap/pheatmap.pdf.
65. Bollinger AL, Bollinger T, Rupp J, Shima K, Gross N, Padayachy L, et al. Annexin V Expression on CD4+ T Cells With Regulatory Function. *Immunology* (2020) 159:205–20. doi: 10.1111/imm.13140
66. Katagiri T, Yamazaki S, Fukui Y, Aoki K, Yagita H, Nishina T, et al. Junb Plays a Crucial Role in Development of Regulatory T Cells by Promoting IL-2 Signaling. *Mucosal Immunol* (2019) 12:1104–17. doi: 10.1038/s41385-019-0182-0
67. Price JG, Idoyaga J, Salmon H, Hogstad B, Bigarella CL, Ghaffari S, et al. CDKN1A Regulates Langerhans Cell Survival and Promotes Treg Cell Generation Upon Exposure to Ionizing Irradiation. *Nat Immunol* (2015) 16:1060–8. doi: 10.1038/ni.3270

68. Lee K, Won HY, Bae MA, Hong JH, Hwang ES. Spontaneous and Aging-Dependent Development of Arthritis in NADPH Oxidase 2 Deficiency Through Altered Differentiation of CD11b+ and Th/Treg Cells. *Proc Natl Acad Sci USA* (2011) 108:9548–53. doi: 10.1073/pnas.1012645108
69. MaruYama T, Kobayashi S, Ogasawara K, Yoshimura A, Chen W, Muta T. Control of IFN-Γ Production and Regulatory Function by the Inducible Nuclear Protein Iκb-Zeta in T Cells. *J Leukoc Biol* (2015) 98:385–93. doi: 10.1189/jlb.2a0814-384r
70. Dai X, Ma W, He XJ, Jha RK. Elevated Expression of Adrenomedullin Is Correlated With Prognosis and Disease Severity in Osteosarcoma. *Med Oncol* (2013) 30:347. doi: 10.1007/s12032-012-0347-0
71. Park SC, Yoon JH, Lee JH, Yu SJ, Myung SJ, Kim W, et al. Hypoxia-Inducible Adrenomedullin Accelerates Hepatocellular Carcinoma Cell Growth. *Cancer Lett* (2008) 271:314–22. doi: 10.1016/j.canlet.2008.06.019
72. Nakata T, Seki N, Miwa S, Kobayashi A, Soeda J, Nimura Y, et al. Identification of Genes Associated With Multiple Nodules in Hepatocellular Carcinoma Using Cdna Microarray: Multicentric Occurrence or Intrahepatic Metastasis? *Hepatogastroenterology* (2008) 55:865–72.
73. Deville JL, Bartoli C, Berenguer C, Fernandez-Sauze S, Kaafarani I, Delfino C, et al. Expression and Role of Adrenomedullin in Renal Tumors and Value of Its Mrna Levels as Prognostic Factor in Clear-Cell Renal Carcinoma. *Int J Cancer* (2009) 125:2307–15. doi: 10.1002/ijc.24568
74. Uemura M, Yamamoto H, Takemasa I, Mimori K, Mizushima T, Ikeda M, et al. Hypoxia-Inducible Adrenomedullin in Colorectal Cancer. *Anticancer Res* (2011) 31:507–14.
75. Rocchi P, Boudouresque F, Zamora AJ, Muracciole X, Lechevallier E, Martin PM, et al. Expression of Adrenomedullin and Peptide Amidation Activity in Human Prostate Cancer and in Human Prostate Cancer Cell Lines. *Cancer Res* (2001) 61:1196–206.
76. Ouafik L, Sauze S, Boudouresque F, Chinot O, Delfino C, Fina F, et al. Neutralization of Adrenomedullin Inhibits the Growth of Human Glioblastoma Cell Lines in Vitro and Suppresses Tumor Xenograft Growth in Vivo. *Am J Pathol* (2002) 160:1279–92. doi: 10.1016/S0002-9440(10)62555-2
77. Kazi JU, Rönnstrand L. Src-Like Adaptor Protein (SLAP) Binds to the Receptor Tyrosine Kinase Flt3 and Modulates Receptor Stability and Downstream Signaling. *PloS One* (2012) 7:e53509–16. doi: 10.1371/journal.pone.0053509
78. Tripodo C, Burocchi A, Piccaluga PP, Chiodoni C, Portararo P, Cappetti B, et al. Persistent Immune Stimulation Exacerbates Genetically Driven Myeloproliferative Disorders Via Stromal Remodeling. *Cancer Res* (2017) 77:3685–99. doi: 10.1158/0008-5472.CAN-17-1098
79. Corrigan DJ, Luchsinger LL, De Almeida MJ, Williams LJ, Strikoudis A, Snoeck HW. PRDM16 Isoforms Differentially Regulate Normal and Leukemic Hematopoiesis and Inflammatory Gene Signature. *J Clin Invest* (2018) 128:3250–64. doi: 10.1172/JCI99862
80. Hua KT, Lee WJ, Yang SF, Chen CK, Hsiao M, Ku CC, et al. Vascular Endothelial Growth Factor-C Modulates Proliferation and Chemoresistance in Acute Myeloid Leukemic Cells Through an Endothelin-1-Dependent Induction of Cyclooxygenase-2. *Biochim Biophys Acta - Mol Cell Res* (2014) 1843:387–97. doi: 10.1016/j.bbamcr.2013.10.015
81. Larrue C, Guiraud N, Mouchel PL, Dubois M, Farge T, Gotanègre M, et al. Adrenomedullin-CALCRL Axis Controls Relapse-Initiating Drug Tolerant Acute Myeloid Leukemia Cells. *Nat Commun* (2021) 12:422–36. doi: 10.1038/s41467-020-20717-9

Conflict of Interest: The authors declare that the research was conducted in the absence of any commercial or financial relationships that could be construed as a potential conflict of interest.

frontiers in Oncology

ORIGINAL RESEARCH
published: 03 June 2021
doi: 10.3389/fonc.2021.685786

Major Differences in Lymphocyte Subpopulations Between Cerebrospinal Fluid and Peripheral Blood in Non-Hodgkin Lymphoma Without Leptomeningeal Involvement: Flow Cytometry Evidence of a Cerebral Lymphatic System

Iole Cordone[1], Serena Masi[1], Diana Giannarelli[1], Alessia Pasquale[1], Laura Conti[1], Stefano Telera[2], Andrea Pace[2], Elena Papa[2], Mirella Marino[1], Paolo de Fabritiis[3] and Andrea Mengarelli[2]*

[1] Department of Research, Advanced Diagnostics and Technological Innovation, IRCCS Regina Elena National Cancer Institute, Rome, Italy, [2] Department of Research and Clinical Oncology, IRCCS Regina Elena National Cancer Institute, Rome, Italy, [3] Hematology, S Eugenio Hospital, ASL Roma2, Tor Vergata University, Rome, Italy

Cerebrospinal fluid (CSF) flow cytometry has a crucial role in the diagnosis of leptomeningeal disease in onco-hematology. This report describes the flow cytometry characterization of 138 CSF samples from patients affected by non-Hodgkin lymphoma, negative for disease infiltration. The aim was to focus on the CSF non-neoplastic population, to compare the cellular composition of the CSF with paired peripheral blood samples and to document the feasibility of flow cytometry in hypocellular samples. Despite the extremely low cell count (1 cell/µl, range 1.0–35) the study was successfully conducted in 95% of the samples. T lymphocytes were the most abundant subset in CSF (77%; range 20–100%) with a predominance of CD4-positive over CD8-positive T cells (CD4/CD8 ratio = 2) together with a minority of monocytes (15%; range 0–70%). No B cells were identified in 90% of samples. Of relevance, a normal, non-clonal B-cell population was documented in 5/7 (71%) patients with primary central nervous system lymphoma at diagnosis ($p<0.0001$), suggesting a possible involvement of blood-brain barrier cell permeability in the pathogenesis of cerebral B-cell lymphomas. The highly significant differences between CSF and paired peripheral blood lymphoid phenotype ($p<0.0001$) confirms the existence of an active mechanism of lymphoid migration through the meninges.

Keywords: cerebrospinal fluid, lymphocytes, flow cytometry, NHL, cerebral lymphatic system

OPEN ACCESS

Edited by:
Alessandro Isidori, AORMN Hospital, Italy

Reviewed by:
Roberta Rudà, University Hospital of the City of Health and Science of Turin, Italy
Silvia Bellesi, Fondazione Policlinico Universitario A. Gemelli IRCCS, Italy

****Correspondence:***
Iole Cordone
iole.cordone@ifo.gov.it

Specialty section:
This article was submitted to Hematologic Malignancies, a section of the journal Frontiers in Oncology

Received: *25 March 2021*
Accepted: *22 April 2021*
Published: *03 June 2021*

Citation:
Cordone I, Masi S, Giannarelli D, Pasquale A, Conti L, Telera S, Pace A, Papa E, Marino M, de Fabritiis P and Mengarelli A (2021) Major Differences in Lymphocyte Subpopulations Between Cerebrospinal Fluid and Peripheral Blood in Non-Hodgkin Lymphoma Without Leptomeningeal Involvement: Flow Cytometry Evidence of a Cerebral Lymphatic System. Front. Oncol. 11:685786. doi: 10.3389/fonc.2021.685786

INTRODUCTION

Neoplastic meningitis is a dramatic complication in cancer patients and the diagnosis of leptomeningeal metastasis represents one of the greatest challenges in neuro-oncology. Cerebrospinal fluid (CSF) analysis has a key role in routine clinical practice however conventional cytology, the gold standard for cell type identification, has considerable limitations regarding sensitivity and specificity, with a reported false-negative rate of up to 40% (1, 2).

In recent years, several studies have demonstrated that CSF flow cytometry is superior to conventional cytology for detection of CNS involvement in non-Hodgkin lymphomas, acute leukemia and multiple myeloma (3–11). Thereafter, flow cytometry is recognized among the basic elements for the diagnosis of leptomeningeal metastasis in hematologic cancers (12, 13), although the low cell count of CSF samples, combined with the rapidly declining leukocyte viability, makes CSF flow cytometry challenging (14). More recently, flow cytometry application and efficiency in diagnosis of solid tumors leptomeningeal metastasis is gaining more evidence (15–18).

However, cancer cells represent only a proportion, often a minority, of the CSF population in neoplastic meningitis. A significant presence of lymphocytes has been documented, together with floating malignant cells, in CSF samples from patients with non-Hodgkin lymphomas and breast cancer leptomeningeal metastasis (18, 19); an active mechanism of reactive CD8 T-lymphocyte migration has been observed in primary central nervous system lymphomas (PCNSL) of B-cell type (20, 21). These findings suggest an active role of the central nervous system (CNS) lymphatic system in both lymphoid and tumor cells migration into and out of the meninges.

Focusing on non-neoplastic populations, we report here the immunophenotype of the CSF leukocytes of patients affected by non-Hodgkin lymphomas without leptomeningeal involvement. The aim was to document the feasibility of flow cytometry in normal, thereafter, extremely hypocellular samples, to document the immunophenotype of CSF non-neoplastic population in non-Hodgkin lymphoma, to compare the cellular composition of the CSF with paired peripheral blood samples. Moreover, a possible correlation between the CSF lymphocyte subpopulations and diagnosis was evaluated.

MATERIALS AND METHODS

Patients

From March 2010 to December 2015 a cohort of 138 samples with non-Hodgkin lymphoma who underwent diagnostic lumbar puncture according to the routine clinical practice entered the study (22). All PCNSL cases diagnosed until December 2019 were also included. Lymphomas were classified according to the World Health Organization (WHO) classification (23).

All CSF samples were analyzed by cytology and flow cytometry and had no evidence of infiltration. Patients with a positive diagnostic lumbar puncture due to CSF infiltration by pathological cells were excluded from this analysis. The Central Ethical Committee IRCCS Lazio, Section I.F.O. approved this retrospective study. Protocol n° 0009524, July 27th 2020.

CSF Collection and Cell Count

CSF was collected in a tube without any transport medium or anticoagulant and processed within 1 to 3 h to minimize cell loss. To avoid peripheral blood contamination, the first 0.2 to 0.4 ml (four to eight drops) of CSF were discarded before sample collection. A standard cell count was performed using the Turk reagent and a Nageotte chamber. CSF was spun at 1,400 rpm for 5 min, the supernatant fluid was discarded and the cell pellet was suspended in 500 µl of phosphate buffered saline (PBS): 100 µl of cell suspension was used for cytomorphology and 100 µl/tube for the flow cytometric study.

CSF Morphological Evaluation

Cytospins were prepared using a Shandon CytoSpin cytocentrifuge. Morphological examination was performed by expert cytopathologists using May–Grünwald–Giemsa staining. All cases were morphologically negative for CNS localization.

CSF Flow Cytometry Assay and Analysis

CSF samples were processed and stained using a 6-color monoclonal antibodies panel, 5 µl of each, and the "Duo-lyse" program of the Becton Dickinson Bioscience (BDB) Lyse-Wash-Assistant according to the following combinations: tube 1) CD3Fitc (BD Biosciences Cat# 345763, RRID : AB_2811220), CD56Pe (BD Biosciences Cat# 345812, RRID : AB_2629216), CD45PerCP-Cy5.5 (BD Biosciences Cat# 332784, RRID : AB_2868632), CD4PE-Cy7 (BD Biosciences Cat# 348809, RRID : AB_2783789), CD19APC (BD Biosciences Cat# 345791, RRID : AB_2868817) and CD8APC-Cy7 (BD Biosciences Cat# 348813, RRID : AB_2868857); tube 2) CD5Fitc (BD Biosciences Cat# 345781, RRID : AB_2868807), CD10Pe (BD Biosciences Cat# 332776, RRID : AB_2868625), CD45PerCP-Cy5.5, CD2PE-Cy7 (BD Biosciences Cat# 335821, RRID : AB_2868684), CD79bAPC (BD Biosciences Cat# 335834, RRID : AB_2868695) and CD20APC-Cy7 (BD Biosciences Cat# 335829, RRID : AB_2868690); tube 3) anti-Lambda Fitc (BD Biosciences Cat# 347247, RRID : AB_2868845, anti-Kappa Pe (BD Biosciences Cat# 347246, RRID : AB_2868844), CD45PerCP-Cy5.5, CD34PE-Cy7 (BD Biosciences Cat# 348811, RRID : AB_2868855), CD22APC (BD Biosciences Cat# 333145, RRID : AB_2868646) and CD14APC-Cy7 (BD Biosciences Cat# 333951, RRID : AB_2868679). All antibodies were from BDB. Prior to sample acquisition, a flow cell cleaning with FACS flow (for 1 to 2 min run) was performed to avoid any event carry over. The whole volume of sample was acquired and analyzed using the FACSCanto II 2L flow cytometer and the FACSDiva software Version 6.1.3 (BDB). Single-stained cellular controls, BD FACS^{TM} 7-color setup beads and BD FACSDiva CS&T IVD Beads have been used to adjust detector voltage, to set fluorescence compensation and to monitor instrument performance.

Data are presented as the percentage of positive cells evaluated on the CD45-positive population. Lymphocytes were identified by CD45-strong/side scatter (SSC)-low. The CD4 and

CD8 subsets were evaluated as a percentage of CD3-positive T lymphocytes. Monocytes were identified using the CD4-weak or CD14 staining. Neutrophils as CD45/SSC-high. Surface immunoglobulins (Ig) kappa and lambda light chain expression was evaluated on CD22-positive B cells. In agreement with the recommendations for the analysis of rare events, a cluster of 10 events was considered to define a positive result and identify a leukocyte subpopulation (10). Disease infiltration of the CSF was excluded, being negative for the lymphoma-associated phenotype identified by histopathology. We defined as CSF negative all sample negative by cytology and flow cytometry.

The peripheral blood lymphocyte characterization, using the CD3 CD56 CD45 CD4 CD19 and CD8 combination (tube n°1), was conducted in 104 paired cases.

Statistical Analysis

Qualitative items were reported as absolute and percentage counts, while quantitative variables were summarized using mean and standard deviation, median and range. The difference in distribution between CSF and PB lymphoid subpopulations was assessed by Wilcoxon rank-sum test. Association between variables was evaluated with the Spearman's ρ coefficient. The test was two-sided with a *p*-value of <0.05 indicating a statistically significant difference. All statistical analyses were performed using SPSS (version 21.0).

RESULTS

Patients

A cohort of 138 samples from 127 non-Hodgkin lymphoma patients, all negative for CNS disease involvement, entered the study (**Table 1**). Eighty-three patients (65%) were male and median age was 60 years (range 18–84). The lumbar puncture for analysis was performed at diagnosis (n=108), at follow up (n=11), at relapse (n=12), or with progressive disease (n=7).

The study focuses on 107 cases; 24 cases (17%) were not included in analysis due to peripheral blood contamination of the CSF documented by the identification of red blood cells in the cytospin assessed morphologically as well as a population of CD45/SSC high (46%; range 30–89%) positive neutrophils. In seven cases the flow cytometry analysis was not evaluable due to the absence of clustered events.

Immunophenotype of CSF Sample

A median volume of 4.0 ml (range 2.0–12.0) of CSF was available for flow cytometry analysis. The CSF cell count was extremely low (1 cell/μl, range 1.0–35); in 9 cases (8%) the CSF cell count was higher than the normal reference value of 4 cell/μl, with a median value of 22 cells/μl (5.0–35). Despite the low absolute cell number, flow cytometry characterization was successfully conducted in 95% of cases (131/138).

Gating on the CD45-positive population in combination with the side scatter, a median of 384 (range 49–23649; mean 1518 ± 3772) events were acquired and analyzed. A positive correlation was found between the volume (ml) of CSF and the number of events analyzed by flow cytometry (Δ 0.36; $p<0.001$) (**Figure 1**).

TABLE 1 | Diagnostic distribution of 127 non-Hodgkin lymphoma patients who underwent diagnostic lumbar puncture according to the routine clinical practice and were negative for leptomeningeal involvement.

Diagnosis	Number of cases
DLBCL	90
MCL	14
PCNSL	11
FL	5
Anaplastic large cell lymphoma	2
Peripheral T-NHL	2
Burkitt lymphoma	1
LBL	1
T-cell rich B-cell lymphoma	1

DLBCL, diffuse large B-cell lymphoma; MCL, mantle cell lymphoma; PCNSL, primary central nervous system lymphoma; FL, follicular lymphoma; LBL, lymphoblastic lymphoma.

The CSF population was represented by lymphocytes (77%; range 20–100%) together with a minor population of monocytes (CD4-weak or CD14-positive 15%; range 0–70%).

The CSF lymphoid population was represented by CD2 CD3 CD5-positive T cells (94%; range 62–100%) with a prevalence of CD4-positive lymphocytes (CD4/CD8 ratio = 2). A minority of CD56-positive cells were also documented (5%; range 0–47%). No B cells (< 10 clustered events) were identified in 90% of cases (**Table 2**).

In 11 patients a subpopulation of CD19 CD20 CD22 CD79b-positive B lymphocytes (4%; range 1–22%), with a normal/balanced Ig kappa/lambda ratio evaluated on the CD22-positive population, was identified: 5 PCNSL, 5 diffuse large B-cell lymphoma (DLBCL), 1 follicular lymphoma (**Table 3**) (**Figures 2A–C**). All 11 patients were at diagnosis. Non-clonal B lymphocytes were documented in 45.5% (5/11) of PCNSL, in 5.5% (5/90) DLBCL and 1/5 FL cases. Seven PCNSL were at diagnosis and 4 in disease progression;

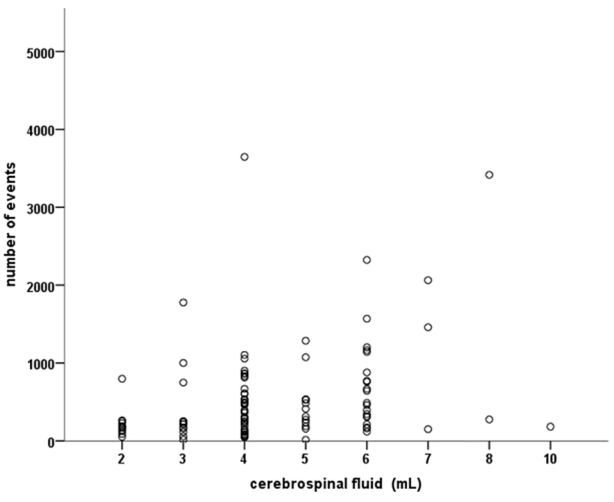

FIGURE 1 | Positive correlation between the ml of cerebrospinal fluid and the number of cells (events) analyzed by flow cytometry (p 0.36; P < 0.001).

TABLE 2 | Cerebrospinal fluid (CSF) and corresponding peripheral blood (PB) lymphoid immunophenotype comparison in 104 non-Hodgkin lymphoma patients negative for leptomeningeal involvement.

%	CSF median	CSF mean	PB median	PB mean	*p* CSF *vs* PB
Lymphocytes	78 (20–100)	71.1 ± 19.8	19 (2–76)	20.9 ± 12.0	<0.0001
CD19+	0 (0–22)	0.4 ± 2.5	4.5 (0–29)	6.5 + 6.6	<0.0001
CD3+	94 (62–100)	92.3 ± 6.9	72 (27–98)	71.8 + 12.7	<0.0001
CD3+/CD4+	65 (3–95)	62.6 ± 16.0	55 (2–86)	53.9 + 14.8	<0.0001
CD3+/CD8+	32 (4–81)	33.5 ± 14.9	38 (15–96)	40.1 + 14.7	<0.0001
CD4/CD8 *ratio*	2 (0.04–23.7)	–	1.4 (0.02–5.7)	–	<0.0001
CD56+	5 (0–47)	7.8 ± 8.9	21(1–61)	23.1 ± 12.8	<0.0001

Values are expresses as a percentage of CD45-positive lymphocytes. Wilcoxon rank-sum test was conducted to evaluate the different distribution between CSF and PB lymphoid subpopulations.

TABLE 3 | Analysis of the cerebrospinal fluid (CSF) and corresponding peripheral blood (PB) lymphocytes of 11/107 non-Hodgkin lymphoma patients, negative for leptomeningeal involvement, where a subpopulation of B cells has been identified at diagnosis by flow cytometry of the CSF sample.

	Diagnosis Case number	PCNSL 1	PCNSL 2	PCNSL 3	PCNSL 4	PCNSL 5	DLBCL 1	DLBCL 2	DLBCL 3	DLBCL 4	DLBCL 5	FL
CSF	**ml of sample**	5	5	5	12	4	4	3.5	7.5	4	7	5.5
	Cell count/ µl	1	16	1	3	35	2	nd	1	5	24	30
	Number of events	412	8583	1286	8285	21000	521	1105	6049	3647	23649	14072
	Lymphocyte %	70	80	77	85	95	80	75	91	90	82	92
	Monocytes %	15	16	17	11	5	19	14	6	8	17	5
	CD2%	86	98	95	95	93	94	95	97	98	76	89
	CD3%	82	91	93	91	90	94	91	97	96	77	87
	CD5%	73	90	95	89	87	90	90	95	96	75	86
	CD56%	3	9	2	4	5	7	7	3	3	1	1
	CD3/CD4%	79	62	47	78	75	66	69	73	79	81	65
	CD3/CD8%	21	32	48	21	24	32	32	25	20	15	31
	T4/T8 ratio	3.7	1.9	1	3.7	3.1	2.1	2.1	2.9	3.9	5.4	2.1
	CD19%	**8**	**1**	**5**	**3**	**6**	**3**	**4**	**1**	**2**	**20**	**12**
	CD20%	**9**	**1**	**4**	**4**	**6**	**4**	**2**	**1**	**3**	**22**	**11**
	CD79b %	**9**	**1**	**3**	**3**	**5**	**4**	**2**	**1**	**3**	**21**	**11**
PB	**Lymphocyte count/ µl**	2300	1120	1350	730	nd	1500	1700	2100	1780	2100	900
	Lymphocyte %	16	11	13	8	nd	20	30	25	37	14	11
	CD3%	71	68	72	88	nd	70	75	64	77	57	64
	CD56%	7	18	13	9	nd	21	11	28	7	55	16
	CD3/CD4%	62	64	40	62	nd	64	54	47	65	38	66
	CD3/CD8%	36	33	55	34	nd	31	45	44	32	60	33
	T4/T8 ratio	1.7	1.9	0.7	1.8	nd	2.0	1.2	1.1	2.0	0.6	2
	CD19%	22	13	17	9	nd	12	11	9	11	2	21

PCNSL, primary central nervous system lymphoma; DLBCL, diffuse large B-cell lymphoma; FL, follicular lymphoma; nd, not done.
The bold value highlights the percentage of B cells, whose relevance is described in the text.

normal B cells were present in 5/7 (71%) PCNSL at diagnosis, identifying a significant correlation between a non-clonal B-cell subpopulation in the CSF and a diagnosis of cerebral B-cell lymphoma ($p<0.0001$).

Immunophenotype of Peripheral Blood Lymphocytes

The peripheral blood lymphocyte subset was evaluated in 104 cases (97%) and compared to the corresponding CSF lymphoid subpopulations. The absolute number of lymphocytes was 1100 cell/µl (range 70–3300), the median percentage was 19% (range 2–76). The analysis documented a population of CD3-positive cells (72%, range 27–98) with a CD4/CD8 ratio of 1.4, CD56-positive (21%; range 1–61) and CD19-positive (5%; range 0–29) lymphocytes. A different distribution of CD3 CD56 and CD19 lymphoid subpopulations was observed between CSF and corresponding peripheral blood samples ($p<0.0001$) (**Table 2**) (**Figure 3**).

DISCUSSION

Leptomeningeal metastasis represents one of the greatest challenges in neuro-oncology and CSF is one of the most promising diagnostic tissues utilized in routine clinical practice (13, 24). In addition to cytology, the diagnostic use of flow cytometry is strongly recommended for CSF samples of patients clinically suspected of neoplastic meningitis (12). This report describes the flow cytometry characterization of 138 CSF samples of non-Hodgkin lymphoma patients who underwent diagnostic lumbar puncture according to the routine clinical

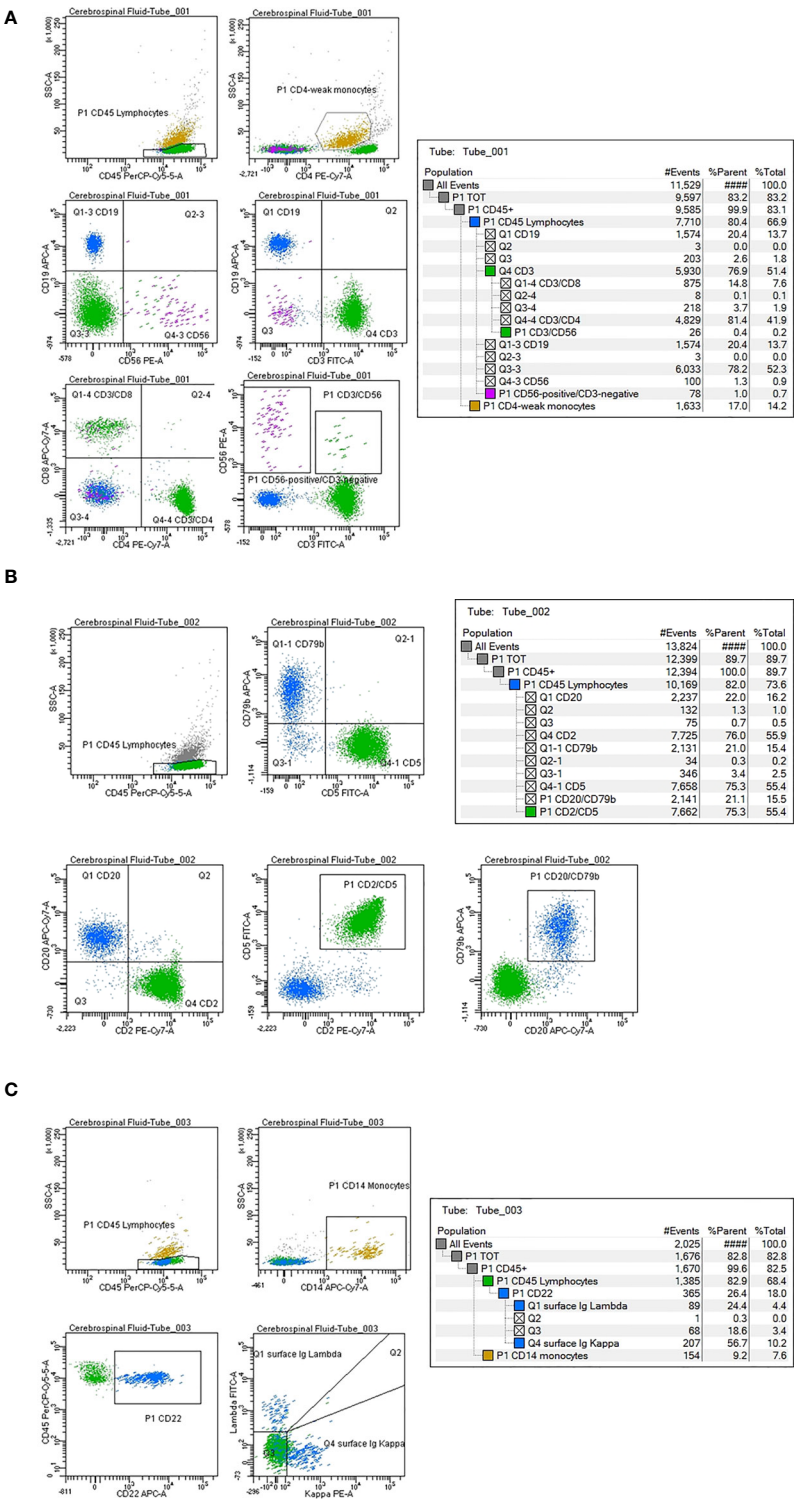

FIGURE 2 | Cerebrospinal fluid (CSF) flow cytometry characterization in a case of diffuse large B-cell lymphoma negative for disease infiltration. Cell count: 24 cells/μl. The CSF lymphocyte immunophenotype is reported as percentage of positive cells within the lymphoid population, identified as CD45-strong/low SSC. **(A)** Tube number 1: Green color has been utilized to mark CD3 CD4 CD8-positive T lymphocytes; purple for CD56-positive cells, blue for CD19-positive B lymphocytes and dark yellow for CD4-weak monocytes. **(B)** Tube number 2: Green color has been utilized to mark CD2 CD5-positive T lymphocytes; blue for CD79b CD20-positive B cells. **(C)** Tube number 3: Blue color has been utilized to mark CD22-positive B lymphocytes. The Ig light chain expression shows a normal kappa/lambda ratio. Dark yellow marks CD14-positive monocytes.

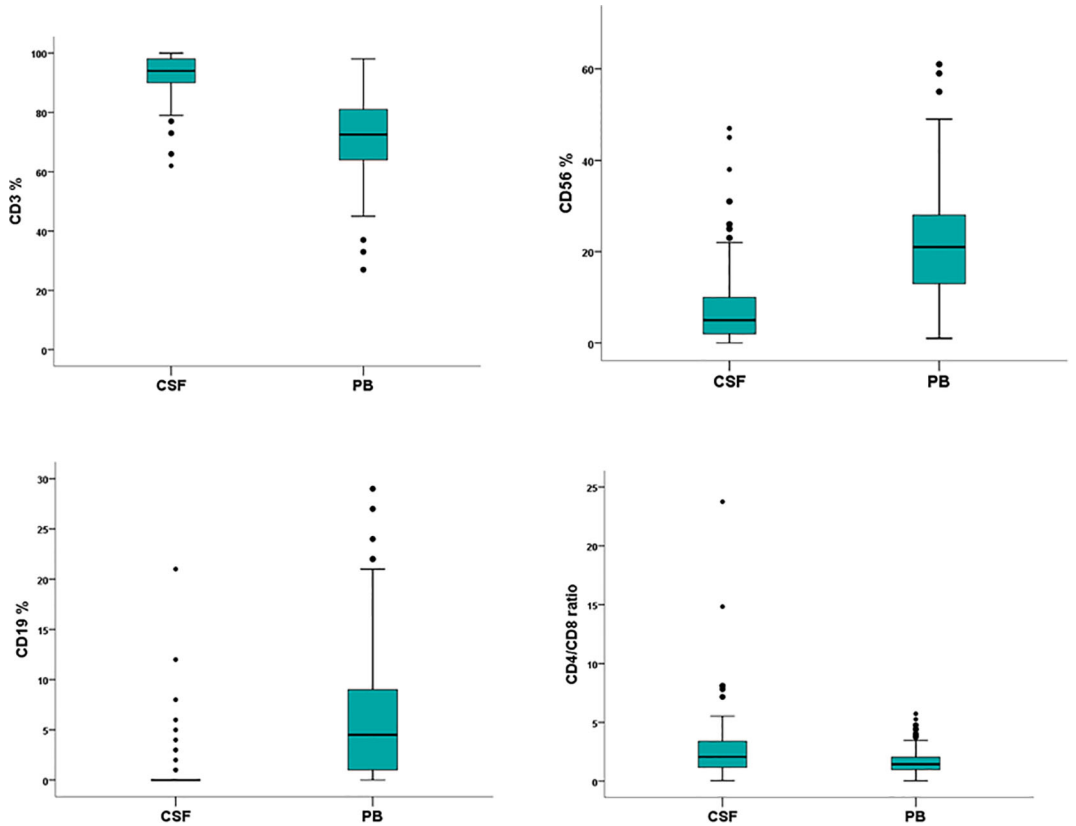

FIGURE 3 | Flow cytometry characterization of cerebrospinal fluid (CSF) and peripheral blood (PB) lymphocytes in 107 non-Hodgkin lymphoma patients negative for leptomeningeal involvement. Wilcoxon rank-sum test documents a significant different distribution between CSF and PB lymphoid subpopulations.

practice and who were negative for disease infiltration. Knowledge of normal values is essential for diagnostic and research interpretation and, to the best of our knowledge, this is the first, single-institution, report on the flow cytometry characterization of CSF non-neoplastic leukocytes in a large cohort of onco-hematology patients.

The normal cell count of the CSF in adults is up to 4 cells/μL and CSF cell count is a diagnostic criterion for leptomeningeal infiltration. The median cellularity in this cohort of patients was extremely low (1 cell/μl, range 1.0–35), but nevertheless flow cytometry was successfully conducted in 95% of cases, confirming its role of a highly sensitive and specific technique for detection of rare cell sub-populations, even in samples with as few as 1 leukocyte per μl of sample. Of note, in 8% of samples (n=9) the CSF cell count was significantly higher than the normal reference value (median 22 cell/μl). In these cases, unequivocal identification of the cell population was mandatory to exclude false positive interpretation: therefore, in addition to cytology, flow cytometry becomes essential. Moreover, the role of an increased number of lymphocytes in the CSF of non-Hodgkin lymphomas patients deserves to be investigated.

High sensitivity has been reported utilizing a volume of 2.0 ml of CSF for flow cytometry characterization (6). The present study was conducted on a median volume of 4 ml of CSF (≤2 ml being withdrawn in six cases only) with a median of 384 (mean 1518 ± 3772) events analyzed. This number is appreciably higher than the minimum number of events, 10 dots, required for minimal disease identification in CSF flow cytometry (6, 25), confirming the feasibility of comprehensive leukocyte characterization in low volume/low count samples. In this series only 7 cases were not evaluable due to the lack of clustered events. However, cancer cells represent only a proportion, often a minority, of the CSF population in neoplastic meningitis (18, 19, 26). Since there is a positive correlation between the volume of CSF (ml) and the number of events available for flow cytometric analysis (Δ 0.36; $p < 0.001$) and taking into account the potentially extremely low cell count of the CSF, as well as some cell loss related to the staining technique, we recommend the withdrawal of not less than 4 ml of sample to ensure an adequate number of events for a reliable identification of minimally represented sub-populations. Moreover, peripheral blood contamination of the CSF, due to difficulty in the execution of the lumbar puncture, can occur. False positive results represent the major pitfall in all cases with peripheral blood infiltration by leukemic/lymphoma cells and blood contamination of the CSF (author statement manuscript in preparation) (12). Thereafter, discarding the first drops of

sample must represent the reference standard in all CSF samples collected for flow cytometry analysis. Moreover, the different distribution of lymphocyte subsets between CSF and peripheral blood can potentially represent a new, useful tool to discriminate between primary and peripheral blood derived populations, particularly at diagnosis or in neutropenic patients.

Studies conducted on normal CSF observed that the vast majority of leucocytes is represented by central memory T lymphocytes with significantly higher percentage compared to blood. The proportion of CD56-positive cells is low while B cells are almost absent (<1%) (27–30). This indicates a selective recruitment of memory T cells into normal CSF. Our study confirms, in a large cohort of samples, that CSF is a tissue rich in CD2 CD3 CD5-positive T lymphocytes with a predominance of CD4-positive over CD8-positive T cells (CD4/CD8 ratio = 2), together with a minority of CD56-positive cells in patients with B-cell non-Hodgkin lymphomas negative for leptomeningeal involvement. The presence of normal T cells in the CSF sample represents not only a strong, reliable internal quality control of the technique but also documents a selective recruitment of T-cell into CSF. The CNS is an immunological sanctuary with restricted access and a unique microenvironment however scientific evidences have recently documented that CNS is no longer an immune-privileged site, but rather a virtual secondary lymphoid organ (31, 32). The tumor inflammatory response is involved in both cancer growth inhibitions as well as in cancer invasiveness (33–37). A relevant proportion of infiltrating T lymphocytes and monocytes beside cancer cells has been documented in patient with breast cancer neoplastic meningitis, with a significant difference in the lymphoid immunophenotype between CSF and peripheral blood (18). Likewise, a sub-population of T cells has been identified in CSF samples positive for B non-Hodgkin lymphoma infiltration (7, 19). Moreover, an active mechanism of reactive CD8 T-lymphocyte migration through the blood-brain barrier has been consistently shown in PCNSL (20, 21). In this study, the ratio between CD4/CD8-positive T cells was shifted significantly in favor of CD4-positive T cells in CSF compared to corresponding peripheral blood (ratio = 2 versus ratio=1.4 respectively; $p < 0.0001$). This different distribution documents that the brain barrier actively selects a sub-population of T lymphocytes, supporting the involvement of the meningeal lymphatic network in lymphoid cell migration into the meninges as a potential alternative route to the cardiovascular system. This finding documents the existence of an active mechanism of lymphocyte localization and provides a promising rationale for the investigation of cellular immunotherapy in brain diseases.

B cells were by far the smallest subset in the CSF of this cohort of B non-Hodgkin lymphoma patients without CNS involvement. The number of B cells is hardly above detection limit in normal CSF (27–29). By contrast, in patients with paraneoplastic neurological syndrome CSF B cell counts showed significantly elevated numbers compared to normal control, suggesting that B lymphocytes are recruited to CSF in certain pathological conditions (38). In the present study, sporadic/no B cells (<10 clustered events) were identified in 90% of the samples and represented a minority (4%) of the lymphoid population in eleven cases (**Table 3**). The normal kappa/lambda *ratio*, evaluated on the CD22-positive population, was crucial for reporting the flow cytometry as negative for infiltration by clonal B cells. A possible correlation between the CSF lymphocyte subpopulations and diagnosis was evaluated. A normal, non-clonal B-cell subpopulation was identified at diagnosis in 71% (5/7) CSF samples of patients with PCNSL ($p < 0.0001$). In contrast with its low frequency in normal CSF and systemic non-Hodgkin lymphomas, the identification of a subpopulation of B cells in the CSF samples of PCNSL cases raises the question of a possible role of blood-brain barrier cell permeability in the pathogenesis of cerebral B-cell lymphomas. Due to the small number of PCNSL cases evaluated, validation on a larger cohort of patients is warranted to confirm this finding and to investigate the role of the CSF B cells in the pathogenesis and diagnosis of the B-cell lymphomas of the brain. A small clonal B-cell population has been described in the CSF of patients with B-cell lymphoproliferative disorders and multiple sclerosis suggesting that this finding is not diagnostic of clinically significant involvement of the CNS by lymphoid malignancy (39, 40). Although a larger prospective study with a long follow-up is required to validate this finding, the identification of a minority of clonal B cells by flow cytometry at diagnosis deserves a careful clinical and instrumental evaluation and more definitive evidence of CNS lymphoid malignancy before a potentially toxic treatment is given (41).

Finally, after (CD4-positive) T lymphocytes, monocytes represent the second most common leukocyte population of the CSF (15%; range 0–70%). Origin and turnover of this medium-size population, well represented in the CSF, is still largely unexplored. The role of monocytes regarding the CNS cellular immune surveillance and their involvement in onco-hematological meningitis deserves in-depth studies and attention.

CONCLUSIONS

The cellular composition of the CSF in non-Hodgkin lymphoma patients negative for leptomeningeal involvement differs profoundly from peripheral blood regarding all major lymphocyte subpopulation. CSF cells are represented by T lymphocytes, in prevalence CD4-positive, and monocytes. B cells are rare and this analysis reveals a possible link with PCNSL. This real-life study confirms the critical role of flow cytometry in routine clinical practice for unequivocal characterization of CSF populations, even in samples with an extremely low cell count. The identification of clusters of normal T cells in the CSF represent a reliable internal quality control of the technique and the significant difference between CSF and paired peripheral blood lymphoid phenotype provides evidence of an independent cerebral lymphatic system. CSF is not an immune-privileged site anymore but a virtual secondary lymphoid organ. An in-depth knowledge of the function and role of the CSF immunological sanctuary is highly needed and has the potential to revolutionize the management of CNS diseases.

DATA AVAILABILITY STATEMENT

The datasets analyzed for this study can be found in the GARRbox (https://gbox.garr.it/garrbox/index.php/s/6BY66PX6n3LaYZP).

ETHICS STATEMENT

The Central Ethical Committee IRCCS Lazio, Section I.F.O. approved this retrospective study. Protocol no 0009524, July 27, 2020. Written informed consent for participation was not required for this study in accordance with the national legislation and the institutional requirements.

AUTHOR CONTRIBUTIONS

IC: designed the study and draft the initial manuscript. SM and APas: flow cytometry studies. IC and SM: analysis, data collection, and quality control. DG: performed the statistical analysis and manuscript revision. MM: histopathological diagnosis and manuscript revision. ST, APac, AM, LC, EP, and PF: patient's clinical management and critical manuscript revision. All authors contributed to the article and approved the submitted version.

ACKNOWLEDGMENTS

IC thanks Federica Falcioni for management support.

REFERENCES

1. Chamberlain MC, Glantz M, Groves MD, Wilson WH. Diagnostic Tools for Neoplastic Meningitis: Detecting Disease, Identifying Patient Risk, and Determining Benefit of Treatment. *Semin Oncol* (2009) 36(4 Suppl 2):S35–45. doi: 10.1053/j.seminoncol.2009.05.005
2. Taillibert S, Chamberlain MC. Leptomeningeal Metastasis. *Handb Clin Neurol* (2018) 149:169–204. doi: 10.1016/B978-0-12-811161-1.00013-X
3. Hegde U, Filie A, Little RF, Janik JE, Grant N, Steinberg SM, et al. High Incidence of Occult Leptomeningeal Disease Detected by Flow Cytometry in Newly Diagnosed Aggressive B-Cell Lymphomas At Risk for Central Nervous System Involvement: The Role of Flow Cytometry Versus Cytology. *Blood* (2005) 105(2):496–502. doi: 10.1182/blood-2004-05-1982
4. Craig FE, Foon KA. Flow Cytometric Immunophenotyping for Hematologic Neoplasms. *Blood* (2008) 111(8):3941–67. doi: 10.1182/blood-2007-11-120535
5. Di Noto R, Scalia G, Abate G, Gorrese M, Pascariello C, Raia M, et al. Critical Role of Multidimensional Flow Cytometry in Detecting Occult Leptomeningeal Disease in Newly Diagnosed Aggressive B-Cell Lymphomas. *Leukemia Res* (2008) 32(8):1196–9. doi: 10.1016/j.leukres.2007.12.016
6. Quijano S, López A, Manuel Sancho J, Panizo C, Debén G, Castilla C. Et Al, Spanish Group for the Study of CNS Disease in NHL (2009). Identification of Leptomeningeal Disease in Aggressive B-Cell Non-Hodgkin's Lymphoma: Improved Sensitivity of Flow Cytometry. *J Clin Oncol Off J Am Soc Clin Oncol* (2009) 27(9):1462–9. doi: 10.1200/JCO.2008.17.7089
7. Ahluwalia MS, Wallace PK, Peereboom DM. Flow Cytometry as a Diagnostic Tool in Lymphomatous or Leukemic Meningitis: Ready for Prime Time? *Cancer* (2012) 118(7):1747–53. doi: 10.1002/cncr.26335
8. Benevolo G, Stacchini A, Spina M, Ferreri AJ, Arras M, Bellio L, et al. Final Results of a Multicenter Trial Addressing Role of CSF Flow Cytometric Analysis in NHL Patients At High Risk for CNS Dissemination. *Blood* (2012) 120(16):3222–8. doi: 10.1182/blood-2012-04-423095
9. Subirá D, Castañón S, Román A, Aceituno E, Jiménez-Garófano C, Jiménez A, et al. Flow Cytometry and the Study of Central Nervous Disease in Patients With Acute Leukaemia. *Br J Haematol* (2001) 112(2):381–4. doi: 10.1046/j.1365-2141.2001.02505.x
10. Del Principe MI, De Bellis E, Gurnari C, Buzzati E, Savi A, Consalvo M, et al. Applications and Efficiency of Flow Cytometry for Leukemia Diagnostics. *Expert Rev Mol Diag* (2019) 19(12):1089–97. doi: 10.1080/14737159.2019.1691918
11. Marchesi F, Masi S, Summa V, Gumenyuk S, Merola R, Orlandi G, et al. Flow Cytometry Characterization in Central Nervous System and Pleural Effusion Multiple Myeloma Infiltration: An Italian National Cancer Institute Experience. *Br J Haematol* (2016) 172(6):980–2. doi: 10.1111/bjh.13549
12. Chamberlain M, Junck L, Brandsma D, Soffietti R, Rudà R, Raizer J, et al. Leptomeningeal Metastases: A RANO Proposal for Response Criteria. *Neuro-oncology* (2017) 19(4):484–92. doi: 10.1093/neuonc/now183
13. Boire A, Brandsma D, Brastianos PK, Le Rhun E, Ahluwalia M, Junck L, et al. Liquid Biopsy in Central Nervous System Metastases: A RANO Review and Proposals for Clinical Applications. *Neuro-oncology* (2019) 21(5):571–84. doi: 10.1093/neuonc/noz012
14. Mlinarić A, Vogrinc Ž, Drenšek Z. Effect of Sample Processing and Time Delay on Cell Count and Chemistry Tests in Cerebrospinal Fluid Collected From Drainage Systems. *Biochem Med* (2018) 28(3):30705. doi: 10.11613/BM.2018.030705
15. Patel AS, Allen JE, Dicker DT, Peters KL, Sheehan JM, Glantz MJ, et al. Identification and Enumeration of Circulating Tumor Cells in the Cerebrospinal Fluid of Breast Cancer Patients With Central Nervous System Metastases. *Oncotarget* (2011) 2(10):752–60. doi: 10.18632/oncotarget.336
16. Le Rhun E, Massin F, Tu Q, Bonneterre J, Bittencourt M, Faure GC. Development of a New Method for Identification and Quantification in Cerebrospinal Fluid of Malignant Cells From Breast Carcinoma Leptomeningeal Metastasis. *BMC Clin Pathol* (2012) 12:21. doi: 10.1186/1472-6890-12-21
17. Stover DG, Parsons HA, Ha G, Freeman SS, Barry WT, Guo H, et al. Association of Cell-Free DNA Tumor Fraction and Somatic Copy Number Alterations With Survival in Metastatic Triple-Negative Breast Cancer. *J Clin Oncol Off J Am Soc Clin Oncol* (2018) 36(6):543–53. doi: 10.1200/JCO.2017.76.0033
18. Cordone I, Masi S, Summa V, Carosi M, Vidiri A, Fabi A, et al. Overexpression of Syndecan-1, MUC-1, and Putative Stem Cell Markers in Breast Cancer Leptomeningeal Metastasis: A Cerebrospinal Fluid Flow Cytometry Study. *Breast Cancer Res: BCR* (2017) 19(1):46. doi: 10.1186/s13058-017-0827-4
19. Masi S, Summa V, Pasquale A, Merola R, Ascani R, Antenucci A, et al. Cerebrospinal Fluid Flow Cytometry for Diagnosis and Monitoring of NHL: A Regina Elena National Cancer Institute Experience. Abstract From XV Sies. *Haematologica* (2018) 103:S117.
20. Cordone I, Masi S, Carosi M, Vidiri A, Marchesi F, Marino M, et al. Brain Stereotactic Biopsy Flow Cytometry for Central Nervous System Lymphoma Characterization: Advantages and Pitfalls. *J Exp Clin Cancer Res: CR* (2016) 35(1):128. doi: 10.1186/s13046-016-0404-1
21. van der Meulen M, Bromberg J, Lam KH, Dammers R, Langerak AW, Doorduijn JK, et al. Flow Cytometry Shows Added Value in Diagnosing Lymphoma in Brain Biopsies. *Cytomet Part B Clin Cytomet* (2018) 94(6):928–34. doi: 10.1002/cyto.b.21641
22. Zelenetz AD, Abramson JS, Advani RH, Andreadis B, Byrd JC, Czuczman MS, et al. NCCN Clinical Practice Guidelines in Oncology: Non-Hodgkin's lymphomas. *J Natl Compr Canc Netw* (2010) 8(3):288–334. doi: 10.6004/jnccn.2010.0021
23. Swerdlow S, Campo E, Harris NL, Jaffe ES, Pileri SA, Stein H, et al. *Who Classification of Tumors of Hematopoietic and Lymphoid Tissues*. Lyon: International Agency for Research on Cancer (IARC) (2017).
24. Sindeeva OA, Verkhovskii RA, Sarimollaoglu M, Afanaseva GA, Fedonnikov AS, Osintsev EY, et al. New Frontiers in Diagnosis and Therapy of Circulating

Tumor Markers in Cerebrospinal Fluid In Vitro and In Vivo. *Cells* (2019) 8 (10):1195. doi: 10.3390/cells8101195
25. Gabelli M, Disarò S, Scarparo P, Francescato S, Zangrando A, Valsecchi MG, et al. Cerebrospinal Fluid Analysis by 8-Color Flow Cytometry in Children With Acute Lymphoblastic Leukemia. *Leukemia Lymphoma* (2019) 60 (11):2825–8. doi: 10.1080/10428194.2019.1602269
26. Sancho JM, Orfao A, Quijano S, García O, Panizo C, Pérez-Ceballos E, et al. Clinical Significance of Occult Cerebrospinal Fluid Involvement Assessed by Flow Cytometry in Non-Hodgkin's Lymphoma Patients At High Risk of Central Nervous System Disease in the Rituximab Era. *Eur J Haematol* (2010) 85(4):321–8. doi: 10.1111/j.1600-0609.2010.01478.x
27. Seehusen DA, Reeves MM, Fomin DA. Cerebrospinal Fluid Analysis. *Am Family Physician* (2003) 68(6):1103–8.
28. Svenningsson A, Andersen O, Edsbagge M, Stemme S. Lymphocyte Phenotype and Subset Distribution in Normal Cerebrospinal Fluid. *J Neuroimmunol* (1995) 63(1):39–46. doi: 10.1016/0165-5728(95)00126-3
29. de Graaf MT, Smitt PA, Luitwieler RL, van Velzen C, van den Broek PD, Kraan J, et al. Central Memory CD4+ T Cells Dominate the Normal Cerebrospinal Fluid. *Cytomet Part B Clin Cytomet* (2011) 80(1):43–50. doi: 10.1002/cyto.b.20542
30. Kleine TO. Cellular Immune Surveillance of Central Nervous System Bypasses Blood-Brain Barrier and Blood-Cerebrospinal-Fluid Barrier: Revealed With the New Marburg Cerebrospinal-Fluid Model in Healthy Humans. *Cytomet Part A J Int Soc Anal Cytol* (2015) 87(3):227–43. doi: 10.1002/cyto.a.22589
31. Louveau A, Smirnov I, Keyes TJ, Eccles JD, Rouhani SJ, Peske JD, et al. Structural and Functional Features of Central Nervous System Lymphatic Vessels. *Nature* (2015) 523(7560):337–41. doi: 10.1038/nature14432
32. Negi N, Das BK. Cns: Not an Immunoprivilaged Site Anymore But a Virtual Secondary Lymphoid Organ. *Int Rev Immunol* (2018) 37(1):57–68. doi: 10.1080/08830185.2017.1357719
33. Disis ML. Immune Regulation of Cancer. *J Clin Oncol Off J Am Soc Clin Oncol* (2010) 28(29):4531–8. doi: 10.1200/JCO.2009.27.2146
34. Chawla A, Alatrash G, Wu Y, Mittendorf EA. Immune Aspects of the Breast Tumor Microenvironment. *Breast Cancer Manage* (2013) 2(3):231–44. doi: 10.2217/bmt.13.15
35. Diakos CI, Charles KA, McMillan DC, Clarke SJ. Cancer-Related Inflammation and Treatment Effectiveness. *Lancet Oncol* (2014) 15(11): e493–503. doi: 10.1016/S1470-2045(14)70263-3
36. Bruno A, Ferlazzo G, Albini A, Noonan DM. A Think Tank of TINK/TANKs: Tumor-Infiltrating/Tumor-Associated Natural Killer Cells in Tumor Progression and Angiogenesis. *J Natl Cancer Inst* (2014) 106(8):dju200. doi: 10.1093/jnci/dju200
37. Zhou W, Bao S. Reciprocal Supportive Interplay Between Glioblastoma and Tumor-Associated Macrophages. *Cancers* (2014) 6(2):723–40. doi: 10.3390/cancers6020723
38. de Graaf M, de Beukelaar J, Bergsma J, Kraan J, van den Bent M, Klimek M, et al. B and T Cell Imbalances in CSF of Patients With Hu-antibody Associated PNS. *J Neuroimmunol* (2008) 195(1-2):164–70. doi: 10.1016/j.jneuroim.2008.01.007
39. Nowakowski GS, Call TG, Morice WG, Kurtin PJ, Cook RJ, Zent CS. Clinical Significance of Monoclonal B Cells in Cerebrospinal Fluid. *Cytomet Part B Clin Cytomet* (2005) 63(1):23–7. doi: 10.1002/cyto.b.20032
40. Greenfield AL, Dandekar R, Ramesh A, Eggers EL, Wu H, Laurent S, et al. Longitudinally Persistent Cerebrospinal Fluid B Cells can Resist Treatment in Multiple Sclerosis. *JCI Insight* (2019) 4(6):e126599. doi: 10.1172/jci.insight.126599
41. Grommes C, Rubenstein JL, DeAngelis LM, Ferreri A, Batchelor TT. Comprehensive Approach to Diagnosis and Treatment of Newly Diagnosed Primary CNS Lymphoma. *Neuro-oncology* (2019) 21(3):296–305. doi: 10.1093/neuonc/noy192

Conflict of Interest: The authors declare that the research was conducted in the absence of any commercial or financial relationships that could be construed as a potential conflict of interest.

frontiers in Oncology

CASE REPORT
published: 29 June 2021
doi: 10.3389/fonc.2021.699886

Case Report: Very Late, Atypical Extra-Medullary Relapse in a Patient With Acute Promyelocytic Leukemia (APL) Rescued With a Transplant-Free Approach

Matteo Molica[1]*, *Carla Mazzone*[1], *Tiziana Ottone*[2], *Pasquale Niscola*[1], *Elisabetta Abruzzese*[1], *Stefano Fratoni*[3], *Maria Teresa Voso*[2] and *Paolo de Fabritiis*[1,2]

[1] Haematology Unit, St. Eugenio Hospital, Rome, Italy, [2] Department of Biomedicine and Prevention, University Tor Vergata, Rome, Italy, [3] Surgical Pathology, Hematopathology Unit, St. Eugenio Hospital, Rome, Italy

OPEN ACCESS

Edited by:
Alessandro Isidori, AORMN Hospital, Italy

Reviewed by:
Hussein A. Abbas, MD Anderson Cancer Center, United States
Leo Ruhnke, University Hospital Carl Gustav Carus Dresden, Germany
Michele Gottardi, Veneto Institute of Oncology (IRCCS), Italy

***Correspondence:**
Matteo Molica
molica@bce.uniroma1.it

Specialty section:
This article was submitted to Hematologic Malignancies, a section of the journal Frontiers in Oncology

Received: 24 April 2021
Accepted: 11 June 2021
Published: 29 June 2021

Citation:
Molica M, Mazzone C, Ottone T, Niscola P, Abruzzese E, Fratoni S, Voso MT and de Fabritiis P (2021) Case Report: Very Late, Atypical Extra-Medullary Relapse in a Patient With Acute Promyelocytic Leukemia (APL) Rescued With a Transplant-Free Approach. Front. Oncol. 11:699886. doi: 10.3389/fonc.2021.699886

Relapses of acute promyelocytic leukemia (APL) beyond 7 years from the first molecular remission are exceptional, and it is unclear whether these relapses represent a new, therapy-related leukemia rather than a delayed relapse of the original leukemic clone. The increase extra-medullary relapses (ER) in the era of all-trans retinoic acid (ATRA) therapy suggests a potential correlation between ATRA therapy and ER, and several potential explanations have been proposed. The gold standard post-remission approach, particularly for patients in late relapse, has not yet been established. The benefit of a transplant approach has been questioned in this setting because continuing ATRA-arsenic trioxide (ATO) might be curative. Here we report on the case of an APL patient who relapsed 9 years after achieving her first molecular complete remission (mCR) and who showed an atypical isolated localization at nodal sites, including the into- and peri-parotid glands. Genomic *PML/RARa* breakpoint analysis detected the same bcr3 *PML/RARa* hybrid gene in DNA purified from bone marrow and lymph nodes, suggesting that the relapse was because of the reemergence of the initial clone. This case shows that APL, treated with ATRA and cytotoxic drugs, may still emerge in extra-medullary sites even after a very prolonged mCR and could be salvaged with an ATO-based protocol, not including a transplant approach.

Keywords: acute promyelocitic leukemia, transplant free approach, bcr3 variant, all-trans retinoic acid and arsenic trioxide combination treatment, very late relapse

CASE REPORT

Late relapses in acute promyelocytic leukemia (APL) patients that occur three or more years from the achievement of complete remission (CR) are very rare, and relapses beyond 7 years from the initial diagnosis are exceptional. A few cases of late APL relapses treated with all-trans retinoic acid (ATRA) in combination with other approaches have been reported (1–10). Most late relapses are the result of the identical immunophenotypic, cytogenetic, and molecular features already present at

diagnosis, suggesting that relapse emerged through the initial leukemic clone (3–5). Approximately 3% to 5% of adult APL presents an extra-medullary relapse (ER) (11, 12). The incidence of ER, which has risen in the era of ATRA therapy, suggests a potential correlation between ATRA therapy and ER (13). Two possible speculative reasons have been contemplated: 1) an increased infiltration of APL leukemic blasts into sanctuary sites because of the effect of ATRA on adhesion molecules and 2) prolonged disease-free survival in treated APL patients (13). However, the main reason is that, in ATRA era, the rate of long-term survivors has increased exponentially, giving far more opportunities to develop late relapses than in the pre-ATRA era. Here we report on the case of an APL patient, treated using the GIMEMA AIDA 2000 protocol, who relapsed 9 years after achieving her first molecular complete remission (mCR) and who showed an atypical presentation at nodal sites into- and peri-parotid gland.

A 43-year-old female was diagnosed with classic APL in March 2011. At diagnosis, peripheral blood count showed WBC 3.6 × 10^9/l with 70% atypical promyelocytes, platelets 15 × 10^9/l, and Hb 12.1 g/dl. The immunophenotypic pattern (CD13+, CD33+, HLA-DR−], karyotypic evaluation [t(15;17) as unique abnormality), and molecular analysis (positivity for *PML/RARa* bcr3) were consistent with APL. The patient was enrolled into the AIDA 2000 protocol and achieved CR following induction with ATRA plus idarubicin (IDA). Molecular remission was achieved after the first consolidation course, and treatment was discontinued in October 2013, after three consolidation cycles and 2 years of maintenance therapy based on oral 6-mercaptopurine (50 mg/m^2) and intramuscular methotrexate (15 mg/m^2) alternating with oral ATRA for 15 days every 3 months. The patient remained in CR^{MRD-} for 9 years. In May 2020, the patient presented with a solid mass in the parotid region: an ultrasound and a computed tomography (CT) scan of the neck showed the presence of four right intra-parotid lymph nodes (maximum diameter 2.5 cm) associated with sub-centimetric peri-parotid, sub-maxillary, and retropharyngeal lymph nodes. The bone marrow was morphologically in CR; however, a molecular relapse of the original bcr3 *PML/RARa* rearrangement was detectable by RT-PCR.

A biopsy of an intra-parotid lymph node was performed. Histopathological examination revealed a lymph node architecture totally effaced by a massive population of atypical promyelocytes with kidney-shaped and/or irregular lobed nuclei,

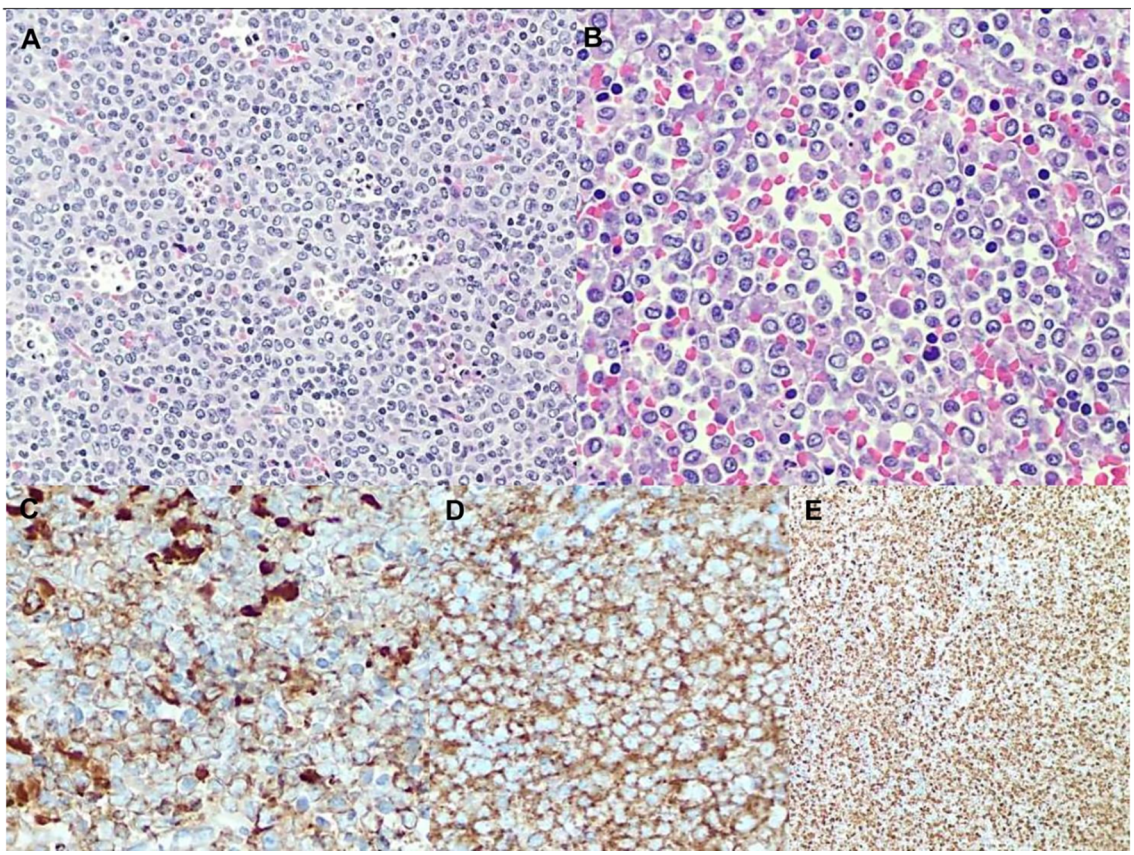

FIGURE 1 | **(A)** low magnification shows a blastic population with diffuse pattern of growth admixed with a lot of tingible body macrophages and apoptotic debris. **(B)** High magnification reveals blastic immature promyelocytes with hypergranular eosinophilic cytoplasm, kidney-shaped or lobed nuclei and prominent central nucleoli. Immunohistochemistry shows a diffuse and strong expression of both MPO **(C)** and CD33 **(D)** along with very high proliferation index Ki67 **(E)**.

prominent central nucleoli, and an eosinophilic cytoplasm that was hypergranulated. Immunohistochemistry revealed a diffuse and strong expression of both MPO and CD33, whereas expression of CD117, CD34, CD68RPGM1, CD14, CD13, CD163, CD56, PAX5, CD3, and large-spectrum cytokeratin AE1/AE3 was absent. Molecular analysis of embedded paraffin tissue showed the presence of the t(15;17) *PML-RARa* fusion gene, confirming the final diagnosis of APL, also defined as a granulocytic sarcoma promyelocytic type, because of its own extramedullary nodal localization (**Figure 1**). To determine the exact chromosomal breakpoint position in the *PML* and *RARa* genes, long-range PCR was performed on DNA samples derived from bone marrow (BM) MNC and the lymph node biopsy. The *PML/RARa* bcr3 isoform was detected using nested real-time polymerase chain reaction (RT-PCR) on the BM sample collected at relapse. DNA extracted from BM-MNC and the lymph node biopsy was also analyzed using long-range PCR. Using different primers combinations, we confirmed the presence of the *PML/RARa* hybrid that was detected in DNA purified from the lymph node sections (**Figure 2**). Sanger sequencing of both PCR products showed the same breakpoints locations in the *PML* and *RARa* genes, at nucleotide position 996 of the PML intron 3 and position 14392 of the *RARa* intron 2 (**Figure 2**). The breakpoint locations were the same as in the original samples harvested at the time of initial APL diagnosis, in 2011.

The patient was treated with an induction treatment based on the following drugs combination: IDA 12 mg/m^2 on days 1 and 3, arsenic trioxide (ATO) 0.15 mg/kg from day 5 to day 28, and ATRA 45 mg/m^2 from day 1 to day 28). A second mCR, assessed by RT-PCR of the *PML/RARa* hybrid, and the complete disappearance of lymph node involvement from a CT-scan were determined after the induction course. According to the radiological response after induction, located radiotherapy on lymph nodes, which was contemplated among potential treatments at relapse, was not performed. ATO and ATRA treatments were continued with three further consolidation courses given at monthly and bi-weekly intervals, respectively. Four doses of intrathecal cytarabine were administered during consolidation. She was closely monitored by RT-PCR throughout the treatment and she will continue to be assessed every two months for at least two years. The patient remains in continuous second mCR until last follow up (May 2021) leading a normal life. To our knowledge, this is one of the latest relapses observed in an APL patient treated with ATRA plus chemotherapy (1, 3, 7). The unusual aspects of this case appear to be due to two main reasons: a relapse after a prolonged period of documented mCR (9 years), and the atypical site of extra-medullary disease. Molecular relapse in this patient was associated with an intra-parotid lymph node involvement, a site infrequently reported in APL relapse and usually present in earlier disease recurrence (3, 14). Genomic *PML/RARa* breakpoint analysis by RT-PCR detected the same bcr3 *PML/RARa* hybrid gene in DNA purified from BM and lymph nodes, suggesting that the relapse was due to reemergence of the initial clone. Whereas central nervous system and skin involvement in APL relapse have been associated with mechanisms mediated by cellular adhesion molecules (CD56, LFA-1, and VLA-4) probably over-expressed in response to ATRA-driven differentiation (15, 16), the issue as to whether ATRA promotes nodal involvement in APL relapses is still unknown. Because patients affected by ATRA syndrome have APL cells that have infiltrated multiple tissues and organs, it has been hypothesized that ATRA could promote the migration of differentiating blasts into several tissues.

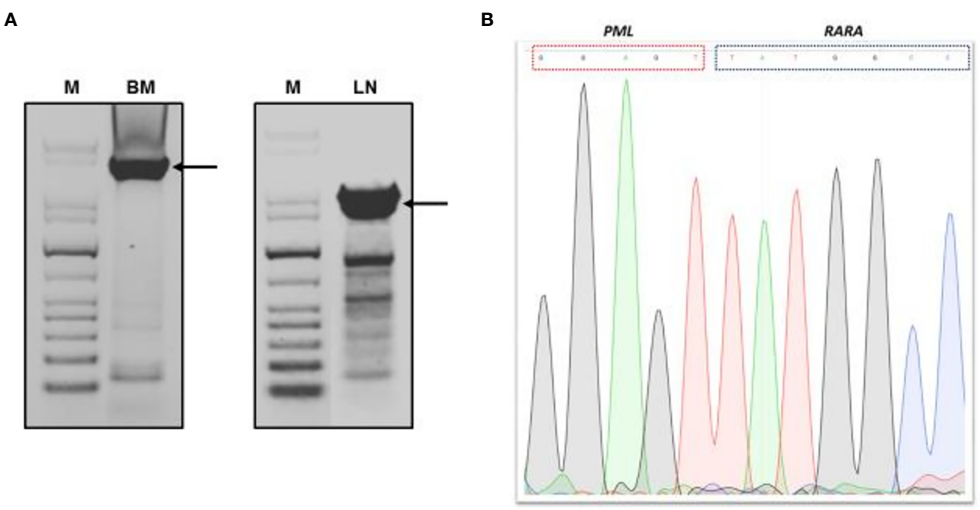

FIGURE 2 | Genomic *PML/RARA* breakpoint analysis by long-range nested PCR. **(A)** Agarose gel electrophoresis of long-range PCR products from bone marrow and lymph node section DNA analysis. **(B)** Sanger sequencing result of long-range PCR product of *PML/RARA* genomic amplification derived from BM analysis. Sequence was aligned to the intronic sequences of *PML* and *RARa* genes. M, GenLadder 1kb DNA Ladder; BM, bone marrow; LN, lymph node. Arrows indicated the long-range PCR products purified from gel.

These blasts could form a reservoir of viable leukemic cells that might later proliferate and result in an extra-medullary recurrence (17, 18). Our patient achieved a second mCR and extra-medullary response after the induction course and three further consolidation courses based on ATO and ATRA combination. Because of the prolonged mCR achieved after the initial treatment, no hematopoietic stem cell transplant (HSCT) option was offered to the patient. The gold standard post-remission approach, especially for late relapse patients, is not yet well established. A registry study of the European Leukemia Net, which analyzed 155 APL relapsed patients showed the efficacy of allogenic and autologous HSCT as a consolidation treatment for patients with early and late relapses who did not achieve a mCR (19).

Based on recent studies (19–23), autologous HSCT should be considered the first choice for eligible patients achieving second molecular remission. However, a recent NCRI report questions the role of transplantation, at least in patients achieving molecular remission with ATO and ATRA who do not have CNS disease at relapse and who have received a full course of consolidation with ATO (24).

However, the benefit of a transplant approach could be questioned in patients relapsing after a very prolonged first CR because continuing ATRA-ATO might in fact be curative. Limited data have been reported for patients who received prolonged ATRA/ATO therapy after a first relapse without a final consolidation with a stem cell transplant. A recent update of 22 patients indicated that only two patients underwent transplant and the rest received additional cycles of ATRA/ATO. The four-year overall survival probability was 85% with a disease-free survival rate of 74%, supporting the potentially curative effect of prolonged ATO treatment especially in patients with a long first mCR (25). In conclusion, this case shows that APL, treated with modern combination therapies including ATRA and cytotoxic drugs, may still emerge in extra-medullary sites even after a very prolonged molecular remission (9 years) and could be salvaged with an ATO-based protocol not including a HSCT.

DATA AVAILABILITY STATEMENT

The original contributions presented in the study are included in the article/supplementary material. Further inquiries can be directed to the corresponding author.

ETHICS STATEMENT

Written informed consent was obtained from the patient for the publication of this case report and the accompanying images.

AUTHOR CONTRIBUTIONS

MM and PF designed the study and wrote the paper. MM, CM, EA, and PN followed the patient. TO and MV performed the molecular studies. SF made histopathological examination. PF supervised the study. All authors contributed to the article and approved the submitted version.

ACKNOWLEDGMENTS

The authors thank Prof. Nathan Tublitz for help in revising the manuscript.

REFERENCES

1. Ferrara F, Selleri C, Mele G, Serio B, Palmieri S, Pocali B, et al. Late Relapse of Acute Promyelocytic Leukemia Treated With All-Trans Retinoic Acid and Chemotherapy: Report of Two Cases. *Ann Hematol* (2004) 83:484–6. doi: 10.1007/s00277-003-0842-7
2. Ebinger M, Schwarze CP, Feuchtinger T, Scheel-Walter HG, Lang P, Hildenbrand S, et al. Long-Term Remission After First-Line Single-Agent Treatment With Arsenic Trioxide of Relapsed Acute Promyelocytic Leukemia in an 8-Year-Old Boy. *Pediatr Hematol Oncol* (2011) 28:334–7. doi: 10.3109/08880018.2010.542557
3. Latagliata R, Carmosino I, Breccia M, Minni A, Testi A, Iorio N, et al. Late Relapses in Acute Promyelocytic Leukaemia. *Acta Haematol* (2007) 117:106–8. doi: 10.1159/000097385
4. Douer D, Zickl LN, Schiffer CA, Appelbaum FR, Feusner JH, Shepherd L, et al. All-Trans Retinoic Acid and Late Relapses in Acute Promyelocytic Leukemia: Very Long Term Follow-Up of the North American Intergroup Study I0129. *Leuk Res* (2013) 37:795–801. doi: 10.1016/j.leukres.2013.03.001
5. Breccia M, Petti MC, Testi AM, Specchia G, Ferrara F, Diverio D, et al. Ear Involvement in Acute Promyelocytic Leukemia at Relapse: A Disease-Associated 'Sanctuary'? *Leukemia* (2002) 16:1127–30. doi: 10.1038/sj.leu.2402497
6. Solano Vercet C, Escudero A, Fernandez-Ranada JM. Meningeal Relapse in Acute Promyelocytic Leukemia. *Acta Haematol* (1982) 70:137– 8. doi: 10.1159/000206708
7. Liso V, Specchia G, Pogliani EM, Palumbo G, Mininni D, Rossi V, et al. Extramedullary Involvement in Patients With Acute Promyelocytic Leukemia: A Report of Seven Cases. *Cancer* (1998) 83:1522–8. doi: 10.1002/(SICI)1097-0142(19981015)83:8<1522::AID-CNCR6>3.0.CO;2-4
8. Kanakura Y, Yonezawa T, Hamaguchi Y, Otsuka A, Matayoshi Y, Kondoh H, et al. Acute Promyelocytic Leukemia With an Intracerebral Mass and Meningeal Involvement After Treatment of Non-Hodgkin's Lymphoma. *Cancer* (1987) 59:94–8. doi: 10.1002/1097-0142(19870101)59:1<94::AID-CNCR2820590121>3.0.CO;2-0
9. Marra R, Storti S, Pagano L, Fioritoni G, Rabitti C, Sica S, et al. Central Nervous System Acute Promyelocytic Leukemia: A Report of Three Cases. *Haematologia* (1989) 22:195– 199.
10. Niazi Z, Molt P, Mittelman A, Arlin ZA, Ahmed T. Leukemic Dermal Infiltrates at Permanent Indwelling Central Venous Catheter Sites. *Cancer* (1991) 68:2281–3. doi: 10.1002/1097-0142(19911115)68:10<2281::AID-CNCR2820681029>3.0.CO;2-I
11. Vega-Ruiz A, Faderl S, Estrov Z, Pierce S, Cortes J, Kantarjian H, et al. Incidence of Extramedullary Disease in Patients With Acute Promyelocytic Leukaemia: A Single-Institution Experience. *Int J Hematol* (2009) 89:489–96. doi: 10.1007/s12185-009-0291-8
12. Pacilli L, Lo Coco F, Ramadan SM, Giannì L, Pingi A, Remotti D, et al. Promyelocytic Sarcoma of the Spine: A Case Report and Review of the Literature. *Adv Hematol* (2010) 2010:137608. doi: 10.1155/2010/137608
13. Testi AM, Moleti ML, Canichella M, Mohamed S, Diverio D, De Propris MS, et al. Very Late Relapse in a Patient With Acute Promyelocytic Leukemia

(APL) Rescued With a Chemotherapy-Free Protocol. *Leuk Lymphoma* (2017) 58(4):999–1001. doi: 10.1080/10428194.2016.1222377
14. Evans GD, Grimwade DJ. Extramedullary Disease in Acute Promyelocytic Leukemia. Leuk. *Lymphoma* (1999) 33(3-4):219–29. doi: 10.3109/10428199909058422
15. Grignani F, Ferrucci PF, Testa U, Talamo G, Fagioli M, Alcalay M, et al. The Acute Promyelocytic Leukemia-Specific PML-RARa Fusion Protein Inhibits Differentiation and Promotes Survival of Myeloid Precursor Cells. *Cell* (1993) 3:423–31. doi: 10.1016/0092-8674(93)80044-F
16. Albano F, Specchia G. Extramedullary Disease in Acute Promyelocytic Leukemia: Two-In-One Disease. *Mediterr J Hematol Infect Dis* (2011) 3(1): e2011066. doi: 10.4084/mjhid.2011.066
17. Raanani P, Shpillberg O, Ben-Bassat I. Extramedullary Disease and Targeted Therapies for Hematological Malignancies—Is the Association Real. *Ann Oncol* (2007) 18:7–12. doi: 10.1093/annonc/mdl129
18. Ko BS, Tang GL, Chen YC, Yao M, Wang CH, Shen MC, et al. Extramedullary Relapse After All-Trans Retinoic Acid Treatment in Acute Promyelocytic Leukemia. The Occurrence of Retinoic Acid Syndrome Is a Risk Factor. *Leukemia* (1999) 13:06–1408. doi: 10.1038/sj.leu.2401495
19. Lengfelder E, Lo Coco F, Ades L, Montesinos P, Grimwade D, Kishore B, et al. Arsenic Trioxide-Based Therapy of Relapsed Acute Promyelocytic Leukemia: Registry Results From the European Leukemianet. *Leukemia* (2015) 29:1084–91. doi: 10.1038/leu.2015.12
20. Yanada M, Tsuzuki M, Fujita H, Fujimaki K, Fujisawa S, Sunami K, et al. Japan Adult Leukemia Study Group. Phase 2 Study of Arsenic Trioxide Followed by Autologous Hematopoietic Cell Transplantation for Relapsed Acute Promyelocytic Leukemia. *Blood* (2013) 121(16):3095–102. doi: 10.1182/blood-2012-11-466862
21. Yanada M, Yano S, Kanamori H, Gotoh M, Emi N, Watakabe K, et al. Autologous Hematopoietic Cell Transplantation for Acute Promyelocytic Leukemia in Second Complete Remission: Outcomes Before and After the Introduction of Arsenic Trioxide. *Leuk Lymphoma* (2017) 58(5):1061–7. doi: 10.1080/10428194.2016.1231406
22. Holter Chakrabarty JL, Rubinger M, Le-Rademacher J, Wang HL, Grigg A, Selby GB, et al. Autologous is Superior to Allogeneic Hematopoietic Cell Transplantation for Acute Promyelocytic Leukemia in Second Complete Remission. *Biol Blood Marrow Transplant* (2014) 20(7):1021–5. doi: 10.1016/j.bbmt.2014.03.025
23. Ganzel C, Mathews V, Alimoghaddam K, Ghavamzadeh A, Kuk D, Devlin S, et al. Autologous Transplant Remains the Preferred Therapy for Relapsed APL in CR2. *Bone Marrow Transplant* (2016) 51(9):1180–3. doi: 10.1038/bmt.2016.96
24. Russell N, Burnett A, Hills R, Betteridge S, Dennis M, Jovanovic J, et al. Ncri AML Working Group. Attenuated Arsenic Trioxide Plus ATRA Therapy for Newly Diagnosed and Relapsed APL: Long-Term Follow-Up of the AML17 Trial. *Blood* (2018) 132(13):1452–4. doi: 10.1182/blood-2018-05-851824
25. Cicconi L, Breccia M, Franceschini L, Latagliata R, Molica M, Divona MD, et al. Prolonged Treatment With Arsenic Trioxide (ATO) and All-Trans-Retinoic Acid (ATRA) for Relapsed Acute Promyelocytic Leukemia Previously Treated With ATRA and Chemotherapy. *Ann Hematol* (2018) 97:1797–802. doi: 10.1007/s00277-018-3400-z

Conflict of Interest: The authors declare that the research was conducted in the absence of any commercial or financial relationships that could be construed as a potential conflict of interest.

frontiers in Oncology

ORIGINAL RESEARCH
published: 04 August 2021
doi: 10.3389/fonc.2021.705627

Decoupling Lineage-Associated Genes in Acute Myeloid Leukemia Reveals Inflammatory and Metabolic Signatures Associated With Outcomes

Hussein A. Abbas[1†], Vakul Mohanty[2†], Ruiping Wang[3†], Yuefan Huang[2,4], Shaoheng Liang[2,5], Feng Wang[3], Jianhua Zhang[3], Yihua Qiu[1], Chenyue W. Hu[1‡], Amina A. Qutub[6‡], Monique Dail[7], Christopher R. Bolen[8], Naval Daver[1], Marina Konopleva[1], Andrew Futreal[3], Ken Chen[2], Linghua Wang[3*] and Steven M. Kornblau[1*]*

[1] Department of Leukemia, The University of Texas MD Anderson Cancer Center, Houston, TX, United States, [2] Department of Bioinformatics and Computational Biology, The University of Texas MD Anderson Cancer Center, Houston, TX, United States, [3] Department of Genomic Medicine, The University of Texas MD Anderson Cancer Center, Houston, TX, United States, [4] Department of Biostatistics & Data Science, School of Public Health, University of Texas Health Science Center at Houston, Houston, TX, United States, [5] Department of Computer Science, Rice University, Houston, TX, United States, [6] Department of Bioengineering, Rice University, Houston, TX, United States, [7] Oncology Biomarker Development, Genentech Inc, South San Francisco, CA, United States, [8] Oncology Bioinformatics, Genentech Inc, South San Francisco, CA, United States

Acute myeloid leukemia (AML) is a heterogeneous disease with variable responses to therapy. Cytogenetic and genomic features are used to classify AML patients into prognostic and treatment groups. However, these molecular characteristics harbor significant patient-to-patient variability and do not fully account for AML heterogeneity. RNA-based classifications have also been applied in AML as an alternative approach, but transcriptomic grouping is strongly associated with AML morphologic lineages. We used a training cohort of newly diagnosed AML patients and conducted unsupervised RNA-based classification after excluding lineage-associated genes. We identified three AML patient groups that have distinct biological pathways associated with outcomes. Enrichment of inflammatory pathways and downregulation of *HOX* pathways were associated with improved outcomes, and this was validated in 2 independent cohorts. We also identified a group of AML patients who harbored high metabolic and mTOR pathway activity, and this was associated with worse clinical outcomes. Using a comprehensive reverse phase protein array, we identified higher mTOR protein expression in the highly metabolic group. We also identified a positive correlation between degree of resistance to venetoclax and mTOR activation in myeloid and lymphoid cell lines. Our approach of integrating RNA, protein, and genomic data

OPEN ACCESS

Edited by:
Alessandro Isidori, AORMN Hospital, Italy

Reviewed by:
Sergio Rutella, Nottingham Trent University, United Kingdom
Antonio Curti, University of Bologna, Italy
Maria Paola Martelli, University of Perugia, Italy

***Correspondence:**
Steven M. Kornblau
skornblau@mdanderson.org
Ken Chen
kchen3@mdanderson.org
Linghua Wang
lwang22@mdanderson.org

[†]These authors have contributed equally to this work

[‡]Present address:
Chenyue W. Hu, Uber Technologies Inc, San Francisco, CA, United States; Amina A. Qutub, Department of Biomedical Engineering, University of Texas San Antonio, San Antonio, TX, United States

Specialty section:
This article was submitted to Hematologic Malignancies, a section of the journal Frontiers in Oncology

Received: *05 May 2021*
Accepted: *07 July 2021*
Published: *04 August 2021*

uncovered lineage-independent AML patient groups that share biologic mechanisms and can inform outcomes independent of commonly used clinical and demographic variables; these groups could be used to guide therapeutic strategies.

Keywords: acute myeloid leukemia, lineage, metabolism, inflammation, multiplatform analysis

INTRODUCTION

Acute myeloid leukemia (AML) is a clinically and morphologically heterogeneous disease with significant variability in treatment responses and outcomes (1–3). Although almost 60-70% of AML patients achieve remission with standard anthracycline (idarubicin or daunorubicin) and cytarabine-based induction chemotherapy, almost 50% of these patients eventually experience relapse within 1 year of diagnosis (2–4). Revealing the underlying biologic processes that contribute to AML heterogeneity and drive outcomes may guide therapeutic strategies.

The French American British (FAB) classification was traditionally used to categorize AML into 8 different morphologic subtypes (M0 to M7) that reflected lineage commitment (2, 5–7). With the advent of cytogenetic and genomic assessments, the European Leukemia Network (ELN) recommendations were widely adopted as it proposed a risk stratification for patients that based on cytogenetics and genomics (2, 8, 9). However, cytogenetic and molecular alterations do not fully account for the heterogeneity of AML because not all patients harbor ELN–pre-defined aberrations (2, 10, 11). Also, there is considerable patient-to-patient variability in response to treatment and clinical outcomes within genomic and ELN subgroups (11). Therefore, there is a need to uncover underlying biologic pathways that are underrepresented in genomic and cytogenetic profiling of AML and may inform outcomes.

To fill this gap, researchers have identified several transcriptomic signatures associated with AML clinical outcomes (10, 12–17). However, RNA-based profiling revealed that this method of grouping AML patients was highly associated with FAB classifications, i.e., related to AML morphology and lineages (15, 16, 18). Yet, the FAB-associated clustering was not accounted for in previous transcriptome-based studies, suggesting that the morphology and lineage of AML were driving patient grouping. Furthermore, although mutations were associated with some transcriptomic-based clustering, there was significant overlap for these mutations in multiple clusters (15, 16). We hypothesized that by decoupling the lineage-related genes from the transcriptomic profiles of AML, we could unmask biologically relevant pathways that are inherent to AML independent of cell of origin and that could inform clinical outcomes. Furthermore, such an approach could identify biologic pathways associated with cluster-specific mutations.

In the current study, we decoupled FAB-associated genes to decipher lineage-independent biologic pathways in 81 newly diagnosed and previously untreated AML patients. We identified distinct biologic AML patient groups and assessed the outcome of patients according to their group membership. To provide further molecular orthogonal characterization of defined groups, we applied a reverse phase protein array (RPPA) in all patient samples and extended panel DNA sequencing in 73 of 81 patients (90%). Using this approach, we identified inflammatory and metabolic pathways associated with outcomes and validated our findings in 2 independent AML cohorts. The findings from this work demonstrate that RNA-based classification could reveal important potentially targetable biologic pathways.

METHODS

Patient Population

A total of 81 newly diagnosed AML patients evaluated at The University of Texas MD Anderson Cancer Center were included in the current study. All patients had bone marrow samples collected and analyzed prior to treatment initiation. Patients provided written informed consent that was approved by the MD Anderson Institutional Review Board. The study was conducted in accordance with the Declaration of Helsinki.

RNA Sequencing and Processing

RNA was isolated and purified from bone marrow mononuclear cells using Qiagen's RNAEasy preparation kits. The purified RNA was used to create cDNA libraries that were assayed using TruSeq (Illumina) RNAAccess. For each sample, 40M 50-bp paired-end reads were sequenced using the Illumina HiSeq sequencer. RNA sequencing (RNA-seq) FASTQ files were processed through FastQC (v0.11.5) and RNA-SeQC (v1.1.8) (1) to generate a series of RNA-seq–related quality control metrics. STAR 2-pass alignment (v2.5.3) (2) was performed with default parameters to generate RNA-seq BAM files. Normalized counts were generated using DESEq2, then $\log_2$-transformed.

Differential Expression and Pathway Analysis

In our cohort and TCGA cohort, gene-level read counts were used to perform differential expression analysis using *DESeq2* (3). The T-statistic from the differential expression analysis was used to perform gene set enrichment analysis (GSEA) using the Bioconductor package *gage* (4), and significantly dysregulated pathways were identified at $q < 0.1$. For the Valk et al. validation cohort, we used single-sample GSEA (ssGSEA) (5, 6) implemented in the Bioconductor package *GSVA* (7) to convert microarray gene expression into pathway activity scores. Pathway activity scores

were compared between groups using the Wilcox Rank Sum test, and p-values were corrected for multiple hypothesis testing using false discovery rate (FDR). Significantly dysregulated pathways were identified at $q < 0.05$. The Hallmark pathways (8) were used in GSEA and ssGSEA.

Unsupervised Clustering Prior to Excluding FAB-Associated Genes

The R package *pheatmap* was used to generate heatmaps and dendrograms for samples from a matrix of variably expressed genes. Euclidian distance and complete clustering were used to perform hierarchical clustering of the data. We used a dynamic tree cutting algorithm implemented in the *cutreeDynamic*() function from the *WGCNA* package (9) to identify optimal clustering of patients. The strength of association between cluster membership and FAB status (M1/M2 and M4/M5) was tested using Fisher's test. Clustering analysis in our dataset was performed using an increasing number of top variably expressed genes (1000, 1500, 2000, 2500, and 3000 genes). Clustering analysis in TCGA cohort was performed as above using the top 1000 variably expressed genes, including only samples with corresponding FAB status (M1/M2 and M4/M5).

Unsupervised Clustering to Identify Patient Clusters Independent of FAB Status

To identify genes with expression associated with FAB status, we excluded genes associated with FAB and lineage commitment. Specifically, for each gene, a p-value was obtained for each of the FAB groups M2, M4, and M5 relative to M1 from the regression analysis. p-values for each of the groups (M2, M4, and M5) were corrected for multiple testing using FDR. A gene's expression was considered associated with FAB status if expression of the gene was significantly different in at least one of the FAB groups M2, M4, and M5 relative to M1 ($q < 0.05$). A total of 4743 genes were found to have expression associated with FAB status. Enrichment of these genes in cell type-specific signatures was quantified using *Enricher (*10, 11). FAB-associated genes were excluded, and the top variably expressed genes (variance > 5, 735 genes) were used to identify clusters (as described above). Three distinct expression clusters were identified using this approach, Group_1, Group_2 and Group_3 (**Figure 1A**)

Survival Analysis

Survival analysis of patient clusters identified from our expression data (**Figures 1D–F**) was performed using multivariant Cox regression implemented in the R package *survival*. First, clinical variables important for survival were identified using univariate Cox regression. The multivariate survival model was built using all variables that were significantly associated with survival in the univariate analysis ($p < 0.05$). Survival analysis reported in **Figures 3A–C** and **Supplementary Figure 4** was performed using the *survminer R* package. p-values for the KM-plots were computed using log-rank test implemented in the function surv_pvalue(). All KM-plots in the study were plotted using the function ggsurplot().

HOX Gene Survival Analysis

Activity of *HOXA* and *HOXB* gene clusters were scored in all datasets using ssGSEA (5, 6) implemented in *GSVA* (7). In each cohort, for each *HOX* gene cluster, the samples were split into 2 groups (the top and bottom 50^{th} percentile) based on the activity scores obtained from ssGSEA. Survival differences between the groups were quantified as described above.

Estimation and Comparison of Metabolic Activity Between Patient Groups

Pathway activity scores were calculated using 91 gene sets, including 85 KEGG (12) metabolic pathways and 5 literature-curated gene sets: glucose deprivation, glycolysis, hypoxia, mTOR, and oxidative phosphorylation. The pathway activity score was calculated using ssGSEA using GSVA (7). Differential activity of pathways among clusters was identified using the Wilcoxon rank-sum test based on each cell's pathway activity scores. p-values were adjusted using the Benjamini-Hochberg method, and the threshold of significance was set to $q < 0.05$.

Foundation Medicine Assay

Samples were submitted to a Clinical Laboratory Improvement Amendments–certified, New York State-accredited, and College of American Pathologists–accredited laboratory (Foundation Medicine, Cambridge, MA) for next-generation sequencing–based genomic profiling. Samples were processed in the protocol defined by hematologic cancers as previously described (13). Briefly, after DNA and RNA extraction from bone marrow aspirate, adaptor-ligated DNA underwent hybrid capture for all coding exons of 465 cancer-related genes. cDNA libraries prepared from RNA underwent hybrid capture for 265 genes known to be rearranged in cancer. Captured libraries were sequenced to a median exon coverage depth of >500× (DNA) or ~3M unique reads (RNA) using Illumina sequencing, and resultant sequences were analyzed for base substitutions, small insertions and deletions (indels), copy number alterations (focal amplifications and homozygous deletions), and gene fusions/rearrangements, as previously described (13, 14). Frequent germline variants from the 1000 Genomes Project (dbSNP142) were removed. To maximize mutation-detection accuracy (sensitivity and specificity) in impure clinical specimens, the test was previously optimized and validated to detect base substitutions at ≥5% mutant allele frequency, indels at ≥10% mutant allele frequency with ≥99% accuracy, and fusions occurring within baited introns/exons with >99% sensitivity (14). Known confirmed somatic alterations deposited in the Catalog of Somatic Mutations in Cancer (COSMIC v62) were called at allele frequencies ≥1% (15). Patients did not provide consent for raw data release. Therefore, associated raw sequence data is not shared. However, variants from a subset of the samples used in this analysis (>18,000) have been deposited in the Genomic Data Commons (accession #phs001179).

Mutational Analysis

Mutation data were binarized to indicate the presence or absence of a mutation. Genes mutated in less than 10% of the samples

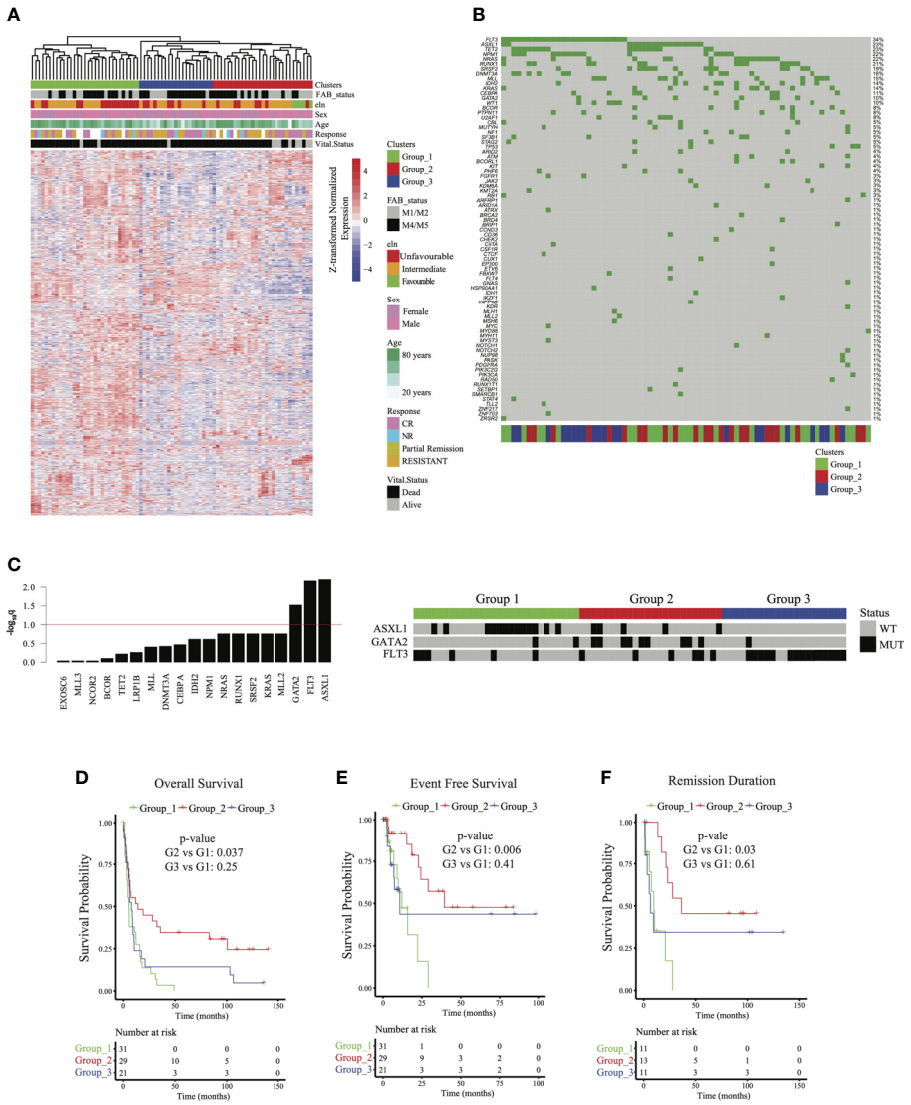

FIGURE 1 | Identifying acute myeloid leukemia patient groups independent of French American British (FAB) classification: **(A)** Clustered gene expression heatmap of top variably expressed genes (variance > 5,735 genes) whose expression was not associated with FAB classification (Fisher p = 0.251). ELN = European Leukemia Network; CR = complete remission. **(B)** Oncoplot of frequently mutated genes in the cohort. **(C)** (**left**) Barplot of $-\log_{10}$ Fisher test q values testing the association of mutations with sample groups. *ASXL1*, *GATA2*, and *FLT3* mutations were associated with groups 1, 2, and 3, respectively (q < 0.1). (**right**) Heatmap showing mutation status of *ASXL1*, *GATA2*, and *FLT3* among patients. WT = wild type; MUT = mutated. **(D)** Overall survival, **(E)** event-free survival, and **(F)** remission duration of patients in groups 1, 2, and 3. p values for **(D–F)** were calculated using a multivariable Cox regression model relative to cluster 1.

were excluded from the analysis. Fisher's test was used to quantify the association between the presence of a gene mutation and cluster membership. p-values were corrected using FDR and mutations significantly associated with a cluster were identified at q < 0.1. Oncoplot was generated using R package *maftools* (16). Gene Mutations that showed significant association with FLT3 mutation were identified using Fisher's test, p-values were corrected for multiple testing using FDR and significant associations were identified at q < 0.1. An odds ratio (OR) > 1 indicates co-occurrence and OR < 1 indicates mutual exclusivity.

Validation Cohorts

Data for the 2 validation datasets TCGA (n= 173) and Valk et al. (n= 293) (17, 18) were downloaded from GEO database (GSE1159) and UCSC Xena (https://xenabrowser.net/datapages/). Clinical data were also available on GEO for the Valk et al. cohort, and from Firehose (https://gdac.broadinstitute.org/) for The Cancer Genome Atlas (TCGA) cohort. To validate survival and pathway patterns observed in Group 2 we performed differential expression analysis between group 2 and groups 1 and 3 combined. Upregulated and downregulated genes were identified as fold-change >2 and

<-2, respectively, at q < 0.05. The activity of these gene sets was scored in each of the validation cohorts using ssGSEA, and each sample was then assigned a score indicating the difference between the activity of the upregulated and downregulated gene sets. In each of the validation cohorts, samples were stratified into 2 groups indicating more Group 2 like (top 50th percentile) and less Group 2 like (bottom 50th percentile). These 2 groups were then used to perform survival analysis as described above. Differential expression between the groups was determined and pathway analysis performed as described above.

Differential Expression of Proteins

RPPA data used in the study were previously published and generated by our group for the cohort of 81 patients (19). To identify differentially expressed proteins between 2 groups, we computed the difference in mean expression of each protein with a p-value using the Wilcoxon rank-sum test. p-values were corrected using FDR. Upregulated and downregulated proteins were identified as difference in mean >75th percentile and <25th percentile, respectively, at q < 0.1.

Cell Line Molecular and Drug Response Data

Cancer cell line drug response data were obtained from Rees et al. (20). The response of each cell to a drug was quantified as the area under the drug response curve (AUC). High AUC indicated poor response and low AUC indicated better response. Protein expression from RPPA for these cell lines was obtained from Cancer Cell Line Encyclopedia (21) using the DepMap portal (https://depmap.org/portal/download/). Correlations between expression data and drug response were computed using Spearman correlation.

RESULTS

Clinical and Demographic Characteristics

A total of 81 newly diagnosed AML patients (58% male and 42% female) with a median age of 67.0 years (range 17.4-85.2 years) were included in the study. All patients had whole transcriptome sequencing and RPPA profiling at the time of diagnosis, and 73 of 81 patients had targeted sequencing of 465 genes using Foundation Medicine's FoundationOne Heme assay. Patient clinical and demographic characteristics are summarized in **Table 1**. Briefly, 46 patients (57%) had intermediate cytogenetic risk per ELN risk assessment (22), 30 (37%) had unfavorable risk, and 5 (6%) had favorable risk. A total of 36 patients (44%) were classified as M1/M2 and 45 patients (56%) were classified as M4/M5 by FAB classification. Thirty-three patients (41%) had antecedent hematologic disorder. Eleven patients were alive at the time of this analysis, with a median follow-up period of 388.1 weeks (range 0-559.5 weeks). Eighty percent of patients (56/70 for whom data were available) were treated with cytarabine-based regimens, 13% were treated with hypomethylating agents (9/70), and 7% with investigational treatments (5/70). Eleven patients had no treatment records at MD Anderson. Of those evaluable for response, 35/63 (56%) had complete remission or a partial response (complete remission: 33/35, 94%; partial response: 2/35, 6%), and 28/63 (44%) had primary refractory disease. Among the patients who had complete remission or a partial response, 20/35 patients (57%) eventually had a relapse. The median overall survival, event free survival, and remission duration for all evaluable patients were 25.4 weeks (range 0-559.6 weeks), 22.4 weeks (range 0-393 weeks), and 42.4 weeks (range 3.3-538.7 weeks), respectively (**Supplementary Figures 1A–C**).

Unsupervised Clustering to Identify Prognostic Clusters Independent of FAB and ELN Classification

Unsupervised clustering of the 81 newly diagnosed AML patients based on the top 1000 variably expressed genes initially revealed two distinct patient clusters. The clustering was highly associated with FAB morphologic classification (Fisher p = 9.2e^{-5}, **Supplementary Figure 2A**). The FAB-associated clustering of patients persisted even when more genes were added to the unsupervised clustering, suggesting a significant impact of lineage and morphology on transcriptomic-based clustering (**Supplementary Figure 2B**). To assess whether this observation was also relevant in other AML cohorts, we conducted unsupervised clustering of expression profiles in M1/M2 and M4/M5 patients from TCGA AML cohort (18). Indeed, unsupervised clustering of TCGA AML cohort revealed similar high dependency on FAB classification (Fisher p = 2.24e^{-10}, **Supplementary Figure 2C**). These findings suggested that the genes associated with lineage morphology in AML were contributing to AML transcriptomic-based clustering, and hence could be masking AML subgroups that share similar underlying biology but different lineages.

To address this concern, we used linear regression models and identified genes whose expression profiles were associated with FAB classification (q < 0.05; see *Methods*). Using enrichment analysis in cell lineage and morphology signatures (10, 11), we found that these genes were highly enriched for myeloid and monocytic lineage differentiation (**Supplementary Figure 3A**). To decouple lineage-associated genes from AML patient clustering and to identify biologically similar AML patients independent of lineage, we excluded the lineage-associated genes and re-clustered AML patients based on the expression of top variable genes (735 genes, variance > 5). This approach led us to identify 3 distinct patient clusters (hereafter referred to as group 1, group 2, and group 3) that clustered independently of FAB classification (Fisher p = 0.251; **Figure 1A** and **Supplementary Figure 2B**). The clinical and demographic characteristics of these 3 clusters are summarized in **Table 1**. Briefly, after correction for multiple hypothesis testing, there were no significant differences in distribution for FAB classification, ELN classification, sex, antecedent hematologic disease, or treatment group. Group 1 patients were the oldest (mean age 68.9 ± 9.9 years), followed by group 2 patients (64.4 ± 15.1 years) and group 3 patients (57.3 ± 15.6 years; p = 0.030, q = 0.073). These findings suggested that the patient grouping was

inherently driven by the transcriptomic signatures independent of lineage or clinical characteristics.

Targeted DNA sequencing of 465 genes using the FoundationOne Heme assay in 73 patients (90%) revealed *FLT3* (37%), *TET2* (30%), *ASXL1* (25%), *NPM1* (22%), and *NRAS* (22%) as the most commonly mutated genes in the cohort (**Figure 1B**). *ASXL1* (q = 0.006), *GATA2* (q = 0.029), and *FLT3* (q = 0.006) mutations were significantly enriched in groups 1, 2, and 3, respectively (**Figure 1C**), but these mutations were not associated with FAB classification (q > 0.4 for all). *FLT3 expression was highest in Group 3, but it was significantly different only when compared to Group 2 (q= 0.018)* (**Supplementary Figure 3B**). We found significant association between mutations in FLT3 and mutations in NPM1 (q = 0.094, OR: 3.82) and ASXL1 (q = 0.094, OR: 0.3) mutations (**Supplementary Figure 3C**). Of note, while a significant fraction of NPM1 mutations co-occur with FLT3, mutations in AXSL1 were largely mutually exclusive. We included this data as **Supplementary Figure 3B**. These findings suggested that mutation profiles were associated with transcriptomic signatures, but not with lineage.

Outcomes of AML Patient Groups

We next evaluated whether the 3 AML groups had distinct clinical outcomes. Univariate Cox survival analysis indicated that sample clustering was associated with differential overall survival, event-free survival, and remission duration ($p < 0.05$). To control for other confounding clinical factors, we first used univariate survival analysis to identify clinical variables associated with survival ($p < 0.05$; **Supplementary Table 1**) and then built a multivariable Cox survival model with these variables. Survival trends observed in the clusters in univariate analysis were re-captured after controlling for other confounding variables associated with survival (see *Methods*). Group 2 was characterized by improved overall survival (median 55.86 weeks; p = 0.037), event-free survival (median 55.85 weeks; p = 0.006), and remission duration (median 111.71 weeks; p = 0.03 relative to group 1, whereas no significant difference was observed between group 1 and group 3 (**Figures 1D–F**).

Inflammatory and Immune Pathways Enriched in Group 2 Patients

To explore transcriptomic signatures that were associated with improved outcomes in group 2, we conducted differential gene expression profiling comparing group 2 with groups 1 and 3, revealing 70 upregulated genes and 322 downregulated genes ($q < 0.05$, absolute $\log_2$ fold change > 2; **Figure 2A** and **Supplementary Table 1**). GSEA of hallmarks pathways demonstrated significant activation of immune signaling in group 2 compared with groups 1 and 3 (**Figure 2B**). To determine whether the signal was confounded by a single group, we next compared group 2 with group 1 and 3 each separately. Indeed, we saw that patients in group 2 consistently had activation of immune and inflammatory pathways, including interferon-alpha and interferon-gamma, compared with each of the other groups, suggesting that intrinsic immune activation in group 2 was associated with improved outcomes (**Figures 2C, D**). *HOXA* and *HOXB* gene clusters were significantly downregulated in group 2 compared with groups 1 and 3 (**Supplementary Table 1**). Furthermore, lower expression of *HOXA* and *HOXB* gene clusters was associated with better outcomes across all patients in our cohort (**Supplementary Figure 4A**).

Validation of Immune Signatures in Independent Cohorts

To validate the finding that immune signatures were associated with improved outcomes in AML, we used 2 independent AML cohorts (17, 18) with available transcriptomic and clinical data (**Supplementary Table 1**; see *Methods*). We then compared outcomes based on median scores derived from ssGSEA (7) from genes differentially expressed in group 2 relative to groups 1 and 3 (see *Methods*). Higher-scoring patients (i.e., more similar to group 2) had improved survival in both validation cohorts (**Figures 3A–C**). Differential pathway activity analysis between these groups revealed activation of immune-associated pathways, consistent with observations in group 2 in our cohort and further validating our finding that immune activity was the main differential factor in outcomes (**Figures 3D, E**). Similarly, patients with lower *HOXA* and *HOXB* gene scores had improved outcomes (**Supplementary Figures 4B, C**). These data indicate that activation of immune-associated pathways and suppression of *HOX* genes in AML are associated with improved outcomes in patients.

Pairwise GSEA Comparisons Revealing Metabolic Signatures in Group 3

To further characterize the biologic pathways that distinguished patient groups, we conducted pairwise GSEA between individual groups of patients. Group 3 patients had significant activation of metabolic activity compared with group 1 and with group 2 patients (**Figures 4A, B**). Although patients in group 3 and group 1 had similarly worse outcomes, activity of metabolic pathways was significantly higher in group 3 patients, especially for oxidative phosphorylation and fatty acid metabolism (**Figure 4B**), suggesting that metabolism was a distinguishing feature between these groups. Furthermore, activity in the mTOR pathway, a major regulator of cancer metabolism (23), was significantly higher in group 3 than in group 1.

To further characterize metabolic activity in group 3, we compared the metabolic pathway activity scores between group 3 and groups 2 and 1. Relative to group 2, group 3 showed significant activation of energy metabolism pathways such as glycolysis, TCA cycle, biosynthesis of unsaturated fatty acids, and gluconeogenesis. Relative to group 1, group 3 was characterized by activation of oxidative phosphorylation, lipid metabolism (ether lipid metabolism, steroid hormone biosynthesis), and pyrimidine metabolism. Group 3 also showed activation of galactose metabolism and linoleic acid metabolism relative to both group 1 and group 2. These findings indicate that patients in group 3 may be characterized by augmented activation of pathways involved in energy production and metabolism (**Figure 4C**).

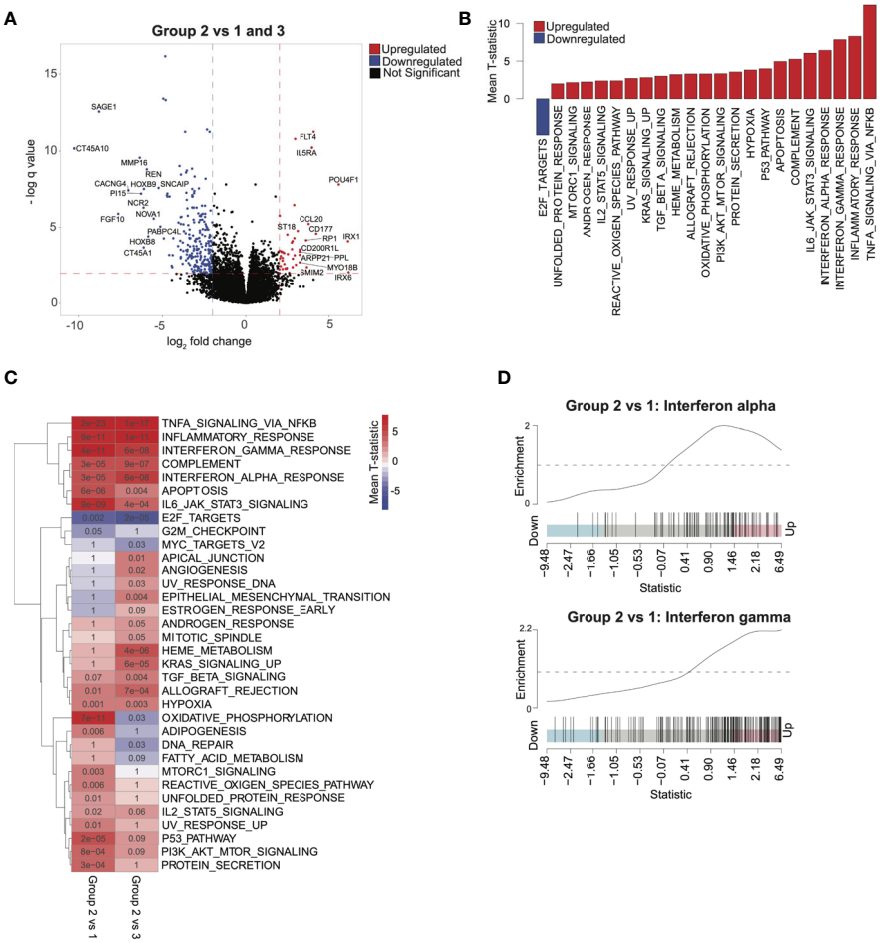

FIGURE 2 | Characterizing transcriptomic features of acute myeloid leukemia patients in group 2: **(A)** Volcano plot corresponding to differential expression analysis comparing the transcriptome of group 2 with that of group 1 and 3 combined (significance based on $\log_2$ fold change > 2 and q < 0.05, in red). **(B)** Pathways identified *via* gene set enrichment analysis (GSEA) of significantly differentially expressed genes from **(A)**. Negative mean T-statistic (blue) indicates downregulation and positive mean T-statistic (red) indicates upregulation of the pathway. **(C)** GSEA mean T-statistic heatmap based on pairwise differential expression comparing group 2 with group 1 and with group 3. Pathways significantly dysregulated (q < 0.1) in at least one comparison are included in the heatmap. Red and blue indicate upregulation and downregulation, respectively. Numbers in the heatmap correspond to q values. **(D)** Barcode plots illustrating upregulation of interferon-alpha and interferon-gamma signaling in group 2 relative to group 1.

Proteomic Assessment to Distinguish Group 3 and Group 1

All 81 AML patients had previously reported RPPA profiling (19) at the same time point of RNA and genomic sequencing. We therefore used this orthogonal molecular platform to delineate protein-based molecular pathways that could differentiate these 3 AML patient groups (**Supplementary Figure 5**). Group 2 had downregulation (q = 0.057 and difference in mean = -0.832) of only CTNNB1 when compared with group 1 (**Supplementary Figure 5A**) and downregulation of MTOR and MTOR.pS2448 compared with group 3 (**Supplementary Figure 5B**). These findings suggested that unlike RNA, RPPA was not able to delineate many proteomic differences between group 2 and groups 1 and 3, most likely owing to the smaller number of genes assayed.

We next evaluated differences in RPPA signatures between group 1 and group 3 patients who had similar outcomes, compared with group 2 patients. We identified 28 upregulated proteins and 19 downregulated proteins (q < 0.1, see *Methods*) in group 3 relative to group 1 (**Figure 5A**). MTOR.pS2448, which signals for activation of both mTOR and PI3K pathways (23–25), was over-expressed in group 3. This was consistent with the mTOR upregulation in the group 3 transcriptomic signature and suggested an active PI3K-AKT-mTOR signaling axis in group 3 patients. In addition, we found over-expression of proteins in the MAPK signaling cascade (MAP2K1_2pS217_211, MAPK9), apoptosis (BAX, CASP8, MCL1, BAK1, BAD.pS155), and BRAF in group 3 compared with group 1 (**Figure 5A**). Overexpression of MCL1, accumulation of total (un-cleaved) CASP8, and lower expression of cleaved caspase-3

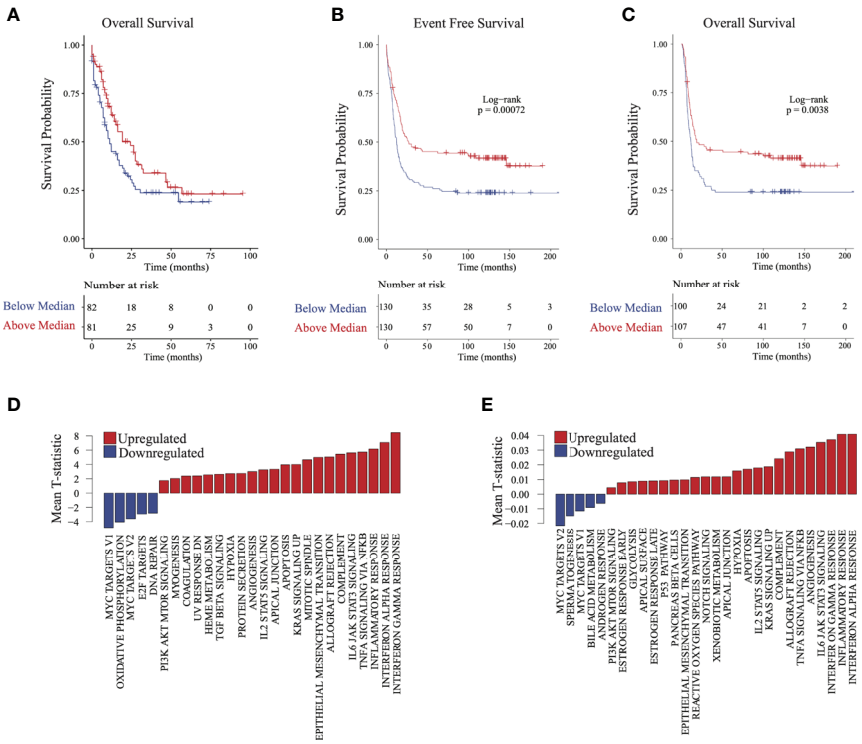

FIGURE 3 | Validating survival and pathway trends observed in group 2 in independent cohorts: Samples in The Cancer Genome Atlas (TCGA) and Valk et al. cohorts were stratified on the basis of their similarity to group 2 (see *Methods*). **(A)** Overall survival and **(B)** event-free survival in TCGA cohort. **(C)** Overall survival in the Valk et al. cohort. **(D, E)** Gene set enrichment analysis barplots of TCGA **(D)** and Valk et al. **(E)** validation cohorts.

(CASP3.cI175) suggested inhibition of apoptosis in group 3 patients (**Figure 5A**), consistent with the higher absolute blast count observed in group 3 (**Table 1**).

MCL1 overexpression is associated with venetoclax resistance and can be seen in *FLT3*-mutated AML (26). We therefore checked for a correlation between mTOR and MCL1 expression. Indeed, MTOR.pS2448 expression was positively correlated with MCL1 expression in RPPA across all patients (**Figure 5B** and **Supplementary Figure 5B**). This is significant because resistance to venetoclax can be mediated *via* MCL1 (26). We therefore evaluated whether resistance to venetoclax in myeloid and lymphoid cell lines is also associated with mTOR overexpression. Phosphorylated S6 p235-236 and p240-244, which are surrogate markers for mTOR activation, were positively correlated with venetoclax AUC ($\rho = 0.36$, $p = 0.001$ and $\rho = 0.32$, $p = 0.003$, respectively), suggesting that mTOR activation was associated with resistance to venetoclax (**Figures 5C, D**).

DISCUSSION

Clinical outcomes of AML patients are largely determined by patient characteristics such as age, performance status, and the underlying cause of the AML (27). ELN classification categorizes AML patients on the basis of cytogenetic and mutational profiles (22, 28). However, almost one-third of AML patients lack prognostic genomic features (29). Also, one-third of AML patients have survival outcomes that deviate more than 20% from their ELN risk category (29). Therefore, identifying orthogonal molecular approaches contributing to AML heterogeneity independent of clinical and genomic features may reveal biologic processes impacting outcomes and identify novel therapeutic strategies.

In previous studies using RNA profiling to classify AML patients (17, 30), gene expression clustering was strongly correlated with mutational and cytogenetic profiles, as well as lineage and morphologic groups as classified by FAB. Similarly, we identified cluster correlation with FAB classification in TCGA and in our cohort. We therefore hypothesized that by excluding the expression profiles of genes associated with lineage and morphologic characteristics in AML, we can potentially uncover AML patient groups that share biologic pathways independent of morphology and lineage. In the current study, we undertook a comprehensive and unique approach to decouple lineage-related genes, combined with RPPA and targeted mutation analysis, and we identified immune and metabolic signatures that contributed to AML heterogeneity and impacted outcomes.

Our analysis identified a group of AML patients (group 2) who had significantly improved overall survival, event-free survival, and remission duration. This patient group was characterized by increased frequency of *GATA2* mutations and an inflammatory and immune phenotype indicated by enrichment for interferon-

TABLE 1 | Clinical and demographic characteristics of patients.

Characteristic	No. (%)					
	Overall, n = 81	Group 1, n = 31	Group 2, n = 29	Group 3, n = 21	p[1]	q[2]
Mean ± SD age, years	64.3±14.1	68.9±9.9	64.4±15.1	57.3±15.6	0.030	0.073
Sex					0.250	0.370
Female	34/81 (42)	12/31 (39)	10/29 (34)	12/21 (57)		
Male	47/81 (58)	19/31 (61)	19/29 (66)	9/21 (43)		
FAB					0.230	0.370
M1/M2	36/81 (44)	16/31 (52)	14/29 (48)	6/21 (29)		
M4/M5	45/81 (56)	15/31 (48)	15/29 (52)	15/21 (71)		
ELN genetic group					0.019	0.073
Favorable	5/81 (6)	0/31 (0)	5/29 (17)	0/21 (0)		
Intermediate	46/81 (57)	15/31 (48)	17/29 (59)	14/21 (67)		
Unfavorable	30/81 (37)	16/31 (52)	7/29 (24)	7/21 (33)		
Recent AHD					0.180	0.360
No	48/81 (59)	16/31 (52)	16/29 (55)	16/21 (76)		
Yes	33/81 (41)	15/31 (48)	13/29 (45)	5/21 (24)		
Treatment					0.280	0.370
AraC-based	56/70 (80)	17/24 (71)	21/25 (84)	18/21 (86)		
HMA-based	9/70 (13)	4/24 (17)	4/25 (16)	1/21 (5)		
Investigational	5/70 (7)	3/24 (13)	0/25 (0)	2/21 (10)		
(Missing)	11	7	4	0		
Response					>0.99	>0.99
CR	33/70 (47)	10/24 (42)	12/25 (48)	11/21 (52)		
Not Evaluable	7/70 (10)	3/24 (13)	2/25 (8)	2/21 (10)		
Partial remission	2/70 (3)	1/24 (4)	1/25 (4)	0/21 (0)		
Resistant	28/70 (40)	10/24 (42)	10/25 (40)	8/21 (38)		
(Missing)	11	7	4	0		
Relapse	20/35 (57)	8/11 (73)	6/13 (46)	6/11 (55)	0.480	0.530
(Missing)	46	20	16	10		
Vital status					0.028	0.073
Alive	11/81 (14)	2/31 (6)	8/29 (28)	1/21 (5)		
Dead	70/81 (86)	29/31 (94)	21/29 (72)	20/21 (95)		
AlloSCT	7/81 (9)	1/31 (3)	4/29 (14)	2/21 (10)	0.370	0.440
Mean ± SD bone marrow blast percentage	60.0±23.1	55.2±22.9	51.9±22.2	79.1±12.2	<0.001	<0.001
(Missing)	1	0	0	1		

[1]*Statistical tests performed: Kruskal-Wallis test; chi-square test of independence; Fisher exact test.*

[2]*False discovery rate correction for multiple testing.*

FAB, French-American-British classification; ELN, European Leukemia Network; AHD, antecedent hematologic disorder; AraC, ara-cytarabine; HMA, hypomethylating agents; CR, complete remission; alloSCT, allogeneic stem cell transplantation.

alpha and interferon-gamma, tumor necrosis factor-alpha, and interleukin-6/JAK/STAT3 signaling pathways. Interestingly, germline deficiencies in *GATA2* leads to myeloid malignancies with an immunodeficient phenotype (31). However, the exact mechanism by which *GATA2* mutations could confer a remodeled immunologic phenotype in AML remains unclear and warrants further investigation. Supported by previous studies demonstrating distinct immune cell activity among AML patients with different outcomes (32). Our findings suggested that the intrinsic inflammatory and immune microenvironment in AML was associated with better outcomes and responses to therapy. Recent work demonstrated the complex immunologic landscape of hematologic malignancies with a subset of AML patients having a distinctively high NK/T cell cytotoxic activity {Dufva:2020bg}. Further, recent work demonstrated that an immune-infiltrated signal was associated with improved outcomes in AML patients but not associated with ELN (33). However, in our results, which were validated in 2 independent cohorts, patients could be grouped by shared biologic characteristics independent of ELN classification or clinical variables such as age.

AML patients in group 2 also had significant downregulation of *HOX* genes, which corresponded with improved outcomes, consistent with previous studies (30, 34, 35). Inflammation and cytokine production in a canine model was associated with reduced *HOXA* gene expression (36), and restoring *HOX* gene expression may oppose inflammation (37) or hamper innate immunity by inhibiting granulopoiesis (38). These studies, although not conducted in a leukemia or cancer model, suggested that inflammation and *HOX* genes may be co-regulated, but the exact mechanism linking these two pathways is still unclear.

Our analysis also revealed 2 distinct patient groups (groups 1 and 3) that had similarly worse outcomes compared with group 2 but distinct underlying biology. Our orthogonal RPPA and genomic analysis coupled with transcriptomic profiling revealed that these 2 groups can be distinguished by increased metabolic activity and overexpression of mTOR and MCL1 proteins in group 3. However, only group 3 had *FLT3* enrichment, contrary to previous transcriptomic studies (17), demonstrating that multiple transcriptional clusters may harbor *FLT3* mutations. Therefore, our approach of decoupling the lineage-associated genes generated

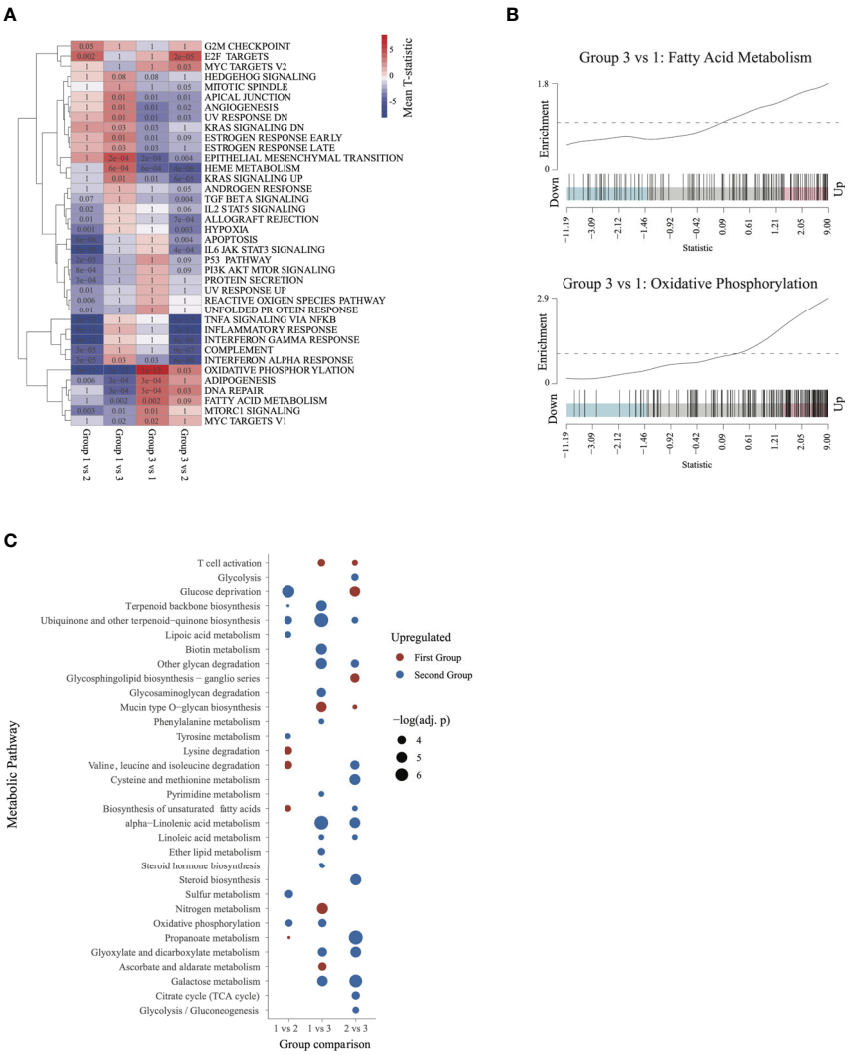

FIGURE 4 | Characterizing the transcriptome of patients in group 3 and group 1: **(A)** Gene set enrichment analysis heatmap, similar to **Figure 2**. Pathways significantly dysregulated (q < 0.1) in at least one of the comparisons were included in the heatmap. **(B)** Barcode plots illustrating upregulation of fatty acid metabolism and oxidative phosphorylation in group 3 relative to group 1 patients. **(C)** Metabolic pathways differentially activated (q ≤ 0.05) in each of the 3 comparisons. Upregulated pathways are shown in red and downregulated pathways in blue (relative to the second group in each comparison).

a better representation of the transcriptomic profile associated with *FLT3* mutations. This is also consistent with the proliferative phenotype conferred by *FLT3* mutations in AML (39). *FLT3* activates downstream mTOR signaling (40, 41), and this signaling is involved in metabolic reprogramming (42). Inhibiting mTOR can also lead to inhibition of MCL1, but the exact mechanism is not clear, although it is thought to involve AKT-dependent regulation of MCL1 (43, 44). mTOR inhibition also has antitumor activity in AML (45–47), and our data suggest that mTOR activation is associated with venetoclax resistance. The finding is of high importance because it suggests an alternative therapeutic target to overcome venetoclax resistance (26). Furthermore, mTOR inhibition could be a surrogate for inhibiting MCL1, especially given that direct MCL1 inhibitors have cardiac and gastrointestinal toxicities that have hampered their recent clinical development.

Our dataset comprised 81 samples from patients mostly treated with intensive chemotherapeutic regimens (80% with cytarabine-based regimens). Given the relatively small sample size, it is likely that we missed subtle transcriptomic and proteomic perturbations that might be biologically important. Furthermore, we used targeted sequencing of AML-associated genes to study DNA lesions in the cohort. Although this approach allowed us to study important AML-associated mutations in these patients, it precluded analysis of the full spectrum of mutations in these patients or the associated mutational processes, although most if not all of the myeloid mutations can be captured by this assay. Outcomes in patients with *FLT3* mutations (primarily group 3) would have been improved had FLT3 inhibitors been used. However, at the time of sample collection and AML diagnosis, none of the FLT3 inhibitors were approved or under investigation

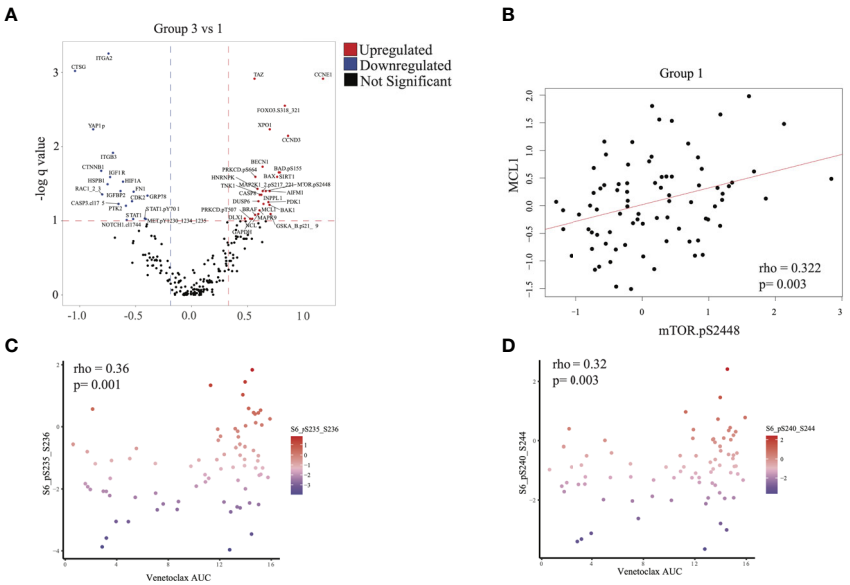

FIGURE 5 | Proteomic analysis: **(A)** Differential protein expression analysis comparing group 3 with group 1. Upregulated proteins (q < 0.1 and difference in mean > 0.32) are shown in red and downregulated proteins (q < 0.1 and difference in mean > -0.188) in blue. **(B)** Scatterplot illustrating the correlation between expression of mTOR.pS2448 (activating phosphorylation) and MCL1 (spearman correlation = 0.322, p = 0.003). **(C, D)** Scatterplot illustrating the expression of phosphorylated S6 (marker of mTOR activation) with venetoclax (higher area under the curve [AUC] indicates more resistance to treatment). Statistics computed using Spearman correlation.

in a trial. Nevertheless, our study, which combined RPPA, genomic profiling, and transcriptomic profiling with extensive and long clinical follow-up data, provided a unique clinical dataset for further interrogation.

Our approach to decouple morphology from lineage-associated genes in AML revealed distinct groups of AML patients that share biologic pathways independent of ELN classification, antecedent hematologic disorders, or other clinical and molecular variables that are known to impact outcomes. We also used orthogonal RPPA analysis to differentiate patients with similarly worse outcomes in groups 1 and 3, revealing an mTOR-associated metabolic profile that can be potentially targeted. Our findings demonstrate that employing alternative classifications for AML patients can provide insight into AML heterogeneity.

DATA AVAILABILITY STATEMENT

The original contributions presented in the study are publicly available. This data can be found at: https://www.ncbi.nlm.nih.gov/geo/query/acc.cgi?acc=GSE165656.

ETHICS STATEMENT

The studies involving human participants were reviewed and approved by IRB approval MD Anderson. The patients/participants provided their written informed consent to participate in this study.

AUTHOR CONTRIBUTIONS

HA, VM, and RW analyzed the data. YH and SL conducted the metabolic profiling. FW and JZ conducted DNA analysis. YQ and CH prepared samples. AQ analyzed RPPA. AQ and CB conducted sequencing. ND, MK, and AF contributed to clinical and integrative analysis. KC, LW, SK, and HA supervised the study. All authors contributed to the article and approved the submitted version.

FUNDING

The work was funded in part by a T32 National Institutes of Health fellowship to HA. This project has been made possible in part by grant RP180248 to KC from Cancer Prevention & Research Institute of Texas and grant U01CA247760 to KC. RNA sequencing and Foundation Medicine assay sequencing were partially done *via* funding from Genentech to SK.

SUPPLEMENTARY MATERIAL

The Supplementary Material for this article can be found online at: https://www.frontiersin.org/articles/10.3389/fonc.2021.705627/full#supplementary-material

Supplementary Table 1 | List of French American British (FAB)-associated genes and differentially expressed genes across all comparisons, in univariate and multivariable analysis, and between groups.

Supplementary Figure 1 | Kaplan-Meier curves for **(A)** overall survival, **(B)** event-free survival, and **(C)** remission duration for all 81 patients in the cohort.

Supplementary Figure 2 | (A) Clustered heatmap of top 1000 variably expressed genes in our cohort. Two patient groups were identified that showed strong association with French American British (FAB) status (Fisher p = $9.2e^{-5}$). **(B)** Clustering of samples performed as in **Supplementary Figure 1A** for various numbers of top variably expressed genes and their association with FAB status, inferred using the Fisher test. The analysis was also performed for clusters corresponding to **Figure 1A** (corrected_clusters). The barplot is the $-\log_{10}$ p values obtained from the Fisher test. **(C)** Transcriptome clustering analysis in The Cancer Genome Atlas (TCGA) acute myeloid leukemia cohort using the top 1000 variably expressed genes. Consistent with observations in our data **(A, B)**, identified clusters showed a strong association with FAB status (Fisher p = 2.24e-10).

Supplementary Figure 3 | (A) Enrichment of cell type markers in genes associated with French American British classification. Strong enrichment was observed for genes associated with myeloid and monocytic lineage. **(B)** boxplot of expression of FLT3 between groups (ANOVA p = 0.025), Tuckey post-hoc test is used to compute q-values for pairwise comparisons. **(C)** Heatmap of mutations that are associated with FLT3 mutations (q < 0.1), identified using Fisher's test followed by correction of p-value by FDR.

Supplementary Figure 4 | Samples stratified on the basis of activity of *HOXA* or *HOXB* clusters and divided into high (above the fiftieth percentile) and low (below the fiftieth percentile) groups. Survival between these groups was compared in **(A)** the MD Anderson cohort (top: overall survival; bottom: event-free survival), **(B)** the Valk et al. cohort (top: overall survival; bottom: event-free survival), and **(C)** The Cancer Genome Atlas (TCGA) cohort (overall survival).

Supplementary Figure 5 | (A) Proteins differentially expressed in group 2 relative to group 1. Upregulated proteins are shown in red (q < 0.1 and difference in mean > 0.149) and downregulated pathways in blue (q < 0.1 and difference in mean < -0.117). **(B)** Proteins differentially expressed in group 2 relative to group 3. Upregulated proteins are shown in red (q < 0.1 and difference in mean > 0.22) and downregulated pathways in blue (q < 0.1 and difference in mean < -0.24).

REFERENCES

1. DeLuca DS, Levin JZ, Sivachenko A, Fennell T, Nazaire M-D, Williams C, et al. RNA-SeQC: RNA-Seq Metrics for Quality Control and Process Optimization. *Bioinformatics* (2012) 28:1530–2. doi: 10.1093/bioinformatics/bts196
2. Dobin A, Davis CA, Schlesinger F, Drenkow J, Zaleski C, Jha S, et al. STAR: Ultrafast Universal RNA-Seq Aligner. *Bioinformatics* (2013) 29:15–21. doi: 10.1093/bioinformatics/bts635
3. Love MI, Huber W, Anders S. Moderated Estimation of Fold Change and Dispersion for RNA-Seq Data With Deseq2. *Genome Biol* (2014) 15:550–21. doi: 10.1186/s13059-014-0550-8
4. Luo W, Friedman MS, Shedden K, Hankenson KD, Woolf PJ. GAGE: Generally Applicable Gene Set Enrichment for Pathway Analysis. *BMC Bioinf* (2009) 10:161–17. doi: 10.1186/1471-2105-10-161
5. Subramanian A, Tamayo P, Mootha VK, Mukherjee S, Ebert BL, Gillette MA, et al. Gene Set Enrichment Analysis: A Knowledge-Based Approach for Interpreting Genome-Wide Expression Profiles. *Proc Natl Acad Sci USA* (2005) 102:15545–50. doi: 10.1073/pnas.0506580102
6. Barbie DA, Tamayo P, Boehm JS, Kim SY, Moody SE, Dunn IF, et al. Systematic RNA Interference Reveals That Oncogenic KRAS-Driven Cancers Require TBK1. *Nature* (2009) 462:108–12. doi: 10.1038/nature08460
7. Hänzelmann S, Castelo R, Guinney J. GSVA: Gene Set Variation Analysis for Microarray and RNA-Seq Data. *BMC Bioinf* (2013) 14:7–15. doi: 10.1186/1471-2105-14-7
8. Liberzon A, Birger C, Thorvaldsdóttir H, Ghandi M, Mesirov JP, Tamayo P. The Molecular Signatures Database (MSigDB) Hallmark Gene Set Collection. *Cell Syst* (2015) 1:417–25. doi: 10.1016/j.cels.2015.12.004
9. Langfelder P, Horvath S. WGCNA: An R Package for Weighted Correlation Network Analysis. *BMC Bioinf* (2008) 9:559–13. doi: 10.1186/1471-2105-9-559
10. Kuleshov MV, Jones MR, Rouillard AD, Fernandez NF, Duan Q, Wang Z, et al. Enrichr: A Comprehensive Gene Set Enrichment Analysis Web Server 2016 Update. *Nucleic Acids Res* (2016) 44:W90–7. doi: 10.1093/nar/gkw377
11. Chen EY, Tan CM, Kou Y, Duan Q, Wang Z, Meirelles GV, et al. Enrichr: Interactive and Collaborative HTML5 Gene List Enrichment Analysis Tool. *BMC Bioinf* (2013) 14:128–14. doi: 10.1186/1471-2105-14-128
12. Kanehisa M, Goto S. KEGG: Kyoto Encyclopedia of Genes and Genomes. *Nucleic Acids Res* (2000) 28:27–30. doi: 10.1093/nar/28.1.27
13. He J, Abdel-Wahab O, Nahas MK, Wang K, Rampal RK, Intlekofer AM, et al. Integrated Genomic DNA/RNA Profiling of Hematologic Malignancies in the Clinical Setting. *Blood* (2016) 127:3004–14. doi: 10.1182/blood-2015-08-664649
14. Frampton GM, Fichtenholtz A, Otto GA, Wang K, Downing SR, He J, et al. Development and Validation of a Clinical Cancer Genomic Profiling Test Based on Massively Parallel DNA Sequencing. *Nat Biotechnol* (2013) 31:1023–31. doi: 10.1038/nbt.2696
15. Forbes SA, Bindal N, Bamford S, Cole C, Kok CY, Beare D, et al. COSMIC: Mining Complete Cancer Genomes in the Catalogue of Somatic Mutations in Cancer. *Nucleic Acids Res* (2011) 39:D945–50. doi: 10.1093/nar/gkq929
16. Mayakonda A, Lin D-C, Assenov Y, Plass C, Koeffler HP. Maftools: Efficient and Comprehensive Analysis of Somatic Variants in Cancer. *Genome Res* (2018) 28:1747–56. doi: 10.1101/gr.239244.118
17. Valk PJM, Verhaak RGW, Beijen MA, Erpelinck CAJ, Barjesteh van Waalwijk van Doorn-Khosrovani S, Boer JM, et al. Prognostically Useful Gene-Expression Profiles in Acute Myeloid Leukemia. *N Engl J Med* (2004) 350:1617–28. doi: 10.1056/NEJMoa040465
18. Cancer Genome Atlas Research Network, Ley TJ, Miller C, Ding L, Raphael BJ, Mungall AJ, et al. Genomic and Epigenomic Landscapes of Adult *De Novo* Acute Myeloid Leukemia. *N Engl J Med* (2013) 368:2059–74. doi: 10.1056/NEJMoa1301689
19. Hu CW, Qiu Y, Ligeralde A, Raybon AY, Yoo SY, Coombes KR, et al. A Quantitative Analysis of Heterogeneities and Hallmarks in Acute Myelogenous Leukaemia. *Nat BioMed Eng* (2019) 3:889–901. doi: 10.1038/s41551-019-0387-2
20. Rees MG, Seashore-Ludlow B, Cheah JH, Adams DJ, Price EV, Gill S, et al. Correlating Chemical Sensitivity and Basal Gene Expression Reveals Mechanism of Action. *Nat Chem Biol* (2016) 12:109–16. doi: 10.1038/nchembio.1986
21. Barretina J, Caponigro G, Stransky N, Venkatesan K, Margolin AA, Kim S, et al. The Cancer Cell Line Encyclopedia Enables Predictive Modelling of Anticancer Drug Sensitivity. *Nature* (2012) 483:603–7. doi: 10.1038/nature11003
22. Dohner H, Estey E, Grimwade D, Amadori S, Appelbaum FR, Buchner T, et al. Diagnosis and Management of AML in Adults: 2017 ELN Recommendations From an International Expert Panel. *Blood* (2017) 129:424–47. doi: 10.1182/blood-2016-08-733196
23. Mossmann D, Park S, Hall MN. mTOR Signalling and Cellular Metabolism Are Mutual Determinants in Cancer. *Nat Rev Cancer* (2018) 18:744–57. doi: 10.1038/s41568-018-0074-8
24. Jung CH, Ro S-H, Cao J, Otto NM, Kim D-H. mTOR Regulation of Autophagy. *FEBS Lett* (2010) 584:1287–95. doi: 10.1016/j.febslet.2010.01.017
25. Kim J, Kundu M, Viollet B, Guan K-L. AMPK and mTOR Regulate Autophagy Through Direct Phosphorylation of Ulk1. *Nat Cell Biol* (2011) 13:132–41. doi: 10.1038/ncb2152
26. Ramsey HE, Fischer MA, Lee T, Gorska AE, Arrate MP, Fuller L, et al. A Novel MCL1 Inhibitor Combined With Venetoclax Rescues Venetoclax-Resistant Acute Myelogenous Leukemia. *Cancer Discov* (2018) 8:1566–81. doi: 10.1158/2159-8290.CD-18-0140
27. Lowenberg B, Downing JR, Burnett A. Acute Myeloid Leukemia. *N Engl J Med* (1999) 341:1051–62. doi: 10.1056/NEJM199909303411407
28. Döhner H, Weisdorf DJ, Bloomfield CD. Acute Myeloid Leukemia. *N Engl J Med* (2015) 373:1136–52. doi: 10.1056/NEJMra1406184
29. Gerstung M, Papaemmanuil E, Martincorena I, Bullinger L, Gaidzik VI, Paschka P, et al. Precision Oncology for Acute Myeloid Leukemia Using a Knowledge Bank Approach. *Nat Genet* (2017) 49(3):332–40. doi: 10.1038/ng.3756
30. Bullinger L, Döhner K, Bair E, Fröhling S, Schlenk RF, Tibshirani R, et al. Use of Gene-Expression Profiling to Identify Prognostic Subclasses in Adult Acute Myeloid Leukemia. *N Engl J Med* (2004) 350:1605–16. doi: 10.1056/NEJMoa031046

31. Alfayez M, Wang SA, Bannon SA, Kontoyiannis DP, Kornblau SM, Orange JS, et al. Myeloid Malignancies With Somatic GATA2 Mutations can be Associated With an Immunodeficiency Phenotype. *Leuk Lymphoma* (2019) 60:2025–33. doi: 10.1080/10428194.2018.1551535
32. Radpour R, Riether C, Simillion C, Höpner S, Bruggmann R, Ochsenbein AF. CD8+ T Cells Expand Stem and Progenitor Cells in Favorable But Not Adverse Risk Acute Myeloid Leukemia. *Leukemia* (2019) 33:2379–92. doi: 10.1038/s41375-019-0441-9
33. Vadakekolathu J, Minden MD, Hood T, Church SE, Reeder S, Altmann H, et al. Immune Landscapes Predict Chemotherapy Resistance and Immunotherapy Response in Acute Myeloid Leukemia. *Sci Transl Med* (2020) 12:eaaz0463. doi: 10.1126/scitranslmed.aaz0463
34. Andreeff M, Ruvolo V, Gadgil S, Zeng C, Coombes K, Chen W, et al. HOX Expression Patterns Identify a Common Signature for Favorable AML. *Leukemia* (2008) 22:2041–7. doi: 10.1038/leu.2008.198
35. Nagy ÄDM, Ősz Á, Budczies J, Krizsán S, Szombath G, Demeter J, et al. Elevated HOX Gene Expression in Acute Myeloid Leukemia is Associated With NPM1 Mutations and Poor Survival. *J Advanced Res* (2019) 20:105–16. doi: 10.1016/j.jare.2019.05.006
36. Hagman R, Rönnberg E, Pejler G. Canine Uterine Bacterial Infection Induces Upregulation of Proteolysis-Related Genes and Downregulation of Homeobox and Zinc Finger Factors. *PloS One* (2009) 4:e8039. doi: 10.1371/journal.pone.0008039
37. Sarno J, Schatz F, Huang SJ, Lockwood C, Taylor HS. Thrombin and Interleukin-1beta Decrease HOX Gene Expression in Human First Trimester Decidual Cells: Implications for Pregnancy Loss. *Mol Hum Reprod* (2009) 15:451–7. doi: 10.1093/molehr/gap030
38. Wang H, Bei L, Shah CA, Hu L, Eklund EA. HoxA10 Terminates Emergency Granulopoiesis by Increasing Expression of Triad1. *J Immunol* (2015) 194:5375–87. doi: 10.4049/jimmunol.1401909
39. Lisovsky M, Estrov Z, Zhang X, Consoli U, Sanchez-Williams G, Snell V, et al. Flt3 Ligand Stimulates Proliferation and Inhibits Apoptosis of Acute Myeloid Leukemia Cells: Regulation of Bcl-2 and Bax. *Blood* (1996) 88:3987–97. doi: 10.1182/blood.V88.10.3987.bloodjournal88103987
40. Han L, Qiu P, Zeng Z, Jorgensen JL, Mak DH, Burks JK, et al. Single-Cell Mass Cytometry Reveals Intracellular Survival/Proliferative Signaling in FLT3-ITD-Mutated AML Stem/Progenitor Cells. *Cytometry A* (2015) 87:346–56. doi: 10.1002/cyto.a.22628
41. Chen W, Drakos E, Grammatikakis I, Schlette EJ, Li J, Leventaki V, et al. mTOR Signaling Is Activated by FLT3 Kinase and Promotes Survival of FLT3-Mutated Acute Myeloid Leukemia Cells. *Mol Cancer* (2010) 9:292–7. doi: 10.1186/1476-4598-9-292
42. Guertin DA, Sabatini DM. Defining the Role of mTOR in Cancer. *Cancer Cell* (2007) 12:9–22. doi: 10.1016/j.ccr.2007.05.008
43. Wei G, Twomey D, Lamb J, Schlis K, Agarwal J, Stam RW, et al. Gene Expression-Based Chemical Genomics Identifies Rapamycin as a Modulator of MCL1 and Glucocorticoid Resistance. *Cancer Cell* (2006) 10:331–42. doi: 10.1016/j.ccr.2006.09.006
44. Li H, Liu L, Chang H, Zou Z, Xing D. Downregulation of MCL-1 and Upregulation of PUMA Using mTOR Inhibitors Enhance Antitumor Efficacy of BH3 Mimetics in Triple-Negative Breast Cancer. *Cell Death Dis* (2018) 9:137–15. doi: 10.1038/s41419-017-0169-2
45. Willems L, Chapuis N, Puissant A, Maciel TT, Green AS, Jacque N, et al. The Dual Mtorc1 and Mtorc2 Inhibitor AZD8055 Has Anti-Tumor Activity in Acute Myeloid Leukemia. *Leukemia* (2019) 26(6):1195–202. doi: 10.1038/leu.2011.339
46. Zeng Z, Wang R-Y, Qiu YH, Mak DH, Coombes K, Yoo SY, et al. MLN0128, a Novel mTOR Kinase Inhibitor, Disrupts Survival Signaling and Triggers Apoptosis in AML and AML Stem/Progenitor Cells. *Oncotarget* (2016) 7:55083–97. doi: 10.18632/oncotarget.10397
47. Zeng Z, Shi YX, Tsao T, Qiu Y, Kornblau SM, Baggerly KA, et al. Targeting of Mtorc1/2 by the mTOR Kinase Inhibitor PP242 Induces Apoptosis in AML Cells Under Conditions Mimicking the Bone Marrow Microenvironment. *Blood* (2012) 120:2679–89. doi: 10.1182/blood-2011-11-393934

Conflict of Interest: ND has received research funding from Daiichi-Sankyo, Bristol-Myers Squibb, Pfizer, Gilead, Sevier, Genentech, Astellas, Daiichi-Sankyo, Abbvie, Hanmi, Trovagene, FATE, Amgen, Novimmune, Glycomimetics, and ImmunoGen and has served in a consulting or advisory role for DaiichiSankyo, Bristol-Myers Squibb, Pfizer, Novartis, Celgene, AbbVie, Astellas, Genentech, Immunogen, Servier, Syndax, Trillium, Gilead, Amgen and Agios. MD and CB are employees of Genentech. MK reports grant support and consulting fees from AbbVie, Genentech, F. Hoffmann La-Roche, Stemline Therapeutics, Forty-Seven, consulting fees from Amgen and Kisoji, grant support from Eli Lilly, Cellectis, Calithera, Ablynx, Agios, Ascentage, AstraZeneca, Rafael Pharmaceutical, Sanofi, royalties and stock options from Reata Pharmaceutical Inc.

The authors declare that this study received funding from Genentech. The funder had the following involvement with the study: the funder was involved in the Foundation Medicine mutation calling.

The remaining authors declare that the research was conducted in the absence of any commercial or financial relationships that could be construed as a potential conflict of interest.

Publisher's Note: All claims expressed in this article are solely those of the authors and do not necessarily represent those of their affiliated organizations, or those of the publisher, the editors and the reviewers. Any product that may be evaluated in this article, or claim that may be made by its manufacturer, is not guaranteed or endorsed by the publisher.

Citation: *Abbas HA, Mohanty V, Wang R, Huang Y, Liang S, Wang F, Zhang J, Qiu Y, Hu CW, Qutub AA, Dail M, Bolen CR, Daver N, Konopleva M, Futreal A, Chen K, Wang L and Kornblau SM (2021) Decoupling Lineage-Associated Genes in Acute Myeloid Leukemia Reveals Inflammatory and Metabolic Signatures Associated With Outcomes.*
Front. Oncol. 11:705627. doi: 10.3389/fonc.2021.705627

frontiers in Oncology

ORIGINAL RESEARCH
published: 18 August 2021
doi: 10.3389/fonc.2021.686156

PD-1 and TIGIT Are Highly Co-Expressed on CD8$^+$ T Cells in AML Patient Bone Marrow

Ling Xu[1,2†‡], Lian Liu[2‡], Danlin Yao[2†‡], Xiangbo Zeng[2], Yikai Zhang[2,3], Jing Lai[2], Jun Zhong[2], Xianfeng Zha[4†], Runhui Zheng[5], Yuhong Lu[2], Minming Li[6], Zhenyi Jin[2], Sudheendra Hebbar Subramanyam[2], Shaohua Chen[2†], Xin Huang[6] and Yangqiu Li[1,2*†]*

[1] The Clinical Medicine Postdoctoral Research Station, Department of Hematology, First Affiliated Hospital; Jinan University, Guangzhou, China, [2] Key Laboratory for Regenerative Medicine of Ministry of Education, Institute of Hematology, School of Medicine; Jinan University, Guangzhou, China, [3] Laboratory Center, Tianhe Nuoya Bio-Engineering Co. Ltd, Guangzhou, China, [4] Department of Clinical Laboratory, First Affiliated Hospital, Jinan University, Guangzhou, China Guangzhou, China, [5] Department of Hematology, First Affiliated Hospital, Guangzhou Medical University, Guangzhou, China, China, [6] Department of Hematology, Guangdong Provincial People's Hospital, Guangdong Academy of Medical Sciences, Guangzhou, China

Despite the great success of immune-checkpoint inhibitor (ICI) treatment for multiple cancers, evidence for the clinical use of ICIs in acute myeloid leukemia (AML) remains inadequate. Further exploration of the causes of immune evasion in the bone marrow (BM) environment, the primary leukemia site, and peripheral blood (PB) and understanding how T cells are affected by AML induction chemotherapy or the influence of age may help to select patients who may benefit from ICI treatment. In this study, we comprehensively compared the distribution of PD-1 and TIGIT, two of the most well-studied IC proteins, in PB and BM T cells from AML patients at the stages of initial diagnosis, complete remission (CR), and relapse-refractory (R/R) disease after chemotherapy. Our results show that PD-1 was generally expressed higher in PB and BM T cells from *de novo* (DN) and R/R patients, while it was partially recovered in CR patients. The expression of TIGIT was increased in the BM of CD8$^+$ T cells from DN and R/R patients, but it did not recover with CR. In addition, according to age correlation analysis, we found that elderly AML patients possess an even higher percentage of PD-1 and TIGIT single-positive CD8$^+$ T cells in PB and BM, which indicate greater impairment of T cell function in elderly patients. In addition, we found that both DN and R/R patients accumulate a higher frequency of PD-1$^+$ and TIGIT$^+$ CD8$^+$ T cells in BM than in corresponding PB, indicating that a more immunosuppressive microenvironment in leukemia BM may promote disease progression. Collectively, our study may help guide the combined use of anti-PD-1 and anti-TIGIT antibodies for treating elderly AML patients and pave the way for the exploration of strategies for reviving the immunosuppressive BM microenvironment to improve the survival of AML patients.

Keywords: PD-1, TIGIT, acute myeloid leukemia, immune-checkpoints, T cell, bone marrow

OPEN ACCESS

Edited by:
Antonio Curti, University of Bologna, Italy

Reviewed by:
Evan F. Lind, Oregon Health and Science University, United States
Rory Shallis, Yale University, United States

***Correspondence:**
Xin Huang
huangmingxin2001@sina.com
Yangqiu Li
yangqiuli@hotmail.com

***ORCID:**
Ling Xu
orcid.org/0000-0002-7044-7663
Danlin Yao
orcid.org/0000-0002-0963-8700
Xianfeng Zha
orcid.org/0000-0002-4970-1305
Shaohua Chen
orcid.org/0000-0003-4945-5914
Yangqiu Li
orcid.org/0000-0002-0974-4036

‡These authors have contributed equally to this work

Specialty section:
This article was submitted to Hematologic Malignancies, a section of the journal Frontiers in Oncology

Received: *31 March 2021*
Accepted: *30 July 2021*
Published: *18 August 2021*

Citation:
Xu L, Liu L, Yao D, Zeng X, Zhang Y, Lai J, Zhong J, Zha X, Zheng R, Lu Y, Li M, Jin Z, Hebbar Subramanyam S, Chen S, Huang X and Li Y (2021) PD-1 and TIGIT Are Highly Co-Expressed on CD8$^+$ T Cells in AML Patient Bone Marrow. Front. Oncol. 11:686156. doi: 10.3389/fonc.2021.686156

INTRODUCTION

In the last few decades, immunotherapy has emerged as the fourth pillar following surgery, radiation/chemotherapy and targeted therapy for solid tumor and leukemia therapy. One of the most effective immunotherapies includes resolving T cell dysfunction with immune checkpoint (IC) inhibitors (ICIs), such as programmed death receptor-1 (PD-1) and its ligand (PD-L1), cytotoxic T lymphocyte-associated antigen-4 (CTLA-4), and T cell immunoglobulin mucin-3 (Tim-3) (1–5). IC proteins are co-inhibitory receptors that distributed on the surface of several immune cells. After ligand binding, these regulators can transducing inhibitory signals to avoid immune injury under physiological conditions. However, under pathological conditions, such as chronic inflamation and cancer, continuous antigen stimulation and several immunosupressive factors could drive T cells to develop into a "unfitness" state called T cell exhaustion. One of the features of T cell exhaustion is the occurrence of elevated expession of several IC proteins. When these proteins bind their ligands, they reduce the anti-virus or anti-tumor effects of T cells, ultimately resulting in the immune escape of pathogens or tumors (3, 6–8).

Acute myeloid leukemia (AML) is a genetically, epigenetically, and clinically heterogeneous disease characterized by a failure in normal hematopoiesis and the accumulation of immature myeloid cells in the bone marrow (BM) and peripheral blood (PB) (9). For all AML patients (except for those with acute promyelocytic leukemia) who are medically able to tolerate chemotherapy, treatment with a 7-day infusion of cytarabine and a 3-day infusion of daunorubicin ("$7^{+}3$"), has not changed in the past 50 years. Additionally, post-remission therapy aimed to prevent relapse of the disease. Additional cytotoxic chemotherapies (such as high or intermediate dose cytarabine), with or without targeted therapies, and allogenic hematopoietic stem cell transplantation (Allo-SCT) are the two commonly employed strategies. Several targeted therapies have been developed and approved for AML patients with special molecular and cytogenetic alterations, including venetoclax to target B-cell lymphoma 2, midostaurin, and gilteritinib to target FLT3, and ivosidenib and enasidenib to target mutant isocitrate dehydrogenase 1 and 2 (IDH1 and IDH2). The outcomes of AML patients who have a favorable or intermediate risk prognostic classification have improved with the addition of various targeted drugs; however, longer-term overall survival (OS) beyond 3–5 years remains low for adverse risk patients, particularly older AML patients (9–14). In recent studies, ICIs have demonstrated encouraging results when combined with hypomethylating agents (HMAs) in relapsed/refractory AML patients, particularly for those who were not exposed to HMA treatment, but most of the other clinical trials did not achieve a satisfactory response when using ICIs alone (15–19). One of the reasons for this discrepancy may be that the patients involved in those trials often experienced failure with multiple lines of conventional therapy, which could have a long-term impact on immunological fitness and clinical responses (20, 21). Therefore, comparing the immune status of T cells in AML patients before and after chemotherapy may help determine which type of patient could benefit from novel immune therapies. Additionally, cancer cells can orchestrate surrounding cells, such as regulatory T cells (Tregs), myeloid-derived suppressor cells (MDSCs), and plasmacytoid dendritic cells (pDCs), to construct an immunosuppressive tumor microenvironment (TME), enabling immune evasion and immunotherapy resistance (22, 23). In the BM, which is the nest of the leukemia progenitors generated and output in AML, the environment is quite complicated and resembles that of the TME in solid tumors to some degree. For example, the BM of AML patients also accumulates Treg, MDSC, and pDC cells that could inhibit the anti-leukemia immune response of T cells (24–27). Increasing evidence has shown that the BM immune environment of AML patients is profoundly altered, contributing to the severity of the disease; however, there have been limited studies comparing differences in T cell dysfunction between PB and BM. Thus, further elucidating the characteristics of the immune microenvironment in the BM of AML patients may help guide the use of immunotherapy drugs and facilitate the exploration of new immune targets.

PD-1, CTLA-4, and Tim-3 are the most well-studied IC proteins, and multiple other IC proteins are also targeted by immune checkpoint blockades or agonists in clinical research, such as lymphocyte activation Gene-3 (LAG-3), T cell immunoreceptor with immunoglobulin, and ITIM domain (TIGIT), and tumor necrosis factor receptor (OX40) (28–31). TIGIT, which is express on activated T cells, Treg cells, and NK cells, has been identified as a promising new target for cancer immunotherapy in recent years (2, 3, 7, 28, 32–34). Previously, high expression of PD-1 and TIGIT on PB T cells from AML patients has been reported (33, 35, 36), and higher PD-1 expression also detected on BM T cells in our previous study (37); however, how the expression of TIGIT and its co-expression with PD-1 changes in the BM of *de novo* (DN) AML patients remains unknown. Thus, we comprehensively compared the single and dual expression of PD-1 and TIGIT in both PB and BM T cells from AML patients at initial diagnosis. In addition, since ICI treatment typically used for patients with relapsed-refractory (R/R) disease, it is necessary to check the fitness of T cells from patients who have received chemotherapy. Thus, we also analyzed the expression of PD-1 and TIGIT in the PB and BM of AML patients at completed remission (CR) and disease relapse after chemotherapy.

MATERIALS AND METHODS

Sample Collection and Preparation

A total of 38 PB samples and 32 BM samples from *de novo* AML patients [(median age, range), (PB: 54.5, 11-88; BM: 57.5, 14-80)] were collected, including 26 paired samples. A total of 17 PB samples and 21 BM samples from AML patients who achieved CR (PB: 46, 13-80; BM: 47, 13-73) were collected, including 16 paired samples. A total of 10 PB samples and 8 BM samples from AML patients with relapsed-refractory disease (PB: 51, 23-80; BM: 49, 23-67) were collected, including 6 paired samples. All of

the patients included in our CR and R/R cohorts are transplant-naïve patients. In addition, 36 PB samples from healthy donors (53, 13-65), and 14 unpaired BM samples from hematopoietic stem cell transplantation donors or iron deficiency anemia patients (47, 17-68) underwent bone marrow aspiration served as the control group. Sample details shown in **Table 1**. All samples collected with informed consent. Ethical approval for the study was obtained from the Ethics Committee of the First Affiliated Hospital of Jinan University. All procedures were conducted according to the guidelines of the Medical Ethics Committees of the Health Bureau of the Guangdong Province in China. All samples were freshly obtained and subjected to immediate preparation.

Flow Cytometry Analysis

Cell surface staining for flow cytometry was performed using the following antibodies: CD45-BUV395 (clone HI30, BD), CD3-AF700 (clone UCHT1, BD), CD4-APC-H7 (clone RPA-T4, BD), CD8-APC-H7 (clone SK1, BD), TIGIT-PE/Dazzle™ 594 (clone A15153G, Biolegend), TIGIT-BV421 (clone A15153G, Biolegend), and PD1-BV421 (clone EH12.2H7, Biolegend). These antibodies were used to analyze surface receptors in two different panels. Isotype-matched antibodies, labeled with the proper fluorochromes, were used as negative controls. Extracellular staining was performed according to the manufacturer's instructions. Briefly, an antibody cocktail was added to whole blood or BM samples, which were then incubated at room temperature for 15 minutes in the dark, followed by red cell lysis with lysis buffer (BD; Cat: 555899). The lysed cells were washed twice with phosphate buffer saline (PBS), and then 350 µl stain buffer was added for further flow cytometer analysis. Twenty microliters of absolute count microsphere (Thermo; Cat: C36950) were added to the samples for absolute number analysis. Cells were analyzed using a BD Fortessa flow cytometer (BD Biosciences), and data analysis performed with Flowjo 10.6 software.

Statistical Analysis

Data were analyzed by correlation, linear regression, independent t-test, or paired t-test depending on the experimental design. Calculations were performed using GraphPad Prism, version 8.02 software. Significance is indicated as $*p < 0.05$, $**p < 0.01$, $***p < 0.001$, $****p < 0.0001$. Values of $p < 0.05$ were considered significant.

RESULTS

The Distribution of PD-1 and TIGIT in the PB and BM of AML Patients During Diagnosis, Complete Remission, and in Relapsed-Refractory Patients

We first compared the PD-1 and TIGIT expression frequency on $CptD4^+$ and $CD8^+$ T cells from the PB and BM of AML patients in the DN, CR, and R/R stages. The results demonstrated that PD-1 expression increased on both PB $CD4^+$ (20.63% *vs* 15.86%, p=0.029) and $CD8^+$ (24.77% *vs* 17.49%, p=0.011) T cells in DN patients when compared with healthy individuls (HIs), while the same result was found when comparing the BM $CD4^+$ (26.17% *vs* 18.48%, p=0.010) and $CD8^+$ (41.17% *vs* 21.68%, p=0.0003) T cell populations. When patients achieved CR, we found that PD-1 expression recovered in most T cell populations except for the PB $CD8^+$ population (27.00% *vs* 17.49%, p=0.014). In addition, we also detected higher PD-1 expression on PB $CD4^+$ (23.22% *vs* 15.86%, p=0.023) and $CD8^+$ (26.84% *vs* 17.49%, p=0.021) T cells as well as BM $CD8^+$ (37.14% *vs* 21.68%, p=0.018) T cells from R/R patients when compared with HIs (**Figure 1A**). Unlike the high expression of PD-1 on both PB and BM T cells in DN AML patients, TIGIT expression was increased only in the BM $CD8^+$ (59.18% *vs* 38.69%, p=0.003) T cell population. Interestingly, the expression of TIGIT was also higher in the BM $CD8^+$ population from CR (55.08% *vs* 38.69%, p=0.002) and R/R (65.94% *vs* 38.69%, p<0.0001) patients compared

TABLE 1 | Clinical characteristics of HIs and AML patients.

Variables	HIs		DN AML		CR AML		R/R AML	
	PB	BM	PB	BM	PB	BM	PB	BM
Number	36	14	38	32	17	21	10	8
Age (years)	53	47	54.5	57.5	46	47	50	49
median, range	(13-84)	(17-68)	(11-88)	(14-80)	(13-80)	(13-73)	(23-80)	(23-67)
Gender, M/F	19/17	6/8	17/21	18/14	10/7	10/11	5/5	5/3
WBC ($\times10^9$/L), mean ± SD	/	/	54.92 ± 135.16	/	4.60 ± 1.77	/	9.29 ± 16.37	/
PLT ($\times10^9$/L), mean ± SD	/	/	81.95 ± 143.85	/	193.69 ± 133.46	/	71.00 ± 58.68	/
Blasts (%) mean ± SD,	/	/	/	63.15 ± 20.03	/	1.64 ± 2.09	/	25.59 ± 27.32
Paired sample (n)	2		27		16		6	
Subtype(n, %)								
MDS-T			3 (7.9%)	2 (6.3%)	1 (5.9%)	1 (4.8%)	2 (20%)	3 (37.5%)
M1			1 (2.6%)	0 (0.0%)	0 (0.0%)	0 (0.0%)	0 (0.0%)	0 (0.0%)
M2			13 (34.2%)	11 (34.4%)	5 (29.4%)	8 (38.1%)	1 (10%)	0 (0.0%)
M3			2 (5.3%)	4 (12.5%)	4 (23.5%)	4 (19.0%)	0 (0.0%)	0 (0.0%)
M4			6 (15.8%)	5 (15.6%)	1 (5.9%)	1 (4.8%)	3 (30%)	3 (37.5%)
M5			11 (28.9%)	9 (28.1%)	5 (29.4%)	4 (23.8%)	2 (20%)	3 (37.5%)
Unclassified			2 (5.3%)	1 (3.1%)	1 (5.9%)	2 (9.52%)	2 (20%)	3 (37.5%)

M/F, male/female; WBC, white blood cell; PLT, platelets; n, number; MDS-T, myelodysplastic syndrome transformed.

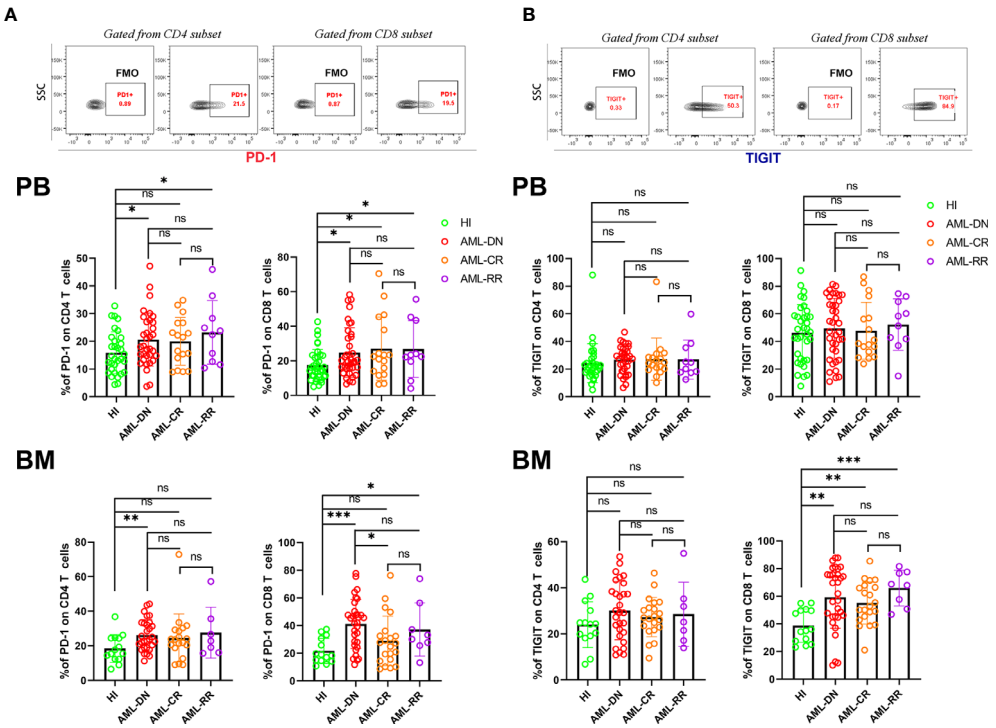

FIGURE 1 | T cells from the PB and BM of DN AML and R/R AML patients generally have high expression of PD-1, and BM CD8$^+$ T cells from DN, CR, and R/R patients have increased TIGIT expression. **(A)** The top figure shows the gating strategy for PD-1 in the CD4$^+$ and CD8$^+$ populations by flow cytometry. The frequency of PD-1 by subset in the PB of HIs (CD4, n=33; CD8, n=36) and patients in the AML-DN (CD4, n=34; CD8, n=38), AML-CR (n=17), and AML-R/R (n=10) cohorts (*Upper*); The frequency of PD-1 by subset in the BM of HIs (n=14), and patients in the AML-DN (CD4, n=29; CD8, n=32), AML-CR (n=21), and AML-R/R (CD4, n=7; CD8, n=8) cohorts (*Lower*). The PD-1 expression frequency generally increased in T cells from DN and R/R patients. **(B)** The top figure shows the gating strategy for TIGIT in the CD4$^+$ and CD8$^+$ populations by flow cytometry. The frequency of TIGIT by subset in the PB (*Upper*) and BM of HIs, and patients in the AML-DN, AML-CR, and AML-R/R cohorts (*Lower*); The TIGIT expression frequency increased in BM CD8$^+$ T cells from DN, CR, and R/R patients compared with HIs. The *p* values shown are from independent t-tests between groups. **p* < 0.05, ***p* < 0.01, ****p* < 0.001, ns denotes not significant.

with HIs (**Figure 1B**). The above results indicated that higher expression of PD-1 in PB and BM T cells is a characteristic of patients with DN AML and might be a sign of disease relapse, while PD-1 expression recovery might be a favorable signal of disease remisson. Whether PD-1 expression could predict the prognosis or survival of AML patients needs to be confirmed in a future study.

Age Correlation of PD-1 and TIGIT Expression on PB and BM T Cells

TIGIT was previously reported to have increased expression in blood T cells of elderly healthy individuals (38); thus, we analyzed the correlation between age and the expression frequency of PD-1 and TIGIT on PB and BM CD4$^+$ and CD8$^+$ T cells in each group. We found that PD-1 had no age correlation with any T cell subset in the HI group; however, in the DN group, the expression of PD-1 on PB and BM CD8$^+$ T cells was positively correlated with age. In addition, the expression of PD-1 on BM CD4$^+$ T cells also demonstrated a trend toward a positive correlation (**Figure 2A**). These results suggest that the expression of PD-1 in elderly AML patients may be even higher than that in young patients, which may weaken the anti-leukemia T cell response of elderly patients. Elderly AML generally defined as AML in a patient who is greater than 60 years of age. Hence, we further compared the expression of PD-1 on CD4$^+$ and CD8$^+$ T cells in the PB and BM of young (< 60 years) and elderly (>= 60 years) AML patients. The results demonstrated that PD-1 is expressed higher on all T cell subsets except for the CD4$^+$ subset in the PB of elderly AML patients (**Figure 2B**). As shown in **Figure 2A**, there was also no correlation between age and PD-1 expression for any of the T cell subsets in the CR and R/R groups.

Regarding the expression of TIGIT, we found the exact age correlation for its expression on CD4$^+$ and CD8$^+$ T cells in HI PB, which was dramatically evident in the CD8$^+$ population. Additionally, we found that the positive correlation between TIGIT and age in the PB CD4$^+$ T cell population lost in the DN, CR, and R/R groups. In contrast, in the PB CD8$^+$ T cell population, it was diminished in the DN group but recovered in the CR group. Considering the strong age correlation of TIGIT in the PB of HIs, we further dissected the HI, DN, and CR groups into young and elderly cohorts and compared the expression of TIGIT on each subset. The results demonstrated that in the cohorts under age 60, the frequency of TIGIT on the CD4$^+$ T cells of DN AML patients was higher than that on HIs (26.31% *vs* 20.14%, p=0.038); however, there was no difference in other comparisons between AML and HIs in the same age cohorts (**Supplementary Figure 1**). Regarding the

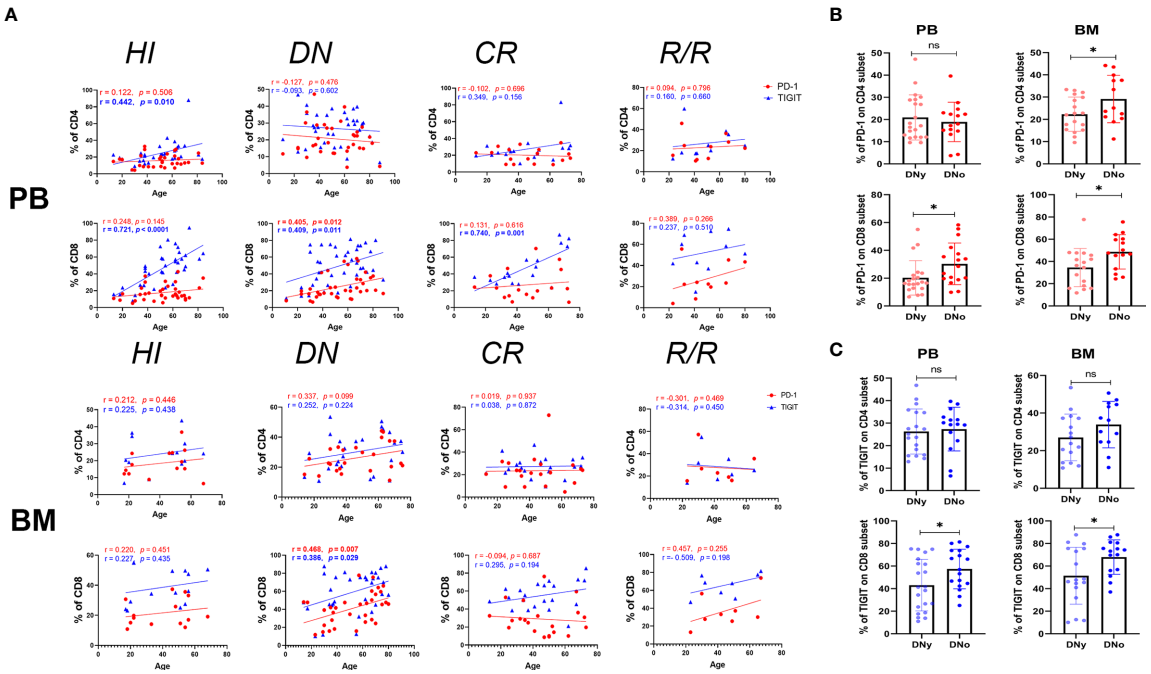

FIGURE 2 | PD-1$^+$ and TIGIT$^+$ CD8$^+$ T cells increase in the BM of older DN-AML patients. **(A)** The upper panel shows the correlation between the frequency of PD-1 (red dots) or TIGIT (blue triangles) and age in the PB CD4$^+$ and CD8$^+$ T cell populations in HIs (CD4, n=33; CD8, n=36) and patients in the AML-DN (CD4, n=34; CD8, n=38), AML-CR (n=17), and AML-R/R (n=10) cohorts; the lower panel shows the correlation between the frequency of PD-1 (the red dots) or TIGIT (blue triangles) and age in the BM CD4$^+$ and CD8$^+$ T cell populations in HIs (n=14) and patients in the AML-DN (CD4, n=29; CD8, n=32), AML-CR (n=21), and AML-R/R (CD4, n=7; CD8, n=8) cohorts. Spearman's nonparametric test used to test for correlations between each group. **(B)** Comparison of the expression of PD-1 on CD4$^+$ and CD8$^+$ T cells from the PB of DNy (CD4, n=19; CD8, n=21) and DNo (CD4, n=15; CD8, n=17) (younger and older than 60 years) patients (Left) from the BM of DNy (CD4, n=16; CD8, n=17) and DNo (CD4, n=13; CD8, n=15) patients (Right). **(C)** Comparison of the expression of TIGIT on CD4$^+$ and CD8$^+$ T cell subsets from the PB and BM of DNy and DNo AML patients. The sample cases used for TIGIT are the same as those used for the PD-1 comparison. The *p* values shown in B and C are from the independent student's t-test. *$p < 0.05$, ns denotes not significant.

expression of TIGIT on HI BM T cells, there was no age correlation found in either the CD4$^+$ or CD8$^+$ population, but a significant age correlation was found for the DN AML group (**Figure 2A**). Further analysis revealed that the frequency of TIGIT in the CD8$^+$ population in BM was higher in elderly *vs.* younger DN AML patients (**Figure 2C**).

In summary, we found that the frequency of PD-1 expression on T cells in HIs had no age correlation in PB or BM; however, strikingly, there was higher PD-1 expression in elderly AML patients. Moreover, the above results confirmed that the expression of TIGIT on T cells is closely correlated with age in PB but not BM. However, higher TIGIT expression is still detected in the CD4$^+$ population of DN patients under 60 years. In addition, relatively higher TIGIT expression was also detected in the BM CD8$^+$ T cell subset of elderly DN patients.

Higher PD-1 and TIGIT Expression Detected in the BM of DN and R/R AML Patients

Previous studies have found that the leukemia BM microenvironment possesses several immune suppressive factors that may protect malignant hematopoietic stem cells from immunological surveillance. We and others have also reported that PD-1 increased in BM CD8$^+$ T cells from DN AML patients, which may promote immune evasion for leukemia cells in the BM (36, 37, 39, 40). In this study, we further compared the expression of PD-1 and TIGIT in paired PB and BM from DN, CR, and R/R patients. The results demonstrated that both the CD4$^+$ and CD8$^+$ T cell subsets in the BM of DN AML patients possessed a higher percentage of PD-1 (**Figure 3A**) and TIGIT (**Figure 3B**) when compared with corresponding PB, and the increase in the CD8$^+$ population was most apparent. In addition, the above differences did not exist for CR patients and remained in the CD8$^+$ population for R/R patients. These results indicate that the BM microenviroment of AML patients possesses an increased number of immunosupressive factors compared with PB, and reviving the immunosupressive microenviroment might be a key factor for treating AML and preventing relapse.

Higher Co-Expression of PD-1 and TIGIT was Detected in the DN and R/R AML Cohorts, and DN-AML Patients Accumulated More PD-1$^+$TIGIT$^+$ CD8$^+$ T Cells in BM Than PB

Co-expression of several IC proteins is a characteristic of exhausted T cells. A high percentage of PD-1$^+$TIGIT$^+$CD8$^+$

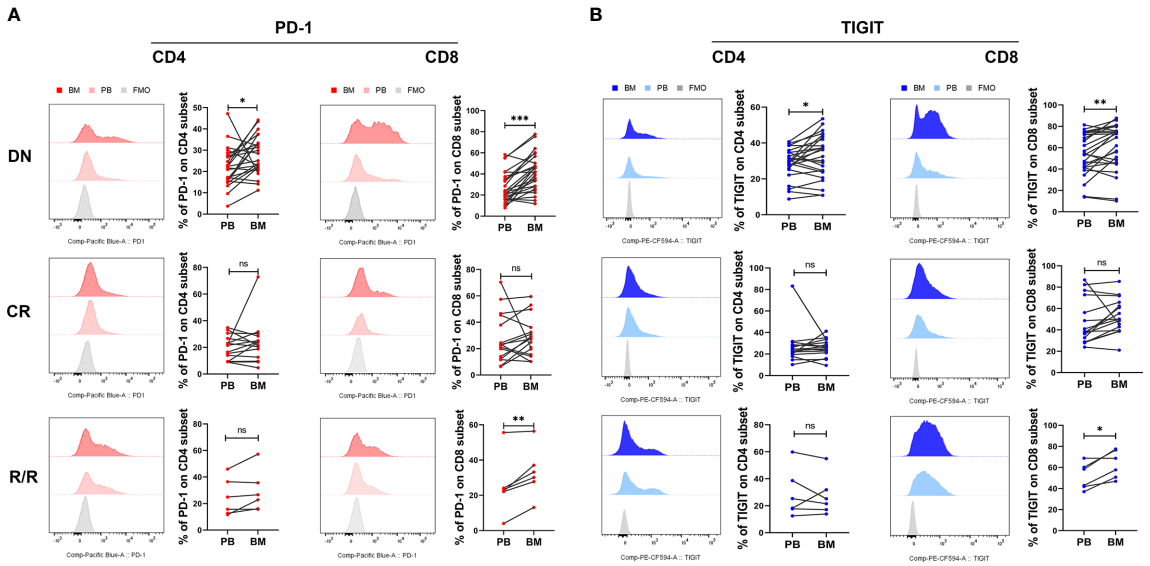

FIGURE 3 | BM CD4$^+$ and CD8$^+$ T cells from DN-AML and R/R-AML patients have a higher percentage of PD-1- and TIGIT-expressing T cells than matched PB. **(A)** The flow-cytometry analysis detected an increase in the frequency of PD-1-expressing CD4$^+$ and CD8$^+$ T cells in the BM of DN-AML patients compared with matched PB (CD4, n=24; CD8, n=27); the expression of PD-1 on CD4$^+$ and CD8$^+$ T cells between PB and BM was not different in the CR-AML cohort (CD4, n=15; CD8, n=16). Increased PD-1 expression was also detected in BM CD8$^+$ T cells from R/R patients (n=6). **(B)** Flow-cytometry analysis detected an increased frequency of TIGIT-expressing CD4$^+$ and CD8$^+$ T cells in the BM of DN-AML patients compared with matched PB (CD4, n=24; CD8, n=27); the expression of TIGIT on CD4$^+$ and CD8$^+$ T cells between PB and BM was not different in the CR-AML cohort (CD4, n=15; CD8, n=16); increased TIGIT expression was also detected in the BM CD8$^+$ T cells of R/R patients (n=6). The *p* values in **(A, B)** were calculated by the paired student's t-test. $^*p < 0.05$, $^{**}p < 0.01$, $^{***}p < 0.001$, ns denotes not significant.

T cells was found in the PB of DN AML patients with the exhaustion phenotype; however, it remains unknown whether they change in the BM and in patients who achieve CR or those with R/R disease. Thus, we further examined the co-expression of PD-1 and TIGIT in the PB and BM of each cohort. As shown in **Figure 4A**, higher co-expression of PD-1 and TIGIT only detected on PB CD4+ T cells from DN patients, while, as shown in **Figure 4B**, higher co-expression detected on PB CD8$^+$ T cells from DN and R/R AML patients but not on the cells in the CR group. However, increased co-expression was also found in the BM CD8$^+$ T cell population of AML patients in all disease conditions. However, statistical significance was found only for DN patients based on the limited CR and R/R patient samples analyzed (**Figure 4B**). We further compared the co-expression of PD-1 and TIGIT between PB and BM in AML patients at different disease stages. We found no significant co-expression difference in the CD4$^+$ population in any of the AML sub-groups (**Figure 4C**, left). In terms of the CD8$^+$ population, higher co-expression was detected in the DN and CR cohorts (**Figure 4C**, right). These results further suggest a more immunosupressive BM microenvironment in AML patients at initial diagnosis and relapse.

DISCUSSION

Previous studies have reported the expression of PD-1 and TIGIT in AML patients at diagnosis and after hematopoietic stem cell transplantation (33, 35–37, 41, 42); however, most of these studies were only concerned about T cells in the PB. Some of these studies ignored the impact of patient age; thus, controversial results exist. In this study, we comprehensively compared the distribution of PD-1 and TIGIT, two of the most well-studied IC proteins in PB and BM T cells from AML patients at different disease stages. The results demonstrated that PD-1 is highly expressed in almost all CD4$^+$ and CD8$^+$ T cells in the PB and BM of DN AML patients and demonstrates higher expression in the elderly than younger patients. Expression in the BM was higher than that in PB. When patients achieve CR after induction chemotherapy, most of T cells can restore the average expression level of PD-1 except for the CD8$^+$ T cells in PB. In addition, patients who were not response to or relapsed from chemotherapy maintained a high expression of PD-1 in most of the T cell subsets except for CD4$^+$ T cells in BM. These results indicated that the function of T cells in elderly patients at first diagnosis might be worse than that in younger patients, which may be a reason for their chemotherapy intolerance, but this may be an advantage for receiving ICI therapy. Although most of the clinical trials using PD-1/PD-L1 inhibitors have been administered to R/R AML patients who experienced intensive induction chemotherapy at least twice (16, 32, 43, 44), a multi-center phase 2 study (NCT02845297) of pembrolizumab (PD-1–blocking antibody) and azacitidine (AZA) in patients with R/R AML and a small cohort of newly diagnosed AML patients (median age and range: 75, 67-83 years) suggested a favorable overall response rate (ORR; 71%) and survival for newly diagnosed and unfit older AML patients.

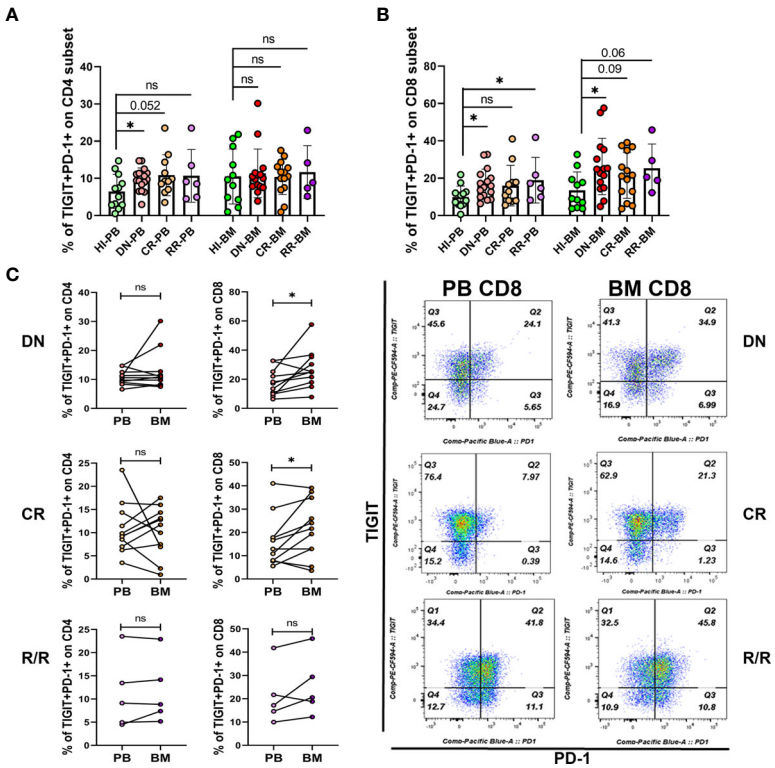

FIGURE 4 | Co-expression of PD-1 and TIGIT is increased in the PB and BM T cells of DN-AML patients. **(A)** Shown is the co-expression of PD-1 and TIGIT in PB and BM CD4$^+$ T cells from HIs (PB, n=12; BM, n=11) and patients in the DN-AML (PB, n=16; BM, n=15), CR-AML (PB, n=11; BM, n=14), and R/R-AML (n=5) cohorts. **(B)** Co-expression of PD-1 and TIGIT in PB and BM CD8$^+$ T cells from HIs and patients in the DN-AML, CR-AML, and R/R-AML cohorts. The cases in the figure are the same as those in the CD4$^+$ population. The *p* values in **(A, B)** were calculated by the independent student's t-test. **(C)** Comparison of PD-1 and TIGIT co-expression between the paired PB and BM CD4$^+$ and CD8$^+$ subsets. Higher co-expression existed in the BM CD8$^+$ T cell from most of the DN-AML and CR-AML patients. The *p* values shown in C were calculated by the paired student's t-test. *$p < 0.05$, ns denotes not significant.

Moreover, this study also found that the AZA/pembro combination is safe, feasible, and well tolerated by these elderly patients (45). Moreover, a higher survival rate when using drugs targeting PD-1 in metastatic melanoma patients between the ages of 70 and 80 was reported in a large population-based Danish patient cohort (1,082 cases) (46). In addition to age, cytogenetic abnormalities are another critical prognostic factor for AML. Thus, analyzing changes in T cell status in patients with different karyotypes and gene mutations is also essential. Previously Williams et al. reported that PD-L1 is higher expressed in BM blasts from patients with *TP53* mutation and also have a higher expression trend in patients with adverse cytogenetics; however, they did not find any correlation between cytogenetic abnormalities and the expression of IC proteins in T cells (36). We also analyzed the expression of PD-1 and TIGIT in patients with or without *FLT3-ITD* mutation and complex karyotype. However, there was no difference to be found in either group (data not shown). To explore the relationship of PD1 and TIGIT expression on T cells with other gene mutations, such as *TP-53* and IDH1/2, would require a larger cohort study in the future.

The high expression of PD-1/PD-L1 is an essential indicator for effective ICI therapy; however, whether sufficient tumor-infiltrating T cells in the tumor microenvironment is also a prerequisite (32). We also analyzed the absolute numbers of T cells in the PB and BM samples included in this study. We found increased numbers of infiltrating T cells in the BM of DN patients, and CR and R/R patients had a lower T cell count in the PB and comparable numbers of T cells in the BM compared with HIs (**Supplementary Figure 2**). These results suggest that the T cells were activated and responded to leukemia antigen stimulation in DN patients. However, most of them may be functionally impaired by expressing IC proteins and other immunosuppressive factors. When receiving induction chemotherapy, most of the T cells were killed simultaneously by the unspecific cytotoxicity of the chemotherapy drugs; thus, there might not be sufficient numbers of T cells to respond to ICI treatment. This reason may be one of the causes for anti-PD-1 treatment without satisfactory effects in R/R patients; however, whether a single anti-PD-1 agent would affect the overall survival (OS) of untreated younger AML patients remains unknown. Recently, a phase 2 study (NCT02464657) using nivolumab combined with induction cytarabine plus idarubicin produced an ORR of 80% and a median OS of 18.54 months in untreated, younger AML patients. Interestingly, responding patients who continued idarubicin, cytarabine, and

nivolumab beyond remission had similar overall survival and event-free survival compared with those bridged to allogeneic stem cell transplantation, suggesting the possibility of nivolumab efficacy in restoring host antitumor immune surveillance. Moreover, the authors also found that a higher prevalence of CD3-positive T cells in the bone marrow before the therapy administration appeared to predict the response (47). This study, combined with our findings here, may shed light on using anti-PD-1 as a single agent or in combination with other drugs for treating DN AML patients, particularly elderly DN AML patients. Previously, two studies also compared the absolute number of T cells in AML patients; one used flow-cytometry and found a higher $CD3^+$ T cell number in the PB of DN AML patients compared with age-matched HIs. The different results reported here may be because we used anti-CD45 to exclude the impact of many leukemia cells in the samples (48). In another study, the authors used immunochemistry to compare the $CD3^+$ T cell number in the BM and found a comparable amount of $CD3^+$ T cells between DN patients and HIs (36). Considering the high sensitivity of flow cytometry in minimal residual disease detection and the greater number of samples analyzed in our study (31 *vs* 14), we believe that our results have higher accuracy. Whether the increased absolute count of T cells in the PB and BM of DN AML patients would predict the outcome and survival of DN AML patients is worth further exploration with a large cohort.

With regards to the expression of TIGIT, we confirmed Yangzi Song's result that the $TIGIT^+$ cell frequencies among PB $CD8^+$ T cells were significant age correlated, whereas $CD4^+$ T cells exhibited exhibited a weak correlation (38). Based on this age-induced change in PB T cells, the different expression of TIGIT in PB T cells between AMLy and AMLo patients is most likely to be a distinction that also exists in the HIy and HIo groups. In 2016, Yaxian Kong had reported that TIGIT expression elevated in the PB $CD8^+$ T cells of AML patients, and high TIGIT was associated with poor clinical outcome in AML (49); however, we only found higher expression of TIGIT on PB $CD4^+$ T cells of DN AML patients compared with HIs in the younger age group and on PB $CD8^+$ T cells in both young and older patients. This inconsistency may arise from the average age of their healthy cohort appears to be younger than that of the AML cohort (51 *vs.* 60). Interestingly, the expression of TIGIT on BM T cells demonstrated no age correlation for HIs. Thus, we speculate that TIGIT function in BM T cells might be different from that in PB. Thus, the elevated TIGIT expression on the BM $CD8^+$ T cells of DN, CR, and R/R patients may be mainly impacted by the leukemia microenvironment itself, while the BM microenvironment of elderly patients may further exacerbate the high expression of TIGIT. Although the immunosupressive functions of TIGIT have been demonstrated many times, whether its high expression on the BM $CD8^+$ T cells of AML patients correlates with prognosis and survival remains to be seen in the future. In addition, further studies should elucidate the functional heterogeneity of $TIGIT^+$ T cells co-expressed with other IC proteins and with its competitive activation receptor CD226, considering the complex mechanisms of TIGIT in suppressing T cell function.

Co-expression of several IC proteins is usually thought to be one of the characteristics of T cell exhaustion. Two previous studies have reported higher dual expression of PD-1 and TIGIT in PB T cells from DN AML patients, and functional experiments supported that $PD\text{-}1^+TIGIT^+$ $CD8^+$ T cells were functionally exhausted (35, 50). In this study, we further found that the percentage of PD-1 and TIGIT double-positive T cells not only increased in PB but also in BM $CD8^+$ T cells from DN AML patients. In addition, it was shown that there was an increase in PB and a trend toward an increase in BM $CD8^+$ T cells in R/R AML patients. All these results indicated that a more immunosuppressive microenvironment might exist in the BM of AML patients. Previously Jia's study found that intracellular expression of Granzyme B in BM $CD8^+$ T cells was significantly lower compared with that of PB, which supports our results (51); however, a study from Lamble et al. reported that there was no significant proliferation difference between BM and PB $CD8^+$ T cells from AML patients (52), which may be due to the high patient-to-patient variability when looking into their data. Such individual differences also existed in our study; thus, to precisely understand the dysfunctional status of BM T cells in each AML patient, a comprehensive assessment of the immune checkpoints expression, cytokine secretion, and proliferation capacity of paired PB and BM samples is needed. In addition, whether these results support the combined use of anti-PD-1 and anti-TIGIT ICIs for treating DN and R/R patients remains to be seen.

Taken together, in addition to the previously reported high expression of PD-1 and co-expression of PD-1 and TIGIT in the PB of DN AML patients and increased PD-1 expression in the BM of DN AML patients, we further identified the accumulation of $TIGIT^+$ $CD8^+$ T cells in the BM of DN, CR, and R/R patients. Moreover, we found a higher percentage of PD-1 and TIGIT co-expressing $CD8^+$ T cells in the BM of DN AML patients. These results support the idea that the BM microenvironment of AML patients possesses many more immunosupressive factors than PB. Future treatment strategies focused on reviving the immunosuppressive BM microenvironment may improve AML patients' survival. Moreover, we also found that increased PD-1 and TIGIT single-positive T cells exist in the PB and BM of older AML patients compared with younger patients, suggesting that T cell function in elderly patients might be even worse than that in younger patients. This finding may partially explain the chemotherapy intolerance of older AML patients, which brings hope for using ICIs to treat DN elderly AML patients who may have sufficient T cells to respond.

DATA AVAILABILITY STATEMENT

The raw data supporting the conclusions of this article will be made available by the authors, without undue reservation.

ETHICS STATEMENT

The studies involving human participants were reviewed and approved by Ethics Committee of the First Affiliated Hospital of

Jinan University. Written informed consent to participate in this study was provided by the participants' legal guardian/next of kin.

AUTHOR CONTRIBUTIONS

YQL and XH contributed to the concept development and study design. LX, LL, DLY, XBZ, YKZ, and SHS performed the laboratory studies. JL, ZYJ, XFZ, RHZ, YHL, MML, and XH collected the clinical samples. LL collected the clinical information of patients. LX and YQL drafted the manuscript. SHC managed the laboratory reagents and financial affairs. LX and YQL helped modify the manuscript. All authors contributed to the article and approved the submitted version.

FUNDING

This study was supported by grants from the National Natural Science Foundation of China (Nos. 82000108, 82070152, 91642111, 81890991, and 81800143), China postdoctoral science foundation (2018M640884), Guangdong Provincial Outstanding Young Medical Talents Supporting Research Foundation (KJ012019459), Guangdong Provincial Natural Science Foundation (2020A1515110310), Guangzhou Science and Technology Project (201807010004 and 201803040017), and Key Laboratory for Regenerative Medicine of Ministry of Education Project (ZSYXM202001).

ACKNOWLEDGMENTS

We would like to acknowledge the Institute of Tumour Pharmacology, College of Pharmacology, College of Pharmacy of Jinan University for providing the flow cytometer for our project. We also would like to thank the healthy volunteers who donated blood or bone marrow for this project.

SUPPLEMENTARY MATERIAL

The Supplementary Material for this article can be found online at: https://www.frontiersin.org/articles/10.3389/fonc.2021.686156/full#supplementary-material

Supplementary Figure 1 | Expression frequency of TIGIT on the PB $CD4^+$ and $CD8^+$ subsets of the HI, DN-AML, and CR-AML cohorts in the young and old age groups. Flow-cytometry analysis shows that the expression frequency of TIGIT increased in the PB $CD4^+$ population of DNy patients when compared with HIy.

Supplementary Figure 2 | The absolute number of $CD3^+$, $CD4^+$, and $CD8^+$ T cells in the PB and BM of the HI and AML cohorts. The total $CD3^+$ T cell number in PB heavily decreased in CR and R/R patients who received induction chemotherapy, and total $CD3^+$ T cells in the BM increased in DN-AML patients when compared with HIs.

REFERENCES

1. Gong J, Chehrazi-Raffle A, Reddi S, Salgia R. Development of PD-1 and PD-L1 Inhibitors as a Form of Cancer Immunotherapy: A Comprehensive Review of Registration Trials and Future Considerations. *J Immunother Cancer* (2018) 6(1):8. doi: 10.1186/s40425-018-0316-z
2. Rotte A. Combination of CTLA-4 and PD-1 Blockers for Treatment of Cancer. *J Exp Clin Cancer Res* (2019) 38(1):255. doi: 10.1186/s13046-019-1259-z
3. Li X, Shao C, Shi Y, Han W. Lessons Learned From the Blockade of Immune Checkpoints in Cancer Immunotherapy. *J Hematol Oncol* (2018) 11(1):31. doi: 10.1186/s13045-018-0578-4
4. Wang JC, Chen C, Kundra A, Kodali S, Pandey A, Wong C, et al. Programmed Cell Death Receptor (PD-1) Ligand (PD-L1) Expression in Philadelphia Chromosome-Negative Myeloproliferative Neoplasms. *Leuk Res* (2019) 79:52–9. doi: 10.1016/j.leukres.2019.02.010
5. Kohler N, Ruess DA, Kesselring R, Zeiser R. The Role of Immune Checkpoint Molecules for Relapse After Allogeneic Hematopoietic Cell Transplantation. *Front Immunol* (2021) 12:634435. doi: 10.3389/fimmu.2021.634435
6. Kim N, Kim HS. Targeting Checkpoint Receptors and Molecules for Therapeutic Modulation of Natural Killer Cells. *Front Immunol* (2018) 9:2041. doi: 10.3389/fimmu.2018.02041
7. Yu X, Gao R, Li Y, Zeng C. Regulation of PD-1 in T Cells for Cancer Immunotherapy. *Eur J Pharmacol* (2020) 881:173240. doi: 10.1016/j.ejphar.2020.173240
8. Tan J, Chen S, Lu Y, Yao D, Xu L, Zhang Y, et al. Higher PD-1 Expression Concurrent With Exhausted $CD8^+$ T Cells in Patients With De Novo Acute Myeloid Leukemia. *Chin J Cancer Res* (2017) 29(5):463–70. doi: 10.1016/j.exphem.2017.06.190
9. Khanal N, Upadhyay Banskota S, Bhatt VR. Novel Treatment Paradigms in Acute Myeloid Leukemia. *Clin Pharmacol Ther* (2020) 108(3):506–14. doi: 10.1002/cpt.1962
10. Xuan L, Wang Y, Huang F, Fan Z, Xu Y, Sun J, et al. Sorafenib Maintenance in Patients With FLT3-ITD Acute Myeloid Leukaemia Undergoing Allogeneic Haematopoietic Stem-Cell Transplantation: An Open-Label, Multicentre, Randomised Phase 3 Trial. *Lancet Oncol* (2020) 21(9):1201–12. doi: 10.1016/S1470-2045(20)30455-1
11. Cerrano M, Itzykson R. New Treatment Options for Acute Myeloid Leukemia in 2019. *Curr Oncol Rep* (2019) 21(2):16. doi: 10.1007/s11912-019-0764-8
12. Kayser S, Levis MJ. Advances in Targeted Therapy for Acute Myeloid Leukaemia. *Br J Haematol* (2018) 180(4):484–500. doi: 10.1111/bjh.15032
13. Perl AE. The Role of Targeted Therapy in the Management of Patients With AML. *Blood Adv* (2017) 1(24):2281–94. doi: 10.1182/bloodadvances.2017009829
14. Bazinet A, Assouline S. A Review of FDA-Approved Acute Myeloid Leukemia Therapies Beyond '7^+3'. *Expert Rev Hematol* (2021) 14(2):185–97. doi: 10.1080/17474086.2021.1875814
15. Giannopoulos K. Targeting Immune Signaling Checkpoints in Acute Myeloid Leukemia. *J Clin Med* (2019) 8(2):236. doi: 10.3390/jcm8020236
16. Daver N, Garcia-Manero G, Basu S, Boddu PC, Alfayez M, Cortes JE, et al. Efficacy, Safety, and Biomarkers of Response to Azacitidine and Nivolumab in Relapsed/Refractory Acute Myeloid Leukemia: A Nonrandomized, Open-Label, Phase II Study. *Cancer Discov* (2019) 9(3):370–83. doi: 10.1158/2159-8290.CD-18-0774
17. Stahl M, Goldberg AD. Immune Checkpoint Inhibitors in Acute Myeloid Leukemia: Novel Combinations and Therapeutic Targets. *Curr Oncol Rep* (2019) 21(4):37. doi: 10.1007/s11912-019-0781-7
18. Przespolewski A, Szeles A, Wang ES. Advances in Immunotherapy for Acute Myeloid Leukemia. *Future Oncol* (2018) 14(10):963–78. doi: 10.2217/fon-2017-0459
19. Gale RP. Will Immune Therapy Cure Acute Myeloid Leukemia? *Blood Sci* (2019) 1: (1):2–3. doi: 10.1097/BS9.0000000000000024
20. Davis JE, Handunnetti SM, Ludford-Menting M, Sharpe C, Blombery P, Anderson MA, et al. Immune Recovery in Patients With Mantle Cell Lymphoma Receiving

Long-Term Ibrutinib and Venetoclax Combination Therapy. *Blood Adv* (2020) 4 (19):4849–59. doi: 10.1182/bloodadvances.2020002810
21. Cooke RE, Quinn KM, Quach H, Harrison S, Prince HM, Koldej R, et al. Conventional Treatment for Multiple Myeloma Drives Premature Aging Phenotypes and Metabolic Dysfunction in T Cells. *Front Immunol* (2020) 11:2153. doi: 10.3389/fimmu.2020.02153
22. Hinshaw DC, Shevde LA. The Tumor Microenvironment Innately Modulates Cancer Progression. *Cancer Res* (2019) 79(18):4557–66. doi: 10.1158/0008-5472.CAN-18-3962
23. Anderson NM, Simon MC. The Tumor Microenvironment. *Curr Biol* (2020) 30(16):R921–5. doi: 10.1016/j.cub.2020.06.081
24. Mendez-Ferrer S, Bonnet D, Steensma DP, Hasserjian RP, Ghobrial IM, Gribben JG, et al. Bone Marrow Niches in Haematological Malignancies. *Nat Rev Cancer* (2020) 20(5):285–98. doi: 10.1038/s41568-020-0245-2
25. Swatler J, Turos-Korgul L, Kozlowska E, Piwocka K. Immunosuppressive Cell Subsets and Factors in Myeloid Leukemias. *Cancers (Basel)* (2021) 13(6):1203. doi: 10.3390/cancers13061203
26. Mu LL, Ke F, Guo XL, Cai JJ, Hong DL. Neoplasms in the Bone Marrow Niches: Disturbance of the Microecosystem. *Int J Hematol* (2017) 105(5):558–65. doi: 10.1007/s12185-017-2193-5
27. Zhu L, Wang P, Zhang W, Li Q, Xiong J, Li J, et al. Plasmacytoid Dendritic Cell Infiltration in Acute Myeloid Leukemia. *Cancer Manag Res* (2020) 12:11411–9. doi: 10.2147/CMAR.S260825
28. Rodriguez-Abreu D, Johnson ML, Hussein MA, Cobo M, Patel AJ, Secen NM, et al. Primary Analysis of a Randomized, Double-Blind, Phase II Study of the Anti-TIGIT Antibody Tiragolumab (Tira) Plus Atezolizumab (Atezo) *Versus* Placebo Plus Atezo as First-Line (1L) Treatment in Patients With PD-L1-Selected NSCLC (CITYSCAPE). *J Clin Oncol* (2020) 38: (15_suppl):9503–3. doi: 10.1200/JCO.2020.38.15_suppl.9503
29. Maruhashi T, Sugiura D, Okazaki IM, Okazaki T. LAG-3: From Molecular Functions to Clinical Applications. *J Immunother Cancer* (2020) 8(2):e001014. doi: 10.1136/jitc-2020-001014
30. Curti BD, Kovacsovics-Bankowski M, Morris N, Walker E, Chisholm L. Floyd K Et Al: OX40 Is a Potent Immune-Stimulating Target in Late-Stage Cancer Patients. *Cancer Res* (2013) 73(24):7189–98. doi: 10.1158/0008-5472.CAN-12-4174
31. Wang Z, Chen J, Wang M, Zhang L, Yu L. One Stone, Two Birds: The Roles of Tim-3 in Acute Myeloid Leukemia. *Front Immunol* (2021) 12:618710. doi: 10.3389/fimmu.2021.618710
32. Vago L, Gojo I. Immune Escape and Immunotherapy of Acute Myeloid Leukemia. *J Clin Invest* (2020) 130(4):1552–64. doi: 10.1172/JCI129204
33. Zhu L, Kong Y, Zhang J, Claxton DF, Ehmann WC, Rybka WB, et al. Blimp-1 Impairs T Cell Function *via* Upregulation of TIGIT and PD-1 in Patients With Acute Myeloid Leukemia. *J Hematol Oncol* (2017) 10(1):124. doi: 10.1186/s13045-017-0486-z
34. Catakovic K, Gassner FJ, Ratswohl C, Zaborsky N, Rebhandl S, Schubert M, et al. TIGIT Expressing $CD4^+$T Cells Represent a Tumor-Supportive T Cell Subset in Chronic Lymphocytic Leukemia. *Oncoimmunology* (2017) 7(1): e1371399. doi: 10.1080/2162402X.2017.1371399
35. Wang M, Bu J, Zhou M, Sido J, Lin Y, Liu G, et al. $Cd8(^+)$T Cells Expressing Both PD-1 and TIGIT But Not CD226 Are Dysfunctional in Acute Myeloid Leukemia (AML) Patients. *Clin Immunol* (2018) 190:64–73. doi: 10.1016/j.clim.2017.08.021
36. Williams P, Basu S, Garcia-Manero G, Hourigan CS, Oetjen KA, Cortes JE, et al. The Distribution of T-Cell Subsets and the Expression of Immune Checkpoint Receptors and Ligands in Patients With Newly Diagnosed and Relapsed Acute Myeloid Leukemia. *Cancer* (2019) 125(9):1470–81. doi: 10.1002/cncr.31896
37. Tan J, Yu Z, Huang J, Chen Y, Huang S, Yao D, et al. Increased PD-1^+Tim-3^+ Exhausted T Cells in Bone Marrow may Influence the Clinical Outcome of Patients With AML. *Biomark Res* (2020) 8:6. doi: 10.1186/s40364-020-0185-8
38. Song Y, Wang B, Song R, Hao Y, Wang D, Li Y, et al. T-Cell Immunoglobulin and ITIM Domain Contributes to CD8(+) T-Cell Immunosenescence. *Aging Cell* (2018) 17(2):e12716. doi: 10.1111/acel.12716
39. Zeidner JF, Knaus HA, Zeidan AM, Blackford AL, Montiel-Esparza R, Hackl H, et al. Immunomodulation With Pomalidomide at Early Lymphocyte Recovery After Induction Chemotherapy in Newly Diagnosed AML and High-Risk MDS. *Leukemia* (2020) 34(6):1563–76. doi: 10.1038/s41375-019-0693-4
40. Zhao E, Xu H, Wang L, Kryczek I, Wu K, Hu Y, et al. Bone Marrow and the Control of Immunity. *Cell Mol Immunol* (2012) 9(1):11–9. doi: 10.1038/cmi.2011.47
41. Knaus HA, Berglund S, Hackl H, Blackford AL, Zeidner JF, Montiel-Esparza R, et al. Signatures of $CD8^+$ T Cell Dysfunction in AML Patients and Their Reversibility With Response to Chemotherapy. *JCI Insight* (2018) 3(21): e120974. doi: 10.1172/jci.insight.120974
42. Schnorfeil FM, Lichtenegger FS, Emmerig K, Schlueter M, Neitz JS, Draenert R, et al. T Cells Are Functionally Not Impaired in AML: Increased PD-1 Expression Is Only Seen at Time of Relapse and Correlates With a Shift Towards the Memory T Cell Compartment. *J Hematol Oncol* (2015) 8:93. doi: 10.1186/s13045-015-0189-2
43. Davids MS, Kim HT, Bachireddy P, Costello C, Liguori R, Savell A, et al. Ipilimumab for Patients With Relapse After Allogeneic Transplantation. *New Engl J Med* (2016) 375(2):143–53. doi: 10.1056/NEJMoa1601202
44. Berger R, Rotem-Yehudar R, Slama G, Landes S, Kneller A, Leiba M, et al. Phase I Safety and Pharmacokinetic Study of CT-011, a Humanized Antibody Interacting With PD-1, in Patients With Advanced Hematologic Malignancies. *Clin Cancer Res Off J Am Assoc Cancer Res* (2008) 14 (10):3044–51. doi: 10.1158/1078-0432.CCR-07-4079
45. Gojo I, Stuart RK, Webster J, Blackford A, Varela JC, Morrow J, et al. Multi-Center Phase 2 Study of Pembroluzimab (Pembro) and Azacitidine (AZA) in Patients With Relapsed/Refractory Acute Myeloid Leukemia (AML) and in Newly Diagnosed (≥65 Years) AML Patients. *Blood* (2019) 134 (Supplement_1):832–2. doi: 10.1182/blood-2019-127345
46. Bastholt L, Schmidt H, Bjerregaard JK, Herrstedt J, Svane IM. Age Favoured Overall Survival in a Large Population-Based Danish Patient Cohort Treated With Anti-PD1 Immune Checkpoint Inhibitor for Metastatic Melanoma. *Eur J Cancer* (2019) 119:122–31. doi: 10.1016/j.ejca.2019.06.022
47. Ravandi F, Assi R, Daver N, Benton CB, Kadia T, Thompson PA, et al. Idarubicin, Cytarabine, and Nivolumab in Patients With Newly Diagnosed Acute Myeloid Leukaemia or High-Risk Myelodysplastic Syndrome: A Single-Arm, Phase 2 Study. *Lancet Haematol* (2019) 6(9):e480–8. doi: 10.1016/S2352-3026(19)30114-0
48. Le Dieu R, Taussig DC, Ramsay AG, Mitter R, Miraki-Moud F, Fatah R, et al. Peripheral Blood T Cells in Acute Myeloid Leukemia (AML) Patients at Diagnosis Have Abnormal Phenotype and Genotype and Form Defective Immune Synapses With AML Blasts. *Blood* (2009) 114(18):3909–16. doi: 10.1182/blood-2009-02-206946
49. Kong Y, Zhu L, Schell TD, Zhang J, Claxton DF, Ehmann WC, et al. T-Cell Immunoglobulin and ITIM Domain (TIGIT) Associates With $CD8^+$ T-Cell Exhaustion and Poor Clinical Outcome in AML Patients. *Clin Cancer Res Off J Am Assoc Cancer Res* (2016) 22(12):3057–66. doi: 10.1158/1078-0432.CCR-15-2626
50. Zhang RJ, Zhai JH, Zhang ZJ, Yang LH, Wang MF, Dong CX. Hypomethylating Agents for Elderly Patients With Acute Myeloid Leukemia: A PRISMA Systematic Review and Meta-Analysis. *Eur Rev Med Pharmaco* (2021) 25(6):2577–90. doi: 10.26355/eurrev_202103_25421
51. Jia B, Wang L, Claxton DF, Ehmann WC, Rybka WB, Mineishi S, et al. Bone Marrow CD8 T Cells Express High Frequency of PD-1 and Exhibit Reduced Anti-Leukemia Response in Newly Diagnosed AML Patients. *Blood Cancer J* (2018) 8(3):34. doi: 10.1038/s41408-018-0069-4
52. Lamble AJ, Kosaka Y, Laderas T, Maffit A, Kaempf A, Brady LK, et al. Reversible Suppression of T Cell Function in the Bone Marrow Microenvironment of Acute Myeloid Leukemia. *Proc Natl Acad Sci USA* (2020) 117(25):14331–41. doi: 10.1073/pnas.1916206117

Conflict of Interest: Author YKZ was employed by company Tianhe Nuoya Bio-Engineerinig Co. Ltd.

The remaining authors declare that the research was conducted in the absence of any commercial or financial relationships that could be construed as a potential conflict of interest.

Publisher's Note: All claims expressed in this article are solely those of the authors and do not necessarily represent those of their affiliated organizations, or those of

the publisher, the editors and the reviewers. Any product that may be evaluated in this article, or claim that may be made by its manufacturer, is not guaranteed or endorsed by the publisher.

frontiers in Oncology

ORIGINAL RESEARCH
published: 23 August 2021
doi: 10.3389/fonc.2021.709543

Ascorbate Inhibits Proliferation and Promotes Myeloid Differentiation in *TP53*-Mutant Leukemia

Carlos C. Smith-Díaz[1], *Nicholas J. Magon*[1], *Judith L. McKenzie*[2], *Mark B. Hampton*[1], *Margreet C. M. Vissers*[1] *and Andrew B. Das*[1*†]

[1] Centre for Free Radical Research, Department of Pathology and Biomedical Science, University of Otago, Christchurch, New Zealand, [2] Haematology Research Group, Christchurch Hospital and Department of Pathology and Biomedical Science, University of Otago, Christchurch, New Zealand

OPEN ACCESS

Edited by:
Charles De Bock,
Children's Cancer Institute Australia, Australia

Reviewed by:
Luisa Cimmino,
University of Miami, United States
Heather Lee,
The University of Newcastle, Australia

***Correspondence:**
Andrew B. Das
Andrew.Das@otago.ac.nz

†Present address:
Andrew B. Das,
Peter MacCallum Cancer Research Centre, Melbourne, VIC, Australia

Specialty section:
This article was submitted to Hematologic Malignancies, a section of the journal Frontiers in Oncology

Received: 14 May 2021
Accepted: 02 August 2021
Published: 23 August 2021

Citation:
Smith-Díaz CC, Magon NJ, McKenzie JL, Hampton MB, Vissers MCM and Das AB (2021) Ascorbate Inhibits Proliferation and Promotes Myeloid Differentiation in TP53-Mutant Leukemia. Front. Oncol. 11:709543. doi: 10.3389/fonc.2021.709543

Loss-of-function mutations in the DNA demethylase TET2 are associated with the dysregulation of hematopoietic stem cell differentiation and arise in approximately 10% of *de novo* acute myeloid leukemia (AML). *TET2* mutations coexist with other mutations in AML, including *TP53* mutations, which can indicate a particularly poor prognosis. Ascorbate can function as an epigenetic therapeutic in pathological contexts involving heterozygous *TET2* mutations by restoring *TET2* activity. How this response is affected when myeloid leukemia cells harbor mutations in both *TET2* and *TP53* is unknown. Therefore, we examined the effects of ascorbate on the SKM-1 AML cell line that has mutated *TET2* and *TP53*. Sustained treatment with ascorbate inhibited proliferation and promoted the differentiation of these cells. Furthermore, ascorbate treatment significantly increased 5-hydroxymethylcytosine, suggesting increased TET activity as the likely mechanism. We also investigated whether ascorbate affected the cytotoxicity of Prima-1^{Met}, a drug that reactivates some p53 mutants and is currently in clinical trials for AML. We found that the addition of ascorbate had a minimal effect on Prima-1^{Met}–induced cytotoxicity, with small increases or decreases in cytotoxicity being observed depending on the timing of treatment. Collectively, these data suggest that ascorbate could exert a beneficial anti-proliferative effect on AML cells harboring both *TET2* and *TP53* mutations whilst not interfering with targeted cytotoxic therapies such as Prima-1^{Met}.

Keywords: epigenetic therapy, differentiation, ascorbate, TET2, Prima-1^{Met}, APR-246, vitamin C, leukemia

INTRODUCTION

Acute myeloid leukemia (AML) is a hematological cancer that harbors a poor prognosis. The disease is highly heterogeneous at the genetic level, with at least 11 distinct subgroups comprising driver mutations in over 100 different genes (1). Epigenetic dysregulation is a key feature of many of these AML subgroups (2, 3). Consequently, therapeutic strategies targeting the mutations that lead to epigenetic dysregulation offer hope for novel forms of treatment.

Ascorbate is an emerging epigenetic therapeutic. This property arises from its co-factor activity for the Fe-containing 2-oxoglutarate-dependent dioxygenases, a large family that includes prolyl hydroxylases (4, 5) numerous histone demethylases (2, 6) and the ten-eleven translocation (TET) enzymes (6–8). The TET proteins are responsible for the active demethylation of DNA *via* the oxidation of 5-methylcytosine (5mC) to 5-hydroxymethylcytosine (5hmC), 5-formylcytosine (5fC), and 5-carboxylcytosine (5caC) (9–11). Ascorbate sustains and promotes TET activity, most likely by reducing Fe^{3+} to Fe^{2+} during the catalytic cycle (8). TET2 activity and cellular levels of 5hmC increase with intracellular ascorbate availability in a dose-dependent manner (12–14). Therefore, ascorbate has the potential to act as an epigenetic therapeutic *via* the stimulation of TET2 activity. This has been demonstrated *in vitro* and using mouse models (3, 15, 16). Furthermore, we have previously reported that supplementation with ascorbate resulted in clinical remission in a patient with AML harboring a *TET2* mutation (17).

TET2 is a major regulator of hematopoiesis, regulating the differentiation and self-renewal of hematopoietic stem cells (HSC) (15). This has been demonstrated in murine studies showing that *Tet2* knockout results in the expansion of the HSC population and skews the peripheral erythrocyte-to-monocyte ratio in favor of increased peripheral monocytes (18). The role of TET2 in hematopoiesis is also evident from the observation that loss-of-function mutations are frequently found in blood disorders such as AML, clonal hematopoiesis of indeterminate potential, chronic myelomonocytic leukemia and myelodysplastic syndrome (19, 20).

TET2 mutations in AML are associated with a significant decrease in 5hmC (21), highlighting the role that this enzyme plays as an epigenetic regulator in hematopoiesis. Emerging insights also suggest that ascorbate supplementation could be beneficial in AML cases associated with decreased *TET2* activity (15, 16). However, *TET2* mutations occur in conjunction with numerous combinations of other mutations (1, 2) and we know relatively little about how other mutations might affect the ascorbate-mediated up-regulation of TET2 activity and subsequent effects on cell differentiation and survival. The epigenetic effects of ascorbate have been explored in some models of leukemia (15, 16, 22–24), but have not been considered in the context of *TP53* and *TET2* mutated AML.

TP53 loss-of-function mutations are of clinical interest as they confer an exceedingly poor prognosis in AML. Three-year survival rates are between 0 – 15% (25) and new treatment options are desperately required. Therefore, we investigated the effects of ascorbate on growth and differentiation using SKM-1 cells - a model of leukemia where both *TET2* and *TP53* mutations co-exist (26). We also investigated the effects of ascorbate in conjunction with Prima-1^{Met} (APR-246), a compound which reactivates some p53 mutants and promotes oxidative stress in cancer cells (27–30). Prima-1^{Met} has been shown to act synergistically with azacitidine to inhibit the proliferation of a number of *TP53*-mutant cell lines, including SKM-1 (31). Given the importance of combination therapy in AML treatment, we investigated the interplay between ascorbate and Prima-1^{Met} to determine whether the antioxidant activity of ascorbate interfered with the cytotoxicity of Prima-1^{Met}.

METHODS

General Cell Culture Methods

SKM-1 cells were provided by the Dawson Lab at the Peter MacCallum Cancer Institute, Melbourne, Australia. These cells were grown in RPMI-1640 medium with penicillin, streptomycin and 10% heat-inactivated fetal bovine serum. Cells were cultured at 37°C with a humidified atmosphere of 5% CO_2. A complete refresh of the media was carried out prior to commencing experiments by centrifugation of the cell suspension, aspiration of media and resuspension in new media.

Validation

SKM-1 DNA was sent for analysis to CellBank Australia, confirming a 98% match between the sample DNA and a reference SKM-1 genome. PCR was used to amplify regions of DNA at the sites of the known *TET2* and *TP53* mutations in the SKM-1 cells. Primers were designed using the Benchling bioinformatics platform. Sanger sequencing at the University of Otago, Dunedin confirmed the presence of a hemizygous *TP53* mutation (c.743G>A, **Supplementary Figure 1**) and a heterozygous *TET2* mutation (c.4253_4254insTT, **Supplementary Figure 2**), consistent with other reports in the literature (26, 31). The 743G>A mutation in *TP53* is a hotspot mutation in patients, translating to a R248Q substitution in the DNA binding domain and is predicted to result in loss-of-function (1). Some studies also suggest that R248Q results in *TP53* gain-of-function attributes (32). The *TET2* mutation results in a frameshift at p.1419 with the truncation of ~600 amino acids. Given that the fundamental 2-OG-dependent dioxygenase domain of TET2 is located at amino acids 1322-2002, this frameshift most likely results in complete loss-of-function (33). Flow cytometry was used to show that the SKM-1 cells were $CD11b^+$, $CD117^+$, $CD13^+$, $CD33^+$, $CD45RA^+$, $CD15^+$, $CD19^-$ and $CD3^-$. The observed cell surface marker data is consistent with data from Deutsche Sammlung von Mikroorganismen und Zellkulturen and reports in the literature (34). In house PCR testing was used to confirm that the SKM-1 cell line was negative for mycoplasma contamination.

Ascorbate and Phosphoascorbate Uptake

Ascorbate or phosphoascorbate was added to SKM-1 cells in a 12-well plate in a final volume of 2 ml containing 0.2 x 10^6 cells/ml and incubated for periods up to 48 hours. At the end of the incubation period, the cells were pelleted by centrifugation at 1000 g for 5 minutes at room temperature and resuspended in PBS. An equal volume of ice cold 0.54 M perchloric acid (PCA) containing 50 μM diethylenetriaminepentaacetic acid (DTPA) was added to supernatant and cell samples. The samples were then mixed by vortex and centrifuged at 12,000 *g* for 2 minutes at 4°C to remove the protein precipitate. Extracted cell lysate and supernatant samples were stored at −20°C and the ascorbate levels were measured using HPLC with electrochemical detection

as previously described (35, 36). Extracts were pre-treated with Tris(2-carboxyethyl)phosphine (TCEP) to reduce any dehydroascorbic acid (DHA) present and the DHA content was determined from the difference between the two measures (35).

Effects of Ascorbate on Cell Proliferation, Cell Cycle and Apoptosis

SKM-1 cells were cultured for 6 days with the addition of sodium ascorbate, bovine liver catalase, and phosphoascorbate (2-phospho-L-ascorbic acid trisodium salt) where indicated. Cells were seeded at 0.2 x 10^6 cells/ml in a volume of 1 ml in a 24-well plate. Ascorbate and phosphoascorbate were added at 0 – 500 μM and catalase at 20 μg/ml. The media was refreshed with a 1:5 dilution at days 2 and 4, with the addition of ascorbate, catalase and phosphoascorbate at the original concentration. The number of cells was recorded after 6 days with a hemocytometer and viability assessed by trypan blue dye exclusion. PI/Annexin V and PI DNA staining were used to assess cell viability/apoptosis and cell cycle status *via* flow cytometry after 6 days with 300 μM ascorbate, with data analysis using CXP Software from Beckman Coulter (Brea, CA, USA).

Analysis of Cell Surface Markers

To assess ascorbate-mediated changes on differentiation, SKM-1 cells were grown for up to 36 days +/- 300 μM phosphoascorbate or ascorbate. Every 2-3 days the medium was refreshed by diluting 1:5 with fresh media and adding phosphoascorbate or ascorbate at the original concentration. At 7, 12/13 days, 22 days and 36 days, cell surface marker expression was analyzed using flow cytometry for CD15, CD33, CD45RA, CD117, CD13, and CD11b. The percentage change in mean fluorescence intensity (MFI) was calculated by taking the ratio of the MFI for the treated cells relative to the control, subtracting 1 and then converting to a percentage. The data was exported using CXP Software. Isotype controls were used to confirm the binding specificity of the antibodies.

Mass Spectrometry Analysis of 5hmC Levels

SKM-1 cells were cultured with 300 μM ascorbate or phosphoascorbate in 12-well plates at 0.4 x 10^6 cells/ml in 2 ml per well for periods up to 4 days. The medium was refreshed by diluting 1:5 in fresh media with the addition of 300 μM ascorbate or phosphoascorbate after 2 days. At the end of the incubation period, the cells were harvested and the DNA was extracted using a DNA extraction kit (DNeasy Blood and Tissue Kit Cat No. 69504, Qiagen, Hilden, Germany).

A stable isotope dilution LC-MS/MS method was used for the detection and quantification of 2'-deoxycytidine, 5-methyl-2'-deoxycytidine and 5-hydroxymethyl-2'-deoxycytidine. Isotopically labeled standards [2'-deoxycytidine (^{13}C, $^{15}N_2$), 5-methyl-2'-deoxycytidine (^{13}C, $^{15}N_2$) and 5-hydroxy-methyl-2'-deoxycytidine (d_3)] were used to control for experimental variations such as recovery, matrix effect, and ionization. Standard calibration curves using the ratio of light to heavy isotopes were used for quantification. One μg of SKM-1 DNA was hydrolyzed using a nucleoside digestion kit M0649S (New England Biolabs, Ipswich, MA, USA) in the presence of internal standards [130 fmoles 2'-deoxycytidine (^{13}C, $^{15}N_2$), 5 fmoles 5-methyl-2'-deoxycytidine (^{13}C, $^{15}N_2$) and 0.013 fmoles 5-hydroxy-methyl-2'-deoxycytidine (d_3)].

Standards and digested SKM-1 DNA samples were analyzed using a 6500 QTrap mass spectrometer (Sciex, Framingham, MA, USA) coupled to an Infinity 1290 LC system (Agilent, Santa Clara, CA, USA). Standards and samples were stored on the autosampler tray at 5°C. An Acclaim RSLC Polar Advantage II 120Å column (150 x 2.1 mm, Thermo Fisher Scientific Inc., Waltham, MA, USA) was used for chromatographic separation using 100% water (0.1% formic acid) as Solvent A and 100% acetonitrile (0.1% formic acid) as Solvent B. A flow rate of 0.2 mL/minute was used. The column temperature was set to 40°C. The analytes were eluted during the initial isocratic phase with 100% Solvent A over 3.5 minutes. The column was then flushed with 5% Solvent A and 95% Solvent B for 2.5 minutes, and then re-equilibrated at initial conditions for 5 minutes. Data were analyzed using Analyst 1.7.1 (Sciex, Framingham, MA, USA). All species were quantified by fragmenting the singly-charged parent ion $[M+H]^+$, monitoring the fragment ion resulting from the loss of the deoxyribose sugar in positive-ion mode (**Table 1**), and measuring the area under the curve of the resulting peak (Fit: Linear, Weighting: None, Regression Parameter: Area). The concentration of deoxycytidine, 5mC and 5hmC in each sample was calculated by relating the peak area ratio of the light to the heavy isotope to standard calibration curves, and then converted to a percentage of the total cytidine species. The assay was validated by measuring the relative composition of cytidine species in frontal cortex and liver tissues (Dunkin Hartley guinea pigs) for comparison. For guinea pig tissue samples, one μg of DNA was hydrolyzed in the presence of 340 fmoles 2'-deoxycytidine (^{13}C, $^{15}N_2$), 10 fmoles 5-methyl-2'-

TABLE 1 | The m/z values for the singly-charged parent and fragment ions and the optimised parameters that were used to quantify each analyte in LC-MS/MS experiments.

Analyte	Parent (m/z)	Fragment (m/z)	DP	EP	CE	CXP
2'-Deoxycytidine (H^+)	228.10	112.05	45	7	15	16
2'-Deoxycytidine (^{13}C, $^{15}N_2$) (H^+)	231.10	115.05	45	7	15	16
5-Methyl-2'-deoxycytidine (H^+)	242.11	126.07	45	7	13	16
5-Methyl-2'-deoxycytidine (^{13}C, $^{15}N_2$) (H^+)	245.11	129.06	45	7	13	16
5-Hydroxy-methyl-2'-deoxycytidine (H^+)	258.11	142.06	50	7	11	16
5-Hydroxy-methyl-2'-deoxycytidine (d_3) (H^+)	261.13	145.08	50	7	11	16

DP, declustering potential; EP, entrance potential; CE, collision energy; CXP, cell exit potential.

deoxycytidine (^{13}C, $^{15}N_2$) and 1.3 fmoles 5-hydroxy-methyl-2'-deoxycytidine (d_3)).

Effects of Prima-1^{Met} and Ascorbate

SKM-1 cells were cultivated in a 24-well plate in 1 ml at a starting concentration of 0.2 x 10^6 cells/ml. Cells were pre-treated with either 300 µM ascorbate or phosphoascorbate for 4 hours before the administration of Prima-1^{Met}. Cell viability was assessed at 24 hours by resuspending the cells in PBS with 20 µg/mL propidium iodide (PI) and analyzed by flow cytometry.

SKM-1 cells were also grown with or without 300 µM ascorbate or phosphoascorbate for 1 week. The cells were seeded at 0.4 x 10^6 cells/ml in 2 ml in a 12-well plate. The media was refreshed with a 1:5 dilution every 2-3 days, with the addition of ascorbate or phosphoascorbate at the original concentration. The cells were then centrifuged at 1000 *g* for 5 minutes and resuspended in fresh media at a cellular concentration of 0.2 x 10^6 cells/ml. The cells were left for 1 hour in the incubator before transfer into a 24-well plate and treatment with Prima-1^{Met}. Cell viability was assessed at 24 hours by resuspending the cells in PBS with 20 µg/mL PI and analyzed by flow cytometry.

Statistical Analysis

The results in this paper are expressed as means ± the standard error of the mean unless indicated otherwise. Prism 9 software (GraphPad, La Jolla, CA, USA) was used for statistical analysis. The ascorbate-mediated inhibition of cell growth and increases in 5hmC levels were analyzed by one-way ANOVAs with Dunnett's multiple comparison post-hoc test. Paired t-tests (2-tailed) were used for comparing the changes in the expression of SKM-1 cell surface proteins and cell viability after growth in ascorbate/phosphoascorbate replete media. Two-way ANOVAs with Tukey's post-hoc tests were used to analyze the combined cytotoxic effect of Prima-1^{Met} and ascorbate/phosphoascorbate, and differences in intracellular ascorbate concentrations. For all tests the statistical significance was set at $p < 0.05$.

Materials

Nucleoside standards were obtained from Toronto Research Chemicals (Toronto, Ontario, Canada). FITC and PE conjugated fluorescent antibodies were obtained from Biolegend (San Diego, CA, USA), CD15 (Cat. 301903), CD33 (Cat. 366619), CD45RA (Cat. 304105), CD117 (Cat. 313203), CD13 (Cat. 301703), CD11b (Cat. 301305), CD3 (Cat. 100203), CD9 (Cat. 312105). The drug Prima-1^{Met} (CAS No: 5291-32-7) was obtained from MedChemExpress, Monmouth Junction, NJ, USA.

RESULTS

Ascorbate and Phosphoascorbate Uptake Dynamics

RPMI cell culture medium does not contain ascorbate, and therefore SKM-1 cells maintained under standard culture conditions lack ascorbate. Following the supplementation of ascorbate to the medium, intracellular ascorbate levels increased in a dose-dependent manner, with levels peaking at 8-24 hours and decreasing again by 48 hours (**Figures 1A, B**). When 300 µM ascorbate was added to the medium, the intracellular levels peaked around 4 nmoles/10^6 cells at 8-24 hours after ascorbate administration, with significant variation between batches of cells. By 48 hours, very little ascorbate remained in the medium,

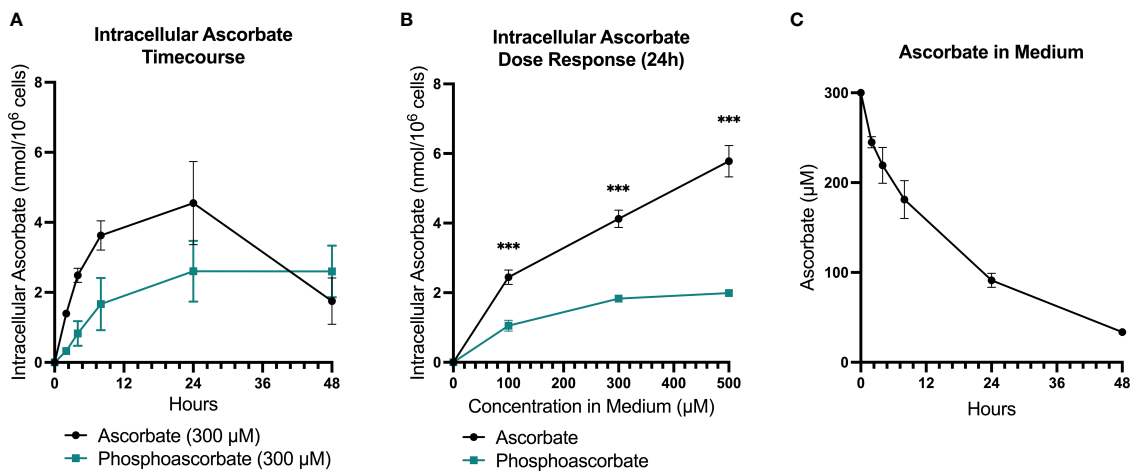

FIGURE 1 | SKM-1 Ascorbate and phosphoascorbate uptake dynamics. The ascorbate content of SKM-1 cells following the addition of varying concentrations of ascorbate or phosphoascorbate to RPMI medium for up to 48 hours. SKM-1 cells were seeded at 0.2 x 10^6 cells/ml in a volume of 2 ml in 12-well plates and were harvested at the times shown. **(A)** The intracellular concentration of ascorbate (n = 6) or phosphoascorbate (n = 3) was measured at different time intervals following the addition of 300 µM ascorbate or phosphoascorbate to the medium. **(B)** Intracellular ascorbate levels at 24 hours following the addition of 0 – 500 µM ascorbate or phosphoascorbate to the medium (n = 3) ***$p < 0.001$, representing a significant difference between the intracellular concentration after ascorbate or phosphoascorbate treatment. **(C)** The ascorbate concentration in the media (containing SKM-1 cells) at different time intervals following the addition of 300 µM ascorbate (n = 3).

although intracellular levels remained around 2 nmol/10^6 cells (**Figures 1A, C**). Most of the cellular ascorbate was present as reduced ascorbate: DHA was estimated to be 5.26 ± 2.4% of the total ascorbate (SEM, n=15), determined by measuring ascorbate with and without pre-treatment of the cell extracts with TCEP.

High ascorbate concentrations in cell culture media result in the generation of extracellular H_2O_2 *via* the reduction of traces of free iron present in solution. This effect can contribute to ascorbate-mediated cytotoxicity in cell culture (37). For this reason, we included controls that mitigated any H_2O_2-induced toxicity by: (i) adding catalase to the medium, or (ii) using the redox-stable molecule phosphoascorbate. Phosphoascorbate is an ascorbate analogue that does not undergo oxidation to DHA and thus circumvents the generation of H_2O_2 in cell culture media (22, 38, 39). When phosphoascorbate was added to the medium instead of ascorbate, SKM-1 intracellular ascorbate levels also increased, but at a slower rate. The maximum intracellular ascorbate concentration after phosphoascorbate administration to the medium was measured at around 2-2.5 nmoles/10^6 cells (**Figures 1A, B**).

Ascorbate Inhibits SKM-1 Cell Proliferation

SKM-1 cell proliferation was significantly decreased when the cells were maintained in ascorbate-replete media for 6 days. With 500 μM ascorbate in the medium, we noted a 75% inhibition of cell growth (**Figure 2A**). When 20 μg/ml catalase was added to the medium to control for the possible contribution of H_2O_2-induced cytotoxicity, cell growth was inhibited in a concentration-dependent manner up to 300 μM ascorbate, with a maximum inhibition of 44% (**Figure 2B**). When phosphoascorbate was added to the medium instead of ascorbate, cell proliferation was decreased at 100 μM, with no further decrease at higher concentrations (**Figure 2C**). Exposure to 300 μM ascorbate for 6 days had no effect on cell viability, apoptosis or the cell cycle (**Figures 3A, B**) and no loss in viability was observed after 28 hours growth in media with 300 μM ascorbate or phosphoascorbate. Furthermore, staining with trypan blue and observation by microscopy indicated that the cells maintained a high degree of viability (between 0-1 trypan blue positive cells per 200 cells). Collectively these data indicate that ascorbate inhibits SKM-1 cell growth without promoting cell death at culture media concentrations between 100 to 300 μM. They also indicate that the inhibition of cell growth is not dependent on H_2O_2 at these concentrations.

Ascorbate Modulates Expression of SKM-1 Cell Surface Proteins

Growth in cell culture media with 300 μM phosphoascorbate promoted changes in cell surface markers consistent with monocytic differentiation (**Figure 4A**). Significant changes in several cell surface proteins were observed, with increases in CD13 (13, 36 days), CD15 (7, 13, 22 days), CD11b (7, 13 days), CD45RA (36 days), and decreases in CD117 (22, 36 days) and CD33 (36 days) (**Figures 4B, C**). Similar changes were also achieved with 300 μM ascorbate at 7 days (**Figure 4C**). The direction of these changes is consistent with monocytic cell differentiation and maturation.

Ascorbate Increases 5hmC Levels

We utilized mass-spectrometry to measure the relative abundance of deoxycytidine, 5mC and 5hmC in untreated cells at 95.5% ± 0.4, 4.5% ± 0.4, 0.003% ± 0.001 of the total cytidine species respectively (average ± SD, n=9). We then observed that

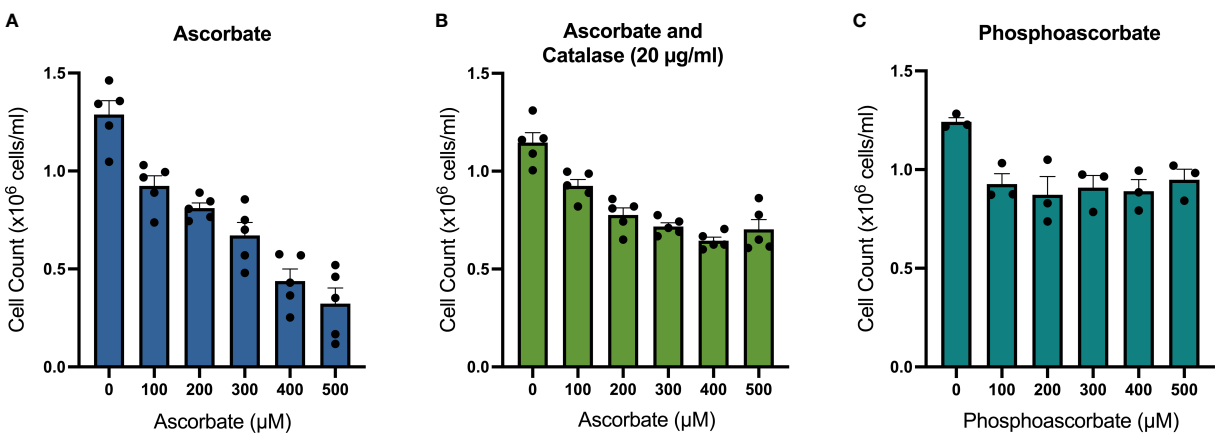

FIGURE 2 | Effect of ascorbate and phosphoascorbate on SKM-1 cell growth. **(A–C)** SKM-1 cell numbers 6 days following treatment with ascorbate (n = 5), ascorbate and catalase (n = 5) or phosphoascorbate (n = 3). Each data point represents the mean of two cells counts recorded with a hemocytometer from two separate wells with the same treatment. The cells were all seeded at a starting concentration of 0.2 x 10^6 cells/ml, with 1:5 dilutions after 2 days and 4 days in cell culture media with re-administration of ascorbate, phosphoascorbate and catalase at the original concentration. The setup of this experiment means that if the cells had not grown at all, then the total cell count after 6 days would be around 8 x 10^3 cells/ml. All treatments resulted in a statistically significant inhibition of cell growth. 100 μM ascorbate +/- catalase $p < 0.01$; 200 - 500 μM ascorbate +/- catalase $p < 0.0001$; 100, 500 μM phosphoascorbate $p < 0.05$; 200 - 400 μM phosphoascorbate $p < 0.01$.

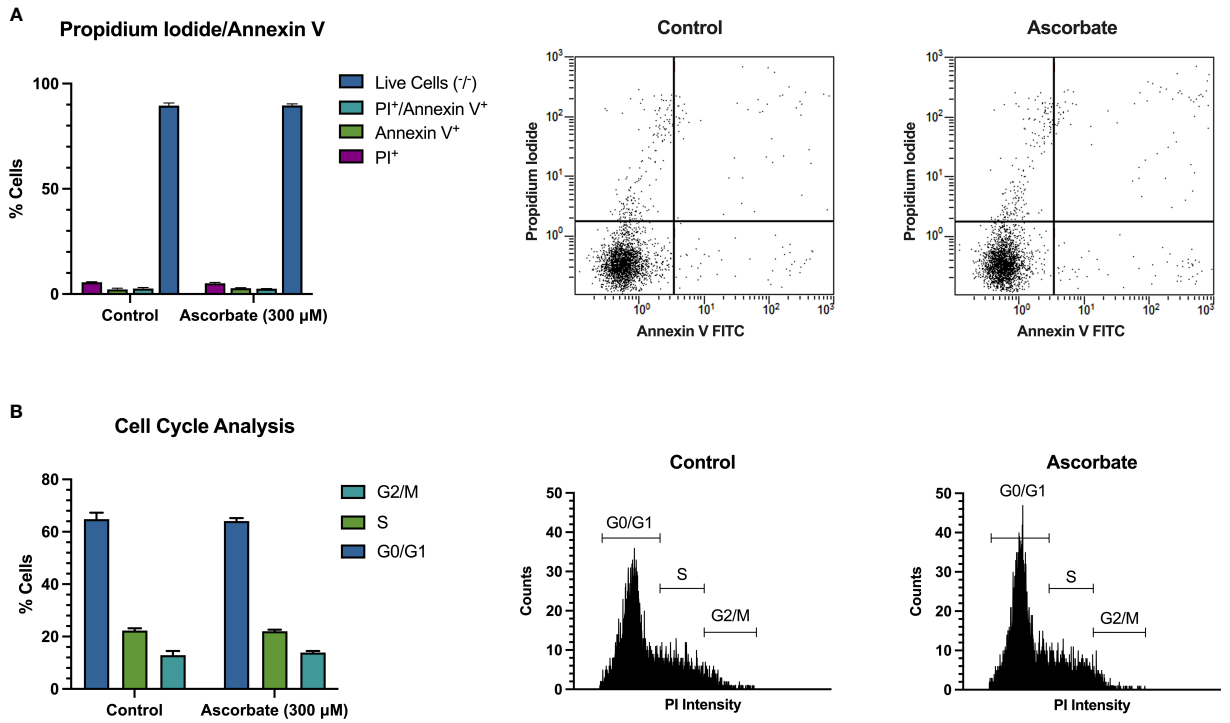

FIGURE 3 | 300 µM ascorbate does not promote cell death or affect the cell cycle. SKM-1 cells were grown for 6 days in media with 300 µM ascorbate. **(A)** Staining with annexin V/FITC and propidium iodide shows that 300 µM ascorbate does not promote cell death or apoptosis (n = 3). **(B)** Cell cycle analysis shows no effect on the cell cycle (n = 3). Representative traces are shown.

the addition of either 300 µM ascorbate or phosphoascorbate to the cell culture media resulted in increased global 5hmC. This effect was time-dependent; culturing the SKM-1 cells with ascorbate or phosphoascorbate for up to 2 days resulted in progressively higher levels of 5hmC (**Figures 5A, B**). After 4 days with phosphoascorbate, 5hmC levels had increased 8-fold relative to untreated cells. Treatment with ascorbate or phosphoascorbate had no observable effect on global methylation in either direction. We observed that SKM-1 5hmC levels, even after growth in media with ascorbate, were still lower than levels measured in tissue samples (**Table 2**).

Effects of Ascorbate on Prima-1^{Met} Induced Cytotoxicity

The addition of 300 µM ascorbate or phosphoascorbate to the culture medium 4 hours prior to the administration of Prima-1^{Met} increased the LC_{50} after 24 hours (**Figure 6A**). In cells pre-incubated with ascorbate or phosphoascorbate for 4 hours the LC_{50} for Prima-1^{Met} was 72 µM and 64 µM respectively whereas the control was 51 µM. However, the reverse effect was observed when cells were grown in ascorbate-replete media for 1 week to induce changes in cell surface differentiation markers, before treatment with Prima-1^{Met} (**Figure 6B**). After 1 week pre-treatment with ascorbate the LC_{50} was 63 µM for the control, 57 µM for ascorbate pre-treated cells and 59 µM for phosphoascorbate pre-treated cells. These differences were small but statistically significant. It is important to note that the LC_{50} differs for the control between the two sets of experiments (51 µM vs 63 µM) which may be due to differences in experimental setup. However, a comparison has been made for each treatment relative to its own control. Overall, ascorbate pre-treatment only exhibited a small influence on Prima-1^{Met} induced cytotoxicity.

DISCUSSION

Dysregulated epigenetics is a known driver of AML (2, 3). Mutations in proteins such as TET2, DNMT, IDH1/2, and WT1 are common in AML, and all affect epigenetic processes (2, 17). Recently, scientists have begun to consider the possibility of employing ascorbate to target epigenetic dysregulation in AML, by harnessing its ability to stimulate TET2 (15, 16). Agathocleous et al. showed that ascorbate availability could affect HSC proliferation and differentiation, demonstrating an increase in HSCs relative to body mass and decreased levels of HSC 5hmC in ascorbate-deficient *Gulo*$^{-/-}$ mice (16). Upon administering ascorbate to a *FLT3*^{ITD} *TET2*$^{+/-}$ *Gulo*$^{-/-}$ murine model of leukemia, overall survival was prolonged and the progression of the disease was suppressed (16). Cimmino et al. also observed that knocking down TET2 with RNAi led to aberrations in the self-renewal capacity of HSC, an effect that was reversed once TET2 activity was restored. The restoration of TET2 activity promoted cell death, myeloid differentiation and

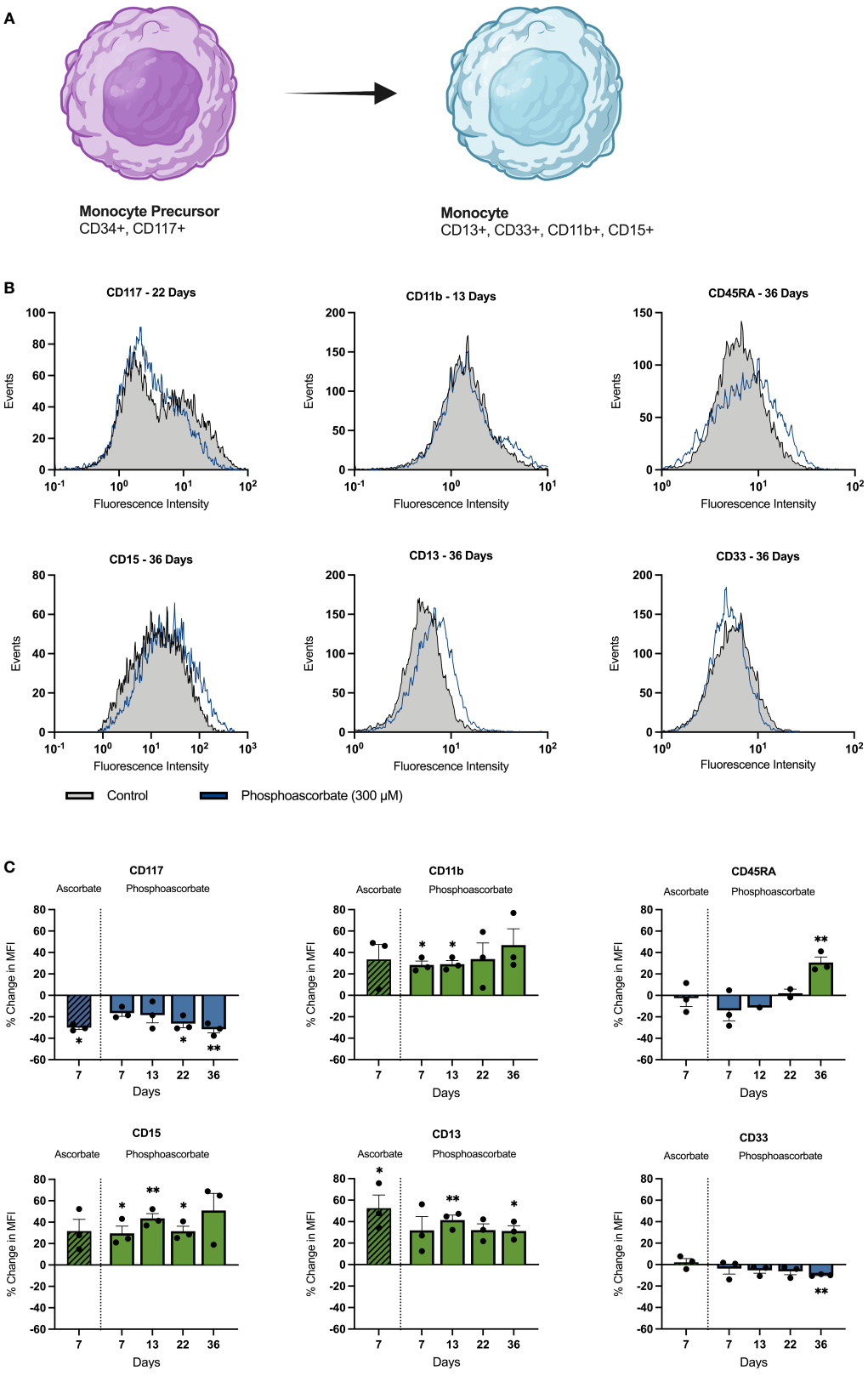

FIGURE 4 | Continued

FIGURE 4 | Ascorbate-induced changes in cell surface antigen expression. **(A)** Changes in cell surface markers associated with monocytic differentiation. Common granulocyte/monocyte precursor cells express immature cell antigens such as CD34 and CD117 which persist up until the monocyte precursor/monoblast differentiation stage. Once these immature cells mature into promonocytes and mature monocytes, CD117 and CD34 expression is lost and the cells begin to express CD15, CD33, CD13 and CD11b along with other characteristic cell surface markers (40). These changes are mirrored by SKM-1 cells following growth in ascorbate-replete media with notable increases in CD15, CD13, CD11b and a decrease in CD177. **(B)** Representative histograms showing shifts in the fluorescence intensity signal for each cell surface marker after treatment with phosphoascorbate, relative to the control. **(C)** Relative changes in cell surface antigen expression following treatment with phosphoascorbate and ascorbate. Measurements are n = 3 except for CD45RA expression, which was measured at n = 1 (at 12 days) and n = 2 (at 22 days). For all other measurements the 13-day timepoint includes one measurement taken at 12 days and two measurements at 13 days. For CD117, when two distinct subpopulations were present, the change in MFI was calculated by gating to select the $CD117^{+}$ subpopulation and calculating the MFI change for this subpopulation. Statistically significant changes are marked as: *p < 0.05, **p < 0.01. Parts of this figure were made using BioRender.com.

DNA demethylation. Moreover, the administration of ascorbate pharmacologically mimicked TET2 restoration (15). These findings suggest that intracellular ascorbate levels are linked to cell differentiation and 5hmC levels.

However, few studies have investigated how additional mutations might affect the TET2-dependent benefit of ascorbate treatment in AML. In a model of AML characterized by *TET2* and *TP53* loss-of-function, we have now shown that ascorbate inhibits proliferation, increases 5hmC and drives cellular differentiation. Ascorbate also had minimal effect on the efficacy of Prima-1^{Met}, a novel cytotoxic reagent currently in clinical trial for AML with *TP53* mutations (31, 42). This is significant given the adverse prognosis associated with *TP53* mutations and the fact that the TP53/complex karyotype subgroup of AML has been identified as comprising 13% of cases (1).

Ascorbate is not generally added to culture media and cultured cells are usually ascorbate deficient (43–45). We observed that supplementing the cell culture medium with ascorbate resulted in rapid uptake into cells and was associated with a significant decrease in proliferation at 6 days. Extended incubation with ascorbate also induced differentiation towards a more mature cell phenotype over a 36-day period. Differentiation is fundamentally an epigenetic process and can be initiated by a variety of cell intrinsic and extrinsic cues. Given that SKM-1 cells carry a heterozygous loss-of-function mutation in the epigenetic eraser *TET2*, we hypothesized that the restoration of TET2 activity was a likely mechanism for these phenotypic changes. Consistent with this hypothesis, we found that treatment with ascorbate increased 5hmC - a proxy for TET activity. These findings highlight the potential for epigenetic therapy in this subtype of leukemia.

In untreated SKM-1 cells, 5hmC levels were very low compared with levels reported in non-cancerous human tissues (46) and the levels we measured in guinea pig frontal cortex and liver samples. This phenomenon has been previously observed in human cell lines and cancers, both of which can have very low levels of 5hmC relative to their tissue of origin (46, 47). For

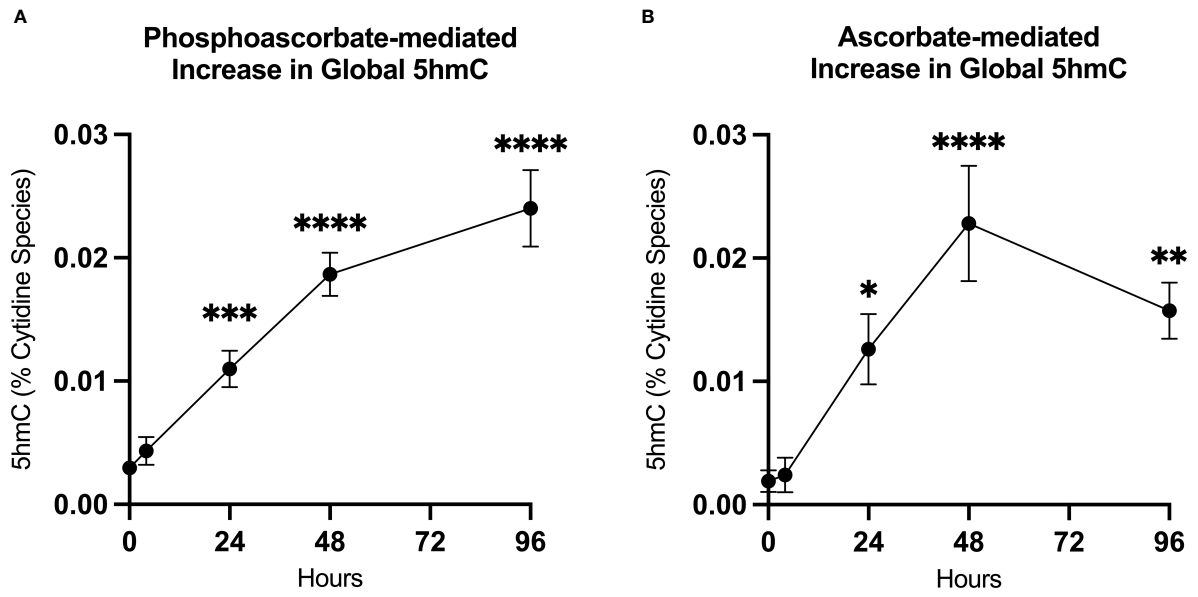

FIGURE 5 | Ascorbate induced changes in 5hmC levels. **(A, B)** Increase in 5hmC in SKM-1 cells following growth in media with 300 μM phosphoascorbate or ascorbate. p-values are displayed for statistically significant increases relative to the control. ****p < 0.0001, ***p < 0.001, **p < 0.01, *p < 0.05. All time points represent at least n = 3 except for ascorbate 4 hours which is n = 2. Treatment with ascorbate or phosphoascorbate had no apparent effect on global methylation.

TABLE 2 | The measured 5mC and 5hmC levels in SKM-1 cells grown with and without ascorbate/phosphoascorbate, and reference tissue samples (average ± SD).

Sample	5mC (% total cytidine species)	5hmC (% total cytidine species)
SKM-1 (n=9)	4.5% ± 0.4	0.003% ± 0.001
SKM-1 (48h phosphoascorbate, n=4)	4.2% ± 0.7	0.019% ± 0.004
SKM-1 (48h ascorbate, n=4)	4.2% ± 0.6	0.023% ± 0.009
Liver (guinea pig, n=4)	3.7% ± 0.7	0.076 ± 0.022
Frontal Cortex (guinea pig, n=4)	4.0% ± 0.3	0.75% ± 0.11

example, in one study, 5hmC levels in healthy colorectal tissue were found to be ~10-fold higher compared with levels in colorectal cancer tissue (47). Moreover, it has been observed that cells may undergo a loss in global 5hmC as they adapt to cell culture conditions (46). The effect may be partially attributed to reduced TET activity in a cell culture environment lacking ascorbate, although Nestor et al. also observed significantly reduced TET expression in human cell lines (46). We observed that supplementing the cell culture media with ascorbate or phosphoascorbate caused a significant increase in 5hmC within 24 hours and an ~8-fold increase in 5hmC after 48 hours growth with ascorbate.

The increased expression of SKM-1 cell surface proteins CD13, CD15, CD11b and decreased expression of CD117 after growth in ascorbate-replete media is consistent with monocytic differentiation (40). CD11b expression increases in the U937 promonocytic cell line following treatment with 12-O-tetradecanoylphorbol-13-acetate to induce cellular differentiation (48). CD117 expression, in contrast, is associated with an immature cell phenotype (40). CD117 is involved in stem cell differentiation and is generally lost as progenitor cells differentiate into mature blood cells, with the exception of dendritic and mast cells (49–51). The significance of the observed decrease in CD33 and increase in CD45RA is less clear. CD33 expression increases in the context of monocytic maturation, however in other cellular contexts, such as neutrophil maturation, a slight decrease in CD33 expression is observed during cellular maturation (40). Overall, the observed changes in cell surface protein expression following growth in ascorbate-replete media are consistent with other findings in the literature. For example, Cimmino et al. reported that reactivating TET2 caused a similar decrease in CD117 expression along with increased CD34 and CD11b expression (15). When the cell surface marker data is considered collectively, the general trend of the changes in surface protein expression points to cellular differentiation and mirrors the changes observed during monocytic differentiation.

The oxidation of ascorbate in solution, and particularly in cell culture media that contain traces of ferrous iron, is known to generate H_2O_2 (3, 52). This can reach cytotoxic levels when ascorbate concentrations approach 1 mM (52–54). We employed two separate strategies to avoid this artefact: we added catalase to the medium to scavenge any extracellular

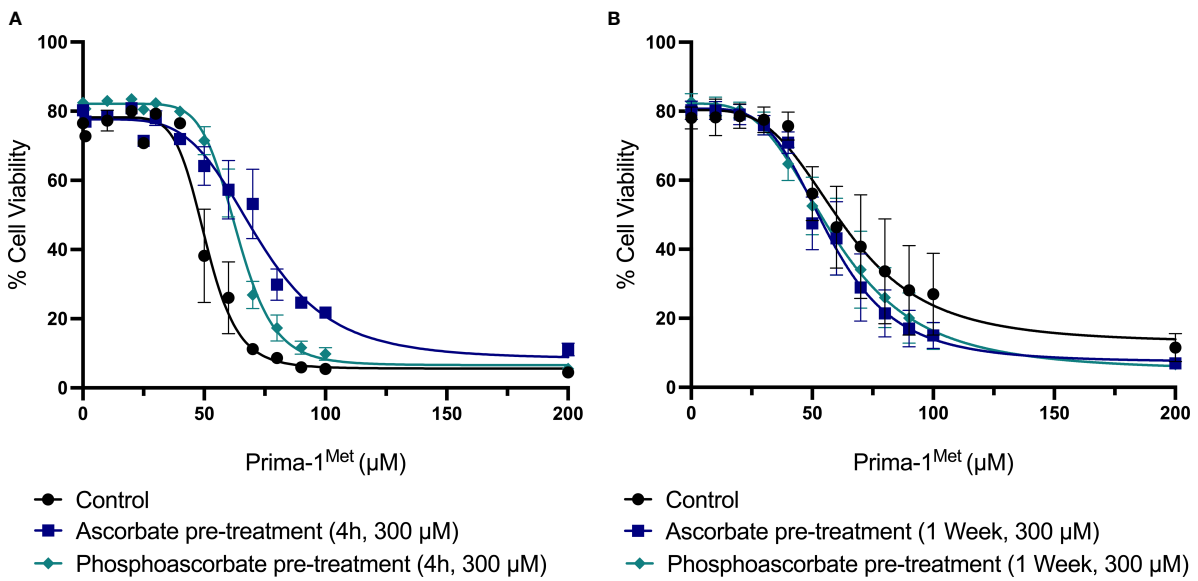

FIGURE 6 | The effect of ascorbate on Prima-1^{Met} cytotoxicity. **(A)** SKM-1 cells were grown for 4 hours +/- ascorbate or phosphoascorbate (300 μM). The cells were all seeded at a starting concentration of 0.2 x 10^6 cells/ml at a depth of 1 ml in a 24 well plate. After 4 hours, Prima-1^{Met} was added and the percentage cell viability was calculated after 24 hours using PI and flow cytometry (n = 3). For reference, clinical studies show that Prima-1^{Met} is tolerated at plasma concentrations up to 250 μM with only relatively minor side effects (41). Pre-treatment with either ascorbate or phosphoascorbate significantly decreased the cytotoxicity of Prima-1^{Met} ($p < 0.0001$). **(B)** SKM-1 cells were grown for 1 week +/- ascorbate or phosphoascorbate (300 μM). The media was refreshed every 2/3 days with a 1:5 dilution. The cells were then resuspended in fresh media, diluted to a concentration of 0.2 x 10^6 cells/ml and left for 1 hour before the addition of Prima-1^{Met}. The percentage cell viability was then measured 24 hours later (n = 4). Pre-treatment with either ascorbate or phosphoascorbate for 1 week significantly increased the cytotoxicity of Prima-1^{Met} (ascorbate $p = 0.0046$, phosphoascorbate $p = 0.0397$).

H_2O_2 and used phosphoascorbate, a redox inert substitute for ascorbate. Phosphoascorbate is hydrolyzed by membrane-bound phosphatases prior to uptake *via* the sodium-vitamin C transporters and accumulates in the cells as reduced ascorbate, with dephosphorylation being the rate limiting step for cellular uptake (55). It is likely that the slower rate of intracellular ascorbate accumulation when phosphoascorbate was used reflects the requirement for phosphoascorbate to be hydrolyzed by membrane-bound phosphatases. Both ascorbate and phosphoascorbate resulted in similar intracellular levels after 48 hours.

Adding 300 μM ascorbate or phosphoascorbate to the medium resulted in intracellular ascorbate levels similar to those measured *in vivo*: Agathocleous et al. measured intracellular ascorbate levels at around 2.5 fmoles/cell (or 2.5 nmoles/10^6 cells) in hematopoietic stem cells from Gulo$^{+/+}$ mice (16), which is comparable to the 2-4 nmoles/10^6 cells measured in the SKM-1 cells. This data gives us confidence that the ascorbate-mediated effects on hydroxymethylation, differentiation, and growth inhibition in the SKM-1 cells were achieved at intracellular ascorbate concentrations comparable to those seen *in vivo* and were not driven by H_2O_2 generated in the cell culture media. Overall, we found that phosphoascorbate was very useful for our cell culture experiments. We recommend that future cell culture studies with ascorbate use phosphoascorbate to limit the pro-oxidant effects of ascorbate in cell culture.

Loss-of-function in p53 can be caused by mutations that result in a truncated protein, disrupted protein folding or a mutation in a DNA contact residue (56). In the case of a protein folding mutation it is sometimes possible to pharmacologically stabilize the mutant protein and restore a functional conformation (57). This exciting prospect has prompted the search for small molecule compounds that can promote functional p53 folding, such as Prima-1^{Met} (41). Prima-1^{Met} is a pro-drug that is converted to methylene quinuclidinone (MQ), which can act as a Michael acceptor, rendering it susceptible to nucleophilic attack from the sulfhydryl moiety of cysteine residues. MQ has been shown to bind Cys124 and Cys277 in p53 to promote the reactivation of R175H and R273H p53 mutants by stabilizing the protein and shifting the equilibrium in favor of an active conformation (58, 59). In addition to p53-dependent effects, MQ targets the cellular redox balance *via* binding to glutathione and thioredoxin reductase, causing the depletion of glutathione and the inhibition of thioredoxin reductase (30, 41).

Interestingly, ascorbate supplementation had divergent effects on Prima-1^{Met} cytotoxicity depending on the order and timing of treatment. The preincubation of SKM-1 cells with ascorbate for 1 week to promote cellular differentiation caused a small, but statistically significant increase in the cytotoxicity of Prima-1^{Met}. In contrast, the reverse effect was observed when cells were preincubated with ascorbate for only 4 hours, with a decrease in the cytotoxicity of Prima-1^{Met}. The protective effect of ascorbate after 4 hours might be rationalized on the basis that dosing with ascorbate just before Prima-1^{Met} allows SKM-1 cells to better survive the generation of reactive oxygen species. On the other hand, the enhanced cytotoxic effect of ascorbate after 1 week could be a result of ascorbate induced cellular differentiation rendering the cells more susceptible to Prima-1^{Met}. However, in all cases the effect size was small and thus the biological significance of these effects remains unclear. Clinical trial data will be required to determine the utility of ascorbate as an adjunct therapy in this scenario.

In addition to *TET2* mutations, there are potentially other scenarios where TP53/complex karyotype AML patients could benefit from ascorbate supplementation. For example, decreased TET2 activity can also arise as a result of mutations in *IDH1, IDH2* or *WT1* (2) and mutations in this pathway collectively occur in around 30-50% of AML (1, 60, 61). Ascorbate-depletion also decreases TET2 activity, with similar effects to loss-of-function mutations (2, 15, 16), and low plasma ascorbate levels are common in AML patients (62, 63). Importantly, in a recent clinical trial, oral ascorbate supplementation increased 5hmC levels in myeloid cancer patients on azacitidine treatment (64).

Overall, we have found that ascorbate has the potential to function as an epigenetic therapeutic in a *TP53*-mutant leukemia model. Moreover, our data does not contraindicate the use of both ascorbate and Prima-1^{Met}, as ascorbate had a negligible effect on cytotoxicity caused by Prima-1^{Met}.

DATA AVAILABILITY STATEMENT

The raw data supporting the conclusions of this article will be made available by the authors, without undue reservation.

AUTHOR CONTRIBUTIONS

AD, MV, and MH conceived the work that led to this manuscript. CS-D, NM, JM, MH, MV, and AD designed the experiments and interpreted the data. CS-D, NM, and AD, carried out the experiments. CS-D, MH, MV, and AD wrote the paper with contributions from all authors. All authors contributed to the article and approved the submitted version.

FUNDING

This study was supported by funding from the Canterbury Medical Research Fund, the Bone Marrow Cancer Research Trust, and a NZSO Roche Translational Cancer Research Fellowship to AD.

SUPPLEMENTARY MATERIAL

The Supplementary Material for this article can be found online at: https://www.frontiersin.org/articles/10.3389/fonc.2021.709543/full#supplementary-material

REFERENCES

1. Papaemmanuil E, Gerstung M, Bullinger L, Gaidzik VI, Paschka P, Roberts ND, et al. Genomic Classification and Prognosis in Acute Myeloid Leukemia. *N Engl J Med* (2016) 374(23):2209–21. doi: 10.1056/NEJMoa1516192
2. Das AB, Smith-Díaz CC, Vissers MCMM. Emerging Epigenetic Therapeutics for Myeloid Leukemia: Modulating Demethylase Activity With Ascorbate. *Haematologica* (2021) 106(1):14–25. doi: 10.3324/haematol.2020.259283
3. Vissers MCM, Das AB. Potential Mechanisms of Action for Vitamin C in Cancer: Reviewing the Evidence. *Front Physiol* (2018) 9(JUL):1–13. doi: 10.3389/fphys.2018.00809
4. Padayatty SJ, Levine M. Vitamin C Physiology: The Know and the Unknown and Goldilocks. *Oral Dis* (2016) 22(6):463–93. doi: 10.1111/odi.12446
5. Kuiper C, Vissers MCM. Ascorbate as a Co-Factor for Fe- and 2-Oxoglutarate Dependent Dioxygenases: Physiological Activity in Tumor Growth and Progression. *Front Oncol* (2014) 4(NOV):1–11. doi: 10.3389/fonc.2014.00359
6. Islam MS, Leissing TM, Chowdhury R, Hopkinson RJ, Schofield CJ. 2-Oxoglutarate-Dependent Oxygenases. *Annu Rev Biochem* (2018) 87(1):585–620. doi: 10.1146/annurev-biochem-061516-044724
7. Flashman E, Davies SL, Yeoh KK, Schofield CJ. Investigating the Dependence of the Hypoxia-Inducible Factor Hydroxylases (Factor Inhibiting HIF and Prolyl Hydroxylase Domain 2) on Ascorbate and Other Reducing Agents. *Biochem J* (2010) 427(1):135–42. doi: 10.1042/BJ20091609
8. Vissers MCM, Das AB. Ascorbate as an Enzyme Cofactor. In: *Vitamin C*. Boca Raton, Florida, United States: CRC Press (2020). p. 71–98.
9. Crawford DJ, Liu MY, Nabel CS, Cao X-J, Garcia BA, Kohli RM. Tet2 Catalyzes Stepwise 5-Methylcytosine Oxidation by an Iterative and *De Novo* Mechanism. *J Am Chem Soc* (2016) 138(3):730–3. doi: 10.1021/jacs.5b10554
10. He Y-F, Li B-Z, Li Z, Liu P, Wang Y, Tang Q, et al. Tet-Mediated Formation of 5-Carboxylcytosine and its Excision by TDG in Mammalian DNA. *Science* (2011) 333(6047):1303–7. doi: 10.1126/science.1210944
11. Kohli RM, Zhang Y. TET enzymes TDG. And the Dynamics of DNA Demethylation. *Nature* (2013) 502(7472):472–9. doi: 10.1038/nature12750
12. Yin R, Mao S-Q, Zhao B, Chong Z, Yang Y, Zhao C, et al. Ascorbic Acid Enhances Tet-Mediated 5-Methylcytosine Oxidation and Promotes DNA Demethylation in Mammals. *J Am Chem Soc* (2013) 135(28):10396–403. doi: 10.1021/ja4028346
13. Monfort A, Wutz A. Breathing-in Epigenetic Change With Vitamin C. *EMBO Rep* (2013) 14(4):337–46. doi: 10.1038/embor.2013.29
14. Young JI, Züchner S, Wang G. Regulation of the Epigenome by Vitamin C. *Annu Rev Nutr* (2015) 35(1):545–64. doi: 10.1146/annurev-nutr-071714-034228
15. Cimmino L, Dolgalev I, Wang Y, Yoshimi A, Martin GH, Wang J, et al. Restoration of TET2 Function Blocks Aberrant Self-Renewal and Leukemia Progression. *Cell* (2017) 170(6):1079–95. doi: 10.1016/j.cell.2017.07.032
16. Agathocleous M, Meacham CE, Burgess RJ, Piskounova E, Zhao Z, Crane GM, et al. Ascorbate Regulates Haematopoietic Stem Cell Function and Leukaemogenesis. *Nature* (2017) 549(7673):476–81. doi: 10.1038/nature23876
17. Das AB, Kakadia PM, Wojcik D, Pemberton L, Browett PJ, Bohlander SK, et al. Clinical Remission Following Ascorbate Treatment in a Case of Acute Myeloid Leukemia With Mutations in TET2 and WT1. *Blood Cancer J* (2019) 9(10):82. doi: 10.1038/s41408-019-0242-4
18. Izzo F, Lee SC, Poran A, Chaligne R, Gaiti F, Gross B, et al. DNA Methylation Disruption Reshapes the Hematopoietic Differentiation Landscape. *Nat Genet* (2020) 52(4):378–87. doi: 10.1038/s41588-020-0595-4
19. Delhommeau F, Dupont S, Della VV, James C, Trannoy S, Massé A, et al. Mutation in TET2 in Myeloid Cancers. *N Engl J Med* (2009) 360(22):2289–301. doi: 10.1056/NEJMoa0810069
20. Ferrone CK, Blydt-Hansen M, Rauh MJ. Age-Associated TET2 Mutations: Common Drivers of Myeloid Dysfunction, Cancer and Cardiovascular Disease. *Int J Mol Sci* (2020) 21(2):626. doi: 10.3390/ijms21020626
21. Ko M, Huang Y, Jankowska AM, Pape UJ, Tahiliani M, Bandukwala HS, et al. Impaired Hydroxylation of 5-Methylcytosine in Myeloid Cancers With Mutant TET2. *Nature* (2010) 468(7325):839–43. doi: 10.1038/nature09586
22. Mingay M, Chaturvedi A, Bilenky M, Cao Q, Jackson L, Hui T, et al. Vitamin C-Induced Epigenomic Remodelling in IDH1 Mutant Acute Myeloid Leukaemia. *Leukemia* (2018) 32(1):11–20. doi: 10.1038/leu.2017.171
23. Liu J, Hong J, Han H, Park J, Kim D, Park H, et al. Decreased Vitamin C Uptake Mediated by SLC2A3 Promotes Leukaemia Progression and Impedes TET2 Restoration. *Br J Cancer.* (2020) 122(10):1445–52. doi: 10.1038/s41416-020-0788-8
24. Guan Y, Greenberg EF, Hasipek M, Chen S, Liu X, Kerr CM, et al. Context Dependent Effects of Ascorbic Acid Treatment in TET2 Mutant Myeloid Neoplasia. *Commun Biol* (2020) 3(1):493. doi: 10.1038/s42003-020-01220-9
25. Dutta S, Pregartner G, Rücker FG, Heitzer E, Zebisch A, Bullinger L, et al. Functional Classification of TP53 Mutations in Acute Myeloid Leukemia. *Cancers (Basel).* (2020) 12(3):637. doi: 10.3390/cancers12030637
26. Cluzeau T, Dubois A, Jacquel A, Luciano F, Renneville A, Preudhomme C, et al. Phenotypic and Genotypic Characterization of Azacitidine-Sensitive and Resistant SKM1 Myeloid Cell Lines. *Oncotarget* (2014) 5(12):4384–91. doi: 10.18632/oncotarget.2024
27. Perdrix A, Najem A, Saussez S, Awada A, Journe F, Ghanem G, et al. PRIMA-1 and PRIMA-1Met (APR-246): From Mutant/Wild Type P53 Reactivation to Unexpected Mechanisms Underlying Their Potent Anti-Tumor Effect in Combinatorial Therapies. *Cancers (Basel)* (2017) 9(12):172. doi: 10.3390/cancers9120172
28. Lambert JMR, Moshfegh A, Hainaut P, Wiman KG, Bykov VJN. Mutant P53 Reactivation by PRIMA-1MET Induces Multiple Signaling Pathways Converging on Apoptosis. *Oncogene* (2010) 29(9):1329–38. doi: 10.1038/onc.2009.425
29. Tessoulin B, Descamps G, Dousset C, Amiot M, Pellat-Deceunynck C. Targeting Oxidative Stress With Auranofin or Prima-1Met to Circumvent P53 or Bax/Bak Deficiency in Myeloma Cells. *Front Oncol* (2019) 9(MAR):1–7. doi: 10.3389/fonc.2019.00128
30. Peng X, Zhang M-Q-Z, Conserva F, Hosny G, Selivanova G, Bykov VJN, et al. APR-246/PRIMA-1MET Inhibits Thioredoxin Reductase 1 and Converts the Enzyme to a Dedicated NADPH Oxidase. *Cell Death Dis* (2013) 4(10): e881. doi: 10.1038/cddis.2013.417
31. Maslah N, Salomao N, Drevon L, Verger E, Partouche N, Ly P, et al. Synergistic Effects of PRIMA-1 Met (APR-246) and 5-Azacitidine in TP53 -Mutated Myelodysplastic Syndromes and Acute Myeloid Leukemia. *Haematologica* (2020) 105(6):1539–51. doi: 10.3324/haematol.2019.218453
32. Zhang C, Liu J, Xu D, Zhang T, Hu W, Feng Z. Gain-of-Function Mutant P53 in Cancer Progression and Therapy. *J Mol Cell Biol* (2020) 12(9):674–87. doi: 10.1093/jmcb/mjaa040
33. Solary E, Bernard OA, Tefferi A, Fuks F, Vainchenker W. The Ten-Eleven Translocation-2 (TET2) Gene in Hematopoiesis and Hematopoietic Diseases. *Leukemia* (2014) 28(3):485–96. doi: 10.1038/leu.2013.337
34. Zeng W, Dai H, Yan M, Cai X, Luo H, Ke M, et al. Decitabine-Induced Changes in Human Myelodysplastic Syndrome Cell Line SKM-1 are Mediated by FOXO3A Activation. *J Immunol Res* (2017) 2017:1–12. doi: 10.1155/2017/4302320
35. Pullar JM, Bayer S, Carr AC. Appropriate Handling, Processing and Analysis of Blood Samples is Essential to Avoid Oxidation of Vitamin C to Dehydroascorbic Acid. *Antioxidants* (2018) 7(2):29. doi: 10.3390/antiox7020029
36. Carr AC, Pullar JM, Moran S, Vissers MCM. Bioavailability of Vitamin C From Kiwifruit in non-Smoking Males: Determination of 'Healthy' and 'Optimal' Intakes. *J Nutr Sci* (2012) 1:e14. doi: 10.1017/jns.2012.15
37. Parrow NL, Leshin JA, Levine M. Parenteral Ascorbate as a Cancer Therapeutic: A Reassessment Based on Pharmacokinetics. *Antioxidants Redox Signal* (2013) 19(17):2141–56. doi: 10.1089/ars.2013.5372
38. Caritá AC, Fonseca-Santos B, Shultz JD, Michniak-Kohn B, Chorilli M, Leonardi GR. Vitamin C: One Compound, Several Uses. Advances for Delivery, Efficiency and Stability. *Nanomedicine Nanotechnology Biol Med* (2020) 24:102117. doi: 10.1016/j.nano.2019.102117
39. Zheng K, Song W, Sun A, Chen X, Liu J, Luo Q, et al. Enzymatic Production of Ascorbic Acid-2-Phosphate by Recombinant Acid Phosphatase. *J Agric Food Chem* (2017) 65(20):4161–6. doi: 10.1021/acs.jafc.7b00612
40. Leach M, Drummond M, Doig A. *Practical Flow Cytometry in Haematology Diagnosis*. Oxford: John Wiley & Sons (2013).
41. Bykov VJN, Zhang Q, Zhang M, Ceder S, Abrahmsen L, Wiman KG. Targeting of Mutant P53 and the Cellular Redox Balance by APR-246 as a Strategy for Efficient Cancer Therapy. *Front Oncol* (2016) 6:21. doi: 10.3389/fonc.2016.00021

42. Sallman DA, DeZern AE, Steensma DP, Sweet KL, Cluzeau T, Sekeres MA, et al. Phase 1b/2 Combination Study of APR-246 and Azacitidine (AZA) in Patients With TP53 Mutant Myelodysplastic Syndromes (MDS) and Acute Myeloid Leukemia (AML). *Blood* (2018) 132(Supplement 1):3091. doi: 10.1182/blood-2018-99-119990
43. Huang A, Vita JA, Venema RC, Keaney JF. Ascorbic Acid Enhances Endothelial Nitric-Oxide Synthase Activity by Increasing Intracellular Tetrahydrobiopterin. *J Biol Chem* (2000) 275(23):17399–406. doi: 10.1074/jbc.M002248200
44. May JM, Qu Z, Meredith ME. Mechanisms of Ascorbic Acid Stimulation of Norepinephrine Synthesis in Neuronal Cells. *Biochem Biophys Res Commun* (2012) 426(1):148–52. doi: 10.1016/j.bbrc.2012.08.054
45. Parker WH, Qu Z, May JM. Ascorbic Acid Transport in Brain Microvascular Pericytes. *Biochem Biophys Res Commun* (2015) 458(2):262–7. doi: 10.1016/j.bbrc.2015.01.096
46. Nestor CE, Ottaviano R, Reddington J, Sproul D, Reinhardt D, Dunican D, et al. Tissue Type Is a Major Modifier of the 5-Hydroxymethylcytosine Content of Human Genes. *Genome Res* (2012) 22(3):467–77. doi: 10.1101/gr.126417.111
47. Li W, Liu M. Distribution of 5-Hydroxymethylcytosine in Different Human Tissues. *J Nucleic Acids* (2011) 2011:1–5. doi: 10.4061/2011/870726
48. Yamamoto T, Sakaguchi N, Hachiya M, Nakayama F, Yamakawa M, Akashi M. Role of Catalase in Monocytic Differentiation of U937 Cells by TPA: Hydrogen Peroxide as a Second Messenger. *Leukemia* (2009) 23(4):761–9. doi: 10.1038/leu.2008.353
49. Frumento G, Zuo J, Verma K, Croft W, Ramagiri P, Chen FE, et al. CD117 (C-Kit) is Expressed During CD8+ T Cell Priming and Stratifies Sensitivity to Apoptosis According to Strength of TCR Engagement. *Front Immunol* (2019) 10(MAR):468. doi: 10.3389/fimmu.2019.00468
50. Abbaspour Babaei M, Kamalidehghan B, Saleem M, Zaman Huri H, Ahmadipour F. Receptor Tyrosine Kinase (C-Kit) Inhibitors: A Potential Therapeutic Target in Cancer Cells. *Drug Des Devel Ther* (2016) 10:2443–59. doi: 10.2147/DDDT.S89114
51. Lennartsson J, Rönnstrand L. Stem Cell Factor Receptor/C-Kit: From Basic Science to Clinical Implications. *Physiol Rev* (2012) 92(4):1619–49. doi: 10.1152/physrev.00046.2011
52. Michels A, Frei B. Myths, Artifacts, and Fatal Flaws: Identifying Limitations and Opportunities in Vitamin C Research. *Nutrients* (2013) 5(12):5161–92. doi: 10.3390/nu5125161
53. Halliwell B. Oxidative Stress in Cell Culture: An Under-Appreciated Problem? *FEBS Lett* (2003) 540(1–3):3–6. doi: 10.1016/S0014-5793(03)00235-7
54. Buettner GR. In the Absence of Catalytic Metals Ascorbate Does Not Autoxidize at Ph 7: Ascorbate as a Test for Catalytic Metals. *J Biochem Biophys Methods* (1988) 16(1):27–40. doi: 10.1016/0165-022X(88)90100-5
55. May JM. The SLC23 Family of Ascorbate Transporters: Ensuring That You Get and Keep Your Daily Dose of Vitamin C. *Br J Pharmacol* (2011) 164 (7):1793–801. doi: 10.1111/j.1476-5381.2011.01350.x
56. Kastenhuber ER, Lowe SW. Putting P53 in Context. *Cell* (2017) 170(6):1062–78. doi: 10.1016/j.cell.2017.08.028
57. Joerger AC, Fersht AR. Structure–Function–Rescue: The Diverse Nature of Common P53 Cancer Mutants. *Oncogene* (2007) 26(15):2226–42. doi: 10.1038/sj.onc.1210291
58. Zhang Q, Bykov VJN, Wiman KG, Zawacka-Pankau J. APR-246 Reactivates Mutant P53 by Targeting Cysteines 124 and 277. *Cell Death Dis* (2018) 9 (5):439. doi: 10.1038/s41419-018-0463-7
59. Omar SI, Tuszynski J. The Molecular Mechanism of Action of Methylene Quinuclidinone and Its Effects on the Structure of P53 Mutants. *Oncotarget* (2018) 9(98):37137–56. doi: 10.18632/oncotarget.26440
60. Wang Y, Xiao M, Chen X, Chen L, Xu Y, Lv L, et al. WT1 Recruits TET2 to Regulate Its Target Gene Expression and Suppress Leukemia Cell Proliferation. *Mol Cell* (2015) 57(4):662–73. doi: 10.1016/j.molcel.2014.12.023
61. Ley TJ, Miller C, Ding L, Raphael BJ, Mungall AJ, Robertson G, et al. Genomic and Epigenomic Landscapes of Adult De Novo Acute Myeloid Leukemia. *N Engl J Med* (2013) 368(22):2059–74. doi: 10.1056/NEJMoa1301689
62. Huijskens MJAJ, Wodzig WKWH, Walczak M, Germeraad WTV, Bos GMJ. Ascorbic Acid Serum Levels are Reduced in Patients With Hematological Malignancies. *Results Immunol* (2016) 6:8–10. doi: 10.1016/j.rinim.2016.01.001
63. Carr AC, Spencer E, Das A, Meijer N, Lauren C, MacPherson S, et al. Patients Undergoing Myeloablative Chemotherapy and Hematopoietic Stem Cell Transplantation Exhibit Depleted Vitamin C Status in Association With Febrile Neutropenia. *Nutrients* (2020) 12(6):1879. doi: 10.3390/nu12061879
64. Gillberg L, Ørskov AD, Nasif A, Ohtani H, Madaj Z, Hansen JW, et al. Oral Vitamin C Supplementation to Patients With Myeloid Cancer on Azacitidine Treatment: Normalization of Plasma Vitamin C Induces Epigenetic Changes. *Clin Epigenetics* (2019) 11(1):143. doi: 10.1186/s13148-019-0739-5

Conflict of Interest: The authors declare that the research was conducted in the absence of any commercial or financial relationships that could be construed as a potential conflict of interest.

Publisher's Note: All claims expressed in this article are solely those of the authors and do not necessarily represent those of their affiliated organizations, or those of the publisher, the editors and the reviewers. Any product that may be evaluated in this article, or claim that may be made by its manufacturer, is not guaranteed or endorsed by the publisher.

frontiers in Oncology

ORIGINAL RESEARCH
published: 26 August 2021
doi: 10.3389/fonc.2021.739171

Prognostic Factors for Overall Survival In Chronic Myeloid Leukemia Patients: A Multicentric Cohort Study by the Italian CML GIMEMA Network

Giorgina Specchia[1†], Patrizia Pregno[2†], Massimo Breccia[3†], Fausto Castagnetti[4], Chiara Monagheddu[5], Massimiliano Bonifacio[6], Mario Tiribelli[7], Fabio Stagno[8], Giovanni Caocci[9], Bruno Martino[10], Luigiana Luciano[11], Michele Pizzuti[12], Antonella Gozzini[13], Anna Rita Scortechini[14], Francesco Albano[15], Micaela Bergamaschi[16], Isabella Capodanno[17], Andrea Patriarca[18], Carmen Fava[19], Giovanna Rege-Cambrin[20], Federica Sorà[21], Sara Galimberti[22], Monica Bocchia[23], Gianni Binotto[24], Giovanni Reddiconto[25], Paolo DiTonno[26], Alessandro Maggi[27], Grazia Sanpaolo[28], Maria Stella De Candia[29], Valentina Giai[2], Elisabetta Abruzzese[30], Maria Cristina Miggiano[31], Gaetano La Barba[32], Giuseppe Pietrantuono[33], Anna Guella[34], Luciano Levato[35], Olga Mulas[9], Fabio Saccona[5], Gianantonio Rosti[4], Pellegrino Musto[15], Francesco Di Raimondo[8], Fabrizio Pane[11], Michele Baccarani[4], Giuseppe Saglio[19†] and Giovannino Ciccone[5†]*

[1] Former Full Professor of Hematology- University of Bari Aldo Moro" Bari GIMEMA WP CML, Bari, Italy, [2] Haematology Unit, Azienda Ospedaliero-Universitaria Città della Salute e della Scienza, Torino, Italy, [3] Department of Cellular Biotechnologies and Hematology, Sapienza University of Rome, Roma, Italy, [4] Department of Experimental, Diagnostic and Specialty Medicine, S. Orsola-Malpighi Hospital, University of Bologna, Bologna, Italy, [5] Clinical Epidemiology Unit and CPO Piemonte, Città della Salute e della Scienza, Torino, Italy, [6] Section of Hematology, Department of Medicine, University of Verona, Verona, Italy, [7] Division of Hematology and BMT, Department of Medical Area, University of Udine, Udine, Italy, [8] Division of Hematology and Bone Marrow Transplant, Azienda Ospedaliera-Universitaria (AOU) Policlinico-V. Emanuele, Catania, Italy, [9] Department of Medical Sciences and Public Health, Businco Hospital, University of Cagliari, Cagliari, Italy, [10] Haematology Unit, Azienda Ospedaliera "Bianchi-Melacrino-Morelli", Reggio Calabria, Italy, [11] Haematology Unit "Federico II", University of Naples, Naples, Italy, [12] Department of Hematology, "San Carlo" Regional Hospital, Potenza, Italy, [13] Haematology Unit, AOU Careggi, University of Florence, Florence, Italy, [14] Division of Hematology, Department of Molecular and Clinical Sciences, Polytechnic University of Marche, Ancona, Italy, [15] Department of Emergency and Transplantation, Hematology Section, University of Bari Medical School, Bari, Italy, [16] Clinical Hematology, Policlinico San Martino, Genua, Italy, [17] Department of Hematology, Azienda UNITà SANITARIA LOCALE (USL)-IRCCS di Reggio Emilia, Viale Risorgimento, Reggio Emilia, Italy, [18] Division of Hematology, Department of Translational Medicine, University of Eastern Piedmont, Novara, Italy, [19] Department of Clinical and Biological Sciences, University of Turin, Turin, Italy, [20] Orbassano Hospital, Turin University, Turin, Italy, [21] Institute of Hematology, Università Cattolica Sacro Cuore, Rome, Italy, [22] Department of Clinical and Experimental Medicine, Unità Operativa (UO) Haematology, AOU Pisana, Pisa, Italy, [23] Haematology Unit, Azienda Ospedaliera Universitaria Senese, University of Siena, Siena, Italy, [24] Padova Hematology and Clinical Immunology, Padua, Italy, [25] Department of Ematologia, Lecce Ematologia Ospedale Vito Fazzi, Lecce, Italy, [26] Haematology Unit, National Cancer Center, IRCCS Istituto Tumori "Giovanni Paolo II", Bari, Italy, [27] Division of Hematology, Hospital "S.G. Moscati", Taranto, Italy, [28] Department of Hematology and Stem Cell Transplantation Unit, IRCCS Casa Sollievo della Sofferenza Hospital, San Giovanni Rotondo, Italy, [29] Hematology, Hospital A. Perrino, Brindisi, Italy, [30] Hemoglobinopathies Unit, Hematology Department, S. Eugenio Hospital (ASL Roma 2), Rome, Italy, [31] Hematology Department, San Bortolo Hospital, Vicenza, Italy, [32] Department of Hematology, "Spirito Santo" Hospital, Pescara, Italy, [33] Hematology Oncology, IRCCS Centro di Riferimento Oncologico della Basilicata, Rionero in Vulture, Italy, [34] Hematology Unit, Santa Chiara Hospital, Trento, Italy, [35] Haematology Unit, A. Pugliese Hospital, Azienda Ospedaliera Pugliese Ciaccio, Catanzaro, Italy

OPEN ACCESS

Edited by:
Walter Fiedler,
University Medical Center
Hamburg-Eppendorf, Germany

Reviewed by:
Juan Carlos Hernandez-Boluda,
Hospital Clínico Universitario de
Valencia, Spain
Mervat Mattar,
Cairo University, Egypt

***Correspondence:**
Giorgina Specchia
giorgina.specchia@gmail.com

[†]These authors have contributed equally to this work

Specialty section:
This article was submitted to Hematologic Malignancies, a section of the journal Frontiers in Oncology

Received: 10 July 2021
Accepted: 06 August 2021
Published: 26 August 2021

An observational prospective study was conducted by the CML Italian network to analyze the role of baseline patient characteristics and first line treatments on overall survival and CML-related mortality in 1206 newly diagnosed CML patients, 608 treated with imatinib (IMA) and 598 with 2nd generation tyrosine kinase inhibitors (2GTKI). IMA-treated patients

were much older (median age 69 years, IQR 58-77) than the 2GTKI group (52, IQR 41-63) and had more comorbidities. Estimated 4-year overall survival of the entire cohort was 89% (95%CI 85.9-91.4). Overall, 73 patients (6.1%) died: 17 (2.8%) in the 2GTKI vs 56 (9.2%) in the IMA cohort (adjusted HR=0.50; 95% CI=0.26-0.94), but no differences were detected for CML-related mortality (10 (1.7%) vs 11 (1.8%) in the 2GTKIs vs IMA cohort (sHR=1.61; 0.52-4.96). The ELTS score was associated to CML mortality (high risk vs low, HR=9.67; 95%CI 2.94-31.74; p<0.001), while age (per year, HR=1.03; 95%CI 1.00-1.06; p=0.064), CCI (4-5 vs 2, HR=5.22; 95%CI 2.56-10.65; p<0.001), ELTS score (high risk vs low, HR=3.11; 95%CI 1.52-6.35, p=0.002) and 2GTKI vs IMA (HR=0.26; 95%CI 0.10-0.65, p=0.004) were associated to an increased risk of non-related CML mortality. The ELTS score showed a better discriminant ability than the Sokal score in all comparisons.

Keywords: chronic myeloid leukemia, tyrosine kinase inhibitors, prognostic factors, ELTs, Sokal score

INTRODUCTION

The treatment landscape of patients with chronic myeloid leukemia (CML) changed dramatically after the approval of imatinib, the first tyrosine kinase inhibitor (TKI), in 2001 (1). Since then, several newer TKIs have also been approved, and 3 different TKIs are currently available as front-line treatments in Italy (2). Due to the remarkable efficacy of TKIs therapy, the life expectancy of newly diagnosed chronic phase (CP) patients is now near to that of age-matched individuals in the general population (3). The improved outcome and long-term safety of these drugs have mainly been demonstrated in sponsored randomized controlled trials (RCTs) (4). However, many questions related to the prognosis and the optimal management of newly diagnosed CML patients remain unanswered, and it is widely accepted that these questions could be addressed by evaluating large prospective cohorts in real world clinical practice. Prognostic evaluation of baseline features has been reported in small single country series (5, 6) or in large datasets including 20 countries in Europe, such as the EUTOS registry (7). Until 2016, three different clinical prognostic scores were in use in clinical practice (Sokal, Euro, Eutos scores) (8), before the EUTOS Long Term survival (ELTS) score (9) was introduced, that stratifies patients in three different risk groups, with significantly different probabilities of dying of CML. The EUTOS score ability to discriminate CML patients in terms of long-term overall survival has been validated several times, but predominantly in patients treated with front-line imatinib (10–12). The score was recently suggested by the European Leukemia Net (ELN) panel in the updated recommendations (13) as a helpful tool to predict the rate of deaths related to CML in TKIs-treated patients.

The Italian CML GIMEMA network promoted an observational cohort study in January 2013, to collect a large series of consecutive newly diagnosed patients and evaluate the management and the long-term outcomes in a real-world perspective.

The aim of this article is to analyze the impact of the baseline patients' characteristics and their front-line treatments on long term overall survival and CML-related deaths.

PATIENTS AND METHODS

The CML Italian GIMEMA network (including 68 Hematology Centers from 19 Italian regions) prospectively recorded, in a dedicated web-based database (https://www.epiclin.it/lmc), the clinical and biological features of all newly diagnosed adult (>18 years) Italian Ph+ CML patients in each phase of disease, diagnosed from January 2013 onwards. All consecutive patients were included, without any exclusion criteria and regardless of their participation in any other clinical trial, to limit the eligibility criteria selection bias typical of experimental studies. All centers followed the ELN guidelines currently available and their updates (13, 14) for the management of patients, without any other predefined recommendations, including the selection of first line TKI treatment and the subsequent monitoring every 3 months.

The study was approved by the local ethics committees and other competent authorities; all patients were registered after obtaining prior informed consent.

Standardized information on all newly diagnosed patients was collected and entered in the database by local staff and centrally checked for completeness and coherence. Baseline information included sociodemographic, clinical, and standard laboratory data. Comorbidities were evaluated by medical staff before the start of treatment according to the Charlson Comorbidity index (CCI) (15). CML was classified as chronic phase (CP), accelerated phase (AP) and blast phase (BP) according to the ELN criteria (13). Cytogenetic analysis was performed according to banding analysis at baseline, as well as qualitative molecular analysis to define the type of BCR-ABL transcript. Sokal (16) and ELTS (9) scores were calculated as previously reported. Any front-line treatment was recorded. Overall survival (OS) and cause-specific survival (CML-related deaths, other causes of death) were calculated from the date of diagnosis. Cause of death was clinically defined as leukemia-related when it occurred after progression to accelerated phase (AP) or blast phase (BP). All other deaths were classified as leukemia-unrelated, and the specific causes of death were recorded.

In this article we present the baseline characteristics (age, sex, comorbidities, prognostic scores), the type of TKI initially

prescribed (Imatinib - IMA or 2nd generation TKIs -2GTKI) and their impact on survival, overall and by cause of death. For OS analyses, Kaplan–Meier curves were calculated. To quantify differences in survival probabilities between groups, the log-rank test was applied. Cox proportional hazard regression models were applied to analyze the influence of all the variables considered on OS. Harrell's C statistic was calculated to assess the discrimination ability of the two prognostic scores.

To analyze the association of prognostic factors and of first-line treatments on CML mortality, deaths due to other causes were considered competitive events. Separate cumulative incidence curves for CML and other causes mortality were estimated with the Gooley method. Adjusted sub–Hazard Ratios (sHR) for prognostic factors and treatment were estimated separately for CML and other causes mortality with the Fine and Gray method.

RESULTS

Baseline Characteristics of the Enrolled Population

A cohort of 1206 patients was prospectively analyzed, 608 (50.4%) of whom received front-line IMA and 598 (49.6%) a 2GTKI (**Table 1**).

The age distribution shows a clear imbalance between treatments. There was no difference of observation time between age groups. Median age in the IMA cohort was 69 years (range 58-77) versus 52 years in the 2GTKI cohort (range 41-63). In the IMA group 28% were under 60 and 49% over 70, while in the 2GTKI the corresponding figures were 68% and 10%. The male/female ratio was 1.70 in the IMA group and 1.35 in the 2GTKI cohort. Regarding the year of diagnosis, 2GTKI were prescribed more frequently in the first period (2013-2015) and less in more recent years (2018-2020). Overall, 98% of patients were in CP, versus 0.4% in blast phase and 1.6% in accelerated phase at baseline.

Results of molecular analysis of the BCR-ABL transcript at baseline showed: b2a2 in 33.1% of patients and b3a2 in 59.9%, while an atypical transcript was found in 7%. No other meaningful differences were observed according to treatments. Cytogenetic analysis at baseline showed additional cytogenetic aberrations (ACA) in 7.3% of patients (5.7% classified as major and 1.6% as minor) in the whole population. According to treatment, there were 5.3% of ACA (32/608) in the IMA cohort and 9.4% (56/598) in the 2GTKIs group respectively. According to the different type of ACA (Major and Minor route), high risk minor route ACA were detected only in 1/10 2GTKI treated patients (del7q) and in none of the IMA cohort.

In the IMA cohort, 27.7%, 57.3% and 15% of patients were stratified as low, intermediate and high risk, according to the Sokal score, whereas according to the ELTS score 51.3%, 35.5% and 13.3% of patients were classified as low, intermediate and high risk, respectively. In the 2GTKI cohort, 44.8%, 34.5% and 20.8%, were low, intermediate and high risk, according to the Sokal score, whereas according to the ELTS score, 66.9%, 22% and 11% were assigned to the respective risk groups.

The prevalence of comorbidity was at least double in the IMA group: at baseline 39% of patients presented cardiovascular comorbidities, 18% had previous pulmonary diseases and 12% a metabolic disorder. In the 2GTKI cohort, baseline cardiovascular comorbidities, pulmonary diseases and metabolic disorders were recorded in 15%, 5.5% and 4.8%, respectively. The CCI was evaluated in 82% of patients treated with IMA, and the resulting scores were 2-3 and 4-5 in 74% and 26% of patients, respectively. In patients treated with 2GTKI the CCI was available in 76% of patients and resulted 2-3 in 89.8%, and 4-5 only in 10.2%.

Overall Survival and Cause-Specific Mortality

Overall, median follow-up of the whole population was 24.7 months (IQR: 13.3-39.3): 23.0 (10.3-37.0) and 33.2 (17.2-47.5) for the IMA and 2GTKI groups, respectively.

In the overall population, 73 patients (6.1%) died (**Table 2**). During follow-up, 56 patients (9.2% of the IMA cohort) died at a median age of 80.5 years (range 73-85), but only 11/56 (19.6%) due to CML-related causes. Indeed, 45/56 patients (80.4%) died of other causes, mostly cardiovascular diseases (19.6%) and a second neoplasia (19.6%). Conversely, in the 2GTKI cohort, only 17 patients (2.8%) died, at a median age of 62 years (range 53-72), 10/17 (58.8%) due to CML-related causes. The principal causes of death in the 2GTKI cohort were a second neoplasia (N=3) and gastro-intestinal disorders (N=2). Estimated 2- and 4-years OS of the entire cohort were 95.2% (95%CI 93.5-96.4) and 89.0% (95%CI 85.9-91.4), respectively (**Figure 1**).

The crude and adjusted effects of prognostic variables and of front-line treatment on OS are reported in **Table 3**. All the variables considered showed strong and statistically clear crude effects on OS. Harrel's C statistic, estimated to compare the discriminant propriety of the two CML risk scores, was 0.705 for the ELTS score and 0.640 for the Sokal score, confirming a better performance of the former. In the multivariable Cox model, the adjusted effects of increasing age, more comorbidities and a high ELTS risk remained clearly associated with poorer survival. Patients treated with 2GTKI showed a substantial reduction of the risk of death for any cause (HR=0.50, 95%CI 0.26-0.94) even after adjustment. When the Sokal score was analyzed in the multivariable Cox model, instead of the ELTS, its impact on OS was weaker and less precise.

Because of the wide differences in age and distribution of comorbidities between the patients receiving the two first-line treatments, and the different causes of deaths that occurred in these groups, a comparison for CML-related deaths was performed, considering other causes of deaths as competing events. The cumulative mortality risk for CML-related causes did not show any meaningful difference between treatments (**Figure 2A**), all the difference being wholly attributable to the other causes of deaths (**Figure 2B**).

The performance of the two CML prognostic scores is described in the graphs in **Figure 3**. The ELTS score showed a good discrimination of the three classes of risk, both for the CML-related deaths (**Figure 3A**) and for the other causes (**Figure 3B**). The discriminant ability of the Sokal score was slightly lower for CML-related causes (**Figure 3C**), but especially for the other causes of death (**Figure 3D**).

TABLE 1 | Baseline CML patient characteristics by front-line TKI treatment.

Patient characteristics	First-line treatment				Total (N=1206)	
	Imatinib (N = 608)		2GTKI (N = 598)			
	N	%	N	%	N	%
Age:						
median (iqr)	69	(58-77)	52	(41-63)	60	(48-71)
mean (sd)	65.7	(14.7)	51.6	(14.0)	58.6	(16.0)
18-29	16	2.6	34	5.7	50	4.1
30-39	23	3.8	94	15.7	117	9.7
40-49	51	8.4	133	22.2	184	15.3
50-59	81	13.3	148	24.7	229	19.0
60-69	139	22.9	129	21.6	268	22.2
70-79	192	31.6	52	8.7	244	20.2
+80	106	17.4	8	1.3	114	9.5
Sex:						
Male	383	63.0	344	57.5	727	60.3
Female	225	37.0	254	42.5	479	39.7
Period of diagnosis:						
2013-2015	113	18.6	172	28.8	285	23.6
2016-2017	257	42.3	261	43.6	518	43.0
2018-2020	238	39.1	165	27.6	403	33.4
Comorbidity:						
Cardiovascular disease	238	39.1	90	15.1	328	27.2
Pulmonary disease	110	18.1	33	5.5	143	11.9
Metabolic disease	75	12.3	29	4.8	104	8.6
Other neoplasm	61	10.0	31	5.2	92	7.6
Charlson index score:						
2	359	59.0	489	81.8	848	70.3
3	104	17.1	48	8.0	152	12.6
4	80	13.2	26	4.3	106	8.8
5	46	7.6	19	3.2	65	5.4
not available	19	3.1	16	2.7	35	2.9
CML Phase:						
chronic	590	97.0	574	96.0	1164	96.5
blastic	3	0.5	2	0.3	5	0.4
accelerated	7	1.2	12	2.0	19	1.6
not available	8	1.3	10	1.7	18	1.5
ELTS score:						
Low	305	51.3	390	66.9	695	59.0
Intermediate	211	35.5	128	22.0	339	28.8
High	79	13.3	65	11.1	144	12.2
not available	13	2.1	15	2.5	28	2.3
Sokal score:						
Low	164	27.7	261	44.8	425	36.1
Intermediate	340	57.3	201	34.5	541	46.0
High	89	15.0	121	20.8	210	17.9
not available	15	2.5	15	2.5	30	2.5

TABLE 2 | Causes of death of CML patients by front-line TKI treatment.

Causes of death	First-line treatment				Total (N = 73)	
	Imatinib (N = 56)		2GTKI (N = 17)			
	N	%	N	%	N	%
CML-related	11	19.6	10	58.8	21	28.8
Other causes:	45	80.4	7	41.2	52	71.2
cardiac	11	19.6	1	5.9	12	16.4
neoplasia	11	19.6	3	17.6	14	19.2
lung	3	5.4	0	0.0	3	4.1
infections	1	1.8	0	0.0	1	1.4
neurologic	5	8.9	0	0.0	5	6.8
gastroenteric	3	5.4	2	11.8	5	6.8
other/unknown	10	17.9	1	5.9	11	15.1

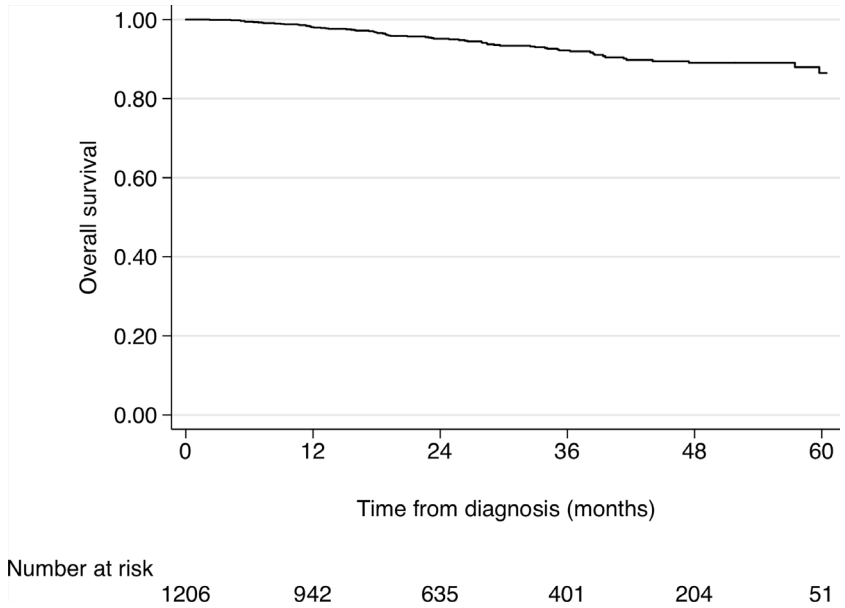

FIGURE 1 | Cumulative Overall Survival of the whole CML cohort.

Finally, the adjusted effects of the variables of interest on the two groups for causes of deaths were estimated with a Fine and Gray model (**Table 4**). The effect of age was similar, but the CCI was a strong prognostic factor for other causes, but not for CML-related deaths. The apparent benefit of the 2GTKI on OS disappeared completely when the CML-related deaths were considered, their effect being completely attributable to a reduced risk of the other causes of deaths, and in particular of age.

The performance of the two CML prognostic scores was much clearer in predicting the risk for CML-related deaths than for the other causes of deaths. For both outcomes, the ELTS showed a better discriminant ability than the Sokal score.

DISCUSSION

In the last decade, the availability of different first line TKIs has changed the clinical management of CML patients, allowing a better diagnostic work-up and careful evaluation of baseline comorbidities to select the best therapeutic option. In fact, the consequence of TKI-related improved survival is an increased probability of dying of other, unrelated causes: for this reason, it is of paramount importance to analyze specific causes of deaths separately, and avoid specific drug-related off-target effects.

In this study we report the overall survival and CML-related death probability of a large CML population, prospectively enrolled in a multicentric Italian observational study, together

TABLE 3 | Role of prognostic variables and front-line treatments on overall survival of CML patients.

	Crude effects			Adjusted effects		
	HR	**95% CI**	**p**	**HR**	**95% CI**	**p**
Age (per year)	1.07	1.05-1.10	<0.001	1.03	1.00-1.05	0.019
Sex (F vs M)	0.59	0.35-0.97	0.040	0.71	0.42-1.21	0.211
Charlson C.I. (ref=2)						
3	2.87	1.50-5.48	0.001	1.73	0.88-3.38	0.111
>=4	6.66	3.98-11.13	<0.001	3.61	2.10-6.22	<0.001
2GTKI (ref=Imatinib)	0.22	0.13-0.39	<0.001	0.50	0.26-0.94	0.025
ELTS risk (ref=low)						
medium	3.45	1.91-6.25	<0.001	1.69	0.88-3.24	0.112
high	7.71	4.22-14.07	<0.001	4.80	2.48-9.30	<0.001
Sokal risk (*)						
medium	3.52	1.77-7.00	<0.001	1.10	0.49-2.46	0.815
high	4.22	1.96-9.08	<0.001	2.19	0.91-5.29	0.080

**Estimated in a model including all the covariates in the tables except the ELTS score.*
Hazard Ratio (HR) and 95% Confidence Intervals (CI) estimated with Cox regression models.

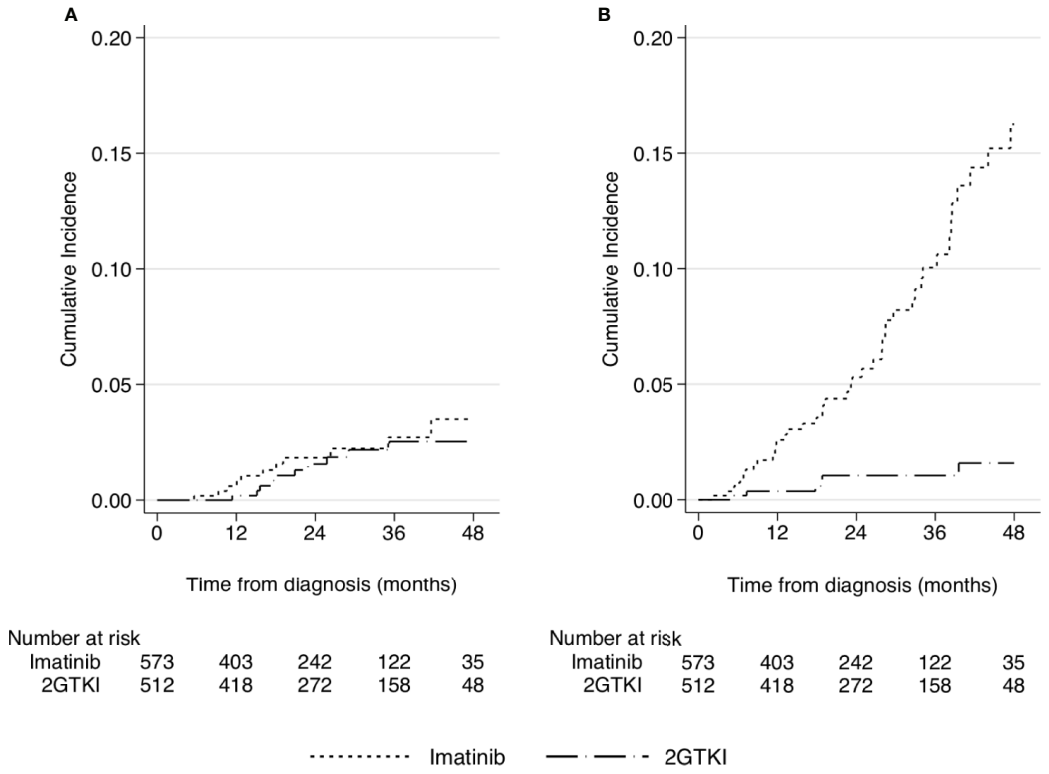

FIGURE 2 | Cumulative incidence of mortality related to CML **(A)** or to other causes of deaths **(B)** treated as a competing event, according to front-line TKI treatment.

with estimates of the role of major prognostic factors and of first line treatments. Prescription preferences by Italian centers clearly showed that imatinib was prevalently chosen for older patients, whose median age was 69 years older, and who had an increased burden of comorbidities, whereas a 2GTKI was reserved to the younger and healthier population. The 4 years OS for the complete cohort was 89%, a result not so different from those reported in randomized controlled trials (RCT) of younger, more selected patients.

Previous reports analyzed large CML cohorts outside clinical trials but prevalently treated with imatinib: the EUTOS group reported a CML population collected in 20 predefined countries and regions in Europe between January 2008 and December 2013, showing an OS probability at 30 months of 92%, with a risk of dying in remission of 1% after 24 months (17). In this population, the ELTS score was tested and showed a significant difference in OS, namely 96%, 89% and 84% in the low, intermediate, and high-risk groups, respectively (8). The EUTOS group reported a subsequent validation of the ELTS score in 2949 CML patients, of whom 236 died, 89 of CML-related causes (12). The overall probability of dying of CML was 5%: applying the ELTS score both the intermediate and high-risk groups had significantly higher probabilities of dying of the disease as compared to the corresponding risk groups defined by the Sokal score. The results of our study are in line with the report by the EUTOS group but are based on a population in which about 50% of patients were treated with a 2GTKI rather than mainly with imatinib.

Since the introduction of imatinib as front-line treatment, older age appears to have lost much of its prognostic relevance. Several experiences have been reported based on age stratification: among them, the MDACC experience showed that older patients had similar cytogenetic response rates and survival compared to younger patients in chronic phase, whereas a worse survival was reported for patients in an advanced phase of the disease (18). Characteristics of CML and rates of responses vary according to age, as demonstrated in a large analysis including 2784 adult patients: the frequency of splenomegaly was more evident in younger patients, as also a high-risk stratification according to prognostic scores, and lower rates of cytogenetic responses with a higher risk of progression (19). In contrast, the German group reported that younger patients do well with imatinib despite baseline prognostic indicators (20). Age may have an influence on the initial dose and compliance to imatinib but the real impact on overall survival was related to comorbidities and to a higher risk of death from other causes, unrelated to CML, confirming the findings of a study on 181 patients aged over 75 years observed in real life practice (21). However, in the EUTOS registry, older age, more peripheral blasts, an enlarged spleen, and low platelet counts were significantly associated with an increased probability of dying of CML (8).

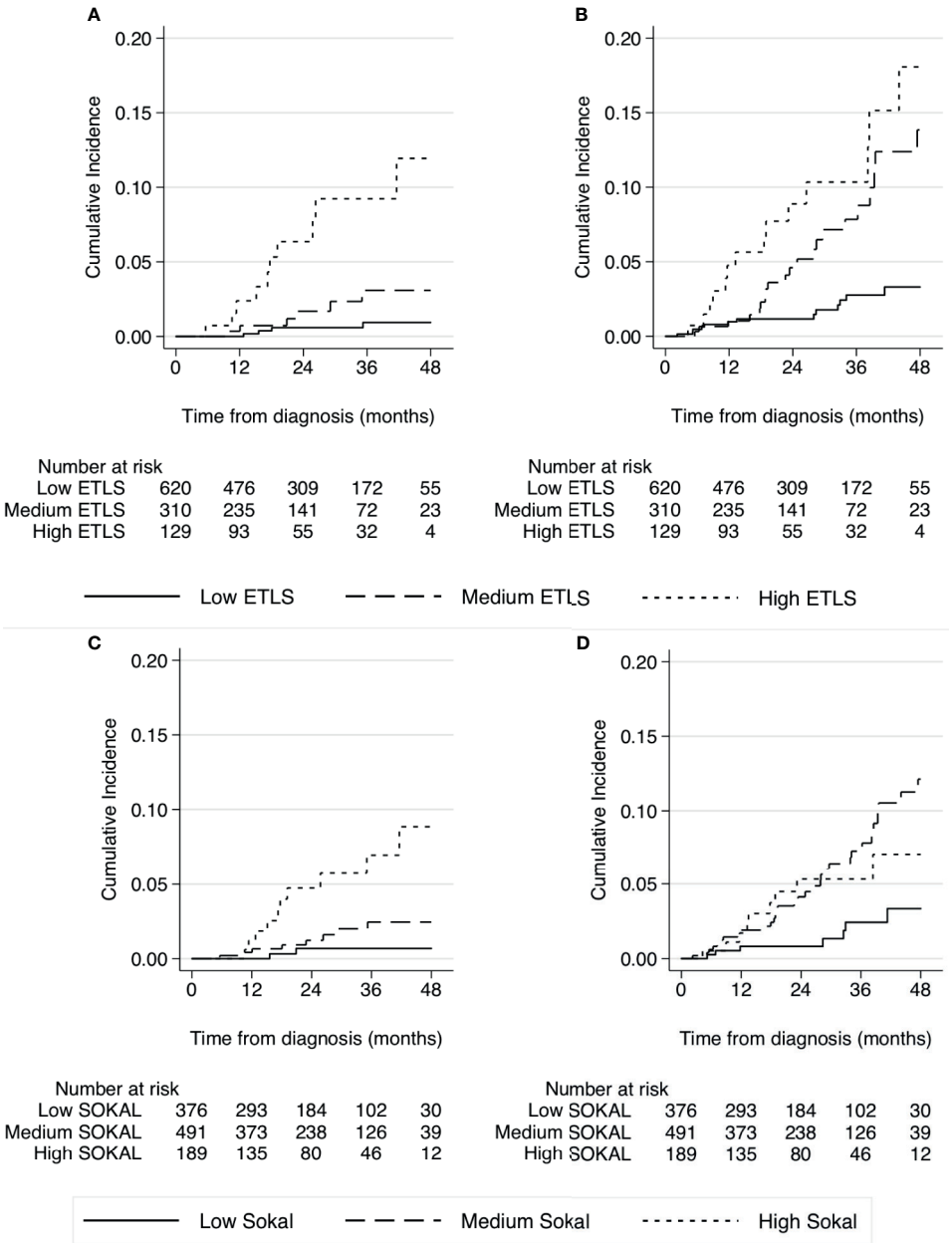

FIGURE 3 | Cumulative incidence of mortality related to CML and other causes of deaths (competing event) by prognostic baseline risk, according to the ELTS **(A, B)** and Sokal score **(C, D)**.

Comorbidities may affect survival and the choice of treatment in CML. A first observation analyzed the Charlson comorbidity index in 125 older CML patients treated with dasatinib in relation to compliance and the onset of pleural effusions, showing a direct association between a higher comorbidity score and drug-related side effects (22). The role of comorbidities and the prognostic role of Charlson index stratification on CML outcomes was further assessed by the German group: 1519 patients entered this analysis, and no differences were detected in terms of cumulative incidences of accelerated and blast phase or remission rates in the different groups. Indeed, higher scores according to the Charlson index were significantly associated with lower overall survival probabilities, with an 8-year survival of only 46.4% in patients with score >7 versus 93.6% in patients with score 2 (23). The presence of comorbidities may also be correlated with the risk of developing adverse events with TKIs. In particular, this association is highlighted by the increasing risk of arterio-occlusive events in patients with other pre-existing cardiovascular risk factors (18). As shown also in our study, in

TABLE 4 | Role of prognostic variables and front-line treatments on survival of CML patients by cause of death (CML related or others).

	CML deaths			Other causes		
	sHR	95% CI	p	sHR	95% CI	p
Age (per year)	1.03	0.99-1.07	0.176	1.03	0.99-1.06	0.064
Sex (F vs M)	0.88	0.32-2.43	0.805	0.65	0.34-1.27	0.207
Charlson C.I. (ref=2)						
3	1.49	0.47-4.71	0.497	1.75	0.73-4.20	0.210
>=4	1.18	0.34-4.07	0.797	5.22	2.56-10.65	<0.001
2GTKI (ref=Imatinib)	1.61	0.52-4.96	0.406	0.26	0.10-0.65	0.004
ELTS risk (ref=low)						
medium	2.36	0.55-10.05	0.245	1.50	0.71-3.15	0.285
high	9.67	2.94-31.74	<0.001	3.11	1.52-6.35	0.002
Sokal risk (*)						
medium	1.76	0.34-9.11	0.498	0.83	0.33-2.08	0.688
high	6.94	1.39-34.54	0.018	1.07	0.35-3.24	0.909

**Estimated in a model including all the covariates in the tables except the ELTS score.*
Sub Hazard Ratio (sHR) and 95% Confidence Intervals (CI) estimated with a multivariable Fine and Gray regression model.

CML patients the assessment of comorbidities and the baseline age may affect TKI selection and dictates close follow-up to optimize the TKI dose.

The estimated crude effects of the variables analyzed were all strongly associated to OS, with a HR of 0.22 in favor of the 2GTKI. Even adjusting the comparison between these drugs by applying a multivariable Cox model, the protective effect of a 2GTKI on overall survival remained remarkable, with an HR of 0.50. However, the proportion of patients who died of CML-related causes was similar in the two cohorts: 1.8% in the imatinib cohort and 1.7% in the 2GTKI cohort. Furthermore, considering the CML-related deaths separately from those due to other causes, treated as competing events, no difference could be detected between treatments in terms of the cumulative risk of CML mortality: all the difference observed for OS was attributable to an increased mortality due to other causes. The analyses performed with the Fine and Gray model, that can account for competing events, clarified the role of the study variables on CML-related death or other causes death. These results did not confirm any advantage of 2GTKIs on CML mortality, in line with the results of the meta-analyses of randomized trials (4). However, these agents induced faster and deeper molecular responses but without differences in overall survival as compared to imatinib (24–26). The rationale to start a 2GTKI was supported by a subanalysis of the ENESTnd, that reported an increased rate of sustained deep molecular response with the 2GTKI when started as front-line treatment as compared to imatinib, allowing an increased proportion of patients to become candidates for a possible discontinuation over time (24). However, the optimization of the dose to reduce the possible long-term off-target events, in particular the cardiovascular side effects associated to these drugs, and the effect of treatment discontinuation, are still a matter of debate.

The principal strength of this large prospective and representative national cohort is that the TKI choice was performed according to a "patient-centered approach", considering at baseline the prognostic role of age, concomitant comorbidities, prognostic score stratification and all the possible concomitant factors that could have influenced the adherence in the long-term (27, 28). Although the comparison between treatments has been adjusted for a set of pre-defined important prognostic factors, and the causes of death analyzed separately, the observational study design does not allow the role of uncontrolled or residual confounding to be excluded.

In conclusion, the analysis conducted showed that some specific clinical factors could be predictive of long-term overall survival in CML patients treated with TKIs. In particular, the comorbidity profile and the stratification by the ELTS score have to be considered at baseline as the mainstay on which to base decisions about the therapeutic strategy best suited to each patient. No difference between IMA and 2GTKI was observed for CML-related mortality.

DATA AVAILABILITY STATEMENT

The data analyzed in this study is subject to the following licenses/restrictions: Observational study. Requests to access these datasets should be directed to gianni.ciccone@cpo.it.

ETHICS STATEMENT

The studies involving human participants were reviewed and approved by University of Bari. The patients/participants provided their written informed consent to participate in this study.

AUTHOR CONTRIBUTIONS

GSp, PP, MBr, GSag, and GCi collected, analyzed and wrote the manuscript. GCa and CM made the statistical analysis. All authors contributed to the article and approved the submitted version.

REFERENCES

1. Hochhaus A, Larson RA, Guilhot F, Radich JP, Branford S, Hughes TP, et al. Long-Term Outcomes of Imatinib Treatment for Chronic Myeloid Leukemia. *New Engl J Med* (2017) 376:917–27. doi: 10.1056/NEJMoa1609324
2. Garcia-Gutierrez V, Hernandez-Boluda JC. Tyrosine Kinase Inhibitors Available for Chronic Myeloid Leukemia: Efficacy and Safety. *Front Oncol* (2019) 9:603. doi: 10.3389/fonc.2019.00603
3. Bower H, Bjorkholm M, Dickman PW, Hoglund M, Lambert PC, Andersson TM. Life Expectancy of Patients With Chronic Myeloid Leukemia Approaches the Life Expectancy of the General Population. *J Clinl Oncol* (2016) 34:2851–57. doi: 10.1200/JCO.2015.66.2866
4. Vener C, Banzi R, Ambrogi F, Ferrero A, Saglio G, Pravettoni G, et al. First-Line Imatinib vs Second- and Third-Generation TKIs for Chronic-Phase CML: A Systematic Review and Meta-Analysis. *Blood Adv* (2020) 4:2723–35. doi: 10.1182/bloodadvances.2019001329
5. Sasaki K, Strom SS, O'Brien S, Jabbour E, Ravandi F, Konopleva M, et al. Relative Survival in Patients With Chronic-Phase Chronic Myeloid Leukaemia in the Tyrosine-Kinase Inhibitor Era: Analysis of Patient Data From Six Prospective Clinical Trials. *Lancet Haematol* (2015) 2:e186–193. doi: 10.1016/S2352-3026(15)00048-4
6. Ylescas-Soria J, de la Torre-Lujian A, Herrera LA, Miranda D, Grimaldo F, Rivas S, et al. Prognostic Factors for Overall Survival in Patients With Chronic Myeloid Leukemia Treated With Imatinib at the National Cancer Institute-Mexici, From 2000 to 2016. *Cancer Med* (2019) 8:2942–9. doi: 10.1002/cam4.2201
7. Hoffmann VS, Baccarani M, Hasford J, Lindoerfer D, Burgstaller S, Sertic D, et al. The EUTOS Population-Based Registry: Incidence and Clinical Characteristics of 2904 CML Patients in 20 European Countries. *Leukemia* (2015) 29:1336–43. doi: 10.1038/leu.2015.73
8. Pfirrmann M, Lauseker M, Hoffmann VS, Hasford J. Prognostic Scores for Patients With Chronic Myeloid Leukemia Under Particular Consideration of Competing Causes of Death. *Ann Hematol* (2015) 94 suppl 2:209–18. doi: 10.1007/s00277-015-2316-0
9. Pfirrmann M, Baccarani M, Saussele S, Guilhot J, Cervantes F, Ossenkoppele G, et al. Prognosis of Long-Term Survival Considering Disease-Specific Death in Patients With Chronic Myeloid Leukemia. *Leukemia* (2016) 30:48–56. doi: 10.1038/leu.2015.261
10. Geelen IGP, Sandin F, Thielen N, Janssen JJWM, Hoogendoorn M, Visser O, et al. Validation of the EUTOS Long-Term Survival Score in a Recent Independent Cohort of "Real World" CML Patients. *Leukemia* (2018) 32:2299–303. doi: 10.1038/s41375-018-0136-7
11. Molica M, Canichella M, Alunni Fegatelli D, Colafigli G, Massaro F, Latagliata R, et al. The Eutos Long-Term Survival Score Accurately Predicts the Risk of Death in Chronic Myeloid Leukaemia Patients Treated Outside of Clinical Trials. *Am J Hematol* (2017) 92:e661–4. doi: 10.1002/ajh.24913
12. Pfirrmann M, Clark RE, Prejzner W, Lauseker M, Baccarani M, Saussele S, et al. The EUTOS Long-Term Survival (ELTS) Score is Superior to the Sokal Score for Predicting Survival in Chronic Myeloid Leukemia. *Leukemia* (2020) 34:2138–49. doi: 10.1038/s41375-020-0931-9
13. Hochhaus A, Baccarani M, Silver RT, Schiffer C, Apperley JF, Cervantes F, et al. European LeukemiaNet 2020 Recommendations for Treating Chronic Myeloid Leukemia. *Leukemia* (2020) 34:966–84. doi: 10.1038/s41375-020-0776-2
14. Baccarani M, Deininger MW, Rosti G, Hochhaus A, Soverini S, Apperley JF, et al. European LeukemiaNet Recommendations for the Management of Chronic Myeloid Leukemia. *Blood* (2013) 122:872–84. doi: 10.1182/blood-2013-05-501569
15. Charlson ME, Pompei P, Ales KL, MacKenzie CR. A New Method of Classifying Prognostic Comorbidity in Longitudinal Studies: Development and Validation. *J Chronic Dis* (1987) 40:373–83. doi: 10.1016/0021-9681(87)90171-8
16. Sokal JE, Cox EB, Baccarani M, Tura S, Gomez GA, Robertson JE, et al. Prognostic Discrimination in "Good-Risk" Chronic Granulocytic Leukemia. *Blood* (1984) 63:789–99. doi: 10.1182/blood.V63.4.789.789
17. Hoffmann VS, Baccarani M, Hasford J, Castagnetti F, Di Raimondo F, Casado LF, et al. Treatment and Outcome of 2904 CML Patients From the EUTOS Population-Based Registry. *Leukemia* (2017) 31:593–601. doi: 10.1038/leu.2016.246
18. Cortes J, Talpaz M, O'Brien S, Giles F, Beth M, Rios J, et al. Effects of Age on Prognosis With Imatinib Mesylate Therapy for Patients With Philadelphia Chromosome-Positive Chronic Myelogenous Leukemia. *Cancer* (2003) 98:1105–13. doi: 10.1002/cncr.11629
19. Castagnetti F, Gugliotta G, Baccarani M, Breccia M, Specchia G, Levato L, et al. Differences Among Young Adults, Adults and Elderly Chronic Myeloid Leukemia Patients. *Ann Oncol* (2015) 26:185–92. doi: 10.1093/annonc/mdu490
20. Kalmanti L, Saussele S, Lauseker M, Proetel U, Muller MC, Hanfstein B, et al. Younger Patients With Chronic Myeloid Leukemia do Well in Spite of Poor Prognostic Indicators: Results From the Randomized CML Study IV. *Ann Hematol* (2014) 93:71–80. doi: 10.1007/s00277-013-1937-4
21. Breccia M, Latagliata R, Stagno F, Luciano L, Gozzini A, Castagnetti F, et al. Charlson Comorbidity Index and Adult Comorbidity Evaluation-27 Scores Might Predict Treatment Compliance and Development of Pleural Effusions in Elderly Patients With Chronic Myeloid Leukemia Treated With Second-Line Dasatinib. *Haematologica* (2011) 96:1457–61. doi: 10.3324/haematol.2011.041251
22. Breccia M, Luciano L, Latagliata R, Castagnetti F, Ferrero D, Cavazzini F, et al. Age Influences Initial Dose and Compliance to Imatinib in Chronic Myeloid Leukemia Elderly Patients But Concomitant Comorbidities Appear to Influence Overall and Event-Free Survival. *Leuk Res* (2014) 38:1173–6. doi: 10.1016/j.leukres.2014.06.020
23. Saussele S, Krauss MP, Hehlmann R, Lauseker M, Proetel U, Kalmanto L, et al. Impact of Comorbidities on Overall Survival in Patients With Chronic Myeloid Leukemia: Results of the Randomized CML Study IV. *Blood* (2015) 126:42–9. doi: 10.1182/blood-2015-01-617993
24. Hochhaus A, Saglio G, Hughes TP, Larson RA, Kim DW, Issaragrisil S, et al. Long-Term Benefits and Risks of Frontline Nilotinib vs Imatinib for Chronic Myeloid Leukemia in Chronic Phase: 5-Year Update of the Randomized ENESTnd Trial. *Leukemia* (2016) 30:1044–54. doi: 10.1038/leu.2016.5
25. Cortes J, Saglio G, Kantarjian HM, Baccarani M, Mayer J, Boquè C, et al. Final 5-Years Study Results of DASISION: The Dasatinib vs Imatinib Study in Treatment-Naïve Chronic Myeloid Leukemia Patients Trial. *J Clin Oncol* (2016) 34:2333–40. doi: 10.1200/JCO.2015.64.8899
26. Cortes JE, Gambacorti-Passerini C, Deininger MW, Mauro MJ, Chuah C, Kim DW, et al. Bosutinib Versus Imatinib for Newly Diagnosed Chronic Myeloid Leukemia: Results From the Randomized BFORE Trial. *J Clin Oncol* (2018) 36:231–7. doi: 10.1200/JCO.2017.74.7162
27. Breccia M, Alimena G. Firstline Treatment for Chronic Phase Chronic Myeloid Leukemia Patients Should be Based on a Holistic Approach. *Expert Rev Hematol* (2015) 8:5–7. doi: 10.1586/17474086.2015.987230
28. Cortes J. How to Manage CML Patients With Comorbidities. *Hematol Am Soc Hematol Educ Program* (2020) 2020(1):237–42. doi: 10.1182/hematology.2020006911

Conflict of Interest: The authors declare that the research was conducted in the absence of any commercial or financial relationships that could be construed as a potential conflict of interest.

Citation: *Specchia G, Pregno P, Breccia M, Castagnetti F, Monagheddu C, Bonifacio M, Tiribelli M, Stagno F, Caocci G, Martino B, Luciano L, Pizzuti M, Gozzini A, Scortechini AR, Albano F, Bergamaschi M, Capodanno I, Patriarca A, Fava C, Rege-Cambrin G, Sorà F, Galimberti S, Bocchia M, Binotto G, Reddiconto G, DiTonno P, Maggi A, Sanpaolo G, De Candia MS, Giai V, Abruzzese E, Miggiano MC, La Barba G, Pietrantuono G, Guella A, Levato L, Mulas O, Saccona F, Rosti G, Musto P, Di Raimondo F, Pane F, Baccarani M, Saglio G and Ciccone G (2021) Prognostic Factors for Overall Survival In Chronic Myeloid Leukemia Patients: A Multicentric Cohort Study by the Italian CML GIMEMA Network.*
Front. Oncol. 11:739171. doi: 10.3389/fonc.2021.739171

frontiers in Oncology

BRIEF RESEARCH REPORT
published: 31 August 2021
doi: 10.3389/fonc.2021.726637

Enrichment of Double RUNX1 Mutations in Acute Leukemias of Ambiguous Lineage

Gabriele Merati[1†], Marianna Rossi[1†], Anna Gallì[1], Elisa Roncoroni[1], Silvia Zibellini[1], Ettore Rizzo[2], Daniela Pietra[1], Cristina Picone[1], Barbara Rocca[1], Claudia Patricia Tobar Cabrera[3], Eleonora Gelli[3], Eugenio Santacroce[3], Luca Arcaini[1,3‡] and Patrizia Zappasodi[1*‡]*

[1] Division of Hematology, Fondazione IRCCS Policlinico San Matteo, Pavia, Italy, [2] enGenome, Pavia, Italy, [3] Department of Molecular Medicine, University of Pavia, Pavia, Italy

Acute leukemia of ambiguous lineage (ALAL) is a rare type of leukemia and represents an unmet clinical need. In fact, due to heterogeneity, substantial rarity and absence of clinical trials, there are no therapeutic guidelines available. We investigated the genetic basis of 10 cases of ALAL diagnosed at our centre from 2008 and 2020, through a targeted myeloid and lymphoid sequencing approach. We show that this rare group of acute leukemias is enriched in myeloid-gene mutations. In particular we found that RUNX1 mutations, which have been found double mutated in 40% of patients and tend to involve both alleles, are associated with an undifferentiated phenotype and with lineage ambiguity. Furthermore, because this feature is typical of acute myeloid leukemia with minimal differentiation, we believe that our data strengthen the idea that acute leukemia with ambiguous lineage, especially those with an undifferentiated phenotype, might be genetically more closer to acute myeloid leukemia rather than acute lymphoblastic leukemia. These data enrich the knowledge on the genetic basis of ALAL and could have clinical implications as an acute myeloid leukemia (AML) – oriented chemotherapeutic approach might be more appropriate.

Keywords: Runx1, acute undifferentiated leukaemia, myeloid genes, acute leukemia of ambiguous lineage, double mutations

OPEN ACCESS

Edited by:
Alessandro Isidori, AORMN Hospital, Italy

Reviewed by:
Deepshi Thakral, All India Institute of Medical Sciences, India
Alice Mims, The Ohio State University, United States

****Correspondence:***
Patrizia Zappasodi
p.zappasodi@smatteo.pv.it
Luca Arcaini
luca.arcaini@unipv.it

[†]These authors have contributed equally to this work and share first authorship

[‡]These authors have contributed equally to this work and share last authorship

Specialty section:
This article was submitted to Hematologic Malignancies, a section of the journal Frontiers in Oncology

Received: *17 June 2021*
Accepted: *05 August 2021*
Published: *31 August 2021*

Citation:
Merati G, Rossi M, Gallì A, Roncoroni E, Zibellini S, Rizzo E, Pietra D, Picone C, Rocca B, Cabrera CPT, Gelli E, Santacroce E, Arcaini L and Zappasodi P (2021) Enrichment of Double RUNX1 Mutations in Acute Leukemias of Ambiguous Lineage. Front. Oncol. 11:726637. doi: 10.3389/fonc.2021.726637

INTRODUCTION

Acute leukemia of ambiguous lineage is a group of rare leukaemia with mixed features of lymphoblastic and myeloid lineage, which represents <4% of all acute leukemias (1).

The 2016 WHO classification of myeloid and lymphoid neoplasms recognizes seven entities under the category of acute leukemias of ambiguous lineage (ALAL), including mixed phenotype acute leukemia (MPAL) with t(9;22)(q34.1;q11.2) *BCR-ABL1*, MPAL with t(v;11q23.3) KMT2A rearranged, MPAL B/myeloid NOS, MPAL T/myeloid NOS, MPAL not otherwise specified (NOS)

rare types, acute undifferentiated leukemia (AUL), and acute leukemia of ambiguous lineage, not otherwise specified (ALAL NOS).

Mixed phenotype acute leukemia (MPAL) is characterized in most cases by a single population of blast cells that express both immunophenotypic features of myeloid origin, as MPO, and markers of B- or T-cell lineage (cCD3 for T cell or CD19 plus CD22 and/or CD79a for B-cell commitment).

MPALs with recurrent cytogenetic abnormalities (BCR-ABL1 and KMT2A rearrangements) represent distinct entities in the last WHO classification; MPALs without these anomalies have been termed MPAL B/myeloid and T/myeloid NOS.

Acute undifferentiated leukemia (AUL) is the rarest type of ALAL. By definition, AUL usually expresses no more than one marker for B-cell, T-cell, or myeloid lineage. Blasts often express the early hematopoietic-associated antigens CD34, CD38, human leukocyte antigen (HLA)-DR, and may be positive for TdT. Attention must be paid in differential diagnosis between AUL and acute myeloid leukemia (AML) with minimal differentiation, which grossly corresponds to the previous M0 by the French–American–British (FAB) classification.

ALALs that do not fulfil the diagnostic criteria for MPAL or AUL should be classified as ALAL NOS.

The immunophenotypic heterogeneity of ALAL likely reflects a heterogeneous mutational profile. Literature data on the mutational landscape of ALAL are sparse and controversial and have been conducted on small cohorts, mainly composed of MPAL (2–4). Overall, they suggest that MPAL share common genetic features with acute lymphoblastic leukemia (ALL). On the other hand, sporadic genetic data on AUL seem to suggest that they are more similar to AML and share a mutational and gene expression profile with AML (3).

An increased biological knowledge on ALAL could have clinical implications such as the choice of an appropriate therapeutic approach: in fact, the treatment of ALAL remains a matter of debate, and it is not clear whether patients benefit from ALL- or AML-oriented chemotherapeutic regimens (5, 6).

Therefore, there is a great need of further studies to better characterize the biology of this group of rare leukemias, which is the first step for setting an effective treatment strategy that is still an unmet clinical need.

METHODS

To address the need of a better biological definition of ALAL, we identified 12 patients who received a diagnosis of ALAL between 2008 and 2020 at the Division of Hematology, Fondazione IRCCS Policlinico San Matteo of Pavia.

All diagnoses have been carefully reviewed according to (1) criteria. The review process was conducted with particular attention to MPALs because the WHO 2016 classification states that some well-defined myeloid leukemia entities have immunophenotypic features that suggest that they be classified as B/myeloid or T/myeloid leukemia. These cases should be classified within their main WHO category, with a secondary annotation that they present a mixed phenotype (1). Therefore, ALAL remains mainly a diagnosis of exclusion. As a result, patients 1 and 8 have been reclassified from MPALs to the AML with myelodysplasia-related changes (AML-MRC) category.

We conducted a mutational analysis on bone marrow samples on the 10 patients with confirmed diagnosis, by using a targeted sequencing approach with a 54 myeloid and a 138 lymphoid gene panels on a HiSeq2500 Illumina (**Supplemental Table 1**). Detailed methods used with each gene panel have been previously published (7, 8). Bone marrow mononuclear cells of patients at diagnosis were analyzed. All variants have been confirmed by whole exome sequencing (WES).

When available, to state the germline or somatic nature of RUNX1 mutations mesenchymal stem cells cultured from bone marrow, skin fibroblasts or cells isolated from buccal rinse were sequenced. The relapse sample of patient 9 was also sequenced.

Copy-number variants (CNVs) calling was performed with ExomeDepth (9), an algorithm that uses a read depth strategy to call CNVs from exome or targeted sequencing data. This approach aims to compare each case with a matched aggregate reference set that is created combining the sequencing results of the study.

In a subset of cases with RUNX1 double mutations, we explored the reads generated from DNA or RNA libraries spanning both positions in order to determine if mutations involved one allele (*cis*) or both alleles (*trans*). The reads presenting only one variant were considered in *trans*, and the reads presenting both variants were considered in *cis*. The fraction of reads with *cis* configuration and the fraction with *trans* configuration were then calculated by dividing the number of in *cis* reads and in *trans* reads by the number of total reads. DNA libraries were prepared using Illumina TruSight Myeloid Panel.

For patients with RUNX1 mutations not covered by unique DNA sequencing reads (i.e., >250 bp distance), an *ad hoc* procedure was developed for the analysis of RNA. Briefly, specific primers with overhang adapter sequences were designed to amplify the region encompassing the two RUNX1 mutations. Illumina sequencing adapters and dual-index barcodes were added to the amplicon target through a limited cycle of PCR. Libraries were normalized, pooled, and loaded onto a 500-cycle MiSeq sequencer flow cell.

RESULTS

Our study cohort resulting from the diagnostic review consists of five AUL, two MPAL B/myeloid NOS, one MPAL T/myeloid NOS, and two ALAL NOS (**Table 1**); the median age at diagnosis was 64.5 years (range, 26–73).

Seven (3 AUL, 2 ALAL-NOS, and 2 MPAL) of 10 patients have been treated with intensive chemotherapy. Two patients were considered unfit for intensive treatment, and one patient was lost to follow-up after diagnosis. Both ALL- and AML-oriented chemotherapeutic regimens showed some efficacy to induce complete remissions, supporting the ambiguous nature of disease. Overall, five patients achieved complete remission, and

TABLE 1 | Flow cytometry and cytogenetic features of the ALAL cohort.

Patient	Diagnosis review (WHO 2016)	Age at diagnosis (year)	Flow Cytometry	Cytogenetic analysis
Pt 2	AUL	66	90% blasts: **CD34+,** CD117–, MPO–, **Tdt+**, **CD13dim**, **CD38+, DR+**, CD19–, CD79a–, CD2–, cCD3–, CD3, CD4–, CD5–, CD7–, CD8–, CD10–, CD14–, CD16–, CD19–, CD20–, CD11b–, CD11c–, CD33–, CD14–, CD15–, CD41–, CD56–, CD61–	46 XY FISH for 5q31/5p15,7q31/cen7, KMT2A, t(8;21) normal
Pt 3	ALAL NOS	71	57% blasts: **CD34+, CD117+**, MPO–, **Tdt+, CD7+, CD5+, CD99+, CD79a+, CD38+, CD33dim**, CD10–, CD19–, CD20–, cyCD22–, FMC7–, CD1a–, CD2–, CD3–, cCD3–, CD4–, CD8–, CD11c–, CD13–, CD15–, CD16–, CD56–	46 XX FISH for 5q31/5p15,7q31/cen7, KMT2A, t(8;21) normal
Pt 4	ALAL NOS	46	50% blasts: **CD34+**, CD117–, MPO–, Tdt–, **CD13+**, **CD33+**, **CD5+, CD7+, DR+, CD10+**, CD19–, CD20, cyCD22–, cyCD79a–, CD2–, CD3–, cyCD3–, CD4–, CD8–, CD11b–, CD11c–, CD14–, CD15–, CD16–, CD56–	46, XX, t(2;3)(p21;q26), del (6q)(q23), t (12);?(p13);?, ins (12);?(p13);? FISH for 5q31/5p15,7q31/cen7, KMT2A, t(8;21) normal, ETV6 and MECOM rearranged with unknown partner genes
Pt 5	AUL	72	27% blasts: **CD34+**, CD117–, MPO–, **Tdt+, CD13+, CD38+**, CD33–, **CD99+, DR+**, CD10–, CD19–, CD20–, cyCD22–, cyCD79a–, CD1a–, CD2–, CD3–, cyCD3–, CD4–, CD5–, CD7–, CD8–, CD11b–, CD11c–, CD14–, CD15–, CD16–, CD41–, CD61–, CD71–, CD25–, CD56–	48, XX, −14, + mar1, + dup(mar1), + mar2 FISH for 5q31/5p15,7q31/cen7, KMT2A, t(8;21) normal
Pt 6	AUL	72	80% blasts: **CD34+, CD117+**, MPO–, Tdt–, **DR+, CD38+**, CD33–, CD13–, CD10–, CD19–, CD20–, cyCD22–, cyCD79a–, CD2–, CD3–, cyCD3–, CD4–, CD5–, CD7–, CD8–, CD11b–, CD11c–, CD14–, CD15–, CD16–, CD56–	46 XY FISH for 5q31/5p15,7q31/cen7, KMT2A, t(8;21) normal, BCR/ABL, rearrangements involving EV1, FGFR1, PDGFRB e JAK2 absent
Pt 7	MPAL B/ myeloid	52	64% blasts: CD34–, CD117–, **MPO+, Tdt+, CD19+, CD79a+, CD10+, CD58+, CD38+, CD33dim**, CD10–, CD19–, cyCD22–, cyCD79a–, CD7–, cyCD3–, CD11c–, CD14–, CD16–	45, X FISH panel for 5q31/5p15,7q31/cen7, KMT2A, t(8;21) normal
Pt 9	MPAL B/ myeloid bilinear	63	40% blasts: **CD34+, CD117+**, MPO–, **Tdt+, CD13+, CD33+, CD25+, DR+**. 28% blasts: **CD34+**, CD117–, MPO–, **Tdt+, CD19+, CD22+, CD25+**; CD10–, CD20–, cyCD79a–, CD2–, CD3–, cyCD3–, CD4–, CD5–, CD7–, CD8–, CD11b–, CD11c–, CD14–, CD15–, CD16–, CD56–	46, XY
Pt 10	MPAL T/myeloid	45	78% blasts: **CD34+, CD117+, MPO+**, Tdt–, **CD13+, CD33+, CD7+, CD5+, cyCD3+, CD3+**, DR–, CD2–, CD4–, CD8–, CD11b–, CD11c–, CD14–, CD15–, CD16–, CD25–, CD56–	Hyperdiploidy
Pt 11	AUL	73	65% blasts: **CD34+**, CD19–, **CD10dim**, **Tdt+,** CD20–, MPO–, **CD38+, CD117+**, CD13–, CD33–, CD3–, cyCD3–, CD2–, CD5–, CD7–, **cyCD22dim**, cyCD79a–	46, XY
Pt 12	AUL	26	91% blasts: **CD34+**, CD19–, **CD10dim, Tdt+**, CD20–, MPO–, **CD38+/**–, CD117–, CD13–, CD33–, CD3–, cyCD3–, CD2–, CD7–/+(dim), CD5–, CD25–, **cyCD22dim**, cyCD79a–	46, XY

Bold values highlight positive flow cytometry markers.

four proceeded to allogeneic bone marrow transplant (**Supplemental Table 2**).

The most frequently mutated genes within the myeloid panel were NRAS (40%; 4/10 patients), RUNX1 (40%; 4/10), ASXL1 (30%; 3/10), DNMT3A (20%; 2/10), BCOR (20%; 2/10), EZH2 (20%; 2/10), and U2AF1 (20%; 2/10). The only recurrently mutated lymphoid gene was KMT2C (25%, 2/8), but mutations within this gene were mainly subclonal (**Supplemental Table 3**). **Table 2** summarizes the mutational profile of the 10 ALAL patients.

The median number of mutations in myeloid genes [3; interquartile range (IQR), 1–4] was superior compared to the lymphoid ones (1; IQR, 0–19) (**Supplemental Figure 1**).

We then focused our attention on the RUNX1 gene, which is a well-known regulator of hematopoiesis and is essential for the development of both lymphoid and myeloid lineages (10).

All four RUNX1-mutated cases presented two mutations, mainly of founding type (**Table 3**): three AUL patients (patients 2, 11, and 12) and one patient (patient 9) with a MPAL B/myeloid bilinear NOS whose immunophenotype profile was a mixture of an AML with minimal differentiation and a B-cell acute lymphoblastic leukemia (B-ALL) (**Table 1**). Patients 2, 9, and 12 presented high RUNX1 variant allele frequency (VAF), suggesting that all variants were clonal (**Table 3**). Patient 11 was the only one who presented oncogenic variants with low allelic burdens, including RUNX1, and this has been addressed to hemodilution of the bone marrow aspirate.

In addition to SNVs and small insertions/deletions (indels), major RUNX1 deletions represent another possible mechanism of loss-of-function alteration. Therefore, we applied a copy number variant (CNV)-targeted approach for the identification of RUNX1 deletions, and we did not identify any larger deletions or insertions along the exons of the RUNX1 wild-type cases.

To investigate whether RUNX1 SNVs and indels were somatically acquired or inherited, we sequenced with the myeloid-gene panel the germline control tissues (bone marrow mesenchymal stem cells, buccal rinse cells, or skin fibroblasts) available in three RUNX1-mutated patients (patients 2, 9, and 12): all samples resulted wild type, thus confirming the somatic

TABLE 2 | Mutational profile of the 10 patients with acute leukemia of ambiguous lineage.

Diagnosis	Pt 2 AUL	Pt 5 AUL	Pt 6 AUL	Pt 11 AUL	Pt 12 AUL	Pt 7 MPAL B/M	Pt 9 MPAL B/M	Pt 10 MPAL T/M	Pt 3 ALAL NOS	Pt 4 ALAL NOS	
ASXL1											Chromatin regulation
BCOR											
EZH2											
KDM6A											
DNMT3A											DNA methilation
IDH2											
FLT3											RTK-RAS signaling
KRAS											
NRAS											
PTPN11											
SETBP1											
PHF6											Transcription factor
IKZF1											
RUNX1											
SF3B1											RNA splicing
SRSF2											
U2AF1											
ARID1A											Chromatin regulation
ATM											Cell cycle apoptosis
FGFR3											RTK-RAS signaling
KMT2C											DNA methylation
KMT2D											
NOTCH1											NOTCH pathway
PDE4DIP											Microtubule assembly

We report only oncogenic and likely oncogenic single nucleotide variants and small indels identified with the 54 myeloid gene and 138 lymphoid gene panels. The green colored boxes indicate that patients 11 and 12 have not been studied with the lymphoid panel. The violet-colored boxes identify myeloid gene mutations. Orange-colored boxed identify lymphoid gene mutations.

TABLE 3 | Pattern of RUNX1 mutations in three AUL patients and one MPAL B/myeloid.

Patient	Gene	Function	Chr	C.	P.	AB	Exon	WT	MT	Allele configuration P.	COSMIC ID	FATHMM pathogenic score
2	RUNX1	Stopgain SNV	21	c.777dupT	p.N260_P261delinsX	42.00	7	–	A	p.[F163Y][N260_P261delinsX]	NA	NA
	RUNX1	Missense	21	c.T488A	p.F163Y	43.30	5	A	T		COSM26023	0.99
9	RUNX1	Frameshift deletion	21	c.492delC	p.V164fs	26.58	5	G	–	NA	NA	NA
	RUNX1	Missense	21	c.A314G	p.H105R	37.40	4	T	C		NA	NA
11	RUNX1	Nonsense	21	c.427T	p.E143X	4.00	5	C	A	p.[E143X;p.A147_T148insRDA]	NA	NA
	RUNX1	Inframe insertion	21	c.442_443insGAGATGCTA	p.A147_T148insRDA	5.30	5	–	TAGCATCTC		NA	NA
12	RUNX1	Frameshift	21	c.382_383insAGAG	p.T128KfsX11	45.90	5	–	CTCT	p.[T128KfsX11];[p.R166G]	NA	NA
	RUNX1	Missense	21	c.496C>G	p.R166G	43.40	5	G	C		COSM24742	0.88

All four RUNX1 mutated patients present both a missense and a nonsense/frameshift variant. All variants were likely to be founding because allele burden (AB) are high in all patients except from patient 11 whose bone marrow sample was highly contaminated with peripheral blood (see also ***Supplemental Table 3****).*

TABLE 4 | Clonal evolution dynamics in patient 9.

Gene	Transcript	CCDS	EX	C.	P.	Allele burden—diagnosis	Allele burden—relapse
PHF6	NM_001015877	CCDS14639.1	9	c.C932G	p.A311G	0.8065	0.4013
RUNX1	NM_001754	CCDS13639.1	4	c.A314G	p.H105R	0.374	0
RUNX1	NM_001754	CCDS13639.1	5	c.492delC	p.V164fs	0.2658	0.3043
SF3B1	NM_012433	CCDS33356.1	13	c.G1774A	p.E592K	0.4347	0.2907
Immunophenotypic features of bone marrow blasts						40%: **CD34+, CD117+**, MPO–, **Tdt+, CD13+, CD33+, CD25+, DR+**. 28%: **CD34+,** CD117–, MPO–, **Tdt+, CD19+, CD22+, CD25+**; CD10–, CD20–, cyCD79a–, CD2–, CD3–, cyCD3–, CD4–, CD5–, CD7–, CD8–, CD11b–, CD11c–, CD14–, CD15–, CD16–, CD56–	15%: **CD34+, CD117+, MPO+, CD13+, CD33+, CD15+, DR+, CD38+**, Tdt–, CD19–, CD20–, CD22–, CD22cy–, CD79a–, CD2–, cyCD3–, CD7–, CD123–, CD10–, CD25–, CD56–, CD11b–

The double RUNX1 mutant genotype at diagnosis confers lineage ambiguity (MPAL B/myeloid NOS), whereas the disappearance of one RUNX1 variant at relapse gives rise to an AML phenotype.
Bold values highlight positive flow cytometry markers.

origin of these variants. Case 11 showed a low allele burden in the tumour sample (4% and 5%), and therefore, even in the absence of a control tissue, we can reasonably conclude that both mutations were somatically acquired.

To better understand the effect of RUNX1 double mutations, we studied the distribution of RUNX1 variants between the two alleles of the gene, as *cis* or *trans* configuration may have different biological implications on gene function and clinical phenotype.

In three samples (samples 2, 11, and 12), we were able to determine the allele configuration of RUNX1 composite mutations (**Table 3**).

The analysis of sequencing reads generated from DNA of the low VAF RUNX1 double mutated case (patient 11, **Table 3**) revealed a *cis* configuration of the two lesions.

The analysis of DNA and RNA sequencing reads in patients 12 and 2, respectively, showed a *trans* configuration of the two mutations; this allele configuration likely reduces the functional form of the gene, since both homologues are altered in nearly all cells.

In addition, the missense mutation identified in patient 2 (c.488T>A, p.F163Y) was predicted, by *in silico* splice site prediction tools (Human Splice Finder and Fruifly with score of 98.4 and 1, respectively), to induce the activation of a cryptic donor site that might affect pre-mRNA processing. Accordingly with this prediction, the analysis of RNA reads showed the presence of a 23-nucleotide deletion in 49% of the reads resulting from a non-canonical splice site recognition (**Supplemental Figure 2**). This event induces a shift in the reading frame that predicts the termination of protein synthesis 41 codons downstream, thus resulting in a truncated protein. Sanger sequencing on complementary DNA (cDNA) confirmed next-generation sequencing (NGS) results (c.486-508del23, p.F163EfsX41). Moreover, the original c.488T>A and c.777dupT variants were found in the remaining 2% and 49% of the RNA reads, respectively. Therefore, wild-type reads were not detected, confirming that the RUNX1 variants are in *trans*, and substantially, no functional RNA was present.

Case 9 was also evaluated at relapse with the targeted myeloid panel. The mutational landscape at relapse showed overlapping with the sample at diagnosis except for the loss of the RUNX1 missense variant c.314A>G. Interestingly, the immunophenotype at relapse showed loss of the lymphoid markers Tdt, CD19, and CD22 and gain of MPO, thus corresponding to the immunophenotypic profile of an AML with minimal differentiation.

DISCUSSION

Our cohort of patients is limited and precludes the possibility of a significant statistical analysis. Despite this intrinsic limitation, the amount of mutations in myeloid genes was clearly exceeding the number of lymphoid ones, with statistical significance (**Supplemental Figure 1**). This imbalance could in part reflect the features of our cohort, which is particularly enriched in AUL, whereas the majority of studies on ALAL have been conducted on MPALs, and AULs were often underrepresented (4, 11, 12).

Overall, ALAL presents a heterogeneous genetic landscape, and both individual genes and pathways do not clearly cluster within the different disease subtypes (**Supplemental Figure 3**).

One of the most frequently mutated genes was RUNX1 (40%; 4/10), which was found double mutated in all cases. To gain insight into this particular feature, which was previously described in AML with minimal differentiation, we further characterized the RUNX1-mutated cases.

All RUNX1 SNV and indels resulted somatically acquired, excluding a familial predisposition leukemia with one inherited RUNX1 mutation, which is an increasingly recognized and often underdiagnosed condition (13). Furthermore, we excluded other major deletions/insertions that could affect RUNX1 gene.

Finally, we studied the *cis/trans* RUNX1 allele configuration in three patients (patient 9 could not be studied due to paucity of the sample) and revealed that two patients (patients 2 and 12) had mutations involving both alleles, while one patient (patient 11) presented both mutations on the same allele. Therefore, while for patients 2 and 12, we can reasonably speculate that there is substantially no functional RUNX1 protein left, patient 11 kept one RUNX1 allele intact.

Other factors can negatively affect RUNX1 protein function in the posttranscriptional phase, such as the dominant-negative effect, which is a well-known mechanism that has been described for some RUNX1 variants (14). Although it has not been demonstrated for patient 9, we cannot exclude that protein function be altered through other posttranscriptional events leading to a complete RUNX1 loss of function.

Patient 2 RUNX1 c.488T>A variant has been previously reported in the literature (15, 16) and has been interpreted as a missense mutation coding for p.F163Y. However, data about the mechanism of action of RUNX1 p.F163Y have not been provided, and we could not find sequences carrying c.486_508del23 in repositories of variants as Cosmic, ClinVar, HGMD, or Lovd.

Therefore, we gained insight into the oncogenic mechanism of c.488T>A variants, which, instead of a missense variant, results in a misplacing event that leads to a truncated protein. This underlines the importance to perform RNA analysis for the full evaluation of exonic mutations close to exon–intron border.

Patient 9 was evaluated at relapse where both the immunophenotypic properties and genetic landscape substantially changed. In particular, the disappearance of one RUNX1 variant at relapse was associated with the loss of lineage ambiguity (**Table 4**), and the immunophenotypic features at that point were coherent with an AML with minimal differentiation.

Taken together, these data suggest that the complete loss of function of RUNX1 correlates with the lack of expression of lineage-defining markers and contributes to lineage ambiguity.

Double RUNX1 mutations have been previously reported to be associated with AML with minimal differentiation (14), and RUNX1 mutations have been described in AUL (17) in up to 40% of cases, consistently with our results. Our data enrich previous knowledge on AUL, suggesting that this rare type of leukemia is genetically more similar to AML, specific to AML with minimal differentiation.

In conclusion, we show that myeloid gene mutations are enriched in a cohort of ALAL cases strictly diagnosed according to WHO 2016 criteria.

Moreover, our data seem to suggest that double RUNX1 mutations are enriched in leukemias with an undifferentiated phenotype and may support the hypothesis that AUL and AML

with minimal differentiation represent a continuum of disease with a similar genetic background. This finding has significant clinical implications, as AUL could be more sensitive to standard AML-oriented therapeutic regimens.

DATA AVAILABILITY STATEMENT

The datasets presented in this study can be found in online repositories. The names of the repository/repositories and accession number(s) can be found in the article/**Supplementary Material**.

ETHICS STATEMENT

The studies involving human participants were reviewed and approved by Ethics committee of IRCCS Fondazione Policlinico San Matteo, Pavia, Italy. The patients/participants provided their written informed consent to participate in this study.

AUTHOR CONTRIBUTIONS

PZ and LA conceived, designed, and supervised the study. GM, MR, AG, SZ, PZ, and LA analyzed and interpreted data and wrote the manuscript. All authors contributed to the article and approved the submitted version.

FUNDING

This work was supported by grants of the Fondazione Regionale Ricerca Biomedica (FRRB), Milan, Italy (FRRB project no. 2015-0042, genomic profiling of rare hematologic malignancies, development of personalized medicine strategies, and their implementation into the Rete Ematologica Lombarda clinical network) and by the Italian Ministry of Education, University and Research (MIUR) to the Departments of Molecular Medicine (DMM) of the University of Pavia under the initiative "Dipartimenti di Eccellenza (2018–2022)". The funder was not involved in the study design, collection, analysis, and interpretation of data, the writing of this article or the decision to submit it for publication.

ACKNOWLEDGMENTS

The authors thank Chiara Chiereghin who helped in the interpretation of data.

SUPPLEMENTARY MATERIAL

The Supplementary Material for this article can be found online at: https://www.frontiersin.org/articles/10.3389/fonc.2021.726637/full#supplementary-material

REFERENCES

1. Arber DA, Orazi A, Hasserjian R, Thiele J, Borowitz MJ, Le Beau MM, et al. The 2016 Revision To The World Health Organization Classification of Myeloid Neoplasms and Acute Leukemia. *Blood* (2016) 127(20):2391–405. doi: 10.1182/blood-2016-03-643544
2. Eckstein OS, Wang L, Punia JN, Kornblau SM, Andreeff M, Wheeler DA, et al. Mixed-Phenotype Acute Leukemia (MPAL) Exhibits Frequent Mutations in DNMT3A and Activated Signaling Genes. *Exp Hematol* (2016) 44(8):740–4. doi: 10.1016/j.exphem.2016.05.003
3. Lao ZT, Ding LW, An O, Hattori N, Sun QY, Tan KT, et al. Mutationa and Transcriptomic Profiling of Acute Leukemia of Ambiguous Lineage Reveals Obscure But Clinically Important Lineage Bias. *Haematologica* (2019) 104 (5):200–3. doi: 10.3324/haematol.2018.202911
4. Takahashi K, Wang F, Morita K, Yan Y, Hu P, Zhao P, et al. Integrative Genomic Analysis Of Adult Mixed Phenotype Acute Leukemia Delineates Lineage Associated Molecular Subtypes. *Nat Commun* (2018) 9(2670):1–12. doi: 10.1038/s41467-018-04924-z
5. Zhang Y, Wu D, Sun A, Qiu H, He G, Jin Z, et al. Clinical Characteristics, Biological Profile, and Outcome of Biphenotypic Acute Leukemia: A Case Series. *Acta Haematol* (2011) 125(4):210–8. doi: 10.1159/000322594
6. Changcheng Z, Jingsheng W, Xin L, Kaiyang D, Xiaoyan C, Weibo Z. What is the Optimal Treatment for Biphenotypic Acute Leukemia? *Haematologica* (2009) 94(12):1778–80. doi: 10.3324/haematol.2009.015594
7. Malcovati L, Gallì A, Travaglino E, Ambaglio I, Rizzo E, Molteni E, et al. Clinical Significance Of Somatic Mutation in Unexplained Blood Cytopenia. *Blood* (2017) 129(25):3371–8. doi: 10.1182/blood-2017-01-763425
8. Defrancesco I, Zibellini S, Boveri E, Frigeni M, Ferretti VV, Rizzo E, et al. Targeted Next-Generation Sequencing Reveals Molecular Heterogeneity In Non-Chronic Lymphocytic Leukemia Clonal B-Cell Lymphocytosis. *Hematol Oncol* (2020) 38(5):689–97. doi: 10.1002/hon.2784
9. Plagnol V, Curtis J, Epstein M, Mok KY, Stebbings E, Grigoriadou S, et al. A Robust Model for Read Count Data in Exome Sequencing Experiments and Implications for Copy Number Variant Calling. *Bioinformatics* (2012) 28 (21):2747–54. doi: 10.1093/bioinformatics/bts526
10. Yoshiaki I. Oncogenic Potential of the RUNX Gene Family: 'Overview'. *Oncogene* (2004) 23(24):4198–208. doi: 10.1038/sj.onc.1207755
11. Quesada A, Hu Z, Routbort M, Patel KP, Luthra R, Loghavi S, et al. Mixed Phenotype Acute Leukemia Contains Heterogeneous Genetic Mutations by Next-Generation Sequencing. *Oncotarget* (2018) 9:8441–9. doi: 10.18632/oncotarget.23878
12. Alexander TB, Gu Z, Iacobucci I, Dickerson K, Choi JK, Xu B, et al. The Genetic Basis and Cell Of Origin Of Mixed Phenotype Acute Leukemia. *Nature* (2018) 562:373–9. doi: 10.1038/s41586-018-0436-0
13. Ernst M, Kavelaars F, Löwenberg B, Valk P, Raaijmakers M. *RUNX1* Germline Variants in *RUNX1*-Mutant AML: How Frequent? *Blood* (2021) 137 (10):1428–31. doi: 10.1182/blood.2020008478
14. Simon L, Lavallèe VP, Bordeleau ME, Krosl J, Baccelli I, Boucher G, et al. Chemogenomic Landscape Of RUNX1-Mutated AML Reveals Importance Of RUNX1 Allele Dosage In Genetics and Glucocorticoid Sensitivity. *Clin Cancer Res* (2017) 23(22):6969–81. doi: 10.1158/1078-0432.CCR-17-1259
15. Chien-Yuan C, Liang-In L, Jih-Luh T, Ko BS, Tsay W, Chou WC, et al. RUNX1 Gene Mutation In Primary Myelodysplastic Syndrome–The Mutation Can Be Detected Early at Diagnosis or Acquired During Disease Progression and Is Associated With Poor Outcome. *Br J Haematol* (2007) 139(3):405–14. doi: 10.1111/j.1365-2141.2007.06811.x
16. Syed AM, Alexander ES, Austin GK, Kizilors A, Mohamedali AM, Lea NC, et al. Spliceosome Mutations Exhibit Specific Associations With Epigenetic Modifiers and Proto-Oncogenes Mutated In Myelodysplastic Syndrome. *Haematologica* (2013) 98(7):1058–66. doi: 10.3324/haematol.2012.075325
17. Weinberg O, Hasserjian R, Baraban E, Ok CY, Geyer JT, Philip JKKS, et al. Clinical, Immunophenotypic, and Genomic Findings of Acute Undifferentiated

Leukemia and Comparison to Acute Myeloid Leukemia With Minimal Differentiation: A Study From The Bone Marrow Pathology Group. *Modern Pathol* (2019) 32:1373–85. doi: 10.1038/s41379-019-0263-3

Conflict of Interest: Author ER was employed by the company enGenome srl.

The remaining authors declare that the research was conducted in the absence of any commercial or financial relationships that could be construed as a potential conflict of interest.

Publisher's Note: All claims expressed in this article are solely those of the authors and do not necessarily represent those of their affiliated organizations, or those of the publisher, the editors and the reviewers. Any product that may be evaluated in this article, or claim that may be made by its manufacturer, is not guaranteed or endorsed by the publisher.

frontiers in Oncology

ORIGINAL RESEARCH
published: 06 September 2021
doi: 10.3389/fonc.2021.740079

Letermovir Prophylaxis for Cytomegalovirus Infection in Allogeneic Stem Cell Transplantation: A Real-World Experience

Massimo Martino[1†], Annalisa Pitino[2†], Mercedes Gori[2†], Benedetto Bruno[3,4], Alessandra Crescimanno[5], Vincenzo Federico[6], Alessandra Picardi[7,8], Stefania Tringali[9], Claudia Ingrosso[10], Paola Carluccio[11], Domenico Pastore[12], Gerardo Musuraca[13], Annalisa Paviglianiti[1], Adriana Vacca[14], Bianca Serio[15], Gabriella Storti[16], Nicola Mordini[17], Salvatore Leotta[18], Michele Cimminiello[19], Lucia Prezioso[20], Barbara Loteta[1], Anna Ferreri[1], Fabrizia Colasante[21], Emanuela Merla[21], Luisa Giaccone[3,4], Alessandro Busca[3], Maurizio Musso[5], Renato Scalone[5], Nicola Di Renzo[6], Serena Marotta[7], Patrizio Mazza[10], Pellegrino Musto[11], Immacolata Attolico[11], Carmine Selleri[15], Filippo Antonio Canale[1], Marta Pugliese[1], Giovanni Tripepi[22], Gaetana Porto[1], Giovanni Martinelli[13], Angelo Michele Carella Jr.[21‡] and Claudio Cerchione[13*‡]*

[1] Centro Unico Regionale Trapianti Cellule Staminali e Terapie Cellulari (CTMO), Grande Ospedale Metropolitano "Bianchi-Melacrino-Morelli", Reggio Calabria, Italy, [2] Istituto di Fisiologia Clinica del Consiglio Nazionale delle Ricerche (CNR), Roma, Italy, [3] Dipartimento di Oncologia, SSD Trapianto Allogenico di Cellule Staminali, AOU Città della Salute e della Scienza di Torino, Torino, Italy, [4] Dipartimento di Biotecnologie Molecolari e Scienze per la Salute, Divisione di Ematologia, Università di Torino, Torino, Italy, [5] Unità Operativa di Oncoematologia e TMO, Istituto "La Maddalena", Palermo, Italy, [6] Ematologia e Trapianto di Cellule Staminali, Polo Ospedaliero "Vito Fazzi", Lecce, Italy, [7] UOC Ematologia con Trapianto CSE, AORN "Antonio Cardarelli", Napoli, Italy, [8] Dipartimento di Biomedicina e Prevenzione, Università di Roma Tor Vergata, Roma, Italy, [9] UOSD UTMO, AOR Villa "Sofia Cervello", Palermo, Italy, [10] Ematologia e Trapianto di Midollo Osseo, Ospedale "San Giuseppe Moscati", Taranto, Italy, [11] UOC di Ematologia con Trapianto, Dipartimento di Emergenza e Trapianti d'Organo, Università degli Studi "Aldo Moro" e AOUC Policlinico di Bari, Bari, Italy, [12] Divisione di Ematologia, Ospedale "Antonio Perrino", Brindisi, Italy, [13] Unità di Ematologia, IRCCS Istituto Romagnolo per lo Studio dei Tumori (IRST) "Dino Amadori", Meldola, Italy, [14] UO Ematologia - CTMO, Polo Ospedaliero "Armando Businco", Cagliari, Italy, [15] Dipartimento di Medicina, Chirurgia e Odontoiatria, Università di Salerno, Salerno, Italy, [16] Unità di Ematologia, Azienda Ospedaliera "San Giuseppe Moscati", Avellino, Italy, [17] SC Ematologia, Azienda Ospedaliera "S. Croce e Carle", Cuneo, Italy, [18] Programma di Trapianto Emopoietico, Azienda Policlinico "Vittorio Emanuele", Catania, Italy, [19] Divisione Universitaria di Ematologia, Ospedale "San Carlo", Potenza, Italy, [20] Ematologia e Centro Trapianti Midollo Osseo (CTMO), Dipartimento ad Attività Integrata Medicina Generale e Specialistica, Azienda Ospedaliero-Universitaria di Parma, Parma, Italy, [21] Ospedale I.R.C.C.S. Casa Sollievo della Sofferenza - Centro Trapianti di Cellule Staminali, San Giovanni Rotondo, Italy, [22] Istituto di Fisiologia Clinica del Consiglio Nazionale delle Ricerche (CNR), Reggio Calabria, Italy

Despite effective treatments, cytomegalovirus (CMV) continues to have a significant impact on morbidity and mortality in allogeneic stem cell transplant (allo-SCT) recipients. This multicenter, retrospective, cohort study aimed to evaluate the reproducibility of the safety and efficacy of commercially available letermovir for CMV prophylaxis in a real-world setting. Endpoints were rates of clinically significant CMV infection (CSCI), defined as CMV disease or CMV viremia reactivation within day +100-+168. 204 adult CMV-seropositive allo-SCT recipients from 17 Italian centres (median age 52 years) were treated with LET 240 mg/day between day 0 and day +28. Overall, 28.9% of patients underwent a haploidentical, 32.4% a matched related, and 27.5% a matched unrelated donor (MUD)

Edited by:
Massimo Gentile, Health Agency of Cosenza, Italy

Reviewed by:
Shin Mineishi, Penn State Milton S. Hershey Medical Center, United States
Jacopo Mariotti, Humanitas Research Hospital, Italy

***Correspondence:**
Massimo Martino
massimo.martino@ospedalerc.it
Claudio Cerchione
claudio.cerchione@irst.emr.it

†These authors have contributed equally to this work and share first authorship

‡These authors have contributed equally to this work and share last authorship

Specialty section:
This article was submitted to Hematologic Malignancies, a section of the journal Frontiers in Oncology

Received: *12 July 2021*
Accepted: *13 August 2021*
Published: *06 September 2021*

Citation:
Martino M, Pitino A, Gori M, Bruno B, Crescimanno A, Federico V, Picardi A, Tringali S, Ingrosso C, Carluccio P, Pastore D, Musuraca G, Paviglianiti A, Vacca A, Serio B, Storti G, Mordini N, Leotta S, Cimminiello M, Prezioso L, Loteta B, Ferreri A, Colasante F, Merla E, Giaccone L, Busca A, Musso M, Scalone R, Di Renzo N, Marotta S, Mazza P, Musto P, Attolico I, Selleri C, Canale FA, Pugliese M, Tripepi G, Porto G, Martinelli G, Carella AM Jr and Cerchione C (2021) Letermovir Prophylaxis for Cytomegalovirus Infection in Allogeneic Stem Cell Transplantation: A Real-World Experience. Front. Oncol. 11:740079. doi: 10.3389/fonc.2021.740079

transplant. 65.7% were considered at high risk of CSCI and 65.2% had a CMV seropositive donor. Low to mild severe adverse events were observed in 40.7% of patients during treatment [gastrointestinal toxicity (36.3%) and skin rash (10.3%)]. Cumulative incidence of CSCI at day +100 and day +168 was 5.4% and 18.1%, respectively, whereas the Kaplan-Meier event rate was 5.8% (95% CI: 2.4-9.1) and 23.3% (95% CI: 16.3-29.7), respectively. Overall mortality was 6.4% at day +100 and 7.3% at day +168. This real-world experience confirms the efficacy and safety of CMV.

Keywords: cytomegalovirus infection, allogeneic stem cell transplantation, prophylaxis, real-world data, Letermovir

INTRODUCTION

Clinically significant cytomegalovirus (CMV) infection (CSCI), defined as CMV disease or CMV viremia reactivation after allogeneic stem-cell transplantation (allo-SCT), is often a serious complication given the delayed immune recovery of the host (1–3). Post-transplant CSCI varies from 30% to 70% and has been associated with higher non-relapse mortality (NRM) (4–10). During the past few decades, both clinical trials and real-world experiences have evaluated the role of CMV prophylaxis, reporting conflicting results (11, 12).

Letermovir (LET) is an antiviral agent with a novel mechanism of action characterized by inhibition of the CMV DNA terminase complex (13, 14). In a pivotal registration Phase 3 clinical trial, prophylaxis with LET significantly reduced the incidence of CSCI after allo-SCT (15). The drug was granted fast-track status by the US Food and Drug Administration (FDA), and orphan drug status by the European Medicines Agency. In the US and Europe, LET was approved for prophylaxis of CSCI in adult CMV-seropositive recipients of allo-SCT (16). FDA considers it a first-in-class medication (17).

The majority of Italian transplant programs adopted prophylaxis with LET as standard policy as soon as the drug became commercially available. The aims of the present multicenter, retrospective, cohort study were to investigate whether the results reported in the aforementioned phase 3 trial could be reproduced in a real-world experience and to assess whether prophylaxis could affect pre-emptive CMV therapy.

METHODS

Seventeen Italian Transplant Centers took part in the study. The observation period began in January 2019 when the Italian Medicines Agency (AIFA) authorized LET for commercial purposes. Prophylaxis was indicated by AIFA for patients aged 18 years or older who had positive CMV serologic status with an undetectable level of CMV DNAemia in whole blood before transplant. Patients received LET 480 mg tablet once daily between day 0 and day +28 after allo-SCT and continued until day +100 if no adverse events occurred during the observation period. If LET was co-administered with cyclosporine, the dosage of LET has been decreased to 240 mg once daily. The intravenous (IV) formulation of LET was not available in Italy. All patients continued herpesvirus prophylaxis as per standard practice.

A high sensitivity and high specificity serologic test was used to detect CMV-IgG before transplant and real-time PCR assay was used for post allo-SCT CMV monitoring (18). DNAemia was determined at least once a week in the first three months, and every other week in the second three-month period. Pre-emptive treatment was initiated when the CMV-DNAemia level was >1,000 copies/mL in plasma or 10,000 copies/mL in whole blood, in two consecutive assessments (18, 19). Patients were evaluated up to day +100 for the primary efficacy endpoint, after which follow-up continued through week 24 post-transplant.

Conditioning intensity was classified according to Working Group definitions (20). Donor selection, conditioning, graft-versus-host disease (GVHD) prophylaxis, and supportive care followed standard institutional operating procedures (21).

Patients were considered at high risk of CSC if one or more of the following criteria were present: human leukocyte antigen (HLA)-related (sibling) donor with at least one mismatch at HLA-A, -B or -DR loci; haploidentical donor; unrelated donor with at least one mismatch at HLA-A, -B, -C or -DRB; use of umbilical cord blood as stem cell source; use of *ex vivo* T-cell-depleted grafts; ≥grade 2 GVHD requiring systemic corticosteroids. Given the retrospective design (i.e., the non-interventional nature) of the study, no sample size calculation was performed.

Endpoints

The primary endpoint was the incidence of CSCI leading to pre-emptive treatment (22) at day +100 (14 weeks) post allo-SCT, and the time to CSCI. The secondary endpoint was the incidence of CSCI at day +168 (24 weeks). Follow-up time was calculated from the transplant date to the first positive CMV DNAemia or its last measurement during the study period, whichever occurred first. Censoring time was the last date of the positive CMV test or the date of death if <14 days from the last negative test. Since endpoints were evaluated at day +100 and day +168, no data on CMV tests were collected after day +168.

Statistical Analysis

The follow-up period (spanning from January 2019 to June 2020) was calculated as the time (in days) spanning from the transplant date to the first positive CMV DNAemia (*i.e.*, the achievement of

Abbreviations: AE, adverse event; allo-SCT, allogeneic stem cell transplant; AML, acute myeloid leukaemia; CMV, cytomegalovirus; CSCI, clinically significant CMV infection; GVHD, graft-versus-host disease; HLA, human leukocyte antigen; LET, letermovir; MRD, matched related; MUD, matched unrelated donor; NRM, non-relapse mortality.

the study endpoint) or the last observation coinciding with 168 days or the date of death or lost to follow-up. Data were summarized as median and interquartile range, or absolute number and percentage. To identify the demographic and clinical correlates of CMV infection and drug discontinuation we did not use a face-to-face comparison of patients' characteristics but the univariate logistic analysis, a method that specifically allows to assess the strength of the risk factor-study outcomes links. Bonferroni's correction was used to minimize the possibility of false-positive findings due to multiple testing. Kaplan-Meier survival analysis was performed for time to infection, overall-survival (OS), and non-relapse mortality (NRM). NRM was defined as death without recurrent or progressive disease after allo-SCT. Probabilities of NRM were estimated with the use of cumulative incidence curves, with relapse viewed as a competing risk. Gray's method was used to evaluate the differences between groups (23). If no competitive risk was found, a standard Kaplan-Meier analysis was applied. Data were analysed with STATA/IC 13.1 for Windows (College Station, TX) and RStudio-1.2.5033.1.

Compliance With Ethical Standards

This multicenter, retrospective, cohort study was approved by the Ethics Committee of the coordinating centre, Grande OspedaleMetropolitano "Bianchi-Melacrino-Morelli" of Reggio Calabria, Italy, and by those of the other participating centres. All procedures were performed according to the principles laid down in the 1964 Helsinki declaration and its later amendments or comparable ethical standards. All patients signed the informed consent.

RESULTS

Overall, 230 patients who underwent an allograft in the participating Italian centres were enrolled; 26 were excluded from the analysis because of incomplete data. Median age of the 204 patients in the study cohort was 52 years, and 53.9% were males (**Table 1**). Acute myeloid leukaemia (AML) was diagnosed in 53.4%. Overall, 28.9% underwent a haploidentical, 32.4% a matched related (MRD), and 27.5% a matched unrelated donor (MUD) transplant. In the majority of patients, stem cell source was G-CSF mobilized peripheral blood (65.7%). 65.7% of patients were considered at high risk of CMV and 65.2% had a CMV seropositive donor. The first patient was enrolled in January 2019 and the last one in June 2020.

Incidence of CMV Infection and Discontinuation

The cumulative incidence of CSCI was 5.4% at day +100 and 18.1% at day +168 after transplant (**Table 2**). Overall, from day +100 to day +168, the cumulative incidence of CSCI was 12.7%. Twenty patients discontinued the trial in the first 100 days, the majority (13 patients) because of death. The percentage of discontinuation was 28.4% at 168 days. Thirteen (6.4%) patients died before day +100 day and 15 (7.3%) before day +168. The Kaplan-Meier event rate of CSCI through 24 weeks was 23.3% (95% CI: 16.3-29.7), 5.8% at day +100 (95% CI: 2.4-9.1). Of note, starting at week +19, the incidence of CMV infection rapidly increased (**Figure 1A**). Given that no competitive risk from drug discontinuation was found on incidence rate by baseline CMV risk categories, low versus high, (competitive risk: 14 weeks, p=0.15; 24 weeks, p=0.84), a standard Kaplan-Meier analysis showed substantially similar curves (**Figure 1B**).

Adverse Events

Over 100 days of treatment, 40.7% of patients treated with LET experienced adverse events (AEs) (**Table 3**). Gastrointestinal AEs were the most frequent (36.3%), followed by skin rash (10.3%). Six cases were CMV-positive; four were CMV negative and died before 100 days. LET was discontinued in 20 patients before 100 days.

Correlates of Time to Drug Discontinuation and CMV Infection

After Bonferroni's correction, no baseline characteristics were significantly associated with time to drug discontinuation or CMV infection at day +100 and at day +168 (**Tables 4** and **5**).

GVHD

Incidences of acute GvHD grades II-IV by 168 days was 2% (4 patients) (**Table 1**). No patients experienced chronic GvHD during the period of follow-up

TABLE 1 | Baseline patients' characteristics.

Median age, years (range)	52 (18-75)
Male gender n. (%)	110 (53.9)
CMV-seropositive donor n. (%)	133 (65.2)
Disease n. (%)	
Acute myeloid leukaemia	109 (53.4)
Myelodysplastic syndrome	19 (9.3)
Non-Hodgkin's lymphoma	15 (7.4)
Acute lymphocytic leukaemia	28 (13.7)
Other disease	33 (16.2)
HLA matching and donor type n. (%)	
Matched unrelated	56 (27.5)
Matched related	66 (32.4)
Mismatched related	68 (33.3)
Mismatched unrelated	14 (6.9)
Haploidentical-related donor n. (%)	59 (28.9)
Stem-cell source n. (%)	
Peripheral blood	175 (85.8)
Bone marrow	27 (13.2)
Cord blood	2 (1)
Myeloablative conditioning regimen n. (%)	134 (65.7)
Acute GVHD grade ≥2 on the day of starting letermovir n. (%)	4 (2)
Risk of CMV disease n. (%)	
High risk	134 (65.7)
Low risk	70 (34.3)
ATG n. (%)	98 (48.0)
Ex vivo T-celldepletion n. (%)	16 (7.8)
Cyclosporine n. (%)	66 (32.4)
Tacrolimus n. (%)	135 (66.2)
Mycophenolate n. (%)	194 (95.1)

CMV, cytomegalovirus; HLA, human leukocyte antigen; GVHD, graft-versus-host disease, ATG, anti-thymocyte globulin.

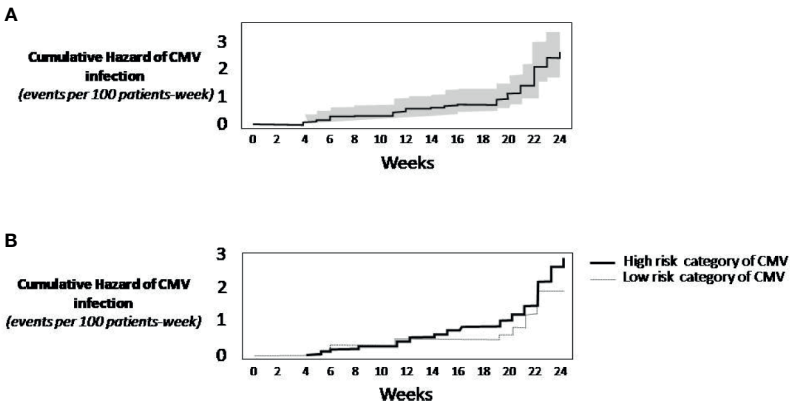

FIGURE 1 | Kaplan-Meier Survival Analysis. **(A)** Cumulative rate of CMV infection (continuous line). The grey area around the continuous line represents the 95% confidence intervals. **(B)** Cumulative incidence of CMV infection by risk category of CMV. The analysis did not consider the competitive risk of mortality. When not considering the competing mortality risk, the practical implication is that the analysis of CMV infection censors patients who die. As this censoring is assumed to be uninformative, the resulting prognosis should be interpreted as the risk of CMV infection in a hypothetical setting in which patients do not die.

Survival

4 patients with incomplete data set for OS and EFS have been excluded from the analysis; 200 patients were eligible for survival analysis. The cumulative incidence of death was 9.9% (95% CI 5.4-14.1) at day +100 and 14.3% (95% CI 8.7-19.5) at day +168 after transplant, respectively. Among patients who died (n=24 patients),10 had relapse. **Figure 2** shows the cumulative incidence of relapse mortality (RM) and non-relapse mortality (NRM), taking into account the competing risk of relapse. Overall, the cumulative incidences of NRM through the first 14 and 24 weeks were 7% (95% CI 4.0-11.0) and 8% (95% CI 4.0-12.0) respectively. The cumulative incidences of RM were 7% (95% CI 4.0-12.0) through the first 14 weeks and 14% (95% CI 9.0-20.0) through 24 weeks.

TABLE 2 | Cumulative incidence of CMV infection and discontinuation at 100 days and at 168 days in 204 patients.

	No.	% (95% CI)
Clinically significant CMV infection through week 14 after transplantation	11	5.4 (2.3-8.5)
Initiation of pre-emptive therapy	4	2.0 (0.1-3.9)
CMV disease	5	2.5 (0.3-4.6)
Discontinued before 100 days without CMV	20	9.8 (5.7-13.9)
Patients who died	13	6.4 (3.0-9.7)
Clinically significant CMV infection through week 24 after transplantation	37	18.1 (12.8-23.4)
Initiation of pre-emptive therapy	17	8.3 (4.5-12.1)
CMV disease	7	3.4 (0.9-5.9)
Discontinued before 168 days without CMV	58	28.4 (22.2-34.6)
Patients who died	15	7.3 (3.8-10.9)

CMV, cytomegalovirus; 95% CI 95%, confidence interval.

TABLE 3 | Adverse events to Letermovir. The frequency is given in percentage.

Adverse events	Frequency
Gastrointestinal	36.3
Rash	10.3
Cough	1.0
Peripheral edema	2.0
Fatigue	4.4
Head pain	2.9
Acute renal damage	3.4
Hypertension	3.9

DISCUSSION

This multicenter, retrospective, cohort study shows that the cumulative incidence of CSCI was 5.4% and 18.1% at day +100 and at day +168 after transplant, respectively. Twenty patients discontinued the trial in the first 100 days, the majority (13 patients) because of death.

CSCI has been associated with increased NRM in transplant patients (2–6). Up until the introduction of LET, no antiviral prophylaxis had proven capable of preventing CSCI in seropositive patients. In randomized studies, prophylaxis with IV ganciclovir reduced the risk of CSCI without improving survival, while high doses of aciclovir or valaciclovir reduced the risk of CMV viremia reactivation but not of CMV disease (24–28). No differences in the risk of CMV disease or in patient survival were observed between prophylaxis with ganciclovir and valaciclovir (29), or between ganciclovir prophylaxis and pre-emptive therapy (9). Prophylaxis with foscarnet has only been used in uncontrolled trials, and its prolonged use is commonly limited by toxicity (30, 31).

In a phase 3 trial, maribavir at 100 mg BID did not prevent CMV disease (32). In another phase 3 trial, brincidofovir did not

TABLE 4 | Univariate logistic regression analysis of treatment discontinuation through first 100 days and through 168 days by baseline characteristics.

		14 weeks				24 weeks			
		No discontinuation	Discontinuation	OR (95% CI)	*p*	No discontinuation	Discontinuation	OR (95% CI)	*p*
Age, years	≤52	97	7	1		79	25	1	
	>52	87	13	2.07 (0.79-5.42)	0.2	67	33	1.55 (0.84-2.87)	0.2
Gender	Female	87	7	1		72	22	1	
	Male	97	13	1.67 (0.64-4.36)	0.3	74	36	1.59 (0.86-2.96)	0.1
CMV donor	Negative	63	8	1		52	19	1	
	Positive	121	12	0.78 (0.30-2.01)	0.6	94	39	1.14 (0.60-2.16)	0.7
Disease*	Acute myeloid leukaemia	99	10	1		80	29	1	
	Myelodysplastic syndrome	19		0.5 (0.11-1.72)	0.3	14	5	0.99 (0.3-2.83)	0.9
	Non-Hodgkin's lymphoma	14	1			9	6	1.84 (0.57-5.56)	0.3
	Acute lymphocytic leukaemia	26	2			23	5	0.6 (0.19-1.62)	0.3
	Other disease	26	7	2.67 (0.89-7.64)	0.07	20	13	1.79 (0.78-4.04)	0.2
HLA	Matched unrelated	47	9	1		37	19	1	
	Matched related	63	3	0.25 (0.05-0.88)	0.04***	50	16	0.62 (0.28-1.37)	0.2
	Mismatched related	63	5	0.41 (0.12-1.28)	0.14	50	18	0.7 (0.32-1.52)	0.4
	Mismatched unrelated	11	3	1.42 (0.28-5.75)	0.64	9	5	1.08 (0.3-3.6)	0.9
Haploidentical-related donor	No	129	16	1		104	41	1	
	Yes	55	4	0.59 (0.19-1.83)	0.4	42	17	1.03 (0.52-1.98)	0.9
Stem source	Peripheral blood	156	19	1		124	51	1	
	Other source	28	1	0.29 (0.04-2.28)	0.2	22	7	0.77 (0.29-1.84)	0.6
Myeloablative regimen	No	60	10	1		43	27	1	
	Yes	124	10	0.48 (0.19-1.22)	0.1	103	31	0.48 (0.26-0.9)	0.02***
ATG	No	99	7	1		79	27	1	
	Yes	85	13	2.16 (0.82-5.67)	0.1	67	31	1.35 (0.74-2.5)	0.3
Ex vivo cell depletion**	No	168	20			132	56	1	
	Yes	16			–	14	2	0.34 (0.05-1.26)	0.1
Cyclosporine	No	125	13	1		98	40	1	
	Yes	59	7	1.14 (0.43-3.01)	0.8	48	18	0.92 (0.48-1.77)	0.8
Tacrolimus	No	62	7	1		51	18	1	
	Yes	122	13	0.94 (0.36-2.49)	0.4	95	40	1.19 (0.62-2.29)	0.6
Mycophenolate	No	8	2	1		8	2	1	
	Yes	176	18	0.41 (0.8-2.07)	0.3	138	56	1.62 (0.33-7.88)	0.5
Risk of CMV disease	Low	66	4	1		49	21	1	
	High	118	16	2.24 (0.72-6.97)	0.2	97	37	0.89 (0.47-1.7)	0.7

CMV, cytomegalovirus; HLA, human leukocyte antigen; ATG, anti-thymocyte globulin; No disc, not discontinued; Disc, discontinued; OR (95% CI) odds radio (95% confidence interval).
**For analysis at 14 weeks, disease was grouped in 3 classes; acute myeloid leukaemia; myelodysplastic syndrome - non-Hodgkin's lymphoma - acute lymphocytic leukaemia; and other.*
***For analysis at 14 weeks, no OR was calculated for ex vivo cell depletion.*
****Not significant after Bonferroni's correction.*

reduce CSCI at week 24 and was associated with significant gastrointestinal toxicity (33). Two systematic reviews focused on the effects of antiviral prophylaxis in allo-SCT recipients (11, 12). In both analyses, none of the drugs previously described showed reduction in all-cause mortality. Moreover, IV immunoglobulins or CMV-specific immunoglobulins are not recommended for prophylaxis of CSCI (34).

In 2017, the FDA approved LET to prevent CSCI in adult allo-SCT recipients (35). In the registration trial, prophylaxis with LET was started a median of 9 days after allo-SCT and administered through week 14. It was significantly associated with lower all-cause mortality than placebo through week 24 after allo-SCT (15). Patients considered at high risk of CSCI benefitted the most from antiviral prophylaxis. However, multiple CYP3A- and OATP1B1/3-mediated drug interactions may occur, especially when LET is co-administered with cyclosporine. Interestingly, LET does not appear to have significant hematologic or extra-hematologic toxicity.

Prospective randomized clinical trials are the statistical "gold standard" to evaluate the safety and efficacy of novel therapeutic agents. However, inclusion criteria are often very stringent, and the reproducibility of their results in real-world practice remains to be confirmed. Real-world studies have become increasingly important in their role of providing evidence of safety and

TABLE 5 | Univariate logistic regression analysis of CMV infection through first 100 days and through 168 days by baseline characteristics.

	Risk categories	14 weeks				24 weeks			
		CMV-	CMV+	OR (95% CI)	*P*	CMV-	CMV+	OR (95% CI)	*P*
Age, years	≤52	99	5	1		88	16	1	
	>52	94	6	1.26 (0.37-4.28)	0.9	79	21	1.46 (0.71-3.00)	0.4
Gender	Female	90	4	1		81	13	1	
	Male	103	7	1.53 (0.43-5.39)	0.5	86	24	1.74 (0.83-3.64)	0.1
CMV donor	Negative	67	4	1		54	17	1	
	Positive	126	7	0.93 (0.26-3.29)	0.9	113	20	0.56 (0.27-1.16)	0.1
Disease*	Acute myeloid leukaemia	100	9	1		94	15	1	
	Myelodysplastic syndrome	19		0.24 (0.04-0.96)	0.07	12	7	3.66 (1.2-10.69)	0.02****
	Non-Hodgkin's lymphoma	15				14	1	0.45 (0.02-2.49)	0.5
	Acute lymphocytic leukaemia	26	2			22	6	1.71 (0.56-4.75)	0.3
	Other disease	33				25	8	2.01 (0.74-5.18)	0.2
HLA**	Matched unrelated	53	3	1		48	8	1	
	Matched related	63	3	0.84 (0.15-4.71)	0.8	56	10	1.07 (0.39-3.01)	0.9
	Mismatched related	63	5	1.15 (0.27-5.78)	0.9	55	13	1.42 (0.55-3.86)	0.5
	Mismatched unrelated	14				8	6	4.5 (1.21-16.82)	0.02****
Haploidentical-related donor	No	139	6	1		120	25	1	
	Yes	54	5	2.15 (0.63-7.32)	0.2	47	12	1.23 (0.57-2.63)	0.6
Stem source	Peripheral blood	165	10	1		142	33	1	
	Other source	28	1	0.59 (0.07-4.78)	0.6	25	4	0.69 (0.22-2.11)	0.5
Myeloablative regimen	No	66	4	1		57	13	1	
	Yes	127	7	0.91 (0.26-3.22)	0.9	110	24	0.96 (0.45-2.02)	0.9
Antimycotic regimen	No	101	5	1		86	20	1	
	Yes	92	6	1.32 (0.39-4.46)	0.7	81	17	0.9 (0.44-1.84)	0.8
*Ex vivo****	No	177	11		—	154	34	1	
	Yes	16				13	3	1.05 (0.28-3.87)	0.9
Cyclosporine	No	132	6	1		115	23	1	
	Yes	61	5	1.8 (0.53-6.14)	0.3	52	14	1.35 (0.64-2.82)	0.4
Tacrolimus	No	64	5	1		55	14	1	
	Yes	129	6	0.6 (0.17-2.02)	0.4	112	23	0.81 (0.38-1.69)	0.6
Mycophenolate	No	9	1	1		7	3	1	
	Yes	184	10	0.49 (0.06-4.25)	0.5	160	34	0.5 (0.12-2.01)	0.3
Risk of CMV disease	Low	67	3	1		60	10	1	
	High	126	8	1.42 (0.36-5.52)	0.5	107	27	1.51 (0.69-3.34)	0.3

CMV, cytomegalovirus; CMV-, no CMV infection; CMV+, CMV infection; HLA, human leukocyte antigen; ATG, anti-thymocyte globulin; OR (95% CI), odds radio (95% confidence interval).
**For analysis at 14 weeks, disease was grouped into 2 classes; acute myeloid leukaemia and all others.*
***For analysis at 14 weeks, HLA-matching donors were grouped into 3 classes; matched unrelated, matched related and mismatched.*
****For analysis at 14 weeks, no OR was calculated for ex vivo cell depletion.*
*****Not significant after Bonferroni's correction.*

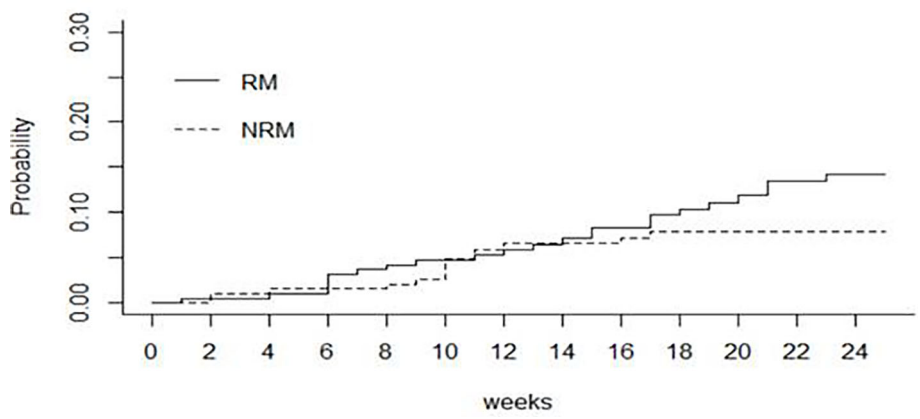

FIGURE 2 | Cumulative incidence by relapse (RM) and non-relapse mortality (NRM).

efficacy in larger and more representative patient populations (36). Overall, they provide physicians with important clinical findings outside the context of clinical trials. Moreover, more rigorous methodology has greatly enhanced their quality, to the point that regulatory agencies such as the FDA and EMA currently recognize their potential value (37). Agencies underline the importance of real-life research in assessing marketed products and their life cycle, including development/monitoring and regulatory decision-making.

Within the setting of CMV prophylaxis, transplant programs will have to determine whether prophylaxis with LET is associated with survival benefits that offset the risk of toxicity and justify costs. In the present study, we described the most extensive real-world experience to date of prophylaxis with LET in allo-SCT patients, highlighting the reproducibility of the safety and efficacy of this commercially available antiviral agent. Although a stringent comparison of our findings with the registration trial is not possible, it is of note that only 40% of the enrolled patients experienced low to mild AEs that were easily managed. In our real-world experience, the efficacy of prophylaxis with LET was confirmed. Despite differences from the registration study in terms of baseline patient characteristics, none were significantly associated with treatment discontinuation or CSCI. Of note, the cumulative incidence of CSCI did not differ between our study and that of the registration trial in both observation periods, *i.e.* 5.4% versus 7.7% within day +100, and 18.1% versus 17.5% within day +168, respectively. In particular, we did not observe an increased frequency of CSCI in patients considered at high risk of this event at baseline versus those at low risk, suggesting that prophylaxis abrogated the impact of this variable on the study endpoint. Of note, the cumulative incidence of mortality at day +100 and at day +168 was higher than that reported in the registration trial (6.4 versus 1.5% and 7.4 versus 1.8%, respectively). This was probably due to differences in baseline prognostic characteristics and/or inclusion criteria between our study and the registration trial.

Other real-world experiences have also been published. An Italian study compared 45 patients undergoing prophylaxis with LET with a retrospective cohort that did not receive prophylaxis (38). Results showed that prophylaxis was highly effective and safe in reducing the incidence of CSCI when administered from day 0 to day +100. The incidence of CSCI at day +100 was significantly lower in patients who received prophylaxis than in those who did not (8% versus 44%, respectively). In another retrospective real-world study on 80 patients, prophylaxis was started after neutrophil engraftment, around the third week after allo-SCT (39). The incidence of CSCI at day +100 was 14%, lower than in the retrospective cohort not administered LET (41%).

The strength of the present study are the sample size, that is probably the largest one published so far, assessing the real word experience of LET prophylaxis, and the multicenter characteristic, comprising 17 centers in Italy. Nevertheless, this study has some limitations: first, the absence of a control group to make a comparison led to difficult interpretation of results; second, the results confirm what has been reported in other real-life studies, without adding new clinical information; and lastly, today we know that the presence of circulating infectious CMV particles is determined by virus isolation and degradation of free-floating viral DNA. For this reason, during LET prophylaxis the clinical relevance of CMV DNAemia should be critically considered, since the presence of DNAemia during letermovir prophylaxis may not represent a real CMV reactivation, but just an abortive infection (40). We don't have this data in the few patients with DNAemia within day 100

There are still several unanswered questions on prophylaxis with LET, including potential benefits of its extension beyond day +100. Our real-life study showed that, after discontinuation of prophylaxis at day +101, some 13% of patients experienced CMV reactivation, supporting the prolongation of its administration. Moreover, a notable increase in reactivation was observed after week +19. An ongoing phase 3 clinical trial is currently evaluating the safety and efficacy of prophylaxis with LET beyond day +100 (41), focusing on the hypothesis that prolonged prophylaxis until day +200 is superior to placebo in preventing long-term CMV reactivation.

Moreover, the use of LET can reduce NRM. In a posthoc analysis performed to investigate the effects of LET on all-cause mortality, the incidence of all-cause mortality in the LET group was similar in patients with or without clinically significant CMV infection (42). In contrast, in the placebo group, all-cause mortality was higher in patients with versus those without clinically significant CMV infection, despite the use of pre-emptive therapy for CMV infection. These results suggest that there may be a benefit to avoiding clinically significant CMV infection and potentially toxic antivirals such as ganciclovir.

There are currently scanty data on the cost-effectiveness of prophylaxis with LET (43). However, in a recent study, prophylaxis in adult patients compared with no-prophylaxis showed favourable cost-effectiveness for the Italian National Health Service (44).

In conclusion, our real-world analysis reports similar efficacy findings to those of the registration trial. However, the costs of CMV prophylaxis may be prohibitive in countries with socioeconomic healthcare issues.

DATA AVAILABILITY STATEMENT

The raw data supporting the conclusions of this article will be made available by the authors, without undue reservation.

ETHICS STATEMENT

The studies involving human participants were reviewed and approved by Ethics Committee of Grande Ospedale Metropolitano "Bianchi-Melacrino-Morelli" of Reggio Calabria, Italy. The patients/participants provided their written informed consent to participate in this study.

AUTHOR CONTRIBUTIONS

Study concepts: MMa, AMC, and CC. Quality control of data and algorithms: MMa, APit, GP, GT, MG, and CC. Data analysis and interpretation: MMa, APit, GP, GT, MG, and CC. Statistical analysis: APit, GT, and MG. Manuscript preparation: MMa, APit, GP, GT, MG, and CC. Manuscript editing: MMa, BB, and CC. Critical revision of the article: MMa, APit, BB, GP, GT, MG, CC, GMa and GMu. Data collection: AC, VF, APic, ST, CI, PC, DP, GMu, APa, AV, BS, GS, NM, SL, MC, LP, BL, AF, FC, EM, LG, AB, MMu, RS, NR, SM, PMa, PMu, IA, CS, FAC, and MP. All authors contributed to the article and approved the submitted version.

ACKNOWLEDGMENTS

The authors would like to thank the medical and nursing staff who cared for the patients at the GITMO (Gruppo Italiano TrapiantoMidollo Osseo) Centers and provided information on the patients.

REFERENCES

1. Cho SY, Lee DG, Kim HJ. Cytomegalovirus Infections After Hematopoietic Stem Cell Transplantation: Current Status and Future Immunotherapy. *Int J Mol Sci* (2019) 20(11):2666. doi: 10.3390/ijms20112666
2. Maffini E, Busca A, Costa C, Giaccone L, Cerrano M, Curtoni A, et al. An Update on the Treatment of Cytomegalovirus Infection After Allogeneic Hematopoietic Stem Cell Transplantation. *Expert Rev Hematol* (2019) 12 (11):937–45. doi: 10.1080/17474086.2019.1657399
3. Maffini E, Giaccone L, Festuccia M, Brunello L, Busca A, Bruno B. Treatment of CMV Infection After Allogeneic Hematopoietic Stem Cell Transplantation. *Expert Rev Hematol* (2016) 9(6):585–96. doi: 10.1080/17474086.2016.1174571
4. Maertens J, Lyon S. Current and Future Current and Future Options for Cytomegalovirus Reactivation in Hematopoietic Cell Transplantation Patients. *Future Microbiol* (2017) 12:839–42. doi: 10.2217/fmb-2017-0095
5. Jeon S, Lee WK, Lee Y, Lee DG, Lee JW. Risk Factors for Cytomegalovirus Retinitis in Patients With Cytomegalovirus Viremia After Hematopoietic Stem Cell Transplantation. *Ophthalmology* (2012) 119(9):1892–8. doi: 10.1016/j.ophtha.2012.03.032
6. Schmidt-Hieber M, Labopin M, Beelen D, Volin L, Ehninger G, Finke J, et al. CMV Serostatus Still has an Important Prognostic Impact in *De Novo* Acute Leukemia Patients After Allogeneic Stem Cell Transplantation: A Report From the Acute Leukemia Working Party of EBMT. *Blood* (2013) 122 (19):3359–64. doi: 10.1182/blood-2013-05-499830
7. Teira P, Battiwalla M, Ramanathan M, Barrett AJ, Ahn KW, Chen M, et al. Early Cytomegalovirus Reactivation Remains Associated With Increased Transplant-Related Mortality in the Current Era: A CIBMTR Analysis. *Blood* (2016) 127(20):2427–38. doi: 10.1182/blood-2015-11-679639
8. Green ML, Leisenring W, Xie H, Mast TC, Cui Y, Sandmaier BM, et al. Cytomegalovirus Viral Load and Mortality After Haemopoietic Stem Cell Transplantation in the Era of Pre-Emptive Therapy: A Retrospective Cohort Study. *Lancet Haematol* (2016) 3(3):e119–27. doi: 10.1016/S2352-3026(15)00289-6
9. Boeckh M, Nichols WG. The Impact of Cytomegalovirus Serostatus of Donor and Recipient Before Hematopoietic Stem Cell Transplantation in the Era of Antiviral Prophylaxis and Preemptive Therapy. *Blood* (2004) 103(6):2003–8. doi: 10.1182/blood-2003-10-3616
10. Ljungman P, de la Camara R, Robin C, Crocchiolo R, Einsele H, Hill JA, et al. Guidelines for the Management of Cytomegalovirus Infection in Patients With Haematological Malignancies and After Stem Cell Transplantation From the 2017 European Conference on Infections in Leukaemia (ECIL 7). *Lancet Infect Dis* (2019) 19(8):e260–72. doi: 10.1016/S1473-3099(19)30107-0
11. Chen K, Cheng MP, Hammond SP, Einsele H, Marty FM. Antiviral Prophylaxis for Cytomegalovirus Infection in Allogeneic Hematopoietic Cell Transplantation. *Blood Adv* (2018) 2(16):2159–75. doi: 10.1182/bloodadvances.2018016493
12. Gagelmann N, Ljungman P, Styczynski J, Kroger N. Comparative Efficacy and Safety of Different Antiviral Agents for Cytomegalovirus Prophylaxis in Allogeneic Hematopoietic Cell Transplantation: A Systematic Review and Meta-Analysis. *Biol Blood Marrow Transplant* (2018) 24(10):2101–9. doi: 10.1016/j.bbmt.2018.05.017
13. Reefschlaeger J, Bender W, Hallenberger S, Weber O, Eckenberg P, Goldmann S, et al. Novel Non-Nucleoside Inhibitors of Cytomegaloviruses (BAY 38-4766): *In Vitro* and *In Vivo* Antiviral Activity and Mechanism of Action. *J Antimicrob Chemother* (2001) 48(6):757–67. doi: 10.1093/jac/48.6.757
14. Weber O, Bender W, Eckenberg P, Goldmann S, Haerter M, Hallenberger S, et al. Inhibition of Murine Cytomegalovirus and Human Cytomegalovirus by a Novel Non-Nucleosidic Compound *In Vivo*. *Antiviral Res* (2001) 49(3):179–89. doi: 10.1016/s0166-3542(01)00127-9
15. Marty FM, Ljungman P, Chemaly RF, Maertens J, Dadwal SS, Duarte RF, et al. Letermovir Prophylaxis for Cytomegalovirus in Hematopoietic-Cell Transplantation. *N Engl J Med* (2017) 377(25):2433–44. doi: 10.1056/NEJMoa1706640
16. Baynes R. *FDA Approves Letermovir for CMV Prophylaxis Post-Transplantation. November 9, 2017*. Available at: https://www.onclive.com/view/fda-approves-letermovir-for-cmv-prophylaxis-posttransplantation.
17. U.S. Food and Drug Administration (FDA). *Advancing Health Trough Innovation. New Drug Therapy Approvals 2017* (2018). Available at: https://www.fda.gov/files/about%20fda/published/2017-New-Drug-Therapy-Approvals-Report.pdf.
18. Girmenia C, Lazzarotto T, Bonifazi F, Patriarca F, Irrera G, Ciceri F, et al. Assessment and Prevention of Cytomegalovirus Infection in Allogeneic Hematopoietic Stem Cell Transplant and in Solid Organ Transplant: A Multidisciplinary Consensus Conference by the Italian GITMO, SITO, and AMCLI Societies. *Clin Transplant* (2019) 33(10):e13666. doi: 10.1111/ctr.13666
19. Sidoti F, Piralla A, Costa C, Scarasciulli ML, Calvario A, Conaldi PG, et al. Collaborative National Multicenter for the Identification of Conversion Factors From Copies/mL to Internationalunits/mL for the Normalization of HCMV DNA Load. *Diagn Microbiol Infect Dis* (2019) 95(2):152–8. doi: 10.1016/j.diagmicrobio.2019.05.012
20. Bacigalupo A, Ballen K, Rizzo D, Giralt S, Lazarus H, Ho V, et al. Defining the Intensity of Conditioning Regimens: Working Definitions. *Biol Blood Marrow Transplant* (2009) 15(12):1628–33. doi: 10.1016/j.bbmt.2009.07.004
21. Gratwohl A, Brand R, McGrath E, van Biezen A, Sureda A, Ljungman P, et al. Use of the Quality Management System "JACIE" and Outcome After Hematopoietic Stem Cell Transplantation. *Haematologica* (2014) 99(5):908–15. doi: 10.3324/haematol.2013.096461
22. Ljungman P, Griffiths P, Paya C. Definitions of Cytomegalovirus *Infection* and Disease in Transplant Recipients. *Clin Infect Dis* (2002) 34(8):1094–7. doi: 10.1086/339329
23. Gray RJ. A Class of K-Sample Tests for Comparing the Cumulative Incidence of a Competing Risk. *Ann Statist* (1988) 16(3):1141–54. doi: 10.1214/aos/1176350951
24. Prentice HG, Gluckman E, Powles RL, Ljungman P, Milpied N, Fernandez Rañada JM, et al. Impact of Long-Term Acyclovir on Cytomegalovirus Infection and Survival After Allogeneic Bone Marrow Transplantation. European Acyclovir for CMV Prophylaxis Study Group. *Lancet* (1994) 343 (8900):749–53. doi: 10.1016/s0140-6736(94)91835-x
25. Ljungman P, de la Camara R, Milpied N, Volin L, Russell CA, Crisp A, et al. Randomized Study of Valacyclovir as Prophylaxis Against Cytomegalovirus Reactivation in Recipients of Allogeneic Bone Marrow Transplants. *Blood* (2002) 99(8):3050–6. doi: 10.1182/blood.v99.8.3050

26. Goodrich JM, Bowden RA, Fisher L, Keller C, Schoch G, Meyers JD. Ganciclovir Prophylaxis to Prevent Cytomegalovirus Disease After Allogeneic Marrow Transplant. *Ann Intern Med* (1993) 118(3):173–8. doi: 10.7326/0003-4819-118-3-199302010-00003
27. Winston DJ, Ho WG, Bartoni K, Du Mond C, Ebeling DF, Buhles WC, et al. Ganciclovir Prophylaxis of Cytomegalovirus Infection and Disease in Allogeneic Bone Marrow Transplant Recipients. Results of a Placebo-Controlled, Double-Blind Trial. *Ann Intern Med* (1993) 118(3):179–84. doi: 10.7326/0003-4819-118-3-199302010-00004
28. Boeckh M, Gooley TA, Myerson D, Cunningham T, Schoch G, Bowden RA. Cytomegalovirus Pp65 Antigenemia-Guided Early Treatment With Ganciclovir Versus Ganciclovir at Engraftment After Allogeneic Marrow Transplantation: A Randomized Double-Blind Study. *Blood* (1996) 88 (10):4063–71. doi: 10.1182/blood.V88.10.4063.bloodjournal88104063
29. Winston DJ, Yeager AM, Chandrasekar PH, Snydman DR, Petersen FB, Territo MC, et al. Randomized Comparison of Oral Valacyclovir and Intravenous Ganciclovir for Prevention of Cytomegalovirus Disease After Allogeneic Bone Marrow Transplantation. *Clin Infect Dis* (2003) 36(6):749–58. doi: 10.1086/367836
30. Bacigalupo A, Tedone E, Van Lint MT, Trespi G, Lonngren M, Sanna MA, et al. CMV Prophylaxis With Foscarnet in Allogeneic Bone Marrow Transplant Recipients at High Risk of Developing CMV Infections. *Bone Marrow Transplant* (1994) 13(6):783–8.
31. Bregante S, Bertilson S, Tedone E, Van Lint MT, Trespi G, Mordini N, et al. Foscarnet Prophylaxis of Cytomegalovirus Infections in Patients Undergoing Allogeneic Bone Marrow Transplantation (BMT): A Dose-Finding Study. *Bone Marrow Transplant* (2000) 26(1):23–9. doi: 10.1038/sj.bmt.1702450
32. Marty FM, Ljungman P, Papanicolaou GA, Winston DJ, Chemaly RF, Strasfeld L, et al. Maribavir Prophylaxis for Prevention of Cytomegalovirus Disease in Recipients of Allogeneic Stem-Cell Transplants: A Phase 3, Double-Blind, Placebo-Controlled, Randomised Trial. *Lancet Infect Dis* (2011) 11 (4):284–92. doi: 10.1016/S1473-3099(11)70024-X
33. Marty FM, Winston DJ, Chemaly RF, Mullane KM, Shore TB, Papanicolaou GA, et al. A Randomized, Double-Blind, Placebo-Controlled Phase 3 Trial of Oral Brincidofovir for Cytomegalovirus Prophylaxis in Allogeneic Hematopoietic Cell Transplantation. *Biol Blood Marrow Transplant* (2019) 25(2):369–81. doi: 10.1016/j.bbmt.2018.09.038
34. Raanani P, Gafter-Gvili A, Paul M, Ben-Bassat I, Leibovici L, Shpilberg O. Immunoglobulin Prophylaxis in Hematopoietic Stem Cell Transplantation: Systematic Review and Meta-Analysis. *J Clin Oncol* (2009) 27(5):770–81. doi: 10.1200/JCO.2008.16.8450
35. U.S. Food & Drug Administration. *PREVYMIS (Letermovir) Tablets and PREVYMIS (Letermovir) Injection*. Available at: https://www.accessdata.fda.gov/drugsatfda_docs/nda/2017/209939Orig1s000,209940Orig1s000TOC.cfm.
36. Blonde L, Khunti K, Harris SB, Meizinger C, Skolnik NS. Interpretation and Impact of Real-World Clinical Data for the Practicing Clinician. *Adv Ther* (2018) 35(11):1763–74. doi: 10.1007/s12325-018-0805-y
37. U.S. Food & Drug Administration. *Real-World Data (RWD) and Real-World Evidence (RWE) Are Playing an Increasing Role in Health Care Decisions*. Available at: https://www.fda.gov/science-research/science-and-research-special-topics/real-world-evidence.
38. Malagola M, Pollara C, Polverelli N, Zollner T, Bettoni D, Gandolfi L, et al. Advances in CMV Management: A Single Center Real-Life Experience. *Front Cell Dev Biol* (2020) 8:534268. doi: 10.3389/fcell.2020.534268
39. Derigs P, Radujkovic A, Schubert ML, Schnitzler P, Schöning T, Müller-Tidow C, et al. Letermovir Prophylaxis Is Effective in Preventing Cytomegalovirus Reactivation After Allogeneic Hematopoietic Cell Transplantation: Single-Center Real-World Data. *Ann Hematol* (2021) 100(8):2087–93. doi: 10.1007/s00277-020-04362-2
40. Cassaniti I, Colombo AA, Bernasconi P, Malagola M, Russo D, Iori AP, et al. Positive HCMV DNAemia in Stem Cell Recipients Undergoing Letermovir Prophylaxis Is Expression of Abortive Infection. *Am J Transplant* (2021) 21 (4):1622–8. doi: 10.1111/ajt.16450
41. Clinical trial. Extension of Letermovir (LET) From Day 100 to Day 200 Post-Transplant for the Prevention of Cytomegalovirus (CMV) Infection in Hematopoietic Stem Cell Transplant (HSCT) Participants (MK-8228-040). Available at: https://clinicaltrials.gov/ct2/show/NCT03930615.
42. Ljungman P, Schmitt M, Marty FM, Maertens J, Chemaly RF, Kartsonis NA, et al. A Mortality Analysis of Letermovir Prophylaxis for Cytomegalovirus (CMV) in CMV-Seropositive Recipients of Allogeneic Hematopoietic Cell Transplantation. *Clin Infect Dis* (2020) 70(8):1525–33. doi: 10.1093/cid/ciz490
43. Chan TS, Cheng SS, Chen WT, Hsu DC, Chau RW, Kang SH, et al. Cost-Effectiveness of Letermovir as Cytomegalovirus Prophylaxis in Adult Recipients of Allogeneic Hematopoietic Stem Cell Transplantation in Hong Kong. *J Med Econ* (2020) 23(12):1485–92. doi: 10.1080/13696998.2020.1843321
44. Restelli U, Croce D, Pacelli V, Ciceri F, Girmenia C. Cost-Effectiveness Analysis of the Use of Letermovir for the Prophylaxis of Cytomegalovirus in Adult Cytomegalovirus Seropositive Recipients Undergoing Allogenic Hematopoietic Stem Cell Transplantation in Italy. *Infect Drug Resist* (2019) 12:1127–38. doi: 10.2147/IDR.S196282

Conflict of Interest: The authors declare that the research was conducted in the absence of any commercial or financial relationship that could be construed as a potential conflict of interest.

frontiers in Oncology

CASE REPORT
published: 09 September 2021
doi: 10.3389/fonc.2021.729106

Case Report: Contrasting BCL2 Upregulation With Venetoclax in a Case of Refractory Lymphomatoid Papulosis and Progressive Chronic Lymphocytic Leukemia

Valerio Guarente, Giovanni Martino, Erica Dorillo, Filomena De Falco, Chiara Rompietti, Daniele Sorcini, Mariangela Brogna, Valeria Cardinali, Stefano Ascani, Andrea Marra† and Paolo Sportoletti*†*

Institute of Hematology-Centro di Ricerca Emato-Oncologica (CREO), Department of Medicine and Surgery, University of Perugia, Perugia, Italy

OPEN ACCESS

Edited by:
Stefano Luminari, University of Modena and Reggio Emilia, Italy

Reviewed by:
Sergiu Pasca, Iuliu Haţieganu University of Medicine and Pharmacy, Romania
Irene Biasoli, Federal University of Rio de Janeiro, Brazil

***Correspondence:**
Paolo Sportoletti
paolo.sportoletti@unipg.it
Andrea Marra
andrea.marra1987@gmail.com

†These authors share last authorship

Specialty section:
This article was submitted to Hematologic Malignancies, a section of the journal Frontiers in Oncology

Received: *22 June 2021*
Accepted: *30 July 2021*
Published: *09 September 2021*

Citation:
Guarente V, Martino G, Dorillo E, De Falco F, Rompietti C, Sorcini D, Brogna M, Cardinali V, Ascani S, Marra A and Sportoletti P (2021) Case Report: Contrasting BCL2 Upregulation With Venetoclax in a Case of Refractory Lymphomatoid Papulosis and Progressive Chronic Lymphocytic Leukemia. Front. Oncol. 11:729106. doi: 10.3389/fonc.2021.729106

A 57-year-old man affected by high-risk progressive chronic lymphocytic leukemia (CLL), primary resistant to first-line chemoimmunotherapy, developed a type A lymphomatoid papulosis (LyP) during a second progression of CLL. The two blood tumor entities were clonally unrelated. LyP presented with a diffuse (>90% body surface area) cutaneous rash and was characterized by intensely pruriginous dusky nodules (n = 10) and red flat-topped papules (n = 60). No response to topical corticosteroids and psoralen plus ultraviolet A (PUVA) phototherapy was observed. In order to effectively treat progressive *TP53*-mutated CLL, the potent BCL2 inhibitor, venetoclax, was initiated with no treatment-related complications. While CLL only achieved a partial response, a complete remission of LyP-associated cutaneous rash and of the intractable pruritus was obtained within 2 months from venetoclax initiation. BCL2 immunostaining of the original cutaneous specimen showed a strong over-expression of the anti-apoptotic protein, restricted to $CD30^+$ lymphoid cells and reactive microenvironment. At 12 months follow-up, the patient is still in complete remission of LyP. Our findings underline the probable pathogenic role of BCL2 in LyP and the potential therapeutic efficacy of venetoclax for the treatment of this primary cutaneous $CD30^+$ lymphoproliferative disorder, especially in the setting of severe and refractory disease.

Keywords: T-cell lymphoma, chronic lymphocytic leukemia, venetoclax (BCL2 inhibitor), lymphomatoid papulosis (LyP), lymphomatoid papulosis treatment

INTRODUCTION

Lymphomatoid papulosis (LyP) is a primary cutaneous $CD30^+$ T-cell lymphoproliferative disorder characterized by chronic, recurrent, and self-healing papulonecrotic or nodular skin lesions, generally localized to the trunk and extremities (1). LyP accounts for ~12% of cutaneous T-cell lymphomas (CTCLs) and usually exhibits a benign course (as some cases can regress

spontaneously), with a 5-year disease-specific survival of 99% (1). In ~20% of patients, LyP may be preceded by, associates with, or followed by another malignant lymphoma such as mycosis fungoides, anaplastic large T-cell lymphoma, or, more rarely, Hodgkin's lymphoma (1); however, LyP has been anecdotally reported in patients with chronic lymphocytic leukemia/small lymphocytic lymphoma (CLL/SLL), only accounting for 11 adult cases previously described (2).

LyP has no approved therapy and can often be very difficult to treat, especially in the presence of extensive and ulcerative lesions or chronic intractable pruritus (1, 3); recently, brentuximab vedotin, a monoclonal antibody directed against CD30, has proved effective in treating refractory LyP in a phase II trial (4, 5), achieving an overall response rate in 12/12 cases [100%] and a complete response rate in 5/12 cases [58%]; however, its use in the clinic might be limited (at least in part) by peripheral neuropathy [10/12 cases (83%) and 5/12 cases (42%) experienced grade 2 neuropathy (5)].

CASE PRESENTATION

In June 2014, a 57-year-old Caucasian man was diagnosed with chronic lymphocytic leukemia (CLL), Rai stage II, Binet stage A, genetically driven by an unmutated immunoglobulin variable heavy-chain (*IGVH*) gene status, with no mutations in *NOTCH1*, *SF3B1*, and *TP53* genes; interphase fluorescence *in situ* hybridization (I-FISH) performed with the peripheral blood lymphocytes identified a IGVH/14q32 deletion and no other cytogenetic aberrations. CLL B cells did not express zeta chain-associated protein kinase 70 (ZAP70) and CD38. Blood counts showed lymphocytosis (lymphocyte absolute count: $8,500 \times 10^9$/L) and no anemia or thrombocytopenia. The patient underwent a careful clinical and laboratory follow-up for ~4.5 years. In January 2019, CLL progressed with notable lymphocytosis ($331,000 \times 10^9$/L) and macrocytic anemia [Hb 11.2 g/dl, mean corpuscular volume (MCV) 112 fl], accompanied with supra-/subdiaphragmatic lymphadenopathies (>3 regions) and splenomegaly (longitudinal spleen diameter of 22 cm); no *TP53* mutations/deletion underlaid disease progression. Chemoimmunotherapy with intravenous bendamustine (90 mg/m^2, days 1 and 2) and rituximab (375 mg/m^2, day 1) was then administered (for 6 cycles, every 28 days, from January to July 2019), achieving a partial response (6). In August 2019, the patient presented with a skin rash of intensely pruritic dusky nodules (n > 10) and red flat-topped papules (n > 300) with erythema involving >90% of body surface area (**Figures 1A–D**).

The punch biopsy specimen obtained from the left arm and stained with hematoxylin and eosin demonstrated an abnormal mixed-lymphoid infiltrate (composed of small lymphocytes and few large-sized Hodgkin-like cells) in the dermis and subcutis, with moderate extension into epidermis (**Figure 2A**). Immunohistochemical analysis showed that pathological Hodgkin-like cells were CD3$^+$, CD4$^+$, CD30$^+$ (**Figure 2B**) and CD8$^-$, and were intermingled with numerous inflammatory cells (mostly of T-cell origin; **Figure 2C**); no monomorphic small

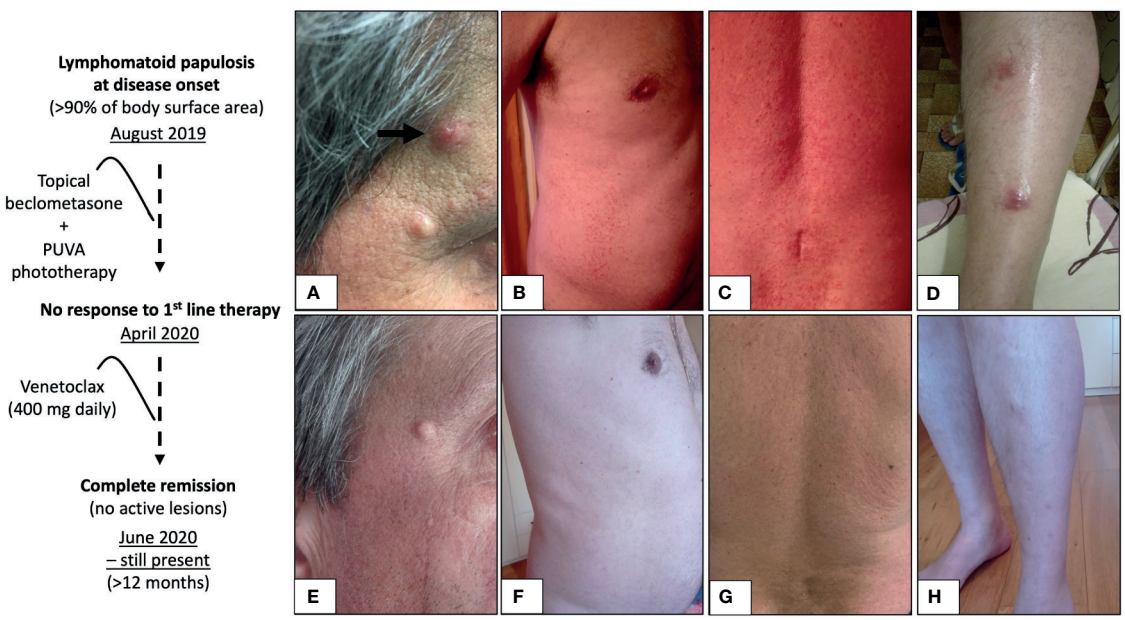

FIGURE 1 | Lymphomatoid papulosis at disease onset **(A–D)** and at 8 weeks from the initiation of venetoclax monotherapy **(E–H)**. Intensely pruritic red flat-topped papules with diffuse erythema spreading on >90% body surface area **(B, C)**, accompanied with sparse nodules (**A**, black arrow, and **D**). At 8 weeks from the initiation of the potent selective BCL2 inhibitor venetoclax (400 mg daily), a complete response was achieved, as defined by no detectable active skin lesions **(E–H)**, and it is still present (in May 2021), lasting more than 12 months.

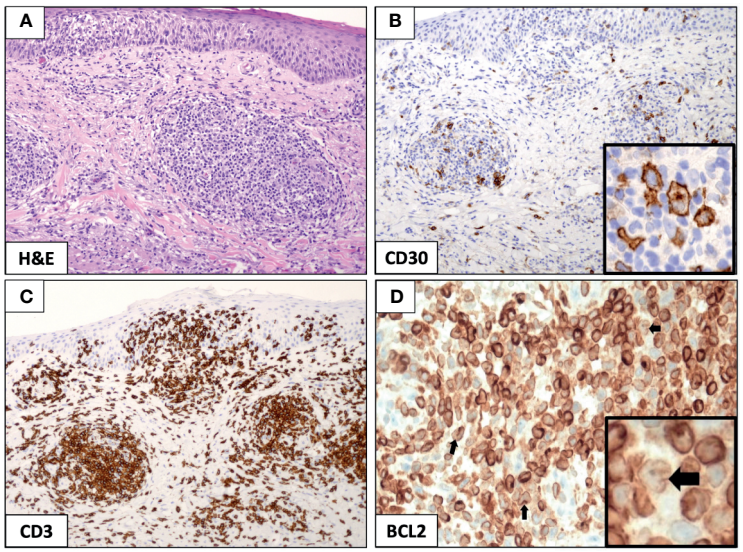

FIGURE 2 | Immunohistochemical analysis of mixed-infiltrate type A lymphomatoid papulosis (LyP). The punch biopsy from the left arm identified a diffuse infiltration of small lymphocytes and few large-sized Hodgkin-like cells that were prevalent in the dermis and subcutis, while largely sparing the epidermis (**A**, *original magnification*, ×10). Hodgkin-like cells stained positive for CD30 (**B**, *original magnification*, ×10; and B, inset, *original magnification*, ×40) and were interspersed in a dense lymphoid infiltrate mostly contributed by $CD3^+$ T cells (**C**, *original magnification*, ×10). The expression of the anti-apoptotic protein BCL2 was strong and pervasive in the LyP tissue (**D**, *original magnification*, ×10), and it was readily recognized in the reactive lymphoid meshwork and large-sized Hodgkin-like cells (**D**, inset, black arrow, *original magnification*, ×40).

neoplastic B cells nor immunoglobulin gene rearrangements were detected in the skin biopsy, thus excluding a diagnosis of B-cell leukemia cutis while proving that the $CD30^+$ cutaneous lymphoproliferative disorder was clonally unrelated to the mature B-cell neoplasm in our case. In conclusion, the clinicopathological picture was consistent with mixed-infiltrate type A LyP (1).

Topical corticosteroid beclomethasone (from August 2019 to January 2020) and psoralen plus ultraviolet A (PUVA) phototherapy were administered (three times per week, from January to April 2020) with no improvement of the diffuse skin papulonodular rash nor of the intractable pruritus associated with scratch lesions [pruritus was defined as of severe entity, according to a visual analogue scale (7)]. In April 2020, a second progression of CLL occurred and it was clinically characterized by progressive lymphadenopathy and, genetically, by the acquisition of a pathogenic nonsense mutation ($TP53^{E294X}$) and of a monoallelic deletion of *TP53* gene (del*TP53*/17p11). A salvage therapy with oral venetoclax (400 mg, daily, following the 5-week ramp-up dosing schedule), a potent selective BCL2 inhibitor, was then started and induced a partial response of CLL (6) with no treatment-related complications (in particular, no tumor lysis syndrome or neutropenia); owing to the risk of cardiotoxicity, the administration of Bruton's tyrosine kinase inhibitor, ibrutinib, was not considered in this patient who had recently suffered acute myocardial infarction. Very surprisingly, LyP-associated skin lesions completely resolved (zero lesions) along with intractable pruritus within 8 weeks from venetoclax initiation (**Figures 1E–H**).

DISCUSSION

In order to search for the molecular underpinning of patient's dramatic response to venetoclax, we stained the original cutaneous biopsy for the BCL2 anti-apoptotic protein and demonstrated its strong expression restricted to the $CD30^+$ Hodgkin-like cells and reactive lymphoid infiltrate (**Figure 2D**); a positive staining for BCL2 has been previously described in 100% of LyP cases studied by immunohistochemistry [8 and 5 cases from two independent studies (8, 9)], and it has been mostly observed within the reactive small T-cell infiltrate of the LyP tissue (13/13); however, only in 1/8 cases (∼12%), BCL2 over-expression has been even detected in the Hodgkin-like cell component (9), as it is for the current case. Notably, BCL2 protein and mRNA expression have shown to have an inverse relationship with *in vitro* sensitivity to venetoclax in primary cells from patients with CTCL, and a higher BCL2 expression at baseline does correlate with a better response to venetoclax (10); these observations are in line with the patient's durable complete response to venetoclax (lasting >12 months from drug initiation and still present in May 2021), which is defined as no detectable active skin lesion (11).

CONCLUDING REMARKS

Our findings underline the probable pathogenic role of BCL2 in LyP and the potential therapeutic efficacy of the BCL2 inhibitor,

venetoclax, for the treatment of this primary cutaneous $CD30^+$ lymphoproliferative disorder, especially in the setting of severe and refractory disease.

DATA AVAILABILITY STATEMENT

The original contributions presented in the study are included in the article, further inquiries can be directed to the corresponding authors.

ETHICS STATEMENT

Ethical review and approval were not required for the study on human participants in accordance with the local legislation and institutional requirements. The patients/participants provided their written informed consent to participate in this study. Written informed consent was obtained from the individual(s) for the publication of any potentially identifiable images or data included in this article.

AUTHOR CONTRIBUTIONS

VG, AM, and PS conceived the study. VG, VC, MB, and PS were involved in patient's clinical management and treatment. VG, GM, SA, AM, and PS performed the pathological examination of the skin biopsy. ED, FDF, CR, and DS performed molecular genetic analyses. VG, AM, and PS wrote the paper. AM and PS supervised the entire study. All authors contributed to the article and approved the submitted version.

FUNDING

This research has received funding from the Associazione Italiana per la Ricerca sul Cancro (AIRC) IG 2018, Project ID 21352, to PS.

REFERENCES

1. Willemze R, Cerroni L, Kempf, Berti E, Facchetti F, Swerdlow SH, et al. The 2018 Update of the WHO-EORTC Classification for Primary Cutaneous Lymphomas. *Blood* (2019) 133(16):1703–14. doi: 10.1182/blood-2018-11-881268
2. Cheng JY, Cohen PR. Lymphomatoid Papulosis in Patients With Chronic Lymphocytic Leukemia/Small Lymphocytic Lymphoma: Case Report and Literature Review. *Dermatol Online J* (2018) 24(5):13030/qt0n77t015.
3. Prieto-Torres L, Rodriguez-Pinilla SM, Onaindia A, Ara M, Requena L, Piris MÁ, et al. CD30-Positive Primary Cutaneous Lymphoproliferative Disorders: Molecular Alterations and Targeted Therapies. *Haematologica* (2019) 104 (2):226–35. doi: 10.3324/haematol.2018.197152
4. Duvic M, Tetzlaff MT, Gangar P, Clos AL, Sui D, Talpur R. Results of a Phase II Trial of Brentuximab Vedotin for $CD30^+$ Cutaneous T-Cell Lymphoma and Lymphomatoid Papulosis. *J Clin Oncol* (2015) 33(32):3759–65. doi: 10.1200/JCO.2014.60.3787
5. Lewis DJ, Talpur R, Huen AO, Tetzlaff MT, Duvic M. Brentuximab Vedotin for Patients With Refractory Lymphomatoid Papulosis: An Analysis of Phase 2 Results. *JAMA Dermatol* (2017) 153(12):1302–6. doi: 10.1001/jamadermatol.2017.3593
6. Hallek M, Cheson BD, Catovsky D, Caligaris-Cappio F, Dighiero G, Döhner H, et al. iwCLL Guidelines for Diagnosis, Indications for Treatment, Response Assessment, and Supportive Management of CLL. *Blood* (2018) 131 (25):2745–60. doi: 10.1182/blood-2017-09-806398
7. Reich A, Heisig M, Phan NQ, Taneda K, Takamori K, Takeuchi S, et al. Visual Analogue Scale: Evaluation of the Instrument for the Assessment of Pruritus. *Acta Derm Venereol* (2012) 92:497–501. doi: 10.2340/00015555-1265
8. Dummer R, Michie SA, Kell D, Gould JW, Haeffner AC, Smoller BR, et al. Expression of Bcl-2 Protein and Ki-67 Nuclear Proliferation Antigen in Benign and Malignant Cutaneous T-Cell Infiltrates. *J Cutan Pathol* (1995) 22(1):11–7.
9. Paulli M, Berti E, Boveri E, Kindl S, Bonoldi E, Gambini C, et al. Cutaneouos CD30+ Lymphoproliferative Disorders: Expression of Bcl-2 and Proteins of the Tumor Necrosis Factor Receptor Superfamily. *Hum Pathol* (1998) 29 (11):1223–30.
10. Cyrenne BM, Lewis JM, Weed GM, Carlson KR, Mirza FN, Foss FM, et al. Synergy of BCL2 and Histone Deacetylase Inhibition Against Leukemic Cells From Cutaneous T-Cell Lymphoma Patients. *Blood* (2017) 130(19):2073–83. doi: 10.1182/blood-2017-06-792150
11. Olsen EA, Whittaker S, Kim YH, Duvic M, Prince HM, Lessin SR, et al. International Society for Cutaneous Lymphomas; United States Cutaneous Lymphoma Consortium; Cutaneous Lymphoma Task Force of the European Organisation for Research and Treatment of Cancer. Clinical End Points and Response Criteria in Mycosis Fungoides and Sézary Syndrome: A Consensus Statement of the International Society for Cutaneous Lymphomas, the United States Cutaneous Lymphoma Consortium, and the Cutaneous Lymphoma Task Force of the European Organisation for Research and Treatment of Cancer. *J Clin Oncol* (2011) 29(18):2598–607. doi: 10.1200/JCO.2010.32.0630

Conflict of Interest: The authors declare that the research was conducted in the absence of any commercial or financial relationships that could be construed as a potential conflict of interest.

frontiers in Oncology

ORIGINAL RESEARCH
published: 28 September 2021
doi: 10.3389/fonc.2021.680411

Off-Label Use of Thrombopoietin Receptor Agonists: Case Series and Review of the Literature

Marco Capecchi[1,2*†], *Fabio Serpenti*[2,3†], *Juri Giannotta*[3,4], *Loredana Pettine*[4], *Gianluigi Reda*[4], *Ida Martinelli*[2], *Andrea Artoni*[2], *Wilma Barcellini*[4] *and Bruno Fattizzo*[3,4]

[1] Department of Biomedical Sciences for Health, Università degli Studi di Milano, Milan, Italy, [2] Fondazione IRCCS Ca' Granda Ospedale Maggiore Policlinico, Angelo Bianchi Bonomi Hemophilia and Thrombosis Center, Milan, Italy, [3] Department of Oncology and Onco-hematology, Università degli Studi di Milano, Milan, Italy, [4] Fondazione IRCCS Ca' Granda Ospedale Maggiore Policlinico, Hematology Unit, Milan, Italy

Since their license in 2008, studies on thrombopoietin receptor agonists (TPO-RAs) are proceeding at a fast pace. Their favorable efficacy and safety profile makes them good candidates for the management of thrombocytopenia in different settings, even beyond their current indications. In the last 10 years, we faced patients with refractory thrombocytopenia that required treatment with off-label TPO-RA, despite the paucity of data in the literature and the possible risks, particularly that of thrombosis. We hereby report our 10-year real-life single-center experience of TPO-RA used off-label. Fourteen patients were divided into three groups according to the etiology of thrombocytopenia: myelodysplastic syndromes, post-transplantation, and lymphoproliferative diseases. Clinical features and results are reported within each group. Overall, TPO-RA proved effective in all these conditions achieving responses also in heavily pretreated patients. The overall response rate (ORR) was 100% in patients with thrombocytopenia after transplantation and in those with lymphoproliferative diseases and 75% in patients with myelodysplastic syndromes. The median duration of therapy was 285 days (range 93–1,513 days). Four patients (29%) discontinued treatment because of lack of response (n=2) or a sustained response (n=2). No grade 3–4 adverse events occurred, particularly no thrombosis. In our real-life experience, TPO-RAs were effective and safe and proved of value in the challenging management of patients with refractory thrombocytopenia associated with different conditions.

Keywords: thrombopoietin receptor agonist, eltrombopag, romiplostim, myelodysplastic syndromes, transplant, lymphoproliferative syndromes

OPEN ACCESS

Edited by:
Luca Laurenti, Agostino Gemelli University Polyclinic, Italy

Reviewed by:
Howard Allen Liebman, University of Southern California, United States
Mohamed Mahmoud Moussa, Ain Shams University, Egypt

***Correspondence:**
Marco Capecchi
marco.capecchi@unimi.it

†These authors have contributed equally to this work

Specialty section:
This article was submitted to Hematologic Malignancies, a section of the journal Frontiers in Oncology

Received: *18 March 2021*
Accepted: *06 September 2021*
Published: *28 September 2021*

Citation:
Capecchi M, Serpenti F, Giannotta J, Pettine L, Reda G, Martinelli I, Artoni A, Barcellini W and Fattizzo B (2021) Off-Label Use of Thrombopoietin Receptor Agonists: Case Series and Review of the Literature. Front. Oncol. 11:680411. doi: 10.3389/fonc.2021.680411

INTRODUCTION

Since thrombopoietin receptor agonists (TPO-RAs) eltrombopag and romiplostim were licensed in the United States for treatment of immune thrombocytopenia (ITP) in 2008, their use has progressively increased, and they are currently available in more than 100 countries (1). Both TPO-RAs bind to the thrombopoietin (TPO) receptor, causing conformational change, activating the JAK2/STAT5 pathway, and resulting in higher megakaryocyte progenitor proliferation and

increased platelet production. Indications for their use are similar in the United States and Europe. Eltrombopag (Revolade®, Promacta®) is approved for second-line therapy of ITP patients older than 1 year of age with a disease lasting at least 6 months (2), for second-line therapy of severe aplastic anemia after failure of immune suppressive therapy (3), and for the treatment of thrombocytopenia in adults with chronic hepatitis C treated with interferon-based regimens (4). Romiplostim (Nplate®) is only approved as second-line treatment for chronic ITP patients (i.e., after 12 months from diagnosis). Two other TPO-RAs have been recently approved, namely avatrombopag (Doptelet®) and lusutrombopag (Mulpleo®), specifically licensed for the treatment of patients with thrombocytopenia secondary to chronic liver disease undergoing invasive procedures (5, 6).

As for safety, the initial concerns on the risk of myelofibrosis induction have not been confirmed. Only a small number of patients develop moderate to severe reticulin and/or collagen fibrosis, which is usually reversible after drug discontinuation (7). A higher rate of venous thromboembolism has been reported, with a two- to threefold increased risk as compared with non-TPO-RA treated ITP patients (8, 9). Cataract and transiminitis are eltrombopag-associated adverse effects, whereas the development of neutralizing antibodies and pain after injection are associated to romiplostim (1).

Emerging evidence is being produced about TPO-RA efficacy and safety profile in different settings other than the registered ones. Overall, it appears relevant to understand which are the main clinical needs and the most promising fields in which to broaden TPO-RA use, given their convenient and safe profile. We hereby report our real-life single-center experience of TPO-RA use in unlabeled conditions and provide inherent literature review.

METHODS

We conducted an observational retrospective study to report the response rates and safety profile of TPO-RA used off-label. All consecutive patients aged >18 years and receiving out-of-label TPO-RA at our center between January 2010 and June 2020 were included. Patients were divided into three main groups according to the underlying cause of thrombocytopenia: post-transplant thrombocytopenia, myelodysplastic syndrome (MDS), and thrombocytopenia associated to lymphoproliferative diseases. All patients were assessed at baseline by whole blood counts with differential, peripheral blood smear, liver and kidney function tests, hemolytic markers (LDH, bilirubin, haptoglobin, reticulocytes), antiplatelet antibodies, and antiphospholipid antibodies and underwent a bone marrow evaluation with cytogenetic studies (karyotype for all patients and FISH for MDS patients), according to clinical practice. In MDS patients, a myeloid gene panel evaluating 69 genes implied in myeloid neoplasms had been performed at diagnosis in two patients; the test was unavailable for the others. Data on underlying disease, previous lines of therapy, drug dosing, discontinuation, bleeding/thrombotic events, and other adverse events were recorded. Clinical status and platelet response were recorded at 1, 3, 6, and 12 months after beginning of the drug. In patients with thrombocytopenia other than the ITP candidate to treatment with TPO-RA, a bone marrow evaluation at baseline is always performed. MDS patients receive further bone marrow assessments every 6 months and whenever clinically indicated. Patient monitoring and education for thrombotic complications and liver function tests evaluation were performed according to current clinical practice for ITP patients treated with TPO-RA. Response criteria were defined as partial response (PR) (platelet count >30,000) and complete response (CR) (platelet count >100,000). Adverse events were defined according to the CTCAE version 5.0.

RESULTS

From January 2010 to June 2020, a total of 81 patients have been treated with a TPO-RA (eltrombopag or romiplostim) at our referral center. A total of 67 patients received the TPO-RA for in-label conditions—ITP (54 patients) or aplastic anemia (13 patients)—while 14 patients received a TPO-RA for unlabeled conditions (**Figure 1** and **Table 1**). Among the latter group, four patients had a transplant-associated thrombocytopenia, eight suffered from MDS, and two had thrombocytopenia associated to a lymphoproliferative neoplasm. The median patient age was 62.5 years (range 36–86). All patients were treated with eltrombopag except for one who received romiplostim. The median duration of therapy was 285 days (range 93–1,513 days) with 4 patients (29%) discontinuing the drug. **Figure 2** shows median platelet trends over time among the different groups (**Figure 2A**) and platelet counts over time for each MDS patient (**Figure 2B**). Regarding responses to TPO-RA treatment, we only observed an increase in platelet counts, while no changes were recorded in erythrocytes and leukocytes in all the three clinical settings. No patient received blood transfusions or myeloid growth factors.

Transplant Group

One patient received an autologous hematopoietic stem cell transplant (HSCT) due to an AL amyloidosis that was complicated by graft failure, leading to persistent thrombocytopenia in the post-transplant period. No more autologous stem cells were available to perform a second transplant procedure, and the patient was not suitable for an allogenic stem cell transplant given the comorbidities. After failure of danazol therapy, she was treated with eltrombopag at the same dose licensed for aplastic anemia (150 mg daily) reaching platelet transfusion independency at 3 months from TPO-RA start.

The other three patients of this group received a solid organ transplant (two liver and one kidney). The median time from transplantation to the onset of thrombocytopenia was 7 days for liver-transplanted patients. The kidney-transplanted patient had instead a late-onset thrombocytopenia (4 years and 2 months after transplantation) associated with graft rejection. Thrombocytopenia in these patients was interpreted as immune-mediated, but all failed steroid therapy. Two of them also received high-dose intravenous

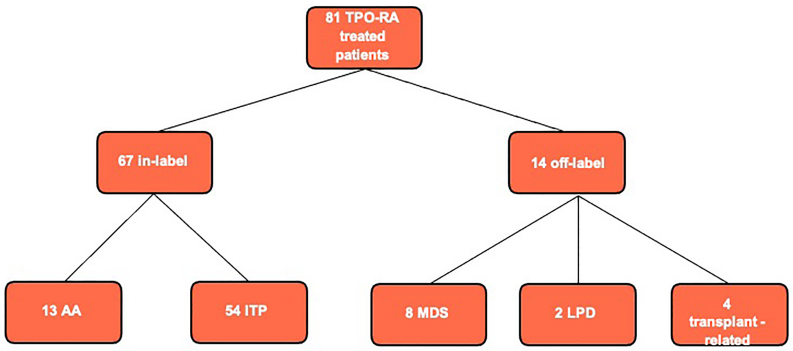

FIGURE 1 | Flowchart of thrombopoietin receptor agonist (TPO-RA) treated patients at our center in the last 10 years. Aplastic anemia (AA) refers to aplastic anemia patients treated in second line after failure of immunosuppressive therapy as for current drug indications; we had no off-label AA patient treated in first line. MDS, myelodysplastic syndrome; LPD, lymphoproliferative disease; ITP, autoimmune thrombocytopenia.

TABLE 1 | Patient outcome stratified by group.

PATIENT ID	GROUP	NUMBER OF PREVIOUS THERAPY LINES	TPO-RA	MAXIMAL DOSE	DURATION OF THERAPY	RESPONSE	TIME TO RESPONSE	ADVERSE EVENT
T-01	TA-T	1	ELTROMBOPAG	150 mg die	181 d	PR	87	0
T-02	TA-T	1	ELTROMBOPAG	75 mg die	1513 d	PR	60	G1 liver
T-03	TA-T	2	ROMIPLOSTIM	6 mcg/kg/w	439 d	CR	119	0
T-04	TA-T	2	ELTROMBOPAG	50 mg die	93 d	CR	17	0
M-01	MDS	1	ELTROMBOPAG	75 mg die	702 d	PR	49	0
M-02	MDS	2	ELTROMBOPAG	75 mg die	1486 d	PR	57	0
M-03	MDS	3	ELTROMBOPAG	75 mg die	93 d	NR	-	PD to AML
M-04	MDS	3	ELTROMBOPAG	50 mg die	354 d	CR	14	0
M-05	MDS	1	ELTROMBOPAG	50 mg die	216 d	PR	40	0
M-06	MDS	2	ELTROMBOPAG	150 mg die	317 d	NR	-	0
M-07	MDS	4	ELTROMBOPAG	150 mg die	252 d	PR	25	0
M-08	MDS	1	ELTROMBOPAG	50 mg die	516 d	PR	44	0
L-01	LPD	4	ELTROMBOPAG	25 mg die	111 d	PR	20	0
L-02	LPD	2	ELTROMBOPAG	50 mg die	158 d	PR	139	0

Each row defines a patient. T-AT, transplant-associated thrombocytopenia; MDS, myelodysplastic syndrome; LPD, lymphoproliferative disease; TPO-RA, thrombopoietin receptor agonist; CR, complete response; PR, partial response; NR, non-response; G1, grade 1; PD to AML, progression to acute myeloid leukemia.

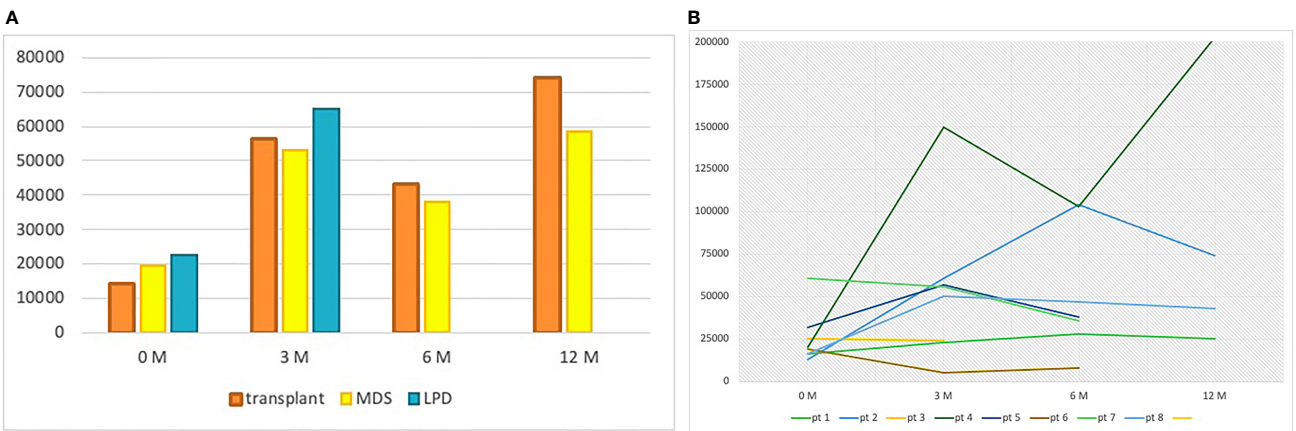

FIGURE 2 | **(A)** Median platelet count at baseline, 3, 6, and 12 months per group of patients. At 6 and 12 months, no data are reported for the lymphoproliferative patients because the median follow-up was inferior to 6 months in this group. LPD, lymphoproliferative disease; MDS, myelodysplastic syndrome; M, months. **(B)** Platelet counts over time for each MDS patient.

immunoglobulins, with only a transient PR in the kidney-transplanted patient. The median time from thrombocytopenia onset to TPO-RA therapy start was only 13 days (10–149 days), as the general clinical conditions of the patients required fast intervention to raise platelet counts. Two patients started eltrombopag 50 mg daily, and one of them had to increase the dose to 75 mg daily due to suboptimal response. The other patient was treated with romiplostim 1 mcg/kg per week, gradually increased to 6 mcg/kg per week to obtain a response. All patients responded, and median platelet counts increased from 8,000/mcl (range 2,000–30,000/mcl) pre-TPO therapy to 62,000/mcl (range 51,000–260,000/mcl), 91,000/mcl (range 43,000–139,000/mcl), and 74,000/mcl (range 64,000–84,000/mcl) at 3, 6, and 12 months, respectively (**Figure 2**).

The overall response rate (ORR) was 100% (1 CR and 3 PR). After 3 years of therapy, one patient who underwent liver transplantation stopped eltrombopag due to grade 1 hepatic toxicity together with a stable PR, which persisted even after TPO-RA discontinuation, until more than 6 months of follow-up (189 days). The median duration of therapy was 310 days (range 93–1,513), and overall survival (OS) was 100% with all patients being alive and in good general conditions at last follow-up visit.

Myelodysplastic Syndrome Group

Eight patients received eltrombopag because of thrombocytopenic MDS. Six patients had low international prognostic scoring system (IPSS)/revised-IPSS, and the other two had intermediate-1 IPSS/revised-IPSS. Only one patient had abnormal cytogenetics with chromosome 8 trisomy. Mutational analysis with NGS was performed in two patients, one bearing a DNMT3A mutation with a variant allele frequency (VAF) of 3.6% and the other showing no detectable mutations. Five patients had a hypocellular bone marrow, three of them showing also reduced megakaryocytes. The other three patients showed an increased number of megakaryocytes, one of them with marked dysplastic features. Antiplatelet antibodies were found in five cases. The median number of therapy lines before TPO-RA was 2 (range 1–4). These included steroids (all patients, 5 PR), Cyclosporin A (3 patients, 2 PR), intravenous immunoglobulin (IVIG, 3 patients, 1 PR and 1 CR), danazol (3 patients, 2 PR), and rituximab (1 patient, transient PR). The median time elapsed from onset of thrombocytopenia to eltrombopag therapy was 1,582 days (range 30–5,878 days), and the median platelet count was 20,000/mcl (range 13,000–230,000/mcl) before therapy. Eltrombopag was started at 50 mg daily and raised according to clinical judgment, with a median steady dose of 75 mg (50–150 mg). The median platelet count was 53,000/mcl (range 5,000–150,000/mcl), 38,000/mcl (range 8,000–104,000/mcl), and 59,000/mcl (25,000–203,000/mcl) at 3, 6, and 12 months, respectively. ORR was 75% (5 PR and 1 CR). Three patients discontinued TPO-RA, two because of failure after 3 (93 days) and 10 months (317 days) of therapy, respectively. Interestingly, these patients were the only ones with intermediate-1 risk score according to IPSS/r-IPSS risk stratification, and both had an increased number of dysplastic megakaryocytes in their bone marrow biopsies. The other patient discontinued the drug due to persisting CR for more than 11 months (340 days). This patient experienced transient drops in platelet counts while tapering TPO-RA but was able to stop the drug keeping a sustained CR for 9 months (279 days). Thereafter, a relapse occurred again, successfully rescued with TPO-RA. No adverse events were observed in this group of patients. The median duration of therapy was 336 days (range 93–1,486 days) and the OS was 88%. The patient who died had a 15-year history of thrombocytopenic MDS heavily pretreated with steroids, IVIG, danazol, cyclosporine, and finally eltrombopag with no response. Three months after TPO-RA start, the patient evolved to AML, received induction chemotherapy and bone marrow transplantation, and thereafter died because of an infection complication. The long history of refractory disease and the short course of eltrombopag therapy before disease progression make it difficult to evaluate a possible cause–effect relationship between TPO-RA treatment and leukemic progression.

Lymphoproliferative Group

Two patients had a lymphoproliferative disorder, one chronic lymphocytic leukemia (CLL) and one indolent non-Hodgkin lymphoma (not histologically classified due to the patient's frailty and comorbidities that contraindicated biopsy).

The CLL patient had a long history (about 10 years) of indolent untreated disease before the development of thrombocytopenia. He received steroids, rituximab, rituximab-bendamustine, and rituximab-idelalisib all without efficacy. Thereafter, eltrombopag 25 mg daily was started, and platelets rose to 60,000/mcl after 3 months of therapy. At last follow-up, he was still on TPO-RA treatment, in good general conditions, and without need for further CLL therapy.

The indolent non-Hodgkin lymphoma patient presented to the emergency department with grade 4 thrombocytopenia (platelet count 1,000/ml) associated with bleeding (grade 3 lower gastrointestinal tract hemorrhage). Steroids and IVIG were started without any improvement in terms of transfusion needs. After 2 weeks, she was put on eltrombopag 50 mg daily with a PR allowing hospital discharge. At 3 months from TPO-RA start, the platelet count was 70,000/mcl without any bleeding symptom and no adverse event reported.

TPO-RA Off Label: Available Literature

Table 2 shows the most important trials and reports of TPO-RA use in a number of unlabeled conditions, including myeloid neoplasms (mainly MDS, but also acute myeloid leukemia and chronic myelomonocytic leukemia), postchemotherapy setting of solid tumors, secondary ITP (associated to both lymphoproliferative syndromes and systemic lupus erythematosus, SLE), graft failure after hematopoietic stem cell transplant, thrombocytopenia after heart and lung transplantation, non-HCV-related chronic liver diseases, and inherited thrombocytopenia (10–52). The majority of these studies are small trials, mostly phase I/II, with less than 50 patients enrolled. The heterogeneity of the study designs and endpoints of the trials makes it difficult to compare their results. Anyway, the overall response rates, reported accordingly to the study primary objective, were high and satisfactory (more than 50%) in most cases. Some discrepancies can be appreciated in the results for the myeloid malignancies group, characterized by high heterogeneity in disease type and severity, ranging from low- to high-risk MDS patients and to acute myeloid leukemia;

TABLE 2 | Published and ongoing studies with TPO-RA used in unlabeled conditions.

TRIAL	AUTHOR	STUDY DESIGN	DISEASE	N° OF PTS	DRUG	RESULTS[1]
	Ramadan et al. (10)	phase I trial	CMML	7	E	ORR 42%
	Gudbrandsdottir et al. (11)	retrospective	miscellaneous	17	E/R	ORR 40%
NCT01481220	Svensson et al. (12)	phase I trial	hgh-risk MDS	12	E + A	ORR 75%
NCT01286038	Duong et al. (13)	phase I trial	high-risk MDS/AML	37	E	ORR 24%
NCT00903422	Platzbecker et al. (14)	phase I/II RCT	high-risk MDS/AML	98	E	ORR 28%*
NCT01440374	Mittelman et al. (15)	phase II RCT	high-risk MDS/AML	145	E	NA^
NCT01893372	Swaminathan et al. (16)	phase II RCT	hgh-risk MDS	28	E +/- A	ORR 11%
NCT02158936	Dickinson et al. (17)	phase III RCT	high risk MDS	356	A +/- E	ORR 16%*
NCT01890746	Frey et al. (18)	phase II RCT	AML	148	E	ORR 70%*
NCT00303472	Kantarjian HM et al. (19)	phase I/II trial	low-risk MDS	44	R	ORR 46%
NCT00303472	Sekeres et al. (20)	phase I/II trial	low-risk MDS	28	R	ORR 61%
2010-022890-33	Oliva et al. (21)	phase I/II RCT	low-risk MDS	90	E	ORR 47%
NCT00321711	Kantarjian et al. (22)	phase II RCT	low-risk MDS	40	R + A	NA^
NCT00418665	Wang et al. (23)	phase II RCT	low-risk MDS	39	R + L	NA^
NCT00321711	Greenberg PL et al. (24)	phase II RCT	hgh-risk MDS	29	R + D	NA^
NCT00614523	Kantarjian et al. (25)	phase II RCT	low-risk MDS	250	R	ORR 38%
NCT00472290	Fenaux et al. (26)	extension study	low-risk MDS	60	R	ORR 57%
NCT04324060	ongoing		low-risk MDS		E/R	
NCT01772420	ongoing		low-risk MDS		E + L	
NCT02912208	ongoing		low-risk MDS		E	
	Parameswaran R et al. (27)	retrospective	solid tumor chemotherapy	20	R	success rate 70%
	García Lagunar et al. (28)	retrospective	solid tumor chemotherapy	6	E	NA^
	Al-Samkari et al. (29)	retrospective	solid tumor chemotherapy	153	R	success rate 79%
NCT01147809	Winer et al. (30)	phase II RCT	solid tumor chemotherapy	26	E	success rate 86%
NCT01147809	Winer et al. (31)	phase II RCT	solid tumor chemotherapy	75	E	NA^
NCT02052882	Soff et al. (32)	phase II RCT	solid tumor chemotherapy	60	R	success rate 93%
NCT02227576	Le Rhun et al. (33)	phase II trial	solid tumor chemotherapy	20	R	success rate 60%
NCT04485416	ongoing	phase I trial	solid tumor chemotherapy		E	
NCT02093325	ongoing	phase III RCT	solid tumor chemotherapy		E	
	Shobha V et al. (34)	retrospective	TP secondary to SLE	12	E	ORR 100%
	Maroun MC et al. (35)	retrospective	TP secondary to SLE	3	E	ORR 100%
	González-López et al. (36)	retrospective	secondary ITP	87	E	ORR 38%
NCT01168921	Paul S et al. (37)	phase II trial	TP secondary to CLL	24	E	ORR 82%
NCT01610180	Visco et al. (38)	phase II trial	TP secondary to LPD	18	E	ORR 78%
NCT01610180	ongoing	phase II trial	TP secondary to CLL		E	
NCT01168921	ongoing	phase II trial	TP secondary to CLL		E	
NCT01610180	ongoing	phase II trial	TP secondary to LPD		E	
	Fu et al. (39)	retrospective	poor graft function after HSCT	38	E	ORR 63%
	Marotta et al. (40)	retrospective	poor graft function after HSCT	13	E	ORR 53%
	Tang et al. (41)	retrospective	poor graft function after HSCT	12	E	ORR 83%
	Tanaka et al. (42)	retrospective	poor graft function after HSCT	12	E	ORR 60%
	Samarkandi et al. (43)	retrospective	poor graft function after HSCT	21	E	ORR 75%
	Hartranft et al. (44)	retrospective	poor graft function after HSCT	13	R	ORR 53%
	Yuan et al. (45)	phase II trial	poor graft function after HSCT	13	E	ORR 62%
NCT01980030	Peffault de Latour et al. (46)	phase I/II trial	poor graft function after HSCT	24	R	ORR 66%
NCT03515447	Vourc'h et al. (47)	before - after study	TP in heart and lung transplant	20	R	NA^
NCT03437603	ongoing	phase II trial	poor graft function after HSCT		E	
NCT00861601	Kawaguchi et al. (48)	phase I/II trial	TP in iver disease - non HCV	8	E	ORR 48%
NCT01133860	Pecci et al. (49)	phase II trial	inherited (MYH9)	12	E	ORR 91%
NCT00909363	Gerrits et al. (50)	phase II trial	inherited (WAS)	8	E	ORR 62%
NCT02422394	Ongoing	phase II trial	inherited		E	
NCT04371939	ongoing	phase II trial	inherited (WAS)		E	
NCT03638817	ongoing	phase II trial	inherited		E	

Studies are grouped according to the indication for TPO-RA use. The number of trial as on ClinicalTrial.gov is reported when available. First author name is reported for published studies. RCT, randomized controlled trial; CMML chronic myelomonocytic leukemia; MDS, myelodysplastic syndrome; AML, acute myeloid leukemia; SLE, systemic lupus erythematosus; CLL, chronic lymphocytic leukemia; TP, thrombocytopenia; HSCT, hematopoietic stem cell transplantation; WAS, Wiskott–Aldrich syndrome; E, eltrombopag; R, romiplostim; A, azacytidine; L, lenalidomide; D, decitabine; ORR, overall response rate.

[1]Response rates are reported according to the primary endpoint of each study and therefore different rates are not comparable between studies. For trials on solid cancer chemotherapy, the term success rate more than ORR is applied, as main objectives were thrombocytopenia prevention and ability not to delay chemotherapy cycles.

**Experimental arm did not show better outcomes compared to placebo arm.*

^Not applicable, due to different aims and outcome measures; among outcome measures: higher PLT counts/nadir, lower PLT transfusion rates, lower clinically relevant thrombocytopenic event (CRTE).

furthermore, medications associated to TPO-RA may also confound the picture. Of note, none of the published or ongoing studies have assessed the use of TPO-RA in the liver or renal post-transplant setting, and none is a real-life study.

The most explored field of investigation for these drugs remains myelodysplastic syndromes, especially in the low-risk setting, where thrombocytopenia is common and can impact the quality of life of patients with a good prognosis. Eight trials have already been completed (19–26) and three are ongoing, including a phase II/III trial, with a cumulative ORR of 45%. Despite some older reports pointing out an increased leukemogenesis risk (53), a recent phase II trial (15) did not confirm these data and showed a reduction in the need of platelet transfusion support and bleeding episodes also in patients with high-risk MDS or AML treated with eltrombopag. Similarly, a phase I/II study (26) found romiplostim to be safe in low-risk MDS patients with a good response rate in terms of platelet count. The biggest study available in MDS is a phase III randomized controlled trial (RCT) (17) conducted in high-risk MDS patients with eltrombopag coupled to azacytidine. This trial failed to show any benefit of eltrombopag and was terminated prematurely.

Regarding chemotherapy-associated thrombocytopenia in solid tumors (27–33), TPO-RA reduced thrombocytopenic adverse events thus decreasing the delay between cycles and the need for chemotherapy dose reduction. A phase III RCT is currently ongoing on the use of eltrombopag for chemotherapy-induced thrombocytopenia in any solid tumor in Taiwan.

ITP secondary to SLE may not respond to disease-specific treatments (steroids, immunosuppressors, and biologics) and further impair patients' quality of life. TPO-RA showed 100% response rates in a total of 15 SLE patients treated in two retrospective studies (34, 35).

ITP secondary to autoimmune and lymphoproliferative diseases (34–38) remains an understudied setting, with the majority of studies being retrospective and including a low number of patients, although with remarkable efficacy. Overall, 144 patients have been reported and the cumulative ORR was 57%. Indeed, thrombocytopenia refractory to first line steroids should be managed with lymphoma-specific treatment (e.g., chemo-immunotherapy in CLL) according to current guidelines.

Reports for the use of TPO-RA in inherited thrombocytopenia, such as MYH9-related disorders or Wiskott–Aldrich syndrome (49, 50), showed benefit on transfusion needs and hemostasis in a total of 80% of patients. There is also one report indicating benefit from TPO-RA in von Willebrand disease type 2B refractory to more conventional lines of therapy in emergency conditions (54).

Lastly, a promising field of interest, with an increasing number of reports in the last years, is the post- HSCT setting. TPO-RA could be of great benefit in prolonged cytopenia secondary to poor graft function that remains nowadays still difficult to manage and accounts for a significant proportion of nonrelapse mortality after transplant. Many recent retrospective series have reported encouraging results (39–46, 51, 52), with the biggest experience of the Spanish Group who reported an ORR of 72% in a cohort of 89 patients (51). Importantly, promising data exist in post-HSCT pediatric cohorts too (52).

DISCUSSION

In this study, we report the safety and efficacy of TPO-RA use outside approved indications in real-life cohort from a single referral center. These clinical settings represent the real life encountered by hematologists handling thrombocytopenia. We found that TPO-RAs are effective and manageable even in off-label settings, despite possible detrimental cofactors linked to underlying conditions such as cancer and transplant. Indeed, all the transplanted patients and those with lymphoproliferative syndromes responded after about 3 months of TPO-RA therapy, and among myelodysplastic patients, six out of eight achieved at least a PR.

Only 1 transplanted patient out of 14 treated with eltrombopag experienced a grade 1 hepatic toxicity, with complete recovery after drug discontinuation. No other TPO-RA-related adverse events were observed during the study.

Of note, one transplanted and one myelodysplastic patient maintained a stable response, partial and complete, respectively, after 189 and 279 days from TPO-RA discontinuation, showing that the achievement of a treatment-free remission is possible even in conditions other than ITP.

The favorable efficacy and safety profile emerging from our cohort is similar to that reported in the increasing number of studies addressing the use of TPO-RA in myeloid neoplasms (mainly MDS, but also acute myeloid leukemia and chronic myelomonocytic leukemia), in the postchemotherapy setting of solid tumors, in secondary ITP (associated to both lymphoproliferative syndromes or systemic lupus erythematosus), in graft failure after HSCT, in thrombocytopenia after heart and lung transplantation, in chronic liver diseases, and in inherited thrombocytopenia (**Table 2**). Thrombocytopenic low-risk MDS was the main clinical condition in which we used off-label eltrombopag. Compared to the biggest phase II trial of eltrombopag in low-risk MDS patients [EQol-MDS study (21)], we experienced a higher ORR (75% *vs* 47%) possibly due to the lower representation of intermediate-1 risk MDS in our cohort (25% *vs* 71%). Interestingly, the only two intermediate-1 risk patients were the ones who did not respond to eltrombopag.

An interesting point is that the employed doses of TPO-RA are extremely heterogeneous, reflecting the uncertainties in off-label conditions. Similarly, in this study, a wide range of doses of eltrombopag has been used, from 25 to 150 mg daily. However, both the lowest (25 mg) and the highest (150 mg) doses were associated with at least a PR, and the two CR occurred on eltrombopag at low dose (50 mg in both cases). This likely reflects the use of the off-label drug at the "minimal effective dose," with the aim to limit toxicities, as currently suggested in ITP (55). On average, higher doses were requested in MDS-associated thrombocytopenia compared to transplant- and lymphoproliferative-associated thrombocytopenia, where the ITP dose (i.e., 50–75 mg daily) seems to be sufficient. This can be explained by the different pathogenesis of thrombocytopenia in these settings. In particular, post-transplant thrombocytopenia is the one that mostly resembles ITP, since the post-transplant period is characterized by a cytokine storm that may be responsible for the onset of cytopenia and may require several lines of immunosuppressive therapies other than steroids and IVIG (56).

In contrast, thrombocytopenia associated with conditions that are characterized by a derangement of the myeloid stem cell, such as myelodysplasia, requires higher doses of TPO-RA to achieve a response. Indeed, TPO-RAs exert their stimulating/differentiating effect also on early hematopoietic stem cells (57); if the latter are dysplastic, the stimulus carried out by standard doses of TPO-RA may not be sufficient (58). As a matter of fact, doses as high as 300 mg daily have been used in RCT (15, 21). Clarifying the best TPO-RA schedule in MDS will be of great value, since 50% of these patients suffer from thrombocytopenia (59), which may be worsened by MDS therapy, and is mainly managed with transfusions and steroids.

The importance of bone marrow reserve is an issue also in lymphoproliferative diseases, where the use of TPO-RA induces an overall response of about 40–50% (58), which increases to 70–80% (the same of primary ITP), if considering only true immune-mediated thrombocytopenia.

Thrombotic events, although infrequent, have been reported in ITP patients treated with TPO-RA with an incidence rate ranging from 1.4 to 4.3 per 100 patient-years (1); if we consider the conditions other than ITP, the majority of studies reported an incidence of venous thromboembolism lower than 2% (range 0–1.6%), while higher rates (≥2%) were reported in MDS/AML and postchemotherapy ITP (conditions *per se* associated with increased thrombotic risk), possibly related to the higher doses of TPO-RA used. Consistently, despite the heterogeneity of available trials, a trend toward increased thrombosis frequency is noted with higher TPO-RA doses; and almost all studies using eltrombopag > 200 mg reported at least one thrombotic event. In our study, no patients developed a thrombotic event, neither venous nor arteriosus. Even if the small number of patients does not allow taking definitive conclusions, the long follow-up and the supramaximal doses of TPO-RA employed in some patients suggest that the risk of thrombosis is not significantly increased.

Finally, some concerns about the potential clonal evolution induced by a sustained stem-cell stimulation under TPO-RA have been raised, particularly in aplastic anemia and MDS. However, in the prospective randomized EQoL-MDS study, leukemic evolution was comparable among the two arms (12% in eltrombopag *versus* 16% in the placebo arm), even if the long-term assessment is still ongoing (21). In our study, only one patient with a long history of heavily pretreated MDS presented a rapid evolution to acute leukemia (3 months after start of eltrombopag), making it difficult to evaluate a possible cause–effect relationship between TPO-RA treatment and leukemic progression. All the other patients were on long-term TPO-RA (range 216–1,486 days) without signs of evolution.

CONCLUSIONS

Our real-life report of TPO-RA off-label use, even though on a small number of patients, highlights their efficacy and safety in difficult-to-manage thrombocytopenia forms, including post-transplant ITP and cases secondary to MDS and lymphoproliferative syndromes. Despite the awareness on thrombotic risk and on the possible clonal evolution should remain high, TPO-RA use in these conditions may have a significant impact on clinical management.

DATA AVAILABILITY STATEMENT

The raw data supporting the conclusions of this article will be made available by the authors, without undue reservation.

ETHICS STATEMENT

The studies involving human participants were reviewed and approved by Comitato Etico Milano Area 2. The patients/participants provided their written informed consent to participate in this study.

AUTHOR CONTRIBUTIONS

MC and FS equally contributed to the manuscript. MC and BF designed the study. FS, JG, LP, and GR assessed the patients for eligibility, collected data, and critically revised the manuscript. MC, FS, BF, IM, AA, and WB contributed to developing the manuscript, and drafting and revising the text, tables, and figure. All authors contributed to the article and approved the submitted version.

FUNDING

This work was supported by the Italian Ministry of Health—Bando Ricerca Corrente.

REFERENCES

1. Ghanima W, Cooper N, Rodeghiero F, Godeau B, Bussel JB. Thrombopoietin Receptor Agonists: Ten Years Later. *Haematologica* (2019) 104(6):1112–23. doi: 10.3324/haematol.2018.212845
2. Birocchi S, Podda GM, Manzoni M, Casazza G, Cattaneo M. Thrombopoietin Receptor Agonists for the Treatment of Primary Immune Thrombocytopenia: A Meta-Analysis and Systematic Review. *Platelets* (2020) 12:1–11. doi: 10.1080/09537104.2020.1745168
3. Desmond R, Townsley DM, Dumitriu B, Olnes MJ, Scheinberg P, Bevans M, et al. Eltrombopag Restores Trilineage Hematopoiesis in Refractory Severe Aplastic Anemia That Can be Sustained on Discontinuation of Drug. *Blood* (2014) 123(12):1818–25. doi: 10.1182/blood-2013-10-534743
4. Mihăilă RG, Cipăian RC. Eltrombopag in Chronic Hepatitis C. *World J Gastroenterol* (2014) 20(35):12517–21. doi: 10.3748/wjg.v20.i35.12517
5. Li C, Li X, Huang F, Yang J, Wu A, Wang L, et al. Efficacy and Safety of Avatrombopag in Patients With Thrombocytopenia: A Systematic Review and Meta-Analysis of Randomized Controlled Trials. *Front Pharmacol* (2019) 10:829. doi: 10.3389/fphar.2019.00829
6. Bussel JB, Kuter DJ, Aledort LM, Kessler CM, Cuker A, Pendergrass KB, et al. A Randomized Trial of Avatrombopag, an Investigational Thrombopoietin-Receptor Agonist, in Persistent and Chronic Immune Thrombocytopenia. *Blood* (2014) 123(25):3887–94. doi: 10.1182/blood-2013-07-514398
7. Brynes RK, Orazi A, Theodore D, Burgess P, Bailey CK, Thein MM, et al. Evaluation of Bone Marrow Reticulin in Patients With Chronic Immune

Thrombocytopenia Treated With Eltrombopag: Data From the EXTEND Study. *Am J Hematol* (2015) 90(7):598–601. doi: 10.1002/ajh.24011
8. Kuter DJ, Bussel JB, Newland A, Baker RI, Lyons RM, Wasser J, et al. Long-Term Treatment With Romiplostim in Patients With Chronic Immune Thrombocytopenia: Safety and Efficacy. *Br J Haematol* (2013) 161(3):411–23. doi: 10.1111/bjh.12260
9. Wong RSM, Saleh MN, Khelif A, Salama A, Portella MSO, Burgess P, et al. Safety and Efficacy of Long-Term Treatment of Chronic/Persistent ITP With Eltrombopag: Final Results of the EXTEND Study. *Blood* (2017) 130 (23):2527–36. doi: 10.1182/blood-2017-04-748707
10. Ramadan H, Duong VH, Al Ali N, Padron E, Zhang L, Lancet JE, et al. Eltrombopag Use in Patients With Chronic Myelomonocytic Leukemia (CMML): A Cautionary Tale. *Clin Lymphoma Myeloma Leuk* (2016) 16 (Suppl):S64–6. doi: 10.1016/j.clml.2016.02.009
11. Gudbrandsdottir S, Frederiksen H, Hasselbalch H. Thrombopoietin-Receptor Agonists in Haematological Disorders: The Danish Experience. *Platelets* (2012) 23(6):423–9. doi: 10.3109/09537104.2011.634931
12. Svensson T, Chowdhury O, Garelius H, Lorenz F, Saft L, Jacobsen SE, et al. A Pilot Phase I Dose Finding Safety Study of the Thrombopoietin-Receptor Agonist, Eltrombopag, in Patients With Myelodysplastic Syndrome Treated With Azacitidine. *Eur J Haematol* (2014) 93(5):439–45. doi: 10.1111/ejh.12383
13. Duong VH, Al Ali N, Zhang L, Padron E, Sallman D, Lancet JE, et al. A Sequential Two-Stage Dose Escalation Study of Eltrombopag in Patients With Myelodysplastic Syndrome and Thrombocytopenia After Hypomethylating Agent Failure. *Leuk Lymphoma* (2020) 61(8):1901–7. doi: 10.1080/10428194.2020.1751841
14. Platzbecker U, Wong RS, Verma A, Abboud C, Araujo S, Chiou TJ, et al. Safety and Tolerability of Eltrombopag *Versus* Placebo for Treatment of Thrombocytopenia in Patients With Advanced Myelodysplastic Syndromes or Acute Myeloid Leukaemia: A Multicentre, Randomised, Placebo-Controlled, Double-Blind, Phase 1/2 Trial. *Lancet Haematol* (2015) 2(10): e417–26. doi: 10.1016/S2352-3026(15)00149-0
15. Mittelman M, Platzbecker U, Afanasyev B, Grosicki S, Wong RSM, Anagnostopoulos A, et al. Eltrombopag for Advanced Myelodysplastic Syndromes or Acute Myeloid Leukaemia and Severe Thrombocytopenia (ASPIRE): A Randomised, Placebo-Controlled, Phase 2 Trial. *Lancet Haematol* (2018) 5(1):e34–43. doi: 10.1016/S2352-3026(17)30228-4
16. Swaminathan M, Borthakur G, Kadia TM, Ferrajoli A, Alvarado Y, Pemmaraju N, et al. A Phase 2 Clinical Trial of Eltrombopag for Treatment of Patients With Myelodysplastic Syndromes After Hypomethylating-Agent Failure. *Leuk Lymphoma* (2019) 60(9):2207–13. doi: 10.1080/10428194.2019.1576873
17. Dickinson M, Cherif H, Fenaux P, Mittelman M, Verma A, Portella MSO, et al. SUPPORT Study Investigators. Azacitidine With or Without Eltrombopag for First-Line Treatment of Intermediate- or High-Risk MDS With Thrombocytopenia. *Blood* (2018) 132(25):2629–38. doi: 10.1182/blood-2018-06-855221
18. Frey N, Jang JH, Szer J, Illés Á, Kim HJ, Ram R, et al. Eltrombopag Treatment During Induction Chemotherapy for Acute Myeloid Leukaemia: A Randomised, Double-Blind, Phase 2 Study. *Lancet Haematol* (2019) 6(3): e122–31. doi: 10.1016/S2352-3026(18)30231-X
19. Kantarjian H, Fenaux P, Sekeres MA, Becker PS, Boruchov A, Bowen D, et al. Safety and Efficacy of Romiplostim in Patients With Lower-Risk Myelodysplastic Syndrome and Thrombocytopenia. *J Clin Oncol* (2010) 28 (3):437–44. doi: 10.1200/JCO.2009.24.7999
20. Sekeres MA, Kantarjian H, Fenaux P, Becker P, Boruchov A, Guerci-Bresler A, et al. Subcutaneous or Intravenous Administration of Romiplostim in Thrombocytopenic Patients With Lower Risk Myelodysplastic Syndromes. *Cancer* (2011) 117(5):992–1000. doi: 10.1002/cncr.25545
21. Oliva EN, Alati C, Santini V, Poloni A, Molteni A, Niscola P, et al. Eltrombopag *Versus* Placebo for Low-Risk Myelodysplastic Syndromes With Thrombocytopenia (EQoL-MDS): Phase 1 Results of a Single-Blind, Randomised, Controlled, Phase 2 Superiority Trial. *Lancet Haematol* (2017) 4 (3):e127–36. doi: 10.1016/S2352-3026(17)30012-1
22. Kantarjian HM, Giles FJ, Greenberg PL, Paquette RL, Wang ES, Gabrilove JL, et al. Phase 2 Study of Romiplostim in Patients With Low- or Intermediate-Risk Myelodysplastic Syndrome Receiving Azacitidine Therapy. *Blood* (2010) 116(17):3163–70. doi: 10.1182/blood-2010-03-274753
23. Wang ES, Lyons RM, Larson RA, Gandhi S, Liu D, Matei C, et al. A Randomized, Double-Blind, Placebo-Controlled Phase 2 Study Evaluating the Efficacy and Safety of Romiplostim Treatment of Patients With Low or Intermediate-1 Risk Myelodysplastic Syndrome Receiving Lenalidomide. *J Hematol Oncol* (2012) 5:71. doi: 10.1186/1756-8722-5-71
24. Greenberg PL, Garcia-Manero G, Moore M, Damon L, Roboz G, Hu K, et al. A Randomized Controlled Trial of Romiplostim in Patients With Low- or Intermediate-Risk Myelodysplastic Syndrome Receiving Decitabine. *Leuk Lymphoma* (2013) 54(2):321–8. doi: 10.3109/10428194.2012.713477
25. Kantarjian HM, Fenaux P, Sekeres MA, Szer J, Platzbecker U, Kuendgen A, et al. Long-Term Follow-Up for Up to 5 Years on the Risk of Leukaemic Progression in Thrombocytopenic Patients With Lower-Risk Myelodysplastic Syndromes Treated With Romiplostim or Placebo in a Randomised Double-Blind Trial. *Lancet Haematol* (2018) 5(3):e117–26. doi: 10.1016/S2352-3026(18)30016-4
26. Fenaux P, Muus P, Kantarjian H, Lyons RM, Larson RA, Sekeres MA, et al. Romiplostim Monotherapy in Thrombocytopenic Patients With Myelodysplastic Syndromes: Long-Term Safety and Efficacy. *Br J Haematol* (2017) 178(6):906–13. doi: 10.1111/bjh.14792
27. Parameswaran R, Lunning M, Mantha S, Devlin S, Hamilton A, Schwartz G, et al. Romiplostim for Management of Chemotherapy-Induced Thrombocytopenia. *Support Care Cancer* (2014) 22(5):1217–22. doi: 10.1007/s00520-013-2074-2
28. García Lagunar MH, Cerezuela Fuentes P, Martínez Penella M, Gutiérrez-Meca Maestre DP, García Coronel M, Martínez Ortiz MJ. Experiencia Del Uso Fuera De Indicación De Eltrombopag En El Tratamiento De La Trombocitopenia Asociada a Tumores Sólidos [Experience of Off-Label Use of Eltrombopag in the Treatment of Thrombocytopenia Associated With Solid Tumors]. *Farm Hosp* (2015) 39 (3):157–60. Spanish. doi: 10.7399/fh.2015.39.3.8580
29. Al-Samkari H, Parnes AD, Goodarzi K, Weitzman JI, Connors JM, Kuter DJ. A Multicenter Study of Romiplostim for Chemotherapy-Induced Thrombocytopenia in Solid Tumors and Hematologic Malignancies. *Haematologica* (2020) 106(4):1148–57 haematol.2020.251900. doi: 10.3324/haematol.2020.251900
30. Winer ES, Safran H, Karaszewska B, Richards DA, Hartner L, Forget F, et al. Eltrombopag With Gemcitabine-Based Chemotherapy in Patients With Advanced Solid Tumors: A Randomized Phase I Study. *Cancer Med* (2015) 4(1):16–26. doi: 10.1002/cam4.326
31. Winer ES, Safran H, Karaszewska B, Bauer S, Khan D, Doerfel S, et al. Eltrombopag for Thrombocytopenia in Patients With Advanced Solid Tumors Receiving Gemcitabine-Based Chemotherapy: A Randomized, Placebo-Controlled Phase 2 Study. *Int J Hematol* (2017) 106(6):765–76. doi: 10.1007/s12185-017-2319-9
32. Soff GA, Miao Y, Bendheim G, Batista J, Mones JV, Parameswaran R, et al. Romiplostim Treatment of Chemotherapy-Induced Thrombocytopenia. *J Clin Oncol* (2019) 37(31):2892–8. doi: 10.1200/JCO.18.01931
33. Le Rhun E, Devos P, Houillier C, Cartalat S, Chinot O, Di Stefano AL, et al. Romiplostim for Temozolomide-Induced Thrombocytopenia in Glioblastoma: The PLATUM Trial. *Neurology* (2019) 93(19):e1799–806. doi: 10.1212/WNL.0000000000008440
34. Shobha V, Sanil S, Roongta R. Eltrombopag: Efficacy and Safety in Steroid Refractory Lupus-Associated Immune Thrombocytopenia. *J Clin Rheumatol* (2020) 26(7):274–8. doi: 10.1097/RHU.0000000000001083
35. Maroun MC, Ososki R, Andersen JC, Dhar JP. Eltrombopag as Steroid Sparing Therapy for Immune Thrombocytopenic Purpura in Systemic Lupus Erythematosus. *Lupus* (2015) 24(7):746–50. doi: 10.1177/0961203314559632
36. González-López TJ, Alvarez-Román MT, Pascual C, Sánchez-González B, Fernández-Fuentes F, Pérez-Rus G, et al. Use of Eltrombopag for Secondary Immune Thrombocytopenia in Clinical Practice. *Br J Haematol* (2017) 178 (6):959–70. doi: 10.1111/bjh.14788
37. Paul S, Jain N, Ferrajoli A, O'Brien S, Burger J, Keating M, et al. A Phase II Trial of Eltrombopag for Patients With Chronic Lymphocytic Leukaemia (CLL) and Thrombocytopenia. *Br J Haematol* (2019) 185(3):606–8. doi: 10.1111/bjh.15581

38. Visco C, Rodeghiero F, Romano A, Valeri F, Merli M, Quaresimini G, et al. Eltrombopag for Immune Thrombocytopenia Secondary to Chronic Lymphoproliferative Disorders: A Phase 2 Multicenter Study. *Blood* (2019) 134(20):1708–11. doi: 10.1182/blood.2019001617
39. Fu H, Zhang X, Han T, Mo X, Wang Y, Chen H, et al. Eltrombopag Is an Effective and Safe Therapy for Refractory Thrombocytopenia After Haploidentical Hematopoietic Stem Cell Transplantation. *Bone Marrow Transpl* (2019) 54(8):1310–8. doi: 10.1038/s41409-019-0435-2
40. Marotta S, Marano L, Ricci P, Cacace F, Frieri C, Simeone L, et al. Eltrombopag for Post-Transplant Cytopenias Due to Poor Graft Function. *Bone Marrow Transpl* (2019) 54(8):1346–53. doi: 10.1038/s41409-019-0442-3
41. Tang C, Chen F, Kong D, Ma Q, Dai H, Yin J, et al. Successful Treatment of Secondary Poor Graft Function Post Allogeneic Hematopoietic Stem Cell Transplantation With Eltrombopag. *J Hematol Oncol* (2018) 11(1):103. doi: 10.1186/s13045-018-0649-6
42. Tanaka T, Inamoto Y, Yamashita T, Fuji S, Okinaka K, Kurosawa S, et al. Eltrombopag for Treatment of Thrombocytopenia After Allogeneic Hematopoietic Cell Transplantation. *Biol Blood Marrow Transpl* (2016) 22 (5):919–24. doi: 10.1016/j.bbmt.2016.01.018
43. Samarkandi H, Al Nahedh M, Alfattani A, Alsharif F, Bakshi N, Rasheed W, et al. Evaluation of Eltrombopag in Thrombocytopenia Post Hematopoietic Cell Transplantation: Rertrospective Observational Trial. *Hematol Oncol Stem Cell Ther* (2020) S1658-3876(20). doi: 10.1016/j.hemonc.2020.07.006
44. Hartranft ME, Clemmons AB, DeRemer DL, Kota V. Evaluation of Romiplostim for the Treatment of Secondary Failure of Platelet Recovery Among Allogeneic Hematopoietic Stem Cell Transplant Patients. *J Oncol Pharm Pract* (2017) 23(1):10–7. doi: 10.1177/1078155215612240
45. Yuan C, Boyd AM, Nelson J, Patel RD, Varela JC, Goldstein SC, et al. Eltrombopag for Treating Thrombocytopenia After Allogeneic Stem Cell Transplantation. *Biol Blood Marrow Transpl* (2019) 25(7):1320–4. doi: 10.1016/j.bbmt.2019.01.027
46. Peffault de Latour R, Chevret S, Ruggeri AL, Suarez F, Souchet L, Michonneau D, et al. Romiplostim in Patients Undergoing Hematopoietic Stem Cell Transplantation: Results of a Phase 1/2 Multicenter Trial. *Blood* (2020) 135 (3):227–9. doi: 10.1182/blood.2019000358
47. Vourc'h M, Senage T, Lepoivre T, Volteau C, Fortuit C, Pattier S, et al. Romiplostim as a Transfusion Saving Strategy in 20 Patients After Heart or Lung Transplantation: A Single Centre Before-After Pilot Study. *Perfusion* (2020) 35(2):121–30. doi: 10.1177/0267659119864814
48. Kawaguchi T, Komori A, Seike M, Fujiyama S, Watanabe H, Tanaka M, et al. Efficacy and Safety of Eltrombopag in Japanese Patients With Chronic Liver Disease and Thrombocytopenia: A Randomized, Open-Label, Phase II Study. *J Gastroenterol* (2012) 47(12):1342–51. doi: 10.1007/s00535-012-0600-5
49. Pecci A, Gresele P, Klersy C, Savoia A, Noris P, Fierro T, et al. Eltrombopag for the Treatment of the Inherited Thrombocytopenia Deriving From MYH9 Mutations. *Blood* (2010) 116(26):5832–7. doi: 10.1182/blood-2010-08-304725
50. Gerrits AJ, Leven EA, Frelinger AL 3rd, Brigstocke SL, Berny-Lang MA, Mitchell WB, et al. Effects of Eltrombopag on Platelet Count and Platelet Activation in Wiskott-Aldrich Syndrome/X-Linked Thrombocytopenia. *Blood* (2015) 126(11):1367–78. doi: 10.1182/blood-2014-09-602573
51. Bento L, Bastida JM, García-Cadenas I, García-Torres E, Rivera D, Bosch-Vilaseca A, et al. Thrombopoietin Receptor Agonists for Severe Thrombocytopenia After Allogeneic Stem Cell Transplantation: Experience of the Spanish Group of Hematopoietic Stem Cell Transplant. *Biol Blood Marrow Transpl* (2019) 25(9):1825–31. doi: 10.1016/j.bbmt.2019.05.023
52. Masetti R, Vendemini F, Quarello P, Girardi K, Prete A, Fagioli F, et al. Eltrombopag for Thrombocytopenia Following Allogeneic Hematopoietic Stem Cell Transplantation in Children. *Pediatr Blood Cancer* (2020) 67(5): e28208. doi: 10.1002/pbc.28208
53. Ogata K, Tamura H. Thrombopoietin and Myelodysplastic Syndromes. *Int J Hematol* (2000) 72(2):173–7.
54. Espitia O, Ternisien C, Agard C, Boisseau P, Denis CV, Fouassier M. Use of a Thrombopoietin Receptor Agonist in Von Willebrand Disease Type 2B (P.V1316M) With Severe Thrombocytopenia and Intracranial Hemorrhage. *Platelets* (2017) 28(5):518–20. doi: 10.1080/09537104.2016.1246717
55. Zaja F, Carpenedo M, Baratè C, Borchiellini A, Chiurazzi F, Finazzi G, et al. Tapering and Discontinuation of Thrombopoietin Receptor Agonists in Immune Thrombocytopenia: Real-World Recommendations. *Blood Rev* (2020) 41:100647. doi: 10.1016/j.blre.2019.100647
56. Pulanic D, Lozier JN, Pavletic SZ. Thrombocytopenia and Hemostatic Disorders in Chronic Graft *Versus* Host Disease. *Bone Marrow Transpl* (2009) 44(7):393–403. doi: 10.1038/bmt.2009.196
57. Imbach P, Crowther M. Thrombopoietin-Receptor Agonists for Primary Immune Thrombocytopenia. *N Engl J Med* (2011) 365(8):734–41. doi: 10.1056/NEJMct1014202
58. Fattizzo B, Levati G, Cassin R, Barcellini W. Eltrombopag in Immune Thrombocytopenia, Aplastic Anemia, and Myelodysplastic Syndrome: From Megakaryopoiesis to Immunomodulation. *Drugs* (2019) 79(12):1305–19. doi: 10.1007/s40265-019-01159-0
59. Alessandrino EP, Amadori S, Barosi G, Cazzola M, Grossi A, Liberato LN, et al. Evidence- and Consensus-Based Practice Guidelines for the Therapy of Primary Myelodysplastic Syndromes. A Statement From the Italian Society of Hematology. *Haematologica* (2002) 87(12):1286–306.

Conflict of Interest: MC reports nonfinancial support from Roche, Novonordisk, and Sobi and honoraria from Daiichi Sankyo. AA reports nonfinancial support from Bayer and Roche and honoraria from Janssen outside of the submitted work. IM reports personal and nonfinancial support from Bayer and Roche outside of the submitted work. WB received consultation honoraria from Novartis, Apellis, Alexion, Agios, and Sanofi. BF received consultation honoraria from Amgen, Novartis, and Momenta.

The remaining authors declare that the research was conducted in the absence of any commercial or financial relationships that could be construed as a potential conflict of interest.

Publisher's Note: All claims expressed in this article are solely those of the authors and do not necessarily represent those of their affiliated organizations, or those of the publisher, the editors and the reviewers. Any product that may be evaluated in this article, or claim that may be made by its manufacturer, is not guaranteed or endorsed by the publisher.

frontiers in Oncology

CASE REPORT
published: 30 September 2021
doi: 10.3389/fonc.2021.728613

Case Report: A Novel Activating FLT3 Mutation in Acute Myeloid Leukemia

Samantha Bruno[1], Lorenza Bandini[2], Agnese Patuelli[2], Valentina Robustelli[1,2], Claudia Venturi[1], Manuela Mancini[2], Dorian Forte[1], Sara De Santis[1], Cecilia Monaldi[1], Alessandra Grassi[2], Gabriella Chiurumbolo[2], Stefania Paolini[2], Gianluca Cristiano[1], Cristina Papayannidis[2], Chiara Sartor[1], Jacopo Nanni[1], Emanuela Ottaviani[2], Antonio Curti[2], Michele Cavo[1,2] and Simona Soverini[1]*

[1] Department of Experimental, Diagnostic and Specialty Medicine, University of Bologna, Bologna, Italy, [2] Istituto di Ricovero e Cura a Carattere Scientifico (IRCCS) Azienda Ospedaliero-Universitaria di Bologna, Istituto di Ematologia "Seràgnoli", Bologna, Italy

FMS-like tyrosine kinase 3 (FLT3) is among the most common driver genes recurrently mutated in acute myeloid leukemia (AML), accounting for approximately 30% of cases. Activating mutations of the FLT3 receptor include internal tandem duplications (ITD) that map to the auto-inhibitory juxtamembrane (JM) domain or point mutations within the tyrosine kinase domain (TKD). Several FLT3 tyrosine kinase inhibitors have been developed in the last few years, but midostaurin is currently the only one approved for the treatment of newly diagnosed patients harboring *FLT3* mutations. Here we describe for the first time a novel in-frame deletion in exon 14 (JM domain) of the *FLT3* gene, that we identified in a young woman with CBFb-MYH11-positive AML. We demonstrated that this novel *FLT3* variant is pathogenic, since it is responsible for constitutive activation of FLT3 receptor. Finally, *ex-vivo* studies demonstrated that this novel mutation is sensitive to midostaurin.

Keywords: acute myeloid leukemia, FLT3 mutation, NGS - next generation sequencing, targeted therapy, midostaurin

OPEN ACCESS

Edited by:
Massimo Breccia, Sapienza University of Rome, Italy

Reviewed by:
Tomasz Stoklosa, Medical University of Warsaw, Poland
Rosa Ayala, Research Institute Hospital 12 de Octubre, Spain

****Correspondence:***
Samantha Bruno
samantha.bruno2@unibo.it

Specialty section:
This article was submitted to Hematologic Malignancies, a section of the journal Frontiers in Oncology

Received: *21 June 2021*
Accepted: *13 September 2021*
Published: *30 September 2021*

Citation:
Bruno S, Bandini L, Patuelli A, Robustelli V, Venturi C, Mancini M, Forte D, De Santis S, Monaldi C, Grassi A, Chiurumbolo G, Paolini S, Cristiano G, Papayannidis C, Sartor C, Nanni J, Ottaviani E, Curti A, Cavo M and Soverini S (2021) Case Report: A Novel Activating FLT3 Mutation in Acute Myeloid Leukemia. Front. Oncol. 11:728613. doi: 10.3389/fonc.2021.728613

INTRODUCTION

Acute myeloid leukemia (AML) is a highly heterogeneous haematological malignancy characterized by a wide range of genomic alterations responsible of defective regulation of the differentiation and self-renewal programs of hematopoietic stem cells. FMS-like tyrosine kinase 3 (FLT3) is a member of class III receptor tyrosine kinases that exhibits activating mutations in approximately 30% of AML patients, making it one of the most recurrently mutated genes (1, 2). Notably, there are two types of *FLT3* mutations which include the internal tandem duplications (ITD) within the auto-inhibitory juxtamembrane (JM) domain, described in about 25-30% of AML patients, and the less frequent gain-of-function mutations occurring in about 8% of AML cases as point mutations in the activation loop of the tyrosine kinase domain (TKD) (1, 2). The leukemogenic relevance and inferior overall survival of *FLT3-ITD* mutations have been shown, although it has been demonstrated that the prognostic impact is affected by both mutant allele burden and presence of co-existing mutations (3, 4). Indeed, high allele ratio (AR>0.5; FLT3-ITD^{high}) is associated with higher disease risk, whereas low AR (<0.5; FLT3-ITD^{low}) is associated with intermediate risk, which becomes favourable in case of co-occurrence of the nucleophosmin 1 (NPM1) mutation (4).

Concerning the *FLT3-TKD* mutations, their prognostic significance still remains unclear, with numerous conflicting data (3, 5–8). The clinical impact of ITD and TKD mutations of *FLT3* is dependent on the subsequent constitutive activation of the tyrosine kinase, that activates its downstream signalling pathways including the signal transducer and activator of transcription 5 (STAT5), RAS/mitogen-activated protein kinase (MAPK)/extracellular-signal-regulated kinase (ERK), phosphoinositide 3-kinase (PI3K)/Serine-Threonine Kinase 1 (AKT) (9–13). These targets have been associated with increased proliferation and survival of the leukemic cell population (14). In light of the crucial pathogenetic role of FLT3 constitutive activation, small molecule inhibitors have been developed as new promising therapies to treat this subset of AML patients.

Here we describe for the first time a novel *FLT3* in-frame deletion and its impact on downstream signalling pathways showing the activation effect of such mutation on FLT3 receptor. Moreover, *ex-vivo* study performed on mutated primary cells sought to demonstrated their sensitivity to midostaurin, a multi-targeted kinase inhibitor active against FLT3, currently approved for first-line treatment of *FLT3*-mutated AML (15).

CASE DESCRIPTION

Clinical Case

A 32 years-old woman which presented with persistent fever associated with marked hyperleukocytosis [white blood cells (WBC), 319,000/mm^3], anemia [hemoglobin (Hb), 5.7 g/dL] and thrombocytopenia [platelets (PLTs), 22,000/mm^3] was admitted to our hospital in July 2019. Morphological analysis of bone marrow (BM) aspirate suggested a diagnosis of acute myelomonocytic leukemia with 80% of myeloid blasts. Computed tomography (TC) examination of the brain detected central nervous system (CNS) localization of blast cells. Immunophenotypic analysis of leukemic cells from the BM aspirate confirmed the expression of several markers of hematopoietic stem and progenitor cells, including CD34, CD13, CD33, CD117, MPO, CD14, CD64, and aberrant expression of CD4. Karyotype and fluorescence *in situ* hybridization (FISH) analyses of BM nuclei identified the inv(16)(p13;q22) chromosome rearrangement in 20/20 metaphases examined. This was confirmed by quantitative RT-PCR that detected the presence of *CBFβ-MYH11* transcript type A (*CBFβ-MYH11*/*ABL**100 = 85.37), along with over-expressed *WT1* (ratio *WT1*/*ABL**10,000 = 1409.53). Therefore, the patient was diagnosed with M4 inv(16) acute myeloid leukemia (AML) according to French-American-British (FAB) classification and was classified as favourable cytogenetic risk based on cytogenetic and molecular biology data according to ELN 2017 (4). However, in light of CNS localization at diagnosis, the patient was considered at high risk of relapse. A FLAI-5 (fludarabine-cytarabine-idarubicin) regimen was selected as induction chemotherapy, which resulted effective and well tolerated. The follow-up evaluation performed after 2 months of induction therapy showed a good response: the patient exhibited a peripheral blood count with WBC levels of 6,100/mm^3, Hb levels of 10.1 g/dL and PLTs of 189,000/mm^3. Accordingly, BM evaluation by morphology, immunophenotyping and molecular biology revealed complete remission (CR; *CBFβ-MYH11*/*ABL**100 = 0.0332; *WT1*/*ABL**10,000 = 13.24) and TC of the brain was negative for SNC localization of blast cells. Therefore, the patient continued with 1 cycle of consolidation therapy with the FLAI-5 regimen. As reported above, due to CNS localization at diagnosis, the patient underwent allogeneic stem cell transplantation (allo-SCT) receiving haploidentical peripheral blood stem cells from her brother. After transplant, she remained in complete remission until the last follow-up. **Figure 1** summarizes relevant clinical course and diagnostic results.

DETECTION OF A NOVEL FLT3 DELETION AND INVESTIGATION OF ITS POTENTIAL ROLE

In light of the clinical utility of next-generation sequencing (NGS) for the assessment of the genetic landscape of AML providing diagnostic and prognostic information, the AmpliSeq Myeloid Panel (Thermofisher) was performed on primary blast cells enriched by density gradient centrifugation from the patient bone marrow sample collected at diagnosis. NGS analysis revealed a *FLT3* mutation with a variant allele frequency (VAF) of 40%, represented by an in-frame deletion at exon 14 of the JM domain (c.1770_1784del15; p.Phe590_Arg595delinsLeu). Interrogation of the COSMIC database indicated that this deletion had never been reported before. The mutation was confirmed by Sanger sequencing (**Figure 2**) and mutant-to-wild-type allelic ratio (AR) was obtained through PCR-electrophoresis and fragment analysis (*FLT3-ITD*-AR=1.1). The *FLT3* mutation became undetectable in the sample collected at the time of CR after induction chemotherapy.

In order to understand whether the newly described FLT3 alteration influenced its cellular activity, we analysed by Western blot (WB) the expression and activation of some target proteins downstream of FLT3. As shown in **Figure 3A**, we observed that the deletion in the JM domain resulted in the constitutive activation of FLT3, with the sample at diagnosis showing increased levels of phosphorylated FLT3 and of its downstream signalling molecules. Five AML patients with wild-type (wt) *FLT-3* and 5 AML patients carrying canonical *FLT3-ITD* mutations (with an AR ranging from 0.8 to 1.5) were used as control for protein expression levels of FLT3 downstream signalling molecules (**Figure 3B**). In particular, the sample at diagnosis, showed increased levels of p21, c-MYC and Cyclin D1, that were associated with the activation of STAT5 signalling pathway, together with the up-regulation of MAPK-activated proteins p-ERK and p38. In addition, the activation of FLT3 induced p27 and BIM expression, which are regulated by AKT and FOXO3A signalling, as well as the up-regulation of 14-3-3 and phosphorylated BAD (serine 112 and 136) that are responsible for the block of cell death. Results were superimposable to what

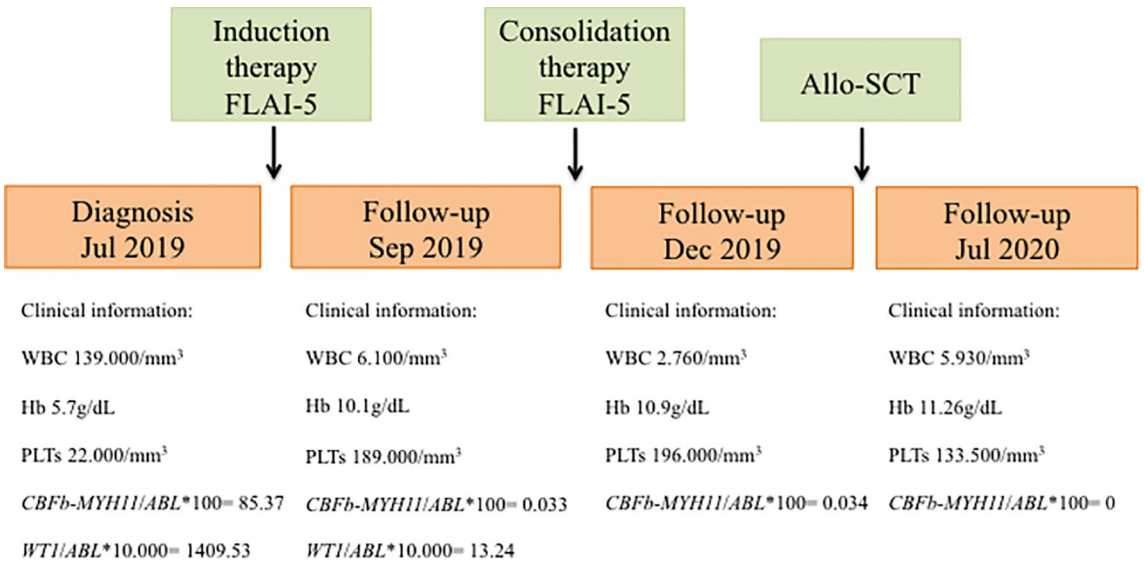

FIGURE 1 | Schematic representation showing timeline of treatment course and clinical information. FLAI-5, fludarabine-cytarabine-idarubicin; Allo-SCT, allogeneic stem cell transplantation; WBC, white blood cells; Hb, hemoglobin; PLTs, platelets.

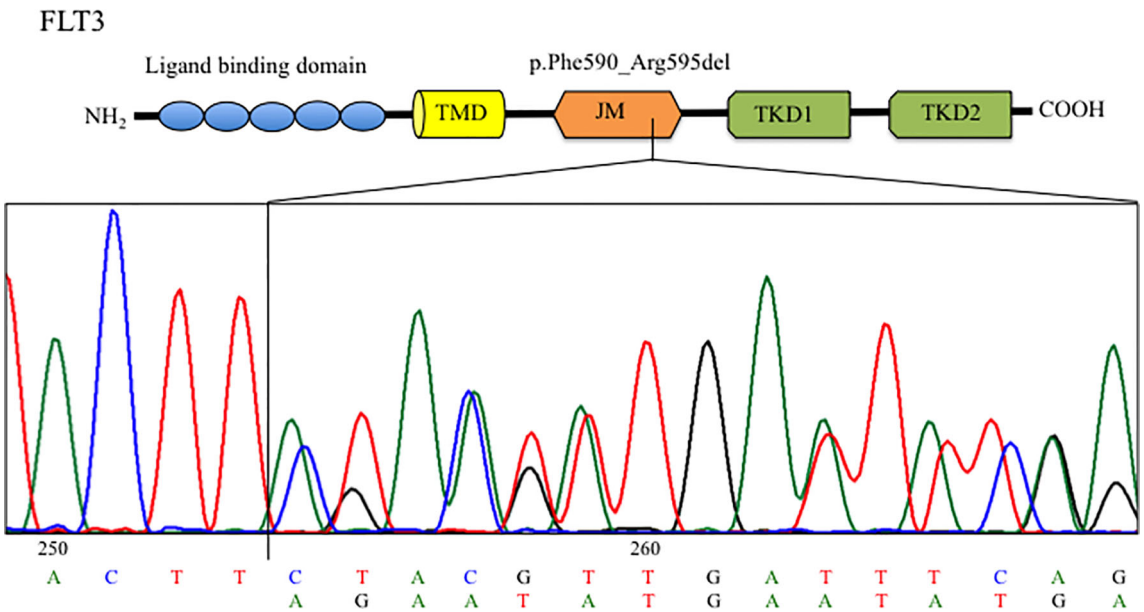

FIGURE 2 | Sanger sequencing chromatogram showing the FLT3 deletion identified in the BM at diagnosis. TMD, transmernbrane domain; JMD, juxtamembrane domain; TKD, tyrosine kinase domain.

we could observe in the 5 *FLT3-ITD* mutated samples as compared to *wt FLT3* samples. As expected, the sample at remission showed a significant reduction of phosphorylated FLT3 and of the activation of all the above mentioned targets, supporting the direct link between activated signalling molecules and the observed FLT3 mutation. Lastly, to investigate the clinical relevance of the described mutation, we assessed the effects of midostaurin on the clonogenic potential of leukemic blasts cells isolated from the patient at diagnosis. Midostaurin induced a dose-dependent reduction in colony formation with an LD_{50} of 100nM, suggesting that the newly reported mutation is sensitive to midostaurin inhibition (**Figure 4**).

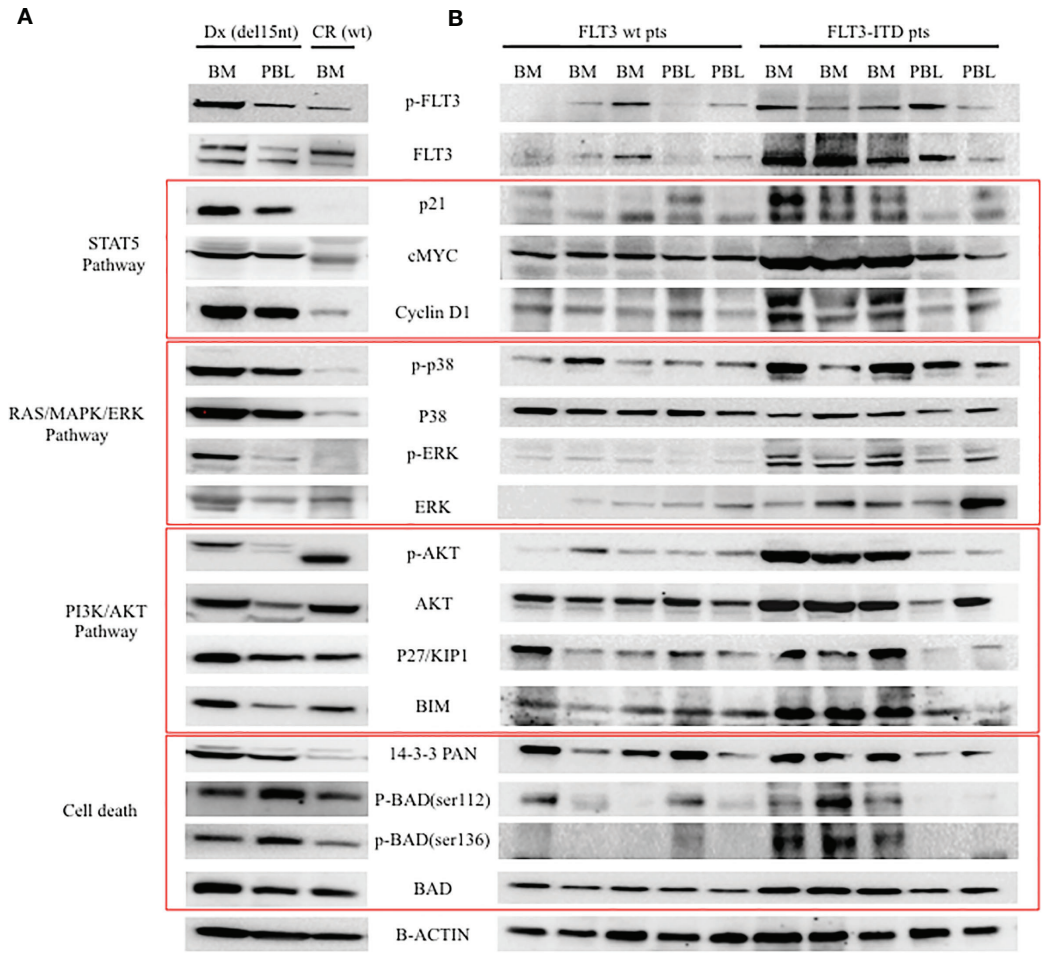

FIGURE 3 | Western blot analysis of FLT-3 expression and of its down-stream signalling pathway. **(A)** Analysis of patient cells at two different time points (Dx: diagnosis with FLT3 carrying the c.1770_1784del15; CR: complete remission with wt FLT3). **(B)** Analysis of 5 AML patients with wt FLT3 along with 5 patients carrying FLT3-ITD, used as control of FLT3 downstream signalling. BM, bone marrow; PBL, peripheral blood.

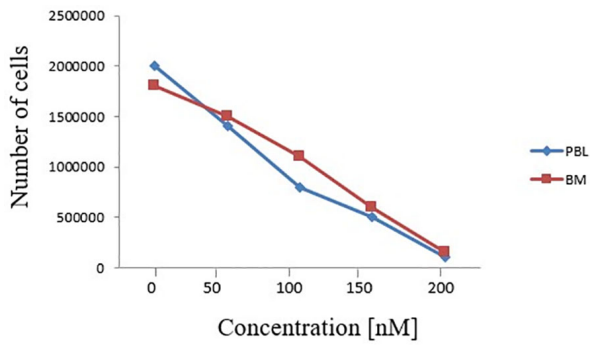

FIGURE 4 | Effects of increasing doses of midostaurin on the clonogenic capacity of primary BM and PBL cells carrying the reported FLT3 deletion (c.1770_1784del15; p.Phe590_Arg595delinsLeu).

CONCLUSION AND DISCUSSION

FLT3 is the most frequently mutated gene in AML patients, with a strong disease specificity (2), and encodes is one of the key molecules involved in the pathogenesis of AML. Indeed, *FLT3* is one of the markers currently used for the molecular genetic diagnosis and risk stratification of AML (4). The clinical relevance of ITD and TKD mutations in AML pathogenesis and progression highlighted the need for specific compounds targeting FLT3 constitutive activation. Consequently, during the last years several inhibitors have been developed as target therapies to improve the outcome of *FLT3*-mutated patients (16, 17). In this study, we describe for the first time a novel *FLT3* mutation identified in an AML patient, consisting in a deletion of 15 nucleotides in the JM domain, where the *FLT3*-ITDs usually localize. Interestingly, other case reports showing noncanonical *FLT3* deletions have

been published, and all these mutations cluster in the JM domain, a highly conserved region that mediates the activation of the FLT3 receptor (18–20). There are limited functional data for deletions in the JM domain, however existing knowledge suggest that any type of mutation, including deletions, in the JM sequence could potentially activate the FLT3 tyrosine kinase receptor, with consequent pathogenetic and clinical impact. In this study, we demonstrated by WB that the newly reported deletion indeed induces the constitutive activation of FLT3 and of its downstream effectors, including STAT5, ERK and AKT pathways. The patient showed a good response to conventional chemotherapy and underwent transplant. However, we also evaluated by *ex-vivo* treatment the efficacy of midostaurin, the TKI currently approved for the treatment of *de novo FLT3*-mutated patients, finding that midostaurin could effectively reduce the clonogenic capacity of primary blast cells. Although additional studies are needed to better characterize the functional consequences and TKI sensitivity of this deletion, our results are corroborated by recent work from Young and colleagues. They used a scanning mutagenesis approach to generated a panel of FLT3 deletions (clustering in the region comprised between K568 to V581) demonstrating that this class of mutations lead to the activation of signalling molecules downstream to FLT3 and are targetable with several TKI inhibitors (20). In conclusion, our results suggest the clinical relevance of the novel *FLT3* deletion herein reported, that acts as a standard activating ITD mutation and can be successfully targeted by midostaurin. Our findings provide useful information for clinicians treating AML patients, highlighting the importance to characterize and monitor the genomic alterations of AML patients.

DATA AVAILABILITY STATEMENT

The original contributions presented in the study are included in the article/supplementary materials. Further inquiries can be directed to the corresponding author.

ETHICS STATEMENT

The studies involving human participants were reviewed and approved by local Ethics Committee (protocol 112/2014/U/Tess of Policlinico Sant'Orsola-Malpighi). The patients/participants provided their written informed consent to participate in this study.

AUTHOR CONTRIBUTIONS

SB, LB, DF, SS, EO and MM contributed to the conception, research design, drafting of the manuscript, and conceptualization methodology. LB and AP performed NGS analysis. VR, CV, SDS, and CM performed sanger sequencing and PCR-electrophoresis and fragment analysis. GaC and AG performed FISH analysis. SB and MM performed WB analysis. SB and DF performed colony-formation assay. SP, GiC, CP, CS, JN, AC, and MC provided clinical data and enrolled the patient for the study. SS and AC reviewed and edited the manuscript. EO, SS, and MC acquired the funding. MM, EO and SS provided the supervision of the study. All authors contributed to the article and approved the submitted version.

ACKNOWLEDGMENTS

The authors acknowledge the supports from AIL Bologna ODV.

REFERENCES

1. Thiede C, Steudel C, Mohr B, Schaich M, Schäkel U, Platzbecker U, et al. Analysis of FLT3-Activating Mutations in 979 Patients With Acute Myelogenous Leukemia: Association With FAB Subtypes and Identification of Subgroups With Poor Prognosis. *Blood* (2002) 99:4326–35. doi: 10.1182/blood.V99.12.4326
2. Papaemmanuil E, Gerstung M, Bullinger L, Gaidzik VI, Paschka P, Roberts ND, et al. Genomic Classification and Prognosis in Acute Myeloid Leukemia. *N Engl J Med* (2016) 374:2209–21. doi: 10.1056/NEJMoa1516192
3. Yanada M, Matsuo K, Suzuki T, Kiyoi H, Naoe T. Prognostic Significance of FLT3 Internal Tandem Duplication and Tyrosine Kinase Domain Mutations for Acute Myeloid Leukemia: A Meta-Analysis. *Leukemia* (2005) 19:1345–9. doi: 10.1038/sj.leu.2403838
4. Döhner H, Estey E, Grimwade D, Amadori S, Appelbaum FR, Büchner T, et al. Diagnosis and Management of AML in Adults: 2017 ELN Recommendations From an International Expert Panel. *Blood* (2017) 129:424–47. doi: 10.1182/blood-2016-08-733196
5. Mead AJ, Linch DC, Hills RK, Wheatley K, Burnett AK, Gale RE, et al. FLT3 Tyrosine Kinase Domain Mutations are Biologically Distinct From and Have a Significantly More Favorable Prognosis Than FLT3 Internal Tandem Duplications in Patients With Acute Myeloid Leukemia. *Blood* (2007) 110:1262–70. doi: 10.1182/blood-2006-04-015826
6. Whitman SP, Ruppert AS, Radmacher MD, Mrózek K, Paschka P, Langer C, et al. FLT3 D835/I836 Mutations are Associated With Poor Disease-Free Survival and a Distinct Gene-Expression Signature Among Younger Adults With *De Novo* Cytogenetically Normal Acute Myeloid Leukemia Lacking FLT3 Internal Tandem Duplications. *Blood* (2008) 111:1552–9. doi: 10.1182/blood-2007-08-107946
7. Boddu P, Kantarjian H, Borthakur G, Kadia T, Daver N, Pierce S, et al. Co-Occurrence of FLT3-TKD and NPM1 Mutations Defines a Highly Favorable Prognostic AML Group. *Blood Adv* (2017) 1:1546–50. doi: 10.1182/bloodadvances.2017009019
8. Perry M, Bertoli S, Rocher C, Hayette S, Ducastelle S, Barraco F, et al. FLT3-TKD Mutations Associated With NPM1 Mutations Define a Favorable-Risk Group in Patients With Acute Myeloid Leukemia. *Clin Lymphoma Myeloma Leuk* (2018) 18:e545–50. doi: 10.1016/j.clml.2018.06.006
9. Takahashi S. Downstream Molecular Pathways of FLT3 in the Pathogenesis of Acute Myeloid Leukemia: Biology and Therapeutic Implications. *J Hematol Oncol* (2011) 4:13. doi: 10.1186/1756-8722-4-13
10. Spiekermann K, Bagrintseva K, Schwab R, Schmieja K, Hiddemann W. Overexpression and Constitutive Activation of FLT3 Induces STAT5 Activation in Primary Acute Myeloid Leukemia Blast Cells. *Clin Cancer Res* (2003) 9:2140–50.
11. Brandts CH, Sargin B, Rode M, Biermann C, Lindtner B, Schwäble J, et al. Constitutive Activation of Akt by Flt3 Internal Tandem Duplications Is Necessary for Increased Survival, Proliferation, and Myeloid Transformation. *Cancer Res* (2005) 65:9643–50. doi: 10.1158/0008-5472.CAN-05-0422
12. Choudhary C, Brandts C, Schwable J, Tickenbrock L, Sargin B, Ueker A, et al. Activation Mechanisms of STAT5 by Oncogenic Flt3-ITD. *Blood* (2007) 110:370–4. doi: 10.1182/blood-2006-05-024018
13. Nogami A, Oshikawa G, Okada K, Fukutake S, Umezawa Y, Nagao T, et al. FLT3-ITD Confers Resistance to the PI3K/Akt Pathway Inhibitors by Protecting the mTOR/4ebp1/Mcl-1 Pathway Through STAT5 Activation in Acute Myeloid Leukemia. *Oncotarget* (2015) 6:9189–205. doi: 10.18632/oncotarget.3279

14. Levis M, Small D. FLT3: ITDoes Matter in Leukemia. *Leukemia* (2003) 17:1738–52. doi: 10.1038/sj.leu.2403099
15. Levis M. Midostaurin Approved for FLT3-Mutated AML. *Blood* (2017) 129:3403–6. doi: 10.1182/blood-2017-05-782292
16. Stone RM, Mandrekar SJ, Sanford BL, Laumann K, Geyer S, Bloomfield CD, et al. Midostaurin Plus Chemotherapy for Acute Myeloid Leukemia With a FLT3 Mutation. *N Engl J Med* (2017) 377:454–64. doi: 10.1056/NEJMoa1614359
17. Zhao J, Song Y, Liu D. Gilteritinib: A Novel FLT3 Inhibitor for Acute Myeloid Leukemia. *Biomark Res* (2019) 7:19. doi: 10.1186/s40364-019-0170-2
18. Chatain N, Perera RC, Rossetti G, Rossa J, Carloni P, Schemionek M, et al. Rare FLT3 Deletion Mutants may Provide Additional Treatment Options to Patients With AML: An Approach to Individualized Medicine. *Leukemia* (2015) 29(12):2434–8. doi: 10.1038/leu.2015.131
19. Shin S-Y, Lee S-T, Park C-H, Kim H-J, Kim S-H. Two Cases of in-Frame Deletion Mutation in Juxtamembrane Domain of the FLT3. *Leuk Lymphoma* (2016) 57(2):486–8. doi: 10.3109/10428194.2015.1065982
20. Young DJ, Nguyen B, Zhu R, Seo J, Li L, Levis MJ, et al. Deletions in FLT-3 Juxtamembrane Domain Define a New Class of Pathogenic Mutations: Case Report and Systematic Analysis. *Blood Adv* (2021) 5:2285–93. doi: 10.1182/bloodadvances.2020002876

Conflict of Interest : AC was employed by Novartis, Pfizer, Abbvie and acted as speaker in Advisory Board for Novartis and Abbvie. CP was employed by Astellas, Amgen and acted as speaker in Advisory Board for Abbvie, Janssen, Novartis, Pfizer and Astellas.

The remaining authors declare that the research was conducted in the absence of any commercial or financial relationships that could be construed as a potential conflict of interest.

Publisher's Note: All claims expressed in this article are solely those of the authors and do not necessarily represent those of their affiliated organizations, or those of the publisher, the editors and the reviewers. Any product that may be evaluated in this article, or claim that may be made by its manufacturer, is not guaranteed or endorsed by the publisher.

frontiers in Oncology

REVIEW
published: 06 October 2021
doi: 10.3389/fonc.2021.752192

From Biology to Clinical Practice: Iron Chelation Therapy With Deferasirox

Giuseppe A. Palumbo[1], Sara Galimberti[2], Wilma Barcellini[3], Daniela Cilloni[4], Nicola Di Renzo[5], Elena Maria Elli[6], Carlo Finelli[7], Luca Maurillo[8], Alessandra Ricco[9], Pellegrino Musto[9,10], Rodolfo Russo[11] and Roberto Latagliata[12]*

[1] Department of Scienze Mediche Chirurgiche e Tecnologie Avanzate "G.F. Ingrassia," University of Catania, Catania, Italy, [2] Section of Hematology, Department of Clinical and Experimental Medicine, University of Pisa, Pisa, Italy, [3] Hematology, Fondazione Istituto di Ricovero e Cura a Carattere Scientifico (IRCCS) Ca' Granda Ospedale Maggiore Policlinico di Milano and University of Milan, Milan, Italy, [4] Department of Clinical and Biological Sciences, University of Turin, Turin, Italy, [5] Hematology and Transplant Unit, Ospedale Vito Fazzi, Lecce, Italy, [6] Division of Hematology and Bone Marrow Unit, Ospedale San Gerardo, Aziende Socio Sanitarie Territoriali (ASST), Monza, Italy, [7] IRCCS Azienda Ospedaliero-Universitaria di Bologna, Istituto di Ematologia "Seràgnoli", Bologna, Italy, [8] Department of Onco-hematology, Fondazione Policlinico Tor Vergata, Rome, Italy, [9] Unit of Hematology and Stem Cell Transplantation, Azienda Ospedaliera Universitaria (AOU) Consorziale Policlinico, Bari, Italy, [10] Department of Emergency and Organ Transplantation, "Aldo Moro" University School of Medicine, Bari, Italy, [11] Clinica Nefrologica, Dialisi e Trapianto, Department of Integrated Medicine with the Territory, IRCCS Ospedale Policlinico San Martino, Genoa, Italy, [12] Unità Operativa Complessa (UOC) Ematologia, Ospedale Belcolle, Viterbo and Division of Cellular Biotechnology and Hematology, Sapienza University, Rome, Italy

OPEN ACCESS

Edited by:
Mohamed A. Yassin, Hamad Medical Corporation, Qatar

Reviewed by:
Yasser Wali, Sultan Qaboos University, Oman
Heather Leitch, St. Paul's Hospital, Canada
Mervat Mattar, Cairo University, Egypt

***Correspondence:**
Giuseppe A. Palumbo
palumbo.ga@gmail.com

Specialty section:
This article was submitted to Hematologic Malignancies, a section of the journal Frontiers in Oncology

Received: *02 August 2021*
Accepted: *08 September 2021*
Published: *06 October 2021*

Citation:
Palumbo GA, Galimberti S, Barcellini W, Cilloni D, Di Renzo N, Elli EM, Finelli C, Maurillo L, Ricco A, Musto P, Russo R and Latagliata R (2021) From Biology to Clinical Practice: Iron Chelation Therapy With Deferasirox. Front. Oncol. 11:752192. doi: 10.3389/fonc.2021.752192

Iron chelation therapy (ICT) has become a mainstay in heavily transfused hematological patients, with the aim to reduce iron overload (IOL) and prevent organ damage. This therapeutic approach is already widely used in thalassemic patients and in low-risk Myelodysplastic Syndrome (MDS) patients. More recently, ICT has been proposed for high-risk MDS, especially when an allogeneic bone marrow transplantation has been planned. Furthermore, other hematological and hereditary disorders, characterized by considerable transfusion support to manage anemia, could benefit from this therapy. Meanwhile, data accumulated on how iron toxicity could exacerbate anemia and other clinical comorbidities due to oxidative stress radical oxygen species (ROS) mediated by free iron species. Taking all into consideration, together with the availability of approved oral iron chelators, we envision a larger use of ICT in the near future. The aim of this review is to better identify those non-thalassemic patients who can benefit from ICT and give practical tips for management of this therapeutic strategy.

Keywords: iron chelation therapy (ICT), deferasirox, myelodysplastic syndromes (MDS), myelofibrosis (MF), radical oxygen species (ROS), iron toxicity, anemia

INTRODUCTION

Iron chelation therapy (ICT) has become a mainstay in heavily transfused hematological patients, with the aim to reduce iron overload (IOL) and prevent organ damage. International and Italian guidelines recommend ICT in low-risk Myelodysplastic Syndrome (MDS) patients (1). ICT should also be considered for transfusion-dependent patients with high-risk disease, when they are

responding to therapies able to modify their life expectancy or if they are candidate for an allogeneic stem cell transplantation (HSCT) in their therapeutic program (2, 3).

Considering hematological and hereditary disorders, characterized by considerable transfusion support to manage anemia, consequent iron toxicity contributes to exacerbate anemia and other clinical comorbidities due to oxidative stress radical oxygen species (ROS) mediated by free iron species. Therefore, ICT has been introduced in the last years also in these additional categories of patients recognizing the importance of this therapy beyond the supportive aim, to counteract iron toxicity itself.

Approved iron chelators in the abovementioned diseases are deferoxamine (subcutaneous route) and deferasirox (oral administration). Unlike thalassemic patients, in whom it should be continued indefinitely, in patients with MDS and other hematological conditions, ICT can usually be continued until resolution of transfusion dependency and/or normalization of iron toxicity available markers (4–8).

THE CURRENT ROLE OF IRON CHELATION THERAPY IN MYELODYSPLASTIC SYNDROMES

Why to Use ICT in Patients With MDS?

Mechanisms That Can Favor Iron Toxicity in Patients With MDS

MDSs belong to a family of clonal dysfunctions of the hematopoietic system, which result in failure of bone marrow hematopoiesis (ineffective hematopoiesis) and in an increased risk of progression to acute myeloid leukemia (AML). A common complication observed in these anemic patients is iron toxicity, which not only causes organ damage in liver, heart, and endocrine glands but also has toxic effects on the bone marrow niche, favoring ineffective hematopoiesis, genomic instability, and eventual clonal evolution towards acute leukemia, with consequent negative implications for survival and quality of life (9, 10).

Dyserythropoiesis affects the regulation of iron homeostasis, favoring increased intestinal absorption and plasma recirculation. In this setting, the two key factors involved in the mechanisms triggered by ineffective erythropoiesis are

- hepcidin, whose generally decreased levels vary in the different forms of MDS, with lower values observed in lower-risk MDS and higher values in higher-risk MDS and in chronic myelomonocytic leukemia (CMML) (11)
- hypoxia, which increases the expression of DMT1, DCYTB, and FPN in the enterocytes, the epithelial cells that form the epithelial lining of the intestinal villi, resulting in increased intestinal iron absorption (12).

These pathological iron load mechanisms are active regardless of the need for transfusions, although transfusion support considerably worsens this pre-existing overload (9, 13–15). Indeed, each unit of packed red cells contains 200–250 mg of iron (approximately 100 times the normal daily intake). Moreover, at diagnosis 80% of patients with MDS present already anemia due to ineffective erythropoiesis and requiring blood transfusions (16–18). Consequently, it is very common that chronic transfusion-dependent patients will develop IOL.

Definition of a Genetic Profile Predisposing for Iron Overload

Different gene mutations and/or alterations that have a direct effect on iron metabolism and accumulation have been reported in certain forms of MDS. These include the following:

- SF3B1 mutations: these mutations, frequently observed in MDS patients and especially when ring sideroblasts (RS) are present, dysregulate the RNA splicing of the erythroid transcription factors TAL1 and GATA1, resulting in increased but ineffective erythropoiesis (19). SF3B1-mutated patients present mitochondrial iron accumulation (20) and increased expression of a specific isoform of SLC25A37 (an important transporter of Fe(2+) into the mitochondria) (21). Splicing alterations have been observed in the key genes associated with iron accumulation.
- 5q deletion: this karyotypic alteration results in considerable ineffective erythropoiesis associated with the heterozygous deletion of RPS14. RPS14 haploinsufficiency activates the innate immune system and increases the expression of S100A8-S100A9, resulting in p53-dependent erythroid differentiation defects (22).
- TET2 mutations: (only in a subset of patients with MDS) may be involved in iron metabolism and in heme biosynthesis in the erythroblasts. Studies using TET2 knockdown mouse models have shown high serum and mitochondrial ferritin levels and dysregulation in a number of genes involved in iron metabolism (23).

Diagnostic Workup for Iron Toxicity in Patients With MDS

The approaches currently employed to diagnose iron overload include

- estimate iron intake following transfusions;
- serum ferritin and transferrin saturation measurements (blood ferritin levels must be monitored monthly, whereas follow-up monitoring of the parameter trends should be performed every 3–6 months);
- magnetic resonance imaging (MRI) of liver, pancreas and heart evaluation when available
- morphological evaluation of bone marrow iron by Perls staining.

Serum ferritin is an indirect and unreliable measurement of the entity of iron deposits in the body; although there is no validated threshold, as for other conditions such as thalassemia,

experts consider a ferritin level >1,000 ng/ml to be suggestive of IOL and suggest serial/periodic evaluation of ferritin to evaluate trends instead of absolute values. However, as high ferritin levels may be secondary to an inflammatory state regardless of iron burden, it is always advisable to assess ferritin trends and transferrin saturation suggesting the presence of unbound iron that is harmful for several organs (24).

Transferrin saturation values >60–70% are correlated with free iron in plasma as non-transferrin-bound iron (NTBI) (5, 25–27). A subcomponent of NTBI, called labile plasma iron (LPI), is a potent redox-active form capable of permeating cells through free cellular ionic channels, inducing enlargement of the amount of labile cellular iron (LCI) that in turns leads to increased levels of intracellular ROS. The consequent intracellular oxidative stress condition cause iron-related cellular damages or even cellular death (10).

Unfortunately, at the time being, measurements of NTBI and LPI are not yet standardized methods, available only in selected research laboratories.

Lower-Risk MDS Patients: How and When to Chelate

When to Start Iron Chelation Therapy

Current guidelines (SIE, ELN, NCCN) (2, 28, 29) consider the following parameters as criteria for the initiation of ICT in patients with lower-risk MDS:

- Transfusion dependency (with transfusion burden of at least 20 units of packed red cells).
- Ferritin level >1,000 ng/ml.
- Life expectancy >12–24 months.
- When the chosen drug is deferasirox, CrCl has to be >60 ml/min; the starting dose of deferasirox is usually 7 mg/kg for the new formulation.

Evidence of oxidative stress due to iron-induced ROS before the conventional limit of 20 transfused units might lead to review current indications for early starting ICT providing a better tolerated lower-dose treatment (for deferasirox, 3.5 mg/kg) for reducing iron overload and thus ROS overproduction promptly (1).

Hence, it is under discussion the ideal approach to candidate patients which might lead to an expansion of the indications for ICT, including the following:

- Patients with transfusion-dependent MDS (and bone marrow failure in general), regardless of the International Prognostic Scoring System (IPSS) risk level, taking into consideration the presumable life expectancy
- Patients with a transfusion history (even if recently started) and/or ferritin ≥500 ng/ml, in the absence of hepatocellular necrosis and/or inflammation

When to Discontinue Iron Chelation Therapy

Although there is currently a divergent opinion on the optimal duration of ICT, some guidelines (NCCN, ELN) (28, 29) recommend considering therapy interruption when serum ferritin levels are <1,000 ng/ml (whereas in the SmPc for deferasirox, the threshold value is <500 ng/ml). A consensus statement issued by the MDS Foundation Working Group in 2008 suggests continuing therapy for the entire duration of transfusion need (1). With the aim to prevent damage induced by free toxic iron exposure rather than iron bulk, it might be useful to consider not only ferritin values but also transferrin saturation, when considering the possibility of discontinuing the chelation treatment. Although the threshold value of transferrin saturation that protects from organ damage is not yet known, the iron chelation optimal goal should be a normal transferrin saturation value. Finally, when ferritin levels during deferasirox therapy goes below 300 μg/L, a temporary discontinuation should be taken into consideration for a potential toxicity increase of chelation therapy itself.

Clinical Outcomes and Iron Chelation With Deferasirox in Lower-Risk MDS

In **Table 1**, response to chelation treatment, rate of discontinuation, and erythroid response observed in the main studies with DFX in MDS low-risk setting are reported.

Possible Effects of Iron Chelation in Addition to the Decrease in Iron Overload

In MDS patients, when assessing iron-induced damage, changes in the dynamic equilibrium between functional iron pool and deposited iron pool must be considered in addition to tissue iron concentrations.

This deposition results in exposure to iron, which causes organ damage mainly to the heart, blood vessels, and bone marrow, a worsening hematopoiesis, and an enhanced clonal instability.

In MDS, further clinical outcomes are observed during chelation treatment with deferasirox, such as the following:

- *Overall survival (OS).* A number of retrospective studies show that chelated MDS patients have a better median survival than those who are not chelated. This finding was subsequently confirmed by a meta-analysis (eight studies for a total of 1,562 patients), which reported an advantage in terms of survival greater than 61.2 months (38). Although these observations may be partly attributed to selected bias, the finding of a positive effect of ICT on the OS of patients with MDS would appear to be fairly consistent. In addition, a Canadian prospective study that collected data from March 2006 to July 2016 demonstrated the advantage in terms of survival in patients with MDS receiving ICT independently by confounding factors such as age, comorbidities, the Revised International Prognostic Scoring System (R-IPSS), and treatment with disease-modifying drugs (39). An improvement in OS for ICT patients was also evidenced in a propensity-score analysis on transfused lower-risk MDS subjects in the European MDS Registry (40).

  In addition to an increase in OS (133 *versus* 105 months; p=0.009), the IRON2 retrospective study reported a significant increase in cardiac event-free survival (EFS) in the 146 patients who received ICT (of whom 72% treated with

TABLE 1 | Response to chelation treatment, rate of discontinuation, and erythroid response in the main studies with deferasirox in MDS low-risk setting.

	N° Pts	Dosage (mg/kg/day)	Ferritin at baseline, ng/ml (median)	Ferritin at 12th month, ng/ml (median)	p	% stop DFX at 12th month	Erythroid response (%)
EPIC (30)	341	10–30	2,730	1,904	0.002	48.7	22.6
GIMEMA MDS0306 (31)	152	10–20	1,966	1,475	<0.0001	55.2	15.5
GERMAN STUDY (32)	50	20–30	2,447	1,685	0.01	52.0	11.0
US STUDY (33)	176	20	2,771	2,210	<0.001	47.0	15.0
Hematology Sapienza (34)	40	10–30	2,878	1,400	<0.001	40.0	10.0
GROM + Basilicata (35)	118	10–20	1,773	1,300	<0.001	35.0	19.0
GRUPPO CAMPANO (36)	55	10–30	2,362	683	0.001	NR	29
STUDY EXTEND (37)	123	10–20	2,679	2,000	0.0002	37.7	NR
STUDY EXJANGE (37)	44	10–30	2,442	2,077	0.06	29.5	NR

deferasirox) compared to those who did not (137 *versus* 90 months; p=0.004) (41).

Focusing on the clinical outcomes, the results of the TELESTO randomized, double-blind prospective study, which evaluated the effects of treatment with deferasirox *versus* placebo in patients with low-/int-1-risk MDS have been reported. The primary endpoint of the study was EFS: of a total of 225 randomized patients, the group treated with deferasirox showed a median EFS (time to the first adverse event, constituted by clinically significant organ toxicity, including cardiac and hepatic events, evolution to leukemia or death) that was significantly longer than that observed in the placebo arm (1,440 *vs.*1,091 days; risk reduction: 36.4; p=0.015) (**Figure 1**). The use of this molecule is therefore supported in patients with low-/int-1-risk MDS with iron overload (42).

- *Evolution to acute leukemia.* Regarding the risk of evolution to leukemia, data are still controversial: preclinical models describe the effect of ICT to reduce genetic instability induced by the greater production of ROS. Indeed, a significant reduction in leukemia-free survival (LFS) has been reported in patients with transfusion-dependent disease (41, 43). The American US22 registry data on 600 patients with transfusion-dependent low-risk MDS [of whom 263 received ICT, the vast majority with deferasirox (44)] provided prospective evidence that ICT has a positive effect. In addition to OS, in this cohort, LFS was also better amongst patients receiving ICT, with a median time to progression of 40.6 *vs* 27.3 months.

Similar results were achieved in an observational study on 97 patients with low-/intermediate-risk MDS, with a trend towards shorter LFS in patients who did not receive ICT: at 30 months,

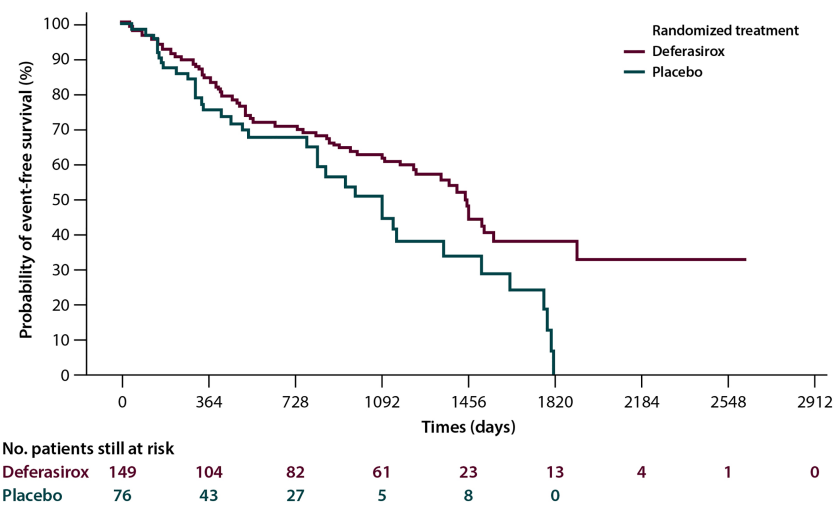

FIGURE 1 | Event-free survival in the Telesto trial according to treatment arm, and 225 myelodysplastic patients were included, 149 in the deferasirox arm and 76 in the placebo one (42).

34% of patients not treated with an iron chelator had progressed to AML *vs* 17% of patients receiving iron chelators (45).

- *Hematological improvement*. In several clinical studies, including the EPIC (Evaluation of Patients' Iron Chelation with Exjade) study, a percentage of patients (10–20%) treated with deferasirox obtained a positive effect on hematopoiesis, with erythroid hematological recovery (30–33), as reported in **Table 1**. Similar results were also observed in Italian and international real-world studies. In the data reported by two Italian regional registries, the Roman Myelodysplasia Group (GROM) and the Basilicata Registry, including a total of 118 patients with transfusion-dependent MDS treated with deferasirox, hematologic improvements in the erythroid, platelet, and neutrophil series were reported in 17.6, 5.9, and 7.1% of cases, respectively (35). In the prospective randomized TELESTO study, 27/127 patients (22.3%) receiving deferasirox obtained hematological improvement; however, it is worth of note that a similar rate of hematological improvement (14/68 patients, 20.6%) was also observed in the placebo arm of the study (42). Although several mechanisms have been postulated, the reduced production of iron-dependent ROS and inhibition of NFk-B activity would appear to be particularly relevant factors (**Figure 2**).

Higher-Risk MDS Patients: How and When to Chelate

According to prognostic scores such as the IPSS, R-IPSS, and WHO Prognostic Scoring System (WPSS), patients with "high-risk" MDS account for 20–30% of the total population. Historically, life expectancy in this group of patients has been reported between 1 and 2 years; however, the introduction of disease-modifying therapies (such as hypomethylating agents) has led to longer survival and better prognosis (16).

The main causes of death in two-thirds of patients with high-risk MDS are strongly correlated with cardiac events and infectious complications (greater risk in transfused patients than in those who do not receive transfusions), at least partly due to the impact of iron-induced toxicity (46).

The main limiting factors to start ICT are the short OS of these patients, the potential higher risk of renal or hepatic impairment and gastrointestinal bleeding.

The data currently available are constituted by a retrospective study on 51 patients with transfusion-dependent intermediate-/high-risk MDS (in 71% azacitidine was co-administered). Treatment with deferasirox in these patients showed a significant clinical benefit in terms of decrease in ferritin levels, liver marker normalization, and (in one case) hematological improvement, without significant additional toxicity (median follow-up was 35.3 months, and median OS 37.5 months) (3). Some registries (US Medicare, SEER) that already reported a higher incidence of infections in transfused than in non-transfused MDS patients (45–47) reported data on deferasirox treatment able to reduce risk of infection in patients more likely suffering these events for iron toxicity exposure due to transfusion. Prospective studies evaluating the combination of azazitidine and deferasirox in HR-MDS are ongoing.

In patients with high-risk MDS, there is also new evidence of a significant effect in terms of genotoxicity accumulation of IOL-induced mutations, which might add a biological strong rationale for the administration of ICT. *In vivo* evidence also shows that oxidative stress may contribute to the hypermethylation of important tumor suppressor genes, suggesting a synergic action of ICT and treatment with hypomethylating agents (48).

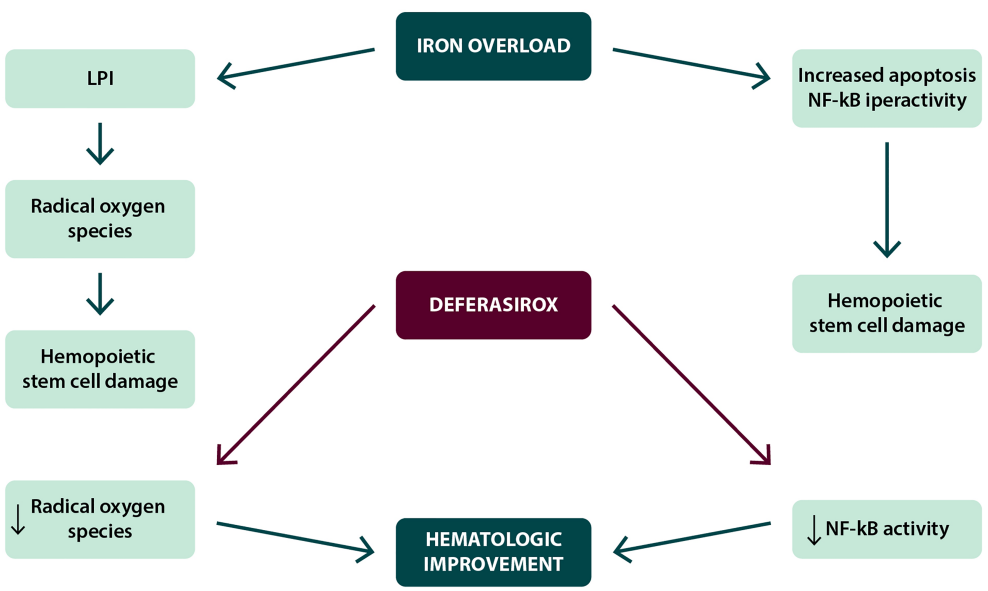

FIGURE 2 | Possible mechanisms in the achievement of hematological improvement during deferasirox treatment.

The ideal candidates for ICT amongst patients with higher-risk MDS are those with a longer life expectancy and more favorable prognostic factors, including

- good general health and age ≤65 years,
- absence of significant comorbidities, and
- patients who are candidates for allogeneic transplantation and/or treatment with demethylating agents.

When to Start Iron Chelation Therapy and When to Discontinue Iron Chelation Therapy

The possible parameters for starting ICT in patients with high-risk MDS are the same as described previously for lower-risk patients. Decisions regarding the duration of the treatment should also be based on the same criteria already described.

Efficacy and Safety of Deferasirox in Patients With MDS: How to Administer Iron Chelation Therapy

How to Measure the Efficacy of Iron Chelation Therapy in Terms of the Reduction in Iron Overload in Patients With MDS

The assessment of the efficacy of the treatment may be based on two types of parameters:

1. Iron toxicity markers
2. Patient clinical outcome

The biochemical and tissue damage markers that indicate a reduction in IOL and constitute the parameters for the administration of deferasirox are

- transferrin saturation,
- serum ferritin,
- aminotransferases (a decrease in aminotransferase with improvement of liver function has been observed in a significant proportion of patients with abnormal values at baseline),
- measurement of labile plasma iron (LPI), where available, and
- T2-weighted MRI (where available).

In the published clinical studies, serum ferritin levels serially measured throughout the observation period were the main used parameters (16, 49).

Clinical outcomes that can be directly measured and therefore compared, alongside cardiac events, infectious complications, and disease progression, were hematologic response rates, in terms of trilinear improvement (erythroid, platelet, and neutrophil compartment). The relationship between these parameters and the reduction in the markers of IOL was significant in some cases, but not in all (46).

Any kind of hematologic responses, which was observed in 20% of patients treated with deferasirox, can be considered an additional clinical benefit constituting a further reason for continuing ICT, and its absence does not constitute an indication for discontinuing treatment and it does not, therefore, represent a criterion for a therapeutic decision-making.

How to Monitor the Safety of the Iron Chelation Therapy

The most important studies in MDS setting reported data on old formulation deferasirox safety profile, and the most common side effects were gastrointestinal (GI) ones due to lactose; in particular, diarrhea, nausea, and abdominal pain could occur. The safety profile of deferasirox's new formulation, now available in film-coated tablets, was studied in ECLIPSE trial: the incidence and type of adverse events (AEs) for the new formulation are similar to the previous one (tablets for oral suspension), whereas the incidence of severe AEs (SAE) is lower (19.5 *versus* 25.6%), especially for GI events such as diarrhea, nausea, and vomiting (50). The study also reports the same similarity also for hepatic and renal safety (the CrCl values to start treatment remained ≥60 ml/min). Patients receiving treatment with deferasirox can be subjected to the same safety monitoring scheme.

Guidance to be Given to Patients on Iron Chelation Therapy

It is essential to provide patients with clear and complete information concerning the main aspects of ICT. These aspects regard

- treatment compliance, which is extremely important for the efficacy of therapy, as the better treatment compliance observed amongst patients treated with the new formulation (92.9 *vs.* 85.3%) coincided with a greater decrease in ferritin levels in this group (median: −14% vs. −4.1%) (50); and
- safety management: it is important to instruct patients how to manage adverse events and eventually refer them promptly to their physician.

Hence, patient education can improve compliance with ICT and reduce the complications associated with IOL (51).

IRON CHELATION THERAPY IN MYELOFIBROSIS AND OTHER CHRONIC ANEMIAS

Pathogenesis and Clinical Significance of Anemia in Myelofibrosis

The Pathogenetic Mechanisms of Anemia in Myelofibrosis

Myelofibrosis (MF) is a rare hematological condition classified in the group of chronic BCR-ABL1- negative myeloproliferative neoplasms (MPN) (52), characterized by bone marrow fibrosis and consequent ineffective hematopoiesis, with the onset of extramedullary hematopoiesis. The signs and symptoms characterizing this condition include

- constitutional symptoms (itching, fever, night sweats and weight loss);
- symptoms associated with splenomegaly;
- symptoms due to anemia (asthenia, dyspnea, palpitations) (53): huge symptom burden, poorer quality of life, and iron

overload associated with transfusion therapy. As bone marrow fibrosis, anemia increases progressively over time from 38% of cases with Hb <10 g/dl at diagnosis to 64% 1 year after diagnosis (54).

Although anemia is caused by bone marrow erythropoietic tissue fibrotic replacement and by ineffective production and maturation of red blood cells generated by a compensatory extramedullary erythropoiesis, these are not the only etiological factors. Other significant pathogenetic mechanisms causing anemia are splenic sequestration and hemodilution, resulting from the increase in plasma volume and abnormal production of bone marrow cytokines. As a consequence, MF is characterized by a considerable local and systemic inflammatory state, with a wide increase of inflammatory bone marrow cytokines, which in turn affect erythropoiesis in the residual functional areas of hematopoietic bone marrow. This pro-inflammatory state includes an increase in circulating hepcidin levels interfering with iron metabolism as observed in other secondary anemias (55).

MF patients present specific genetic changes too likely anemia-related: patients with Calreticulin (CALR) or MPL thrombopoietin receptor (MPL) gene mutations would appear to have a lower likelihood of developing anemia than triple-negative patients (CALR, MPL, and JAK2 wild types), with underlying unknown mechanisms at this time.

The presence of anemia is a negative variable recognized in all the scores that stratify MF patient risk from a prognostic standpoint (56), with a negative impact on life expectancy (by stratifying patients with primary MF according to the degree of anemia, we observe median OS values that range from 7.9 years in patients without anemia to 2.1 years in cases with severe anemia) (57).

Anemia and thrombocytopenia in patients with MF could worsen with treatment with ruxolitinib, the first Janus Kinase 1/2 (JAK) inhibitor approved on the basis of the COMFORT and JUMP study results (58, 59). Ruxolitinib acts directly on the hyperactivation of the JAK-STAT pathway that underlies the disease, by selectively inhibiting the JAK-1 and JAK-2 kinases and suppressing residual bone marrow function (55). The anemia due to ruxolitinib treatment has not to be considered as negative prognostic factor, as it is often transient and does not worsen the patient's overall outcome, unlike pre-existing anemia. Most cases of anemia during ruxolitinib therapy appear within the first 6 months and are Grade 1/2, rarely requiring the discontinuation of therapy. In general, it is advisable to strictly monitor patients during the first weeks of therapy when the Hb levels could decrease rapidly to promptly evaluate the possible transfusion need, before increasing again in the following months, and stabilize on average approximately 10% below the baseline value (60).

The onset of anemia does not reduce the efficacy of ruxolitinib on splenomegaly and symptoms (58, 61), and consequently treatment is strongly recommended in anemic patients too. Similarly, it is not advisable to reduce the dose of ruxolitinib in patients who develop anemia, as this side effect seems not dose-dependent: the treatment should be continued at the doses required to control the disease and established on the basis of the platelet count.

Therefore, three types of patients can be identified:

- Patients who are not transfusion-dependent at baseline
- Patients who are already transfusion-dependent at baseline and who usually remain so throughout treatment
- Patients just above the dependency threshold at baseline, who become transfusion-dependent after therapy (these borderline patients can be the most difficult to manage, as they are not used to receiving transfusion support)

Iron Toxicity and Transfusion Need in Myelofibrosis

The Pathogenic Mechanisms of Oxidative Stress Iron-Mediated in Myelofibrosis and Organ Toxicity

The main treatment for anemia consists of RBC transfusions: approximately a quarter of patients with MF are transfusion-dependent at diagnosis (when dependency is defined as the administration of >6 units of RBC over a period of 12 weeks for Hb levels <8.5 g/dl), and many more become so during the course of their illness (55).

In patients with MF, characterized by a significant pro-inflammatory state, hepcidin levels are usually higher, with a consequent unbalance of iron metabolism and showing a negative prognostic value (62).

Although the vascular effects of free iron species have been less extensively studied, it has been observed that high circulating iron levels can worsen the atherosclerotic phenotype, especially in elderly patients: the macrophages on the vessel wall accumulate the iron produced by the increased destruction of red blood cells and abnormal iron homeostasis, with an increase in the production of ROS and decreased cholesterol outflow. The resulting oxidative stress promotes the formation of foamy cells, inflammation, apoptosis, and the deterioration of the atherosclerotic plaque. Furthermore, the high hepcidin levels typical of MF contribute to this process by blocking ferroportin and, therefore, the exportation of iron from plaque (63).

ICT can have a beneficial effect on iron-mediated endothelial dysfunction, because the binding of the labile cell iron in the vessel wall may reduce the formation of ROS and the inactivation of nitric oxide, another consequence of iron-induced toxicity. It was observed that deferasirox can significantly improve the dilation of the brachial artery and reduce carotid artery stiffness in patients with beta-thalassemia (64).

In bone marrow, IOL and the consequent oxidative stress cause an increase of genetic instability of the hematopoietic cells and the production of pro-inflammatory cytokines by bone marrow stromal cells that, in turn, may play a role on bone marrow failure in patients with MF, as it was reported in MDS (15). However, iron-induced toxicity and its negative impact on the hematopoietic microenvironment (65) might have an impact on the dysregulation of the JAK-STAT pathway itself, which is able to induce an increase in pro-inflammatory and fibrogenic cytokines and increased ROS production. In addition, patients with MF present significant NF-kB pathway activation, which

induces the production of inflammatory cytokines (IL6, TNFα) and interacts with the dysregulation of the JAK-STAT pathway to amplify the oxidative damage (66, 67).

Assessment and Monitoring of Iron-Induced Toxicity in Patients With Myelofibrosis

As for other conditions ferritin remains the main parameter for the evaluation of IOL although relatively less reliable in MF, due to inflammatory state. In these patients, therefore, a more significant role is played by transferrin saturation (marker of free iron release, which causes organ damage), and it should be tested together with ferritin level trends at the onset of the disease.

The role of imaging techniques (T2-weighted MRI) in patients with MF is more controversial, due both to the difficulties in distinguishing between fibrosis-induced organ damage and iron-induced toxicity and because toxic iron-induced damage and exposure to ROS may clinically occur even before iron accumulation will be evident in the hepatocytes and myocardial cells.

Iron Chelation Therapy and Myelofibrosis: Iron Chelation Response

Impact of Deferasirox Treatment in Reducing Ferritin and Inducing Erythroid Response in Transfusion-Dependent Myelofibrosis

Although the observation of potentially harmful iron-induced toxicity has suggested the utility of ICT in MF in the management of anemia, the clinical evidence regarding the use of iron-chelating agents is still limited. In fact, only single case reports regarding the use of ICT in MF were available until few years ago. Recently the results of two Italian multicenter studies became available with the following results (**Table 2**):

- 45 patients with primary MF or Post Polycythemia Vera MF (PPV-MF)/Post Essential Thrombocythemia MF (PET-MF) treated between 2010 and 2018 in the Lombardy Hematological Network (IRON-M Study) (68)
- 48 patients with primary MF or PPV-MF/PET-MF treated by the Lazio Group (69)

These two studies report the impact of treatment with deferasirox in terms of induction of iron chelation response (ICR) and erythroid response. Based on these data, an ICR was obtained with deferasirox in approximately 30–40% of patients with MF, whereas complete or partial hematological response (usually not accompanied by an increase in platelets and neutrophils) was observed in 20–40% of cases.

The results show that in both studies, patients who obtained an ICR experienced a progressive reduction in ferritin levels at 6, 12, and 18 months, compared to non-responders (68). As regards the identification of factors predictive of an ICR to deferasirox, in the study by Elli et al. (68), patients who obtained efficacious ICR presented statistically lower ferritin levels at baseline than non-responders. Similarly, the median number of prior transfusions and the duration of the history of transfusion dependence were statistically lower/shorter amongst responders. These data highlight that an earlier access to iron chelation therapy constitutes an advantage in terms of efficacious iron chelation. On the other hand, other than the statistically significant relationship between the achievement of ICR and the obtainment of hematological improvement, it was not possible to identify factors predictive of hematological response (68).

The achievement of ICR, defined both by reduction in ferritin levels and by prolonged OS, are closely related in patients with MF treated with deferasirox (69): 2-years OS after the start of treatment was 100% in patients who responded to the ICT, compared to 70% in patients who did not experience a reduction in ferritin levels (68) (95% CI: 46.5–84.8%, p=0.007). In patients who presented a reduction in ferritin levels, median survival from the start of therapy with deferasirox was 61.0 months (95% CI: 18.4–103.6) compared to 15.8 months (95% CI: 5.9–25.6) in patients who did not respond to the ICT (p=0.001) (69). Therefore, by reducing the IOL, treatment with deferasirox seems to provide a significant advantage in terms of the survival in patients with MF. The rate of leukemia evolution or

TABLE 2 | Iron chelation efficacy and erythroid responses during deferasirox treatment in myelofibrosis patients.

Institution	Lombardy Hematological Network (68) (*)	Lazio Group (69) (**)
Evaluable patients	41/45 pts	47/48 pts
Median duration of treatment	17.2 months (IR 3–59.5)	27.6 months
Iron chelating response (ICR)	Ferritin <1,000 ng/ml or ≥50% decrease of baseline ferritin: 29.3% (12 pts) No response: 70.7% (29 pts)	Global response: 41% (19 pts) of which: • Ferritin <500 ng/ml: 5 pts • Ferritin <1,000 ng/ml: 11 pts • ≥50% decrease of baseline ferritin but with ferritin level >1,000 ng/ml: 3 pts No response: 59% (28 pts)
Erythroid responses (ER)	17% (7 pts)	12,8%
• Transfusion independence	26.9% (11 pts)	6.4%
• ↑Hb ≥1,5 g/dl or decrease ≥50% of transfusional rate	56.1% (23 pts)	80.8%
• No response		
Median time to ER	2.4 months (IR 1–8.5)	6.3 months (IR 4.3–12.1)

(*) starting dose 750 mg/day (10 mg/kg/day); (**): Starting dose 20 mg/kg in 23 patients, 15 mg/kg in 20 patients, and 10 mg/kg in 5 patients.
IR, interquartile; pts, patients.

progression disease seems to be lower in ICR group, with a better 2-year leukemia free survival (LFS, p=0.039) (68), but this result needs to be confirmed in a larger and prospective cohort.

Patients with MF in Whom There is an Indication for Initiating Iron Chelation Therapy

The data currently available allow us to identify the eligible patient profile for ICT, for subjects with a life expectancy >6 months:

1. Patients with anemia not treated with ruxolitinib, when they become transfusion-dependent
2. Patients with transfusion-dependent anemia and significant symptoms and/or splenomegaly who start treatment with ruxolitinib, whose IOL is already significant at the start of therapy and will probably increase after the administration of ruxolitinib itself, as transfusion needs will increase
3. Transfusion-dependent anemic patients with an indication for HSCT, who require ICT in preparation for the transplant procedure

On the contrary, in non-anemic MF patients and who develop transfusion dependency in the early months after starting of ruxolitinib, the administration of an iron chelator may not be necessary due to the likelihood of Hb level recovery.

When a Patient With MF Treated With Deferasirox Must Be Considered a Responder

ICR to deferasirox is usually evaluated by taking into account ferritin value trends compared to the baseline. In the absence of standardized response criteria, ferritin levels <1,000 ng/ml or <500 ng/ml can be considered indicative of the achievement of ICR, as can a ≥50% decrease in ferritin levels compared to the baseline, regardless of the final levels.

As mentioned previously, given the inflammatory nature of the condition, although on the one hand these values are sufficient for MDS, they would appear to be less conclusive in patients with MF. Transferrin saturation rate could represent a more reliable marker of chelation efficacy useful also as markers of iron toxicity and ROS-induced damage; a threshold of 70% might be considered for this evaluation.

Safety Profile of Deferasirox in Myelofibrosis

Treatment with deferasirox in patients with MF can be associated with the onset of extra-hematological adverse events (AEs), which are primarily constituted by renal impairment: 17.7% (70), hepatic impairment: 8.9% (68), gastrointestinal symptoms: 11.1–21.4% (68, 69), and skin reactions: 6.7–7.2% (68, 69). Overall, a definitive discontinuation of ICT secondary to toxicity of grade ≥2 of DFX was reported in about a quarter of patients. Of note, no difference in term of number of AEs was seen between ICR and no ICR group; among the patients achieving ICR, no grade 3–4 toxicity was reported (68).

Therapies for Myelofibrosis and Iron Chelation

Clinical Evidence Regarding Ruxolitinib-Deferasirox Combinations

In recent years the advent of the specific JAK-1/JAK-2 inhibitor ruxolitinib represented the only real innovation in the treatment of MF. The use of concomitant therapy with deferasirox in MF patients treated with ruxolitinib would appear based on a clinical need and a strong biological rationale (both drugs work synergically by reducing the oxidative damage in the bone marrow and interacting with the NF-kB and JAK-STAT pathways). The limited evidence currently available (70) suggests that this combination is feasible in terms of tolerability and efficacious in reducing iron overload.

Iron-Induced Toxicity, Transfusion Requirements, and Iron Chelation Therapy in Patients With Aplastic Anemia and Other Chronic Anemias

Utility of Iron Chelation in Aplastic Anemia

Aplastic anemia (AA), a rare blood disorder, is considered the paradigm of bone marrow failure (BMF) syndromes. The disease is caused by an aberrant immune response, which causes the oligoclonal expansion of cytotoxic T cells, resulting in the destruction of haemopoietic stem cells (71). Clinically, it results in different grade pancytopenia (AA classified as "severe," "very severe," or "not severe" depending on bone marrow cellularity and peripheral cytopenia status).

Current treatment for AA (indicated in cases that are severe, very severe, or become transfusion-dependent) is based on allogeneic stem cell transplantation (in eligible patients) and on immunosuppressive therapy [cyclosporine, anti-thymocyte globulin (ATG)]. Patients who are not eligible due to old age or comorbidities and those who do not obtain clinical response can be managed with supportive care that includes the use of growth factors, antibiotic treatments, and transfusion therapy (54).

IOL, defined as a ferritin value >1,000 ng/ml, is present in almost 20% of patients who receive transfusions and in 6% of non-transfused patients (72). In a *post-hoc* analysis of the EPIC study, patients with AA were seen to have had an average of between 8 and 15 transfusion sessions in the previous year, and their median ferritin levels were 3,600–3,700 ng/ml (73). Using imaging techniques (MRI), IOL was observed in the liver in 76.4% of patients (including AA) and in the heart in 19.2% (74). The presence of an IOL in patients with severe AA reduces the efficacy of the immunosuppressive therapy and increases the risk of a relapse, confirming that it is a negative prognostic factor for the outcome of these patients (75).

Therefore, in AA there is a significant incidence of IOL, and its negative impact on clinical outcomes constitutes the rationale for using ICT in this setting. Furthermore, high ferritin levels might have a negative impact on the response to therapy and on the risk of toxicity in patients with AA undergoing a HSCT (76).

At the current time, there are no specific standardized criteria for starting ICT in patients with AA. The serum ferritin threshold value >1,000 ng/ml can be used as a rule of thumb (75, 77–80).

The EPIC prospective study evaluated the efficacy and safety of ICT with deferasirox in 116 patients with AA (74). The analysis showed that therapy with deferasirox efficaciously reduced median serum ferritin levels: this efficacy was associated with the transfusional iron load and the dose of

deferasirox, with higher doses of medicinal product needed to reduce the iron load in subjects with a high intake (79).

In patients with AA, as in other blood disorders, IOL is associated with the observation of hematological response in patients that became transfusion-independent (73). In an Italian multicenter prospective study (81), hematological responses were observed with transfusion independence, associated with a significant increase in platelets, in a cohort of eight patients with AA treated with deferasirox in a real-life setting.

Other Types of Anemia in Which Iron Overload Occurs Regardless of the Transfusion Load

IOL is a common complication in patients with congenital hemolytic anemias (CHAs), a heterogeneous group of disorders that include hereditary spherocytosis, G6PD deficiency, and pyruvate-kinase (PK) deficiency. These patients can experience an IOL regardless of transfusion therapy due to the hyperhemolysis caused by the hereditary deficiency, as demonstrated by MRI evaluation that showed IOL also reported in patients with ferritin levels <1,000 ng/ml (82). In patients with PK deficiency who do not have regular transfusions, a total prevalence of IOL (based on ferritin values) of 38% was observed, which increases (to 82%) when MRI is used as the detection technique.

In an analysis conducted on a population of 37 cases of CHAs (26), the presence of IOL was seen to be common in patients with congenital hemolytic anemias, especially in those with PK deficiency and with congenital dyserythropoietic anemia type II (CDAII), who presented particularly high ferritin and transferrin saturation levels, even regardless of transfusion dependency. Moreover, hepatic iron overload (LIC) was observed in patients with not excessively high ferritin levels also in this study.

A specific sub-analysis of the EPIC study on a total population of 57 patients including 23 cases of hemolytic anemia (of which five cases of PK deficiency, two cases of congenital erythropoietic protoporphyria, and one patient with hereditary hemolytic anemia) showed efficacy of deferasirox in decreasing median serum ferritin levels (−617 ng/ml at 1 year), confirming the durable response after 1 year of treatment, regardless of the underlying pathogenic mechanisms (83).

MANAGEMENT OF SIDE EFFECTS AND COMORBIDITIES

Frailty of Elderly Hematological Oncology Patients and Comorbidities

When considering a new treatment approach, it is important to consider the patient age, which is often high, and the likely presence of comorbidities; the latter must not be seen as a contraindication for ICT, rather a supplementary factor to be taken into consideration in order to support its indication. Iron-mediated toxicity caused by excess free iron can even worsen an existing dysfunction or result in the emergence of concomitant subclinical conditions.

Impact of Iron-Induced Toxicity on Renal Function

Impaired renal function is closely correlated to the age of the patient; over 40 years of age, 2/3 of the population present a progressive decrease in glomerular filtration rate (especially in males) (84). Changes in renal function are therefore more common in elderly patients and cardiac, hepatic or metabolic comorbidities (85).

The concomitant presence of anemia, hypoxia, and iron overload may impair the kidneys, especially in the tubular region. Moreover, these factors can cause oxidative stress in the tubular cells responsible for the resorption of water and solutes, which have a consistent ATP-dependent metabolic activity, with consequent histological and functional damage that, in turn, results in increased urinary excretion of certain solutes, including albumin, proteins, potassium, uric acid, calcium, phosphorus and bicarbonate. This excretion inevitably leads to conditions such as metabolic acidosis, bone changes, and kidney stones (85–91).

Chelation agents such as deferoxamine and deferasirox are thought to be responsible for the onset of renal changes and, in a small percentage of cases, also for severe forms of acute renal impairment, although the pathogenetic mechanism of this effect is still unclear. The onset of Fanconi syndrome (generalized proximal convoluted tubule defect) has also been observed, associated, not necessarily concomitantly, with polyuria, proteinuria, hypouricemia, hypopotassemia, hypercalciuria, hypophosphatemia, metabolic acidosis (caused by decreased bicarbonate resorption), and bone demineralization (due to the buffer effect of bone that binds with the acids) (92, 93).

As demonstrated by pivotal clinical studies on the use of deferasirox (94–96), up to one-third of cases present renal function changes, most of which are mild and within range of normality. These changes should not be considered clinically significant, as they are slight, non-progressive fluctuations in creatinine levels, with a less than 33% increase compared to the baseline, reversible (in most cases), and transient. In the GIMEMA MDS0306 study (31) just one in 15 cases of renal function changes was grade 3. In most cases, the change in renal function resolves spontaneously.

IOL leads to kidney injury secondary to oxidative stress. However, iron constitutes an important co-factor in prostaglandin synthesis and in the production of ATP in the kidney tubule cells by the mitochondria (85). This results in decreased sodium and chlorine resorption localized in the proximal convoluted tubules, which in turn causes increased resorption of both electrolytes in the distal portion of the tubules (macula densa) anatomically adjacent to the glomerulus. This process transmits a vasoconstriction signal to the afferent arteriole of the glomerulus, triggering a reduction in glomerular filtration (tubuloglomerular feedback).

The decreased levels of prostaglandins, caused by the lack of production, induce vasoconstriction on the afferent arteriole that leads to the impairment of glomerular blood flow. This results in a reduction in glomerular filtration rate that, together with renal flow, normalizes when treatment is discontinued, even after 2 years of treatment (97, 98). When the benefits of the treatment are

considered to outweigh the risks associated with the increase in creatinine (which is non-progressive and lower than 33% compared to the baseline) and/or proteinuria (values lower than 0.5 g/24 h), it is possible to continue treatment with deferasirox without dose adjustments.

All patients should then undergo (also with the aid of a nephrology specialist) renal function laboratory monitoring, including assessments of glomerular and tubular function.

When changes in renal function in patients with chronic anemia eligible for ICT are observed, it is necessary to consider all factors potentially responsible for renal injury as

- anemia;
- IOL;
- viral infections (HBV, HCV, HIV);
- comorbidities (heart and liver disease, diabetes mellitus, arterial hypertension, dyslipidemia);
- smoking habits; and
- patients, especially elderly ones, who are co-administered nephrotoxic drugs (non-steroidal analgesics, antibiotics, proton pump inhibitors, and allopurinol) (99, 100).

How to Monitor Renal Function at the Start of and During Therapy With Deferasirox

In patients with IOL (regardless of treatment with deferasirox), it is important to monitor renal function by taking into consideration factors such as:

- albumin-to-creatinine ratio,
- protein-to-creatinine ratio.

Both tests are simple to perform on the first morning urine sample of the day, and the results correlate with those over 24 h.

Other important, but less extensively studied, aspects are

- tubular function and
- venous blood gas analysis (to identify states of metabolic acidosis).

Table 3 provides a possible monitoring schedule during treatment with deferasirox.

Hepatic Comorbidities and Iron Chelation

The presence of hepatic comorbidities needs to be carefully considered for appropriate multidisciplinary management: the free iron can lead to functional changes in liver parenchyma that, if not appropriately managed, can result in cirrhosis and liver cancer.

Treatment with deferasirox is not recommended in patients with severe hepatic impairment (Child-Pugh class C), whereas for Child-Pugh class B patients, who present moderate hepatic impairment, the dose should be considerably decreased and progressively increased if needed. However, baseline hypertransaminase should not be considered an absolute contraindication to start therapy, as it may be sign of iron-induced toxicity that will be reduced by ICT (101, 102). For a correct management of hepatic enzymes, it is important to perform baseline tests and constant monitoring of AST/ALT, bilirubin and alkaline phosphatase, and of the transfusion burden (main cause of transaminase elevation, which conditions the adjustment of the dose of iron chelator). In order to identify the cause of the liver disease, it is therefore essential to work closely with a hepatology specialist.

The Role of T2-Weighted MRI in Establishing the Relationship Between Liver Disease and Iron Overload

MRI and the transverse relaxation rate (R2*) are non-invasive methods for a quantitative assessment of the iron content of almost the whole organ, unlike biopsy. While these methods are well established in thalassemic patients, the use of MRI in transfusion-dependent patients is increasing in recent years (103, 104). This can be limited by the fact that most of transfusion-dependent patients are elderly ones, in whom the organ damage may occur even before iron accumulates in liver and heart cells; this may correlate with higher mortality in this group of patients (105). A recently published Italian cooperative study (MIOMED) well demonstrated the fundamental role of T2*-MRI in detecting IOL: amongst 50 patients affected by low-/intermediate-1 MDS, 13 showed a hepatic and 13 a cardiac IOL. The hepatic involvement was significantly conditioned by transfusion load that, at the contrary, did not influence the cardiac status. When patients were prospectively evaluated,

TABLE 3 | Optimum renal monitoring schedule.

Tests	Baseline	First months	First 6 months	Every 6 months
Nephrology consultation	X			
General functional markers:				
■ Creatinine	X	X	X	X
■ Urinalysis	X	X (every week for first month)	X	X
■ Cystatin C	X			X
■ Urinary protein/creatinine ratio (mg/g)	X		X (every month for 6 months)	X
Markers of glomerular function:	X		X (every month for 6 months)	X
■ Urinary albumin/creatinine ratio (mg/g)				X
Markers of tubular function:				
■ Urinary Beta2-microglobulin/creatinine ratio (mcg/g)	X			X
■ Urinary calcium/creatinine ratio (mg/g)	X			X
■ Urinary phosphorus/creatinine ratio (mg/g)	X			X
■ Urinary NGAL/creatinine ratio (mcg/g)	X			X
■ Venous blood gas analysis	X			X

after 12 months two (non-chelated) developed hepatic IO and other two heart damage (106).

Patients on Polytherapy: The Most Common Pharmacological Interactions With Deferasirox

The Clinical Role of and Rationale for Plasma Deferasirox Testing

From a pharmacokinetic standpoint, deferasirox is characterized by a somewhat reduced volume of distribution, circulation that is 99% bound to serum proteins, especially albumin, metabolism that occurs largely by UGT1A1-mediated glucuronidation (and 8% in the liver by cytochromes), and fecal elimination (107).

It has been observed (108, 109) that the plasma levels of deferasirox are closely influenced by different polymorphisms, such as the levels of enzymes involved in the metabolism of the medicinal product and of efflux pumps (UTG1A1, CYP1A1, CYP1A2, CYP2D6, ABCG2), which therefore directly influence the safety and efficacy profile of the medicinal product. For example, toxicity in patients with homozygosity for UGT1A1*6 is some 14 times greater than wild-type patients.

Given the number of genes involved, typing is challenging in clinical practice; this difficulty also regards hepatic transporters like MRP2, involved in the biliary excretion of the medicinal product, whose polymorphisms can increase hepatotoxicity seven-fold (108).

One solution could be to test plasma deferasirox levels, although this approach is not currently used in clinical practice.

Products That May Interact With Deferasirox

For patients with MF and MDS, concomitant use of medicinal products is an important issue. As mentioned previously, great care is required when using medicinal products such as non-steroidal anti-inflammatory drugs (NSAIDs) and angiotensin converting enzyme (ACE) inhibitors, whereas there is no literature evidence available for other interactions, such as deferasirox + erythropoietin, lenalidomide, and demethylating agents (azacitidine and decitabine).

In literature, there are comforting data regarding the synergistic use of deferasirox with other medicinal products: for example, the use of this treatment with anti-leukemia therapy would appear to improve its efficacy.

In patients with MDS on treatment with demethylating agents, which have an epigenetic effect, deferasirox has been reported to be additive or synergistic with azacitidine and decitabine (an association that reduces proliferation, increases apoptosis, and halts the cell cycle in leukemia cell lines and has a more potent effect than the individual products) (110). Moreover, treatment with deferasirox results in the upregulation of the HJV gene that encodes for hemojuvelin, suggesting that deferasirox might play a role in the demethylation of certain agents together with decitabine (110).

The other therapeutic effects of deferasirox regard the upregulation of TP53 oncosuppressor gene expression (111) and reduction in the outflow proteins, such as the P-glycoprotein, the levels of which are increased by iron through the production of ROS, which decreases after treatment with deferasirox and increases the efficacy of chemotherapy agents (112).

Synergistic use of deferasirox and eltrombopag increases the mobilization of cell iron by the latter, which acts as a shuttle that removes the iron present in the tissues and rapidly transfers it to the former (113, 114).

In patients undergoing HSCT, special attention must be dedicated to busulfan and specific inhibitors (ibrutinib, ruxolitinib), as concomitant use with deferasirox can increase the plasma levels of these agents.

CONCLUSIONS

In patients with MF and MDS, but also with AA and hemolytic anemias, the prognosis is not merely associated with individual factors such as age, comorbidities, or underlying condition, but also with complications associated with the degree of cytopenia present (severity of anemia, hemorrhages, and infections) and the treatment that they receive (blood transfusions, allogeneic transplants, etc.). In these patients, any therapeutic interventions should also face not only the management of comorbidities but also complications caused by the evolution of disease and adverse effects of primary treatments.

The excess iron, associated with direct and indirect toxicity on the various tissues, leads to a worsening in age-related comorbidities, ultimately resulting in cumulative organ damage. Iron-induced toxicity also affects the evolution of the MDS or MF, by increasing cellular genomic instability and altering the bone marrow stroma through the oxidative stress, thus favoring progression to acute leukemia (15, 65).

The performance of a multidisciplinary evaluation of patients treated with deferasirox, at baseline and during follow-up, makes it possible to improve the therapeutic approach and optimally manage elderly patients with MF and MDS, consequently avoiding the need to discontinue specific therapy and reducing the risk of developing organ damage.

AUTHOR CONTRIBUTIONS

GP, SG, RR, and RL conceived the manuscript and prepared the first draft. All authors critically revised the article for important intellectual content. All authors gave final approval of the version to be published and agreed to be accountable for all aspects of the work in ensuring that questions related to the accuracy or integrity of any part of the work are appropriately investigated and resolved. All authors contributed to the article and approved the submitted version.

FUNDING

Medical writing assistance for the preparation of this article was funded by Novartis Pharma, Italy. The funder was not involved in the writing of this article or the decision to submit it for publication.

ACKNOWLEDGMENTS

We thank Forum Service s.r.l. for their medical editorial assistance with this manuscript.

REFERENCES

1. Bennett JM. MDS Foundation's Working Group on Transfusional Iron Overload. Consensus Statement on Iron Overload in Myelodysplastic Syndromes. *Am J Hematol* (2008) 83(11):858–61. doi: 10.1002/ajh.21269
2. Santini V, Alessandrino PE, Angelucci E, Barosi G, Billio A, Di Maio M, et al. Clinical Management of Myelodysplastic Syndromes: Update of SIE, SIES, GITMO Practice Guidelines. *Leuk Res* (2010) 34(12):1576–88. doi: 10.1016/j.leukres.2010.01.018
3. Musto P, Maurillo L, Simeon V, Poloni A, Finelli C, Balleari, et al. Iron-Chelating Therapy With Deferasirox in Transfusion-Dependent, Higher Risk Myelodysplastic Syndromes: A Retrospective, Multicenter Study. *Br J Hematol* (2017) 177(5):741–50. doi: 10.1111/bjh.14621
4. Leitch HA. Controversies Surrounding Iron Chelation Therapy for MDS. *Blood Rev* (2011) 25(1):17–31. doi: 10.1016/j.blre.2010.09.003
5. Vinchi F, Hell S, Platzbecker U. Controversies on the Consequences of Iron Overload and Chelation in MDS. *Hemasphere* (2020) 4(3):e357. doi: 10.1097/HS9.0000000000000357
6. Gattermann N. Do Recent Randomized Trial Results Influence Which Patients With Myelodysplastic Syndromes Receive Iron Chelation? *Hematol Oncol Clin North Am* (2020) 34(2):465–73. doi: 10.1016/j.hoc.2019.10.006
7. Liu H, Yang N, Meng S, Zhang Y, Zhang H, Zhang W. Iron Chelation Therapy for Myelodysplastic Syndrome: A Systematic Review and Meta-Analysis. *Clin Exp Med* (2020) 20(1):1–9. doi: 10.1007/s10238-019-00592-5
8. Zeidan AM, Giri S, DeVeaux M, Ballas SK, Duong VH. Systematic Review and Meta-Analysis of the Effect of Iron Chelation Therapy on Overall Survival and Disease Progression in Patients With Lower-Risk Myelodysplastic Syndromes. *Ann Hematol* (2019) 98(2):339–50. doi: 10.1007/s00277-018-3539-7
9. Angelucci E, Cianciulli P, Finelli C, Mecucci C, Voso MT, Tura S. Unraveling the Mechanisms Behind Iron Overload and Ineffective Hematopoiesis in Myelodysplastic Syndromes. *Leuk Res* (2017) 62:108–15. doi: 10.1016/j.leukres.2017.10.001
10. Pilo F, Angelucci E. A Storm in the Niche: Iron, Oxidative Stress and Haemopoiesis. *Blood Rev* (2018) 32:29–35. doi: 10.1016/j.blre.2017.08.005
11. Santini V, Girelli D, Sanna A, Martinelli N, Duca L, Campostrini, et al. Hepcidin Levels and Their Determinants in Different Types of Myelodysplastic Syndromes. *PloS One* (2011) 6:e23109. doi: 10.1371/journal.pone.0023109
12. Camaschella C, Nai A. Ineffective Erythropoiesis and Regulation of Iron Status in Iron Loading Anemias. *Br J Hematol* (2016) 172:512–23. doi: 10.1111/bjh.13820
13. Shenoy N, Vallumsetla N, Rachmilewitz E, Verma A, Ginzburg Y. Impact of Iron Overload and Potential Benefit From Iron Chelation in Low-Risk Myelodysplastic Syndrome. *Blood* (2014) 124(6):873–81. doi: 10.1182/blood-2014-03-563221
14. Weber S, Parmon A, Kurrle N, Schnütgen F, Serve H. The Clinical Significance of Iron Overload and Iron Metabolism in Myelodysplastic Syndrome and Acute Myeloid Leukemia. *Front Immunol* (2021) 11:627662. doi: 10.3389/fimmu.2020.627662
15. Gattermann N. Iron Overload in Myelodysplastic Syndromes (MDS). *Int J Hematol* (2018) 107(1):55–63. doi: 10.1007/s12185-017-2367-1
16. Zeidan AM, Griffiths EA. To Chelate or Not to Chelate in MDS: That Is the Question! *Blood Rev* (2018) 32(5):368–77. doi: 10.1016/j.blre.2018.03.002
17. Platzbecker U, Kubasch AS, Homer-Bouthiette C, Prebet T. Current Challenges and Unmet Medical Needs in Myelodysplastic Syndromes. *Leukemia* (2021) 35(8):2182–98. doi: 10.1038/s41375-021-01265-7
18. Germing U, Oliva EN, Hiwase D, Almeida A. Treatment of Anemia in Transfusion-Dependent and Non-Transfusion-Dependent Lower-Risk MDS: Current and Emerging Strategies. *Hemasphere* (2019) 3(6):e314. doi: 10.1097/HS9.0000000000000314
19. Jin S, Su H, Tran NT, Song J, Lu SS, Li Y, et al. Splicing Factor SF3B1K700E Mutant Dysregulates Erythroid Differentiation *via* Aberrant Alternative Splicing of Transcription Factor TAL1. *PloS One* (2017) 12:e0175523. doi: 10.1371/journal.pone.0175523
20. Malcovati L, Stevenson K, Papaemmanuil E, Neuberg D, Bejar R, Boultwood J, et al. SF3B1-Mutant MDS as a Distinct Disease Subtype: A Proposal From the International Working Group for the Prognosis of MDS. *Blood* (2020) 136(2):157–70. doi: 10.1182/blood.2021012067
21. Visconte V, Avishai N, Mahfouz R, Tabarroki A, Cowen J, Sharghi-Moshtaghin R, et al. Distinct Iron Architecture in SF3B1-Mutant Myelodysplastic Syndrome Patients Is Linked to an SLC25A37 Splice Variant With a Retained Intron. *Leukemia* (2015) 29(1):188–95. doi: 10.1038/leu.2014.170
22. Schneider RK, Schenone M, Ferreira MV, Kramann R, Joyce CE, Hartigan C, et al. Rps14 Haploinsufficiency Causes a Block in Erythroid Differentiation Mediated by S100A8 and S100A9. *Nat Med* (2016) 22(3):288–97. doi: 10.1038/nm.4047
23. Inokura K, Fujiwara T, Saito K, Iino T, Hatta S, Okitsu Y, et al. Impact of TET2 Deficiency on Iron Metabolism in Erythroblasts. *Exp Hematol* (2017) 49:56–67.e5. doi: 10.1016/j.exphem.2017.01.002
24. Angelucci E, Pilo F. Iron Chelation Therapy in MDS – The Final Answer. *Clin Lymphoma Myeloma* (2019) 19(S1):S75–6. doi: 10.1016/j.clml.2019.07.425
25. de Swart L, Hendriks JC, van der Vorm LN, Cabantchik ZI, Evans PJ, Hod EA, et al. Second International Round Robin for the Quantification of Serum Non-Transferrin-Bound Iron and Labile Plasma Iron in Patients With Iron-Overload Disorders. *Haematologica* (2016) 101(1):38–45. doi: 10.3324/haematol.2015.133983
26. Barcellini W, Zaninoni A, Gregorini AI, Soverini G, Duca L, Fattizzo B, et al. Iron Overload in Congenital Haemolytic Anemias: Role of Hepcidin and Cytokines and Predictive Value of Ferritin and Transferrin Saturation. *Br J Hematol* (2019) 185(3):523–31. doi: 10.1111/bjh.15811
27. Brissot P, Ropert M, Le Lan C, Loréal O. Non-Transferrin Bound Iron: A Key Role in Iron Overload and Iron Toxicity. *Biochim Biophys Acta* (2012) 1820(3):403–10. doi: 10.1016/j.bbagen.2011.07.014
28. Greenberg PL, Stone RM, Al-Kali A, Barta SK, Bejar R, Bennett JM, et al. Myelodysplastic Syndromes, Version 2.2017, NCCN Clinical Practice Guidelines in Oncology. *J Natl Compr Canc Netw* (2017) 15(1):60–87. doi: 10.6004/jnccn.2017.0007
29. Malcovati L, Hellström-Lindberg E, Bowen D, Adès L, Cermak J, Del Cañizo C, et al. Diagnosis and Treatment of Primary Myelodysplastic Syndromes in Adults: Recommendations From the European LeukemiaNet. *Blood* (2013) 122(17):2943–64. doi: 10.1182/blood-2013-03-492884
30. Gattermann N, Finelli C, Porta MD, Fenaux P, Ganser A, Guerci-Bresler A, et al. Deferasirox in Iron-Overloaded Patients With Transfusion-Dependent Myelodysplastic Syndromes: Results From the Large 1-Year EPIC Study. *Leuk Res* (2010) 34(9):1143–50. doi: 10.1016/j.leukres.2010.03.009
31. Angelucci E, Santini V, Di Tucci AA, Quaresmini G, Finelli C, Volpe A, et al. Deferasirox for Transfusion-Dependent Patients With Myelodysplastic Syndromes: Safety, Efficacy, and Beyond (GIMEMA MDS0306 Trial). *Eur J Hematol* (2014) 92(6):527–36. doi: 10.1111/ejh.12300
32. Nolte F, Höchsmann B, Giagounidis A, Lübbert M, Platzbecker U, Haase D, et al. Results From a 1-Year, Open-Label, Single Arm, Multi-Center Trial Evaluating the Efficacy and Safety of Oral Deferasirox in Patients Diagnosed With Low and Int-1 Risk Myelodysplastic Syndrome (MDS) and Transfusion-Dependent Iron Overload. *Ann Hematol* (2013) 92(2):191–8. doi: 10.1007/s00277-012-1594-z
33. List AF, Baer MR, Steensma DP, Raza A, Esposito J, Martinez-Lopez N, et al. Deferasirox Reduces Serum Ferritin and Labile Plasma Iron in RBC Transfusion-Dependent Patients With Myelodysplastic Syndrome. *J Clin Oncol* (2012) 30(17):2134–9. doi: 10.1200/JCO.2010.34.1222
34. Breccia M, Finsinger P, Loglisci G, Federico V, Santopietro M, Colafigli G, et al. Deferasirox Treatment for Myelodysplastic Syndromes: "Real-Life" Efficacy and Safety in a Single-Institution Patient Population. *Ann Hematol* (2012) 91(9):1345–9. doi: 10.1007/s00277-012-1481-7
35. Maurillo L, Breccia M, Buccisano F, Voso MT, Niscola P, Trapè G, et al. Deferasirox Chelation Therapy in Patients With Transfusion-Dependent MDS: A 'Realworld' Report From Two Regional Italian Registries: Gruppo Romano Mielodisplasie and Registro Basilicata. *Eur J Hematol* (2015) 95(1):52–6. doi: 10.1111/ejh.12476
36. Improta S, Villa MR, Volpe A, Lombardi A, Stiuso P, Cantore N, et al. Transfusion-Dependent Low-Risk Myelodysplastic Patients Receiving Deferasirox: Long-Term Follow-Up. *Oncol Lett* (2013) 6(6):1774–8. doi: 10.3892/ol.2013.1617

37. Gattermann N, Jarisch A, Schlag R, Blumenstengel K, Goebeler M, Groschek M, et al. Deferasirox Treatment of Iron-Overloaded Chelation-Naïve and Prechelated Patients With Myelodysplastic Syndromes in Medical Practice: Results From the Observational Studies Extend and Exjange. *Eur J Hematol* (2012) 88(3):260–8. doi: 10.1111/j.1600-0609.2011.01726.x
38. Mainous AG3rd, Tanner RJ, Hulihan MM, Amaya M, Coates TD. The Impact of Chelation Therapy on Survival in Transfusional Iron Overload: A Meta-Analysis of Myelodysplastic Syndrome. *Br J Hematol* (2014) 167 (5):720–3. doi: 10.1111/bjh.13053
39. Leitch HA, Parmar A, Wells RA, Chodirker L, Zhu N, Nevill TJ, et al. Overall Survival in Lower IPSS Risk MDS by Receipt of Iron Chelation Therapy, Adjusting for Patient-Related Factors and Measuring From Time of First Red Blood Cell Transfusion Dependence: An MDS-CAN Analysis. *Br J Hematol* (2017) 179:83–97. doi: 10.1111/bjh.14825
40. Hoeks M, Yu G, Langemeijer S, Crouch S, de Swart L, Fenaux P, et al. EUMDS Registry Participants. Impact of Treatment With Iron Chelation Therapy in Patients With Lower-Risk Myelodysplastic Syndromes Participating in the European MDS Registry. *Hematologica* (2020) 105 (3):640–51. doi: 10.3324/hematol.2018.212332
41. Remacha ÁF, Arrizabalaga B, Villegas A, Durán MS, Hermosín L, de Paz R, et al. Evolution of Iron Overload in Patients With Low-Risk Myelodysplastic Syndrome: Iron Chelation Therapy and Organ Complications. *Ann Hematol* (2015) 94(5):779–87. doi: 10.1007/s00277-014-2274-y
42. Angelucci E, Li J, Greenberg P, Wu D, Hou M, Montano Figueroa EH, et al. Chelation in Transfusion-Dependent Patients With Low- to Intermediate-1-Risk Myelodysplastic Syndromes: A Randomized Trial. *Ann Intern Med* (2020) 172(8):513–22. doi: 10.7326/M19-0916
43. Malcovati L, Della Porta MG, Cazzola M. Predicting Survival and Leukemic Evolution in Patients With Myelodysplastic Syndrome. *Hematologica* (2006) 91(12):588–1590.
44. Lyons RM, Marek BJ, Paley C, Esposito J, Garbo L, DiBella N, et al. Comparison of 24-Month Outcomes in Chelated and non-Chelated Lower-Risk Patients With Myelodysplastic Syndromes in a Prospective Registry. *Leuk Res* (2014) 38(2):149–54. doi: 10.1016/j.leukres.2013.11.004
45. Rose C, Brechignac S, Vassilief D, Pascal L, Stamatoullas A, Guerci A, et al. Does Iron Chelation Therapy Improve Survival in Regularly Transfused Lower Risk MDS Patients? A Multicenter Study by the GFM (Groupe Francophone Des Myelodysplasies). *Leuk Res* (2010) 34(7):864–70. doi: 10.1016/j.leukres.2009.12.004
46. Goldberg SL, Chen E, Corral M, Guo A, Mody-Patel N, Pecora AL, et al. Incidence and Clinical Complications of Myelodysplastic Syndromes Among United States Medicare Beneficiaries. *J Clin Oncol* (2010) 28 (17):2847–52. doi: 10.1200/JCO.2009.25.2395
47. Fenaux P, Mufti GJ, Hellstrom-Lindberg E, Santini V, Finelli C, Giagounidis A, et al. Efficacy of Azacitidine Compared With That of Conventional Care Regimens in the Treatment of Higher-Risk Myelodysplastic Syndromes: A Randomised, Open-Label, Phase III Study. *Lancet Oncol* (2009) 10(3):223–32. doi: 10.1016/S1470-2045(09)70003-8
48. Gonçalves AC, Cortesão E, Oliveiros B, Alves V, Espadana AI, Rito L, et al. Oxidative Stress Levels Are Correlated With P15 and P16 Gene Promoter Methylation in Myelodysplastic Syndrome Patients. *Clin Exp Med* (2016) 16 (3):333–43. doi: 10.1007/s10238-015-0357-2
49. Porter JB, Elalfy M, Taher A, Aydinok Y, Lee SH, Sutcharitchan P, et al. Limitations of Serum Ferritin to Predict Liver Iron Concentration Responses to Deferasirox Therapy in Patients With Transfusion-Dependent Thalassaemia. *Eur J Hematol* (2017) 98(3):280–8. doi: 10.1111/ejh.12830
50. Taher AT, Origa R, Perrotta S, Kourakli A, Ruffo GB, Kattamis A, et al. New Film-Coated Tablet Formulation of Deferasirox Is Well Tolerated in Patients With Thalassemia or Lower-Risk MDS: Results of the Randomized, Phase II ECLIPSE Study. *Am J Hematol* (2017) 92(5):420–8. doi: 10.1002/ajh.24668
51. Zeidan AM, Pullarkat VA, Komrokji RS. Overcoming Barriers to Treating Iron Overload in Patients With Lower-Risk Myelodysplastic Syndrome. *Crit Rev Oncol Hematol* (2017) 117:57–66. doi: 10.1016/j.critrevonc.2017.07.002
52. Palumbo GA, Stella S, Pennisi MS, Pirosa C, Fermo E, Fabris S, et al. Role of New Technologies in Myeloproliferative Neoplasms. *Front Oncol* (2019) 9:321. doi: 10.3389/fonc.2019.00321
53. Komrokji RS, Verstovsek S, Padron E, List AF. Advances in the Management of Myelofibrosis. *Cancer Control* (2012) 19(4 Suppl):4–15. doi: 10.1177/107327481201904s04
54. Tefferi A, Lasho TL, Jimma T, Finke CM, Gangat N, Vaidya R, et al. One Thousand Patients With Primary Myelofibrosis: The Mayo Clinic Experience. *Mayo Clin Proc* (2012) 87(1):25–33. doi: 10.1016/j.mayocp.2011.11.001
55. Naymagon L, Mascarenhas J. Myelofibrosis-Related AnemiaAnemia: Current and Emerging Therapeutic Strategies. *HemaSphere* (2017) 1(1):e1. doi: 10.1097/HS9.0000000000000001
56. Carreau N, Tremblay D, Savona M, Kremyanskaya M, Mascarenhas J. Ironing Out the Details of Iron Overload in Myelofibrosis: Lessons From Myelodysplastic Syndromes. *Blood Rev* (2016) 30(5):349–56. doi: 10.1016/j.blre.2016.04.003
57. Nicolosi M, Mudireddy M, Lasho TL, Hanson CA, Ketterling RP, Gangat N, et al. Sex and Degree of Severity Influence the Prognostic Impact of Anemia in Primary Myelofibrosis: Analysis Based on 1109 Consecutive Patients. *Leukemia* (2018) 32(5):1254–8. doi: 10.1038/s41375-018-0028-x
58. Verstovsek S, Mesa RA, Gotlib J, Levy RS, Gupta V, DiPersio JF, et al. A Double-Blind, Placebo-Controlled Trial of Ruxolitinib for Myelofibrosis. *N Engl J Med* (2012) 366(9):799–807. doi: 10.1056/NEJMoa1110557
59. Al-Ali HK, Griesshammer M, Foltz L, Palumbo GA, Martino B, Palandri F, et al. Primary Analysis of JUMP, a Phase 3b, Expanded-Access Study Evaluating the Safety and Efficacy of Ruxolitinib in Patients With Myelofibrosis, Including Those With Low Platelet Counts. *Br J Hematol* (2020) 189(5):888–903. doi: 10.1111/bjh.16462
60. Cervantes F, Vannucchi AM, Kiladjian JJ, Al-Ali HK, Sirulnik A, Stalbovskaya V, et al. Three-Year Efficacy, Safety, and Survival Findings From COMFORT-II, a Phase 3 Study Comparing Ruxolitinib With Best Available Therapy for Myelofibrosis. *Blood* (2013) 122(25):4047–53. doi: 10.1182/blood-2013-02-485888
61. Palandri F, Tiribelli M, Benevolo G, Tieghi A, Cavazzini F, Breccia M, et al. Efficacy and Safety of Ruxolitinib in Intermediate-1 IPSS Risk Myelofibrosis Patients: Results From an Independent Study. *Hematol Oncol* (2018) 36 (1):285–90. doi: 10.1002/hon.2429
62. Pardanani A, Finke C, Abdelrahman RA, Lasho TL, Tefferi A. Associations and Prognostic Interactions Between Circulating Levels of Hepcidin, Ferritin and Inflammatory Cytokines in Primary Myelofibrosis. *Am J Hematol* (2013) 88(4):312–6. doi: 10.1002/ajh.23406
63. Vinchi F, Muckenthaler MU, Da Silva MC, Balla G, Balla J, Jeney V. Atherogenesis and Iron: From Epidemiology to Cellular Level. *Front Pharmacol* (2014) 5:94. doi: 10.3389/fphar.2014.00094
64. Cheung YF, Chan GC, HA SY. Effect of Deferasirox (ICL670) on Arterial Function in Patients With Beta-Thalassaemia Major. *Br J Hematol* (2008) 141(5):728–33. doi: 10.1111/j.1365-2141.2008.07092.x
65. Isidori A, Borin L, Elli E, Latagliata R, Martino B, Palumbo G, et al. Iron Toxicity - Its Effect on the Bone Marrow. *Blood Rev* (2018) 32(6):473–9. doi: 10.1016/j.blre.2018.04.004
66. Fisher DAC, Malkova O, Engle EK, Miner CA, Fulbright MC, Behbehani GK, et al. Mass Cytometry Analysis Reveals Hyperactive NF Kappa B Signaling in Myelofibrosis and Secondary Acute Myeloid Leukemia. *Leukemia* (2017) 31(9):1962–74. doi: 10.1038/leu.2016.377
67. Elli EM, Baratè C, Mendicino F, Palandri F, Palumbo GA. Mechanisms Underlying the Anti-Inflammatory and Immunosuppressive Activity of Ruxolitinib. *Front Oncol* (2019) 9:1186. doi: 10.3389/fonc.2019.01186
68. Elli EM, Iurlo A, Aroldi A, Caramella M, Malato S, Casartelli, et al. Deferasirox in the Management of Iron-Overload in Patients With Myelofibrosis: A Multicenter Study From the Rete Ematologica Lombarda (IRON-M Study). *Br J Hematol* (2019) 186(5):e123–6. doi: 10.1111/bjh.15964
69. Di Veroli A, Campagna A, De Muro M, Maurillo L, Trawinska MM, LeonettiCrescenzi S, et al. Deferasirox in the Treatment of Iron Overload During Myeloproliferative Neoplasms in Fibrotic Phase: Does Ferritin Decrement Matter? *Leuk Res* (2019) 76:65–9. doi: 10.1016/j.leukres.2018.11.012
70. Elli EM, Di Veroli A, Iurlo A, Carmosino I, Benevolo G, Abruzzese E, et al. Concomitant Treatment With Ruxolitinib and Deferasirox in the Management of Iron Overload in Patients With Myelofibrosis: A Multicenter Italian Experience. *Blood* (2019) 134(Suppl_1):839. doi: 10.1182/blood-2019-127488
71. Young NS, Calado RT, Scheinberg P. Current Concepts in the Pathophysiology and Treatment of Aplastic Anemia. *Blood* (2006) 108 (8):2509–19. doi: 10.1182/blood-2006-03-010777

72. Jin P, Shi J, Li XX, Shao YQ, Nie N, Ge ML, et al. Study on Abnormal Iron Metabolism and Iron Overload in Patients With Aplastic Anemia. *ZhonghuaXue Ye Xue Za Zhi* (2013) 348(10):877–82. doi: 10.3760/cma.j.issn.0253-2727.2013.10.011
73. Lee JW, Yoon SS, Shen ZX, Ganser A, Hsu HC, El-Ali A, et al. Hematologic Responses in Patients With Aplastic Anemia Treated With Deferasirox: A Post Hoc Analysis From the EPIC Study. *Hematologica* (2013) 98(7):1045–8. doi: 10.3324/hematol.2012.077669
74. Cancado R, Watman NP, Lobo C, Chona Z, Manzur F, Traina F, et al. Assessment of Liver and Cardiac Iron Overload Using MRI in Patients With Chronic Anemias in Latin American Countries: Results From ASIMILA Study. *Hematology* (2018) 23(9):676–82. doi: 10.1080/10245332.2018.1461292
75. Pawelec K, Salamonowicz M, Panasiuk A, Leszczynska E, Krawczuk-Rybak M, Demkow U, et al. Influence of Iron Overload on Immunosuppressive Therapy in Children With Severe Aplastic Anemia. *Adv Exp Med Biol* (2015) 866:83–9. doi: 10.1007/5584_2015_148
76. Zhang X, Shi Y, Huang Y, Zhang G, He Y, Jiang E, et al. Serum Ferritin Is a Different Predictor From Transfusion History for Allogeneic Transplantation Outcome in Patients With Severe Aplastic Anemia. *Hematology* (2018) 23(5):291–8. doi: 10.1080/10245332.2017.1390929
77. Taher AT, Porter JB, Viprakasit V, Kattamis A, Chuncharunee S, Sutcharitchan P, et al. Defining Serum Ferritin Thresholds to Predict Clinically Relevant Liver Iron Concentrations for Guiding Deferasirox Therapy When MRI Is Unavailable in Patients With Non-Transfusion-Dependent Thalassaemia. *Br J Haematol* (2015) 168(2):284–90. doi: 10.1111/bjh.13119
78. Scheinberg P. Acquired Severe Aplastic Anaemia: How Medical Therapy Evolved in the 20th and 21st Centuries. *Br J Haematol* (2021) 194(6):954–69. doi: 10.1111/bjh.17403
79. Lee JW, Yoon SS, Shen ZX, Ganser A, Hsu HC, Habr D, et al. Iron Chelation Therapy With Deferasirox in Patients With Aplastic Anemia: A Subgroup Analysis of 116 Patients From the EPIC Trial. *Blood* (2010) 116(14):2448–54. doi: 10.1182/blood-2010-01-261289
80. Lee JW. Iron Chelation Therapy in the Myelodysplastic Syndromes and Aplastic Anemia: A Review of Experience in South Korea. *Int J Hematol* (2008) 88(1):16–23. doi: 10.1007/s12185-008-0117-0
81. Messa E, Biale L, Castiglione A, Lunghi M, Bonferroni M, Salvi F, et al. Erythroid Response During Iron Chelation Therapy in a Cohort of Patients Affected by Hematologic Malignancies and Aplastic Anemia With Transfusion Requirement and Iron Overload: A FISM Italian Multicenter Retrospective Study. *Leuk Lymphoma* (2017) 58(11):2752–4. doi: 10.1080/10428194.2017.1312385
82. van Beers EJ, van Straaten S, Morton DH, Barcellini W, Eber SW, Glader B, et al. Prevalence and Management of Iron Overload in Pyruvate Kinase Deficiency: Report From the Pyruvate Kinase Deficiency Natural History Study. *Hematologica* (2019) 104(2):e51–3. doi: 10.3324/hematol.2018.196295
83. Porter JB, Lin KH, Beris P, Forni GL, Taher A, Habr D, et al. Response of Iron Overload to Deferasirox in Rare Transfusion-Dependent Anemias: Equivalent Effects on Serum Ferritin and Labile Plasma Iron for Haemolytic or Production Anemias. *Eur J Hematol* (2011) 87(4):338–48. doi: 10.1111/j.1600-0609.2011.01660.x
84. Wesson LGJr. Renal Hemodynamics in Physiological States. In: Wesson LG, editor. *Physiology of the Human Kidney*. New York: Grune & Stratton (1969). p. 98–100.
85. Ponticelli C, Musallam KM, Cianciulli P, Cappellini MD. Renal Complications in Transfusion-Dependent Beta Thalassaemia. *Blood Rev* (2010) 24(6):239–44. doi: 10.1016/j.blre.2010.08.004
86. Ige AO, Ongele FA, Adele BO, Emediong IE, Odetola AO, Adewoye EO. Pathophysiology of Iron Overload-Induced Renal Injury and Dysfunction: Roles of Renal Oxidative Stress and Systemic Inflammatory Mediators. *Pathophysiology* (2019) 26(2):175–80. doi: 10.1016/j.pathophys.2019.03.002
87. Demosthenous C, Vlachaki E, Apostolou C, Eleftheriou P, Kotsiafti A, Vetsiou E, et al. Beta-Thalassemia: Renal Complications and Mechanisms: A Narrative Review. *Hematology* (2019) 24(1):426–38. doi: 10.1080/16078454.2019.1599096
88. Mallat NS, Mallat SG, Musallam KM, Taher AT. Potential Mechanisms for Renal Damage in Beta-Thalassemia. *J Nephrol* (2013) 26(5):821–8. doi: 10.5301/jn.5000253
89. Cetin T, Oktenli C, Ozgurtas T, Yenicesu M, Sanisoglu SY, Oguz Y, et al. Renal Tubular Dysfunction in Beta-Thalassemia Minor. *Am J Kidney Dis* (2003) 42(6):1164–8. doi: 10.1053/j.ajkd.2003.08.016
90. Quinn CT, Johnson VL, Kim HY, Trachtenberg F, Vogiatzi MG, Kwiatkowski JL, et al. Renal Dysfunction in Patients With Thalassaemia. *Br J Haematol* (2011) 153(1):111–7. doi: 10.1111/j.1365-2141.2010.08477.x
91. Bakr A, Al-Tonbary Y, Osman G, El-Ashry R. Renal Complications of Beta-Thalassemia Major in Children. *Am J Blood Res* (2014) 4(1):1–6.
92. Hall AM, Bass P, Unwin RJ. Drug-Induced Renal Fanconi Syndrome. *QJM* (2014) 107(4):261–9. doi: 10.1093/qjmed/hct258
93. Dell'Orto VG, Bianchetti MG, Brazzola P. Hyperchloraemic Metabolic Acidosis Induced by the Iron Chelator Deferasirox: A Case Report and Review of the Literature. *J Clin Pharm Ther* (2013) 38(6):526–7. doi: 10.1111/jcpt.12095
94. Cappellini MD, Cohen A, Piga A, Bejaoui M, Perrotta S, Agaoglu L, et al. A Phase 3 Study of Deferasirox (ICL670), a Once-Daily Oral Iron Chelator, in Patients With Beta-Thalassemia. *Blood* (2006) 107(9):3455–62. doi: 10.1182/blood-2005-08-3430
95. Cappellini MD, Taher A. Deferasirox (Exjade) for the Treatment of Iron Overload. *Acta Hematol* (2009) 122(2-3):165–73. doi: 10.1159/000243801
96. Cappellini MD, Porter J, El-Beshlawy A, Li CK, Seymour JF, Elalfy M, et al. Tailoring Iron Chelation by Iron Intake and Serum Ferritin: The Prospective EPIC Study of Deferasirox in 1744 Patients With Transfusion-Dependent Anemias. *Hematologica* (2010) 95(4):557–66. doi: 10.3324/hematol.2009.014696
97. Piga A, Fracchia S, Lai ME, Cappellini MD, Hirschberg R, Habr D, et al. Deferasirox Effect on Renal Haemodynamic Parameters in Patients With Transfusion-Dependent Beta Thalassaemia. *Br J Hematol* (2015) 168 (6):882–90. doi: 10.1111/bjh.13217
98. Al-Khabori M, Bhandari S, Al-Rasadi K, Mevada S, Al-Dhuhli H, Al-Kemyani N, et al. Correlation of Iron Overload and Glomerular Filtration Rate Estimated by Cystatin C in Patients With Beta-Thalassemia Major. *Hemoglobin* (2014) 38 (5):365–8. doi: 10.3109/03630269.2014.944314
99. Brewster UC, Perazella MA. Acute Kidney Injury Following Proton Pump Inhibitor Therapy. *Kidney Int* (2007) 71(6):589–93. doi: 10.1038/sj.ki.5002038
100. Esposito AJ, Murphy RC, Toukatly MN, Amro OW, Kestenbaum BR, Najafian B. Acute Kidney Injury in Allopurinol-Induced DRESS Syndrome: A Case Report of Concurrent Tubulointerstitial Nephritis and Kidney-Limited Necrotizing Vasculitis. *Clin Nephrol* (2017) 87(6):316–9. doi: 10.5414/CN108966
101. Kattamis A, Aydinok Y, Taher A. Optimising Management of Deferasirox Therapy for Patients With Transfusion-Dependent Thalassaemia and Lower-Risk Myelodysplastic Syndromes. *Eur J Haematol* (2018) 101 (3):272–82. doi: 10.1111/ejh.13111
102. Saliba AN, El Rassi F, Taher AT. Clinical Monitoring and Management of Complications Related to Chelation Therapy in Patients With β-Thalassemia. *Expert Rev Hematol* (2016) 9(2):151–68. doi: 10.1586/17474086.2016.1126176
103. Zhang Y, Xiao C, Li J, Song LX, Zhao YS, Han S, et al. Comparative Study on Iron Content Detection by Energy Spectral CT and MRI in MDS Patients. *Front Oncol* (2021) 11:646946. doi: 10.3389/fonc.2021.646946
104. Mantovani LF, Santos FPS, Perini GF, Nascimento CMB, Silva LP, Wroclawski CK, et al. Hepatic and Cardiac and Iron Overload Detected by T2* Magnetic Resonance (MRI) in Patients With Myelodisplastic Syndrome: A Cross-Sectional Study. *Leuk Res* (2019) 76:53–7. doi: 10.1016/j.leukres.2018.12.001
105. Angelucci E, Urru SA, Pilo F, Piperno A. Myelodysplastic Syndromes and Iron Chelation Therapy. *Mediterr J Hematol Infect Dis* (2017) 9(1):e2017021. doi: 10.4084/MJHID.2017.021
106. Pepe A, Rizzo M, Galimberti S, Baratè C, Oliva EN, Arcioni F, et al. Prospective Cardiac Magnetic Resonance Imaging Survey in Myelodysplastic Syndrome Patients: Insights From an Italian Network. *Ann Hematol* (2021) 100(5):1139–47. doi: 10.1007/s00277-021-04495-y
107. Tanaka C. Clinical Pharmacology of Deferasirox. *Clin Pharmacokinet* (2014) 53(8):679–94. doi: 10.1007/s40262-014-0151-4
108. Lee JW, Kang HJ, Choi JY, Kim NH, Jang MK, Yeo CW, et al. Pharmacogenetic Study of Deferasirox, an Iron Chelating Agent. *PloS One* (2013) 8(5):e64114. doi: 10.1371/journal.pone.0064114
109. Cusato J, Allegra S, Massano D, De Francia S, Piga A, D'Avolio A. Influence of Single-Nucleotide Polymorphisms on Deferasirox C Trough Levels and Effectiveness. *Pharmacogenom J* (2015) 15(3):263–71. doi: 10.1038/tpj.2014.65

110. Li N, Chen Q, Gu J, Li S, Zhao G, Wang W, et al. Synergistic Inhibitory Effects of Deferasirox in Combination With Decitabine on Leukemia Cell Lines SKM-1, THP-1, and K-562. *Oncotarget* (2017) 8(22):36517–30. doi: 10.18632/oncotarget.16583
111. Choi JH, Kim JS, Won YW, Uhm J, Park BB, Lee YY. The Potential of Deferasirox as a Novel Therapeutic Modality in Gastric Cancer. *World J Surg Oncol* (2016) 14:77. doi: 10.1186/s12957-016-0829-1
112. Sechaud R, Robeva A, Belleli R, Balez S. Absence of an Effect of a Single-Dose Deferasirox on the Steady-State Pharmacokinetics of Digoxin. *Int J Clin Pharmacol Ther* (2008) 46(10):519–26. doi: 10.5414/cpp46519
113. Vlachodimitropoulou E, Chen YL, Garbowski M, Koonyosying P, Psaila B, Sola-Visner M, et al. Eltrombopag: A Powerful Chelator of Cellular or Extracellular Iron(III) Alone or Combined With a Second Chelator. *Blood* (2017) 130(17):1923–33. doi: 10.1182/blood-2016-10-740241
114. Fattizzo B, Cavallaro F, Milesi G, Barcellini W. Iron Mobilization in a Real Life Cohort of Aplastic Anemia Patients Treated With Eltrombopag. *Am J Hematol* (2019) 94(9):E237–9. doi: 10.1002/ajh.25550

Conflict of Interest: GP has received honoraria and/or served on the scientific advisory boards for Abbvie, Amgen, AOP, AstraZeneca, BMS Celgene, Janssen, and Novartis. WB: Consultant Novartis. EE: Participation to advisory board Novartis. CF: Novartis: advisory committees, speaker fees; Celgene: research funding, advisory committees, speaker fees; Takeda: consultancy. PM has received honoraria and/or served on the scientific advisory boards for Celgene, Janssen, Takeda, Bristol-Myers Squibb, Amgen, Novartis, Gilead, Jazz, Sanofi, Abbvie, Incyte, and Glaxo-Smith-Kline.

The remaining authors declare that the research was conducted in the absence of any commercial or financial relationships that could be construed as a potential conflict of interest.

Publisher's Note: All claims expressed in this article are solely those of the authors and do not necessarily represent those of their affiliated organizations, or those of the publisher, the editors and the reviewers. Any product that may be evaluated in this article, or claim that may be made by its manufacturer, is not guaranteed or endorsed by the publisher.

frontiers in Oncology

ORIGINAL RESEARCH
published: 12 October 2021
doi: 10.3389/fonc.2021.760732

[^{18}F](2*S*,4*R*)-4-Fluoroglutamine as a New Positron Emission Tomography Tracer in Myeloma

Silvia Valtorta[1,2†], Denise Toscani[3†], Martina Chiu[3†], Andrea Sartori[4], Angela Coliva[2], Arianna Brevi[5], Giuseppe Taurino[3], Matteo Grioni[5], Livia Ruffini[6], Federica Vacondio[4], Franca Zanardi[4], Matteo Bellone[5], Rosa Maria Moresco[1,2,7], Ovidio Bussolati[3*] and Nicola Giuliani[3,8*]*

[1] Department of Medicine and Surgery and Tecnomed Foundation, University of Milan Bicocca, Milano, Italy, [2] Department of Nuclear Medicine, San Raffaele Scientific Institute, Istituto di Ricovero e Cura a Carattere Scientifico (IRCCS), Milano, Italy, [3] Department of Medicine and Surgery, University of Parma, Parma, Italy, [4] Department of Food and Drug, University of Parma, Parma, Italy, [5] Division of Immunology, Transplantation and Infectious Diseases, San Raffaele Scientific Institute, Istituto di Ricovero e Cura a Carattere Scientifico (IRCCS), Milano, Italy, [6] Nuclear Medicine, "Azienda Ospedaliero-Universitaria di Parma", Parma, Italy, [7] Institute of Bioimaging and Molecular Physiology, National Research Council (IBFM-CNR), Milano, Italy, [8] Hematology, "Azienda Ospedaliero-Universitaria di Parma", Parma, Italy

The high glycolytic activity of multiple myeloma (MM) cells is the rationale for use of Positron Emission Tomography (PET) with ^{18}F-fluorodeoxyglucose ([^{18}F]FDG) to detect both bone marrow (BM) and extramedullary disease. However, new tracers are actively searched because [^{18}F]FDG-PET has some limitations and there is a portion of MM patients who are negative. Glutamine (Gln) addiction has been recently described as a typical metabolic feature of MM cells. Yet, the possible exploitation of Gln as a PET tracer in MM has never been assessed so far and is investigated in this study in preclinical models. Firstly, we have synthesized enantiopure (2*S*,4*R*)-4-fluoroglutamine (4-FGln) and validated it as a Gln transport analogue in human MM cell lines, comparing its uptake with that of ^{3}H-labelled Gln. We then radiosynthesized [^{18}F]4-FGln, tested its uptake in two different *in vivo* murine MM models, and checked the effect of Bortezomib, a proteasome inhibitor currently used in the treatment of MM. Both [^{18}F]4-FGln and [^{18}F]FDG clearly identified the spleen as site of MM cell colonization in C57BL/6 mice, challenged with syngeneic Vk12598 cells and assessed by PET. NOD.SCID mice, subcutaneously injected with human MM JJN3 cells, showed high values of both [^{18}F]4-FGln and [^{18}F]FDG uptake. Bortezomib significantly reduced the uptake of both radiopharmaceuticals in comparison with vehicle at post treatment PET. However, a reduction of glutaminolytic, but not of glycolytic, tumor volume was evident in mice showing the highest response to Bortezomib. Our data indicate that [^{18}F](2*S*,4*R*)-4-FGln is a new PET tracer in preclinical MM models, yielding a rationale to design studies in MM patients.

Keywords: myeloma, glutamine, metabolism, positron-emission tomography, mouse model, nuclear medicine

OPEN ACCESS

Edited by:
Massimo Gentile, Health Agency of Cosenza, Italy

Reviewed by:
Antonia Dimitrakopoulou-Strauss, German Cancer Research Center (DKFZ), Germany
Xiaoxia Xu, Peking University Cancer Hospital, China

****Correspondence:***
Nicola Giuliani
nicola.giuliani@unipr.it
Ovidio Bussolati
ovidio.bussolati@unipr.it
Rosa Maria Moresco
rosa.moresco@unimib.it

†These authors have contributed equally to this work and share first authorship

Specialty section:
This article was submitted to Hematologic Malignancies, a section of the journal Frontiers in Oncology

Received: *18 August 2021*
Accepted: *20 September 2021*
Published: *12 October 2021*

Citation:
Valtorta S, Toscani D, Chiu M, Sartori A, Coliva A, Brevi A, Taurino G, Grioni M, Ruffini L, Vacondio F, Zanardi F, Bellone M, Moresco RM, Bussolati O and Giuliani N (2021) [^{18}F](2S,4R)-4-Fluoroglutamine as a New Positron Emission Tomography Tracer in Myeloma. Front. Oncol. 11:760732. doi: 10.3389/fonc.2021.760732

INTRODUCTION

Multiple myeloma (MM) is a hematological disease characterized by the accumulation of malignant plasma cells (PC) into and, more rarely, outside the bone marrow (BM) (1). In the last years, 2-deoxy-2-[^{18}F]fluoro-D-glucose positron emission tomography/computed tomography ([^{18}F]FDG PET/CT) in MM has attained significant relevance, and it is considered the cornerstone of MM imaging at the initial diagnosis as well as in staging, prognostic evaluation, and monitoring response to therapy (2). Thus, [^{18}F]FDG PET/CT is currently used to assess active bone lesions and extramedullary localizations in MM patients (3). However, [^{18}F]FDG uptake yields both false positive and false negative lesions, and only 60–70% of patients with active MM are positive for [^{18}F]FDG PET (4, 5). These data support the need for additional imaging methods to assess skeletal involvement and monitoring the effect of treatment. To this purpose, several other PET tracers, such as choline and methionine, have been proposed (6, 7).

[^{18}F](2*S*,4*R*)-4-fluoroglutamine ([^{18}F]4-FGln) has been recently tested in different types of glutamine (Gln)-dependent tumors (8–10). MM is a Gln-addicted cancer that strictly relies on extracellular Gln uptake, and the use of Gln for anaplerosis has been also confirmed in patients (11, 12). However, [^{18}F]4-FGln as a PET tracer in MM has not been investigated yet.

Previous studies showed that [^{18}F]4-FGln is taken up by Gln transporters, including ASCT2, in solid tumors (13). Since we have already demonstrated that MM cells have increased expression of several Gln transporters and mainly depend on ASCT2 for Gln transport (11), we hypothesized that [^{18}F]4-FGln could be exploited to image MM. In the present study, we firstly documented that 4-FGln and Gln share the same transporters in human MM cell lines. Then, we investigated the sensitivity of [^{18}F]4-FGln in comparison to [^{18}F]FDG for the detection of MM cells using either a syngeneic murine model or a xenograft model of MM. Lastly, we explored the use of [^{18}F]4-FGln to monitor the effects of Bortezomib against MM.

MATERIALS AND METHODS

Chemical Synthesis and Characterization

The synthesis of the four stereoisomers of 4-FGln and their ^{18}F-labeled counterparts, together with data on the uptake of these compounds in 9L and SF188-Bcl-xL tumor cells (Gln-addicted glioblastoma-derived tumor cells), has been previously reported (14). In that work, the radiolabeled (2*S*,4*R*)-configured 4-fluoroglutamine [^{18}F]4-FGln (^{18}F-**1**), a fluorinated analogue of natural L-glutamine, displayed the best uptake properties in tumor cells as compared to the other stereoisomers.

Based on these precedents, we carried out the stereospecific synthesis of 4-FGln (1), to be used both for *in vitro* biological assays and as a reference compound in radio-HPLC analyses.

The synthesis procedure moved upon the previously reported footsteps (14), apart from some optimization variants. Thus, as shown in **Supplemental Figure 1**, starting from commercially available 2*S*-configured protected homoserine **2**, the synthesis path proceeded uneventfully, providing the tosyl product **10** in 29% overall yield. This advanced intermediate was ready for either the subsequent radiofluorination step to [^{18}F]4-FGln, or its transformation to "cold" target **1**.

Following the reported procedure for fluorination step of **10** to **11**, we were able to isolate but low amounts of the desired product (32% yield instead of the reported 77%). Thus, we proceeded to slightly modify the procedure by adopting the following conditions: (*i*) TASF (5 equiv) and $Et_3N{\cdot}(HF)_3$ (3 equiv) till reaching pH 5; (*ii*) solution concentration was a critical parameter and 0.1 M was judged optimal; and (*iii*) dry solvents were necessary to avoid C2 epimerization. Under these conditions, compound **11** was isolated in a very good 86% yield with complete stereochemical integrity.

Finally, global removal of the acid-sensitive protecting groups within **11** was carried out by employing trifluoroacetic acid and dimethyl sulfide, to provide crude fluoroglutamine **1**. The purification procedure of the target compound **1** turned out to be more troublesome than expected. According to the reported procedure, a first column purification step using Dowex 50WX8-200 (H^+ form) resin followed by recrystallization from EtOH/H_2O should have provided the final product in a good yield. In our hands, this method did not furnish any precipitate; after resin column, the eluted fraction was purified by reverse phase HPLC (using H_2O/TFA 0.1% and acetonitrile as eluent mixture), giving an unknown fluorinated product whose mass spectrum (ESI^+) coincided with that of the target, but the characterization data ($^1H/^{13}C/^{19}F$ NMR spectra, HPLC retention time), though similar, did not perfectly matched those reported for the target. Further attempts of purifications of the crude using the same acidic resin and avoiding the HPLC analysis gave, again, unsuccessful results. The ^{19}F-NMR analysis performed directly on the fraction eluted from the Dowex, without concentrating it, revealed the presence of several byproducts. Therefore, the purification procedure was modified, and it was found that evaporation of the reaction mixture to eliminate TFA and direct purification *via* reverse-phase HPLC eluting with H_2O (+0.1% formic acid) and acetonitrile lastly provided the desired fluoroglutamine **1** (41% yield), which was perfectly consistent with the reported data (optical activity, $^1H/^{13}C/^{19}F$ NMR spectra, HPLC retention time, **Figures S2** and **S3**).

It was concluded that the coexistence of many reactive functional groups (amide, carboxylic acid, amine, fluorine) within the small molecule, together with the presence of two stereocenters, renders the purification of this molecule highly challenging, and particular caution to both basic and acidic conditions has to be paid. We may hypothesize that the use of the acidic Dowex resin in the last stage and/or the 5% aqueous ammonia used to elute the product could be responsible for the undesired formation of less polar, cyclic imide product **12** (**Supplemental Figures 1**, **4–5**), possibly deriving from **1** *via* intramolecular dehydration closure. The data collected for the unknown compound are compatible with the structure of putative imide **12**, while its mass spectrum, coinciding with

that of target **1**, could be generated by reopening of imide **12** under the mass source conditions.

In conclusion, 4-FGln **1** was obtained in 10% overall yield over six steps from homoserine **2**.

(2*S*,4*S*)-*tert*-Butyl 2-(*tert*-Butoxycarbonylamino)-4-Hydroxy-5-Oxo-5-(2,4,6-Trimethoxybenzylamino) Pentanoate (9)

The title compound was prepared from compound **8**, thiourea and sodium bicarbonate, according to a reported procedure (*1*). The crude reaction mixture containing a 1:1 mixture of two diastereoisomeric alcohols **9** and **9'** was purified by flash chromatography on silica gel using CH_2Cl_2/MeOH as eluent (gradient from 99:1 to 98.5:1.5). Pure product **9** was isolated in a 44% yield as a white solid.

R_f: 0.5 (EtOAc/hexane 50:50); $[\alpha]_D^{25}$: −29.8 (c = 1.95, MeOH); lit. (*1*) $[\alpha]_D^{26}$: −28.7 (c = 1.06, MeOH).

^{1}H-NMR: (400 MHz, $CDCl_3$) δ 7.27 (bs, J = 5.4 Hz, 1H, NH), 6.13 (s, 2H, Ar-H), 5.47 (d, J = 7.7 Hz, 1H, NHBoc), 4.8 (bs, s, 1H, OH), 4.55 (dd, J = 13.7, 5.8 Hz, 1H, Ar-CH_A), 4.43 (dd, J = 13.7, 5.3 Hz, 1H, Ar-CH_B), 4.33 (ddd, J = 11.6, 7.8, 3.1 Hz, 1H, CH-NHBoc), 4.06 (dd, J = 11.7, 2.4 Hz, 1H, CHOH), 3.83 (s, 9H, OCH_3), 2.14 (ddd, J = 14.0, 12.6, 2.6 Hz, 1H, CH_2), 1.99 (ddd, J = 14.0, 11.9, 3.3 Hz, 1H), 1.46 (s, 9H, *t*-Bu), 1.43 (s, 9H, *t*-Bu).

^{13}C-NMR: (100 MHz, $CDCl_3$) δ 171.8 (C=O), 171.2 (C=O *t*-Bu), 160.9 (Cq), 159.4 (Cq), 157.3 (C=O Boc), 106.5 (Cq), 90.5 (CH), 82.8 (Cq Boc), 80.9 (Cq *t*-Bu), 68.2 (CH), 55.8 (CH3), 55.3 (CH_3), 50.8 (CH), 39.1 (CH_2), 31.7 (CH_2), 28.1 (3C, CH_3).

(2*S*,4*R*)-*tert*-Butyl 2-(*Tert*-Butoxycarbonylamino)-4-Fluoro-5-Oxo-5-(2,4,6-Trimethoxybenzylamino) Pentanoate (11)

To a stirred solution of tris(dimethylamino)sulfonium difluorotrimethylsilicate (TASF, 160 mg, 0.582 mmol) in dry DCM/THF (0.7:0.7 ml), under nitrogen atmosphere, $Et_3N{\cdot}(HF)_3$ (6 µl) was added. After that, tosylate **10** (76 mg, 0.116 mmol) in dry DCM/THF (0.7:0.7 ml) was added to the TASF solution. The reaction mixture was heated to 50°C and kept under inert atmosphere. Some of the solvent was removed by a nitrogen flux in order to have a final volume of 1 ml (final concentration 0.1 M). After 16 h, the oil bath was removed and EtOAc (8 ml) was added. The organic phase was extracted with $NaHCO_3$ solution (0.5 M) (1×), water (1×), and brine (1×). The organic phase was dried with $MgSO_4$, filtered and evaporated under reduced pressure. The residue was purified by silica gel flash chromatography (EtOAc/Petroleum Ether 20:80 to 30:70) to give product **11** as a white foam (58.3 mg, 86%).

$[\alpha]_D^{25}$: +1.7 (*c* = 1.10, MeOH); *lit (1):* $[\alpha]_D^{24}$: +1.7 (*c* = 1.14, MeOH)

^{1}H-NMR: (400 MHz, $CDCl_3$) δ (ppm) 6.70 (bs, 1H, NH), 6.13 (s, 2H, ArH), 5.33 (d, J = 7.4 Hz, 1H, NHBoc) 5.01 (ddd, $^2J_{HF}$ = 49.6 Hz, $^3J_{HH}$ = 8.9, 3.3 Hz, 1H, CHF), 4.61 (dd, J = 13.7, 5.9 Hz, 1H, ArCH_A) 4.40-4.36 (m, 2H, ArCH_B + CH_2), 3.82 (s, 9H, OCH_3), 2.52 (dddd, $^3J_{HF}$ = 34.0, J_{HH} = 15.0, 5.3, 3.4 Hz, 1H, CH_{2A}) 2.22-2.17 (m, 1H, CH_{2B}) 1.46 (s, 9H, *t*-Bu) 1.44 (s, 9H, *t*-Bu). ^{13}C-NMR: (100 MHz, $CDCl_3$) δ (ppm) 170.7 (C=O), 168.4 (d, $^2J_{CF}$ = 19.0 Hz), 161.1 (Cq), 159.3 (Cq), 106.1 (Cq), 90.6 (CH), 90.1 (d, $^1J_{CF}$ = 186.2 Hz, CF), 55.7 (CH_3), 55.3 (CH_3) 35.3 (d, $^2J_{CF}$ =20.1 Hz, CH_2), 31.9 (CH_2), 28.3 (3C, CH_3), 27.9 (3C, CH_3). ^{19}F-NMR: (376 MHz, $CDCl_3$) δ (ppm) −189.2 (ddd, J = 49.5, 37.0, 19.1 Hz).

(2*S*,4*R*)-4-Fluoroglutamine (1)

Protected 4-fluoroglutamine **11** (0.104 g, 0.208 mmol) was put in a two-neck flask, kept under N_2 atmosphere and cooled at 0°C with an ice bath. Dimethylsulfide was added (53 µl, 0.726 mmol), and immediately after TFA was added dropwise (5 ml, 3.53 mmol). The reaction was then removed by the ice bath and kept under stirring for 2.5 h at room temperature. TFA was evaporated, and the crude was washed with DCM (2 × 1 ml) and Et_2O (2 × 1 ml) removing the solvent with a Pasteur pipette. The crude was purified by a HPLC-RP ([C_{18}-10 µm column, 21.2 × 250 mm); solvent A H_2O (0.1% v/v formic acid); solvent B: ACN; flow rate 8.0 ml/min; detection 210 nm] using the following gradient elution: 0–1 min 0% B, 1–14 min 0–30% B, 14–23 min 30 B, 23–29 min 30–0% B (R_t = 11.4 min), obtaining the product 4-F-Gln **1** as a white solid (14 mg, 41%).

$[\alpha]_D^{25}$: +45.8 (*c* = 0.15, H_2O); *lit (1):* $[\alpha]_D^{24}$: +46.2 (*c* = 0.16, H_2O)

^{1}H-NMR: (400 MHz, D_2O) δ (ppm) 5.25 (ddd, $^2J_{H\text{-}F}$ = 48.9 Hz, $J_{H\text{-}H}$ = 10.2, 2.9 Hz, 1H, CHF), 3.94 (dd, J = 6.4, 6.4 Hz, 1H, C*H*NH_2), 2.56 (dddd, $^3J_{H\text{-}F}$ = 37.6 Hz, $^3J_{H\text{-}H}$ = 15.6, 6.0, 3.0 Hz, 1H, CH_A), 2.33 (dddd, $^3J_{H\text{-}F}$ = 15.8 Hz, $J_{H\text{-}H}$ = 15.8, 10.3, 7.1 Hz, 1H, CH_B). ^{13}C-NMR: (75 MHz, CD_3OD) δ (ppm) 174.8 (d, $^2J_{C\text{-}F}$ = 20.0 Hz), 174.2 (C=O), 90.1 (d, $^1J_{C\text{-}F}$ = 183 Hz, CF), 53.1 (CH), 34.4 (d, $^2J_{C\text{-}F}$ = 20.0 Hz, CH_2). ^{19}F-NMR: (376 MHz, D_2O) δ (ppm) -188.1 (ddd, J = 48.9, 37.6, 15.8 Hz). MS (ESI^+) = 165.06 $(M+H)^+$.

In Vitro Characterization of Glutamine and 4-FGln Transport

The human MM cell lines (HMCLs) RPMI8226 and JJN3 were purchased from Leibniz Institute Deutsche Sammlung von Mikroorganismen und Zellkulturen GmbH (Braunschweig, Germany). Cells were seeded in 24-well multidish plates (Falcon, Becton Dickinson Biosciences, Franklin Lakes, NJ, USA) at $750{\times}10^3$ cells/well 48 h before performing [^{3}H]-Gln (L-(3,4-^{3}H(N))-Gln, PerkinElmer, Groningen, Netherlands), and 4-FGln uptake. Cells were rinsed with Earle's Balanced Salt Solution (EBSS, NaCl 117 mM, TrisHCl 26 mM; KCl 5.3 mM, $CaCl_2$ 1.8 mM, $MgSO_4{\cdot}7H_2O$ 0.81 mM, choline phosphate 0.9 mM, glucose 5.5 mM, supplemented with 0.02% Phenol Red, adjusted at pH 7.4).

For the kinetic analysis of 4-FGln and Gln inhibition on Gln transport, cells were incubated for 30 s at pH 7.4 in EBSS in the presence of [^{3}H]-Gln (2 µCi/ml, 0.1 mM) and of increasing concentrations (0.05, 0.25, 1, 5, or 10 mM) of 4-FGln or Gln. At the end of the uptake, cells were rapidly washed with ice-cold urea (300 mM), to block amino acid trans-membrane fluxes, and extracted with absolute ethanol. Extracts were mixed with 200 µl of scintillation fluid and counted with a scintillation

spectrometer (Microbeta2, PerkinElmer, Milan, Italy). [3H]-Gln influx data, obtained at the different concentrations of the inhibitors, were fit to the equation for competitive inhibition:

$$v = v_0 - \frac{I_{max} \cdot [4 - FG\,ln]}{[I]_{0.5} + [4 - FG\,ln]}$$

For the discrimination of the transporters involved in 4-FGln uptake, cells were incubated for 1 min at pH 7.4 in EBSS in the presence of [3H]-Gln (10 μCi/ml, 0.1 mM) or 4-FGln (0.1 mM), and the influx was measured in the absence or in the presence of α-methylaminoisobutyric acid (MeAIB, 5 mM), L-threonine (Thr, 5 mM), or 2-aminobicyclo[2.2.1]heptane-2-carboxylic acid (BCH, 5 mM), as specific or preferential competitive inhibitors of SNAT1/2, ASCT2, or LAT1 transporters, respectively (11). At the end of the uptake, cells were rapidly washed with ice-cold urea (300 mM), and the intracellular amino acid content was extracted with 100 μl of cold absolute ethanol. For cells incubated with radiolabeled Gln, extracts were mixed with 200 μl of scintillation fluid and counted as described above, while the intracellular content of 4-FGln was quantified by high performance liquid chromatography coupled to tandem mass spectrometry (HPLC-MS/MS, see below). For both Gln and 4-FGln, influx data are expressed as pmol/mg prot/min.

Quantification of 4-FGln Intracellular Content

An Accela HPLC system (Thermo, USA) coupled to a TSQ Quantum Access Max Triple Quadrupole mass spectrometer (Thermo, USA), equipped with a heated electrospray (H-ESI) ion source, was employed for 4-FGln detection. HPLC separation occurred by a linear gradient employing a Phenomenex HILIC Luna column (2.1 × 100 mm; 3 μm particle size; Phenomenex, USA). Eluent A: 90:10 acetonitrile: HCOONH4 1 mM, pH 3.2; eluent B: 50:40:10 acetonitrile: water: $HCOONH_4$ 1 mM, pH 3.2). HPLC Gradient was as follows: t=0 min: 90%A; t=0.5 min: 90%A; t=7 min: 50%A; t=8 min: 90%A; with 8 min reconditioning time. Total run time: 16 min. Flow rate: 0.30 ml/min; injection volume: 10 μl. Instrumental parameters were set as follows: ion source voltage: 4,000 V; Capillary temperature: 270°C; sheath gas (N_2): 35 psi; auxiliary gas (N_2): 15 psi; collision gas (Ar) pressure: 1.5 mtorr. Mass spectrometer operated in positive ion (ESI+) and in Multiple Reaction Monitoring (MRM) mode. Tube lens voltages (TL) and collision energies (CE) for each parent-product ion transition were optimized by Flow Injection Analysis (FIA). The following transitions were employed: 4-FGln: m/z = 165.07 $[M+H]^+ \rightarrow$ m/z = 148.08, 102.16, 82.20 (TL: 47 V; CE: 5, 16, 22 eV, respectively; Internal Standard: *N*-acetylcysteine m/z = 136.04 $[M+H]^+ \rightarrow$ m/z = 119.07, 90.16, 77.15 (TL: 38 V; CE: 5, 13, 16 eV).

Ethanol cell extracts containing 4-FGln were dried by gentle nitrogen flow and reconstituted in HPLC eluent (90:10 acetonitrile: $HCOONH_4$ 1 mM) immediately before HPLC-MS/MS analysis. Calibration curves for 4-FGln were built employing seven calibration standards (CS) in the concentration range 100 nM–10 μM starting from 4-FGln stock solutions in water. Coefficients of correlations (r^2) were > 0.99 for all curves. The specificity of the method was evaluated by comparison of HPLC-ESI-MS/MS traces of 4-FGln at the Lower Limit of quantification to those of blank cell extracts. Xcalibur software version 2.2 (Thermo, USA) was employed for both data acquisition and processing.

Radiosynthesis of [18F]4-FGln

Radiosynthesis of [18F]4-FGln was obtained as described in literature (15), adapting the reported procedure to the in-house modified GE TRACERlab FX Module. [18F]Fluoride was produced *via* the $^{18}O(p,n)^{18}F$ nuclear reaction by irradiation of $[^{18}O]H_2O$ water in a Niobium target (2 ml) using an 18 MeV cyclotron (18 Twin, IBA RadioPharma Solutions, Louvain-la-Neuve, Belgium). The radionuclide was transferred from target in a water bolus by means of helium flow and trapped in a Chromafix® PS-HCO_3 cartridge (ABX, Radeberg, Germany) to separate $[^{18}O]H_2O$. [18F]Fluoride was eluted with 1 ml of 18-crown-6 in methanol (8 mg/ml) and 0.18 ml of $KHCO_3$ in water (8 mg/ml). Solvents were evaporated by heating to 75°C under reduced pressure. After azeotropic distillation, the precursor *tert*-butyl-(2S,4S)-2-[(tert-butoxycarbonyl)amino]-5-oxo-4-tosyloxy-5-[(2,4,6-trimethoxybenzyl)amino] pentanoate [Tosyl Precursor, compound **10**, **Supplementary Figure 1** (3.5 mg)], dissolved in 0.6 ml of acetonitrile, was added to the dried residue in the reaction vessel. The reaction mixture was heated at 70°C for 15 min without stirring. After quenching by addition of 0.6 ml of water and dilution with 3.5 ml of HPLC solvents (MeOH/H_2O 75:25+0.1% HCOOH), the reaction mixture was injected in a semipreparative C18 HPLC column (Luna, Phenomenex) for separation of the radiolabeled intermediate (retention time: 18 min) from unreacted [18F]Fluoride and other by-products. The intermediate peak was collected in the round bottom flask containing 20 ml of water and loaded on an Oasis HLB cartridge (Waters SPA, Milan, Italy). After washing with water, product was eluted with 1.2 ml of ethanol into the second reaction vessel. The evaporation of the solvent was followed by the addition to the dried residue of 1 ml of trifluoroacetic acid (TFA) containing 20 μl of anisole. Hydrolysis was achieved by heating at 60°C for 5 min, and excess TFA and volatile impurities were removed by evaporation. Radiolabeled product was dissolved in 10 ml of Phosphate Buffered Saline (PBS) and finally recovered in a sterile vial.

Quality Controls of [18F]4-FGln and Stability

Chiral analytical HPLC column Chirex 3126 (Phenomenex, CA, USA) was employed for determination of radiochemical and enantiomeric purity. [18F]4-FGln was eluted at 6.5–7.0 min with $CuSO_4$ 1 mM at 1 ml/min. pH was measured with indicator strips. The residual anisole in the final solution was quantified by analytical C18 HPLC (Luna, Phenomenex), mobile phase MeOH: H_2O = 75: 25 + 0.1% HCOOH, flow rate 1 ml/min, λ = 269 nm. The concentration was obtained by fitting to a calibration curve of standard anisole solution. TFA content was obtained by analytical C18 HPLC (Luna, Phenomenex), mobile phase 4.5 mM TBAOH: MeOH = 60: 40 pH 3, flow rate 1 ml/min, λ = 200 nm by fitting to a calibration curve of standard TFA solution. Residual ethanol content was quantified by GC by fitting to a calibration curve of standard ethanol solution.

In-vial stability of [18F]4-FGln was evaluated at different time points (1 h, 2 h, 3 h) by chiral HPLC analysis and pH measurements.

Animal Models and Treatments

Mice were maintained under specific pathogen-free conditions (SPF) in the San Raffaele Scientific Institute facility. Experiments were performed according to national rules and authorized by the Italian Ministry of Health (n. 34/2018-PR).

C57BL/6J mice (6–8 weeks, Charles River Breeding Laboratories, Calco, Italy) were injected intravenously (i.v.). with 0.5×10^6 Vk12598 cells in 200 µl of PBS. Mice were monitored weekly for M-spike and MM progression by retro-orbital bleeding. At weeks 3, 4, and 5, mice underwent PET with [18F]FDG and [18F]4-FGln on consecutive days.

For xenograft experiments, female NOD.SCID mice (4–6 weeks, Charles River Breeding Laboratories, Calco, Italy) were subcutaneously injected with 5×10^6 JJN3 HMCL in 100 µl of PBS. Tumors were measured twice a week with caliper, and tumor volume was calculated as $(a \times b^2)/2$; a: long side, b: short side. For evaluation of tracer biodistribution, 6 and 12 days after cell inoculation seven mice underwent PET scans with [18F]FDG and [18F]4-FGln in consecutive days. An additional group of mice was randomly assigned to two groups: vehicle- (n = 8) and Bortezomib-treated (n = 7). Bortezomib (1 mg/kg) was administered by intravenous injections on d1 and d4. Before (d-1 and d0) and after treatment (d5 and d6), animals underwent PET with [18F]FDG and [18F]4-FGln and sacrificed on d7. Efficacy was determined according to the adapted RECIST score (16). This index was defined as Tumor Volume Response (TVR) and calculated as the percentage change in median tumor volume measured by caliper at the end of treatment over the median tumor volume before treatment. Treatment response was defined as Partial Response (PR) (TVR > −30%); Stable Disease (SD) (TVR < −30% and < +20%), and Progressive Disease (PD), (TVR > +20%). In this study, PR and SD mice were grouped as responders.

PET Acquisition

PET studies were performed on a YAP-(S)-PET II (ISE S.r.l., Pisa, Italy) (17). [18F]FDG is routinely prepared in our facility for clinical use (European Pharmacopoeia X Edition), whereas [18F]4-FGln preparation was described above. [18F]FDG (4.32 ± 0.23 MBq) and [18F]4-FGln (4.46 ± 0.41 MBq) were injected in a tail vein of fasted mice (>6 h). Dynamic [18F]FDG acquisitions started at 60 min post injection and lasted 30 min (six scans of 5 min each) (18, 19). Mice were positioned prone on a "hand-made" mold on the PET bed to maintain the position with the tumor centered in field of view. For [18F]4-FGln pilot study, mice (n = 3) underwent a 90-min dynamic acquisition (frames: 4 of 2.5 min, 4 of 5 min, 6 of 10 min each) to determine the optimal imaging time for uptake measures. In the subsequent studies, dynamic PET acquisitions started at 15 min lasting 30 min (six scans of 5 min each). Mice were positioned with the tumor centered in field of view (20) and anesthetized (isoflurane 2%) during acquisition.

Images Quantification

All images were calibrated with a dedicated phantom, corrected for the radionuclide half-life decay, and then quantified with PMOD 3.2 (Zurich, Switzerland). To set acquisition time and verify reversibility of [18F]4-FGln (21), we applied the simplified Logan analyses using muscle as input function (21, 22) to three JJN3 mice. Regions of interest (ROIs) were drawn on tumor and thorax muscle and data expressed as %ID/g to obtain time-activity curves (TACs) of [18F]4-FGln. TACs of T/B revealed a time window of 15 to 60 min after injection when the T/B reached stable values. For comparison studies, images were processed as previously described (20), and maximum tumor to muscle ratios (Tmax/M), standardized uptake value (SUV), volume of radioactivity uptake ([18F]FDG and [18F]4-FGln metabolic tumor volume), total lesion glycolysis (TLG), and total lesion glutaminolysis (TLGln) were calculated. To this aim, PET images were thresholded, as previously validated and described by Krak et al., to create masks for the automatic extraction of the volume of tracer distribution (23). Using Region of Interest (ROI), we first calculated maximum radioligands concentration in tumor (MBq/g) (upper threshold value) and mean radioligands distribution in background (thorax muscle, MBq/g, ROI dimension 0.022 cm^3) (background value). Then, lower threshold was calculated as the halfway value between upper threshold value and background value. This method allowed to automatically extract the metabolic tumor volume (cm^3) within of the threshold values and the maximum and mean uptake of the tumor. Thanks to the positioning in the mold, [18F]4-FGln images were co-registered with [18F]FDG images using PMOD 3.2 and subsequently [18F]4-FGln mask of metabolic volume was co-registered to that of [18F]FDG and overlapped, so that exclusive radiotracer uptake regions were identified. The profile of backbone visible both with [18F]FDG, and [18F]4-FGln was used as anatomic landmark and co-registration quality judged and confirmed by an expert in the field (S.V.). For syngeneic model, ROIs were manually drawn on spleen, thorax muscle (0.02 cm^3), and femur (0.02 cm^3), and Tmax/M and SUV were calculated.

Murine Serum Protein Electrophoresis

Blood was collected in Eppendorf by retro-orbital sampling. Semiautomated electrophoresis was performed on the Hydrasys instrument (Sebia, Lissex, France). According to the manufacturer's instructions, 10 µl of undiluted serum were manually applied to the Hydragel agarose gels (Sebia). The subsequent steps, electrophoresis (pH 9.2, 20 W constant current at 20°C), drying, amidoblack staining, de-staining, and final drying, were carried out automatically. The use of Hydrasys densitometer and Phoresis software (Sebia) for scanning resulting profiles provided accurate relative concentrations (percentage) of individual protein zones. M-spike levels were calculated as total gamma globulins/albumin ratio (G/A).

Western Blot of ASCT2 in Murine MM

BM samples of either Vk12598-injected or non-injected C57BL/6J mice were lysed in RIPA buffer (Cell Signaling Technology).

Immunoblotting was performed as previously described (11). Anti-ASCT2 (rabbit, polyclonal, 1:1,000, Cell Signaling Technology) and anti-β-tubulin (mouse, polyclonal, 1:1,000, Sigma) were used as primary antibodies.

Statistics

In vivo data are presented as means ± standard deviation (SD). All statistical analyses were performed using Prism 8 (GraphPad Software, Inc., USA). Statistics are detailed in figure legends. Differences were considered significant when $p < 0.05$.

RESULTS

Chemical and Radiochemical Syntheses

Based on previously reported procedures (14), we carried out the stereospecific synthesis of 4-FGln (**Supplementary Figures 1–5**) to be used both for *in vitro* biological assays and as a reference compound in radio-HPLC analyses. This section as well as radiolabeling have been extensively described in *Methods*. For radiochemical synthesis, 2.5 ± 1.4 GBq of [^{18}F]4-FGln were obtained in about 100 min by automated synthesis [see above, *(2S,4R)-4-Floroglutamine (1)*]. Radiochemical yield was 12.3 ± 5.4% n.d.c (n=16). Radiochemical purity was 98.9 ± 0.9%, and stereochemical purity was 95 ± 3.5%. The pH of the solution was 6.9–7. Residual solvents are below the admitted limit (Anisole 0.3 ± 0.1 μg/ml, TFA 78.6 ± 60 μg/ml, Ethanol 2.5 ± 0.4 mg/ml).

Characterization of 4-FGln Uptake

Gln and 4-FGln were rapidly accumulated in either RPMI8226 or JJN3 HMCLs, reaching a maximum at 5 min of incubation (**Figure 1A**). 4-FGln accumulation remained fairly stable up to 60 min, while showed a partial decrease at 120 min (**Figure 1B**). To verify if 4-FGln enters MM cells through the same transporters used by Gln, radiolabeled Gln uptake was performed in the presence of increasing doses of either 4-FGln or Gln in RPMI8226. As shown in **Figure 1C**, 4-FGln inhibited [^{3}H]-Gln with a potency comparable to that of the natural amino acid (4-FGln [I]0.5 = 143 ± 35 μM; Gln [I]0.5 = 193 ± 33 μM). The maximal inhibition was around 70% of the total control uptake for both Gln and 4-FGln. Then, the 1-min influx of 4-FGln (0.1 mM) and [^{3}H]-Gln (0.1 mM, 2 μCi/mL) was determined in the presence of MeAIB, a specific substrate of System A carriers, Thr, a preferential substrate of the ASCT2 transporter, or BCH, a substrate of System L transporters. Although determined with different analytical techniques, the uninhibited uptakes of Gln and 4-FGln were fairly comparable (**Figures 1D–E**). Moreover, all the inhibitors tested were able to hinder both 4-FGln and Gln uptake, with Thr showing the highest and MeAIB the lowest inhibitory activity (**Figures 1D–E**). BCH inhibited more 4-FGln than Gln uptake, suggesting that 4-FGln exploits sodium-independent system L transporters more than the natural amino acid.

Tumor and Muscle Time Activity Curves of [^{18}F]4-FGln

Firstly, we characterized [^{18}F]4-FGln kinetics *in vivo* using the NOD.SCID JJN3 xenograft model (**Figure 2**). **Figure 2A** shows JJN3 tumor and muscle TACs. In tumor, [^{18}F]4-FGln uptake peaked at 25 min slowly declining thereafter (**Figure 2B**). The Logan plot (**Figure 2C**) confirmed linearity starting at 15 min from injection, consistent with largely reversible tracer exchange (21). The R^2 value for the fits of data from JJN3-grafted mice was 0.9989. For this reason, acquisition time was set between 15 and 45 min p.i. for subsequent studies.

In Vivo [^{18}F]4-FGln and [^{18}F]FDG Distribution in MM Models

[^{18}F]4-FGln and [^{18}F]FDG were compared in two MM models: a syngeneic model (murine Vk12598 cells) and a xenograft model (JJN3 cells).

Upon injection into C57BL/6 mice, Vk12598 cells colonize the BM, without lytic lesions, and the spleen, generating an aggressive MM (24). The expression of the glutamine transporter ASCT2 was checked in the BM (femur) of Vk12598 MM bearing mice. As shown in **Figure 3A**, the expression of the transporter increased along with MM progression, monitored with M-spike in blood samples collected at weeks 3, 4, and 5 after cell injection (**Figure 3B**) (25). Uptake of both tracers was measurable in the spleen of MM mice by week 3, reached a peak at week 4 [[^{18}F]4-FGln (T/M: 2.51 ± 0.69); [^{18}F]FDG (T/M: 5.73 ± 3.26)] and declined thereafter (**Figures 3C–E**). At the 4th week, T/M values of [^{18}F]FDG were definitely higher than that of [^{18}F]4-FGln. We performed also a quantification of the femur uptake. Healthy mice displayed a similar uptake of both radiotracers, whereas at the 4th week we observed a significant increase of [^{18}F]4-FGln uptake. The uptake of [^{18}F]FDG was more heterogeneous (**Figures 3F, G**).

In the JJN3 cells model, mice underwent a first scan at the tumor size of 72.8 ± 35.95 mm^3, displaying both [^{18}F]4-FGln (T/M: 1.6 ± 0.1) and [^{18}F]FDG (T/M: 3.5 ± 1.1) uptake. Tumor volume (896.8 ± 349.00 mm^3), [^{18}F]4-FGln uptake, and [^{18}F]FDG uptake (T/M: 2.3 ± 0.3 and 7.1 ± 2.6, respectively) increased after 1 week (**Figures 4A, B**). In any case, [^{18}F]FDG displayed a higher uptake than [^{18}F]4-FGln. Similar results were obtained considering SUVmax (**Figure 4C**).

In Vivo [^{18}F]4-FGln and [^{18}F]FDG Displayed Different Response After Bortezomib Administration in Mice

Administration of Bortezomib to JJN3-challenged mice caused a dramatic reduction in tumor growth when compared to vehicle-treated MM mice (172.0 ± 86.6 *vs* 687.9 ± 286.5 mm^3; $p = 0.0006$) (**Figure 5A**). In vehicle-treated mice at day 6, PET demonstrated only a positive, not significant trend of [^{18}F]4-FGln uptake (T/M pre: 1.86 ± 0.48, post: 2.08 ± 0.59; $p > 0.05$), but a significant increase of [^{18}F]4-FGln-derived tumor volume (pre: 0.024 ± 0.016 cm^3, post: 0.105 ± 0.069 cm^3; $p = 0.016$) and total lesion glutamine (pre: 0.021 ± 0.016, post: 0.092 ± 0.061; $p = 0.016$) (**Figures 5B–D**). In parallel, we observed a significant increase of [^{18}F]FDG uptake (pre: 2.66 ± 0.78, post: 6.58 ± 2.08; $p = 0.0078$), [^{18}F]FDG-derived tumor volume (pre: 0.026 ± 0.010 cm^3, post: 0.144 ± 0.061 cm^3; $p = 0.008$) and TLG (pre: 0.017 ± 0.007, post: 0.208 ± 0.114; $p = 0.008$) (**Figures 5E–G**). In Bortezomib-treated animals, we did not observe any increase of [^{18}F]4-FGln uptake

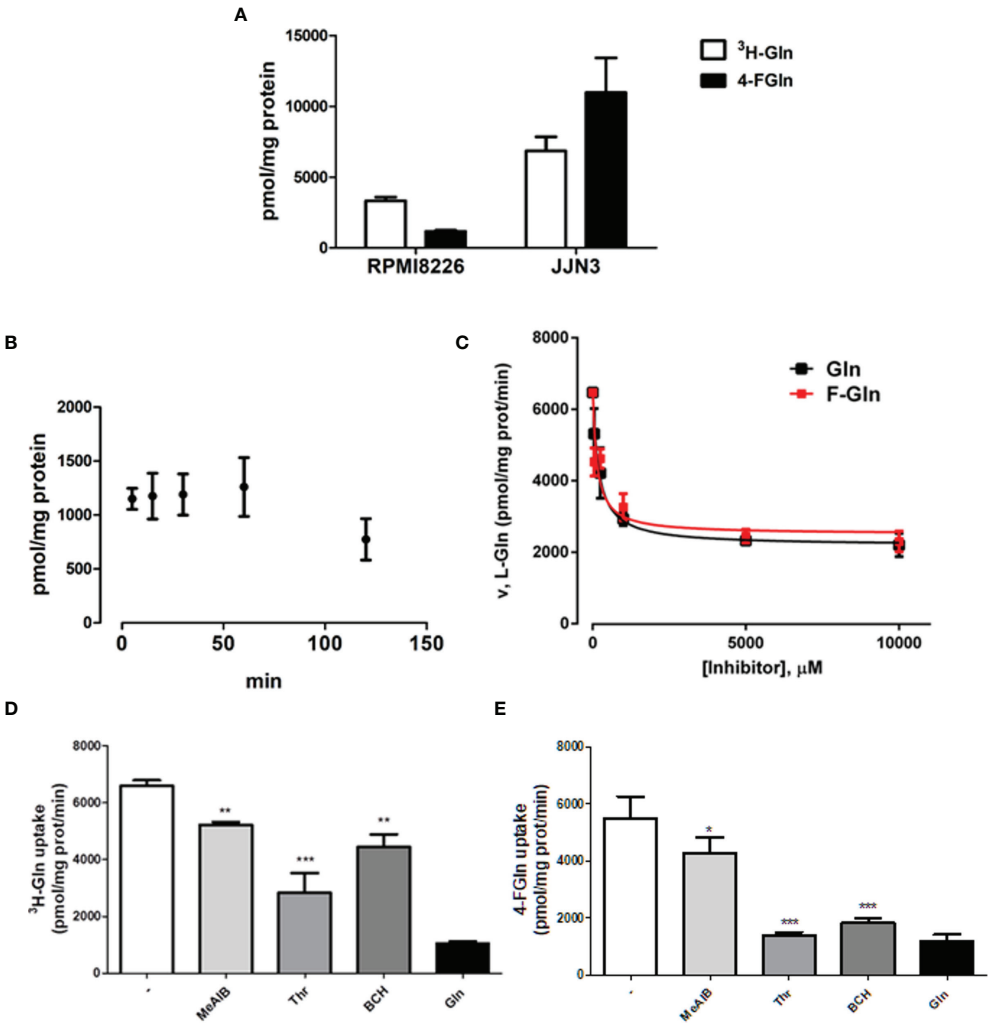

FIGURE 1 | Gln and F-Gln accumulation and uptake in MM cells. **(A)** RPMI8226 and JJN3 cells were incubated in EBSS containing L-[3,4-^{3}H(N)]-Gln (0.1 mM, 2 µCi/ml, ^{3}H-Gln) or 4-FGln (0.1 mM) for 5 min. Means ± SD of two experiments with five independent determinations each are shown. **(B)** RPMI8226 cells were incubated in EBSS containing 4-FGln (0.1 mM) for 5, 15, 30, 60, and 120 min. Means ± SD of two experiments with five independent determinations each are shown. **(C)** RPMI8226 cells were incubated for 30 s in EBSS containing L-[3,4-^{3}H(N)]-Gln (0.1 mM, 2 µCi/ml) in the presence of increasing doses (0.050, 0.25, 1, 5, or 10 mM) of cold 4-FGln or Gln. Means ± SD of two experiments with five independent determinations each are shown. **(D–E)** 1-min 4-FGln **(D)** or Gln **(E)** uptake in RPMI8226 cells in the presence of the indicated inhibitors, used at 5 mM. Means ± SD of two experiments with five independent determinations each are shown. *p < 0.05, **p < 0.01, ***p < 0.001. as assessed with a two-tailed t test.

(T/M), [^{18}F]4-FGln metabolic tumor volume, and TLGln after treatment (**Figures 5B–D**). In addition, SUVmax values highlighted a significant reduction of [^{18}F]4-FGln (**Figure 5H**). On the contrary, using [^{18}F]FDG we observed a significant increase of the radiotracer tumor volume (pre: 0.02 ± 0.006 cm^{3}, post: 0.06 ± 0.04 cm^{3}; p = 0.016), TLG (pre: 0.01 ± 0.005, post: 0.05 ± 0.03; p = 0.016) (**Figures 5F, G**), and also SUVmax (pre: 0.79 ± 0.14, post: 1.19 ± 0.24; p = 0.016) (**Figure 5I**). For both radiotracers and for all the considered parameters, Bortezomib-treated mice displayed significant lower values than vehicle-treated mice (**Figures 5B–G**).

To verify if metabolic modifications were related with tumor response, mice in the Bortezomib-treated group were classified as responders and non-responders based upon the adapted RECIST score (**Figure 6A**). Three Bortezomib-treated mice were classified as responders (#7G, #10G, #5G). These mice displayed a reduction of [^{18}F]4-FGln T/M ratio, [^{18}F]4-FGln-related tumor volume, and TLGln (**Figure 6B**). On the contrary, independently from the response, all mice displayed increased [^{18}F]FDG parameters (**Figure 6C**). These results indicate that [^{18}F]4-FGln better highlights MM response to Bortezomib than [^{18}F]FDG.

The quantitative volumetric analysis of exclusive areas of [^{18}F]FDG and [^{18}F]4-FGln uptake, as well as of regions of tracer overlap, was performed (**Figures 7A, B**). This strategy was applied to analyze *in vivo*, in the same animals, the modification in the volume of distribution of the two radiotracers and the presence of regional

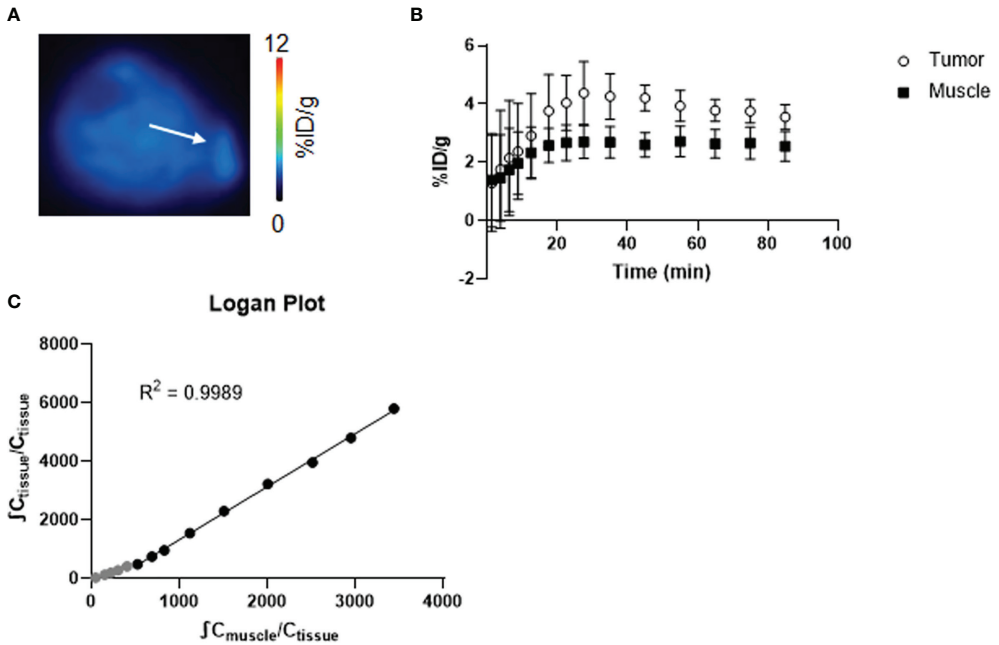

FIGURE 2 | Kinetic study of [^{18}F]4-FGln. **(A)** Coronal PET image summed from 15 to 50 min of dynamic scan of a representative JJN3 tumor-bearing mouse expressed as %ID/g. The white arrow indicates tumor. **(B)** Time-activity curves of the muscle and tumor of JJN3 tumor-bearing mice (n = 3). **(C)** Logan graphical analysis of TACs of JJN3 tumor-bearing mice. Data points used for the graphical fits are denoted in black, and unused data points are gray.

treatment-related differences in metabolism. Overlapping regions showed the part of the tumor with cells that are both glycolytic and glutaminolytic, while in the other regions one of the two types of metabolism is prevalent. The total metabolic tumor volume (the sum of [^{18}F]FDG and [^{18}F]4-FGln) increased in all groups (**Figure 7D**). The tracer overlap increased from 32 to 43% after 6 days in control and from 26 to 45% in non-responder mice. On the contrary, the area of tracer overlap decreased at about 9% in responder mice. After 6 days, the area of exclusive [^{18}F]4-FGln and [^{18}F]FDG uptake of vehicle-treated and non-responder mice remained fairly stable. Conversely, the area of relative exclusive uptake of [^{18}F]4-FGln significantly decreased at 9% ($p = 0.04$) in responders compared to 32% in non-responders, while that of [^{18}F]FDG uptake significantly increased at 82% ($p = 0.04$) compared to 23% in non-responders (**Figures 7B, C**).

DISCUSSION

Currently, [^{18}F]FDG is the standard tracer for the PET/CT scan in MM patients, and the role of this imaging is well established for checking skeletal involvement and extramedullary disease. Recently, the prognostic role of [^{18}F]FDG has been further highlighted (2, 26, 27). However, [^{18}F]FDG in CT/PET scans may have some limitations due to the presence of MM patients negative but with the presence of the disease. Moreover, [^{18}F]FDG carries its own limitations as a radiopharmaceutical, including a rather poor sensitivity for the detection of diffuse bone marrow infiltration, a relatively low specificity, and the lack of widely applied, established criteria for image interpretation (4, 5). Overall, this evidence have led to the development of alternative PET tracers, such as choline and methionine (6, 28), with promising results regarding MM detection. Other tracers are under evaluation (29).

Growing evidence suggests the possible use of [^{18}F]4-FGln as a new tracer in cancer patients taking advantage by the Gln-dependent metabolic profile of several tumors. Some preclinical and clinical studies have been published on *in vivo* testing of [^{18}F]4-FGln (8, 9, 21, 30–32), supporting its possible use as imaging biomarker. Moreover, [^{18}F]4-FGln could be used to study the metabolic profile and the Gln addiction of MM cells in order to design a metabolic-based therapeutic approach.

Recently, we have demonstrated that MM cells are strictly Gln addicted and lack of a sizable expression of the enzyme Glutamine Synthetase (11). Therefore, MM cells only rely on extracellular Gln. Consequently, MM cells are endowed with fast Gln uptake due to high expression of at least three different types of Gln transporters and, in particular, of the sodium-dependent carrier ASCT2, which is overexpressed in several types of Gln-dependent cancers (33). Moreover, we have also recently shown that the massive Gln uptake by MM cells decreases Gln concentration in the tumor microenvironment, contributing to the bone remodeling process induced by MM cells (34). Overall, this evidence provides a rational basis to exploit Gln metabolism in the design of a PET tracer for MM diagnosis and patient stratification.

Here, the possible role of [^{18}F]4-FGln as radiotracer for imaging in MM has been evaluated either *in vitro* or *in vivo*. First, we assessed 4-FGln transport *in vitro*, showing that 4-FGln

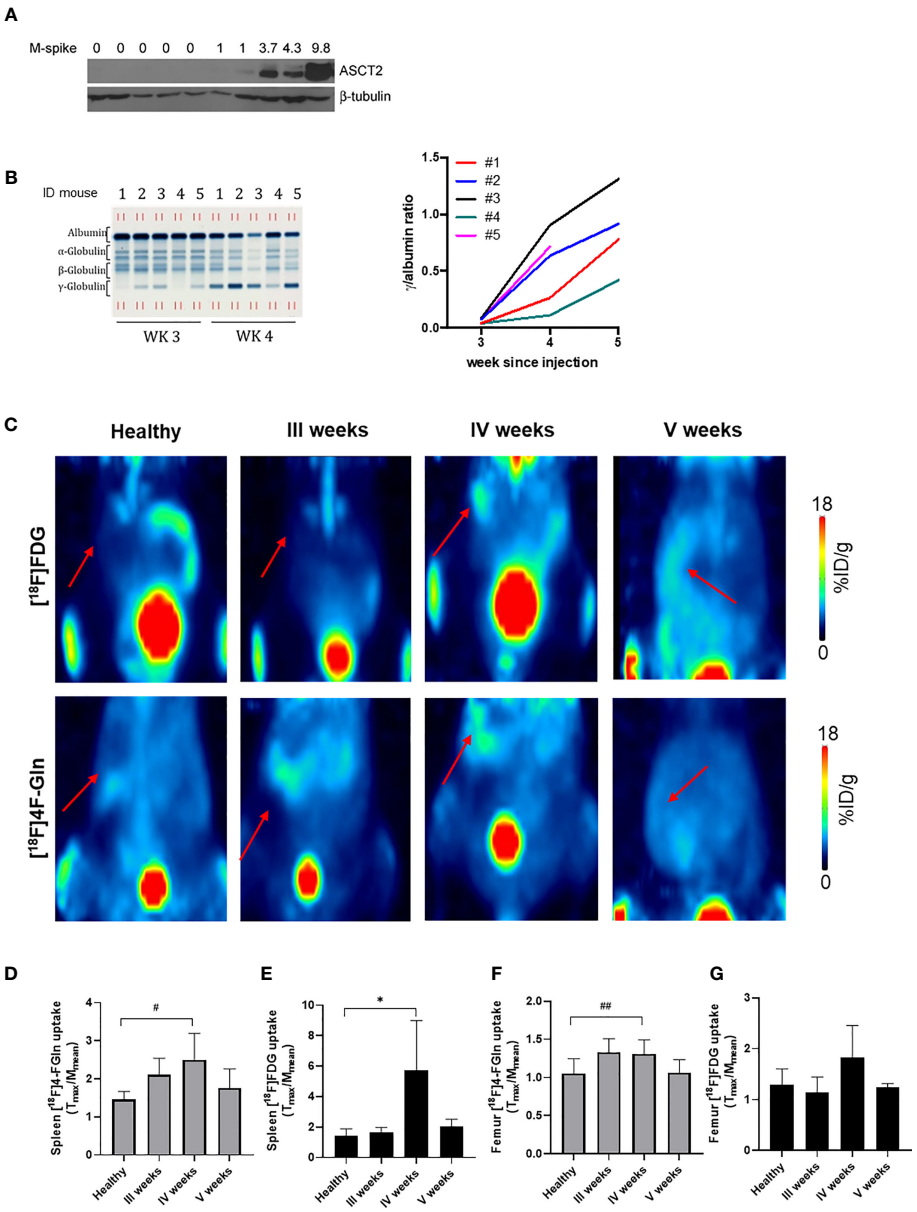

FIGURE 3 | Radiotracers distribution in a syngeneic MM model. **(A)** ASCT2 expression in the bone marrow (femurs) of control (lanes 1–5) and Vk12598 injected mice 5 weeks after injection (lanes 5–10). Numbers indicate the M-spike level at the time of the analysis. **(B)** Representative serum protein electrophoresis gel (left) and tumor growth curves represented as total gamma/albumin ratio (right) of mice from 1 to 5 measured at 3, 4, and 5 weeks after Vk12598 injection. **(C)** Representative maximum intensity projection (MIP) images of from [^{18}F]FDG and [^{18}F]4-FGln of a healthy mouse and at III, IV, and V weeks from the injection of Vk12598 cells. The red arrows indicate the spleen. **(D, E)** Quantitative analysis of radiotracers uptake expressed as T/M in the spleen. Differences intragroups were tested for significance using paired t test. *p = 0.03; $^{\#}$p = 0.04. **(F, G)** Quantitative analysis of radiotracers uptake expressed as T/M in the femur. Differences intragroups were tested for significance using paired t test. $^{\#\#}$p = 0.002.

is a reliable Gln transport analogue in human MM cell lines, with a potency as an inhibitor of Gln even larger than the natural amino acid. More importantly, most of the uptake of 4-FGln by MM cells occurs through the ASCT2 transporter, the same carrier exploited preferentially by Gln.

Applicability of [^{18}F]4-FGln to *in vivo* studies was confirmed in two models: the well-established syngeneic model, based on the inoculation of murine MM cells Vk12598 and extensively used to provide the rationale for novel therapeutic intervention (24, 25, 35), and a xenograft model based on human JJN3 cells. Our data suggest that in Vk12598 model both [^{18}F]4-FGln and [^{18}F]FDG can be used to follow disease progression, as indicated by M-spike measurement, in sites of extramedullary disease, despite higher uptake of [^{18}F]FDG in extramedullary lesion in

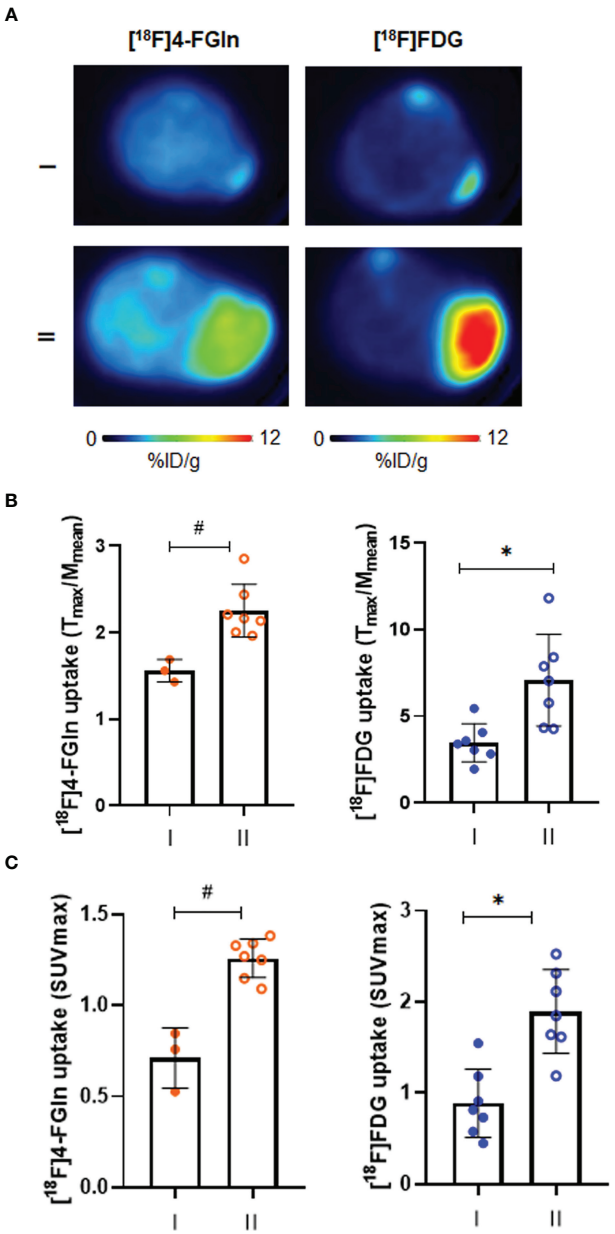

FIGURE 4 | Characterization of [18F]FDG and [18F]4-FGln uptake in JJN3 tumor model. **(A)** Transaxial [18F]FDG and [18F]4-FGln PET images of a representative JJN3 tumor-bearing mouse acquired on days 5–6 (I) and 12–13 (II) expressed as %ID/g. **(B)** Quantitative analysis of radiotracers uptake expressed as T/M. Differences intra- and intergroups were tested for significance using Wilcoxon matched-pairs signed rank-test and Unpaired Mann-Whitney test. *p = 0.0156; #p = 0.0167. **(C)** Quantitative analysis of radiotracers uptake expressed as SUVmax. Differences intra- and intergroups were tested for significance using Wilcoxon matched-pairs signed rank-test and Unpaired Mann-Whitney test. *p = 0.0156; #p = 0.0167.

comparison with [18F]4-FGln, as shown by ROIs analysis. MM can develop disease also in bone marrow, but one possible limit of [18F]4-FGln for the detection of medullary disease is the high uptake found in the bone after 60 min from injection (36). In our study, with the signal acquired between 15 and 45 min, bone signal was not evident. To better understand this issue, we analyzed femur uptake in the syngeneic model. We performed a quantification of uptake in femur of the syngeneic mice where bone signal could be increased also by the presence of myeloma. We did not observe any significant difference between the two radiotracers when myeloma was not present (healthy condition). However, at the 4th week we observed a significant increase of [18F]4-FGln whereas the uptake of [18F]FDG was more heterogeneous. Unfortunately, due to the low sensitivity of the PET system used for the acquisition with our PET system, it is not possible to distinguish the uptake between bone and bone marrow. Further analyses are needed to address this issue.

Also the xenograft model demonstrated the capacity of [18F]4-FGln and [18F]FDG to be taken up by subcutaneous plasmocytomas. Interestingly, in this model, we observed minimal radiotracer trapping and largely reversible tracer exchange despite the high glutaminase (GLS) activity of the JJN3 line (11) that should lead to F-Gln hydrolysis. On the other hand, [18F]4-FGln uptake could reflect glutamine pool rather than GLS activity (8). Indeed, [18F]4-FGln tumor kinetics reflects Logan plot confirming the presence of a reversible tracer exchange also in this MM model. Although uptake of [18F]4-FGln was lower than [18F]FDG uptake also in JJN3 tumors, as observed in the Vk12598 model, variability of [18F]4-FGln was remarkably smaller.

To better define the role of [18F]4-FGln as radiopharmaceutical, we evaluated the effect of Bortezomib. Our most intriguing finding was that [18F]4-FGln and [18F]FDG differently perceived the metabolic changes imposed to the tumor by Bortezomib. Indeed, independently from response, Bortezomib increased [18F]FDG uptake and volume of distribution, whereas [18F]4-FGln parameters were more closely associated with the response, suggesting that [18F]4-FGln based PET scan reliably delineates tumor sensitivity to the drug. In line with our observations, it has been reported that [18F]FDG uptake may persist in MM patients who achieved complete response to Bortezomib (37). The drug has been reported to stimulate aerobic glycolysis, thus possibly indicating that changes in tumor volume are masked by increased glycolytic flux (38–40). Overall, we showed a marked effect of Bortezomib on tumor cell metabolic phenotype, as indicated by the reduction of volume of exclusive [18F]4-FGln uptake in responder mice.

Previous studies suggested that [18F]4-FGln labels the intracellular Gln pool and, indirectly, is a glutaminolytic marker (8). This was recently supported by a kinetic analysis applied on murine breast cancer models (21) and confirmed here by the demonstration that [18F]4-FGln uptake in JJN3 tumors is described by a one-compartment, reversible tissue model with no trapping. Thus, [18F]4-FGln proves a dynamic tool for research and potential clinical use in MM. Moreover, Bortezomib caused a significant reduction of volume of exclusive [18F]4-FGln uptake in responder mice, indicating a drug effect on tumor metabolic phenotype. These results suggest that glutaminolysis impairment

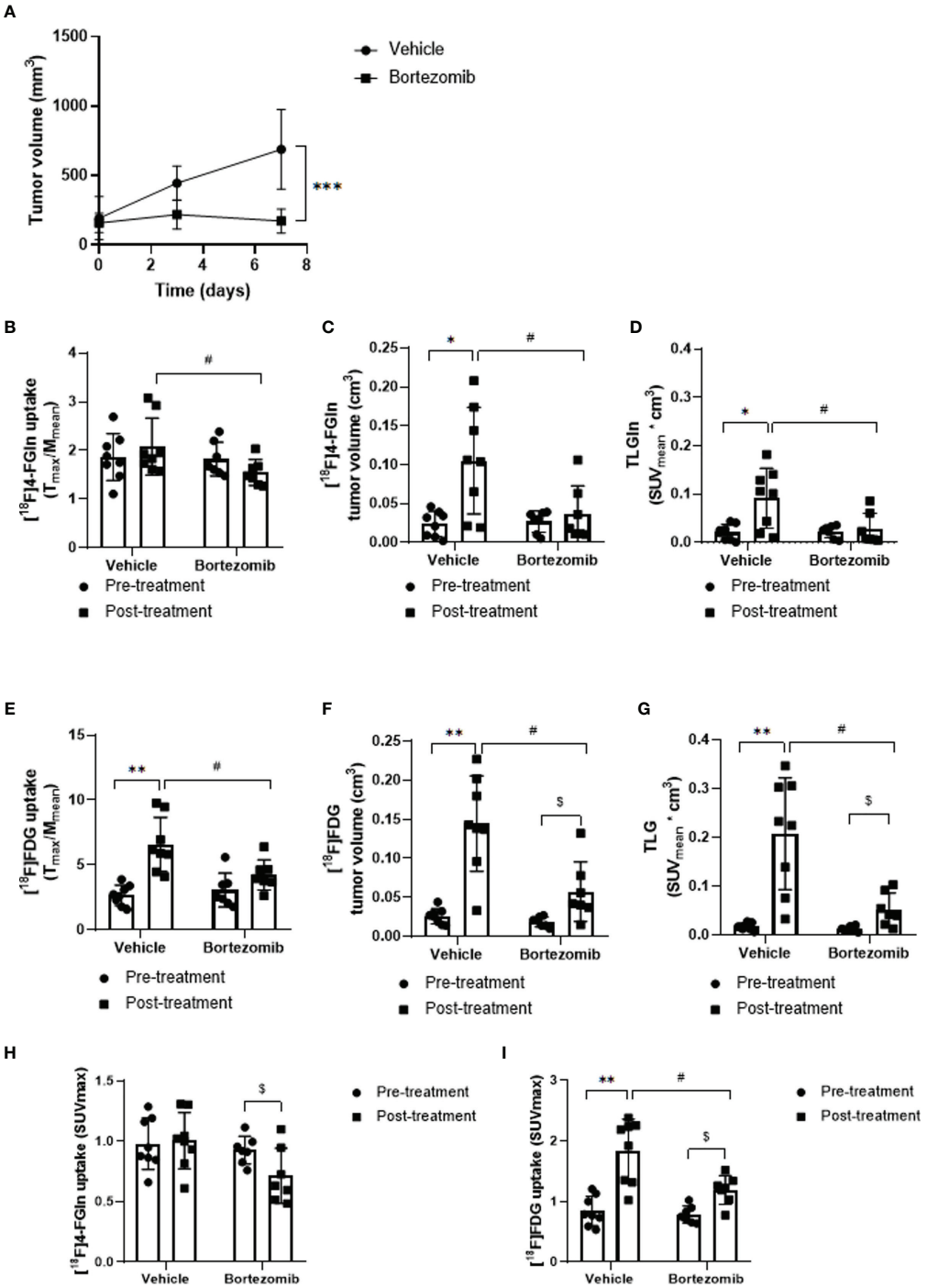

FIGURE 5 | Effect of Bortezomib treatment on [18F]FDG and [18F]4-FGln uptake measured by PET. **(A)** Tumor volume measured by caliper in vehicle and Bortezomib-treated mice. Data are expressed as mean ± SD and were analyzed by Unpaired Mann-Whitney test. ***p = 0.0006. **(B, E)** Quantitative analysis of [18F]FDG and [18F]4-FGln T/M uptake ratio before and after treatment with vehicle and Bortezomib. **(C, F)** Volumetric analysis of [18F]FDG and [18F]4-FGln uptake within the tumor region, pre- and post-therapy. **(D, G)** Quantification of total lesion glycolysis (TLG) and total lesion glutamine (TLGln) within the tumor region, pre- and post-therapy. Differences intra- and intergroups were tested for significance using Wilcoxon matched-pairs signed rank-test and Unpaired Mann-Whitney test. *, #, $, $p < 0.05$; **$p < 0.01$. **(H)** Quantitative analysis of [18F]4-FGln and **(I)** [18F]FDG SUVmax uptake before and after treatment with vehicle and Bortezomib. Differences intra- and intergroups were tested for significance using Wilcoxon matched-pairs signed rank-test and Unpaired Mann-Whitney test. #, $, $p < 0.05$; **$p < 0.01$.

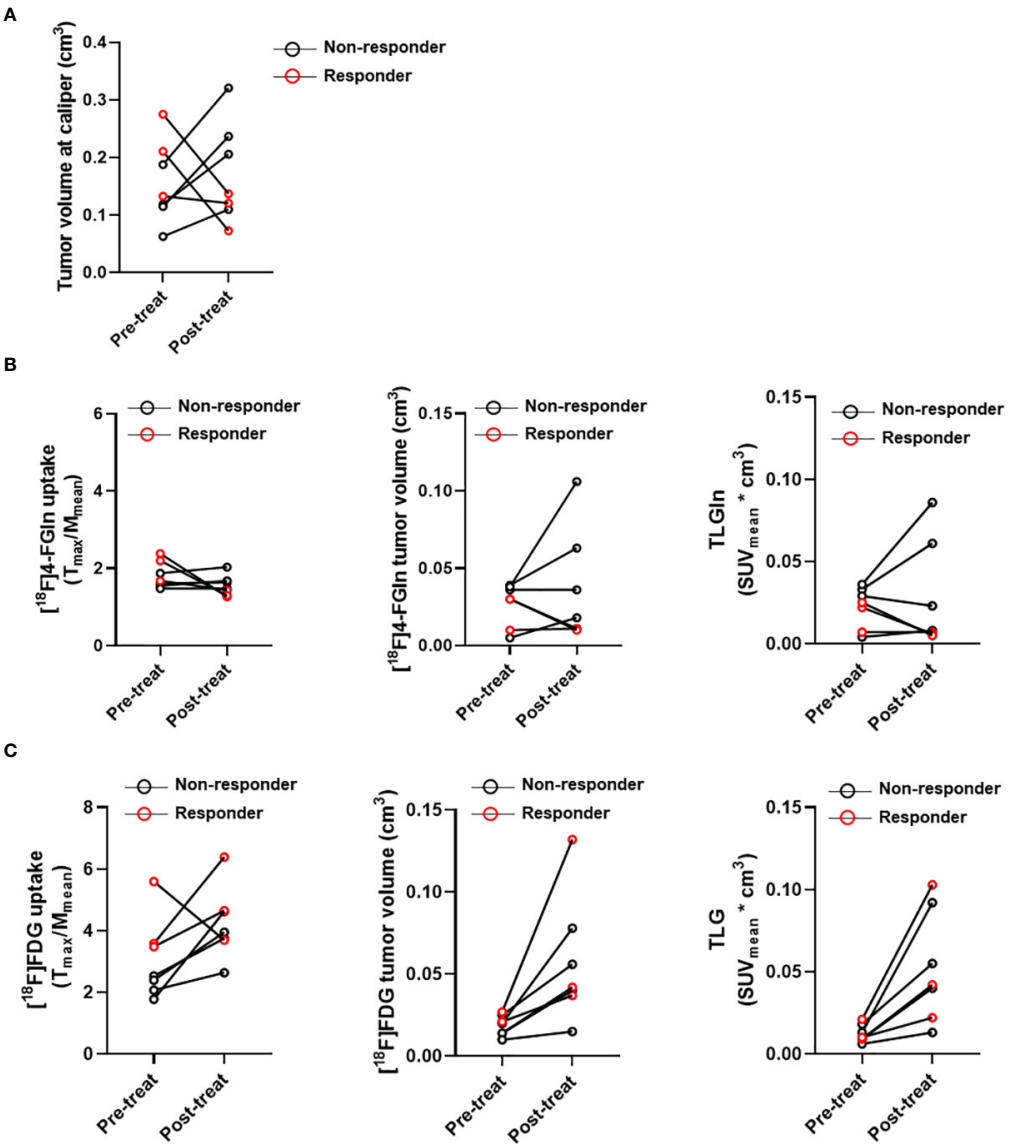

FIGURE 6 | Case by case analysis of "responders" and "non-responders." **(A)** Tumor volume measured at caliper, **(B)** T/M ratios and tumor volume relative to [^{18}F]4-FGln uptake and TLGln, and **(C)** T/M ratios and tumor volume relative to [^{18}F]FDG uptake and TLG pre- and post-treatment with Bortezomib in responder (red circles) and non-responder cases (black circles).

represents a major factor in Bortezomib efficacy. This confirms the metabolic heterogeneity of MM and suggests that modification in glutaminolysis represents a major event in Bortezomib efficacy. For the reasons above, our results suggest that [^{18}F]4-FGln may be a promising radiopharmaceutical for PET molecular imaging of the outcome of metabolically based target therapy acting on glutaminolysis.

Metabolic changes parallel MM progression (41). For instance, glutamine-dependent anaplerosis of the TCA cycle increases from MGUS to myeloma (12). Moreover, a sizable degree of metabolic heterogeneity may be present in the same MM (42), suggesting that subpopulations of MM cells may respond in a different way to therapeutic treatments. For these reasons, the combined use of distinct metabolically related probes, such as [^{18}F]4-FGln and [^{18}F]FDG, may yield clinically important information.

In conclusion, our data indicate that [^{18}F]4-FGln may be a new tracer to detect MM cells in preclinical *in vivo* models. [^{18}F]4-FGln might help to explore the potential use of PET to better define the metabolic phenotype of the tumor and the modifications induced by therapy, particularly as a potential marker of treatment response to proteasome inhibitors. Moreover the *in vivo* study of the metabolic profile of myeloma cells by [^{18}F]4-FGln could be useful to design future metabolic-based therapeutic approach and for the clinical management of MM patients.

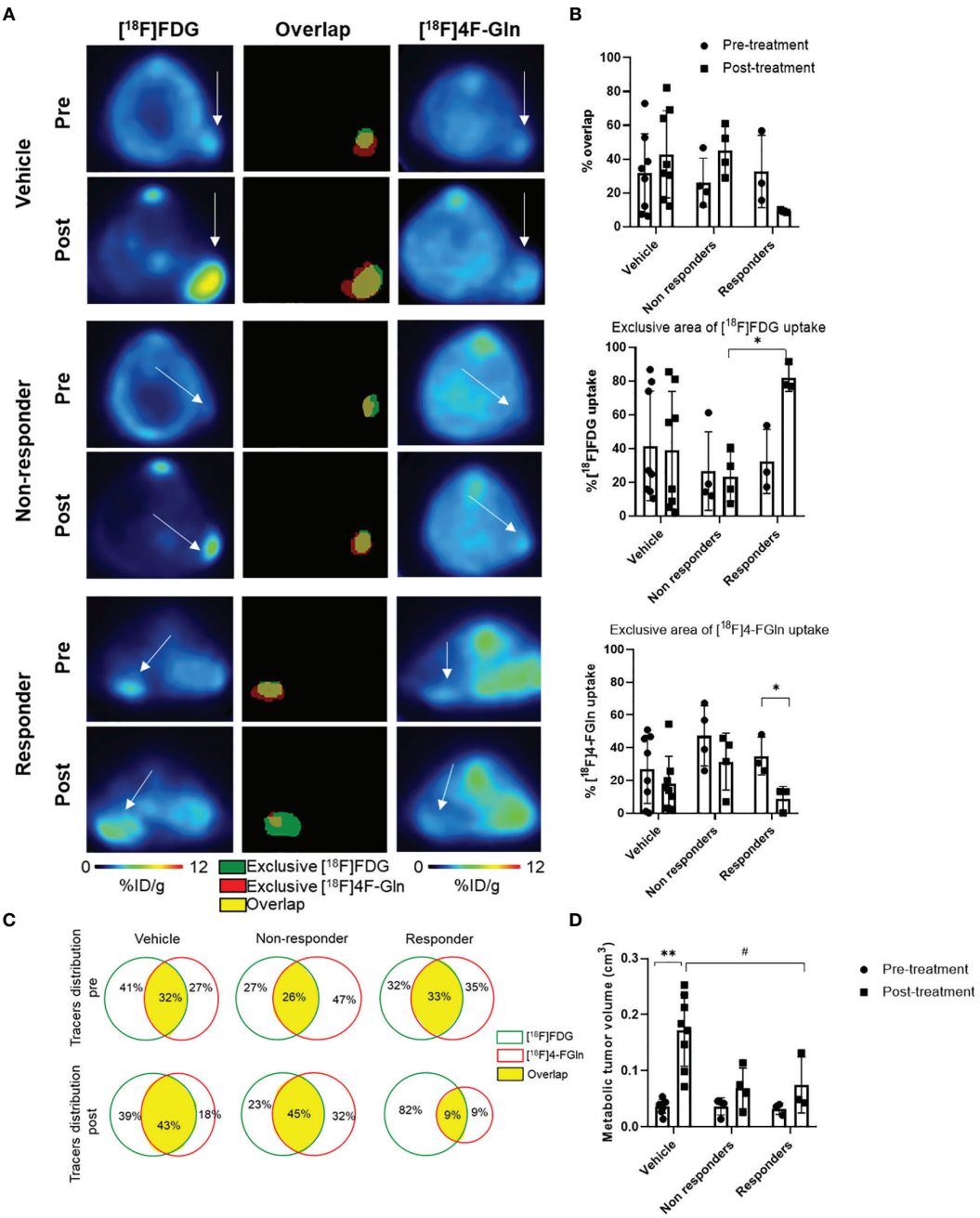

FIGURE 7 | Volumetric analysis defines the distribution of tracers in the tumor and highlights specific therapy-induced alterations in the uptake of individual tracers. **(A)** representative transaxial PET images from [^{18}F]FDG and [^{18}F]4-FGln and the overlay image of [^{18}F]FDG and [^{18}F]4-FGln masks in the same mice (vehicle, Bortezomib-non-responder and responder) pre- and post-treatment. White arrows indicate tumor. In overlay images, green color represents exclusive [^{18}F]FDG uptake, red color represents exclusive [^{18}F]4-FGln uptake, and yellow color represents co-distribution of both radiopharmaceuticals. **(B)** % of overlap, exclusive [^{18}F]FDG and [^{18}F]4-FGln tracer uptake volumes in vehicle- and Bortezomib-treated responder and non-responder groups. Differences intra- and intergroups were tested for significance using one-way ANOVA with multiple comparisons corrected with Tukey's test and Wilcoxon matched pairs signed rank test. *$p < 0.05$. **(C)** Quantitative analysis of single tracers uptake and total distribution pre-and post-treatment in vehicle- and Bortezomib-treated non-responder and responder groups; the green lines represent [^{18}F]FDG unique area, red lines represent [^{18}F]4-FGln unique area, and the yellow filled space is the overlap of both tracers. **(D)** Metabolic tumor volume (sum of [^{18}F]FDG and [^{18}F]4-FGln volume of biodistribution) pre- and post-treatment with vehicle and Bortezomib in responders and non-responders. Differences intra- and intergroups were tested for significance using one-way ANOVA with multiple comparisons corrected with Tukey's test and Wilcoxon matched pairs signed rank test. $^{\#}p = 0.027$; $^{**}p = 0.008$.

DATA AVAILABILITY STATEMENT

The original contributions presented in the study are included in the article/**Supplementary Material**. Further inquiries can be directed to the corresponding authors.

ETHICS STATEMENT

The animal study was reviewed and approved by Italian Ministry of Health (n. 34/2018-PR).

AUTHOR CONTRIBUTIONS

All authors contributed to the study conception and design. Material preparation, data collection, and analysis were performed by SV, DT, MC, AS, AC, AB, GT, MG, FV, FZ, MB, RM, OB, and NG. The first draft of the manuscript was written by NG and DT, and all authors commented on previous versions of the manuscript. All authors read and approved the final manuscript.

FUNDING

The research leading to these results has received funding from: Associazione Italiana per la Ricerca sul Cancro (AIRC) under IG IG2017 ID. 20299 project and International Myeloma Society (IMS) under "Paula and Rodeger Riney Foundation Translational Research Grant" (PI NG) and AIRC under IG 2018, ID. 210808 project (PI BM). The Italian Ministry for Education and Research (MIUR) is gratefully acknowledged for yearly FOE funding to the Euro-BioImaging Multi-Modal Molecular Imaging Italian Node (MMMI). Translational Research Program Grant ID 6618-21 (PI BM) from the Leukemia & Lymphoma Society (L&LS).

ACKNOWLEDGMENTS

We thank Associazione Italiana contro Leucemie, Linfomi e Mielomi ONLUS, ParmAIL for the support. We thank Dr. Stefania Battaglia and Mr. Pasquale Simonelli for technical support in PET acquisitions. We thank Drs. Marta Chesi and Leif Bergsagel (Mayo Clinic Arizona, Scottsdale) for the generous gift of Vk12598 cells.

SUPPLEMENTARY MATERIAL

The Supplementary Material for this article can be found online at: https://www.frontiersin.org/articles/10.3389/fonc.2021.760732/full#supplementary-material

REFERENCES

1. Roodman GD. Pathogenesis of Myeloma Bone Disease. *Leukemia* (2009) 23 (3):435–41. doi: 10.1038/leu.2008.336
2. Cavo M, Terpos E, Nanni C, Moreau P, Lentzsch S, Zweegman S, et al. Role of (18)F-FDG PET/CT in the Diagnosis and Management of Multiple Myeloma and Other Plasma Cell Disorders: A Consensus Statement by the International Myeloma Working Group. *Lancet Oncol* (2017) 18(4):e206–17. doi: 10.1016/S1470-2045(17)30189-4
3. Lu YY, Chen JH, Lin WY, Liang JA, Wang HY, Tsai SC, et al. FDG PET or PET/CT for Detecting Intramedullary and Extramedullary Lesions in Multiple Myeloma: A Systematic Review and Meta-Analysis. *Clin Nucl Med* (2012) 37(9):833–7. doi: 10.1097/RLU.0b013e31825b2071
4. Rasche L, Angtuaco E, McDonald JE, Buros A, Stein C, Pawlyn C, et al. Low Expression of Hexokinase-2 is Associated With False-Negative FDG-Positron Emission Tomography in Multiple Myeloma. *Blood* (2017) 130(1):30–4. doi: 10.1182/blood-2017-03-774422
5. Abe Y, Ikeda S, Kitadate A, Narita K, Kobayashi H, Miura D, et al. Low Hexokinase-2 Expression-Associated False-Negative (18)F-FDG PET/CT as a Potential Prognostic Predictor in Patients With Multiple Myeloma. *Eur J Nucl Med Mol Imaging* (2019) 46(6):1345–50. doi: 10.1007/s00259-019-04312-9
6. Nanni C, Zamagni E, Cavo M, Rubello D, Tacchetti P, Pettinato C, et al. 11C-Choline vs. 18F-FDG PET/CT in Assessing Bone Involvement in Patients With Multiple Myeloma. *World J Surg Oncol* (2007) 5:68. doi: 10.1186/1477-7819-5-68
7. Nakamoto Y, Kurihara K, Nishizawa M, Yamashita K, Nakatani K, Kondo T, et al. Clinical Value of (1)(1)C-Methionine PET/CT in Patients With Plasma Cell Malignancy: Comparison With (1)(8)F-FDG PET/CT. *Eur J Nucl Med Mol Imaging* (2013) 40(5):708–15. doi: 10.1007/s00259-012-2333-3
8. Zhou R, Pantel AR, Li S, Lieberman BP, Ploessl K, Choi H, et al. [(18)F](2S,4R)4-Fluoroglutamine PET Detects Glutamine Pool Size Changes in Triple-Negative Breast Cancer in Response to Glutaminase Inhibition. *Cancer Res* (2017) 77(6):1476–84. doi: 10.1158/0008-5472.CAN-16-1945
9. Miner MW, Liljenback H, Virta J, Merisaari J, Oikonen V, Westermarck J, et al. (2s, 4r)-4-[(18)F]Fluoroglutamine for In Vivo PET Imaging of Glioma Xenografts in Mice: An Evaluation of Multiple Pharmacokinetic Models. *Mol Imaging Biol* (2020) 22(4):969–78. doi: 10.1007/s11307-020-01472-1
10. Xu XX, Zhu H, Liu F, Li N, Zhu L, Kung H, et al. Preliminary Clinical Trasnationl Study of F-18-(2S, 4R) 4-Fluoroglutamine PET/CT Imaging in 17 Breast Cancer Patients. *J Nucl Med* (2018) 59.
11. Bolzoni M, Chiu M, Accardi F, Vescovini R, Airoldi I, Storti P, et al. Dependence on Glutamine Uptake and Glutamine Addiction Characterize Myeloma Cells: A New Attractive Target. *Blood* (2016) 128(5):667–79. doi: 10.1182/blood-2016-01-690743
12. Gonsalves WI, Jang JS, Jessen E, Hitosugi T, Evans LA, Jevremovic D, et al. In Vivo Assessment of Glutamine Anaplerosis Into the TCA Cycle in Human Pre-Malignant and Malignant Clonal Plasma Cells. *Cancer Metab* (2020) 8 (1):29. doi: 10.1186/s40170-020-00235-4
13. Ploessl K, Wang L, Lieberman BP, Qu W, Kung HF. Comparative Evaluation of 18F-Labeled Glutamic Acid and Glutamine as Tumor Metabolic Imaging Agents. *J Nucl Med* (2012) 53(10):1616–24. doi: 10.2967/jnumed.111.101279
14. Qu W, Zha Z, Ploessl K, Lieberman BP, Zhu L, Wise DR, et al. Synthesis of Optically Pure 4-Fluoro-Glutamines as Potential Metabolic Imaging Agents for Tumors. *J Am Chem Soc* (2011) 133(4):1122–33. doi: 10.1021/ja109203d
15. Zhang X, Basuli F, Shi ZD, Xu B, Blackman B, Choyke PL, et al. Automated Synthesis of [(18)F](2S,4R)-4-Fluoroglutamine on a GE TRACERlab FX-N Pro Module. *Appl Radiat Isotopes: Including Data Instrumentation Methods Use Agriculture Industry Med* (2016) 112:110–4. doi: 10.1016/j.apradiso.2016.02.016
16. Amendt C, Staub E, Friese-Hamim M, Storkel S, Stroh C. Association of EGFR Expression Level and Cetuximab Activity in Patient-Derived Xenograft Models of Human non-Small Cell Lung Cancer. *Clin Cancer Res* (2014) 20 (17):4478–87. doi: 10.1158/1078-0432.CCR-13-3385
17. Lo Dico A, Martelli C, Valtorta S, Raccagni I, Diceglie C, Belloli S, et al. Identification of Imaging Biomarkers for the Assessment of Tumour Response to Different Treatments in a Preclinical Glioma Model. *Eur J Nucl Med Mol Imaging* (2015) 42(7):1093–105. doi: 10.1007/s00259-015-3040-7

18. Duncan K, Rosean TR, Tompkins VS, Olivier A, Sompallae R, Zhan F, et al. (18)F-FDG-PET/CT Imaging in an IL-6- and MYC-Driven Mouse Model of Human Multiple Myeloma Affords Objective Evaluation of Plasma Cell Tumor Progression and Therapeutic Response to the Proteasome Inhibitor Ixazomib. *Blood Cancer J* (2013) 3:e165. doi: 10.1038/bcj.2013.61
19. Bailly C, Gouard S, Lacombe M, Remaud-Le Saec P, Chalopin B, Bourgeois M, et al. Comparison of Immuno-PET of CD138 and PET Imaging With (64) CuCl2 and (18)F-FDG in a Preclinical Syngeneic Model of Multiple Myeloma. *Oncotarget* (2018) 9(10):9061–72. doi: 10.18632/oncotarget.23886
20. Curtarello M, Zulato E, Nardo G, Valtorta S, Guzzo G, Rossi E, et al. VEGF-Targeted Therapy Stably Modulates the Glycolytic Phenotype of Tumor Cells. *Cancer Res* (2015) 75(1):120–33. doi: 10.1158/0008-5472.CAN-13-2037
21. Viswanath V, Zhou R, Lee H, Li S, Cragin A, Doot RK, et al. Kinetic Modeling of (18)F-(2s,4r)4-Fluoroglutamine in Mouse Models of Breast Cancer to Estimate Glutamine Pool Size as an Indicator of Tumor Glutamine Metabolism. *J Nucl Med* (2020) 62:1154–62. doi: 10.2967/jnumed.120.250977
22. Logan J, Fowler JS, Volkow ND, Wang GJ, Ding YS, Alexoff DL. Distribution Volume Ratios Without Blood Sampling From Graphical Analysis of PET Data. *J Cereb Blood Flow Metabolism: Off J Int Soc Cereb Blood Flow Metab* (1996) 16(5):834–40. doi: 10.1097/00004647-199609000-00008
23. Krak NC, Boellaard R, Hoekstra OS, Twisk JW, Hoekstra CJ, Lammertsma AA. Effects of ROI Definition and Reconstruction Method on Quantitative Outcome and Applicability in a Response Monitoring Trial. *Eur J Nucl Med Mol Imaging* (2005) 32(3):294–301. doi: 10.1007/s00259-004-1566-1
24. Chesi M, Robbiani DF, Sebag M, Chng WJ, Affer M, Tiedemann R, et al. AID-Dependent Activation of a MYC Transgene Induces Multiple Myeloma in a Conditional Mouse Model of Post-Germinal Center Malignancies. *Cancer Cell* (2008) 13(2):167–80. doi: 10.1016/j.ccr.2008.01.007
25. Calcinotto A, Brevi A, Chesi M, Ferrarese R, Garcia Perez L, Grioni M, et al. Microbiota-Driven Interleukin-17-Producing Cells and Eosinophils Synergize to Accelerate Multiple Myeloma Progression. *Nat Commun* (2018) 9(1):4832. doi: 10.1038/s41467-018-07305-8
26. Zamagni E, Patriarca F, Nanni C, Zannetti B, Englaro E, Pezzi A, et al. Prognostic Relevance of 18-F FDG PET/CT in Newly Diagnosed Multiple Myeloma Patients Treated With Up-Front Autologous Transplantation. *Blood* (2011) 118(23):5989–95. doi: 10.1182/blood-2011-06-361386
27. Moreau P, Attal M, Caillot D, Macro M, Karlin L, Garderet L, et al. Prospective Evaluation of Magnetic Resonance Imaging and [(18)F]Fluorodeoxyglucose Positron Emission Tomography-Computed Tomography at Diagnosis and Before Maintenance Therapy in Symptomatic Patients With Multiple Myeloma Included in the IFM/DFCI 2009 Trial: Results of the IMAJEM Study. *J Clin Oncol: Off J Am Soc Clin Oncol* (2017) 35(25):2911–8. doi: 10.1200/JCO.2017.72.2975
28. Matteucci F, Paganelli G, Martinelli G, Cerchione C. PET/CT in Multiple Myeloma: Beyond FDG. *Front Oncol* (2020) 10:622501. doi: 10.3389/fonc.2020.622501
29. Lapa C, Schreder M, Schirbel A, Samnick S, Kortum KM, Herrmann K, et al. [(68)Ga]Pentixafor-PET/CT for Imaging of Chemokine Receptor CXCR4 Expression in Multiple Myeloma - Comparison to [(18)F]FDG and Laboratory Values. *Theranostics* (2017) 7(1):205–12. doi: 10.7150/thno.16576
30. Venneti S, Dunphy MP, Zhang H, Pitter KL, Zanzonico P, Campos C, et al. Glutamine-Based PET Imaging Facilitates Enhanced Metabolic Evaluation of Gliomas *In Vivo*. *Sci Trans Med* (2015) 7(274):274ra17. doi: 10.1126/scitranslmed.aaa1009
31. Li C, Huang S, Guo J, Wang C, Huang Z, Huang R, et al. Metabolic Evaluation of MYCN-Amplified Neuroblastoma by 4-[(18)F]FGln PET Imaging. *Mol Imaging Biol* (2019) 21(6):1117–26. doi: 10.1007/s11307-019-01330-9
32. Dunphy MPS, Harding JJ, Venneti S, Zhang H, Burnazi EM, Bromberg J, et al. In Vivo PET Assay of Tumor Glutamine Flux and Metabolism: In-Human Trial of (18)F-(2s,4r)-4-Fluoroglutamine. *Radiology* (2018) 287(2):667–75. doi: 10.1148/radiol.2017162610
33. Liu Y, Zhao T, Li Z, Wang L, Yuan S, Sun L. The Role of ASCT2 in Cancer: A Review. *Eur J Pharmacol* (2018) 837:81–7. doi: 10.1016/j.ejphar.2018.07.007
34. Chiu M, Toscani D, Marchica V, Taurino G, Costa F, Bianchi MG, et al. Myeloma Cells Deplete Bone Marrow Glutamine and Inhibit Osteoblast Differentiation Limiting Asparagine Availability. *Cancers* (2020) 12(11). doi: 10.3390/cancers12113267
35. Saltarella I, Frassanito MA, Lamanuzzi A, Brevi A, Leone P, Desantis V, et al. Homotypic and Heterotypic Activation of the Notch Pathway in Multiple Myeloma-Enhanced Angiogenesis: A Novel Therapeutic Target? *Neoplasia* (2019) 21(1):93–105. doi: 10.1016/j.neo.2018.10.011
36. Zhu H, Liu F, Zhang Y, Yang J, Xu X, Guo X, et al. (2s,4r)-4-[(18)F] Fluoroglutamine as a PET Indicator for Bone Marrow Metabolism Dysfunctional: From Animal Experiments to Clinical Application. *Mol Imaging Biol* (2019) 21(5):945–53. doi: 10.1007/s11307-019-01319-4
37. Li Y, Liu J, Huang B, Chen M, Diao X, Li J. Application of PET/CT in Treatment Response Evaluation and Recurrence Prediction in Patients With Newly-Diagnosed Multiple Myeloma. *Oncotarget* (2017) 8(15):25637–49. doi: 10.18632/oncotarget.11418
38. Ludman T, Melemedjian OK. Bortezomib-Induced Aerobic Glycolysis Contributes to Chemotherapy-Induced Painful Peripheral Neuropathy. *Mol Pain* (2019) 15:1744806919837429. doi: 10.1177/1744806919837429
39. Sanchez WY, McGee SL, Connor T, Mottram B, Wilkinson A, Whitehead JP, et al. Dichloroacetate Inhibits Aerobic Glycolysis in Multiple Myeloma Cells and Increases Sensitivity to Bortezomib. *Br J Cancer* (2013) 108(8):1624–33. doi: 10.1038/bjc.2013.120
40. Soriano GP, Besse L, Li N, Kraus M, Besse A, Meeuwenoord N, et al. Proteasome Inhibitor-Adapted Myeloma Cells are Largely Independent From Proteasome Activity and Show Complex Proteomic Changes, in Particular in Redox and Energy Metabolism. *Leukemia* (2016) 30(11):2198–207. doi: 10.1038/leu.2016.102
41. Whitburn J, Edwards CM. Metabolism in the Tumour-Bone Microenvironment. *Curr Osteoporosis Rep* (2021). doi: 10.1007/s11914-021-00695-7
42. Dalva-Aydemir S, Bajpai R, Martinez M, Adekola KU, Kandela I, Wei C, et al. Targeting the Metabolic Plasticity of Multiple Myeloma With FDA-Approved Ritonavir and Metformin. *Clin Cancer Res* (2015) 21(5):1161–71. doi: 10.1158/1078-0432.CCR-14-1088

Conflict of Interest: NG received research funding and honoraria from Bristol Mayers Squibb, Celgene, Millenium Pharmaceutical, GSK, Takeda, and Janssen Pharmaceutical.

The remaining authors declare that the research was conducted in the absence of any commercial or financial relationships that could be construed as a potential conflict of interest.

Publisher's Note: All claims expressed in this article are solely those of the authors and do not necessarily represent those of their affiliated organizations, or those of the publisher, the editors and the reviewers. Any product that may be evaluated in this article, or claim that may be made by its manufacturer, is not guaranteed or endorsed by the publisher.

frontiers in Oncology

ORIGINAL RESEARCH
published: 14 October 2021
doi: 10.3389/fonc.2021.733848

Protein Kinase CK1α Sustains B-Cell Receptor Signaling in Mantle Cell Lymphoma

Sabrina Manni[1,2], Anna Fregnani[1,2], Laura Quotti Tubi[1,2], Zaira Spinello[1,2], Marco Carraro[1,2], Greta Scapinello[1,2], Andrea Visentin[1,2], Gregorio Barilà[1,2], Marco Pizzi[3], Angelo Paolo Dei Tos[3], Fabrizio Vianello[1], Renato Zambello[1,2], Carmela Gurrieri[1,2], Gianpietro Semenzato[1,2], Livio Trentin[1,2] and Francesco Piazza[1,2]**

[1] Department of Medicine-DIMED, Hematology and Clinical Immunology Section, University of Padova, Padova, Italy, [2] Laboratory of Myeloma and Lymphoma Pathobiology, Veneto Institute of Molecular Medicine, Padova, Italy, [3] Department of Medicine-DIMED, Surgical Pathology and Cytopathology Unit, University of Padova, Padova, Italy

OPEN ACCESS

Edited by:
Luca Agnelli,
Istituto Nazionale dei Tumori (IRCCS), Italy

Reviewed by:
Antonello Domenico Cabras,
Istituto Nazionale dei Tumori (IRCCS), Italy
Vaclav Seda,
Central European Institute of Technology (CEITEC), Czechia

***Correspondence:**
Sabrina Manni
sabrina.manni@unipd.it
Francesco Piazza
francesco.piazza@unipd.it

Specialty section:
This article was submitted to Hematologic Malignancies, a section of the journal Frontiers in Oncology

Received: 30 June 2021
Accepted: 06 September 2021
Published: 14 October 2021

Citation:
Manni S, Fregnani A, Quotti Tubi L, Spinello Z, Carraro M, Scapinello G, Visentin A, Barilà G, Pizzi M, Dei Tos AP, Vianello F, Zambello R, Gurrieri C, Semenzato G, Trentin L and Piazza F (2021) Protein Kinase CK1α Sustains B-Cell Receptor Signaling in Mantle Cell Lymphoma. Front. Oncol. 11:733848. doi: 10.3389/fonc.2021.733848

Mantle Cell Lymphoma (MCL) is still an incurable B-cell malignancy characterized by poor prognosis and frequent relapses. B Cell Receptor (BCR) signaling inhibitors, in particular of the kinases BTK and PI3Kγ/δ, have demonstrated clinically meaningful anti-proliferative effects in B cell tumors. However, refractoriness to these drugs may develop, portending a dismal prognosis. Protein kinase CK1α is an emerging pro-growth enzyme in B cell malignancies. In multiple myeloma, this kinase sustains β-catenin and AKT-dependent survival and is involved in the activation of NF-κB in B cells. In this study, we analyzed the role of CK1α on MCL cell survival and proliferation, on the regulation of BCR-related BTK, NF-κB, PI3K/AKT signaling cascades and the effects of CK1α chemical inhibition or gene silencing in association with the BTK inhibitor Ibrutinib or the PI3Kγ/δ inhibitor Duvelisib. CK1α was found highly expressed in MCL cells as compared to normal B cells. The inactivation/loss of CK1α caused MCL cell apoptosis and proliferation arrest. CK1α sustained BCR signaling, in particular the NF-κB, AKT and BTK pathways by modulating the phosphorylation of Ser 652 on CARD11, Ser 536 p65 on NF-κB, Ser 473 on AKT, Tyr 223 on BTK, as well as the protein levels. We also provided evidence that CK1α-mediated regulation of CARD11 and BTK likely implicates a physical interaction. The combination of CK1α inhibition with Ibrutinib or Duvelisib synergistically increased cytotoxicity, leading to a further decrease of the activation of BCR signaling pathways. Therefore, CK1α sustains MCL growth through the regulation of BCR-linked survival signaling cascades and protects from Ibrutinib/Duvelisib-induced apoptosis. Thus, CK1α could be considered as a rational molecular target for the treatment of MCL, in association with novel agents.

Keywords: mantle cell lymphoma, CK1α, BCR inhibitors, ibrutinib, duvelisib, targeted therapy

INTRODUCTION

Mantle Cell Lymphoma (MCL) is a B-cell neoplasm - characterized by clinical and morphological variants (1) - that accounts for about 6% of all Non-Hodgkin Lymphoma (NHL) in the United States, and 7–9% in Europe (2). It is characterized by a high incidence of relapse, even after the introduction of novel drugs in the therapeutic armamentarium (3).

Recent studies have shown that MCL cells display an aberrant activation of survival signaling pathways. These include the B-Cell Receptor (BCR)-related signaling cascades, such as Phosphatidylinositide 3-Kinases/AKT (PI3K/AKT)/mammalian Target Of Rapamycin (mTOR), the Nuclear Factor kappa-light-chain-enhancer of activated B cells (NF-κB) and the Extracellular signal-Regulated Kinase (ERK) cascades, as well as signals elicited by Tumor Necrosis Factor alpha (TNFα), Hedgehog and Wingless (WNT) pathways. Moreover, the B-Cell Lymphoma 2 (BCL-2) family of apoptosis regulators have also been implicated in MCL growth (4).

In normal B cells, after the engagement of the BCR by the antigen, Immunoreceptor Tyrosine-based Activation Motifs (ITAMs) are phosphorylated and this event in turn recruits the cytosolic Src Family tyrosine Kinases (SFKs) Lyn and Spleen Tyrosine Kinase (SYK). Next, the phosphorylation of Bruton Tyrosine Kinase (BTK) on Tyr 551 leads to its autophosphorylation at Tyr 223, necessary for the full activation of this kinase. A subsequent cascade of events follows, through the activation of Phospholipase Cγ2 (PLCγ2) generation of inositol triphosphate (IP_3) and diacylglycerol (DAG), the release of calcium and the stimulation of Protein Kinase C β (PKCβ) (5). PKCβ phosphorylates caspase recruitment domain-containing protein 11 (CARD11) on Ser 652, enabling it to recruit B cell CLL/lymphoma 10 (BCL10) and Mucosa-associated lymphoid tissue lymphoma translocation protein 1 (MALT1) into a multiprotein CARD11-BCL10-MALT1 (CBM1) complex that facilitates the activation of the NF-κB inhibitor (IκB) kinase (IKK), thereby initiating NF-κB signaling (6). Moreover, upon BCR engagement, the stimulation of the PI3K/AKT signal transduction pathway results in the activating AKT phosphorylation on Ser 473.

Ibrutinib is an oral drug, which inhibits BTK enzymatic activity and it is currently employed in the therapy of relapsed/refractory MCL. Even though Ibrutinib has shown an overall response rate of 68% (7), approximately 30% of MCL patients display a primary resistance to the drug, maybe due to a lack of normal BTK expression or presence of mutated BTK (5, 8, 9). Along with Ibrutinib, other BTK inhibitors such as Acalabrutinib and Zanubrutinib are now approved in the relapsed setting in MCL (10). Duvelisib is a PI3Kγ/δ inhibitor approved for the treatment of Chronic Lymphocytic Leukemia (LLC) and Follicular Lymphoma (FL) (11, 12). Its use in MCL is controversial and, to date, there are limited studies regarding the potential use in the therapy of MCL.

Protein kinase CK1 consists of a family of multiple isoforms with distinct biochemical characteristics. In mammalians, seven isoforms are encoded by different genes (α, β, γ1, γ2, γ3, δ and ϵ), which have highly conserved kinase domains, but differ significantly in length and primary structure of their N-terminal and C-terminal regulatory non-catalytic domains (13, 14). CK1 takes part in many cellular processes, such as stress response, DNA damage response, cell cycle progression, spindle-dynamics and chromosome segregation and apoptosis (13, 15).

The isoform α (CK1α) is encoded by the *CSNK1A1* gene, mapping on chromosome 5q32. It regulates a broad range of cellular processes, and it modulates several signaling pathways such as PI3K/AKT, NF-κB, WNT/β-catenin (13, 16). We and others, recently demonstrated that CK1α sustains multiple myeloma (MM) cell growth (17, 18) positively regulating β-catenin and AKT signaling (17) and supporting a prosurvival autophagy (19, 20). CK1α was found highly expressed in MM patients in a large microarray data set series (17). This protein level is reduced by lenalidomide in MM cells and stromal cells, indicating a role in therapy. A recent study has described CK1α as a tumor growth-propeller in Diffuse Large B-cell Lymphoma (DLBCL), by regulating NF-κB signaling intensity (21). In T cells, after antigen receptor engagement, CK1α physically interacts with CARD11 (21) and phosphorylates MALT1 on ser 562, being important for the assembly of the CBM1 complex and the fully activation of NF-κB signaling (22). Several highly potent CK1-specific, ATP competitive, small molecule inhibitors have been identified. D4476 {4-[4(2,3-Dihydro-1,4-benzodioxin-6-yl)-5-(2-pyridinyl)-1H-imidazol-2-yl] benzamide} is one of the best commercially available cell permeant inhibitor specific for CK1 isoforms α and δ (23). Very recently, the compound A-51 was discovered as a novel dual inhibitor of CK1α and the kinase CDK7/9 with an anti-leukemic effect in preclinical models (24).

Given the putative role of CK1α in signal transduction pathways crucial for MCL, in the present study, we investigated its function in MCL downstream of the BCR signaling. We aimed at i) assessing the effect of CK1α inactivation on the proliferation, survival, sensitivity to therapeutic agents and intracellular signaling of MCL cells, ii) evaluating CK1α involvement in the BCR cascade and in sustaining MCL cell "addiction" to the BCR; iii) evaluating if CK1α inhibition could empower BCR inhibitors (such as Ibrutinib and Duvelisib) cytotoxicity for the treatment of MCL.

MATERIAL AND METHODS

Patients and Cell Cultures

PBMC, MCL cell lines Jeko-1, Rec-1, Granta-519 and primary PBMC from patients were isolated and cultured as previously described (25). Malignant and healthy B cells were isolated with EasySep™ kits (STEMCELL Technologies, USA), after achieving informed consent according to the declaration of Helsinki, with approval of the internal Institutional Board (protocol # 4089/AO/17). The clinical features of the patients analyzed are described in **Table 1**.

Chemicals

IPTG was from Sigma-Aldrich, (Italy); Ibrutinib, Duvelisib, Bortezomib and Z-VAD-FMK was from Selleck chemicals (USA); D4476 (4-[4-(2,3-Dihydro-1,4-benzodioxin-6-yl)-5-(2-pyridinyl)-1*H*-imidazol-2-yl]benzamide) was from abcam (UK). Working dilution of D4476 was prepared using Fugene VI reagent (Promega, Italy).

Evaluation of Growth and Apoptosis

Cell viability was measured through Trypan blue exclusion dye assay. Apoptosis was assessed by Annexin V/Propidium Iodide (PI) staining (IMMUNOSTEP, Spain) and FACS analysis as in (17).

TABLE 1 | Clinical and pathological features of MCL cases analyzed.

Patient	Age/sex	Stage/MIPI	IHC					IgH/CCND1 FISH	karyotype	outcome
			CD5	CD20	CD23	Ciclina D1	Ki-67%			
MCL#1	68/M	IVA	+	+	–	+	10-15	nd	nd	A
MCL#2	66/F	IVA	+	+	–	+	nd	nd	nd	A
MCL#3	70/M	IVB	+	+	+	nd	nd	nd	normal	D
MCL#4	76/F	IVA/MIPI 5.9 (*intermediate risk*)	–	+	nd	+	nd	+	normal	A
MCL#5	78/M	IVA	+	+	–	+	40	–	normal	D
MCL#6	51/F	IVB/MIPI 6.6 (*high risk*)	–	nd	–	+	nd	–	normal	A
MCL#7	74/M	IVA/MIPI 9 (*high risk*)	+	+	–	+	40	+	complex*	A
MCL#8	81/F	IVA	+	+	–	+	nd	nd	normal	D
MCL#9	81/M	IVA	+	++	–	+	nd	–	nd	D
MCL#10	65/M	IVA/MIPI6.1 (*intermediate risk*)	+	–	–	+	10	–	normal	A
MCL#11	55/F	IVA	+	++	–	+	nd	nd	nd	A
MCL#12	74/F	IVA/MIPI 6.4 (*high risk*)	+	+	–	+	nd	+	Complex**	A
MCL#13	72/F	IVA/MIPI 6.1 (*intermediate risk*)	+	+	–	+	nd	nd	complex***	D
MCL#14	71/M	nd	+	+	–	+	nd	+	complex****	D
MCL#15	85/F	IVA	+	+	–	+	nd	–	normal	D
MCL#16	71/M	IVA/MIPI 6.1 (*intermediate risk*)	+	+	–	+	nd	+	normal	A
MCL#17	79/M	IVA	+	++	+	+	nd	+	complex°	D
MCL#18	68/M	IVB/MIPI *high risk*	+	++	–	+	nd	+	nd	A
MCL#19	58/M	IVA/MIPI 5.6 (*intermediate risk*)	+	+	–	+	nd	+	complex°°	A
MCL#20	61/M	IVA	+	+	–	+	nd	+	normal	A

MIPI, Mantle cell International Prognostic Index; IHC, immunohistochemistry; nd, not determined; A, alive; D, death. M, male; F, female.

**43,XY,add(1)(q4)?,+3,del(6)(q13),-8,-9,der(10)t(10;13)(p13;q12),del(11)(q13),-13,-13,-14,+mar[13]/46,XY[12].ish add(1)(IGH++,CCND1++),der(11)t(11;14)(CCND1+,IGH+),add(?)(IGH+,CCND1+)[10].*

***47XX,+3,del(6),t(10;15),t(11;14).*

****62,XX,-X,-3,-5,+8,-12,-16,-17,dup(17)(p11p13),-18,+21,i(22)(q10),+mar[cp6]/46,XX[4].*

*****hyperdiploid karyotype due to a low number of mytosis with del(17)(p13) by FISH.*

°42,X,-Y,+3,der(6;17)(q12;p11)?t(6;19)(q12;p13),i(8)(q10),der(11)t(11;14)(q13;q32),-13,-14,-15,add(15)(p13),add(20)(q13)[22]/46,XY[6].nuc ish(CCND1,IGH)x3(CCND1conIGHx2)[233/300].

°°43,C,-Y,+der(3)del(3)(p22)add(3)(q26),dic(4;6)(p16;q13),add(7)(p21),i(8)(q10),-10,t(11;14)(q13;q32),-13.der(15)t(10;15)(q21;q21),-20,-r[cp14]/46,XY[14].

Cell Cycle Analysis

It was performed as described in (17).

Assessment of Drug Concentration-Effect and Calculation of the Combination Index

Jeko-1 and Granta-519 cells were plated into 96 well plates in 100 µl media. D4476, Ibrutinib, and Duvelisib were added at different concentrations for 72 h alone or in combination. Cell viability was analyzed with 3-(4,5-dimethylthiazol-2-yl)- 2,5-diphenyltetrazolium bromide (MTT) and the CI was calculated as in (26).

Immunofluorescence

It was performed as in (26) with the following antibodies: anti-CK1α (abcam, UK), secondary Alexa-Fluor 594-conjugated goat anti-rabbit (Life technologies, Italy), MALT1 and CARD11, (Santa Cruz Biotechnology, Inc (USA) using Alexa-Fluor 488 conjugated anti-mouse. Specimens were mounted in Vectashield medium with DAPI (Vector Laboratories, USA) and analyzed using Zeiss LSM 700 E90 confocal microscope, oil objective 63x (Italy).

Western Blot

WB was performed as described (27). Antibodies used were the following: CK1α, PARP, Mcl1, total β-catenin, Ser 473 AKT, total AKT, Ser 176/180, Ser 177/181 IKKα/α, total IKKα, IKKβ, Ser 536 NF-κB p65, Ser 652 CARD11, Tyr 223 BTK, total BTK, Ser 32 Ikbα, BCL10 (Cell signaling Technology, MA, USA); GAPDH (Ambion, USA), β-actin (Sigma-Aldrich, Italy); p21 (Becton Dickinson, Italy); Caspase 3 (Enzo Life Science, UK); total p65 (abcam, UK), DEPTOR (Millipore, Itlay); CARD11 and BTK for immunoprecipitation (Santa Cruz Biotechnology, Inc; Italy). Images were acquired using the Image Quant LAS 500 chemiluminescence detection system (GE Healthcare, USA).

Immunoprecipitation

Cells were lysed in immunoprecipitation (IP) buffer containing Tris 50mM, NaCl 150 mM, Triton 1%, NP-40 1%, EDTA 2mM, phosphatases and proteases inhibitors (Life technologies and SIGMA Aldrich). 500-800 µg of total protein lysates were precleared for 30 min at 4°C with anti-mouse or anti-goat agarose beads (e-bioscience, Italy), according to the antibody used for the IP. After centrifugation, the supernatant was incubated overnight 4°C with the dedicated antibody (BTK, CARD11 or CK1α) or with the corresponding pre-immune serum. Agarose beads were added to the protein suspension for 2h at 4°C. After extensive washes in IP buffer the immunocomplex was resuspended in Laemmli buffer with β-mercaptoethanol and processed for WB analysis.

RNA Interference

RNA interference (RNAi) was performed with nucleofection of double strand (ds) siRNA and by the generation of inducible

shRNA MCL cell clones. Nucleofection was performed by electroporation of Jeko-1 using the Amaxa system (Lonza, Rockland, Inc.) with 100 pmol of scrambled siRNAs or CK1α targeting siRNAs ON-TARGET plus SMARTpool siRNA (Thermo Scientific, USA), as described (17) through the nucleofector solution R with the program A-023. Cells were harvested at 48h after nucleofection. Cells were simultaneously electroporated with a fluorescent oligonucleotide (siGLO green). The transfection rate, evaluated by FACS analysis, has always been around 95%. To perform shRNA lentiviral transduction, Jeko-1 and Granta-519 cells were transduced with the IPTG inducible lentiviral particles carrying *CSNK1A1*-specific shRNA (pLKO_IPTG_3XLacO, Sigma-Aldrich, Italy) with the sequence TRCN0000006044. $2x10^4$ cells were infected with a multiplicity of infection of 12, using the spinfection method, in the presence of 8μg/ml polybrene (Sigma-Aldrich, Italy). Puromycin selection (1μg/ml) was initiated two days after transduction. A titration curve for puromycin resistance was performed for Jeko-1 and Granta-519 cells by an Antibiotic Kill Curve Assay. Once a cellular clone was established, to induce CK1α silencing, cells were incubated with 500/1000μM IPTG every two/three day for a total of one (in the case of Granta-519) or two (in the case of Jeko-1) weeks, time lapse in which the best knockdown efficacy was obtained.

Quantitative Real-Time PCR

Performed as in (25) using the QuantStudio 5 detection system (Applied Biosystem, CA, USA) with the QuantStudio™ Design and Analysis Software v.1.4.3. The primers used are the following: *BTK* Forward 5'-3' GGGGTTTGCTCAGACTGTCC and Reverse 5'-3' AATCACTGCGGCCATAGCTT; *RELA* Forward 5'-3' CCCCA CGAGCTTGTAGGAAAG and Reverse 5'-3' CCAGGTT CTGGAAACTGTGGAT; *BIRC3* Forward 5'-3' GACA GGAGTTCATCCGTCAAG and Reverse 5'-3' TTCCACGGCA GCATTAAT; *GAPDH* Forward 5'-3' AATGGAAATCCC ATCACCATCT and Reverse 5'-3' CGCCCCACTTGATTTTGG.

Statistical Analysis

Data were examined for their statistical significance with the two-tail unpaired Student's *t* test or ANOVA analysis of variance with *post-hoc* corrections. Values were considered statistically significant at *p* values below 0.05.

RESULTS

CK1α Is Overexpressed in MCL Samples Compared to Healthy B Cells

We analyzed CK1α mRNA expression in different subtypes of B cell derived cancers (through the publicly available database Oncomine), finding that *CSNK1A1* mRNA is highly expressed in MCL human samples as compared to normal B lymphocytes (www.oncomine.org, "Basso Lymphoma" data set). Thus, we evaluated CK1α protein level in purified B lymphocytes from healthy controls, MCL patients and the MCL cell lines Jeko-1, Granta-519 and Rec-1.

Immunoblot and densitometric analysis revealed that all the MCL cell lines and most of MCL patients overexpressed CK1α when compared to normal B lymphocytes, even if with some variability between different MCL samples (**Figure 1A**). Among a total of fifteen MCL patients analyzed, eleven showed CK1α overexpression in malignant B cells at variance from what seen in B cells from healthy controls. CK1α was overexpressed in 100% of patients in **Figure 1A** left, in 80% of patients in **Figure 1A** middle, and in 50% of patients in **Figure 1A** right. On average, 77% of MCL patients and 100% of the MCL cell lines tested showed overexpressed CK1α at the protein level.

To study the localization of the kinase inside B cells, we performed a confocal immunofluorescence analysis in purified B lymphocytes from a healthy control, a MCL patient and in Jeko-1 cells. CK1α localized both in the cytoplasm and in the nucleus of Jeko-1 and MCL patient cells while it was restricted in cytoplasm in healthy B lymphocytes (**Figure 1B**). These data, which are similar to what we observed in another B cell malignancy like MM (17), suggest an abnormal localization of CK1α in MCL cells.

CK1α Sustains MCL Growth and Proliferation

To examine if CK1α is essential for MCL cell growth, Jeko-1, Granta-519, Rec-1 and B cells isolated from 7 MCL patients, were treated with increasing concentrations of the CK1 chemical inhibitor D4476 or with the vehicle DMSO. Apoptosis was investigated through Annexin V (AV) and PI labelling and FACS analysis. Treatment with DMSO alone did not produce any significant changes in cell viability compared to untreated cells. All the MCL cell lines were sensitive to D4476, starting from the 20 μM concentration for Granta-519 and Rec-1 cells and 30 μM for Jeko-1 (**Figures 2A**, **S1**). Even if with some variability, malignant B cells from most of MCL patients proved to be sensitive to D4476 (6 out of 7) used at 40 μM. Of note, B cells from 3 patients were responsive also to the 20 μM D4476 concentration (**Figure 2B**). We previously showed that D4476 is not toxic for healthy B lymphocytes at any concentration used (17).

To validate the results obtained with the chemical inhibitor of CK1 and to investigate the specific role of the α isoform, we used RNAi to knockdown CK1α protein in Jeko-1 cells. CK1α knockdown was obtained through the generation of IPTG-inducible *CSNK1A1* specific shRNAs or with electroporation of double-strand (ds) *CSNK1A1* directed siRNAs (**Figures 2C**, **S1**). The number of apoptotic cells was assessed by FACS analysis of AV/PI positive cells, which showed increased apoptotic rate upon silencing. To exclude off-target effects induced by IPTG *per se*, wt Jeko-1 cells were treated with the same concentration of IPTG and this treatment did not increase apoptosis. The proapoptotic effect of CK1α inhibition or silencing was confirmed by a reduction of uncleaved PARP, pro-caspase 3 and Mcl1 (**Figure 2D**). An effective decrease of CK1α protein levels upon silencing (around 40-50% with both the techniques used) was confirmed (**Figure 2E**). As expected, IPTG treatment did not affect the expression level of CK1α and of pro- and anti-

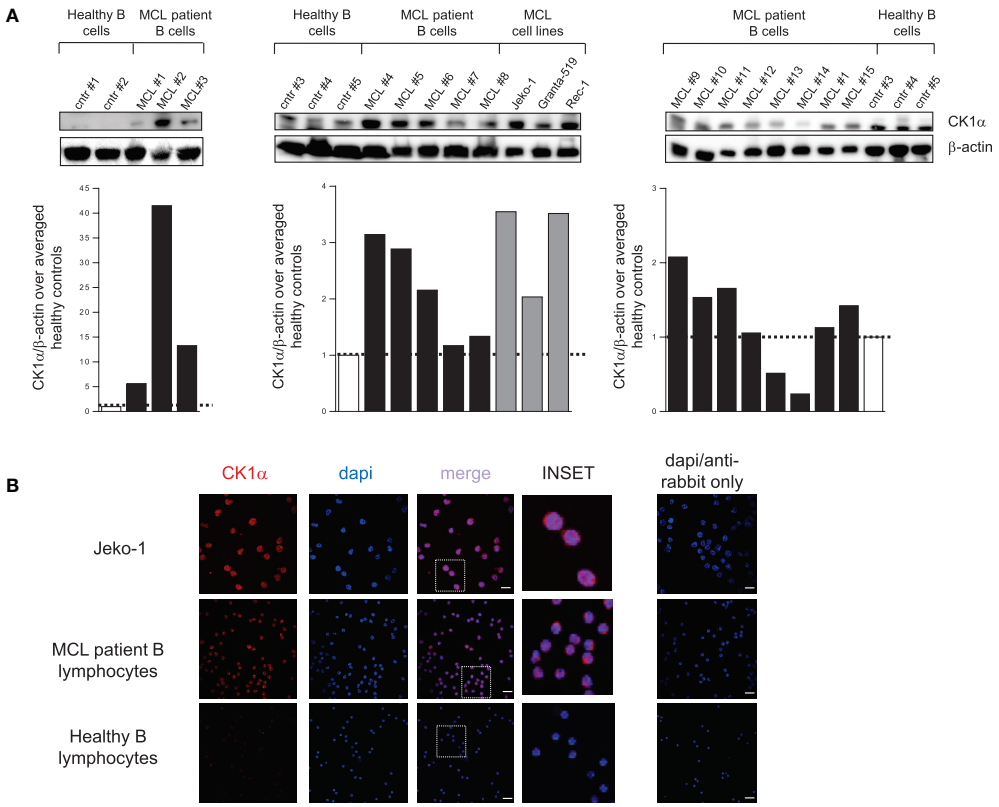

FIGURE 1 | CK1α protein is overexpressed in MCL patients and cell lines compared to controls. **(A)** WB analysis (upper panel) and the corresponding densitometric values (lower panel) of CK1α protein expression in purified B lymphocytes from 5 healthy buffy coats (white bars), from 15 MCL patients (black bars) and from the MCL cell lines Jeko-1, Granta-519 and Rec-1 (grey bars). β-actin was used as a loading control. For each blot, the densitometric values of CK1α in MCL patients and cell lines are reported as arbitrary units over averaged healthy controls within the blot. **(B)** CK1α cellular distribution along with DAPI staining in Jeko-1 cell lines, a MCL patient sample and healthy lymphocytes from buffy coat. CK1α is detected by red fluorescence and nuclei by DAPI. On the right panel staining with only Alexa fluor 594-conjugated goat anti-rabbit secondary antibody merged with dapi is shown. Images were collected with 63X magnification, oil objective. The insert shows a detail of the image. Scale bars = 25μm.

apoptotic proteins in wt Jeko-1 cells, confirming the efficacy/specificity of the silencing strategy. To evaluate the effect of CK1α silencing on MCL cell proliferation, we performed cell cycle analysis of Jeko-1 wt and CK1α–silenced clones treated with IPTG (**Figure 2F**). The pro-apoptotic effect of CK1α knockdown was confirmed by the observation of a substantial increase in the fraction of CK1α-directed inducible shRNA-bearing Jeko-1 cells in the sub-G_1 (apoptotic) phase of the cell cycle upon IPTG treatment. Alongside with the prevalent accumulation of sub-G1 (likely apoptotic) cells, CK1α silencing in the same cellular clone determined a minimal accumulation of cells in G_0/G_1 phase and a more evident reduction of cells in the S phase, suggesting an impairment also of proliferation upon CK1α knockdown. As expected, IPTG treatment of wt cells did not affect cell cycle. Moreover, CK1α silencing, through IPTG treatment for 6 days and for 13 days caused a reduction in the total count of live cells as judged by Trypan blue exclusion assay analysis, indicating a proliferation dysregulation (**Figure 2G**).

CK1α Sustains Chronic Active BCR Dependent Signaling Pathways

CK1α is known to be involved in the regulation of several survival signaling pathways associated with BCR to which MCL cells are addicted for their growth. Bidere et al. (21) defined CK1α as a "conditionally essential malignancy" gene demonstrating that CK1α is required for constitutive NF-κB pathway in DLBCL. To understand if this holds true also for MCL cells, we treated three different MCL cell lines with D4476 40μM or DMSO for 48h and analyzed the NF-κB signaling pathway, in particular the activating phosphorylation of CARD11 on Ser 652, of NF-κB p65 on Ser 536, of the upstream IKKα/β, and of IkBα on Ser 32. Remarkably, the results showed a significant reduction of the activation of the NF-κB pathway upon CK1 chemical inhibition (**Figure 3A**). Most importantly, the specific effects of the inhibition on NF-κB were confirmed also by RNAi, both with IPTG-inducible shRNA transduced Jeko-1 and Granta-519 cells, and with electroporation of ds *CSNK1A1*-directed siRNA in Jeko-1 cells (**Figures 3B, C**). Surprisingly, CK1α inactivation not only

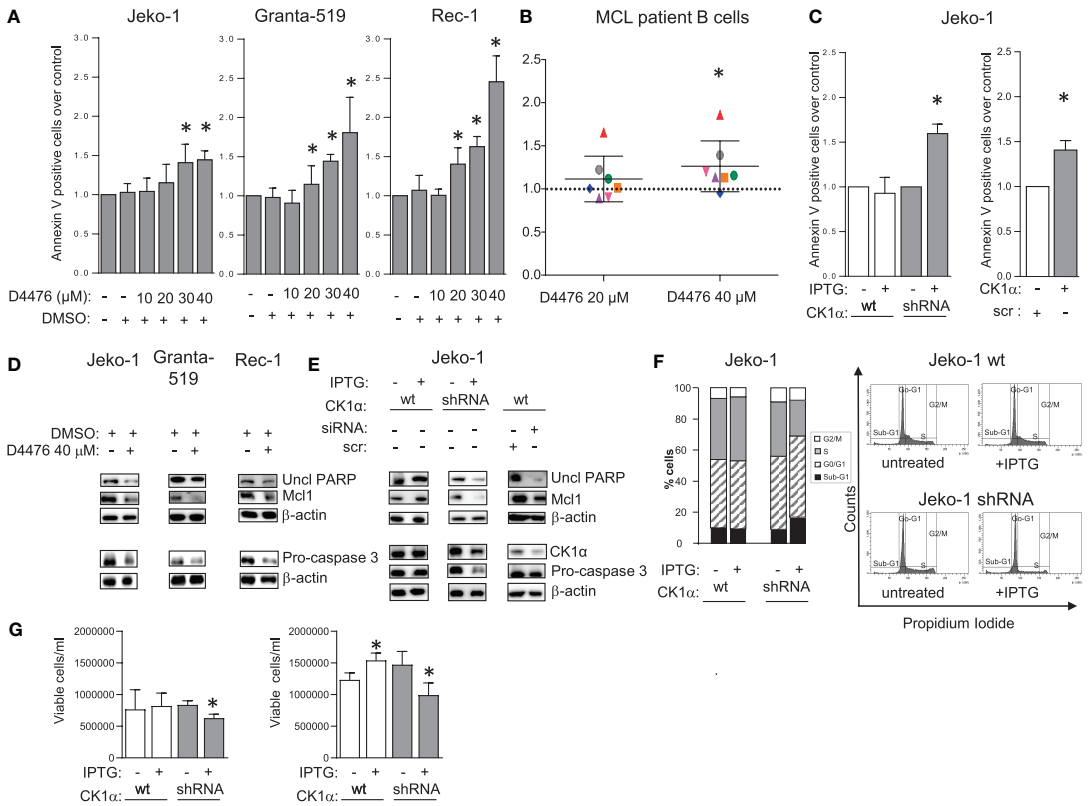

FIGURE 2 | CK1α sustains MCL cell survival and proliferation. Histogram showing annexin V positive cells of MCL cell lines Jeko-1 Granta-519 and Rec-1 **(A)**, 7 independent MCL patients B cells **(B)** treated with different concentration of D4476 for 48h **(A)** or 24h **(B)**, Jeko-1 IPTG inducible *CSNK1A1* directed shRNA clone (named CK1α shRNA) and Jeko-1 wt treated with IPTG 500μM for 13 days (**C** left panel) or Jeko-1 cells electroporated with *CSNK1A1* directed siRNAs for 48h (**C** right panel). Data are expressed as mean ± SD of n=3 **(A)**, n=7 **(B)** n=4 (**C** left panel) and n=3 (**C** right panel) independent experiments. * indicates $p < 0.05$ compared to the untreated cell population. The silencing efficacy and the expression of anti-apoptotic proteins are showed in **(D, E)** In WB panels, β-actin was used as loading control. Uncl PARP= Uncleaved PARP. **(F)** cell cycle distribution with PI staining and FACS analysis of the same cells as in **(C)**. Left: bar graph representing the average of four independent experiments of the sub-G1 (black), G0/G1 (striped, gray), S (grey) and G2/M (white) phases of the cell cycle. Right: representative FACS histogram plots. **(G)** Trypan blue negative (viable) Jeko-1 wt (white bars) and Jeko 1 shRNA cellular clone (grey bars) treated with IPTG 500μM for 6 days (left panel) or 13 days (right panel). Data are expressed as mean ± SD of n=3 experiments (wt and shRNA clone, left panel), n=4 experiments (wt Jeko-1 right panel) and n=8 experiments (Jeko-1 shRNA clone, right panel). * indicates $p < 0.05$ compared to the corresponding untreated cell population.

caused a decrease in the activating phosphorylations of CARD11 on Ser 652, NF-κB-p65 on Ser 536, IKKα/β on Ser 176/180, Ser 177/181, but also in their total protein levels. Consequently, CK1α loss-of-function determined a reduced mRNA expression of the NF-κB-p65 target *BIRC3* (**Figure 3D**). *BIRC3* encodes for c-IAP-2 (cellular inhibitor of apoptosis), which confers resistance to apoptosis.

It has previously been demonstrated that CK1α controls canonical NF-κB activation in stimulated T and in DLBCL cells, participating to the activation of the upstream CBM1 complex (CARD11, BCL10, MALT1), through the phosphorylation of CARD11 and MALT1 (21, 22). We therefore evaluated a possible interaction between CK1α and the CBM1 complex in MCL cells. We stimulated Jeko-1, Granta-519 and MCL patients B cells with anti-IgM to fully activate the BCR and NF-κB signaling, and we performed immunoprecipitation and immunofluorescence experiments using CARD11 and CK1α antibodies. We found that CK1α associates with the CBM1 complex at basal and anti-IgM stimulated conditions (**Figures 4A–C**), as evidenced by coimmunoprecipitation of CK1α and CARD11 and as suggested by cellular colocalization studies of CK1α with CARD11 and MALT1 (**Figure S2**). Of note, CK1α silencing in Jeko-1 determined a reduction of CARD11 and BCL10 protein levels (**Figure 4D**) accompanied by a decrease in basal and anti-IgM-induced NF-κB pathway activation (**Figure 4E**). Of note, the perturbation of NF-κB signaling is achieved also within 72h (shorter) incubation time with IPTG treatment (silencing), indicating an acute/direct effect of CK1α silencing.

As previously mentioned, PI3K/AKT is an essential cascade constitutively active in a subset of MCL, including all the aggressive blastoid variants and in MCL cell lines (28). It is known that CK1α may impinge on the PI3K/AKT pathway (17). Therefore, we sought to investigate whether CK1α could regulate this cascade also in MCL. CK1 chemical inhibition with D4476 in Jeko-1, Granta-519, Rec-1 MCL cells (**Figure 5A**) and CK1α silencing through the IPTG inducible method in Jeko-1 and

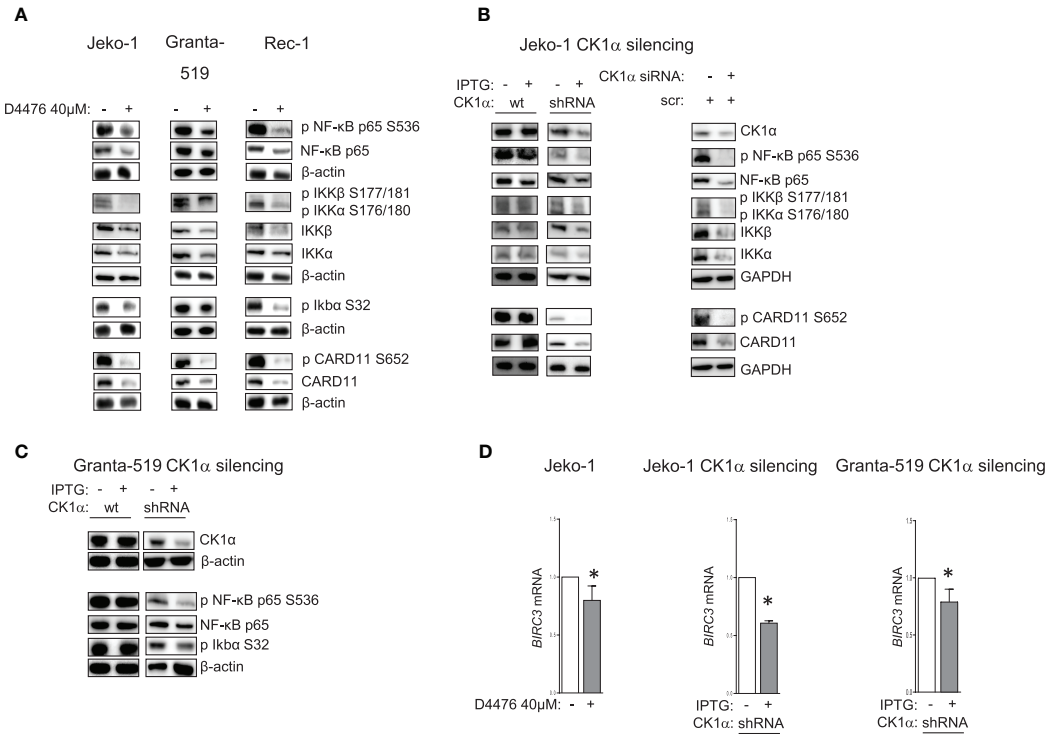

FIGURE 3 | CK1α sustains NF-kB signaling pathway. Representative WB of NF-κB dependent signaling in MCL cell lines Jeko-1, Granta-519 and Rec-1, treated with D4476 40uM for 48h **(A)**, in Jeko-1 IPTG inducible *CSNK1A1* directed shRNA clone (named CK1α shRNA) and in Jeko-1 wt treated with IPTG 500μM for 13 days (**B** left panel) or Jeko -1 cells electroporated with *CSNK1A1* directed siRNAs (**B** right panel), or in Granta-519 IPTG inducible *CSNK1A1* directed shRNA clone (named CK1α shRNA) treated with IPTG 500μM for 72h **(C)**. Membranes for WB analysis were probed with antibodies listed in the figure. GAPDH or β actin were used as loading control. Experiments were repeated at least three times **(D)**. *BIRC3* mRNA expression in Jeko-1 treated with D4476 40uM for 48h, (left panel) or in Jeko-1 IPTG inducible *CSNK1A1* directed shRNA clone treated with IPTG 500μM for 13 days (middle panel) or in Granta-519 IPTG inducible *CSNK1A1* directed shRNA clone treated with IPTG 500μM for 7 days (right panel). Data represent mean ± SD of at least 3 independent experiments. * indicates $p < 0.05$.

Granta-519 led to a reduction of the phosphorylation of AKT on Ser 473 and of total AKT (**Figures 5B, C**). Wild-type Jeko-1 or Granta-519 cells treated with IPTG did not show any changes in the phosphorylated/total AKT protein content. It is known that CK1α phosphorylates the mTOR inhibitor DEPTOR, leading to its proteasomal degradation. As expected, as a consequence of CK1α silencing, DEPTOR level increased (**Figure 5B**). The reduction in AKT activating cascade is present also in *CSNK1A1* directed siRNA transiently transfected Jeko-1 cells (**Figure 5B**).

Since CK1α may have a broader regulative role on the BCR-transduced signal, we next investigated whether CK1α inhibition could affect other BCR-triggered events, such as BTK activation. **Figure 5** shows that both the BTK activating phosphorylation on Tyr 223 and the total amount of the BTK protein are downregulated when CK1α is chemically inhibited or silenced, indicating that CK1α could sustain BTK activity in MCL cells.

The observed CK1α modulation of some BCR dependent signaling cascades was present also at early time points of D4476 treatment, such as 6h (activating phosphorylation of AKT and CARD11) and 24h (activating phosphorylation of AKT and BTK) (**Figure S3**). To exclude a global rewiring of survival signaling events downstream the BCR as a direct effect of CK1α inhibition dependent cytotoxicity, and to selectively ascribe the effects observed on NF-κB, AKT and BTK cascades directly to the activity of CK1α, we also evaluated the effects of CK1α inactivation on ERK/MAP kinase signaling. To note, neither the chemical inhibition nor silencing of CK1α modified ERK 1,2 activating phosphorylation on Thr 202, Tyr 204, (**Figures 5** and **S3**), pointing to a role of CK1α in sustaining specifically NF-κB, AKT and BTK BCR dependent cascades. Altogether, the observation of early signaling changes upon CK1α inactivation indicates that they are very unlikely due to the ongoing apoptotic process. To investigate the mechanism of CK1α dependent regulation of BTK and NF-κB p65 stability, we checked whether the effects observed upon CK1α inactivation were due to transcriptional or post-translational mechanisms. Interestingly, we found that the mRNA expression of *BTK* and *REL A (p65)* did not change upon CK1α chemical inhibition or silencing, suggesting a post-translational mechanism of regulation of these two proteins (**Figures S4A, B**). We next asked whether this mechanism could be proteasome- or caspase-dependent. To this aim, the CK1α-directed shRNA transduced Jeko-1 clone was treated with Bortezomib (7.5nM), a clinically

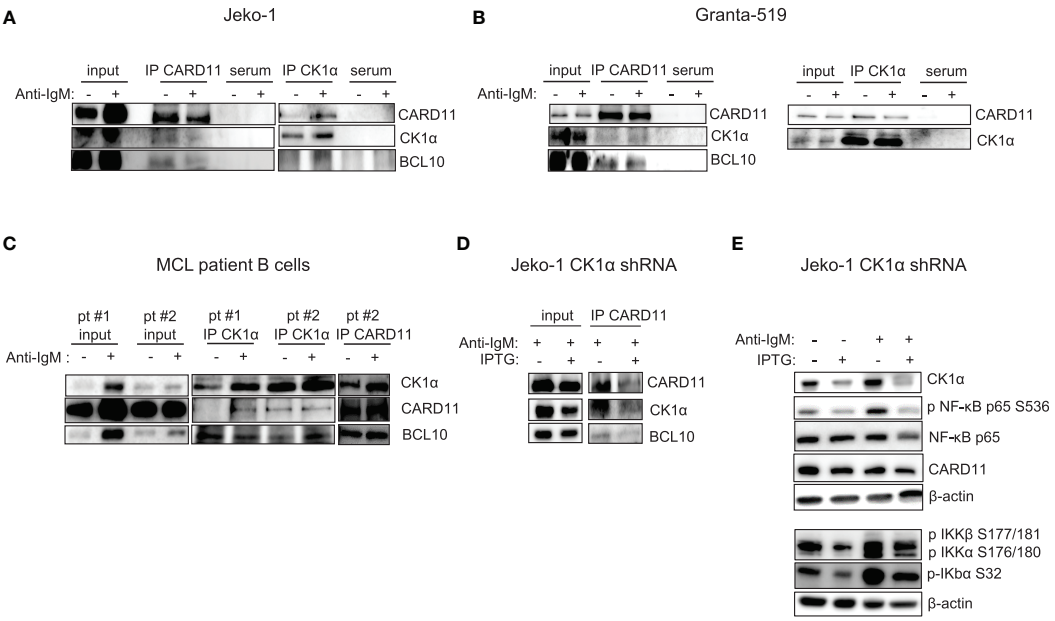

FIGURE 4 | CK1α associates with the CBM1 complex, and its silencing reduces basal and anti-IgM induced NF-kB activation. **(A)** Immunoprecipitation (IP) of CARD11 and CK1α in Jeko-1 **(A)**, Granta- 519 **(B)**, purified B lymphocytes from two MCL patients (pt#1 and pt#2) **(C)**, stimulated with anti-IgM 10μg/ml for 5 min (serum= preimmune serum). **(D)** CK1α silencing reduces the binding of CK1α to CARD11 and BCL10 in the CBM1 complex in anti-IgM stimulated Jeko-CK1α shRNA inducible clone. Untreated and IPTG treated (500μM for 72h) Jeko-1 cells from the CK1α shRNA cellular clone were stimulated with anti-IgM 10μg/ml for 5 min and IP was carried out using CARD11 antibody. **(E)** CK1α silencing affects basal and anti-IgM stimulated NF-κB activation. Cells were treated as in **(D)**. WB was probed with antibodies listed in the figure. β-actin was used as loading control.

used proteasome inhibitor or with Z-VAD-FMK (2μM), a cell permeant pan-caspase inhibitor, along with IPTG to silence CK1α. Remarkably, p65 and BTK protein levels remained downregulated with the association of CK1α and bortezomib, while the CK1α silencing dependent reduction was rescued by Z-VAD-FMK treatment, suggesting that BTK and p65 degradation might be due to a caspase- rather than to a proteasome-dependent mechanism (**Figure S4C**).

Given the novel, unanticipated potential role of CK1α in regulating BTK function, we analyzed if these two kinases could physically interact. To this aim, we treated MCL cells with anti-IgM for 5 min and BTK was subsequently immunoprecipitated. Strikingly, CK1α was present in the immunocomplex (**Figure 5D**). To test specificity and BCR activation, phosphorylated AKT on Ser 473, indicative of fully activated BCR, was evaluated. Interestingly, CK1α physically interacts with BTK also at basal condition in patient isolated B cells from a particularly aggressive form of MCL. Thus, CK1α physically interacts with BTK downstream from the BCR in MCL cells.

CK1α Inactivation Empowers BCR Inhibitor-Induced Cytotoxic Effects on MCL

Given the aforementioned role of CK1α on BCR related signaling cascades, we next asked whether CK1α could interfere with BCR inhibitors (such as Ibrutinib or Duvelisib) -induced MCL cell apoptosis. Since we showed an unprecedented role of CK1α in sustaining BTK levels and activity and given the known role of CK1α on the BTK downstream CBM1 complex, we reasoned that its inhibition or silencing combined with direct BTK targeting would produce cooperative/synergic cytotoxic effects. Therefore, we treated three MCL cell lines, primary MCL B cells and healthy B lymphocytes with different doses of D4476 and Ibrutinib, alone or in combination. Annexin V staining and FACS analysis showed a cooperative effect of D4476 and Ibrutinib in inducing cell death in MCL cells (**Figures 6A, B** and **S5A**). This did not hold true for normal B cells, which were spared by the cytotoxic activity of D4476 (**Figure 6C**). The therapeutic potential of the association of Ibrutinib with CK1α inactivation was confirmed also in the models of CK1α silencing. Treatment with IPTG of *CSNK1A1*-directed shRNA transduced Jeko-1 clones significantly empowered Ibrutinib induced apoptosis (**Figures 6D** and **S5B**). Of note IPTG-treated wt Jeko-1 cells did not show increase in apoptosis compared to Ibrutinib-only treated cells, confirming the efficacy and the specificity of the silencing method. These results were confirmed also in experiments of nucleofection of *CSNK1A1*-directed siRNAs in Jeko-1 cells (**Figure 6D**). The rise in apoptosis in the combination treatments was confirmed by immunoblot analysis of PARP cleavage (**Figure S5C**). Moreover, MTT viability assays in the presence of increasing concentrations of Ibrutinib, D4476 or the combination of the two drugs for 72 h showed a strong synergic effect of the two compounds, as judged by the calculated Combination Index (CI) below 1 (**Figure 6E**). Of note, the

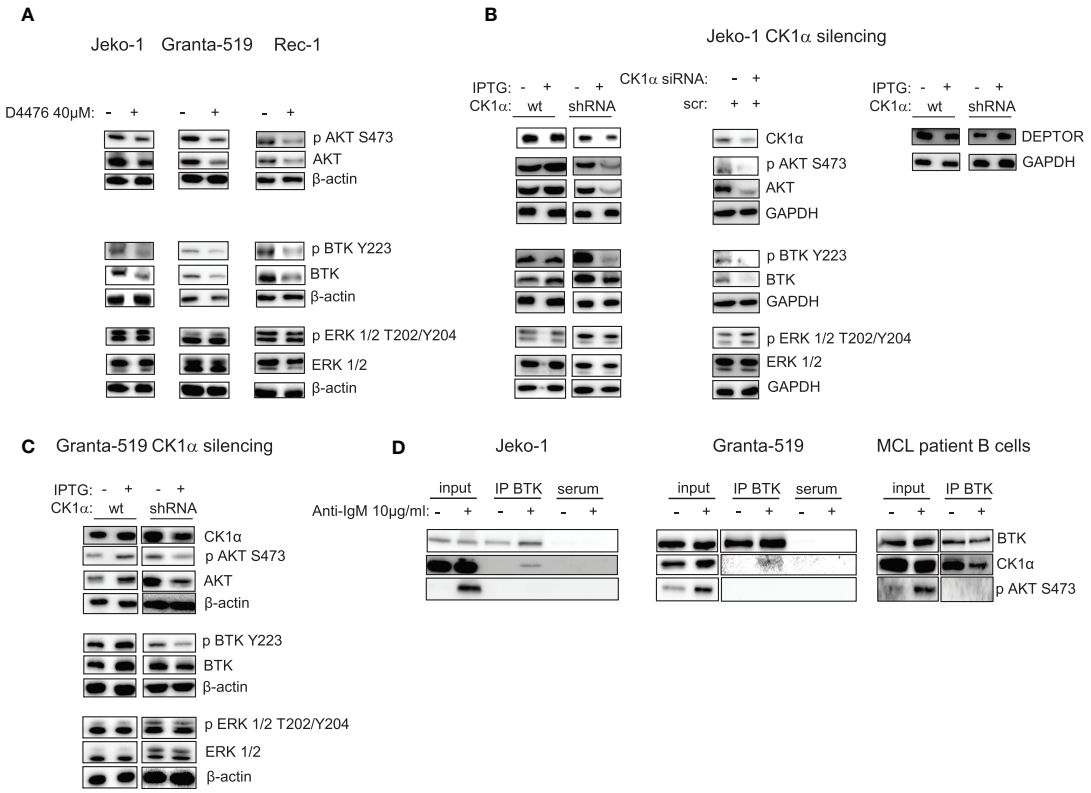

FIGURE 5 | CK1α inactivation reduces AKT and BTK signaling pathways activation without affecting ERK/MAPK kinase and CK1α interacts with BTK in MCL cells. Representative WB of AKT, BTK and ERK1/2 dependent signaling in MCL cell lines Jeko-1 Granta-519 and Rec-1 treated with D4476 40uM for 48h **(A)** or in Jeko-1 IPTG inducible *CSNK1A1* directed shRNA clone (named CK1α shRNA) and in Jeko-1 wt treated with IPTG 500μM for 13 days (**B** left and right panel) or Jeko -1 cells electroporated with *CSNK1A1* directed siRNAs (**B** middle panel), or in Granta-519 IPTG inducible *CSNK1A1* directed shRNA clone (named CK1α shRNA) treated with IPTG 500μM for 72h **(C)**. Membranes for WB analysis were probed with antibodies listed in the figure. GAPDH or β actin was used as loading control. Experiments were repeated at least three times. **(D)** Immunoprecipitation (IP) of BTK in Jeko-1 (left panel), Granta-519 (middle panel), or purified B lymphocytes from one MCL patient (pt#2) (right panel), stimulated with anti-IgM 10μg/ml for 5 min. WB was probed with anti-CK1α and anti-BTK antibodies. To ensure BCR activation AKT phosphorylation on S473 (pAKT S473) was detected after anti-IgM stimulation in the total cell lysate (input).

synergy was present also in Granta-519 cells, a line known to be less sensitive to Ibrutinib (IC50 in Granta-519 28 μM *versus* 11 μM for Jeko-1), suggesting that CK1α inhibition could partly overcome Ibrutinib resistance.

Analysis of intracellular signaling revealed that Ibrutinib cooperated with CK1 inactivation (both chemical inhibition with D4476 and gene silencing) in modulating NF-κB, AKT and BTK-dependent cascades by further reducing the levels of phosphorylated NF-κB-p65 on Ser 536, AKT on Ser 473 and BTK on Tyr 223, without affecting ERK1/2 MAP kinase activity (**Figures 7A, B**). To note, we noticed that in Ibrutinib-treated Jeko-1 cells CK1α expression was decreased. We therefore treated all the MCL cell lines available with different concentrations of Ibrutinib for 24h. Strikingly, Ibrutinib effectively caused a reduction of CK1α protein expression in Jeko-1, Rec-1 and - even if to a lower extent - in Granta-519 cells (**Figure 7C**). The effectiveness of Ibrutinib was confirmed by the abolition of phosphorylated BTK on Tyr 223.

We next tested the interaction of CK1α inhibition with Duvelisib, a PI3Kγ/δ inhibitor approved for the treatment of Chronic Lymphocytic Leukemia (CLL) and Follicular Lymphoma (FL). However, its use in MCL is still under scrutiny (29, 30).

We first verified the efficacy of Duvelisib on a panel of MCL cell lines and purified B cells from six MCL patients. Cells were treated with different doses of Duvelisib for 24 and 48 h. Duvelisib caused MCL cell apoptosis in a dose and time dependent manner. The efficacy of the drug was monitored by assessing the levels of phosphorylated AKT on Ser 473, which were always reduced in all the cells treated (**Figure S6**). Next, the effects on apoptosis of the combination of CK1α inhibition together with Duvelisib was analyzed through Annexin V staining and FACS analysis. Jeko-1, Granta- 519, Rec-1 MCL cells were treated with D4467 and Duvelisib alone or in combination (**Figures 8A** and **S7**). Also, Jeko-1 CK1α silenced cells were treated with Duvelisib (**Figure 8B**). The combination of Duvelisib and CK1α inactivation cooperatively increased the cytotoxicity induced by the single agents. Of note, this cooperation was absent in healthy normal B cells, which were spared by D4476-induced cytotoxicity (**Figure 8C**). The higher rate of apoptosis obtained in the combination experiments was

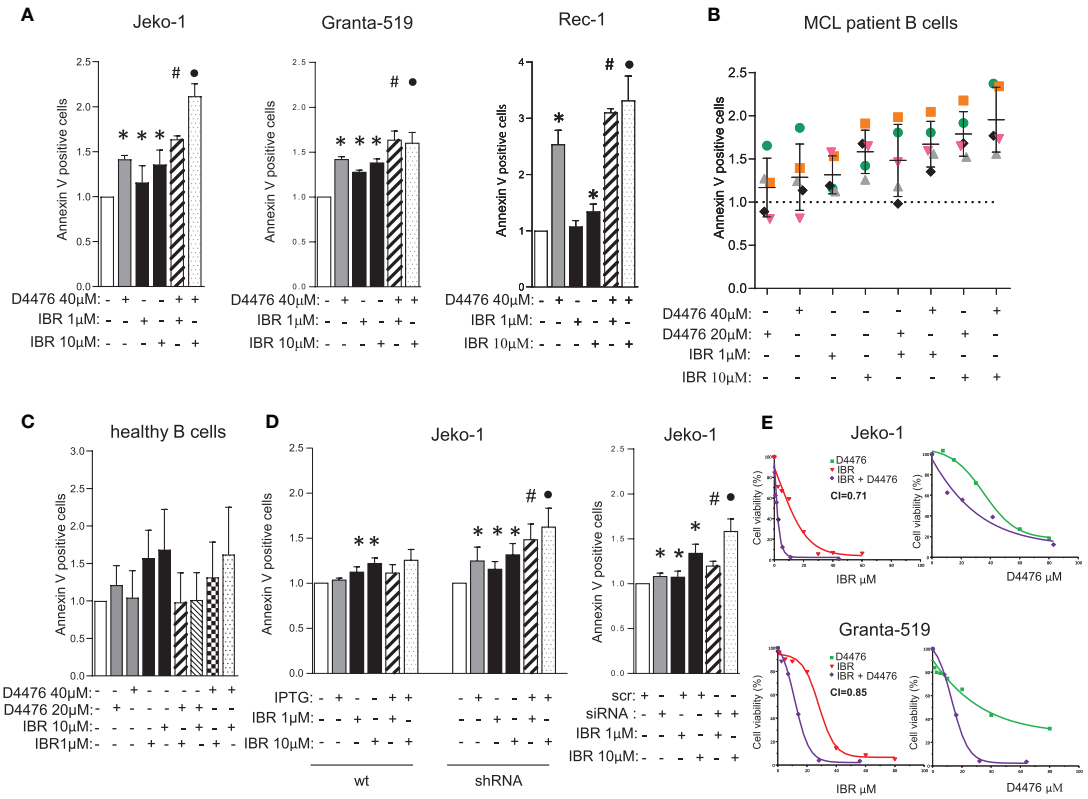

FIGURE 6 | CK1α inactivation empowers Ibrutinib induced cytotoxicity. **(A–D)** Annexin V staining and FACS analysis of MCL and healthy B cells in which CK1α inactivation was associated with Ibrutinib (IBR) treatment. MCL cell lines Jeko-1, Granta-519, Rec-1 **(A)**, were treated with D4476 40 μM for 48h, B cells derived from MCL patients (n=5, **B**), or healthy B cells (n=4, **C**), were treated with D4476 20 μM or D4476 40 μM for 24h. From A to C, Ibrutinib 1 μM or 10 μM, alone or in combination with D4476 was added for the last 24h. Jeko-1 wt or Jeko-1 IPTG inducible *CSNK1A1* directed shRNA clone (named CK1α shRNA) were treated with IPTG 500μM for 13 days (**D** left panel), Jeko-1 wt cells were electroporated with *CSNK1A1* directed siRNAs oligo for 48h (**D** right panel), and treated with Ibrutinib 1 μM or 10 μM, alone or in combination with CK1α silencing for the last 24h. Data represent the mean ± SD of at least three independent experiments. * indicates $p < 0.05$; # indicates $p < 0.05$ between samples treated with Ibrutinib 1 μM together with D4476 (or CK1α silencing) and Ibrutinib 1 μM or D4476/CK1α silencing alone; • indicates $p < 0.05$ between samples treated with Ibrutinib 10 μM together with D4476 (or CK1α silencing) and Ibrutinib 10 μM or D4476/CK1α silencing alone. **(E)** Synergistic effect of D4476 and Ibrutinib in reducing cell viability. Dose response curve of Jeko-1 (upper) and Granta-519 (bottom) incubated for 72 hours with increasing concentrations of D4476 alone, (green squared curve), of Ibrutinib alone (red tringle curve), and with the combination of D4476 and Ibrutinib (purple squared curve). Cell viability was assessed with MTT test and reported as percentage over untreated cells. In Jeko-1, IC50 for D4476 alone was 41.5μM and for Ibrutinib alone was 11μM. IC50 for D4476 used in combination with Ibrutinib was 24μM, while IC50 for Ibrutinib used together with D4476 was 1.6μM. The CI between D4476 and Ibrutinib was calculated as to be 0.71. In Granta-519, IC50 for D4476 alone was 32μM and for Ibrutinib alone was 28μM. IC50 for D4476 used in combination with Ibrutinib was 14μM, while IC50 for Ibrutinib used together with D4476 was 12μM. The CI between D4476 and Ibrutinib was calculated as to be 0.85.

confirmed also by immunoblot analysis of PARP, pro-caspase 3 and Mcl1 protein cleavage (**Figure 8D**). The effect was synergic since the calculated combination index was lower than 1 (**Figure 8E**). Of note, CK1α inactivation caused a significant reduction of the IC50 of Duvelisib in the more resistant Granta-519 cells (**Figure 8E**). Interestingly, as observed with Ibrutinib, treatment with Duvelisib at different concentrations caused a reduction of CK1α protein expression in MCL cells (**Figure S8**).

DISCUSSION

In this work we have provided evidence that the Ser/Thr kinase CK1α is a pivotal regulator of the BCR cascades and may be targeted to enhance the cytotoxic effects of BCR inhibitors, suggesting the rationale for innovative therapeutic strategies for patients with MCL in association with novel agents.

Our findings suggest that CK1α has a pro-survival role in MCL cells, through the regulation of BCR-linked signaling cascades and protects from Ibrutinib/Duvelisib-induced apoptosis indicating that CK1α could be a novel targetable molecule in this malignancy. We described here that CK1α inactivation disrupts the activity of specific critical cascades, namely NF-κB, PI3K/AKT, BTK, which sustain BCR addiction in MCL. Therefore, CK1α inhibition may be a powerful way to boost BCR inhibitors -mediated cell death in MCL.

We showed here that the expression of CK1α, even with a variable outcome, was elevated in most of MCL patients' B cells

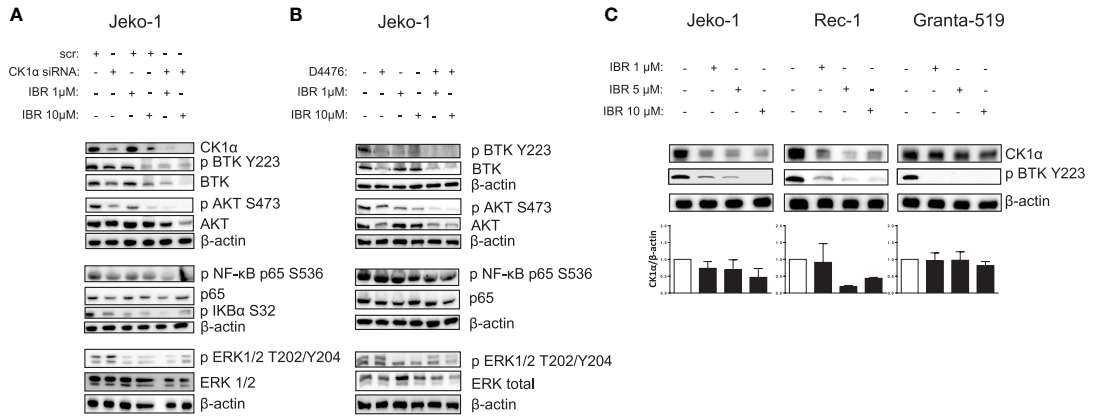

FIGURE 7 | Ibrutinib cooperates with CK1 inactivation in modulating BCR dependent signaling cascades, reducing also CK1α expression. **(A, B)** Representative WB of NF-kB p65, BTK, AKT, ERK1/2 dependent phosphorylation and total protein expression in Jeko-1 cells electroporated with *CSNK1A1* directed siRNA for 48h **(A)**, and in Jeko- 1 exposed to D4476 40 μM for 48h **(B)**, treated with Ibrutinib (IBR) 1 μM or 10 μM for the last 24h. β actin was used as loading control. The figure shows a representative WB, that was performed on at least 3 independent experiments. **(C)** Representative WB (upper panel) and densitometric analysis (lower panel) of CK1α protein expression in Jeko-1, Rec-1, Granta-519 MCL cells, treated with Ibrutinib 1μM, 5μM and 10 μM for 24h, of three (Jeko-1), two (Rec-1), four (Granta-519) independent experiments. β actin was used as loading control.

and in all the MCL cell lines analyzed compared to B cells from healthy controls. At variance with normal B cells, we found an atypical nuclear diffuse microspeckled localization in MCL cells, similar to what we already observed in MM (17). Several reports have established that CK1α is associated with distinct structures and factors in the cell and has a cell-cycle-dependent subcellular distribution (31). The nuclear diffusion of CK1α in MCL and MM samples suggests that this localization could be a feature of CK1α in B-cell derived tumors. CK1α might have nuclear roles dependent on the transformed status. However, at present there are no data that allow to speculate whether this kinase takes part in the regulation of gene transcription, DNA metabolism or chromatin dynamics in MCL.

We also demonstrated that CK1α sustains MCL survival and proliferation. The alterations of the cell cycle and the arrest of proliferation, seen upon CK1α silencing, suggest that CK1α has a role in cell division. Indeed it has been previously demonstrated that CK1α might participate in mitosis regulating spindle placing (32). Moreover, phosphoproteomics data suggest a putative regulative role for CK1α in phosphorylation of about 50% of mitosis-related phosphopeptides (33).

In addition, the prosurvival effects of CK1α might depend on its known role in the regulation of the intensity of NF-κB activation downstream the BCR (21, 22) and, as suggested by our observation in MM cells, in the upholding of the PI3K/AKT pathway (17). The relevance of these two pathways in MCL are well-established. Aberrant NF-κB activation is associated with maintenance and progression of a range of lymphoid malignancies, including MCL (34, 35). Moreover, a constitutive activation of the PI3K/AKT pathway contributes to the pathogenesis of MCL likely due to loss of PTEN expression (28). Ibrutinib resistance in CLL and DLBCL could be attributed to aberrant activation of the AKT pathway (36). Indeed, initial reports indicate that targeting PI3K may overcome Ibrutinib intolerance/resistance in CLL (37) and Richter syndrome (38).

Indeed, our experiments demonstrated that CK1α sustains the NF-kB dependent signaling (**Figure 3**). Inhibition or silencing of CK1α led to a reduction of both phosphorylated and total NF-kB p65. The level at which CK1α seems to act in the NF-kB signaling is upstream of p65, since phosphorylation and total IKKα/IKKβ protein levels were also reduced. Importantly, the demonstration that CK1α inhibition/silencing significantly causes a reduction of CARD11 phosphorylation and levels and that CK1α is present in the CBM1 complex, both at resting and at BCR-stimulated conditions (**Figure 4**), suggests that this kinase might regulate the IKK/NF-κB activation by sustaining the activity of CARD11, as shown in DLBCL (22).

Moreover, we have also provided evidence that CK1α regulates other pivotal signaling molecules in MCL cells (**Figure 5**). Indeed, CK1α inhibition or silencing led to a reduction of AKT phosphorylation on Ser 473 and total AKT and of BTK phosphorylation on Tyr 223 and total BTK. Instead, the MAPK/ERK pathway was unaffected. The regulative role of CK1α on the PI3K/AKT signaling axis was already documented in previous works. For instance, CK1α is known to phosphorylate DEPTOR, targeting it for proteasomal degradation (39). This would leave mTOR free to phosphorylate AKT, with the consequent activation of the downstream survival pathway. The inhibition of the kinase would therefore cause an increase in DEPTOR activity. However, the reduction of AKT expression could be also a consequence of p53 activation upon CK1α inhibition, since previous work established that cells undergoing p53-dependent apoptosis downregulate AKT in a caspase-dependent mechanism (40). Along this line, we showed that in MM CK1α inactivation caused a p53/caspase dependent reduction of AKT (17). Thus, the observed AKT decrease upon CK1α inactivation in MCL cells could

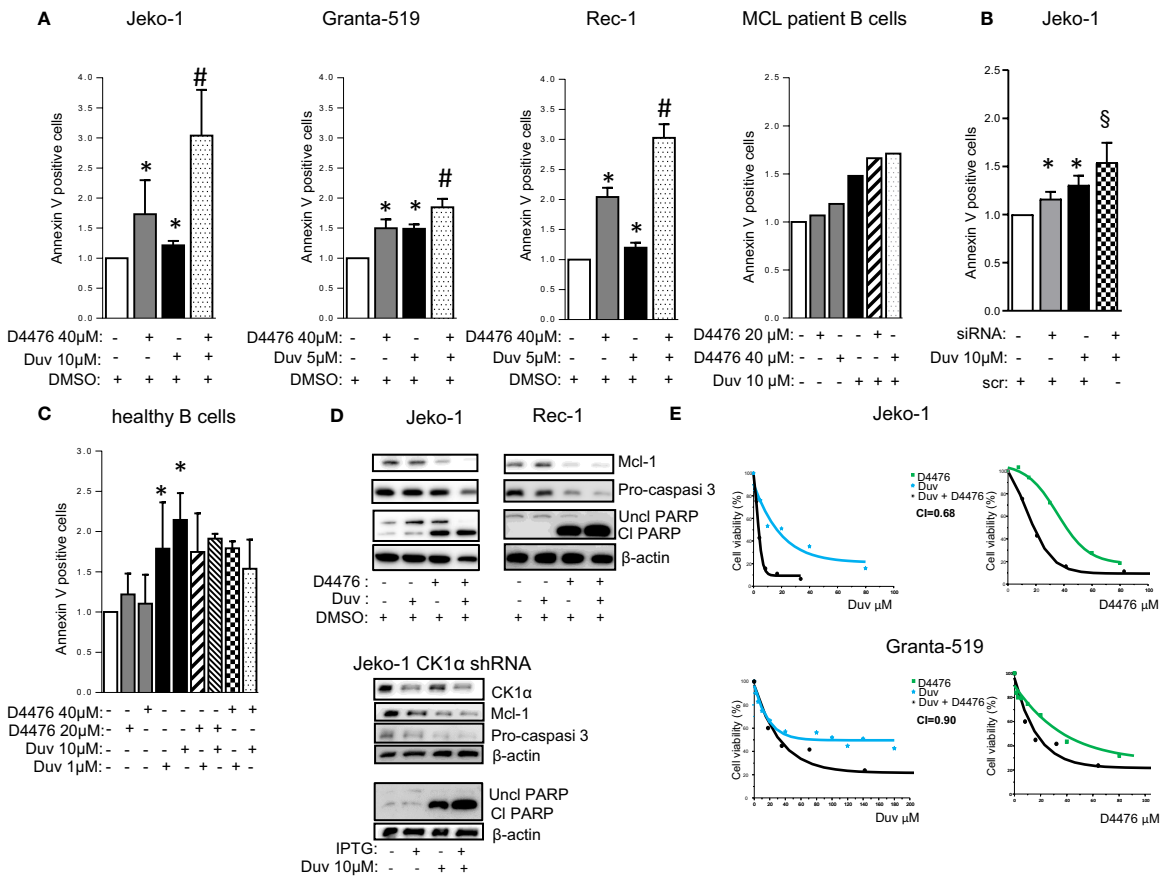

FIGURE 8 | CK1α inactivation empowers Duvelisib induced cytotoxicity. **(A–C)** Annexin V staining and FACS analysis of MCL and healthy B cells in which CK1α inactivation was associated with Duvelisib (Duv) treatment. **(A)**, MCL cell lines Jeko-1, Granta-519, Rec-1, were treated with Duv for 48h and with D4476 for the last 24h at the indicated concentrations. Purified B cells derived from 1 MCL patient were treated with Duv and D4476 for 24h. **(B)** Jeko-1 wt cells were electroporated with *CSNK1A1* directed siRNAs for 48h and treated with Duv 10μM alone or in combination with CK1α silencing for the last 24h. **(C)** Healthy B cells (n=4) were treated with Duv 1μM or 10μM, D4476 20μM or 40μM or the combination of both compounds for 24h. Data represent the mean ± SD of at least n=6 (Jeko-1), n=9 (Granta-519), n=3 (Rec-1) independent experiments normalized over control. * indicates $p < 0.05$ compared to DMSO treated cells, # indicates $p < 0.05$ between samples treated with Duvelisib together with D4476 and Duvelisib or D4476 alone; § indicates $p < 0.05$ between samples treated with Duvelisib together with CK1α silencing and Duvelisib or CK1α silencing alone. **(D)** Representative WB analysis of Mcl1, Procaspase-3, and PARP cleavage in Jeko-1 and Rec-1 treated with Duv (10 μM for Jeko-1 and 5μM for Rec-1) for 48h and with D4476 40 μM for the last 24h (upper panel) and Jeko-1 IPTG inducible *CSNK1A1* directed shRNA clone (named CK1α shRNA) treated with IPTG 500μM for 13 days and with Duv 10 μM for the last 24h, (lower panel). CK1α antibody was used to monitor the silencing efficacy. β actin was used as loading control. The figure shows a representative WB, that was performed on at least 3 independent experiments. **(E)** Synergistic effect of D4476 and Duv in reducing cell viability. Dose response curve of Jeko-1 (upper) and Granta-519 (bottom) incubated for 72 hours with increasing concentrations of D4476 alone, (green squared curve), of Duv alone (light blue star curve), and with the combination of D4476 and Duv (black filled circle curve). Cell viability was assessed with MTT test and reported as percentage over untreated cells. In Jeko-1, IC50 for D4476 alone was 41.5μM and for Duv alone was 16,85μM. IC50 for D4476 used in combination with Duv was 18,63μM, while IC50 for Duv used together with D4476 was 3,95 μM. The CI between D4476 and Duv was calculated as to be 0.68. In Granta-519, IC50 for D4476 alone was 32μM and for Duv alone was 71μM. IC50 for D4476 used in combination with Duv was 14,41 μM, while IC50 for Duv used together with D4476 was 32,27μM. The CI between D4476 and Ibrutinib was calculated as to be 0.90.

still rely on the inhibitory effects exerted by the unleashed p53/caspase axis.

Remarkably, we have also demonstrated an unanticipated novel role of CK1α on BTK function. CK1α chemical inactivation and gene silencing caused a reduction of activating phosphorylation and of total BTK levels. It has been previously reported that BTK is needed for BCR-induced activation of NF-κB (41, 42) and BTK dependent phosphorylation of IKBα is associated to NF-κB-p65 nuclear translocation and activation, independently from IKK (43). On the other hand, the activity of the NF-κB subunit p65, which directly interacts with the BTK promoter, may cause an increase of BTK activity in B cells (44). Our findings suggest that CK1α could be involved in the autoregulatory loop between BTK and NF-κB in MCL. Mechanistically, we provide evidence that CK1α might control BTK protein stability through a post-translational mechanism that does not involve the proteasome but instead relies on caspases (**Figure S4**). Remarkably, we also showed that CK1α

physically interacts with BTK, thus making it possible that CK1α facilitates BTK activating phosphorylation on Tyr 223. Even if it needs to be further investigated, this new finding is particularly relevant in the context of the therapy of MCL and other BTK-addicted NHL. To this regard, our data indicate that the molecular effects of CK1α on BTK and PI3K/AKT might impinge on the action of different classes of BCR inhibitors. Indeed, CK1α loss of function synergically potentiated Ibrutinib or Duvelisib cytotoxicity, compared to single treatments, in all the models tested, including cells less sensitive to Ibrutinib and Duvelisib (Granta-519 cells). Our results showed that CK1α inhibition could boost the Ibrutinib dependent NF-κB and AKT inactivation, impinging on crucial survival pathways important for MCL clonal expansion such as AKT, NF-κB and BTK. This is particularly meaningful since it has been shown that Ibrutinib resistance is associated to an increase of mTOR and NF-κB mediated signaling (9). CK1α-dependent activation of these pathways could be therefore usefully targeted in a therapeutic perspective and the design of novel inhibitors of CK1α would be suitable for a use in the clinical setting to overcome MCL therapy resistance. Indeed, a successful example of such an approach is the development of the dual PI3Kδ/CK1ϵ inhibitor Umbralisib, which has shown clinical efficacy in relapsed/refractory CLL and lymphomas, alone, or in combination with BTK inhibitors (45–47).

We have herein provided compelling evidence that CK1α sustains chronic active BCR-linked signaling cascades in MCL, namely the AKT, NF-κB and BTK-dependent pathways, and promotes tumor survival and proliferation. CK1α genetic and chemically inhibition causes MCL cell death and synergically empowered Ibrutinib and Duvelisib induced apoptosis. Our results are particularly meaningful in the perspective of developing novel strategies that abrogate BCR activation. Therefore, CK1α may be a key target opening new perspectives in the treatment of MCL patients, especially those with relapsed/refractory disease.

DATA AVAILABILITY STATEMENT

The original contributions presented in the study are included in the article/**Supplementary Material**. Further inquiries can be directed to the corresponding authors.

ETHICS STATEMENT

The studies involving human participants were reviewed and approved by Ethic Committee of the Padova University Hospital internal Institutional Board. The patients/participants provided their written informed consent to participate in this study.

AUTHOR CONTRIBUTIONS

SM and FP conceived, designed the experiments, and wrote the paper. SM, AF, LQT, ZS, and MC performed the experiments. SM, ZS, AF, MC, and FP analyzed the data. GSc, AV, GB, MP, AD, FV, RZ, CG, GSe, and LT provided patient samples and clinical data. SM, GSe, LT, and FP contributed reagents/materials/analysis tools. All authors contributed to the article and approved the submitted version.

FUNDING

Supported by Italian Gilead Oncohematology Fellowship Program to FP, LT, FV, Associazione Italiana per la Ricerca sul Cancro (AIRC) to FP (IG 18387) and LT (IG 25024), PRIN (Progetti di rilevante interesse nazionale)-MIUR Prot. 2017ZXT5WR to SM, Ricerca per Credere nella vita (R.C.V) ODV to LT.

ACKNOWLEDGMENTS

The authors thank AIRC, Italian Ministry of University for grant support and "Ricerca per Credere nella Vita" (R.C.V) ODV. The authors are grateful to patients for donating samples, to past and present members of the Padova Hematology Unit, including students that helped during their thesis.

SUPPLEMENTARY MATERIAL

The Supplementary Material for this article can be found online at: https://www.frontiersin.org/articles/10.3389/fonc.2021.733848/full#supplementary-material

REFERENCES

1. Tabe Y, Jin L, Konopleva M, Shikami M, Kimura S, Andreeff M, et al. Class IA PI3K Inhibition Inhibits Cell Growth and Proliferation in Mantle Cell Lymphoma. *Acta Haematol* (2014) 131:59–69. doi: 10.1159/000353164
2. Sandoval-Sus JD, Sotomayor EM, Shah BD. Mantle Cell Lymphoma: Contemporary Diagnostic and Treatment Perspectives in the Age of Personalized Medicine. *Hematol/Oncol Stem Cell Ther* (2017) 10:99–115. doi: 10.1016/j.hemonc.2017.02.003
3. Hanel W, Epperla N. Emerging Therapies in Mantle Cell Lymphoma. *J Hematol Oncol* (2020) 13:79. doi: 10.1186/s13045-020-00914-1
4. Perez-Galan P, Dreyling M, Wiestner A. Mantle Cell Lymphoma: Biology, Pathogenesis, and the Molecular Basis of Treatment in the Genomic Era. *Blood* (2011) 117:26–38. doi: 10.1182/blood-2010-04-189977
5. Ma J, Lu P, Guo A, Cheng S, Zong H, Martin P, et al. Characterization of Ibrutinib-Sensitive and -Resistant Mantle Lymphoma Cells. *Br J Haematol* (2014) 166:849–61. doi: 10.1111/bjh.12974
6. Davis RE, Ngo VN, Lenz G, Tolar P, Young RM, Romesser PB, et al. Chronic Active B-Cell-Receptor Signalling in Diffuse Large B-Cell Lymphoma. *Nature* (2010) 463:88–92. doi: 10.1038/nature08638
7. Myklebust JH, Brody J, Kohrt HE, Kolstad A, Czerwinski DK, Walchli S, et al. Distinct Patterns of B-Cell Receptor Signaling in Non-Hodgkin Lymphomas Identified by Single-Cell Profiling. *Blood* (2017) 129:759–70. doi: 10.1182/blood-2016-05-718494
8. Inamdar AA, Goy A, Ayoub NM, Attia C, Oton L, Taruvai V, et al. Mantle Cell Lymphoma in the Era of Precision Medicine-Diagnosis, Biomarkers and Therapeutic Agents. *Oncotarget* (2016) 7:48692–731. doi: 10.18632/oncotarget.8961

9. Zhao X, Wang MY, Jiang H, Lwin T, Park PM, Gao J, et al. Transcriptional Programming Drives Ibrutinib-Resistance Evolution in Mantle Cell Lymphoma. *Cell Rep* (2021) 34:108870. doi: 10.1016/j.celrep.2021.108870
10. Bond DA, Martin P, Maddocks KJ. Relapsed Mantle Cell Lymphoma: Current Management, Recent Progress, and Future Directions. *J Clin Med* (2021) 10:1207. doi: 10.3390/jcm10061207
11. Visentin A, Frezzato F, Severin F, Imbergamo S, Pravato S, Romano Gargarella L, et al. Lights and Shade of Next-Generation Pi3k Inhibitors in Chronic Lymphocytic Leukemia. *Oncol Targets Ther* (2020) 13:9679–88. doi: 10.2147/OTT.S268899
12. Patel K, Danilov AV, Pagel JM. Duvelisib for CLL/SLL and Follicular Non-Hodgkin Lymphoma. *Blood* (2019) 134:1573–7. doi: 10.1182/blood.2019001795
13. Knippschild U, Kräger M, Richter J, Xu P, Garcãa-Reyes B, Peifer C, et al. The CK1 Family: Contribution to Cellular Stress Response and Its Role in Carcinogenesis. *Front Oncol* (2014) 4:96. doi: 10.3389/fonc.2014.00096
14. Fulcher LJ, Sapkota GP. Functions and Regulation of the Serine/Threonine Protein Kinase CK1 Family: Moving Beyond Promiscuity. *Biochem J* (2020) 477:4603–21. doi: 10.1042/BCJ20200506
15. Knippschild U, Gocht A, Wolff S, Huber N, Löhler J, Stöter M. The Casein Kinase 1 Family: Participation in Multiple Cellular Processes in Eukaryotes. *Cell Signall* (2005) 17:675–89. doi: 10.1016/j.cellsig.2004.12.011
16. Spinello Z, Fregnani A, Quotti Tubi L, Trentin L, Piazza F, Manni S. Targeting Protein Kinases in Blood Cancer: Focusing on CK1α and CK2. *IJMS* (2021) 22:3716. doi: 10.3390/ijms22073716
17. Manni S, Carrino M, Manzoni M, Gianesin K, Nunes SC, Costacurta M, et al. Inactivation of CK1α in Multiple Myeloma Empowers Drug Cytotoxicity by Affecting AKT and β-Catenin Survival Signaling Pathways. *Oncotarget* (2017) 8:14604–19. doi: 10.18632/oncotarget.14654
18. Hu Y, Song W, Cirstea D, Lu D, Munshi NC, Anderson KC. Csnk1α1 Mediates Malignant Plasma Cell Survival. *Leukemia* (2015) 29:474–82. doi: 10.1038/leu.2014.202
19. Carrino M, Quotti Tubi L, Fregnani A, Canovas Nunes S, Barilà G, Trentin L, et al. Prosurvival Autophagy Is Regulated by Protein Kinase CK1 Alpha in Multiple Myeloma. *Cell Death Discovery* (2019) 5:98. doi: 10.1038/s41420-019-0179-1
20. Manni S, Carrino M, Piazza F. Role of Protein Kinases CK1α and CK2 in Multiple Myeloma: Regulation of Pivotal Survival and Stress-Managing Pathways. *J Hematol Oncol* (2017) 10:157. doi: 10.1186/s13045-017-0529-5
21. Bidere N, Ngo VN, Lee J, Collins C, Zheng L, Wan F, et al. Casein Kinase 1alpha Governs Antigen-Receptor-Induced NF-kappaB Activation and Human Lymphoma Cell Survival. *Nature* (2009) 458:92–6. doi: 10.1038/nature07613
22. Gehring T, Erdmann T, Rahm M, Graß C, Flatley A, O'Neill TJ, et al. MALT1 Phosphorylation Controls Activation of T Lymphocytes and Survival of ABC-DLBCL Tumor Cells. *Cell Rep* (2019) 29:873–88.e10. doi: 10.1016/j.celrep.2019.09.040
23. Rena G, Bain J, Elliott M, Cohen P. D4476, A Cell-Permeant Inhibitor of CK1, Suppresses the Site-Specific Phosphorylation and Nuclear Exclusion of FOXO1a. *EMBO Rep* (2004) 5:60–5. doi: 10.1038/sj.embor.7400048
24. Minzel W, Venkatachalam A, Fink A, Hung E, Brachya G, Burstain I, et al. Small Molecules Co-Targeting Ckiα and the Transcriptional Kinases CDK7/9 Control AML in Preclinical Models. *Cell* (2018) 175:171–85.e25. doi: 10.1016/j.cell.2018.07.045
25. Manni S, Brancalion A, Mandato E, Tubi LQ, Colpo A, Pizzi M, et al. Protein Kinase CK2 Inhibition Down Modulates the NF-κb and STAT3 Survival Pathways, Enhances the Cellular Proteotoxic Stress and Synergistically Boosts the Cytotoxic Effect of Bortezomib on Multiple Myeloma and Mantle Cell Lymphoma Cells. *PloS One* (2013) 8:e75280. doi: 10.1371/journal.pone.0075280
26. Manni S, Brancalion A, Tubi LQ, Colpo A, Pavan L, Cabrelle A, et al. Protein Kinase CK2 Protects Multiple Myeloma Cells From ER Stress–Induced Apoptosis and From the Cytotoxic Effect of HSP90 Inhibition Through Regulation of the Unfolded Protein Response. *Clin Cancer Res* (2012) 18:1888–900. doi: 10.1158/1078-0432.CCR-11-1789
27. Piazza F, Manni S, Tubi LQ, Montini B, Pavan L, Colpo A, et al. Glycogen Synthase Kinase-3 Regulates Multiple Myeloma Cell Growth and Bortezomib-Induced Cell Death. *BMC Cancer* (2010) 10:526. doi: 10.1186/1471-2407-10-526
28. Rudelius M, Pittaluga S, Nishizuka S, Pham TH, Fend F, Jaffe ES, et al. Constitutive Activation of Akt Contributes to the Pathogenesis and Survival of Mantle Cell Lymphoma. *Blood* (2006) 108:1668–76. doi: 10.1182/blood-2006-04-015586
29. Wang J, Zhang V, Bell T, Liu Y, Guo H, Zhang L. The Effects of PI3K-δ/γ Inhibitor, Duvelisib, in Mantle Cell Lymphoma *In Vitro* and in Patient-Derived Xenograft Studies. *Blood* (2016) 128:3016–6. doi: 10.1182/blood.V128.22.3016.3016
30. Flinn IW, O'Brien S, Kahl B, Patel M, Oki Y, Foss FF, et al. Duvelisib, A Novel Oral Dual Inhibitor of PI3K-δ,γ, Is Clinically Active in Advanced Hematologic Malignancies. *Blood* (2018) 131:877–87. doi: 10.1182/blood-2017-05-786566
31. Gross SD, Anderson RA. Casein Kinase I: Spatial Organization and Positioning of a Multifunctional Protein Kinase Family. *Cell Signall* (1998) 10:699–711. doi: 10.1016/S0898-6568(98)00042-4
32. Fulcher LJ, He Z, Mei L, Macartney TJ, Wood NT, Prescott AR, et al. FAM83D Directs Protein Kinase CK1α to the Mitotic Spindle for Proper Spindle Positioning. *EMBO Rep* (2019) 20:e47495. doi: 10.15252/embr.201847495
33. Ly T, Whigham A, Clarke R, Brenes-Murillo AJ, Estes B, Madhessian D, et al. Proteomic Analysis of Cell Cycle Progression in Asynchronous Cultures, Including Mitotic Subphases, Using PRIMMUS. *Elife* (2017) 6:e27574. doi: 10.7554/eLife.27574
34. Nishikori M. Classical and Alternative NF-kB Activation Pathways and Their Roles in Lymphoid Malignancie. *J Clin Exp Hematopathol* (2005) 45:15–24. doi: 10.3960/jslrt.45.15
35. Martinez N, Camacho FI, Algara P, Rodriguez A, Dopazo A, Ruiz-Ballesteros E, et al. The Molecular Signature of Mantle Cell Lymphoma Reveals Multiple Signals Favoring Cell Survival. *Cancer Res* (2003) 63:8226–32.
36. Kapoor I, Li Y, Sharma A, Zhu H, Bodo J, Xu W, et al. Resistance to BTK Inhibition by Ibrutinib can be Overcome by Preventing FOXO3a Nuclear Export and PI3K/AKT Activation in B-Cell Lymphoid Malignancies. *Cell Death Dis* (2019) 10:924. doi: 10.1038/s41419-019-2158-0
37. Mato AR, Ghosh N, Schuster SJ, Lamanna N, Pagel JM, Flinn IW, et al. Phase 2 Study of the Safety and Efficacy of Umbralisib in Patients With CLL Who Are Intolerant to BTK or PI3Kδ Inhibitor Therapy. *Blood* (2021), 137 (20):2817–26. doi: 10.1182/blood.2020007376
38. Visentin A, Imbergamo S, Scomazzon E, Pravato S, Frezzato F, Bonaldi L, et al. BCR Kinase Inhibitors, Idelalisib and Ibrutinib, Are Active and Effective in Richter Syndrome. *Br J Haematol* (2019) 185:193–7. doi: 10.1111/bjh.15440
39. Duan S, Skaar JR, Kuchay S, Toschi A, Kanarek N, Ben-Neriah Y, et al. mTOR Generates an Auto-Amplification Loop by Triggering the βtrcp- and CK1α-Dependent Degradation of DEPTOR. *Mol Cell* (2011) 44:317–24. doi: 10.1016/j.molcel.2011.09.005
40. Gottlieb TM, Leal JF, Seger R, Taya Y, Oren M. Cross-Talk Between Akt, P53 and Mdm2: Possible Implications for the Regulation of Apoptosis. *Oncogene* (2002) 21:1299–303. doi: 10.1038/sj.onc.1205181
41. Petro JB, Rahman SMJ, Ballard DW, Khan WN. Bruton's Tyrosine Kinase Is Required for Activation of Iκb Kinase and Nuclear Factor κb in Response to B Cell Receptor Engagement. *J Exp Med* (2000) 191:1745–54. doi: 10.1084/jem.191.10.1745
42. Doyle SL, Jefferies CA, O'Neill LA. Bruton's Tyrosine Kinase Is Involved in P65-Mediated Transactivation and Phosphorylation of P65 on Serine 536 During Nfκb Activation by Lipopolysaccharide. *J Biol Chem* (2005) 280:23496–501. doi: 10.1074/jbc.C500053200
43. Pontoriero M, Fiume G, Vecchio E, de Laurentiis A, Albano F, Iaccino E, et al. Activation of NF-κb in B Cell Receptor Signaling Through Bruton's Tyrosine Kinase-Dependent Phosphorylation of Iκb-α. *J Mol Med* (2019) 97:675–90. doi: 10.1007/s00109-019-01777-x
44. Mohamed AJ, Yu L, Backesjo CM, Vargas L, Faryal R, Aints A, et al. Bruton's Tyrosine Kinase (Btk): Function, Regulation, and Transformation With Special Emphasis on the PH Domain. *Immunol Rev* (2009) 228:58–73. doi: 10.1111/j.1600-065X.2008.00741.x
45. Burris HA, Flinn IW, Patel MR, Fenske TS, Deng C, Brander DM, et al. Umbralisib, A Novel PI3Kδ and Casein Kinase-1ε Inhibitor, in Relapsed or Refractory Chronic Lymphocytic Leukaemia and Lymphoma: An Open-Label, Phase 1, Dose-Escalation, First-in-Human Study. *Lancet Oncol* (2018) 19:486–96. doi: 10.1016/S1470-2045(18)30082-2
46. Davids MS, Kim HT, Nicotra A, Savell A, Francoeur K, Hellman JM, et al. Umbralisib in Combination With Ibrutinib in Patients With Relapsed or Refractory Chronic Lymphocytic Leukaemia or Mantle Cell Lymphoma: A Multicentre Phase 1-1b Study. *Lancet Haematol* (2019) 6:e38–47. doi: 10.1016/S2352-3026(18)30196-0

47. Lunning M, Vose J, Nastoupil L, Fowler N, Burger JA, Wierda WG, et al. Ublituximab and Umbralisib in Relapsed/Refractory B-Cell Non-Hodgkin Lymphoma and Chronic Lymphocytic Leukemia. *Blood* (2019) 134:1811–20. doi: 10.1182/blood.2019002118

Conflict of Interest: FP is in the Advisory Board of Roche and Janssen. LT reports grants, personal fees from Janssen, personal fees from Abbvie, grants from Gilead. AV is in the Scientific Board of Janssen and Takeda and in the Speaker Bureaux of Janssen, Italfarmaco, Gilead and Abbvie. GS has reported consultancy or advisory board for Janssen and Celgene and has received research support from Roche and Novartis, all outside of the submitted work.

The remaining authors declare that the research was conducted in the absence of any commercial or financial relationships that could be construed as a potential conflict of interest.

Publisher's Note: All claims expressed in this article are solely those of the authors and do not necessarily represent those of their affiliated organizations, or those of the publisher, the editors and the reviewers. Any product that may be evaluated in this article, or claim that may be made by its manufacturer, is not guaranteed or endorsed by the publisher.

frontiers in Oncology

ORIGINAL RESEARCH
published: 26 October 2021
doi: 10.3389/fonc.2021.753465

A Murine Model With JAK2V617F Expression in Both Hematopoietic Cells and Vascular Endothelial Cells Recapitulates the Key Features of Human Myeloproliferative Neoplasm

Haotian Zhang[1], *Amar Yeware*[2], *Sandy Lee*[3] *and Huichun Zhan*[2,4]*

[1] Graduate Program in Molecular & Cellular Biology, Stony Brook University, Stony Brook, NY, United States, [2] Department of Medicine, Stony Brook School of Medicine, Stony Brook, NY, United States, [3] Graduate Program in Molecular & Cellular Pharmacology, Stony Brook University, Stony Brook, NY, United States, [4] Medical Service, Northport VA Medical Center, Northport, NY, United States

OPEN ACCESS

Edited by:
Cyrus Khandanpour, University Hospital Münster, Germany

Reviewed by:
Angela Fleischman, University of California, Irvine, United States
Nicolas Chatain, University Hospital Aachen, Germany
Jonathan Tan, Bond University, Australia

***Correspondence:**
Huichun Zhan
Huichun.Zhan@stonybrookmedicine.edu

Specialty section:
This article was submitted to Hematologic Malignancies, a section of the journal Frontiers in Oncology

Received: *04 August 2021*
Accepted: *07 October 2021*
Published: *26 October 2021*

Citation:
Zhang H, Yeware A, Lee S and Zhan H (2021) A Murine Model With JAK2V617F Expression in Both Hematopoietic Cells and Vascular Endothelial Cells Recapitulates the Key Features of Human Myeloproliferative Neoplasm. Front. Oncol. 11:753465. doi: 10.3389/fonc.2021.753465

The myeloproliferative neoplasms (MPNs) are characterized by an expansion of the neoplastic hematopoietic stem/progenitor cells (HSPC) and an increased risk of cardiovascular complications. The acquired kinase mutation *JAK2V617F* is present in hematopoietic cells in a majority of patients with MPNs. Vascular endothelial cells (ECs) carrying the *JAK2V617F* mutation can also be detected in patients with MPNs. In this study, we show that a murine model with both *JAK2V617F*-bearing hematopoietic cells and *JAK2V617F*-bearing vascular ECs recapitulated all the key features of the human MPN disease, which include disease transformation from essential thrombocythemia to myelofibrosis, extramedullary splenic hematopoiesis, and spontaneous cardiovascular complications. We also found that, during aging and MPN disease progression, there was a loss of both HSPC number and HSPC function in the marrow while the neoplastic hematopoiesis was relatively maintained in the spleen, mimicking the advanced phases of human MPN disease. Different vascular niche of the marrow and spleen could contribute to the different *JAK2V617F* mutant stem cell functions we have observed in this *JAK2V617F*-positive murine model. These results indicate that the spleen is functionally important for the JAK2V617F mutant neoplastic hematopoiesis during aging and MPN disease progression. Compared to other MPN murine models reported so far, our studies demonstrate that JAK2V617F-bearing vascular ECs play an important role in both the hematologic and cardiovascular abnormalities of MPN.

Keywords: myeloproliferative neoplasm, cardiovascular diseases, endothelial cells, JAK2V617F, murine model

HIGHLIGHTS

- A murine model in which *JAK2V617F* is expressed in both hematopoietic cells and ECs recapitulated the key features of the human MPN disease
- Different vascular niche of the marrow and spleen could contribute to different *JAK2V617F* mutant HSC functions during MPN disease progression

INTRODUCTION

The Philadelphia chromosome-negative myeloproliferative neoplasms (MPNs), which include polycythemia vera (PV), essential thrombocythemia (ET), and primary myelofibrosis (PMF), are clonal stem cell disorders characterized by hematopoietic stem/progenitor cell (HSPC) expansion, overproduction of mature blood cells, a tendency to extramedullary hematopoiesis, an increased risk of transformation to acute leukemia or myelofibrosis, and an increased risk of vascular thrombosis (1, 2). The incidence of MPNs increases significantly with aging and MPN is uncommon before the age of 50 years (3). Older age and longer disease duration are also associated with higher risk of disease transformation to myelofibrosis or secondary acute myeloid leukemia, as well as increased morbidity and mortality in these patients (4). These observations suggest that aging plays an important role in MPN development.

The acquired signaling kinase mutation *JAK2V617F* is present in most patients with MPNs and aberrant JAK-STAT signaling plays a central role in these disorders (5). Although *JAK2V617F*-positive murine models have provided unequivocal evidence that *JAK2V617F* is able to cause MPNs, there is significant heterogeneity in disease phenotypes between different murine models, and none has been able to recapitulate both the myeloproliferative phenotype and the cardiovascular pathology in patients with MPNs (6). In addition, these murine models were mostly followed for less than 3-9 months (7–18) and how aging affects MPN disease progression has not been studied.

Endothelial cells (ECs) are an essential component of the hematopoietic niche and most HSPCs reside close to a marrow sinusoid (the "perivascular niche") (19). Vascular ECs also play critical roles in the regulation of hemostasis and thrombosis (20). The *JAK2V617F* mutation can be detected in microvascular ECs isolated from liver and spleen (by laser microdissection), and marrow (by flow cytometry sorting) in 60-70% of patients with MPNs (21, 22). The mutation can also be detected in 60-80% of EC progenitors derived from the hematopoietic lineage and, in some reports based on *in vitro* culture assays, in endothelial colony-forming cells from patients with MPNs (22–26). Previously, we reported that the *JAK2V617F*-bearing vascular endothelium promotes the expansion of the *JAK2V617F* mutant HSPCs in preference to wild-type HSPCs (27–31) and contributes to the development of cardiovascular complications (32) in a murine model of MPN. In the present study, we investigated how MPN progresses in the *JAK2V617F*-bearing vascular niche during aging.

MATERIALS AND METHODS

Experimental Mice

JAK2V617F Flip-Flop (FF1) mice (12) was provided by Radek Skoda (University Hospital, Basal, Switzerland) and *Tie2-Cre* mice (33) by Mark Ginsberg (University of California, San Diego). FF1 mice were crossed with Tie2-Cre mice to express *JAK2V617F* specifically in all hematopoietic cells (including HSPCs) and vascular ECs ($Tie2^{+/-}FF1^{+/-}$, or Tie2FF1), so as to model the human diseases in which both the hematopoietic stem cells and ECs harbor the mutation. All mice used were crossed onto a C57BL/6 background and bred in a pathogen-free mouse facility at Stony Brook University. Animal experiments were performed in accordance with the guidelines provided by the Institutional Animal Care and Use Committee.

Marrow and Spleen Cell Isolation

Murine femurs and tibias were first harvested and cleaned thoroughly. Marrow cells were flushed into PBS with 2% fetal bovine serum using a 25G needle and syringe. Remaining bones were crushed with a mortar and pestle followed by enzymatic digestion with DNase I (25U/ml) and Collagenase D (1mg/ml) at 37°C for 20 min under gentle rocking. Tissue suspensions were thoroughly homogenized by gentle and repeated mixing using 10ml pipette to facilitate dissociation of cellular aggregates. Resulting cell suspensions were then filtered through a 40uM cell strainer.

Murine spleens were collected and placed into a 40uM cell strainer. The plunger end of a 1ml syringe was used to mash the spleen through the cell strainer into a collecting dish. 5ml PBS with 2% FBS was used to rinse the cell strainer and the resulting spleen cell suspension was passed through a 5ml syringe with a 23G needle several times to further eliminate small cell clumps.

Complete Blood Counts and *In Vitro* Assays

Complete blood counts and hematopoietic colony formation assays were performed as we previously described (34). Mouse methylcellulose complete media (Stem Cell Technologies, Vancouver, BC) was used to assay hematopoietic colony formation, which was enumerated according to the manufacturer's protocol.

For Lineage negative (Lin^-) cell culture, marrow or splenic Lin^- cells were first enriched using the Lineage Cell Depletion Kit (Miltenyi Biotec). On Day 0, 1,000 Lin^- cells were seeded in a 48-well plate and cultured in 150ul StemSpan serum-free expansion medium (SFEM) containing recombinant mouse Stem cell factor (100 ng/ml), recombinant mouse Interleukin-3 (6 ng/ml) and recombinant human Interleukin-6 (10 ng/ml) (all from Stem Cell Technologies). 200ul fresh SFEM medium with cytokines was added on Day 5 and 8 and cells were counted on Day 5 and 10.

Histology

Femur and spleen tissues were fixed in cold 4% paraformaldehyde for 6hr at 4°C while shaking. The tissues were washed with PBS for 8-16hrs at room temperature to remove paraformaldehyde. Femurs were then decalcified and paraffin sections (5-μm thickness) were stained with hematoxylin and eosin or reticulin (Reticulum II Staining Kit, Roche, Tucson, AZ) to assess fibrosis. Images were taken using a Nikon Eclipse TS2R inverted microscope (Nikon, Melville, NY).

Flow Cytometry

All samples were analyzed by flow cytometry using a FACSAriaTM III or a LSR II (BD biosciences, San Jose, CA, USA). Lineage cocktail (include CD3, B220, Gr1, CD11b, Ter119; Biolegend), cKit (Clone 2B8, Biolegend), Sca1 (Clone D7, Biolegend), CD150 (Clone mShad150, eBioscience), CD48 (Clone HM48-1, Biolegend), CD45 (Clone 104) (Biolegend, San Diego, CA, USA), and CD31 (Clone 390, BD biosciences) antibodies were used.

BrdU Incorporation Analysis

Mice were injected intraperitoneally with a single dose of 5-bromo-2′-deoxyuridine (BrdU; 100 mg/kg body weight) and maintained on 1mg BrdU/ml drinking water for two days. Mice were then euthanized and marrow cells isolated as described above. For analysis of HSC ($Lin^-cKit^+Sca1^+CD150^+CD48^-$) proliferation, Lin^- cells were first enriched using the Lineage Cell Depletion Kit (Miltenyi Biotec) before staining with fluorescent antibodies specific for cell surface HSC markers, followed by fixation and permeabilization using the Cytofix/Cytoperm kit (BD Biosciences, San Jose, CA), DNase digestion (Sigma, St. Louis, MO), and anti-BrdU antibody (Biolegend, San Diego, CA) staining to analyze BrdU incorporation (31).

Analysis of Apoptosis by Active Caspase-3 Staining

Marrow cells were stained with fluorescent antibodies specific for cell surface HSC markers, followed by fixation and permeabilization using the Cytofix/Cytoperm kit (BD Biosciences). Cells were then stained using a rabbit anti-activated caspase-3 antibody (31). Data were acquired using a LSR II flow cytometer.

Analysis of Senescence by Senescence Associated β-Galactosidase Activity

Marrow cells were stained with fluorescent antibodies specific for cell surface HSC markers. Cells were then washed and fixed using 2% paraformaldehyde and incubated with CellEvent™ Senescence Green Probe (ThermoFisher Scientific, Waltham, MA) according to the manufacturer's instruction. Data were acquired using a LSR II flow cytometer.

VE-Cadherin *In Vivo* Staining and Immunofluorescence Imaging

25ug Alexa Fluor 647-conjugated monoclonal antibodies that target mouse VE-cadherin (clone BV13, Biolegend) were injected retro-orbitally into 2yr old Tie2FF1 or control mice under anesthesia (35). Ten minutes after antibody injection, the mice were euthanized. Mouse femurs and spleens were dissected out and washed in PBS. After fixation in 4% paraformaldehyde (PFA) (Affymetrix) for 6hr at 4°C while rotating, the samples were washed in PBS overnight to remove PFA, cryoprotected in 20% sucrose, embedded in OCT compound (Tissue-Tek), and flash frozen at -80°C. Frozen samples were cryosectioned (~10uM) using a Leica CM1510S Cryostat. Images were acquired using a Nikon Eclipse Ts2R inverted fluorescence microscope.

Transthoracic Echocardiography

Transthoracic echocardiography was performed on mildly anesthetized spontaneously breathing mice (sedated by inhalation of 1% isoflurane, 1 L/min oxygen), using a Vevo 3100 high-resolution imaging system (VisualSonics Inc., Toronto, Canada). Both parasternal long-axis and sequential parasternal short-axis views were obtained to assess global and regional wall motion. Left ventricular (LV) dimensions at end-systole and end-diastole and fractional shortening (percent change in LV diameter normalized to end-diastole) were measured from the parasternal long-axis view using linear measurements of the LV at the level of the mitral leaflet tips during diastole. LV ejection fraction (EF), volume, and mass are measured and calculated using standard formulas for the evaluation of LV systolic function (32, 36).

Histology

Hearts and lungs were fixed in 4% PFA overnight at 4°C while rotating. The tissues were then washed multiple times with PBS at room temperature to remove PFA. Paraffin sections (5-μm thickness) were stained with Hematoxylin/Eosin (H&E) following standard protocols. Images were taken using a Nikon Eclipse Ts2R inverted microscope.

Statistical Analysis

Statistical analyses were performed using Student's unpaired, 2-tailed *t* tests using Excel software (Microsoft). A *p* value of less than 0.05 was considered significant. For all bar graphs, data are presented as mean ± standard error of the mean (SEM).

RESULTS

The Tie2FF1 Mice Develop ET to PMF Transformation During Aging

To study the effects of the *JAK2V617F*-bearing vascular niche on MPN disease development *in vivo*, we crossed mice that bear a Cre-inducible human *JAK2V617F* gene (FF1) (12) with Tie2-Cre mice (33) to express *JAK2V617F* specifically in all hematopoietic cells and ECs (Tie2FF1). The Tie2FF1 mice developed an ET-like phenotype with neutrophilia (3.8 vs 1.8 x 10^3/uL, P=0.014), thrombocytosis (1068 vs 558 x 10^3/uL, P=0.036), and normal hemoglobin at 2mo of age, results consistent with previous reports (28, 37). We followed these mice up to 18mo of age to evaluate how the *JAK2V617F* mutant vascular niche regulate

MPN neoplastic hematopoiesis and disease transformation during aging. The Tie2FF1 mice continued to develop increasing neutrophilia and thrombocytosis, both of which plateaued at ~1 yr of age. In addition, the mice developed significant lymphocytosis and anemia after 6mo of age (**Figures 1A, B**). At 18mo of age, there was significant splenomegaly (spleen weight 611mg vs 89mg, $P<0.001$), increased total spleen cell counts (267 vs 153 x 10^6 cells per spleen, $P=0.031$), and decreased total marrow cell counts (23 vs 58 x 10^6 cells per femur, $P<0.001$) in the Tie2FF1 mice compared to age-matched Tie2-cre control mice (**Figures 1C–E**). Histology examination revealed extensive marrow osteopetrosis and destroyed splenic architecture, as well as increased fibrosis in both the marrow and spleen of the old Tie2FF1 mice compared to age matched control mice (**Figures 1F–I**). No evidence of leukemia transformation was observed in the Tie2FF1 mice. These findings indicate that the Tie2FF1 mice developed ET to PMF disease transformation with extramedullary splenic hematopoiesis during aging.

Decreased Marrow Hematopoiesis During Aging in the Tie2FF1 Mice

Previously, we and others reported that marrow HSCs were significantly expanded in young Tie2FF1 mice compared to age-matched Tie2-cre control mice (28, 31, 38). To examine how aging affects the neoplastic hematopoiesis in MPN, we first measured the numbers of marrow hematopoietic progenitor cells using colony formation assays. We found that the total hematopoietic progenitor cells were significantly increased in young (4-5mo) Tie2FF1 mice compared to age-matched control

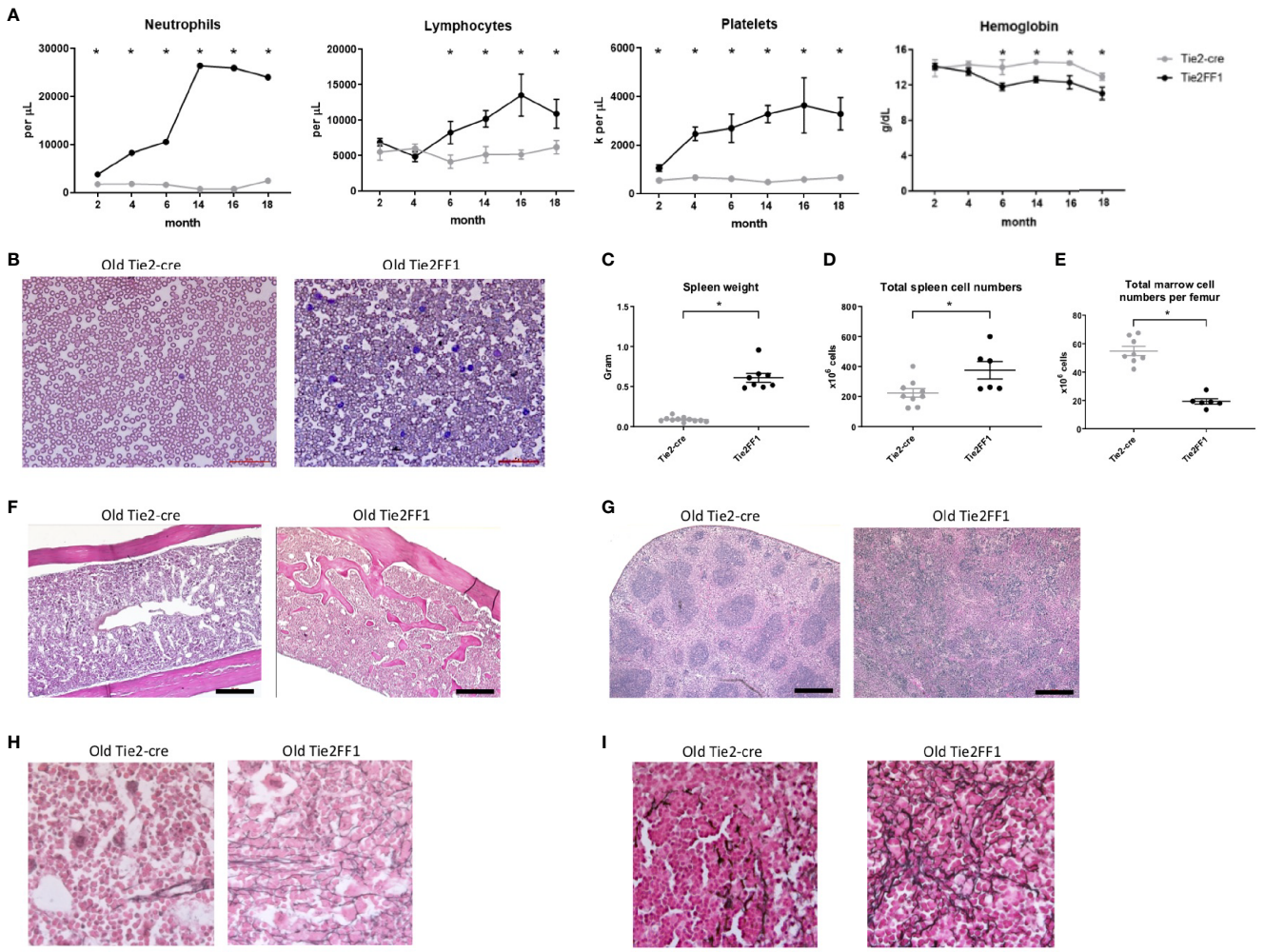

FIGURE 1 | The Tie2FF1 mice develop ET to PMF transformation during aging. **(A)** Peripheral blood cell counts of Tie2FF1 (black line) and Tie2-cre control mice (grey line). (n=5-10 mice in each group at 2mo and 4mo; n=6-7 mice in each group at 6mo, 12mo, and 15mo; n=10 mice in each group at 18mo). **(B)** Representative peripheral blood smear of 18mo old Tie2-cre and Tie2FF1 mice (40X magnification). **(C–E)** Spleen weight **(C)**, total spleen cell counts **(D)**, and total femur cell counts **(E)** in 18mo old Tie2-cre and Tie2FF1 mice (n=10 mice in each group). **(F, G)** Representative hematoxylin and eosin sections of marrow **(F)** and spleen **(G)** from 18mo old Tie2-cre and Tie2FF1 mice [**F**: 10X magnification, scale bar: 100uM; **(G)** 4X magnification, scale bar: 500uM]. **(H, I)** Representative reticulin stain of marrow **(H)** and spleen **(I)** from 18mo old Tie2-cre and Tie2FF1 mice (40X magnification). *$P < 0.05$.

mice (2.6-fold, *P*=0.005); in contrast, there was no significant difference in progenitor cell numbers between old (18mo) Tie2FF1 mice and age-matched control mice (**Figure 2A**). Consistent with these findings, flow cytometry analysis revealed that marrow Lin$^-$cKit$^+$Sca1$^+$CD150$^+$CD48$^-$ HSCs (39) were significantly expanded in young Tie2FF1 mice compared to age-matched control mice (9.7-fold, *P*<0.001), while there was no significant difference in HSC frequency between old Tie2FF1 and control mice (0.125% vs. 0.184%, *P*=0.087) (**Figure 2B**). Considering that the total marrow cells were decreased 2.5-fold in the old Tie2FF1 mice (**Figure 1E**), there was a 3.7-fold decrease in the absolute marrow HSC cell numbers in old Tie2FF1 mice compared to age-matched control mice.

To test whether the decreased phenotypic HSC number was associated with altered HSC function, we isolated marrow Lin$^-$ HSPCs from Tie2-cre control and Tie2FF1 mice and measured their cell proliferation *in vitro* in serum-free liquid medium. At the end of a ten-day culture, while *JAK2V617F* mutant HSPCs from young Tie2FF1 mice displayed a higher proliferation rate than wild-type HSPCs from young control mice (1.6-fold, *P*=0.012), mutant HSPCs from old Tie2FF1 mice proliferated less than old control HSPCs (2.0-fold, *P*=0.043) (**Figures 2C, D**). Taken together, these data indicated that there was a loss of both HSPC number and HSPC function in the marrow of old Tie2FF1 mice during aging, mimicking the advanced phases of myelofibrosis (3).

Expanded Splenic Extramedullary Hematopoiesis in the Tie2FF1 Mice

Spleen is the most frequent organ involved in extramedullary hematopoiesis in patients with MPNs (3). To examine how the splenic hematopoiesis changes during aging and MPN disease progression in the old Tie2FF1 mice, we first measured the numbers of splenic hematopoietic progenitor cells using colony formation assays. We found that splenic hematopoietic progenitor cells were markedly increased in both young (19-fold, *P*<0.001) and old (19-fold, *P*<0.001) Tie2FF1 mice compared to age-matched control mice (**Figure 3A**). In line with this finding, flow cytometry analysis revealed that spleen HSCs were expanded in both young (53-fold *P* = 0.046) and old (6.2-fold, *P* = 0.004) Tie2FF1 mice compared to age-matched control mice (**Figure 3B**). Considering that the total spleen cells were increased 1.7-fold in old Tie2FF1 mice (**Figure 1D**), there was a 10.5-fold increase in the absolute spleen HSC numbers in old Tie2FF1 mice compared to age-matched control mice. When we isolated spleen Lin$^-$ HSPCs from young and old Tie2-cre control and Tie2FF1 mice and cultured them *in vitro*, we found that both young (12.9-fold, *P*=0.005) and old (4.3-fold, *P*=0.022) *JAK2V617F* mutant spleen HSPCs displayed a higher proliferation rate than age-matched wild-type control spleen HSPCs (**Figures 3C, D**). These results suggest that, in contrast to the decreased HSPC number and HSPC function we have observed in the marrow (**Figure 2**), the spleen of old Tie2FF1 mice was able to maintain the expansion of *JAK2V617F* mutant hematopoiesis during aging and MPN disease progression.

Different HSC Functions in the Marrow and Spleen of Old Tie2FF1 Mice

The differences between marrow (**Figure 2**) and spleen (**Figure 3**) hematopoiesis in the old Tie2FF1 mice prompted us to further investigate how aging and MPN disease progression

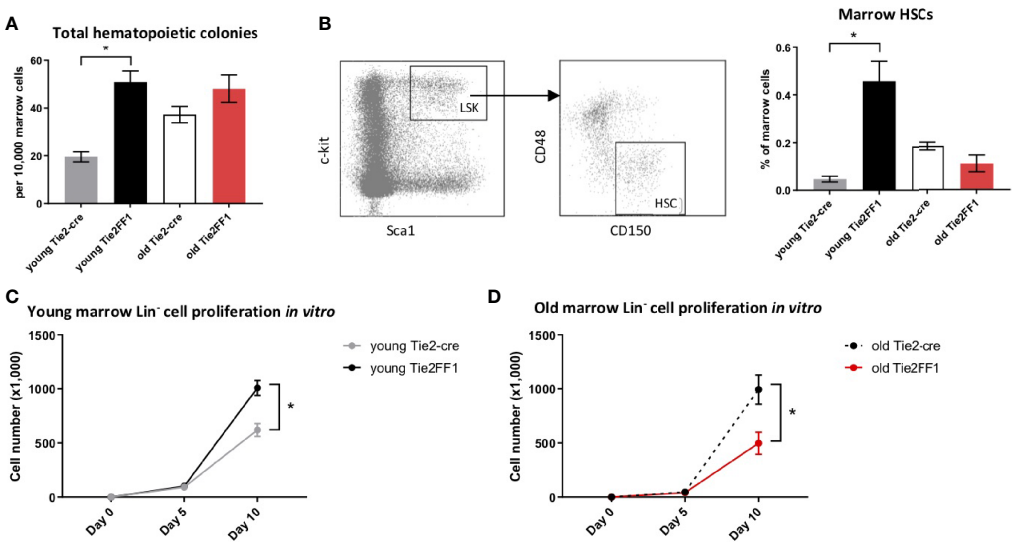

FIGURE 2 | Decreased marrow hematopoiesis in the Tie2FF1 mice during aging. **(A)** Colony formation assays in marrow cells isolated from young (n=4 mice in each group) and old (n=6-7 mice in each group) Tie2-cre control and Tie2FF1 mice. **(B)** Representative flow cytometry plots showing gating strategy (left) of marrow Lin cKit$^+$Sca1$^+$CD150$^+$CD48$^-$ HSCs frequency (right) in young (n=7 mice in each group) and old (n=5-6 mice in each group) Tie2-cre control and Tie2FF1 mice. **(C, D)** Cell proliferation of marrow Lin- HSPCs isolated from young **(C)** and old **(D)** Tie2-cre control and Tie2FF1 mice. Cells were cultured on SFEM medium containing recombinant mouse SCF (1OOng/mL), recombinant mouse IL3 (6ng/mL), and recombinant human IL6 (1Ong/mL). Data are from one of two independent experiments (with triplicates in each experiment) that gave similar results. *$P < 0.05$.

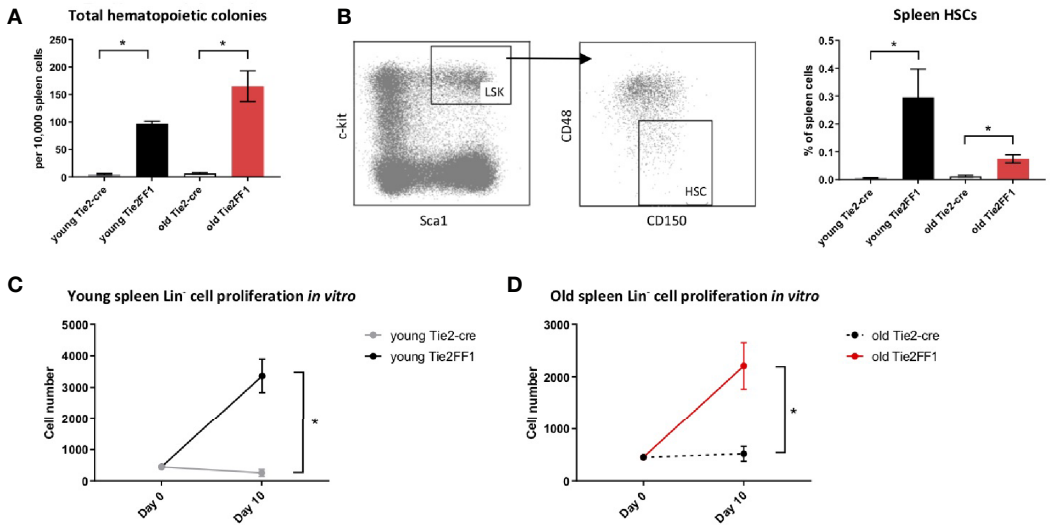

FIGURE 3 | Expanded splenic extramedullary hematopoiesis in the Tie2FF1 mice. **(A)** Colony formation assays in spleen cells isolated from young (n=3 mice in each group) and old (n=5-6 mice in each group) Tie2-cre control and Tie2FF1 mice. **(B)** Spleen Lin-cKit$^+$Sca1$^+$CD150$^+$CD48$^-$ HSCs frequency in young (n=3 mice in each group) and old (n=5 mice in each group) Tie2-cre control and Tie2FF1 mice. **(C, D)** Cell proliferation of spleen Lin HSPCs isolated from young **(C)** and old **(D)** Tie2-cre control and Tie2FF1 mice. Cells were cultured in SFEM medium containing recombinant mouse SCF (1OOng/mL), recombinant mouse IL3 (6ng/mL), and recombinant human IL6 (1Ong/mL). Data are from one of two independent experiments (with triplicates in each experiment) that gave similar results. *P < 0.05.

affect the *JAK2V617F* mutant HSC function differently in the marrow and spleen. First, we measured HSC proliferation *in vivo* by BrdU labeling (31). We found that *JAK2V617F* mutant HSCs from old Tie2FF1 mice proliferated more rapidly than wild-type HSCs from age-matched control mice in both the marrow (58% vs 21%, *P*=0.001) and the spleen (41% vs 22%, *P*=0.042) (**Figures 4A, B**). Next, we measured HSC cell apoptosis by assessing their activated caspase-3 levels using flow cytometry analysis (31). We found that *JAK2V617F* mutant marrow HSCs from old Tie2FF1 mice displayed higher level of apoptosis compared to wild-type marrow HSCs from age-matched control mice (3.0% vs 0.8%, *P*=0.006); in contrast, mutant spleen HSCs from old Tie2FF1 mice displayed significantly less apoptosis compared to wild-type spleen HSCs from control mice (1.8% vs 11.6%, *P*=0.002) (**Figures 4C, D**). Since oncogenic mutation is a major stress to induce cellular senescence (40) and the JAK-STAT signaling has been reported to induce cellular senescence (41–44), we assessed HSC senescence by measuring their senescence associated β-galactosidase (SA-β-Gal) activity, which is a hallmark of cellular senescence (40). *JAK2V617F* mutant marrow HSCs from old Tie2FF1 mice demonstrated significantly higher senescence rates compared to wild-type marrow HSCs from age-matched control mice (18% vs 9%, *P*=0.011); in contrast, there was no difference in the cellular senescence rate between the mutant spleen HSCs from old Tie2FF1 mice and wild-type spleen HSCs from control mice (**Figures 4E, F**). Taken together, although the *JAK2V617F* mutant HSCs from old Tie2FF1 mice were more proliferative than wild-type HSCs in both the marrow and spleen, mutant HSCs were more apoptotic and senescent than wild-type HSCs in the marrow while the mutant cells were relatively protected in the spleen.

Most HSCs reside close to a perivascular niche in the marrow and spleen (19, 45). To understand how different vascular niches contribute to different HSC functions in the old Tie2FF1 mice, we measured marrow and spleen ECs (CD45-CD31+) by flow cytometry analysis. We found that marrow ECs were significantly decreased in old Tie2FF1 mice compared to age-matched control mice; in contrast, spleen ECs were significantly expanded in old Tie2FF1 mice. These results were also confirmed by in vivo VE-cadherin labeling and immunofluorescence imaging of the marrow and spleen tissue samples (**Figures 4G, H**). In addition, while there was no difference in marrow EC senescence rate between old Tie2FF1 mice and old control mice, the *JAK2V617F* mutant splenic ECs from old Tie2FF1 mice were much less senescent compared to wild-type splenic ECs from age-matched control mice (**Figures 4I, J**). Therefore, the different vascular niche of the marrow and spleen could contribute to the decreased marrow hematopoiesis and expanded splenic hematopoiesis we have observed in the Tie2FF1 mice during aging.

Persistent But Compensated Cardiomyopathy in the Old Tie2FF1 Mice

Cardiovascular complications are the leading cause of morbidity and mortality in patients with MPNs. Previously, we reported that the Tie2FF1 mice developed spontaneous heart failure with thrombosis, vasculopathy, and cardiomyopathy at 20wk of age (32). Here, we followed the cardiovascular function of Tie2FF1 mice during aging. At 18mo of age, the Tie2FF1 mice continued to demonstrate a phenotype of dilated cardiomyopathy with a

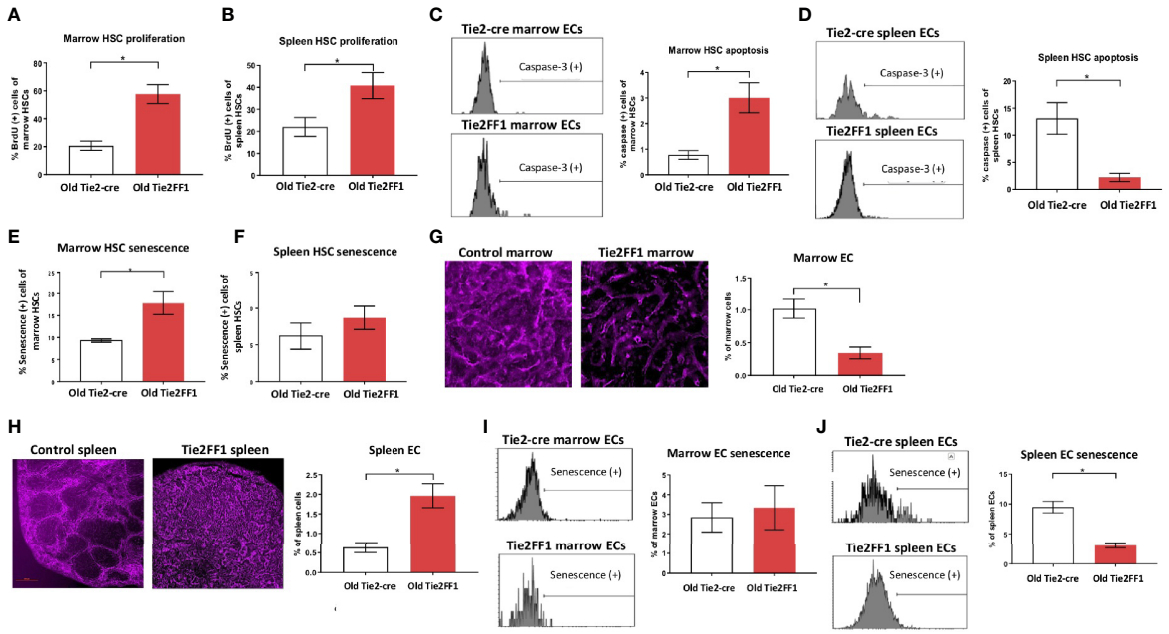

FIGURE 4 | Different HSC functions in the marrow and spleen of old Tie2FF1 mice **(A, B)** Cell proliferation rate of HSCs in the marrow **(A)** and spleen **(B)** measured by *in vivo* BrdU labeling (A: n=4-5 mice in each group; B: n=4 mice in each group). **(C, D)** Representative flow cytometry histograms (left) and quantitative analysis of cellular apoptosis rate of HSCs in the marrow **(C)** and spleen **(D)** measured by activated caspase-3 staining using flow cytometry analysis (**C**: n=5 mice in each group; **D**: n=5-6 mice in each group). **(E, F)** Cellular senescence rate of HSCs in the marrow **(E)** and spleen **(F)** measured by SA-β-Gal activity using flow cytometry analysis **(E)**: n=5 mice in each group; **(F)** n=5-6 mice in each group). **(G, H)** Representative immunofluorescent images of VE cadherin (+) vasculatures (magnification 10x for femur marrow and 4x for spleen) (left) and flow cytometry quantitative analysis of $CD45^{-}CD31^{+}$ ECs (right) of the marrow **(G)** and spleen **(H)** from 18mo Tie2-cre control and Tie2FF1 mice **(G)**: n=8 mice in each group; **(H)** n=5 mice in each group). **(I)** Representative flow cytometry histograms (left) and quantitative analysis of cellular senescence of marrow ECs (n=4 mice in each group). **(J)** Representative flow cytometry histograms (left) and quantitative analysis of cellular senescence of spleen ECs (n=3 mice in each group).*$P < 0.05$.

moderate but significant decrease in LV EF (56% versus 66%, P=0.043), an increase in LV end-diastolic volume (84μL vs 71μL, P=0.086) and end-systolic volume (38 μL vs 25 μL, P=0.041), and an increase in LV mass (156mg vs 113mg, P=0.021) compared to age-matched control mice (**Figure 5A**). Pathological evaluation confirmed the diagnosis of dilated cardiomyopathy in old Tie2FF1 mice with significantly increased heart weight-to-tibia length ratio compared to age-matched control mice (0.014 vs 0.011 gram/mm, P=0.004) (**Figure 5B**). Increased lung weight in old Tie2FF1 mice compared to control mice (0.287 vs 0.226 gram) further indicated the presence of pulmonary edema commonly associated with heart failure (**Figure 5C**). Similar to what we previously reported in the young Tie2FF1 mice (32), there was spontaneous thrombosis in the right ventricle and pulmonary arteries in the old Tie2FF1 mice, while age-matched Tie2-cre control mice had no evidence of spontaneous thrombosis in their heart or lungs (**Figures 5D, E**). Despite these cardiovascular dysfunctions, there was no difference in body weight between old Tie2FF1 mice and control mice (**Figure 5F**), nor was there any significantly increased incidence of sudden death in the old Tie2FF1 mice compared to age-matched control mice. These findings suggested that there was a persistent but compensated cardiomyopathy and heart failure in the Tie2FF1 mice during aging.

DISCUSSIONS

With heterozygous human *JAK2V617F* transgene expression in both the hematopoietic cells and vascular ECs, the Tie2FF1 mice developed an ET-like phenotype at young age (2mo old) which transformed to PMF during aging. The mice also demonstrated features of extramedullary splenic hematopoiesis, spontaneous vascular thrombosis, cardiovascular dysfunction, which persisted during the aging process. Compared to other MPN murine models reported so far (7–18), the Tie2FF1 mice is the first MPN murine model that faithfully recapitulated almost all the key features of the human MPN diseases. Considering the presence of the *JAK2V617F* mutation in microvascular ECs isolated from patients with MPNs (21, 22, 26) and the recapitulation of all the key features of human MPN diseases by the Tie2FF1 mice, the roles of endothelial dysfunction in the hematologic and cardiovascular pathogenesis of MPN and whether the MPN vascular niche can be targeted to provide more effective therapeutic strategies for patients with these diseases shall be further investigated.

Extramedullary splenic hematopoiesis often compensates for normal hematopoietic suppression in neoplastic conditions (46, 47). Splenomegaly is a common feature in patients with MPNs as a result of extramedullary hematopoiesis, in which HSCs

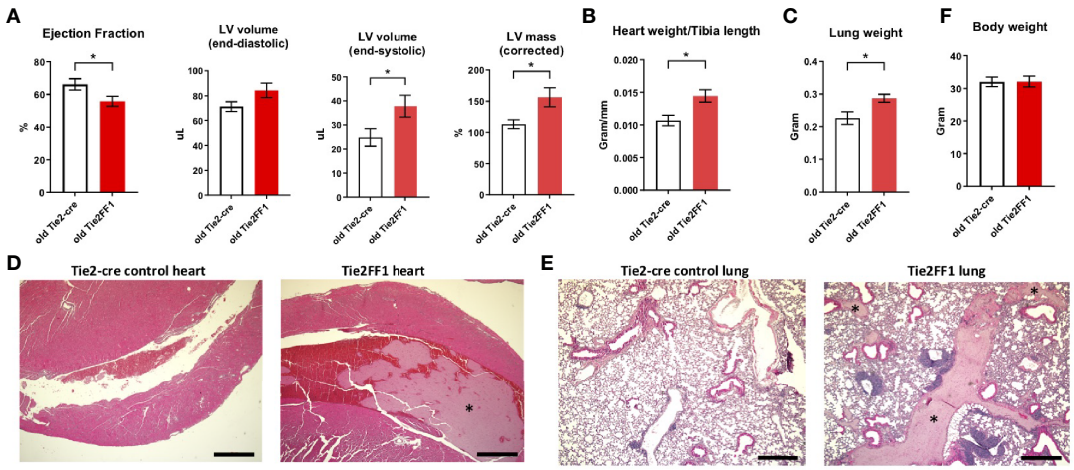

FIGURE 5 | Persistent cardiomyopathy and congestive heart failure in the old Tie2FF1 mice. **(A)** Measurements of left ventricular (LV) ejection fraction, end-diastolic and end-systolic volume, and mass by transthoracic echocardiography in 18mo old Tie2-cre control and Tie2FF1 mice. **(B)** Heart weight adjusted by tibia length of 18mo old Tie2-cre control and Tie2FF1 mice. **(C)** Lung weight of 18mo old Tie2-cre control and Tie2FF1 mice. **(D)** Representative H&E staining of transverse sections of heart from Tie2-cre control and Tie2FF1 mice. Note the presence of thrombus (*) in right ventricle (magnification 4x, scale bar: 500uM). **(E)** Representative H&E staining of coronal sections of lung from Tie2-cre control and Tie2FF1 mice. Note the presence of thrombus (star*) in segment pulmonary arteries of the Tie2FF1 mice (magnification 4x, scale bar: 500uM). **(F)** Body weight of 18mo old Tie2-cre control and Tie2FF1 mice. n=8-11 mice in each group.*$P < 0.05$.

are mobilized to sites outside the marrow to expand hematopoiesis. Our study showed that the extramedullary splenic hematopoiesis could also compensate/maintain MPN neoplastic hematopoiesis during disease transformation/progression. Together with a previous report that the spleens of PMF patients contain the neoplastic stem cells for MPN development (48), these findings indicate that effective targeting of the splenic neoplastic hematopoiesis might be necessary for successful MPN therapies.

ECs are an essential component of the perivascular niche in the marrow and spleen (19, 45). It is known that vascular ECs within different tissues have unique gene expression profile and cellular function (49). Results from our previous studies and current work demonstrated that there was a significant heterogeneity of the *JAK2V617F* mutant ECs in different parts of the circulation (e.g., marrow, spleen, heart32). How the same *JAK2V617F* mutation results in different EC functions in different tissues is not fully understood. Since flow shear stress has key roles in endothelial function (50) and biomechanical forces can regulate HSC function (51), it is possible that different e.g. flow rate, shear stress, or hydrostatic pressure in different tissues can contribute to different *JAK2V617F* -bearing EC functions.

In summary, our previous (27–32) and current work have demonstrated that *JAK2V617F*-bearing vascular ECs play an important role in both the hematologic and cardiovascular disease processes of MPNs. Results from our studies also revealed a significant heterogeneity of the *JAK2V617F* mutant ECs in different parts of the circulation and the spleen is functionally important for MPN neoplastic hematopoiesis during aging and disease progression. Therefore, the Tie2FF1 mice provide a unique *in vivo* model to screen or test potential preventive and therapeutic interventions for patients with MPNs.

DATA AVAILABILITY STATEMENT

The datasets presented in this article are not readily available because none. Requests to access the datasets should be directed to Huichun.zhan@stonybrookmedicine.edu.

ETHICS STATEMENT

The animal study was reviewed and approved by Stony Brook Institutional Animal Care and Use Committee

AUTHOR CONTRIBUTIONS

HZhang performed various *in vitro* and *in vivo* experiments of the project, and analyzed the data. AY assisted various *in vitro* culture experiments. SL provided technical assistance in various parts of the project. HZhan conceived the projects, analyzed the data, interpreted the results, and wrote the manuscript. All authors contributed to the article and approved the submitted version.

FUNDING

This research was supported by the National Heart, Lung, and Blood Institute grant NIH R01 HL134970 (HZhan) and VA Merit Award BX003947 (HZhang).

REFERENCES

1. Landolfi R, Di Gennaro L, Falanga A. Thrombosis in Myeloproliferative Disorders: Pathogenetic Facts and Speculation. *Leukemia* (2008) 22:2020–8. doi: 10.1038/leu.2008.253
2. Zhan H, Spivak JL. The Diagnosis and Management of Polycythemia Vera, Essential Thrombocythemia, and Primary Myelofibrosis in the JAK2 V617F Era. *Clin Adv Hematol Oncol* (2009) 7:334–42.
3. Spivak JL. Myeloproliferative Neoplasms. *N Engl J Med* (2017) 376:2168–81. doi: 10.1056/NEJMra1406186
4. Stein BL, Oh ST, Berenzon D, Hobbs GS, Kremyanskaya M, Rampal RK, et al. Polycythemia Vera: An Appraisal of the Biology and Management 10 Years After the Discovery of JAK2 V617F. *J Clin Oncol* (2015) 33:3953–60. doi: 10.1200/JCO.2015.61.6474
5. Nangalia J, Green AR. Myeloproliferative Neoplasms: From Origins to Outcomes. *Hematol Am Soc Hematol Educ Program* (2017) 2017:470–9. doi: 10.1182/asheducation-2017.1.470
6. Dunbar A, Nazir A, Levine R. Overview of Transgenic Mouse Models of Myeloproliferative Neoplasms (MPNs). *Curr Protoc Pharmacol* (2017) 77:14 40 1–14 40 19. doi: 10.1002/cpph.23
7. Bumm TG, Elsea C, Corbin AS, d M, Sherbenou D, Wood L, et al. Characterization of Murine JAK2V617F-Positive Myeloproliferative Disease. *Cancer Res* (2006) 66:11156–65. doi: 10.1158/0008-5472.CAN-06-2210
8. Lacout C, Pisani DF, Tulliez M, Gachelin FM, Vainchenker W, Villeval JL. JAK2V617F Expression in Murine Hematopoietic Cells Leads to MPD Mimicking Human PV With Secondary Myelofibrosis. *Blood* (2006) 108:1652–60. doi: 10.1182/blood-2006-02-002030
9. Wernig G, Mercher T, Okabe R, Levine RL, Lee BH, Gilliland DG. Expression of Jak2V617F Causes a Polycythemia Vera-Like Disease With Associated Myelofibrosis in a Murine Bone Marrow Transplant Model. *Blood* (2006) 107:4274–81. doi: 10.1182/blood-2005-12-4824
10. Zaleskas VM, Krause DS, Lazarides K, Patel N, Hu Y, Li S, et al. Molecular Pathogenesis and Therapy of Polycythemia Induced in Mice by JAK2 V617F. *PloS One* (2006) 1:e18. doi: 10.1371/journal.pone.0000018
11. Shide K, Shimoda HK, Kumano T, Karube K, Kameda T, Takenaka K, et al. Development of ET, Primary Myelofibrosis and PV in Mice Expressing JAK2 V617F. *Leukemia* (2008) 22:87–95. doi: 10.1038/sj.leu.2405043
12. Tiedt R, Hao-Shen H, Sobas MA, Looser R, Dirnhofer S, Schwaller J, et al. Ratio of Mutant JAK2-V617F to Wild-Type Jak2 Determines the MPD Phenotypes in Transgenic Mice. *Blood* (2008) 111:3931–40. doi: 10.1182/blood-2007-08-107748
13. Xing S, Wanting TH, Zhao W, Ma J, Wang S, Xu X, et al. Transgenic Expression of JAK2V617F Causes Myeloproliferative Disorders in Mice. *Blood* (2008) 111:5109–17. doi: 10.1182/blood-2007-05-091579
14. Akada H, Yan D, Zou H, Fiering S, Hutchison RE, Mohi MG. Conditional Expression of Heterozygous or Homozygous Jak2V617F From Its Endogenous Promoter Induces a Polycythemia Vera-Like Disease. *Blood* (2010) 115:3589–97. doi: 10.1182/blood-2009-04-215848
15. Mullally A, Lane SW, Ball B, Megerdichian C, Okabe R, Al-Shahrour F, et al. Physiological Jak2V617F Expression Causes a Lethal Myeloproliferative Neoplasm With Differential Effects on Hematopoietic Stem and Progenitor Cells. *Cancer Cell* (2010) 17:584–96. doi: 10.1016/j.ccr.2010.05.015
16. Marty C, Lacout C, Martin A, Hasan S, Jacquot S, Birling MC, et al. Myeloproliferative Neoplasm Induced by Constitutive Expression of JAK2V617F in Knock-in Mice. *Blood* (2010) 116:783–7. doi: 10.1182/blood-2009-12-257063
17. Li J, Spensberger D, Ahn JS, Anand S, Beer PA, Ghevaert C, et al. JAK2 V617F Impairs Hematopoietic Stem Cell Function in a Conditional Knock-in Mouse Model of JAK2 V617F-Positive Essential Thrombocythemia. *Blood* (2010) 116:1528–38. doi: 10.1182/blood-2009-12-259747
18. Li J, Kent DG, Godfrey AL, Manning H, Nangalia J, Aziz A, et al. JAK2V617F Homozygosity Drives a Phenotypic Switch in Myeloproliferative Neoplasms, But Is Insufficient to Sustain Disease. *Blood* (2014) 123:3139–51. doi: 10.1182/blood-2013-06-510222
19. Crane GM, Jeffery E, Morrison SJ. Adult Haematopoietic Stem Cell Niches. *Nat Rev Immunol* (2017) 17:573–90. doi: 10.1038/nri.2017.53
20. Wu KK, Thiagarajan P. Role of Endothelium in Thrombosis and Hemostasis. *Annu Rev Med* (1996) 47:315–31. doi: 10.1146/annurev.med.47.1.315
21. Sozer S, Fiel MI, Schiano T, Xu M, Mascarenhas J, Hoffman R. The Presence of JAK2V617F Mutation in the Liver Endothelial Cells of Patients With Budd-Chiari Syndrome. *Blood* (2009) 113:5246–9. doi: 10.1182/blood-2008-11-191544
22. Rosti V, Villani L, Riboni R, Riboni R, Poletto V, Bonetti E, Tozzi, et al. Spleen Endothelial Cells From Patients With Myelofibrosis Harbor the JAK2V617F Mutation. *Blood* (2013) 121:360–8. doi: 10.1182/blood-2012-01-404889
23. Yoder MC, Mead LE, Prater D, Krier TR, Mroueh KN, Li F, et al. Redefining Endothelial Progenitor Cells *via* Clonal Analysis and Hematopoietic Stem/Progenitor Cell Principals. *Blood* (2007) 109:1801–9. doi: 10.1182/blood-2006-08-043471
24. Teofili L, Martini M, Iachininoto MG, Capodimonti S, Nuzzolo ER, Torti L, et al. Endothelial Progenitor Cells Are Clonal and Exhibit the JAK2(V617F) Mutation in a Subset of Thrombotic Patients With Ph-Negative Myeloproliferative Neoplasms. *Blood* (2011) 117:2700–7. doi: 10.1182/blood-2010-07-297598
25. Piaggio G, Rosti V, Corselli M, Bertolotti F, Bergamaschi G, Pozzi S, et al. Endothelial Colony-Forming Cells From Patients With Chronic Myeloproliferative Disorders Lack the Disease-Specific Molecular Clonality Marker. *Blood* (2009) 114:3127–30. doi: 10.1182/blood-2008-12-190991
26. Helman R, Pereira WO, Marti LC, Campregher PV, Puga RD, Hamerschlak N, et al. Granulocyte Whole Exome Sequencing and Endothelial JAK2V617F in Patients With JAK2V617F Positive Budd-Chiari Syndrome Without Myeloproliferative Neoplasm. *Br J Haematol* (2018) 180:443–5. doi: 10.1111/bjh.14327
27. Lin CH, Kaushansky K, Zhan H. JAK2V617F-Mutant Vascular Niche Contributes to JAK2V617F Clonal Expansion in Myeloproliferative Neoplasms. *Blood Cells Mol Dis* (2016) 62:42–8. doi: 10.1016/j.bcmd.2016.09.004
28. Zhan H, Lin CHS, Segal Y, Kaushansky K. The JAK2V617F-Bearing Vascular Niche Promotes Clonal Expansion in Myeloproliferative Neoplasms. *Leukemia* (2018) 32:462–9. doi: 10.1038/leu.2017.233
29. Lin CHS, Zhang Y, Kaushansky K, Zhan H. JAK2V617F-Bearing Vascular Niche Enhances Malignant Hematopoietic Regeneration Following Radiation Injury. *Haematologica* (2018) 103:1160–8. doi: 10.3324/haematol.2017.185736
30. Mazzeo C, Quan M, Wong H, Castiglione M, Kaushansky K, Zhan H. JAK2V617F Mutant Endothelial Cells Promote Neoplastic Hematopoiesis in a Mixed Vascular Microenvironment. *Blood Cells Mol Dis* (2021) 90:102585. doi: 10.1016/j.bcmd.2021.102585
31. Castiglione M, Zhang H, Kaushansky K, Zhan H. Cell Competition Between Wild-Type and JAK2V617F Mutant Cells in a Murine Model of a Myeloproliferative Neoplasm. *Exp Hematol* (2021). doi: 10.1101/2020.08.26.267070
32. Castiglione M, Jiang YP, Mazzeo C, Lee S, Chen JS, Kaushansky K, et al. Endothelial JAK2V617F Mutation Leads to Thrombosis, Vasculopathy, and Cardiomyopathy in a Murine Model of Myeloproliferative Neoplasm. *J Thromb Haemost* (2020). doi: 10.1101/2019.12.31.891721
33. Constien R, Forde A, Liliensiek B, Grone HJ, Nawroth P, Hammerling G, et al. Characterization of a Novel EGFP Reporter Mouse to Monitor Cre Recombination as Demonstrated by a Tie2 Cre Mouse Line. *Genesis* (2001) 30:36–44. doi: 10.1002/gene.1030
34. Zhan H, Ma Y, Lin CH, Kaushansky K. JAK2V617F-Mutant Megakaryocytes Contribute to Hematopoietic Stem/Progenitor Cell Expansion in a Model of Murine Myeloproliferation. *Leukemia* (2016) 30:2332–41. doi: 10.1038/leu.2016.114
35. Guo P, Poulos MG, Palikuqi B, Badwe CR, Lis R, Kunar B, et al. Endothelial Jagged-2 Sustains Hematopoietic Stem and Progenitor Reconstitution After Myelosuppression. *J Clin Invest* (2017) 127:4242–56. doi: 10.1172/JCI92309
36. Gao S, Ho D, Vatner DE, Vatner SF. Echocardiography in Mice. *Curr Protoc Mouse Biol* (2011) 1:71–83. doi: 10.1002/9780470942390.mo100130
37. Etheridge SL, Roh ME, Cosgrove ME, Sangkhae V, Fox NE, Chen J, et al. JAK2V617F-Positive Endothelial Cells Contribute to Clotting Abnormalities in Myeloproliferative Neoplasms. *Proc Natl Acad Sci USA* (2014) 111:2295–300. doi: 0.1073/pnas.1312148111
38. Sangkhae V, Etheridge SL, Kaushansky K, Hitchcock IS. The Thrombopoietin Receptor, MPL, Is Critical for Development of a JAK2V617F-Induced Myeloproliferative Neoplasm. *Blood* (2014) 124:3956–63. doi: 10.1182/blood-2014-07-587238

39. Kiel MJ, Yilmaz OH, Iwashita T, Yilmaz OH, Terhorst C, Morrison SJ. SLAM Family Receptors Distinguish Hematopoietic Stem and Progenitor Cells and Reveal Endothelial Niches for Stem Cells. *Cell* (2005) 121:1109–21. doi: 10.1016/j.cell.2005.05.026
40. Sharpless NE, Sherr CJ. Forging a Signature of *In Vivo* Senescence. *Nat Rev Cancer* (2015) 15:397–408. doi: 10.1038/nrc3960
41. Xu M, Tchkonia T, Ding H, Ogrodnik M, Lubbers ER, Pirtskhalava T, et al. JAK Inhibition Alleviates the Cellular Senescence-Associated Secretory Phenotype and Frailty in Old Age. *Proc Natl Acad Sci USA* (2015) 112: E6301–10. doi: 10.1073/pnas.1515386112
42. Xu M, Palmer AK, Ding H, Weivoda MM, Pirtskhalava T, White TA, et al. Targeting Senescent Cells Enhances Adipogenesis and Metabolic Function in Old Age. *Elife* (2015) 4:e12997. doi: 10.7554/eLife.12997
43. Novakova Z, Hubackova S, Kosar M, Janderova-Rossmeislova L, Dobrovolna J, Vasicova P, et al. Cytokine Expression and Signaling in Drug-Induced Cellular Senescence. *Oncogene* (2010) 29:273–84. doi: 10.1038/onc.2009.318
44. Griveau A, Wiel C, Ziegler DV, Bergo MO, Bernard D. The JAK1/2 Inhibitor Ruxolitinib Delays Premature Aging Phenotypes. *Aging Cell* (2020) 19:e13122. doi: 10.1111/acel.13122
45. Inra CN, Zhou BO, Acar M, Murphy MM, Richardson J, Zhao Z, et al. A Perisinusoidal Niche for Extramedullary Haematopoiesis in the Spleen. *Nature* (2015) 527:466–71. doi: 10.1038/nature15530
46. Cheng H, Hao S, Liu Y, Pang Y, Ma S, Dong F, et al. Leukemic Marrow Infiltration Reveals a Novel Role for Egr3 as a Potent Inhibitor of Normal Hematopoietic Stem Cell Proliferation. *Blood* (2015) 126:1302–13. doi: 10.1182/blood-2015-01-623645
47. Zhang TY, Dutta R, Benard B, Zhao F, Yin R, Majeti R. IL-6 Blockade Reverses Bone Marrow Failure Induced by Human Acute Myeloid Leukemia. *Sci Transl Med* (2020) 12:538. doi: 10.1126/scitranslmed.aax5104
48. Wang X, Prakash S, Lu M, Tripodi J, Ye F, Najfeld V, et al. Spleens of Myelofibrosis Patients Contain Malignant Hematopoietic Stem Cells. *J Clin Invest* (2012) 122:3888–99. doi: 10.1172/JCI64397
49. Nolan DJ, Ginsberg M, Israely E, Palikuqi B, Poulos MG, James D, et al. Molecular Signatures of Tissue-Specific Microvascular Endothelial Cell Heterogeneity in Organ Maintenance and Regeneration. *Dev Cell* (2013) 26:204–19. doi: 10.1016/j.devcel.2013.06.017
50. Chiu JJ, Chien S. Effects of Disturbed Flow on Vascular Endothelium: Pathophysiological Basis and Clinical Perspectives. *Physiol Rev* (2011) 91:327–87. doi: 10.1152/physrev.00047.2009
51. Lee HJ, Li N, Evans SM, Diaz MF, Wenzel PL. Biomechanical Force in Blood Development: Extrinsic Physical Cues Drive Pro-Hematopoietic Signaling. *Differentiation* (2013) 86:92–103. doi: 10.1016/j.diff.2013.06.004

Conflict of Interest: The authors declare that the research was conducted in the absence of any commercial or financial relationships that could be construed as a potential conflict of interest.

Publisher's Note: All claims expressed in this article are solely those of the authors and do not necessarily represent those of their affiliated organizations, or those of the publisher, the editors and the reviewers. Any product that may be evaluated in this article, or claim that may be made by its manufacturer, is not guaranteed or endorsed by the publisher.

frontiers in Oncology

REVIEW
published: 29 October 2021
doi: 10.3389/fonc.2021.769628

Recent Progress in Interferon Therapy for Myeloid Malignancies

Fiona M. Healy[1], *Lekh N. Dahal*[1], *Jack R.E. Jones*[1], *Yngvar Floisand*[2,3] *and John F. Woolley*[1]*

[1] Department of Pharmacology & Therapeutics, University of Liverpool, Liverpool, United Kingdom, [2] Department of Molecular & Clinical Cancer Medicine, University of Liverpool, Liverpool, United Kingdom, [3] The Clatterbridge Cancer Centre NHS Foundation Trust, Liverpool, United Kingdom

OPEN ACCESS

Edited by:
Simona Soverini,
University of Bologna, Italy

Reviewed by:
Ken Mills,
Queen's University Belfast, United Kingdom
Fabio Stagno,
University Hospital Polyclinic Vittorio Emanuele, Italy

***Correspondence:**
John F. Woolley
john.woolley@liverpool.ac.uk

Specialty section:
This article was submitted to Hematologic Malignancies, a section of the journal Frontiers in Oncology

Received: 14 September 2021
Accepted: 13 October 2021
Published: 29 October 2021

Citation:
Healy FM, Dahal LN, Jones JRE, Floisand Y and Woolley JF (2021) Recent Progress in Interferon Therapy for Myeloid Malignancies. Front. Oncol. 11:769628. doi: 10.3389/fonc.2021.769628

Myeloid malignancies are a heterogeneous group of clonal haematopoietic disorders, caused by abnormalities in haematopoietic stem cells (HSCs) and myeloid progenitor cells that originate in the bone marrow niche. Each of these disorders are unique and present their own challenges with regards to treatment. Acute myeloid leukaemia (AML) is considered the most aggressive myeloid malignancy, only potentially curable with intensive cytotoxic chemotherapy with or without allogeneic haematopoietic stem cell transplantation. In comparison, patients diagnosed with chronic myeloid leukaemia (CML) and treated with tyrosine kinase inhibitors (TKIs) have a high rate of long-term survival. However, drug resistance and relapse are major issues in both these diseases. A growing body of evidence suggests that Interferons (IFNs) may be a useful therapy for myeloid malignancies, particularly in circumstances where patients are resistant to existing front-line therapies and have risk of relapse following haematopoietic stem cell transplant. IFNs are a major class of cytokines which are known to play an integral role in the non-specific immune response. IFN therapy has potential as a combination therapy in AML patients to reduce the impact of minimal residual disease on relapse. Alongside this, IFNs can potentially sensitize leukaemic cells to TKIs in resistant CML patients. There is evidence also that IFNs have a therapeutic role in myeloproliferative neoplasms (MPNs) such as polycythaemia vera (PV) and primary myelofibrosis (PMF), where they can restore polyclonality in patients. Novel formulations have improved the clinical effectiveness of IFNs. Low dose pegylated IFN formulations improve pharmacokinetics and improve patient tolerance to therapies, thereby minimizing the risk of haematological toxicities. Herein, we will discuss recent developments and the current understanding of the molecular and clinical implications of Type I IFNs for the treatment of myeloid malignancies.

Keywords: interferon, myeloid malignancies, interferon alfa, interferon beta, type I interferon (IFN) signaling, myeloid neoplasia

CLONAL MALIGNANCIES IN MYELOID LINEAGES

Myeloid malignancies, consisting of myeloproliferative neoplasms (MPNs), myelodysplastic syndrome (MDS), and acute myeloid leukaemia (AML), are a heterogeneous group of clonal haematopoietic disorders caused by abnormalities in HSCs and myeloid progenitor cells, originating in the bone marrow niche (1, 2). Each myeloid malignancy is unique and therefore presents different challenges with regards to treatment. MPNs have been categorized by the WHO as: chronic myeloid leukaemia (CML), polycythaemia vera (PV), primary myelofibrosis(PMF) and essential thrombocythemia (ET) and are characterized by the presence of the *BCR-ABL* gene, *JAK2*, *MPL* or *CALR* mutations, excessive erythrocyte production, fibrotic bone marrow degeneration, and excessive megakaryocyte lineage proliferation, respectively (3). MDS is characterized by abnormalities in normal haematopoiesis with resulting progression to bone marrow failure and genetic instability with potential to develop into AML (4) which is often considered the most aggressive myeloid malignancy. Older AML patients, those with poor-risk associated karyotypes, or with an unfavourable mutational burden (e.g. *TP53* mutations) have a median survival as low as 4-6 months (5–7). In comparison, patients who are diagnosed with CML and treated with tyrosine kinase inhibitors (TKIs), such as imatinib, have an overall long-term (8-year) survival rate as high as 93% (8–10). This vast difference in survival between different malignancies warrants a novel and innovative approach to the treatment of certain myeloid malignancies.

There are currently a variety of therapies available for myeloid malignancies, dependent on the disease in question. Most CML patients will experience long term responses with tyrosine kinase inhibitors (TKIs) targeting the *BCR-ABL* oncogene and can in many cases be considered functionally cured of their disease (9, 11). PV is associated with blood hyperviscosity due to the expansion of the erythrocyte mass, and therefore standard therapy involves blood withdrawal to reduce mass as well as treatment with hydroxyurea, or ruxolitinib (Janus activated kinase 1/2 (JAK1/JAK2) inhibitor) as a second-line chemotherapy option (12, 13). PMF can also be treated using JAK2 inhibitors, however this is considered only a symptom relieving measure – PMF is only potentially curable with an allogeneic haematopoietic stem cell transplant (HCT) and is associated with a substantial risk of treatment-related mortality (14). Finally, MDS and AML can also be treated with high dose, aplasia-inducing chemotherapy and consolidated with HCT. However, relapse remains a problem and many factors such as poor cytogenetic risk (15); monosomal karyotype (16); measurable residual disease (MRD) positivity (17, 18); FLT3-ITD and other mutations (19–21) can influence the risk of relapse in AML patients after HCT.

A large portion of AML patients are elderly and are considered unfit to undergo intensive chemotherapy (22). Current treatment for these malignancies is therefore unfavourable for many patients. Alternatively, hypomethylating agents in combination with BCL2 inhibitors (23, 24) are becoming an increasingly better option to reduce toxicity (25), although a new treatment for MDS and AML is still urgently required.

For decades, cytokines belonging to the Interferon (IFN) family have been shown to play an integral role in co-ordinating immune responses against viruses, intracellular pathogens and tumour control (26). IFNs are divided into three types: Type I (including IFN-α and IFN-β), Type II (IFN-γ only) and Type III (IFN-λ). A summary of these subtypes and potential therapeutics is described in **Table 1** (27–29). Type I IFNs are produced by most cells, following detection of pathogen-associated molecular patterns (PAMPs), such as foreign or self-nucleic acids (30). Interestingly, Type I IFNs differ in their binding affinity to the same cell surface receptor (IFNAR1/IFNAR2) and consequently trigger different antiviral, antiproliferative, and immunomodulatory outcomes (31). It is these antiproliferative and immunomodulatory outcomes which highlight IFNs as a potential treatment for myeloid malignancies (32). Herein we discuss to what extent IFNs can be used therapeutically to manage myeloid malignancies.

TYPE I INTERFERON SIGNALING

Following binding of Type I IFNs to the IFNAR1/IFNAR2 receptor complex, the associated JAK1 and tyrosine kinase 2 (TYK2) activation causes the tyrosine phosphorylation of STAT1 (signal transducer and activator of transcription 1) and STAT2 (**Figure 1**). This ultimately results in the formation of an IFN-stimulated gene factor 3 (ISGF3) complex which is translocated to the nucleus. Here, it binds IFN-stimulated response elements (ISREs), initiating transcription of IFN-stimulated genes (ISGs) (33). These ISGs have a wide range of functions, and can be involved in immune system regulation and cell death, amongst

Abbreviations: ABL, Abelson proto-oncogene; AML, Acute Myeloid Leukaemia; ara-C, Cytarabine; bFGF, basic fibroblast growth factor; BCR, Breakpoint cluster region gene; cGAMP, 2'3'-Cyclic GMP-AMP; cGAS, cyclic GMP-AMP synthase; CML, Chronic Myeloid Leukaemia; cMyc, cellular Myc protein; COX, Cyclooxygenase; DNA, Deoxyribonucleic acid; DR5, Death receptor 5; ET, Essential thrombocythaemia; GVHD, Graft versus host disease; GVL, Graft versus leukaemia; HCT, Haematopoietic stem cell transplant; HSCs, Haematopoietic stem cells; IFNAR1/2, Interferon-alpha/beta receptor 1/2; IFNs, Interferons; IFN-α/β/γ, Interferon alpha/beta/gamma; IRF3/9, Interferon regulatory factor 3/9; ISGF3, Interferon-stimulated gene factor 3; ISGs, Interferon-stimulated genes; ISREs, Interferon-stimulated response elements; IκB, Inhibitor of kappa B kinase; JAK1/2, Janus Kinase 1/2; LSCs, Leukaemic stem cells; MDS, Myelodysplastic syndrome; MMR, Molecular response rate; MPNs, Myeloproliferative neoplasms; MRD, Measurable/minimal residual disease; MSCs, Mesenchymal stromal cells; NF-κB, Nuclear factor-kappa B; NSAIDs, Non-steroidal anti-inflammatory drugs; PAMPs, Pathogen-associated molecular patterns; PMF, Primary myelofibrosis; PV, Polycythaemia Vera; Rig-G, Retinoic acid-induced gene G; RUNX1, Runt-related transcription factor 1; STAT1/2, Signal transducer and activator of transcription 1/2; STING, Stimulator of interferon genes; TKIs, Tyrosine Kinase Inhibitors; TNF-α, Tumour necrosis factor alpha; TRAIL, Tumour necrosis factor-related apoptosis inducing ligand; TYK2, Tyrosine kinase 2; VEGF, vascular epidermal growth factor.

TABLE 1 | Summary of the Canonical Functions of Type I Interferons and Therapeutic Potential.

Type	Expressed in humans?	Function/Key Processes	Therapeutically used?	Cancer therapeutic?
IFN-α	Yes	Apoptosis, CD8+ T cell priming, antigen presentation, pro-inflammatory cytokine production	Yes- IFN-α2a, IFN- α2b IFN- α14	IFN- α2a, IFN- α2b
IFN-β	Yes	Anti-proliferative, anti-angiogenic, stimulation of immune response	Yes	Yes
IFN-δ	No	Anti-proliferative effects	No	No
IFN-ϵ	Yes	TNF- α pathway activation, ROS generation	No	No
IFN-ζ (Limitin)	No	MHC class I expression, increases cytotoxic T lymphocyte activity, anti-proliferative effects	No	No
IFN-κ	Yes	Increases IFN-β production	No	No
IFN-τ	No	IL-6/IL-8 expression and secretion	No	No
IFN-ω	Yes	MHC I molecule production, innate immune cytokine production, phagocytosis	Yes - veterinary uses	No

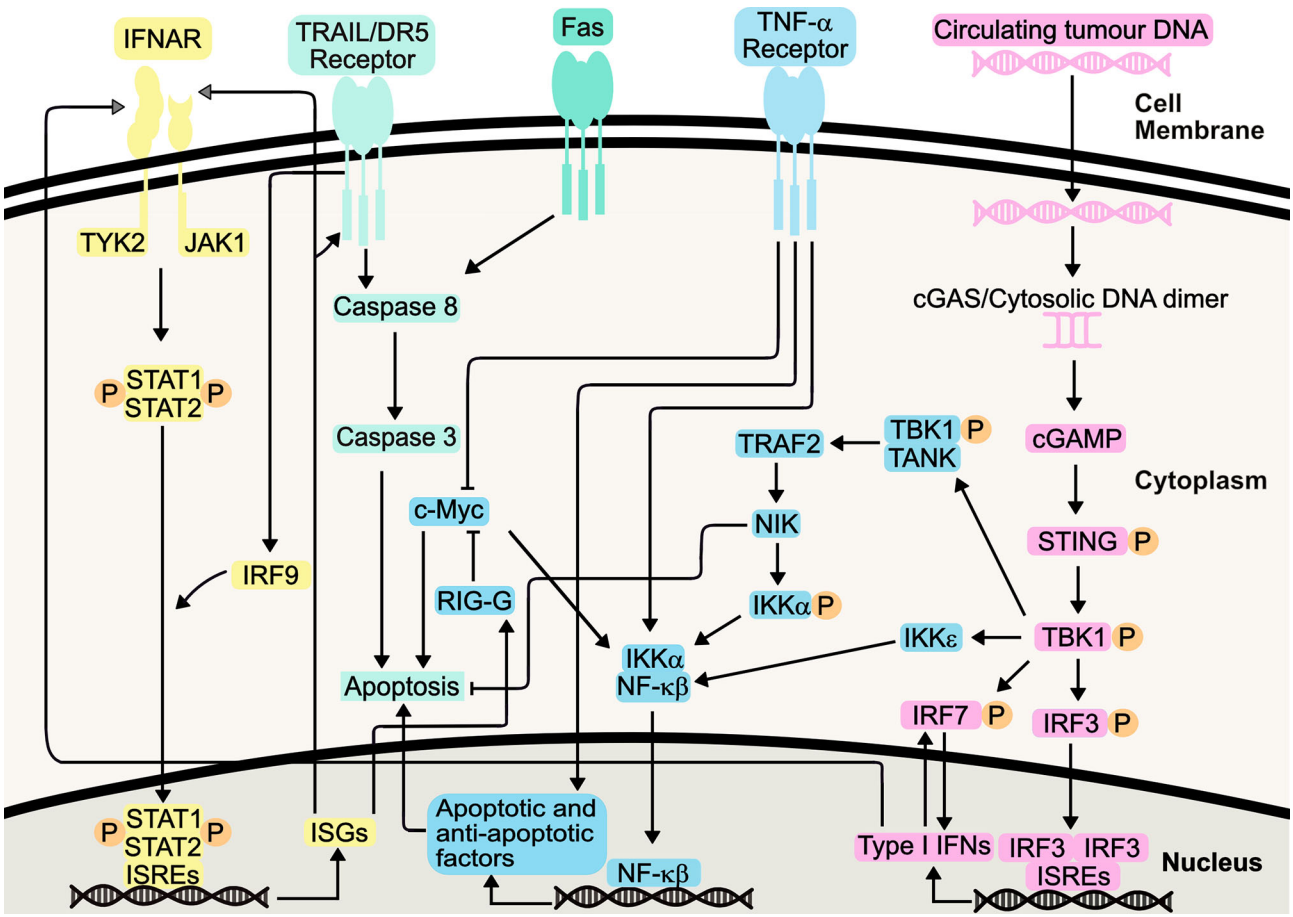

FIGURE 1 | Type I Interferon Signalling Pathways. Type I IFNs bind the IFNAR1/IFNAR2 receptors, causing heterodimerization and TYK2 and JAK1 activation, initiating STAT1/STAT2 heterodimerization and phosphorylation. Following IRF-9-mediated translocation of this heterodimer to the nucleus, it binds interferon-stimulated response elements (ISREs), resulting in transcription of interferon-stimulated genes (ISGs). Resulting proteins include death receptor ligands (including TRAIL and Fas), which bind their respective receptors. Apoptosis is induced, either directly, or indirectly *via* NF-κβ signalling. These pathways also synergize with TNF-α pathway, increasing apoptosis. The STING pathway, initiated by detection of circulating tumour DNA, can mediate production of Type I IFNs or induce apoptosis, through canonical and non-canonical pathways following TBK1 activation. This includes its role in positive feedback loops involving IRF7, further increasing Type I IFN production.

other processes. ISGs are also involved in both positive and negative feedback loops within the IFN signalling system, with the potential to increase or decrease IFN signalling, depending on cellular context such as mutational status (34).

IFN signaling results in the transcription and translation of cell death-inducing ISGs, and it has been hypothesized that IFN-α works by potentiating Tumour Necrosis Factor (TNF)-induced apoptosis through suppression of nuclear factor-κβ (NF-κβ) (35). Co-treatment of AML cell lines with TNF-α and IFN-α increased apoptosis compared to IFN-α alone, indicating IFN-α enhancement of TNF-α apoptosis *via* distinct and common pathways (36). Increased IFN production has been shown to inhibit activity of NF-κβ through the NIK/TRAF2 pathway, yet, this can be somewhat of a 'double-edged sword', with this pathway also implicated in cellular protection against IFN-mediated apoptosis (37). Furthermore, IFN-mediated NF-κβ inhibition leads to downregulation of cellular Myc (c-Myc) by increasing *IFIT3* (*RIG-G*) gene expression, promoting apoptosis and inducing cell cycle arrest, *via* enhancement of CD95/Fas expression, triggering increased cellular caspase 3 activity (38–40). Indeed, IFN-α has been known to sensitize cells to TRAIL-induced apoptosis, through activation of DR5 receptor-mediated death signaling and subsequent suppression of TRAIL-mediated NF-κβ activation (41).

NF-κβ is also responsible for the production of cytokines in response to the detection of cytosolic DNA. Through the stimulator of interferon genes (STING) pathway, activation of interferon regulatory factor 3 (IRF-3) and NF-κβ leads to transcription of ISGs and cytokines. This includes IFN-α and IFN-β, and STING activation ultimately promotes varying mechanisms of cell death, including apoptosis (42–44). It can therefore be argued that the STING pathway activation of NF-κβ forms an opposing mechanism, perhaps to maintain homeostasis as well as desensitizing the body to further IFN stimulation (45). This could also explain why some IFN therapies require frequent administration of IFNs to maintain a therapeutic effect. Nevertheless, the STING pathway presents itself as a promising target to promote immunity in cancer, including the treatment of AML (46).

It has been proposed that antiproliferative effects stimulated by Type I IFN on cancerous cells can enhance the immune response in mouse models of haematological malignancies (47), through induction of cell cycle arrest. This is largely through an increase in p21 activity, as well as CDK2 inhibition, though perhaps to a lesser extent (48, 49). Type I IFN-mediated cell cycle arrest in S phase appears to be regulated through IRF9 (48–50). Increased levels of IRF9 have been attributed to increased *TRAIL* activity, which itself is an ISG (50, 51).

Type I IFNs can also negatively regulate angiogenesis, thereby reducing oxygen supply to malignant cells. This can be through increased transcription of anti-angiogenic factors, including the ISGs *IRF7* and *PML*. Alternatively, Type I IFNs can reduce production of pro-angiogenic factors, including basic fibroblast growth factor (bFGF), a factor increased in myeloid leukaemia (52, 53). Furthermore, it has been suggested that IFN therapy could reduce levels of pro-angiogenic vascular epidermal growth factor (VEGF), which is a biomarker used for CML severity (54, 55). Again, this primarily occurs through IFN-mediated reduction in *VEGFA* and *HIF1α* transcription, with lower levels of *VEGF* mRNA detected in tumour samples following Type I IFN therapy, as compared to diagnostic samples (52, 56).

Immunomodulatory effects of Type I IFNs can be mediated through dendritic cells, with Type I IFNs driving activation and maturation of dendritic cells (57). Following IFN-stimulated dendritic cell maturation, there can be an increase in MHC molecule production and antigen presentation to CD8+ T cells, thereby promoting CD8+ T cell mediated responses, ultimately leading to tumour destruction (58). Furthermore, IFN-stimulated dendritic cell maturation also induces expression of costimulatory ligands CD80 and CD86 (59–61). CD80 and CD86 are needed for full T cell activation, through their binding to CD28. Furthermore, increased CD80 expression induces IRF-7 expression, thereby stimulating further Type I IFN production, in somewhat of a positive feedback mechanism. Such pathway can be mediated by TRADD, TRAF3 and TANK activation, as well as IFN-β and IRF3 (31, 60, 62). Aside from these aforementioned signalling pathways, IFN-α also increases production of pro-inflammatory cytokines, including IL-1β, IFN-γ and TNF-α (31, 63). As previously stated, increased TNF-α contributes to increased apoptosis seen in response to Type I IFN. Thus, it can be deduced that, unsurprisingly, there is synergy between the various IFN-stimulated pathways, converging in key elements responsible for the apoptotic, anti-angiogenic, immunomodulatory and antiproliferative responses.

DO IFNs REDUCE THE RATES OF AML RELAPSE?

Treatment options for AML patients rely heavily on a combination of anthracyclines (e.g. daunorubicin, idarubicin) and the pyrimidine nucleoside cytarabine (64), which deliver an unsatisfactory 5-year survival rate of <20% in older patients (65–68). A goal of treating AML is obtaining a complete remission and preferably eradicating MRD, which is defined as the presence of residual leukaemic cells in bone marrow (BM) or peripheral blood (PB) in patients who have achieved morphologic complete remission (69). MRD positivity is associated with increased relapse risk and shorter survival in AML (70–73). One recent study found that measuring the transcript levels of *RUNX1/RUNX1T1* fusion gene in AML patients with MRD (post-HCT) allowed for a significant discrimination between patients that would continue remission or enter relapse (74). Other studies have supported this finding and argue that monitoring MRD using transcript levels of *RUNX1/RUNX1T1* fusion gene is favourable over the measurement of other mutations including *c-KIT* mutations for the risk stratification of AML patients with MRD (75). IFN therapy could potentially target the leukaemic stem cells (LSCs) at the root of AML development and relapse. It has been

demonstrated that IFN-α triggers cell cycle entry in dormant HSCs (76). This raises the possibility that treating AML patients with IFN could force quiescent LSCs to proliferate, and thus amenable to standard chemotherapy. It has been shown that MRD-directed IFN-α treatment was able to significantly decrease the risk of cumulative incidence of relapse and improve survival in MRD-positive AML patients post-HCT, compared to MRD patients with no intervention (77, 78). Indeed, a recent retrospective study examined the use of IFN maintenance therapy following induction and consolidation chemotherapy in favourable-risk AML patients. Of patients who were MRD positive at baseline measurements, 78% of those treated with IFN-α2b became MRD negative, after a median time of 5.5 months. In contrast, only 27% of patients not treated with IFN-α2b (monitored only) showed MRD conversion from positive to negative. This corresponded to an increase in relapse-free survival, with 87% IFN-α2b treated patients relapse free after 4 years, compared to 56% in the control group (79). An ongoing phase I/II trial has demonstrated that pegylated IFN-α, when administered prophylactically after myeloablative conditioning in an AML cohort at high risk for relapse, did not significantly alter toxicity or acute graft *versus* host disease (GVHD) risk and produced relatively low rates of relapse suggesting a robust graft *versus* leukaemia (GVL) response (80). Separately a recent trial has explored the use of IFN-α2b therapy following MRD detection post induction and consolidation chemotherapy. A significant decrease in the number of patients with MRD in the IFN-α2b treated group was reported after a median follow-up time of 5 months, compared to a significant increase in patients with MRD detection in the trial arm that did not receive IFN after chemotherapy (patients observed only) (81). Importantly, event-free survival was also considerably higher in the IFN-α2b treated patients. IFN therapies to prevent relapse in AML potentially offer significant benefit to AML patients and this warrants further study.

IFNs FOR TKI RESISTANT CML PATIENTS

TKIs including imatinib, nilotinib, dasatinib, bosutinib, and most recently ponatinib, are the current preferred treatment for CML patients, and have dramatically improved the outcome of CML patients (82). Despite the success of TKIs, there is still a possibility that some CML patients become resistant to front-line treatment with imatinib, and to second generation TKIs (e.g. nilotinib, dasatinib) through the *BCR-ABL* T315I mutation wherein only third generation TKIs (e.g. ponatinib) are efficacious. Even still, resistance to imatinib has been seen since the earliest trials and has recently been shown for third-generation TKIs (83, 84). IFN therapy for the treatment of CML pre-dates TKI therapy, and is characterized by its ability to induce haematologic remission and durable cytogenetic response (85). Combination therapy of IFNs with cytarabine for many CML patients showed promising results, however the advent of TKIs meant that IFN therapy was largely replaced (86). The IRIS trial compared the use of imatinib or IFN-α plus cytarabine. Whilst there was no significant difference in survival after 18 months between either group, patients treated with IFN-α and cytarabine showed a markedly poorer cytogenetic response, coupled with a greater risk of disease progression, compared to those who received imatinib alone. Indeed, many patients who initially received IFN-α and cytarabine crossed over to imatinib therapy (9, 87, 88). Response to imatinib continued over 5 years, with a complete cytogenetic response seen in 69% of all patients who received imatinib (and up to 96% in those still taking imatinib after 5 years) (87). However, approximately 17% patients did lose complete cytogenetic response over the follow-up period (9).

This is in line with current understanding which suggests that TKIs are not entirely curative as monotherapies in CML, as LSC exposure to many TKIs fails to induce apoptosis in the most primitive quiescent CML LSCs (89, 90). Combined therapy of IFN-α with TKIs could address this issue by stimulating cytotoxic T cells to target LSCs refractory to standard TKI therapy. Initial studies comparing patients treated with imatinib and IFNα, to those treated with imatinib alone, showed that the combination therapy resulted in a higher rate of complete cytogenetic remission at 6 months, and similar rates at 4 years (91). Similarly, a trial of imatinib and IFN-α combination therapy showed 75% of patients showed sustained remission following imatinib discontinuation at 2.4 years (92). However, other trials involving the combination of IFNs with imatinib have shown mixed results, with no improvement in cytogenetic response rates or progression-free survival and increased adverse events (93, 94). For example, in extended (10 year) follow-up of the aforementioned IRIS trial, patients treated with imatinib alone had similar overall and progression-free survival than those treated with imatinib and IFN-α (95).

Whilst imatinib is considered a 'game-changing' drug for the extremely high survival rate it is associated with, second generation TKIs have shown further improvements in these rates in certain cases (10). IFN-α combination therapy with the second generation TKI dasatinib has also shown promising results (96). Low dose pegylated IFN-α following dasatinib treatment was well tolerated, and demonstrated rapid increased response rates with major molecular response (MMR) rate of 89% after 18 months. Encouragingly pegylated IFN-α was well tolerated in this study, and further investigation is warranted with second generation TKIs. Earlier studies of combination therapy comprising pegylated IFN-α formulations with imatinib, had shown good clinical response (significantly higher MMR of 82% compared to 54% for imatinib monotherapy after 12 months), yet were associated with toxicity also in a majority of patients (54). NiloPeg, a small 2011 phase II trial looking at the use of nilotinib and IFN-α2a showed a good molecular response in patients treated with this regimen (64% after 12 months), although adverse effects were, again, a frequent occurrence (97). The currently ongoing TIGER trial of nilotinib combination therapy with pegylated IFN-α is attempting to address these concerns, and will evaluate the feasibility of discontinuing drug

therapy in patients showing stable deep molecular response after nilotinib *versus* IFN maintenance therapy (98).

TREATING MPNs WITH IFNs

The WHO classification system for MPNs includes seven subcategories (3), but more commonly this refers to the *JAK2* mutation-enriched diseases polycythaemia vera (PV), essential thrombocythaemia (ET) and primary myelofibrosis (PMF). PV is characterized by an elevated red blood cell mass (and potentially overproduction of white blood cells and platelets). PV is also associated with an increased risk for thromboembolic events, leukaemic transformation, and/or myelofibrosis.

Type I IFN signalling can contribute to the pathology of MPN, as well as being used as a therapeutic, as mentioned previously. In PMF, levels of IFN-α, and associated proinflammatory cytokines such as IL-1β, can be increased compared to healthy bone marrow or plasma. This contributes to the inflammatory phenotype associated with PMF (99). This coincides with the effects of *TET2* mutations, which are common in MPNs and are also associated with inflammation (100). In a similar way, whilst myelodysplastic syndrome (MDS) has a vast range of causes, increased pro-inflammatory signalling is thought to be a key driver, again mediated by Type I IFNs. Type I IFN-associated genes were found to be upregulated in MDS patients' bone marrow, including *IRF-7* and *ISG-15*, suggesting their involvement in MDS pathology (101).

Standard therapy for PV involves phlebotomy and cytoreductive drugs (hydroxyurea, busulfan) but recently IFN-α and JAK1/2 inhibitors have been examined as potential treatments (102, 103). Although busulfan has been effective over long periods (104), resistance to hydroxyurea is associated with increased mortality and progression to more advanced MPNs or secondary AML (13). IFN therapy is an accepted alternative to hydroxyurea or busulfan in PV, and is particularly useful for younger patients or those who are pregnant (105, 106). In fact, IFN-α2 has been shown to induce haematological responses in about 80% of PV patients while also reducing splenomegaly, and relieving pruritus (107). A study of patients treated with IFN-α compared to a control group showed an MMR of 89%, with a stable circulating *JAK2* mutated allele (% V617F) in the other 11% of patients (108).

Recent trial data have demonstrated that 76% of advanced PV patients treated with IFN-α2a showed complete haematologic response, while the complete molecular response rate was 19% at 42 months (109). Similarly, good efficacy for pegylated IFN-α in hydroxyurea resistant patients was seen, with an overall response rate of 60% at 12 months (110). Significantly this trial was based on relatively broad inclusion criteria e.g., advanced age, prolonged disease duration, and a high prevalence of splenomegaly. However, 14% of patients discontinued therapy due to adverse events. However, the PROUD-PV and Continuation-PV trials revealed a need for prolonged IFN-α therapy as a means of reaching both molecular response and complete haematological response. Whilst therapy with ropeginterferon-alfa-2b (pegylated form of IFN-α2b) increased the proportion of patients achieving complete haematological response and improved disease burden after 36 months compared to those patients treated with hydroxyurea (53% *versus* 38%), this was not the case after shorter time periods (46% *versus* 51% at 12 months). Thus, there is a need for sustained treatment with IFN-α to achieve best response). Importantly, the toxicity profile associated with prolonged ropeginterferon-alfa-2b therapy was not significantly worse than that of hydroxyurea (111).

Primary Myelofibrosis (PMF) can be classified into two stages: pre-fibrotic (pre-PMF) and fibrotic PMF (overt-PMF) diagnosed by bone marrow morphology, fibrosis grade and clinical features including leukoerythroblastosis, anaemia and splenomegaly (112). Aside from HCT, there are limited treatment options for very high- and high-risk patients and 10-year survival is estimated at <13%. The use of JAK2 inhibitors is considered mostly palliative, and the treatment of clinical features includes the use of androgens, hydroxyurea and ruxolitinib (113). However, IFNs may provide a means of increasing the survival of patients with PMF. Preliminary results of a Phase II study using a combination therapy between pegylated IFN-α and ruxolitinib on 50 MPN patients (32 PV and 18 PMF patients), most of whom were resistant and/or intolerant to IFN-α as a monotherapy, saw complete haematologic responses in 44% and 58% of PV and PMF patients respectively (114). Despite a 20% discontinuation rate for this trial, there is clear indication that the inflammatory mediated toxicity which often limits IFN-α was reduced by ruxolitinib, known for its potent anti-inflammatory properties. It is also reported that levels of the V617F allele declined significantly in both groups. This supports previous findings that monitoring the %V617F is a reliable marker for MPNs and the detection of MRD.

Essential thrombocythaemia (ET) is a clonal MPN characterized by excess production of platelets and mature hyperlobulated megakaryocytes, with the presence of mutations in *JAK2*, *CALR*, or *MPL* and the absence of *BCR-ABL* (3). Most ET patients have a normal life expectancy, and the goals of treatment are the prevention of thrombotic and bleeding complications while minimizing the risk of progression, the effective control of systemic symptoms, and the appropriate management of complications and risk situations (105). Treatment of ET typically involves combinations of aspirin, ticlopidine, hydroxyurea and anagrelide to reduce platelet number and manage clotting (115, 116). IFN therapy in ET is also effective for reducing platelet numbers while also reducing the risk of thrombotic complications (107, 117) but does not appear to restore polyclonal haematopoiesis (118). Studies that will directly compare pegylated IFN-α2a to hydroxyurea in ET and PV are currently ongoing (110). Initial reports show an overall response rate of 69% for pegylated IFN-α2a in ET patients at 12 months, with acceptable safety profile (major thrombotic events at 1 year was 1%, with no major bleeding events).

A recent study comprising patients with PV, PMF or ET indicated IFN-α has a stronger effect on HSCs than mature blood cells. Within this compartment, those with *JAK2* V617F-mutated HSCs responded better than those with other mutations, such as *CALR*. This is thought to be a result of the *JAK2* V617F increasing the sensitivity of HSCs to IFN signalling, through increased ISG activation (119). Whilst it has been widely understood that IFN-α can reduce the HSC compartment through cell cycle activation and subsequent HSC exhaustion, recent findings suggest this is only the case in *JAK2* V617F mutated HSCs. In contrast, JAK2 wild-type HSCs generally remain quiescent in the presence of IFN-α. This is consistent with the ability of IFN-α to arrest the cell cycle in bulk tumor cells (48). Current understanding suggests IFN-α-mediated promotion of *JAK2* V617F-mutated HSC cell cycle not only exhausts the cells, but uses induces differentiation to the erythroid lineage, making them susceptible to IFN-α-mediated apoptosis (120). Nevertheless, the effects of IFN-α demonstrated here may not be wholly specific to the V617F mutant, since stem cell derived erythrocytes containing *JAK2* with exon 12 mutations (also causing constitutive JAK2 activation, as seen in PV) were also sensitive to IFN-α treatment (121).

CONCLUSIONS & FUTURE DIRECTIONS

Similar to symptoms experienced during normal IFN release in the presence of a foreign pathogen, acute toxicity to IFN therapy usually presents as flu-like symptoms including nausea, fatigue, and myalgia (122). Most side effects associated with IFN therapy are dose-dependent, and these can be mitigated by administering low dose pegylated-IFNs in addition to managing inflammation with NSAIDs. Acute toxicity is experienced by nearly all patients, while sub-acute and chronic side effects have been reported in almost all organ systems throughout the body. A 2018 study conducted by Mo et al. using IFN-α for the treatment for MRD in AML for example, reported that all patients reported transient fevers and six patients (14%) showed grade ≥3 toxicity, two of which were haematological (77). A study of CML patients treated with low-dose pegylated IFN-α reported that 20% and 25% of patients experienced grade 3-4 neutropenia and thrombocytopenia in the first 12 months respectively (96). While some toxicity is still observed, pegylated IFNs show increased patient tolerance, and modify the immunological, pharmacokinetic and pharmacodynamic properties of the drug to minimize off-target adverse effects and increase efficacy (123). Pegylated IFN-α lengthens plasma half-life and reduces sensitivity to proteolysis, allowing it to be administered less frequently (122).

It is important that other adverse events in IFN therapy including flu-like symptoms and myalgia are also controlled using anti-inflammatory drugs. A common trend throughout the studies discussed herein is a high percentage of patients who do not complete IFN therapy because it is not well tolerated alongside chemotherapy, which can be as high as 61% of patients discontinuing treatment (54).

Another confounding factor for IFN therapy is the variability of the bone marrow niche between patients. IFN therapy relies on the innate, non-specific immune system to induce an immune response meaning it is not well tailored to one specific individual. This may partially explain why the responsiveness to IFN therapy in a small patient group varies greatly. To account for this, larger studies such as the TIGER study (98) are vital to better understand the causes for intolerance and resistance to therapy.

There is also a considerable economic barrier for uptake of IFN therapy. Analysis has shown that imatinib is a cost-effective first line therapy *versus* IFN-α plus low-dose cytarabine for newly diagnosed CML (124). If significant cohorts of patients will ultimately discontinue IFN therapy in favour of TKIs, then coupled with cost-based concerns, then IFNs become less favourable drugs to develop.

It is apparent in AML that carefully targeted IFN therapy can provide a significant improvement to patient outcome especially in the management of MRD (27, 77, 78). The sensitization of leukaemic cells in the bone marrow niche by IFNs to classic chemotherapy agents will possibly improve the prospects of many AML patients should the treatment become more widely available (**Figure 2**), especially in patients post-HCT for the eradication of MRD. This is an extremely important goal, as multiple studies have shown the presence of MRD is associated with increased relapse risk and shorter survival in both paediatric and adult AML (71).

Similarly in CML, further development of IFN therapy provides an opportunity alongside current standards. Continuing focus on development of novel TKIs targeting BCR-ABL has meant that IFN therapy has not advanced greatly over the last decade for CML patients. There is potential for IFN therapy as a combination therapy with TKIs to sensitize cells and aid the action of the primary treatment. Just as in the case of AML, targeting the LSC to overcome resistance to TKIs is a fundamental goal and essential to achieving long-term remissions.

In PV and PMF, where the side effects of IFNs are tolerated, treatment using IFNs in combination with JAK2 inhibitors is certainly a possibility for the prevention of disease progression to other myeloid malignancies. As in AML, the use of IFNs for the treatment of PV and PMF to control MRD post-HCT would be beneficial for patients.

In conclusion, the benefits of using IFN therapy for the treatment of myeloid malignancies warrants further research. Despite intolerance seen in many small studies, IFNs are to be considered as an alternative therapy to traditional chemotherapy regimens or in combination with existing regimens for the sensitization of leukaemic cells to treatment and the reduction of MRD. It is important that other formulations of IFNs are developed in addition to pegylation, as this will determine whether pharmaceutical companies recognize this therapy as a reliable candidate for future treatment – the findings of large, ongoing Phase III trials will become a critical turning point. In short, the re-emergence of IFN therapy does indeed provide new

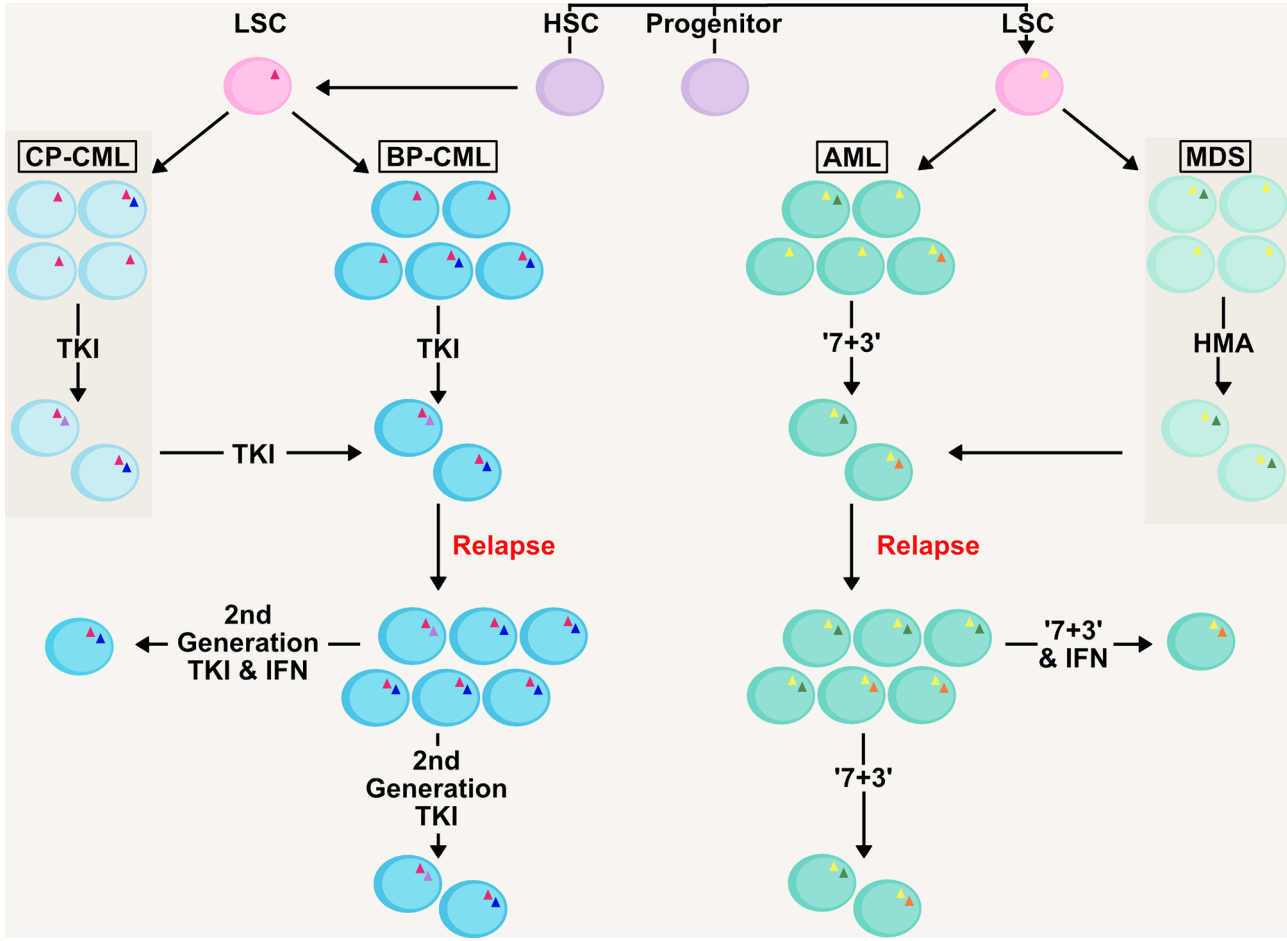

FIGURE 2 | Management of Clonality and MRD in AML/CML with IFN therapy. AML and CML are clonal diseases, presenting at diagnosis with a major immature blast clone and minor clones (denoted by mutations as triangles within cells) which develop due to mutations in the haematopoietic stem and progenitor pool generating the LSC. Initial therapy in both chronic-phase (CP-CML) and blast-phase (BP-CML) patients with a first-generation tyrosine kinase inhibitor (TKI) against the *BCR-ABL* oncogene (pink triangle), such as imatinib, will reduce the bulk of CML blasts in the bone marrow and peripheral blood. However, it is not uncommon for resistant clones to persist that are refractory to this treatment. Later generation TKIs (e.g. nilotinib, dasatanib, ponatinib) may eradicate these clones but some mutations (e.g. *BCR-ABL* T315I; green circle) drive resistance to novel TKIs. Similarly, initial '7+3' therapy in AML (7 day treatment with the pyrimidine analogue cytarabine, in conjunction with an anthracycline, such as daunorubicin, for the first 3 days) and HMA-therapy (hypomethylating agent) in MDS will eradicate the bulk of leukaemic blasts (such as those containing initiating mutations; yellow triangle) in the patient. However, clones refractory to these therapies (including those with signalling mutations; blue and orange circles) will drive relapse in MDS/AML patients, as well as transformation from MDS to AML. Management of measurable residual disease (MRD) in myeloid malignancies is critical to preventing relapse. Therapies based on IFNs could target the clones resistant to front-line therapies and deliver longer remissions.

hope for leukaemia patients, more specifically in the treatment of MRD.

AUTHOR CONTRIBUTIONS

JW conceived the study. FH, JJ, and JW wrote the manuscript. FH and JW produced the figures. YF and LD edited and contributed to the final submitted manuscript, and provided critical insights. All authors contributed to the article and approved the submitted version.

FUNDING

JW and LD are supported by North West Cancer Research.

REFERENCES

1. Korn C, Méndez-Ferrer S. Myeloid Malignancies and the Microenvironment. *Blood* (2017) 129(7):811–22. doi: 10.1182/blood-2016-09-670224
2. Zeidner JR,D, Perl A, Gojo I. *The American Cancer Society's Oncology in Practice: Clinical Management*. Newark, United States: John Wiley & Sons, Incorporated (2018).
3. Arber DA, Orazi A, Hasserjian R, Thiele J, Borowitz MJ, Le Beau MM, et al. The 2016 Revision to the World Health Organization Classification of Myeloid Neoplasms and Acute Leukemia. *Blood* (2016) 127(20):2391–405. doi: 10.1182/blood-2016-03-643544
4. Haferlach T. The Molecular Pathology of Myelodysplastic Syndrome. *Pathobiology* (2019) 86(1):24–9. doi: 10.1159/000488712
5. Rücker FG, Schlenk RF, Bullinger L, Kayser S, Teleanu V, Kett H, et al. TP53 Alterations in Acute Myeloid Leukemia With Complex Karyotype Correlate With Specific Copy Number Alterations, Monosomal Karyotype, and Dismal Outcome. *Blood* (2012) 119(9):2114–21. doi: 10.1182/blood-2011-08-375758
6. Hou HA, Chou WC, Kuo YY, Liu CY, Lin LI, Tseng MH, et al. TP53 Mutations in De Novo Acute Myeloid Leukemia Patients: Longitudinal Follow-Ups Show the Mutation Is Stable During Disease Evolution. *Blood Cancer J* (2015) 5:e331 p. doi: 10.1038/bcj.2015.59
7. Welch JS, Petti AA, Miller CA, Fronick CC, O'Laughlin M, Fulton RS, et al. TP53 and Decitabine in Acute Myeloid Leukemia and Myelodysplastic Syndromes. *N Engl J Med* (2016) 375(21):2023–36. doi: 10.1056/NEJMoa1605949
8. Sacha T. Imatinib in Chronic Myeloid Leukemia: An Overview. *Mediterr J Hematol Infect Dis* (2014) 6(1):e2014007–e. doi: 10.4084/mjhid.2014.007
9. Hughes TP, Hochhaus A, Branford S, Müller MC, Kaeda JS, Foroni L, et al. Long-Term Prognostic Significance of Early Molecular Response to Imatinib in Newly Diagnosed Chronic Myeloid Leukemia: An Analysis From the International Randomized Study of Interferon and STI571 (IRIS). *Blood* (2010) 116(19):3758–65. doi: 10.1182/blood-2010-03-273979
10. García-Gutiérrez V, Hernández-Boluda JC. Tyrosine Kinase Inhibitors Available for Chronic Myeloid Leukemia: Efficacy and Safety. *Front Oncol* (2019) 9(603). doi: 10.3389/fonc.2019.00603
11. Suttorp M, Bornhäuser M, Metzler M, Millot F, Schleyer E. Pharmacology and Pharmacokinetics of Imatinib in Pediatric Patients. *Expert Rev Clin Pharmacol* (2018) 11(3):219–31. doi: 10.1080/17512433.2018.1398644
12. Dale E, Davis M, Faustman DL. A Role for Transcription Factor NF-kappaB in Autoimmunity: Possible Interactions of Genes, Sex, and the Immune Response. *Adv Physiol Educ* (2006) 30(4):152–8. doi: 10.1152/advan.00065.2006
13. Nazha A, Gerds AT. Where to Turn for Second-Line Cytoreduction After Hydroxyurea in Polycythemia Vera? *Oncologist* (2016) 21(4):475–80. doi: 10.1634/theoncologist.2015-0380
14. Tefferi A, Guglielmelli P, Pardanani A, Vannucchi AM. Myelofibrosis Treatment Algorithm 2018. *Blood Cancer J* (2018) 8(8):72. doi: 10.1038/s41408-018-0109-0
15. Cornelissen JJ, Breems D, van Putten WL, Gratwohl AA, Passweg JR, Pabst T, et al. Comparative Analysis of the Value of Allogeneic Hematopoietic Stem-Cell Transplantation in Acute Myeloid Leukemia With Monosomal Karyotype *Versus* Other Cytogenetic Risk Categories. *J Clin Oncol* (2012) 30(17):2140–6. doi: 10.1200/JCO.2011.39.6499
16. Fang M, Storer B, Estey E, Othus M, Zhang L, Sandmaier BM, et al. Outcome of Patients With Acute Myeloid Leukemia With Monosomal Karyotype Who Undergo Hematopoietic Cell Transplantation. *Blood* (2011) 118(6):1490–4. doi: 10.1182/blood-2011-02-339721
17. Leung W, Pui CH, Coustan-Smith E, Yang J, Pei D, Gan K, et al. Detectable Minimal Residual Disease Before Hematopoietic Cell Transplantation Is Prognostic But Does Not Preclude Cure for Children With Very-High-Risk Leukemia. *Blood* (2012) 120(2):468–72. doi: 10.1182/blood-2012-02-409813
18. Walter RB, Gyurkocza B, Storer BE, Godwin CD, Pagel JM, Buckley SA, et al. Comparison of Minimal Residual Disease as Outcome Predictor for AML Patients in First Complete Remission Undergoing Myeloablative or Nonmyeloablative Allogeneic Hematopoietic Cell Transplantation. *Leukemia* (2015) 29(1):137–44. doi: 10.1038/leu.2014.173
19. Brunet S, Labopin M, Esteve J, Cornelissen J, Socié G, Iori AP, et al. Impact of FLT3 Internal Tandem Duplication on the Outcome of Related and Unrelated Hematopoietic Transplantation for Adult Acute Myeloid Leukemia in First Remission: A Retrospective Analysis. *J Clin Oncol* (2012) 30(7):735–41. doi: 10.1200/JCO.2011.36.9868
20. Schmid C, Labopin M, Socié G, Daguindau E, Volin L, Huynh A, et al. Outcome of Patients With Distinct Molecular Genotypes and Cytogenetically Normal AML After Allogeneic Transplantation. *Blood* (2015) 126(17):2062–9. doi: 10.1182/blood-2015-06-651562
21. Estey EH. Acute Myeloid Leukemia: 2019 Update on Risk-Stratification and Management. *Am J Hematol* (2018) 93(10):1267–91. doi: 10.1002/ajh.25214
22. Heiblig M, Elhamri M, Tigaud I, Plesa A, Barraco F, Labussière H, et al. Treatment With Low-Dose Cytarabine in Elderly Patients (Age 70 Years or Older) With Acute Myeloid Leukemia: A Single Institution Experience. *Mediterr J Hematol Infect Dis* (2016) 8(1):e2016009–e. doi: 10.4084/mjhid.2016.009
23. DiNardo CD, Pratz K, Pullarkat V, Jonas BA, Arellano M, Becker PS, et al. Venetoclax Combined With Decitabine or Azacitidine in Treatment-Naive, Elderly Patients With Acute Myeloid Leukemia. *Blood* (2019) 133(1):7–17. doi: 10.1182/blood-2018-08-868752
24. Pollyea DA, Pratz K, Letai A, Jonas BA, Wei AH, Pullarkat V, et al. Venetoclax With Azacitidine or Decitabine in Patients With Newly Diagnosed Acute Myeloid Leukemia: Long Term Follow-Up From a Phase 1b Study. *Am J Hematol* (2021) 96(2):208–17. doi: 10.1002/ajh.26039
25. Gerds AT, Gooley TA, Estey EH, Appelbaum FR, Deeg HJ, Scott BL. Pretransplantation Therapy With Azacitidine *vs* Induction Chemotherapy and Posttransplantation Outcome in Patients With MDS. *Biol Blood Marrow Transplant* (2012) 18(8):1211–8. doi: 10.1016/j.bbmt.2012.01.009
26. Parkin J, Cohen B. An Overview of the Immune System. *Lancet* (2001) 357(9270):1777–89. doi: 10.1016/S0140-6736(00)04904-7
27. Li S, Gong M, Zhao F, Shao J, Xie Y, Zhang Y, et al. Type I Interferons: Distinct Biological Activities and Current Applications for Viral Infection. *Cell Physiol Biochem* (2018) 51(5):2377–96. doi: 10.1159/000495897
28. Pestka S, Krause CD, Walter MR. Interferons, Interferon-Like Cytokines, and Their Receptors. *Immunol Rev* (2004) 202:8–32. doi: 10.1111/j.0105-2896.2004.00204.x
29. Budhwani M, Mazzieri R, Dolcetti R. Plasticity of Type I Interferon-Mediated Responses in Cancer Therapy: From Anti-Tumor Immunity to Resistance. *Front Oncol* (2018) 8(322). doi: 10.3389/fonc.2018.00322
30. Musella M, Manic G, De Maria R, Vitale I, Sistigu A. Type-I-Interferons in Infection and Cancer: Unanticipated Dynamics With Therapeutic

Implications. *Oncoimmunology* (2017) 6(5):e1314424. doi: 10.1080/2162402X.2017.1314424
31. Medrano RFV, Hunger A, Mendonça SA, Barbuto JAM, Strauss BE. Immunomodulatory and Antitumor Effects of Type I Interferons and Their Application in Cancer Therapy. *Oncotarget* (2017) 8(41):71249–84. doi: 10.18632/oncotarget.19531
32. Alsufyani A, Alanazi R, Woolley JF, Dahal LN. Old Dog, New Trick: Type I IFN-Based Treatment for Acute Myeloid Leukemia. *Mol Cancer Res* (2021) 19(5):753–6. doi: 10.1158/1541-7786.MCR-20-0871
33. Platanias LC. Mechanisms of Type-I- and Type-II-Interferon-Mediated Signalling. *Nat Rev Immunol* (2005) 5(5):375–86. doi: 10.1038/nri1604
34. Porritt RA, Hertzog PJ. Dynamic Control of Type I IFN Signalling by an Integrated Network of Negative Regulators. *Trends Immunol* (2015) 36 (3):150–60. doi: 10.1016/j.it.2015.02.002
35. Manna SK, Mukhopadhyay A, Aggarwal BB. IFN-α Suppresses Activation of Nuclear Transcription Factors NF-κb and Activator Protein 1 and Potentiates TNF-Induced Apoptosis. *J Immunol* (2000) 165(9):4927. doi: 10.4049/jimmunol.165.9.4927
36. Nakashima A, Kumakura S, Mishima S, Ishikura H, Kobayashi S. IFN-Alpha Enhances TNF-Alpha-Induced Apoptosis Through Down-Regulation of C-Myc Protein Expression in HL-60 Cells. *J Exp Clin Cancer Res* (2005) 24(3):447–56.
37. Pfeffer LM. The Role of Nuclear Factor κb in the Interferon Response. *J Interferon Cytokine Res* (2011) 31(7):553–9. doi: 10.1089/jir.2011.0028
38. Kimura M, Haisa M, Uetsuka H, Takaoka M, Ohkawa T, Kawashima R, et al. TNF Combined With IFN-Alpha Accelerates NF-kappaB-Mediated Apoptosis Through Enhancement of Fas Expression in Colon Cancer Cells. *Cell Death Differ* (2003) 10(6):718–28. doi: 10.1038/sj.cdd.4401219
39. Sarkar D, Park ES, Fisher PB. Defining the Mechanism by Which IFN-β Dowregulates C-Myc Expression in Human Melanoma Cells: Pivotal Role for Human Polynucleotide Phosphorylase (Hpnpaseold-35). *Cell Death Differ* (2006) 13(9):1541–53. doi: 10.1038/sj.cdd.4401829
40. Xiao S, Li D, Zhu HQ, Song MG, Pan XR, Jia PM, et al. RIG-G as a Key Mediator of the Antiproliferative Activity of Interferon-Related Pathways Through Enhancing P21 and P27 Proteins. *Proc Natl Acad Sci USA* (2006) 103(44):16448–53. doi: 10.1073/pnas.0607830103
41. Shigeno M, Nakao K, Ichikawa T, Suzuki K, Kawakami A, Abiru S, et al. Interferon-Alpha Sensitizes Human Hepatoma Cells to TRAIL-Induced Apoptosis Through DR5 Upregulation and NF-Kappa B Inactivation. *Oncogene* (2003) 22(11):1653–62. doi: 10.1038/sj.onc.1206139
42. Gulen MF, Koch U, Haag SM, Schuler F, Apetoh L, Villunger A, et al. Signalling Strength Determines Proapoptotic Functions of STING. *Nat Commun* (2017) 8(1):427. doi: 10.1038/s41467-017-00573-w
43. Chen D, Tong J, Yang L, Wei L, Stolz DB, Yu J, et al. PUMA Amplifies Necroptosis Signaling by Activating Cytosolic DNA Sensors. *Proc Natl Acad Sci USA* (2018) 115(15):3930–5. doi: 10.1073/pnas.1717190115
44. Sun F, Liu Z, Yang Z, Liu S, Guan W. The Emerging Role of STING-Dependent Signaling on Cell Death. *Immunol Res* (2019) 67(2-3):290–6. doi: 10.1007/s12026-019-09073-z
45. Schneider WM, Chevillotte MD, Rice CM. Interferon-Stimulated Genes: A Complex Web of Host Defenses. *Annu Rev Immunol* (2014) 32:513–45. doi: 10.1146/annurev-immunol-032713-120231
46. Curran E, Chen X, Corrales L, Kline DE, Dubensky TWJr., Duttagupta P, et al. STING Pathway Activation Stimulates Potent Immunity Against Acute Myeloid Leukemia. *Cell Rep* (2016) 15(11):2357–66. doi: 10.1016/j.celrep.2016.05.023
47. Escobar G, Barbarossa L, Barbiera G, Norelli M, Genua M, Ranghetti A, et al. Interferon Gene Therapy Reprograms the Leukemia Microenvironment Inducing Protective Immunity to Multiple Tumor Antigens. *Nat Commun* (2018) 9(1):2896. doi: 10.1038/s41467-018-05315-0
48. Murphy D, Detjen KM, Welzel M, Wiedenmann B, Rosewicz S. Interferon-Alpha Delays S-Phase Progression in Human Hepatocellular Carcinoma Cells *via* Inhibition of Specific Cyclin-Dependent Kinases. *Hepatology* (2001) 33(2):346–56. doi: 10.1053/jhep.2001.21749
49. Szeps M, Erickson S, Gruber A, Castro J, Einhorn S, Grandér D. Effects of Interferon-α on Cell Cycle Regulatory Proteins in Leukemic Cells. *Leukemia Lymphoma* (2003) 44(6):1019–25. doi: 10.1080/1042819031000077133
50. Tsuno T, Mejido J, Zhao T, Schmeisser H, Morrow A, Zoon KC. IRF9 Is a Key Factor for Eliciting the Antiproliferative Activity of IFN-Alpha. *J Immunother* (2009) 32(8):803–16. doi: 10.1097/CJI.0b013e3181ad4092
51. Leaman DW, Chawla-Sarkar M, Jacobs B, Vyas K, Sun Y, Ozdemir A, et al. Novel Growth and Death Related Interferon-Stimulated Genes (ISGs) in Melanoma: Greater Potency of IFN-Beta Compared With IFN-Alpha2. *J Interferon Cytokine Res* (2003) 23(12):745–56. doi: 10.1089/107999003772084860
52. Borden EC. Interferons α and β in Cancer: Therapeutic Opportunities From New Insights. *Nat Rev Drug Discovery* (2019) 18(3):219–34. doi: 10.1038/s41573-018-0011-2
53. Song M-Z, Mao Y-M, Wu J, Pan H-F, Ye Q-L. Increased Circulating Basic Fibroblast Growth Factor Levels in Acute Myeloid Leukemia: A Meta-Analysis. *Hematology* (2020) 25(1):186–93. doi: 10.1080/16078454.2020.1766865
54. Simonsson B, Gedde-Dahl T, Markevärn B, Remes K, Stentoft J, Almqvist A, et al. Combination of Pegylated IFN-α2b With Imatinib Increases Molecular Response Rates in Patients With Low- or Intermediate-Risk Chronic Myeloid Leukemia. *Blood* (2011) 118(12):3228–35. doi: 10.1182/blood-2011-02-336685
55. Legros L, Guilhot J, Huault S, Mahon FX, Preudhomme C, Guilhot F, et al. Interferon Decreases VEGF Levels in Patients With Chronic Myeloid Leukemia Treated With Imatinib. *Leukemia Res* (2014) 38(6):662–5. doi: 10.1016/j.leukres.2014.01.010
56. von Marschall Z, Scholz A, Cramer T, Schäfer G, Schirner M, Öberg K, et al. Effects of Interferon Alpha on Vascular Endothelial Growth Factor Gene Transcription and Tumor Angiogenesis. *JNCI: J Natl Cancer Institute* (2003) 95(6):437–48. doi: 10.1093/jnci/95.6.437
57. Gardner A, Ruffell B. Dendritic Cells and Cancer Immunity. *Trends Immunol* (2016) 37(12):855–65. doi: 10.1016/j.it.2016.09.006
58. Schiavoni G, Mattei F, Gabriele L. Type I Interferons as Stimulators of DC-Mediated Cross-Priming: Impact on Anti-Tumor Response. *Front Immunol* (2013) 4:483–. doi: 10.3389/fimmu.2013.00483
59. Simmons DP, Wearsch PA, Canaday DH, Meyerson HJ, Liu YC, Wang Y, et al. Type I IFN Drives a Distinctive Dendritic Cell Maturation Phenotype That Allows Continued Class II MHC Synthesis and Antigen Processing. *J Immunol* (2012) 188(7):3116–26. doi: 10.4049/jimmunol.1101313
60. Peteranderl C, Herold S. The Impact of the Interferon/TNF-Related Apoptosis-Inducing Ligand Signaling Axis on Disease Progression in Respiratory Viral Infection and Beyond. *Front Immunol* (2017) 8:313. doi: 10.3389/fimmu.2017.00313
61. Mehrotra A, D'Angelo JA, Romney-Vanterpool A, Chu T, Bertoletti A, Janssen HLA, et al. IFN-α Suppresses Myeloid Cytokine Production, Impairing IL-12 Production and the Ability to Support T-Cell Proliferation. *J Infect Dis* (2020) 222(1):148–57. doi: 10.1093/infdis/jiaa064
62. Bauvois B, Nguyen J, Tang R, Billard C, Kolb JP. Types I and II Interferons Upregulate the Costimulatory CD80 Molecule in Monocytes *via* Interferon Regulatory Factor-1. *Biochem Pharmacol* (2009) 78(5):514–22. doi: 10.1016/j.bcp.2009.05.005
63. Rozera C, Carlei D, Lollini PL, De Giovanni C, Musiani P, Di Carlo E, et al. Interferon (IFN)-Beta Gene Transfer Into TS/A Adenocarcinoma Cells and Comparison With IFN-Alpha: Differential Effects on Tumorigenicity and Host Response. *Am J Pathol* (1999) 154(4):1211–22. doi: 10.1016/S0002-9440(10)65373-4
64. Büchner T, Schlenk RF, Schaich M, Döhner K, Krahl R, Krauter J, et al. Acute Myeloid Leukemia (AML): Different Treatment Strategies *Versus* a Common Standard Arm–Combined Prospective Analysis by the German AML Intergroup. *J Clin Oncol* (2012) 30(29):3604–10. doi: 10.1200/JCO.2012.42.2907
65. Burnett AK, Milligan D, Prentice AG, Goldstone AH, McMullin MF, Hills RK, et al. A Comparison of Low-Dose Cytarabine and Hydroxyurea With or Without All-Trans Retinoic Acid for Acute Myeloid Leukemia and High-Risk Myelodysplastic Syndrome in Patients Not Considered Fit for Intensive Treatment. *Cancer* (2007) 109(6):1114–24. doi: 10.1002/cncr.22496
66. Fernandez HF, Sun Z, Yao X, Litzow MR, Luger SM, Paietta EM, et al. Anthracycline Dose Intensification in Acute Myeloid Leukemia. *N Engl J Med* (2009) 361(13):1249–59. doi: 10.1056/NEJMoa0904544
67. Löwenberg B, Ossenkoppele GJ, van Putten W, Schouten HC, Graux C, Ferrant A, et al. High-Dose Daunorubicin in Older Patients With Acute Myeloid Leukemia. *New Engl J Med* (2009) 361(13):1235–48. doi: 10.1056/NEJMoa0901409
68. De Angelis R, Sant M, Coleman MP, Francisci S, Baili P, Pierannunzio D, et al. Cancer Survival in Europe 1999-2007 by Country and Age: Results of

EUROCARE–5-A Population-Based Study. *Lancet Oncol* (2014) 15(1):23–34. doi: 10.1016/S1470-2045(13)70546-1
69. Schuurhuis GJ, Heuser M, Freeman S, Béné M-C, Buccisano F, Cloos J, et al. Minimal/Measurable Residual Disease in AML: A Consensus Document From the European LeukemiaNet MRD Working Party. *Blood* (2018) 131 (12):1275–91. doi: 10.1182/blood-2017-09-801498
70. Walter RB, Ofran Y, Wierzbowska A, Ravandi F, Hourigan CS, Ngai LL, et al. Measurable Residual Disease as a Biomarker in Acute Myeloid Leukemia: Theoretical and Practical Considerations. *Leukemia* (2021) 35 (6):1529–38. doi: 10.1038/s41375-021-01230-4
71. Hourigan CS, Gale RP, Gormley NJ, Ossenkoppele GJ, Walter RB. Measurable Residual Disease Testing in Acute Myeloid Leukaemia. *Leukemia* (2017) 31(7):1482–90. doi: 10.1038/leu.2017.113
72. Grimwade D, Freeman SD. Defining Minimal Residual Disease in Acute Myeloid Leukemia: Which Platforms are Ready for "Prime Time"? *Blood* (2014) 124(23):3345–55. doi: 10.1182/blood-2014-05-577593
73. Ossenkoppele GJ, van de Loosdrecht AA, Schuurhuis GJ. Review of the Relevance of Aberrant Antigen Expression by Flow Cytometry in Myeloid Neoplasms. *Br J Haematol* (2011) 153(4):421–36. doi: 10.1111/j.1365-2141.2011.08595.x
74. Qin YZ, Wang Y, Xu LP, Zhang XH, Chen H, Han W, et al. The Dynamics of RUNX1-RUNX1T1 Transcript Levels After Allogeneic Hematopoietic Stem Cell Transplantation Predict Relapse in Patients With T (8,21) Acute Myeloid Leukemia. *J Hematol Oncol* (2017) 10(1):44. doi: 10.1186/s13045-017-0414-2
75. Wang Y, Wu DP, Liu QF, Qin YZ, Wang JB, Xu LP, et al. In Adults With T (8;21)AML, Posttransplant RUNX1/RUNX1T1-Based MRD Monitoring, Rather Than C-KIT Mutations, Allows Further Risk Stratification. *Blood* (2014) 124(12):1880–6. doi: 10.1182/blood-2014-03-563403
76. Essers MA, Offner S, Blanco-Bose WE, Waibler Z, Kalinke U, Duchosal MA, et al. IFNalpha Activates Dormant Haematopoietic Stem Cells *In Vivo*. *Nature* (2009) 458(7240):904–8. doi: 10.1038/nature07815
77. Mo X-D, Wang Y, Zhang X-H, Xu L-P, Yan C-H, Chen H, et al. Interferon-α Is Effective for Treatment of Minimal Residual Disease in Patients With T (8;21) Acute Myeloid Leukemia After Allogeneic Hematopoietic Stem Cell Transplantation: Results of a Prospective Registry Study. *Oncologist* (2018) 23(11):1349–57. doi: 10.1634/theoncologist.2017-0692
78. Mo X-D, Zhang X-H, Xu L-P, Wang Y, Yan C-H, Chen H, et al. IFN-A Is Effective for Treatment of Minimal Residual Disease in Patients With Acute Leukemia After Allogeneic Hematopoietic Stem Cell Transplantation: Results of a Registry Study. *Biol Blood Marrow Transplant* (2017) 23 (8):1303–10. doi: 10.1016/j.bbmt.2017.04.023
79. Jiang H, Liu X-H, Kong J, Wang J, Jia J-S, Lu S-Y, et al. Interferon-α as Maintenance Therapy can Significantly Reduce Relapse in Patients With Favorable-Risk Acute Myeloid Leukemia. *Leukemia Lymphoma* (2021) 1–8. doi: 10.1080/10428194.2021.1948027
80. Magenau JM, Pawarode A, Riwes MM, Parkin B, Anand S, Ghosh M, et al. A Phase I/II Clinical Trial of Type 1 Interferon for Reduction of Relapse After HCT in High Risk AML. *Biol Blood Marrow Transplant* (2019) 25(3, Supplement):S12–S3. doi: 10.1016/j.bbmt.2018.12.078
81. Liu X, Duan W, Wang J, Jia J, Gong L , Lu >S-Y, et al. Interferon-A-2b As a Maintenance Therapy Significantly Improves Disease-Free Survival in Patients With Low-Risk Acute Myeloid Leukemia. *Blood* (2019) 134 (Supplement_1):3823–. doi: 10.1182/blood-2019-128505
82. Kannaiyan R, Mahadevan D. A Comprehensive Review of Protein Kinase Inhibitors for Cancer Therapy. *Expert Rev Anticancer Ther* (2018) 18 (12):1249–70. doi: 10.1080/14737140.2018.1527688
83. Gorre ME, Mohammed M, Ellwood K, Hsu N, Paquette R, Rao PN, et al. Clinical Resistance to STI-571 Cancer Therapy Caused by BCR-ABL Gene Mutation or Amplification. *Science* (2001) 293(5531):876–80. doi: 10.1126/science.1062538
84. Lu L, Kok CH, Saunders VA, Wang J, McLean JA, Hughes TP, et al. Modelling Ponatinib Resistance in Tyrosine Kinase Inhibitor-Naïve and Dasatinib Resistant BCR-ABL1+ Cell Lines. *Oncotarget* (2018) 9(78):34735–47. doi: 10.18632/oncotarget.26187
85. Talpaz M, Kantarjian H, Kurzrock R, Trujillo JM, Gutterman JU. Interferon-Alpha Produces Sustained Cytogenetic Responses in Chronic Myelogenous Leukemia. Philadelphia Chromosome-Positive Patients. *Ann Intern Med* (1991) 114(7):532–8. doi: 10.7326/0003-4819-114-7-532
86. Kujawski LA, Talpaz M. The Role of Interferon-Alpha in the Treatment of Chronic Myeloid Leukemia. *Cytokine Growth Factor Rev* (2007) 18(5-6):459–71. doi: 10.1016/j.cytogfr.2007.06.015
87. Druker BJ, Guilhot F, O'Brien SG, Gathmann I, Kantarjian H, Gattermann N, et al. Five-Year Follow-Up of Patients Receiving Imatinib for Chronic Myeloid Leukemia. *New Engl J Med* (2006) 355(23):2408–17. doi: 10.1056/NEJMoa062867
88. O'Brien SG, Guilhot F, Larson RA, Gathmann I, Baccarani M, Cervantes F, et al. Imatinib Compared With Interferon and Low-Dose Cytarabine for Newly Diagnosed Chronic-Phase Chronic Myeloid Leukemia. *New Engl J Med* (2003) 348(11):994–1004. doi: 10.1056/NEJMoa022457
89. Copland M, Hamilton A, Elrick LJ, Baird JW, Allan EK, Jordanides N, et al. Dasatinib (BMS-354825) Targets an Earlier Progenitor Population Than Imatinib in Primary CML But Does Not Eliminate the Quiescent Fraction. *Blood* (2006) 107(11):4532–9. doi: 10.1182/blood-2005-07-2947
90. Graham SM, Jørgensen HG, Allan E, Pearson C, Alcorn MJ, Richmond L, et al. Primitive, Quiescent, Philadelphia-Positive Stem Cells From Patients With Chronic Myeloid Leukemia Are Insensitive to STI571 *In Vitro*. *Blood* (2002) 99(1):319–25. doi: 10.1182/blood.V99.1.319
91. Palandri F, Castagnetti F, Iacobucci I, Martinelli G, Amabile M, Gugliotta G, et al. The Response to Imatinib and Interferon-Alpha Is More Rapid Than the Response to Imatinib Alone: A Retrospective Analysis of 495 Philadelphia-Positive Chronic Myeloid Leukemia Patients in Early Chronic Phase. *Haematologica* (2010) 95(8):1415–9. doi: 10.3324/haematol.2009.021246
92. Burchert A, Müller MC, Kostrewa P, Erben P, Bostel T, Liebler S, et al. Sustained Molecular Response With Interferon Alfa Maintenance After Induction Therapy With Imatinib Plus Interferon Alfa in Patients With Chronic Myeloid Leukemia. *J Clin Oncol* (2010) 28(8):1429–35. doi: 10.1200/JCO.2009.25.5075
93. Preudhomme C, Guilhot J, Nicolini FE, Guerci-Bresler A, Rigal-Huguet F, Maloisel F, et al. Imatinib Plus Peginterferon Alfa-2a in Chronic Myeloid Leukemia. *N Engl J Med* (2010) 363(26):2511–21. doi: 10.1056/NEJMoa1004095
94. Hanfstein B, Müller MC, Hehlmann R, Erben P, Lauseker M, Fabarius A, et al. Early Molecular and Cytogenetic Response Is Predictive for Long-Term Progression-Free and Overall Survival in Chronic Myeloid Leukemia (CML). *Leukemia* (2012) 26(9):2096–102. doi: 10.1038/leu.2012.85
95. Hehlmann R, Lauseker M, Saußele S, Pfirrmann M, Krause S, Kolb HJ, et al. Assessment of Imatinib as First-Line Treatment of Chronic Myeloid Leukemia: 10-Year Survival Results of the Randomized CML Study IV and Impact of Non-CML Determinants. *Leukemia* (2017) 31(11):2398–406. doi: 10.1038/leu.2017.253
96. Hjorth-Hansen H, Stentoft J, Richter J, Koskenvesa P, Höglund M, Dreimane A, et al. Safety and Efficacy of the Combination of Pegylated Interferon-α2b and Dasatinib in Newly Diagnosed Chronic-Phase Chronic Myeloid Leukemia Patients. *Leukemia* (2016) 30(9):1853–60. doi: 10.1038/leu.2016.121
97. Nicolini FE, Etienne G, Dubruille V, Roy L, Huguet F, Legros L, et al. Nilotinib and Peginterferon Alfa-2a for Newly Diagnosed Chronic-Phase Chronic Myeloid Leukaemia (NiloPeg): A Multicentre, Non-Randomised, Open-Label Phase 2 Study. *Lancet Haematol* (2015) 2(1):e37–46. doi: 10.1016/S2352-3026(14)00027-1
98. Hochhaus A. *TKI and Interferon Alpha Evaluation Initiated by the German Chronic Myeloid Leukemia Study Group - the TIGER Study (TIGER) Clinicaltrials.Gov2012* (2021). Available at: https://ClinicalTrials.gov/show/NCT01657604.
99. Tefferi A, Vaidya R, Caramazza D, Finke C, Lasho T, Pardanani A. Circulating Interleukin (IL)-8, IL-2r, IL-12, and IL-15 Levels Are Independently Prognostic in Primary Myelofibrosis: A Comprehensive Cytokine Profiling Study. *J Clin Oncol* (2011) 29(10):1356–63. doi: 10.1200/JCO.2010.32.9490
100. Hasselbalch HC, Holmström MO. Perspectives on Interferon-Alpha in the Treatment of Polycythemia Vera and Related Myeloproliferative Neoplasms: Minimal Residual Disease and Cure? *Semin Immunopathol* (2019) 41(1):5–19. doi: 10.1007/s00281-018-0700-2
101. Kim M, Hwang S, Park K, Kim SY, Lee YK, Lee DS. Increased Expression of Interferon Signaling Genes in the Bone Marrow Microenvironment of

Myelodysplastic Syndromes. *PloS One* (2015) 10(3):e0120602. doi: 10.1371/journal.pone.0120602
102. Pardanani A, Vannucchi AM, Passamonti F, Cervantes F, Barbui T, Tefferi A. JAK Inhibitor Therapy for Myelofibrosis: Critical Assessment of Value and Limitations. *Leukemia* (2011) 25(2):218–25. doi: 10.1038/leu.2010.269
103. Muller EW, de Wolf JT, Egger R, Wijermans PW, Huijgens PC, Halie MR, et al. Long-Term Treatment With Interferon-Alpha 2b for Severe Pruritus in Patients With Polycythaemia Vera. *Br J Haematol* (1995) 89(2):313–8. doi: 10.1111/j.1365-2141.1995.tb03306.x
104. Brodsky I. Busulfan Versus Hydroxyurea in the Treatment of Polycythemia Vera (PV) and Essential Thrombocythemia (ET). *Am J Clin Oncol* (1998) 21 (1):105–6. doi: 10.1097/00000421-199802000-00024
105. Barbui T, Barosi G, Birgegard G, Cervantes F, Finazzi G, Griesshammer M, et al. Philadelphia-Negative Classical Myeloproliferative Neoplasms: Critical Concepts and Management Recommendations From European LeukemiaNet. *J Clin Oncol* (2011) 29(6):761–70. doi: 10.1200/JCO.2010.31.8436
106. Kiladjian JJ, Mesa RA, Hoffman R. The Renaissance of Interferon Therapy for the Treatment of Myeloid Malignancies. *Blood* (2011) 117(18):4706–15. doi: 10.1182/blood-2010-08-258772
107. Kiladjian JJ, Chomienne C, Fenaux P. Interferon-Alpha Therapy in Bcr-Abl-Negative Myeloproliferative Neoplasms. *Leukemia* (2008) 22(11):1990–8. doi: 10.1038/leu.2008.280
108. Jones AV, Silver RT, Waghorn K, Curtis C, Kreil S, Zoi K, et al. Minimal Molecular Response in Polycythemia Vera Patients Treated With Imatinib or Interferon Alpha. *Blood* (2006) 107(8):3339–41. doi: 10.1182/blood-2005-09-3917
109. Quintás-Cardama A, Abdel-Wahab O, Manshouri T, Kilpivaara O, Cortes J, Roupie AL, et al. Molecular Analysis of Patients With Polycythemia Vera or Essential Thrombocythemia Receiving Pegylated Interferon α-2a. *Blood* (2013) 122(6):893–901. doi: 10.1182/blood-2012-07-442012
110. Yacoub A, Mascarenhas J, Kosiorek H, Prchal JT, Berenzon D, Baer MR, et al. Pegylated Interferon Alfa-2a for Polycythemia Vera or Essential Thrombocythemia Resistant or Intolerant to Hydroxyurea. *Blood* (2019) 134(18):1498–509. doi: 10.1182/blood.2019000428
111. Gisslinger H, Klade C, Georgiev P, Krochmalczyk D, Gercheva-Kyuchukova L, Egyed M, et al. Ropeginterferon Alfa-2b Versus Standard Therapy for Polycythaemia Vera (PROUD-PV and CONTINUATION-PV): A Randomised, Non-Inferiority, Phase 3 Trial and Its Extension Study. *Lancet Haematol* (2020) 7(3):e196–208. doi: 10.1016/S2352-3026(19)30236-4
112. Rumi E, Sant'Antonio E, Boveri E, Pietra D, Cavalloni C, Roncoroni E, et al. Diagnosis and Management of Prefibrotic Myelofibrosis. *Expert Rev Hematol* (2018) 11(7):537–45. doi: 10.1080/17474086.2018.1484280
113. Tefferi A. Primary Myelofibrosis: 2019 Update on Diagnosis, Risk-Stratification and Management. *Am J Hematol* (2018) 93(12):1551–60. doi: 10.1002/ajh.25230
114. Mikkelsen SU, Kjaer L, Bjørn ME, Knudsen TA, Sørensen AL, Andersen CBL, et al. Safety and Efficacy of Combination Therapy of Interferon-α2 and Ruxolitinib in Polycythemia Vera and Myelofibrosis. *Cancer Med* (2018) 7 (8):3571–81. doi: 10.1002/cam4.1619
115. Harrison CN, Campbell PJ, Buck G, Wheatley K, East CL, Bareford D, et al. Hydroxyurea Compared With Anagrelide in High-Risk Essential Thrombocythemia. *N Engl J Med* (2005) 353(1):33–45. doi: 10.1056/NEJMoa043800
116. Gisslinger H, Gotic M, Holowiecki J, Penka M, Thiele J, Kvasnicka HM, et al. Anagrelide Compared With Hydroxyurea in WHO-Classified Essential Thrombocythemia: The ANAHYDRET Study, a Randomized Controlled Trial. *Blood* (2013) 121(10):1720–8. doi: 10.1182/blood-2012-07-443770
117. Radin AI, Kim HT, Grant BW, Bennett JM, Kirkwood JM, Stewart JA, et al. Phase II Study of Alpha2 Interferon in the Treatment of the Chronic Myeloproliferative Disorders (E5487): A Trial of the Eastern Cooperative Oncology Group. *Cancer* (2003) 98(1):100–9. doi: 10.1002/cncr.11486
118. Sacchi S, Gugliotta L, Papineschi F, Liberati AM, Rupoli S, Delfini C, et al. Alfa-Interferon in the Treatment of Essential Thrombocythemia: Clinical Results and Evaluation of Its Biological Effects on the Hematopoietic Neoplastic Clone. *Ital Cooperative Group ET Leukemia* (1998) 12(3):289–94. doi: 10.1038/sj.leu.2400931
119. Mosca M, Lamrani L, Marzac C, Tisserand A, Edmond V, Dagher T, et al. Differential Impact of Interferon Alpha on JAK2V617F and Calr Mutated Hematopoietic Stem and Progenitor Cells in Classical MPN. *Blood* (2018) 132(Supplement 1):4333–. doi: 10.1182/blood-2018-99-114744
120. Mullally A, Bruedigam C, Poveromo L, Heidel FH, Purdon A, Vu T, et al. Depletion of Jak2V617F Myeloproliferative Neoplasm-Propagating Stem Cells by Interferon-α in a Murine Model of Polycythemia Vera. *Blood* (2013) 121(18):3692–702. doi: 10.1182/blood-2012-05-432989
121. Nilsri N, Jangprasert P, Pawinwongchai J, Israsena N, Rojnuckarin P. Distinct Effects of V617F and Exon12-Mutated JAK2 Expressions on Erythropoiesis in a Human Induced Pluripotent Stem Cell (iPSC)-Based Model. *Sci Rep* (2021) 11(1):5255. doi: 10.1038/s41598-021-83895-6
122. Sleijfer S, Bannink M, Van Gool AR, Kruit WH, Stoter G. Side Effects of Interferon-Alpha Therapy. *Pharm World Sci* (2005) 27(6):423–31. doi: 10.1007/s11096-005-1319-7
123. Aghemo A, Rumi MG, Colombo M. Pegylated IFN-Alpha2a and Ribavirin in the Treatment of Hepatitis C. *Expert Rev Anti Infect Ther* (2009) 7(8):925–35. doi: 10.1586/eri.09.70
124. Reed SD, Anstrom KJ, Li Y, Schulman KA. Updated Estimates of Survival and Cost Effectiveness for Imatinib *Versus* Interferon-Alpha Plus Low-Dose Cytarabine for Newly Diagnosed Chronic-Phase Chronic Myeloid Leukaemia. *Pharmacoeconomics* (2008) 26(5):435–46. doi: 10.2165/00019053-200826050-00007

Conflict of Interest: The authors declare that the research was conducted in the absence of any commercial or financial relationships that could be construed as a potential conflict of interest.

frontiers in Oncology

REVIEW
published: 29 October 2021
doi: 10.3389/fonc.2021.736758

CCR7 in Blood Cancers – Review of Its Pathophysiological Roles and the Potential as a Therapeutic Target

Carlos Cuesta-Mateos[1,2,3*†], *Fernando Terrón*[2,3] *and Marco Herling*[4†]

[1] Immunology Department, Hospital Universitario de La Princesa, Instituto de Investigación Sanitaria- Instituto la Princesa (IIS-IP), Madrid, Spain, [2] Immunological and Medicinal Products (IMMED S.L.), Madrid, Spain, [3] Catapult Therapeutics BV, Lelystad, Netherlands, [4] Clinic of Hematology and Cellular Therapy, University of Leipzig, Leipzig, Germany

According to the classical paradigm, CCR7 is a homing chemokine receptor that grants normal lymphocytes access to secondary lymphoid tissues such as lymph nodes or spleen. As such, in most lymphoproliferative disorders, CCR7 expression correlates with nodal or spleen involvement. Nonetheless, recent evidence suggests that CCR7 is more than a facilitator of lymphatic spread of tumor cells. Here, we review published data to catalogue CCR7 expression across blood cancers and appraise which classical and novel roles are attributed to this receptor in the pathogenesis of specific hematologic neoplasms. We outline why novel therapeutic strategies targeting CCR7 might provide clinical benefits to patients with CCR7-positive hematopoietic tumors.

Keywords: CCR7, lymph node, lymphoma, leukemia, immunotherapy

OPEN ACCESS

Edited by:
Mohamed A. Yassin,
Hamad Medical Corporation, Qatar

Reviewed by:
Emilia Jaskula,
Hirszfeld Institute of Immunology and Experimental Therapy (PAN), Poland
Christine Moussion,
Genentech, Inc., United States
Lydia Scarfò,
Vita-Salute San Raffaele University, Italy

***Correspondence:**
Carlos Cuesta-Mateos
carlos.cuesta@salud.madrid.org

†These authors have contributed equally to this work

Specialty section:
This article was submitted to Hematologic Malignancies, a section of the journal Frontiers in Oncology

Received: *05 July 2021*
Accepted: *12 October 2021*
Published: *29 October 2021*

Citation:
Cuesta-Mateos C, Terrón F and Herling M (2021) CCR7 in Blood Cancers – Review of Its Pathophysiological Roles and the Potential as a Therapeutic Target. Front. Oncol. 11:736758. doi: 10.3389/fonc.2021.736758

1 INTRODUCTION

Lymph nodes (LN) function as major immunological hubs, being essential for immune homeostasis and the generation of effective immune responses (1). LNs are also fundamental sites-of-origin in disease development and progression as well as in treatment failure of several hematological malignancies. Growing evidence suggests that cell trafficking orchestrated by the C-C chemokine receptor 7 (CCR7) plays a critical role in the pathophysiology of several leukemias and lymphomas. This receptor assists malignant cells in access to niches that provide proliferating cues and enable escape from therapy-induced death, hence, promoting disease progression and resistance. In this review we provide a summary of insights towards a better understanding in which blood cancers, particularly B-cell, T-cell, and myeloid-cell malignancies, CCR7 mediates which pathogenetic functions. We further appraise how this chemokine receptor is of great potential for the development of rational and effective therapies in some of these conditions.

2 CCR7: A SINGLE RECEPTOR LINKING INNATE AND THE ADAPTIVE IMMUNITY IN THE LN

The homeostatic chemokine receptor CCR7 (also known as Epstein–Barr virus-induced gene 1 (EBI1), Burkitt's lymphoma receptor 2 (BLR2), or CD197) is a G-protein coupled receptor (GPCR) (2–4). CCR7 is expressed by various immune cells including double negative (DN) and single

positive (SP) thymocytes, naïve, central memory, and regulatory T-cells (T_N, T_{CM}, T_{REG}) as well as naïve B-cells, $CD56^+CD16^-$ regulatory NK cells, and semi-mature and fully mature dendritic cells (DC) (5–7). Generally, T-cell subsets and mature B-cells constitutively express CCR7 whereas NK cells and DC acquire CCR7 expression upon pathogen encounter (5). In homeostasis CCR7 specifically drives cell homing into LN and other secondary lymphoid organs (SLO) (8–10). This single GPCR orchestrates efficient interactions between different CCR7-expressing cell types that belong to both the innate and the adaptive functional axis of immunity and which immigrated to the LN from different peripheral environments. As part of this, CCR7 directs central aspects of immune cell migration into the LN: cell trafficking, firm arrest at the endothelium, extravasation, positioning within SLO, activation, differentiation, survival, and egress. All these processes mediated by CCR7 take place upon binding to either of its two cognate ligands, the chemokines CCL19 (also known as ELC or MIP-3β) and CCL21 (also known as SLC or 6CK), which are constitutively expressed by stroma cells in SLO and which are present on lymphatic vessels, high-endothelial venules (HEVs), and fibroblastic reticular cells (FBR) of the T-cell zones (5, 6, 11). Different signaling pathways downstream of CCR7 and several mechanisms differentially ignited by CCL19 or CCL21 signaling determine the overall outcome of CCR7 engagement in each cell type. A detailed review on those mechanisms is provided by Hauser et al. (11).

3 CCR7 EXPRESSION AND FUNCTIONS IN DISTINCT BLOOD CANCERS

Most of CCR7's roles in homeostasis (e.g. cell trafficking, interstitial migration, or survival) are particularly relevant for leukemias and lymphomas, which very often express CCR7 because of their lymphoid origin and/or maturation stage. In this section we will appraise the current knowledge on CCR7 biology in several B-cell and T-cell cancers and in selected myeloid neoplasms. In addition, we will review the evidence that associates expression profiles of CCR7 with functionality and pathological findings such as LN infiltration or spread to the central nervous system (CNS).

3.1 B-Cell Malignancies

B-cell malignancies consist of distinct diseases that can arise throughout the developmental lifespan of a B-cell. From pro-B-cells in the bone marrow (BM), through circulating mature memory B-cells, each stage of B-cell development is prone to oncogenic alterations and transformation. The corresponding entities carry characteristic protein profiles, including differential expression of CCR7. In some diseases, expression can differ between malignant cells and the corresponding normal ontogenetic counterpart. In others, tumor-associated CCR7 expression can be unaltered, but may trigger different cellular functions.

3.1.1 B-Cell Acute Lymphoblastic Leukemia (B-ALL)

B-ALL is the most common childhood malignancy and represents the leading cause of cancer-related deaths in children and young adults (12). B-ALL arises from a monoclonal or oligoclonal expansion of malignant B-cell precursors in the BM. Normally, CCR7 is not expressed by precursor B-cells (6, 13) and scant information is available on CCR7 expression and function in childhood and adult B-ALL. Indeed, reports are somehow controversial since gene expression profiles showed both unchanged (14, 15) or upregulated CCR7 mRNA (especially in pediatric B-ALL) (16, 17). Similarly, some protein studies performed in a low number of cases showed no CCR7 in B-ALL (18, 19) while, in others series, expression was detected in specific subtypes of B-ALL, mainly in pediatric Burkitt´s-like B-ALL and in one third of pediatric pro-B, early-pre-B, and pre-B ALL (20). In most cases, the surface levels of CCR7 tested by flow cytometry were low-to-moderate. In our hands, adult B-ALL showed detectable CCR7 in only a minor tumor cell fraction of 10-40% (13, 21).

Related to differential CCR7 functionality, isolated early pre-B-ALL cells showed spontaneous migration towards CCL19 (20) whereas normal pre-B and pro-B-cells showed chemotactic responses to this ligand only after a previous exposure to soluble recombinant CD40 ligand (CD40L). In fact, engagement of CD40 seems a common mechanism to up-regulate CCR7 in lymphoblastic cells from patients potentiating the migration towards CCL19 (22, 23). Interestingly, this phenomenon seems highly specific to CCR7 since pre-incubation with CD40L did not affect chemotaxis mediated by other chemokine receptors (e.g. CXCR4) (20). Nonetheless, robust expression data confirm that, in general, CCR7 is absent or found at variably low levels in B-ALL suggesting a rather low impact in mediating migration of this malignancy into LN or other lymphoid niches. This is in accordance with the low incidence of lymphadenopathy in B-ALL. However, CCR7 may provide competitive advantages to the minor fraction of leukemic cells that express this receptor, potentially enabling them to escape to non-lymphoid protective tissues. Indeed, a recent study on a cohort of 160 B-ALL could associate expression of CCR7 and of zeta-chain-associated protein kinase 70 (ZAP-70) protein with enhanced migration (24). These authors also showed that CCR7 expression at diagnosis correlated with cerebral manifestation, which led to the hypothesis that CCR7 is involved in preferred CNS homing in the first phases of the disease. Notably, similar mechanisms have been previously proposed for T-ALL (25). We will address the more established contribution of the CCR7/CCL19 axis in CNS infiltration and survival of T-ALL cells below.

Once at their protective niches, the minor fraction of homed CCR7-expressing B-ALL cells could utilize CCR7 also as a mediator of survival signals. In this context, synergisms between CCR7/CCL19 and CXCR5/CXCL13 were shown to mediate resistance of B-ALL cells to tumor necrosis factor alpha (TNF-α)-mediated apoptosis through activation of paternally expressed gene 10 (PEG10) (26, 27). Moreover, both ligands also synergistically regulated CD40-CD40L crosstalk between B-ALL cells and $CD8^+$ T-cells leading to a PEG10-mediated enhanced production of IL-10 in CD40-activated leukemic cells, which impaired tumor-specific cytotoxic T-cell

(CTL) responses (28). Similarly, CD40-acivated B-ALL cells can deplete IL-12 from the local milieu and block the differentiation process of CCR7-expressing naïve T-cells towards active T_H1 effectors (22). Therefore, CCR7 is likely involved in the creation of tolerogenic niches and its expression might confer escape of B-ALL cells from immune surveillance.

3.1.2 Chronic Lymphocytic Leukemia (CLL)

CLL is the most common leukemia in Western countries (29). It is characterized by the clonal proliferation and accumulation of mature, typically CD5-positive B-cells within the peripheral blood (PB), BM, LN, and spleen. Typically, blood circulating CLL cells are arrested in the G_0/G_1 cell-cycle phase, whereas leukemic cells within LN proliferate and receive protective anti-apoptotic signals (30, 31). CCR7 overexpression, as mRNA (14, 32–34) and as surface protein (in comparison to normal pan-B-cells and $CD5^+CD19^+$ B-cells), is consistently found in virtually all CLL, irrespective whether sampled from PB, BM, or LN (13, 19, 21, 35–48). In agreement, migration in response to CCR7 ligands is enhanced in CLL cells as compared to its normal cell counterparts (13, 35, 40, 46) and both expression and functionality have been associated with nodal disease involvement (13, 27, 35, 36, 38, 46, 47).

In CLL, genetic factors or polymorphisms involved in the overexpression of CCR7 remain uncovered but one single-nucleotide polymorphism (SNP) in the *CCR7* gene was strongly associated with the risk of acquiring CLL. Out of 6 tested SNPs (including rs11574665, rs2023906, rs2290065, rs3136685, rs3136687, and rs588019) (49, 50), the major G allele in the SNP rs3136687, which is located at the first intron and is in linkage disequilibrium with rs11574665, was associated with a higher risk towards CLL whereas the minor A allele resulted in a protective effect (49). The authors found no differences in CCR7 expression for such allelic variants. This lack of association between *CCR7* polymorphisms and receptor over-expression suggests that other proteins might ultimately determine different signaling pathways controlling *CCR7* gene transcription and/or surface protein expression. Accordingly, activating mutations at Notch1 intracellular domain were shown to repress the dual specificity protein phosphatase 22 (*DUSP22*) tumor suppressor gene that encodes a phosphatase that dephosphorylates STAT3 (51). Because of this, STAT3 is constitutively activated resulting in increased CCR7 levels in CLL cells. Another STAT family member, STAT-4, which is profoundly reduced in CLL cells (52), was implicated in *in vivo* down-regulation of CCR7 in T-cells (53). Different B-cell receptor (BCR) signaling pathways have been implicated as well in the aberrant up-regulation of CCR7. For instance, after BCR engagement, the ZAP-70 protein has been shown to up-regulate CCR7 through an extracellular signal-regulated kinase 1/2 (ERK1/2)-dependent mechanism (42). Similarly, the transcription factors NFATC1 (nuclear factor of activated T-cells), NF-κB (nuclear factor kappa B), and AP-1 (activator protein 1) are known to regulate CCR7 expression in CLL following activation *via* the BCR or other receptors (54–56).

In CLL, the normal LN architecture is effaced by the malignant infiltrate (57). Different studies confirm CCR7 as the main receptor involved in nodal entry of CLL cells. Mechanistically, binding to CCL21 on the surface of HEVs activates α4β1 (CD49d/CD29; VLA-4) and αLβ2 (CD11a/CD18; LFA-1) (35, 58), which respectively bind to ICAM-1 and VCAM-1. Whether β1 and β2 integrins are equally relevant in CCR7-mediated homing of CLL cells is still unknown. By one hand, Till et al. showed spontaneous active conformation (without chemokine-induced clustering) of LFA-1 on CLL cells (59). On the other hand, circulating CLL cells usually express low levels of these integrins (60). Therefore, few CLL cells are able to arrest in ICAM-1 expressing endothelium *in vitro* and to migrate to lymph nodes of NOD/SCID mice *in vivo* (60). However, a significantly higher expression of both types of integrins (thus facilitated access to LN) is detected in CLL cells derived from high-risk patients with unfavorable cytogenetic abnormalities such as deletion 17p, deletion 11q and, specially, with trisomy 12 (47, 61, 62). Recently, Legler et al. have shown on trisomy-12 carrying OSU-CLL cells that CCR7-mediated inside-out signaling to the β1 integrinVLA-4 and the β2 integrin LFA-1 is controlled by Src and ZAP-70 kinases (58, 63). This process is critical for static and dynamic cell adhesions to endothelium and subsequent migration, but did not seem to impact the speed of migration velocity, and was dispensable for chemokine-mediated crawling and diapedesis. Further studies are needed to know which are the molecular mechanisms driving the latter processes.

Activation of integrins promotes the production and release of MMP-9 (64) and the subsequent transmigration of CLL cells through the endothelial cell wall into the LN [transendothelial migration (TEM)]. This ability of CLL cells to eventually accumulate at these sites may be determined by the genetic background of CLL. The more aggressive *immunoglobulin heavy variable chain* (*IGHV)* gene unmutated CLL subset displays higher CCR7 expression (35, 36, 43, 46, 65). In support, the presence of adverse factors such as *IGHV* unmutated status or expression of CD38 or ZAP-70 was shown to be associated with increased responsiveness of CLL cells to CCR7 ligands in both chemotactic and TEM assays (38, 47, 60, 66, 67).

There is data that indicate CCR7 to drive interstitial migration within the lymphoid tissue and to facilitate the positioning of leukemic cells close to accessory $CD40L^+CD4^+$ T_H cells, follicular DC (FDC), and stromal cells (e.g. stromal-like cells and nurse-like cells), which are all known to promote the survival and growth of the malignant clone (9, 38, 68, 69). This crosstalk with accessory cells can induce the release of high levels of CCL19 and CCL21, which among others, has two functional consequences. First, it causes the establishment of a self-enhancing loop that recruits more CCR7-expressing tumor and accessory cells favoring the creation of a protective and tolerogenic microenvironment. Secondly, CCR7 ligands directly promote survival of CLL cells. In these scenarios CCL19 and CCL21 can act as single factors that activate mitogen-activated protein kinase (MAPK) and phosphatidylinositol-3-kinase (PI3K)-AKT signaling (40, 70) or in a cooperative fashion with CXCL13 which contributes to resistance of CLL cells (but not normal $CD5^+$ B-cells) to TNF-α-mediated apoptosis through up-regulation of PEG10 which in turn stabilizes caspases-3 and -8 (26, 27).

Finally, besides its role in homing and survival within SLO, CCR7 along with sphingosine-1-phosphate receptor 1 (S1P1) are crucial molecules in the egress of lymphocytes from lymphoid organs to PB. As shown in CCR7-deficient mice, cells lacking CCR7 left LN quicker than wild-type cells. In contrast, overexpression of CCR7 retarded emigration from LN to PB (71). Evidence implicates the characteristic high CCR7 expression in CLL alongside the low expression of the egress receptor S1P1 to contribute to nodal retention (43, 46, 72), driving a scenario of lymphadenopathy that favors homing and accumulation in SLO. Remarkably, driving leukemic cells out of LN into PB induces death by deprivation of milieu-derived signals and is one of the modes of action (MOA) of a very efficient treatment option in CLL, ibrutinib, the first approved Bruton´s tyrosine kinase (BTK) inhibitor with activities on multiple other kinases (73). Recent work suggests ibrutinib to down-modulate CCR7 expression and function in CLL (e.g. integrin activation and receptor recycling) and by that to restore the balance between CCR7 and S1P1 and to enforce nodal egress of leukemic cells (44, 46).

3.1.3 Mantle Cell Lymphoma (MCL)

MCL is a B-cell tumor that originates from the clonal expansion of a naïve $CD5^+$ B-cell localized in the mantle cell zone surrounding the germinal center (GC) in secondary follicles of the LN (74). Lymphadenopathy and BM infiltration are the most common clinical manifestations, followed by splenomegaly and PB lymphocytosis. Gastrointestinal and CNS involvement have been reported as well (75–77). This preferential pattern of dissemination can be attributed to the high surface expression of CCR7 by MCL cells as per flow cytometry, second to those levels observed in CLL (13, 21, 78, 79). In most of these studies, MCL cells from LN, PB, BM, and pleural effusions expressed higher levels of CCR7 than their proposed normal counterparts. The underlying causes of this overexpression are largely unknown. Comparative transcript analysis between MCL and normal B-cells have shown CCR7 mRNA to be significantly up-regulated in lymphoma cells (32). The fact that CCR7 was not among the top differentially regulated RNAs in MCL (80) suggests that additional mechanisms such as altered protein turn-over (46) are responsible for overexpression of surface CCR7 in MCL. Nevertheless, MCL and normal B-cells differ in their migratory behavior towards CCR7 ligands. In chemotaxis assays, MCL cells, but not their normal counterparts, migrated in response to CCL19, which was selectively potentiated by pre-exposure to CXCL12 (78). These results suggested CCR7-driven migration to be of relevance in the dissemination pattern seen in MCL patients. We corroborated this hypothesis in pre-clinical *in vivo* models in which the inhibition of CCR7 by anti-CCR7 antibodies abrogated infiltration of CCR7-expressing MCL cell lines into LN, spleen, lung, or CNS, all of them tissues in which CCR7 ligands are found (21). Moreover, this neutralization of the CCR7 axis also induced a strong reduction in viability of lymphoma cells within tumor masses, confirming that in MCL CCR7 overexpression is not only involved in orchestrating migration, but also in directly promotion of survival.

3.1.4 Follicular Lymphoma (FL)

FL is the second most common type of non-Hodgkin´s lymphoma (NHL) and despite its indolent nature, it is essentially incurable (81). FL encompasses lymphomas emerging from a GC B-cell, which can vary in presentation from indolent to aggressive courses (82). Similar to normal GC lymphocytes, which physiologically down-regulate CCR7 and up-regulate CXCR5 (83), FL cells express low to moderate levels of CCR7. Moreover, the proportions of CCR7-expressing cells were reported to be low and, in some patients, no expression of CCR7 was detected at all (13, 19, 21, 79). In agreement, mRNA levels in FL cells did not differ from those of their normal counterparts (32, 84–87). The genetic variants of CCR7 rs2023906, rs2290065, rs3136685, and rs588019, were not associated with differential expression or with clinical course in FL (50). The fact that CCR7 is not prominently found in most FL suggests that it has a limited role in the pathophysiology of this lymphoma, which is supported by recent evidence. In fact, comparative analyses of LN from FL *versus* reactive LN revealed that CCL21 and CXCL12 were neither over- nor differentially expressed, whereas FL-LN nearly lacked expression of CCL19. In addition, in FL lymphoid tissues in which both CCR7 ligands were detected, they were preferentially found in HEVs and in lymphatic vessels of T-cell zones, but on average at 3-fold lower levels than in reactive LN (88). Conceivably, the reduced abundance of CCL19/CCL21 in LN of FL is lymphoma instructed and contributes to evasion from anti-tumor immunity. Accordingly, FL progression may be associated with reduced numbers of perifollicular $CCR7^+$ gamma-delta T-lymphocytes due to a shortage of attracting CCR7 ligands (88).

3.1.5 Burkitt`s Lymphoma (BL)

CCR7 was first characterized in EBV infected BL cell lines, hence the initially coined term Epstein-Barr-induced 1 (EBI-1) for CCR7 (4). CCR7 upregulation was shown to rely on the viral transactivator EBV nuclear antigen 2 (EBNA-2), which after binding to centromere-binding factor 1 (CBF-1, also known as RBP-jκ), a highly conserved cellular DNA binding repressor, gains access to regulatory regions of CCR7 target genes and activates transcription in infected (previously EBV-negative) BL4 BL cells (4, 89). Information on CCR7 expression in primary BL material is scarce. No upregulated mRNA levels were seen in 22 patient samples (32, 84) and, to our knowledge, only one work studied CCR7 expression by flow cytometry in another 9 patients (79). The receptor was found in all cases, but in a fraction of ~53% of tumor cells per sample with no disclosed results on receptor surface levels. Interestingly, in the NC37 BL cell line, *in vitro* chemotaxis and TEM was modulated by a cooperative activity of CXCL12 with CCL19 or CCL21, suggesting that the CCR7 axis is involved in BL cell homing to LN (90). Accordingly, in the syngeneic *Eμ-Myc* mouse model of BL, CCR7 was found necessary for lymphoma cells to home to LN (9). These results also indicated that CCR7 guides tumor cells to distinct microanatomic sites in spleen and LN, especially to their T-cell zones. Cross-talk with resident stromal and accessory cells at

these sites contributed to the creation and preservation of pro-tumor niches that conferred a survival advantage to CCR7-positive lymphoma cells over CCR7-deficient lymphoma cells (9). In a proposed model, stromal cells (e.g. fibroblastic reticular cells, FRC, and HEV endothelial cells) secrete CCL21 through which CCR7-expressing lymphoma cells home through HEV into the LN (or spleen) and migrate towards FRC in the T-cell region. Upon interaction with FRC, lymphoma cells secrete lymphotoxin through which they stimulate lymphotoxin-β-receptor expressing FRC. In turn, BL cells receive survival signals, presumably including Indian hedgehog (Ihh) secreted by FRC and CD40 stimulation through CD40 ligand-expressing $CD4^+$ T-cells located in the T-zones. The importance of this cross-talk was demonstrated by showing that genetic deletion of CCR7 impaired lymphoma growth (9). Therefore, this model not only established the basis for a better understanding of the pathogenic role of CCR7 in BL, but also in many other blood cancers with a high dependence on the nodal or splenic microenvironments.

3.1.6 Subsets of Diffuse Large B-Cell Lymphoma (DLBCL)

DLBCL, the most common type of malignant lymphoma, accounts for ~30% of adult NHL (91). DLBCL can arise at multiple anatomical sites and comprises two major groups: activated B-cell like (ABC) and GC B-cell like (GCB) DLBCL. Therefore, it is not surprising that chemokine receptor (CKR) expression varies between these subtypes and in association with disease location (91, 92). Up to 62% of DLBCL express CCR7, both in analyses of flow cytometry and immunohistochemistry (IHC), with a preferential mRNA and protein expression in the non-GCB subtypes, especially in patients with both LN and BM involvement (79, 85, 93, 94). In EBV-positive DLBCL of the elderly, in primary effusion lymphoma, in gastric extranodal DLBCL, and in transformation of gastric mucosa-associated lymphoid tissue (MALT) lymphomas to gastric extranodal DLBCL, up-regulation of CCR7 mRNA, among other CKR, was reported (32, 91, 94–96). Notably, in EBV-associated DLBCL recurrent mutations in the *CCR7* gene are found in 11% of patients (94). These alterations seem exclusive to this subtype and could enable homing of tumor cells to SLOs where the virus in turn propagates infection or establishes latency, thereby driving lymphomagenesis (97). In other related primary lymphomas such as intravascular large B-cell lymphoma and mediastinal large B-cell lymphoma a characteristic decrease in immunodetected CCR7 was described (32, 98, 99). As these types typically show sparing of LN manifestation, this corroborates the role of CCR7 in nodal homing. The genetic polymorphisms in *CCR7* that were disclosed in FL did not associate with the risk of acquiring DLBCL (50). CCR7 expression, both at mRNA and protein levels, was an independent prognostic factor for disease progression, advanced clinical stages, shorter median survival times, and poorer survival rates in GC and ABC DLBCL (93, 100). First functional data on CCR7 in DLBCL indicate that receptor expression facilitates CCR7-mediated *in vitro* migration in EBV-positive DLBCL cell lines with functional analyses on primary samples still missing (91).

3.1.7 Primary Central Nervous System Lymphomas (PCNSL)

Immunohistochemical staining of PCNSL and secondary CNS lymphoma (sCNSL) showed these disorders to present CKR profiles that were different from those of systemic DLBCL. CCR7 was detected in the malignant B-cells of specimens of PCNSL (101) and in CNS relapses of DLBCL (102). However, and opposed to lymphomas with peripheral involvement, CCR7 was present in the cytoplasm rather than at the cell surface indicating that the receptor may not respond to its corresponding ligands in the same conventional fashion (101). It is tempting to associate this loss of surface CCR7 with the absence of nodal involvement, which defines PCNSL (103). However, one should also take into account that the restricted intracellular CCR7 expression pattern may in part be a consequence of a milieu that is highly enriched in CCR7 ligands, especially in CCL19, the most potent inducer of CCR7 endocytosis (11). In agreement, a recent study addressing the role of gliosis in lymphoma cell retention in the CNS found that astrocyte-derived CCL19 was required for gliosis-promoted CNSL *via* enhancing parenchymal retention of lymphoma cells (104).

3.1.8 Marginal Zone Lymphoma (MZL)

MZL comprises three entities that arise from the marginal zone surrounding the follicular GC of the LN: extranodal MZL or MALT lymphoma, splenic MZL, and nodal MZL. Analyses on MALT lymphoma samples showed more than 50% of malignant cells to express CCR7 (79). In extragastric MALT lymphoma or malignant transformation from *Helycobacter pylori*-associated gastritis to MALT lymphoma, up-regulation of CCR7 mRNA, among other CKRs, was a common finding (91, 95, 96). In splenic MZL, no changes were seen at the mRNA level (87) whereas flow cytometry revealed significantly reduced expression of CCR7 as compared to normal B-cells (13, 19, 21, 79). The low CCR7 expression in extranodal or splenic MZL suggest a minor role of this receptor in their pathobiology. This in turn might explain the minimal lymphadenopathy seen in these types of MZL (13) and reports on CCR7 expression in nodal MZL are still missing. Accordingly, one study in salivary gland MALT lymphoma samples selectively implicated the chemokine CCL21 in the organization of ectopic reactive lymphoid tissue whereas no significant expression of the ligand was detected in the malignant lymphoid aggregate (105). The authors concluded that CCR7 plays no major role in the infiltration of the epithelium or in the regulation of malignant cell survival.

3.1.9 Hairy Cell Leukemia (HCL)

HCL is an indolent, rare disease that accounts for approximately 2% of leukemias and is typically defined by the B-raf kinase mutation pV600E (106). Cell surface expression of CCR7 is low (or absent) in HCL cells when compared to normal B-cells (13, 19, 21, 107). Similarly, CCR7 transcription in HCL samples is reduced (32). This would explain why nodal dissemination is not a key feature in this disease.

3.1.10 Lymphoplasmacytic Lymphoma (LPL) and Multiple Myeloma (MM)

LPL and its subgroup Waldenstroem´s macroglobulinemia (WM) are rare and indolent lymphomas that arise from terminally differentiated B-cells that physiologically do not express CCR7 (82). Analyses on very few clinical samples did not shed light on the expression profile of CCR7 in LPL, as some cases did express the receptor (21) while others did not (13). Available evidence does not link CCR7 to an altered genetic profile in plasma cell leukemia (PCL) (108). Normal plasma cells and those of MM do not typically express surface CCR7, and if expressed, it is found in a minor proportion of cells as demonstrated in samples from BM or extramedullary sites (PB and pleural effusions) (13, 21, 109, 110). Curiously, in non-Hispanic Caucasian subjects the genetic CCR7 variant s3136685 was reported to be associated with an elevated risk for MM (110). Since this genotype was not associated with MM in further permutation-based tests and since previous evidence did not link CCR7 to MM (108, 111), these findings should be interpreted with caution and further investigation is required to clarify this issue. Finally, gene expression profiles of monoclonal gammopathy of undetermined significance (MGUS) and of smoldering myeloma seem to discard a prominent role of CCR7 in these conditions as well (108, 111, 112).

3.1.11 Hodgkin Lymphoma (HL)

HL is a unique type of B-cell lymphoma characterized by the presence of a minority (<1%) of neoplastic cells in a background of infiltrating reactive cells (113). The microenvironment is considered to be shaped by the malignant cells and provides survival signals and protection against anti-tumor immune responses (114). Based on differences in histopathology, HL is classified in two subgroups: the classical form (cHL) that accounts for 95% of all HL cases and the nodular lymphocyte predominant variant (NLPHL) that represents only 5% of all cases (113). Tumor cells in cHL are termed Reed/Sternberg (RS) cells, which generally express CD30, whereas tumor cells in NLPHL are called lymphocytic and histiocytic (L&H) cells and lack CD30.

CCR7 expression has been observed in cHL-derived tumor cell lines and in primary tissue. In the majority of cell lines expression was moderate-high and CCR7 was functional in inducing migration towards both of its ligands (115). In patient samples, IHC revealed a differential expression of CCR7 between cHL and NLPHL. The classical form, located in the interfollicular zones, showed strong CCR7 expression whereas NLPHL, regularly associated to follicles, was shown to be CCR7 negative (115). Accordingly, mRNA levels were highly expressed in cHL when compared to NLPHL and normal B-cells (84, 116). Moreover, CCL19/CCL21 were found in tumor infiltrates of cHL, whereas the tumor nodules in NLPHD almost completely lacked these chemokines (115).

In cHL, CCR7 upregulation might be a consequence of two, or more, altered pathways that are partially interconnected. For example, the *CCR7* gene contains binding sites in its promoter region for the transcription factors AP-1 and NF-κB (3), and both axes have been shown to be constitutively active in cHL and to upregulate CCR7, individually or cooperatively (3, 117). Notably, the combined constitutive activation of AP-1 and NF-κB mimics a state of chronic inflammation that involves the production of cytokines by RS cells. Whether CCR7 up-regulation is part of the prominent NF-κB program in cHL, as it is the case for CD30 expression (115, 118), remains to be investigated.

At the functional level, constitutively active WNT signaling in cHL is important in CCR7-mediated migration and generation of protumorigeneic milieus. Binding of the WNT protein to the low-density lipoprotein receptor-related protein 5/6 (LRP5/6) regulates CCL19-guided chemotaxis through the β-catenin and lymphocyte enhancer-binding factor-1 (LEF-1) pathways (119). WNT signaling is commonly involved in metastasis and angiogenesis in various tumors (120). In tumor cells of cHL canonical WNT/β-catenin/LEF-1 signaling is also required to secrete vascular endothelial growth factor A (VEGF-A), and by that, to attract endothelial cells as well as to enhance their migration, sprouting and tube formation. Therefore, canonical WNT signaling is a regulator of the endothelium-lymphoma interplay. WNT is a prerequisite for secretion of VGEF-A by cHL cells which stimulates biogenesis of vascular endothelium which in turn presents CCR7 ligands that direct movement of cHL cells towards vascular niches. Thus homing and interstitial movement of tumor cells within the affected LN is facilitated by constitutive WNT. Moreover, CCR7's ligand, CCL21, was shown to be absent on RS cells, but was detected on the majority of small vessels (including HEV) with a luminal membranous localization (121).

The CCR7 axis not only seems to play a pathogenic role by recruiting cHL tumor cells, it is also implicated in recruiting pro-tumorigenic CCR7-expressing immune cells from the circulation. Within infiltrating immune cells in cHL, CCR7 (and the related homing markers CD62 and lymphocyte function-associated antigen 1, LFA1) were demonstrated to be expressed on a large proportion (~33%) of reactive T-cells, which showed receptor-mediated chemotaxis that was similar to PBMC from healthy donors (121). Notably, in cHL the infiltrate is commonly enriched by $CCR7^+$ T_{REG} and activated T-cells (122–126). In contrast, in NLPHL these T-cell subsets are less abundant and are found outside the tumor area (115, 127). Together, these findings suggest different immune escape mechanisms in both subtypes of HL that may be related to the different expression profiles of CCR7 in tumor-associated cells and of CCR7 ligands in the surrounding tissue.

3.2 CCR7 in T-Cell Malignancies

As described for B-cell malignancies, T-cell neoplasms consist of multiple entities that are thought to arise from particular stages of T-cell development. For instance, T-cell acute lymphoblastic leukemia (T-ALL) originates from thymic stages of T-cell evolution while peripheral (post-thymic) T-cell neoplasms show features of mature T-cells with distinct phenotypes of differentiation, e.g. T-cell prolymphocytic leukemia (T-PLL) mostly resembling T_{CM} or unconventional transitional stages between T_N and T_{CM}; adult T-cell leukemia/lymphoma (ATLL) resembling T_{REG}; Mycosis fungoides (MF) resembling T_{EM}; Sézary syndrome (SS) resembling T_{CM}; or T-cell large granular

lymphocytic leukemia (T-LGL) resembling activated cytotoxic T-cells (113, 128–130). Based on this phenotypic characterization, CCR7 expression would follow its physiological T-lineage pattern and be highest in those diseases resembling a DN or SP thymocyte, T_N, T_{REG}, or T_{CM} and to show LN or CNS involvement. A low number of studies limits the knowledge on the role of CCR7 in some of these disorders. However, in light of the restricted armamentarium of available efficient therapies for T-cell malignancies, such insights are highly desired. In this section we will address our current knowledge on CCR7 biology in several T-cell cancers and will try to associate reported expression profiles with CCR7 functionality and pathological findings.

3.2.1 T-Cell Acute Lymphoblastic Leukemia (T-ALL)

T-ALL mainly afflicts children and adolescents. It presents with increased white blood cell counts and often with hepatosplenomegaly. At relapse, there is an increased incidence of CNS manifestations (131, 132). A seminal report showed CCR7 to be a functional receptor that is highly expressed in 4 of 5 T-ALL cell lines and in PB tumor cells of 8 of 11 T-ALL patients (25). A recent study in a larger cohort of 130 patients (24) and unpublished data from our laboratory confirm these results. In T-ALL, CCR7 expression is controlled by the activity of the oncogene *Notch1*. Significantly up-regulated CCR7 was found in human T-ALL cells that harbor *Notch1*-activating mutations while receptor expression was repressed by Notch1-specific γ-secretase inhibitors (DBZ or compound E), both at mRNA and at protein levels (25). Mechanistically, Notch receptor engagement initiated the PI3K/mammalian target of rapamycin complex 2 (mTORC2) pathway, which transmitted through NF-κB to regulate expression of the *CCR7* gene in leukemic cells (25, 133). Notably, in pre-clinical *in vivo* T-ALL models generated by overexpression of the intracellular cleaved form of Notch1 (ICN1), CCR7 overexpression led to enhanced chemotaxis and invasion into different tissues, especially to leptomeningeal spaces of brain and spinal cord, in which endothelial cells were shown to produce CCL19 (25). This CCR7-driven homing into CNS facilitated leukemic cell survival and was associated with reduced animal survival. Similarly, CCL19 promoted T-ALL cell invasion of spleen in syngeneic *in vivo* models and shortened host survival (134). Inside cerebral or spleen parenchyma, cross-talk between stromal cells and leukemic cells mediates the production of higher levels of tissue CCL19 (25, 134, 135). In CNS, these positive loops and the concomitant alteration of drainage from cerebrospinal fluid facilitated lymphoblastic meningeal infiltration (25). Nonetheless, it is likely that CCR7 is not the sole mediator of this process as meningeal infiltration is also detected in ICN1-induced T-ALL with CCR7-deficient hematopoietic progenitors (135). A recent study suggested that CNS infiltration in xenograft models is regulated by ZAP-70 which positively correlated with the overexpression of both CCR7 and CXCR4 and with migratory abilities towards CCL19 and CXCL12 (24). This study also confirmed, in a large cohort of 130 T-ALL patients, the positive correlation between ZAP-70 and CCR7 expression and, importantly, high CCR7 expression in tumor cells from BM biopsies at diagnosis was associated with a significant 11-fold increased risk of CNS involvement (24). Together, despite some T-ALL patients showing low or absent expression of CCR7 in their tumor cells from BM (135), the herein presented evidence supports CCR7 as a key element responsible of high-risk features such as CNS infiltration.

3.2.2 T-Cell Prolymphocytic Leukemia (T-PLL)

Although being the most frequent mature T-cell leukemia in Western countries, T-PLL represents only ~3% of all T-cell malignancies (136–138). Its clinical course is typically aggressive with poor responses to conventional chemotherapies resulting in a median overall survival (OS) of usually <2-3 years (139, 140). An inevitably rapid proliferation of mostly $CD4^+$ prolymphocytes involves the PB, BM, spleen, liver, LN as well as skin and effusions (136, 137, 141). Not uncommon are CNS involvements (136, 137, 142). This pattern of dissemination suggests chemokine receptors to play an important role in T-PLL, however, little is known about their relevance and the role of their ligands in the pathophysiology of T-PLL (143). Although previous evidence did not show overexpression of CCR7 mRNA in six primary T-PLL samples (144), a recent study by our groups focused on CCR7 in T-PLL biology and its interventional potential (130). We assayed CCR7 surface levels at diagnosis by flow cytometry in 109 patients and found that receptor overexpression in malignant cells is seen in a very high proportion of cases (86.5%). CCR7 expression profiles were also instrumental in assigning T-PLL to stages of memory T-cell differentiation (130, 145). The proportion of CCR7-expressing T-PLL cells in PB at diagnosis was associated with a shorter OS and a higher risk of death within an 8-year follow-up period (130). CCR7 was a fully functional receptor upon CCL19 and CCL21 binding and its downstream signaling pathways activated PI3K and ERK (130), two axes that have shown to be relevant in T-PLL pathogenesis (145–147). We further showed that receptor activation triggered chemotaxis, invasion trough biological matrices or endothelial cells, and T-PLL cell survival (130). In *in vivo* pre-clinical studies, we confirmed CCR7 to play critical roles in enabling tumor cells to access tumor microenvironments in CNS and lymphoid organs, especially in LN (130). In agreement, prominent HEV are often infiltrated by neoplastic cells in T-PLL (148), which suggests CCL21 as a major route for homing into lymphoid tissues and in mediating the dissemination of T-PLL cells to different organs. Our results demonstrated CCR7 to promote a rapid niche colonization as well as survival and proliferation in these environments.

3.2.3 Adult T-Cell Leukemia/Lymphoma (ATLL)

ATLL is an aggressive peripheral T-cell malignancy associated with human T-cell leukemia virus, type 1 (HTLV-1) infection and predominantly occurs in HTLV-1 endemic areas such as South-Western Japan, the Caribbean Islands, Central and South America, intertropical Africa, and the Middle East (149, 150). The prognosis of ATLL is very poor with a 4-year OS rate of 11%, 16%, 36%, and 52%, in the subtypes of acute, lymphoma, chronic, and smoldering ATLL, respectively (151, 152). In the majority of cases, ATLL cells express CD4 and CD25 and often lack CD7 (152–154). Forkhead box P3 (FoxP3) expression is

detected and led to concepts of ATLL cells to resemble T_{REG} (155) which, however, remains a subject of debate (156). The malignant cells of ATLL express surface CCR7 (157) and up-regulated CCR7 transcripts are associated with the aggressive acute ATLL subset, which distinguishes these cases from the less aggressive chronic ATLL (158, 159). Studies in larger cohorts confirmed upregulated CCR7 mRNA and protein, especially in patients with acute, progressive, or treatment refractory acute disease. These reports also associated higher CCR7 expression levels with a poor prognosis and nodal involvement (154, 160, 161). Accordingly, ATLL cells from patients with lymphadenopathy and splenomegaly showed enhanced ability to adhere to surfaces coated with intercellular adhesion molecule 1 (ICAM-1) and to migrate towards CCL19 or CCL21 (157). Recent whole-exome sequencing studies revealed gain-of-function mutations in the receptor (162, 163). The *CCR7* gene was recurrently and significantly affected in 11% of ATLL with a majority of cases harboring mutations that led to truncated protein forms at the C-terminal cytoplasmic domain, which regulates multiple biological processes. Of special interest were the mutations at CCR7 Trp355, which prevented receptor turnover and internalization upon ligand stimulation resulting in increased surface receptor expression. These mutations led to an enhanced ligand-induced chemotaxis and PI3K/AKT signaling (162, 163). More recently, *CCR7* gene mutations were mutually associated with mutations at *phospholipase C gamma 1* (*PLCG1*) and *caspase recruitment domain family member 11* (*CARD11*) genes, which are frequent alterations in TCR/NF-κB signaling (164). The pathological implications of this coexistence in ATLL remain unaddressed.

3.2.4 Mycosis Fungoides (MF)

MF is the most common type of cutaneous T-cell lymphoma (CTCL), in which a protracted clonal expansion of atypical dermatotropic $CD3^+CD4^+$ T-lymphocytes underlies a chronic cutaneous manifestation (165). The majority of patients with early-stage (i.e. limited patch/plaque) disease have a normal life expectancy, while in advanced (i.e. ubiquitous, tumor, nodal) stages survival is drastically reduced, which in addition to a marked symptomatology requires multimodal treatments (166–168). Available data emphasize a complementary, prominent pro-tumorigenic role of distinct factors present within the skin or LN milieus of CTCL, such as chemokines (CCL21 or CXCL12) (169), cytokines (IL-13) (170) or antigens able to entertain chronic T-cell receptor stimulation (171).

Expression of CCR7 has been considered a marker of advanced MF and a component involved in the spread of cutaneous lesions to lymphoid tissues. Indeed, single-cell RNA sequencing of skin biopsies from one patient with aggressive disease showed that malignant clones in PB and LN displayed a transcriptional program reminiscent of a more central $CCR7^+$ memory-like phenotype, while retaining tissue-homing receptors (i.e. CLA, CCR10) (172). Nonetheless, evidence of CCR7 protein expression in MF samples is scarce. Kallinich et al. analyzed expression of several CKRs in MF (165). They studied CCR7 expression in skin biopsies from six patients with early disease and six patients at the tumor stage. Using IHC, they found no expression of CCR7 in any tested sample, however, two skin samples of advanced disease showed strong and uniform expression of CCR7 on tumor cells by flow cytometry. A more recent study reported CCR7 expression in 62% (13/21) of specimens as per IHC, and indicated that CCR7 expression strongly correlated with subcutaneous extension of lymphoma cells (173). The CCR7-expressing MF cell line MyLa shows enhanced *in vitro* migration towards CCL21 in an mTOR-dependent manner (161) and through up-regulation of *metastasis-associated lung adenocarcinoma transcript 1* (*MALAT1*) (174), a long noncoding RNA that is also associated with migration of several solid tumor types (175). These authors also concluded that CCR7 promotes subcutaneous involvement of MF. In agreement, total RNAs from skin biopsies of epidermis *versus* those from involved dermis of MF associated the presence of tumor cells in the dermis with the CCR7/CCL21 axis (161). Accompanying IHC analyses confirmed that expression of CCR7 was high in infiltrating lymphoma cells. It also demonstrated CCL21 in the cytoplasm of epidermal keratinocytes and to be diffusely distributed in the dermal extracellular matrix.

3.2.5 Sézary Syndrome (SS)

SS is a mature systemic T-cell malignancy in which skin-homing T-lymphocytes also accumulate in PB and LN. Patients are highly symptomatic (e.g. pruritus, staphylococcal infections) and prognosis is poor with a median of survival of 63 months (166, 167). Despite increasingly better knowledge on disease biology, currently applied therapies show short-lived responses (168). By convention, SS has been regarded as a systemic variant of MF based on identical cytologic and immunophenotypic features. In addition, long-standing MF may subsequently develop into a secondary SS-like disease that exhibits circulating neoplastic cells, indistinguishable from those of primary de-novo SS. Nonetheless, several studies provide clues to consider SS and MF as two separate entities. First, patients with primary SS typically experience a more aggressive disease course, characterized by frequent involvement of LN (166–168). Second, MF and SS tumor cells show different molecular and CKR profiles (176–178). SS is thought to arise from expansions of mature long-lived $CD4^+CD7^-$ T-cells with a $CD45RO^+CD27^+CD62L^+$ T_{CM} phenotype accompanied by a consistently high CCR7 mRNA and protein expression, whereas CCR7 expression in the predominantly T_{EM} cells from cutaneous MF lesions is controversial (165, 178–182). Admittedly, biases by the different sources of sampling, e.g. skin preferentially for MF *versus* blood and LN for SS might attribute to the observed differences.

Although CCR7 gene expression could not be significantly correlated with lymphoid organ involvement or patient survival in SS (179), it appears plausible that production of CCL19 and CCL21 by stromal and endothelial cells in lymphoid tissues contributes to the lymphotropism of SS cells. In support, the chemokine CXCL13, mainly produced in lymphoid tissues, promotes a synergistic CCR7-mediated migration that was of higher efficiency in SS cells than in normal T-cells (183). Additionally, CCR7 activation enhanced invasion by modulating adhesion and secretion of metalloproteases in

clinical samples and in SS cell lines (183, 184). CCR7-induced integrin activation and metalloprotease secretion are processes that in other CCR7-expressing blood cancers are known to be required for CCR7-mediated TEM and for homing (35, 130).

Epidermotropism and tumor growth within the skin environment of SS are features that had been attributed to CCR7 function, but the exact mechanisms are poorly characterized. A first report found no function for CCR7 in promoting *in vitro* survival or proliferation of primary SS tumor cells (183). Another study on a cohort of 43 SS cases found contradictory results (169). This more recent investigation demonstrated that overexpressed CCL21 (and CXCL12) in skin tissue induced activation of PI3K/AKT/mTORC1 signaling in skin-resident SS cells. SS samples frequently show a recurrent loss of the phosphatase PTEN (phosphatase and tensin homolog) and the liver kinase B1 (LKB1) (169), two proteins that under normal conditions attenuate upstream activation of mTORC1 in low energy conditions (185). Therefore, these defects might result in a constitutive TORC1 activation that promotes protein translation and a metabolic shift from oxidative phosphorylation (mainly observed in quiescent/memory lymphocytes) toward aerobic glycolysis (typically observed in activated lymphocytes) (185). This increase in glucose demand (also known as Warburg effect) might be energetically beneficial during the recruitment of SS cells to skin and/or LN by CCL21, with the latter being able to further enhance mTORC1 activation and by that SS cell growth (169). Indeed, among other, in part stronger stimuli such as IL-2/IL-7, CCL21-mTORC1 also promoted up-regulation of the Ki67 proliferative protein in SS-derived cell lines and in primary SS cells (169).

3.2.6 T-Cell Large Granular Lymphocytic Leukemia (T-LGL)

T-LGL is characterized by the chronic low-level expansion of mostly $CD8^+$ T-cells in blood, BM, and spleen. Nodal disease is infrequent. T-LGL cells express pan-T-antigens, programmed cell death 1 (PD-1), some NK-cell associated molecules, cytotoxic granules (containing perforin and granzymes) and lack the CD28 co-stimulatory receptor. Detection of CD45RA and further markers of T-cell differentiation suggest a terminally differentiated effector memory (T_{EM-RA}) phenotype (128, 186–188). T_{EM-RA} cells are featured by the absence of CCR7, and accordingly, most T-LGL cases in these studies did not show tumor cell expression of CCR7.

3.2.7 Other T-Cell Malignancies

In other types of T-cell neoplasms such as peripheral T-cell lymphoma not otherwise specified (PTCL-NOS), extra-nodal NK/T-cell lymphoma (ENKTL), anaplastic large cell lymphoma (ALCL), and angioimmunoblastic T-cell lymphoma (AITL) expression of CCR7 remains poorly studied and controversial (including the source of expression, namely tumor cells *versus* local bystander cells). Two studies in a total of 41 ALCL patient samples and in 7 ALCL cell lines found the anaplastic-lymphoma kinase (ALK)-negative ALCL variant to overexpress CCR7 genes (compared to ALK-positive or primary cutaneous ALCL) (116, 189) while another series on LN biopsies associated ALCL to a $CD4^+CD45RO^+CD27^-$ T_{EM} phenotype that lacks CCR7 (190). In contrast, PTCL-NOS showed CCR7 expression as part of its T_{CM} signature (190). However, gene expression profiles showed no upregulation of CCR7 transcripts in PTCL-NOS as compared to normal T-cells; as also observed for AITL (191). A subsequent study reported expression of CCR7 by IHC in an overall of 83% of samples that contained PTCL-NOS, ENKTL, ALCL, and AILT, but without disclosed resolution for the proportions of CCR7 positive cases per entity (184). Despite this shortcoming, this work corroborated the expression of CCR7 in a high proportion of mature T-cell malignancies and, importantly, significantly associated CCR7 staining with lymphatic or hematogeneous dissemination as well as with clinical stage. As in B-cell malignancies, constitutive activation of the transcription factor AP-1 is a proposed mechanism underlying CCR7 overexpression and CCR7-mediated cell survival in some of these conditions, particularly ALCL (117).

In other, very rare T-cell lymphomas, studies on CCR7 have been sporadically reported. In a case of primary cutaneous aggressive epidermotropic CD8+ T-cell lymphoma transformation from an indolent to an aggressive phase was accompanied by a shift to CCR7 expression (177). A case of enteropathy-associated T-cell lymphoma (EATL) showed no lymphoma-cell associated CCR7 (178), fitting its cytotoxic T-cell nature, similar to CCR7-negative T-LGL.

3.2.8 Natural Killer (NK) Cell-Type Lymphoproliferative Diseases

NK-cell cancers can be subdivided into aggressive NK cell leukemia (ANKL) and indolent chronic NK cell lymphocytosis (CNKL), both characterized by leukemic infiltration into multiple organs (192). In a cohort composed of PB samples of nine ANKL and six CNKL cases several CKR were investigated by flow cytometry (193). In both types of leukemia, CCR7 was detected in a small proportion of tumorous NK-cells (<25%), a lower proportion than the relative number of CCR7-positive NK-cells the authors found in six healthy controls. Together, these results suggested that CCR7 might not play an important role in the pathophysiology of ANKL or CNKL.

3.3 CCR7 in Myeloid-Cell Malignancies

Description of CCR7 in myeloid-cell derived cancers is anecdotal and, as opposed to lymphoid disorders, myeloid neoplasms seem to be mainly characterized by downregulated CCR7, although this aspect still remains controversial.

3.3.1 Myelodysplastic Syndrome (MDS)

MDS constitutes a heterogeneous group of clonal hematopoietic stem cell diseases that share ineffective hematopoiesis, increased risk of developing acute myeloid leukemia (AML), and augmented prevalence of immune deregulation. To our knowledge no studies have addressed the expression or functions of CCR7 in myeloid cells from MDS patients. A comparative study of a cohort of 33 MDS, a condition with a known prominent inflammasome, patients with healthy controls found that in MDS CD8+ T-cells exhibited decreased levels of

CCR7 and a concomitant upregulation of CCR3, CCR5, or CX3CR1 (194). Hence, a central pathogenic relevance of CCR7 and other CKR in MDS still has to be shown.

3.3.2 Acute Myeloid Leukemia (AML)

AML is a heterogeneous group of aggressive proliferations with variable genetic make-up and differential responses to therapy (195). In clinical practice, CCR7 is sporadically detected by flow cytometry in AML samples from PB and BM in a small proportion of tumor cells (unpublished data). In agreement, CCR7 mRNA is not highly abundant in AML in several transcriptome analyses (14, 16, 196, 197). Only one study reported CCR7 transcript over-expression (~3-fold) in 148 human AML samples as compared to 12 samples of normal cord blood-derived CD34+CD45RA- cells (198). Protein expression to confirm high membrane levels of CCR7 was not studied. Potential associations of CCR7 mRNA with the most frequent genetic aberrations were also not investigated (198).

3.3.3 Blastic Plasmacytoid Dendritic Cell Neoplasm (BPDCN)

BPDCN is a rare and clinically aggressive hematologic tumor derived from cells of immature PDC differentiation (199). The clinical course of BPDCN shows progressive systemic expansion, partially attributed to the local production of chemokine ligands of CKR expressed by the tumor cells (CXCR3, CXCR4, CCR6, CCR7) (200). Beyond expression data, no clues are available on the pathogenic roles of CCR7 in BPDCN.

3.3.4 Langerhans Cell Histiocytosis (LCH)

In LCH pathological $CD207^+$ DC show constitutively activated MAPK pathway signaling. In *in vivo* and *in vitro* models, the B-raf V600E activating mutation impaired the Raf/ERK-mediated CCR7-induced migration of DC (201). This in turn caused their retention in the tissue lesions and, by promoting expression of BCL2-like protein 1 (BCL2L1), this resulted in enhanced resistance to apoptosis.

3.3.5 Myeloproliferative Disorders

Chronic myeloid leukemia (CML) is a clonal disease characterized by premature release of aberrant cells from the BM alongside their substantial accumulation in PB, spleen, and BM (202). In CML, the presence of the Philadelphia chromosome and its oncogenic product, the fusion oncoprotein BCR/ABL, is directly linked to multiple pathways involved in cell survival, growth promotion, and disease progression (203, 204). Similarly to LCH, an impaired adhesion and motility towards CCR7 was first reported for CML cells (14, 205) though this effect remains controversial since more recent reports showed *in vitro* and *in vivo* how a positive activation loop between BCR-ABL and the signal-transducing adaptor protein-2 (STAP-2) led to enhanced ERK signaling resulting in overexpression of CCR7, LN enlargement, and hepatosplenomegaly (203, 204). Whether these contradictory outcomes are a result of differential *in vitro versus in vivo* settings, or a consequence of artifacts associated to the use of cell lines *versus* primary tumor cells, needs clarification.

4 PATHOPHYSIOLOGICAL ROLE OF CCR7 IN HEMATOLOGIC MALIGNANCIES

Chemokines obey Stephen Paget's 'seed and soil' paradigm, proposing that the microenvironments of different organs are different from each other, and that certain tumor cells have specific attraction to the milieu of specific organs (206). As reviewed above, CCR7 is a single receptor driving immune cells into LN, and for this reason this receptor assumes a central role in the pathogenesis of many leukemia and lymphomas, which very often express CCR7 due to their lymphoid or myeloid origin (**Table 1**).

In lymphoid malignancies, the role of CCR7 in hallmark deregulations of cancer such as enhanced migration or death resistance, can be associated to functional differences between CCR7-expressing normal and malignant cells. In some cases, gain-of-function in CCR7 is a consequence of an upregulated transcription and/or protein translation (**Figure 1**). For example, tonic signaling through the BCR or CD40 activates transcription factors such as NFATC1, NF-κB, and AP-1, which target the CCR7 gene, a mechanism found in CLL and B-ALL (22, 23, 42, 54–56, 208, 211). Similarly, CD30 down-stream signaling seems to increase CCR7 gene transcription in cHL and ALCL likely through NF-κB and AP-1 (3, 115, 117). Moreover, constitutive activation of the Notch1 oncoprotein increases CCR7 expression in T-ALL through the mTORC2/NF-κB cascade (25, 133), or in CLL through down-modulation of the DUSP22 phosphatase levels and the subsequent increase in STAT3 activation (51). In other instances, CCR7 up-regulation is promoted by a viral machinery that suppresses CCR7 gene repressor factors like CBF-1. This is described for the viral transactivator EBNA-2 in BL and DLBCL (89, 91) and it could be hypothesized that a similar mechanism governs HTLV-1-induced transformation in ATLL. Notably, downregulation of CCR7 expression and reduction of associated chemotaxis during viral infections, have been reported (11, 212). The EBV (213), the murine lymphocytic choriomeningitis virus (LCMV) (214), the human immunodeficiency virus type 1(HIV-1) (215), or the influenza virus (216) are examples of CCR7-downmodulating viruses. In other cases, e.g. during HIV-1 infection, primary $CD4^+$ T-cells showed and enhancement of CCR7-mediated motility, leading to efficient propagation of HIV-1 (217, 218). Based on this, one might be tempted to associate these changes of the CKR expression profile to particular needs of each virus' cycle. Therefore, discrepancies between outcomes in CCR7 expression after viral infections might be also a consequence of distinct cell-to-cell aspects such as the time elapsed after cell infection, the cell development stage at which the infection takes place, or baseline CCR7 expression by host cell. For example, the impact of *in vitro* EBV infection on CCR7 expression was very different between tonsillar or PB B-cells, being milder (if at all) in the last cell type (213). Moreover, the presence of additional tumorigeneic events in the infected tumor cells may synergize with the viral machinery to induce CCR7 gene expression (219, 220). In agreement, expression of CKR and chemokines in immortalized cell lines differs from that of EBV-infected PB

TABLE 1 | Summary of blood cancers with reported CCR7 expression studies (following 2016 WHO classification of blood neoplasms) (207).

				CCR7	
				GEP	**Protein**
Lymphoid neoplasms	**Precursor lymphoid neoplasms**	B-ALL and B-lymphoblastic lymphoma		-/+	-/+
		T-ALL and T-lymphoblastic lymphoma		+	+
	Mature B-cell neoplasms	Chronic lymphocytic leukemia/small lymphocytic lymphoma		+	+
		Monoclonal B-cell lymphocytosis		na	+
		Splenic marginal zone lymphoma		–	–
		Hairy cell leukemia		–	–
		Lymphoplasmacytic lymphoma/Waldenström macroglobulinemia		na	-/+
		Monoclonal gammopathy of undetermined significance		–	na
		Plasma cell myeloma		–	-/+
		Plasma cell myeloma variants	Smoldering myeloma	–	na
			Non-secretory myeloma	na	–
			Plasma cell leukemia	–	na
		Extranodal marginal zone lymphoma of mucosa-associated lymphoid tissue (MALT lymphoma)		-/+	+
		Nodal marginal zone lymphoma		na	na
		Follicular lymphoma		-/+	-/+
		Primary cutaneous follicle center lymphoma		-/+	na
		Mantle cell lymphoma		+	+
		Diffuse large B-cell lymphoma	GCB type	-/+	-/+
			ABC type	+	+
		T-cell/histiocyte-rich large B-cell lymphoma		-/+	na
		Primary diffuse large B-cell lymphoma of the central nervous system		na	+
		EBV-positive diffuse large B-cell lymphoma		-/+	na
		Primary effusion lymphoma		+	na
		Burkitt lymphoma		-/+	+
	Mature T- and NK-cell neoplasms	T-cell prolymphocytic leukemia		+	+
		T-cell large granular lymphocytic leukemia		na	–
		Chronic lymphoproliferative disorder of NK cells		na	–
		Aggressive NK-cell leukemia		na	–
		Adult T-cell leukemia/lymphoma		+	+
		Extranodal NK-/T-cell lymphoma		na	-/+
		Mycosis fungoides		+	+
		Sézary syndrome		+	+
		Primary cutaneous $CD30^+$ T-cell lymphoproliferative disorders	Primary cutaneous anaplastic large cell lymphoma	-/+	na
		Primary cutaneous peripheral T-cell lymphomas, rare subtypes	Pimary cutaneous $CD8^+$ aggressive epidermotropic cytotoxic T-cell lymphoma	na	–
		Peripheral T-cell lymphoma, not otherwise specified		-/+	+
		Angioimmunoblastic T-cell lymphoma		-/+	-/+
		Anaplastic large-cell lymphoma	ALK-positive	-/+	-/+
			ALK-negative	+	+
	Hodgkin lymphoma	Nodular lymphocyte predominant Hodgkin lymphoma		-/+	–
		Classical Hodgkin lymphoma		+	+
Histiocytic and DC neoplasms	**Tumors derived from Langerhans cells**	Langerhans cell histiocytosis		–	–
Myeloid neoplasms	**Myelodysplastic syndromes**			na	na
	Acute myeloid leukemia and related neoplasms			-/+	-/+
	Blastic plasmacytoid dendritic cell neoplasm			na	+
	Myeloproliferative neoplasms	Chronic myeloid leukemia		–	–

ABC, activated B-cell like; ALK, anaplastic-lymphoma kinase; DC, dendritic cells; EBV, Epstein-Barr virus; GCB, germinal center B-cell like; GEP, gene expression profile; na, not available.

B-cells (89, 213) and different growth requirements, such as the oestrogens, are known to positively regulate viral factors like EBNA2, which subsequently activate CCR7 gene expression (4, 213).

Finally, CCR7 up-regulation may be also promoted by mutations in the C-terminal cytoplasmic region of CCR7 or dysregulation of its endocytic machinery both affect receptor turn-over. For example, in ATLL or CLL cells impaired internalization upon ligand stimulation results in increased surface receptor expression (43, 46, 162, 163). Whatever the underlying reasons for the upregulation of CCR7, in the majority of diseases that are reviewed here, all these events lead to increased numbers of functional receptors at the surface of the tumor cells, which endows them with an increased migratory

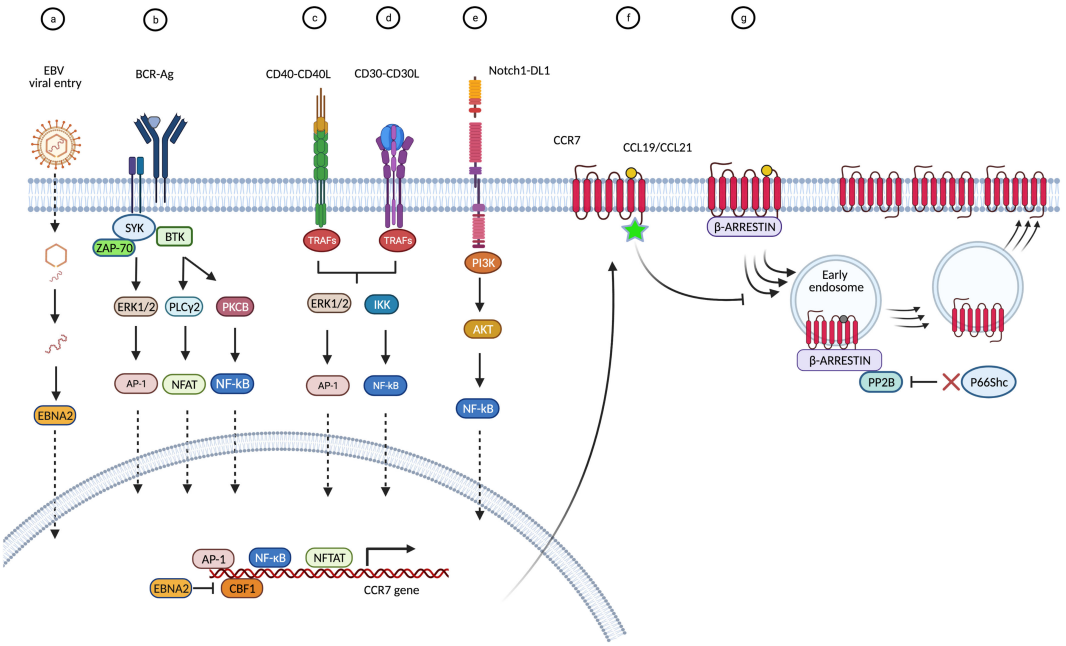

FIGURE 1 | Causes and modes that underlie CCR7 overexpression in blood cancers. Overview of proposed signaling cascades with reported data. **(A)** CCR7 upregulation may be promoted by EBV. In BL and DLBCL cells, following viral endocytosis, the virion and packaged proteins are released into the cytoplasm. The viral transactivator EBNA-2 binds to and inhibits the *CCR7* gene repressor factor CBF-1 (also known as RBP-Jκ) thus promoting *CCR7* gene transcription (4, 89, 91). **(B)** In B-cell malignancies (CLL, B-ALL) tonic signaling through the BCR activates transcription factors such as NFATC1, NF-κB, and AP-1, which target the *CCR7* gene (42, 54, 56). **(C)** When engaged by CD40L, the receptor CD40 recruits tumor necrosis factor receptor-associated proteins (TRAF) to the membrane, which initiate different signaling pathways leading to activation of NFκB or AP-1 (22, 23, 208, 209). **(D)** In cHL and ALCL, binding of CD30L (CD153) or sCD30 to CD30 can result in trimerization and signal mediation through TRAF proteins to stimulate the NFκB pathway resulting in *CCR7* gene expression (3, 210). In addition, CD30 can signal through MAPK pathways, including ERK1/2 and the nuclear transcription factor AP-1, all leading to enhanced *CCR7* transcription (3, 115, 117). **(E)** In T-ALL cells, release of intracellular Notch1 (ICN1) from membrane-tethered heterodimeric Notch1 protein upregulates PI3K/mTORC2/NF-κB pathways and activation of the *CCR7* gene (25, 133). In CLL cells, activating mutations in Notch1 intracellular domain favor the downmodulation of DUSP22 phosphatase thus facilitating the accumulation of activated STAT3 which mediates *CCR7* gene transcription (51). **(F)** Mutations in the C-terminal amino acid Trp355, located in the cytoplasmic region of CCR7, impair internalization upon ligand stimulation resulting in increased expression of the surface receptor in ATLL cells (162, 163). **(G)** Dysregulation of the endocytic machinery of CCR7, e.g. in CLL, impacts receptor turn-over and increases CCR7 membrane expression. Deficiency of the cytoplasmic p66Shc protein causes enhanced activity of the PP2B/calcineurin phosphatase on the endosomal CCR7 pool, which enhances its recycling back to the plasma membrane (43, 46).

capacity (13, 20, 35, 40, 46, 99, 115, 173). CCR7-mediated migratory abilities can be selectively potentiated in leukemia/lymphoma cells (as opposed to their normal counterparts) by pre-exposure or co-incubation with other homeostatic chemokines like CXCL12 or CXCL13, as demonstrated in MCL, BL, or SS (78, 90, 183). Although in many entities the molecular mechanisms of CCR7 upregulation remain unknown, it is consistently found across various diseases, e.g. B-ALL, T-ALL, or CLL. Therein, its overexpression is associated with the presence of adverse prognostic factors, e.g. ZAP-70, which seem to directly cooperate with CCR7 towards facilitation of homing to survival niches such as LN or CNS (24, 38, 47). In fact, in CLL ZAP-70 has been shown to govern integrin activation upon CCR7 stimulation, in a G-protein independent fashion and through oligomerization of four CCR7 molecules (58, 63). Nevertheless, some associations of CCR7 expression with markers of disease subsets, hence aggressiveness or outcome, might be of indirect nature and just represent indicators of different inherent cellular programs (e.g. higher migratory potential), as suggested for the histogenetic subsets of CLL with unmutated *IGHV* and/or with trisomy 12 that show higher responsiveness to CCR7 ligands (35, 36, 38, 46, 47, 66).

Generally, in most blood cancers, CCR7 expression correlates with nodal or spleen involvement. In the conditions of B-ALL, MCL, T-ALL, or T-PLL it is also associated with infiltration of the CNS and in CTCL it correlates with the degree of epidermotropism (21, 24, 25, 130, 134, 161, 169, 221, 222). Therefore, it is consistently proposed that overexpression of CCR7 confers an invasive phenotype that contributes to lymphatic and hematogenous spread and promotes homing into target tissues (**Figure 2**). This $CCR7^{+}$ transmigrating phenotype is further characterized by activation of α4β1 and αLβ2 integrins that facilitate adhesion of malignant cells to HEV or stromal proteins, and that promote the secretion of matrix metalloproteases MMP-2 and/or MMP-9, which degrade extracellular matrix (35, 58, 64, 130, 157, 183, 184). Both

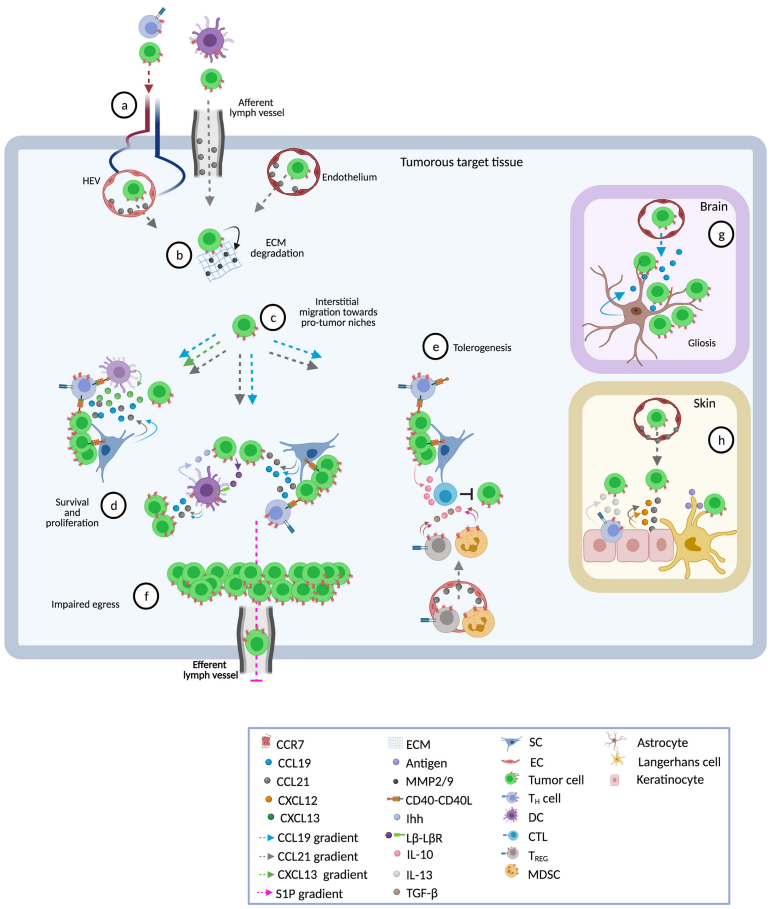

FIGURE 2 | Pathophysiological roles of CCR7 in blood cancers. Shown are different tissues and ways in which the receptor contributes to disease progression. **(A)** Following CCL21 gradients, CCR7-expressing tumor and accessory cells enter into target tissues through high endothelial venules (HEV, in LN and other SLO), afferent lymphatic vessels (in LN), or endothelial cells (BM, spleen, skin, CNS) (8–10, 24, 25, 104, 130, 134). CCL21 on the surface of endothelial cells (EC) activates α4β1 and αLβ2 integrins thus facilitating transmigration (35, 58, 64, 130, 157). **(B)** Subsequently, activated CCR7 promotes invasive phenotypes that secrete metalloproteinases 2 and 9 (MMP-2/9) and promotes extracellular matrix (ECM) degradation (64, 130, 183, 184). **(C)** Within the tissue, CCR7 drives interstitial migration of tumor cells to distinct sites such as T-zones or B-zones in spleen and LN (9), or to lymphoid-like (tertiary) structures in skin or CNS (104, 169). Some tumor cells have inherent abilities to migrate towards CCL19/CCL21 gradients whereas others need cooperative signaling by other chemokines (e.g. CXCL12 or CXCL13) or a previous stimulus, such as exposure to CD40L, to initiate this process (20, 22, 23, 78, 90, 183, 209). **(D)** CCR7-driven interstitial migration assists tumor cells in their right positioning adjacent to accessory cells such as $CD40L^{+}CD4^{+}$ T_H cells, DC, and stromal cells (SC) which foster growth and resistance to spontaneous or drug-induced cell death (9, 68). Cross-talk with accessory cells induces the release of CCL19 and CCL21 (9, 25, 134) directly promoting survival and proliferation of tumor cells *via* MAP-kinase and PI3K signaling pathways (9, 40, 70, 223). CCL19 can also act in cooperation with CXCL13 to confer resistance to TNF-α-mediated apoptosis *via* up-regulation of PEG10 (26, 27). Other pro-tumor factors delivered by accessory cells include the Indian hedgehog (Ihh) secreted by fibroblastic reticular cells (FRC) and CD40 stimulation through CD40 ligand-expressing $CD4^{+}$ T_H cells (9). In turn, malignant cells secrete factors that stimulate and protect accessory cells. One of these factors is lymphotoxin through which tumor cells stimulate lymphotoxin-β-receptor (LβR) expressing FRC (9). Finally, in these niches enhanced production of CCR7 ligands establishes a self-enhancing loop that recruits more tumor and accessory CCR7-expressing cells favoring the continuation of pro-tumor microenvironments (9, 25, 134, 161, 169, 221). **(E)** CCR7 ligands may attract $CCR7^{+}$ immunosuppressive cells such as T_{REG} and myeloid-derived suppressor cells (MDSC) (224, 225). These suppressor cells inhibit anti-tumor effector cells (e.g. CTL) through cell-cell interactions or by creating a tolerant milieu enriched in suppressor cytokines like IL-10 and tumor growth factor beta (TGF-β) (22, 28, 225, 226). Similarly, CCL19 and CXCL13 may synergistically regulate CD40-CD40L cross-talk between cancer cells and $CD8^{+}$ T-cells leading to a PEG10-mediated enhanced production of IL-10 in CD40-activated tumor cells that inhibits tumor-specific CTL (28). Together, these CCR7-induced mechanisms facilitate permissive milieus within tumor target tissues. **(F)** CCR7 also prolongs the time of residence of CCR7-expressing cells in lymphoid tissues (i.e. LN) thus favoring proliferative cycles and providing niches of escape from systemic therapies. In the steady state, internalization of CCR7 activates the transcription and surface expression of S1P1, facilitating the egress of lymph-node-homed immune cells through efferent lymphatic vessels (71). Tumor-associated overexpression of CCR7 impairs S1P1 upregulation thus retaining tumor cells within the LNs, reducing the egress and causing lymphadenopathy (43, 46, 72). **(G)** In CNS, astrocyte-derived CCL19 attracts tumor cells and enhances their parenchymal retention thus contributing to gliosis (24, 25, 104). Inside cerebral or spleen parenchyma, cross-talk between stromal cells and leukemic cells mediates the production of higher levels of tissue CCL19 (25, 134) facilitating the infiltration of tumor cells. **(H)** In the skin, CCL21 in the cytoplasm of epidermal keratinocytes and to be diffusely distributed in the dermal extracellular matrix may lead tumor cells to milieus enriched in growth factors such as CXCL12, IL-13 or antigens able to entertain chronic T-cell receptor stimulation (169).

events result in transmigration of tumor cells into protective niches at which, particularly in T-zones, CCR7 contributes to disease progression in four major ways:

1) In 'homing' tumor cells, CCR7 drives interstitial migration within the tissue and assists in optimal positioning, e.g. adjacent to accessory cells such as $CD40L^+CD4^+$ T_H cells, DC, and stromal cells, which foster growth and resistance to spontaneous or drug-induced cell death. As described, this positioning can be controlled by local factors including gradients of CCR7 ligands (9, 69, 104, 121), CD40-CD40L interactions (9, 68), BCR/ZAP-70 signal transduction (38, 42), or canonical WNT signaling (119).

2) Crosstalk with accessory cells can induce the release of high levels of the chemokines CCL19 and CCL21, which engage and activate CCR7 to provide pro-survival signals (9, 25, 134). In addition, stromal cells can produce CCR7 ligands in a constitutive manner (35, 46, 121, 161, 169, 223). Whatever the source of CCR7 ligands, they promote survival, e.g. by acting as trophic factors that induce MAPK and PI3K-AKT signaling (9, 25, 40, 70, 134, 223). They can also act in cooperation with CXCL13, which contributes to resistance to TNFα-mediated apoptosis preferentially in malignant over normal B-cells, *via* upregulation of *PEG10* and stabilization of caspases-3 and -8 (26, 27). In some entities, e.g. MCL, T-PLL, or SS, CCR7 ligands have also shown to trigger proliferation (21, 130, 169).

3) Besides promoting influx, CCR7 (together with S1P1) also contributes to LN enlargement by regulating egress from lymphoid tissues, hence accumulation. It prolongs the time of residence of CCR7-expressing cells in lymphoid tissues, by that favoring proliferative cycles and providing niches of escape from systemic therapies. In CLL, the characteristic high expression of CCR7 can be attributed to abnormalities in the surface membrane recycling machinery as a consequence of abnormally low production of the cytoplasmatic p66Shc protein (43, 46). Deficiency of the cytoplasmic p66Shc protein causes enhanced activity of the PP2B/calcineurin phosphatase on the endosomal CCR7 pool, which enhances its recycling back to the plasma membrane. Likewise, ATLL cells carry mutations in the C-terminal cytoplasmic domain of CCR7 that impairs proper recycling (162, 163).

4) CCR7 participates in the creation of permissive tumor microenvironments within tumorous target tissues (SLOs, CNS, or skin). As part of the involved tissue interactions between tumor cells and stromal or other accessory cells, an increased production of CCR7 ligands is stimulated (9, 25, 134). For example, cooperative CCR7/WNT signaling is needed for secretion of VGEF-A by cHL cells, which leads to *de novo* generation of vascular endothelium which, in turn, presents CCR7 ligands that direct movement of cHL towards vascular niches (119). Similarly, BL cells can secrete lymphotoxin through which they stimulate lymphotoxin-β-receptor expressing $gp38^+$ FRC that secrete the survival factors Ihh and CCL21 (9). These patterns and higher amounts of chemokines establish a feed-forward loop that not only recruits additional CCR7-expressing malignant cells, but also further supportive bystander cells (9, 25, 105, 134, 161, 221). Moreover, in B-ALL CCR7 ligands potentiate secretion of immunosuppressive IL-10 by tumor cells leading to impaired specific anti-tumor CTL responses (28). CCR7 can also recruit regulatory cells that hamper anti-tumor immunity. For example, an increase of functional T_{REG} has been established for patients with blood cancers (226). Expansion of T_{REG} is needed to generate and sustain a tolerogenic TME (227). Indeed, higher numbers of T_{REG} associate with progressive disease in cHL, CLL, MGUS, MM, or DLBCL (228–232).

5 BIASED SIGNALING OF CCR7 LIGANDS IN BLOOD CANCERS

In the field of GPCRs, knowledge on the diversity in signaling pathways has promoted the concept of "biased signaling", which involves a context-specific preference for one intracellular signaling pathway over another (233). This concept can be considered as either receptor bias (the same ligand has different actions through different receptors), ligand bias (more than one or naturally modified ligands act on the same receptor and induce different outcomes), or tissue bias (the cellular effect depends on the tissue/cell type) (234). How biased signaling enables different downstream pathways that eventually will determine the overall outcome of CCR7 engagement in different immune cell types has been recently, and deeply, reviewed by Hauser et al. (11). The role(s) of biased signaling of CCR7 in the pathophysiology of blood cancers is not clear, although a scarce number of studies comparing CCR7 activation in healthy *versus* malignant cells indicate that a differential regulation is plausible. For example, in CLL we demonstrated that PI3K and ROCK, but not MAPK, were involved in migration of CLL cells toward CCL19 and CCL21, whereas normal B-cells relied more on PI3K, ROCK, and p38-SAPK pathways (40). Moreover, while CLL cells showed an enhanced, similar migratory response to both CCR7 ligands, normal B-cells showed a moderate response, and preferentially towards CCL21 (13, 35, 40, 46). Likewise, CLL and normal B-cells showed a different signaling to migrate through the endothelium (35, 235). Finally, it is worth mentioning that in the last years CCR7 has been shown to form heterodimers with CXCR4 (217). This process affects CCR7 signaling and might explain a poorly understood, but important, mechanism of chemokine biology that allows synergistic and/or inhibitory outputs produced by simultaneous activation or inhibition of multiple CKRs. Interestingly, CCR7/CXCR4 dimers may enhance tumor B-cell homing to LN by potentiating the TEM upon simultaneous exposure to CXCL12, CCL19, and CCL21 (90) while in healthy, mature B-cells CCR7 acts as a selective allosteric modulator that inactivates CXCR4 thus impairing retention in the BM (236). Together, these findings support the existence of a functional and phenotypic diversity as a result of a biased signaling of CCR7 in homeostasis and blood cancers. Nonetheless, other studies show identical mechanisms in both healthy and neoplastic cells. For example, CCL19-specific translation of S1P1 is mediated by ERK-5/Krüppel-like factor-2 in the HuT78 SS cell line and healthy

primary T-cells (237). Therefore, additional comparative studies addressing biased signaling in both healthy and tumor tissues are mandatory to better understand the pathophysiological roles of these regulatory mechanisms in CCR7 and other CKRs.

6 CCR7 AS A THERAPEUTIC TARGET IN BLOOD CANCERS

The circumstantial and direct evidence presented in this review suggests that the tumor-associated CCR7-ligand interaction is an actionable vulnerability. At CCR7-ligand permissive sites, e.g. LN or brain, malignant cells evade spontaneous or drug-induced apoptosis as well as escape immune cell control or proliferate, all in a CCR7-mediated manner. Therefore, interfering in CCR7-signalling promises to be of therapeutic potential in many CCR7 expressing and CCR7 promoted blood cancers. Nonetheless, targeting CCR7 in cancer has the potential downsite of activating and/or potentiating alternative pathways that would eventually allow homing of tumor cells to protective niches. For instance, to adhere to HEVs of peripheral and mesenteric LNs T-cells rely on CCR7 and partially on CXCL12/CXCR4 whereas normal B-cells can exploit the CXCR4 and CXCL13/CXCR5 axes to induce integrin-mediated arrest on HEVs and homing to the LN (238–243). To avoid this scenario, it is desirable that anti-CCR7 drugs feature a double MOA including both, neutralization of the target and tumoricidal capacities. In this regard, we and others have demonstrated that approaches based on we and others have demonstrated that approaches based on blocking (non-activating) monoclonal antibodies (mAbs) that target CCR7 or its ligands, are highly effective in *in vitro* and *in vivo* preclinical models, including B-ALL (24), CLL (37, 40, 45), MCL (21), T-ALL (24, 25), or T-PLL (130). In these studies, such anti-CCR7 therapies reduced tumor cell migration and infiltration into CCR7-specific environments and additionally impaired survival/proliferation. Overall, the combined neutralizing and killing activities of anti-CCR7 mAbs led to retarded tumor implantation, reduced tumor burden, and significantly extended host survival in *in vivo* models.

Taken together, there is ample data on target expression and mechanistic rationales as well as sufficient proof of principle and feasibility data that strongly encourage the therapeutic application of anti-CCR7 therapies in blood cancers. Consequently, first clinical-grade anti-CCR7 antibodies have been developed during the last years. Novartis is enrolling patients into a phase-I trial with JBH492 an antibody-drug conjugate (ADC) targeting CCR7 (NCT042140704). Moreover, Catapult Therapeutics presented first pre-clinical results of an antagonist mAb called CAP-100 that will be evaluated in first-in-human clinical trials in 2021 (NCT04704323) (244). In preclinical settings, both compounds have shown to be highly effective as a single agent and at least CAP-100 revealed the potential for combinations with current standard-of-care drugs (245). Owing to their particular MOA, antagonisticanti-CCR7 mAbs may be likely combined with other standard-of-care drugs to obtain additive or synergistic effects while reducing the likelihood of treatment resistances. For example, by blocking ligand-receptor interactions, anti-CCR7 therapies may displace tumor cells out of protective niches, forcing them to accumulate in blood where they may become more accessible to other cytotoxic drugs such antibodies against established targets (e.g. CD20, CD30, CCR4, etc), or chemotherapeutics (e.g. fludarabine), or small molecule inhibitors (e.g. BCL2 inhibitors). Along with the BTK inhibitor ibrutinib or with the PI3Kδ inhibitor idelalisib, anti-CCR7 mAbs would additively or synergistically target CCR7-mediated adhesion to lymphoid stroma or endothelium, thus favoring an enhanced cell egress from lymphoid tissues into circulation (44, 46, 48, 246). In fact, we have recently demonstrated that CCR7 expression and functionality is not impaired during ibrutinib treatment in CLL patients and that the anti-CCR7 CAP-100 and ibrutinib show complementary activities (245). Moreover, while the antibody would block recirculation and loops of LN homing, ibrutinib would also interfere with CXCR4- and CXCR5-mediated signaling and with the production of chemokines (CXCL12, CXCL13, CCL19) by myeloid stroma cells (44, 247), thus acting against potential redundant chemotactic pathways. Finally, it is worth mentioning that immune checkpoint blockade and CAR-T-cells have revolutionized the field of cancer therapy during the last decades. Whether anti-CCR7 therapy may complement such treatments is uncertain since for avoiding negative interactions it seems necessary that therapeutic T-cells to express an effector or effector memory CCR7-negative phenotype.

Given the various roles in tumor development and progression, adhesion molecules are promising targets to block the access of tumor cells to tumor-permissive niches like the LN (248, 249). For instance, LFA-1 and VLA-4 are involved in the development of hematological malignancies and tumor cells require their expression to migrate into lymphoid tissues (250, 251). Therefore, it is plausible to speculate that targeting these leukocyte adhesion molecules might be an alternative way to target the CCR7 axis. Like anti-CCR7 assets do, targeting cell adhesion exerts direct effects to the tumor cell (e.g. reduction of motility, invasiveness, and proliferation) that may impair homing to SLO (252, 253). In addition, cell adhesion molecules are common downstream players activated by several CKRs, including CCR7 (254), hence, their inhibition would potentially inhibit CCR7 along with several other receptors, thus overcoming the redundancy of CKRs (255). Yanguas et al. showed in murine melanoma models that an increased number of intra-tumorally injected tumor-specific T-cells migrated into the draining LN when treated with anti-ICAM-1 or anti-LFA-1 mAbs (256). This indicates that specific approaches, such as anti-CCR7 mAbs, are needed to block LN homing. Moreover, since integrins play diverse roles in immunity and anti-tumor responses, targeting the function of these molecules *in vivo* may be a difficult task in cancer therapy (254, 257, 258). Accordingly, multiple clinical trials that involve the targeting of αV or β1 integrins have shown disappointing results with low therapeutic efficacies (249), while anti-LFA-1 strategies have been associated with an increased risk of malignancies,

infections, and rare, but severe, systemic adverse events such as immune-mediated thrombocytopenia and hemolytic anemia (259, 260). To overcome these deleterious effects, novel approaches aiming to target the integrin and/or ligands on tumor cells or tumor vessels, but not in immune cells, are needed. Bispecific antibodies simultaneously directed against LFA-1 and a tumor specific antigen may contribute to specifically block LFA-1-mediated tumor cell adhesion without affecting immune responses, as shown in mice (261). Since targeting CCR7 shares both overlapping and differentiating MOAs with such therapies that target adhesion, combining both of these strategies could provide clinical benefits and needs to be further investigated.

7 SAFETY OF NOVEL THERAPIES TARGETING CCR7 IN BLOOD CANCERS

Currently, two clinical trials aim to validate anti-CCR7 approaches in hematologic diseases with an urgent need for more rationally based and efficient therapies. These studies will also allow us to learn the real risks that are associated with blocking CCR7 and/or depleting CCR7-expressing immune cell subsets as this receptor is critical for activation steps in the adaptive immune system and for the homeostasis of T_{REG}, which limit self-reactive events and autoimmunity (262). In one hand, several mouse models revealed that deficiency of CCR7 signaling was not a life-threatening condition, as it was associated with a moderate impact on immunity by retarded, but preserved, T-cell and B-cell responses (8, 240, 263–265), especially against infections with replicating antigens (266–269). However, in different vaccinations approaches (e.g. HIV, HSV, or HCV) adjuvant CCL19 was relevant for augmenting the trafficking of T-cells and DC (270–272). Therefore, anti-CCR7 therapy may reduce priming of antigen-specific T-cells and the production of Abs in a virus-dependent manner. From pre-clinical models, we know that the use of anti-CCR7 mAbs selectively inhibited and/or depleted tumor cells while sparing healthy counterparts (37, 45, 244, 273, 274). Notably, $CD4^+$ T_N and T_{CM} cells were preferentially impacted while other CCR7-expressing subsets such as DC or B-cells were not. Lower target density in non-tumor cells or lower affinity of these antibodies for CCR7 expressed in these cell types could explain these observations which also suggests that anti-CCR7 therapy might impair new immunization processes dependent on T_N cells, but not memory effector responses against infections (273–275). In this regard, CCR7-negative T_{EFF} and T_{EM} rather than CCR7-expressing T_N or T_{CM} are necessary for effective anti-tumour responses (276). Moreover, naïve tumor-specific $CD8^+$ T-cells, which seem less susceptible to anti-CCR7 therapy (244, 273, 274), can also become activated and gain effector-cell phenotypes directly at the tumor site, suggesting that cross-presenting DC are also able to prime $CD8^+$ T-cells within the tumor (277). These results indicate that DC migration into LN may not even be completely necessary for DC-mediated anti-tumor responses.

Targeting CCR7 could also affect B-cell homing during antigen-dependent and independent B-cell differentiation; however, CCR7-deficient mice show splenic B-cell responses upon bacterial challenge (240). In addition, normal B-cells are less dependent on CCR7 than leukemic cells for the arrest on HEVs and for homing (71, 238, 278) while BM B-cell precursors and plasma cells lack CCR7 (13), suggesting that CCR7 therapy would not suppress B-cell lymphopoiesis nor immunoglobulin secretory function (8, 240).

Related to unwanted autoimmune side-effects, lack of CCR7 signaling in T_{REG} hampered central and peripheral tolerance (224, 279–282) and led to generalized multi-organ autoimmunity. Whether anti-CCR7 therapies will resemble phenotypes in CCR7-deficient animals will remain unknown until first evidence in patients becomes available. Until then, clinical results with the therapeutic antibody mogamulizumab (which removes $CCR4^+$ T-cell subsets, including T_{REG}) (283) allow us to speculate that anti-CCR7 can be safe and well-tolerated. In line with this, anti-CCR7 therapy in pre-clinical syngeneic mouse models of cancer, autoimmunity, GVHD, or inflammation did not uncover treatment-associated side effects (225, 273, 275) and CAP-100 toxicology studies in NHP did not reveal overt toxicities or autoimmune disease, all indicating superior tolerability of this novel therapy (244). In the coming months, first data in patients receiving a chronic administration of an anti-CCR7 mAb will be available and, hopefully, results from clinical studies will shed light into the safety and utility of targeting CCR7, and more importantly, will validate anti-CCR7 approaches in hematologic diseases with an urgent need for more rationally based and efficient therapies.

8 CONCLUSIONS

Classically, the pathogenic role of CCR7 as a cancer-associated receptor in hematology has been attributed to its unique ability to drive tumor cells into the LN and other SLO. Accordingly, CCR7 expression has been strongly linked to bulky disease in these lymphoid tissues. Nonetheless, this canonical (and somehow narrow) view of CCR7 as a migratory receptor is changing thanks to recent evidence that supports additional pathogenic functions of CCR7. Beyond cancer cell lymphotropism, we have disclosed that CCR7 expression is also associated to neurotropism and epidermotropism, to interstitial migration within tumor tissues, to juxta-positioning to accessory cells, and to cell survival and proliferation. Moreover, CCR7 also guides different accessory cell types that are needed to create and preserve pro-tumor niches and to protect cancer cells from spontaneous or drug-induced apoptosis. Likewise, immunosuppressive cells take advantage of CCR7 to locate themselves close to innate or adaptative anti-tumor immune cells, thus facilitating their tolerogenic or their inhibitory participation in the TME.

However, our knowledge on CCR7 biology in blood cancers is still scant and additional efforts are needed to solve relevant questions such as around the major mechanisms regulating CCR7 (over)expression, how CCR7 contributes to tumor

growth during the first tumorigeneic events, or what the exact contributions of CCR7 in accessory cells in early cancer events or during different stages of target tissue colonization are.

CCR7 is currently postulated as a potential therapeutic target for some blood cancers and novel antibody(conjugate)-based strategies targeting CCR7 are being evaluated in early-phase clinical trials. It is also tempting to speculate that modulation of CCR7 expression and signaling in therapeutic lymphocytes might allow manipulation of the performance (e.g. migratory potential, longevity) of T- or NK-cells carrying chimeric-antigen receptors. If such direct or indirect modulation of tumor-cell or milieu-derived CCR7-signaling stands out as a promising approach it is likely that in the coming years an extensive collection of novel evidence will help to better understand its biology and to refine CCR7-based translational applications.

AUTHOR CONTRIBUTIONS

CC-M conceived the manuscript, wrote the manuscript, and conceived and created the figures and tables. FT co-wrote the manuscript. MH co-wrote the manuscript, conceived and edited tables and figures. All authors contributed to the article and approved the submitted version.

ACKNOWLEDGMENTS

The authors would like to thank Marty Wulferink and Wim Mol for language editing and proofreading of the manuscript. In addition, we would like to thank BioRender.com for figure editing.

REFERENCES

1. Riedel A, Shorthouse D, Haas L, Hall BA, Shields J. Tumor-Induced Stromal Reprogramming Drives Lymph Node Transformation. *Nat Immunol* (2016) 17(9):1118–27. doi: 10.1038/ni.3492
2. Birkenbach M, Josefsen K, Yalamanchili R, Lenoir G, Kieff E. Epstein-Barr Virus-Induced Genes: First Lymphocyte-Specific G Protein-Coupled Peptide Receptors. *J Virol* (1993) 67(4):2209–20. doi: 10.1128/jvi.67.4.2209-2220.1993
3. Schweickart VL, Raport CJ, Godiska R, Byers MG, Eddy RLJr., Shows TB, et al. Cloning of Human and Mouse EBI1, a Lymphoid-Specific G-Protein-Coupled Receptor Encoded on Human Chromosome 17q12-Q21.2. *Genomics* (1994) 23(3):643–50. doi: 10.1006/geno.1994.1553
4. Burgstahler R, Kempkes B, Steube K, Lipp M. Expression of the Chemokine Receptor BLR2/EBI1 is Specifically Transactivated by Epstein-Barr Virus Nuclear Antigen 2. *Biochem Biophys Res Commun* (1995) 215(2):737–43. doi: 10.1006/bbrc.1995.2525
5. Comerford I, Harata-Lee Y, Bunting MD, Gregor C, Kara EE, McColl SR. A Myriad of Functions and Complex Regulation of the CCR7/CCL19/CCL21 Chemokine Axis in the Adaptive Immune System. *Cytokine Growth Factor Rev* (2013) 24(3):269–83. doi: 10.1016/j.cytogfr.2013.03.001
6. Forster R, Davalos-Misslitz AC, Rot A. CCR7 and its Ligands: Balancing Immunity and Tolerance. *Nat Rev Immunol* (2008) 8(5):362–71. doi: 10.1038/nri2297
7. Legler DF, Uetz-von Allmen E, Hauser MA. CCR7: Roles in Cancer Cell Dissemination, Migration and Metastasis Formation. *Int J Biochem Cell Biol* (2014) 54:78–82. doi: 10.1016/j.biocel.2014.07.002
8. Forster R, Schubel A, Breitfeld D, Kremmer E, Renner-Muller I, Wolf E, et al. CCR7 Coordinates the Primary Immune Response by Establishing Functional Microenvironments in Secondary Lymphoid Organs. *Cell* (1999) 99(1):23–33. doi: 10.1016/S0092-8674(00)80059-8
9. Rehm A, Mensen A, Schradi K, Gerlach K, Wittstock S, Winter S, et al. Cooperative Function of CCR7 and Lymphotoxin in the Formation of a Lymphoma-Permissive Niche Within Murine Secondary Lymphoid Organs. *Blood* (2011) 118(4):1020–33. doi: 10.1182/blood-2010-11-321265
10. Wiley HE, Gonzalez EB, Maki W, Wu MT, Hwang ST. Expression of CC Chemokine Receptor-7 and Regional Lymph Node Metastasis of B16 Murine Melanoma. *J Natl Cancer Inst* (2001) 93(21):1638–43. doi: 10.1093/jnci/93.21.1638
11. Hauser MA, Legler DF. Common and Biased Signaling Pathways of the Chemokine Receptor CCR7 Elicited by its Ligands CCL19 and CCL21 in Leukocytes. *J Leukoc Biol* (2016) 99(6):869–82. doi: 10.1189/jlb.2MR0815-380R
12. Pui CH, Robison LL, Look AT. Acute Lymphoblastic Leukaemia. *Lancet* (2008) 371(9617):1030–43. doi: 10.1016/S0140-6736(08)60457-2
13. Lopez-Giral S, Quintana NE, Cabrerizo M, Alfonso-Perez M, Sala-Valdes M, De Soria VG, et al. Chemokine Receptors That Mediate B Cell Homing to Secondary Lymphoid Tissues Are Highly Expressed in B Cell Chronic Lymphocytic Leukemia and Non-Hodgkin Lymphomas With Widespread Nodular Dissemination. *J Leukoc Biol* (2004) 76(2):462–71. doi: 10.1189/jlb.1203652
14. Haferlach T, Kohlmann A, Wieczorek L, Basso G, Kronnie GT, Béné M-C, et al. Clinical Utility of Microarray-Based Gene Expression Profiling in the Diagnosis and Subclassification of Leukemia: Report From the International Microarray Innovations in Leukemia Study Group. *J Clin Oncol Off J Am Soc Clin Oncol* (2010) 28(15):2529–37. doi: 10.1200/JCO.2009.23.4732
15. Maia S, Haining WN, Ansén S, Xia Z, Armstrong SA, Seth NP, et al. Gene Expression Profiling Identifies BAX-Delta as a Novel Tumor Antigen in Acute Lymphoblastic Leukemia. *Cancer Res* (2005) 65(21):10050–8. doi: 10.1158/0008-5472.CAN-05-1574
16. Andersson A, Ritz C, Lindgren D, Edén P, Lassen C, Heldrup J, et al. Microarray-Based Classification of a Consecutive Series of 121 Childhood Acute Leukemias: Prediction of Leukemic and Genetic Subtype as Well as of Minimal Residual Disease Status. *Leukemia* (2007) 21(6):1198–203. doi: 10.1038/sj.leu.2404688
17. Coustan-Smith E, Song G, Clark C, Key L, Liu P, Mehrpooya M, et al. New Markers for Minimal Residual Disease Detection in Acute Lymphoblastic Leukemia. *Blood* (2011) 117(23):6267–76. doi: 10.1182/blood-2010-12-324004
18. Dürig J, Schmucker U, Duhrsen U. Differential Expression of Chemokine Receptors in B Cell Malignancies. *Leukemia* (2001) 15(5):752–6. doi: 10.1038/sj.leu.2402107
19. Wong S, Fulcher D. Chemokine Receptor Expression in B-Cell Lymphoproliferative Disorders. *Leuk Lymphoma* (2004) 45(12):2491–6. doi: 10.1080/10428190410001723449
20. Corcione A, Arduino N, Ferretti E, Pistorio A, Spinelli M, Ottonello L, et al. Chemokine Receptor Expression and Function in Childhood Acute Lymphoblastic Leukemia of B-Lineage. *Leuk Res* (2006) 30(4):365–72. doi: 10.1016/j.leukres.2005.07.009
21. Somovilla-Crespo B, Alfonso-Perez M, Cuesta-Mateos C, Carballo-de Dios C, Beltran AE, Terron F, et al. Anti-CCR7 Therapy Exerts a Potent Anti-Tumor Activity in a Xenograft Model of Human Mantle Cell Lymphoma. *J Hematol Oncol* (2013) 6:89. doi: 10.1186/1756-8722-6-89
22. D'Amico G, Vulcano M, Bugarin C, Bianchi G, Pirovano G, Bonamino M, et al. CD40 Activation of BCP-ALL Cells Generates IL-10-Producing, IL-12-Defective APCs That Induce Allogeneic T-Cell Anergy. *Blood* (2004) 104(3):744–51. doi: 10.1182/blood-2003-11-3762
23. Luczynski W, Ilendo E, Kovalchuk O, Krawczuk-Rybak M, Malinowska I, Koltan A, et al. Acute Lymphoblastic Leukaemia Cells Express CCR7 But Not Higher Amounts of IL-10 After CD40 Ligation. *Scand J Clin Lab Invest* (2006) 66(8):695–703. doi: 10.1080/00365510600931098
24. Alsadeq A, Fedders H, Vokuhl C, Belau NM, Zimmermann M, Wirbelauer T, et al. The Role of ZAP70 Kinase in Acute Lymphoblastic Leukemia

Infiltration Into the Central Nervous System. *Haematologica* (2017) 102 (2):346–55. doi: 10.3324/haematol.2016.147744
25. Buonamici S, Trimarchi T, Ruocco MG, Reavie L, Cathelin S, Mar BG, et al. CCR7 Signalling as an Essential Regulator of CNS Infiltration in T-Cell Leukaemia. *Nature* (2009) 459(7249):1000–4. doi: 10.1038/nature08020
26. Chunsong H, Yuling H, Li W, Jie X, Gang Z, Qiuping Z, et al. CXC Chemokine Ligand 13 and CC Chemokine Ligand 19 Cooperatively Render Resistance to Apoptosis in B Cell Lineage Acute and Chronic Lymphocytic Leukemia CD23+CD5+ B Cells. *J Immunol* (2006) 177(10):6713–22. doi: 10.4049/jimmunol.177.10.6713
27. Hu C, Xiong J, Zhang L, Huang B, Zhang Q, Li Q, et al. PEG10 Activation by Co-Stimulation of CXCR5 and CCR7 Essentially Contributes to Resistance to Apoptosis in CD19+CD34+ B Cells From Patients With B Cell Lineage Acute and Chronic Lymphocytic Leukemia. *Cell Mol Immunol* (2004) 1 (4):280–94.
28. Wang X, Yuling H, Yanping J, Xinti T, Yaofang Y, Feng Y, et al. CCL19 and CXCL13 Synergistically Regulate Interaction Between B Cell Acute Lymphocytic Leukemia CD23+CD5+ B Cells and CD8+ T Cells. *J Immunol (Baltimore Md 1950)* (2007) 179(5):2880–8. doi: 10.4049/jimmunol.179.5.2880
29. Hallek M, Cheson BD, Catovsky D, Caligaris-Cappio F, Dighiero G, Dohner H, et al. iwCLL Guidelines for Diagnosis, Indications for Treatment, Response Assessment, and Supportive Management of CLL. *Blood* (2018) 131(25):2745–60. doi: 10.1182/blood-2017-09-806398
30. Hayden RE, Pratt G, Roberts C, Drayson MT, Bunce CM. Treatment of Chronic Lymphocytic Leukemia Requires Targeting of the Protective Lymph Node Environment With Novel Therapeutic Approaches. *Leuk Lymphoma* (2012) 53(4):537–49. doi: 10.3109/10428194.2011.610014
31. Ponzoni M, Doglioni C, Caligaris-Cappio F. Chronic Lymphocytic Leukemia: The Pathologist's View of Lymph Node Microenvironment. *Semin Diagn Pathol* (2011) 28(2):161–6. doi: 10.1053/j.semdp.2011.02.014
32. Basso K, Margolin AA, Stolovitzky G, Klein U, Dalla-Favera R, Califano A. Reverse Engineering of Regulatory Networks in Human B Cells. *Nat Genet* (2005) 37(4):382–90. doi: 10.1038/ng1532
33. Rosenwald A, Wright G, Chan WC, Connors JM, Campo E, Fisher RI, et al. The Use of Molecular Profiling to Predict Survival After Chemotherapy for Diffuse Large-B-Cell Lymphoma. *N Engl J Med* (2002) 346(25):1937–47. doi: 10.1056/NEJMoa012914
34. Haslinger C, Schweifer N, Stilgenbauer S, Döhner H, Lichter P, Kraut N, et al. Microarray Gene Expression Profiling of B-Cell Chronic Lymphocytic Leukemia Subgroups Defined by Genomic Aberrations and VH Mutation Status. *J Clin Oncol Off J Am Soc Clin Oncol* (2004) 22(19):3937–49. doi: 10.1200/JCO.2004.12.133
35. Till KJ, Lin K, Zuzel M, Cawley JC. The Chemokine Receptor CCR7 and Alpha4 Integrin Are Important for Migration of Chronic Lymphocytic Leukemia Cells Into Lymph Nodes. *Blood* (2002) 99(8):2977–84. doi: 10.1182/blood.V99.8.2977
36. Ghobrial IM, Bone ND, Stenson MJ, Novak A, Hedin KE, Kay NE, et al. Expression of the Chemokine Receptors CXCR4 and CCR7 and Disease Progression in B-Cell Chronic Lymphocytic Leukemia/ Small Lymphocytic Lymphoma. *Mayo Clin Proc* (2004) 79(3):318–25. doi: 10.4065/79.3.318
37. Alfonso-Perez M, Lopez-Giral S, Quintana NE, Loscertales J, Martin-Jimenez P, Munoz C. Anti-CCR7 Monoclonal Antibodies as a Novel Tool for the Treatment of Chronic Lymphocyte Leukemia. *J Leukoc Biol* (2006) 79 (6):1157–65. doi: 10.1189/jlb.1105623
38. Richardson SJ, Matthews C, Catherwood MA, Alexander HD, Carey BS, Farrugia J, et al. ZAP-70 Expression is Associated With Enhanced Ability to Respond to Migratory and Survival Signals in B-Cell Chronic Lymphocytic Leukemia (B-CLL). *Blood* (2006) 107(9):3584–92. doi: 10.1182/blood-2005-04-1718
39. Calissano C, Damle RN, Hayes G, Murphy EJ, Hellerstein MK, Moreno C, et al. *In Vivo* Intraclonal and Interclonal Kinetic Heterogeneity in B-Cell Chronic Lymphocytic Leukemia. *Blood* (2009) 114(23):4832–42. doi: 10.1182/blood-2009-05-219634
40. Cuesta-Mateos C, Lopez-Giral S, Alfonso-Perez M, de Soria VG, Loscertales J, Guasch-Vidal S, et al. Analysis of Migratory and Prosurvival Pathways Induced by the Homeostatic Chemokines CCL19 and CCL21 in B-Cell Chronic Lymphocytic Leukemia. *Exp Hematol* (2010) 38(9):756–64, 64 e1-4. doi: 10.1016/j.exphem.2010.05.003
41. Calissano C, Damle RN, Marsilio S, Yan XJ, Yancopoulos S, Hayes G, et al. Intraclonal Complexity in Chronic Lymphocytic Leukemia: Fractions Enriched in Recently Born/Divided and Older/Quiescent Cells. *Mol Med* (2011) 17(11-12):1374–82. doi: 10.2119/molmed.2011.00360
42. Calpe E, Codony C, Baptista MJ, Abrisqueta P, Carpio C, Purroy N, et al. ZAP-70 Enhances Migration of Malignant B Lymphocytes Toward CCL21 by Inducing CCR7 Expression *via* IgM-ERK1/2 Activation. *Blood* (2011) 118 (16):4401–10. doi: 10.1182/blood-2011-01-333682
43. Capitani N, Patrussi L, Trentin L, Lucherini OM, Cannizzaro E, Migliaccio E, et al. S1P1 Expression is Controlled by the Pro-Oxidant Activity of p66Shc and is Impaired in B-CLL Patients With Unfavorable Prognosis. *Blood* (2012) 120(22):4391–9. doi: 10.1182/blood-2012-04-425959
44. de Rooij MF, Kuil A, Geest CR, Eldering E, Chang BY, Buggy JJ, et al. The Clinically Active BTK Inhibitor PCI-32765 Targets B-Cell Receptor- and Chemokine-Controlled Adhesion and Migration in Chronic Lymphocytic Leukemia. *Blood* (2012) 119(11):2590–4. doi: 10.1182/blood-2011-11-390989
45. Cuesta-Mateos C, Loscertales J, Kreutzman A, Colom-Fernandez B, Portero-Sainz I, Perez-Villar JJ, et al. Preclinical Activity of Anti-CCR7 Immunotherapy in Patients With High-Risk Chronic Lymphocytic Leukemia. *Cancer Immunol Immunother* (2015) 64(6):665–76. doi: 10.1007/s00262-015-1670-z
46. Patrussi L, Capitani N, Martini V, Pizzi M, Trimarco V, Frezzato F, et al. Enhanced Chemokine Receptor Recycling and Impaired S1P1 Expression Promote Leukemic Cell Infiltration of Lymph Nodes in Chronic Lymphocytic Leukemia. *Cancer Res* (2015) 75(19):4153–63. doi: 10.1158/0008-5472.CAN-15-0986
47. Ganghammer S, Hutterer E, Hinterseer E, Brachtl G, Asslaber D, Krenn PW, et al. CXCL12-Induced VLA-4 Activation is Impaired in Trisomy 12 Chronic Lymphocytic Leukemia Cells: A Role for CCL21. *Oncotarget* (2015) 6(14):12048–60. doi: 10.18632/oncotarget.3660
48. Patrussi L, Capitani N, Cattaneo F, Manganaro N, Gamberucci A, Frezzato F, et al. p66Shc Deficiency Enhances CXCR4 and CCR7 Recycling in CLL B Cells by Facilitating Their Dephosphorylation-Dependent Release From Beta-Arrestin at Early Endosomes. *Oncogene* (2018) 37(11):1534–50. doi: 10.1038/s41388-017-0066-2
49. Enjuanes A, Benavente Y, Bosch F, Martin-Guerrero I, Colomer D, Perez-Alvarez S, et al. Genetic Variants in Apoptosis and Immunoregulation-Related Genes are Associated With Risk of Chronic Lymphocytic Leukemia. *Cancer Res* (2008) 68(24):10178–86. doi: 10.1158/0008-5472.CAN-08-2221
50. Chen Q, Zheng T, Lan Q, Lerro C, Zhao N, Qin Q, et al. Single-Nucleotide Polymorphisms in Genes Encoding for CC Chemokines Were Not Associated With the Risk of Non-Hodgkin Lymphoma. *Cancer Epidemiology Biomarkers Prev Publ Am Assoc Cancer Research cosponsored by Am Soc Prev Oncol* (2013) 22(7):1332–5. doi: 10.1158/1055-9965.EPI-13-0328
51. Arruga F, Gizdic B, Bologna C, Cignetto S, Buonincontri R, Serra S, et al. Mutations in NOTCH1 PEST Domain Orchestrate CCL19-Driven Homing of Chronic Lymphocytic Leukemia Cells by Modulating the Tumor Suppressor Gene DUSP22. *Leukemia* (2017) 31(9):1882–93. doi: 10.1038/leu.2016.383
52. Cattaneo F, Patrussi L, Capitani N, Frezzato F, D'Elios MM, Trentin L, et al. Expression of the p66Shc Protein Adaptor is Regulated by the Activator of Transcription STAT4 in Normal and Chronic Lymphocytic Leukemia B Cells. *Oncotarget* (2016) 7(35):57086–98. doi: 10.18632/oncotarget.10977
53. Kim SH, Gunst KV, Sarvetnick N. STAT4/6-Dependent Differential Regulation of Chemokine Receptors. *Clin Immunol* (2006) 118(2-3):250–7. doi: 10.1016/j.clim.2003.10.002
54. Wolf C, Garding A, Filarsky K, Bahlo J, Robrecht S, Becker N, et al. NFATC1 Activation by DNA Hypomethylation in Chronic Lymphocytic Leukemia Correlates With Clinical Staging and can be Inhibited by Ibrutinib. *Int J Cancer* (2017) 2017(18):31057. doi: 10.1002/ijc.31057
55. Macian F, Lopez-Rodriguez C, Rao A. Partners in Transcription: NFAT and AP-1. *Oncogene* (2001) 20(19):2476–89. doi: 10.1038/sj.onc.1204386
56. Rodriguez A, Martinez N, Camacho FI, Ruiz-Ballesteros E, Algara P, Garcia JF, et al. Variability in the Degree of Expression of Phosphorylated IkappaBalpha in Chronic Lymphocytic Leukemia Cases With Nodal Involvement. *Clin Cancer Res* (2004) 10(20):6796–806. doi: 10.1158/1078-0432.CCR-04-0753

57. Faguet GB. Chronic Lymphocytic Leukemia: An Updated Review. *J Clin Oncol* (1994) 12(9):1974–90. doi: 10.1200/JCO.1994.12.9.1974
58. Laufer JM, Lyck R, Legler DF. ZAP70 Expression Enhances Chemokine-Driven Chronic Lymphocytic Leukemia Cell Migration and Arrest by Valency Regulation of Integrins. *FASEB J* (2018) 32(9):4824–35. doi: 10.1096/fj.201701452RR
59. Till KJ, Harris RJ, Linford A, Spiller DG, Zuzel M, Cawley JC. Cell Motility in Chronic Lymphocytic Leukemia: Defective Rap1 and Alphalbeta2 Activation by Chemokine. *Cancer Res* (2008) 68(20):8429–36. doi: 10.1158/0008-5472.CAN-08-1758
60. Hartmann TN, Grabovsky V, Wang W, Desch P, Rubenzer G, Wollner S, et al. Circulating B-Cell Chronic Lymphocytic Leukemia Cells Display Impaired Migration to Lymph Nodes and Bone Marrow. *Cancer Res* (2009) 69(7):3121–30. doi: 10.1158/0008-5472.CAN-08-4136
61. Riches JC, O'Donovan CJ, Kingdon SJ, McClanahan F, Clear AJ, Neuberg DS, et al. Trisomy 12 Chronic Lymphocytic Leukemia Cells Exhibit Upregulation of Integrin Signaling That is Modulated by NOTCH1 Mutations. *Blood* (2014) 123(26):4101–10. doi: 10.1182/blood-2014-01-552307
62. Hutterer E, Asslaber D, Caldana C, Krenn PW, Zucchetto A, Gattei V, et al. CD18 (ITGB2) Expression in Chronic Lymphocytic Leukaemia is Regulated by DNA Methylation-Dependent and -Independent Mechanisms. *Br J haematology* (2015) 169(2):286–9. doi: 10.1111/bjh.13188
63. Hauser MA, Schaeuble K, Kindinger I, Impellizzieri D, Krueger WA, Hauck CR, et al. Inflammation-Induced CCR7 Oligomers Form Scaffolds to Integrate Distinct Signaling Pathways for Efficient Cell Migration. *Immunity* (2016) 44(1):59–72. doi: 10.1016/j.immuni.2015.12.010
64. Redondo-Munoz J, Jose Terol M, Garcia-Marco JA, Garcia-Pardo A. Matrix Metalloproteinase-9 is Up-Regulated by CCL21/CCR7 Interaction *via* Extracellular Signal-Regulated Kinase-1/2 Signaling and is Involved in CCL21-Driven B-Cell Chronic Lymphocytic Leukemia Cell Invasion and Migration. *Blood* (2008) 111(1):383–6. doi: 10.1182/blood-2007-08-107300
65. Zucchetto A, Cattarossi I, Nanni P, Zaina E, Prato G, Gilestro M, et al. Cluster Analysis of Immunophenotypic Data: The Example of Chronic Lymphocytic Leukemia. *Immunol Lett* (2011) 134(2):137–44. doi: 10.1016/j.imlet.2010.09.017
66. Zucchetto A, Caldana C, Benedetti D, Tissino E, Rossi FM, Hutterer E, et al. CD49d is Overexpressed by Trisomy 12 Chronic Lymphocytic Leukemia Cells: Evidence for a Methylation-Dependent Regulation Mechanism. *Blood* (2013) 122(19):3317–21. doi: 10.1182/blood-2013-06-507335
67. Brachtl G, Sahakyan K, Denk U, Girbl T, Alinger B, Hofbauer SW, et al. Differential Bone Marrow Homing Capacity of VLA-4 and CD38 High Expressing Chronic Lymphocytic Leukemia Cells. *PloS One* (2011) 6(8): e23758. doi: 10.1371/journal.pone.0023758
68. Girbl T, Hinterseer E, Grossinger EM, Asslaber D, Oberascher K, Weiss L, et al. CD40-Mediated Activation of Chronic Lymphocytic Leukemia Cells Promotes Their CD44-Dependent Adhesion to Hyaluronan and Restricts CCL21-Induced Motility. *Cancer Res* (2013) 73(2):561–70. doi: 10.1158/0008-5472.CAN-12-2749
69. Catusse J, Leick M, Groch M, Clark DJ, Buchner MV, Zirlik K, et al. Role of the Atypical Chemoattractant Receptor CRAM in Regulating CCL19 Induced CCR7 Responses in B-Cell Chronic Lymphocytic Leukemia. *Mol Cancer* (2010) 9:297. doi: 10.1186/1476-4598-9-297
70. Ticchioni M, Essafi M, Jeandel PY, Davi F, Cassuto JP, Deckert M, et al. Homeostatic Chemokines Increase Survival of B-Chronic Lymphocytic Leukemia Cells Through Inactivation of Transcription Factor FOXO3a. *Oncogene* (2007) 26(50):7081–91. doi: 10.1038/sj.onc.1210519
71. Pham TH, Okada T, Matloubian M, Lo CG, Cyster JG. S1P1 Receptor Signaling Overrides Retention Mediated by G Alpha I-Coupled Receptors to Promote T Cell Egress. *Immunity* (2008) 28(1):122–33. doi: 10.1016/j.immuni.2007.11.017
72. Borge M, Remes Lenicov F, Nannini PR, de los Rios Alicandu MM, Podaza E, Ceballos A, et al. The Expression of Sphingosine-1 Phosphate Receptor-1 in Chronic Lymphocytic Leukemia Cells is Impaired by Tumor Microenvironmental Signals and Enhanced by Piceatannol and R406. *J Immunol* (2014) 193(6):3165–74. doi: 10.4049/jimmunol.1400547
73. Cameron F, Sanford M. Ibrutinib: First Global Approval. *Drugs* (2014) 74 (2):263–71. doi: 10.1007/s40265-014-0178-8
74. Herrmann A, Hoster E, Zwingers T, Brittinger G, Engelhard M, Meusers P, et al. Improvement of Overall Survival in Advanced Stage Mantle Cell Lymphoma. *J Clin Oncol* (2009) 27(4):511–8. doi: 10.1200/JCO.2008.16.8435
75. Barista I, Romaguera JE, Cabanillas F. Mantle-Cell Lymphoma. *Lancet Oncol* (2001) 2(3):141–8. doi: 10.1016/S1470-2045(00)00255-2
76. Argatoff LH, Connors JM, Klasa RJ, Horsman DE, Gascoyne RD. Mantle Cell Lymphoma: A Clinicopathologic Study of 80 Cases. *Blood* (1997) 89 (6):2067–78. doi: 10.1182/blood.V89.6.2067
77. Perez-Galan P, Dreyling M, Wiestner A. Mantle Cell Lymphoma: Biology, Pathogenesis, and the Molecular Basis of Treatment in the Genomic Era. *Blood* (2011) 117(1):26–38. doi: 10.1182/blood-2010-04-189977
78. Corcione A, Arduino N, Ferretti E, Raffaghello L, Roncella S, Rossi D, et al. CCL19 and CXCL12 Trigger *In Vitro* Chemotaxis of Human Mantle Cell Lymphoma B Cells. *Clin Cancer Res* (2004) 10(3):964–71. doi: 10.1158/1078-0432.CCR-1182-3
79. Bryson MS. *The Role of Chemokines and Their Receptors in Non-Hodgkin's Lymphoma*. Glasgow, Scotland, United Kingdom: PhD Thesis University of Glasgow (2011).
80. Ek S, Hogerkorp CM, Dictor M, Ehinger M, Borrebaeck CA. Mantle Cell Lymphomas Express a Distinct Genetic Signature Affecting Lymphocyte Trafficking and Growth Regulation as Compared With Subpopulations of Normal Human B Cells. *Cancer Res* (2002) 62(15):4398–405.
81. Friedberg JW, Taylor MD, Cerhan JR, Flowers CR, Dillon H, Farber CM, et al. Follicular Lymphoma in the United States: First Report of the National LymphoCare Study. *J Clin Oncol* (2009) 27(8):1202–8. doi: 10.1200/JCO.2008.18.1495
82. Nugent A, Proia RL. The Role of G Protein-Coupled Receptors in Lymphoid Malignancies. *Cell Signal* (2017) 39:95–107. doi: 10.1016/j.cellsig.2017.08.002
83. Bowman EP, Campbell JJ, Soler D, Dong Z, Manlongat N, Picarella D, et al. Developmental Switches in Chemokine Response Profiles During B Cell Differentiation and Maturation. *J Exp Med* (2000) 191(8):1303–18. doi: 10.1084/jem.191.8.1303
84. Brune V, Tiacci E, Pfeil I, Döring C, Eckerle S, van Noesel CJM, et al. Origin and Pathogenesis of Nodular Lymphocyte-Predominant Hodgkin Lymphoma as Revealed by Global Gene Expression Analysis. *J Exp Med* (2008) 205(10):2251–68. doi: 10.1084/jem.20080809
85. Compagno M, Lim WK, Grunn A, Nandula SV, Brahmachary M, Shen Q, et al. Mutations of Multiple Genes Cause Deregulation of NF-kappaB in Diffuse Large B-Cell Lymphoma. *Nature* (2009) 459(7247):717–21. doi: 10.1038/nature07968
86. Rosenwald A, Alizadeh AA, Widhopf G, Simon R, Davis RE, Yu X, et al. Relation of Gene Expression Phenotype to Immunoglobulin Mutation Genotype in B Cell Chronic Lymphocytic Leukemia. *J Exp Med* (2001) 194(11):1639–47. doi: 10.1084/jem.194.11.1639
87. Storz MN, van de Rijn M, Kim YH, Mraz-Gernhard S, Hoppe RT, Kohler S. Gene Expression Profiles of Cutaneous B Cell Lymphoma. *J Invest Dermatol* (2003) 120(5):865–70. doi: 10.1046/j.1523-1747.2003.12142.x
88. Braza MS, Caraux A, Rousset T, Lafaye de Micheaux S, Sicard H, Squiban P, et al. Gammadelta T Lymphocytes Count is Normal and Expandable in Peripheral Blood of Patients With Follicular Lymphoma, Whereas it is Decreased in Tumor Lymph Nodes Compared With Inflammatory Lymph Nodes. *J Immunol (Baltimore Md 1950)* (2010) 184(1):134–40. doi: 10.4049/jimmunol.0901980
89. Maier S, Santak M, Mantik A, Grabusic K, Kremmer E, Hammerschmidt W, et al. A Somatic Knockout of CBF1 in a Human B-Cell Line Reveals That Induction of CD21 and CCR7 by EBNA-2 is Strictly CBF1 Dependent and That Downregulation of Immunoglobulin M is Partially CBF1 Independent. *J Virol* (2005) 79(14):8784–92. doi: 10.1128/JVI.79.14.8784-8792.2005
90. Zabel BA, Lewén S, Berahovich RD, Jaén JC, Schall TJ. The Novel Chemokine Receptor CXCR7 Regulates Trans-Endothelial Migration of Cancer Cells. *Mol Cancer* (2011) 10:73. doi: 10.1186/1476-4598-10-73
91. Wu L, Ehlin-Henriksson B, Zhou X, Zhu H, Ernberg I, Kis LL, et al. Epstein-Barr Virus (EBV) Provides Survival Factors to EBV(+) Diffuse Large B-Cell Lymphoma (DLBCL) Lines and Modulates Cytokine Induced Specific Chemotaxis in EBV(+) DLBCL. *Immunology* (2017) 152(4):562–73. doi: 10.1111/imm.12792
92. Alizadeh AA, Eisen MB, Davis RE, Ma C, Lossos IS, Rosenwald A, et al. Distinct Types of Diffuse Large B-Cell Lymphoma Identified by Gene

Expression Profiling. *Nature* (2000) 403(6769):503–11. doi: 10.1038/35000501
93. Du H, Zhang L, Li G, Liu W, Tang W, Zhang H, et al. CXCR4 and CCR7 Expression in Primary Nodal Diffuse Large B-Cell Lymphoma-A Clinical and Immunohistochemical Study. *Am J Med Sci* (2019) 357(4):302–10. doi: 10.1016/j.amjms.2019.01.008
94. Gebauer N, Künstner A, Ketzer J, Witte HM, Rausch T, Benes V, et al. Genomic Insights Into the Pathogenesis of Epstein-Barr Virus-Associated Diffuse Large B-Cell Lymphoma by Whole-Genome and Targeted Amplicon Sequencing. *Blood Cancer J* (2021) 11(5):102. doi: 10.1038/s41408-021-00493-5
95. Deutsch AJ, Aigelsreiter A, Steinbauer E, Fruhwirth M, Kerl H, Beham-Schmid C, et al. Distinct Signatures of B-Cell Homeostatic and Activation-Dependent Chemokine Receptors in the Development and Progression of Extragastric MALT Lymphomas. *J Pathol* (2008) 215(4):431–44. doi: 10.1002/path.2372
96. Deutsch AJ, Steinbauer E, Hofmann NA, Strunk D, Gerlza T, Beham-Schmid C, et al. Chemokine Receptors in Gastric MALT Lymphoma: Loss of CXCR4 and Upregulation of CXCR7 is Associated With Progression to Diffuse Large B-Cell Lymphoma. *Mod Pathol* (2013) 26(2):182–94. doi: 10.1038/modpathol.2012.134
97. Kocks JR, Adler H, Danzer H, Hoffmann K, Jonigk D, Lehmann U, et al. Chemokine Receptor CCR7 Contributes to a Rapid and Efficient Clearance of Lytic Murine Gamma-Herpes Virus 68 From the Lung, Whereas Bronchus-Associated Lymphoid Tissue Harbors Virus During Latency. *J Immunol* (2009) 182(11):6861–9. doi: 10.4049/jimmunol.0801826
98. Kasuya A, Fujiyama T, Shirahama S, Hashizume H, Tokura Y. Decreased Expression of Homeostatic Chemokine Receptors in Intravascular Large B-Cell Lymphoma. *Eur J Dermatol* (2012) 22(2):272–3. doi: 10.1684/ejd.2012.1639
99. Rehm A, Anagnostopoulos I, Gerlach K, Broemer M, Scheidereit C, Johrens K, et al. Identification of a Chemokine Receptor Profile Characteristic for Mediastinal Large B-Cell Lymphoma. *Int J Cancer* (2009) 125(10):2367–74. doi: 10.1002/ijc.24652
100. Li S, Huang S, Peng SB. Overexpression of G Protein-Coupled Receptors in Cancer Cells: Involvement in Tumor Progression. *Int J Oncol* (2005) 27 (5):1329–39. doi: 10.3892/ijo.27.5.1329
101. Jahnke K, Coupland SE, Na IK, Loddenkemper C, Keilholz U, Korfel A, et al. Expression of the Chemokine Receptors CXCR4, CXCR5, and CCR7 in Primary Central Nervous System Lymphoma. *Blood* (2005) 106(1):384–5. doi: 10.1182/blood-2005-01-0324
102. Lemma SA, Pasanen AK, Haapasaari K-M, Sippola A, Sormunen R, Soini Y, et al. Similar Chemokine Receptor Profiles in Lymphomas With Central Nervous System Involvement - Possible Biomarkers for Patient Selection for Central Nervous System Prophylaxis, a Retrospective Study. *Eur J haematology* (2016) 96(5):492–501. doi: 10.1111/ejh.12626
103. Han CH, Batchelor TT. Diagnosis and Management of Primary Central Nervous System Lymphoma. *Cancer* (2017) 123(22):4314–24. doi: 10.1002/cncr.30965
104. O'Connor T, Zhou X, Kosla J, Adili A, Garcia Beccaria M, Kotsiliti E, et al. Age-Related Gliosis Promotes Central Nervous System Lymphoma Through CCL19-Mediated Tumor Cell Retention. *Cancer Cell* (2019) 36(3):250–67.e9. doi: 10.1016/j.ccell.2019.08.001
105. Barone F, Bombardieri M, Rosado MM, Morgan PR, Challacombe SJ, De Vita S, et al. CXCL13, CCL21, and CXCL12 Expression in Salivary Glands of Patients With Sjogren's Syndrome and MALT Lymphoma: Association With Reactive and Malignant Areas of Lymphoid Organization. *J Immunol (Baltimore Md 1950)* (2008) 180(7):5130–40. doi: 10.4049/jimmunol.180.7.5130
106. Grever MR, Blachly JS, Andritsos LA. Hairy Cell Leukemia: Update on Molecular Profiling and Therapeutic Advances. *Blood Rev* (2014) 28(5):197–203. doi: 10.1016/j.blre.2014.06.003
107. Basso K, Liso A, Tiacci E, Benedetti R, Pulsoni A, Foa R, et al. Gene Expression Profiling of Hairy Cell Leukemia Reveals a Phenotype Related to Memory B Cells With Altered Expression of Chemokine and Adhesion Receptors. *J Exp Med* (2004) 199(1):59–68. doi: 10.1084/jem.20031175
108. Agnelli L, Mosca L, Fabris S, Lionetti M, Andronache A, Kwee I, et al. A SNP Microarray and FISH-Based Procedure to Detect Allelic Imbalances in Multiple Myeloma: An Integrated Genomics Approach Reveals a Wide Gene Dosage Effect. *Genes Chromosomes Cancer* (2009) 48(7):603–14. doi: 10.1002/gcc.20668
109. Trentin L, Miorin M, Facco M, Baesso I, Carraro S, Cabrelle A, et al. Multiple Myeloma Plasma Cells Show Different Chemokine Receptor Profiles at Sites of Disease Activity. *Br J Haematol* (2007) 138(5):594–602. doi: 10.1111/j.1365-2141.2007.06686.x
110. Purdue MP, Lan Q, Menashe I, Zheng T, Zhang Y, Yeager M, et al. Variation in Innate Immunity Genes and Risk of Multiple Myeloma. *Hematol Oncol* (2011) 29(1):42–6. doi: 10.1002/hon.954
111. Zhan F, Hardin J, Kordsmeier B, Bumm K, Zheng M, Tian E, et al. Global Gene Expression Profiling of Multiple Myeloma, Monoclonal Gammopathy of Undetermined Significance, and Normal Bone Marrow Plasma Cells. *Blood* (2002) 99(5):1745–57. doi: 10.1182/blood.V99.5.1745
112. Zhan F, Barlogie B, Arzoumanian V, Huang Y, Williams DR, Hollmig K, et al. Gene-Expression Signature of Benign Monoclonal Gammopathy Evident in Multiple Myeloma is Linked to Good Prognosis. *Blood* (2007) 109(4):1692–700. doi: 10.1182/blood-2006-07-037077
113. Swerdlow SHC, E., Harris NL, Jaffe ES, Pileri SA, Stein H, Thiele J, et al. *WHO Classification of Tumours of Haematopoietic and Lymphoid Tissues. 4th ed* Vol. 2008. Geneva, Switzerland: World Health Organization (2008) p. 323–5.
114. Liu Y, Sattarzadeh A, Diepstra A, Visser L, van den Berg A. The Microenvironment in Classical Hodgkin Lymphoma: An Actively Shaped and Essential Tumor Component. *Semin Cancer Biol* (2014) 24:15–22. doi: 10.1016/j.semcancer.2013.07.002
115. Hopken UE, Foss HD, Meyer D, Hinz M, Leder K, Stein H, et al. Up-Regulation of the Chemokine Receptor CCR7 in Classical But Not in Lymphocyte-Predominant Hodgkin Disease Correlates With Distinct Dissemination of Neoplastic Cells in Lymphoid Organs. *Blood* (2002) 99 (4):1109–16. doi: 10.1182/blood.V99.4.1109
116. Eckerle S, Brune V, Döring C, Tiacci E, Bohle V, Sundström C, et al. Gene Expression Profiling of Isolated Tumour Cells From Anaplastic Large Cell Lymphomas: Insights Into its Cellular Origin, Pathogenesis and Relation to Hodgkin Lymphoma. *Leukemia* (2009) 23(11):2129–38. doi: 10.1038/leu.2009.161
117. Mathas S, Hinz M, Anagnostopoulos I, Krappmann D, Lietz A, Jundt F, et al. Aberrantly Expressed C-Jun and JunB Are a Hallmark of Hodgkin Lymphoma Cells, Stimulate Proliferation and Synergize With NF-Kappa B. *EMBO J* (2002) 21(15):4104–13. doi: 10.1093/emboj/cdf389
118. Bleul CC, Wu L, Hoxie JA, Springer TA, Mackay CR. The HIV Coreceptors CXCR4 and CCR5 Are Differentially Expressed and Regulated on Human T Lymphocytes. *Proc Natl Acad Sci USA* (1997) 94(5):1925–30. doi: 10.1073/pnas.94.5.1925
119. Linke F, Harenberg M, Nietert MM, Zaunig S, von Bonin F, Arlt A, et al. Microenvironmental Interactions Between Endothelial and Lymphoma Cells: A Role for the Canonical WNT Pathway in Hodgkin Lymphoma. *Leukemia* (2017) 31(2):361–72. doi: 10.1038/leu.2016.232
120. Zhong Z, Yu J, Virshup DM, Madan B. Wnts and the Hallmarks of Cancer. *Cancer Metastasis Rev* (2020) 39(3):625–45. doi: 10.1007/s10555-020-09887-6
121. Machado L, Jarrett R, Morgan S, Murray P, Hunter B, Hamilton E, et al. Expression and Function of T Cell Homing Molecules in Hodgkin's Lymphoma. *Cancer Immunol Immunother* (2009) 58(1):85–94. doi: 10.1007/s00262-008-0528-z
122. Atayar C, Poppema S, Visser L, van den Berg A. Cytokine Gene Expression Profile Distinguishes CD4+/CD57+ T Cells of the Nodular Lymphocyte Predominance Type of Hodgkin's Lymphoma From Their Tonsillar Counterparts. *J Pathol* (2006) 208(3):423–30. doi: 10.1002/path.1894
123. Bosler DS, Douglas-Nikitin VK, Harris VN, Smith MD. Detection of T-Regulatory Cells has a Potential Role in the Diagnosis of Classical Hodgkin Lymphoma. *Cytometry B Clin Cytom* (2008) 74(4):227–35. doi: 10.1002/cyto.b.20407
124. Quesada AE, Assylbekova B, Jabcuga CE, Zhang R, Covinsky M, Rios A, et al. Expression of Sirt1 and FoxP3 in Classical Hodgkin Lymphoma and Tumor Infiltrating Lymphocytes: Implications for Immune Dysregulation, Prognosis and Potential Therapeutic Targeting. *Int J Clin Exp Pathol* (2015) 8(10):13241–8.

125. Greaves P, Clear A, Owen A, Iqbal S, Lee A, Matthews J, et al. Defining Characteristics of Classical Hodgkin Lymphoma Microenvironment T-Helper Cells. *Blood* (2013) 122(16):2856–63. doi: 10.1182/blood-2013-06-508044
126. Wu R, Sattarzadeh A, Rutgers B, Diepstra A, van den Berg A, Visser L. The Microenvironment of Classical Hodgkin Lymphoma: Heterogeneity by Epstein-Barr Virus Presence and Location Within the Tumor. *Blood Cancer J* (2016) 6:e417. doi: 10.1038/bcj.2016.26
127. Visser L, Wu R, Rutgers B, Diepstra A, van den Berg A. Characterization of the Microenvironment of Nodular Lymphocyte Predominant Hodgkin Lymphoma. *Int J Mol Sci* (2016) 17(12):pii:E2127. doi: 10.3390/ijms17122127
128. Moura J, Rodrigues J, Santos AH, Teixeira Mdos A, Queiros ML, Santos M, et al. Chemokine Receptor Repertoire Reflects Mature T-Cell Lymphoproliferative Disorder Clinical Presentation. *Blood Cells Mol Dis* (2009) 42(1):57–63. doi: 10.1016/j.bcmd.2008.08.002
129. Foucar K. Mature T-Cell Leukemias Including T-Prolymphocytic Leukemia, Adult T-Cell Leukemia/Lymphoma, and Sezary Syndrome. *Am J Clin Pathol* (2007) 127(4):496–510. doi: 10.1309/KWJYBCCGTB90B6AE
130. Cuesta-Mateos C, Fuentes P, Schrader A, Juárez-Sánchez R, Loscertales J, Mateu-Albero T, et al. CCR7 as a Novel Therapeutic Target in T-Cell PROLYMPHOCYTIC Leukemia. *Biomark Res* (2020) 8:54. doi: 10.1186/s40364-020-00234-z
131. Aifantis I, Raetz E, Buonamici S. Molecular Pathogenesis of T-Cell Leukaemia and Lymphoma. *Nat Rev Immunol* (2008) 8(5):380–90. doi: 10.1038/nri2304
132. Pui CH, Howard SC. Current Management and Challenges of Malignant Disease in the CNS in Paediatric Leukaemia. *Lancet Oncol* (2008) 9(3):257–68. doi: 10.1016/S1470-2045(08)70070-6
133. Lee K, Nam KT, Cho SH, Gudapati P, Hwang Y, Park D-S, et al. Vital Roles of mTOR Complex 2 in Notch-Driven Thymocyte Differentiation and Leukemia. *J Exp Med* (2012) 209(4):713–28. doi: 10.1084/jem.20111470
134. Ma S, Shi Y, Pang Y, Dong F, Cheng H, Hao S, et al. Notch1-Induced T Cell Leukemia can be Potentiated by Microenvironmental Cues in the Spleen. *J Hematol Oncol* (2014) 7:71. doi: 10.1186/s13045-014-0071-7
135. Jost TR, Borga C, Radaelli E, Romagnani A, Perruzza L, Omodho L, et al. Role of CXCR4-Mediated Bone Marrow Colonization in CNS Infiltration by T Cell Acute Lymphoblastic Leukemia. *J Leukoc Biol* (2016) 99(6):1077–87. doi: 10.1189/jlb.5MA0915-394R
136. Matutes E, Brito-Babapulle V, Swansbury J, Ellis J, Morilla R, Dearden C, et al. Clinical and Laboratory Features of 78 Cases of T-Prolymphocytic Leukemia. *Blood* (1991) 78(12):3269–74. doi: 10.1182/blood.V78.12.3269.3269
137. Dearden C. How I Treat Prolymphocytic Leukemia. *Blood* (2012) 120 (3):538–51. doi: 10.1182/blood-2012-01-380139
138. Bellone M, Svensson AM, Zaslav AL, Spitzer S, Golightly M, Celiker M, et al. Pediatric T-Cell Prolymphocytic Leukemia With an Isolated 12(P13) Deletion and Aberrant CD117 Expression. *Exp Hematol Oncol* (2012) 1 (1):7. doi: 10.1186/2162-3619-1-7
139. Hopfinger G, Busch R, Pflug N, Weit N, Westermann A, Fink AM, et al. Sequential Chemoimmunotherapy of Fludarabine, Mitoxantrone, and Cyclophosphamide Induction Followed by Alemtuzumab Consolidation is Effective in T-Cell Prolymphocytic Leukemia. *Cancer* (2013) 119(12):2258–67. doi: 10.1002/cncr.27972
140. Ravandi F, O'Brien S, Jones D, Lerner S, Faderl S, Ferrajoli A, et al. T-Cell Prolymphocytic Leukemia: A Single-Institution Experience. *Clin Lymphoma myeloma* (2005) 6(3):234–9. doi: 10.3816/CLM.2005.n.051
141. Herling M, Khoury JD, Washington LT, Duvic M, Keating MJ, Jones D. A Systematic Approach to Diagnosis of Mature T-Cell Leukemias Reveals Heterogeneity Among WHO Categories. *Blood* (2004) 104(2):328–35. doi: 10.1182/blood-2004-01-0002
142. Bennett JM, Catovsky D, Daniel MT, Flandrin G, Galton DA, Gralnick HR, et al. Proposals for the Classification of Chronic (Mature) B and T Lymphoid Leukaemias. French-American-British (FAB) Cooperative Group. *J Clin Pathol* (1989) 42(6):567–84. doi: 10.1136/jcp.42.6.567
143. Schrader A, Crispatzu G, Oberbeck S, Mayer P, Putzer S, von Jan J, et al. Actionable Perturbations of Damage Responses by TCL1/ATM and Epigenetic Lesions Form the Basis of T-PLL. *Nat Commun* (2018) 9 (1):697. doi: 10.1038/s41467-017-02688-6
144. Dürig J, Bug S, Klein-Hitpass L, Boes T, Jöns T, Martin-Subero JI, et al. Combined Single Nucleotide Polymorphism-Based Genomic Mapping and Global Gene Expression Profiling Identifies Novel Chromosomal Imbalances, Mechanisms and Candidate Genes Important in the Pathogenesis of T-Cell Prolymphocytic Leukemia With Inv(14)(Q11q32). *Leukemia* (2007) 21(10):2153–63. doi: 10.1038/sj.leu.2404877
145. Oberbeck S, Schrader A, Warner K, Jungherz D, Crispatzu G, von Jan J, et al. Non-Canonical Effector Functions of the T-Memory-Like T-PLL Cell Are Shaped by Cooperative TCL1A and TCR Signaling. *Blood* (2020) 107 (10):2786–08. doi: 10.1182/blood.2019003348
146. Despouy G, Joiner M, Le Toriellec E, Weil R, Stern MH. The TCL1 Oncoprotein Inhibits Activation-Induced Cell Death by Impairing PKCtheta and ERK Pathways. *Blood* (2007) 110(13):4406–16. doi: 10.1182/blood-2006-11-059501
147. Herling M, Patel KA, Teitell MA, Konopleva M, Ravandi F, Kobayashi R, et al. High TCL1 Expression and Intact T-Cell Receptor Signaling Define a Hyperproliferative Subset of T-Cell Prolymphocytic Leukemia. *Blood* (2008) 111(1):328–37. doi: 10.1182/blood-2007-07-101519
148. Graham RL, Cooper B, Krause JR. T-Cell Prolymphocytic Leukemia. *Proc (Bayl Univ Med Cent)* (2013) 26(1):19–21. doi: 10.1080/08998280.2013.11928902
149. Iwanaga M, Watanabe T, Yamaguchi K. Adult T-Cell Leukemia: A Review of Epidemiological Evidence. *Front Microbiol* (2012) 3:322. doi: 10.3389/fmicb.2012.00322
150. Ishitsuka K, Tamura K. Human T-Cell Leukaemia Virus Type I and Adult T-Cell Leukaemia-Lymphoma. *Lancet Oncol* (2014) 15(11):e517–26. doi: 10.1016/S470-2045(14)70202-5[doi]LID-S1470-2045(14)-5[pii
151. Katsuya H, Ishitsuka K, Utsunomiya A, Hanada S, Eto T, Moriuchi Y, et al. Treatment and Survival Among 1594 Patients With ATL. *Blood* (2015) 126 (24):2570–7. doi: 10.1182/blood-2015-03-632489
152. Watanabe T. Adult T-Cell Leukemia: Molecular Basis for Clonal Expansion and Transformation of HTLV-1-Infected T Cells. *Blood* (2017) 129(9):1071–81. doi: 10.1182/blood-2016-09-692574
153. Dahmoush L, Hijazi Y, Barnes E, Stetler-Stevenson M, Abati A. Adult T-Cell Leukemia/Lymphoma: A Cytopathologic, Immunocytochemical, and Flow Cytometric Study. *Cancer* (2002) 96(2):110–6. doi: 10.1002/cncr.10480
154. Kagdi HH, Demontis MA, Fields PA, Ramos JC, Bangham CR, Taylor GP. Risk Stratification of Adult T-Cell Leukemia/Lymphoma Using Immunophenotyping. *Cancer Med* (2017) 6(1):298–309. doi: 10.1002/cam4.928
155. Yoshie O, Fujisawa R, Nakayama T, Harasawa H, Tago H, Izawa D, et al. Frequent Expression of CCR4 in Adult T-Cell Leukemia and Human T-Cell Leukemia Virus Type 1-Transformed T Cells. *Blood* (2002) 99(5):1505–11. doi: 10.1182/blood.V99.5.1505
156. Toulza F, Nosaka K, Takiguchi M, Pagliuca T, Mitsuya H, Tanaka Y, et al. FoxP3+ Regulatory T Cells Are Distinct From Leukemia Cells in HTLV-1-Associated Adult T-Cell Leukemia. *Int J Cancer* (2009) 125(10):2375–82. doi: 10.1002/ijc.24664
157. Hasegawa H, Nomura T, Kohno M, Tateishi N, Suzuki Y, Maeda N, et al. Increased Chemokine Receptor CCR7/EBI1 Expression Enhances the Infiltration of Lymphoid Organs by Adult T-Cell Leukemia Cells. *Blood* (2000) 95(1):30–8. doi: 10.1182/blood.V95.1.30.001k09_30_38
158. Kohno T, Moriuchi R, Katamine S, Yamada Y, Tomonaga M, Matsuyama T. Identification of Genes Associated With the Progression of Adult T Cell Leukemia (ATL). *Jpn J Cancer Res* (2000) 91(11):1103–10. doi: 10.1111/j.1349-7006.2000.tb00892.x
159. Choi YL, Tsukasaki K, O'Neill MC, Yamada Y, Onimaru Y, Matsumoto K, et al. A Genomic Analysis of Adult T-Cell Leukemia. *Oncogene* (2007) 26 (8):1245–55. doi: 10.1038/sj.onc.1209898
160. Harasawa H, Yamada Y, Hieshima K, Jin Z, Nakayama T, Yoshie O, et al. Survey of Chemokine Receptor Expression Reveals Frequent Co-Expression of Skin-Homing CCR4 and CCR10 in Adult T-Cell Leukemia/Lymphoma. *Leuk Lymphoma* (2006) 47(10):2163–73. doi: 10.1080/10428190600775599
161. Hashikawa K, Yasumoto S, Nakashima K, Arakawa F, Kiyasu J, Kimura Y, et al. Microarray Analysis of Gene Expression by Microdissected Epidermis and Dermis in Mycosis Fungoides and Adult T-Cell Leukemia/Lymphoma. *Int J Oncol* (2014) 45(3):1200–8. doi: 10.3892/ijo.2014.2524

162. Kataoka K, Nagata Y, Kitanaka A, Shiraishi Y, Shimamura T, Yasunaga J, et al. Integrated Molecular Analysis of Adult T Cell Leukemia/Lymphoma. *Nat Genet* (2015) 47(11):1304–15. doi: 10.1038/ng.3415
163. Nakagawa M, Schmitz R, Xiao W, Goldman CK, Xu W, Yang Y, et al. Gain-Of-Function CCR4 Mutations in Adult T Cell Leukemia/Lymphoma. *J Exp Med* (2014) 211(13):2497–505. doi: 10.1084/jem.20140987
164. Sakihama S, Morichika K, Saito R, Miyara M, Miyagi T, Hayashi M, et al. Genetic Profile of Adult T-Cell Leukemia/Lymphoma in Okinawa: Association With Prognosis, Ethnicity, and HTLV-1 Strains. *Cancer Sci* (2021) 112(3):1300–9. doi: 10.1111/cas.14806
165. Kallinich T, Muche JM, Qin S, Sterry W, Audring H, Kroczek RA. Chemokine Receptor Expression on Neoplastic and Reactive T Cells in the Skin at Different Stages of Mycosis Fungoides. *J Invest Dermatol* (2003) 121 (5):1045–52. doi: 10.1046/j.1523-1747.2003.12555.x
166. Scarisbrick JJ, Prince HM, Vermeer MH, Quaglino P, Horwitz S, Porcu P, et al. Cutaneous Lymphoma International Consortium Study of Outcome in Advanced Stages of Mycosis Fungoides and Sézary Syndrome: Effect of Specific Prognostic Markers on Survival and Development of a Prognostic Model. *J Clin Oncol Off J Am Soc Clin Oncol* (2015) 33(32):3766–73. doi: 10.1200/JCO.2015.61.7142
167. Olsen EA, Whittaker S, Kim YH, Duvic M, Prince HM, Lessin SR, et al. Clinical End Points and Response Criteria in Mycosis Fungoides and Sézary Syndrome: A Consensus Statement of the International Society for Cutaneous Lymphomas, the United States Cutaneous Lymphoma Consortium, and the Cutaneous Lymphoma Task Force of the European Organisation for Research and Treatment of Cancer. *J Clin Oncol Off J Am Soc Clin Oncol* (2011) 29(18):2598–607. doi: 10.1200/JCO.2010.32.0630
168. Wilcox RA. Cutaneous T-Cell Lymphoma: 2017 Update on Diagnosis, Risk-Stratification, and Management. *Am J Hematol* (2017) 92(10):1085–102. doi: 10.1002/ajh.24876
169. Cristofoletti C, Bresin A, Picozza M, Picchio MC, Monzo F, Helmer Citterich M, et al. Blood and Skin-Derived Sezary Cells: Differences in Proliferation-Index, Activation of PI3K/AKT/mTORC1 Pathway and its Prognostic Relevance. *Leukemia* (2019) 33(5):1231–42. doi: 10.1038/s41375-018-0305-8
170. Geskin LJ, Viragova S, Stolz DB, Fuschiotti P. Interleukin-13 is Overexpressed in Cutaneous T-Cell Lymphoma Cells and Regulates Their Proliferation. *Blood* (2015) 125(18):2798–805. doi: 10.1182/blood-2014-07-590398
171. Wang T, Lu Y, Polk A, Chowdhury P, Murga-Zamalloa C, Fujiwara H, et al. T-Cell Receptor Signaling Activates an ITK/NF-κb/GATA-3 Axis in T-Cell Lymphomas Facilitating Resistance to Chemotherapy. *Clin Cancer Res an Off J Am Assoc Cancer Res* (2017) 23(10):2506–15. doi: 10.1158/1078-0432.CCR-16-1996
172. Rindler K, Bauer WM, Jonak C, Wielscher M, Shaw LE, Rojahn TB, et al. Single-Cell RNA Sequencing Reveals Tissue Compartment-Specific Plasticity of Mycosis Fungoides Tumor Cells. *Front Immunol* (2021) 12:666935. doi: 10.3389/fimmu.2021.666935
173. Hu SC, Lin CL, Hong CH, Yu HS, Chen GS, Lee CH. CCR7 Expression Correlates With Subcutaneous Involvement in Mycosis Fungoides Skin Lesions and Promotes Migration of Mycosis Fungoides Cells (MyLa) Through mTOR Activation. *J Dermatol Sci* (2016) 74(1):31–8. doi: 10.1016/j.jdermsci.2013.12.003
174. Hong C-H, Lin S-H, Lee C-H. CCL21 Induces mTOR-Dependent MALAT1 Expression, Leading to Cell Migration in Cutaneous T-Cell Lymphoma. *In Vivo (Athens Greece)* (2019) 33(3):793–800. doi: 10.21873/invivo.11541
175. Zhou Y, Xu X, Lv H, Wen Q, Li J, Tan L, et al. The Long Noncoding RNA MALAT-1 Is Highly Expressed in Ovarian Cancer and Induces Cell Growth and Migration. *PloS One* (2016) 11(5):e0155250. doi: 10.1371/journal.pone.0155250
176. Shin J, Monti S, Aires DJ, Duvic M, Golub T, Jones DA, et al. Lesional Gene Expression Profiling in Cutaneous T-Cell Lymphoma Reveals Natural Clusters Associated With Disease Outcome. *Blood* (2007) 110(8):3015–27. doi: 10.1182/blood-2006-12-061507
177. van Doorn R, van Kester MS, Dijkman R, Vermeer MH, Mulder AA, Szuhai K, et al. Oncogenomic Analysis of Mycosis Fungoides Reveals Major Differences With Sezary Syndrome. *Blood* (2009) 113(1):127–36. doi: 10.1182/blood-2008-04-153031
178. Campbell JJ, Clark RA, Watanabe R, Kupper TS. Sezary Syndrome and Mycosis Fungoides Arise From Distinct T-Cell Subsets: A Biologic Rationale for Their Distinct Clinical Behaviors. *Blood* (2010) 116(5):767–71. doi: 10.1182/blood-2009-11-251926
179. Capriotti E, Vonderheid EC, Thoburn CJ, Bright EC, Hess AD. Chemokine Receptor Expression by Leukemic T Cells of Cutaneous T-Cell Lymphoma: Clinical and Histopathological Correlations. *J Invest Dermatol* (2007) 127 (12):2882–92. doi: 10.1038/sj.jid.5700916
180. Morice WG, Katzmann JA, Pittelkow MR, el-Azhary RA, Gibson LE, Hanson CA. A Comparison of Morphologic Features, Flow Cytometry, TCR-Vbeta Analysis, and TCR-PCR in Qualitative and Quantitative Assessment of Peripheral Blood Involvement by Sezary Syndrome. *Am J Clin Pathol* (2006) 125(3):364–74. doi: 10.1309/25E9Y7RRAY84HTAT
181. Sokolowska-Wojdylo M, Wenzel J, Gaffal E, Lenz J, Speuser P, Erdmann S, et al. Circulating Clonal CLA(+) and CD4(+) T Cells in Sezary Syndrome Express the Skin-Homing Chemokine Receptors CCR4 and CCR10 as Well as the Lymph Node-Homing Chemokine Receptor CCR7. *Br J Dermatol* (2005) 152(2):258–64. doi: 10.1111/j.1365-2133.2004.06325.x
182. Narducci MG, Scala E, Bresin A, Caprini E, Picchio MC, Remotti D, et al. Skin Homing of Sezary Cells Involves SDF-1-CXCR4 Signaling and Down-Regulation of CD26/dipeptidylpeptidase Iv. *Blood* (2006) 107(3):1108–15. doi: 10.1182/blood-2005-04-1492
183. Picchio MC, Scala E, Pomponi D, Caprini E, Frontani M, Angelucci I, et al. CXCL13 is Highly Produced by Sezary Cells and Enhances Their Migratory Ability *via* a Synergistic Mechanism Involving CCL19 and CCL21 Chemokines. *Cancer Res* (2008) 68(17):7137–46. doi: 10.1158/0008-5472.CAN-08-0602
184. Yang J, Wang S, Zhao G, Sun B. Effect of Chemokine Receptors CCR7 on Disseminated Behavior of Human T Cell Lymphoma: Clinical and Experimental Study. *J Exp Clin Cancer Res* (2011) 30:51. doi: 10.1186/1756-9966-30-51
185. Zeng H, Chi H. mTOR and Lymphocyte Metabolism. *Curr Opin Immunol* (2013) 25(3):347–55. doi: 10.1016/j.coi.2013.05.002
186. Lima M, Almeida J, Dos Anjos Teixeira M, Alguero Md Mdel C, Santos AH, Balanzategui A, et al. TCRalphabeta+/CD4+ Large Granular Lymphocytosis: A New Clonal T-Cell Lymphoproliferative Disorder. *Am J Pathol* (2003) 163 (2):763–71. doi: 10.1016/S0002-9440(10)63703-0
187. Wlodarski MW, Schade AE, Maciejewski JP. T-Large Granular Lymphocyte Leukemia: Current Molecular Concepts. *Hematology* (2006) 11(4):245–56. doi: 10.1080/10245330600774793
188. Caperton C, Agrawal S, Gupta S. Good Syndrome Presenting With $CD8^+$ T-Cell Large Granular Lymphocyte Leukemia. *Oncotarget* (2015) 6(34):36577–86. doi: 10.18632/oncotarget.5369
189. Lamant L, de Reynies A, Duplantier MM, Rickman DS, Sabourdy F, Giuriato S, et al. Gene-Expression Profiling of Systemic Anaplastic Large-Cell Lymphoma Reveals Differences Based on ALK Status and Two Distinct Morphologic ALK+ Subtypes. *Blood* (2007) 109(5):2156–64. doi: 10.1182/blood-2006-06-028969
190. Geissinger E, Bonzheim I, Krenacs L, Roth S, Reimer P, Wilhelm M, et al. Nodal Peripheral T-Cell Lymphomas Correspond to Distinct Mature T-Cell Populations. *J Pathol* (2006) 210(2):172–80. doi: 10.1002/path.2046
191. Piccaluga PP, Agostinelli C, Califano A, Rossi M, Basso K, Zupo S, et al. Gene Expression Analysis of Peripheral T Cell Lymphoma, Unspecified, Reveals Distinct Profiles and New Potential Therapeutic Targets. *J Clin Invest* (2007) 117(3):823–34. doi: 10.1172/JCI26833
192. Suzuki R, Suzumiya J, Nakamura S, Aoki S, Notoya A, Ozaki S, et al. Aggressive Natural Killer-Cell Leukemia Revisited: Large Granular Lymphocyte Leukemia of Cytotoxic NK Cells. *Leukemia* (2004) 18(4):763–70. doi: 10.1038/sj.leu.2403262
193. Makishima H, Ito T, Asano N, Nakazawa H, Shimodaira S, Kamijo Y, et al. Significance of Chemokine Receptor Expression in Aggressive NK Cell Leukemia. *Leukemia* (2005) 19(7):1169–74. doi: 10.1038/sj.leu.2403732
194. Sand KE, Rye KP, Mannsåker B, Bruserud O, Kittang AO. Expression Patterns of Chemokine Receptors on Circulating T Cells From Myelodysplastic Syndrome Patients. *Oncoimmunology* (2013) 2(2):e23138. doi: 10.4161/onci.23138
195. Voso MT, Ottone T, Lavorgna S, Venditti A, Maurillo L, Lo-Coco F, et al. MRD in AML: The Role of New Techniques. *Front Oncol* (2019) 9:655. doi: 10.3389/fonc.2019.00655
196. Stegmaier K, Ross KN, Colavito SA, O'Malley S, Stockwell BR, Golub TR. Gene Expression-Based High-Throughput Screening(GE-HTS) and

Application to Leukemia Differentiation. *Nat Genet* (2004) 36(3):257–63. doi: 10.1038/ng1305
197. Valk PJM, Verhaak RGW, Beijen MA, Erpelinck CAJ, Barjesteh van Waalwijk van Doorn-Khosrovani S, Boer JM, et al. Prognostically Useful Gene-Expression Profiles in Acute Myeloid Leukemia. *N Engl J Med* (2004) 350(16):1617–28. doi: 10.1056/NEJMoa040465
198. Maiga A, Lemieux S, Pabst C, Lavallée VP, Bouvier M, Sauvageau G, et al. Transcriptome Analysis of G Protein-Coupled Receptors in Distinct Genetic Subgroups of Acute Myeloid Leukemia: Identification of Potential Disease-Specific Targets. *Blood Cancer J* (2016) 6(6):e431. doi: 10.1038/bcj.2016.36
199. Falcone U, Sibai H, Deotare U. A Critical Review of Treatment Modalities for Blastic Plasmacytoid Dendritic Cell Neoplasm. *Crit Rev Oncol/Hematol* (2016) 107:156–62. doi: 10.1016/j.critrevonc.2016.09.003
200. Bendriss-Vermare N, Chaperot L, Peoc'h M, Vanbervliet B, Jacob MC, Briere F, et al. *In Situ* Leukemic Plasmacytoid Dendritic Cells Pattern of Chemokine Receptors Expression and *In Vitro* Migratory Response. *Leukemia* (2004) 18 (9):1491–8. doi: 10.1038/sj.leu.2403452
201. Hogstad B, Berres M-L, Chakraborty R, Tang J, Bigenwald C, Serasinghe M, et al. RAF/MEK/extracellular Signal-Related Kinase Pathway Suppresses Dendritic Cell Migration and Traps Dendritic Cells in Langerhans Cell Histiocytosis Lesions. *J Exp Med* (2018) 215(1):319–36. doi: 10.1084/jem.20161881
202. Hehlmann R. Chronic Myeloid Leukemia in 2020. *Hemasphere* (2020) 4(5): e468. doi: 10.1097/HS9.0000000000000468
203. Kubo K, Iwakami M, Muromoto R, Inagaki T, Kitai Y, Kon S, et al. CCR7 is Involved in BCR-ABL/STAP-2-Mediated Cell Growth in Hematopoietic Ba/F3 Cells. *Biochem Biophys Res Commun* (2015) 463(4):825–31. doi: 10.1016/j.bbrc.2015.06.020
204. Sekine Y, Ikeda O, Mizushima A, Ueno Y, Muromoto R, Yoshimura A, et al. STAP-2 Interacts With and Modulates BCR-ABL-Mediated Tumorigenesis. *Oncogene* (2012) 31(40):4384–96. doi: 10.1038/onc.2011.604
205. Jongen-Lavrencic M, Salesse S, Delwel R, Verfaillie CM. BCR/ABL-Mediated Downregulation of Genes Implicated in Cell Adhesion and Motility Leads to Impaired Migration Toward CCR7 Ligands CCL19 and CCL21 in Primary BCR/ABL-Positive Cells. *Leukemia* (2005) 19(3):373–80. doi: 10.1038/sj.leu.2403626
206. Ben-Baruch A. Organ Selectivity in Metastasis: Regulation by Chemokines and Their Receptors. *Clin Exp Metastasis* (2008) 25(4):345–56. doi: 10.1007/s10585-007-9097-3
207. Swerdlow SH, Campo E, Pileri SA, Harris NL, Stein H, Siebert R, et al. The 2016 Revision of the World Health Organization Classification of Lymphoid Neoplasms. *Blood* (2016) 127(20):2375–90. doi: 10.1182/blood-2016-01-643569
208. D'Amico G, Frascaroli G, Bianchi G, Transidico P, Doni A, Vecchi A, et al. Uncoupling of Inflammatory Chemokine Receptors by IL-10: Generation of Functional Decoys. *Nat Immunol* (2000) 1(5):387–91. doi: 10.1038/80819
209. Luczynski W, Stasiak-Barmuta A, Piszcz J, Ilendo E, Kowalczuk O, Krawczuk-Rybak M. B-Cell Chronic Lymphocytic Leukemia-Derived Dendritic Cells Stimulate Allogeneic T-Cell Response and Express Chemokines Involved in T-Cell Migration. *Neoplasma* (2007) 54(6):527–35.
210. Xie P, Kraus ZJ, Stunz LL, Bishop GA. Roles of TRAF Molecules in B Lymphocyte Function. *Cytokine Growth Factor Rev* (2008) 19(3-4):199–207. doi: 10.1016/j.cytogfr.2008.04.002
211. Pei L, Choi JH, Liu J, Lee EJ, McCarthy B, Wilson JM, et al. Genome-Wide DNA Methylation Analysis Reveals Novel Epigenetic Changes in Chronic Lymphocytic Leukemia. *Epigenetics* (2012) 7(6):567–78. doi: 10.4161/epi.20237
212. Yan Y, Chen R, Wang X, Hu K, Huang L, Lu M, et al. CCL19 and CCR7 Expression, Signaling Pathways, and Adjuvant Functions in Viral Infection and Prevention. *Front Cell Dev Biol* (2019) 7:212. doi: 10.3389/fcell.2019.00212
213. Ehlin-Henriksson B, Liang W, Cagigi A, Mowafi F, Klein G, Nilsson A. Changes in Chemokines and Chemokine Receptor Expression on Tonsillar B Cells Upon Epstein-Barr Virus Infection. *Immunology* (2009) 127(4):549–57. doi: 10.1111/j.1365-2567.2008.03029.x
214. Potsch C, Vohringer D, Pircher H. Distinct Migration Patterns of Naive and Effector CD8 T Cells in the Spleen: Correlation With CCR7 Receptor Expression and Chemokine Reactivity. *Eur J Immunol* (1999) 29(11):3562–70. doi: 10.1002/(SICI)1521-4141(199911)29:11<3562::AID-IMMU3562>3.0.CO;2-R
215. Ramirez PW, Famiglietti M, Sowrirajan B, DePaula-Silva AB, Rodesch C, Barker E, et al. Downmodulation of CCR7 by HIV-1 Vpu Results in Impaired Migration and Chemotactic Signaling Within CD4+ T Cells. *Cell Rep* (2014) 7(6):2019–30. doi: 10.1016/j.celrep.2014.05.015
216. Debes GF, Bonhagen K, Wolff T, Kretschmer U, Krautwald S, Kamradt T, et al. CC Chemokine Receptor 7 Expression by Effector/Memory CD4+ T Cells Depends on Antigen Specificity and Tissue Localization During Influenza A Virus Infection. *J Virol* (2004) 78(14):7528–35. doi: 10.1128/JVI.78.14.7528-7535.2004
217. Hayasaka H, Kobayashi D, Yoshimura H, Nakayama EE, Shioda T, Miyasaka M. The HIV-1 Gp120/CXCR4 Axis Promotes CCR7 Ligand-Dependent CD4 T Cell Migration: CCR7 Homo- and CCR7/CXCR4 Hetero-Oligomer Formation as a Possible Mechanism for Up-Regulation of Functional CCR7. *PloS One* (2015) 10(2):e0117454. doi: 10.1371/journal.pone.0117454
218. Saleh S, Lu HK, Evans V, Harisson D, Zhou J, Jaworowski A, et al. HIV Integration and the Establishment of Latency in CCL19-Treated Resting CD4(+) T Cells Require Activation of NF-κb. *Retrovirology* (2016) 13(1):49. doi: 10.1186/s12977-016-0284-7
219. Spender LC, Lucchesi W, Bodelon G, Bilancio A, Karstegl CE, Asano T, et al. Cell Target Genes of Epstein-Barr Virus Transcription Factor EBNA-2: Induction of the P55alpha Regulatory Subunit of PI3-Kinase and its Role in Survival of EREB2.5 Cells. *J Gen Virol* (2006) 87(Pt 10):2859–67. doi: 10.1099/vir.0.82128-0
220. Nakayama T, Fujisawa R, Izawa D, Hieshima K, Takada K, Yoshie O. Human B Cells Immortalized With Epstein-Barr Virus Upregulate CCR6 and CCR10 and Downregulate CXCR4 and CXCR5. *J Virol* (2002) 76(6):3072–7. doi: 10.1128/JVI.76.6.3072-3077.2002
221. Hopken UE, Rehm A. Homeostatic Chemokines Guide Lymphoma Cells to Tumor Growth-Promoting Niches Within Secondary Lymphoid Organs. *J Mol Med (Berl)* (2012) 90(11):1237–45. doi: 10.1007/s00109-012-0906-z
222. Pals ST, de Gorter DJ, Spaargaren M. Lymphoma Dissemination: The Other Face of Lymphocyte Homing. *Blood* (2007) 110(9):3102–11. doi: 10.1182/blood-2007-05-075176
223. Link A, Vogt TK, Favre S, Britschgi MR, Acha-Orbea H, Hinz B, et al. Fibroblastic Reticular Cells in Lymph Nodes Regulate the Homeostasis of Naive T Cells. *Nat Immunol* (2007) 8(11):1255–65. doi: 10.1038/ni1513
224. Schneider MA, Meingassner JG, Lipp M, Moore HD, Rot A. CCR7 Is Required for the *In Vivo* Function of CD4+ CD25+ Regulatory T Cells. *J Exp Med* (2007) 204(4):735–45. doi: 10.1084/jem.20061405
225. Shields JD, Kourtis IC, Tomei AA, Roberts JM, Swartz MA. Induction of Lymphoidlike Stroma and Immune Escape by Tumors That Express the Chemokine CCL21. *Science* (2010) 328(5979):749–52. doi: 10.1126/science.1185837
226. Yang ZZ, Novak AJ, Stenson MJ, Witzig TE, Ansell SM. Intratumoral CD4+ CD25+ Regulatory T-Cell-Mediated Suppression of Infiltrating CD4+ T Cells in B-Cell Non-Hodgkin Lymphoma. *Blood* (2006) 107(9):3639–46. doi: 10.1182/blood-2005-08-3376
227. Strauss L, Bergmann C, Szczepanski M, Gooding W, Johnson JT, Whiteside TL. A Unique Subset of CD4+CD25highFoxp3+ T Cells Secreting Interleukin-10 and Transforming Growth Factor-Beta1 Mediates Suppression in the Tumor Microenvironment. *Clin Cancer Res* (2007) 13 (15 Pt 1):4345–54. doi: 10.1158/1078-0432.CCR-07-0472
228. Alvaro T, Lejeune M, Salvado MT, Bosch R, Garcia JF, Jaen J, et al. Outcome in Hodgkin's Lymphoma can be Predicted From the Presence of Accompanying Cytotoxic and Regulatory T Cells. *Clin Cancer Res* (2005) 11(4):1467–73. doi: 10.1158/1078-0432.CCR-04-1869
229. Beyer M, Kochanek M, Darabi K, Popov A, Jensen M, Endl E, et al. Reduced Frequencies and Suppressive Function of CD4+CD25hi Regulatory T Cells in Patients With Chronic Lymphocytic Leukemia After Therapy With Fludarabine. *Blood* (2005) 106(6):2018–25. doi: 10.1182/blood-2005-02-0642
230. Beyer M, Kochanek M, Giese T, Endl E, Weihrauch MR, Knolle PA, et al. *In Vivo* Peripheral Expansion of Naive CD4+CD25high FOXP3+ Regulatory T Cells in Patients With Multiple Myeloma. *Blood* (2006) 107(10):3940–9. doi: 10.1182/blood-2005-09-3671
231. Mittal S, Marshall NA, Duncan L, Culligan DJ, Barker RN, Vickers MA. Local and Systemic Induction of CD4+CD25+ Regulatory T-Cell Population

by Non-Hodgkin Lymphoma. *Blood* (2008) 111(11):5359–70. doi: 10.1182/blood-2007-08-105395
232. Lee NR, Song EK, Jang KY, Choi HN, Moon WS, Kwon K, et al. Prognostic Impact of Tumor Infiltrating FOXP3 Positive Regulatory T Cells in Diffuse Large B-Cell Lymphoma at Diagnosis. *Leuk Lymphoma* (2008) 49(2):247–56. doi: 10.1080/10428190701824536
233. Lefkowitz RJ, Shenoy SK. Transduction of Receptor Signals by Beta-Arrestins. *Science* (2005) 308(5721):512–7. doi: 10.1126/science.1109237
234. Steen A, Larsen O, Thiele S, Rosenkilde MM. Biased and G Protein-Independent Signaling of Chemokine Receptors. *Front Immunol* (2014) 5:277. doi: 10.3389/fimmu.2014.00277
235. Till KJ, Spiller DG, Harris RJ, Chen H, Zuzel M, Cawley JC. CLL. But Not Normal, B Cells Are Dependent on Autocrine VEGF and Alpha4beta1 Integrin for Chemokine-Induced Motility on and Through Endothelium. *Blood* (2005) 105(12):4813–9. doi: 10.1182/blood-2004-10-4054
236. McHeik S, Van Eeckhout N, De Poorter C, Galés C, Parmentier M, Springael J-Y. Coexpression of CCR7 and CXCR4 During B Cell Development Controls CXCR4 Responsiveness and Bone Marrow Homing. *Front Immunol* (2019) 10:2970. doi: 10.3389/fimmu.2019.02970
237. Shannon LA, McBurney TM, Wells MA, Roth ME, Calloway PA, Bill CA, et al. CCR7/CCL19 Controls Expression of EDG-1 in T Cells. *J Biol Chem* (2012) 287(15):11656–64. doi: 10.1074/jbc.M111.310045
238. Okada T, Ngo VN, Ekland EH, Forster R, Lipp M, Littman DR, et al. Chemokine Requirements for B Cell Entry to Lymph Nodes and Peyer's Patches. *J Exp Med* (2002) 196(1):65–75. doi: 10.1084/jem.20020201
239. Muller G, Lipp M. Shaping Up Adaptive Immunity: The Impact of CCR7 and CXCR5 on Lymphocyte Trafficking. *Microcirculation* (2003) 10(3-4):325–34. doi: 10.1080/mic.10.3-4.325.334
240. Hopken UE, Achtman AH, Kruger K, Lipp M. Distinct and Overlapping Roles of CXCR5 and CCR7 in B-1 Cell Homing and Early Immunity Against Bacterial Pathogens. *J Leukoc Biol* (2004) 76(3):709–18. doi: 10.1189/jlb.1203643
241. Velaga S, Herbrand H, Friedrichsen M, Jiong T, Dorsch M, Hoffmann MW, et al. Chemokine Receptor CXCR5 Supports Solitary Intestinal Lymphoid Tissue Formation, B Cell Homing, and Induction of Intestinal IgA Responses. *J Immunol* (2009) 182(5):2610–9. doi: 10.4049/jimmunol.0801141
242. Warnock RA, Campbell JJ, Dorf ME, Matsuzawa A, McEvoy LM, Butcher EC. The Role of Chemokines in the Microenvironmental Control of T *Versus* B Cell Arrest in Peyer's Patch High Endothelial Venules. *J Exp Med* (2000) 191(1):77–88. doi: 10.1084/jem.191.1.77
243. Ebisuno Y, Tanaka T, Kanemitsu N, Kanda H, Yamaguchi K, Kaisho T, et al. Cutting Edge: The B Cell Chemokine CXC Chemokine Ligand 13/B Lymphocyte Chemoattractant is Expressed in the High Endothelial Venules of Lymph Nodes and Peyer's Patches and Affects B Cell Trafficking Across High Endothelial Venules. *J Immunol* (2003) 171(4):1642–6. doi: 10.4049/jimmunol.171.4.1642
244. Cuesta-Mateos C, Juárez-Sánchez R, Mateu-Albero T, Loscertales J, Mol W, Terrón F, et al. Targeting Cancer Homing Into the Lymph Node With a Novel Anti-CCR7 Therapeutic Antibody: The Paradigm of CLL. *mAbs* (2021) 13(1):1917484. doi: 10.1080/19420862.2021.1917484
245. Mateu-Albero T, Juárez-Sánchez R, Loscertales J, Mol W, Terrón F, Muñoz-Calleja C, et al. Effect of Ibrutinib on CCR7 Expression and Functionality in Chronic Lymphocytic Leukemia and its Implication for the Activity of CAP-100, a Novel Therapeutic Anti-CCR7 Antibody. *Cancer Immunol Immunother CII.* (2021). doi: 10.1007/s00262-021-03014-2
246. Fiorcari S, Brown WS, McIntyre BW, Estrov Z, Maffei R, O'Brien S, et al. The PI3-Kinase Delta Inhibitor Idelalisib (GS-1101) Targets Integrin-Mediated Adhesion of Chronic Lymphocytic Leukemia (CLL) Cell to Endothelial and Marrow Stromal Cells. *PloS One* (2013) 8(12):e83830. doi: 10.1371/journal.pone.0083830
247. Ping L, Ding N, Shi Y, Feng L, Li J, Liu Y, et al. The Bruton's Tyrosine Kinase Inhibitor Ibrutinib Exerts Immunomodulatory Effects Through Regulation of Tumor-Infiltrating Macrophages. *Oncotarget* (2017) 8(24):39218–29. doi: 10.18632/oncotarget.16836
248. Lafouresse F, Groom JR. A Task Force Against Local Inflammation and Cancer: Lymphocyte Trafficking to and Within the Skin. *Front Immunol* (2018) 9:2454. doi: 10.3389/fimmu.2018.02454
249. Harjunpää H, Llort Asens M, Guenther C, Fagerholm SC. Cell Adhesion Molecules and Their Roles and Regulation in the Immune and Tumor Microenvironment. *Front Immunol* (2019) 10:1078. doi: 10.3389/fimmu.2019.01078
250. Reina M, Espel E. Role of LFA-1 and ICAM-1 in Cancer. *Cancers (Basel)* (2017) 9(11):153. doi: 10.20944/preprints201709.0146.v1
251. San Sebastián E, Zimmerman T, Zubia A, Vara Y, Martin E, Sirockin F, et al. Design, Synthesis, and Functional Evaluation of Leukocyte Function Associated Antigen-1 Antagonists in Early and Late Stages of Cancer Development. *J Medicinal Chem* (2013) 56(3):735–47. doi: 10.1021/jm3016848
252. Lin Y-C, Shun C-T, Wu M-S, Chen C-C. A Novel Anticancer Effect of Thalidomide: Inhibition of Intercellular Adhesion Molecule-1-Mediated Cell Invasion and Metastasis Through Suppression of Nuclear Factor-Kappab. *Clin Cancer Res an Off J Am Assoc Cancer Res* (2006) 12(23):7165–73. doi: 10.1158/1078-0432.CCR-06-1393
253. Yu JA, Sadaria MR, Meng X, Mitra S, Ao L, Fullerton DA, et al. Lung Cancer Cell Invasion and Expression of Intercellular Adhesion Molecule-1 (ICAM-1) Are Attenuated by Secretory Phospholipase A_2 Inhibition. *J Thorac Cardiovasc Surg* (2012) 143(2):405–11. doi: 10.1016/j.jtcvs.2011.10.026
254. Laufer JM, Legler DF. Beyond Migration-Chemokines in Lymphocyte Priming, Differentiation, and Modulating Effector Functions. *J Leukoc Biol* (2018) 104(2):301–12. doi: 10.1002/JLB.2MR1217-494R
255. Ma J, Wang JH, Guo YJ, Sy MS, Bigby M. *In Vivo* Treatment With Anti-ICAM-1 and Anti-LFA-1 Antibodies Inhibits Contact Sensitization-Induced Migration of Epidermal Langerhans Cells to Regional Lymph Nodes. *Cell Immunol* (1994) 158(2):389–99. doi: 10.1006/cimm.1994.1285
256. Yanguas A, Garasa S, Teijeira Á, Aubá C, Melero I, Rouzaut A. ICAM-1-LFA-1 Dependent CD8+ T-Lymphocyte Aggregation in Tumor Tissue Prevents Recirculation to Draining Lymph Nodes. *Front Immunol* (2018) 9:2084. doi: 10.3389/fimmu.2018.02084
257. Schmits R, Kündig TM, Baker DM, Shumaker G, Simard JJ, Duncan G, et al. LFA-1-Deficient Mice Show Normal CTL Responses to Virus But Fail to Reject Immunogenic Tumor. *J Exp Med* (1996) 183(4):1415–26. doi: 10.1084/jem.183.4.1415
258. Mukai S, Kagamu H, Shu S, Plautz GE. Critical Role of CD11a (LFA-1) in Therapeutic Efficacy of Systemically Transferred Antitumor Effector T Cells. *Cell Immunol* (1999) 192(2):122–32. doi: 10.1006/cimm.1998.1439
259. Seminara NM, Gelfand JM. Assessing Long-Term Drug Safety: Lessons (Re) Learned From Raptiva. *Semin Cutaneous Med Surg* (2010) 29(1):16–9. doi: 10.1016/j.sder.2010.01.001
260. Talamonti M, Spallone G, Di Stefani A, Costanzo A, Chimenti S. Efalizumab. *Expert Opin Drug Saf* (2011) 10(2):239–51. doi: 10.1517/14740338.2011.524925
261. Cohen S, Haimovich J, Hollander N. Anti-Idiotype X Anti-LFA-1 Bispecific Antibodies Inhibit Metastasis of B Cell Lymphoma. *J Immunol (Baltimore Md 1950)* (2003) 170(5):2695–701. doi: 10.4049/jimmunol.170.5.2695
262. Moschovakis GL, Forster R. Multifaceted Activities of CCR7 Regulate T-Cell Homeostasis in Health and Disease. *Eur J Immunol* (2012) 42(8):1949–55. doi: 10.1002/eji.201242614
263. Moschovakis GL, Bubke A, Dittrich-Breiholz O, Braun A, Prinz I, Kremmer E, et al. Deficient CCR7 Signaling Promotes TH2 Polarization and B-Cell Activation *In Vivo*. *Eur J Immunol* (2012) 42(1):48–57. doi: 10.1002/eji.201141753
264. Vassileva G, Soto H, Zlotnik A, Nakano H, Kakiuchi T, Hedrick JA, et al. The Reduced Expression of 6Ckine in the Plt Mouse Results From the Deletion of One of Two 6Ckine Genes. *J Exp Med* (1999) 190(8):1183–8. doi: 10.1084/jem.190.8.1183
265. Luther SA, Tang HL, Hyman PL, Farr AG, Cyster JG. Coexpression of the Chemokines ELC and SLC by T Zone Stromal Cells and Deletion of the ELC Gene in the Plt/Plt Mouse. *Proc Natl Acad Sci USA* (2000) 97(23):12694–9. doi: 10.1073/pnas.97.23.12694
266. Junt T, Scandella E, Forster R, Krebs P, Krautwald S, Lipp M, et al. Impact of CCR7 on Priming and Distribution of Antiviral Effector and Memory CTL. *J Immunol* (2004) 173(11):6684–93. doi: 10.4049/jimmunol.173.11.6684
267. Junt T, Nakano H, Dumrese T, Kakiuchi T, Odermatt B, Zinkernagel RM, et al. Antiviral Immune Responses in the Absence of Organized Lymphoid T Cell Zones in Plt/Plt Mice. *J Immunol* (2002) 168(12):6032–40. doi: 10.4049/jimmunol.168.12.6032

268. Kursar M, Hopken UE, Koch M, Kohler A, Lipp M, Kaufmann SH, et al. Differential Requirements for the Chemokine Receptor CCR7 in T Cell Activation During Listeria Monocytogenes Infection. *J Exp Med* (2005) 201 (9):1447–57. doi: 10.1084/jem.20041204
269. Scandella E, Fink K, Junt T, Senn BM, Lattmann E, Forster R, et al. Dendritic Cell-Independent B Cell Activation During Acute Virus Infection: A Role for Early CCR7-Driven B-T Helper Cell Collaboration. *J Immunol* (2007) 178 (3):1468–76. doi: 10.4049/jimmunol.178.3.1468
270. Aritomi K, Kuwabara T, Tanaka Y, Nakano H, Yasuda T, Ishikawa F, et al. Altered Antibody Production and Helper T Cell Function in Mice Lacking Chemokines CCL19 and CCL21-Ser. *Microbiol Immunol* (2010) 54(11):691–701. doi: 10.1111/j.1348-0421.2010.00266.x
271. Hartoonian C, Sepehrizadeh Z, Tabatabai Yazdi M, Jang YS, Langroudi L, Amir Kalvanagh P, et al. Enhancement of Immune Responses by Co-Delivery of CCL19/MIP-3beta Chemokine Plasmid With HCV Core DNA/Protein Immunization. *Hepat Mon* (2014) 14(3):e14611. doi: 10.5812/hepatmon.14611
272. Hu K, Luo S, Tong L, Huang X, Jin W, Huang W, et al. CCL19 and CCL28 Augment Mucosal and Systemic Immune Responses to HIV-1 Gp140 by Mobilizing Responsive Immunocytes Into Secondary Lymph Nodes and Mucosal Tissue. *J Immunol (Baltimore Md 1950)* (2013) 191(4):1935–47. doi: 10.4049/jimmunol.1300120
273. Moschovakis GL, Bubke A, Friedrichsen M, Ristenpart J, Back JW, Falk CS, et al. The Chemokine Receptor CCR7 is a Promising Target for Rheumatoid Arthritis Therapy. *Cell Mol Immunol* (2019) 16(10):791–9. doi: 10.1038/s41423-018-0056-5
274. Cuesta-Mateos C, Portero-Sainz I, García-Peydró M, Alcain J, Fuentes P, Juárez-Sánchez R, et al. Evaluation of Therapeutic Targeting of CCR7 in Acute Graft-*Versus*-Host Disease. *Bone Marrow Transplant* (2020) 55 (10):1935–45. doi: 10.1038/s41409-020-0830-8
275. Fowler KA, Vasilieva V, Ivanova E, Rimkevich O, Sokolov A, Abbasova S, et al. R707, a Fully Human Antibody Directed Against CC-Chemokine Receptor 7, Attenuates Xenogeneic Acute Graft-*Versus*-Host Disease. *Am J Transplant.* (2019) 19(7):1941–54. doi: 10.1111/ajt.15298
276. Soudja SM, Henri S, Mello M, Chasson L, Mas A, Wehbe M, et al. Disrupted Lymph Node and Splenic Stroma in Mice With Induced Inflammatory Melanomas is Associated With Impaired Recruitment of T and Dendritic Cells. *PloS One* (2011) 6(7):e22639. doi: 10.1371/journal.pone.0022639
277. Thompson ED, Enriquez HL, Fu YX, Engelhard VH. Tumor Masses Support Naive T Cell Infiltration, Activation, and Differentiation Into Effectors. *J Exp Med* (2010) 207(8):1791–804. doi: 10.1084/jem.20092454
278. Forster R, Mattis AE, Kremmer E, Wolf E, Brem G, Lipp M. A Putative Chemokine Receptor, BLR1, Directs B Cell Migration to Defined Lymphoid Organs and Specific Anatomic Compartments of the Spleen. *Cell* (1996) 87 (6):1037–47. doi: 10.1016/S0092-8674(00)81798-5
279. Hintzen G, Ohl L, del Rio ML, Rodriguez-Barbosa JI, Pabst O, Kocks JR, et al. Induction of Tolerance to Innocuous Inhaled Antigen Relies on a CCR7-Dependent Dendritic Cell-Mediated Antigen Transport to the Bronchial Lymph Node. *J Immunol* (2006) 177(10):7346–54. doi: 10.4049/jimmunol.177.10.7346
280. Worbs T, Bode U, Yan S, Hoffmann MW, Hintzen G, Bernhardt G, et al. Oral Tolerance Originates in the Intestinal Immune System and Relies on Antigen Carriage by Dendritic Cells. *J Exp Med* (2006) 203(3):519–27. doi: 10.1084/jem.20052016
281. Davalos-Misslitz AC, Rieckenberg J, Willenzon S, Worbs T, Kremmer E, Bernhardt G, et al. Generalized Multi-Organ Autoimmunity in CCR7-Deficient Mice. *Eur J Immunol* (2007) 37(3):613–22. doi: 10.1002/eji.200636656
282. Kurobe H, Liu C, Ueno T, Saito F, Ohigashi I, Seach N, et al. CCR7-Dependent Cortex-to-Medulla Migration of Positively Selected Thymocytes is Essential for Establishing Central Tolerance. *Immunity* (2006) 24(2):165–77. doi: 10.1016/j.immuni.2005.12.011
283. Lewis DJ, Rook AH. Mogamulizumab in the Treatment of Advanced Mycosis Fungoides and Sézary Syndrome: Safety and Efficacy. *Expert Rev Anticancer Ther* (2020) 20(6):447–52. doi: 10.1080/14737140.2020.1760096

Conflict of Interest: CC-M is an employee of Catapult Therapeutics and of Immunological and Medical Products (IMMED S.L.), and a shareholder in this last company. FT declares that he is CEO and a shareholder in the same companies.

The remaining author declares that the research was conducted in the absence of any commercial or financial relationships that could be construed as a potential conflict of interest.

Publisher's Note: All claims expressed in this article are solely those of the authors and do not necessarily represent those of their affiliated organizations, or those of the publisher, the editors and the reviewers. Any product that may be evaluated in this article, or claim that may be made by its manufacturer, is not guaranteed or endorsed by the publisher.

frontiers in Oncology

BRIEF RESEARCH REPORT
published: 05 November 2021
doi: 10.3389/fonc.2021.730194

CNS Prophylaxis: How Far Is Routine Practice From the Guidelines? Focus on a Nationwide Survey by the Fondazione Italiana Linfomi (FIL)

Guido Gini[1], Alice Di Rocco[2]*, Luca Nassi[3]*, Annalisa Arcari[4]*, Maria Chiara Tisi[5]*, Giacomo Loseto[6]*, Attilio Olivieri[1]*, Massimo Gentile[7]*, Ombretta Annibali[8]*, Maria Giuseppina Cabras[9]*, Annalisa Chiappella[10]*, Chiara Rusconi[11]*, Andrés José María Ferreri[12]* and Monica Balzarotti[13]* on behalf of the Fondazione Italiana Linfomi (FIL)*

[1] Clinic of Hematology, Ospedali Riuniti, Ancona, Italy, [2] Department of Traslational and Precision Medicine, Sapienza University, Roma, Italy, [3] Hematology, Department of Translational Medicine, University of Eastern Piedmont and AOU Maggiore della Carità, Novara, Italy, [4] Division of Hematology, Guglielmo da Saliceto Hospital, Piacenza, Italy, [5] Department of Hematology and Cell Therapy, San Bortolo Hospital, Vicenza, Italy, [6] Division of Hematology, IRCCS Ospedale Oncologico, Bari, Italy, [7] Department of Onco-Hematology, Hematology Unit, A.O of Cosenza, Cosenza, Italy, [8] Unit of Hematology and Stem Cell Transplantation, University "Campus Bio-Medico", Rome, Italy, [9] Division of Hematology, Ospedale Oncologico Armando Businco, Cagliari, Italy, [10] Department of Hematology, Azienda Ospedaliero Universitaria Citta`della Salute e della Scienza di Torino, Torino, Italy, [11] Division of Hematology, Ospedale Niguarda Ca' Granda, Milan, Italy, [12] San Raffaele Hospital, IRCCS, Milano, Italy, [13] Hematology Unit, IRCCS Humanitas Cancer Center, Milan, Italy

Keywords: diffuse large B cell lymphoma (DLBCL), central nervous system involvement, survey, risk assessment, prophylaxis

OPEN ACCESS

Edited by:
Weili Zhao,
Shanghai Jiao Tong University, China

Reviewed by:
Wenbin Qian,
Zhejiang University, China
Monica Bocchia,
University of Siena, Italy

****Correspondence:***
Guido Gini
Guido.Gini@ospedaliriuniti.marche.it
Alice Di Rocco
dirocco@bce.uniroma1.it
Luca Nassi
luca.nassi@gmail.com
Annalisa Arcari
a.arcari@ausl.pc.it
Maria Chiara Tisi
mchiara.tisi@gmail.com
Giacomo Loseto
loseto.giacomo@gmail.com
Massimo Gentile
massimogentile@virgilio.it
Andrés José María Ferreri
ferreri.andres@hsr.it
Monica Balzarotti
monica.balzarotti@cancercenter.humanitas.it
Attilio Olivieri
a.olivieri@univpm.it
Ombretta Annibali
o.annibali@unicampus.it
Maria Giuseppina Cabras
cabras.giuseppina@tiscali.it
Annalisa Chiappella
annalisa.chiappella@istitutotumori.mi.it
Chiara Rusconi
chiara.rusconi@ospedaleniguarda.it

Specialty section:
This article was submitted to Hematologic Malignancies, a section of the journal Frontiers in Oncology

Received: *24 June 2021*
Accepted: *27 August 2021*
Published: *05 November 2021*

Central nervous system (CNS) prophylaxis in patients with diffuse large B-cell lymphoma (DLBCL) (1) remains at matter of facts an unmeet clinical need.

In a recent paper, McKay et al. for the British Society of Haematology (BSH) published a good practice in this field (2).

Authors should be commended for the relevant effort to draw management recommendations for routine practice. In brief, they suggested that CNS prophylaxis should be offered to patients with any factor among high (4–6) CNS-IPI, involvement of three or more extranodal sites irrespective of CNS-IPI, involvement of certain extranodal organs (i.e., testes, kidney/adrenal), and in intravascular large B-cell lymphoma; they advise to consider CNS prophylaxis in patients with involvement of breast or uterus. Authors recommend the use of two to three cycles of methotrexate (MTX) at 3 g/m^2 in infusion over 2–4 hours as early as possible, perhaps intercalating it with R-CHOP therapy, leaving intrathecal chemotherapy only for patients unfit for high-dose MTX. These recommendations resulted from an extensive literature research and followed the BSH guidelines, with the aim to recommend good practice in an area where there is a limited evidence. Literature on CNS prophylaxis in DLBCL (3–10) is mostly based on retrospective studies, where high-risk patients were defined usually by homemade, not validated prognostic factors. Anyway, it is interestingly to understand how much this growing, low-level evidence influenced prophylaxis strategies, and definition and management of high-risk patients in the clinical practice. In other words, it would be important to establish how far routine practice from proposed guidelines and supportive literature is. With this aim, we designed a National survey focused on algorithms used in routine practice to identify DLBCL

patients at high CNS risk and on strategies to prevent CNS dissemination in Italian cancer centers. A questionnaire designed after consultation with specialist clinicians and a review of published literature was sent to cancer centers referring to the Fondazione Italiana Linfomi (FIL) in July 2018. The primary objectives of this study were to establish strategies used to detect CNS dissemination and to identify high CNS risk patients and preferred CNS prophylaxis in real-life practice, between 2014 and 2018. More in detail, each center was asked to specify the characteristics of the patients considered at high CNS risk (i.e., CNS-IPI > 4, extranodal sites, biological parameters, and chromosomal abnormalities) as well as the list of extranodal organs considered at high risk of CNS relapse (i.e., paravertebral, kidney, adrenal, massive facial, nasopharynx, testicle, and uterus). Information on procedures routinely used to exclude CNS disease (i.e., type of neuroimaging and/or lumbar puncture) and availability of exams on the cerebrospinal fluid (physico-chemical, cytological, flow cytometric) was requested. Information on the routinely use of genetic and molecular tools like cell of origin, chromosomal translocations, and myc/bcl-2/bcl-6 immunostaining was also collected.

Sixty-three (57%) of the 110 invited FIL centers fulfilled the survey.

The survey suggest a concordance between guidelines and clinical practice regarding the criteria used to define patients with high risk of CNS dissemination: CNS-IPI is considered in 87% of centers, and 71% of centers considered the involvement of extranodal organs with reported risk of CNS dissemination. These findings reflect a diffuse acceptance of CNS-IPI in routine practice, whereas a lower use of high-risk extranodal sites may be due to uncertainties in literature on the prognostic value of some sites.

In fact, 92% of centers considered at high risk for CNS relapse the involvement of at least one of the following extranodal organs: kidney, adrenal gland, nasopharynx, and testicle, which is in line with ESMO guidelines (11). Conversely, consensus is lacking for involvement of breast, orbit, paranasal sinus, and skeleton; probably because assessed series were small, included varied lymphoma entities and were treated with different approaches (12). In agreement with BSH guidelines, only 5% of Italian centers use genetic abnormalities to define CNS risk, which reflects inconsistent results in available literature on double hit lymphoma (13–15) and double expresser lymphoma (16, 17). Although the combined assessment of CNS-IPI and cell of origin by gene expression profiling seems to be associated with a high predictive sensitivity (18), a diffuse use of this strategy to guide CNS prophylaxis indication will require independent confirmatory studies and a wider use of gene-expression profiling in routine practice (19). Patients with double/triple and/or ABC and/or double expresser lymphomas were considered at high risk of CNS relapse in in 38 (60%) centers, whereas only those with double\triple hit lymphoma were considered really high risk in six centers (9%).

CNS disease status was assessed by imaging even among asymptomatic patients in 73% of centers, but only half of them use MRI routinely, the others used the less sensitive whole-brain CT scan. Complete diagnostics in cerebrospinal fluid analysis (CSF; physical-chemical, cytological, flow cytometric) are used in 79% of centers, whereas CSF flow cytometry is not routinely performed in 10 (16%) centers. Meningeal/CSF involvement was defined exclusively by positive CSF cytology examination in 19 (30%) centers, whereas the only positive flow cytometry was enough to define this event in 41 (65%) centers. Noteworthy, this is not discussed on international guidelines, but a large retrospective study suggests that most patients with positive CSF flow cytometry and negative CSF cytology will develop more evident CNS disease early (20).

There is gap between guidelines and routine practice regarding the type of CNS prophylaxis; only 40% of participating centers use intravenous MTX at a dose of 1.5 to 3 gr/sqm), with or without intrathecal drug delivery, as CNS prophylaxis, whereas 58% of centers use only intrathecal chemotherapy. This may reflect discrepancies between previously published guidelines: NCCN suggests equally intrathecal and intravenous chemotherapy (21), while ESMO guidelines recognize that intrathecal injections of methotrexate may not be an optimal method, and that intravenous high-dose methotrexate is associated with a lower CNS recurrence rate (11).

This survey shows real-life practice in a representative group of Italian hematological centers. However, it exhibits a few limitations. In particular, prevalently large- or medium-size centers participated, which could have introduced an interpretation bias, mostly in the case small center could show a lower adherence to international guidelines. This survey was produced in Italy and compared with recommendations written by UK colleagues, with consequent weakness regarding differences in patient managements, reimbursement of therapies, among others. With these limitations, this survey highlights the substantial inter-center differences in the use of methods of diagnosis and prophylaxis of CNS involvement in DLBCL patients. The growing literature has been progressively incorporated in international guidelines, but level of evidence of available studies should be improved to draw undebatable recommendations. These achievements should be followed by educational efforts to disseminate these recommendations so that they will soon be incorporated into routine practice.

DATA AVAILABILITY STATEMENT

The original contributions presented in the study are included in the article/supplementary material. Further inquiries can be directed to the corresponding authors.

AUTHOR CONTRIBUTIONS

GG, AR, MS, LN, AA, MT, GL, MG, OA, AF, and MB contributed to conception and design of the study. All authors contributed to manuscript revision, read, and approved the submitted version.

REFERENCES

1. Bernstein SH, Unger JM, Leblanc MJ, Friedberg J, Miller TP, Fisher RI, et al. Natural History of CNS Relapse in Patients With Aggressive Non-Hodgkin's Lymphoma: A 20-Year Follow-Up Analysis of SWOG 8516 - the Southwest Oncology Group. *J Clin Oncol* (2009) 27:114–9. doi: 10.1200/JCO.2008.16.8021
2. McKay P, Wilson MR, Chaganti S, Smith J, Fox CP, Cwynarski K, et al. The Prevention of Central Nervous System Relapse in Diffuse Large B-Cell Lymphoma: A British Society for Haematology Good Practice Paper. *Br J Haematol* (2020) 190(5):708–14. doi: 10.1111/bjh.16866
3. Boehme V, Schmitz N, Zeynalova S, Loeffler M, Pfreundschuh M. CNS Events in Elderly Patients With Aggressive Lymphoma Treated With Modern Chemotherapy (CHOP-14) With or Without Rituximab: An Analysis of Patients Treated in the RICOVER-60 Trial of the German High-Grade Non-Hodgkin Lymphoma Study Group (DSHNHL). *Blood* (2009) 113:3896–902. doi: 10.1182/blood-2008-10-182253
4. Zahid MF, Khan N, Hashmi SK, Kizilbash SH, Barta SK. Central Nervous System Prophylaxis in Diffuse Large B-Cell Lymphoma. *Eur J Haematol* (2016) 97:108–20. doi: 10.1111/ejh.12763
5. Schmitz N, Zeynalova S, Nickelsen M, Kansara R, Villa D, Sehn LH, et al. CNS International Prognostic Index: A Risk Model for CNS Relapse in Patients With Diffuse Large B-Cell Lymphoma Treated With R-CHOP. *J Clin Oncol* (2016) 34(26):3150–6. doi: 10.1200/JCO.2015.65.6520
6. Calimeri T, Lopedote P, Ferreri AJM. Risk Stratification and Management Algorithms for Patients With Diffuse Large B-Cell Lymphoma and CNS Involvement. *Ann Lymphoma* (2019) 3:7. doi: 10.21037/aol.2019.06.01
7. Tai WM, Chung J, Tang PL, Koo YX, Hou KW, Tay R, et al. Central Nervous System (CNS) Relapse in Diffuse Large B Cell Lymphoma (DLBCL): Pre- and Post-Rituximab. *Ann Hematol* (2011) 90:809–18. doi: 10.1007/s00277-010-1150-7
8. Oki Y, Noorani M, Lin P, Davis RE, Neelapu SS, Ma L, et al. Double Hit Lymphoma: The MD Anderson Cancer Center Clinical Experience. *Br J Haematol* (2014) 166:891–901. doi: 10.1111/bjh.12982
9. Petrich AM, Gandhi M, Jovanovic B, Castillo JJ, Rajguru S, Yang DT, et al. Impact of Induction Regimen and Stem Cell Transplantation on Outcomes in Double-Hit Lymphoma: A Multicenter Retrospective Analysis. *Blood* (2014) 124:2354–61. doi: 10.1182/blood-2014-05-578963
10. Abramson JS, Hellmann M, Barnes JA, Hammerman P, Toomey C, Takvorian T, et al. Intravenous Methotrexate as Central Nervous System (CNS) Prophylaxis Is Associated With a Low Risk of CNS Recurrence in High-Risk Patients With Diffuse Large B-Cell Lymphoma. *Cancer* (2010) 116:4283–90. doi: 10.1002/cncr.25278
11. Tilly H, Gomez da Silva M, Vitolo U, Jack A, Meignan M, Lopez-Guillermo A, et al. Guidelines Committee. Diffuse Large B-Cell Lymphoma (DLBCL): ESMO Clinical Practice Guidelines for Diagnosis, Treatment and Follow-Up. *Ann Oncol* (2015) Suppl 5:v116–25. doi: 10.1093/annonc/mdv304
12. Ferreri AJM. Risk of CNS Dissemination in Extranodal Lymphomas. *Lancet Oncol* (2014) 15(4):e159–69. doi: 10.1016/S1470-2045(13)70568-0
13. Gleeson M, Counsell N, Cunningham D, Chadwick N, Lawrie A, Hawkes EA, et al. Central Nervous System Relapse of Diffuse Large B-Cell Lymphoma in the Rituximab Era: Results of the UK NCRI R-CHOP-14 Versus 21 Trial. *Ann Oncol* (2017) 28(10):2511–6. doi: 10.1093/annonc/mdx353
14. Petrich AM, Nabhan C, Smith SM. MYC-Associated and Double-Hit Lymphomas: A Review of Pathobiology, Prognosis, and Therapeutic Approaches. *Cancer* (2014) 120(24):3884–95. doi: 10.1002/cncr.28899
15. Oki Y, Noorani M, Lin P, Davis RE, Neelapu SS, Ma L, et al. Double Hit Lymphoma: The MD Anderson Cancer Center Clinical Experience. *Br J Haematol* (2014) 166(6):891–901. doi: 10.1111/bjh.12982
16. Klanova M, Sehn LH, Bence-Bruckler I, Trneny M. Integration of Cell of Origin Into the Clinical CNS International Prognostic Index Improves CNS Relapse Prediction in DLBCL. *Blood* (2019) 133(9):919–26. doi: 10.1182/blood-2018-07-862862
17. Savage K, Kerry J, Slack G, Mottok A, Sehn LH, Villa D, et al. Impact of Dual Expression of MYC and BCL2 by Immunohistochemistry on the Risk of CNS Relapse in DLBCL. *Blood* (2016) 127:2182–8. doi: 10.1182/blood-2015-10-676700
18. Klanova M, Sehn LH, Bence-Bruckler I, Cavallo F, Jin J, Martelli M, et al. Integration of Cell of Origin Into the Clinical CNS International Prognostic Index Improves CNS Relapse Prediction in DLBCL. *Blood* (2019) 133(9):919–26. doi: 10.1182/blood-2018-07-862862
19. Ferreri AJM. Secondary CNS Lymphoma: The Poisoned Needle in the Haystack. *Ann Oncol* (2017) 28(10):2335–7. doi: 10.1093/annonc/mdx515
20. Benevolo G, Stacchini A, Spina M, Ferreri AJM, Arras M, Bellio L, et al. Final Results of a Multicenter Trial Addressing Role of CSF Flow Cytometric Analysis in NHL Patients at High Risk for CNS Dissemination. *Blood* (2012) 120(16):3222–8. doi: 10.1182/blood-2012-04-423095
21. National Comprehensive Cancer Network. *Non-Hodgkin's Lymphoma. Version 5*. (2017).

Conflict of Interest: The authors declare that the research was conducted in the absence of any commercial or financial relationships that could be construed as a potential conflict of interest.

Citation: *Gini G, Di Rocco A, Nassi L, Arcari A, Tisi MC, Loseto G, Olivieri A, Gentile M, Annibali O, Cabras MG, Chiappella A, Rusconi C, Ferreri AJM and Balzarotti M (2021) CNS Prophylaxis: How Far Is Routine Practice From the Guidelines? Focus on a Nationwide Survey by the Fondazione Italiana Linfomi (FIL). Front. Oncol. 11:730194. doi: 10.3389/fonc.2021.730194*

frontiers in Oncology

PERSPECTIVE
published: 08 November 2021
doi: 10.3389/fonc.2021.720704

Monitoring and Managing BTK Inhibitor Treatment-Related Adverse Events in Clinical Practice

Susan M. O'Brien[1*], *Jennifer R. Brown*[2], *John C. Byrd*[3], *Richard R. Furman*[4], *Paolo Ghia*[5], *Jeff P. Sharman*[6] *and William G. Wierda*[7]

[1] *Chao Family Comprehensive Cancer Center, University of California, Orange, CA, United States,* [2] *Chronic Lymphocytic Leukemia (CLL) Center, Dana-Farber Cancer Institute, Boston, MA, United States,* [3] *James Cancer Hospital and Solove Research Institute, The Ohio State University Comprehensive Cancer Center and Division of Hematology, Columbus, OH, United States,* [4] *Chronic Lymphocytic Leukemia (CLL) Research Center, New York-Presbyterian/Weill Cornell Medical Center, New York, NY, United States,* [5] *Division of Experimental Oncology, Università Vita-Salute San Raffaele and IRCCS Ospedale San Raffaele, Milano, Italy,* [6] *Division of Hematology Research for US Oncology, Willamette Valley Cancer Institute/US Oncology, Eugene, OR, United States,* [7] *Department of Leukemia, The University of Texas MD Anderson Cancer Center, Houston, TX, United States*

OPEN ACCESS

Edited by:
Rakesh Verma, Consultant, San Francisco, CA, United States

Reviewed by:
Yi Miao, Nanjing Medical University, China
Jian Hou, Shanghai JiaoTong University, China
Tanja Nicole Hartmann, University of Freiburg Medical Center, Germany

***Correspondence:**
Susan M. O'Brien
obrien@uci.edu

Specialty section:
This article was submitted to Hematologic Malignancies, a section of the journal Frontiers in Oncology

Received: *04 June 2021*
Accepted: *18 October 2021*
Published: *08 November 2021*

Citation:
O'Brien SM, Brown JR, Byrd JC, Furman RR, Ghia P, Sharman JP and Wierda WG (2021) Monitoring and Managing BTK Inhibitor Treatment-Related Adverse Events in Clinical Practice. Front. Oncol. 11:720704. doi: 10.3389/fonc.2021.720704

Bruton tyrosine kinase (BTK) inhibitors represent an important therapeutic advancement for B cell malignancies. Ibrutinib, the first-in-class BTK inhibitor, is approved by the US FDA to treat patients with chronic lymphocytic leukemia (CLL)/small lymphocytic lymphoma (SLL), and mantle cell lymphoma (MCL; after ≥1 prior therapy); and by the European Medicines Agency (EMA) for adult patients with relapsed/refractory (R/R) MCL and patients with CLL. Ibrutinib treatment can be limited by adverse events (AEs) including atrial fibrillation, arthralgias, rash, diarrhea, and bleeding events, leading to drug discontinuation in 4%–26% of patients. Acalabrutinib, a second-generation BTK inhibitor, is approved by the FDA to treat adult patients with CLL/SLL or MCL (relapsed after 1 prior therapy); and by the EMA to treat adult patients with CLL or R/R MCL. The most common AE associated with acalabrutinib is headache of limited duration, which occurs in 22%–51% of patients, and is mainly grade 1–2 in severity, with only 1% of patients experiencing grade ≥3 headache. Furthermore, acalabrutinib is associated with a low incidence of atrial fibrillation. Zanubrutinib, a selective next-generation covalent BTK inhibitor, is approved by the FDA to treat adult patients with MCL who have received ≥1 prior therapy, and is under investigation for the treatment of patients with CLL. In the phase 3 SEQUOIA trial in patients with CLL, the most common grade ≥3 AEs were neutropenia/neutrophil count decreased and infections. This review provides an overview of BTK inhibitor-related AEs in patients with CLL, and strategies for their management.

Keywords: acalabrutinib, adverse events, Bruton tyrosine kinase inhibitor, chronic lymphocytic leukemia, ibrutinib

INTRODUCTION

Ibrutinib, the first-in-class Bruton tyrosine kinase (BTK) inhibitor, is approved by the US Food and Drug Administration (FDA) for the treatment of patients with chronic lymphocytic leukemia (CLL)/small lymphocytic lymphoma (SLL), mantle cell lymphoma (MCL) after at least 1 prior therapy, Waldenstrom's macroglobulinemia, marginal zone lymphoma in patients who have

received at least 1 prior anti-CD20-based therapy, and chronic graft-versus-host disease after failure of at least 1 systemic therapy (1); and by the European Medicines Agency (EMA) for adult patients with relapsed or refractory (R/R) MCL, and patients with CLL (2). Ibrutinib consistently demonstrated benefit in clinical trials, with improved progression-free survival (PFS) and overall survival (OS) in patients with CLL/SLL and R/R MCL, compared to outcomes with conventional therapies (3, 4). However, ibrutinib treatment can be limited by adverse events (AEs) including atrial fibrillation, arthralgias, rash, diarrhea, and bleeding events (3, 5, 6) leading to drug discontinuation in 4% to 26% of patients (3, 6).

Acalabrutinib is a second-generation BTK inhibitor approved by the US FDA for the treatment of patients with CLL/SLL, and patients with MCL who have received at least 1 prior therapy (7), and by the EMA for patients with CLL (8). Zanubrutinib is a selective next-generation covalent BTK inhibitor approved by the FDA for the treatment of adult patients with MCL who have received at least 1 prior therapy (9); it is under investigation for the treatment of patients with CLL (10, 11). This review will discuss the mechanisms of BTK inhibition, review AEs associated with ibrutinib therapy, together with their possible underlying molecular basis, and AEs reported with acalabrutinib therapy in patients with CLL, including recommendations for the management of acalabrutinib-related AEs. Acalabrutinib-associated AEs will be described using data from the phase 3 ASCEND (12) and ELEVATE-TN (13) trials, long-term safety data from the phase 2 ACE-CL-001 study in patients with CLL who were either treatment naïve or who became R/R (14, 15), and from reports of the most common acalabrutinib-related AEs observed in clinical practice. AEs associated with the use of zanubrutinib in the treatment of patients with treatment-naïve or R/R CLL will also be presented (10, 11). In addition, we will discuss AE management strategies based on the authors' experiences.

MOLECULAR MECHANISMS OF BTK INHIBITION FOR THE TREATMENT OF CLL/SLL

Targeting key signaling proteins responsible for driving cancer cell growth and differentiation has provided a revolution in cancer drug development. The B cell receptor (BCR)-signaling pathway is fundamental to CLL cell growth and survival; hence, antagonists have proven highly effective for the treatment of patients with CLL (16). In normal B cells, BCR ligation first induces activation, proliferation, and expansion. Certain B cells generate plasma cells, while others become anergic or undergo apoptosis (17, 18). Following antigen stimulation and activation, certain B cells become memory B cells, and stop proliferation and differentiation (18). When these memory B cells subsequently re-encounter the same antigen, they are activated and proliferate and differentiate into plasma cells (18). In CLL, there is chronic stimulation through the BCR-signaling pathway leading to proliferation, propagation, and increased prosurvival signals, contributing to expansion and prolonged survival of clonal B cells (19). BTK is an important downstream protein in the BCR-signaling pathway, and plays a major role in immune regulation, as indicated by the severe immunodeficiency occurring in patients with X-linked agammaglobulinemia (XLA) who do not express BTK due to the presence of a mutation in this gene (20–22). BTK is uniformly overexpressed at the transcriptional level and constitutively phosphorylated in patients with CLL (19).

BTK is not only a signaling component downstream of the BCR-signaling pathway but it is also involved in additional signaling pathways (i.e., chemokine receptor [e.g., CXCR4], Toll-like receptor [TLR], and activating Fcγ receptor signaling [e.g., FcγRI]) (23). Upon chemokine binding to the extracellular domain of G-protein-coupled chemokine receptors, a conformation change leads to dissociation of the Gα and Gβγ subunits, which independently activate phosphoinositide 3-kinase (PI3K), leading to activation of BTK, protein kinase B (AKT), and mitogen-activated protein kinase (MAPK)-dependent pathways (23). Following ligand recognition, TLRs recruit several proteins (e.g., myeloid differentiation primary response 88 [MYD88], interleukin-1-receptor associated kinase 1 [IRAK1], and TIR-domain-containing adaptor protein [TIRAP]/MyD88 adapter-like [MAL]) (23). These interact with BTK to induce nuclear factor-κB (NFκB) activation, leading to activation, proliferation, antibody secretion, and proinflammatory cytokine production in B cells (23). Following FcγRI cross-linking, Src-kinases, SYK, PI3K-γ, and BTK are activated, while inhibitory Fc-receptors (e.g., FcγRIIB) recruit phosphatases and reduce BTK activation (23). However, it is not clear if BTK inhibition interferes with the signaling of these various receptors.

All covalently binding BTK inhibitors currently in clinical use irreversibly bind to the cysteine at position 481 (CYS-481), blocking the ATP binding pocket of BTK, preventing autophosphorylation at tyrosine residue 223 and full BTK activation (24). Ibrutinib is a highly potent, irreversible BTK inhibitor, which is rapidly absorbed following oral administration, with a pharmacodynamic profile that is maintained over a 24-hour period (25). Ibrutinib also irreversibly binds other kinases possessing an analogous cysteine with varying affinity (interleukin-2-inducible T-cell kinase [ITK] and tyrosine kinase expressed in hepatocellular carcinoma [TEC]-family kinases), thereby potentially disrupting normal T-cell, macrophage, and platelet function (15, 24, 26, 27). These off-target effects may influence the AE profile associated with ibrutinib therapy (26) (**Figure 1**); bleeding is attributed to effects on BTK and TEC; rash and diarrhea are possibly related to effects on epidermal growth factor receptor (EGFR), while a molecular target leading to the development of atrial fibrillation has been shown to be the C-terminal Src kinase (CSK) (28) (**Figure 1**).

Based on the toxicity profile observed with ibrutinib, more selective second-generation BTK inhibitors were developed for the treatment of hematological malignancies (7, 24). Acalabrutinib is a highly selective, potent, second-generation BTK inhibitor, with reduced off-target activity (12, 15), rapid absorption, and a short pharmacokinetic half-life (15). An advantage of a short half-life is that there is no lasting impact upon noncovalently bound enzymes. Furthermore, acalabrutinib has an extended pharmacodynamic

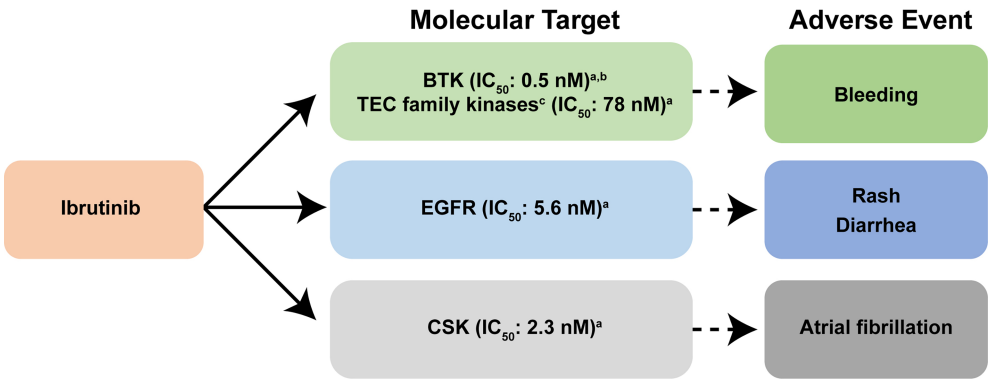

FIGURE 1 | Reported molecular targets of ibrutinib and their associated adverse events. In addition to covalently binding to BTK, ibrutinib also targets other cellular processes regulated by other kinases including EGFR, and TEC family kinases, thereby disrupting normal T-lymphocyte, macrophage, and platelet function (15, 24, 26). Ibrutinib also inhibits other enzymes that contain cysteine residues that are homologous to CYS-481 present within BTK (27). Collectively, these additional off-target effects on cellular process are thought to influence the adverse event profile associated with ibrutinib therapy (26). Bleeding is attributed to effects on BTK and TEC family proteins; rash and diarrhea are related to effects on EGFR; and the molecular target leading to the development of atrial fibrillation is CSK (28). [a]Data are from reference (29). [b]Data are from reference (30). [c]Kinases that contain a cysteine residue that aligns with CYS-481 are present in BTK (29). BTK, Bruton tyrosine kinase; CSK, C-terminal Src kinase; EGFR, epidermal growth factor receptor; IC_{50}, the half maximal inhibitory concentration; TEC, tyrosine kinase expressed in hepatocellular carcinoma.

response (15), such that in patients with B cell malignancies, a 100-mg dose of acalabrutinib every 12 hours led to a mean steady-state BTK occupancy of ≥95% in peripheral blood cells, which was maintained over the 12-hour period, thereby ensuring BTK inhibition during the entire dosing period (7). Acalabrutinib, and its major active metabolite, ACP-5862, form a covalent bond with the CYS-481 residue in the active site of BTK, thereby irreversibly inhibiting BTK enzymatic activity (7, 31). In preclinical studies, acalabrutinib inhibited BTK-mediated activation of downstream signaling proteins; and in mouse xenograft models, acalabrutinib inhibited malignant B cell proliferation and tumor growth (7). Further, acalabrutinib does not inhibit Src-family kinases, and demonstrated less inhibition of TEC kinases compared with that observed with ibrutinib, and displayed no *in vitro* activity against EGFR or ERBB2 (27) (**Table 1**), consistent with a low frequency of skin rash and diarrhea (27). However, exposure of acalabrutinib is decreased in the presence of proton-pump inhibitors (PPIs), with a 43% reduction in the area under the concentration-time curve (AUC) observed with coadministration of 40 mg omeprazole for 5 days (7). Consequently, patients are advised to avoid coadministration of acalabrutinib with PPIs (7).

The mean steady-state BTK occupancy by zanubrutinib in peripheral blood was maintained at 100% over 24 hours at a dose of 320 mg once daily in patients with B cell malignancies (9). *In vitro* half-maximal inhibitory concentration (IC_{50}) values for zanubrutinib for off-target kinases and BTK are presented in **Table 1** (32). The median T_{max} of zanubrutinib is 2 hours, and mean half-life is 2–4 hours following a single oral dose of 160 mg or 320 mg. No clinically significant differences in the pharmacokinetics of zanubrutinib were observed when coadministered with PPIs (9).

TABLE 1 | A comparison of half maximal inhibitory concentrations of BTK and members of the TEC protein kinase family by acalabrutinib, ibrutinib, and zanubrutinib.

Kinase	Acalabrutinib IC_{50} (nM)[a]	Ibrutinib IC_{50} (nM)[a]	Zanubrutinib IC_{50} (nM)[b]
BLK	>1000	0.1 + 0.0	1.13[c]
BMX	46 ± 12	0.8 ± 0.1	0.62[c]
BTK	5.1 ± 1.0	1.5	0.3 ± 0.06
EGFR	>1000	5.3 ± 1.3	2.6 ± 1.0[c]
ERBB2	~1000	6.4 ± 1.8	530 ± 273
ERBB4	16 ± 5	3.4 ± 1.4	1.58[c]
ITK	>1000	4.9 ± 1.25	56 ± 12
JAK3	>1000	32 ± 15.0	580 ± 21
TEC	126 ± 11	10 ± 2.0	2.0 ± 0.8
TXK	368 ± 141	2.0 ± 0.3	2.95[c]

[a]Data are reproduced with permission from reference (27), and are presented as the mean ± SD of at least 3 independent experiments.
[b]Data are reproduced with permission from reference (32) and represent triplicate determinations except where noted.
[c]n = 1 determination.
B-lymphoid tyrosine kinase; BMX, bone marrow kinase on X; BTK, Bruton tyrosine kinase; BLK, EGFR, epidermal growth factor receptor; ERBB2, Erb-B2 receptor tyrosine kinase; ERBB4, Erb-B4 receptor tyrosine kinase; IC_{50}, half-maximal inhibitory concentration; ITK, interleukin-2 inducible T-cell kinase; JAK3, Janus kinase 3; TEC, tyrosine kinase expressed in hepatocellular carcinoma; TXK, nonreceptor tyrosine protein kinase encoded by the TXK gene.

ADVERSE EVENTS ASSOCIATED WITH BTK INHIBITOR THERAPY OBSERVED IN CLINICAL TRIALS

The efficacy and safety of ibrutinib was evaluated in 3 pivotal phase 3 trials: RESONATE (5), RESONATE-2 (3), and ILLUMINATE (33).

RESONATE (PCYC-1112), a multicenter, open-label, phase 3 study in patients with R/R CLL, compared the efficacy and safety of ibrutinib versus the anti-CD20 antibody, ofatumumab (5). The median age of patients was 67 years (range, 30–86) (5). At a median follow-up point of 9.4 months, the most common AEs of any grade occurring in >20% of patients following ibrutinib monotherapy were diarrhea (48%), fatigue (28%), nausea (26%), pyrexia (24%), anemia (23%), and neutropenia (22%) (5). The most common grade ≥3 AEs occurring in ≥5% of patients were neutropenia (16%), pneumonia (7%), thrombocytopenia (6%), and anemia (5%) (5). In addition, atrial fibrillation (any grade) was noted in 5% of ibrutinib-treated patients; and grade ≥3 atrial fibrillation occurred in 3% of ibrutinib-treated patients (5). A subdural hematoma was noted in 1 patient as an AE of interest following ibrutinib monotherapy (5).

RESONATE-2 (PCYC-1115-CA) was a multicenter, open-label, randomized, phase 3 study to evaluate the efficacy and safety of ibrutinib compared with chlorambucil in treatment-naïve patients with CLL who were ≥65 years of age (3). The median age of patients in the ibrutinib-treated group was 73 years (range, 65–89) (3). At a median follow-up point of 18.4 months, the most common AEs of any grade were consistent with those observed in RESONATE (diarrhea, 42%; fatigue, 30%; cough, 22%; and nausea, 22%) (3). Grade ≥3 AEs were neutropenia (10%), anemia (6%), hypertension (4%), pneumonia (4%), and diarrhea (4%) (3). Atrial fibrillation was noted in 6% of patients in the ibrutinib-treated group (grade 2, n = 6; grade 3, n = 2) (3).

ILLUMINATE, a multicenter, randomized, open-label, phase 3 study, evaluated the efficacy and safety of ibrutinib plus obinutuzumab versus chlorambucil plus obinutuzumab in treatment-naïve patients with CLL/SLL, aged either ≥65 or <65 years (33). Overall median age was 71 years (range, 66–76), and 81% of the patients in the ibrutinib plus obinutuzumab group were ≥65 years of age (33). After a median follow-up duration of 31.3 months, the most common grade ≥3 treatment-emergent AEs occurring in ≥5% of patients in the ibrutinib plus obinutuzumab group were neutropenia (36%), thrombocytopenia (19%), pneumonia (7%), and atrial fibrillation (5%) (33). Serious ibrutinib-related AEs occurred in 27% of patients in the ibrutinib plus obinutuzumab group; these AEs were pneumonia (n=5), atrial fibrillation (n=5), and febrile neutropenia (n=4) (33). An ibrutinib treatment-related death was reported in 1 patient in the ibrutinib plus obinutuzumab group (33).

The efficacy and safety of acalabrutinib in patients with CLL were investigated in 2 pivotal phase 3 studies: ELEVATE-TN (13) and ASCEND (12).

ELEVATE-TN was a randomized, multicenter, open-label, controlled study that compared the efficacy and safety of acalabrutinib monotherapy, acalabrutinib plus obinutuzumab, and obinutuzumab plus chlorambucil (1:1:1) in treatment-naïve patients with CLL (13). The median age across treatment groups was 70 years (range, 66–75); 84% of patients were aged ≥65 years (13). After a median follow-up of 28.3 months, the most common AEs of any grade observed for acalabrutinib monotherapy included headache (37%), diarrhea (35%), fatigue (18%), cough (18%), upper respiratory tract infection (18%), arthralgia (16%), and contusion (15%) (13). AEs of grade ≥3 severity that occurred with acalabrutinib monotherapy included neutropenia (10%), anemia (7%), thrombocytopenia (3%), urinary tract infection (2%), pneumonia (2%), dyspnea (2%), headache (1%), fatigue (1%), and back pain (1%) (13). In patients who received acalabrutinib monotherapy, predefined events of clinical interest included atrial fibrillation (4%), any-grade hypertension (5%), grade ≥3 hypertension (2%), and bleeding events (any grade: 39%; grade 1–2: 37%); the most common of which were contusion (15%) and petechiae (9%) (13). Grade ≥3 bleeding events occurred in 2% of patients (13). In total, 9% (16/179) of patients discontinued acalabrutinib treatment because of AEs (e.g., acute myocardial infarction, brain injury, cardiac failure, and fatigue, n=1 each) (13).

The incidence of grade ≥3 AEs in patients receiving acalabrutinib plus obinutuzumab was 70% compared with 50% for patients receiving acalabrutinib monotherapy (13). Grade ≥3 neutropenia was 3 times more frequent in patients treated with acalabrutinib plus obinutuzumab (30%) compared with patients treated with acalabrutinib monotherapy (10%) (13). Grade 4–5 neutropenia occurred in 20% of patients receiving acalabrutinib plus obinutuzumab compared with 6% of patients receiving acalabrutinib monotherapy (13). In addition, grade ≥3 thrombocytopenia occurred in 8% of patients receiving acalabrutinib plus obinutuzumab compared with 3% of those receiving acalabrutinib monotherapy; and grade ≥3 pneumonia occurred in 6% of patients receiving acalabrutinib plus obinutuzumab compared with 2% in patients who received acalabrutinib monotherapy (13). Predefined events of clinical interest in the acalabrutinib plus obinutuzumab group included atrial fibrillation and grade ≥3 hypertension (3% each) (13).

ASCEND, a randomized phase 3 trial, compared the efficacy and safety of acalabrutinib monotherapy versus intestigator's choice of idelalisib plus rituximab or bendamustine plus rituximab in patients with R/R CLL (12). The median age across treatment groups was 67 years (range, 32–90); 22% of patients in the acalabrutinib group were aged ≥75 years (12). In patients who received acalabrutinib monotherapy, the most common AEs of any grade were headache (22%), neutropenia (19%), diarrhea (18%), cough (15%), upper respiratory tract infection and anemia (14% each), after a median follow-up of 16.1 months (12). In total, 82% of patients had ≥1 treatment-emergent AE of clinical interest, which included infection (57%), atrial fibrillation (5%), hepatotoxicity (5%), hypertension (3%), and major bleeding (2%) (12). Additionally, 19% (30/155) of patients discontinued treatment, 11% (17/155) were ascribed to an AE (e.g., alanine aminotransferase level increased, headache, respiratory tract infection, n=1 each) (12).

Recently, mature results from the phase 2 ACE-CL-001 study provided the longest duration safety follow-up data for

acalabrutinib in treatment-naïve and R/R patients with CLL with a median follow-up of 53 months and 41 months, respectively (14, 15). The median age of the patients with treatment-naïve CLL in this study was 64 years (range, 33–85) (14); and 66 years (range, 42–85) for patients with R/R CLL (20% of whom were aged ≥75 years) (15). In treatment-naïve patients, the most common AEs of any grade were diarrhea (51%), headache (45%), upper respiratory tract infection (44%), arthralgia (42%), and contusion (42%) (14). Any-grade and grade ≥3 severity AEs of clinical interest included infection (84% and 15%, respectively), bleeding event (66%/3%), and hypertension (22%/11%) (14). Atrial fibrillation (all grades) occurred in 5% of treatment-naïve patients (14). Serious AEs were reported in 38% of treatment-naïve patients, including pneumonia (n=4) and sepsis (n=3) (14). In total, 6% of patients discontinued due to an AE (14). No new long-term safety issues were reported in treatment-naïve patients (14). In patients with R/R CLL, most AEs were mild or moderate and included: diarrhea (all grades: 52%; grade 1: 31%; grade 2: 16%; grade 3: 5%), headache (all grades: 51%; grade 1: 44%; grade 2; 7%), upper respiratory tract infection (all grades: 37%; grade 1: 10%; grade 2: 26%; grade 3: 1%), and fatigue (all grades: 31%; grade 1: 17%; grade 2: 13%; grade 3: 3%) (15). Treatment discontinuation occurred in 11% of patients due to AEs, including infections that occurred early during treatment (15). No patients with R/R CLL discontinued acalabrutinib treatment because of atrial fibrillation, hypertension, or bleeding events (15).

The phase 3 head-to-head comparison to evaluate the efficacy and safety of acalabrutinib versus ibrutinib in previously treated patients with high-risk CLL was recently completed (NCT02477696; ELEVATE-RR) (34). Patient median age was 66 years (range, 28–89) (34). The results demonstrated that acalabrutinib met the primary efficacy endpoint with noninferior PFS compared to ibrutinib in previously treated patients with high-risk CLL after a median follow-up period of 40.9 months (range, 0.0–59.1) (34). The key secondary endpoint for safety was also met, with a statistically significant lower incidence of atrial fibrillation with acalabrutinib compared to that seen with ibrutinib (9.4% *vs* 16.0%, $P = 0.02$) (34). Acalabrutinib treatment was also associated with a lower incidence of any-grade hypertension compared with ibrutinib (8.6% *vs* 22.8%), as well as incidences of arthralgia (15.8% *vs* 22.8%) and diarrhea (34.6% *vs* 46.0%), but there was a higher incidence of headache (34.6% *vs* 20.2%) and cough (28.9% *vs* 21.3%) (34). Overall, AEs leading to discontinuation were numerically lower in acalabrutinib-treated patients compared with ibrutinib-treated patients (14.7% *vs* 21.3%) (34).

In a phase 2 single-arm study, zanubrutinib was generally well tolerated by Chinese patients with R/R CLL/SLL (median age, 61 years [range, 35–87]), after a median follow-up period of 15.1 months (range, 0.8 to 21.1) (11). The most common grade ≥3 AEs were neutropenia (44%), thrombocytopenia (15.4%), lung infection/pneumonia (13.2%), upper respiratory infection (9.9%), and anemia (8.8%) (11). Eight (9%) patients discontinued zanubrutinib treatment due to AEs, and 7 (8%) patients required ≥1 dose reduction (11).

The SEQUOIA trial (NCT03336333), an open-label, global, multicenter, phase 3 study, included a nonrandomized cohort of treatment-naïve patients with del(17p) CLL/SLL who were treated with zanubrutinib 160 mg twice daily (10). Patient median age was 70 years (range, 42–86) (10). After a median follow-up period of 18.2 months (range, 5.0–26.3 months), AEs (of any grade; reported in ≥10% of treated patients) were contusion (20.2%), upper respiratory tract infection (19.3%), neutropenia/neutrophil count decreased (17.4%), diarrhea (16.5%), nausea (14.7%), constipation (13.8%), rash (13.8%), back pain (12.8%), cough (11.9%), arthralgia (11.0%), and fatigue (10.1%) (10). Grade ≥3 AEs occurring in ≥2% of patients were neutropenia/neutrophil count decreased (12.8%) and pneumonia (3.7%) (10). AEs of interest (any grade) reported in ≥10% of patients were infections (64.2%; grade ≥3, 13.8%), minor bleeding (26.6%), bruising (24.8%), neutropenia (18.3%; grade ≥3, 13.8%), diarrhea (15.6%; grade ≥3, 0.9%), nausea (13.8%), arthralgia (11.0%), and fatigue (10.1%; grade ≥3, 0.9%) (10). Dermatological malignancies were reported in 9.2% of patients, and nonskin second malignancies were reported in 4.6% of patients (10). Atrial fibrillation was reported in 3 (2.8%) patients, 2 events of which occurred in the setting of sepsis (10). Four (3.7%) patients discontinued zanubrutinib due to AEs (i.e., pneumonia, sepsis secondary to pseudomonas, melanoma, and acute renal failure [associated with disease progression]), and 2 of these patients died (10). No sudden deaths or deaths of unknown cause were reported (10).

The ALPINE trial was an open-label, global, randomized, phase 3 study that compared zanubrutinib versus ibrutinib treatment in patients with R/R CLL/SLL (NCT03734016) (35, 36). Data from a pre planned interim analysis for the first 12 months after randomization of the first 415 patients was recently reported (35, 36). Patients ≥65 years of age comprised 62.3% of the zanubrutinib-treated group and 61.5% of the ibrutinib-treated group (35). With a median follow-up period of 15 months, grade ≥3 AEs occurred in 55.9% of patients in the zanubrutinib group compared with 51.2% of patients in the ibrutinib group (37). Atrial fibrillation/flutter, a prespecified safety endpoint, was observed at lower rates in patients in the zanubrutinib group versus the ibrutinib group (2.5% *vs* 10.1%, respectively, $P = 0.0014$) (35). Rates of other AEs that were lower in the zanubrutinib group versus the ibrutinib group included major bleeding (2.9% *vs* 3.9%), cardiac disorders of any grade (13.7% *vs* 25.1%) or grade ≥3 (2.5% *vs* 6.8%), and AEs leading to discontinuation (7.8% *vs* 13.0%) or death (3.9% *vs* 5.8%), respectively (35, 37). The rate of neutropenia was higher with zanubrutinib versus ibrutinib treatment (28.4% *vs* 21.7%, respectively); however, grade ≥3 infections were lower with zanubrutinib than with ibrutinib (12.7% *vs* 17.9%, respectively) (35). Because this is an interim analysis, additional data are needed before these results can be fully evaluated.

MANAGING BTK INHIBITOR-INDUCED AEs IN CLINICAL PRACTICE

Headache, occurring in 22% to 51% of patients, is the most common AE experienced by patients receiving acalabrutinib therapy (12, 13, 15). Acalabrutinib treatment-related headaches usually occur early in the course of treatment, are mild, and of

limited duration (38). These headaches typically occur within 30 minutes of dosing and in many cases do not need medical intervention, or can be effectively managed with acetaminophen or caffeine, while avoiding the use of nonsteroidal anti-inflammatory drugs (NSAIDs), if possible (**Table 2**) (39). Only 1% of headaches lead to treatment discontinuation (12). In clinical practice, patient education prior to initiation of therapy (i.e., advising that acalabrutinib-induced headaches are easily managed and should abate over a period of up to 4 weeks) helps to reassure the patient that it is not a long-term consequence. The mechanism(s) for these headaches is unclear, but could include calcitonin gene-related peptide (CGRP) agonism, which is of interest given the new class of migraine medications designed to work by antagonizing CGRP (42).

Atrial fibrillation has been reported in 6%–10% of untreated patients with CLL (43–45). Furthermore, the prevalence of atrial fibrillation increases with age (46). In clinical trials, the incidence rate of atrial fibrillation with ibrutinib treatment, after a 9-month follow-up, was 3% (5), and 6% after a median follow-up of 18 months (3); the 2-year incidence rate—based on randomized and observational studies—was estimated at between 10%–16% (44, 47). With a follow-up ranging from 14 to 28 months in clinical trials, the incidence rate of atrial fibrillation with acalabrutinib was approximately 0%–5% (12, 13, 48), with a time to onset of atrial fibrillation in the range of 23 days to >1–3 years after treatment initiation (15). The slope is slightly higher in the first 6 months, but is then stable, perhaps suggesting minimal risk associated with drug initiation. Monitoring for atrial fibrillation while receiving acalabrutinib therapy is indicated (7). Appropriate management of atrial fibrillation, such as the administration of direct oral anticoagulants, is recommended without necessarily withholding acalabrutinib, and discontinuation should be considered if the atrial fibrillation is not medically controllable (**Table 2**) (39).

Grade ≥3 hypertension was reported in 38% of patients treated with ibrutinib, including 18% in patients who did not have previous hypertension at baseline (49). In contrast, grade ≥3 hypertension was reported in 2%–7% of patients treated with acalabrutinib, with a median follow-up ranging from 14 to 28 months (12, 13, 48). Further, the updated results from the long-term follow-up (41 months) of the ACE-CL-001 phase 2 study, reported that 18% of patients experienced hypertension (all grades), 10% of which were grade 1–2, and 7% were grade ≥3 (15). In patients treated with ibrutinib, hypertension (all grades) was observed in 14% of patients; 4% of which were grade 3, after a median follow-up of 18 months (3). Patients should be monitored for treatment-emergent hypertension, which should be managed with antihypertensive medication (**Table 2**). It should be noted that antihypertensive medication dosages may need to be adjusted once any BTK inhibitor therapy is discontinued.

Although a moderate incidence of diarrhea was reported with acalabrutinib treatment in clinical trials and in a long-term follow-up study (18%–52%) (12, 13, 15), it appeared not to be drug-related. Diarrhea usually resolves quickly without the need for further intervention. If intervention is required, patients can be simply treated with an antidiarrheal medication (e.g., loperamide) (**Table 2**) (40).

Thrombocytopenia is frequently observed in patients with unfavorable biological risk factors for CLL, and is commonly caused by splenomegaly, bone marrow failure secondary to tumor infiltration, recent chemotherapy, or megakaryocyte dysplasia (50).

TABLE 2 | Management of adverse events associated with BTK inhibitor therapy.

Adverse Event	Management Strategy	References
Atrial fibrillation	• Monitor for atrial fibrillation during treatment • Administer direct oral anticoagulants • Discontinue BTK inhibitor therapy if atrial fibrillation is not medically controllable	(7, 39)
Bleeding events	• Monitor for signs of bleeding • Use direct oral anticoagulants if anticoagulation therapy is needed • Withhold BTK inhibitor for 3 to 7 days before and after surgery, depending upon the type of surgery, and the risk of a bleeding event	(7)
Diarrhea	• Use antidiarrheal medication (e.g., loperamide) as needed	(40)
Headache	• Prior to treatment initiation: advise patients that headaches should abate quickly, are easily managed, and are not a long-term consequence of treatment • After treatment initiation: recommend the use of acetaminophen or caffeine and avoid NSAIDs if possible	(39)
Hypertension	• Monitor for treatment-emergent hypertension • Manage with antihypertensive medication • Reduce antihypertensive medication dose once BTK inhibitors are discontinued	
Infection	• Consider prophylaxis for patients at increased risk of opportunistic infection • Monitor for signs and symptoms • Treat as needed	(1, 7, 9)
Musculoskeletal pain (myalgia, arthralgia, etc)	• Grade 1 myalgias/arthralgias may not need intervention • Dose reduction or dose interruption should be used as appropriate	(41)
Neutropenia	• First to third occurrence of grade 3 or 4: dose interruptions are recommended • Fourth occurrence: discontinuation of BTK inhibitor is recommended	(7, 9)
Thrombocytopenia	• First to third occurrence of grade 3 or 4: dose interruptions are recommended • Fourth occurrence: discontinuation of BTK inhibitor is recommended (unless thrombocytopenia is related to CLL infiltration of the bone marrow)	(7)

BTK, Bruton tyrosine kinase; CLL, chronic lymphocytic leukemia; NSAID, nonsteroidal anti-inflammatory drug.

In patients with CLL who were treated with acalabrutinib monotherapy, thrombocytopenia of any grade and grade ≥3 were reported in 7%–11% and 3%–4% of patients, respectively (12, 13). In patients with R/R CLL who were treated with zanubrutinib, all-grade and grade ≥3 thrombocytopenia was reported in 42% and 15% of patients, respectively (11). Thrombocytopenia (all grades) was reported in 6% of patients with treatment-naïve CLL who were treated with zanubrutinib, with 1% of cases of grade ≥3 severity (10). Dose interruptions are recommended for the first to third occurrences of grade 3 or 4 thrombocytopenia, and dose discontinuation is recommended for the fourth occurrence, unless thrombocytopenia is related to CLL infiltration of the marrow (**Table 2**) (7, 9).

Neutropenia is also commonly observed in patients treated with BTK inhibitors due to an on-target toxicity effect (11). Between 10%–16% of patients treated with acalabrutinib monotherapy developed grade ≥3 neutropenia, although this number can be higher with combination therapies (e.g., 30% of patients experienced grade ≥3 neutropenia when treated with acalabrutinib plus obinutuzumab) (12, 13, 26). When treated with ibrutinib, 10% of patients experienced grade ≥3 neutropenia (3); and 44% of patients treated with zanubrutinib experienced grade ≥3 neutropenia (11). As with thrombocytopenia, dose interruptions are recommended for the first to third occurrences of grade 3 or 4 neutropenia, and dose discontinuation is recommended after a fourth occurrence (**Table 2**) (7, 9).

Infections were common in patients with CLL who were treated with zanubrutinib; 39% of patients with R/R CLL reported ≥1 grade ≥3 infection (11), and 64% of patients with treatment-naive CLL reported an infection of any grade, 13.8% of which were grade ≥3 (10). Most were respiratory tract infections and were effectively managed without the need for a dose reduction or treatment discontinuation (11). Grade ≥3 infections occurred at similar rates in patients receiving acalabrutinib monotherapy (14%) (13). However, 17.9% of ibrutinib-treated patients developed grade ≥3 infections (35). Prophylactic treatment should be considered for patients at a higher risk of developing opportunistic infections, and all patients should be monitored for signs and symptoms of infection and treated promptly (**Table 2**) (1, 7, 9).

Monitoring for signs of bleeding is important in patients receiving acalabrutinib therapy (7). Data suggest that BTK inhibitors increase the risk of bleeding by impairing collagen-induced platelet activation, akin to the effects of aspirin (51, 52). Inhibition of Src-kinases is suggested to be associated with bleeding (52). Acalabrutinib has less inhibitory potential with respect to Src-family kinases compared with that seen with ibrutinib (**Table 1**) (27). Preliminary studies suggest that BTK and TEC kinases have overlapping roles in platelets, which would explain why patients with XLA do not demonstrate a bleeding phenotype (53, 54). In ibrutinib-treated and acalabrutinib-treated patients, BTK and TEC kinases are both irreversibly inhibited (52). The lower affinity of acalabrutinib for TEC kinase (53) may preserve some platelet activity. Further, differences in bleeding events may be related to a greater selectivity of acalabrutinib for BTK over TEC compared to ibrutinib (54). Minor bleeding tends to be less evident, and patients treated with acalabrutinib report fewer minor bleeding occurrences. There is also evidence that major bleeding events are rare in patients treated with acalabrutinib (54). However, in our experience, the risk for a major bleeding event is equal for both acalabrutinib and ibrutinib. The risk of bleeding in acalabrutinib-treated patients can be mitigated as for those treated with ibrutinib. Further, in patients with treatment-naive CLL, grade 1/2 minor bleeding was observed in 27% of patients, and grade ≥3 major bleeding was observed in 5% of patients—2 of whom experienced a grade 3 major bleeding event following a surgical procedure for which there was no per protocol dose hold (10). Minor bleeding events were relatively common in patients with R/R CLL treated with zanubrutinib: 1% of patients experienced grade 1-2 major bleeding, and 1% of patients experienced grade ≥3 major bleeding (gastrointestinal hemorrhage following diagnosis of colon cancer, and posttraumatic right-thalamic hemorrhage) (11). Patients treated with warfarin were excluded early from the ibrutinib studies after complications, and, as such, coadministration of warfarin and acalabrutinib has not been studied. Jones and colleagues assessed the use of anticoagulant or antiplatelet agents and bleeding events in patients with CLL who were treated with ibrutinib monotherapy in 2 multicenter studies (55). In the PCYC-1102 study (median follow-up of 22 months), 9% of patients who received ibrutinib treatment plus an anti-coagulant agent and 4% who received ibrutinib plus an antiplatelet agent reported a major bleeding event (55). In the RESONATE study with a median follow-up of 10 months, 2% and 1% of patients, respectively, reported a major bleeding event (55). Major bleeding events in these patients were typically observed in conjunction with other factors (i.e., coexisting medical conditions, concurrent medications) (55). Therefore, the risk-versus-benefit profile for coadministration of a BTK inhibitor with antiplatelet or anticoagulant therapy should be carefully considered, and the patient should be monitored for signs of bleeding (**Table 2**) (7, 39). If anticoagulation therapy is required, we generally prefer to use direct oral anticoagulants (**Table 2**). In addition, we recommend withholding acalabrutinib administration for 3 to 7 days before and after surgery, depending upon the type of surgery, and the potential risk of a bleeding event (**Table 2**) (7).

Although musculoskeletal pain, including myalgias and arthralgias, is a less serious AE reported with BTK inhibitor therapy, it can be troublesome for the patient and lead to treatment discontinuation (11, 41). Musculoskeletal pain is one of the most common AEs (i.e., occurring in ≥30% of patients) observed with ibrutinib treatment (1). A retrospective analysis of patients with CLL who received ibrutinib treatment reported that 36% of patients developed new or worsening arthralgias/myalgias, with a median time to occurrence of 34.5 months (41). Musculoskeletal pain, of any grade, was reported in 14% of patients treated with zanubrutinib, with grade ≥3 AEs observed in 3.4% (9), and myalgia was also observed in acalabrutinib-treated patients (all grades, 21%; grade ≥3, 0.8%) (7). Interrupting ibrutinib therapy, as recommended, alleviated symptoms in 14% of patients, while a dose reduction alleviated symptoms in 60% of patients (41). Although avoiding the use of NSAIDs has been recommended

because this class of drugs may exacerbate the risk of bleeding, 50% of patients who used NSAIDs reported improvements in arthralgia/myalgia symptoms (41). Additionally, 54% of patients who developed arthralgias/myalgias had spontaneous resolution of their symptoms with no changes to ibrutinib treatment, although most patients had grade 1 arthralgias/myalgias (41). Ultimately 22% of patients with arthralgias/myalgias discontinued ibrutinib treatment; however, this increased to 63% in patients with grade 3 events (41).

DISCUSSION

Treatment options for patients with CLL have evolved considerably over recent years (39). Small-molecule inhibitor-based therapies have significantly improved PFS outcomes in patients with CLL compared with chemoimmunotherapy outcomes, especially in patients with high-risk disease characteristics (e.g., del(17p) or *TP53* mutations) (39, 56, 57). Current National Comprehensive Cancer Network and the European Society for Medical Oncology practice guidelines recommend that first-line treatment for patients with CLL should be based on the presence or absence of del(17p) or mutated *TP53*, regardless of patient age and comorbidities (39, 58), and preference should be given to small molecules. The shift from chemoimmunotherapy to oral targeted therapy provides patients with CLL/SLL convenient options with fewer toxicities. However, since oral therapy can be administered away from the clinic, there must be vigilant monitoring of safety considerations and thorough adverse event management.

Acalabrutinib is well-tolerated and associated with low rates of treatment discontinuation due to AEs [8, 9, 18], which may provide some advantages in routine practice. However, patients taking proton-pump inhibitors might have impaired absorption of acalabrutinib (7).

Long-term data from the phase 2 ACE-CL-001 study reaffirmed that acalabrutinib monotherapy for patients with treatment-naïve and R/R CLL provided durable responses with a favorable safety profile, with no new safety concerns reported (14, 15). Several clinically relevant AEs considered to be associated with BTK inhibition in the clinical setting appear to be present at a low frequency in patients treated with acalabrutinib. The most common AE associated with the use of acalabrutinib is a headache (12, 13, 26). Headaches are mild, easily managed, and of limited duration, lasting only a few days (39, 59).

Zanubrutinib is associated with an overall favorable safety profile, with a low incidence of major bleeding or arrythmias observed in patients with CLL (60). The National Comprehensive Cancer Network guidelines recommend the use of zanubrutinib as a first-line or second-line therapy for patients with CLL/SLL with del (17p)/*TP53* mutations who have a contraindication to other BTK inhibitors, and as second-line and subsequent therapy for patients without del(17p)/*TP53* mutations who are intolerant of, or have a contraindication to, other BTK inhibitors (61). However, zanubrutinib is currently approved by the FDA only for the treatment of MCL in patients who have received ≥1 prior therapy (9).

In summary, BTK inhibitors are highly effective options for the treatment of patients with CLL, and selection is driven by patient and physician personal choice, as well as available efficacy and tolerability data from clinical trials and clinician experience. Acalabrutinib is safe and effective and provides an additional FDA-approved option for the treatment of patients with CLL.

AUTHOR CONTRIBUTIONS

All authors contributed to the discussion of the content, reviewed each draft, and approved the final version for submission.

ACKNOWLEDGMENTS

Medical writing and editorial support, conducted in accordance with Good Publication Practice 3 (GPP3) and the International Committee of Medical Journal Editors (ICMJE) guidelines, were provided by Marie-Louise Ricketts, PhD, of Oxford PharmaGenesis Inc., Newtown, PA, and funded by AstraZeneca, Gaithersburg, MD.

REFERENCES

1. *Imbruvica® (Ibrutinib) [Prescribing Information]*. Sunnyvale, CA: Pharmacyclics LLC (2020).
2. *Imbruvica® [Summary of Product Characteristics]*. Beerse, Belgium: Janssen-Cilag International NV (2021).
3. Burger JA, Tedeschi A, Barr PM, Robak T, Owen C, Ghia P, et al. Ibrutinib as Initial Therapy for Patients With Chronic Lymphocytic Leukemia. *N Engl J Med* (2015) 373:2425–37. doi: 10.1056/NEJMoa1509388
4. Dreyling M, Jurczak W, Jerkeman M, Silva RS, Rusconi C, Trneny M, et al. Ibrutinib Versus Temsirolimus in Patients With Relapsed or Refractory Mantle-Cell Lymphoma: An International, Randomised, Open-Label, Phase 3 Study. *Lancet* (2016) 387:770–8. doi: 10.1016/S0140-6736(15)00667-4
5. Byrd JC, Brown JR, O'Brien S, Barrientos JC, Kay NE, Reddy NM, et al. Ibrutinib Versus Ofatumumab in Previously Treated Chronic Lymphoid Leukemia. *N Engl J Med* (2014) 371:213–23. doi: 10.1056/NEJMoa1400376
6. Byrd JC, Furman RR, Coutre SE, Flinn IW, Burger JA, Blum K, et al. Ibrutinib Treatment for First-Line and Relapsed/Refractory Chronic Lymphocytic Leukemia: Final Analysis of the Pivotal Phase Ib/II PCYC-1102 Study. *Clin Cancer Res* (2020) 26:3918–27. doi: 10.1158/1078-0432.CCR-19-2856
7. *Calquence® (Acalabrutinib) [Prescribing Information]*. Wilmington, DE: AstraZeneca Pharmaceuticals LP (2019).
8. *AstraZeneca. Calquence Recommended for Approval in the EU by CHMP for Chronic Lymphocytic Leukaemia* (2020). Available at: https://www.astrazeneca.com/media-centre/press-releases/2020/calquence-recommended-for-approval-in-the-eu-by-chmp-for-chronic-lymphocytic-leukaemia.html (Accessed May 12, 2021).
9. *Brukinsa™ (Zanubrutinib) [Full Prescribing Information]*. San Mateo, CA: BeiGene USA, Inc (2019).
10. Tam CS, Robak T, Ghia P, Kahl BS, Walker P, Janowski W, et al. Zanubrutinib Monotherapy for Patients With Treatment Naive Chronic Lymphocytic Leukemia and 17p Deletion. *Haematologica* (2020) 106:2354–63. doi: 10.3324/haematol.2020.259432
11. Xu W, Yang S, Zhou K, Pan L, Li Z, Zhou J, et al. Treatment of Relapsed/Refractory Chronic Lymphocytic Leukemia/Small Lymphocytic Lymphoma With the BTK Inhibitor Zanubrutinib: Phase 2, Single-Arm, Multicenter Study. *J Hematol Oncol* (2020) 13:48. doi: 10.1186/s13045-020-00884-4

12. Ghia P, Pluta A, Wach M, Lysak D, Kozak T, Simkovic M, et al. ASCEND: Phase III, Randomized Trial of Acalabrutinib Versus Idelalisib Plus Rituximab or Bendamustine Plus Rituximab in Relapsed or Refractory Chronic Lymphocytic Leukemia. *J Clin Oncol* (2020) 38:2849–461. doi: 10.1200/JCO.19.03355
13. Sharman JP, Egyed M, Jurczak W, Skarbnik A, Pagel JM, Flinn IW, et al. Acalabrutinib With or Without Obinutuzumab Versus Chlorambucil and Obinutuzmab for Treatment-Naive Chronic Lymphocytic Leukaemia (ELEVATE TN): A Randomised, Controlled, Phase 3 Trial. *Lancet* (2020) 395:1278–91. doi: 10.1016/S0140-6736(20)30262-2
14. Byrd JC, Woyach JA, Furman RR, Martin P, O'Brien S, Brown JR, et al. Acalabrutinib in Treatment-Naive Chronic Lymphocytic Leukemia. *Blood* (2021) 137:3327–38. doi: 10.1182/blood.2020009617
15. Byrd JC, Wierda WG, Schuh A, Devereux S, Chaves JM, Brown JR, et al. Acalabrutinib Monotherapy in Patients With Relapsed/Refractory Chronic Lymphocytic Leukemia: Updated Phase 2 Results. *Blood* (2020) 135:1204–13. doi: 10.1182/blood.2018884940
16. Byrd JC, Furman RR, Coutre SE, Flinn IW, Burger JA, Blum KA, et al. Targeting BTK With Ibrutinib in Relapsed Chronic Lymphocytic Leukemia. *N Engl J Med* (2013) 369:32–42. doi: 10.1056/NEJMoa1215637
17. Tan C, Hiwa R, Mueller JL, Vykunta V, Hibiya K, Noviski M, et al. NR4A Nuclear Receptors Restrain B Cell Responses to Antigen When Second Signals Are Absent or Limiting. *Nat Immunol* (2020) 21:1267–79. doi: 10.1038/s41590-020-0765-7
18. Wen Y, Jing Y, Yang L, Kang D, Jiang P, Li N, et al. The Regulators of BCR Signalling During B Cell Activation. *Blood Sci* (2019) 1:119–29. doi: 10.1097/BS9.0000000000000026
19. Woyach JA, Bojnik E, Ruppert AS, Stefanovski MR, Goettl VM, Smucker KA, et al. Bruton's Tyrosine Kinase (BTK) Function is Important to the Development and Expansion of Chronic Lymphocytic Leukemia (CLL). *Blood* (2014) 123:1207–13. doi: 10.1182/blood-2013-07-515361
20. Vetrie D, Vořechovský I, Sideras P, Holland J, Davies A, Flinter F, et al. The Gene Involved in X-Linked Agammaglobulinaemia is a Member of the Src Family of Protein-Tyrosine Kinases. *Nature* (1993) 361:226–33. doi: 10.1038/361226a0
21. Tsukada S, Saffran DC, Rawlings DJ, Parolini O, Allen RC, Klisak I, et al. Deficient Expression of a B Cell Cytoplasmic Tyrosine Kinase in Human X-Linked Agammaglobulinemia. *Cell* (1993) 72:279–90. doi: 10.1016/0092-8674(93)90667-f
22. Ponader S, Burger JA. Bruton's Tyrosine Kinase: From X-Linked Agammaglobulinemia Toward Targeted Therapy for B-Cell Malignancies. *J Clin Oncol* (2014) 32:1830–9. doi: 10.1200/JCO.2013.53.1046
23. Pal Singh S, Dammeijer F, Hendriks RW. Role of Bruton's Tyrosine Kinase in B Cells and Malignancies. *Mol Cancer* (2018) 17:57. doi: 10.1186/s12943-018-0779-z
24. Wu J, Liu C, Tsui ST, Liu D. Second-Generation Inhibitors of Bruton Tyrosine Kinase. *J Hematol Oncol* (2016) 9:80. doi: 10.1186/s13045-016-0313-y
25. Parmar S, Patel K, Pinilla-Ibarz J. Ibrutinib (Imbruvica): A Novel Targeted Therapy for Chronic Lymphocytic Leukemia. *Pharm Ther* (2014) 39:483–519.
26. Awan FT, Schuh A, Brown JR, Furman RR, Pagel JM, Hillmen P, et al. Acalabrutinib Monotherapy in Patients With Chronic Lymphocytic Leukemia Who Are Intolerant to Ibrutinib. *Blood Adv* (2019) 3:1553–62. doi: 10.1182/bloodadvances.2018030007
27. Barf T, Covey T, Izumi R, van de Kar B, Gulrajani M, van Lith B, et al. Acalabrutinib (ACP-196): A Covalent Bruton Tyrosine Kinase Inhibitor With a Differentiated Selectivity and *In Vivo* Potency Profile. *J Pharmacol Exp Ther* (2017) 363:240–52. doi: 10.1124/jpet.117.242909
28. Xiao L, Salem JE, Clauss S, Hanley A, Bapat A, Hulsmans M, et al. Ibrutinib-Mediated Atrial Fibrillation Due to Inhibition of CSK. *Circulation* (2020) 142:2443–55. doi: 10.1161/CIRCULATIONAHA.120.049210
29. Honigberg LA, Smith AM, Sirisawad M, Verner E, Loury D, Chang B, et al. The Bruton Tyrosine Kinase Inhibitor PCI-32765 Blocks B-Cell Activation and Is Efficacious in Models of Autoimmune Disease and B-Cell Malignancy. *Proc Natl Acad Sci U.S.A.* (2010) 107:13075–80. doi: 10.1073/pnas.1004594107
30. Akinleye A, Chen Y, Mukhi N, Song Y, Liu D. Ibrutinib and Novel BTK Inhibitors in Clinical Development. *J Hematol Oncol* (2013) 6:59. doi: 10.1186/1756-8722-6-59
31. Herman SEM, Montraveta A, Niemann CU, Mora-Jensen H, Gulrajani M, Krantz F, et al. The Bruton Tyrosine Kinase (BTK) Inhibitor Acalabrutinib Demonstrates Potent on-Target Effects and Efficacy in Two Mouse Models of Chronic Lymphocytic Leukemia. *Clin Cancer Res* (2017) 23:2831–41. doi: 10.1158/1078-0432.CCR-16-0463
32. Guo Y, Liu Y, Hu N, Yu D, Zhou C, Shi G, et al. Discovery of Zanubrutinib (BGB-3111), A Novel, Potent, and Selective Covalent Inhibitor of Bruton's Tyrosine Kinase. *J Med Chem* (2019) 62:7923–40. doi: 10.1021/acs.jmedchem.9b00687
33. Moreno C, Greil R, Demirkan F, Tedeschi A, Anz B, Larratt L, et al. Ibrutinib Plus Obinutuzumab Versus Chlorambucil Plus Obinutuzumab in First-Line Treatment of Chronic Lymphocytic Leukaemia (iLLUMINATE): A Multicentre, Randomised, Open-Label, Phase 3 Trial. *Lancet Oncol* (2019) 20:43–56. doi: 10.1016/S1470-2045(18)30788-5
34. Byrd JC, Hillmen P, Ghia P, Kater AP, Chanan-Khan A, Furman RR, et al. Acalabrutinib Versus Ibrutinib in Previously Treated Chronic Lymphocytic Leukemia: Results of the First Randomized Phase III Trial. *J Clin Oncol* (2021), JCO2101210. doi: 10.1200/JCO.21.01210
35. Hillmen P, Eichhorst B, Brown JR, Lamanna N, O'Brien SM, Tam CS, et al. First Interim Analysis of ALPINE Study: Results of a Phase 3 Randomized Study of Zanubrutinib vs Ibrutinib in Patients With Relapsed/Refractory Chronic Lymphocytic Leukemia/Small Lymphocytic Lymphoma. *Eur Hematol Assoc* (2021).
36. Hillmen P, Brown JR, Eichhorst BF, Lamanna N, O'Brien SM, Qiu L, et al. ALPINE: Zanubrutinib Versus Ibrutinib in Relapsed/Refractory Chronic Lymphocytic Leukemia/Small Lymphocytic Lymphoma. *Future Oncol* (2020) 16:517–23. doi: 10.2217/fon-2019-0844
37. Helwick C. *Zanubrutinib vs Ibrutinib in Relasped/Refractory CLL/SLL: ALPINE Trial* (2021). Available at: https://ascopost.com/news/june-2021/zanubrutinib-vs-ibrutinib-in-relapsedrefractory-cllsll-alpine-trial/ (Accessed August 13, 2021).
38. Dolan S, Christofides A, Doucette S, Shafey M. Highlights From ASCO 2020: Updates on the Treatment of Chronic Lymphocytic Leukemia. *Curr Oncol* (2020) 27:e420–e32. doi: 10.3747/co.27.7009
39. Wierda WG, Byrd JC, Abramson JS, Bilgrami SF, Bociek G, Brander D, et al. Chronic Lymphocytic Leukemia/Small Lymphocytic Lymphoma, Version 4.2020, NCCN Clinical Practice Guidelines in Oncology. *J Natl Compr Canc Netw* (2020) 18:185–217. doi: 10.6004/jnccn.2020.0006
40. Badillo M, Nava D, Rosa M, Chen W, Guerrero M, Wang M. Acalabrutinib: Managing Adverse Events and Improving Adherence in Patients With Mantle Cell Lymphoma. *Clin J Oncol Nurs* (2020) 24:392–8. doi: 10.1188/20.CJON.392-398
41. Rhodes JM, LoRe VA3rd, Mato AR, Chong EA, Barrientos JC, Gerson JN, et al. Ibrutinib-Associated Arthralgias/Myalgias in Patients With Chronic Lymphocytic Leukemia: Incidence and Impact on Clinical Outcomes. *Clin Lymphoma Myeloma Leuk* (2020) 20:438–44 e1. doi: 10.1016/j.clml.2020.02.001
42. Carmine Belin A, Ran C, Edvinsson L. Calcitonin Gene-Related Peptide (CGRP) and Cluster Headache. *Brain Sci* (2020) 10:30. doi: 10.3390/brainsci10010030
43. Shanafelt TD, Parikh SA, Noseworthy PA, Goede V, Chaffee KG, Bahlo J, et al. Atrial Fibrillation in Patients With Chronic Lymphocytic Leukemia (CLL). *Leuk Lymphoma* (2017) 58:1630–9. doi: 10.1080/10428194.2016.1257795
44. Baptiste F, Cautela J, Ancedy Y, Resseguier N, Aurran T, Farnault L, et al. High Incidence of Atrial Fibrillation in Patients Treated With Ibrutinib. *Open Heart* (2019) 6:e001049. doi: 10.1136/openhrt-2019-001049
45. Larsson K, Mattsson M, Ebrahim F, Glimelius I, Hoglund M. High Prevalence and Incidence of Cardiovascular Disease in Chronic Lymphocytic Leukaemia: A Nationwide Population-Based Study. *Br J Haematol* (2020) 190:e245–e8. doi: 10.1111/bjh.16859
46. Aronow WS, Banach M. Atrial Fibrillation: The New Epidemic of the Ageing World. *J Atr Fibrillation* (2009) 1:154. doi: 10.4022/jafib.154
47. Ganatra S, Sharma A, Shah S, Chaudhry GM, Martin DT, Neilan TG, et al. Ibrutinib-Associated Atrial Fibrillation. *JACC Clin Electrophysiol* (2018) 4:1491–500. doi: 10.1016/j.jacep.2018.06.004
48. Byrd JC, Harrington B, O'Brien S, Jones JA, Schuh A, Devereux S, et al. Acalabrutinib (ACP-196) in Relapsed Chronic Lymphocytic Leukemia. *N Engl J Med* (2016) 374:323–32. doi: 10.1056/NEJMoa1509981
49. Dickerson T, Wiczer T, Waller A, Philippon J, Porter K, Haddad D, et al. Hypertension and Incident Cardiovascular Events Following Ibrutinib Initiation. *Blood* (2019) 134:1919–28. doi: 10.1182/blood.2019000840

50. Visco C, Barcellini W, Maura F, Neri A, Cortelezzi A, Rodeghiero F. Autoimmune Cytopenias in Chronic Lymphocytic Leukemia. *Am J Hematol* (2014) 89:1055–62. doi: 10.1002/ajh.23785
51. Goldmann L, Duan R, Kragh T, Wittmann G, Weber C, Lorenz R, et al. Oral Bruton Tyrosine Kinase Inhibitors Block Activation of the Platelet Fc Receptor CD32a (FcgammaRIIA): A New Option in HIT? *Blood Adv* (2019) 3:4021–33. doi: 10.1182/bloodadvances.2019000617
52. Series J, Garcia C, Levade M, Viaud J, Sié P, Ysebaert L, et al. Differences and Similarities in the Effects of Ibrutinib and Acalabrutinib on Platelet Functions. *Haematologica* (2019) 104:2292–9. doi: 10.3324/haematol.2018.207183
53. Chen J, Kinoshita T, Gururaja T, Sukbuntherng J, James D, Lu D, et al. The Effect of Bruton's Tyrosine Kinase (BTK) Inhibitors on Collagen-Induced Platelet Aggregation, BTK, and Tyrosine Kinase Expressed in Hepatocellular Carcinoma (TEC). *Eur J Haematol* (2018) 101:604–12. doi: 10.1111/ejh.13148
54. Nicolson PLR, Hughes CE, Watson S, Nock SH, Hardy AT, Watson CN, et al. Inhibition of Btk by Btk-Specific Concentrations of Ibrutinib and Acalabrutinib Delays But Does Not Block Platelet Aggregation Mediated by Glycoprotein VI. *Haematologica* (2018) 103:2097–108. doi: 10.3324/haematol.2018.193391
55. Jones JA, Hillmen P, Coutre S, Tam C, Furman RR, Barr PM, et al. Use of Anticoagulants and Antiplatelet in Patients With Chronic Lymphocytic Leukaemia Treated With Single-Agent Ibrutinib. *Br J Haematol* (2017) 178:286–91. doi: 10.1111/bjh.14660
56. Shanafelt TD, Wang V, Kay NE, Hanson CA, O'Brien SM, Barrientos JC, et al. A Randomized Phase III Study of Ibrutinib (PCI-32765)-Based Therapy vs. Standard Fludarabine, Cyclophosphamide, and Rituximab (FCR) Chemoimmunotherapy in Untreated Younger Patients With Chronic Lymphocytic Leukemia (CLL): A Trial of the ECOG-ACRIN Cancer Research Group (E1912) [Abstract]. *Blood* (2018) 132(Suppl 1):LBA–4. doi: 10.1182/blood-2018-120779
57. Woyach J, Ruppert AS, Perez G, Booth AM, Feldman D, Dib EG, et al. Alliance A041702: A Randomized Phase III Study of Ibrutinib Plus Obinutuzumab Versus Ibrutinib Plus Venetoclax and Obinutuzumab in Untreated Older Patients (≥ 70 Years of Age) With Chronic Lymphocytic Leukemia (CLL) [Abstract]. *Blood* (2019) 134(Suppl 1):1751. doi: 10.1182/blood-2019-127102
58. Eichhorst B, Robak T, Montserrat E, Ghia P, Niemann CU, Kater AP, et al. Chronic Lymphocytic Leukemia: ESMO Clinical Practice Guidelines for Diagnosis, Treatment and Follow-Up. *Ann Oncol* (2021) 31:23–33. doi: 10.1016/j.annonc.2020.09.019
59. Seymour C. *Acalabrutinib Demonstrates Activity in Frontline CLL* (2019). Available at: https://www.targetedonc.com/view/acalabrutinib-demonstrates-activity-in-frontline-cll (Accessed May 12, 2021).
60. Rhodes JM, Mato AR. Zanubrutinib (BGB-3111), a Second-Generation Selective Covalent Inhibitor of Bruton's Tyrosine Kinase and Its Utility in Treating Chronic Lymphocytic Leukemia. *Drug Des Devel Ther* (2021) 15:919–26. doi: 10.2147/DDDT.S250823
61. National Comprehensive Cancer Network. *NCCN Guidelines Version 4.2021. Chronic Lymphocytic Leuekemia/Small Lymphocytic Lymphoma*. National Comprehensive Cancer Network, Plymouth Meeting, PA (2021).

Conflict of Interest: SO has served as a consultant for Amgen, Astellas, Celgene, GlaxoSmithKline, Janssen Oncology, Aptose Biosciences Inc, Vaniam Group LLC, AbbVie, and Alexion; has received research support from Kite Pharma, Regeneron, and Acerta Pharma; and has been a consultant and received research support from Gilead, Pharmacyclics, TG Therapeutics, Pfizer, and Sunesis. JBr has served as a consultant for AbbVie, Acerta, AstraZeneca, BeiGene, Catapult, Dynamo Therapeutics, Eli Lilly, Juno/Celgene, Kite, MEI Pharma, Nextcea, Novartis, Octapharma, Pfizer, Rigel, Sunesis, TG Therapeutics, and Verastem; received honoraria from Janssen; received research funding from Gilead, Loxo, Sun, and Verastem; and served on data safety monitoring committees (DSMC) for Invectys. JBy reports personal fees from Acerta Pharma (a member of the AstraZeneca Group), Genentech, Janssen, and Pharmacyclics. RF reports consulting fees from AbbVie, Acerta, AstraZeneca, BeiGene, Genentech, Janssen, Loxo Oncology, Morphosys, OncoTarget, Pharmacyclics, Sanofi, Sunesis, TG Therapeutics, and Verastem; DSMC: Incyte; and speaker fees from Janssen. PG reports consulting or advisory fees from AbbVie, BeiGene, Janssen Oncology, Gilead Sciences, Juno Therapeutics, Sunesis Pharmaceuticals, ArQule, Adaptive Biotechnologies, MEI Pharma, and Acerta Pharma/AstraZeneca; and research funding from: AbbVie, Janssen Oncology, Gilead Sciences, and Novartis. JS reports personal fees from AbbVie, Acerta Pharma (a member of the AstraZeneca Group), AstraZeneca, Genentech, Pharmacyclics, Sunesis, and TG Therapeutics. WW has received research funding from AbbVie, Acerta Pharma, Genentech, Gilead, GlaxoSmithKline/Novartis, Janssen, Juno, Kite, and Pharmacyclics.

Publisher's Note: All claims expressed in this article are solely those of the authors and do not necessarily represent those of their affiliated organizations, or those of the publisher, the editors and the reviewers. Any product that may be evaluated in this article, or claim that may be made by its manufacturer, is not guaranteed or endorsed by the publisher.

frontiers in Oncology

ORIGINAL RESEARCH
published: 06 December 2021
doi: 10.3389/fonc.2021.755188

High Expression of *BCL11A* Predicts Poor Prognosis for Childhood *MLL*-r ALL

Lu-Lu Wang[1†], Dehong Yan[2†], Xue Tang[1], Mengqi Zhang[2], Shilin Liu[1], Ying Wang[1], Min Zhang[1], Guichi Zhou[1], Tonghui Li[1], Feifei Jiang[1], Xiaowen Chen[1], Feiqiu Wen[1], Sixi Liu[1] and Huirong Mai[1*]*

[1] Department of Hematology and Oncology, Shenzhen Children's Hospital, Shenzhen, China, [2] Guangdong Immune Cell Therapy Engineering and Technology Research Center, Center for Protein and Cell-Based Drugs, Institute of Biomedicine and Biotechnology, Shenzhen Institutes of Advanced Technology, Chinese Academy of Sciences, Shenzhen, China

OPEN ACCESS

Edited by:
Shimin Hu,
University of Texas MD Anderson Cancer Center, United States

Reviewed by:
Habibe Kurt,
Warren Alpert Medical School of Brown University, United States
Richard K. Yang,
University of Texas, United States

***Correspondence:**
Sixi Liu
tiger647@126.com
Huirong Mai
maihuirong@163.com

[†]These authors have contributed equally to this work and share first authorship

Specialty section:
This article was submitted to Hematologic Malignancies, a section of the journal Frontiers in Oncology

Received: 08 August 2021
Accepted: 15 November 2021
Published: 06 December 2021

Citation:
Wang LL, Yan D, Tang X, Zhang M, Liu S, Wang Y, Zhang M, Zhou G, Li T, Jiang F, Chen X, Wen F, Liu S and Mai H (2021) High Expression of BCL11A Predicts Poor Prognosis for Childhood MLL-r ALL. Front. Oncol. 11:755188. doi: 10.3389/fonc.2021.755188

Background: Despite much improvement in the treatment for acute lymphoblastic leukemia (ALL), childhood ALLs with *MLL*-rearrangement (*MLL*-r) still have inferior dismal prognosis. Thus, defining mechanisms underlying *MLL*-r ALL maintenance is critical for developing effective therapy.

Methods: GSE13159 and GSE28497 were selected *via* the Oncomine website. Differentially expressed genes (DEGs) between *MLL*-r ALLs and normal samples were identified by R software. Next, functional enrichment analysis of these DEGs were carried out by Gene Ontology (GO), Kyoto Encyclopedia of Genes and Genomes (KEGG), Gene Set Enrichment Analysis (GSEA), and Search Tool for the Retrieval of Interacting Genes/Proteins (STRING). Then, the key hub genes and modules were identified by Weighted Gene Co-expression Network Analysis (WGCNA). Therapeutically Applicable Research to Generate Effective Treatments (TARGET) ALL (Phase I) of UCSC Xena analysis, qPCR, and Kaplan-Meier analysis were conducted for validating the expression of key hub genes from bone marrow cells of childhood ALL patients or ALL cell lines.

Results: A total of 1,045 DEGs were identified from GSE13159 and GSE28497. Through GO, KEGG, GSEA, and STRING analysis, we demonstrated that *MLL*-r ALLs were upregulating "nucleosome assembly" and "B cell receptor signal pathway" genes or proteins. WGCNA analysis found 18 gene modules using hierarchical clustering between *MLL*-r ALLs and normal. The Venn diagram was used to filter the 98 hub genes found in the key module with the 1,045 DEGs. We identified 18 hub genes from this process, 9 of which were found to be correlated with *MLL*-r status, using the UCSC Xena analysis. By using qPCR, we validated these 9 hub key genes to be upregulated in the *MLL*-r ALLs (RS4;11 and SEM) compared to the non-*MLL*-r ALL (RCH-ACV) cell lines. Three of these genes, *BCL11A*, *GLT8D1* and NCBP2, were shown to be increased in *MLL*-r ALL patient bone marrows compared to the non-*MLL*-r ALL patient. Finally, Kaplan–Meier analysis indicated that childhood ALL patients with high *BCL11A* expression had significantly poor overall survival.

Conclusion: These findings suggest that upregulated *BCL11A* gene expression in childhood ALLs may lead to *MLL*-r ALL development and *BCL11A* represents a new potential therapeutic target for childhood *MLL*-r ALL.

Keywords: acute lymphoblastic leukemia, *MLL* rearrangement, *BCL11A*, differentially expressed gene, WGCNA

INTRODUCTION

Acute lymphoblastic leukemia (ALL) is the most common childhood malignancy, which is characterized by recurrent chromosomal and molecular abnormalities of immature lymphoid cells (1). About 9% of adult and 3%–5% of children ALL cases harbor rearrangements of the mixed-lineage leukemia (*MLL*) gene (2, 3). Despite the much improvement in treatment for ALL, childhood ALL with *MLL*-rearrangement (*MLL*-r) still displays inferior prognosis attributed to hyperleukocytosis, aggressive form with early relapse, and central nervous system involvement (4–6), distinguishing itself from other leukemia subgroups.

MLL-r genes form fusions with more than 80 partner genes, of which the most common ones are AF4, AF9, ELL, and ENL (7). *MLL*-AF4 fusion represents the largest subgroup and is associated with a particular poor prognosis (8). Recently, much progress has been made in understanding the *MLL*-r leukemia process by using array-based technologies. A subset of dysregulated genes were found in *MLL*-r ALL, especially posterior *HOXA* genes and *MEIS1* genes (9, 10). Previous studies demonstrated that the *MLL* fusion proteins directly stimulated the histone methylation and target genes transcriptional elongation with the cooperation of *DOT1L*, *PAFc*, and *pTEFb*, leading to the persistent expression of genes that are important for the cell signaling, regulation of hematopoiesis, and transcription (11–13). Thus, exploring novel genes and pathways associated with *MLL*-r ALL may help to identify potential molecular mechanisms, diagnostic markers, and therapeutic targets in this special subgroup.

In this study, weighted gene co-expression network analysis (WGCNA) was first used to analyze the hub genes of *MLL*-r ALL samples mined from the Gene Expression Omnibus (GEO) database. The hub genes closely associated with *MLL*-r ALL were further confirmed in the data of Therapeutically Applicable Research to Generate Effective Treatments (TARGET) ALL (Phase I), ALL cell lines, and childhood ALL patients. We also evaluated the prognostic significance of hub gene expressions in the overall survival (OS) for childhood ALL patients. Our results provided the framework of co-expression gene modules of *MLL*-r ALL, which would be beneficial to the clinical diagnosis and treatment of childhood *MLL*-r ALL.

MATERIALS AND METHODS

ONCOMINE Analysis

ONCOMINE database (https://www.oncomine.org) is an integrated data-mining platform that analyzes previously published or open-access cancer microarray data. Using the keywords "acute lymphoblastic leukemia" and "Cancer vs. Normal Analysis" for searching ALL databases, we identified two GEO Series (GSE, ID GSE13159 and GSE28497), which could be analyzed based on the same annotation platform. The GSE28497 was analyzed by the GPL96, while the GSE13159 was analyzed by GPL570. As described by the GEO website, all probe sets represented on the GPL96 are identically replicated on GPL570. Thus, we could analyze both GSEs by the same annotation platform GPL570.

Data Collection and Preprocessing

GSE13159 contains 74 normal samples and 70 *MLL*-r ALL samples while GSE28497 includes 4 normal samples and 17 *MLL*-r ALL samples. Gene expression data from GSE13159 and GSE28497 were integrated manually to two parts, respectively, one containing 78 normal samples and another containing 87 leukemia samples for bioinformatics analysis. The combat function in the sva package was applied to remove the batch effects (**Supplementary Figure 1**) (14).

Differentially Expressed Genes Screening

The robust multi-array average (RMA) in R software (version 3.6.5) was applied to explore the gene expression data (15). Differentially expressed genes (DEGs) between *MLL*-r ALL and normal cases were identified using the Bayesian method by the linear models for microarray expression data (LIMMA) package in R software (16). $|\text{Log}_2$ fold change (FC)$| > 1$ and a p-value <0.01 were considered as threshold points. All the above operations were run with scripts in the R software Ggplot2 package was conducted to show the heatmap and volcano map.

Protein–Protein Interaction Network Building

DEGs were taken into Search Tool for the Retrieval of Interacting Genes/Proteins (STRING) with the maximum number of interactors = 0 and a confidence score ≥ 0.4 as the cutoff criterion. Then, the result was analyzed by Cytoscape (17). Top 40 genes were screened using the plug-in CytoHubba in Cytoscape (18). CytoHubba provides a simple interface to analyze the node essentiality on the selected network with 11 scoring methods. Then, the bio-functional modules in the top 40 genes were explored using a plug-in MCODE in Cytoscape with a Node Score Cutoff of 0.2, a degree cutoff of 2, and a k-Core of 2. Then, the genes in the three modules were taken into the DAVID website. Gene ontology (GO) and The Kyoto Encyclopedia of Genes and Genomes (KEGG) enrichment analyses were carried out based on DAVID (http://david.ncifcrf.gov/summary.jsp). The significance threshold was $p < 0.05$.

Gene Set Enrichment Analysis

Gene set enrichment analysis (GSEA) was conducted between *MLL*-r ALL and normal samples. Expression dataset from GSE13159 and GSE28497 was converted to the tab delimited gene cluster text (GCT) format following the operations according to the protocol (http://www.gsea-msigdb.org/gsea/). False discovery rate (FDR) < 0.05 and |normalized enrichment score (NES)| > 1 were regarded as the cutoff criteria.

WGCNA

WGCNA package of R software was applied to uncover the correlation among genes. Firstly, gene expression data from GSE13159 and GSE28497 were input into R software to inspect good genes and samples. Sample clustering was used to detect outliers and match the samples with their characteristics. The soft thresholding power of β was set at 6 to ensure a scale-free network. The minimum number of module genes was set at 30. The hierarchical clustering dendrogram summarized the gene modules with different colors. Heatmap and topological overlap matrix (TOM) plot were used to visualize the module structure. The clinical traits were classified into two subtypes, "Normal" and "Leukemia", for constructing module–trait relationships. For each expression profile, the gene significance (GS) and module membership (MM) were defined as the correlation value for each trait and each module eigengene, respectively. Hub genes are a class of highly connected genes, which have high connectivity with other genes in the same gene module and clinical trait.

UCSC Xena Analysis

The gene expression data of TARGET ALL (Phase I) were analyzed by the University of California, Santa Cruz (UCSC) Xena (http://xena.ucsc.edu/). Hub gene expression levels were calculated between *MLL*-r and non-*MLL*-r ALL patients. The minimal residual disease (MRD) status on Day 8 and Day 29 of patients were also detected. The TARGET ALL (Phase I) project was obtained from patients enrolled on biology studies and clinical trials managed through the COG, POG 9906 (clinical trial for patients with newly diagnosed ALL between March 2000 and April 2003 that were defined as high risk for relapse). Patient samples for full characterization were chosen based on the following criteria: the disease onset at >9 years of age; did not have white blood cell count > 50,000/μl; did not express BCR/ABL fusion gene; were not known to be hypodiploid (DNA index > 0.95); and achieved remission (fewer than 5% blasts) following the standard two rounds of induction therapy. The primary patient samples were collected at diagnosis and gene expressions were analyzed following the protocol of Human Genome U133 Plus 2.0 Array (Affymetrix).

Patients

Five childhood *MLL*-r ALL and 30 childhood non-*MLL*-r ALL bone marrow (BM) samples were procured from the newly diagnosed patients being treated in Shenzhen Children's Hospital from 2018 to 2020. Informed consent was obtained from all patients or their parents. Experiments involving human materials were approved by the ethics committee of Shenzhen Children's Hospital (approval number 202105102) and carried out according to the Declaration of Helsinki. Primary mononuclear cells were collected from the bone marrow samples by Ficoll density gradient centrifugation.

Cell Culture

RS4;11 and RCH-ACV cells (ATCC) were maintained in RPMI 1640 with 10% fetal bovine serum (FBS) supplemented with 1% penicillin and streptomycin. SEM cells (ATCC) were maintained in IMDM with 10% FBS, 1% penicillin, and streptomycin. Cells were cultured in a cell incubator and maintained at 5% CO_2 and 37°C.

Quantitative Real-Time PCR

Total RNA of cells were reverse transcribed to cDNA with equal RNA volume (1 μg) using the PrimeScript™ RT Master Mix (Takara). Quantitative real-time PCR (qPCR) was performed using SYBR Green qPCR Master Mix (MedChem Express, USA) and detected on CFX96™ Real-Time System (BIO-RAD). Primer sequences for mRNA expression detection are shown in **Supplementary Table 1**. All experiments were repeated at least in triplicate. Gene expression levels were calculated relative to the housekeeping gene β-actin.

Kaplan–Meier Analysis

The gene expression data of TARGET ALL (Phase I) were obtained from USCS Xena, and the clinical information was downloaded from the official website of the TARGET program (https://ocg.cancer.gov/programs/target). Finally, a total of 207 patients with gene expression data were analyzed by Kaplan–Meier analysis. The ggplot2 of R software was used to plot the Kaplan–Meier survival curve. The population was stratified by the upper 25th percentile (high) versus the lower 25th percentile (low) expression for key hub genes mRNA. The correlations between hub gene expression and OS, the hazard ratio (HR) with 95% confidence intervals, and *p*-value were determined by the Log-rank test. Log-rank test $p < 0.05$ was considered a significant difference. The results published here are in whole or part based on data generated by the TARGET (https://ocg.cancer.gov/programs/target) initiative, phs000218.

Statistical Analysis

Student's *t*-test of variance was used for comparing the statistical differences of mRNA expression of BM samples and ALL cell lines. All the analyses were two-sided and $p < 0.05$ was considered to be a significant difference.

RESULTS

Identification of DEGs in *MLL*-r ALL vs. Normal Samples

Using the keywords "acute lymphoblastic leukemia" and "Cancer vs. Normal Analysis" for searching ALL databases in ONCOMINE website, we identified two GEO Series

(GSE13159 and GSE28497) based on the same annotation platform. Gene expression data from GSE13159 and GSE28497 were integrated manually to two datasets (*MLL*-r ALL dataset containing 87 leukemia samples and normal samples dataset containing 78 normal samples, respectively). The gene expression data were analyzed using LIMMA package of R software and its extension packages. After removing the batch effect, we identified a total of 1,045 DEGs, 301 of which were upregulated genes while 744 were downregulated genes using adjusted |logFC| > 1 and p-value < 0.01 as cutoff threshold points. The most aberrantly expressed DEGs were marked in the volcano map, such as upregulated genes *LAMP5*, *CSRP2*, *GPM6B*, *SOCS2*, *MEF2C*, *MEIS1*, and *FLT3* and downregulated genes *NGFRAP1*, *PDXK*, and *DEF8* (**Figure 1A**). The heatmap of DEGs is shown in **Figure 1B**.

GO, KEGG, GSEA, and STRING Pathway Analysis of DEGs from *MLL*-r ALL vs. Normal Samples

To gain insight into a more comprehensive knowledge of DEGs of *MLL*-r ALL vs. normal samples, the GO and KEGG pathway analysis of DEGs was carried out *via* DAVID online analysis tool. GO analysis showed that *MLL*-r ALLs were mainly upregulating "transcription from RNA polymerase II promoter, cell proliferation, nucleosome assembly" genes and downregulating "immune response, inflammatory response, cell adhesion" genes (**Figure 2A**). KEGG analysis showed upregulation in "transcriptional misregulation in cancer, pathways in cancer, PI3K-Akt signaling pathway" and downregulation in "cytokine-cytokine receptor interaction, hematopoietic cell lineage, chemokine signaling pathways" (**Figure 2B**). Additionally, GSEA showed *MLL*-r ALLs to be enriched in "primary immunodeficiency, B cell receptor signaling pathway" pathways (**Figure 3A**) and negatively correlated with "complement and coagulation cascades, cytokine-cytokine receptor interaction, leukocyte transendothelial migration" pathways (**Figure 3B**).

Based on the STRING website, we built a protein–protein interaction network of up- and downregulated DEGs from *MLL*-r ALL vs. normal samples (**Figures 4A**, **5A**). In order to identify the key up- and downregulated DEGs between *MLL*-r ALL and normal samples, we adopted all the 11 methods in CytoHubba application, a plug-in of Cytoscape. *Via* calculation and analysis, the top 40 genes of up- and downregulated DEGs were identified separately (**Figure 4B** and **Supplementary Figure 2A**). Afterwards, the MCODE was employed to calculate the k-core of each gene and identify the critical networks in the top 40 genes. The upregulated gene with the highest k-core comprised three networks, which were involved in three important KEGG pathways: nucleosome assembly, B-cell proliferation, and transcriptional misregulation in cancer (**Figure 4C**). The top 40 downregulated DEGs with the highest k-score made up one important network, which was enriched in siderophore-dependent iron import into cell (**Supplementary Figure 2B**). Through GO, KEGG, GSEA, and STRING analysis, we demonstrated that *MLL*-r ALLs were upregulating "nucleosome assembly" and "B cell receptor signal pathway" genes or proteins and downregulating "complement and

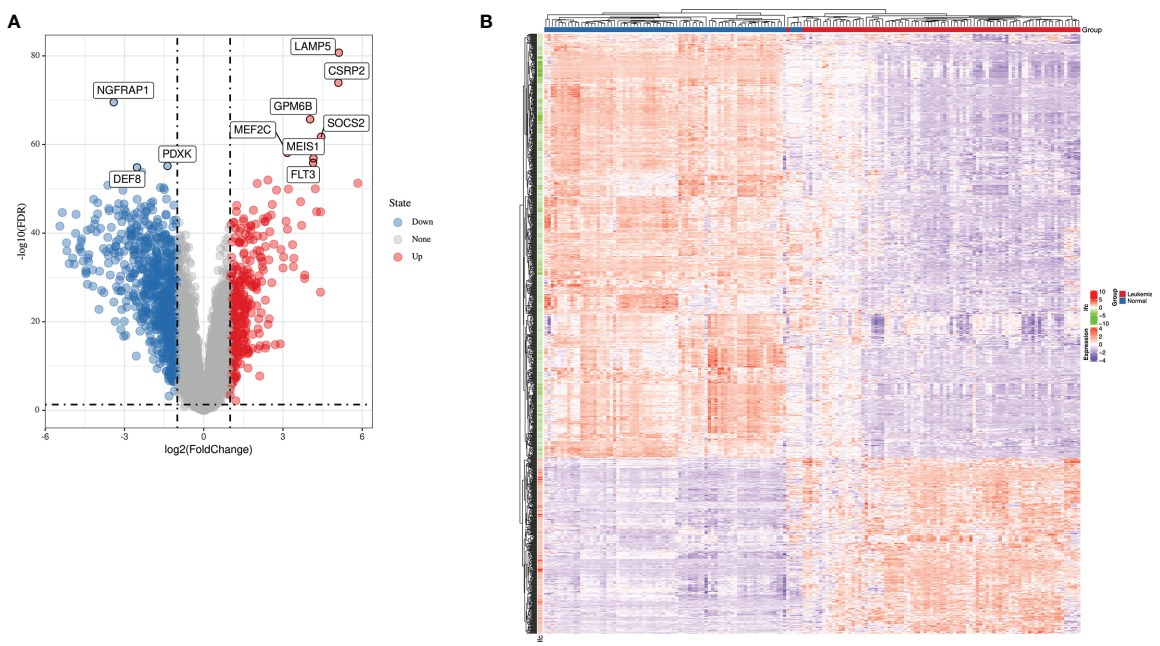

FIGURE 1 | The expression profiles of *MLL*-r ALL. **(A)** Volcano map of differently expressed genes between *MLL*-r ALL and normal samples. **(B)** Heatmap of the DEGs according to the value of |logFC|.

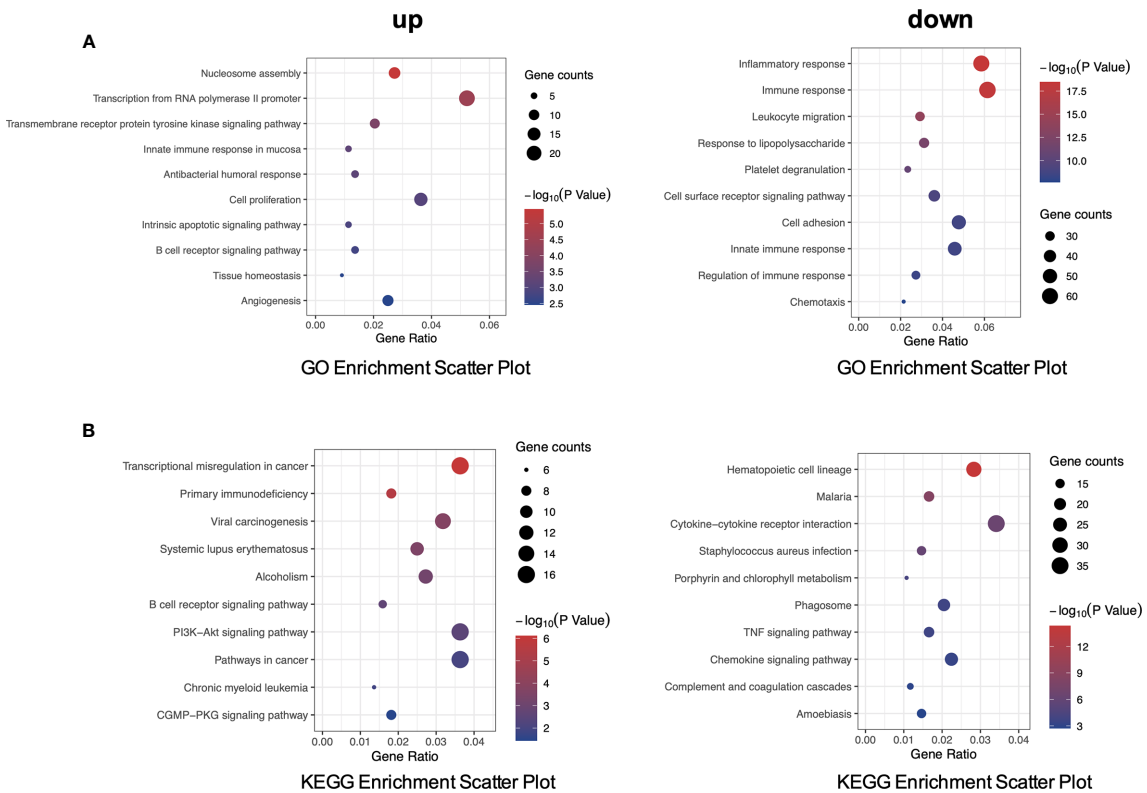

FIGURE 2 | PPI network by STRING. **(A)** GO enrichment analysis of up- and downregulated DEGs. **(B)** KEGG pathway analysis of up- and downregulated DEGs.

coagulation cascades" and "cytokine-cytokine receptor interaction" genes or proteins. These pathways were identified by at least two different biostatistics methods.

Identification of Hub Genes and Modules of *MLL*-r ALL by WGCNA

WGCNA has been widely and successfully used to identify candidate biomarkers and therapeutic targets in various complicated diseases (19–21). To clarify the key modules and hub genes in *MLL*-r ALL, a total of 165 samples from GSE13159 and GSE28497 were input into R software for WGCNA, which was employed to uncover the highly correlated genes and the coexpression networks of *MLL*-r ALL. One GEO sample (GSM), GSM331691, was excluded from the analysis due to poor quality (**Figure 5A**). The power of $\beta = 6$ was set as the soft threshold for a scale-free network (**Figure 5B**). Subsequently, 18 gene modules were generated by the hierarchical clustering dendrogram, ranging in size from 2,947 (blue module) to 41 (gray module) (**Figure 5C**). After analyzing the interactions between the 18 modules, the TOM plot of a gene network was constructed with the corresponding hierarchical clustering dendrogram and the modules (**Figure 5D**). Based on the correlation between module eigengenes and clinical traits, the co-expressed genes were found primarily clustered in the green and steel blue modules. Among the modules, the green module was the most relevant with leukemia traits (**Figure 5E**). The heatmap of gene expression in the green module is shown in **Figure 5F**. We also explored the gene significance and module membership of the genes in the 18 modules. As shown in **Figure 5G**, the green module had significant correlations with leukemia trait. Eventually, 98 genes in the green module were selected for hub genes with a cutoff of intra-modular connectivity >0.85, demonstrating that these genes were not only the key components in module but also highly correlated with the leukemia trait. Taken together, we found 18 gene modules using hierarchical clustering between *MLL*-r ALLs and normal samples by WGCNA. The "Green" module was found to be most relevant with leukemia, 98 genes of which having the highest correlation with leukemia traits were selected for hub genes.

Validation of Key Hub Genes in *MLL*-r ALL vs. non-*MLL*-r ALL Patients

To gain insight into the valuable hub genes in the green module, we used a Venn diagram to filter the 98 hub genes found in the "Green" module with the 1,045 DEGs from **Figure 1**. As shown in the Venn diagram, we identified 18 hub genes from this process (**Figure 6A**). Since the higher expression of 18 hub genes in *MLL*-r ALL is compared to the normal samples, we wondered which hub genes were also highly expressed in *MLL*-r ALL compared to non-*MLL*-r ALL. Thus, we further selected the TARGET ALL (Phase I) dataset

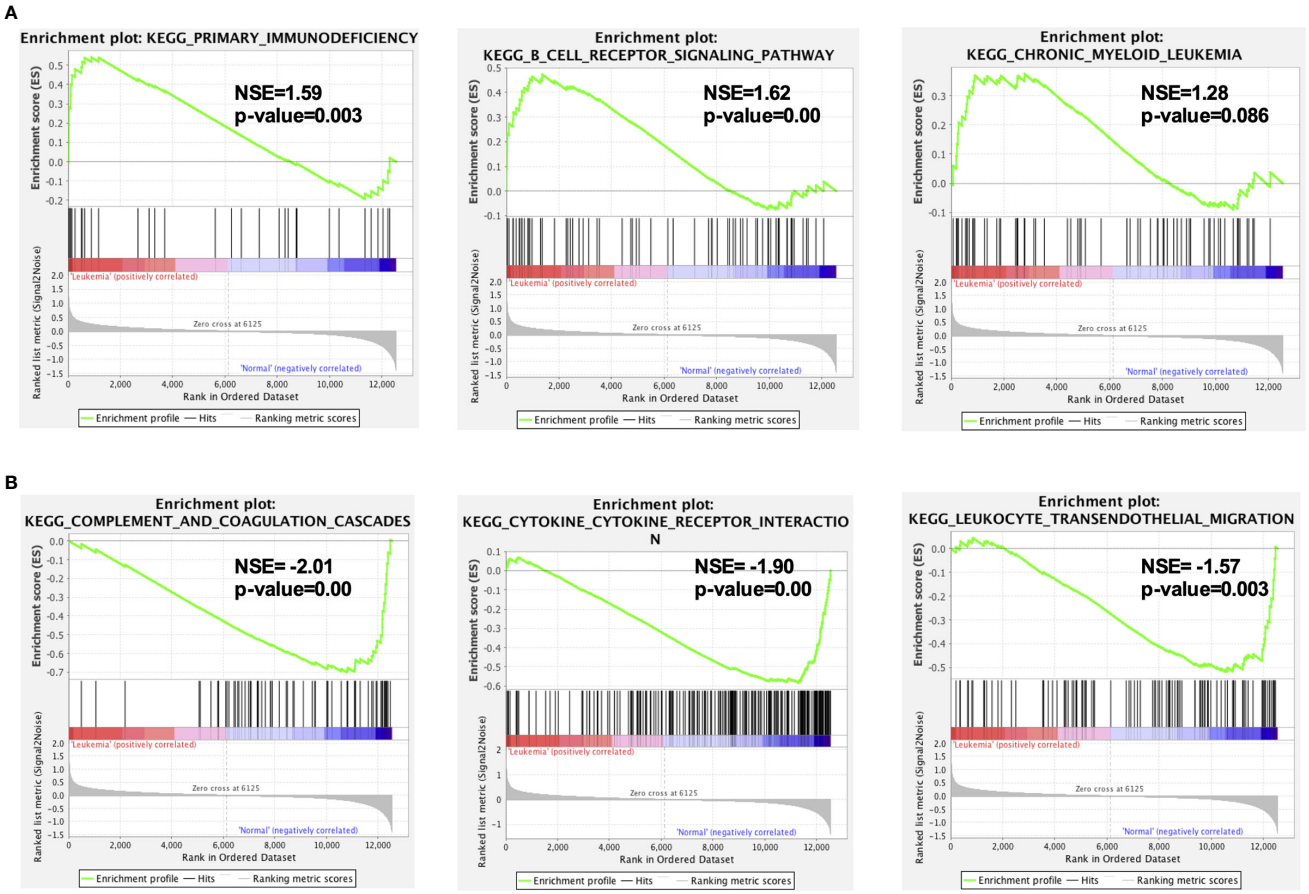

FIGURE 3 | GSEA indicated the KEGG pathways in *MLL*-r ALL. **(A)** The gene sets enriched in *MLL*-r ALL samples were related to primary immunodeficiency and B-cell receptor signaling pathway ($p < 0.05$). **(B)** The gene sets enriched in normal samples were mainly related to complement and coagulation cascades, cytokine–cytokine receptor interaction, and leukocyte transendothelial migration ($p < 0.05$).

to verify the differential expression of 18 hub genes between *MLL*-r and non-*MLL*-r ALL patients (22). Based on the results from UCSC Xena browser, nine key hub genes (*AKR1A1*, *BCL11A*, *DCLRE1C*, *DHTKD1*, *GLT8D1*, *NCBP2*, *PARP1*, *PTER*, and *STK39*) were found highly expressed in the *MLL*-positive samples compared to the *MLL*-negative samples (**Figure 6B**). Accordingly, to further determine the potential biomarkers for *MLL*-r ALL, we assessed hub gene expression in ALL cell lines and childhood ALL bone marrow samples. We found that the higher expression level of nine key hub genes were also observed in *MLL*-AF4 ALL cell lines (RS4;11 and SEM) compared to the non-*MLL*-r ALL cell line (RCH-ACV) (**Figure 7A**). Moreover, in our single clinical center, *MLL*-r ALLs had significantly higher mRNA expressions of *BCL11A*, *GLT8D1*, and *NCBP2* than non-*MLL*-r ALL patients (**Figure 7B**). However, there was no difference in *AKR1A1*, *DCLRE1C*, *DHTKD1*, *PARP1*, *PTER*, and *STK39* expression levels between *MLL*-r ALL and non-*MLL*-r ALL patients (not shown). These data suggest that upregulated *BCL11A*, *GLT8D1*, and *NCBP2* gene expression may be associated with the rearrangement of *MLL* in childhood ALL.

High *BCL11A* Expression Correlated With Poor Overall Survival of ALL Patients

Given the relationship between key hub genes and MLL status, we next examined the prognostic significance of hub genes in TARGET ALL (Phase I) datasets. We identified by Kaplan–Meier analysis that the high level of *BCL11A* mRNA expression was associated with inferior OS [HR = 0.35 (0.15–0.84), $p = 0.014$] (**Figure 8**). Nevertheless, there was no significant difference between the survival rate and the expression of *AKR1A1*, *DCLRE1C*, *DHTKD1*, *GLT8D1*, *NCBP2*, *PARP1*, *PTER*, and *STK39* (**Supplementary Figure 3**). Together, these results demonstrated that childhood ALL patients with high *BCL11A* expression had significantly poor OS, and *BCL11A* represents a new potential therapeutic target for pediatric *MLL*-r ALL.

DISCUSSION

Previous studies highlight the simple landscape of gene mutation, low DNA copy-number abnormalities, and limited

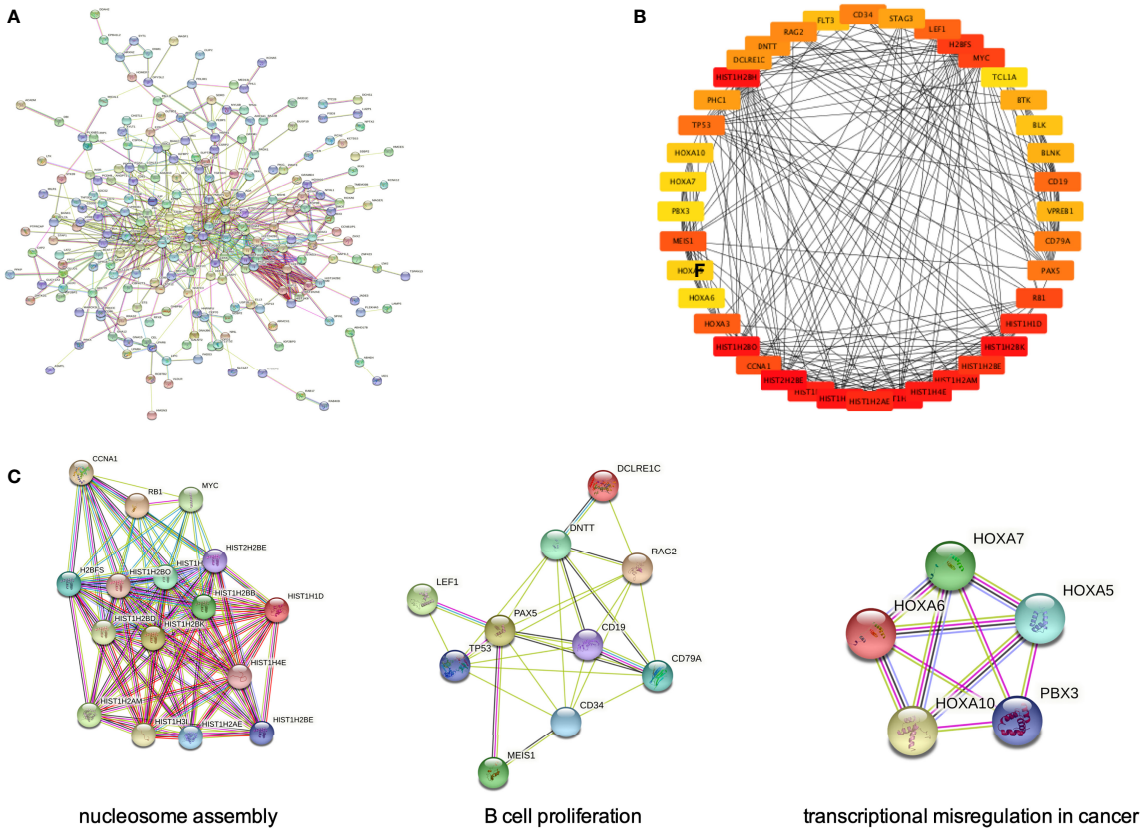

FIGURE 4 | PPI networks of upregulated DEGs by STRING Search Tool. **(A)** The PPI network was constructed by STRING based on upregulated DEGs. **(B)** The 40 genes with highest CytoHubba scores were shown in a circle. The color scheme of each node from red to yellow represents the scores from high to low, respectively. **(C)** The genes with highest CytoHubba scores made up three critical subnetworks.

window of genetic therapeutic targets for infant *MLL*-r ALLs (10, 23, 24). Transcriptional subversion and global gene expression alternation of *MLL*-r ALL play a greater role in this disease (25). Several microarray studies have already demonstrated the identification of DEGs related to distinct clinical and therapeutically relevant classes of leukemias (26, 27). However, the molecular alternation observed in *MLL*-r leukemia patients is rather complex and requires a more differentiated view. To gain a larger sample size, we combined two gene microarray expression datasets from GEO and conduct R software to analyze the DEGs in combined dataset.

As analyzed, in the upregulated gene or protein in *MLL*-r ALL samples, "B cell receptor signal pathway" was found to be significant in GO, KEGG pathway, and GSEA (**Figures 2**, **3A**), while "nucleosome assembly" was significant in GO and PPI network (**Figures 2**, **4C**). These results indicated that nucleosome assembly and B-cell receptor signal pathway were playing a core role in *MLL*-r ALLs. It is reported that *MLL* fusion genes enhance the process of transcriptional elongation by directly or indirectly binding to RNA polymerase II, leading to the alternation of whole genetic expression (28, 29). With the help of RNA polymerase II, *MLL* fusion genes drive the proliferation and self-renewal of immature hematopoietic cells by upregulating posterior *HOXA* genes and their cofactor *MEIS1* (30, 31). Similarly, GO analysis in our study demonstrated that the upregulated DEGs were significantly related with RNA polymerase II pathway (**Figure 2A**). *HOXA* and *MEIS1* were also identified in our PPI analysis (**Figure 4C**). Thus, the "transcription from RNA polymerase II" pathway may also be involved in the *MLL*-r ALL pathogenesis in this study.

WGCNA is widely used to explore the huge and complex relationships among genes across microarray or RNA sequence data. It provides a convenient and effective solution for screening core genes (32). Here, we first used WGCNA to explore the relationship of gene modules and clinical traits in *MLL*-r ALLs. As shown in the result, 18 upregulated genes were screened as hub genes by conducting WGCNA (**Figure 7A**), among which 9 key hub genes were confirmed to be highly associated with the *MLL*-r status in the TARGET ALL (Phase I) dataset (**Figure 7B**). In our childhood *MLL*-r ALL patients, *BCL11A*, *GLT8D1*, and *NCBP2* had significantly higher expression in *MLL*-r ALL patients than that in the non-*MLL*-r ALL patients. One limitation of this study is that there were only five *MLL*-r ALL BM patients for qPCR in the data analysis of our single center.

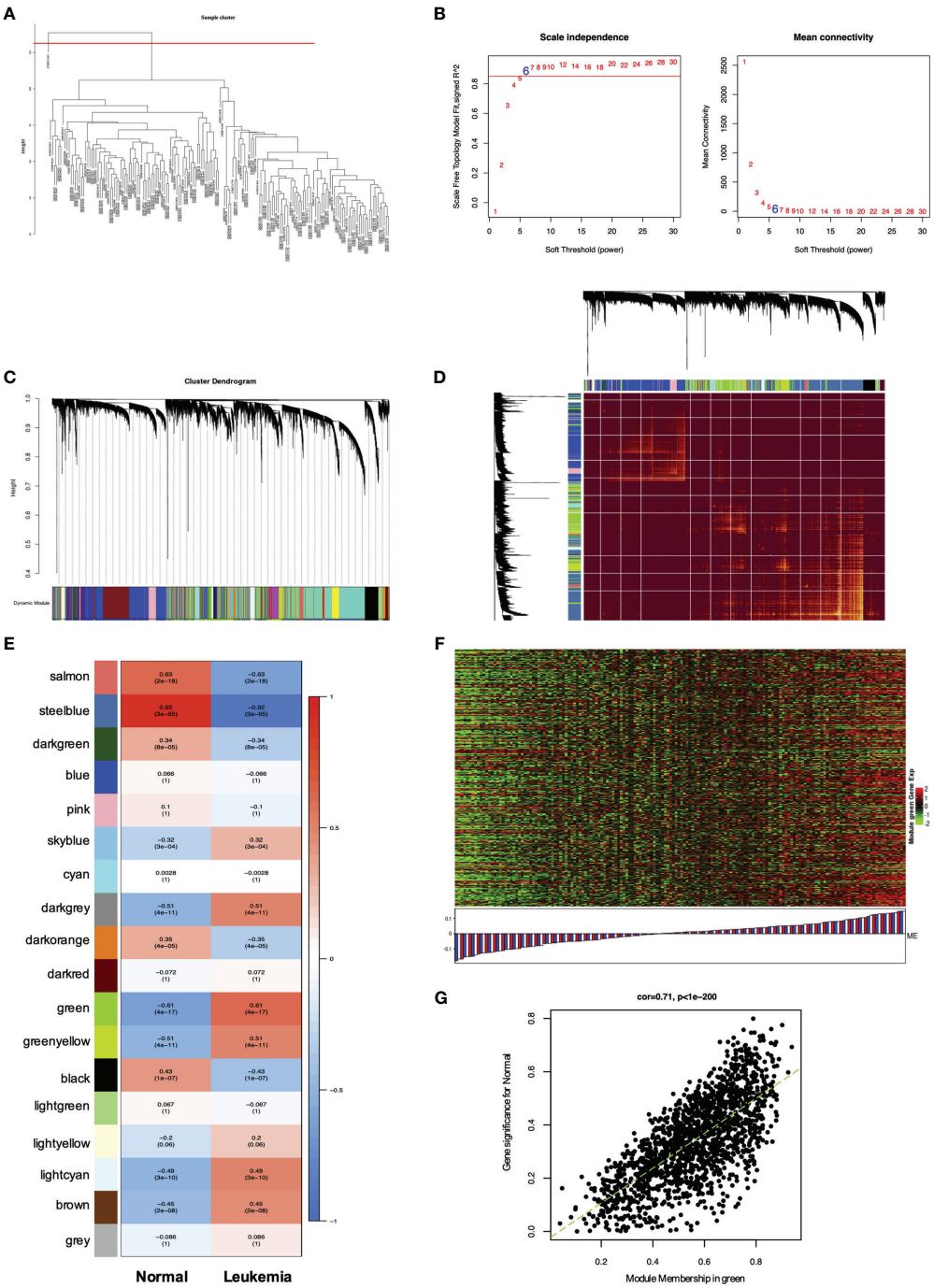

FIGURE 5 | WGCNA of genes and modules in *MLL*-r ALL. **(A)** Cluster dendrogram of 165 samples. **(B)** Analysis of the scale-free fit index for various soft thresholding powers (β) and the mean connectivity for soft threshold power. **(C)** Hierarchical cluster tree showing adjacency modules based on topological overlap. **(D)** Heatmap of all DEGs formed a TOM plot to visualize the module structure. In the TOM plot, light yellow color represents low overlap and darker yellow color indicates higher overlap. Left side and the top side of the heatmap show the gene dendrogram and module assignment. **(E)** Correlation between each module and trait. Each row represents a module eigengene and each column represents a clinic trait. Each cell contains the correlation and *p*-value of each module. **(F)** Heatmap for the DEGs in the green module. **(G)** A scatter plot of eigengenes significance versus modular membership in the green module. Intramodular analysis of the genes found in the green module showed a high correlation with leukemia, with $p <$ 1e-200 and correlation = 0.71.

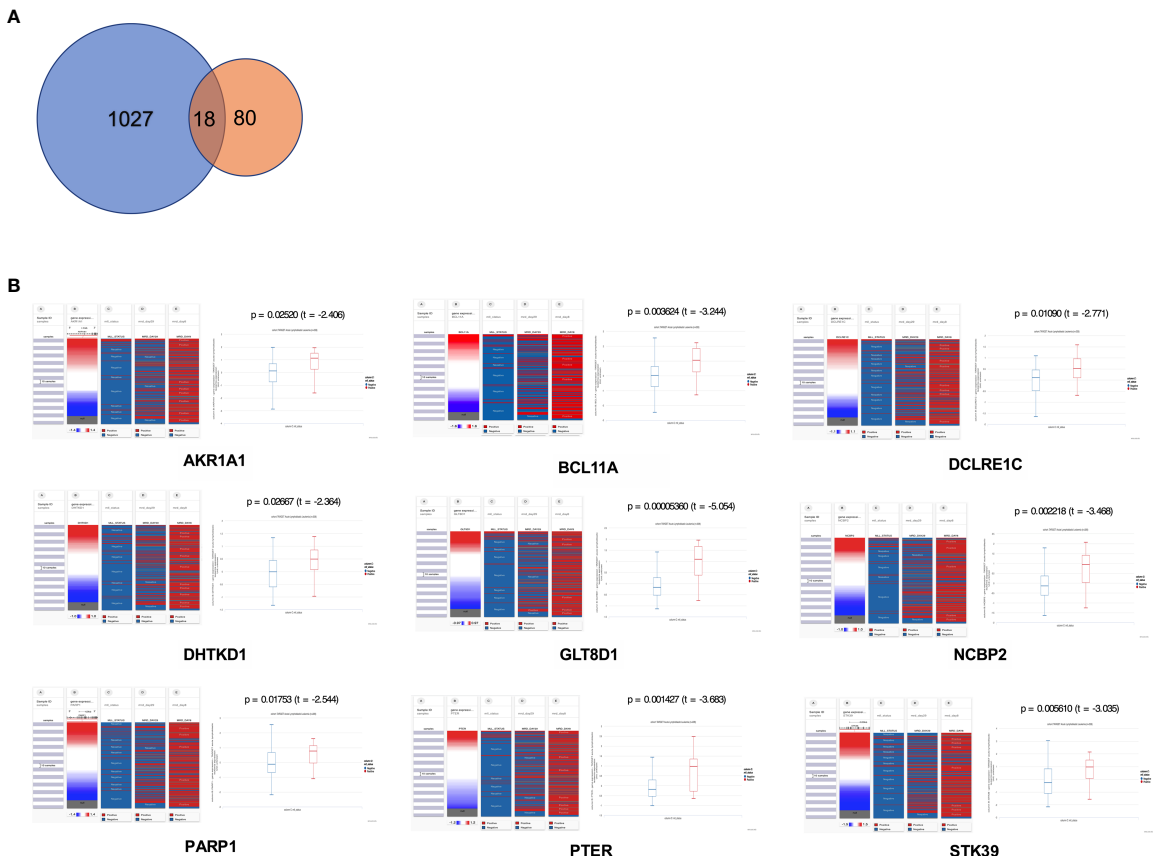

FIGURE 6 | The expression level of key hub genes in childhood *MLL*-r ALL. **(A)** The Venn diagram showed hub genes identified from DEGs and WGCNA. **(B)** Expression of *AKR1A1*, *BCL11A*, *DCLRE1C*, *DHTKD1*, *GLT8D1*, *NCBP2*, *PARP1*, *PTER*, and *STK39* in *MLL*-r ALL was highly correlated with the *MLL* status in the TARGET ALL (Phase I) dataset ($p < 0.05$). The red color represents positive status and the blue color represents negative status of *MLL* fusion and MRD.

Thus, further investigation is required to demonstrate the relationship of *MLL*-r ALL patients and DEGs with high-throughput sequencing for multi-center data analysis.

It is noteworthy to mention that *BCL11A*, a C2H2 zinc finger transcription factor, was initially identified as a chromosomal translocation oncogene in B-cell malignancies (33, 34). It modulated hemoglobin switching by directing γ-globin gene promoter repression (35). Recent studies uncovered that *BCL11A* was a critical oncogene in many other cancers like triple-negative breast cancer, lung squamous carcinoma, colorectal cancer, and laryngeal squamous cell carcinoma (36–39). In acute myeloid leukemia, high expression of *BCL11A* and *MDR1* was significantly associated with the poor prognosis (40). As analyzed using Kaplan–Meier, we reported that childhood ALL patients with high *BCL11A* expression showed inferior OS (**Figure 8**). Given the significant difference of *BCL11A* found by integrated analyses, we proposed that *BCL11A* could be considered as a potential target for ALL treatment and the molecular mechanisms study should be necessary to elucidate the role of *BCL11A* in *MLL*-r ALLs.

The high sensitivity of MRD has a profound influence on the treatment adjustment and the outcome of ALL patients during follow-up. MRD monitoring has been used to determine the ALL stratification in all childhood ALL. It was reported that MRD-positive status in Day 8 and Day 29 was associated with shorter event-free survival (EFS) in all risk groups (41). *MLL*-r ALL with positive MRD has significant worse EFS compared to those with negative MRD (42). To determine whether the poor prognosis that occurs with positive MRD is because of the hub gene expression, we examined the Day 8 and Day 29 MRD status of childhood ALL patients in the TARGET ALL (Phase I) dataset and their relationship with hub gene expression. However, there was no significant relationship between gene expression and MRD status (**Figure 6B**), neither in our single-center clinical data (not shown).

In the current study, we first integrated the information on DEGs through different bioinformatics analysis and identified that the nuclear assembly and B-cell receptor signaling pathway were the key pathways in *MLL*-r leukemia. Furthermore, we combined the results of WGCNA and DEGs, validated by clinical samples, and found that *BCL11A*, *GLT8D1*, and *NCBP2* were the key hub genes highly associated with the *MLL* status in childhood *MLL*-r ALL patients. Childhood ALL patients with high *BCL11A* expression had significantly poor OS. These findings suggest that upregulated *BCL11A* hub gene expression in childhood ALLs may lead to *MLL*-r ALL development and

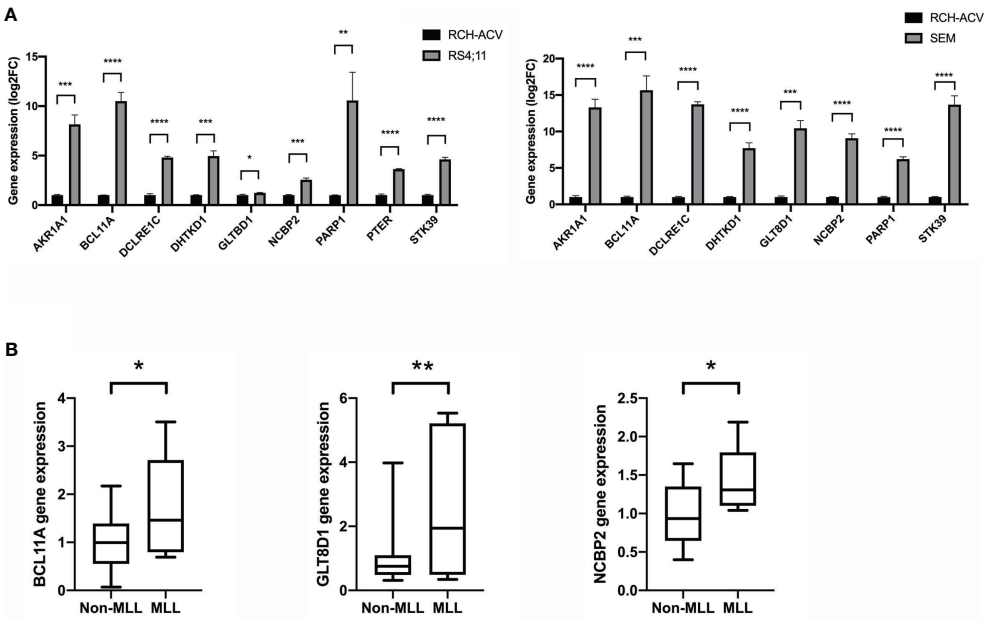

FIGURE 7 | The gene expression level of key hub genes in *MLL*-r ALL and non-*MLL*-r ALL patients. **(A)** The mRNA expression of key hub genes were measured in RS4:11, SEM, and RCH-ACV cell lines. Data are normalized to *β*-actin and are representative of three independent experiments (*$p < 0.05$; **$p < 0.01$; ***$p < 0.001$; ****$p < 0.0001$). **(B)** The mRNA expression was detected in the BM of *MLL*-r ALL and non-*MLL*-r ALL patients. Results are expressed as a fold of the non-*MLL*-r ALL that is set as 1 (*$p < 0.05$; **$p < 0.01$).

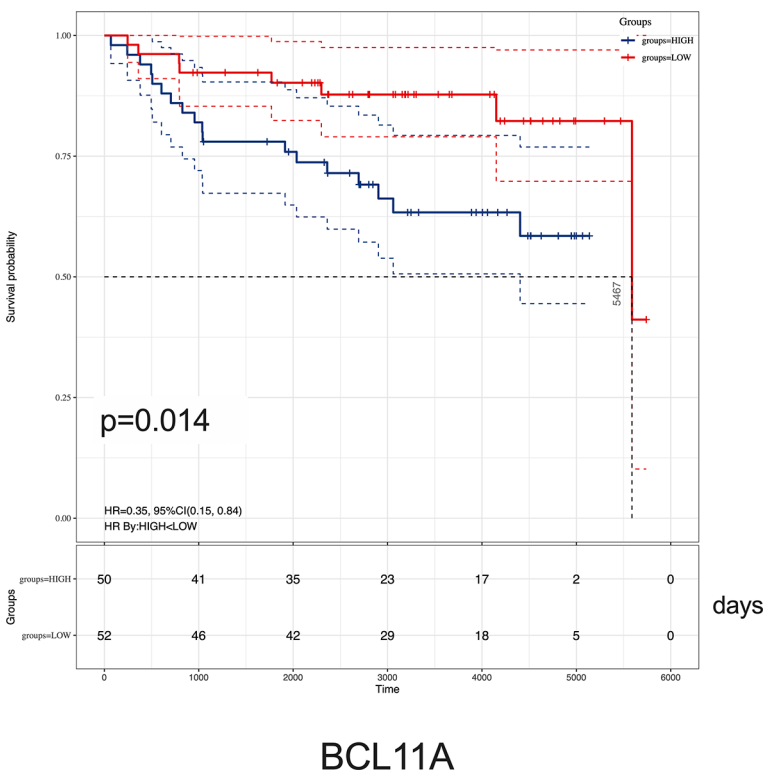

FIGURE 8 | Kaplan–Meier analysis of *BCL11A* expression in childhood ALL. Survival cure comparing patients with high (blue) vs. low (red) *BCL11A* expression were plotted using a Log-rank test [HR = 0.35 (0.15–0.84), $p = 0.014$]. The unit of time is measured in days. The median survival time is 5,467 days.

BCL11A represents a new potential therapeutic target for childhood *MLL*-r ALL.

DATA AVAILABILITY STATEMENT

Publicly available datasets were analyzed in this study. This data can be found here: https://www.ncbi.nlm.nih.gov/geo/query/acc.cgi?acc=GSE13159; https://www.ncbi.nlm.nih.gov/geo/query/acc.cgi?acc=GSE28497; https://ocg.cancer.gov/programs/target/resources.

ETHICS STATEMENT

The studies involving human participants were reviewed and approved by the ethics committee of Shenzhen Children's Hospital. Written informed consent was obtained from all patients or their parents.

AUTHOR CONTRIBUTIONS

L-LW and DY conceived the project, analyzed the datasets, and wrote the manuscript. XT, MQZ, and MZ performed the experiments. SLL, YW, GZ, TL, and FJ contributed analysis tools. XC, FW, SXL, and HM revised the manuscript and discussed the data. All authors contributed to the article and approved the submitted version.

ACKNOWLEDGMENTS

We appreciate the GEO datasets (GSE13159 and GSE28497) and TARGET ALL project for free using. This work was supported by Sanming Project of Medicine in Shenzhen (SZSM201512033), Guangdong Medical Science and Technology Research Project (A2020101), Shenzhen Fund for Guangdong Provincial High-level Clinical Key Specialties (SZGSP012), Shenzhen Key Medical Discipline Construction Fund (SZXK034), Shenzhen Healthcare Research Project (SZLY2018015), National Key R&D Program of China (2019YFA0906100), National Natural Science Foundation of China (82071772), and Shenzhen Basic Science Research Project (JCYJ20190807161419228).

SUPPLEMENTARY MATERIAL

The Supplementary Material for this article can be found online at: https://www.frontiersin.org/articles/10.3389/fonc.2021.755188/full#supplementary-material

REFERENCES

1. Dores GM, Devesa SS, Curtis RE, Linet MS, Morton LM. Acute Leukemia Incidence and Patient Survival Among Children and Adults in the United States, 2001-2007. *Blood* (2012) 119(1):34–43. doi: 10.1182/blood-2011-04-347872
2. Moorman AV, Ensor HM, Richards SM, Chilton L, Schwab C, Kinsey SE, et al. Prognostic Effect of Chromosomal Abnormalities in Childhood B-Cell Precursor Acute Lymphoblastic Leukaemia: Results From the UK Medical Research Council ALL97/99 Randomised Trial. *Lancet Oncol* (2010) 11 (5):429–38. doi: 10.1016/S1470-2045(10)70066-8
3. Armstrong SA, Look AT. Molecular Genetics of Acute Lymphoblastic Leukemia. *J Clin Oncol Off J Am Soc Clin Oncol* (2005) 23(26):6306–15. doi: 10.1200/JCO.2005.05.047
4. Stam RW, den Boer ML, Schneider P, Nollau P, Horstmann M, Beverloo HB, et al. Targeting FLT3 in Primary MLL-Gene-Rearranged Infant Acute Lymphoblastic Leukemia. *Blood* (2005) 106(7):2484–90. doi: 10.1182/blood-2004-09-3667
5. Pieters R, Schrappe M, De Lorenzo P, Hann I, De Rossi G, Felice M, et al. A Treatment Protocol for Infants Younger Than 1 Year With Acute Lymphoblastic Leukaemia (Interfant-99): An Observational Study and a Multicentre Randomised Trial. *Lancet (London England)* (2007) 370 (9583):240–50. doi: 10.1016/S0140-6736(07)61126-X
6. Tomizawa D, Koh K, Hirayama M, Miyamura T, Hatanaka M, Saikawa Y, et al. Outcome of Recurrent or Refractory Acute Lymphoblastic Leukemia in Infants With MLL Gene Rearrangements: A Report From the Japan Infant Leukemia Study Group. *Pediatr Blood Cancer* (2009) 52(7):808–13. doi: 10.1002/pbc.21975
7. Meyer C, Burmeister T, Gröger D, Tsaur G, Fechina L, Renneville A, et al. The MLL Recombinome of Acute Leukemias in 2017. *Leukemia* (2018) 32(2):273–84. doi: 10.1038/leu.2017.213
8. Thomas M, Gessner A, Vornlocher H-P, Hadwiger P, Greil J, Heidenreich O. Targeting MLL-AF4 With Short Interfering RNAs Inhibits Clonogenicity and Engraftment Of T (-Positive Human Leukemic Cells. *Blood* (2005) 106 (10):3559–66. doi: 10.1182/blood-2005-03-1283
9. Krivtsov AV, Armstrong SA. MLL Translocations, Histone Modifications and Leukaemia Stem-Cell Development. *Nat Rev Cancer* (2007) 7(11):823–33. doi: 10.1038/nrc2253
10. Andersson AK, Ma J, Wang J, Chen X, Gedman AL, Dang J, et al. The Landscape of Somatic Mutations in Infant MLL-Rearranged Acute Lymphoblastic Leukemias. *Nat Genet* (2015) 47(4):330–7. doi: 10.1038/ng.3230
11. Muntean AG, Tan J, Sitwala K, Huang Y, Bronstein J, Connelly JA, et al. The PAF Complex Synergizes With MLL Fusion Proteins at HOX Loci to Promote Leukemogenesis. *Cancer Cell* (2010) 17(6):609–21. doi: 10.1016/j.ccr.2010.04.012
12. Lin C, Smith ER, Takahashi H, Lai KC, Martin-Brown S, Florens L, et al. AFF4, a Component of the ELL/P-TEFb Elongation Complex and a Shared Subunit of MLL Chimeras, can Link Transcription Elongation to Leukemia. *Mol Cell* (2010) 37(3):429–37. doi: 10.1016/j.molcel.2010.01.026
13. Yokoyama A, Lin M, Naresh A, Kitabayashi I, Cleary ML. A Higher-Order Complex Containing AF4 and ENL Family Proteins With P-TEFb Facilitates Oncogenic and Physiologic MLL-Dependent Transcription. *Cancer Cell* (2010) 17(2):198–212. doi: 10.1016/j.ccr.2009.12.040
14. Leek JT, Johnson WE, Parker HS, Jaffe AE, Storey JD. The Sva Package for Removing Batch Effects and Other Unwanted Variation in High-Throughput Experiments. *Bioinformatics* (2012) 28(6):882–3. doi: 10.1093/bioinformatics/bts034
15. Gautier L, Cope L, Bolstad BM, Irizarry RA. Affy–Analysis of Affymetrix GeneChip Data at the Probe Level. *Bioinformatics* (2004) 20(3):307–15. doi: 10.1093/bioinformatics/btg405
16. Ritchie ME, Phipson B, Wu D, Hu Y, Law CW, Shi W, et al. Limma Powers Differential Expression Analyses for RNA-Sequencing and Microarray Studies. *Nucleic Acids Res* (2015) 43(7):e47. doi: 10.1093/nar/gkv007
17. Franceschini A, Szklarczyk D, Frankild S, Kuhn M, Simonovic M, Roth A, et al. STRING V9.1: Protein-Protein Interaction Networks, With Increased Coverage

and Integration. *Nucleic Acids Res* (2013) 41(Database issue):D808–15. doi: 10.1093/nar/gks1094
18. Chin C-H, Chen S-H, Wu H-H, Ho C-W, Ko M-T, Lin C-Y. Cytohubba: Identifying Hub Objects and Sub-Networks From Complex Interactome. *BMC Syst Biol* (2014) 8 Suppl 4(Suppl 4):S11. doi: 10.1186/1752-0509-8-S4-S11
19. Liu H, Liu M, You H, Li X, Li X. Oncogenic Network and Hub Genes for Natural Killer/T-Cell Lymphoma Utilizing WGCNA. *Front Oncol* (2020) 10:223. doi: 10.3389/fonc.2020.00223
20. Li X, Liu Z, Mi M, Zhang C, Xiao Y, Liu X, et al. Identification of Hub Genes and Key Pathways Associated With Angioimmunoblastic T-Cell Lymphoma Using Weighted Gene Co-Expression Network Analysis. *Cancer Manag Res* (2019) 11:5209–20. doi: 10.2147/CMAR.S185030
21. Liu Z, Sun T, Zhang Z, Bi J, Kong C. An 18-Gene Signature Based on Glucose Metabolism and DNA Methylation Improves Prognostic Prediction for Urinary Bladder Cancer. *Genomics* (2021) 113(1 Pt 2):896–907. doi: 10.1016/j.ygeno.2020.10.022
22. Mullighan CG, Zhang J, Harvey RC, Collins-Underwood JR, Schulman BA, Phillips LA, et al. JAK Mutations in High-Risk Childhood Acute Lymphoblastic Leukemia. *Proc Natl Acad Sci U.S.A.* (2009) 106(23):9414–8. doi: 10.1073/pnas.0811761106
23. Dobbins SE, Sherborne AL, Ma YP, Bardini M, Biondi A, Cazzaniga G, et al. The Silent Mutational Landscape of Infant MLL-AF4 Pro-B Acute Lymphoblastic Leukemia. *Genes Chromosomes Cancer* (2013) 52(10):954–60. doi: 10.1002/gcc.22090
24. Bardini M, Spinelli R, Bungaro S, Mangano E, Corral L, Cifola I, et al. DNA Copy-Number Abnormalities do Not Occur in Infant ALL With T (/MLL-Af4. *Leukemia* (2010) 24(1):169–76. doi: 10.1038/leu.2009.203
25. Agraz-Doblas A, Bueno C, Bashford-Rogers R, Roy A, Schneider P, Bardini M, et al. Unraveling the Cellular Origin and Clinical Prognostic Markers of Infant B-Cell Acute Lymphoblastic Leukemia Using Genome-Wide Analysis. *Haematologica* (2019) 104(6):1176–88. doi: 10.3324/haematol.2018.206375
26. Krivtsov AV, Feng Z, Lemieux ME, Faber J, Vempati S, Sinha AU, et al. H3K79 Methylation Profiles Define Murine and Human MLL-AF4 Leukemias. *Cancer Cell* (2008) 14(5):355–68. doi: 10.1016/j.ccr.2008.10.001
27. Armstrong SA, Golub TR, Korsmeyer SJ. MLL-Rearranged Leukemias: Insights From Gene Expression Profiling. *Semin Hematol* (2003) 40(4):268–73. doi: 10.1016/S0037-1963(03)00196-3
28. Bitoun E, Oliver PL, Davies KE. The Mixed-Lineage Leukemia Fusion Partner AF4 Stimulates RNA Polymerase II Transcriptional Elongation and Mediates Coordinated Chromatin Remodeling. *Hum Mol Genet* (2007) 16(1):92–106. doi: 10.1093/hmg/ddl444
29. Basu S, Nandy A, Biswas D. Keeping RNA Polymerase II on the Run: Functions of MLL Fusion Partners in Transcriptional Regulation. *Biochim Biophys Acta Gene Regul Mech* (2020) 1863(8):194563. doi: 10.1016/j.bbagrm.2020.194563
30. Armstrong SA, Staunton JE, Silverman LB, Pieters R, den Boer ML, Minden MD, et al. MLL Translocations Specify a Distinct Gene Expression Profile That Distinguishes a Unique Leukemia. *Nat Genet* (2002) 30(1):41–7. doi: 10.1038/ng765
31. Rozovskaia T, Feinstein E, Mor O, Foa R, Blechman J, Nakamura T, et al. Upregulation of Meis1 and HoxA9 in Acute Lymphocytic Leukemias With the T(4 : 11) Abnormality. *Oncogene* (2001) 20(7):874–8. doi: 10.1038/sj.onc.1204174
32. Langfelder P, Horvath S. WGCNA: An R Package for Weighted Correlation Network Analysis. *BMC Bioinf* (2008) 9:559. doi: 10.1186/1471-2105-9-559
33. Satterwhite E, Sonoki T, Willis TG, Harder L, Nowak R, Arriola EL, et al. The BCL11 Gene Family: Involvement of BCL11A in Lymphoid Malignancies. *Blood* (2001) 98(12):3413–20. doi: 10.1182/blood.V98.12.3413
34. Yin B, Delwel R, Valk PJ, Wallace MR, Loh ML, Shannon KM, et al. A Retroviral Mutagenesis Screen Reveals Strong Cooperation Between Bcl11a Overexpression and Loss of the Nf1 Tumor Suppressor Gene. *Blood* (2009) 113(5):1075–85. doi: 10.1182/blood-2008-03-144436
35. Liu N, Hargreaves VV, Zhu Q, Kurland JV, Hong J, Kim W, et al. Direct Promoter Repression by BCL11A Controls the Fetal to Adult Hemoglobin Switch. *Cell* (2018) 173(2):430–442.e17. doi: 10.1016/j.cell.2018.03.016
36. Seachrist DD, Hannigan MM, Ingles NN, Webb BM, Weber-Bonk KL, Yu P, et al. The Transcriptional Repressor BCL11A Promotes Breast Cancer Metastasis. *J Biol Chem* (2020) 295(33):11707–19. doi: 10.1074/jbc.RA120.014018
37. Lazarus KA, Hadi F, Zambon E, Bach K, Santolla M-F, Watson JK, et al. BCL11A Interacts With SOX2 to Control the Expression of Epigenetic Regulators in Lung Squamous Carcinoma. *Nat Commun* (2018) 9(1):3327. doi: 10.1038/s41467-018-05790-5
38. Park SY, Lee S-J, Cho HJ, Kim J-T, Yoon HR, Lee KH, et al. Epsilon-Globin HBE1 Enhances Radiotherapy Resistance by Downregulating BCL11A in Colorectal Cancer Cells. *Cancers (Basel)* (2019) 11(4):498. doi: 10.3390/cancers11040498
39. Zhou J, Zhou L, Zhang D, Tang W-J, Tang D, Shi X-L, et al. BCL11A Promotes the Progression of Laryngeal Squamous Cell Carcinoma. *Front Oncol* (2020) 10:375. doi: 10.3389/fonc.2020.00375
40. Xutao G, PengCheng S, Yin L, Huijuan D, Yan W, Haiqing Z, et al. BCL11A and MDR1 Expressions Have Prognostic Impact in Patients With Acute Myeloid Leukemia Treated With Chemotherapy. *Pharmacogenomics* (2018) 19(4):343–8. doi: 10.2217/pgs-2017-0157
41. Borowitz MJ, Devidas M, Hunger SP, Bowman WP, Carroll AJ, Carroll WL, et al. Clinical Significance of Minimal Residual Disease in Childhood Acute Lymphoblastic Leukemia and its Relationship to Other Prognostic Factors: A Children's Oncology Group Study. *Blood* (2008) 111(12):5477–85. doi: 10.1182/blood-2008-01-132837
42. Tomizawa D, Miyamura T, Imamura T, Watanabe T, Moriya Saito A, Ogawa A, et al. A Risk-Stratified Therapy for Infants With Acute Lymphoblastic Leukemia: A Report From the JPLSG MLL-10 Trial. *Blood* (2020) 136 (16):1813–23. doi: 10.1182/blood.2019004741

Conflict of Interest: The authors declare that the research was conducted in the absence of any commercial or financial relationships that could be construed as a potential conflict of interest.

frontiers in Oncology

CLINICAL TRIAL
published: 06 December 2021
doi: 10.3389/fonc.2021.789891

Venetoclax Shows Low Therapeutic Activity in BCL2-Positive Relapsed/Refractory Peripheral T-Cell Lymphoma: A Phase 2 Study of the Fondazione Italiana Linfomi

*Laura Ballotta[1,2], Pier Luigi Zinzani[3,4], Stefano Pileri[5], Riccardo Bruna[6], Monica Tani[7], Beatrice Casadei[3,4], Valentina Tabanelli[5], Stefano Volpetti[8], Stefano Luminari[9,10], Paolo Corradini[11], Elisa Lucchini[2], Maria Chiara Tisi[12], Michele Merli[13], Alessandro Re[14], Marzia Varettoni[15], Emanuela Anna Pesce[16] and Francesco Zaja[1,2]**

[1] Dipartimento Clinico di Scienze Mediche, Chirurgiche e della Salute, Università degli Studi di Trieste, Trieste, Italy, [2] Struttura Complessa (SC) Ematologia, Azienda Sanitaria Universitaria Giuliano Isontina, Trieste, Italy, [3] Istituti di Ricovero e Cura a Carattere Scientifico (IRCSS) Azienda Ospedaliero-Universitaria di Bologna, Istituto di Ematologia "Seragnoli", Bologna, Italy, [4] Dipartimento di Medicina Specialistica, Diagnostica e Sperimentale, Università degli Studi di Bologna, Bologna, Italy, [5] Divisione di Emolinfopatologia, Istituto Europeo di Oncologia Istituti di Ricovero e Cura a Carattere Scientifico (IRCSS), Milano, Italy, [6] Divisione di Ematologia, Dipartimento di Medicina Traslazionale, Università del Piemonte Orientale e Azienda Ospedaliera Universitaria (AOU) Maggiore della Carità, Novara, Italy, [7] Unità Operativa Complessa (UOC) Ematologia, Ospedale Santa Maria delle Croci, Ravenna, Italy, [8] Clinica Ematologica, Azienda Sanitaria Universitaria (AOU) Friuli Centrale, Udine, Italy, [9] Ematologia, Azienda Unita Sanitaria Locale Istituti di Ricovero e Cura a Carattere Scientifico (IRCSS) Reggio Emilia, Arcispedale Santa Maria Nuova, Reggio Emilia, Italy, [10] Dipartimento Chirurgico Medico Odontoiatrico e di Scienze Morfologiche con interesse Trapiantologico Oncologico e di Medicina Rigenerativa (CHIMOMO), Università di Modena e Reggio Emilia, Modena, Italy, [11] Struttura Complessa (SC) Ematologia, Fondazione Istituti di Ricovero e Cura a Carattere Scientifico (IRCSS) Istituto Nazionale dei Tumori, Milano, Italy, [12] Ematologia e Terapie Cellulari, Ospedale S. Bortolo, Vicenza, Italy, [13] Ematologia "Ospedale di Circolo e Fondazione Macchi-Azienda Socio Sanitaria Territoriale (ASST) Sette Laghi", Varese, Italy, [14] Ematologia, Azienda Socio Sanitaria Territoriale (ASST) Spedali Civili di Brescia, Brescia, Italy, [15] Divisione di Ematologia, Fondazione Istituti di Ricovero e Cura a Carattere Scientifico (IRCSS) Policlinico San Matteo, Pavia, Italy, [16] Fondazione Italiana Linfomi, Modena, Italy*

OPEN ACCESS

Edited by:
Varsha Gandhi,
University of Texas MD Anderson Cancer Center, United States

Reviewed by:
Constantine Tam,
Peter MacCallum Cancer Centre, Australia
John Seymour,
Peter MacCallum Cancer Centre, Australia

***Correspondence:**
Francesco Zaja
francesco.zaja@asugi.sanita.fvg.it

Specialty section:
This article was submitted to Hematologic Malignancies, a section of the journal Frontiers in Oncology

Received: 05 October 2021
Accepted: 15 November 2021
Published: 06 December 2021

Citation:
Ballotta L, Zinzani PL, Pileri S, Bruna R, Tani M, Casadei B, Tabanelli V, Volpetti S, Luminari S, Corradini P, Lucchini E, Tisi MC, Merli M, Re A, Varettoni M, Pesce EA and Zaja F (2021) Venetoclax Shows Low Therapeutic Activity in BCL2-Positive Relapsed/Refractory Peripheral T-Cell Lymphoma: A Phase 2 Study of the Fondazione Italiana Linfomi. Front. Oncol. 11:789891. doi: 10.3389/fonc.2021.789891

Patients with relapsed/refractory (R/R) peripheral T-cell lymphoma (PTCL) have a poor prognosis, with an expected survival of less than 1 year using standard salvage therapies. Recent advances in our understanding of the biology of PTCL have led to identifying B-Cell Lymphoma 2 (BCL2) protein as a potential therapeutic target. BLC2 inhibitor venetoclax was investigated in a prospective phase II trial in patients with BCL2-positive R/R PTCL after at least one previous standard line of treatment (NCT03552692). Venetoclax given alone at a dosage of 800 mg/day resulted in one complete response (CR) and two stable diseases (SDs) among 17 enrolled patients. The majority of patients (88.2%) interrupted the treatment due to disease progression. No relationship with BCL2 expression was documented. At a median follow-up of 8 months, two patients are currently still on treatment (one CR and one SD). No case of tumor lysis syndrome was registered. Therefore, venetoclax monotherapy shows activity in a minority of patients whose biological characteristics have not yet been identified.

Clinical Trial Registration: www.clinicaltrials.gov (NCT03552692, EudraCT number 2017-004630-29).

Keywords: peripheral T-cell lymphoma, BCL2 protein, venetoclax, BCL2 inhibition, relapsed/refractory

INTRODUCTION

Peripheral T-cell lymphomas (PTCLs) are a rare and heterogeneous group of T-cell neoplasms, accounting for 5%–10% of all non-Hodgkin lymphomas in Western countries. PTCL arises from mature post-thymic lymphocytes, and the most represented subtypes are PTCL not otherwise specified (PTCL-NOS), angioimmunoblastic T-cell lymphoma (AITL) and other nodal T-cell lymphomas of T-follicular helper origin (TFH), and anaplastic large cell lymphoma (ALCL) ALK-positive (ALCL-ALK+) and ALK-negative (ALCL-ALK-) (1). With few exceptions, PTCLs share an aggressive clinical behavior and poor prognosis; the response to induction chemotherapy is often inadequate and/or short-term (2).

The standard of care for PTCL is based on anthracycline-containing regimens [cyclophosphamide, doxorubicin, vincristine, prednisolone ± etoposide (CHOP/CHOEP)], resulting in a 5-year overall survival (OS) of only 30%–40% (3). High-dose chemotherapy followed by autologous stem cell transplantation (ASCT) is recommended in younger chemosensitive patients, but many of them do not receive the transplant because of ineffective disease control or, eventually, relapse soon after (4).

Following the promising results of a phase 3 clinical trial, the US Food and Drug Administration (FDA) recently approved the use of brentuximab vedotin (BV) in combination with cyclophosphamide, doxorubicin, and prednisolone (CHP) as first-line treatment for CD30-positive PTCL (5). However, only a minority of patients in this study had PTCL-NOS, AITL, or TFH, and the benefit of the addition of BV was not demonstrated in this small population.

Relapsed or refractory (R/R) PTCLs are characterized by a dismal prognosis, and treatment in this setting is an unmet medical need. There is no standard of care in R/R patients; gemcitabine-based regimens are frequently used in this setting, ensuring an overall response rate (ORR) of 30%–70% and median progression-free survival (PFS) of 4–11 months (6).

Romidepsin, belinostat, and pralatrexate received FDA approval for the treatment of R/R PTCLs, but the ORR with these agents is 30%, with a median PFS of a few months (6–8). More promising results were reported with BV, which showed remarkable activity in ALCLs (9), but no similar activity was registered in other PTCLs (10). Other compounds are under investigation in clinical trials alone or in combination (e.g., lenalidomide, copanlisib, duvelisib, 5-azacitidine) (11).

Recent advances in understanding the biology of PTCLs led to identifying BCL2, Cluster of differentiation 38 (CD38), and Programmed death-1 (PD-1) as potential therapeutic targets. Regarding BCL2, an immunohistochemical analysis conducted within the Fondazione Italiana Linfomi (FIL) indicated that BCL2, an antiapoptotic protein, is overexpressed in 88% of patients with AITL, 80% of patients with PTCL-NOS, 58% of patients with ALK- ALCL, and 31% of patients with ALK+ ALCL (12). Moreover, an inverse correlation between BCL2 expression and the apoptotic rate has been demonstrated in PTCL (13), and BCL2 overexpression in PTCLs seems to correlate with disease progression through interactions with the p53-dependent pathway (14). Thus, BCL2 may represent a potential therapeutic target.

Venetoclax is an anti-BCL2 agent approved in Europe for the treatment of chronic lymphocytic leukemia (CLL) that has shown therapeutic activity in mantle cell lymphoma (MCL) and other hematological malignancies (15–17). We report the results of a study from FIL that evaluated the activity of venetoclax monotherapy in BCL2-positive R/R PTCL.

PATIENTS AND METHODS

FIL_VERT is an open-label, multicenter, single-arm phase II trial with a two-stage Simon design that aimed to evaluate the activity and safety of venetoclax as a single agent in patients with BCL2-positive PTCL-NOS, AITL, or TFH who were R/R after at least one previous standard line of treatment.

Twenty-one Italian centers belonging to FIL were involved in the present study. Patients aged ≥18 years with a diagnosis of R/R PTCL-NOS, AITL, or TFH and an Eastern Cooperative Oncology Group (ECOG) performance status ≤2 were enrolled. Relapse biopsy, if available, or otherwise the initial biopsy was centrally revised (Division of Haematopathology, European Institute of Oncology, Milan, Italy) according to the revised fourth edition of the WHO classification of hematopoietic and lymphoid tumors (1). The percentage of BCL2-positive tumor cells was scored as follows, according to Bossard et al. (18): 4, >75%; 3, 50%–75%; 2, 25%–49%; 1, 5%–24%; 0, <5%. For central review and confirmation of the diagnosis, fresh sections were cut from the paraffin block(s) and used for immunohistochemistry to assess the expression of BCL2. Only patients with ≥25% BCL2-positive tumor cells in the relapse or initial biopsy were included in the study. For all inclusion and exclusion criteria, see **Supplement 1**.

All patients provided written informed consent, and the study was conducted in accordance with the Declaration of Helsinki. The study protocol was approved by the ethical committee of each participating site. The trial was registered at www.clinicaltrials.gov (NCT03552692) and given EudraCT number 2017-004630-29.

The primary objective of the study was to evaluate the efficacy of venetoclax in terms of ORR [complete response (CR) and partial response (PR)] using the Revised Response Criteria for Malignant Lymphoma (Lugano Classification) (19), which was evaluated after three treatment cycles. Secondary objectives included assessment of the CR rate, PR rate, stable disease (SD) rate, overall survival (OS), time to response (TTR), PFS,

duration of treatment, and safety. Finally, the explorative objective was to assess the possible relationship between response and BLC2 expression.

Thirty-five patients were planned to be enrolled. Given the two-stage design of the study, a stop in recruitment was planned after the enrollment of 18 patients to perform interim efficacy analysis. To proceed to the second stage, the minimum number of patients with an ORR had to be 3/18. Treatment consisted of oral venetoclax (800 mg/day for 28 days/cycle) administered continuously as a single agent until disease progression, unacceptable toxicity, withdrawal of consent, and/or the investigator determined that further therapy is not in the patient's best interest. To reduce the risk of tumor lysis syndrome (TLS), the dosage of venetoclax was gradually increased in an initial ramp-up phase (**Supplement 2**). Patients were also hospitalized for the first 72 h of treatment, and intravenous hydration and antihyperuricemic drugs were administered.

OS and PFS were estimated using the Kaplan–Meier product-limit-method. Adverse events (AEs) were encoded according to National Cancer Institute (NCI) Common Terminology Criteria for Adverse Events v. 4.03.

RESULTS

Between May 2018 and November 2019, 22 patients were enrolled and 17 were determined to be eligible; the diagnosis was not centrally confirmed in one patient, BCL2 was <25% in two patients, one patient withdrew consent, and one patient died before starting the treatment. Patient characteristics are summarized in **Table 1**. Two of the 17 patients had received ASCT before venetoclax monotherapy. BCL2 positivity in lymphoma cells was 25%–50% in nine patients (53%), 51%–75% in one patient (5.8%), and >75% in seven patients (41.2%).

Overall therapeutic activity was observed in 3/17 patients (18%). These included one 81-year-old patient in PR after three cycles of treatment with venetoclax (**Figure 1**) that converted to CR at cycle 9 and was maintained 24 months from the beginning of treatment; this patient had PTCL-NOS histology with 50% BCL2 lymphoma cell positivity. He was previously treated with six cycles of age-adjusted CHOP, achieving CR that was maintained for 12 months. Two additional patients had evidence of improvement even without achieving the criteria for PR and for this reason, according to the Lugano classification, were defined as SD. These included a 58-year-old female with relapsed AITL (BCL2 positivity 30%) who received venetoclax for 4 months and experienced disease progression and a 77-year-old male with refractory PTCL-NOS (BCL2 positivity 40%) who is still receiving venetoclax 15 months since the beginning of treatment.

At a median follow-up of 8 months (range, 1–24 months), two patients are currently still receiving treatment (one CR and one SD). Fifteen patients (88.2%) interrupted the treatment due to disease progression, all but one within five cycles of therapy. Twelve patients (70.6%) died: eight (66.7%) due to Progression of disease (PD) and four (40%) due to worsening of clinical condition and infectious complications. Median OS and PFS were 9 months (95% CI, 7.1–14.2) and 3.8 months (95% CI 2.0–4.8), respectively (**Figure 2**).

A total of 12 patients experienced grade 3–4 hematological toxicities: neutropenia (42%), thrombocytopenia (25%), and anemia (25%). Nine patients (52.9%) experienced grade 3 extrahematological toxicities (two metabolism and nutrition disorders, particularly hyponatremia and hypocalcemia, three cases of pneumonia, one asthenia, two general disorders, and one acute renal failure), whereas no cases of TLS were registered.

Because of the ORR rate <30%, enrollment was stopped at the 17 patients.

TABLE 1 | Patient's characteristics at the time of enrollment.

Patient's characteristics	Patients (N = 17)
Age, median (range)	70 (29–86)
Age ≥60 years, n (%)	11 (64.7)
Age ≥70 years, n (%)	9 (52.9)
Sex	
Male, n (%)	10 (58.8)
Female, n (%)	7 (41.2)
Histology	
PTCL-NOS, n (%)	13 (76.5)
AITL, n (%)	4 (23.5)
Ann Arbor stage	
I, n (%)	0 (0)
II, n (%)	1 (5.9)
III, n (%)	4 (23.5)
IV, n (%)	12 (70.6)
ECOG performance status	
0	6 (35.3)
1	6 (35.3)
2	5 (29.4)
Systemic symptoms	
Absent, n (%)	14 (82.3)
Present, n (%)	3 (17.7)
Bone marrow involvement	
Negative, n (%)	7 (41.2)
Positive, n (%)	10 (58.8)
Bone marrow involvement ≥20%, n (%)	4 (23.5)
TLS risk group*	
Missing data, n (%)	1 (5.9)
Low risk, n (%)	9 (52.9)
Intermediate risk, n (%)	7 (41.2)
Status of disease	
Relapse	5 (29.4)
Refractory	12 (70.5)
Prior therapy, n (%)	
1	8 (47.1)
2	7 (41.2)
3	1 (5.9)
4+	1 (5.9)
Previous ASCT	2 (11.7)
Number of cycles, median (min–max)	2 (1–16)
1, n (%)	3 (17.6)
2, n (%)	6 (35.3)
3, n (%)	5 (29.4)
≥4, n (%)	3 (17.6)

**TLS risk group is defined by lymph node (LN) size and absolute lymphocyte count (ALC) defining low-risk group for LN <5 cm and ALC <25 × 10^9/L, intermediate-risk group for LN >5 cm and <10 cm or ALC ≥25 × 10^9/L, and high-risk group for LN >10 cm or ALC ≥25 × 10^9/L associated with LN ≥5 cm. PTCL NOS, Peripheral T-cell Lymphoma not otherwise specified; AITL, Angioimmunoblastic T-cell Lymphoma; ECOG, Eastern Cooperative Oncology Group; TLS, tumor lysis syndrome.*

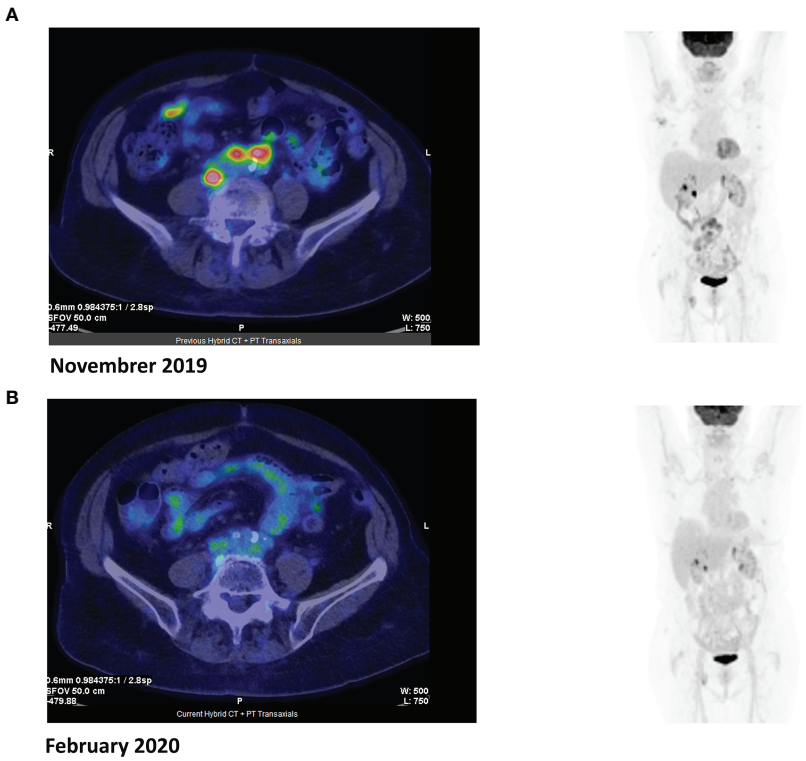

FIGURE 1 | Positron emission tomography (PET) images before **(A)** and after **(B)** three cycles of venetoclax.

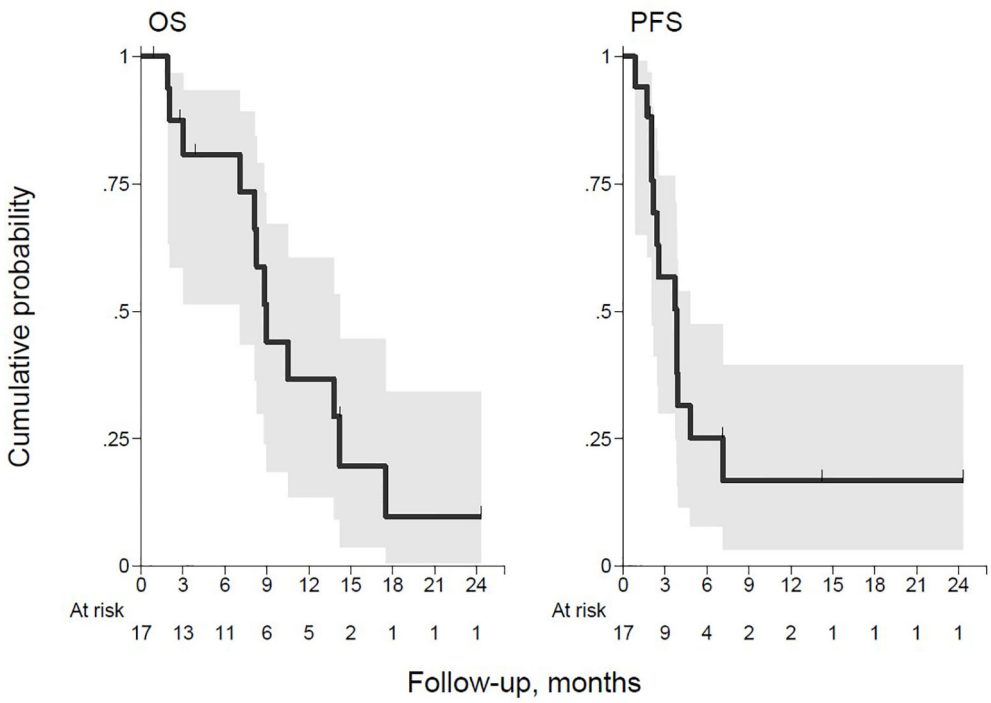

FIGURE 2 | Overall survival (OS) and progression-free survival (PFS).

DISCUSSION

FIL_VERT was designed as a proof-of-concept study to evaluate the activity of venetoclax monotherapy in the setting of R/R BCL2-positive PTCLs with the aim of performing a subsequent trial with venetoclax in combination with other agents in case of positive results. Considering that this was the first therapeutic experience with the use of venetoclax in PTCL, the study was designed in two stages according to Simon.

The characteristics of the 17 patients enrolled in the study indicated high risk/poor prognosis. Unfortunately, despite the biologic rationale and efficacy demonstrated by BCL2 inhibition in other hematological malignancies, our preliminary experience showed that venetoclax monotherapy had therapeutic activity in only 18% of patients, with one case of CR. For this reason, the study was stopped after enrollment of the first 17 patients. It is important to point out that two patients (one CR and one SD) experienced a durable therapeutic effect and are still receiving venetoclax 17 and 18 months after beginning treatment, respectively. No apparent relationship could be found, in our small survey, between the level of BCL2 expression and response. The safety profile was in line with previous studies of other hematological malignancies, and no TLS was observed.

The lack of observed response could be due to cellular mechanisms of resistance that have already been observed in other hematological and solid neoplasms. The major determinants of resistance to venetoclax in MCL and CLL patients have been identified as the overexpression and *de novo* synthesis of BCL-X_L and MCL-1, antiapoptotic proteins belonging to the BCL2 family (20). Other mechanisms of resistance observed in CLL patients treated with venetoclax included early outgrowth of clones with complex karyotype, mutations in BTG1, aberrations of CDKN2A/B (21), and BCL2 mutation Gly101Val alone or associated with other additional acquired BCL2 resistance mutations, as recently reported (22, 23).

A possible strategy for circumventing resistance could be the association with other agents (chemotherapy and/or monoclonal antibodies or biological agents), as reported below.

In R/R follicular lymphoma (FL), despite a high level of BCL2 expression, venetoclax monotherapy has shown limited efficacy, with an ORR of 38% and only 14% CR rate (17). Several trials are ongoing that combine venetoclax with other molecules and/or chemotherapy in both previously untreated patients and in the setting of R/R FL (e.g., NCT04722601, NCT03980171, NCT02956382).

Increased BCL2 levels are also reported in acute myeloid leukemia (AML) patients, and a majority of AML blasts depend on BCL2 for survival. Furthermore, high expression of BCL2 is associated with poor prognosis with an inferior response to chemotherapy (24). Though single-agent venetoclax has had modest activity in AML, the association with azacitidine in previously untreated patients has shown a synergistic effect, with an incidence of a CR and a CR with incomplete hematological recovery of 71% and a median response duration of 21.1 months (25).

Similarly, in the 15%–20% of R/R multiple myeloma patients who carry chromosomal translocation t(11;14), venetoclax has demonstrated promising activity, with an ORR of 40% and 27%, achieving at least a very good partial response (VGPR) (26). To increase the rate of response, several trials of venetoclax in combination with other agents are ongoing and some preliminary results are available (e.g., venetoclax in association with dexamethasone plus/minus bortezomib) (27).

In conclusion, our data suggest that a small number of R/R patients with PTCL may benefit from venetoclax monotherapy. Similarly to what has been observed in other hematological malignancies, it is possible that the combination of venetoclax plus other cytotoxic or biological agents may translate into a synergistic activity and a higher response rate. BCL2 expression alone seems to not be predictive of the response. Further studies should attempt to identify the mechanisms of response and resistance in this setting and define the predictive markers of venetoclax efficacy.

DATA AVAILABILITY STATEMENT

The raw data supporting the conclusions of this article will be made available by the authors without undue reservation.

ETHICS STATEMENT

The study protocol was approved by the ethics committee of each participating site. The trial was registered at www.clinicaltrials.gov, NCT03552692, and given the EudraCT number 2017-004630-29. The patients/participants provided their written informed consent to participate in this study.

AUTHOR CONTRIBUTIONS

FZ designed the study. FZ and LB wrote the article. All other authors contributed to data collection and data analysis, critically revised the article, and approved the final version of the paper.

FUNDING

The study was supported by Abbvie. The funder was not involved in the study design, collection, analysis, interpretation of data, the writing of this article or the decision to submit it for publication.

ACKNOWLEDGMENTS

We thank Gianni Ciccone and Luigi Marcheselli for statistical analysis and reporting.

SUPPLEMENTARY MATERIAL

The Supplementary Material for this article can be found online at: https://www.frontiersin.org/articles/10.3389/fonc.2021.789891/full#supplementary-material

REFERENCES

1. Swerdlow SH, Campo E, Harris NL, Jaffe ES, Pileri SA, Stein H. *WHO Classification of Tumours of Haematopoietic and Lymphoid Tissues. 4th ed.* Lyon, France: IARC (2008). Available at: http://apps.who.int/bookorders/anglais/detart1.jsp?sesslan=1&codlan=1&codcol=70&codcch=4002.
2. Foss FM, Zinzani PL, Vose JM, Gascoyne RD, Rosen ST, Tobinai K. Peripheral T-Cell Lymphoma. *Blood* (2011) 117(25):6756–67. doi: 10.1182/blood-2010-05-231548
3. Abouyabis AN, Shenoy PJ, Sinha R, Flowers CR, Lechowicz MJ. A Systematic Review and Meta-Analysis of Front-Line Anthracycline-Based Chemotherapy Regimens for Peripheral T-Cell Lymphoma. *ISRN Hematol* (2011) 2011:623924. doi: 10.5402/2011/623924
4. D'Amore F, Relander T, Lauritzsen GF, Jantunen E, Hagberg H, Anderson H, et al. Up-Front Autologous Stem-Cell Transplantation in Peripheral T-Cell Lymphoma: NLG-T-01. *J Clin Oncol* (2012) 30(25):3093–9. doi: 10.1200/JCO.2011.40.2719
5. Horwitz S, O'Connor OA, Pro B, Illidge T, Fanale M, Advani R, et al. ECHELON-2 Study Group. Brentuximab Vedotin With Chemotherapy for CD30-Positive Peripheral T-Cell Lymphoma (ECHELON-2): A Global, Double-Blind, Randomised, Phase 3 Trial. *Lancet* (2019) 393(10168):229–40. doi: 10.1016/S0140-6736(18)32984-2
6. Zinzani PL, Venturini F, Stefoni V, Fina M, Pellegrini C, Derenzini E, et al. Gemcitabine as Single Agent in Pretreated T-Cell Lymphoma Patients: Evaluation of the Long-Term Outcome. *Ann Oncol* (2010) 21(4):860–3. doi: 10.1093/annonc/mdp508
7. Coiffier B, Pro B, Prince HM, Foss F, Sokol L, Greenwood M, et al. Romidepsin for the Treatment of Relapsed/Refractory Peripheral T-Cell Lymphoma: Pivotal Study Update Demonstrates Durable Responses. *J Hematol Oncol* (2014) 7:11. doi: 10.1186/1756-8722-7-11
8. O'Connor OA, Pro B, Pinter-Brown L, Bartlett N, Popplewell L, Coiffier B, et al. Pralatrexate in Patients With Relapsed or Refractory Peripheral T-Cell Lymphoma: Results From the Pivotal PROPEL Study. *J Clin Oncol* (2011) 29 (9):1182–9. doi: 10.1200/JCO.2010.29.9024
9. Pro B, Advani R, Brice P, Bartlett NL, Rosenblatt JD, Illidge T, et al. Brentuximab Vedotin (SGN-35) in Patients With Relapsed or Refractory Systemic Anaplastic Large-Cell Lymphoma: Results of a Phase II Study. *J Clin Oncol* (2012) 30(18):2190–6. doi: 10.1200/JCO.2011.38.0402
10. Horwitz SM, Advani RH, Bartlett NL, Jacobsen ED, Sharman JP, O'Connor OA, et al. Objective Responses in Relapsed T-Cell Lymphomas With Single-Agent Brentuximab Vedotin. *Blood* (2014) 123(20):3095–100. doi: 10.1182/blood-2013-12-542142
11. Broccoli A, Argnani L, Zinzani PL. Peripheral T-Cell Lymphomas: Focusing on Novel Agents in Relapsed and Refractory Disease. *Cancer Treat Rev* (2017) 60:120–9. doi: 10.1016/j.ctrv.2017.09.002
12. Zaja F, Tabanelli V, Agostinelli C, Calleri A, Chiappella A, Varettoni M, et al. CD38, BCL-2, PD-1, and PD-1L Expression in Nodal Peripheral T-Cell Lymphoma: Possible Biomarkers for Novel Targeted Therapies? *Am J Hematol* (2017) 92(1):E1–2. doi: 10.1002/ajh.24571
13. Rassidakis GZ, Jones D, Lai R, Ramalingam P, Sarris AH, McDonnell TJ, et al. BCL-2 Family Proteins in Peripheral T-Cell Lymphomas: Correlation With Tumour Apoptosis and Proliferation. *J Pathol* (2003) 200(2):240–8. doi: 10.1002/path.1346
14. Jung JT, Kim DH, Kwak EK, Kim JG, Park TI, Sohn SK, et al. Clinical Role of Bcl-2, Bax, or P53 Overexpression in Peripheral T-Cell Lymphomas. *Ann Hematol* (2006) 85(9):575–81. doi: 10.1007/s00277-006-0127-z
15. Roberts AW, Davids MS, Pagel JM, Kahl BS, Puvvada SD, Gerecitano JF, et al. Targeting BCL2 With Venetoclax in Relapsed Chronic Lymphocytic Leukemia. *N Engl J Med* (2016) 374(4):311–22. doi: 10.1056/NEJMoa1513257
16. Fischer K, Al-Sawaf O, Fink AM, Dixon M, Bahlo J, Warburton S, et al. Venetoclax and Obinutuzumab in Chronic Lymphocytic Leukemia. *Blood* (2017) 129(19):2702–5. doi: 10.1182/blood-2017-01-761973
17. Davids MS, Roberts AW, Seymour JF, Pagel JM, Kahl BS, Wierda WG, et al. Phase I First-In-Human Study of Venetoclax in Patients With Relapsed or Refractory Non-Hodgkin Lymphoma. *J Clin Oncol* (2017) 35(8):826–33. doi: 10.1200/JCO.2016.70.4320
18. Bossard C, Dobay MP, Parrens M, Lamant L, Missiaglia E, Haioun C, et al. Immunohistochemistry as a Valuable Tool to Assess CD30 Expression in Peripheral T-Cell Lymphomas: High Correlation With mRNA Levels. *Blood* (2014) 124(19):2983–6. doi: 10.1182/blood-2014-07-584953
19. Cheson BD, Fisher RI, Barrington SF, Cavalli F, Schwartz LH, Zucca E, et al. Alliance, Australasian Leukaemia and Lymphoma Group; Eastern Cooperative Oncology Group; European Mantle Cell Lymphoma Consortium; Italian Lymphoma Foundation; European Organisation for Research; Treatment of Cancer/Dutch Hemato-Oncology Group; Grupo Español De Médula Ósea; German High-Grade Lymphoma Study Group; German Hodgkin's Study Group; Japanese Lymphorra Study Group; Lymphoma Study Association; NCIC Clinical Trials Group; Nordic Lymphoma Study Group; Southwest Oncology Group; United Kingdom National Cancer Research Institute. Recommendations for Initial Evaluation, Staging, and Response Assessment of Hodgkin and Non-Hodgkin Lymphoma: The Lugano Classification. *J Clin Oncol* (2014) 32 (27):3059–68. doi: 10.1200/JCO.2013.54.8800
20. Bose P, Gandhi V, Konopleva M. Pathways and Mechanisms of Venetoclax Resistance. *Leuk Lymphoma* (2017) 58(9):1–17. doi: 10.1080/10428194.2017.1283032
21. Herling CD, Abedpour N, Weiss J, Schmitt A, Jachimowicz RD, Merkel O, et al. Clonal Dynamics Towards the Development of Venetoclax Resistance in Chronic Lymphocytic Leukemia. *Nat Commun* (2018) 9(1):727. doi: 10.1038/s41467-018-03170-7
22. Blombery P, Anderson MA, Gong JN, Thijssen R, Birkinshaw RW, Thompson ER, et al. Acquisition of the Recurrent Gly101Val Mutation in BCL2 Confers Resistance to Venetoclax in Patients With Progressive Chronic Lymphocytic Leukemia. *Cancer Discovery* (2019) 9(3):342–53. doi: 10.1158/2159-8290.CD-18-1119
23. Blombery P, Thompson ER, Nguyen T, Birkinshaw RW, Gong JN, Chen X, et al. Multiple BCL2 Mutations Cooccurring With Gly101Val Emerge in Chronic Lymphocytic Leukemia Progression on Venetoclax. *Blood* (2020) 135 (10):773–7. doi: 10.1182/blood.2019004205
24. Campos L, Rouault JP, Sabido O, Oriol P, Roubi N, Vasselon C, et al. High Expression of Bcl-2 Protein in Acute Myeloid Leukemia Cells Is Associated With Poor Response to Chemotherapy. *Blood* (1993) 81(11):3091–6. doi: 10.1182/blood.V81.11.3091.3091
25. DiNardo CD, Pratz KW, Letai A, Jonas BA, Wei AH, Thirman M, et al. Safety and Preliminary Efficacy of Venetoclax With Decitabine or Azacitidine in Elderly Patients With Previously Untreated Acute Myeloid Leukaemia: A non-Randomised, Open-Label, Phase 1b Study. *Lancet Oncol* (2018) 19 (2):216–28. doi: 10.1016/S1470-2045(18)30010-X
26. Kumar S, Kaufman JL, Gasparetto C, Mikhael J, Vij R, Pegourie B, et al. Efficacy of Venetoclax as Targeted Therapy for Relapsed/Refractory T(11;14) Multiple Myeloma. *Blood* (2017) 130(22):2401–9. doi: 10.1182/blood-2017-06-788786
27. Kumar SK, Harrison SJ, Cavo M, de la Rubia J, Popat R, Gasparetto C, et al. Venetoclax or Placebo in Combination With Bortezomib and Dexamethasone in Patients With Relapsed or Refractory Multiple Myeloma (BELLINI): A Randomised, Double-Blind, Multicentre, Phase 3 Trial. *Lancet Oncol* (2020) 21(12):1630–42. doi: 10.1016/S1470-2045(20)30525-8

Conflict of Interest: PZ has received advisory board fees from Secura Bio, Celltrion, Gilead, Janssen-Cilag, BMS, Servier, Sandoz, MSD, TG Therapeutics, Takeda, Roche, Eusapharma, Kyowa Kirin, Novartis, ADC Therapeutics, Incyte, and Beigene; received consultant fees from MSD, Eusapharma, and Novartis; and received speaker's bureau fees from Celltrion, Gilead, Janssen-Cilag, BMS, Servier, MSD, TG Therapeutics, Takeda, Roche, Eusapharma, Kyowa Kirin, Novartis, Incyte, and Beigene. SL has received advisory board fees from Roche, BMS/Celgene, Gilead/kite, Jannsen, Genmab, and Regeneron. MV has received advisory board fees from Janssen, Beigene, and Roche and travel expenses from Abbvie. FZ has received advisory board fees from Roche, Celgene, Janssen, Sandoz, Gilead, Novartis, Abbvie, Amgen, Sobi, Argenx, and Grifols and received honoraria for giving lectures to medical meetings from Celgene, Janssen, Gilead, Novartis, Roche, Amgen, Abbvie, and Grifols.

The remaining authors declare that the research was conducted in the absence of any commercial or financial relationships that could be construed as a potential conflict of interest.

Publisher's Note: All claims expressed in this article are solely those of the authors and do not necessarily represent those of their affiliated organizations, or those of

the publisher, the editors and the reviewers. Any product that may be evaluated in this article, or claim that may be made by its manufacturer, is not guaranteed or endorsed by the publisher.

frontiers in Oncology

CASE REPORT
published: 23 December 2021
doi: 10.3389/fonc.2021.795330

Case Report: Phenotypic Switch in High-Grade B-Cell Lymphoma With *MYC* and *BCL6* Rearrangements: A Potential Mechanism of Therapeutic Resistance in Lymphoma?

Hui Liu[1], *Qi Shen*[2], *Chung-Che Chang*[2] *and Shimin Hu*[3]*

[1] Department of Pathology, The Affiliated Hospital of Xuzhou Medical University, Xuzhou, China, [2] Department of Pathology & Laboratory Medicine, AdventHealth Cancer Institute, Orlando, FL, United States, [3] Department of Hematopathology, The University of Texas MD Anderson Cancer Center, Houston, TX, United States

Lineage switch between myeloid and lymphoid in acute leukemia is well established as a mechanism for leukemic cells to escape chemotherapy. Cross-lineage transformation is also recognized in some solid tumors on targeted therapy, such as adenocarcinomas of the lung and prostate that transforms to neuroendocrine carcinoma on targeted therapy. Now lineage plasticity is increasingly recognized in mature lymphomas, such as small B-cell lymphomas transforming to histiocytic/dendritic cell sarcoma. However, there is no report of aggressive mature B-cell lymphoma switching from one histologic category to another upon targeted therapy. We report here a case of high-grade B-cell lymphoma with *MYC* and *BCL6* rearrangements relapsing as a high-grade plasmablastic neoplasm with *MYC* and *BCL6* rearrangements after R-CHOP and R-EPOCH therapy. Being aware of this rare scenario will help improve our understanding of the underlying mechanisms of therapeutic resistance and progression of lymphoma.

Keywords: High-grade B-cell lymphoma, MYC, BCL2, BCL6, plasmablastic lymphoma, lineage switch, plasticity, therapeutic resistance

OPEN ACCESS

Edited by:
Alessandro Isidori, AORMN Hospital, Italy

Reviewed by:
Lorenzo Leoncini, University of Siena, Italy
Pier Paolo Piccaluga, University of Bologna, Italy

***Correspondence:**
Shimin Hu
shu1@mdanderson.org

Specialty section:
This article was submitted to Hematologic Malignancies, a section of the journal Frontiers in Oncology

Received: *14 October 2021*
Accepted: *03 December 2021*
Published: *23 December 2021*

Citation:
Liu H, Shen Q, Chang C-C and Hu S (2021) Case Report: Phenotypic Switch in High-Grade B-Cell Lymphoma With MYC and BCL6 Rearrangements: A Potential Mechanism of Therapeutic Resistance in Lymphoma? Front. Oncol. 11:795330. doi: 10.3389/fonc.2021.795330

INTRODUCTION

Significant advances have been made in cancer targeted therapy in the past decade. Unfortunately, some patients who undergo targeted therapy experience relapse after a brief remission. Accumulating evidence indicates that cancer cells change their identity by antigen remodeling and phenotypic or lineage switching to cope with the adverse microenvironment and achieve therapeutic resistance and tumor relapse and progression. Newly published data has shown that up to 5% of EGFR-mutated adenocarcinomas of the lung on targeted therapy transform their histologic subtype to neuroendocrine carcinoma. Similar trans-differentiation has also been reported in at least 20% of prostatic adenocarcinomas on antiandrogen therapy and some melanomas on MAPK inhibitor treatment (1).

In hematopoietic neoplasms, lineage switch is not uncommon, mostly in immature tumors, as the tumor cells have not yet fully differentiated and are multipotent like their normal counterparts. Cases

of acute leukemia demonstrating lineage switch between myeloid and lymphoid lineages during therapy have been increasingly reported, particularly in those with *KMT2A*/*MLL* rearrangement and/or after CD19-targeted immunotherapies including blinatumomab and CAR-T cells (2–4). In contrast, lymphomas deriving from mature lymphoid cells are considered lineage stable. Nevertheless, evidence has emerged that mature lymphomas could transform from one lineage to another at recurrence. Patients with several types of small B-cell lymphomas, including follicular lymphoma, chronic lymphocytic leukemia/small lymphocytic lymphoma, mantle cell lymphoma, and marginal zone lymphoma, can develop clonally-related histiocytic/dendritic cell sarcomas (5–17). Recently, Zhang et al. and Kawashima et al. each reported one case of mantle cell lymphoma switching lineage to non-hematopoietic sarcoma with neuromuscular immunophenotypic features (18, 19). Besides the lineage switch to non-hematopoietic neoplasms in mature B-cell lymphomas, clonally-related classic Hodgkin lymphoma can be seen at relapse in patients with non-Hodgkin lymphomas including primary mediastinal large B-cell lymphoma and follicular lymphoma (FL), and vice versa (20, 21).

Among non-Hodgkin lymphomas, other than the histologic progression from small B-cell lymphoma to large B-cell lymphoma (LBCL) with a similar immunophenotype or verse visa, such as FL progressing to LBCL or LBCL relapsing as FL (22), however, there is no report so far of aggressive mature B-cell neoplasms switching from one histologic category to another. Here we report a patient with a high-grade B-cell lymphoma (HGBL) with *MYC* and *BCL6* rearrangements. The patient received multiple intensive treatments combined with Rituximab and achieved complete remission, but quickly developed a high-grade plasmablastic neoplasm with retained *MYC* and *BCL6* rearrangements. To the best of our knowledge, this is the first report of histologic subtype switch of high-grade non-Hodgkin lymphoma, which provides further evidence that fully differentiated mature B-cell lymphoma cells retain the lineage plasticity to escape chemotherapy.

CASE DESCRIPTION

A 42-year-old man who had a 4-year history of HIV infection and was not compliant with HAART therapy presented with night sweat and progressive lymphadenopathy in the bilateral neck and groin regions in May 2017. His complete blood count was WBC 4.17 x 10^{3}/ul, Hgb 9.3 g/dL, and PLT 180 x 10^{3}/ul, with a CD4 count of 161/ul. Position-emission tomography/computed tomography (PET/CT) scan showed extensive hypermetabolic lymphadenopathy involving bilateral cervical, bilateral axillary, subpectoral, mediastinal, bilateral hilar, gastro-hepatic, portacaval, periportal, retroperitoneal, mesenteric, bilateral iliac, and bilateral inguinal chains as well as diffuse hypermetabolism in the adenoidal soft tissue and palatine tonsils, hypermetabolism in the left parotid region, focal hypermetabolism in the left T8 paravertebral region, and splenomegaly.

A right inguinal lymph node biopsy showed a large cell lymphoma with starry sky appearance and frequent mitoses (**Figure 1**). The lymphoma cells demonstrated frequent distinct nucleoli and pale cytoplasm. They were positive for PAX5, CD20, BCL6, MUM1 (subset), MYC, and BCL2, and were negative for CD5, CD10, CD30, CD138, cyclin D1, and EBER. The Ki-67 proliferation rate was ~70%. Fluorescence *in situ* hybridization (FISH) revealed *MYC* and *BCL6* rearrangements. No *BCL2* rearrangement was detected. PCR clonality assay showed polyclonal *IgH* rearrangement. However, the quality of DNA was low. A bone marrow biopsy was negative for lymphoma. The patient was diagnosed with HGBL with *MYC* and *BCL6* rearrangements. He was treated with 2 cycles of R-CHOP (rituximab, cyclophosphamide, hydroxydaunorubicin,

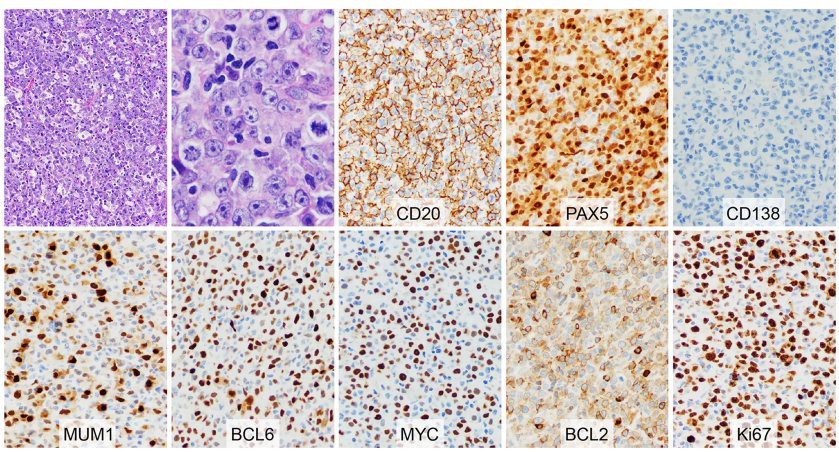

FIGURE 1 | Morphology and immunophenotype of high-grade B-cell lymphoma with *MYC* and *BCL6* rearrangements at initial diagnosis. The H&E showed a large cell lymphoma with starry sky appearance. The lymphoma cells demonstrated distinct nucleoli and pale cytoplasm. Frequent mitoses were present. The lymphoma cells were positive for CD20, PAX5, MUM1 (subset), BCL6, MYC, and BCL2, and were negative for CD138. The Ki-67 proliferation rate was ~70%.

vincristine, and prednisone), 4 cycles of R-EPOCH (rituximab, etoposide, prednisone, vincristine, cyclophosphamide, and hydroxydaunorubicin), and methotrexate for central nerve system prophylaxis. PET/CT scan performed in January 2018 revealed no residual disease.

Unfortunately, he developed multiple masses on the right thigh in July 2018. MRI of the right thigh without contrast showed a 23 x 10 x 9 cm mass centering in the vastus intermedius muscle and a 19 x 6 x 5 cm mass centering in the distal aspect of the sartorius muscle as well as signal abnormalities involving the greater trochanter, tibial plateau, and femoral condyle. A core biopsy of one of the thigh masses showed a large cell neoplasm with starry sky appearance and multi-focal necrosis (**Figure 2**). The tumor cells demonstrated eccentric nuclei and pink cytoplasm. They were positive for MYC, BCL2, MUM1, EMA, CD138, and Kappa, and were negative for PAX5, CD20, BCL6, CD5, CD30, CD56, ALK1, Lambda, and EBER. The Ki-67 proliferation rate was ~90%. A diagnosis of high-grade neoplasm with plasmablastic differentiation was entertained, with a differential diagnosis of plasmablastic lymphoma vs high-grade plasma cell neoplasm. Again, PCR clonality assay showed polyclonal *IgH* rearrangement based on a low-quality DNA. He was treated with 2 cycles of ICE (ifosfamide, carboplatin, and etoposide).

About 1-2 months later, PET/CT restaging revealed multiple hypermetabolic lesions within the chest, abdomen, and pelvis. An excisional biopsy of the abdominal wall mass showed a high-grade neoplasm morphologically and immunophenotypically similar to the thigh neoplasm. FISH analysis showed *MYC* and *BCL6* gene rearrangements. A diagnosis of plasmablastic lymphoma was reached. He was treated with CEOP (cyclophosphamide, etoposide, vincristine, and prednisone), then Gemcitabine plus oxaliplatin, and palliative radiation due to hydronephrosis caused by tumor compression.

Bone marrow biopsy performed in April 2019 was morphologically negative for lymphoma. However, chromosomal analysis detected in 2 of 20 cells a complex karyotype including two concurrent rearrangements involving the *BCL6* and *MYC* genes in the form of t(3;14) and t(8;14): 47,X, dic(Y;1)(q12;p12),+1,t(3;14)(q27;q32),dup(6)(p21.1p25),+7,t(8;14)(q24.2;q32),dup(12)(q13q22),add(18)(q21.3)[2]/46,XY[18]. He died in July 2019, 26 months after the initial diagnosis of HGBL.

DISCUSSION

We report here a case of HGBL with *MYC* and *BCL6* rearrangements switching to high-grade plasmablastic neoplasm/lymphoma with retained *MYC* and *BCL6* rearrangements at relapse. The initial lymphoma demonstrated the typical morphology and phenotype of a mature LBCL. Despite the extensive involvement of lymphoma initially, the patient responded well to chemotherapy combined with Rituximab and achieved complete remission. After a brief remission, the patient had an extensive relapse. The recurrent tumor demonstrated plasmablastic morphology and immunophenotype, losing B-cell markers (CD20, PAX5, and BCL6) and gaining plasmacytic markers (CD138, EMA, and MUM1). The presence of both *MYC* and *BCL6* rearrangements in both tumors support the clonal relatedness. Interestingly, despite retaining *BCL6* rearrangement, BCL6, a molecule that is required to be repressed for plasmacytic differentiation, was not expressed in the recurrent tumor.

From the view of development, pluripotent stem cells progressively lose their plasticity as they mature into differentiated cells and maintain lineage stability after maturation. Correspondingly, immature tumors have multi-

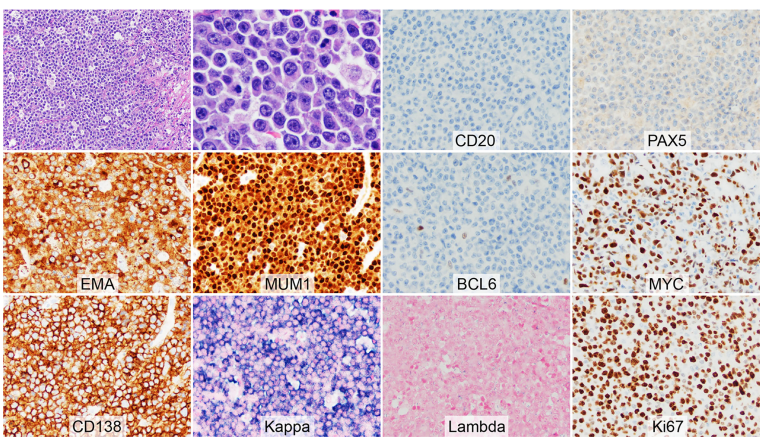

FIGURE 2 | Morphology and immunophenotype of high-grade plasmablastic neoplasm with *MYC* and *BCL6* rearrangements at relapse. The H&E showed a large cell neoplasm with starry sky appearance and focal necrosis. The tumor cells demonstrated eccentric nuclei and pink cytoplasm. Frequent mitoses were present. The tumor cells were positive for EMA, MUM1 (diffuse strong), MYC, CD138, and Kappa, and were negative for CD20, PAX5, BCL6, and Lambda. The Ki-67 proliferation rate was ~90%.

directional differentiation potential whereas mature tumors typically show specific differentiation directions. However, this traditional view has been challenged by the growing evidence that terminally differentiated tumor cells do retain plasticity (23). These cells have the potential to modify their molecular, phenotypic, and histologic characteristics to cope with the selective stresses from the microenvironment, especially after targeted therapy. This plasticity is increasingly recognized as one of the critical mechanisms involving tumor relapse, metastasis, and therapeutic resistance (1).

In general, tumor cells change their identity along the path of differentiation, backward or forward. Differentiated tumor cells de-differentiating to an earlier stage, or even progenitor phenotype, is commonly seen in soft tissue sarcoma (23–25). Sometimes small B-cell lymphomas, such as marginal zone B-cell lymphoma, demonstrate differentiation toward terminally differentiated plasma cells, or even overwhelmed by plasma cells, particularly after therapy (26, 27). Plasmacytic differentiation requires downregulation of PAX5 and BCL6 expression mediated through upregulated MUM1 and BLIMP1 (28, 29). BCL6 is a master regulator for initiation of germinal center reaction and maintenance of germinal center immunophenotype in normal B-cells, and its downregulation is required for their exit of germinal centers. PAX5 controls the identity of B-cells and its downregulation leads to loss of expression of other B-markers, facilitating upregulation of genes for plasmacytic differentiation. Generally, B-cell lymphoma loses only CD20 expression and retains B-cell identity after Rituximab treatment. However, the recurrent lymphoma in our patient lost expression of not only CD20 but also PAX5 and BCL6. In addition, it gained expression of MUM1, CD138, and EMA, indicating a switch to plasmacytic immunophenotype. The loss of B-cell identify renders the lymphoma cells less susceptible to the chemotherapeutic regimens for B-cell lymphomas. Interestingly, PCR analyses both at initial diagnosis and at relapse failed to detect monoclonal *IgH* rearrangements based on low-quality of DNA. Additional pathology material was not available for us to repeat PCR analyses for *IgH* or immunoglobulin light chains. The false-negative *IgH* rearrangement is well known in B-cell lymphomas with translocations involving *IgH*. In such scenarios, *V*, *D* and *J* segments are disrupted. In our case, both *MYC* and *BCL6* had *IgH* as the fusion partners. Another well-documented possibility for the false-negative *IgH* analyses is the presence of extensive somatic hypermutations of *IgH* gene prevents PCR amplification (30). This possibility is supported by the findings of BCL6 negativity by immunohistochemistry in the relapsed tumor despite the presence of *BCL6* rearrangement. However, both initial and relapsed tumors showed *MYC* and *BCL6* rearrangements, supporting that both tumors share a common precursor lesion but diverge to two different histologic subtypes of tumors at initial diagnosis and at relapse, somewhat analogous to acute leukemia switching between myeloid and lymphoid lineages, or analogous to branch evolution of FL (3, 4, 31, 32).

CONCLUSION

In summary, we report here a case of HGBL with *MYC* and *BCL6* rearrangements switching to high-grade plasmablastic neoplasm with *MYC* and *BCL6* rearrangements. This is the first report of aggressive mature B-cell neoplasm switching from one histologic category to another, supporting the notion that fully differentiated mature B-cell lymphoma retains plasticity, and expanding the spectrum of lineage or phenotypic switch in B-cell lymphoma. Being aware of this particular scenario will help improve our understanding of the underlying mechanisms of tumor escape from chemotherapy and develop novel anti-tumor therapy.

DATA AVAILABILITY STATEMENT

The original contributions presented in the study are included in the article/supplementary material. Further inquiries can be directed to the corresponding author.

ETHICS STATEMENT

The studies involving human participants were reviewed and approved by IRB Committee at MD Anderson Cancer Center. Written informed consent for participation was not required for this study in accordance with the national legislation and the institutional requirements.

AUTHOR CONTRIBUTIONS

HL and SH wrote the manuscript. QS and JC prepared the data. All authors contributed to the article and approved the submitted version.

REFERENCES

1. Quintanal-Villalonga ÁVerifytat, Chan JM, Yu HA, Pe'er D, Sawyers CL, Sen T, et al. Lineage Plasticity in Cancer: A Shared Pathway of Therapeutic Resistance. *Nat Rev Clin Oncol* (2020) 17(6):360–71. doi: 10.1038/s41571-020-0340-z
2. Thankamony AP, Subbalakshmi AR, Jolly MK, Nair R. Lineage Plasticity in Cancer: The Tale of a Skin-Walker. *Cancers (Basel)* (2021) 13(14):3602. doi: 10.3390/cancers13143602
3. Liao W, Kohler ME, Fry T, Ernst P. Does Lineage Plasticity Enable Escape From CAR-T Cell Therapy. Lessons from MLL-r leukemia. *Exp Hematol* (2021) 100:1–11. doi: 10.1016/j.exphem.2021.07.002
4. Schultz L, Gardner R. Mechanisms of and Approaches to Overcoming Resistance to Immunotherapy. *Hematol Am Soc Hematol Educ Program* (2019) 2019(1):226–32. doi: 10.1182/hematology.2019000018
5. Feldman AL, Arber DA, Pittaluga S, Martinez A, Burke JS, Raffeld M, et al. Clonally Related Follicular Lymphomas and Histiocytic/Dendritic Cell

Sarcomas: Evidence for Transdifferentiation of the Follicular Lymphoma Clone. *Blood* (2008) 111(12):5433–9. doi: 10.1182/blood-2007-11-124792
6. Shao H, Xi L, Raffeld M, Feldman AL, Ketterling RP, Knudson R, et al. Clonally Related Histiocytic/Dendritic Cell Sarcoma and Chronic Lymphocytic Leukemia/Small Lymphocytic Lymphoma: A Study of Seven Cases. *Mod Pathol* (2011) 24(11):1421–32. doi: 10.1038/modpathol.2011.102
7. Wang E, Papalas J, Hutchinson CB, Kulbacki E, Huang Q, Sebastian S, et al. Sequential Development of Histiocytic Sarcoma and Diffuse Large B-Cell Lymphoma in a Patient With a Remote History of Follicular Lymphoma With Genotypic Evidence of a Clonal Relationship: A Divergent (Bilineal) Neoplastic Transformation of an Indolent B-Cell Lymphoma in a Single Individual. *Am J Surg Pathol* (2011) 35(3):457–63. doi: 10.1097/PAS.0b013e3182098799
8. West DS, Dogan A, Quint PS, Tricker-Klar ML, Porcher JC, Ketterling RP, et al. Clonally Related Follicular Lymphomas and Langerhans Cell Neoplasms: Expanding the Spectrum of Transdifferentiation. *Am J Surg Pathol* (2013) 37(7):978–86. doi: 10.1097/PAS.0b013e318283099f
9. Farris M, Hughes RT, Lamar Z, Soike MH, Menke JR, Ohgami RS, et al. Histiocytic Sarcoma Associated With Follicular Lymphoma: Evidence for Dramatic Response With Rituximab and Bendamustine Alone and a Review of the Literature. *Clin Lymphoma Myeloma Leuk* (2019) 19(1):e1–8. doi: 10.1016/j.clml.2018.10.004
10. Péricart S, Waysse C, Siegfried A, Struski S, Delabesse E, Laurent C, et al. Subsequent Development of Histiocytic Sarcoma and Follicular Lymphoma: Cytogenetics and Next-Generation Sequencing Analyses Provide Evidence for Transdifferentiation of Early Common Lymphoid Precursor-a Case Report and Review of Literature. *Virchows Arch* (2020) 476(4):609–14. doi: 10.1007/s00428-019-02691-w
11. Fraser CR, Wang W, Gomez M, Zhang T, Mathew S, Furman RR, et al. Transformation of Chronic Lymphocytic Leukemia/Small Lymphocytic Lymphoma to Interdigitating Dendritic Cell Sarcoma: Evidence for Transdifferentiation of the Lymphoma Clone. *Am J Clin Pathol* (2009) 132 (6):928–39. doi: 10.1309/AJCPWQ0I0DGXBMHO
12. Burger JA, Landau DA, Taylor-Weiner A, Bozic I, Zhang H, Sarosiek K, et al. Clonal Evolution in Patients With Chronic Lymphocytic Leukaemia Developing Resistance to BTK Inhibition. *Nat Commun* (2016) 207:11589. doi: 10.1038/ncomms11589
13. Rassidakis GZ, Stromberg O, Xagoraris I, Jatta K, Sonnevi K. Trametinib and Dabrafenib in Histiocytic Sarcoma Transdifferentiated From Chronic Lymphocytic Leukemia With a K-RAS and a Unique BRAF Mutation. *Ann Hematol* (2020) 99(3):649–51. doi: 10.1007/s00277-020-03941-7
14. Hure MC, Elco CP, Ward D, Hutchinson L, Meng X, Dorfman DM, et al. Histiocytic Sarcoma Arising From Clonally Related Mantle Cell Lymphoma. *J Clin Oncol* (2012) 30(5):e49–53. doi: 10.1200/JCO.2011.38.8553
15. Wang E, Hutchinson CB, Huang Q, Sebastian S, Rehder C, Kanaly A, et al. Histiocytic Sarcoma Arising in Indolent Small B-Cell Lymphoma: Report of Two Cases With Molecular/Genetic Evidence Suggestive of a 'Transdifferentiation' During the Clonal Evolution. *Leuk Lymphoma* (2010) 51(5):802–12. doi: 10.3109/10428191003699845
16. Ambrosio MR, De Falco G, Rocca BJ, Barone A, Amato T, Bellan C, et al. Langerhans Cell Sarcoma Following Marginal Zone Lymphoma: Expanding the Knowledge on Mature B Cell Plasticity. *Virchows Arch* (2015) 467(4):471–80. doi: 10.1007/s00428-015-1814-8
17. Sabatini PJB, Tremblay-LeMay R, Ahmadi Moghaddam P, Delabie JMA, Sakhdari A. Marginal Zone Lymphoma Transdifferentiated to Histiocytic Sarcoma. *Br J Haematol* (2021) 194(6):1090–4. doi: 10.1111/bjh.17582
18. Zhang Q, Orlando EJ, Wang HY, Bogusz AM, Liu X, Lacey SF, et al. Transdifferentiation of Lymphoma Into Sarcoma Associated With Profound Reprogramming of the Epigenome. *Blood* (2020) 136(17):1980–3. doi: 10.1182/blood.2020005123
19. Kawashima I, Oishi N, Kasai K, Inoue T, Hosokawa E, Nakadate A, et al. Transdifferentiation of Mantle Cell Lymphoma Into Sarcoma With Limited Neuromuscular Differentiation After Conventional Chemotherapy. *Virchows Arch* (2021) 9. doi: 10.1007/s00428-021-03148-9
20. Trecourt A, Mauduit C, Szablewski V, Fontaine J, Balme B, Donzel M, et al. Plasticity of Mature B Cells Between Follicular and Classic Hodgkin Lymphomas: A Series of 22 Cases Expanding the Spectrum of Transdifferentiation. *Am J Surg Pathol* (2021). doi: 10.1097/PAS.0000000000001780
21. Aussedat G, Traverse-Glehen A, Stamatoullas A, Molina T, Safar V, Laurent C, et al. Composite and Sequential Lymphoma Between Classical Hodgkin Lymphoma and Primary Mediastinal Lymphoma/Diffuse Large B-Cell Lymphoma, a Clinico-Pathological Series of 25 Cases. *Br J Haematol* (2020) 189(2):244–56. doi: 10.1111/bjh.16331
22. Kridel R, Mottok A, Farinha P, Ben-Neriah S, Ennishi D, Zheng Y, et al. Cell of Origin of Transformed Follicular Lymphoma. *Blood* (2015) 126(18):2118–27. doi: 10.1182/blood-2015-06-649905
23. Yuan S, Norgard RJ, Stanger BZ. Cellular Plasticity in Cancer. *Cancer Discovery* (2019) 9(7):837–51. doi: 10.1158/2159-8290.CD-19-0015
24. Lucas DR, Shukla A, Thomas DG, Patel RM, Kubat AJ, McHugh JB. Dedifferentiated Liposarcoma With Inflammatory Myofibroblastic Tumor-Like Features. *Am J Surg Pathol* (2010) 34(6):844–51. doi: 10.1097/PAS.0b013e3181db34d8
25. Ferreira I, Droop A, Edwards O, Wong K, Harle V, Habeeb O, et al. The Clinicopathologic Spectrum and Genomic Landscape of De-/Trans-Differentiated Melanoma. *Mod Pathol* (2021) 34(11):2009–19. doi: 10.1038/s41379-021-00857-z
26. Geyer JT, Ferry JA, Longtine JA, Flotte TJ, Harris NL, Zukerberg LR. Characteristics of Cutaneous Marginal Zone Lymphomas With Marked Plasmacytic Differentiation and a T Cell-Rich Background. *Am J Clin Pathol* (2010) 133(1):59–69. doi: 10.1309/AJCPW64FFBTTPKFN
27. Swerdlow SH, Kuzu I, Dogan A, Dirnhofer S, Chan JKC, Sander B, et al. The Many Faces of Small B Cell Lymphomas With Plasmacytic Differentiation and the Contribution of MYD88 Testing. *Virchows Arch* (2016) 468(3):259–75. doi: 10.1007/s00428-015-1858-9
28. Klein U, Dalla-Favera R. Germinal Centres: Role in B-Cell Physiology and Malignancy. *Nat Rev Immunol* (2008) 8(1):22–33. doi: 10.1038/nri2217
29. Basso K, Dalla-Favera R. Germinal Centres and B Cell Lymphomagenesis. *Nat Rev Immunol* (2015) 15(3):172–84. doi: 10.1038/nri3814
30. Langerak AW, Groenen PJ, Bruggemann M, Beldjord K, Bellan C, Bonello L, et al. EuroClonality/BIOMED-2 Guidelines for Interpretation and Reporting of Ig/TCR Clonality Testing in Suspected Lymphoproliferations. *Leukemia* (2012) 26(10):2159–71. doi: 10.1038/leu.2012.246
31. Pasqualucci L, Khiabanian H, Fangazio M, Vasishtha M, Messina M, Holmes AB, et al. Genetics of Follicular Lymphoma Transformation. *Cell Rep* (2014) 6 (1):130–40. doi: 10.1016/j.celrep.2013.12.027
32. Okosun J, Montoto S, Fitzgibbon J. The Routes for Transformation of Follicular Lymphoma. *Curr Opin Hematol* (2016) 23(4):385–91. doi: 10.1097/MOH.0000000000000255

Conflict of Interest: The authors declare that the research was conducted in the absence of any commercial or financial relationships that could be construed as a potential conflict of interest.

Publisher's Note: All claims expressed in this article are solely those of the authors and do not necessarily represent those of their affiliated organizations, or those of the publisher, the editors and the reviewers. Any product that may be evaluated in this article, or claim that may be made by its manufacturer, is not guaranteed or endorsed by the publisher.

frontiers in Oncology

ORIGINAL RESEARCH
published: 04 January 2022
doi: 10.3389/fonc.2021.770988

Initial Treatment Patterns and Survival Outcomes of Mantle Cell Lymphoma Patients Managed at Chinese Academic Centers in the Rituximab Era: A Real-World Study

Meng Wu[1†], Yun Li[2,3†], Huiqiang Huang[4†], Wei Xu[5†], Yanyan Wang[6†], Haiwen Huang[2,3†], Weili Zhao[6], Shuo Liu[2,3], Pengpeng Xu[6], Zhengming Chen[7], Jun Zhu[1], Yuqin Song[1], Jia Ruan[7*] and Depei Wu[2,3*]*

[1] Key Laboratory of Carcinogenesis and Translational Research (Ministry of Education), Department of Lymphoma, Peking University Cancer Hospital & Institute, Beijing, China, [2] National Clinical Research Center for Hematologic Diseases, Jiangsu Institute of Hematology, The First Affiliated Hospital of Soochow University, Suzhou, China, [3] Collaborative Innovation Center of Hematology, Soochow University, Suzhou, China, [4] Department of Medical Oncology, Sun Yat-Sen University Cancer Center, Guangzhou, China, [5] Department of Hematology, The First Affiliated Hospital of Nanjing Medical University, Jiangsu Province Hospital, Nanjing, China, [6] Shanghai Institute of Hematology, State Key Laboratory of Medical Genomics, National Research Center for Translational Medicine at Shanghai, Ruijin Hospital Affiliated to Shanghai Jiao Tong University School of Medicine, Shanghai, China, [7] Weill Cornell Medicine and New York Presbyterian Hospital, New York, NY, United States

Purpose: The aim of the study was to delineate the disease characteristics, the initial treatment patterns, and survival in patients with mantle cell lymphoma (MCL) managed in the real world.

Methods: Data of 518 MCL patients from 5 major Chinese Hematology Centers in the period from 2007 to 2017 were retrospectively analyzed.

Results: The median age was 58 years. Of the patients, 88.6% had Eastern Cooperative Oncology Group Performance Status (ECOG PS) 0–1 and 80.7% had advanced-stage disease. Ki67 expression was <30% in 39.6% of the patients, and 43.2% of patients were categorized into a low-risk group based on the Mantle Cell Lymphoma International Prognostic Index (MIPI) scoring system. Overall, 73.4% of the patients received rituximab as their first-line therapy. The most commonly used chemotherapy was the CHOP-like (cyclophosphamide, hydroxydaunomycin, oncovin, and prednisone) regimen (45.2%), followed by high-dose cytarabine-containing chemotherapy (31.3%) and bendamustine (3.3%). Of the patients, 13.7% (n = 71) underwent consolidative autologous stem cell transplantation (ASCT), and 19.3% (n = 100) received novel agents containing first-line regimens. With a median follow-up time of 52 months, the 3- and 5-year overall survival (OS) rates were 73.7% and 61.4%, respectively. Age ≤60 years, ECOG PS 0–1, stages I–II, normal lactate dehydrogenase (LDH), absence of bone marrow involvement, Ki67 <30%, and lower-risk IPI/MIPI scores were significantly associated with improved OS ($p < 0.05$). The inclusion of rituximab improved the 5-year OS, with borderline significance (62.5% *vs.* 55.2%, $p = 0.076$). High-dose cytarabine-containing chemotherapy showed significant

OPEN ACCESS

Edited by:
Onder Alpdogan, Thomas Jefferson University, United States

Reviewed by:
Wenbin Qian, Zhejiang University, China
Beth Christian, The Ohio State University, United States

***Correspondence:**
Jia Ruan
jruan@med.cornell.edu
Yuqin Song
songyuqin@bjmu.edu.cn
Depei Wu
drwudepei@163.com

[†]These authors have contributed equally to this work and share first authorship

Specialty section:
This article was submitted to Hematologic Malignancies, a section of the journal Frontiers in Oncology

Received: *05 September 2021*
Accepted: *06 December 2021*
Published: *04 January 2022*

Citation:
Wu M, Li Y, Huang H, Xu W, Wang Y, Huang H, Zhao W, Liu S, Xu P, Chen Z, Zhu J, Song Y, Ruan J and Wu D (2022) Initial Treatment Patterns and Survival Outcomes of Mantle Cell Lymphoma Patients Managed at Chinese Academic Centers in the Rituximab Era: A Real-World Study. Front. Oncol. 11:770988. doi: 10.3389/fonc.2021.770988

clinical benefit in 5-year OS (72.1% *vs*. 55.9%, $p = 0.010$). Patients with ASCT had better 5-year OS in the younger (≤60 years) age group (87.2% *vs*. 64.8%, $p = 0.002$).

Conclusion: This large retrospective dataset unequivocally confirmed the survival advantage afforded by cytarabine-containing regimen and ASCT in a first-line setting under real-world management in the rituximab era.

Keywords: mantle cell lymphoma, initial treatment, real-world data, the rituximab era, multicenter research

1 INTRODUCTION

Mantle cell lymphoma (MCL) is an incurable and heterogeneous disease characterized by chromosomal t(11:14)(q13;32) translocation and cyclin D1 overexpression (1). It represents about 6%–9% of all newly diagnosed cases of non-Hodgkin's lymphomas (NHLs) in Western countries (1, 2). It has been reported that the incidence in Asian countries is lower (about 1.5%–3.4%) (3, 4). Whether the clinical features in the Asian population are the same as those of the Western population is unknown. The clinical outcomes of MCL are associated with disease biology and patient factors. About 10%–20% of MCL patients present with an indolent course and can be managed with the "watch-and-wait" strategy for a period of time (5). In patients with symptomatic and aggressive course, intensive chemotherapy containing high-dose cytarabine followed by consolidative autologous stem cell transplantation (ASCT) have been used in younger and fit patients, while less intensive chemo-immunotherapy and maintenance therapy are suitable for older or physically unfit patients. Many Chinese patients cannot tolerate full-dose intensive chemotherapy or may choose the less intensive chemotherapy as the first-line therapy due to personal preference. There is a paucity of reported data on the initial treatment patterns and clinical outcomes in Chinese patient populations managed in the rituximab era. The aim of the study was to delineate the disease characteristics, treatment strategies, and survival in real-world Chinese MCL patients.

2 METHODS

2.1 Patients and Data Collection

Retrospective data of newly diagnosed MCL patients were collected from 5 major Chinese Hematology Centers in Beijing, Guangzhou, Nanjing, Shanghai, and Suzhou in the period from 2007 to 2017. The diagnosis for MCL was based on characteristic immunophenotype and cyclin D1 immunohistochemistry staining. The stage was evaluated by PET/CT or CT scan of the neck, chest, abdomen, and pelvis and by bone marrow biopsy. For patients with gastrointestinal involvement indicated during imaging examination, gastrointestinal endoscopy was conducted. Patients with unconfirmed diagnostic histology, unknown initial treatment, or missing outcome data were excluded. The analysis was approved by the Institutional Review Board of the lead institution of The First Affiliated Hospital of Soochow University and all other participating institutions. Data cut for the last follow-up occurred on 31 October 2019.

In total, 518 cases were included in the final analysis, out of 605 cases initially diagnosed with MCL. Of the 87 cases that were excluded, 51 cases were subsequently determined by the Pathology Department at each center to be non-MCL in December 2019 based on the 2016 revision of the World Health Organization Classification of lymphoid neoplasms (6). Another 36 cases were excluded due to conflicting survival data between the first and the second follow-up, conducted between July 2018 and October 2019.

2.2 Statistical Analysis

Median follow-up time was estimated for overall survival (OS) using the reverse Kaplan–Meier method. OS time was calculated from the date of diagnosis to the date of death or date of the last follow-up, whichever comes first. Differences between the clinical characteristics and therapy strategies were analyzed with the chi-square test. The Kaplan–Meier estimator was used to estimate survival probability. Survival differences between groups were calculated using the log-rank test for statistical significance. The confidence intervals of the survival rates were calculated using Greenwood's formula. Univariate and multivariate analyses with the Cox proportional hazards model were conducted to estimate the effects of prognostic factors on survival. All statistical tests were two-sided, with an alpha level of 0.05 as the significance cutoff. All analyses were performed in SAS statistical software, version 9.4 (SAS Institute, Cary, NC, USA).

3 RESULTS

3.1 Patient Characteristics

A total of 518 newly diagnosed MCL patients with a confirmed diagnosis and longitudinal treatment history and outcome data were included in the analysis. The median age was 58 years (range = 28–83 years), with 59.7% of the patients not older than 60 years; the male-to-female ratio was 3.35:1. Of all patients, 88.6% had Eastern Cooperative Oncology Group Performance Status (ECOG PS) 0–1 and 80.7% had advanced-stage disease. Ki67 expression was <30% in 39.6% and was ≥30% in 44.6% of the patients. About 27.6% of the patients presented with International Prognostic Index (IPI) of 3–5, and 37.8% had intermediate- and high-risk Mantle Cell Lymphoma International Prognostic Index (MIPI) scores (**Table 1**).

TABLE 1 | Patient characteristics in different age groups.

	Total *N* (%)	Age (years)		*p*-value
		≤60, *N* (%)	>60, *N* (%)	
No. of patients	518	309 (59.7)	209 (40.3)	–
Age	median (range)	58.00	(28.00–83.00)	–
Gender				
Male	399 (77.0)	243 (78.6)	156 (74.6)	0.288
Female	119 (23.0)	66 (21.4)	53 (25.4)	
ECOG PS				
0–1	459 (88.6)	284 (91.9)	175 (83.7)	0.003
>1	44 (8.5)	17 (5.5)	27 (12.9)	
Missing	15 (2.9)	8 (2.6)	7 (3.3)	
Ann Arbor stage				
I–II	62 (12.0)	34 (11.0)	28 (13.4)	0.480
III–IV	418 (80.7)	249 (80.6)	169 (80.9)	
Missing	38 (7.3)	26 (8.4)	12 (5.7)	
MIPI				
High risk	96 (18.5)	24 (7.8)	72 (34.4)	<0.001
Intermediate risk	100 (19.3)	23 (7.4)	77 (36.8)	
Low risk	224 (43.2)	191 (61.8)	33 (15.8)	
Missing	98 (18.9)	71 (23.0)	27 (12.9)	
IPI				
0–1	142 (27.4)	129 (41.7)	13 (6.2)	<0.001
2	138 (26.6)	75 (24.3)	63 (30.1)	
3	112 (21.6)	31 (10.0)	81 (38.8)	
4–5	31 (6.0)	2 (0.6)	29 (13.9)	
Missing	95 (18.3)	72 (23.3)	23 (11.0)	
LDH				
Elevated	96 (18.5)	49 (15.9)	47 (22.5)	0.043
Normal	220 (42.5)	139 (45.0)	81 (38.8)	
Missing	202 (39.0)	121 (39.2)	81 (38.8)	
BM positive				
No	247 (47.7)	165 (53.4)	82 (39.2)	0.002
Yes	217 (41.9)	115 (37.2)	102 (48.8)	
Missing	54 (10.4)	29 (9.4)	25 (12.0)	
Ki67				
<30%	205 (39.6)	136 (44.0)	69 (33.0)	0.032
≥30%	231 (44.6)	130 (42.1)	101 (48.3)	
Missing	82 (15.8)	43 (13.9)	39 (18.7)	

ECOG PS, Eastern Cooperative Oncology Group Performance Status; MIPI, Mantle Cell Lymphoma International Prognostic Index; IPI, International Prognostic Index; LDH, lactate dehydrogenase; BM, bone marrow.

The elderly group (patients over 60 years, 40.3%) was similar to the younger group (patients younger than 60 years) in gender distribution and stage status. Patients in the elderly group had a higher rate of poor ECOG PS, Ki67 expression ≥30%, elevated lactate dehydrogenase (LDH), and bone marrow involvement compared with younger patients. Since age was an important factor in both MIPI and IPI scores, the proportions of patients with intermediate- and high-risk MIPI and with IPI scores of 3–5 in the elderly group were higher than that in the younger group (71.2% *vs*. 15.2%, $p < 0.001$; 52.7% *vs*. 10.6%, $p < 0.001$, respectively) (**Table 1**).

3.2 Treatment Description

In the entire cohort, 73.4% ($n = 380$) of patients received rituximab as their first-line therapy. The use of rituximab was similar in the different age groups. A total of 162 (31.3%) patients were treated with high-dose cytarabine-containing chemotherapy. The most commonly used cytarabine-containing regimens were Hyper-CVAD (cyclophosphamide, vincristine, adriamycin, and dexamethasone) (83 cases) and DHAP (dexamethasone, Ara C, and cisplatin) (73 cases). The proportion of patients receiving high-dose cytarabine-containing chemotherapy was higher in the younger group than that in the elderly group (42.4% *vs*. 14.8%, $p < 0.001$).

Apart from the high-dose cytarabine-containing chemotherapy regimens, the most commonly used chemotherapy regimen was the CHOP-like (cyclophosphamide, hydroxydaunomycin, oncovin, and prednisone) regimen (45.2%). The proportions of patients using other regimens, such as bendamustine-based, CVP-like (cyclophosphamide, vincristine, and prednisolone), GemOx (gemcitabine and oxaliplatin), and FC (fludarabine and cyclophosphamide), were all less than 5%.

A total of 71 patients (13.7%) received ASCT as consolidation therapy. In the younger group, 68 patients (22.0%) received ASCT as consolidation therapy. Three patients over 60 years received ASCT, including a 68-year-old patient.

Among the 518 patients, 100 (19.3%) received regimens containing new drugs as their first-line therapy, such as bortezomib ($n = 28$, 5.4%), ibrutinib ($n = 20$, 3.9%), lenalidomide ($n = 18$, 3.5%), and thalidomide ($n = 34$, 6.6%) (**Table 2**).

3.3 Comparison of Survival Between Different Patient Characteristics

The median follow-up time was 52 months. During the analysis, 188 (36.3%) patients had died. The 3- and 5-year OS rates were 73.7% and 61.4%, respectively. Based on log-rank test analysis, the median OS for patients in the younger group was 119 months compared with 59 months in the elderly group (3-year OS = 81.3% *vs*. 62.8%, 5-year OS = 70.7% *vs*. 48.2%, $p < 0.001$). Except for gender, the stratification of all other baseline characteristics (including ECOG PS, Ann Arbor stage, LDH, bone marrow status, Ki67, IPI, and MIPI) provided a reliable prediction of the OS rates ($p < 0.001$, $p = 0.025$, $p < 0.001$, $p < 0.001$, $p < 0.001$, $p < 0.001$, and $p < 0.001$, respectively) (**Figure 1**).

3.4 Comparison of Individual Treatment Regimens

3.4.1 Rituximab

Patients receiving rituximab trended toward better outcomes compared with those without rituximab in the entire cohort (3-year OS = 74.4% *vs*. 69.0%, 5-year OS = 62.5% *vs*. 55.2%, $p = 0.076$) (**Figure 2A**). The inclusion of rituximab had similar efficacy in both the younger group and the elderly group (younger group: 3-year OS = 81.0% *vs*. 79.0%, 5-year OS = 72.7% *vs*. 64.9%, $p = 0.169$; elderly group: 3-year OS = 64.6% *vs*. 53.5%, 5-year OS = 48.6% *vs*. 39.9%, $p = 0.142$).

3.4.2 First-Line Chemotherapy

The use of high-dose cytarabine showed significant clinical benefit in OS (3-year OS = 77.2% *vs*. 71.1%, 5-year OS = 72.1% *vs*. 55.9%, $p = 0.010$) (**Figure 2B**). Nearly half of the patients (45.2%) received CHOP-like regimens, with the 3- and 5-year OS at 73.9% and 58.0%, respectively. In addition, patients receiving moderate regimens, such as CVP-like regimen, had a

TABLE 2 | Treatment summary in different age groups.

	Total *N* (%)	Age (years)		*p*-value
		≤60, *N* (%)	>60, *N* (%)	
No. of patients	518	309 (59.7%)	209 (40.3%)	–
Rituximab-containing regimen				
No	109 (21.0)	65 (21.0)	44 (21.1)	0.945
Yes	380 (73.4)	228 (73.8)	152 (72.7)	
Missing	29 (5.6)	16 (5.2)	13 (6.2)	
HDAC regimen				
No	326 (62.9)	161 (52.1)	165 (78.9)	<0.001
Yes	162 (31.3)	131 (42.4)	31 (14.8)	
Missing	30 (5.8)	17 (5.5)	13 (6.2)	
ASCT				
No	419 (80.9)	225 (72.8)	194 (92.8)	<0.001
Yes	71 (13.7)	68 (22.0)	3 (1.4)	
Missing	28 (5.4)	16 (5.2)	12 (5.7)	
First-line chemotherapy				
CHOP-like	234 (45.2)	140 (45.3)	94 (45.0)	<0.001
Hyper-CVAD	83 (16.0)	62 (20.1)	21 (10.0)	
DHAP	73 (14.1)	62 (20.1)	11 (5.3)	
V-CAP	18 (3.5)	6 (1.9)	12 (5.7)	
Bendamustine-based	17 (3.3)	1 (0.3)	16 (7.7)	
CVP-like	12 (2.3)	4 (1.3)	8 (3.8)	
GemOx	12 (2.3)	0 (0.0)	12 (5.7)	
FC	9 (1.7)	5 (1.6)	4 (1.9)	
Others	23 (4.4)	10 (3.2)	13 (6.2)	
Missing	37 (7.1)	19 (6.1)	18 (8.6)	
First-line novel agents				
Bortezomib	28 (5.4)	14 (4.5)	14 (6.7)	<0.001
Ibrutinib	20 (3.9)	4 (1.3)	16 (7.7)	
Lenalidomide	18 (3.5)	9 (2.9)	9 (4.3)	
Thalidomide	34 (6.6)	14 (4.5)	20 (9.6)	
No	418 (80.7)	268 (86.7)	150 (71.8)	

HDAC, high-dose cytarabine-containing; ASCT, autologous stem cell transplantation; CHOP, cyclophosphamide, hydroxydaunomycin, oncovin, and prednisone; CVAD, cyclophosphamide, vincristine, adriamycin, and dexamethasone; DHAP, dexamethasone, Ara C, and cisplatin; V-CAP, bortezomib, cyclophosphamide, adriamycin, and prednisone; CVP, cyclophosphamide, vincristine, and prednisolone; GemOx, gemcitabine and oxaliplatin; FC, fludarabine and cyclophosphamide.

3-year OS of 50.0%. Among the patients who received bendamustine-based regimens (n = 17, 3.3%), the 3- and 5-year OS rates were 88.2% and 69.1%, respectively. The 3- and 5-year OS rates were 81.4% and 74.0% in patients receiving the V-CAP (bortezomib, cyclophosphamide, adriamycin, and prednisone) regimen (n = 18, 3.5%) (**Table 3**).

3.4.3 Autologous Stem Cell Transplant

In the entire cohort, patients with consolidative ASCT achieved 3- and 5-year OS rates of 87.8% and 84.5%, respectively, which were significantly higher than those in patients without ASCT (3-year OS = 70.6%, 5-year OS = 56.3%, $p < 0.001$) (**Figure 2C**). In the younger group, patients with consolidative ASCT had better survival outcomes (3-year OS = 87.2% *vs.* 78.4%, 5-year OS = 87.2% *vs.* 64.8%, $p = 0.002$).

3.5 Prognostic Factors

The results of the univariate analysis of independent factors are listed in **Table 4**. Based on the multivariate analysis, high-risk MIPI [hazard ratio (HR) = 2.32, 95% CI = 1.30–4.14, $p = 0.0042$), Ki67 ≥30% (HR = 2.11, 95% CI = 1.37–3.24, $p = 0.0007$), treatment with a rituximab-containing regimen (HR = 0.55, 95% CI = 0.33–0.91, $p = 0.0197$), and treatment with a high-dose cytarabine-containing regimen (HR = 0.50, 95% CI = 0.27–0.92, $p = 0.0252$) were independent risk factors for the prediction of OS.

4 DISCUSSION

This retrospective, multicenter, real-world study presents the largest Chinese patient cohort of MCL to date. MCL is a heterogeneous and incurable type of lymphoma with highly varied clinical courses. The treatment strategies for MCL have evolved rapidly during the last decade, while the implementation of treatment guidelines remains variable globally due to local practices and access to care. In our study, we investigated the association between the clinical features, initial treatment strategies, and outcomes of MCL patients seeking initial treatment at major academic hematology centers within China.

The 3- and 5-year OS rates of the entire cohort were 73.7% and 61.4% in this study. In the younger group, the 3- and 5-year OS rates were 81.3% and 70.7%, respectively. In contrast, these were 62.8% and 48.2% in the elderly group, respectively. The survival rate appeared to be higher than other real-world data reported from the UK (3-year OS = 43.9%) (7) or Scandinavia (3-year OS = 51%–61%) (8). Several factors potentially account for the differences. Patients with complete diagnosis and treatment data available in this study had a median age of 58 years, which was younger than the median age of patients in Western populations (9). The majority of patients seeking care at major medical centers had good performance status, and nearly half of the patients had low-risk MIPI/IPI scores, which correlated with favorable survival. In comparison to population-based studies, the improved survival from the current study may reflect referral and treatment decisions that were selected for younger and fit patients at the major urban referral centers. Nonetheless, the clinical parameters retained robust prognostic significance within the study cohort.

Combining rituximab in the CHOP regimen had been confirmed to improve the objective response rate and the complete remission rate compared to chemotherapy alone in a prospective randomized trial in young MCL patients in 2005 (10). Rituximab chemotherapy has since been incorporated into the National Comprehensive Cancer Network (NCCN) guideline. The recommended frontline treatment for younger patients was intensive chemotherapy with a high-dose cytarabine-containing regimen with rituximab. The survival benefit of adding rituximab to the CHOP regimen has also been demonstrated in previous randomized (11) and observational (12) studies for elderly MCL patients. The bendamustine plus rituximab regimen conferred better progression-free survival (PFS) in elderly patients compared with the R-CHOP regimen in the StiL and BRIGHT studies (13, 14). Since the expense of rituximab could not be covered by

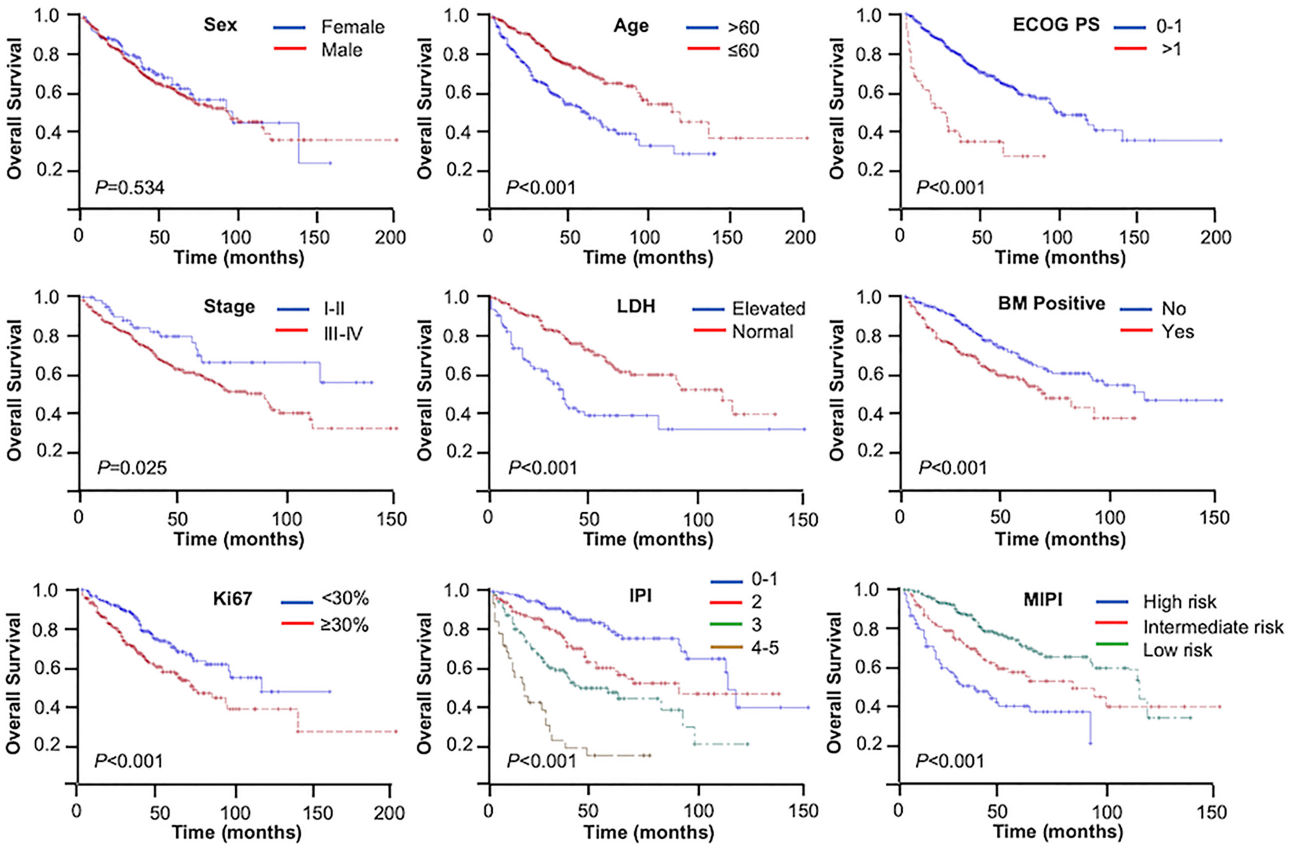

FIGURE 1 | Kaplan–Meier curves: overall survival (OS) in different patient characteristics.

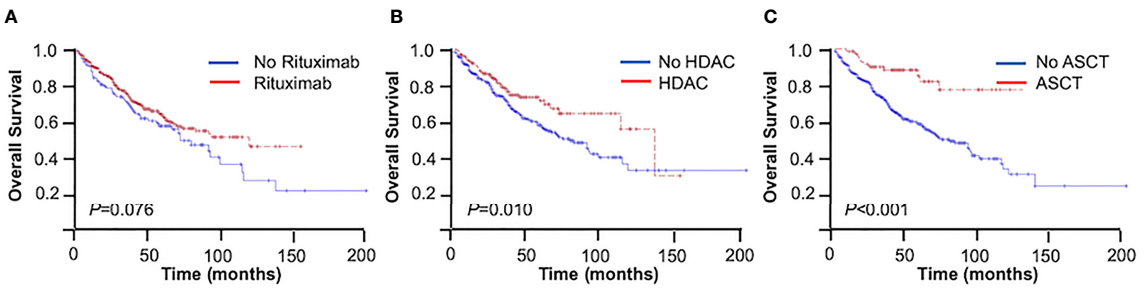

FIGURE 2 | Overall survival (OS) of mantle cell lymphoma (MCL) patients. **(A)** With or without rituximab. **(B)** With or without high-dose cytarabine-containing (HDAC) regimen. **(C)** With or without autologous stem cell transplantation (ASCT).

government-sponsored medical insurance until September 2017, a number of patients enrolled before 2017 opted not to use rituximab for economic reasons. In addition, China has been an endemic area for hepatitis B virus (HBV) infection. Thus, some patients had a high level of HBV DNA and could not receive rituximab treatment. Consequently, only 73.4% of patients received rituximab as part of their initial therapy in our study. Compared to those without rituximab, patients receiving rituximab in our study had superior OS with borderline significance (3-year OS = 74.4% *vs.* 69.0%, 5-year OS = 62.5% *vs.* 55.2%, p = 0.076). The benefit of rituximab on survival was consistent with the results of other real-world studies (7, 8). Our data supported that immunochemotherapy was the cornerstone of MCL induction in the rituximab era. The survival data with rituximab maintenance after induction therapy or consolidative ASCT were not collected in this

TABLE 3 | Overall survival (OS) stratified by clinical features and therapy strategies in mantle cell lymphoma (MCL).

	Total (event)	Median (95% CI)	3-year OS (95% CI)	5-year OS (95% CI)	*p*-value
Overall	514 (188)	95.0 (73.0–119.0)	73.7 (69.7–77.8)	61.4 (56.4–66.4)	
Gender					
Male	399 (149)	95.0 (69.0–119.0)	72.6 (67.9–77.3)	60.9 (55.3–66.6)	0.534
Female	119 (40)	95.0 (64.0–)	77.4 (69.4–85.5)	62.8 (52.2–73.4)	
Age (years)					
≤60	309 (87)	119.0 (96.0–)	81.3 (76.5–86.0)	70.7 (64.6–76.8)	<0.001
>60	209 (102)	59.0 (42.0–73.0)	62.8 (55.9–69.7)	48.2 (40.3–56.1)	
ECOG PS					
0–1	459 (154)	97.0 (76.0–124.0)	77.5 (73.4–81.6)	64.4 (59.1–69.7)	<0.001
>1	44 (30)	19.0 (5.0–35.0)	34.1 (19.6–48.6)	31.1 (16.8–45.5)	
Ann Arbor stage					
I–II	62 (16)	(62.0–)	81.2 (70.6–91.8)	71.9 (58.2–85.6)	0.025
III–IV	418 (166)	74.0 (64.0–97.0)	71.6 (67.0–76.2)	58.1 (52.5–63.6)	
MIPI					
High risk	96 (55)	28.0 (18.0–47.0)	47.5 (37.0–58.0)	36.5 (25.3–47.8)	<0.001
Intermediate risk	100 (43)	86.0 (42.0–)	67.4 (57.7–77.1)	54.8 (43.6–66.0)	
Low risk	224 (60)	120.0 (95.0–)	83.5 (78.2–88.8)	69.7 (62.1–77.3)	
IPI					
0–1	142 (30)	120.0 (99.0–)	89.8 (84.5–95.1)	80.0 (71.9–88.1)	<0.001
2	138 (47)	95.0 (53.0–)	76.5 (68.7–84.3)	58.8 (48.4–69.2)	
3	112 (56)	42.0 (29.0–97.0)	57.8 (48.2–67.4)	45.7 (34.9–56.5)	
4–5	31 (25)	16.0 (7.0–27.0)	20.3 (4.9–35.6)	12.2 (0.0–24.8)	
LDH					
Elevated	96 (51)	37.0 (26.0–48.0)	50.7 (39.8–61.6)	36.7 (25.2–48.2)	<0.001
Normal	220 (67)	119.0 (72.0–)	81.4 (75.8–86.9)	65.9 (58.0–73.7)	
BM positive					
No	247 (74)	119.0 (76.0–)	80.2 (74.7–85.7)	66.5 (59.1–73.8)	<0.001
Yes	217 (92)	69.0 (48.0–98.0)	66.9 (60.4–73.4)	54.7 (47.0–62.4)	
Ki67					
<30%	205 (56)	119.0 (82.0–)	84.9 (79.6–90.2)	69.1 (61.2–76.9)	<0.001
≥30%	231 (94)	71.0 (53.0–95.0)	68.3 (61.8–74.7)	55.7 (48.1–63.4)	
Rituximab-containing regimen					
No	109 (54)	74.0 (46.0–103.0)	69.0 (60.0–78.0)	55.2 (44.9–65.5)	0.076
Yes	380 (128)	97.0 (69.0–)	74.4 (69.7–79.1)	62.5 (56.6–68.3)	
HDAC regimen					
No	326 (137)	74.0 (59.0–96.0)	71.1 (65.9–76.3)	55.9 (49.7–62.2)	0.010
Yes	162 (44)	143.0 (119.0–)	77.2 (70.2–84.1)	72.1 (64.3–79.9)	
First-line chemotherapy					
CHOP-like	234 (93)	73.0 (62.0–143.0)	73.9 (67.9–79.9)	58.0 (50.7–65.3)	<0.001
Hyper-CVAD	83 (31)	119.0 (60.0–)	68.8 (58.4–79.3)	63.6 (52.4–74.9)	
DHAP	73 (9)	(74.0–)	85.8 (76.3–95.3)	85.8 (76.3–95.3)	
V-CAP	18 (5)	(37.0–)	81.4 (62.2–100.0)	74.0 (51.7–96.2)	
Bendamustine-based	17 (5)	(47.0–)	88.2 (72.9–100.0)	69.1 (46.4–91.7)	
CVP-like	12 (8)	40.5 (5.0–57.0)	50.0 (21.7–78.3)	–	
GemOx	12 (5)	42.0 (1.0–)	65.6 (38.1–93.1)	43.8 (4.2–83.3)	
FC	9 (8)	26.0 (3.0–103.0)	44.4 (12.0–76.9)	22.2 (0.0–49.4)	
ASCT					
No	419 (173)	73.0 (62.0–96.0)	70.6 (65.9–75.2)	56.3 (50.7–62.0)	<0.001
Yes	71 (11)	(–)	87.8 (79.8–95.8)	84.5 (74.5–94.4)	

ECOG PS, Eastern Cooperative Oncology Group Performance Status; MIPI, Mantle Cell Lymphoma International Prognostic Index; IPI, International Prognostic Index; LDH, lactate dehydrogenase; BM, bone marrow; HDAC, high-dose cytarabine-containing; ASCT, autologous stem cell transplantation; CI, confidence interval; CHOP, cyclophosphamide, hydroxydaunomycin, oncovin, and prednisone; CVAD, cyclophosphamide, vincristine, adriamycin, and dexamethasone; DHAP, dexamethasone, Ara C, and cisplatin; V-CAP, bortezomib, cyclophosphamide, adriamycin, and prednisone; CVP, cyclophosphamide, vincristine, and prednisolone; GemOx, gemcitabine and oxaliplatin; FC, fludarabine and cyclophosphamide.

analysis; therefore, their impact on PFS and OS in MCL Chinese patients is undefined (15, 16).

Apart from rituximab, intensive chemotherapy and cytarabine-containing regimens were the most important factors in induction therapy for younger MCL patients, as demonstrated in regimens such as R-DHAP or R-DHAx (rituximab, dexamethasone, cytarabine, and oxaliplatin) alternating with R-CHOP, R-Hyper-CVAD, or Nordic MCL studies (15, 17–22). Our study demonstrated the benefits of high-dose cytarabine-containing regimens in MCL patients (3-year OS = 77.2% *vs*. 71.1%, 5-year OS = 72.1% *vs*. 55.9%, $p = 0.010$). Data on the efficacy of and tolerance to cytarabine-containing regimens of elderly Chinese patients remain scanty and deserve attention in future studies.

TABLE 4 | Univariate and multivariate predictor analyses.

	Univariable Cox		Multivariable Cox	
Variable	**HR (95%CI)**	***p*-value**	**HR (95%CI)**	***p*-value**
Ann Arbor stages III–IV	3.26 (1.32–8.04)	0.0104	2.22 (0.88–5.63)	0.0914
BM positive	1.86 (1.25–2.78)	0.0022	1.49 (0.96–2.32)	0.0749
MIPI				
High risk	4.18 (2.49–6.99)	<0.0001	2.32 (1.30–4.14)	0.0042
Intermediate risk	1.73 (1.10–2.72)	0.0183	1.31 (0.79–2.15)	0.2937
Ki67 ≥30%	2.32 (1.52–3.54)	<0.0001	2.11 (1.37–3.24)	0.0007
Rituximab regimen	0.62 (0.38–1.00)	0.0505	0.55 (0.33–0.91)	0.0197
HDAC regimen	0.34 (0.20–0.61)	0.0002	0.50 (0.27–0.92)	0.0252
ASCT	0.39 (0.19–0.80)	0.0102	0.65 (0.30–1.42)	0.2858

ECOG PS, Eastern Cooperative Oncology Group Performance Status; LDH, lactate dehydrogenase; BM, bone marrow; MIPI, Mantle Cell Lymphoma International Prognostic Index; IPI, International Prognostic Index; HDAC, high-dose cytarabine-containing; ASCT, autologous stem cell transplantation; CI, confidence interval.

The survival benefit of ASCT in MCL has been well demonstrated (23, 24). In our study, consolidative ASCT was significantly associated with improved OS in the younger group (3-year OS = 87.2% *vs*. 78.4%, 5-year OS = 87.2% *vs*. 64.8%, $p = 0.002$). However, less than one-third of the young MCL patient group underwent ASCT in the real world (22.0% from our dataset and 17%–31% from other real-world studies) (7, 8, 25). Several factors may have limited broad access to ASCT, including: 1) comorbidities contraindicating ASCT; 2) failure in achieving remission; 3) unsuccessful harvest of stem cells; 4) patient preference due to treatment costs; and 5) availability of local expertise for ASCT.

Novel agents have made their way into real-world practice, first through the introduction of global clinical trials, followed by market access for approved new drugs in relapsed and refractory diseases. Bortezomib, lenalidomide, bendamustine, and Bruton's tyrosine kinase (BTK) inhibitors have all been approved for the treatment of relapsed and refractory MCL. In recent years, VR-CAP (bortezomib, rituximab, cyclophosphamide, adriamycin, and prednisone) and lenalidomide + rituximab regimens have shown favorable survival outcomes when compared with the R-CHOP regimen directly or with historical data (26–28). Compared with other drugs, BTK inhibitors as single agents have shown higher overall response rates, complete remission rates, and PFS, contributing to improved survival of relapsed and refractory MCL patients (29, 30). The survival benefits conferred by BTK inhibitors in Chinese patients have also been reported (31). In addition, BTK inhibitors are being incorporated into first-line regimens in multiple global phase 3 studies. In our study, 100 patients (19.3%) received regimens containing new drugs, namely, VR-CAP containing bortezomib, bendamustine and rituximab (BR) with ibrutinib, and CHOP or GemOx with either lenalidomide or thalidomide, in the context of either global trials or off-label uses. With accelerated new drug approvals for market access in China, Chinese oncologists will be equipped with an increasing number of treatment strategies to benefit patients.

There were several limitations of our study, mostly pertaining to the retrospective nature of a hospital-based cohort. Firstly, our study did not include temporal data of the earliest diagnosis and the commencement of first-line therapy before hospitalization; therefore, the data did not contain information on the "watch-and-wait" strategy. Secondly, the lack of a prior standardization in the induction regimen and drug dosage among the different centers resulted in heterogeneity in first-line treatment. Thirdly, the limited number of patients who received novel agents was suboptimal for a thorough evaluation of their therapeutic benefits.

In conclusion, this large retrospective dataset of MCL patients who received contemporaneous real-world management in Chinese hematology centers confirmed the survival advantage afforded by high-dose cytarabine-containing chemotherapy and consolidative autologous stem cell transplantation in a first-line setting. The majority of patients in this series were not older than 60 years with good performance status and lower-risk MIPI/IPI scores, which correlated with more favorable survival in response to chemo-immunotherapy. The incorporation of novel agents signals infrastructural readiness to explore novel agents and combinations in both first-line and relapsed settings. It remains to be seen whether a broader demographic population of MCL patients would be attracted to the Chinese academic centers for longitudinal follow-up in the novel agent era, including those more elderly and with comorbidities who are unfit for chemotherapy and those asymptomatic who can be initially managed with expectant watch-and-wait.

DATA AVAILABILITY STATEMENT

The raw data supporting the conclusions of this article will be made available by the authors, without undue reservation.

ETHICS STATEMENT

The studies involving human participants were reviewed and approved by the Institutional Review Board of the lead institution of The First Affiliated Hospital of Soochow University and all other participating institutions. Written informed consent for participation was not required for this study, in accordance with the national legislation and the institutional requirements.

AUTHOR CONTRIBUTIONS

MW collected the data and drafted and revised the paper. YL prepared the data and drafted the paper. HuH, WX, HaH, WZ, JZ, and DW participated in designing and revising the paper. SL, YW, and PX collected the data. ZC performed statistical analyses. JR and YS designed the study, interpreted the results, and revised the paper. DW provided logistic support for the study. All authors provided critical comments on the manuscript. All authors contributed to the article and approved the submitted version.

FUNDING

This work was supported by grants from National Natural Science Foundation of China (81730003, 81828001, 81972807, and 81970179), National Science and Technology Major Project (2017ZX09304021), National Science and Technology Major Project for "Significant New Drug Development" (2020zx09201-023), National Key R&D Program of China (2019YFC0840604 and 2017YFA0104502), Key R&D Program of Jiangsu Province (BE2019798), Priority Academic Program Development of Jiangsu Higher Education Institutions (PAPD), Jiangsu Medical Outstanding Talents Project (JCRCA2016002), Jiangsu Provincial Key Medical Center (YXZXA2016002), Suzhou Science and Technology Program Project (SLT201911), the Translational Research Grant of NCRCH (no. 2020ZKMB02), and Suzhou Science and Technology Development Project (no. SYS2019039).

ACKNOWLEDGMENTS

The authors thank all clinicians of the five participating centers for entering data into this study and Sicheng Ai (New York University, New York, NY, USA) for the grammar review.

REFERENCES

1. Teras LR, DeSantis CE, Cerhan JR, Morton LM, Jemal A, Flowers CR. 2016 US Lymphoid Malignancy Statistics by World Health Organization Subtypes. *CA: A Cancer J Clin* (2016) 66(6):443–59. doi: 10.3322/caac.21357
2. The Non-Hodgkin's Lymphoma Classification Project. A Clinical Evaluation of the International Lymphoma Study Group Classification of Non-Hodgkin's Lymphoma. *Blood* (1997) 89(11):3909–18. doi: 10.1182/blood.V89.11.3909
3. Nair R, Arora N, Mallath MK. Epidemiology of Non-Hodgkin's Lymphoma in India. *Oncology* (2016) 91(suppl 1):18–25. doi: 10.1159/000447577
4. Sun J, Yang Q, Lu Z, He M, Gao L, Zhu M, et al. Distribution of Lymphoid Neoplasms in China: Analysis of 4,638 Cases According to the World Health Organization Classification. *Am J Clin Pathol* (2012) 138(3):429–34. doi: 10.1309/AJCP7YLTQPUSDQ5C
5. Abrisqueta P, Scott DW, Slack GW, Steidl C, Mottok A, Gascoyne RD, et al. Observation as the Initial Management Strategy in Patients With Mantle Cell Lymphoma. *Ann Oncol* (2017) 28(10):2489–95. doi: 10.1093/annonc/mdx333.
6. Swerdlow SH, Campo E, Pileri SA, Harris NL, Stein H, Siebert R, et al. The 2016 Revision of the World Health Organization Classification of Lymphoid Neoplasms. *Blood* (2016) 127(20):2375–90. doi: 10.1182/blood-2016-01-643569.
7. Smith A, Roman E, Appleton S, Howell D, Johnson R, Burton C, et al. Impact of Novel Therapies for Mantle Cell Lymphoma in the Real World Setting: A Report From the UK UK 'S Haematological Malignancy Research Network (HMRN HMRN). *Br J Haematol* (2018) 181(2):215–28. doi: 10.1111/bjh.15170
8. Abrahamsson A, Albertsson-Lindblad A, Brown PN, Baumgartner-Wennerholm S, Pedersen LM, D'Amore F, et al. Real World Data on Primary Treatment for Mantle Cell Lymphoma: A Nordic Lymphoma Group Observational Study. *Blood* (2014) 124(6):1288–95. doi: 10.1182/blood-2014-03-559930
9. Jain P, Wang M. Mantle Cell Lymphoma: 2019 Update on the Diagnosis, Pathogenesis, Prognostication, and Management. *Am J Hematol* (2019) 94(6):710–25. doi: 10.1002/ajh.25487
10. Lenz G, Dreyling M, Hoster E, Wörmann B, Dührsen U, Metzner B, et al. Immunochemotherapy With Rituximab and Cyclophosphamide, Doxorubicin, Vincristine, and Prednisone Significantly Improves Response and Time to Treatment Failure, But Not Long-Term Outcome in Patients With Previously Untreated Mantle Cell Lymphoma: Results of a Prospective Randomized Trial of the German Low Grade Lymphoma Study Group (GLSG). *J Clin Oncol* (2005) 23(9):1984–92. doi: 10.1200/JCO.2005.08.133
11. Rule S, Smith P, Johnson PW, Bolam S, Follows G, Gambell J, et al. The Addition of Rituximab to Fludarabine and Cyclophosphamide Chemotherapy Results in a Significant Improvement in Overall Survival in Patients With Newly Diagnosed Mantle Cell Lymphoma: Results of a Randomized UK National Cancer Research Institute Trial. *Haematologica* (2016) 101(2):235–40. doi: 10.3324/haematol.2015.128710
12. Griffiths R, Mikhael J, Michelle G, Danese M, Dreyling M. Addition of Rituximab to Chemotherapy Alone as First-Line Therapy Improves Overall Survival in Elderly Patients With Mantle Cell Lymphoma. *Blood* (2011) 118(18):4808–16. doi: 10.1182/blood-2011-04-348367
13. Rummel MJ, Niederle N, Maschmeyer G, Banat GA, von Grünhagen U, Losem C, et al. Bendamustine Plus Rituximab Versus CHOP Plus Rituximab as First-Line Treatment for Patients With Indolent and Mantle-Cell Lymphomas: An Open-Label, Multicentre, Randomised, Phase 3 non-Inferiority Trial. *Lancet* (2013) 381(9873):1203–10. doi: 10.1016/S0140-6736(12)61763-2
14. Flinn IW, van der Jagt R, Kahl B, Wood P, Hawkins T, MacDonald D, et al. First-Line Treatment of Patients With Indolent Non-Hodgkin Lymphoma or Mantle-Cell Lymphoma With Bendamustine Plus Rituximab Versus R-CHOP or R-CVP: Results of the BRIGHT 5-Year Follow-Up Study. *J Clin Oncol* (2019) 37(12):984–91. doi: 10.1200/JCO.18.00605
15. Le Gouill S, Thieblemont C, Oberic L, Moreau A, Bouabdallah K, Dartigeas C, et al. Rituximab After Autologous Stem-Cell Transplantation in Mantle-Cell Lymphoma. *N Engl J Med* (2017) 377(13):1250–60. doi: 10.1056/NEJMoa1701769
16. Kluin-Nelemans HC, Hoster E, Hermine O, Walewski J, Geisler CH, Trneny M, et al. Treatment of Older Patients With Mantle Cell Lymphoma (MCL): Long-Term Follow-Up of the Randomized European MCL Elderly Trial. *J Clin Oncol* (2019) 38(3):248–56. doi: 10.1200/JCO.19.01294
17. Hermine O, Hoster E, Walewski J, Bosly A, Stilgenbauer S, Thieblemont C, et al. Addition of High-Dose Cytarabine to Immunochemotherapy Before Autologous Stem-Cell Transplantation in Patients Aged 65 Years or Younger With Mantle Cell Lymphoma (MCL Younger): A Randomised, Open-Label, Phase 3 Trial of the European Mantle Cell Lymphoma Network. *Lancet* (2016) 388(10044):565–75. doi: 10.1016/S0140-6736(16)00739-X
18. Geisler CH, Kolstad A, Laurell A, Andersen NS, Pedersen LB, Jerkeman M, et al. Long-Term Progression-Free Survival of Mantle Cell Lymphoma After Intensive Front-Line Immunochemotherapy With *In Vivo*-Purged Stem Cell Rescue: A Nonrandomized Phase 2 Multicenter Study by the Nordic Lymphoma Group. *Blood* (2008) 112(7):2687–93. doi: 10.1182/blood-2008-03-147025
19. Geisler CH, Kolstad A, Laurell A, Jerkeman M, Räty R, Andersen NS, et al. Nordic MCL2 Trial Update: Six-Year Follow-Up After Intensive Immunochemotherapy for Untreated Mantle Cell Lymphoma Followed by BEAM or BEAC + Autologous Stem-Cell Support: Still Very Long Survival But Late Relapses do Occur. *Br J Haematol* (2012) 158(3):355–62. doi: 10.1111/j.1365-2141.2012.09174.x

20. Eskelund CW, Kolstad A, Jerkeman M, Räty R, Laurell A, Eloranta S, et al. 15-Year Follow-Up of the Second Nordic Mantle Cell Lymphoma Trial (MCL2): Prolonged Remissions Without Survival Plateau. *Br J Haematol* (2016) 175 (3):410–8. doi: 10.1111/bjh.14241
21. Merli F, Luminari S, Ilariucci F, Petrini M, Visco C, Ambrosetti A, et al. Rituximab Plus HyperCVAD Alternating With High Dose Cytarabine and Methotrexate for the Initial Treatment of Patients With Mantle Cell Lymphoma, a Multicentre Trial From Gruppo Italiano Studio Linfomi. *Br J Haematol* (2012) 156(3):346–53. doi: 10.1111/j.1365-2141.2011.08958.x
22. Chihara D, Cheah CY, Westin JR, Fayad LE, Rodriguez MA, Hagemeister FB, et al. Rituximab Plus Hyper-CVAD Alternating With MTX/Ara-C in Patients With Newly Diagnosed Mantle Cell Lymphoma: 15-Year Follow-Up of a Phase II Study From the MD Anderson Cancer Center. *Br J Haematol* (2016) 172(1):80–8. doi: 10.1111/bjh.13796
23. Dreyling M, Lenz G, Hoster E, Van Hoof A, Gisselbrecht C, Schmits R, et al. Early Consolidation by Myeloablative Radiochemotherapy Followed by Autologous Stem Cell Transplantation in First Remission Significantly Prolongs Progression-Free Survival in Mantle-Cell Lymphoma: Results of a Prospective Randomized Trial of the European MCL Network. *Blood* (2005) 105(7):2677–84. doi: 10.1182/blood-2004-10-3883
24. Gerson JN, Handorf E, Villa D, Gerrie AS, Chapani P, Li S, et al. Survival Outcomes of Younger Patients With Mantle Cell Lymphoma Treated in the Rituximab Era. *J Clin Oncol* (2019) 37(6):471–80. doi: 10.1200/JCO.18.00690
25. Sawalha Y, Radivoyevitch T, Tullio K, Dean RM, Pohlman B, Hill BT, et al. The Role of Upfront Autologous Hematopoietic Cell Transplantation in the Treatment of Mantle Cell Lymphoma, a Population Based Study Using the National Cancer Data Base (NCDB). *Blood* (2017) 130(Supplement 1):2009–9. doi: 10.1182/blood.V130.Suppl_1.2009.2009
26. Robak T, Huang H, Jin J, Zhu J, Liu T, Samoilova O, et al. Bortezomib-Based Therapy for Newly Diagnosed Mantle-Cell Lymphoma. *N Engl J Med* (2015) 372(10):944–53. doi: 10.1056/NEJMoa1412096
27. Ruan J, Martin P, Christos P, Cerchietti L, Tam W, Shah B, et al. Five-Year Follow-Up of Lenalidomide Plus Rituximab as Initial Treatment of Mantle Cell Lymphoma. *Blood* (2018) 132(19):2016–25. doi: 10.1182/blood-2018-07-859769
28. Ruan J, Martin P, Shah B, Schuster SJ, Smith SM, Furman RR, et al. Lenalidomide Plus Rituximab as Initial Treatment for Mantle-Cell Lymphoma. *N Engl J Med* (2015) 373(19):1835–44. doi: 10.1056/NEJMoa1505237
29. Wang ML, Blum KA, Martin P, Goy A, Auer R, Kahl BS, et al. Long-Term Follow-Up of MCL Patients Treated With Single-Agent Ibrutinib: Updated Safety and Efficacy Results. *Blood* (2015) 126(6):739–45. doi: 10.1182/blood-2015-03-635326.
30. Wang M, Rule S, Zinzani PL, Goy A, Casasnovas O, Smith SD, et al. Acalabrutinib in Relapsed or Refractory Mantle Cell Lymphoma (ACE-LY-004): A Single-Arm, Multicentre, Phase 2 Trial. *Lancet* (2018) 391 (10121):659–67. doi: 10.1016/s0140-6736(17)33108-2.
31. Song Y, Zhou K, Zou D, Zhou J, Hu J, Yang H, et al. Treatment of Patients With Relapsed or Refractory Mantle-Cell Lymphoma With Zanubrutinib, a Selective Inhibitor of Bruton's Tyrosine Kinase. *Clin Cancer Res* (2020) 26 (16):4216–24. doi: 10.1158/1078-0432.Ccr-19-3703.

Conflict of Interest: The authors declare that the research was conducted in the absence of any commercial or financial relationships that could be construed as a potential conflict of interest.

Publisher's Note: All claims expressed in this article are solely those of the authors and do not necessarily represent those of their affiliated organizations, or those of the publisher, the editors and the reviewers. Any product that may be evaluated in this article, or claim that may be made by its manufacturer, is not guaranteed or endorsed by the publisher.

frontiers in Oncology

BRIEF RESEARCH REPORT
published: 05 January 2022
doi: 10.3389/fonc.2021.708915

CXCR4 Mediates Enhanced Cell Migration in *CALM-AF10* Leukemia

Shelby A. Fertal[1†], *Sayyed K. Zaidi*[2,3†], *Janet L. Stein*[2,3], *Gary S. Stein*[2,3] *and Jessica L. Heath*[1,2,3*]

[1] Department of Pediatrics, Larner College of Medicine, University of Vermont, Burlington, VT, United States, [2] Department of Biochemistry, Larner College of Medicine, University of Vermont, Burlington, VT, United States, [3] University of Vermont Cancer Center, Burlington, VT, United States

Leukemia transformed by the *CALM-AF10* chromosomal translocation is characterized by a high incidence of extramedullary disease, central nervous system (CNS) relapse, and a poor prognosis. Invasion of the extramedullary compartment and CNS requires leukemia cell migration out of the marrow and adherence to the cells of the local tissue. Cell adhesion and migration are increasingly recognized as contributors to leukemia development and therapeutic response. These processes are mediated by a variety of cytokines, chemokines, and their receptors, forming networks of both secreted and cell surface factors. The cytokines and cytokine receptors that play key roles in *CALM-AF10* driven leukemia are unknown. We find high cell surface expression of the cytokine receptor CXCR4 on leukemia cells expressing the CALM-AF10 oncogenic protein, contributing to the migratory nature of this leukemia. Our discovery of altered cytokine receptor expression and function provides valuable insight into the propagation and persistence of *CALM-AF10* driven leukemia.

Keywords: CXCR4, CXCL12, leukemia, migration, adhesion, CALM-AF10 leukemia

OPEN ACCESS

Edited by:
Chung Hoow Kok,
University of Adelaide, Australia

Reviewed by:
Federica Barbieri,
University of Genoa, Italy
Stefania Scala,
IRCCS Istituto Nazionale Tumori Napoli "G. Pascale", Italy

****Correspondence:***
Jessica L. Heath
jessica.l.heath@med.uvm.edu

†Present address:
Shelby A. Fertal,
Department of Cell and Regenerative Biology, University of Wisconsin, Madison, WI, United States
Sayyed K. Zaidi,
Senior Scientific Writer, American Association for Cancer Research, Philadelphia, PA, United States

Specialty section:
This article was submitted to Hematologic Malignancies, a section of the journal Frontiers in Oncology

Received: *12 May 2021*
Accepted: *07 December 2021*
Published: *05 January 2022*

Citation:
Fertal SA, Zaidi SK, Stein JL, Stein GS and Heath JL (2022) CXCR4 Mediates Enhanced Cell Migration in CALM-AF10 Leukemia. Front. Oncol. 11:708915. doi: 10.3389/fonc.2021.708915

1 INTRODUCTION

The *t(10;11)(p13;q14-21)* chromosomal translocation results in the fusion of *CALM* (encoding the gene for the clathrin assembly lymphoid myeloid protein, also known as phosphatidylinositol-CALM (PICALM)) to *MLLT10* (also known as AF10) and is a recurrent genetic abnormality in acute lymphoid and myeloid leukemia. Nearly all of each individual gene is retained in this translocation. The endogenous CALM protein is primarily involved in intracellular trafficking. It associates with AP2 and clathrin, and functions to stabilize the clathrin-coated endocytic pit, allowing for efficient cellular uptake of growth factors and other receptor-bound molecules (1). Haploinsufficiency of CALM, as is found in cells expressing CALM-AF10, results in decreased endocytic efficiency (2). It has been reported that CALM contains a nuclear export signal (NES), allowing interaction with the CRM1/XPO1 nuclear export receptor. The NES is retained in the CALM-AF10 fusion construct, where it facilitates nucleocytoplasmic shuttling, and is necessary for leukemogenesis (3). AF10 is a transcription factor, binding to DNA through its leucine zipper domain, which is necessary for leukemogenesis (4–6). AF10 binds Dot1L, the only known H3K79 methyltransferase, and recruits Dot1L to its target genes, including the *HOXA* gene cluster (7). Upregulation of *HOXA* genes in *CALM-AF10* leukemias is a driving factor in *CALM-AF10* mediated leukemogenesis (8, 9).

The *CALM-AF10* translocation was first identified in a patient with histiocytic sarcoma but is more commonly seen in T acute lymphoblastic leukemia (T-ALL), where it makes up about 15% of pediatric and adult cases (10–12). *CALM-AF10* translocated T-ALL is characterized by the presence of extramedullary disease, CNS relapse, and poor response to therapy (12). This translocation is also seen in acute myeloid leukemia (AML), where it is associated with bulky hepatosplenomegaly, mediastinal disease, and central nervous system (CNS) leukemia (13).

Extramedullary and CNS leukemia development relies on migration of the leukemia cell out of the bone marrow compartment, and adhesion of the leukemia cells to cells of the target organ (CNS, liver, spleen, or lymph nodes). Multiple proteins have been implicated in this process, including several members of the integrin and chemokine families (14–16). More recently, interactions between leukemia cells and components of the bone marrow microenvironment have been shown to be critical for leukemic cell survival as well as resistance to chemotherapy [reviewed in (17)]. Interactions of leukemic cells with their microenvironment are mediated both by direct cellular contact and via soluble factors. One such factor is C-X-C motif chemokine receptor 4 (CXCR4), a cell surface G-protein coupled chemokine receptor that is bound and activated by C-X-C motif chemokine ligand 12 (CXCL12). CXCL12 can also enter the vascular system, and its interaction with CXCR4+ circulating hematopoietic stem cells (HSCs) is vital for HSC homing to the bone marrow compartment (18). The CXCR4/CXCL12 interaction plays a role in malignant hematopoiesis as well. Binding of CXCL12 to CXCR4 on leukemia cells activates multiple proliferative and survival pathways (reviewed in (19)), and high CXCR4 expression on leukemic blasts has been identified as a poor prognostic factor in both ALL and AML (20, 21). Finally, increased CXCR4 expression predicts the development of extramedullary disease in pediatric ALL (22).

We report an increase in cell surface expression of CXCR4, and a concomitant increase in the migratory behavior of cells transformed by *CALM-AF10*. Using both human and mouse cell line models, we examine the relationship between CXCR4 expression and phenotype in *CALM-AF10* transformed leukemias. Surprisingly, we do not find synergistic effect of CXCR4 inhibition with traditional chemotherapy in these leukemias, strongly suggesting caution in the broad use of these inhibitors, and a more tailored approach to this targeted therapy.

2 METHODS

2.1 Cell Culture

Human leukemia cell lines were cultured in RPMI 1640 (Fisher Scientific, Waltham, MA, USA) supplemented with 100 units/mL penicillin, and 100ug/mL streptomycin. U937 and Fujioka cells were additionally supplemented with 10% fetal bovine serum (Atlanta, USA) and 2mM L-glutamine. Kasumi-1 cells were additionally supplemented with 20% fetal bovine serum and MEM non-essential amino acids. Human mesenchymal stem cells (hMSC) were cultured in α-MEM (ThermoFisher Scientific, Waltham, MA, USA) media supplemented with 16.5% FBS, 2mM L-glutamine, 100 units/mL penicillin, and 100ug/mL streptomycin. Murine leukemia cell lines were derived from cells isolated from the marrow of leukemic mice (a generous gift from Catherine Lavau, Duke University, North Carolina). *Hoxa9-Meis1* and *CALM-AF10* transformed cells were cultured in RPMI 1640 with 20% fetal bovine serum (Atlanta, USA), 100units/mL of penicillin and streptomycin, and 10ng/mL mouse recombinant IL-3 (Stem Cell Technologies). Murine embryonic fibroblasts (MEFs) were generated from *Picalm*$^{fit1\text{-}5R}$ E14 embryos, immortalized with SV40, as previously described (2). Plat-E cells were transiently transfected with the MSCV-IRES-GFP encoding *CALM-AF10* (3), or the MSCV-IRES-GFP empty control vector using calcium phosphate. MEFs were then retrovirally infected with these constructs by co-culture with filtered Plat-E supernatant. Infection efficiency was measured by flow cytometry at the time of cell line genesis, and intermittently confirmed using fluorescent microscopy and western blot analysis. All cell lines were incubated at 37°C with 5 percent CO_2. All human cell lines and were validated continually by assessment of morphology and annually by short tandem repeat (STR) analysis. Murine cell lines were validated continually by assessment of morphology in cell culture and periodically by western blot assessment of the presence or absence of the CALM-AF10 fusion protein. In addition, all cells were confirmed negative for Mycoplasma infection with the Mycoalert detection kit (Lonza, Basel, CH) annually, or if any morphologic or growth changes were identified.

2.2 Immunofluorescence

Samples of 5x10^5 cells per condition (CXCR4 stained and negative control) for human and murine cell lines were spun down at 1500 rpm for 5 minutes at room temperature, washed twice with PBS and fixed with 3.7% formaldehyde while rotating for 10 minutes. Fixed cells were washed twice with PBS, and resulting pellets were resuspended in 200uL of sterile filtered PBS per condition and transferred onto slides using the Shandon Cytospin 4 (ThermoFisher Scientific, Waltham, MA, USA). Cells were not permeabilized prior to staining, in order to specifically evaluate presence of CXCR4 at the plasma membrane. Slides were air dried for 5 minutes, washed in PBS with 0.5% BSA (PBSA), and either incubated in primary antibody against CXCR4, diluted 1:100 in PBSA (Abcam, Cambridge, UK), or PBSA for 1hr at 37°C in the dark. Samples were washed once in PBSA and incubated in secondary antibody anti-rabbit IgG Alexa Fluor 488, diluted 1:800 (ThermoFisher Scientific, Waltham, MA, USA), for 1hr at 37°C in the dark. Samples were washed in PBSA and stained with 0.5ug/mL DAPI for 5 minutes in the dark and washed once with PBSA. Slides were imaged using Zeiss Imager.Z2.

2.3 Western Blot

Total cellular protein was extracted from 1 x 10^6 cells by boiling in 70uL of 1X protein loading buffer for 15 minutes. Protein samples were resolved in a 10% SDS gel at 140 V for 1.15hr, and

the resolved proteins were transferred to a nitrocellulose membrane at 100 V for 2 hr. Membranes were blocked in 5% milk in Tris-Buffered Saline (TBS) for 1hr, then incubated overnight at 4°C in primary antibody against CXCR4 (Abcam Cambridge, UK) or CALM (Sigma, St. Louis, MI, USA), diluted 1:1000 in TBS containing 0.1% TWEEN. Following primary antibody incubation, membranes were washed 3x in TBST for 5 minutes and incubated with HRP-conjugated anti-rabbit antibodies (1:10,000) for 1 hour. After washing as above, membranes were developed with BioRad Molecular Imager ChemDoc XRS+ system using a Clarity Western ECL substrate kit (BioRad, Hercules, CA, USA). To confirm equal loading of proteins across the experimental conditions, membranes were subsequently incubated with a primary antibody against β-actin at 1:1,000 (Cell Signaling Technologies, Danvers, MA, USA), developed, and imaged as described above.

For co-culture experiments, 1.5x 10^5/mL hMSC cells were plated on 10cm plates and incubated at 37°C with 5% CO_2 for 24hrs. 4.5x 10^5/mL U937 cells were added to previously cultured hMSCs and incubated at 37°C with 5% CO_2 for 24hrs. Following the 24hr incubation, co-cultured cells were exposed to 1uM of AMD3465, a CXCR4 inhibitor (Selleck Chemicals, Houston, TX, USA), for 4hrs. Suspension U937 cells were harvested at 1x 10^6/70uL of 1X loading buffer and boiled for 15 minutes. Samples were loaded on 15% SDS gel, run at 140 V for 3.36hr, and transferred to a nitrocellulose membranes at 100 V for 2 hr. Five percent BSA in Tris-Buffered Saline (TBS) was used to block membranes for 1hr. Membranes were incubated in primary antibody solutions with TBS containing 0.1% TWEEN for p44/42 (ERK) at 1:1,000 (Cell Signaling Technologies, Danvers, MA, USA) and phospho-p44/42 (phospho-ERK) at 1:2000 (Cell Signaling Technologies, Danvers, MA, USA) overnight at 4°C. Membranes were developed and imaged as stated above, and subsequently incubated in β-actin as described above.

All western blots are done in duplicate with one representative experiment shown.

2.4 Real-Time qPCR

Cells (1x 10^6) were harvested in 300uL of Trizol reagent and RNA was extracted using Directzol RNA MiniPrep Plus kit (Zymo Research, Irvine, CA, USA) and quantified using the Thermo Scientific Nanodrop 2000. cDNA was synthesized using SuperScript III Reverse Transcriptase kit (Fisher Scientific, Waltham, MA, USA). Real-time PCR was performed on a ViiA 7 Real-time PCR with the ITaq Universal SYBR Green Supermix and probes for: human GAPDH forward (5' ACCCACTCCTCCACCTTTGAC 3'), reverse (5' TGTTG CTGTAGCCAAATTCGTT 3'); CXCR4 forward (5' CACTTCAGATAACTACACCG 3'), and reverse (5' ATCCAGACGCCAACATAGAC 3'); CXCL12 forward (5' GGACTTTCCGCTAGACCCAC 3'), and reverse (5' GTCCTCATGGTTAAGGCCCC 3').

2.5 Scratch Assay

One million MEFs were plated in a 6 well tissue culture plate 24 hours prior to the experiment, allowing growth to confluence. At hour 24, a single scratch was made using a 200uL pipette tip. The media was aspirated off, each well was gently rinsed with PBS, and 2mL fresh media slowly added. Cells were photographed at hours 0, 4, and 8. Given the short time course of this experiment, anti-mitotic agents were not used. Photographs were processed by ImageJ to measure the area of the scratch at each time point.

2.5 Transwell Migration Assay

Corning transwell plates (8μm pore size, Fisher Scientific, Waltham, MA, USA) were used to assess migration. CXCL12 (R&D Systems, Minneapolis, MA, USA), or control (PBS), was added at 100ng/uL to 1.5x 10^5 Kasumi-1 and U937 cells and incubated for 24hrs at 37°C with 5% CO_2. After 24hrs, inserts were removed, each well was agitated *via* pipette, and cells were incubated for 30 minutes prior to imaging. Three images were taken of each corresponding well and representative areas of each image were analyzed *via* ImageJ (23). Two independent investigators performed each analysis to assure reproducibility. The above was repeated in U937 cells following a 4hr incubation in 0.25uM, 0.5uM, or 1uM AMD3465 (Selleck Chemicals, Houston, TX, USA) or control (water). Following a 4hr, 8hr, and 24hr incubation in transwell plates, images were taken and analyzed as detailed above.

2.6 Cytotoxicity Assays

2.6.1 Flow Cytometry

Human MSC cells were plated at 1x 10^5 cells/mL per well of a 6-well plate. Cells were cultured for 8hrs, then 3x 10^5/mL U937 cells were added to the hMSCs culture. Co-cultures were maintained for 16hrs at 37°C with 5% CO_2. Twenty-four hours from initial hMSC plating, Doxorubicin (1uM) and AMD3465 (1uM) (Selleck Chemicals, Houston, TX, USA) were added to co-cultured cells and allowed to incubate 37°C with 5% CO_2 for 24hrs. Suspension cells were removed from wells and combined with corresponding adherent cells trypsinized with 0.25% trypsin. Samples were washed once in phenol free RPMI 1640 media. Non-specific binding was blocked with normal mouse IgG 1:200 (Santa Cruz Biotechnology, Dallas, TX, USA) in 1% BSA (50uL per 1x 10^6 cells) for 30 minutes in the dark at 4°C. Primary antibody APC-conjugated mouse, anti-human CD45 (BD Pharmingen, San Diego, CA, USA) was added to cell solutions at 1:10, and incubated on ice for 30 minutes in the dark. Cells were washed once with phenol free RPMI 1640 and resuspended in 1uM DAPI solution. Samples were run on BD LSRII and analyzed using FlowJo software.

2.6.2 BrdU Assay

Cells were plated at 5x10^5 cells/mL media and treated with one of the following conditions: vehicle control (sterile water), 1uM AMD3465, 2uM AMD3465, 2.5uM cytarabine, 100nM cytarabine, 1uM AMD3465 + 2.5uM cytarabine, 1uM AMD3465 followed four hours later by 2.5uM cytarabine, 1uM AMD3465 + 100nM cytarabine, 1uM AMD3465 followed four hours later by 100nM cytarabine, 2uM AMD3465 + 100nM cytarabine, and 2uM AMD3465 followed four hours later by 100nM cytarabine. Treated cells were incubated at 37 degrees with 5% CO2 for 48 hours and were then analyzed by BrdU staining (Cell Signaling Technology, Danvers, MA, USA).

Absorbance was read at 450nM on a Perkin Elmer multimode plate reader.

2.7 Statistical Analysis

All data are expressed as the mean ± Standard Error of the Mean (SEM), unless otherwise noted. Differences between two experimental groups were analyzed by unpaired t-test. Ordinary one-way ANOVA was used to compare differences between multiple groups. A p-value ≤ 0.05 was considered significant.

3 RESULTS

3.1 Enhanced Cell Migration in CALM-AF10 Transformed Cells

Murine embryonic fibroblasts (MEFs) were stably infected with *CALM-AF10* or an empty vector (**Figure 1A**), and scratch assays were performed to assess the impact of the CALM-AF10 fusion oncoprotein on cell migration. Cells were plated the day prior to achieve confluence at the time of scratch. Closure of the wound was examined at four and eight hours post scratch infliction, and percent wound closure calculated. The *CALM-AF10* transformed MEFs showed a 35 percent wound closure at 4 hours, compared to 19% closure in the empty vector cells ($p<0.05$). This difference was magnified at the 8-hour time point, with CALM-AF10 transformed cells showing a 85% closure, compared with 61% in the empty vector cells ($p=0.04$) (**Figures 1B, C**).

We then examined the migratory behavior of human leukemia cell lines and sought to identify cytokines that could be involved in the migration of *CALM-AF10* leukemias. Because CXCL12 is the primary ligand for the CXCR4 receptor, we investigated the migratory behavior of *CALM-AF10* translocated leukemias when treated with CXCL12. We found that CALM-AF10 translocated U937 cells demonstrated an increase in cell migration upon stimulation with CXCL12, whereas the CALM-AF10 negative Kasumi-1 cells did not have a significant change in cell migration with the addition of CXCL12. U937 cells exhibited a nearly 3-fold increase in migration compared to Kasumi-1 cells when treated with 100ng/mL CXCL12 over a 24hr period (**Figures 1D, E**, n=3, $p< 0.001$). CXCL12 is measured in U937 and Kasumi1 cells by qPCR and reveals that CXCL12 is not expressed in either cell line at any significant level (**Figure 1F**: CXCR4 expression is shown as a reference). When analyzing the effects of a CXCR4 inhibitor, we found that AMD3465 treatment decreased the migration of *CALM-AF10* translocated leukemias. Following a 4hr treatment with 1uM AMD3465, U937 cells treated with 100ng/mL of CXCL12 for 24 hours had a 6-fold decrease in migration compared to cells exposed to vehicle control (**Figure 1G**, n=3, $p< 0.01$). Dose and time response curves with and without CXCL12 as a chemoattractant reveal migration of U937 cells over time (normalized to the 0 AMD3465 condition) is minimally impacted by increasing concentrations of AMD3465 in the absence of CXCL12. There is a trend toward diminished migration with low doses of AMD3465 in the presence of CXCL12 (**Figure 1H**). Time course experiments reveal a trend toward a greater impact of CXCL12 with short exposures to chemoattractant (**Figure 1I**: 0uM AMD3465 at 4 hour *vs* 24 hour, $p=0.06$). These observations indicate that AMD3465 exerts an inhibitory effect on migration of *CALM-AF10* expressing leukemia cells.

3.2 Increased Expression of CXCR4 in CALM-AF10 Leukemia

We assessed CXCR4 expression in U937 and Fujioka, two myeloid leukemia cell lines containing the *CALM-AF10* translocation, and compared it with that in Kasumi-1, a myeloid leukemia cell line that does not express *CALM-AF10*. The mRNA expression of CXCR4 in the U937 and Fujioka cells was 100-fold greater when compared with the Kasumi-1 cells (**Figure 2A**, $p< 0.001$). Consistent with the elevated transcript levels, total CXCR4 protein was also increased in *CALM-AF10*-translocated cell lines (**Figure 2B**). Immunofluorescence microscopy further revealed that CXCR4 was primarily localized at the plasma membrane, to a greater degree in *CALM-AF10* translocated leukemias (**Figure 2C**).

We determined the *CXCR4* expression in secondary murine cell line models, characterized by either *CALM-AF10* or *Hoxa9-Meis1* chromosomal translocations, to further validate the relationship between CALM-AF10 and increased *CXCR4* expression in human AML cell lines. In concordance with our findings in the human cell line models, we found an increase in total protein expression and plasma membrane receptor expression in the murine *CALM-AF10* leukemia cells relative to the *Hoxa9-Meis1* translocated cells (**Figures 2D, E**).

3.3 Effect of CXCR4 Inhibition in Combination With Doxorubicin

We next examined the potential of CXCR4 as a therapeutic target in *CALM-AF10*-driven leukemia. We co-cultured the *CALM-AF10* expressing U937 cell line with human mesenchymal stem cells (hMSCs) to model the interaction between the bone marrow microenvironment and leukemia cells. With CD45 as a marker for leukemia cells, we employed dual color flow cytometry to separate and analyze the effect of targeted and cytotoxic treatments on leukemia cells in co-culture. We utilized this system to investigate the possible synergistic effect of AMD3465, a CXCR4 inhibitor, in combination with doxorubicin, a standard chemotherapeutic agent. We first assessed the ability of AMD3465 to inhibit CXCR4 activation by examining its effect on the MAPK pathway, a known downstream effector of CXCR4 signaling. U937 cells were cultured with hMSCs for 24hrs before treatment with 1uM of AMD3465 for 4hrs. hMSCs are known to express the ligand for CXCR4, CXCL12. We confirmed expression of CXCL12, as well as lack of CXCR4 expression, in our hMSCs *via* qPCR (**Figure 3A**). Western blot analysis revealed a decrease specifically in the phosphorylated ERK after AMD3465 treatment (**Figure 3B**), confirming an active CXCR4 signaling cascade in *CALM-AF10* expressing leukemia cells. We then examined the impact of AMD3465 on activation of the ERK pathway on U937 cells that were cultured in charcoal stripped,

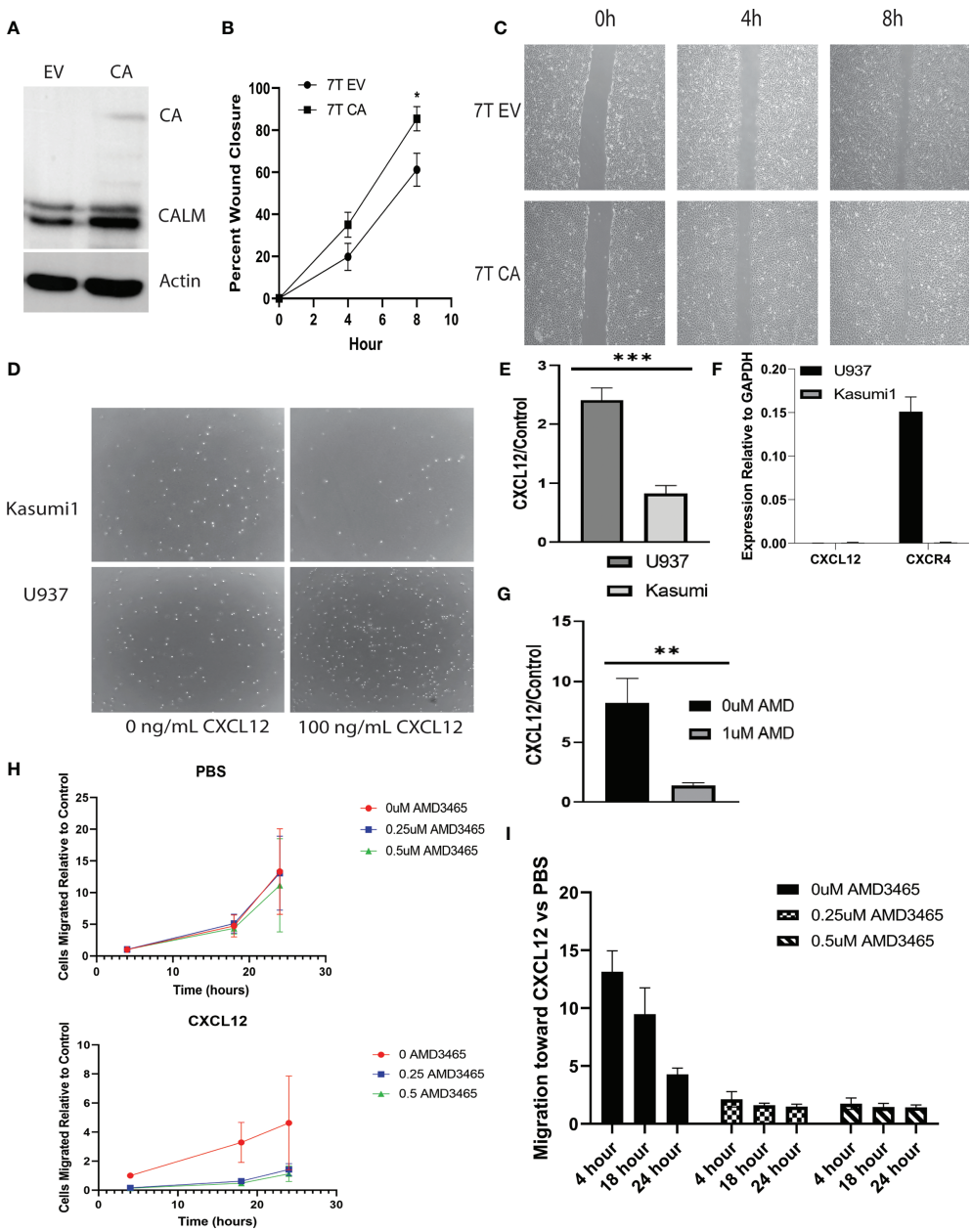

FIGURE 1 | *CALM-AF10* leukemia cells show enhanced migration, influenced by CXCL12. **(A)** A Western blot of MEFs transformed by empty vector (EV) or CALM-AF10 (CA) confirms the presence of the CA oncoprotein. **(B)** Accelerated wound closure in murine embryonic fibroblasts (MEFs) transformed by *CALM-AF10*. **(C)** Representative images from one replicate of scratch assay demonstrate more rapid wound closure in *CALM-AF10* transduced MEFs. **(D)** Representative images from one transwell assay are shown. **(E)** The impact of CXCL12 as a stimulant for cell migration is examined in U937 and Kasumi cells. **(F)** qPCR of CXCL12 and CXCR4 in U937 and Kasumi1. **(G)** The impact of the CXCR4 inhibitor AMD3465 on the migration of U937 cells is evaluated. **(H)** Dose and time response curves of U937 cells exposed to AMD3465 with and without CXCL12 stimulation reveal migration U937 cells over time (normalized to the 0 AMD3465 condition). **(I)** Dose and time response experiments in U937 cells using AMD3465 in the present or absence of CXCL12 as a chemoattractant. *p < 0.05; **p < 0.01; ***p < 0.001.

phenol-free RPMI and treated with CXCL12 in order to further examine the impact of specific CXCR4 inhibition. Western blot analysis again revealed a decrease in pERK/ERK in the AMD3465 treated cells (**Figure 3C**). Total ERK levels were used as a control and remained unchanged.

We next sought to evaluate the cytotoxic effect of CXCR4 inhibition. Following 16hrs of co-culture, cells were exposed to either 1uM AMD3465, 1uM doxorubicin, or the combination for 24hrs and analyzed for cell viability using flow cytometry. One micromolar dosing of doxorubicin is known to be cytotoxic to

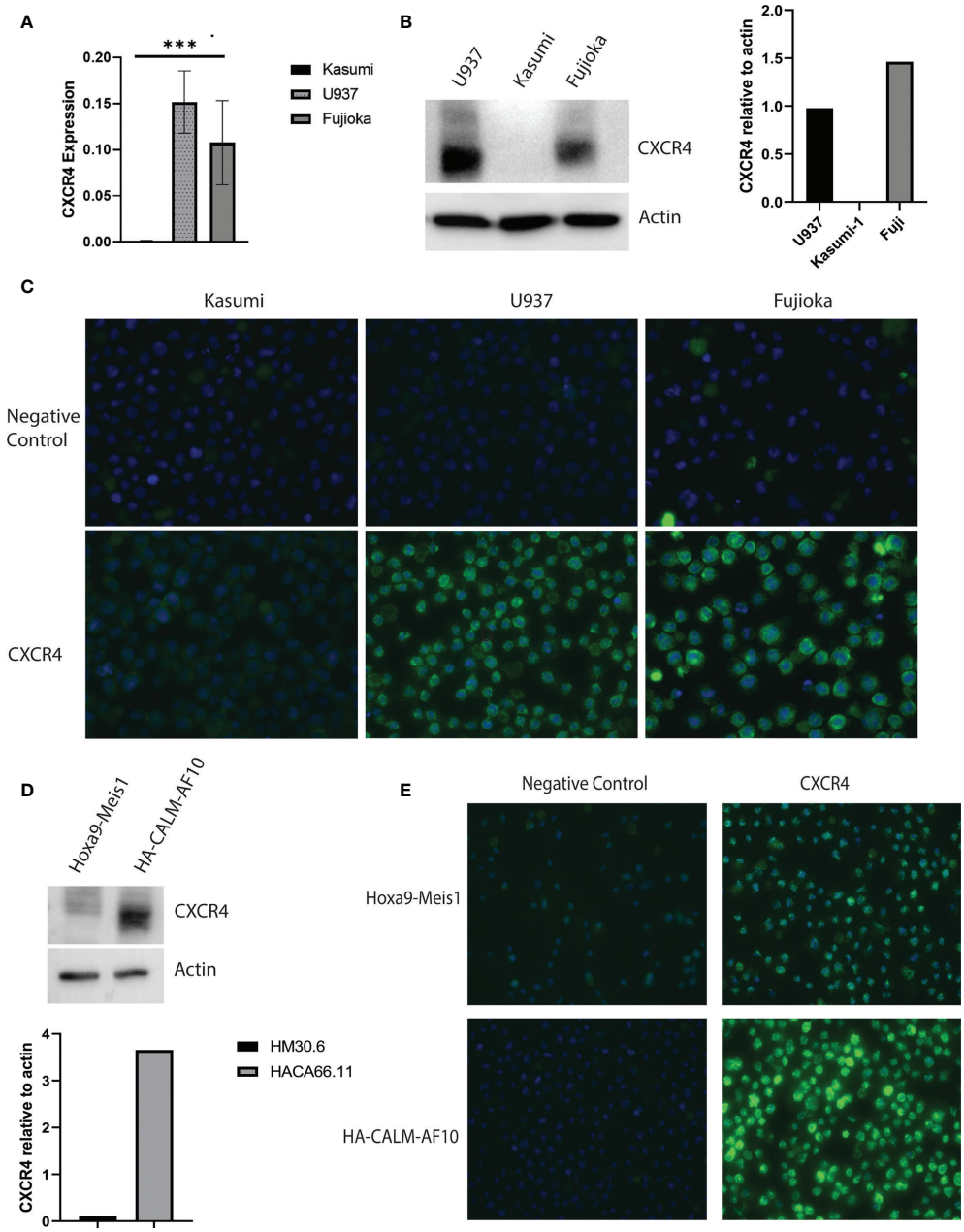

FIGURE 2 | Increased CXCR4 expression in *CALM-AF10* transformed leukemia cells. CXCR4 expression is evaluated in human myeloid leukemia cell lines characterized by the *CALM-AF10* translocation (U937 and Fujioka) and compared with a myeloid leukemia cell line not containing the *CALM-AF10* translocation. Expression is examined by transcript quantification, with values shown relative to *GAPDH* **(A)**, and protein evaluation by Western blot, with corresponding densitometry normalized to actin **(B)**. Immunofluorescence staining of human leukemia cells reveals increased CXCR4 expression is concentrated on the plasma membrane **(C)**. **(D)** High CXCR4 protein expression is confirmed by Western blot in a murine leukemia induced by *CALM-AF10*, compared with a murine leukemia characterized by the *Hoxa9-Meis*1 translocation, with corresponding densitometry shown, normalized to actin. **(E)** Immunofluorescence staining in the *CALM-AF10* translocated murine leukemia cells reveals increased CXCR4 expression is concentrated on the plasma membrane. ***$p < 0.001$.

U937 cells and this was confirmed in our lab (24), and data not shown). We found that the AMD3465 treatment alone did not have a significant cytotoxic effect; the control and AMD3465 treated cells showed 89.53 percent and 90.04 percent cell viability, respectively (n=4). We also did not find a significant difference in cell viability between the AMD3465 in combination with doxorubicin (75.63 percent) and doxorubicin alone (75.33 percent) (**Figures 3D, E**).

We then investigated the potential anti-proliferative effect of CXCR4 inhibition alone or in combination with traditional

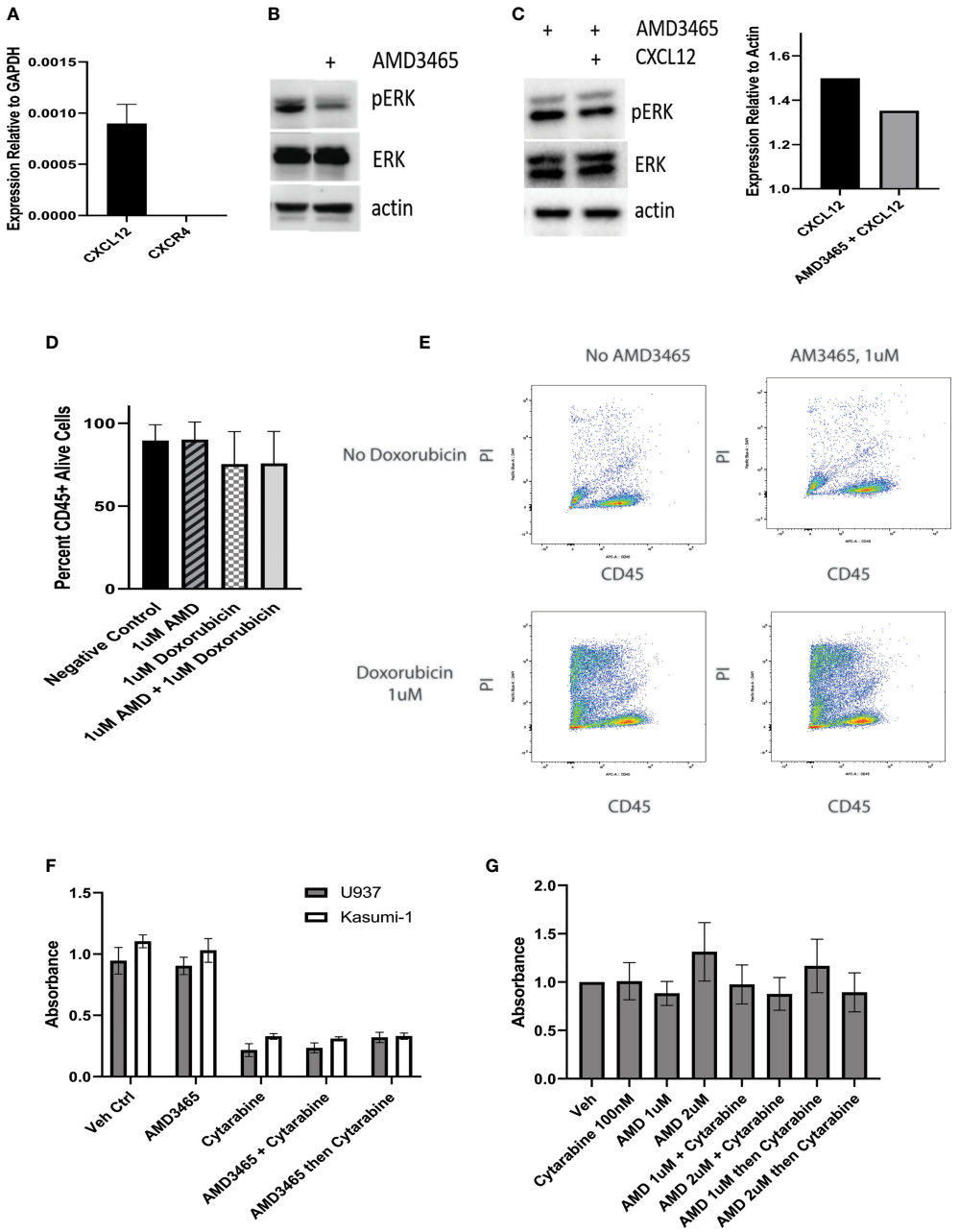

FIGURE 3 | Effect of CXCR4 inhibition on cell proliferation. U937 cells are kept in co-culture with human mesenchymal stem cells (hMSCs) and the cytotoxic effect of a CXCR4 inhibitor, AMD3465 is examined. **(A)** The expression of CXCL12 and CXCR4 in hMSCs is shown, normalized to GAPDH. **(B)** AMD3465 produces a decrease in pERK/ERK in U937 cells kept in co-culture in regular media. **(C)** The impact of AMD3465 on pERK/ERK in U937 cells kept in co-culture in charcoal stripped, phenol-free media in the presence of CXCL12 is shown by western blot, with corresponding densitometry. **(D)** The cytotoxic effect of AMD3465 is examined, both with and without doxorubicin. **(E)** Representative FACS data is shown. Propidium iodide (PI) staining delineates live versus dead cells, and CD45 positivity separates the CD45+ leukemia cells from the CD45- hMSCs. **(F)** The anti-proliferative effect of CXCR4 inhibition is evaluated by BrdU assay, with and without treatment dose cytarabine. **(G)** The anti-proliferative effect of high dose and low dose CXCR4 inhibition is evaluated by BrdU assay, with and without subtoxic dose cytarabine.

chemotherapy. Cells were treated with either 1uM AMD3465, 2.5uM cytarabine, AMD3465 and cytarabine together, or AMD3465 followed by cytarabine 4 hours later. This dose of cytarabine has previously been reported to be cytotoxic to U937 cells, and we found a 77% reduction in U937 cell proliferation with 2.5uM cytarabine (25). Human leukemia cells lines U937 (*CALM-AF10+*) or Kasumi-1 (*CALM-AF10* negative) were treated for 48 hours, and cell proliferation was quantified via BrdU assay. The

cytarabine treatment produced the expected anti-proliferative effect with a 70-80% decrease in absorbance in both cell lines examined. However, AMD3465 showed no anti-proliferative effect in either cell line. This was true when cells were treated with AMD3465 alone, and when AMD3465 was used in combination with cytarabine, either simultaneously or sequentially (**Figure 3F**). We then performed additional cell proliferation assays with low dose cytarabine (100nM), to evaluate whether a subtoxic dose of cytarabine would uncover a potential therapeutic effect of AMD3465. These experiments additionally incorporated AMD3465 at 2uM to assess the potential therapeutic impact of a higher dose of the CXCR4 inhibitor. We found no additive nor synergistic effect of AMD3465 at 1uM or at 2uM in combination with subtoxic doses of cytarabine, when used simultaneously or sequentially (**Figure 3G**).

4 DISCUSSION

4.1 CALM-AF10 Transformed Cells Exhibit Enhanced Cell Migration

The *t(10;11)(p13;q14-21)* chromosomal translocation encodes the leukemogenic CALM-AF10 fusion oncoprotein. The *CALM-AF10* translocation is found in both acute myeloid and acute lymphoid leukemias and are found most frequently in T-ALL at an incidence of about 15%. *CALM-AF10* leukemia is driven by overexpression of HOX homeobox cluster genes (26, 27). The upregulation of *HOXA* genes in *CALM-AF10* leukemia is dependent on AF10's recruitment of DOT1L, and resultant focal H3K79 hypermethylation specifically at the *HOXA* locus (8, 9). CALM-AF10 also interacts with the CRM1/XPO1 nuclear export receptor via CALM's nuclear export signal peptide sequence, which is retained in the fusion protein, and is necessary for leukemogenesis. This interaction is required for localization of CALM-AF10 to the *HOXA* cluster, and for resultant *HOXA* overexpression (3). The PHD1-zinc-knuckle-PHD2 (PZP) domain of *AF10* is consistently interrupted in *CALM-AF10* translocations. It has been recently identified that the disruption of the PZP domain of AF10 disrupts the normal localization of DOT1L across the genome, allowing DOT1L to be tethered to the *HOXA* locus by CALM-AF10 (28).

CALM-AF10 leukemias typically show a poor response to therapy, have an increased propensity to relapse and have a worse overall prognosis. The poor clinical outcome of *CALM-AF10*-driven leukemia necessitates the need for better understanding of how the translocation affects the behavior of the disease so that novel targeted therapies may be developed. Interestingly, *CALM-AF10* leukemias have a high prevalence of extramedullary disease, including bulky mediastinal disease, and a propensity for central nervous system relapse. Emerging evidence reveals a role for factors influencing cell adhesion and migration in these processes. While these processes may be separate from the fundamental mechanisms of tumorigenesis, they are potentially critical to tumor development, metastasis and chemotherapeutic response.

We therefore examined the migratory properties of cells transformed by *CALM-AF10* and found that MEFs transformed by *CALM-AF10* exhibited enhanced cell migration in scratch assays, compared with controls. We then examined cell migration in *CALM-AF10*+ leukemia cells via transwell migration assays and discovered that *CALM-AF10*+ U937 cells show enhanced migration in transwell assays, compared with *CALM-AF10* negative Kasumi-1 cells. Furthermore, the U937 cells showed a robust increase in cell migration toward a CXCL12 stimulus; whereas the presence of CXCL12 did not influence Kasumi-1 cell migration. Neither leukemia cell line expresses significant amounts of CXCL12, thus CXCL12 secretion and autocrine signaling are not impacting this differential response.

4.2 Increased CXCR4 Expression Is Seen in CALM-AF10 Leukemia and Contributes to Cell Migration

CXCL12 is the primary ligand for the chemokine receptor CXCR4, found on cell surface of HSCs and some leukemia cells. The interaction between CXCR4 on HSCs, and its ligand CXCL12, leads to HSC migration and subsequent homing to the bone marrow (29). Evidence suggests that CXCR4 plays a role in leukemia cell migration as well, and one study correlated increased CXCR4 expression on lymphoblasts with a trend toward bulky extramedullary disease in pediatric ALL (22). We investigated whether the increased cell migration we observed in *CALM-AF10* transformed cells correlated with CXCR4 expression.

Following the discovery that CALM-AF10 expressing leukemia cells migrate toward a CXCL12 stimulus, we tested whether blocking this interaction could halt migration. We found that the CXCR4 inhibitor AMD3465 abrogated this migration, confirming that CXCR4 was the integral mediator of this effect. Consistent with this finding, we found an increase in CXCR4 expression specifically in human leukemia cell lines carrying the *CALM-AF10* translocation. This finding was noted at both the transcript and protein levels. To ensure broader validity of these observations, we also confirmed our findings in murine leukemia cell lines previously generated in our lab.

CXCL12 is not only present in the bone marrow but is found in every tissue in the body, except in the CNS. CXCL12 is highly expressed in other lymphoid tissues such as the thymus, lymph nodes and spleen. It is also expressed in the liver and testes. These are all sites of potential leukemic involvement, with extramedullary involvement being characteristic of *CALM-AF10* leukemias (30). It is possible that high CXCR4 expression on the plasma membrane of *CALM-AF10* leukemias contributes to the development of extramedullary disease. Additional *in vivo* studies are needed to definitively establish the relationship between CXCR4 expression and extramedullary disease development in *CALM-AF10* leukemia.

4.3 The Effect of CXCR4 Inhibition on CALM-AF10 Leukemia Cells

Based on our findings of increased CXCR4 expression on *CALM-AF10* leukemic blasts, and the contribution of CXCR4

to *CALM-AF10*+ cell migration, we hypothesized that these cells would be particularly sensitive to CXCR4 inhibition as a chemosensitizer. We first established that CALM-AF10 expressing leukemia cells have an active CXCR4 signaling cascade by observing a reduction in phophoERK to ERK after CXCR4 inhibition. We then sought to examine the potential of CXCR4 inhibition to contribute to either cytostatic or cytotoxic chemotherapy effects.

Cytarabine is commonly used in the treatment of both ALL and AML. It is a pyrimidine analog and competes with cytidine for incorporation into DNA during repair and replication. When cytarabine is incorporated into DNA, it halts replication, exerting a cytostatic effect. Intriguingly, despite an intact CXCR4 signaling cascade, we found no decrease in cell proliferation upon exposure of U937 cells to AMD3465 in combination with either subtoxic or therapeutic concentrations of cytarabine.

Doxorubicin is another chemotherapy agent commonly used for the treatment of both ALL and AML. It is a cytotoxic agent, intercalating with DNA and causing double strand DNA breaks. Doxorubicin also inhibits topoisomerase II and results in apoptosis. We studied the effects of doxorubicin in combination with AMD3465 in U937 cells, and surprisingly found no synergistic nor additive effect of the combination.

Binding of CXCR4 by its ligand may result in activation of a multitude of signaling cascades, including those involved in cell survival and proliferation, such as the PI3K and ERK signaling pathways. CXCR4 inhibition is therefore an attractive target as a chemotherapeutic adjunct. CXCR4 inhibition has been examined in acute leukemia, both as a potential therapy and as a stem cell mobilizer. Previous studies have demonstrated decreased cell proliferation in AML cells *in vitro*, and decreased AML engraftment *in vivo* with the use of CXCR4 inhibitors (31, 32). A prior study reported that lymphoblastic leukemia cells in co-culture were sensitized to vincristine by a CXCR4 inhibitor through the upregulation of Bax (33). However, there are conflicting data in the published literature. For example, a 2013 study revealed that CXCL12 stimulation resulted in increased apoptosis in AML cell lines, mediated by Bcl2 family members (34). In addition, an examination of childhood ALL patient samples revealed variability in chemotactic and proliferative response to CXCR4 inhibition (35).

The factors contributing to these variable and sometimes conflicting findings are not well elucidated. CXCR4 expression and signaling is regulated through a variety of mechanisms. At a transcriptional level, CXCR4 expression may be modified through DNA methylation, directly activated by multiple transcription factors, and impacted by a range of physiologic stimuli (19, 36). Protein expression may be impacted by tyrosine sulfation or glycosylation or modified by oligomerization. There are multiple processes which separately regulate CXCR4 signaling once bound by ligand, impacting receptor internalization, degradation, and recycling (19).

Ultimately, CXCR4 expression on leukemic blasts varies, and the factors influencing differences in expression, function, and downstream signaling in leukemia are unknown. It is also not known whether degree of CXCR4 expression influences therapeutic response to CXCR4 inhibition. Herein, we identify a genetically defined a subtype of leukemia, which is characterized by high CXCR4 expression and has an intact CXCR4 signaling pathway. We report the novel findings that despite an intact CXCR4 signaling pathway, CALM-AF10 carrying leukemia cells do not show additive nor synergistic cytotoxic or anti-proliferative effects upon combinatorial inhibition of CXCR4 and traditional chemotherapeutics.

Jost et al. present a model of CNS meningeal infiltration by T-lymphoblasts through CXCR4 mediated bone marrow colonization (37). Others have provided evidence that CXCR4 inhibition prevented homing of multiple myeloma cells to the bone marrow compartment (38). It is possible the use of CXCR4 inhibitors in specific clinicopathologic scenarios may yet provide clinical benefit. The studies presented here are limited by the use of cell lines, and future studies examining CXCR4 expression and the use of CXCR4 inhibitors in patient samples will add valuable insight to the biology of *CALM-AF10* leukemia. Additional studies are needed to establish whether CXCR4 inhibition impacts other characteristics of *CALM-AF10* leukemia, including CNS invasion. We utilized a co-culture system to simulate the bone marrow microenvironment; however, additional insight would be gleaned utilizing three dimensional bone marrow scaffolds or *in vivo* models of disease (39, 40).

4.4 Summary

Due to its status as a G-protein coupled receptor, CXCR4 plays a role in many downstream pathways controlling cell adhesion, migration, survival and proliferation. Previous studies have reported therapeutic effect of CXCR4 inhibition in some acute leukemias in the preclinical setting, as described above. However, clinical trials of CXCR4 inhibitors have not shown promising results, particularly in ALL (41–43). Specific factors that determine response to CXCR4 inhibition have not been discovered. In this study, we demonstrate that *CALM-AF10* translocated leukemias show an increased expression of CXCR4, as well as an increase in CXCL12-stimulated cell migration. We posited that this increase would lead to an enhanced sensitivity to CXCR4 inhibitors. However, we observed no decrease in cell proliferation nor cytotoxic effect with CXCR4 inhibition. We have therefore identified a subtype of leukemia that is not sensitive to anti-proliferative or cytotoxic effect CXCR4 inhibitors, despite high levels of CXCR4 expression and an intact CXCR4 signaling pathway. This finding strongly suggests caution moving forward with CXCR4 inhibition as a therapeutic adjunct. By elucidating factors that influence response to CXCR4 inhibition, these targeted therapeutics can be better tailored to specific diseases.

DATA AVAILABILITY STATEMENT

The original contributions presented in the study are included in the article/supplementary material. Further inquiries can be directed to the corresponding author.

AUTHOR CONTRIBUTIONS

SF and JH performed the experiments. SF and JH wrote the paper. SZ, GS, and JS provided input into experimental design and analysis, and critically reviewed the manuscript. All authors contributed to the article and approved the submitted version.

FUNDING

This work was supported by a contribution from Donna and Martin Waldron (JH). The research reported here was supported by grant U54 GM115516 from the National Institutes of Health for the Northern New England Clinical and Translational Research network (GS, JH). This work was also supported in part by the Emily M. Lyman Pediatric Leukemia Research Fund (JH), the Children's Leukemia Research Association (JH), the Pediatric Cancer Research Fund, the Keegan Bradley Charity Golf Classic, the University of Vermont Health Network Group (JH), and the Charlotte Perelman Fund (GS). Donna and Martin Waldron were not involved in the study design, collection, analysis, interpretation of data, the writing of this article or the decision to submit it for publication.

ACKNOWLEDGMENTS

The flow cytometry was performed in the Harry Hood Bassett Flow Cytometry and Cell Sorting (FCCS) Facility at the University of Vermont Larner College of Medicine. We acknowledge Roxana del Rio-Guerra PhD, SCYM (ASCP) for her expertise and guidance during these experiments.

REFERENCES

1. Tebar F, Bohlander SK, Sorkin A. Clathrin Assembly Lymphoid Myeloid Leukemia (CALM) Protein: Localization in Endocytic-Coated Pits, Interactions With Clathrin, and the Impact of Overexpression on Clathrin-Mediated Traffic. *Mol Biol Cell* (1999) 10(8):2687–702. doi: 10.1091/mbc.10.8.2687
2. Scotland PB, Heath JL, Conway AE, Porter NB, Armstrong MB, Walker JA, et al. The PICALM Protein Plays a Key Role in Iron Homeostasis and Cell Proliferation. *PloS One* (2012) 7(8):e44252. doi: 10.1371/journal.pone.0044252
3. Conway AE, Scotland PB, Lavau CP, Wechsler DS. A CALM-Derived Nuclear Export Signal is Essential for CALM-AF10-Mediated Leukemogenesis. *Blood* (2013) 121(23):4758–68. doi: 10.1182/blood-2012-06-435792
4. Aasland R, Gibson TJ, Stewart AF. The PHD Finger: Implications for Chromatin-Mediated Transcriptional Regulation. *Trends Biochem Sci* (1995) 20(2):56–9. doi: 10.1016/S0968-0004(00)88957-4
5. Aravind L, Landsman D. AT-Hook Motifs Identified in a Wide Variety of DNA-Binding Proteins. *Nucleic Acids Res* (1998) 26(19):4413–21. doi: 10.1093/nar/26.19.4413
6. Chaplin T, Bernard O, Beverloo HB, Saha V, Hagemeijer A, Berger R, et al. The T(10;11) Translocation in Acute Myeloid Leukemia (M5) Consistently Fuses the Leucine Zipper Motif of AF10 Onto the HRX Gene. *Blood* (1995) 86 (6):2073–6. doi: 10.1182/blood.V86.6.2073.bloodjournal8662073
7. Deshpande AJ, Deshpande A, Sinha AU, Chen L, Chang J, Cihan A, et al. AF10 Regulates Progressive H3K79 Methylation and HOX Gene Expression in Diverse AML Subtypes. *Cancer Cell* (2014) 26(6):896–908. doi: 10.1016/j.ccell.2014.10.009
8. Okada Y, Jiang Q, Lemieux M, Jeannotte L, Su L, Zhang Y. Leukaemic Transformation by CALM-AF10 Involves Upregulation of Hoxa5 by Hdot1l. *Nat Cell Biol* (2006) 8(9):1017–24. doi: 10.1038/ncb1464
9. Lin YH, Kakadia PM, Chen Y, Li YQ, Deshpande AJ, Buske C, et al. Global Reduction of the Epigenetic H3K79 Methylation Mark and Increased Chromosomal Instability in CALM-AF10-Positive Leukemias. *Blood* (2009) 114(3):651–8. doi: 10.1182/blood-2009-03-209395
10. Nakamura F, Maki K, Arai Y, Nakamura Y, Mitani K. Monocytic Leukemia With CALM/AF10 Rearrangement Showing Mediastinal Emphysema. *Am J Hematol* (2003) 72(2):138–42. doi: 10.1002/ajh.10265
11. Huh JY, Chung S, Oh D, Kang MS, Eom HS, Cho EH, et al. Clathrin Assembly Lymphoid Myeloid Leukemia-AF10-Positive Acute Leukemias: A Report of 2 Cases With a Review of the Literature. *Korean J Lab Med* (2010) 30(2):117–21. doi: 10.3343/kjlm.2010.30.2.117
12. Asnafi V, Radford-Weiss I, Dastugue N, Bayle C, Leboeuf D, Charrin C, et al. CALM-AF10 is a Common Fusion Transcript in T-ALL and is Specific to the TCRgammadelta Lineage. *Blood* (2003) 102(3):1000–6. doi: 10.1182/blood-2002-09-2913
13. Borel C, Dastugue N, Cances-Lauwers V, Mozziconacci MJ, Prebet T, Vey N, et al. PICALM-MLLT10 Acute Myeloid Leukemia: A French Cohort of 18 Patients. *Leukemia Res* (2012) 36(11):1365–9. doi: 10.1016/j.leukres.2012.07.008
14. Williams MT, Yousafzai Y, Cox C, Blair A, Carmody R, Sai S, et al. Interleukin-15 Enhances Cellular Proliferation and Upregulates CNS Homing Molecules in Pre-B Acute Lymphoblastic Leukemia. *Blood* (2014) 123(20):3116–27. doi: 10.1182/blood-2013-05-499970
15. Yao H, Price TT, Cantelli G, Ngo B, Warner MJ, Olivere L, et al. Leukaemia Hijacks a Neural Mechanism to Invade the Central Nervous System. *Nature* (2018) 560(7716):55–60. doi: 10.1038/s41586-018-0342-5
16. Kupsa T, Horacek JM, Jebavy L. The Role of Cytokines in Acute Myeloid Leukemia: A Systematic Review. *BioMed Pap Med Fac Univ Palacky Olomouc Czech Repub* (2012) 156(4):291–301. doi: 10.5507/bp.2012.108
17. Becker PS. Dependence of Acute Myeloid Leukemia on Adhesion Within the Bone Marrow Microenvironment. *TheScientificWorldJournal* (2012) 2012:856467. doi: 10.1100/2012/856467
18. Jo DY, Rafii S, Hamada T, Moore MA. Chemotaxis of Primitive Hematopoietic Cells in Response to Stromal Cell-Derived Factor-1. *J Clin Invest* (2000) 105(1):101–11. doi: 10.1172/JCI7954
19. Busillo JM, Benovic JL. Regulation of CXCR4 Signaling. *Biochim Biophys Acta* (2007) 1768(4):952–63. doi: 10.1016/j.bbamem.2006.11.002
20. Konoplev S, Jorgensen JL, Thomas DA, Lin E, Burger J, Kantarjian HM, et al. Phosphorylated CXCR4 is Associated With Poor Survival in Adults With B-Acute Lymphoblastic Leukemia. *Cancer* (2011) 117(20):4689–95. doi: 10.1002/cncr.26113
21. Rombouts EJ, Pavic B, Lowenberg B, Ploemacher RE. Relation Between CXCR-4 Expression, Flt3 Mutations, and Unfavorable Prognosis of Adult Acute Myeloid Leukemia. *Blood* (2004) 104(2):550–7. doi: 10.1182/blood-2004-02-0566
22. Crazzolara R, Kreczy A, Mann G, Heitger A, Eibl G, Fink FM, et al. High Expression of the Chemokine Receptor CXCR4 Predicts Extramedullary Organ Infiltration in Childhood Acute Lymphoblastic Leukaemia. *Br J Haematol* (2001) 115(3):545–53. doi: 10.1046/j.1365-2141.2001.03164.x
23. Schneider CA, Rasband WS, Eliceiri KW. NIH Image to ImageJ: 25 Years of Image Analysis. *Nat Methods* (2012) 9(7):671–5. doi: 10.1038/nmeth.2089
24. Ortiz-Lazareno PC, Bravo-Cuellar A, Lerma-Diaz JM, Jave-Suarez LF, Aguilar-Lemarroy A, Dominguez-Rodriguez JR, et al. Sensitization of U937 Leukemia Cells to Doxorubicin by the MG132 Proteasome Inhibitor Induces an Increase in Apoptosis by Suppressing NF-Kappa B and Mitochondrial Membrane Potential Loss. *Cancer Cell Int* (2014) 14(1):13. doi: 10.1186/1475-2867-14-13
25. Cheong JW, Kim Y, Eom JI, Jeung HK, Min YH. Enhanced Autophagy in Cytarabine Arabinoside-Resistant U937 Leukemia Cells and its Potential as a Target for Overcoming Resistance. *Mol Med Rep* (2016) 13(4):3433–40. doi: 10.3892/mmr.2016.4949
26. Bach C, Buhl S, Mueller D, Garcia-Cuellar MP, Maethner E, Slany RK. Leukemogenic Transformation by HOXA Cluster Genes. *Blood* (2010) 115 (14):2910–8. doi: 10.1182/blood-2009-04-216606
27. Dik WA, Brahim W, Braun C, Asnafi V, Dastugue N, Bernard OA, et al. CALM-AF10+ T-ALL Expression Profiles are Characterized by Overexpression of HOXA and BMI1 Oncogenes. *Leukemia* (2005) 19 (11):1948–57. doi: 10.1038/sj.leu.2403891

28. Klein BJ, Deshpande A, Cox KL, Xuan F, Zandian M, Barbosa K, et al. The Role of the PZP Domain of AF10 in Acute Leukemia Driven by AF10 Translocations. *Nat Commun* (2021) 12(1):4130. doi: 10.1038/s41467-021-24418-9
29. Peled A, Petit I, Kollet O, Magid M, Ponomaryov T, Byk T, et al. Dependence of Human Stem Cell Engraftment and Repopulation of NOD/SCID Mice on CXCR4. *Science* (1999) 283(5403):845–8. doi: 10.1126/science.283.5403.845
30. Caudell D, Aplan PD. The Role of CALM-AF10 Gene Fusion in Acute Leukemia. *Leukemia* (2008) 22(4):678–85. doi: 10.1038/sj.leu.2405074
31. Sison EA, McIntyre E, Magoon D, Brown P. Dynamic Chemotherapy-Induced Upregulation of CXCR4 Expression: A Mechanism of Therapeutic Resistance in Pediatric AML. *Mol Cancer Res: MCR* (2013) 11(9):1004–16. doi: 10.1158/1541-7786.MCR-13-0114
32. Zeng Z, Shi YX, Samudio IJ, Wang RY, Ling X, Frolova O, et al. Targeting the Leukemia Microenvironment by CXCR4 Inhibition Overcomes Resistance to Kinase Inhibitors and Chemotherapy in AML. *Blood* (2009) 113(24):6215–24. doi: 10.1182/blood-2008-05-158311
33. Wang S, Wang X, Liu S, Zhang S, Wei X, Song Y, et al. The CXCR4 Antagonist, AMD3100, Reverses Mesenchymal Stem Cell-Mediated Drug Resistance in Relapsed/Refractory Acute Lymphoblastic Leukemia. *Oncol Targets Ther* (2020) 13:6583–91. doi: 10.2147/OTT.S249425
34. Kremer KN, Peterson KL, Schneider PA, Meng XW, Dai H, Hess AD, et al. CXCR4 Chemokine Receptor Signaling Induces Apoptosis in Acute Myeloid Leukemia Cells *via* Regulation of the Bcl-2 Family Members Bcl-XL, Noxa, and Bak. *J Biol Chem* (2013) 288(32):22899–914. doi: 10.1074/jbc.M113.449926
35. Juarez J, Dela Pena A, Baraz R, Hewson J, Khoo M, Cisterne A, et al. CXCR4 Antagonists Mobilize Childhood Acute Lymphoblastic Leukemia Cells Into the Peripheral Blood and Inhibit Engraftment. *Leukemia* (2007) 21(6):1249–57. doi: 10.1038/sj.leu.2404684
36. Stuckel AJ, Zhang W, Zhang X, Zeng S, Dougherty U, Mustafi R, et al. Enhanced CXCR4 Expression Associates With Increased Gene Body 5-Hydroxymethylcytosine Modification But Not Decreased Promoter Methylation in Colorectal Cancer. *Cancers (Basel)* (2020) 12(3):539–56. doi: 10.3390/cancers12030539
37. Jost TR, Borga C, Radaelli E, Romagnani A, Perruzza L, Omodho L, et al. Role of CXCR4-Mediated Bone Marrow Colonization in CNS Infiltration by T Cell Acute Lymphoblastic Leukemia. *J Leukoc Biol* (2016) 99(6):1077–87. doi: 10.1189/jlb.5MA0915-394R
38. Alsayed Y, Ngo H, Runnels J, Leleu X, Singha UK, Pitsillides CM, et al. Mechanisms of Regulation of CXCR4/SDF-1 (CXCL12)-Dependent Migration and Homing in Multiple Myeloma. *Blood* (2007) 109(7):2708–17. doi: 10.1182/blood-2006-07-035857
39. Sola A, Bertacchini J, D'Avella D, Anselmi L, Maraldi T, Marmiroli S, et al. Development of Solvent-Casting Particulate Leaching (SCPL) Polymer Scaffolds as Improved Three-Dimensional Supports to Mimic the Bone Marrow Niche. *Mater Sci Eng C Mater Biol Appl* (2019) 96:153–65. doi: 10.1016/j.msec.2018.10.086
40. Heath JL, Weiss JM, Lavau CP, Wechsler DS. Effects of Iron Depletion on CALM-AF10 Leukemias. *Exp Hematol* (2014) 42(12):1022–30 e1. doi: 10.1016/j.exphem.2014.08.004
41. Cooper TM, Sison EAR, Baker SD, Li L, Ahmed A, Trippett T, et al. A Phase 1 Study of the CXCR4 Antagonist Plerixafor in Combination With High-Dose Cytarabine and Etoposide in Children With Relapsed or Refractory Acute Leukemias or Myelodysplastic Syndrome: A Pediatric Oncology Experimental Therapeutics Investigators' Consortium Study (POE 10-03). *Pediatr Blood Cancer* (2017) 64(8):e26414–33. doi: 10.1002/pbc.26414
42. Martinez-Cuadron D, Boluda B, Martinez P, Bergua J, Rodriguez-Veiga R, Esteve J, et al. A Phase I-II Study of Plerixafor in Combination With Fludarabine, Idarubicin, Cytarabine, and G-CSF (PLERIFLAG Regimen) for the Treatment of Patients With the First Early-Relapsed or Refractory Acute Myeloid Leukemia. *Ann Hematol* (2018) 97(5):763–72. doi: 10.1007/s00277-018-3229-5
43. Roboz GJ, Ritchie EK, Dault Y, Lam L, Marshall DC, Cruz NM, et al. Phase I Trial of Plerixafor Combined With Decitabine in Newly Diagnosed Older Patients With Acute Myeloid Leukemia. *Haematologica* (2018) 103(8):1308–16. doi: 10.3324/haematol.2017.183418

Conflict of Interest: The authors declare that the research was conducted in the absence of any commercial or financial relationships that could be construed as a potential conflict of interest.

Publisher's Note: All claims expressed in this article are solely those of the authors and do not necessarily represent those of their affiliated organizations, or those of the publisher, the editors and the reviewers. Any product that may be evaluated in this article, or claim that may be made by its manufacturer, is not guaranteed or endorsed by the publisher.

frontiers in Oncology

ORIGINAL RESEARCH
published: 17 January 2022
doi: 10.3389/fonc.2021.790481

Mutations in *JAK/STAT* and *NOTCH1* Genes Are Enriched in Post-Transplant Lymphoproliferative Disorders

Alexandra Butzmann[1,2], Kaushik Sridhar[2], Diwash Jangam[3], Hanbing Song[2], Amol Singh[3], Jyoti Kumar[3], Karen M. Chisholm[4], Benjamin Pinsky[3], Franklin Huang[2] and Robert S. Ohgami[2]*

[1] Agilent Technologies, Santa Clara, CA, United States, [2] Department of Pathology, University of California, San Francisco, San Francisco, CA, United States, [3] Department of Pathology, Stanford University, Stanford, CA, United States, [4] Department of Laboratories, Seattle Children's Hospital, Seattle, WA, United States

Post-transplant lymphoproliferative disorders (PTLD) are diseases occurring in immunocompromised patients after hematopoietic stem cell transplantation (HCT) or solid organ transplantation (SOT). Although PTLD occurs rarely, it may be associated with poor outcomes. In most cases, PTLD is driven by Epstein-Barr virus (EBV) infection. Few studies have investigated the mutational landscape and gene expression profile of PTLD. In our study, we performed targeted deep sequencing and RNA-sequencing (RNA-Seq) on 16 cases of florid follicular hyperplasia (FFH) type PTLD and 15 cases of other PTLD types that include: ten monomorphic (M-PTLD), three polymorphic (P-PTLD), and two classic Hodgkin lymphoma type PTLDs (CHL-PTLD). Our study identified recurrent mutations in *JAK3* in five of 15 PTLD cases and one of 16 FFH-PTLD cases, as well as 16 other genes that were mutated in M-PTLD, P-PTLD, CHL-PTLD and FFH-PTLD. Digital image analysis demonstrated significant differences in single cell area, major axis, and diameter when comparing cases of M-PTLD and P-PTLD to FFH-PTLD. No morphometric relationship was identified with regards to a specific genetic mutation. Our findings suggest that immune regulatory pathways play an essential role in PTLD, with the *JAK/STAT* pathway affected in many PTLDs.

Keywords: PTLD, Epstein-Barr Virus (EBV), florid follicular hyperplasia, targeted sequencing, next generation (deep) sequencing (NGS), whole transcriptome sequencing

OPEN ACCESS

Edited by:
Alessandro Isidori, AORMN Hospital, Italy

Reviewed by:
Pier Paolo Piccaluga, University of Bologna, Italy
Teresa Calimeri, San Raffaele Hospital (IRCCS), Italy

****Correspondence:***
Alexandra Butzmann
alexandra.butzmann@gmail.com

Specialty section:
This article was submitted to Hematologic Malignancies, a section of the journal Frontiers in Oncology

Received: *06 October 2021*
Accepted: *13 December 2021*
Published: *17 January 2022*

Citation:
Butzmann A, Sridhar K, Jangam D, Song H, Singh A, Kumar J, Chisholm KM, Pinsky B, Huang F and Ohgami RS (2022) Mutations in JAK/STAT and NOTCH1 Genes Are Enriched in Post-Transplant Lymphoproliferative Disorders. Front. Oncol. 11:790481. doi: 10.3389/fonc.2021.790481

INTRODUCTION

Post-transplant lymphoproliferative disorders (PTLD) are abnormal lymphoid proliferations that develop in immunosuppressed patients after hematopoietic stem cell transplantation (HCT) or solid organ transplantation (SOT). The current 2017 revised World Health Organization (WHO) classification of hematopoietic neoplasms describes four subtypes of PTLD based on histological features: non-destructive, polymorphic, monomorphic and classic Hodgkin lymphoma type. These four subtypes reflect the phenotypic heterogeneity of PTLD (1). An important driver of PTLD

pathogenesis is thought to be Epstein-Barr virus (EBV). About 70% of PTLD cases are reported to be associated with an EBV infection (2) and recent studies have investigated whether EBV positive and EBV negative PTLDs are distinct entities.

Other studies discuss the progression of PTLD from more benign subtypes, such as the early lesions (florid follicular hyperplasia, FFH) or polymorphic subtypes to more malignant subtypes of PTLD (i.e. monomorphic and classic Hodgkin lymphoma types) (3). Early lesions may be nearly indistinguishable from a reactive inflammatory response. However, next generation sequencing data may provide information about the molecular landscape and genetic profiles in PTLD, allowing for diagnostic subtyping, while also offering insight into the molecular pathogenesis and development of these diseases. To date, the published literature evaluating the genetic landscape of PTLD has been limited. These studies have shown distinct gene expression patterns and copy number aberrations in EBV positive PTLD as compared to EBV negative PTLD (3–5). Additional analyses have demonstrated distinct genetic mutations in monomorphic PTLDs with diffuse large B-cell lymphoma (DLBCL) (6, 7) or T-cell lymphoma phenotypes (8) compared to the corresponding lymphomas arising in immunocompetent patients.

Our study investigates the genetic DNA landscape and RNA gene expression profiles of ten cases of monomorphic, three cases of polymorphic and two cases of classic Hodgkin type PTLD. We compare these cases to the genetic landscape and gene expression profiles of 16 cases of early lesion FFH-PTLD using deep targeted DNA sequencing and RNA-profiling. We additionally evaluate nine cases of PTLD and FFH-PTLD by digital image analysis.

STUDY DESIGN

Patient Cohort

For our study, we selected ten cases of monomorphic, three cases of polymorphic, and two cases of classic Hodgkin lymphoma type PTLD, and 16 cases of FFH-PTLD from the archives (2003-2018) of the Department of Pathology, University of California, San Francisco, Department of Pathology, Stanford University, and Department of Laboratories, Seattle Children's Hospital. All cases and slides were reviewed and diagnoses were confirmed. Patient medical record charts, clinical and laboratory data as well as treatment data were re-reviewed. This study was approved by Institutional Review Boards at each site.

Targeted Deep Sequencing

We extracted DNA from formalin fixed and paraffin embedded (FFPE) tissue using the DNA Storm Kit (Cell Data Science, CA, USA). For our DNA libraries, we developed a customized SureSelect$^{XT\ HS}$ (Agilent Technologies, CA, USA) Heme Malignancies Evaluation and Infectious Detection panel (HeME-ID), which includes 354 genes that are important for lympho- or leukemogenesis in addition to 13 viruses and bacteria associated with hematolymphoid diseases (9, 10). 100 base-pair paired-end targeted deep sequencing was performed at an average coverage depth of 1500-fold on a high-throughput sequencing platform (HiSeq4000). We performed alignment using the Burrows-Wheeler Aligner – maximum exact matches (BWA-MEM) algorithm following the Genome Analysis Toolkit (GATK) best practices for alignment, single-nucleotide variant, and structural variant analysis. For variant calling, we used SureCall (version 4.1, Agilent Technologies). Analysis was run at a variant allele frequency (VAF) of 2%, which was justified by the high read depth and the usage of molecular barcodes in the Sureselect$^{XT\ HS}$ kit. In order to call a mutation, a 20x read coverage per base and a minimum coverage in forward and reverse direction were also required. We applied the same filters for small insertion and deletions (indel) analysis. Annotation of variants was performed using SureCall and wAnnovar (11). For further curation we applied filters of a maximum VAF of 40% and a minimum Combined Annotation Dependent Depletion (CADD) score of 20. Synonymous mutations and mutations outside of exons where excluded. We also used SureCall for analysis of structural variants. For further downstream analysis, such as enrichment or depletion analysis in the promoter region, promoter flanking regions and transcription factor binding sites (CTCF), as well as the analysis of the mutational signature, we used the MutationalPatterns (12) Package from R. Pathway Analysis along with EnrichR (13), Gene Set Enrichment Analysis (GSEA) (14, 15) and ConsensusPathDB-human (CPDB) (16). Evaluation of microorganisms was performed using the subtraction method as described for shotgun metagenomic sequencing (17, 18). For viruses, we interpreted the results based on percent coverage of the targeted regions and average depth. Based on our previous studies, we classified samples as: negative, equivocal, and positive. In order to be interpreted as equivocal, all three viral targeted regions must have a coverage of at least 10% up to 75% and the average read depth must be at least 1. For a sample to be classified as positive, all three targeted regions of a sample required a coverage minimum of 75% and an average read depth of at least 9.

RNA-Sequencing and Data Analysis

RNA was extracted from FFPE tissue blocks with the RNA Storm FFPE DNA Extraction kit (Cell Data Science). The quality and quantity of extracted nucleic acids was assessed by Qubit analysis and 2100 Bioanalyzer (Agilent). We used 200ng of RNA to prepare our RNA library with the SureSelect^{XT} RNA Direct kit (with SureSelect Exome V6 + UTR Capture Library) for strand-specific sequencing libraries (Agilent Technologies). We performed 150 base-pair paired-end whole transcriptome sequencing on a high-throughput sequencing platform from Illumina (HiSeq4000) for an average coverage of 300 million reads per sample. For downstream processing of our output files, we used Hisat2 (version 2.1.0) for alignment and HT-Seq (version 0.11.1) for generation of the count files. Gene expression analysis was performed in RStudio (version 3.5.3). Primary analysis of expression data was performed with ClustVis (19). We used the DeSeq2 package for differential gene expression analysis (20). For fusion analysis, we used STAR-Fusion (version 0.1.1) (21). The immunologic environment was analyzed by CIBERSORT (22).

Computational Digital Image Analysis

We performed digital imaging analysis of representative cases from both the M-PTLD, P-PTLD (n=9) and FFH groups (n=9). MATLAB (v2019B) was used to analyze the RGB images acquired from an Aperio AT2 scanner at an optical magnification of 40X. K-means clustering was used to differentiate the different cellular components and segment the images (23). The image processing toolbox from MATLAB was used to extract eight parameters from the image datasets, which include: area, circularity, major axis, minor axis, eccentricity, equivalent diameter, solidity, and perimeter. Welch's t-test was used to perform a two-tailed test on these parameters.

Statistical Analysis

All statistical analysis was done in RStudio (R version 3.6.0 and RStudio Version 1.2.1335). Student's t-test was performed to evaluate differences between datasets. A p-value < 0.05 was considered statistically significant.

RESULTS

Patient Cohort

Our study included 15 patients diagnosed with advanced PTLD and 16 patients with FFH. The cases of advanced PTLD included ten cases of monomorphic, three cases of polymorphic, and two cases of classic Hodgkin lymphoma type PTLD. The diagnoses for all cases were reconfirmed and classified by R.S.O., B.P., J.K. and K.C. and A.B. based on the 2017 revised WHO classification of lymphoid neoplasms. Our patient cohort consisted of 12 females and 19 males. The average age of the non-FFH PTLD group was 40 years old (range 6 to 67 years) and the average age in the FFH group, 8 years old (range 2 to 20 years). Twelve patients were positive for EBV by *in-situ* hybridization (ISH) in the non-FFH PTLD group, and six patients were positive for EBV by ISH in the FFH group. The clinical characteristics of the non-FFH PTLD and FFH groups are provided in **Tables 1**, **2**, respectively.

Mutational Analysis Reveals Recurrent JAK3 Mutations in Monomorphic, Polymorphic, and Classic Hodgkin Lymphoma PTLD Cases

We performed targeted deep sequencing to gain insight into the mutational landscape of M-PTLD, P-PTLD, and CHL-PTLD in comparison to FFH. The average number of mutations after curation in our M-PTLD, P-PTLD and CHL-PTLD cases was 10.8 and in the FFH cases was 2.8 (with only 10 of 16 FFH cases carrying mutations). The mutations found in the non-FFH PTLD cases were significantly more deleterious than the mutations found in FFH based on the CADD score (average CADD score 28.52 vs. average CADD score 18, p-value 0.01). Among the histological subtypes, the polymorphic subtype had the smallest number of mutations, and the somatic mutations were less damaging. In comparison, other histological subtypes, including monomorphic (DLBCL histology), and classical Hodgkin lymphoma, had a higher number of mutations with more damaging somatic mutations (**Table 3**). Variants for the PTLD cases had a VAF ranging from 2 to 37% with an average of 4.7%, whereas the VAF for the alterations detected in the FFH cases ranged from 2 to 6% with an average of 2.8%.

We also discovered *JAK3* and *BCL11B* mutations in three M-PTLD cases, two CHL-PTLD cases, and *PIK3CD* mutations in four M-PTLD cases. Other genes found to be mutated in more than one case are illustrated in **Figure 1**. Of the genes mutated in greater than three patients, *JAK3* mutations were classified as deleterious based on CADD scores, whereas *BCL11B* mutations had lower CADD scores. *JAK3* mutations were seen in the SH2 and JH2 domains (**Figure 2**). Pathway analysis of the recurrently mutated genes revealed that those genes are key in the *JAK/STAT* pathway and cytokine signaling pathways. Genes affecting the *JAK/STAT* pathway were marked in **Figures 1**, **3**. These genes were also involved in IL-2, IL-3, IL-5 and IL-7 and GM-CSF signaling pathways and signaling events mediated by T-cell Protein Tyrosine Phosphatase (TCPTP).

Overlapping Gene Mutations in M-PTLD, P-PTLD, CHL-PTLD and FFH From Post-Transplant Patients

We identified somatic mutations in 17 overlapping genes between the M-PTLD, P-PTLD, CHL-PTLD and FFH groups (**Figure 3**). The genes recurrently mutated in both groups include *NOTCH1* (four patients), *CREBBP*, and *BCL11B*. All but one mutation in the *NOTCH1* gene were deleterious. The pathogenicity of the somatic mutations involving genes mutated in more than three patients is shown in **Figure 4**.

More Mutations Than Expected in Non-Coding Gene Regions in M-PTLD, P-PTLD, CHL-PTLD and FFH

In order to better understand the overall mutational burden and the distribution of somatic mutations within our samples and groups, we also evaluated the non-coding gene regions, such as promoter, promoter flanking and transcription factor binding sites (CTCF). Here we noted an overall higher number of mutations in M-PTLD, P-PTLD, and the CHL-PTLDs versus FFH, in the promoter regions compared to three non-coding regions (**Figure 5**).

The Mutational Landscape and Gene Expression Profile in M-PTLD, P-PTLD, and CHL-PTLD Is Unrelated to EBV Infection

We performed mutational analysis and evaluated the EBV infection status for M-PTLD, P-PTLD, CHL-PTLD and FFH cases. EBV infection status was determined by ISH and NGS using our targeted HeME-ID panel. By NGS, ten non-FFH PTLD cases and eight FFH cases were positive for EBV infection in the analyzed tissue (**Table 2**). There was no difference in the number of mutations identified between the groups of EBV infected and non-infected patients (**Table 3**). The somatic mutations found in

TABLE 1 | Clinical and histological characteristics of the PTLD patients included in study.

Case	PTLD subtype	EBV status (ISH)	EBV Status (NGS)	Sex	Age	HCT/SOT Indication	Treatment
4	CHL	+	+	F	48	Relapsed HL	Rituximab
6	Monomorphic (DLBCL)	+	+	M	66	BPDCN	Rituximab
28	Polymorphic	+	+	M	24	Relapsed HL	NA
30	T-cell	+	–	M	67	High risk CLL	Nilotinib
32	Monomorphic (DLBCL)	Scattered +	–	M	18	CM	POG 9219
27	Monomorphic (DLBCL)	+	+	M	52	Pre-B-ALL	Rituximab
8	Monomorphic (DLBCL)	–	–	M	56	Cirrhosis	R-CHOP
25	CHL	Scattered +	+	M	24	CM	Stanford V chemotherapy followed by involved field radiotherapy 30 Gy in 20 fractions directed at the pre-chemotherapy disease
13	Polymorphic	+	+	M	22	Relapsed HL	Rituximab
11	Monomorphic (DLBCL)	+	+	F	58	PCKD	R-CHOP
17	Monomorphic (DLBCL)	+	+	F	44	Cirrhosis	Rituximab
29			+				
21	Polymorphic	+	equivocal	M	23	Aplastic Anemia	NA
24	Monomorphic (DLBCL)	–	–	F	40	ESRD	R-CHOP
23	T-cell	+	+	M	6	ESRD	CHOP + high-dose cytarabine with asparaginase
20	Monomorphic (DLBCL)	–	–	F	54	Cirrhosis	Rituximab

PTLD, post-transplant lymphoproliferative disorder; pre-B-ALL, pre-B-cell acute lymphoblastic leukemia; BPDCN, blastic plasmacytoid dendritic cell neoplasm; CHL, classic Hodgkin lymphoma; CLL, chronic lymphoblastic leukemia; CM, cardiomyopathy; HL, Hodgkin lymphoma; DLBCL, diffuse large B-cell lymphoma; ESRD, end-stage renal disease; PCKD, polycystic kidney disease; R-CHOP, rituximab-cyclophosphamide, doxorubicin, vincristine, prednisone. N/A, not applicable.

TABLE 2 | Clinical and histological characteristics of the patients with florid follicular hyperplasia included in study.

Case	PTLD subtype	EBV status (ISH)	EBV Status (NGS)	Sex	Age	HCT/SOT Indication
15	FFH	–	–	M	20	ESRD
14	FFH	–	+	M	5	CM
26	FFH	–	–	M	8	ESRD
22	FFH	–	–	F	4	ESRD
7	FFH	–	–	F	2	Cirrhosis
16	FFH	–	–	F	4	PCKD
3	FFH	+	+	F	6	NEC
19	FFH	+	+	M	4	Biphenotypic AML
2	FFH	+	+	M	2	Cirrhosis
10	FFH	Scattered +	+	F	13	CM
18	FFH	–	–	F	20	ESRD
12	FFH	+	+	M	9	Cirrhosis
5	FFH	–	–	M	2	ESRD
31	FFH	–	equivocal	M	14	ESRD
9	FFH	+	+	M	18	CM
1	FFH	–	+	F	3	CM

PTLD, post-transplant lymphoproliferative disorder; FFH, florid follicular hyperplasia; AML, acute myeloid leukemia; CM, cardiomyopathy; ESRD, end-stage renal disease; NEC, necrotizing enterocolitis; PCKD, polycystic kidney disease.

TABLE 3 | Summary of average number of mutations identified and average CADD score for PTLD subtypes and EBV infection status.

	CHL	T-cell	Monomorphic (DLBCL)	polymorphic	PTLD EBV+	PTLD EBV-	FFH EBV+	FFH EBV-
Average number of mutations	31.5	9	8.4	5.3	10.73	10.8	3	2.57
Average CADD score	30.34	28.86	28.62	25.51	27.88	29.16	15.59	20.42

CHL, classic Hodgkin lymphoma; DLBCL, diffuse large B-cell lymphoma; PTLD, post-transplant lymphoproliferative disorder; FFH, florid follicular hyperplasia; EBV, Epstein-Barr virus.

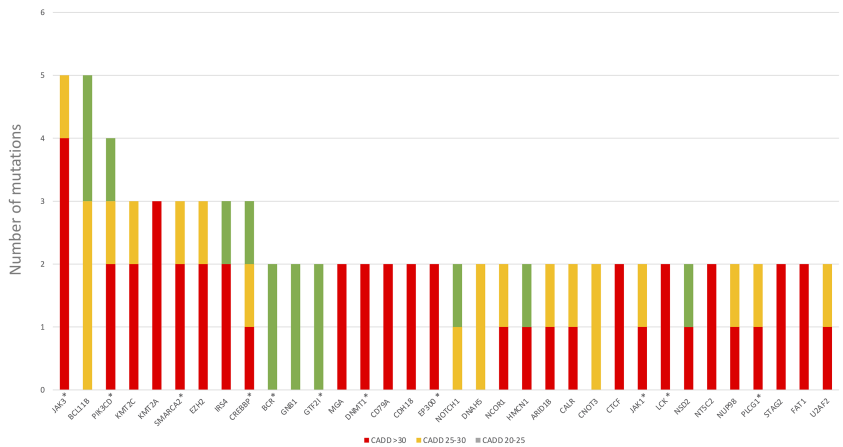

FIGURE 1 | Genes mutated in more than one PTLD sample. *Genes affecting the *JAK/STAT* pathway.

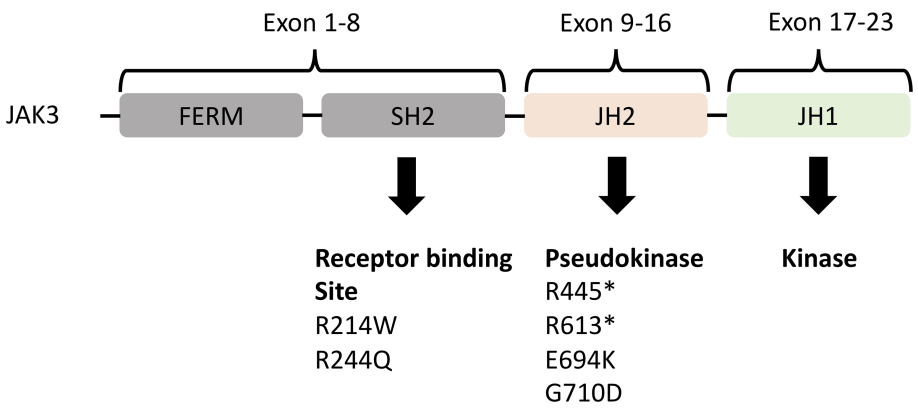

FIGURE 2 | Representation of the JAK3 domains and their encoding exons (24, 25) with JH2 (pseudokinase domain) and JH1 (kinase domain) being the most important. Below the domains are the somatic mutations identified in both M-PTLD, P-PTLD, CHL-PTLD and FFH-PTLD patients. *nonsense mutation.

infected patients had similar CADD scores of pathogenicity, p-value 0.69 (**Table 3**). Discrepancies between the ISH and NGS findings can be explained by two primary factors. The layer of tissue obtained from sectioning the block is variable and may account for the differences between the ISH and NGS studies (i.e. sampling variability). Secondly, interpretation of ISH is subjective, whereas NGS uses predefined parameters with less variation.

Hierarchical clustering of the gene expression profiles shows primary clustering based on the diagnosis of mpc-PTLD and FFH. We also looked for a distinct transcriptional profile based on EBV infection status and noted that EBV negative cases had a tendency to cluster together (**Figure 6**). However, there was no clear separation between EBV positive and negative cases in the gene expression profiles, which was further confirmed using principal component analysis (PCA) (**Supplementary Figure 1**). The different expression patterns did not appear to be associated with any of the other factors we investigated, including batch, mean coverage, gender, race/ethnicity, age, organ transplanted, SOT/HCT, PTLD subtype, or tissue type.

Genes Involved in Regulatory or Innate and Adaptive Immune System Are Upregulated in mpc-PTLD

We performed RNA-sequencing to understand the gene expression profiles of mpc-PTLD compared to FFH. In our exploratory analysis, we saw that mpc-PTLD patients have a different gene expression profile as compared to FFH patients with a subset of mpc-PTLD cases falling in between (cases 6, 8, 17 and 23), as demonstrated in **Figure 6**. We looked at the differentially expressed genes by gene set enrichment analysis and found that genes involved in regulatory or innate and adaptive immune system are overexpressed in mpc-PTLD as compared to FFH.

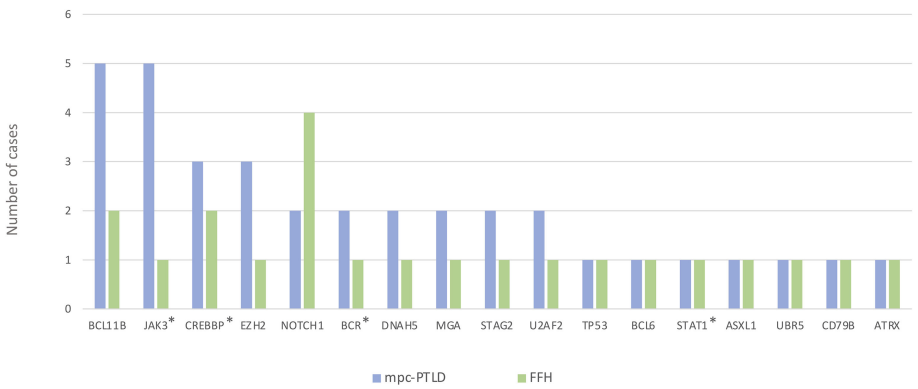

FIGURE 3 | Genes mutated in the mpc-PTLD and FFH-PTLD groups. *Genes affecting the *JAK/STAT* pathway.

	C4_CHL_PTLD	C6_DLBCL_PTLD	C8_DLBCL_PTLD	C11_DLBCL_PTLD	C13_Polymorphic_PTLD	C17_DLBCL_PTLD	C29_DLBCL_PTLD	C20_DLBCL_PTLD	C21_Polymorphic_PTLD	C23_T-cell_PTLD	C24_DLBCL_PTLD	C25_CHL_PTLD	C27_DLBCL_PTLD	C32_DLBCL_PTLD	C9_FFH	C16_FFH	C18_FFH	C19_FFH	C31_FFH
JAK3*	R445*	R214W					R244Q					G710D		R613*			E694K		
BCLB11B					H317Y	R294Q	E432K					E481K		E817K			E297K		P20L
PIK3CD*							D138N			S118N	G252D			D868N					
KMT2C			C385F	A381T									A286V						
KMT2A						R3822C						M3887K		R3232*					
SMARCA2*						R194Q						P775L							
EZH2								Y590N			A262V	T349M						R634C	
IRS4									P903Q			Q621*							
CREBBP*										Q125K	Q329*	E1524K			R1340Q		G1083R		
NOTCH1								V1726M						G1034S		D1517N	P2512L	E1789K	C2140Y

FIGURE 4 | Overview of somatic mutations in recurrently mutated genes in the mpc-PTLD and FFH-PTLD groups. Somatic mutations with a CADD score of >30 are shown in red, CADD score of 25-30 in orange, and CADD score of 20-25 indicated in green. *Genes affecting the *JAK/STAT* pathway.

mpc-PTLD Cases Have More T-Cell Involvement and Fewer B-Cell Involvement Than FFH Cases

Using the gene expression profile of our samples, we looked at the immune cell composition within the mpc-PTLD and FFH group. As shown in **Figure 7**, there is a greater B-cell component (naïve and memory) within the FFH group, whereas the mpc-PTLD group has a stronger overall CD8 and CD4 T-cell component. In general, the mpc-PTLD cases have a more heterogenous immune cell infiltration with more T-follicular helper cells and a greater mast cell component in some of the cases. The mpc-PTLD cases diagnosed with a T-cell subtype show strong signal for T-cells, while lacking a significant B-cell component.

Digital Imaging Analysis Demonstrates That mpc-PTLD Cells Are Larger Than FFH Cells

We performed digital imaging analysis of nine representative cases of both the mpc-PTLD and FFH groups. In our analysis, we found that mpc-PTLD cells have a significant larger area, diameter, and major axis (**Figure 8**) ($p<0.0001$). There was no significant difference in the circularity, minor axis, eccentricity, or perimeter. We were particularly interested in cases that seems to have a molecular overlap. Cases 6, 8 and 23 were analyzed by digital imaging and their transcriptional profile appears more similar to the transcriptional profile of FFH (**Figure 6**). We were unable to identify differentiating features among cases 6, 8, and 23 as well as the remaining cases of the mpc-PTLD group.

DISCUSSION

In our study, we investigated and compared the molecular landscape of 15 cases of advanced PTLD and 16 cases of FFH. Here we performed a high-throughput molecular comparison and conducted digital imaging analysis of mpc-PTLD and FFH cases.

Our mutational analysis showed a higher number of mutations for the mpc-PTLD cases with somatic mutations that were more deleterious than those in the FFH cases. We identified somatic mutations in all of the mpc-PTLD cases but

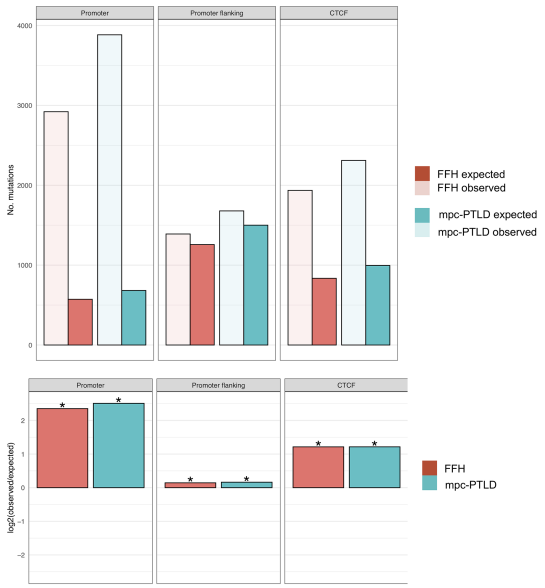

FIGURE 5 | Enrichment analysis for promoter region, promoter flanking regions, and transcription binding sites (CTCF). The top part of the figure shows the observed versus expected number of mutations. In the bottom part of the figure, the mutational burden within the same non-coding gene regions for both groups are demonstrated as the log2 ratio of the number of observed and expected point mutations indicating the effect size of the enrichment or depletion within each region. (*) = statistical significance ($p<0.05$; two-sided binomial test).

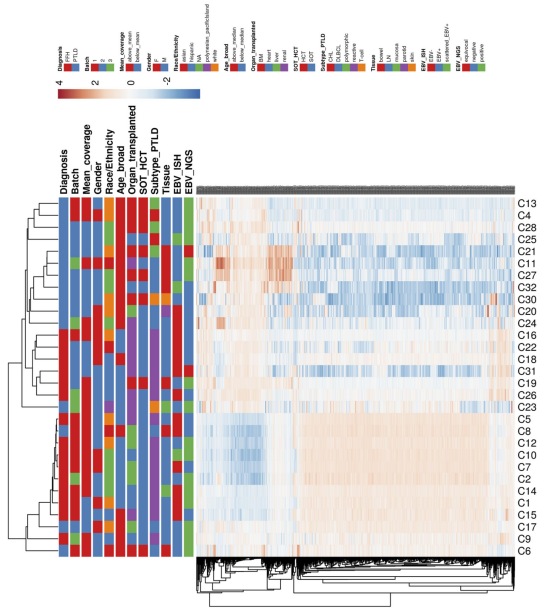

FIGURE 6 | Heatmap hierarchically clustered by Euclidean distance of gene expression for all of the investigated groups (see legend).

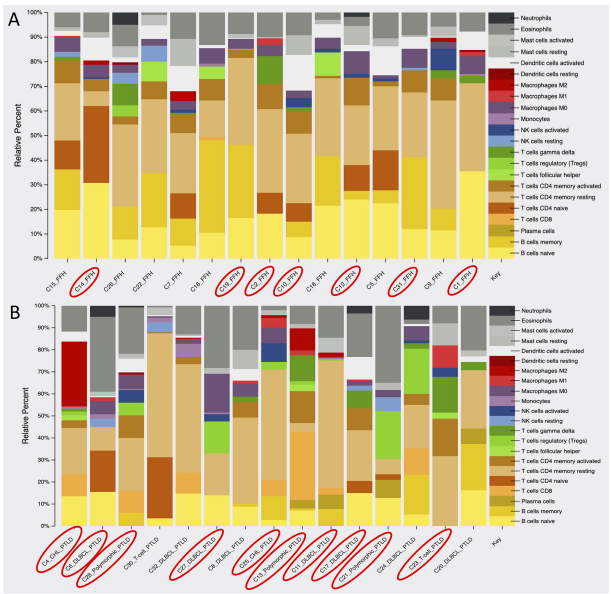

FIGURE 7 | Analysis of the immune cell composition within **(A)** the FFH-PTLD cases and **(B)** the monomorphic, polymorphic, and classic Hodgkin (mpc)-PTLD cases based on gene expression profile. EBV positive cases are circled in red.

only in 10 of 16 FFH cases. These findings were further confirmed by evaluating the mutational burden of the specific non-coding regions: promoter region, promoter flanking and transcription factor binding sites (CTCF) region. Here we again saw a higher number of mutations within the mpc-PTLD group. Interestingly, we observed more promoter region mutations than expected for both mpc-PTLD and FFH. Overall, we found both groups to be very heterogenic with respect to the number of mutations identified and the mutational landscapes.

Previous studies reported on PTLD arising from early lesions, such as FFH (26, 27). Our analysis further corroborates these findings and we identified 17 overlapping genes mutated in both the PTLD and FFH groups. The majority of these genes were mutated in more than one mpc-PTLD case. Among the overlapping genes detected in both mpc-PTLD and FFH, *JAK3*, *BCL11B*, and *PIK3CD* were recurrently mutated in mpc-PTLD in four or more cases. Five of the six detected mutations in *JAK3* were deleterious, all with very low VAF (3-10%). Although we used FFPE tissue for targeted deep sequencing, we were able to detect very low VAF based on a high read depth and the use of molecular barcodes in our library chemistry. *JAK3* is a cytokine receptor and plays a critical role in the *JAK/STAT* pathway. The *JAK/STAT* pathway plays an important role in the regulation of cell proliferation and immune system response, especially by involvement of cytokine and interleukin signaling (28). *JAK3* mutations have been reported in mainly T-cell neoplasms (29,) (30), immunodeficiency syndromes (31, 32), and B-cell neoplasms (33). The mutations found in our PTLD and FFH cases fall into the SH2 and JH2 domains of the *JAK3* gene. The JH2 pseudokinase domain is the most commonly affected

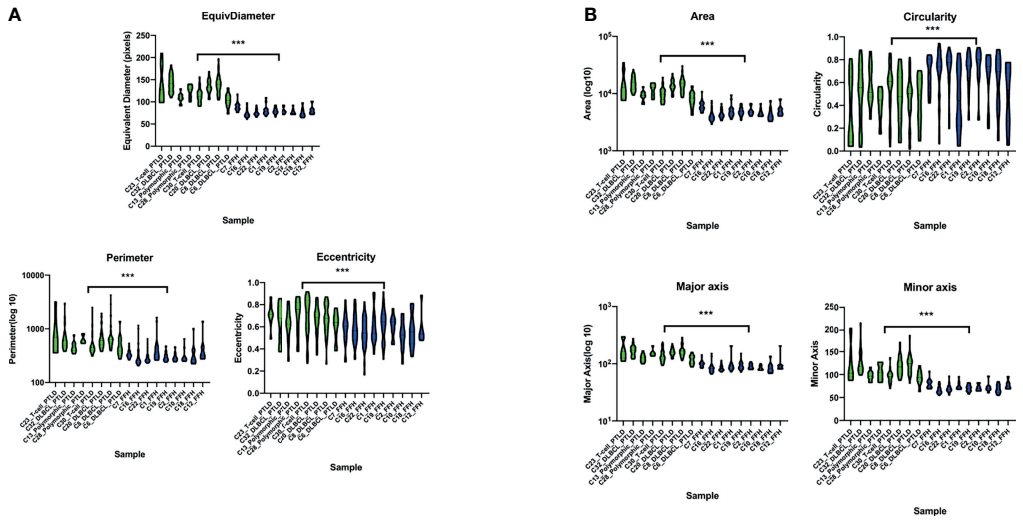

FIGURE 8 | Violin plot of the digital imaging analysis of M-PTLD, P-PTLD, CHL-PTLD, and FFH-PTLD cases. **(A)** Violin plots of cellular parameters of equivalent diameter, perimeter and eccentricity. **(B)** Violin plots of cellular parameters of area, circularity, major axis, and minor axis. Displayed are nine representative samples of each group. Green represents M-PTLD and P-PTLD cases, blue indicates FFH-PTLD cases. (***) = statistical significance ($p<0.0001$).

domain within all the *JAK* mutated genes involved in hematolymphoid diseases, with most mutations functioning as activating mutations (34). The pseudokinase domain suppresses the directly adjacent kinase domain JH1 (24). The SH2 domain is located in the receptor binding domain where kinase activity is initiated and the JAK receptor specificity is determined (35,) (36). Given that current drugs, such as tofacitinib and peficitinib, target the *JAK3* signaling pathway, our findings support the potential role of JAK3-targeted therapy to improve treatment options for PTLD (37–39). However, more cases are necessary to confirm the recurrence of *JAK3* mutations in PTLD. Further, functional studies are necessary to determine if the discovered mutations are activating or inactivating mutations.

Within the FFH group, *NOTCH1* was recurrently mutated. *NOTCH1* mutations often occur in T-cell acute lymphoblastic leukemia/lymphoma (T-ALL) (40) and multiple studies have demonstrated the importance of NOTCH1 signaling for the induction of lymphomagenesis (41–43). A recent study by Kimura et al. suggested that activating *NOTCH1* mutations play a role in the genetic evolution of pediatric T-ALL (44). The mutation detected in our cases are mostly deleterious with two of five cases involving the PEST domain of *NOTCH1* (exon 34). This PEST domain is one of the two most frequently affected domains, often a result of activating mutations (41). Our findings of recurrent *NOTCH1* and overlapping mutational landscapes support the published literature suggesting possible progression of FFH to monomorphic, polymorphic, and classic Hodgkin lymphoma type PTLD. Our FFH study group was younger than the mpc-PTLD group which may lead to differences in outcome and genetic landscape between the two study groups (45).

We performed RNA-sequencing to compare the gene expression profiles of our mpc-PTLD cases with FFH. We found that the FFH cases show a distinct gene expression profile as compared to the mpc-PTLD cases. However, some mpc-PTLD cases exhibited a hybrid expression profile relative to the FFH cases, indicative of a possible relationship between the two groups. Differential gene expression analysis showed an overexpression of genes involved in the innate and adaptive immune system as well as complement activating genes. These results underline our mutational findings of recurrently mutated *JAK3* and *NOTCH1*, both of which are important in immune system regulation.

Through our targeted deep sequencing analysis, we found that the variants for the PTLD cases had a greater average VAF as compared to the VAF for the alterations detected in the FFH cases. These findings suggest that the lower average VAF in cases of FFH may represent gene expression of a benign or reactive background environment whereas the higher average VAF in the mpc-PTLD group may indicate a gene expression pattern of neoplastic cells. Although the majority of the mpc-PTLD group consisted of monomorphic PTLDs, we also compared the number of mutations of the other histological PTLD subtypes. We found that the polymorphic subtype had the smallest number of mutations with less damaging somatic mutations. In concordance with the current literature, we noted that polymorphic PTLD may be a precursor lesion to the other subtypes and we believe our data supports these findings (3). However, given the small sample size within this group, interpretation of these results is limited. In addition, as mentioned before the FFH study group was younger than the mpc-PTLD study group which may cause a difference in genetic landscapes.

Using our HeME-ID panel that targets 13 viruses and bacteria, we evaluated the EBV infection status of all 31 patients. EBV infection was seen in ten out of 15 mpc-PTLD tissues and nine of 16 FFH tissues. Through mutational analysis, we identified a similar number of mutations for EBV positive and

EBV negative cases. The pathogenicity of the mutations found in the EBV positive cases was lower than in the EBV negative cases. Our results support the findings of Menter et al., who found that EBV positive monomorphic PTLD cases had a less pathogenic mutational landscape as compared to EBV negative cases and suggested that EBV induces lymphomagenesis through its oncogenic properties, behaving as a substitute for deleterious mutations (7). When comparing the gene expression profiles, two studies found differences in the gene expression pattern of EBV positive and EBV negative PTLD cases (4, 5), whereas another study did not detect any differentially expressed genes (27). We also noted that the EBV negative cases clustered in between the positive cases in the hierarchical clustering analysis. However, no genes were significantly differentially expressed based on EBV infection status.

To study the immunologic environment of our mpc-PTLD and FFH cases, we looked at the immune cell composition based on the gene expression profiles of the two groups. We found that B-cells were the predominant cell type within the FFH group, whereas the mpc-PTLD group consisted of a large proportion of CD4 and CD8 cells, T-follicular helper cells, and mast cells. Overall, the immune cell composition of the mpc-PTLD cases was more heterogenic and was also unrelated to the EBV infection status, as noted in **Figure 7**. This finding is important to note since the dominating CD4/CD8 T-cell component within the mpc-PTLD group has been associated with EBV infection status due to the naturally occurring T-cell immune response seen in EBV positive immunocompetent patients (8, 46). Based on our molecular findings, we hypothesize that a change of the immune cell composition in PTLD may be due to the dysregulated immune response. *JAK/STAT* and *NOTCH1* pathway defects are often seen in T-cell malignancies (28) and may explain the distinction in B-cell and T-cell composition between the mpc-PTLD and FFH groups. Moreover, *JAK/STAT* is a major regulator of cytokine pathways and dysregulation may also lead to increased mast cells in the immunologic environment. Overall, our immune cell composition findings support our molecular findings. Future studies are also warranted to determine whether the cell of origin in PTLD is recipient- or donor-derived as this may provide further insight into the immune-mediated pathways involved in PTLD.

To our knowledge, this is the first study to perform digital analysis on whole slide images of PTLD samples. The histologic presentation of PTLD is very heterogenic, and it can be difficult to distinguish from other benign or malignant processes of the lymph node (47). Thus, we utilized digital analysis of whole slide images to determine if the cells from monomorphic, polymorphic, or classical Hodgkin type PTLD can be distinguished from FFH cells. mpc-PTLD cells were significantly larger in area, diameter, and major axis as compared to the FFH lymphocytes ($p<0.0001$). These results were expected as mpc-PTLD lymphocytes can be enlarged and can be confused with other entities, such as a plasma cell neoplasm (48). Surprisingly, mpc-PTLD and FFH lymphocytes showed no significant differences in circularity, eccentricity, perimeter, and minor axis since we anticipated mpc-PTLD and FFH lymphocytes to be more distinguishable. Our findings support the molecular data and show similarities between m-PTLD, p-PTLD, CHL-PTLD and FFH lesions. Of note, our imaging analysis was limited by the number of cases and disease entities in this study. Greater sample sizes are needed to perform an in-depth analysis of the morphological hallmarks of PTLD pathology.

CONCLUSION

Our study is the first comprehensive analysis evaluating the molecular landscapes of monomorphic, polymorphic, or classic Hodgkin type PTLD and FFH. Limitations of this study are the small sample size as well as the age difference between mpc-PTLD and FFH group. However, our findings contribute to a better understanding of the pathogenesis of PTLD and will help guide future functional studies for these disease processes.

DATA AVAILABILITY STATEMENT

The data presented in the study are deposited in the Genbank repository, accession numbers SAMN24663821-SAMN24663850 or available upon request to the corresponding author.

ETHICS STATEMENT

The studies involving human participants were reviewed and approved by the UCSF Institutional review board. Written informed consent from the participants' legal guardian/next of kin was not required to participate in this study in accordance with the national legislation and the institutional requirements.

AUTHOR CONTRIBUTIONS

RO conceived of and designed the study, analyzed data, and edited the manuscript. BP conceived of and designed the study, and edited the manuscript. AB designed the study, performed research, designed experiments, analyzed data, and wrote the manuscript. KS, DJ, HS, AS, JK, KC, and FH analyzed data and edited the manuscript. All authors contributed to the article and approved the submitted version.

SUPPLEMENTARY MATERIAL

The Supplementary Material for this article can be found online at: https://www.frontiersin.org/articles/10.3389/fonc.2021.790481/full#supplementary-material

Supplementary Figure 1 | PCA plot of the transcriptional profile of **(A)** EBV positive and EBV negative monomorphic, polymorphic, and classic Hodgkin (mpc)-PTLD cases and **(B)** EBV positive and EBV negative FFH-PTLD samples. EBV status was determined by NGS.

REFERENCES

1. Swerdlow SH, Campo E, Harris NL, Jaffe ES, Pileri SA, Stein H, et al. *WHO Classification of Tumors of Haematopoietic and Lymphoid Tissues, Revised 4th Ed*. Lyon, France: International Agency for Research on Cancer (2017).
2. Morscio J, Tousseyn T. Recent Insights in the Pathogenesis of Post-Transplantation Lymphoproliferative Disorders. *World J Transplant* (2016) 6:505–16. doi: 10.5500/wjt.v6.i3.505
3. Vakiani E, Basso K, Klein U, Mansukhani MM, Narayan G, Smith PM, et al. Genetic and Phenotypic Analysis of B-Cell Post-Transplant Lymphoproliferative Disorders Provides Insights Into Disease Biology. *Hematol Oncol* (2008) 26:199–211. doi: 10.1002/hon.859
4. Craig FE, Johnson LR, Harvey SAK, Nalesnik MA, Luo JH, Bhattacharya SD, et al. Gene Expression Profiling of Epstein-Barr Virus-Positive. *Diagn Mol Pathol* (2007) 16:158–68. doi: 10.1097/PDM.0b013e31804f54a9
5. Morscio J, Dierickx D, Ferreiro JF, Herreman A, Van Loo P, Bittoun E, et al. Gene Expression Profiling Reveals Clear Differences Between EBV-Positive and EBV-Negative Posttransplant Lymphoproliferative Disorders. *Am J Transplant* (2013) 13:1305–16. doi: 10.1111/ajt.12196
6. Ferreiro JF, Morscio J, Dierickx D, Vandenberghe P, Gheysens O, Verhoef G, et al. EBV-Positive and EBV-Negative Posttransplant Diffuse Large B Cell Lymphomas Have Distinct Genomic and Transcriptomic Features. *Am J Transplant* (2016) 16:414–25. doi: 10.1111/ajt.13558
7. Menter T, Juskevicius D, Alikian M, Steiger J, Dirnhofer S, Tzankov A, et al. Mutational Landscape of B-Cell Post-Transplant Lymphoproliferative Disorders. *Br J Haematol* (2017) 178:48–56. doi: 10.1111/bjh.14633
8. Martinez OM. Biomarkers for PTLD Diagnosis and Therapies. *Pediatr Nephrol* (2020) 35:1173–81. doi: 10.1007/s00467-019-04284-w
9. Butzmann A, Sridhar K, Jangam D, Kumar J, Sahoo MK, Shahmarvand N, et al. A Comprehensive Analysis of RHOA Mutation Positive and Negative Angioimmunoblastic T-Cell Lymphomas by Targeted Deep Sequencing, Expression Profiling and Single Cell Digital Image Analysis. *Int J Mol Med* (2020) 46:1466–76. doi: 10.3892/ijmm.2020.4686
10. Jangam D, Butzmann A, Sridhar K, Deresinski S, Banaei N, Ohgami RS. Significance of Bacterial and Viral Genotypes as a Risk Factor in Driving Cancer. *Mol Clin Oncol* (2020) 13:3–12. doi: 10.3892/mco.2020.2043
11. Yang H, Wang K. Genomic Variant Annotation and Prioritization With ANNOVAR and Wannovar. *Nat Protoc* (2015) 10:1556–66. doi: 10.1038/nprot.2015.105
12. Blokzijl F, Janssen R, Van Boxtel R, Cuppen E. Mutationalpatterns: Comprehensive Genome-Wide Analysis of Mutational Processes. *Genome Med* (2018) 10:1–11. doi: 10.1186/s13073-018-0539-0
13. Chen EY, Tan CM, Kou Y, Duan Q, Wang Z, Meirelles GV, et al. Enrichr: Interactive and Collaborative HTML5 Gene List Enrichment Analysis Tool. *BMC Bioinf* (2013) 14:128. doi: 10.1186/1471-2105-14-128
14. Subramanian A, Tamayo P, Mootha VK, Mukherjee S, Ebert BL Gillette MA, et al. Gene Set Enrichment Analysis: A Knowledge-Based Approach for Interpreting Genome-Wide Expression Profiles. *Proc Natl Acad Sci USA* (2005) 102:15545–50. doi: 10.1073/pnas.0506580102
15. Mootha VK, Lindgren CM, Eriksson K-F, Subramanian A, Sihag S, Lehar J, et al. Pgc-1α-Responsive Genes Involved in Oxidative Phosphorylation Are Coordinately Downregulated in Human Diabetes. *Nat Genet* (2003) 34:267–73. doi: 10.1038/ng1180
16. Kamburov A, Stelzl U, Lehrach H, Herwig R. The Consensuspathdb Interaction Database: 2013 Update. *Nucleic Acids Res* (2013) 41:D793–800. doi: 10.1093/nar/gks1055
17. Gyarmati P, Kjellander C, Aust C, Song Y, Öhrmalm L, Giske CG. Metagenomic Analysis of Bloodstream Infections in Patients With Acute Leukemia and Therapy-Induced Neutropenia. *Sci Rep* (2016) 6:23532. doi: 10.1038/srep23532
18. Baheti S, Tang X, O'Brian DR, Chia N, Roberts LR, Nelson H, et al. HGT-ID: An Efficient and Sensitive Workflow to Detect Human-Viral Insertion Sites Using Next-Generation Sequencing Data. *BMC Bioinf* (2018) 19:271. doi: 10.1186/s12859-018-2260-9
19. Metsalu T, Vilo J. Clustvis: A Web Tool for Visualizing Clustering of Multivariate Data Using Principal Component Analysis and Heatmap. *Web Serv issue Publ Online* (2015) 43:W566–70. doi: 10.1093/nar/gkv468
20. Love MI, Huber W, Anders S. Moderated Estimation of Fold Change and Dispersion for RNA-Seq Data With Deseq2. *Genome Biol* (2014) 15:1–21. doi: 10.1186/s13059-014-0550-8
21. Haas BJ, Dobin A, Li B, Stransky N, Pochet N, Regev A. Accuracy Assessment of Fusion Transcript Detection via Read-Mapping and De Novo Fusion Transcript Assembly-Based Methods. *Genome Biol* (2019) 20:213. doi: 10.1186/s13059-019-1842-9
22. Newman AM, Liu CL, Green MR, Gentles AJ, Feng W, Xu Y, et al. Robust Enumeration of Cell Subsets From Tissue Expression Profiles. *Nat Methods* (2015) 12:453–7. doi: 10.1038/nmeth.3337
23. Fouad S, Randell D, Galton A, Mehanna H, Landini G. Unsupervised Morphological Segmentation of Tissue Compartments in Histopathological Images. *PloS One* (2017) 12:e0188717. doi: 10.1371/journal.pone.0188717
24. Raivola J, Hammarén HM, Virtanen AT, Bulleeraz V, Ward AC, Silvennoinen O. Hyperactivation of Oncogenic JAK3 Mutants Depend on ATP Binding to the Pseudokinase Domain. *Front Oncol* (2018) 8:560. doi: 10.3389/fonc.2018.00560
25. Brooimans RA, van der Slot AJ, van den Berg A, Zegers BJ. Revised Exonð Intron Structure of Human JAK3 Locus. *Eur J Hum Genet* (1999) 7:837–40. doi: 10.1038/sj.ejhg.5200375
26. Nelson BP, Nalesnik MA, Bahler DW, Locker J, Fung JJ, Swerdlow SH. Epstein-Barr Virus-Negative Post-Transplant Lymphoproliferative Disorders: A Distinct Entity? *Am J Surg Pathol* (2000) 24:375–85. doi: 10.1097/00000478-200003000-00006
27. Vakiani E, Nandula SV, Subramaniyam S, Keller CE, Alobeid B, Murty VV. Cytogenetic Analysis of B-Cell Posttransplant Lymphoproliferations Validates the World Health Organization Classification and Suggests Inclusion of Florid Follicular Hyperplasia as a Precursor Lesion. *Hum Pathol* (2007) 38:315–25. doi: 10.1016/j.humpath.2006.08.014
28. Shahmarvand N, Nagy A, Shahryari J, Ohgami RS. Mutations in the Signal Transducer and Activator of Transcription Family of Genes in Cancer. *Cancer Sci* (2018) 109:926–33. doi: 10.1111/cas.13525
29. Degryse S, Bornschein S, De Bock CE, Leroy E, Bempft MV, Demeyer S, et al. Mutant JAK3 Signaling Is Increased by Loss of Wild-Type JAK3 or by Acquisition of Secondary JAK3 Mutations in T-ALL. *Blood* (2018) 131:421–5. doi: 10.1182/blood-2017-07-797597
30. Greenplate A, Wang K, Tripathi RM, Palma N, Ali SM, Stephens PJ, et al. Genomic Profiling of T-Cell Neoplasms Reveals Frequent JAK1 and JAK3 Mutations With Clonal Evasion From Targeted Therapies. *JCO Precis Oncol* (2019) 2018. doi: 10.1200/PO.17.00019
31. Aluri J, Desai M, Gupta M, Dalvi A, Terance A, Rosenzweig SD, et al. Clinical, Immunological, and Molecular Findings in 57 Patients With Severe Combined Immunodeficiency (SCID) From India. *Front Immunol* (2019) 10:1–16. doi: 10.3389/fimmu.2019.00023
32. Di Matteo G, Chiriaco M, Scarselli A, Cifaldi C, Livadiotti S, Cesare SD, et al. JAK3 Mutations in Italian Patients Affected by SCID: New Molecular Aspects of a Long-Known Gene. *Mol Genet Genomic Med* (2018) 6:713–21. doi: 10.1002/mgg3.391
33. Batista CR, Lim M, LaraméeLaram A-S, Abu-Sardanah F, Xu LS, Hossain R, et al. Driver Mutations in Janus Kinases in a Mouse Model of B-Cell Leukemia Induced by Deletion of PU.1 and Spi-B. *Blood Adv* (2018) 2:2798–810. doi: 10.1182/bloodadvances.2018019950
34. Babon JJ, Lucet IS, Murphy JM, Nicola NA, Varghese LN. The Molecular Regulation of Janus Kinase (JAK) Activation. *Biochem J* (2014) 462:1–13. doi: 10.1042/BJ20140712
35. Wallweber HJA, Tam C, Franke Y, Starovasnik MA, Lupardus PJ. Structural Basis of Ifnα Receptor Recognition by TYK2. *Nat Struct Mol Biol* (2014) 21:443–8. doi: 10.1038/nsmb.2807
36. Ferrao R, Lupardus P. The Janus Kinase (JAK) Ferm and SH2 Domains: Bringing Specificity to JAK-Receptor Interactions. *Front Endocrinol* (2017) 8:1–11. doi: 10.3389/fendo.2017.00071
37. Roskoski R. Invited Review Janus Kinase (JAK) Inhibitors in the Treatment of Inflammatory and Neoplastic Diseases. *Pharmacol Res* (2016) 111:784–803. doi: 10.1016/j.phrs.2016.07.038
38. Ge Y, Wang C, Song S, Huang J, Liu Z, Li Y, et al. Identification of Highly Potent BTK and JAK3 Dual Inhibitors With Improved Activity for the Treatment of B-Cell Lymphoma. *Eur J Med Chem* (2018) 143:1847–57. doi: 10.1016/j.ejmech.2017.10.080

39. Gomez-Arteaga A, Margolskee E, Wei MT, Van Besien K, Inghirami G, Horwitz S. Combined Use of Tofacitinib (Pan-JAK Inhibitor) and Ruxolitinib (a JAK1/2 Inhibitor) for Refractory T-Cell Prolymphocytic Leukemia (T-PLL) With a JAK3 Mutation. *Leuk Lymphoma* (2019) 60:1626–31. doi: 10.1080/10428194.2019.1594220
40. Aster JC, Blacklow SC, Pear WS. Notch Signalling in T-Cell Lymphoblastic Leukaemia/Lymphoma and Other Haematological Malignancies. *J Pathol* (2011) 223:262–73. doi: 10.1002/path.2789
41. Grabher C, Von Boehmer H, Look AT. Notch 1 Activation in the Molecular Pathogenesis of T-Cell Acute Lymphoblastic Leukaemia. *Nat Rev Cancer* (2006) 6:347–59. doi: 10.1038/nrc1880
42. Weng AP, Ferrando A, Lee W, Morris 4JP, Siverman LB, Sanchez-Irrizary C, et al. Activating Mutations of NOTCH1 in Human T Cell Acute Lymphoblastic Leukemia. *Science* (2004) 306:269–71. doi: 10.1126/science.1102160
43. Wang H-C, Peng V, Zhao Y, Sun X-H. Enhanced Notch Activation Is Advantageous But Not Essential for T Cell Lymphomagenesis in Id1 Transgenic Mice. *PloS One* (2012) 7:e32944. doi: 10.1371/journal.pone.0032944
44. Kimura S, Seki M, Yoshida K, Shiraishi Y, Akiyama M, Koh K, et al. NOTCH1 Pathway Activating Mutations and Clonal Evolution in Pediatric T-Cell Acute Lymphoblastic Leukemia. *Cancer Sci* (2019) 110:784–94. doi: 10.1111/cas.13859
45. Eman M, Navallas M, Navarro OM, Punnet A, Shammas A, Gupta A, et al. Posttransplant Proliferative Disorder in Children: A 360-Degree Perspective. *RadoGraphics* (2019) 40:241–65. doi: 10.1148/rg.2020190103
46. Martinez OM, Krams SM. The Immune Response to Epstein Barr Virus and Implications for Posttransplant Lymphoproliferative Disorder. *Transplantation* (2017) 101:2009–16. doi: 10.1097/TP.0000000000001767
47. Abbas F, El Kossi M, Sakr Shaheen I, Sharma A, Halawa A. Post-Transplantation Lymphoproliferative Disorders: Current Concepts and Future Therapeutic Approaches. *World J Transplant* (2020) 10:29–46. doi: 10.5500/wjt.v10.i2.29
48. Parker A, Bowles K, Bradley JA, Emery V, Featherstone C, Gupte G, et al. Diagnosis of Post-Transplant Lymphoproliferative Disorder in Solid Organ Transplant Recipients - BCSH and BTS Guidelines. *Br J Haematol* (2010) 149:675–92. doi: 10.1111/j.1365-2141.2010.08161.x

Conflict of Interest: The authors declare that the research was conducted in the absence of any commercial or financial relationships that could be construed as a potential conflict of interest.

Publisher's Note: All claims expressed in this article are solely those of the authors and do not necessarily represent those of their affiliated organizations, or those of the publisher, the editors and the reviewers. Any product that may be evaluated in this article, or claim that may be made by its manufacturer, is not guaranteed or endorsed by the publisher.

frontiers in Oncology

BRIEF RESEARCH REPORT
published: 20 January 2022
doi: 10.3389/fonc.2021.773397

Implementation of an Outpatient HD-MTX Initiative

*Kelsey Sokol[1], Kelley Yuan[2], Maria Piddoubny[3], Ellen Sweeney[4], Anne Delengowski[4], Katlin Fendler[4], Gloria Espinosa[3], Judith Alberto[3], Patricia Galanis[4], Carol Gung[3], Meghan Stokley[3], Mercy George[3], Mary Harris[3], Ubaldo Martinez-Outschoorn[5], Onder Alpdogan[5], Pierluigi Porcu[5] and Adam F. Binder[5]**

[1] Department of Medical Oncology, Thomas Jefferson University, Philadelphia, PA, United States, [2] Sidney Kimmel Medical College, Philadelphia, PA, United States, [3] Department of Pharmacy, Thomas Jefferson University, Philadelphia, PA, United States, [4] Department of Nursing, Thomas Jefferson University, Philadelphia, PA, United States, [5] Division of Hematologic Malignancies and Hematopoietic Stem Cell Transplant, Department of Medical Oncology, Sidney Kimmel Cancer Center, Thomas Jefferson University, Philadelphia, PA, United States

OPEN ACCESS

Edited by:
Jean El Cheikh,
American University of Beirut Medical Center, Lebanon

Reviewed by:
Laura B. Ramsey,
Cincinnati Children's Hospital Medical Center, United States
Rajan Kapoor,
Command Hospital, India

***Correspondence:**
Adam F. Binder
adam.binder@jefferson.edu

Specialty section:
This article was submitted to Hematologic Malignancies, a section of the journal Frontiers in Oncology

Received: 09 September 2021
Accepted: 30 December 2021
Published: 20 January 2022

Citation:
Sokol K, Yuan K, Piddoubny M, Sweeney E, Delengowski A, Fendler K, Espinosa G, Alberto J, Galanis P, Gung C, Stokley M, George M, Harris M, Martinez-Outschoorn U, Alpdogan O, Porcu P and Binder AF (2022) Implementation of an Outpatient HD-MTX Initiative. Front. Oncol. 11:773397. doi: 10.3389/fonc.2021.773397

Introduction: Methotrexate (MTX) a folate antagonist is often given in high doses (≥500 mg/m^2) to treat a variety of disease processes. While inpatient administration has been the norm, outpatient administration, has been shown to be safe, effective, and patient centered. Here in we describe development of an outpatient HDMTX protocol and our initial experience.

Methods: All patients were to receive their first cycle of HDMTX in the hospital to ensure they tolerate it well and also to use this time to assist in training for home administration. The outpatient protocol involved continuous IV sodium bicarbonate, along with oral leucovorin and acetazolamide. Patients were required to visit the infusion center daily for labs and methotrexate levels. Clear criteria for admission were developed in the case of delayed clearance or methotrexate toxicity.

Results: Two patients completed the safety run-in phase. Both patients tolerated treatment well. There were no associated toxicity. Methotrexate cleared within 3 days for all cycles. Both patients were able to follow the preadmission instructions for sodium bicarbonate and acetazolamide. The patients reported adequate teaching on the protocol and were able to maintain frequency of urine dipstick checks.

Conclusion: We developed and implemented an outpatient protocol for high dose methotrexate. This study largely details the development of this protocol and its initial safety evaluation. More work needs to be done to assess its feasibility on a larger number of patients who receive more cycles in the outpatient setting.

Keywords: health care delivery, diffuse large B cell lymphoma, CNS prophylactic treatment, quality improvement, chemotherapy – oncology

INTRODUCTION

Methotrexate (MTX) is a folate antagonist used across a wide range of diseases, with dose levels classified as low or high (1). High-dose methotrexate (HDMTX) consists of doses ≥500 mg/m^2, used for the treatment of primary and secondary CNS lymphoma (PCNSL), leptomeningeal metastases, and osteosarcoma, as well as central nervous system (CNS) prophylaxis in patients with leukemia and high-risk lymphoma. These doses are potentially lethal without administration of intravenous and/or oral leucovorin to rescue normal cells from apoptosis, specifically in the bone marrow and GI tract (2, 3). In addition to leucovorin, normal renal clearance of MTX is required to quickly eliminate the drug, supported by aggressive hydration and urinary alkalinization. Toxicities often occur as a result of the high dose and duration of exposure, and include renal toxicity, hepatotoxicity, stomatitis, myelosuppression, rash, pneumonitis, and encephalopathy (4). To ensure safe administration, HDMTX is most often administered in the hospital setting with an average length of stay around 4-5 days, barring any treatment complications. For patients receiving HDMTX for Primary CNS lymphoma or CNS prophylaxis for DLBCL, these inpatient hospital admissions, which most commonly are scheduled every 2 weeks, have the potential to negatively impact a patient's quality of life and contribute to the growing financial burden on the health care system.

There is experience with outpatient administration of HDMTX in the pediatric population. Two small prospective studies, one in pediatric acute lymphoblastic leukemia (ALL) and one in pediatric osteosarcoma, showed the safety and feasibility of this approach in the appropriate patient population, reducing cost and increasing quality of life by allowing patients to remain out of the hospital (5, 6). Two large, retrospective studies in pediatric populations from Memorial Sloan Kettering Cancer Center (MSKCC) and the Children's Hospital at Montefiore support these findings (7, 8). While NCCN has published a toolkit to implement outpatient HDMTX (9), few studies have been published and none of these include the adult patient population, presenting a significant gap in the literature (10, 11). Studies are needed to examine the feasibility and safety in this population, as comorbidities, organ dysfunction, and social challenges seen in adults differ greatly from the pediatric population (12).

Prior to the development of an outpatient HDMTX protocol in the adult population, we performed a retrospective review of all patients receiving inpatient HDMTX at Thomas Jefferson University, an urban academic tertiary care medical center, between January 1, 2018 and October 31, 2019 to determine the distribution and rate of toxicities in adult patients at our institution. Details of this study have been presented (13). The most common toxicity observed in this population was acute kidney injury (AKI), with an incidence of 21% in patients receiving HDMTX as prophylaxis [median dose 3.5 g/m2 (1-3.5 g/m2)] compared to 33% in patients receiving HDMTX as treatment [median dose 3.5 g/m2 (range 0.25-12 g/m2)] for CNS disease. Additionally, all AKI in the prophylactic group was grade II (>1.5 - 3.0 x baseline; >1.5 - 3.0 x ULN) or lower according to CTCAE version 5.0 and resolved. Other toxicities in patients receiving HDMTX for CNS prophylaxis was minimal. Based on these results, we initiated an outpatient HDMTX program in patients requiring CNS prophylaxis for diffuse large B-cell lymphoma (DLCBL). Herein we present the development of our outpatient HDMTX protocol and results of the safety run-in phase.

METHODS

We created an inter-professional, multi-disciplinary team to develop the outpatient HD-MTX protocol. Our team included an oncologist, oncology fellow, infusion center managers, nurse educators, inpatient and outpatient nursing staff, advanced practice providers, oncology pharmacists and home infusion service nurses and pharmacists. Protocol development followed an iterative process and the final protocol is referenced in **Appendix A**. Once developed, the protocol was implemented and modified through an iterative process with each cycle of HD-MTX administered.

Complete patient eligibility criteria are listed in the protocol, including a diagnosis of DLBCL requiring CNS prophylaxis (as determined by their provider), age 18-70 years, ECOG performance status ≤ 2, normal renal function (CrCl ≥60 mL/min), no history of color blindness (to be able to read the urine dipstick), and adequate social support. Patients who clear their first administration of HDMTX within 3-5 days without complications qualify to receive cycles 2 and 3 in the outpatient setting. Both the patient and caregiver are educated on reading the urine dipsticks. While the optimal method of CNS prophylaxis has yet to be defined by prospective randomized studies, each patient receives a currently accepted standard of 3 cycles of HDMTX at a dose of 3.5 gm/m^2. HDMTX can be given alternating with R-CHOP after even cycles (i.e. 2, 4, and 6) or at the end of 6 cycles of systemic treatment. All patients complete cycle 1 of the protocol as an inpatient to ensure clearance of the MTX without complications on the outpatient protocol.

During the inpatient stay for cycle 1, nursing and pharmacy education is performed. Patients are taught how to use the urine dipstick for pH monitoring. The frequency of monitoring is discussed and reinforced. Scheduled medications are reviewed. Pharmacists discuss with patients concomitant medications such as sulfonamides, non-steroidal anti-inflammatory drugs, and proton pump inhibitors should be avoided until after methotrexate clearance. The home infusion team visits with the patient, ensures insurance will cover all related costs, reviews the process for delivery of materials and supplies and also provides an emergency number for 24 hour access in case the infusion pump malfunctions or other questions arise. Patients are also encouraged to call the cancer center at any time to speak with a physician if any concerns or questions arise during the home infusion process.

The protocol is initiated as follows. Oral sodium bicarbonate 1950mg every 6 hours and oral acetazolamide 500mg every 6 hours is initiated at home, three and one days prior to MTX infusion, respectively. On treatment day, patients receive HDMTX, given over 4 hours, in the infusion center, and continuous IV fluids with normal saline (later changed to IV sodium bicarbonate allowing discontinuation of oral sodium bicarbonate) through central venous catheter is initiated. No recommendations were made on minimum or maximum daily oral fluid intake as the patient will receive the necessary daily volume of fluids intravenously. Patients monitor urine pH at home *via* urine dipstick every 2 hours on day 1 followed by every

4 hours thereafter while awake. Nightly acetazolamide 500mg is continued, with additional dose every 6 hours as needed for urine pH <7.5. Starting 24 hours after MTX infusion, patients begin oral leucovorin 25 mg every 6 hours. A record is kept of side effects, timing of medications, and urine pH levels (see **Appendix B**). Patients present daily to the infusion center for toxicity check, medication review, and blood draw including complete blood count, comprehensive metabolic panel, and methotrexate levels (starting on day 3, but this was later modified to day 2). Urine pH is checked daily through central laboratory to ensure correlation with urine dipsticks. Oral leucovorin is increased to 25mg every 3 hours as needed based on the nomogram (**Appendix C**). According to our standard of care practice, if the patient fails to show up for a scheduled appointment, they will be called by the care team to investigate further. Indications for admission to the hospital include serum Cr ≥1.5x baseline, toxicity unable to be managed as outpatient, or need to increase leucovorin dose to >25mg every 3 hours (given limit on oral bioavailability) (14). Once methotrexate level is ≤0.1μmol/L, patients are disconnected from IV fluid infusion and stop oral acetazolamide. Oral leucovorin is continued and oral sodium bicarbonate is restarted for 3 additional days.

As part of the implementation process, a safety run-in phase was designed such that the first 5 cycles on the outpatient protocol were administered in the inpatient setting. This run-in was implemented to allow for any necessary changes to the protocol to be made if unexpected barriers arose.

RESULTS

Two patients completed the safety run-in phase. The first patient, a 46-year-old man with no comorbidities, received all three cycles of HDMTX for CNS prophylaxis as an inpatient on the outpatient protocol. Time to methotrexate clearance was ≤ 2 days for all three cycles. No AKI or other toxicity was observed. During these cycles, the bedside urine dipsticks that were utilized reported urine pH readings 0.5 higher than the lab urine pH. As a result, an alternative urine dipstick test was used for the second patient during the run-in phase.

The second patient, a 28-year-old man with no comorbidities, received cycle 1 and 2 inpatient on the outpatient protocol, with the third cycle completed outpatient. Time to methotrexate clearance was ≤ 3 days for all three cycles. Again, no AKI or other toxicity was observed. With the change in urine dipstick, the lab-based pH values and those obtained at the bedside correlated.

Both patients were able to follow the preadmission instructions for sodium bicarbonate and acetazolamide. The patients reported adequate teaching on the protocol and were able to maintain frequency of urine dipstick checks. Several logistical improvements were made to the protocol based on patient feedback and process review.

DISCUSSION

Care models for the administration of outpatient chemotherapy are becoming increasingly popular, implemented with the goal to improve patient quality of life and decrease costs to the patient and health care system. While the safety and feasibility of outpatient HDMTX has been published in pediatric populations, and a toolkit has been suggested by NCCN, this protocol is one of the few publication we are aware of detailing implementation of outpatient HDMTX administration in adult patients. Our safety run-in phase demonstrated feasibility and safety of the outpatient protocol for patients with DLBCL requiring CNS prophylaxis, although we acknowledge the small sample size (n=2) and young age of these patients may bias the initial results. As the next phase of this implementation initiative, a prospective observational study is being performed with the primary objective to evaluate the rate of methotrexate toxicity, particularly renal toxicity, in the outpatient setting as compared to the rate of toxicity of our historical control. Secondary objectives include comparing the effects on treatment burden and cost burden for these care models, the total cost and out-of-pocket cost for patients, as well as quality of life of inpatient versus outpatient treatment modalities. This is being assessed through use of the patient reported Treatment Burden Questionnaire (TBQ) (15), the Cost Burden Survey (16), revenue cycle evaluation, and the EORTC-qlq-c30 quality of life survey tool (17).

MSKCC has recently demonstrated feasibility of an outpatient HDMTX protocol integrating glucarpidase into the treatment of primary CNS lymphoma (18). Glucarpidase, a carboxypeptidase enzyme, rapidly inactivates methotrexate to reduce toxicity without crossing the blood brain barrier. Use of glucarpidase for this patient population in the outpatient setting is appropriate given the high risk of AKI and other toxicity seen in our retrospective analysis. However, patients receiving HD-MTX for CNS prophylaxis are a different patient population with lower risk for adverse events including acute kidney injury and thus may not need glucarpidase to effectively receive treatment as an outpatient as has been described in these studies (10, 11). The use of glucarpidase is often restricted to patients who meet specific criteria due to its high cost. Our protocol aims to provide a patient centered approach while at the same time limits cost and financial burden of this outpatient regimen. We recognize that our protocol requires significant effort and commitment on behalf of the patient and their family, and is therefore limited to a subset of patients with adequate social support and transportation resources. Additionally, the success of outpatient chemotherapy care models requires a supportive, multidisciplinary team.

DATA AVAILABILITY STATEMENT

The raw data supporting the conclusions of this article will be made available by the authors, without undue reservation.

AUTHOR CONTRIBUTIONS

All authors listed have made a substantial, direct, and intellectual contribution to the work, and approved it for publication.

SUPPLEMENTARY MATERIAL

The Supplementary Material for this article can be found online at: https://www.frontiersin.org/articles/10.3389/fonc.2021.773397/full#supplementary-material

REFERENCES

1. *Methotrexate Injection*. FDA (2015). Available at: https://www.accessdata.fda.gov/drugsatfda_docs/label/2015/011719s122lbl.pdf. (Accessed 12/02/2021)
2. Visentin M, Zhao R, Goldman ID. The Antifolates. *Hematol/Oncol Clin N Am* (2012) 26(3):629–ix. doi: 10.1016/j.hoc.2012.02.002
3. Newman AC, Maddocks ODK. One-Carbon Metabolism in Cancer. *Br J Cancer* (2017) 116(12):1499–504. doi: 10.1038/bjc.2017.118
4. Howard SC, McCormick J, Pui CH, Buddington RK, Harvey RD. Preventing and Managing Toxicities of High-Dose Methotrexate. *Oncologist* (2016) 21(12):1471–82. doi: 10.1634/theoncologist.2015-0164
5. Bartholomew JL, Dai H, August KJ, Ryan RE, Stegenga KA. Feasibility of Outpatient High-Dose Methotrexate Infusions in Pediatric Patients With B-Lineage Acute Lymphoblastic Leukemia. *J Adv Pract Oncol* (2018) 9(4):381–6. doi: 10.6004/jadpro.2018.9.4.2
6. Hendershot E, Volpe J, Taylor T, Nicksy D, Mills D, Ramachandran N, et al. Outpatient High-Dose Methotrexate for Osteosarcoma: It's Safe and Feasible, If You Want It. *J Pediatr Hematol/Oncol* (2019) 41(5):394–8. doi: 10.1097/MPH.0000000000001238
7. Zelcer S, Kellick M, Wexler LH, Gorlick R, Meyers PA. The Memorial Sloan Kettering Cancer Center Experience With Outpatient Administration of High Dose Methotrexate With Leucovorin Rescue. *Pediatr Blood Cancer* (2008) 50 (6):1176–80. doi: 10.1002/pbc.21419
8. Mahadeo KM, Santizo R, Baker L, Curry JO, Gorlick R, Levy AS. Ambulatory High-Dose Methotrexate Administration Among Pediatric Osteosarcoma Patients in an Urban, Underserved Setting Is Feasible, Safe, and Cost-Effective. *Pediatr Blood Cancer* (2010) 55(7):1296–9. doi: 10.1002/pbc.22772
9. Network NCC. *NCCN Best Practices Committee Infusion Efficiency Workgroup Toolkit: Providing Oncology Treatments in the Outpatient Setting* (2020). Available at: https://www.nccn.org/docs/default-source/covid-19/2021-covid-nccn-providing-oncology-treatments-outpatient.pdf?sfvrsn=d7c9efd7_5.
10. Pampín R, Labeaga Y, Rodríguez B, Fernández B, Fernández R, Carbajales M. Experience With Ambulatory High-Dose Methotrexate Administration as CNS Prophylaxis in Patients With Non-Hodgkin Lymphoma. *J Oncol Pharm Pract* (2019) 26(3):549–55. doi: 10.1177/1078155219852412
11. Bernard S, Hachon L, Diasonama JF, Madaoui C, Aguinaga L, Miekoutima, et al. Ambulatory High-Dose Methotrexate Administration as Central Nervous System Prophylaxis in Patients With Aggressive Lymphoma. *Ann Hematol* (2021) 100(4):979–86. doi: 10.1007/s00277-020-04341-7
12. Kawakatsu S, Nikanjam M, Lin M, Le S, Saunders I, Kuo DJ, et al. Population Pharmacokinetic Analysis of High-Dose Methotrexate in Pediatric and Adult Oncology Patients. *Cancer Chemother Pharmacol* (2019) 84(6):1339–48. doi: 10.1007/s00280-019-03966-4
13. Sokol K, Yuan K, Fendler K, Burdette S, Galanis P, Piddoubny M, et al. Toxicity of High-Dose Methotrexate Administration at the Sidney Kimmel Cancer Center (SKCC): A Retrospective Review to Guide Establishment of an Outpatient Treatment Program. *J Clin Oncol* (2020) 38(29_suppl):30–0. doi: 10.1200/JCO.2020.38.29_suppl.30
14. McGuire BW, Sia LL, Haynes JD, Kisicki JC, Gutierrez ML, Stokstad EL. Absorption Kinetics of Orally Administered Leucovorin Calcium. *NCI Monogr* (1987) (5):47–56
15. Tran V-T, Montori VM, Eton DT, Baruch D, Falissard B, Ravaud P. Development and Description of Measurement Properties of an Instrument to Assess Treatment Burden Among Patients With Multiple Chronic Conditions. *BMC Med* (2012) 10(1):68. doi: 10.1186/1741-7015-10-68
16. Huntington SF, Weiss BM, Vogl DT, Cohen AD, Garfall AL, Mangan PA, et al. Financial Toxicity in Insured Patients With Multiple Myeloma: A Cross-Sectional Pilot Study. *Lancet Haematol* (2015) 2(10):e408–16. doi: 10.1016/S2352-3026(15)00151-9
17. Sprangers MAG, Bonnetain F. EORTC QLQ-C30. In: AC Michalos, editor. *Encyclopedia of Quality of Life and Well-Being Research*. Dordrecht: Springer Netherlands (2014). p. 1933–5.
18. Schaff L, Lobbous M, Bozza A, Carlow D, Nabors L, Grommes C. Covd-23. Planned-Use Glucarpidase for Outpatient High Dose Methotrexate (HD-MTX) Administration in Patients With CNS Lymphoma (CNSL) During the COVID-19 Pandemic. *Neuro-Oncology* (2020) 22(Supplement_2):ii25–6. doi: 10.1093/neuonc/noaa215.105

Conflict of Interest: The authors declare that the research was conducted in the absence of any commercial or financial relationships that could be construed as a potential conflict of interest.

Advantages of publishing in Frontiers

OPEN ACCESS
Articles are free to read for greatest visibility and readership

FAST PUBLICATION
Around 90 days from submission to decision

HIGH QUALITY PEER-REVIEW
Rigorous, collaborative, and constructive peer-review

TRANSPARENT PEER-REVIEW
Editors and reviewers acknowledged by name on published articles

Frontiers
Avenue du Tribunal-Fédéral 34
1005 Lausanne | Switzerland

Visit us: www.frontiersin.org
Contact us: frontiersin.org/about/contact

REPRODUCIBILITY OF RESEARCH
Support open data and methods to enhance research reproducibility

DIGITAL PUBLISHING
Articles designed for optimal readership across devices

FOLLOW US
@frontiersin

IMPACT METRICS
Advanced article metrics track visibility across digital media

EXTENSIVE PROMOTION
Marketing and promotion of impactful research

LOOP RESEARCH NETWORK
Our network increases your article's readership